World Materials Congress

1988

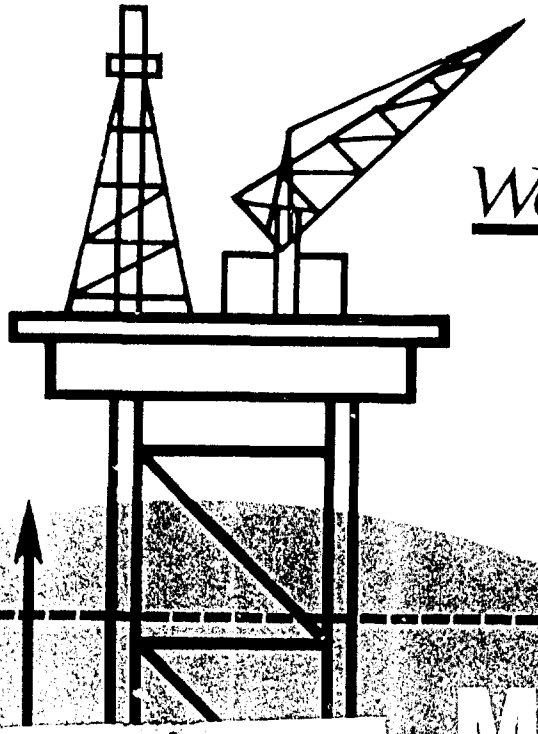



# Microalloyed HSLA Steels



## Conference Proceedings

Published by
ASM

UNCLASSIFIED

SECURITY CLASSIFICATION OF THIS PAGE (When Data Entered)

| REPORT DOCUMENTATION PAGE | | READ INSTRUCTIONS BEFORE COMPLETING FORM |
|---|---|---|
| 1. REPORT NUMBER<br>ARO 25297.6-MS-CF | 2. GOVT ACCESSION NO.<br>N/A | 3. RECIPIENT'S CATALOG NUMBER<br>N/A |
| 4. TITLE (and Subtitle)<br>1988 World Materials Congress Proceedings<br>24-30 Sep 88, Chicago Eight Volumes | | 5. TYPE OF REPORT & PERIOD COVERED<br>Final<br>1 Oct 87 - 31 Mar 89<br>6. PERFORMING ORG. REPORT NUMBER<br>N/A |
| 7. AUTHOR(s)<br>S. G. Fishman and A. K. Dhingra, editors | | 8. CONTRACT OR GRANT NUMBER(s)<br>DAAL03-87-G-0128 |
| 9. PERFORMING ORGANIZATION NAME AND ADDRESS<br>ASM International<br>Detroit, MI 48202 | | 10. PROGRAM ELEMENT, PROJECT, TASK AREA & WORK UNIT NUMBERS<br>N/A |
| 11. CONTROLLING OFFICE NAME AND ADDRESS<br>U. S. Army Research Office<br>P. O. Box 12211<br>Research Triangle Park, NC 27709 | | 12. REPORT DATE<br>1988<br>13. NUMBER OF PAGES |
| 14. MONITORING AGENCY NAME & ADDRESS (if different from Controlling Office) | | 15. SECURITY CLASS. (of this report)<br>Unclassified<br>15a. DECLASSIFICATION DOWNGRADING SCHEDULE |

16. DISTRIBUTION STATEMENT (of this Report)

Submitted for announcement only.

17. DISTRIBUTION STATEMENT (of the abstract entered in Block 20, if different from Report)

18. SUPPLEMENTARY NOTES

The view, opinions, and/or findings contained in this report are those of the author(s) and should not be construed as an official Department of the Army position, policy, or decision, unless so designated by other documentation.

19. KEY WORDS (Continue on reverse side if necessary and identify by block number)

Composites, Sheet Steels, Electronic Materials, Wear Resistance, Precipitation Phenomena, High Integrity Castings, Inclusions, HSLA Steels

20. ABSTRACT (Continue on reverse side if necessary and identify by block number)

The proceedings of the 1988 World Materials Congress were published by ASM and consits of the following volumes:

1. Microalloyed HSLA Sttels Conference Proceedings
2. Inclusions and Their Influence on Material Behavior
3. High Integrity Castings
4. Precipitation Phenomena: Deformation and Aging
5. Wear Resistance of Metals and Alloys

(over)

DD FORM 1 JAN 73 1473 EDITION OF 1 NOV 65 IS OBSOLETE



UNCLASSIFIED

SECURITY CLASSIFICATION OF THIS PAGE (When Data Entered)

ABSTRACT CONTINUED:

6. Electronic Materials and Processing
7. Corrosion-Resistant Automotive Sheet Steels
8. Cast Reinforced Metal Composites

# MICROALLOYED HSLA STEELS

*Proceedings of*

**Microalloying '88**

*held in conjunction with the*

**1988 World Materials Congress**

**Chicago, Illinois, USA**

**24–30 September 1988**

*Sponsored by the*

Microalloying '88 Organizing Committee

*Published by*

ASM INTERNATIONAL

The Publication of this Conference Proceedings of the 1988 World Materials Congress has been made possible by the generous contribution of Dofasco Inc.



Library of Congress Catalog Card Number: 88-071985
ISBN: 0-87170-337-8
SAN: 204-7586

Printed in the United States of America

## ORGANIZING COMMITTEE

Dr. Harry Stuart, Chairman
Niobium Products Company Inc.

Mr. E. A. Loria, Secretary
Consultant

Dr. Jack Bucher
Lukens Steel Company

Dr. Anthony J. DeArdo
University of Pittsburgh

Dr. Issac Garcia
University of Pittsburgh

Dr. J. Malcolm Gray
Microalloying International

Dr. Steven Hansen
Bethlehem Steel Corp.

Mr. John Held
LTV Steel Corp.

Mr. John Hiam
Inland Steel Company

Dr. Jay Koo
Exxon Research

Dr. Konrad Kundig
Consultant

Mr. Roger Laible
Bethlehem Steel Corp.

Dr. Paul Repas
USX Corporation

Dr. Peter D. Southwick
Inland Steel Company



Sold by:
ASM International
9639 Kinsman Road
Metals Park, OH 44073
Price:

# TABLE OF CONTENTS

## Introductory



## Oil and Gas Industry



## Offshore Installation

## Marine, Military and Pressure Vessels

## Automotive and Off-Highway

## Machinery, Engineering and Construction



## Abstract Session
## Research in Progress—Future Applications

# AN INTRODUCTION

**H. Stuart**
Niobium Products Company Inc.
Pittsburgh, Pennsylvania, USA

## AN INTRODUCTION

This present symposium represents an important milestone in a series of symposia which have, over the years, taken the subject of high strength low alloy steels as their theme. Looking back, this series of conferences probably started in 1963 when the British Iron and Steel Research Associate (BISRA) and the British Iron and Steel Institute held a conference in Harrogate, England, called "Metallurgical Developments in Carbon Steels". The proceedings of this conference contain a number of papers which refer to the effects of microalloys, or, in the words of I. M. Mackenzie in his foreword "elements such as nitrogen, niobium, aluminum and boron". In the 25 years that have followed, many conference proceedings have cronicled the developments of this microalloying technology and the applications for steels which develop their properties on its basis. Some of the most auspicious meetings were held in Scarborough, England (1967); Nuremburg, West Germany (1970); Cleveland, Ohio (1972 & 1975); Washington, DC (1985); Pittsburgh, Pennsylvania (1981); Philadelphia, Pennsylvania (1983); Wollongong, Australia (1984); and Beijing, China (1985). It has become clear from these conferences that there are essentially three microalloying elements of primary importance - niobium, vanadium and titanium. In 1963, Mackenzie wrote "Carbon steels are produced in vastly greater tonnages than any other type of steel and thus, from an economic point of view, carbon steels can be classified as the most important product of the steel industry. This remains true today. Probably more than 500 million tonnes of carbon steel are consumed annually by the world's industries, and yet, less than ten percent of this total benefits from the use of microalloying to increase its strength and toughness. Is there some fundamental engineering reason why this is the case? Are microalloyed steels too expensive or is it simply a matter of time before microalloyed steels are more universally adopted in structures. It remains a fact that microalloying appears to have reached some degree of stagnacy during the last few years, certainly if we use world niobium shipments as a barometer, and I hope that one result of this present conference might be a clarification of the current and future status of applications for this class of steels. We know much about how the steels are made by the steelmaker and we are knowledgeable in their applications in the fields of pipelines and automobiles. But what of other applications? Is it unrealistic to expect much more carbon steel to be made using microalloying? That is my question, and I hope in the next five days our symposium will provide the answer.

# METALLURGICAL FUNDAMENTS FOR HSLA STEELS

**Paul E. Repas**
USS Technical Center
Monroeville, Pennsylvania 15146 USA

ABSTRACT

The continuing development and application of HSLA steels has evolved in part because of the constantly increasing technology base associated with these steels as well as the constantly increasing sophistication in the equipment and techniques used to produce such steels. The properties and service performance of HSLA steels depend for the most part on the compositions and microstructures of these steels which, in turn, are controlled by steelmaking and steel processing. Because there are extensive differences in property requirements within and among various steel product forms, numerous steel compositions and processing paths have evolved to satisfy various product applications. A review of the effects of steel composition and microstructure on steel properties is given, followed by an examination of the basic processing factors that control microstructure. The control of microstructure through steel composition, slab heating, roughing and finish rolling, controlled transformation after rolling, and, in some products, during subsequent processing is shown to be of fundamental importance to the successful production and application of microalloyed HSLA steels.

NUMEROUS REVIEWS of the historical development and of the fundamental metallurgy of microalloyed high-strength low-alloy (HSLA) steels have appeared in various conference proceedings over the past 25 years (1-18). Through these references one may follow the development and production of HSLA steels from rather empirical beginnings to the present more scientific basis. This evolution of microalloyed steels, both in production and in application, has resulted because of the constantly improving technology base, because of the sophistication in equipment and techniques for steelmaking, casting, hot working, and subsequent processing, and, because of the user's persistence in learning how to design with, form, and fabricate this class of steels. The end result is obvious: HSLA steels have become widely accepted and, in many applications, totally dominate the market, as will be discussed by others in this conference. The acceptance of these steels is a direct result of the attractive combinations of properties that can be developed in these steels, and it is the metallurgical fundamentals that allow these properties to be controlled, which will be addressed in this paper.

The control of properties in HSLA steels is accomplished by the control of the composition and microstructure of these steels. The term "microstructure" here is meant to include all aspects of the steel structure--from the atomic scale of interstitial and substitutional atoms in the iron matrix, through dislocations and finely dispersed precipitates, through coarser second-phase particles and inclusions, and the conventional description of ferrite and carbide phases (grain size and shape, carbide type and distribution, etc.). The control of this "microstructure" in specific steels depends on the control of both steel composition and steel processing and allows the development of specific sets of mechanical properties for individual applications. The mechanical properties of most common interest include strength, ductility or formability, and notch toughness, whereas specific applications may, for example, require steels with improved weldability, improved levels of through-thickness ductility, improved corrosion resistance, or improved resistance to hydrogen-induced cracking (HIC), and sulfide stress cracking (SSC). The properties required for specific applications are associated with improved fabricability of the steels and/or improved service performance. Naturally, design considerations play an equally important role in determining the service performance of any steel component or structure, but design will not be discussed in

this paper.

Because various product forms (e.g., plates, structurals, sheets, bars, tubular goods, forgings) can undergo significantly different processing histories, it is useful to first review the relationships among properties and microstructure and then examine the relationships among processing and microstructure so that an overall picture can be gained of the important microstructural features that need to be controlled and of how they may be controlled. By knowing the required properties and microstructure for a given application, a combination of steel composition and thermomechanical processing conditions can be better defined to achieve the particular microstructure/property objectives.

## MICROSTRUCTURE/PROPERTY RELATIONSHIPS

For the mechanical properties of general interest, empirical relationships have been developed between composition and microstructural features and specific properties as briefly outlined below.

STRENGTH - A modified Hall-Petch relationship can generally be used to describe the yield or tensile strength of low-carbon steels in terms of compositional and microstructural features, Eq. (1).

$$\sigma = \sigma_o + \sigma_{SSS} + \sigma_{ISS} + \sigma_{PPT} + \sigma_{DSL} + \sigma_{SUB} + \sigma_{SPH} + k_y\, d^{-1/2} \qquad (1)$$

In this equation, $\sigma_o$ and ky are constants, and the various sigma ($\sigma$) terms represent the intrinsic matrix hardening ($\sigma_o$), substitutional solid solution strengthening ($\sigma_{SSS}$), interstitial solid solution strengthening ($\sigma_{ISS}$), precipitation strengthening ($\sigma_{PPT}$), dislocation strengthening ($\sigma_{DSL}$), substructure strengthening ($\sigma_{SUB}$), and second phase strengthening ($\sigma_{SPH}$). The term d is the ferrite grain diameter. Of all the terms on the right-hand side of the equation, only $\sigma_o$ and $\sigma_{SSS}$ are independent of the processing history of the steel. The substitutional solid solution strengthening term [$k^{Mn}$(%Mn) + $k^{Si}$(%Si) + $k^{P}$(%P) + $k^{Cu}$(%Cu) + $k^{Ni}$(%Ni) + .....] for ferrite depends only on the amount of each element present (%x) and its relative strengthening effect ($k^x$) and can be consistently relied on in hot rolled, thermomechanically controlled processed (TMCP), normalized, or annealed products. All the remaining terms are dependent both on composition and processing history and will be discussed in more detail in the section on Processing/Microstructure Relationships.

To provide some insight into the relative contributions of each term in Eq. (1) to yield strength, Figures 1-3 and Table 1 give representative values or ranges for the magnitude of these terms for hot-rolled (or TMCP) steels with ferritic microstructures. As shown, refined ferrite grain sizes, and precipitation hardening can provide substantial increases in strength in such steels and, in fact, are the primary contributors to strength in many hot-rolled HSLA steels. The contribution of $\sigma_{ISS}$ and $\sigma_{DSL}$ are generally small in most hot-rolled products, but there are exceptions to this rule in that nitrogenized steels can contain a significant $\sigma_{ISS}$ term, and dislocation strengthening ($\sigma_{DSL}$ and $\sigma_{SUB}$) can be present in inter-critically rolled products or steels transformed to acicular or bainitic ferrite. Second-phase hardening, for example by pearlite in ferrite-pearlite steels, does not contribute to yield strength but does contribute significantly to tensile strength in low-carbon steels. Other second phases, such as martensite or the martensite-austenite (MA) constituent in dual-phase ferrite-martensite steels, can actually decrease yield strength while increasing tensile strength.

It should be noted that even simple changes in the composition or processing practice of HSLA steels generally produce multiple effects in terms of the various factors in Eq. (1). For example, if a small Ni addition is made to a microalloyed steel, no solid-solution hardening is expected, but as will be described in a later section, the austenite-to-ferrite transformation is affected, and changes in both grain size and precipitation hardening can occur. Similarly, changes in processing practices can simultaneously influence several of the terms in Eq. (1).

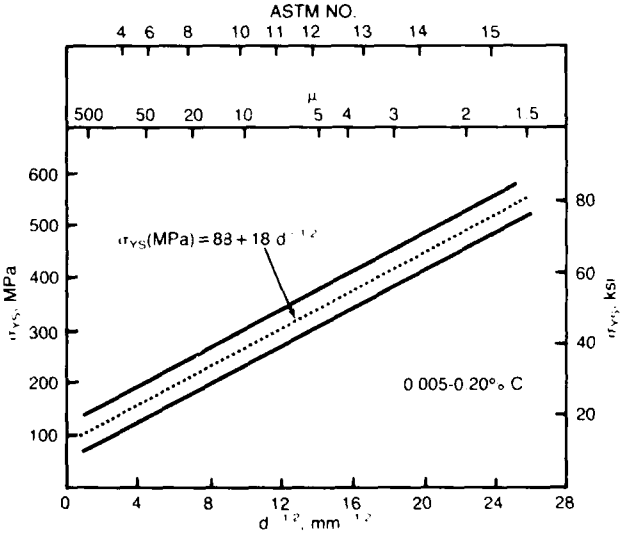


Fig. 1 - Relationship between conventional lower yield stress and (grain diameter)$^{-1/2}$ (Ref. 19)

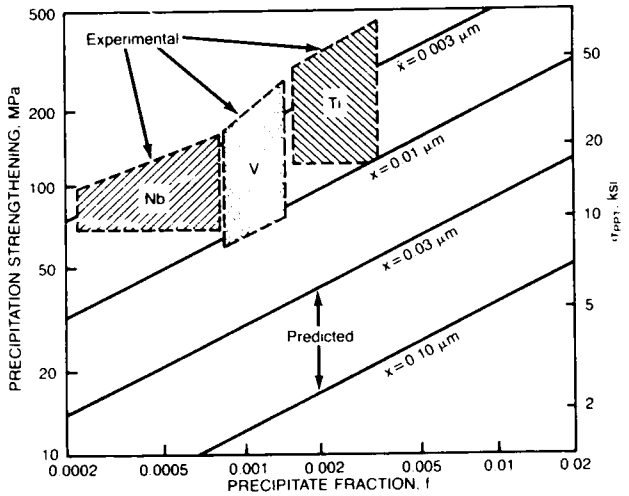


Fig. 2 - The dependence of precipitation strengthening on precipitate size (x) and fraction according to theory compared with experimental observations for given microalloying additions (Ref. 20-21)

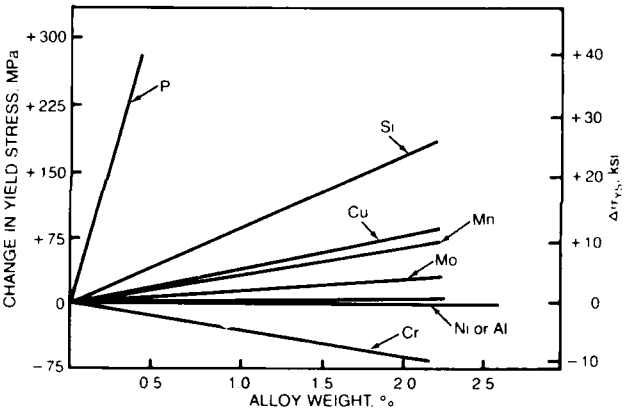


Fig. 3 - Solid-solution strengthening of ferrite (Ref. 22)

Table 1

Representative Contributions to Yield Strength in Hot-Rolled Microalloyed Low-Carbon Ferritic Steels, MPa

| | Polygonal Ferrite | Acicular or Bainitic Ferrite | Intercritically Rolled Ferrite |
|---|---|---|---|
| σ0 | 80 | 80 | 80 |
| σSSS | 10-150 | 10-150 | 10-150 |
| σISS | 0-70 | 0-70 | 0-70 |
| σPPT | 70-250 | 70-250 | 70-250 |
| σDSL | - | 0-200 | - |
| σSUB | - | - | 0-150 |
| σSPH | - | - | - |
| $k_{yd}^{-1/2}$ | 150-300 | 150-300 | 150-300 |

DUCTILITY - The term "ductility" has a variety of meanings to the steel producer or steel user, including uniform or total tensile elongation, reduction of area, strain-hardening exponent (n-value), stretchability, drawability, bendability, and forming limit. Regardless of the measure of ductility selected, increasing strength levels invariably produce lower tensile elongation values and decreased formability. However, different types of steels may have different strength-ductility relationships on an absolute scale so that at any given strength level, steels with different ductility levels can be found. As shown in Figures 4 and 5 for hot- and cold-rolled sheet products, different levels of ductility can be obtained at any given strength level depending on the strengthening mechanism(s) employed.

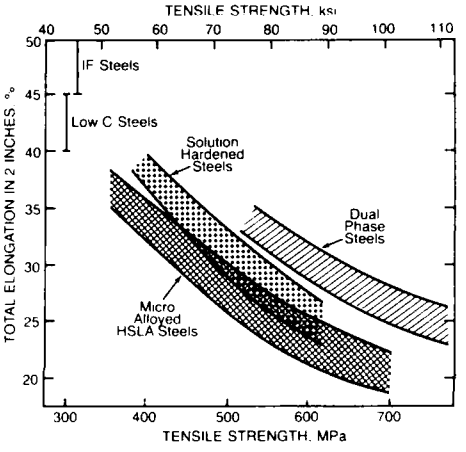


Fig. 4 - Strength-elongation relationships for various hot-rolled sheet steels

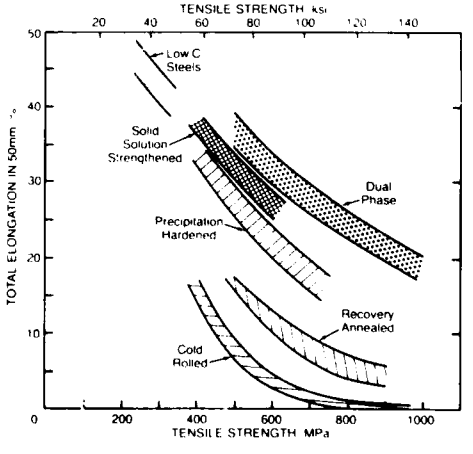


Fig. 5 - Strength-elongation relationships for various cold-rolled sheet steels (Ref. 23, 24, 25)

Thus, judicious choice of or avoidance of particular strengthening mechanisms must be made in the design of alloy and processing practices for specific applications. For example, dual-phase (ferrite-martensite) steels offer the maximum elongation for a given tensile strength for both hot- and cold-rolled sheet products, but such steels may only be required for the most difficult forming application and could be an unnecessarily expensive choice of steels. Cold working is probably the least expensive strengthening mechanism (cold rolling of an unalloyed low-carbon steel), but such steels provide little residual ductility for further cold forming during fabrication. The major portion of HSLA steels in all product forms use combinations of solid solution elements and microalloying elements for strengthening.

NOTCH TOUGHNESS - The resistance to brittle failure or notch toughness of steels is commonly measured by Charpy V-notch impact testing and is an extremely important consideration for high-strength plate and structural products intended for constructional, shipbuilding, line pipe, offshore, pressure vessel, and other applications. The ductile-to-brittle impact transition temperature (ITT) can generally be described by an equation similar to the Hall-Petch type equation given earlier for strength, Eq. (2), and, as

$$ITT = T_o + \Delta T_{SSS} + \Delta T_{ISS} + \Delta T_{PPT} + \Delta T_{DSL} + \Delta T_{SPH} - kd^{-1/2} \quad (2)$$

shown in Figure 6 for some common strengthening mechanisms, the impact transition temperature is raised by all factors except grain refinement, which, as shown, can significantly lower (improve) the transition temperature. The ductile shelf energy, or impact energy absorption, of a steel depends primarily on strength level, steel cleanness, the presence of second phases (such as pearlite), and, of course, test specimen orientation. Figure 7 shows a schematic set of CVN curves that illustrate the major factors controlling the ductile-to-brittle transition curve and the energy absorption curve. Generally, the strength level is fixed for a particular application and carbon contents (pearlite contents) are low so that impact transition temperature can only be lowered significantly by refining the ferrite grain size. The shelf energy for a fixed strength level and carbon content range is controlled basically by control of inclusion content and inclusion morphology. Numerous papers in the symposiums already referenced have documented the importance of sulfur content and sulfide shape on the anisotropy of CVN energy absorption, anisotropy of ductility in the longitudinal, transverse, and through-thickness directions, and in the resistance of certain steel products to hydrogen-assisted cracking (HIC and SSC).

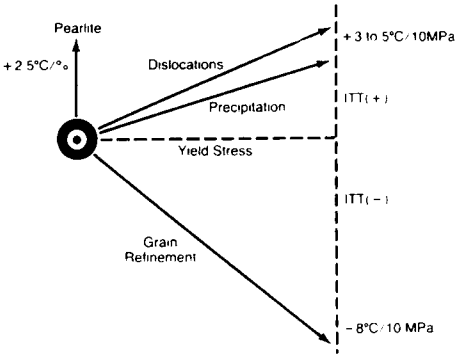


Fig. 6 - Microstructural factors affecting yield strength and impact transition temperature (Ref. 22)

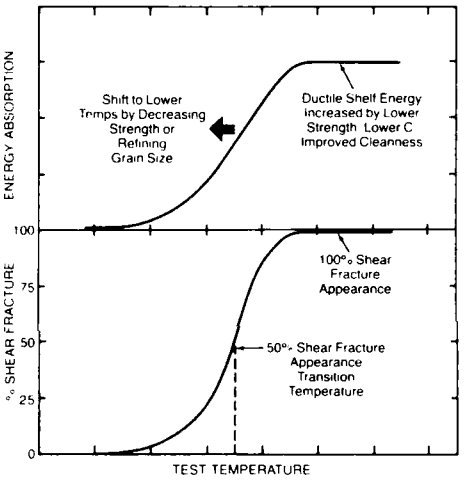


Fig. 7 - Schematic CVN curves

## FABRICABILITY/SERVICE PERFORMANCE REQUIREMENTS

Over and above the strength, ductility and toughness requirements, additional metallurgical constraints on the design and production of microalloyed HSLA steels are imposed by fabrication and service performance requirements. Because of the wide variety of product forms and applications for HSLA steels, these additional constraints can also vary widely.

The two major fabrication requirements are formability and weldability. Service performance requirements can include numerous factors, usually in combination, such as resistance to static loading, dynamic loading, fatigue failure, laminar tearing, corrosion, hydrogen-induced cracking, stress-corrosion cracking, ballistic penetration, etc. It is not the intent of this paper to review each of these factors associated with fabrication and

service performance, but it should be noted that the control of steel composition and cleanness during steelmaking and casting and the control of microstructure during steel processing are used to impart specific characteristics to the steel to meet specific fabrication and service performance requirements.

## MICROSTRUCTURE/PROCESSING RELATIONSHIPS

As noted earlier, the final microstructure in any steel product depends both on steel composition and processing history. The following sections will briefly describe the interaction between composition and processing in controlling the austenitic microstructure during heating prior to hot working and during the hot deformation steps, in controlling the austenite-to-ferrite transformation, and where applicable, in controlling the microstructure during subsequent processing steps.

STEEL HEATING - The heating of steel slabs, billets, etc., prior to hot working accomplishes several purposes including softening the steel for hot working, providing a sufficiently high initial temperature so that finishing passes are completed in the fully austenitic temperature region for some products (e.g., hot-strip mill sheet), and dissolving carbides or nitrides that need to be precipitated at some later stage of processing. Along with these positive effects, the austenite grain size may be significantly coarsened and these grains must then be sufficiently refined during hot deformation to produce the required ferrite grain size during transformation.

Examining the solubility relationships of various carbides and nitrides in austenite, Figure 8, it is apparent that a wide range of compound stabilities exist from the very stable or highly insoluble titanium nitride to the very soluble vanadium carbide. During the reheating of steel, a fine dispersion of precipitated carbonitride particles acts to pin austenite grain boundaries and prevent grain growth. However, at sufficiently high temperature and/or sufficiently long times, the particles dissolve and/or coarsen so that boundary pinning effects diminish and grain coarsening occurs. Examples of the grain coarsening behavior of various microalloyed steels are shown in Figures 9 and 10, and these data suggest, as one might expect, that the most stable compounds are more effective in preventing grain growth at higher temperatures. It is to be noted that, in addition to the solubility considerations, the volume fraction and size of the precipitate particles are obviously important inasmuch as the grain boundary pinning can be described by Eq. (3).

$$D = A \frac{p}{f_v} \qquad (3)$$

where D is the austenite grain diameter, A is a constant, p the precipitate diameter, and $f_v$ the volume fraction of precipitate particles.

HSLA steels often employ multiple microalloying additions in order to achieve a balance of microstructural control. For example, titanium nitrides can be used for austenite grain size control during slab heating, niobium can be used to control recrystal-

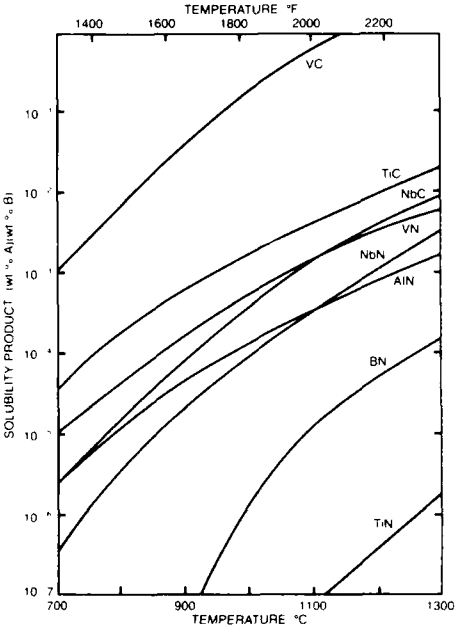


Fig. 8 - Solubility product vs. temperature for eight compounds in austenite

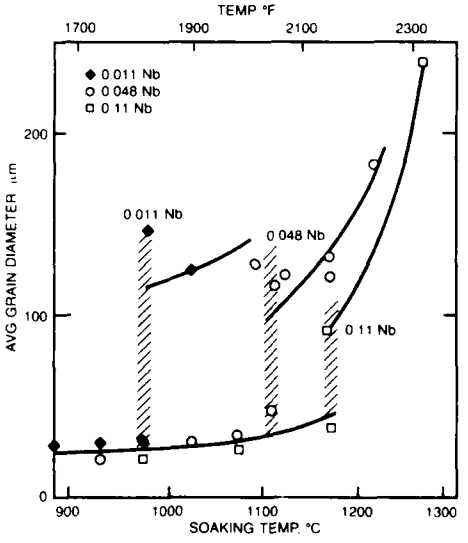


Fig. 9 - Austenite grain-coarsening characteristic of several Nb-containing steels (Ref. 26)

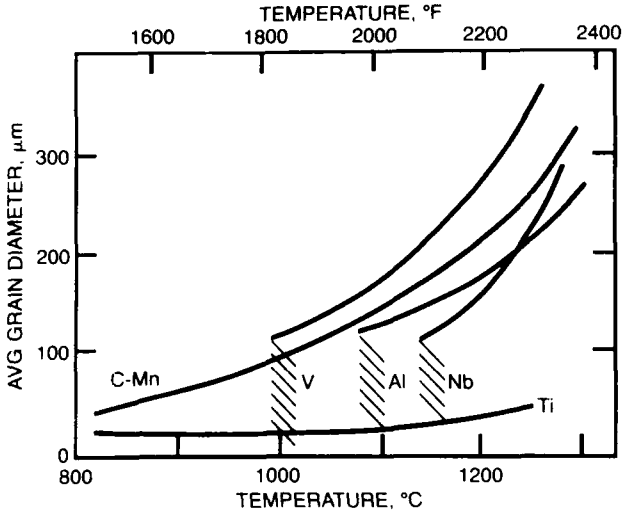


Fig. 10 - Austenite grain-coarsening characteristics of various microalloyed steels (Ref. 27)

lization of austenite during rolling, and niobium and/or vanadium can be used to achieve precipitation strengthening of ferrite.

DEFORMATION OF AUSTENITE - The deformation of austenite is generally divided into several ranges as schematically illustrated in Figure 11. At the highest temperatures, recrystallization is generally rapid and complete before subsequent deformation steps. Following recrystallization, grain growth may occur depending on time, temperature, and the presence or absence of precipitate particles. At lower temperatures, recrystallization may be partially or totally suppressed so that grain flattening and strain accumulation occurs. At very low temperatures, deformation may be extended into the two-phase austenite-plus-ferrite region so that both austenite and ferrite are deformed (intercritical rolling). As will be shown, these temperature ranges are sensitive to steel composition and to processing variables.

For the precipitate compounds that were dissolved during slab heating, the continual decrease of temperature in the workpiece eventually causes the austenite to become supersaturated with respect to compound formation so that precipitate nucleation may occur (particularly during straining) followed by particle growth.

RECRYSTALLIZATION DEFORMATION - The general objective of the initial high-temperature deformation steps after reheating of microalloyed steels (aside from shape changes) is to continually refine the austenite grain structure developed at the reheat temperature. The recrystallization and grain growth steps associated with each deformation step have been

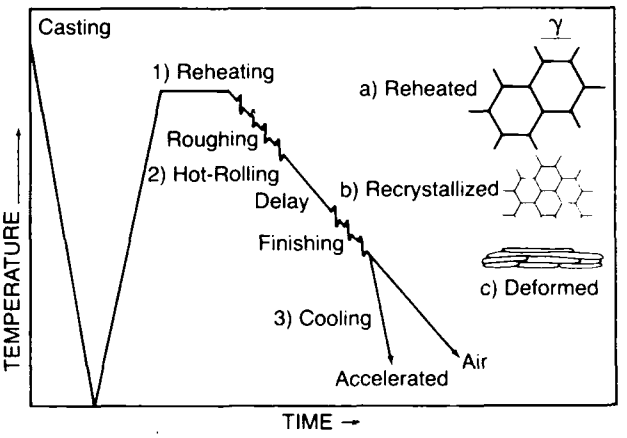


Fig. 11 - Schematic representation of the TMCP process (Ref. 28)

extensively studied in various steels, and microstructural models have been developed (29-32) that allow the calculation of the final recrystallized austenite grain size as a function of starting grain size, deformation strain, strain rate, deformation temperature, time sequence of the deformation steps, and the presence of fine dispersions of grain boundary pinning particles. Finer initial austenite grain sizes, higher strains and strain rates, and lower temperatures act to produce finer recrystallized grain sizes. A representative result of such a calculation for recrystallization rolling is shown in Figure 12. As shown, in the presence of effective pinning particles, grain growth between deformation steps is suppressed in the Nb steel. In general, such precipitates may pre-exist in the steel at the heating temperature or may be introduced by strain-induced precipitation during deformation.

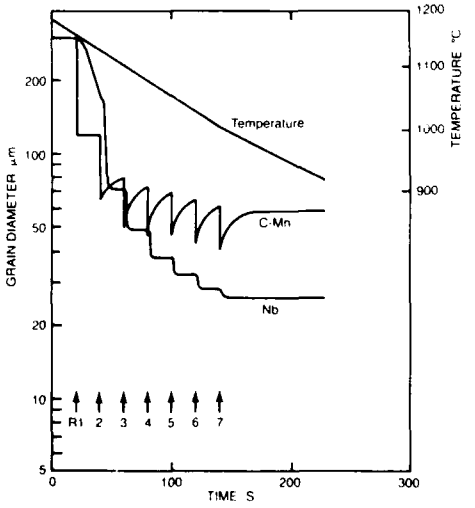


Fig. 12 - Calculated grain sizes in recrystallization rolled C-Mn and C-Mn-Nb Steels (Ref. 29)

The ranges of strains, strain rate, temperatures, and times associated with the recrystallization deformation of various steel products are fairly broad. For some steel products, recrystallization deformation may represent the entire austenite deformation cycle. For example, for very thick plates, the temperature may decrease by a relatively small amount over the entire deformation cycle and strains in each rolling pass will be relatively small. Similarly, heavy structural sections, seamless pipe, and large forgings may be deformed only at high temperatures, although deformation strains can be large. To offset the generally undesirable effect of very high final deformation temperatures on austenite grain size, consideration can be given to using stable precipitates to control the starting austenite grain size, reducing the reheat temperature, adding time delays to achieve additional radiation cooling, and/or introducing one or more accelerated cooling steps (for example, by water spray cooling) between deformation steps. The choice of technique used will depend on the microalloying system in use and the particular product form and manufacturing facility available.

For thermomechanically processed (TMCP) plates and hot-strip-mill products, which receive only a portion of their total deformation at the highest temperatures (the so-called roughing passes), the same objective of producing as fine an austenite grain size as possible at this point generally applies. For plate products, somewhat greater flexibility in the specification of slab reheating temperature is available, whereas for hot-strip-mill products, the slab-heating temperature is relatively fixed and usually high (to achieve required minimum finishing temperatures). Offsetting the higher slab-heating temperatures and consequent higher rolling temperatures are the considerably higher strains per pass used on hot-strip mills in contrast to plate mills.

Bar and rod mills can produce increases in product temperature during the finishing passes (and consequent undesirable microstructural effect), because of the very high strains and strain rates and short interpass times. To offset this adiabatic heating, interstand cooling sprays are employed for temperature (and microstructural) control (33).

DELAYS FOR TEMPERATURE REDUCTION - Because of the major influence of temperature on recrystallization and grain growth for recrystallization controlled rolling (RCR) and because it can be advantageous to deform a given steel at low RCR temperatures or even below the RCR temperature, it is desirable to hold the partially rolled steel and simply allow it to air cool to some predetermined lower temperature before continuation of rolling, or to accelerate cool the steel with water sprays. Accelerated cooling can also be conducted before and/or during the initial rolling passes (roughing passes), the objective, of course, being to force the deformation and recrystallization to lower temperatures and thereby maximize austenite grain refinement (34), especially at the center portions of thick sections. A potentially undesirable feature of decreasing the deformation temperature is that the deformation resistance of steels increases substantially, Figure 13, thereby increasing power requirements and, in some instances, going beyond the capabilities of specific plant equipment, or requiring a greater number of deformation steps (reduced mill throughput) to achieve final dimensions.

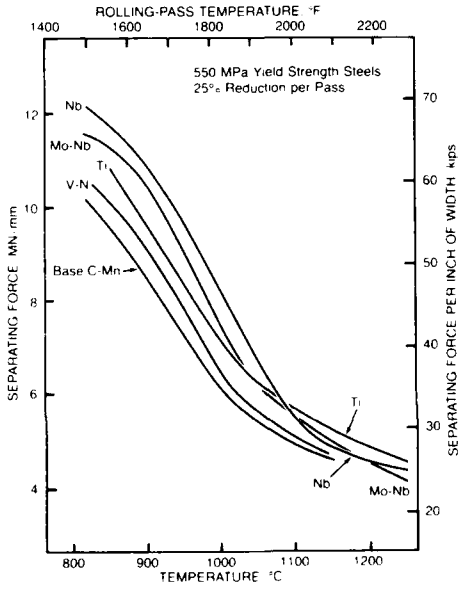


Fig. 13 - Comparison of roll-separating forces of steels that achieve an 80 ksi yield strength.

FINISHING DEFORMATION - The final deformation of various steel products can occur over a very wide temperature range, depending on product dimensions, heating, and rolling practice, and can occur above or below the austenite recrystallization temperature depending to a great extent on microalloy content, Figure 14. For steels and deformation conditions that promote austenite recrystallization, discussion of the finishing deformation is simply an extension of the recrystallization deformation section given earlier. However, as temperature decreases, as interpass times become short between subsequent passes, and as microalloying effects are encountered, recrystallization of the austenite is either incomplete or nonexistent from one particular pass to the next. As shown in Figure 15, for

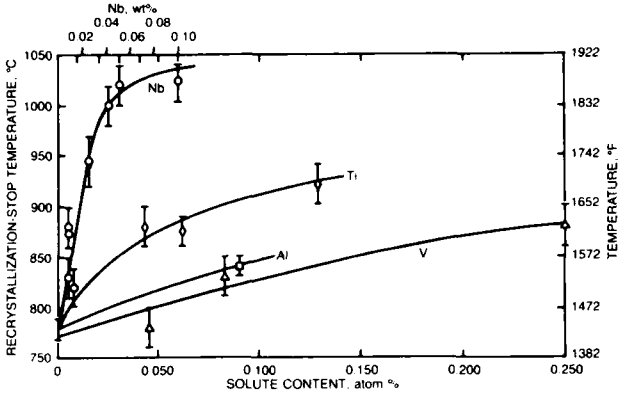


Fig. 14 - The increase in recrystallization stop temperature with increase in the level of microalloy solutes for an interpass time of 10 sec (Ref. 35)

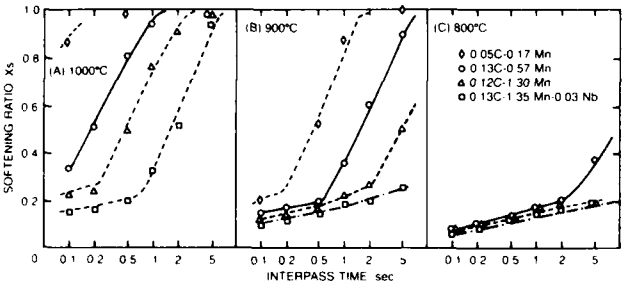


Fig. 15 - Effect of interpass time and steel chemistry on the softening (recrystalliztion) at three deformation temperatures (A) 1000°C, (B) 900°C, (C) 800°C (Ref. 36)

several steels deformed under specific conditions, the recovery and recrystallization of austenite, as determined by relative softening measurements, can be highly time, temperature, and compositional dependent. For a given steel composition, when rolling with these conditions on a reversing plate mill with interpass times of at least five seconds, recrystallization may be essentially complete before the next pass, while on a high-speed bar, rod, or strip mill with interpass times of less than one second, only partial recovery will occur (the next pass or passes, however, may give enough cumulative strain to produce at least partial recrystallization). These differences in behavior of various steels on specific processing equipment actually afford the metallurgist with an opportunity to design the steel alloy and microalloy content to produce desired austenite microstructures throughout and at the end of deformation for the particular product form and required final mechanical properties.

A useful concept in discussing the relative condition of the austenite at the end of the total deformation schedule is the surface area of grain boundaries per unit volume ($S_v$), which is considered as a measure of potential nucleation sites for ferrite during the austenite-to-ferrite transformation. As shown in Figure 16, the value of $S_v$ increases with increased reduction below the recrystallization temperature and would also increase with finer initial grain diameter ($S_v = 2000/D\gamma$ where $S_v$ is in $mm^{-1}$ and $D\gamma$ is in μm). The $S_v$ value is additionally raised by the introduction of deformation bands within the austenite grains as indicated in the figure.

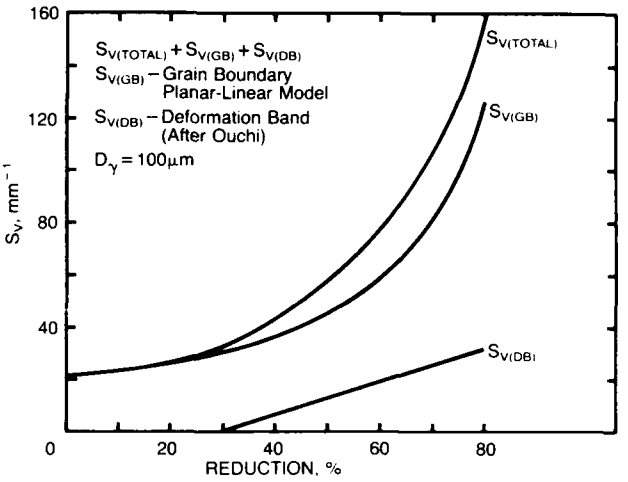


Fig. 16 - Effect of grain flattening and deformation band formation on $S_v$ (Ref. 37)

AUSTENITE TRANSFORMATION - The final step in controlling the microstructure in many products is during cooling from the last deformation step to room temperature. This transformation is basically controlled by the cooling path taken through the continuous-cooling-transformation (CCT) diagram for the particular steel of interest. Although this sounds relatively simple, the CCT diagram for a given steel is strongly influenced by the condition of the austenite prior to transformation (the grain size of recrystallized austenite or the extent of deformation of unrecrystallized austenite), and the fact that the cooling rate is often not continuous (for example, with interrupted accelerated cooled plate and with hot-strip-mill coils). The task then becomes the design of alloy, microalloying, and austenite processing combinations to fit an existing facility capability, or the design of new facilities usually to accommodate modified steel compositions and processing practices to produce desired microstructures and properties.

By briefly examining some of the basic factors that control austenite transformation, a general understanding of microstructural control can be gained. The schematic

continuous-cooling-transformation diagrams (dashed and solid lines) given in Figure 17 illustrate the general effects of composition and austenite condition on transformation.

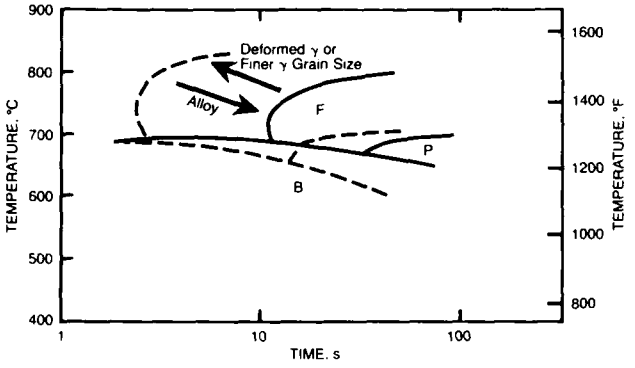


Fig. 17 - Schematic effects of alloy content and of austenite conditioning on the continuous cooling-transformation diagram

Alloying additions that increase austenite hardenability suppress transformation to lower temperatures thereby promoting ferrite nucleation over ferrite growth and leading to finer ferrite grain diameters. Opposing this alloying effect, the refinement of austenite grain size and the deformation of austenite below the austenite recrystallization temperature both tend to accelerate transformation so that for a fixed cooling rate, transformation starts at a high temperature. The magnitude of the increase in transformation temperature is shown in Figure 18 for a Nb steel rolled by various reductions below the austenite recrystallization temperature and is seen to be quite significant. In that same study (38), the effects of composition on the start of transformation was determined as shown in Eq. (4).

$$A_{r3}(°C) = 910 - 310C - 80Mn - 20Cu - 15Cr - 55Ni - 80Mo \quad (4)$$

Superimposed on the phase transformation diagrams are precipitation reactions that can occur either simultaneously with (interphase precipitation) or subsequent to (general matrix precipitation) the formation of ferrite (39). Clearly, the precipitate sizes, and therefore strengthening effects, are controlled by the time and temperature of formation.

The cooling rate through the transformation range is also extremely important to the development of the final microstructure, Figure 19. Higher cooling rates suppress transformation to lower temperatures and allow significantly less time for overall transformation, thereby favoring ferrite nucleation over ferrite growth. As shown in Figure 20 for one specific steel, both the condition of the austenite (grain size or $S_v$) and cooling rate through transformation strongly influence the final ferrite grain size. Recent studies (41) have shown that for interrupted accelerated cooled plate, a two-stage cooling process, which produces more rapid cooling during ferrite formation and slower cooling during bainite formation, will produce higher strengths and equivalent toughness to steels cooled at a single rate. Finally, direct quenching followed by tempering, or interrupted quenching with self tempering, can be used to

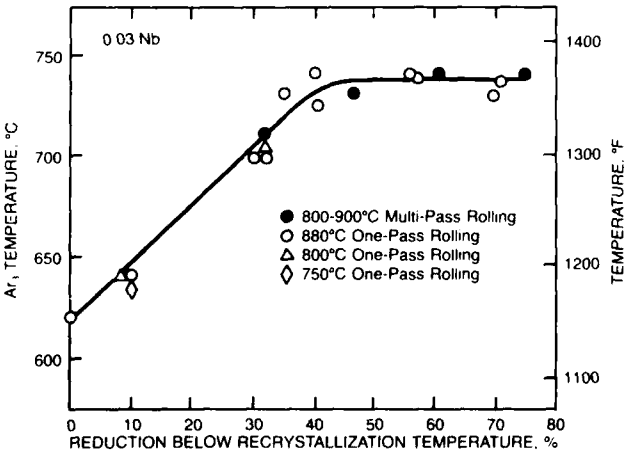


Fig. 18 - The effect of rolling reduction below recrystallization temperature of γ on $Ar_3$ in Nb steel (Ref. 38)

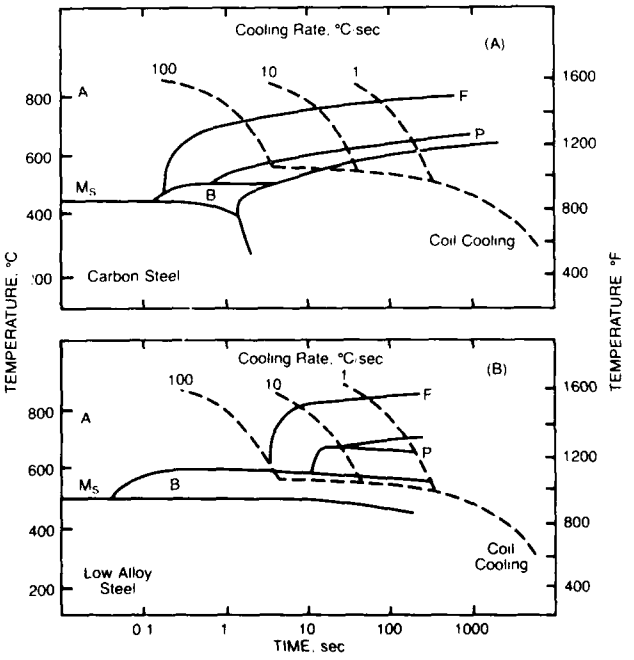


Fig. 19 - Schematic differences in transformation behavior of two steels as a function of runout-table cooling rate

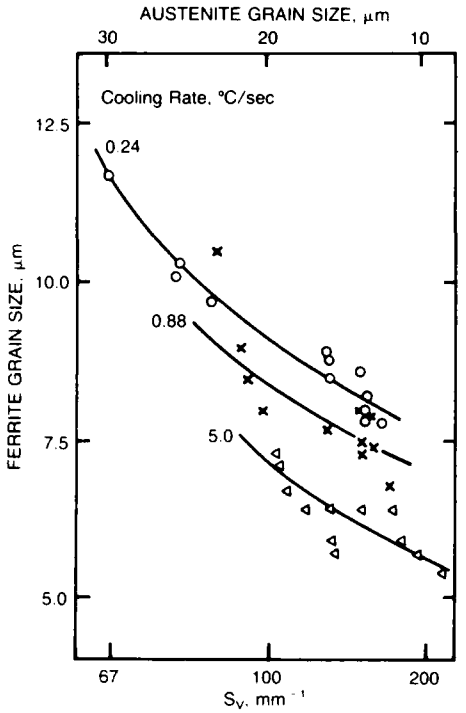


Fig. 20 - Effect of prior austenite grain size and cooling rate during transformation on the final ferrite grain size (Ref. 40)

produce martensitic or bainitic microstructures either in the full section or as a case around a softer core (14).

FURTHER PROCESSING - Although many HSLA steels are used directly after hot rolling or thermomechanical processing, other microalloyed grades will receive further mechanical and/or thermal treatments. High-strength cold-rolled sheet steels are one obvious example of such subsequent processing where cold reduction is followed by a batch- or continuous-annealing treatment. Because precipitate coarsening will accompany the annealing treatment, such steels rely on grain refinement and substitutional solid-solution strengthening to achieve intermediate strength levels. Very high-strength cold-rolled steels are produced by cold rolling high-strength hot-rolled steels followed by recovery annealing so that most of the dislocation strengthening is retained. Bake-hardening steels represent a relatively low-strength class of "high-strength" cold-rolled steels that utilize carbon retained in interstitial solid solution to produce a strain aging effect in formed and paint-baked parts, particularly automotive panels. Such bake-hardening steels are generally not microalloyed steel, but are simple C-Mn steels with or without solid-solution-hardening elements such as silicon or phosphorus. A final class of microalloyed sheet steels that may be mentioned is interstitial-free (IF) steels which contain very low carbon and nitrogen levels (<0.005% each) and have added Ti and/or Nb to effectively combine with all carbon and nitrogen atoms, thereby producing a very soft, continuous yielding ferrite.

Normalizing of steels, particularly structural grades, represents a common processing step following hot rolling and is conducted primarily to improve the toughness of steel products (primarily by grain refinement) that are deformed only at relatively high temperatures (because of product thickness and/or limitations in mill processing equipment). The most common microalloying additions to steels that are normalized are Nb (for austenite grain size control at the normalizing temperature), and V or V plus N (for precipitation strengthening of ferrite formed during cooling from the austenitizing temperature). Various society codes may require a normalizing treatment for specific applications; however, it should be noted that various combinations of steel composition, thermomechanical rolling, and air or accelerated cooling can be used to produce equivalent strength and toughness levels to those of various normalized steels. Such interrupted accelerated cooled steels offer the advantage of lower carbon equivalent values at any given strength level when compared with normalized steels, Figure 21.

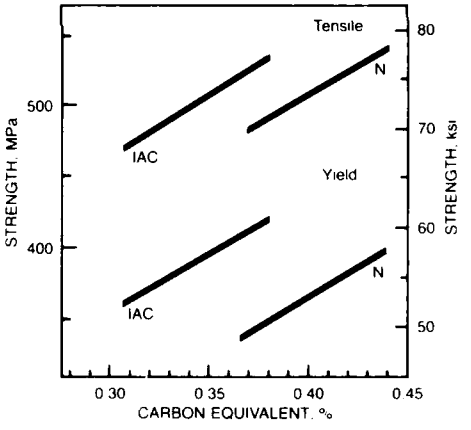


Fig. 21 - Representative data for the effect of carbon equivalent on the strength of normalized (N) and interrupted accelerated cooled (IAC) heavy-gage plate steels (Ref. 42)

Quenching and tempering may also be used as a subsequent treatment to produce specific properties in hot-rolled products. For example, very low-carbon Cu-Ni-Cr-Mo-Nb steels (ASTM A710, HSLA 80, or HSLA 100 types) with 550 to 690 MPa yield strengths are used in naval ship construction and have fine-grained polygonal- or acicular-ferrite microstructures strengthened by fine Cu precipitates that form

during aging (43, 44). The Nb microalloy addition serves primarily as a grain refiner during austenitizing. Similar lower strength (345 to 450 MPa yield strength), polygonal, or acicular-ferrite steels can be produced by quenching and tempering of low-carbon Mn-Nb or Mn-Nb-V steels with possible small alloy additions for hardenability control (42).

## SUMMARY

A brief review of the metallurgical fundamentals associated with microstructural and mechanical-property control in microalloyed HSLA steels has been presented. Specific applications generally dictate the required properties, and specific steel compositions and thermomechanical processing treatments can be combined to attain these properties. Total microstructural control is achieved only with careful attention to control of steel composition followed by control of each processing step from steel heating prior to processing through steel cooling following processing. The basic studies conducted in laboratories throughout the world have been translated into production techniques and facilities to supply the HSLA steel marketplace. Continuing studies will doubtless lead to the refinement of existing products and the development of new microalloyed steels.

## REFERENCES

1. "Metallurgical Developments in Carbon Steels," The Iron and Steel Institute, Special Report No. 81, London (1963).

2. "Strong Tough Structural Steels," The Iron and Steel Institute, Special Report No. 104, London (1967).

3. "Symposium, Low Alloy High Strength Steels," The Metallurg Companies, Dusseldorf (1970).

4. "Processing and Properties of Low Carbon Steels," The Metallurgical Society of AIME, New York (1973).

5. "Microalloying '75," Union Carbide Corporation, New York (1977).

6. "The Hot Deformation of Austenite," The Metallurgical Society of AIME, New York (1977).

7. "Welding of HSLA Structural Steels," American Society for Metals, Metals Park (1978).

8. "Formable HSLA and Dual Phase Steels," The Metallurgical Society of AIME, New York (1979).

9. "Thermomechanical Processing of Microalloyed Austenite," The Metallurgical Society of AIME, New York (1982).

10. "Steels for Line Pipe and Pipeline Fittings," The Metals Society, Book 285, London (1983).

11. "HSLA Steels: Technology and Applications," American Society for Metals, Metals Park (1984).

12. "High Strength Low Alloy Steels," AIME Metallurgical Society and the Australian Institute of Metals (1985).

13. "Accelerated Cooling of Steel," The Metallurgical Society of AIME, Warrendale (1986).

14. "HSLA Steels: Metallurgy and Applications," ASM International, Metals Park (1986).

15. "Welding Metallurgy of Structural Steels," The Metallurgical Society of AIME, Warrendale (1987).

16. "Accelerated Cooling of Rolled Steel," Pergamon Press (1988).

17. "Processing, Microstructure, and Properties of HSLA Steels," The Metallurgical Society of AIME, Warrendale (1988).

18. "Physical Metallurgy of Thermomechanical Processing of Steels and Other Metals," (THERMEC-88), to be published by The Iron and Steel Institute of Japan.

19. Morrison, W. B., Transactions ASM, 59, 824-46 (1966).

20. Gladman, T., Dulieu, D., and McIvor, I. D., "Microalloying '75," Union Carbide Corporation, New York, 9-30 (1977).

21. Grozier, J. D., "Microalloying '75," Union Carbide Corporation, New York, 241-50 (1977).

22. Pickering, F. B., "Microalloying '75," Union Carbide Corporation, New York, 9-30 (1977).

23. Hayami, S. and Furukawa, T., "Microalloying '75," Union Carbide Cororation, New York, 311-20 (1977).

24. Takechi, H. and Akisue, O., "HSLA Steels: Metallurgy and Applications," ASM International, Metals Park, 977-84 (1986).

25. Davies, R. G., and Magee, C. L., "Dual Phase and Cold Pressing Vanadium Steels in the Automotive Industry," Vanitec, London, 25-30 (1978).

26. Cuddy, L. J. and Raley, J. C., Met. Trans. A., 14A, 1989-95 (1983).

27. Cuddy, L. J., "Encyclopedia of Materials Science and Engineering," Pergamon, Oxford (1984).

28. Speich, G. R., Cuddy, L. J., Gordon, C. R., and DeArdo, A. J., "Phase Transformations in Ferrous Alloys," The Metallurgical Society of AIME, Warrendale, 341-89 (1984).

29. Sellars, C. M., "Hot Working and Forming Processes," The Metals Society, London, 3-15 (1980).

30. Roberts, W., Sandberg, A., Siwecki, T., and Werlefors, T., "HSLA Steels: Technology and Applications," American Society for Metals, Metals Park 67-84 (1984).

31. Yada, H., "Accelerated Cooling of Rolled Steel," Pergamon Press, 105-19 (1988).

32. Hofgen, H., Zouhar, G., Birnstock, F., and Bathelt, J., "4th International Steel Rolling Conference," Deauville, France, B2.1-B2.10 (1987).

33. Hostetter, R. S., Kranenberg, H., and Ronemus, D. C., "Mechanical Working and Steel Processing XVII," The Iron and Steel Society of AIME, 107-26, 1979.

34. Williams, J. G., Killmore, C. R., Barrett, J. F., and Church, A. K., "Processing, Microstructure, and Properties of HSLA Steels," Metallurgical Society of AIME, Warrendale (1988).

35. Cuddy, L. J., "Thermomechanical Processing of Microalloyed Austenite," The Metallurgical Society of AIME, Warrendale, 129-39 (1982).

36. Ouchi, C., Okita, T., Okado, M., and Noma, Y., "International Conference on Steel Rolling," The Iron and Steel Institute of Japan, Tokyo, 1272-85 (1980).

37. Kozasu, I., Ouchi, C., Sampei, T., and Okita, T., "Microalloying '75," Union Carbide Corporation, New York, 120-34 (1977).

38. Ouchi, C., Sampei, T., and Kozasu, I., "Trans. ISIJ 22 214-222 (1982).

39. Honeycombe, R. W. K, "HSLA Steels: Metallurgy and Applications," ASM International, Metals Park, 243-50 (1986).

40. Siwecki, T., Sandberg, A., Roberts, W., and Lagneborg, R., "Thermomechanical Processing of Microalloyed Austenite," The Metallurgical Society of AIME, Warrendale, 163-92.

41. Amano, K., Hatomura, T., Shiga, C., Enami, T., and Tanaka, T., "Accelerated Cooling of Rolled Steel," Pergamon Press, 43-56 (1988).

42. Repas, P. E., "Processing, Microstructure and Properties of HSLA Steels," The Metallurgical Society of AIME, Warrendale (1988).

43. Montemarano, T. W., Sack, B. P., Gudas, J. P., Vassilaros, M. G., and Vanderveldt, H. H., Journal of Ship Production, 2, 145-62 (1986).

---

# HIGH STRENGTH LOW ALLOY STEELS— INTERNATIONAL IRON AND STEEL INSTITUTE REPORT FROM THE COMMITTEE FOR TECHNOLOGY

**J. Lessells**
British Steel Corporation
Swinden Laboratories
Rotherham
South Yorkshire, Great Britain

ABSTRACT

This paper introduces a report which was prepared under the auspices of the Committee for Technology of the International Iron and Steel Institute. The report can be ordered at this congress.

Studies in the report illustrate:

- The range of HSLA steels available for particular applications and how they have developed in response to market requirements
- The role of HSLA steel in reducing the cost of steel based constructions
- Production facilities required for the successful manufacture of HSLA steel

The types of HSLA steel differ substantially between market sectors or even product forms and linepipe, structural and pressure vessel, shipbuilding, offshore and cold forming strip steels are therefore separately examined. In each case there is a commentary on the types of steel used and specifications that are relevant together with information on their properties and other characteristics that relate to particular end uses. General aspects of steel production and metallurgy are briefly dealt with in a separate chapter.

The report concludes with a section on the economic advantages of HSLA steels and the part they play in responding to the challenge of competing materials. In this it is concluded that for steel users specific economies can be obtained from the use of HSLA steels both in construction and operational areas

THIS PAPER INTRODUCES A REPORT which was prepared under the auspices of the Committee for Technology of the International Iron and Steel Institute.

Steel as a constructional material has been virtually unrivalled since the late 19th century because of its strength, relative ease of fabrication and low cost. While this remains true today, competition from other materials such as concrete, plastic and non-ferrous materials is growing and steel must continue to develop its virtues if it is to remain competitive. Further improvements in strength were an obvious goal and have received much attention from steelmakers during the past 50 years in particular. In more recent steels it has been recognised that the fabrication and design of modern structures calls in particular for high standards of weldability and fracture toughness as well as low production costs. The category of steels commonly referred to as HSLA (high strength low alloy) incorporate these virtues and has been the steel producers' response to updating the versatility of steel. The steels have proved to be extremely successful.

The Committee for Technology of the Iron and Steel Institute considered a review of HSLA steels as timely and set up a special Study Team (see Apendix I) to prepare a report on the subject. The objective set for the study was to examine the significance of HSLA steel for IISI members, with particular reference to their role in developing markets for steel products. It was recognised also that manufacturing techniques for HSLA steels would in many cases be different from those required for more normal grades of steel and these aspects were also to be highlighted in the study.

In its deliberations the Study Team noted that there was already in existence a very substantial technical literature on the subject of HSLA steels particularly on metallurgical topics and took the view that there was no need in its report to restate basic metallurgy.

Because the types of HSLA steel differ quite markedly between the various product forms, it was considered desirable to separately examine the situation in linepipe, structural and pressure vessel, shipbuilding and offshore and cold forming strip steels. The report therefore contains separate chapters for each of these markets.

Before moving on to more detailed consideration of these steels it is worth drawing attention to two relevant points.

Although the cost of manufacturing steel is generally only a small proportion of the total cost of constructing any particular structural component, the delivered price of raw steel remains an important consideration. The Steel Industry has met this challenge by the adoption of new high productivity and energy efficient methods of steelmaking to ensure that the cost of steel in real terms remains competitive. Fig. 1 illustrates this point in quite a dramatic way relative to examples of competing materials and it will be seen that of these constructional materials only steel has actually decreased in cost over the past decade.

The extent of present use of HSLA steels for the various applications that will be considered in this report is illustrated in Table I which throws up some interesting points. Firstly the adoption of HSLA steels in linepipe is almost complete in

Europe, North America and Japan for reasons which will become more apparent in a subsequent chapter. In shipbuilding, Japanese builders have made extensive use of these steels, while the application in Europe and North American shipyards is much less, indicating perhaps a less advanced state of technology in these shipyards but perhaps an opportunity for advance.

Table I - Proportion of HSLA Produced Worldwide (%) 1986

| | Europe | North America | Japan |
|---|---|---|---|
| Linepipe | 95 | 95 | 95 |
| Shipbuilding | 40 | 20 | 75 |
| Offshore steels | | | |
| Plates | 90 | 30 | 70 |
| Sections | 70 | 20 | 10 |
| Pressure vessels | 30 | 25 | 85 |
| Structural | | | |
| Sections | 30 | 20 | 10 |
| Sections, automotive | 70 | 70 | 30 |
| Sections, ships | 15-30 | 20 | 10 |
| Sheet piling | 25 | 15 | 100 |
| Rebar | 100 | 5 | 10 |
| Plates | 25 | 20 | 10-30 |
| Sheet and coil (inc. galv) | | | |
| Automotive | 20 | 10 | 20 |
| Building (not rebar) | 95 | 80 | 70 |

Almost conversely the use of high strength offshore steels in Europe is at a higher level than in Japan and this is due in very large measure to the particular demands of the European Continental Shelf oil and gas platform production programme which almost of necessity makes extensive use of HSLA steels

Perhaps the most graphic way of illustrating the much improved metallurgy and properties of modern HSLA steels and their user friendliness in terms of ease of fabrication, particularly welding, is seen in the contrast between the material used about 50 years ago for the Sydney Harbour Bridge relative to those used for structural purposes in the offshore environment today. The comparison is shown in the table below

Table II

| Steel Application | Composition C% | Si% | Mn% | Mechanical Properties Yield Stress N/mm² | Tensile Strength N/mm² |
|---|---|---|---|---|---|
| Sydney Harbour c1932 | 0.32/0.42 | 0.15/0.25 | 0.60/1.00 | 323 (min) | 551/659 |
| Typical Offshore Structure c1987 | 0.11 | 0.35 | 1.50 | 325 (min) | 490 |

## METALLURGY AND STEEL PRODUCTION

1. METALLURGY - As mentioned earlier the metallurgy of HSLA steels is extremely well documented, particularly through the microalloy series of conferences, the latest of which we have started today. For the purposes of this presentation, therefore, it is sufficient simply to say that the essential characteristics of the HSLA steels that we are concerned with are fine grain size for good yield strength and fracture toughness, low carbon and indeed carbon equivalent value, again for good toughness and for weldability. The most notable microalloying elements used today are niobium and vanadium with an increasing contribution from titanium, while the important role of aluminium and nitrogen as perhaps the original mircoalloying elements, should not be neglected.

The effects of these microalloying elements have been exploited to the full by the intelligent application of metallurgical principles to the finishing operations used for the various product forms with which we are concerned. Among these, normalising and quenching and tempering were the first to be used and indeed are still indispensable for many products today. Controlled rolling, particularly of plates but more recently of shapes, has clearly been the most notable development in rolling technology and has just about reached its 30th birthday in terms of practical application.

A further extension of the recent application of metallurgical principles to finishing operations has been the use of accelerated cooling immediately after the rolling process in a variety of product forms starting with bars and plates, but moving on more recently to rails and shapes.

The metallurgy of each of these process routes has already been rather well established in the literature and much more information is available at this conference. Further comment here would therefore be superfluous.

2. STEEL PRODUCTION ASPECTS - The first point that needs to be recognised is that the simpler types of HSLA steel can be made in almost any production plant. Special requirements for steelmaking or rolling and heat treatment only arise for the most sophisticated HSLA steels such as high grade linepipe or offshore structural steels.

It is becoming evident, however, that the cost of achieving high accuracy of production, low impurity levels and consistency of properties may be offset by very substantial through cost savings because the cost of their achievement is often much less than the savings obtained in subsequent fabrication or service conditions. There is, therefore, a strong trend towards the use of more sophisticated steel manufacturing techniques as discussed further below.

3. STEELMAKING

Optimum property levels in HSLA steels depend on

- Control of significant alloying elements (e.g. C,Mn, Nb, V, Al)
- Reducing the content of impurities (e.g. S, P, $N_2$) to justifiable levels
- Reducing the content of non metallicinclusions (sulphides and oxides)
- Ensuring uniformity of composition and properties throughout a cast which can be as large as 300 tonnes

The techniques used to achieve these objectives are described in the report, but the essence of the steelmaking requirements is to adopt practices which will achieve very accurate control of the state of oxidation of steel and thereafter, to take specific steps for the limitation of impurity elements using various steelmaking techniques and ladle treatment processes as required

Fig. 2 illustrates the range of steelmaking and casting possibilities that are presently used, while Table III below gives some indication of the kind of composition changes that might be required in moving from mild steel through normal to very high duty HSLA steels.

Table III - Typical Compositions

(a) Composition (%)

| Steel Application | C | Si | S | P | Mn | Nb | Al | $N_2$ |
|---|---|---|---|---|---|---|---|---|
| Normal Structural Use | 0.16 | 0.30 | 0.015 | 0.02 | 1.40 | 0.03 | 0.03 | 0.07 |
| Special Structural Steel (e.g. for Offshore Constructions) | 0.10 | 0.30 | 0.003 | 0.010 | 1.50 | 0.02 | 0.03 | 0.006 |
| | (Plus additions of Ni and Cu) | | | | | | | |

(b) Mechanical Properties

| Steel Application | Yield Stress | Tensile Strength | Charpy Vee Notch Toughness |
|---|---|---|---|
| Normal Structural Use | 345 | 490 | 27 J at -0°C |
| Special Structural Steel (e.g. for Offshore Constructions) | 345 | 460 | 27 J at -60°C |

An essential point that has to be remembered is that for supply to a given customer order, the level of tensile properties achieved is governed by the minimum composition of steel supplied, while on the other hand the customer must set his weldability precautions, notably preheat levels, on the basis of the maximum composition supplied within the consignment. These points are illustrated in the schematic illustration in Fig 3 which clearly shows that the closer the composition control achieved, the greater the optimisation between tensile strength properties and weldability.

The problem of lamellar tearing in the region of welds has made it necessary for the sulphur and other non-metallic inclusion content of steel to be dramatically reduced for many HSLA steels.

There has, therefore, been a considerable demand within the production of HSLA steels to seek highly sophisticated production methods not just to meet the requirements of steels for particularly severe service requirements, but also to produce steels that will reduce the cost of welding.

## LINEPIPE STEELS

Probably the most prominent and successful exploitation of HSLA steels is that concerned with the distribution lines for oil and gas. An historical summary is shown in Table IV below.

Table IV - Development of Gas Transport Via Pipeline

| Year | Operating Pressure bar | Dia. mm | Annual Transportation Capacity $Mm^3$ | Fuel Gas Used For Pumping (6,000 km) % |
|---|---|---|---|---|
| 1910 | 2 | 400 | 80 | 48.8 |
| 1930 | 20 | 500 | 648 | 31.3 |
| 1965 | 66 | 900 | 8,320 | 14.1 |
| 1980 | 80 | 1,420 | 26,000 | 10.6 |
| About 1990 | 120 | 1,620 | 52,000 | 8.2 |

This table is a particularly graphic illustration of what has been achieved over the past 70 to 80 years for gas pipelines. The adoption of HSLA steels associated with greater pipe diameters and operating pressures, has meant that the yield of piped gas (input less the proportion burnt as fuel to power gas pumping stations) has moved from 51.2% to 91.8%, together with a vast increase in gas transportation capacity for each pipeline.

While increased tensile strength has been the dominant feature of linepipe steels, other property aspects have been no less critical to successful fabrication and operation of oil and gas linepipe and these are weldability, fracture toughness and resistance to sour gas attack. These are referred to in some detail in the text of the report, but some summary comments will be appropriate here.

1. WELDABILITY - There are two main welding operations to be considered. The first during manufacture of the pipe, for example the longitudinal seam which is made using the submerged arc process and the girth weld carried out on site or on the lay barge for sub-sea lines.

The longitudinal seam is carried out at relatively high heat input such that HAZ cold cracking should not be a problem. Because pipe toughness is important however it is essential that both the weld HAZ and the weld metal itself have adequate toughness. HAZ toughness has generally been adequate even for increasingly severe service requirements now down to -30°C because HSLA steel development has moved to progressively lower carbon levels and the welding process itself has (mainly for productivity reasons) moved from single to two, to three and even five wire submerged arc systems with attendant reductions in effective heat input.

Probably the main welding problem has been the girth weld which needs to be deposited at high speed and is a low heat input operation. These are circumstances where maximum advantage can be taken of the lowest available carbon equivalent steels which have been developed using advanced thermomechanical rolling or accelerated cooling. Fig 4 illustrates this point.

2. FRACTURE TOUGHNESS - It is clearly of the greatest importance that catastrophic failure of linepipe be avoided because of the major cost and environmental considerations involved.

Possible failure mechanisms are either of the brittle or ductile variety and both have to be legislated for in the design of the steel and weld metal.

Avoidance of brittle fracture is dealt with by the conventional approaches of reduced carbon content and fine grain size achieved in modern steels by microalloying with Nb, V or Ti and thermomechanically rolling or accelerated cooling. Essentially design has to be on the basis of avoidance of

crack initiation because although a leak before break situation may have some validity for oil pipelines, the explosive decompression of gas makes the risk of brittle fracture severe over a potentially long length of linepipe. There is incomplete agreement yet about the most important test critical for linepipe steels to avoid brittle crack propagation under any particular set of design pressure, diameter and operating temperature conditions and Charpy, drop weight and COD tests are used. The position may be clarified by the results of full-scale burst tests being carried out in various parts of the world.

An important consideration in the resistance to brittle fracture is the fracture toughness of the weld metal itself. Since in a normal longitudinal seam weld in pipe, dilution from the parent plate may provide as much as 60% of the weld volume, it will be obvious that the composition of the parent steel is an essential contributing factor. Research over recent years, for example, has clearly demonstrated the important deleterious effects of higher carbon, manganese and nitrogen contents in weld metal. Fortunately modern steels tend to reduce these elements to comparatively low levels. Even so, it has been necessary to carry out detailed metallurgical analyses of the factors that affect weld metal toughness and from these weld consumables have evolved that are capable, in conjunction with modern low carbon steels, of giving weld metal toughness down to operating temperatures of -30°C or lower.

The risk of propagating a ductile crack through a gas linepipe is also well recognised and although full-scale burst tests are still being evaluated to improve predictive capability of steel proving tests, the main factor identified todate has been the need to reduce sulphur content to levels below 0.005%. There is some evidence to suggest that very low sulphur contents in themselves may not be sufficient to eliminate the risk of a running ductile crack particularly in steels with strength levels above about X65 and more information on this aspect is essential to point the way forward for new steel developments.

3. RESISTANCE TO $H_2S$ ENVIRONMENTS (SOUR GAS) - One of the most difficult service problems for steel producers to deal with has been that caused by the increasing incidence of transporting so called sour oil or gas in linepipe.

The sour environment arises from a content of moisture in the oil or gas (arising either naturally or as a consequence of water drives to extract oil) and the subsequent combination with $H_2S$ to react corrossively with the steel to generate atomic hydrogen. The hydrogen then difuses into the steel until it reaches voids, generally non-metallic inclusions, where it is trapped. Given sufficient hydrogen, pressure can build up to the extent of causing cracking along the line of inclusions that are parallel to the plate surface. If such cracks link up in a step wise fashion then pipe failure through the thickness becomes inevitable, leading to the possibility of a running fracture particularly in a gas line.

Fig. 5 indicates the main elements of the problem. One solution is clearly to fully dry the oil or gas before transmission through the main transportation pipelines. For offshore developments this is extremely expensive because the purification plant has to be installed at the well head on vastly expensive production platforms. There is, therefore, a very clear pressure from oil companies on steel producers to provide steels that are resistant to this form of attack.

It has now been established by extensive testing that resistance to sour oil attack can be confined by reducing sulphur content to extremely low levels in the region of 0.002%, ensuring that residual sulphide inclusions are of modified round rather than elongated shape by calcium treatment. Virtual elimination of all other non-metallic inclusions, particularly oxides, and reduction or elimination of segregation by a combination of modified casting practices and reduction in the content of the main segregating elements, carbon and manganese is also important.

The very lean compositions required to operate successfully in sour environments are now becoming available, but only by virtue of the most rigorous steelmaking and casting operations and the use of advanced thermomechanical treatment of plates particularly by the accelerated cooling method.

More detailed information on steel production and property aspects is given in the report but in closing this section it is worth picking out one particular point and that is that at present and for the foreseeable future, there is no viable alternative to steel for constructing linepipe. The drive for improved steels has, therefore, come not from the threat of competing materials but from a need to reduce the operating costs of steel users through more efficient transmission systems.

## SHIPBUILDING AND OFFSHORE STEELS

Despite the almost complete failure of various reputable bodies to forecast world shipbuilding requirements (Fig.6), there remains a very substantial market for steel as the dominant construction material other than for small and specialised vessels. The greatest proportion of new tonnage is provided by Japanese and Korean shipyards and it is in these areas therefore that most modern developments in design, fabrication and material technology might be expected. Reference to Table 1 in fact confirms a much greater use of HSLA steels in Japan than in Europe or North America.

HSLA steels were used for ship hull construction in the 1960's but were slightly inhibited by the need for welding preheat because of the relatively high carbon equivalent levels of about 0.45 that were common in the normalised steels of that time. Shipyards were not then easily able to apply preheat at all, nor even to use low hydrogen welding electrodes.

Steels for shipbuilding have however now been designed to reduce the need for weld preheat in the most common hull plate thicknesses and the most recent accelerated cooled steels reputedly eliminate the need entirely. This point is illustrated in Table V which demonstrates the reduction in composition that has been made possible in modern steels.

Table V - Examples of Ship Plate Produced by a Range of Procedures

(a) Composition

| Grade | Process | C | Si | Mn | P | S | Nb | Al | $C_{eq}$ |
|---|---|---|---|---|---|---|---|---|---|
| EH32 | AC | 0.10 | 0.33 | 1.44 | 0.016 | 0.004 | | 0.035 | 0.34 |
| | N | 0.13 | 0.40 | 1.35 | 0.015 | 0.005 | 0.030 | 0.035 | 0.40 |
| DH36 | CR | 0 15 | 0.36 | 1.36 | 0.018 | 0.014 | 0.029 | 0.033 | 0.39 |
| | N | 0.14 | 0.39 | 1.36 | 0.020 | 0.018 | 0.030 | 0.029 | 0.38 |

(b) Mechanical Properties

| Grade | Process | Gauge mm | Yield Strength MPa | UTS MPa | J | Charpy Temp. °C |
|---|---|---|---|---|---|---|
| EH32 | AC | 25-35 | 372 | 529 | 220 | -40 |
| | N | 20-30 | 355 | 485 | 160 | -40 |
| DH36 | CR | 15-30 | 411 | 546 | 86 | -20 |
| | N | 15-30 | 389 | 517 | 152 | -20 |

There is, of course, a limit to the strength of steel acceptable for ship hull structures and ship classification societies. Generally the benefits of higher yield strength in terms of hull plate thickness reduce substantially above a yield strength of about 350 N/mm$^2$.

This apparently conservative approach is based on concern about the fatigue behaviour of higher strength steels and potential problems with hull rigidity because the elastic modulus of HSLA steels is the same as for mild steel so that reduced overall scantling thickness would give lower elastic rigidity. Additionally, of course, the corrosion characteristics of HSLA steels are broadly similar to mild steel so that the design corrosion allowance should remain constant in terms of plate thickness and will, therefore, reduce the benefit of HSLA steels.

Even so, the benefits of HSLA steels for ship hull structures is significant, as illustrated in Fig. 7, and Japanese shipbuilders are now making economic use of easily welded HSLA steels made by the accelerated cooling route with yield strength levels up to 400 N/mm$^2$.

A further advantage of some modern HSLA shipbuilding steels which make use of Ti additions to maintain fine weld HAZ grain size and very low carbon content for the same reason, is that very high heat input and, therefore, high productivity welding can be used. Such steels permit the use of single pass welding for 20 mm plate.

## OFFSHORE STRUCTURAL STEELS

The developments in steel that have been necessitated by the difficult fabrication and service behaviour requirements posed by the very large oil and gas production platforms used in the North Sea have led to advances in steel production just as dramatic as those required for linepipe.

The essential characteristics of steels for offshore constructional purposes can be summarised as:

- Yield strength in the region of 350 N/mm$^2$
- Good welding characteristics
  (a) High resistance to lamellar tearing
  (b) Low composition to minimise preheat
  (c) High toughness in the weld HAZ
- Good fracture toughness at the designated operating temperature
- Well documented fatigue properties

Table VI shows typical compositions for normalised steels presently in extensive use for this type of construction together with the composition of accelerated cooled type of steel that is of particular current interest although not heavily used todate.

Table VI - Examples of Structural Steel Produced by a Range of Procedures

(a) Composition

| Grade | Process | C | Si | Mn | P | S | Nb | Al | $C_{eq}$ |
|---|---|---|---|---|---|---|---|---|---|
| 50D | AC | 0.08 | 0.34 | 1.49 | 0.011 | 0.002 | 0.015 | 0.025 | 0.35 |
| | N | 0.11 | 0.39 | 1.55 | 0.014 | 0.002 | 0.030 | 0.025 | 0.39 |
| 50E | N | 0.12 | 0.45 | 1.53 | 0.014 | 0.002 | 0.026 | 0.034 | 0.40 |

(b) Mechanical Properties

| Grade | Process | Gauge mm | Yield Strength MPa | UTS MPa | J | Charpy Temp. °C |
|---|---|---|---|---|---|---|
| 50D | AC | <75 | 434 | 517 | 331 | -10 |
| | N | <75 | 376 | 517 | 328 | -10 |
| 50E | N | 40-63 | 384 | 513 | 277 | -40 |

The particular points to note relative to conventional structural steels are the substantially lower carbon levels which are necessary for weldability and toughness reasons and the very low sulphur contents now typical of lamellar tear resistant steels.

Weld heat affected zone toughness is an essential requirement in these steels and is commonly tested for using the fracture toughness crack tip opening displacement (CTOD) test developed by the Welding Institute. A difficulty that has arisen in this context however is that despite the lack of structural failures in offshore structures, a worst case approach to CTOD testing has tended to be adopted. In effect it is required by some relevant specifications that the CTOD crack tip must be located in the most brittle region of the HAZ regardless of how small that region might be or whether it is near the surface or relatively safely buried near the plate mid-thickness. It will be a matter of some interest to see whether this particular problem is solved by the steel development efforts of producers and there is much activity in this area or whether a more pragmatic view can be taken of the risk involved which may well be statistically insignificant. On present evidence, the steel solution is likely to come first.

Finally, the operating conditions of those structures is such that a very full appreciation of their fatigue behaviour is essential to safe design. Certainly in Europe, the expenditure on testing to accumulate the required data has amounted to some millions of pounds and has, together with the weldability and fracture data accumulated, made these steels probably the best documented of any steel type made todate.

For the future, increasing water depths and general efficiency of operation particularly in relation to reducing the weight of deck structures, clearly indicates that further developments will inevitably require HSLA steels of still higher strength and much work on these steels is already underway. Such developments will be essential to maintain the pre-eminent role of steel as the constructional material.

## PRESSURE VESSEL AND STRUCTURAL STEELS

This category includes plates, rolled sections and bars for structural and pressure vessel application. HSLA bars for reinforcement were in fact one of the earliest uses of HSLA steels in general and of accelerated cooling (from the rolling temperature) concept in particular.

Some typical examples of applications for HSLA steels are:

Bridges
Buildings
Electricity pylons
Penstocks
Steel piling
Railway tracks
Trucks
Trailers
Earthmoving equipment
Mining equipment
Tanks
Reinforcement bars

The types of steel used include the microalloyed grades using Nb V and Ti as well as steels intended for higher temperature service where Cr and Mo additions are common.

Process routes include controlled rolling, normalising quenching and tempering as well as the direct accelerated cooling from the rolling temperature already in use for bars, plates and rails and under investigation for rolled shapes.

A particular problem that arises in many applications

is that some of the more recent thermomechanical processing techniques used for plates in particular are not suitable where hot forming will be used during fabrication. The kind of property deterioration so obtained is illustrated in Fig. 8 for a thermomechanically treated steel. Similar effects can be predicted for AC steels. This problem has been neatly circumvented by the use of a modified thermomechanical rolling system referred to as "normalising rolling". In this process the rolling finishing temperature is designed to coincide with the hot forming temperature (900-930°C). Subsequent hot forming therefore simply repeats this operation and deterioration in properties is then small or even absent.

In the report specific examples are given of the cost benefits that can be derived in this area by the use of HSLA steels. These refer to penstock, bridges and the steel frames for buildings.

This last application (steel frames for buildings) is particularly interesting because there are clear opportunities for steel to compete strongly with other building construction materials particularly in situ, or reinforced concrete. A number of examples of benefits are given including increased load bearing capacity for columns, reduced weight light industrial buildings and a multi-storey car park where weight savings of 30/40% and space gains of 11-30% are claimed for HSLA steels.

Illustrating the point that composite construction techniques may be very advantageous for steel is the concept of using HSLA rolled sections and reinforcement bar bonded together with concrete. Such composites (Fig. 9) have the advantages of great strength in compression, high building strength and very good properties when exposed to fire.

## COLD FORMING AND COATED STRIP STEELS

Something like 40% of the world steel production is in the form of strip steel in its various forms - hot or cold rolled sheets and coil, galvanised, tin plate, black plate and coated sheets. This is, therefore, a key area of use for steel and is the subject of a separate chapter in the report which particularly considers the use of those steels in automative and building applications.

The main reason for using HSLA steels in this product area is, of course, the potential for making cold formed products using a thinner gauge than would normally be necessary, leading to weight savings that can be very significant in many areas and particularly in automobiles.

The ability of the material to cold form satisfactorily is an essential attribute for nearly all potential applications and conditions the routes taken in steel development. This requirement is substantially different from those in heavier product forms where weldability and fracture toughness, for example, have usually been dominant. Strip steels are welded for very many applications, but the problems that then arise are more often dealt with by welding process or surface treatment considerations rather than as a fundamental characteristic of the steels themselves.

The metallurgical development of HSLA steels in the cold forming strip area does however overlap with other products so far discussed in their use of microalloying elements, but those steels have also adopted somewhat additional metallurgical and process routes which are interesting.

Table VII - Cold Forming Strip Steels

| Steel Type | Processing | Range of min. Strength YS MPa | Range of min. Strength TS MPa | Chemical Composition Carbon % | Chemical Composition Alloying Elements % |
|---|---|---|---|---|---|
| Precipitation strengthened and grain refined | Hot rolled | 280-600 | 400-700 | 0.05-0.15 | Mn up to 1.5 max. plus Ti, Nb or V |
| | Cold rolled | 240-440 | 340-550 | 0.05-0.15 | Mn up to 1.5 max. plus Ti, Nb or V |
| Solid solution strengthened | Hot or cold rolled C Mn | 230-338 | 370-520 | 0.10-0.20 | Mn up to 1.5 max. |
| | Cold rolled Al killed | 220-300 | 340-435 | <0.05 | P up to 0.1 |
| | Cold rolled interstitial free | 220-300 | 300-400 | [illegible] | P up to 0.1 Ti or Nb B |
| Bake hardening | Cold rolled Al killed | 200-230 max. 240-300 after baking | 310-380 | 0.01-0.02 | P up to 0.1 max. possibly Si |
| | Cold rolled Nb | 210 max. 240 after baking | 360-380 | <0.005 | P up to 0.1 plus Nb |
| Dual phase | Hot and cold rolled | 200-900 | 350-1300 | 0.02-0.15 | Mn up to 1.5 |
| Transformation strengthened | Hot and cold rolled | Up to 1400 | Up to 1500 | Up to 0.20 | Mn up to 1.5 |
| Cold work strengthened | Cold rolled | Up to 1000 | Up to 1100 | Up to 0.20 | Mn up to 1.5 Ti, Nb, V possible |

Table VII briefly summarises the various types of HSLA steel that are considered in the report, while Table VIII gives an indication of their relative formability. These steels, therefore, make use of a wider range of strengthening mechanisms than other product forms and each has its own particular merits.

Table VIII - Forming Properties of Various Steel Types

| Primary Strengthening Mechanism | Stretch-ability | Draw-ability | Strength Range |
|---|---|---|---|
| Cold worked | Very poor | Poor | Large |
| Recovery annealed | Poor | Poor | Large |
| Transformation strengthened | Moderate | Moderate | Large |
| HSLA precipitation grain refined | Moderate | Moderate | Fairly large |
| Solid solution Al killed | Good | Good | Limited |
| Bake hardenable | Good | Good | Limited |
| Dual phase | Good | Moderate | Large |

Since cold forming strip steels have a yield strength substantially lower than heavier product steels, the definition adopted for HSLA steels is of steels above a yield stress of 220 N . The micro-alloyed grades using Nb V Ti derive their higher yield stress from a combination of grain refinement and precipitation strengthening. Such steels are normally produced in the hot rolled or cold rolled and annealed condition. Because they have limited forming ability, they are mostly used for structures and reinforcement parts of automobiles as well as buildings and various items of domestic equipment. Their composition will generally be within the range:

| C% | Mn% | S% | P% | Al% | Nb% |
|---|---|---|---|---|---|
| 0.03/0.15 | 0.50/1.5 | 0.015 Max. | 0.02 Max. | 0.05 | 0.03 |

with substitution of Nb by V or Ti in many cases.

Solid solution strengthened HSLA steels can be of considerable interest because for a given strength level, formability may be better than precipitation strengthened steels. The most common alloying elements used are manganese, silicon with recent interest in phosphorus up to about 0.10% above which it tends to give problems with electric resistance welding. Such steels can be used for automobile body panels.

Interesting HSLA steels used in cold forming strip are the bake hardened steels, so called because they strengthen significantly during the paint baking operation which takes place at about 170°C. These steels have simply harnessed the well-known quench ageing mechanisms whereby carbon is quenched into solution at the cooling rates obtained after batch or particularly continuous annealing and precipitated during the bake hardening operation.

Transformation strengthened steels include the well-known dual phase alloys where the second phase can be martensite bainite or even pearlite depending on strength requirement. These steels can have very good formability and weldability and they have found extensive application in their rolled form.

For the highest strengths up to 1600 N/mm$^2$ yield strength, alloying to ensure transformation to martensite can be employed for components like door impact beams or rear bumper supports. Obviously such steels have quite limited formability.

As mentioned earlier, HSLA steels have corrosion properties that are not significantly improved over normal grades. Fortunately there is now a very great availability of strip coatings nearly all of which are designed to inhibit corrosion and/or to provide a decorative appearance to the steel where it will be used for exterior parts of automobiles or buildings. These include zinc galvanised or aluminised coatings specifically for corrosion protection and applied by the hot dip or continuous processes. To these can be added the very wide range of coloured organic coatings.

Considerable effort has to be expended on the evaluation of performance aspects including fabrication, direct resistance, fatigue behaviour and so on. These aspects are too detailed to be discussed here but are well documented in the report.

## ECONOMIC ASSESSMENT

HSLA steels will only be used in applications where there is a clear cost advantage to the steel purchaser. There has however been an widespread tendency for HSLA steels to be assessed on the basis of their initial cost resulting frequently in the comment that they are too expensive.

The report makes the point that the benefits of HSLA steels only become apparent if full account is taken of all the advantages that accrue from design, fabrication and operational features of these steels. (Fig. 10).

Numerous examples of such advantages are given in the report and a few of these are quoted here.

Fig. 11 was based on a particular set of cost figures but will be broadly true whichever specifications and costs are used. The interesting point is that taking due account of the kind of design code limitations that will be encountered, the main area where savings will occur for structural steel is in the medium (350 N/mm$^2$) yield strength region, i.e. precisely the area that has been so targeted by the microalloyed and thermomechanically processed steels. Above this strength range increasing alloy content tends to raise both initial and fabrication, particularly welding costs. It is, of course, quite likely that the low cost region will be pushed to higher strength yet through the use of the most modern thermomechanical rolling and cooling systems.

Fig. 12 carries this comparison through to the case for bridge construction where it is apparent that the case for HSLA steels can only be made then if full account is taken of fabrication and construction costs.

Finally, in Fig. 13 there is a fairly graphic illustration of the operating costs that can be achieved through the use of HSLA steels in large tanker ships.

## SUMMARY AND CONCLUSIONS

HSLA steels have been available to steel users for many years and except for particular areas, notably linepipe, have been less exploited than their obvious merit would suggest.

This situation is likely to change as steel users become more aware of the through cost advantages of modern HSLA steels although this will only happen through the advocacy of technical staff who can carry out the necessary technical assessment.

Steel producers have developed their steelmaking control to a degree where steel purity and accuracy of manufacture have been dramatically improved over the past ten years. These improvements linked to the metallurgical HSLA developments should help maintain steel in the forefront of

engineering materials.

Much has been written about the metallurgy and development of HSLA steels. It is questionable how much of this information reaches or is comprehended by steel users, admirable though it may be from the scientific standpoint. It is suggested however that we should turn much more of our attention to direct and convincing advocacy of HSLA steels to customers rather than those already converted - that is ourselves.

## ACKNOWLEDGMENT

This paper has been prepared on behalf of the Committee for Technology of the International Iron and Steel Institute. The special report was prepared by the Special Study Team whose names are listed in the Appendix and whose efforts are gratefully acknowledged.

The permission of Dr. R. Baker, Director Research and Development, British Steel Corporation to publish this paper, is also gratefully acknowledged.

## APPENDIX I

### HSLA SPECIAL STUDY TEAM

Chairman: J. Lessells, British Steel Corporation

### MEMBERSHIP OF THE DIFFERENT WORKING GROUPS

Linepipe

Leader: Dr.-Ing. K. Kaup, Hoesch Stahl AG, FR Germany

Members: M. Lafrance, USINOR-Aciers/TFK, France
Dr. Ingo von Hagen, Mannesmann Forschungsinstitut GmbH, FR Germany
Dr. V. Ramaswamy, R&D, Ranchi, Steel Authority of India Ltd., India
Dr. Giuliano Buzzichelli, Centro Sviluppo Materiale SpA, Italy
Masatoki Nakayama, Nippon Steel Corporation, Japan

Shipbuilding and Offshore Steels

Leader: Dr. Chiaki Shiga, Kawasaki Steel Corporation, Japan

Members: Dr. Peter Sandvik, Rautaruukki Oy, Finland
Dr. Joachim Degenkolbe, Thyssen Stahl AG, FR Germany
Dr. Piero Bufalini, Italsider SpA, Italy
M. Kameda, Kawasaki Steel Corporation, London
J. Lessells, British Steel Corporation, United Kingdom

Pressure Vessels and Structural Steels

Leader: J. de la Hamette, ARBED SA, Luxembourg

Members: Dr. S. Watanabe, Sumitomo Metal Industries Ltd., Japan
Dr. M. Ota, Sumitomo Metal Industries Ltd., Dusseldorf
Y. Ando, Sumitomo Metal Industries Ltd., London
T. Nills
T. Nillsson, SSAB Svenskt Stal AB, Sweden
Dr. Paul Repas, USS Technical Center, USA

Cold Forming and Coated Steels

Leader: Dr. B. Baldwin, British Steel Corporation, United Kingdom

Members: Vincent Leroy, Centre de Recherches Metallurgiques ASBL, Belgium
Charles Brun, USINOR, France
Michel Entringer, SOLLAC Produits Plats, France
Dr. Pierluigi Antoniucci, Italsider SpA. Italy
Yukio Hashimoto, Nippon Kokan KK, Japan
M. Nakashima, Nippon Kokan KK, Dusseldorf
R. C. Hudd, British Steel Corporation, United Kingdom

IISI Tsunemi Matsuda
Martin Brooks (Secretary)

Mr. Louis Roesch, IRSID, also made a contribution to the Linepipe Group at the start of the study.

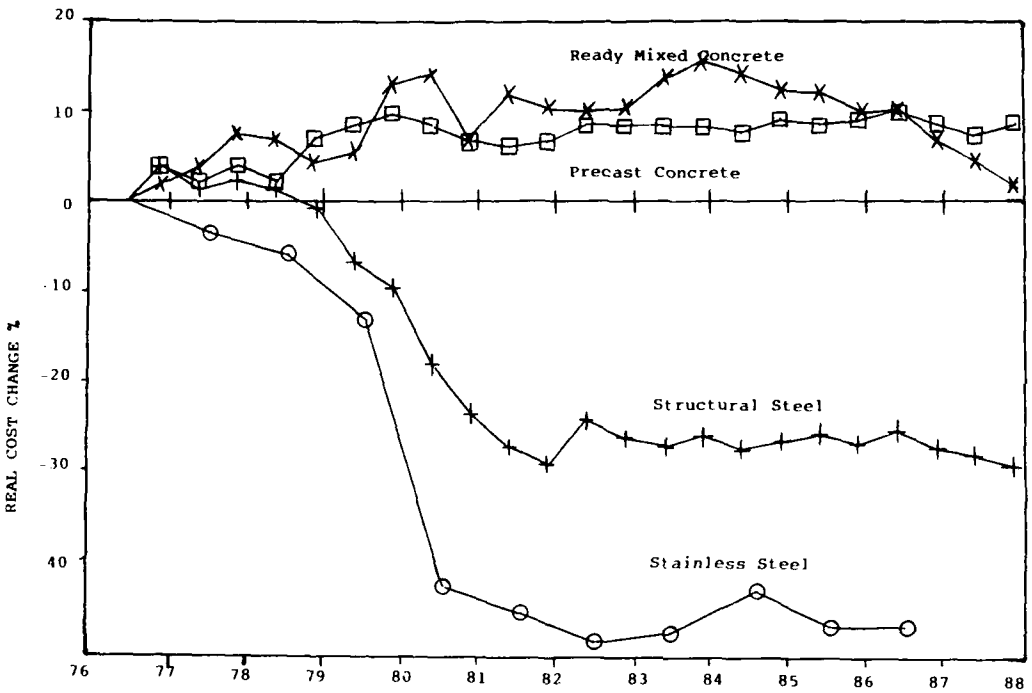


Fig. 1 - COST INDICES STRUCTURAL STEEL, RMC & PRECAST CONCRETE RELATED TO INFLATION

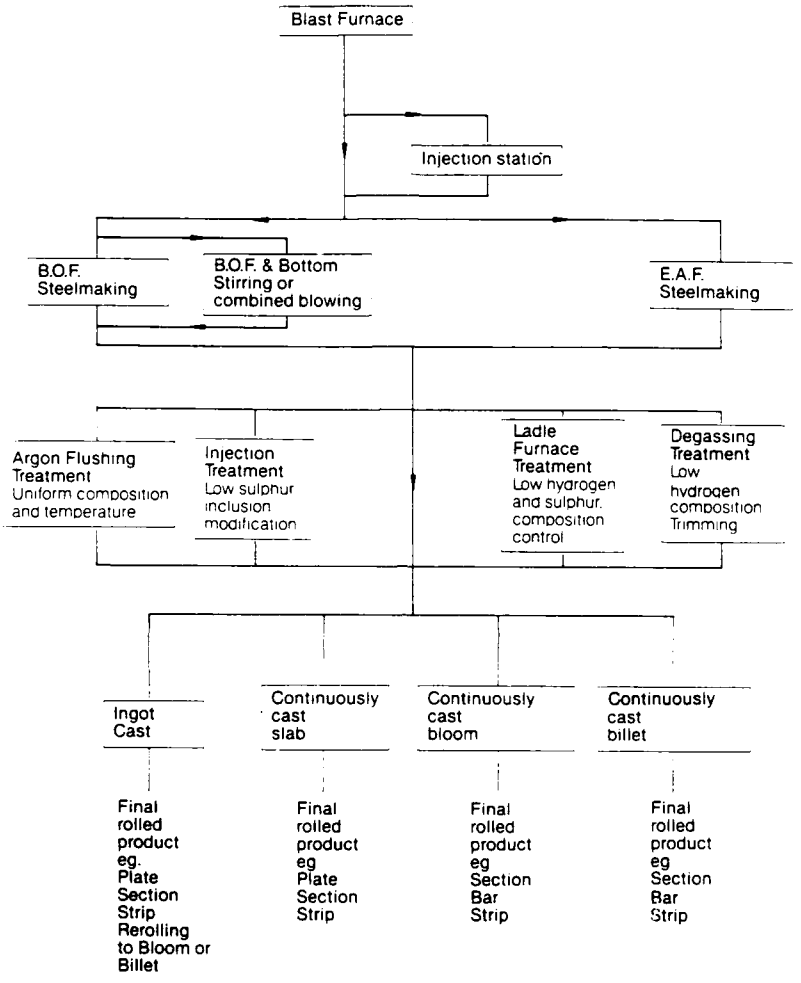


Fig. 2 - STEELMAKING AND CASTING OPTIONS

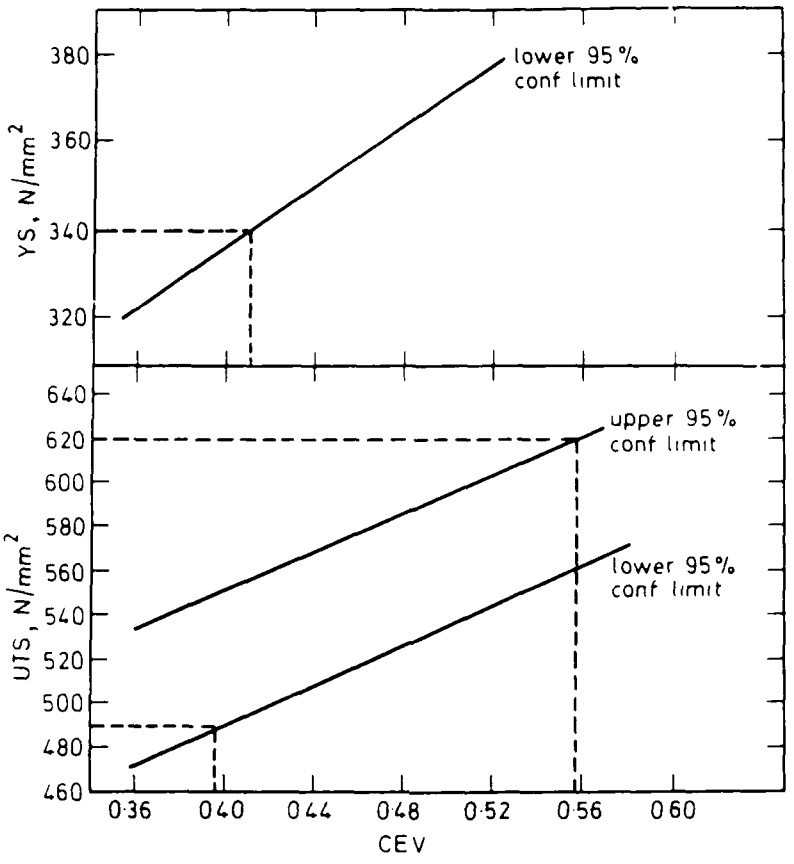


Fig. 3 - EFFECT OF CEV ON YIELD STRESS AND TENSILE STRENGTH FOR NORMALISED C-Mn-Nb-Al PLATE (40-63 mm THICK)

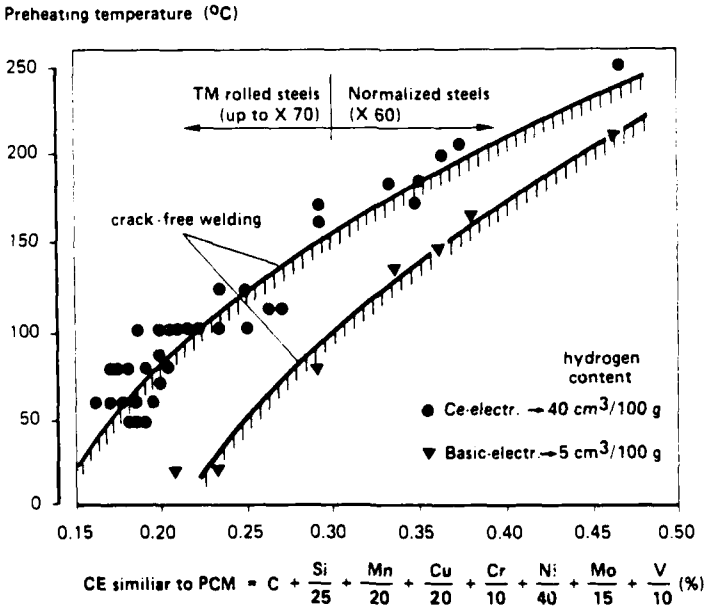


Fig. 4 - PREHEATING TEMPERATURE FOR CRACK RESISTANT WELDS RELATED TO THE CARBON EQUIVALENT

Implant test heat input 0.8 to 0.9 kJ/mm

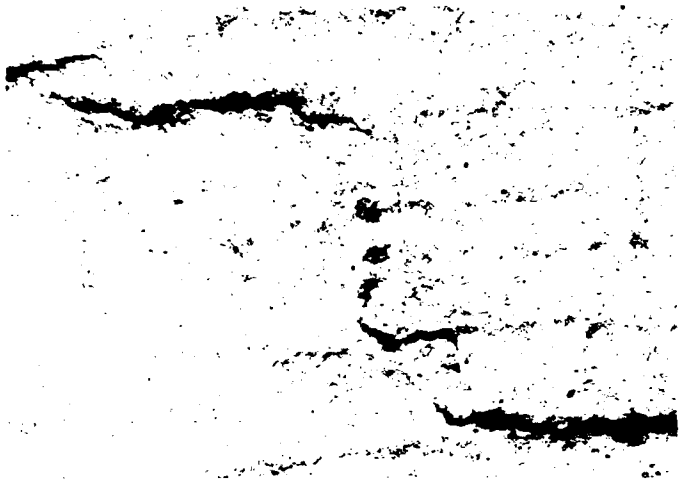

| | HIC | SSCC |
|---|---|---|
| | Formation of blisters | Formation of transverse cracks |
| | Early Stage | |
| Mechanism | Hydrogen internal pressure (H embrittlement) | Nucleation of transverse cracks H embrittlement |
| Necessary conditions | High H activity Stress raisers | High H activity Applied stress (Stress raisers) |
| Site | Elongated inclusions Planar arrays of globular inclusions | Brittle phases (carbides, martensite islands, 'hard' inclusions) |
| | Later Stage | |
| Event | Propagation in hard phase segregated bands Stepwise cracking | Growth of transverse cracks |
| Mechanism | H embrittlement | H embrittlement |

Fig. 5 - THE STAGES OF HIC AND SSCC

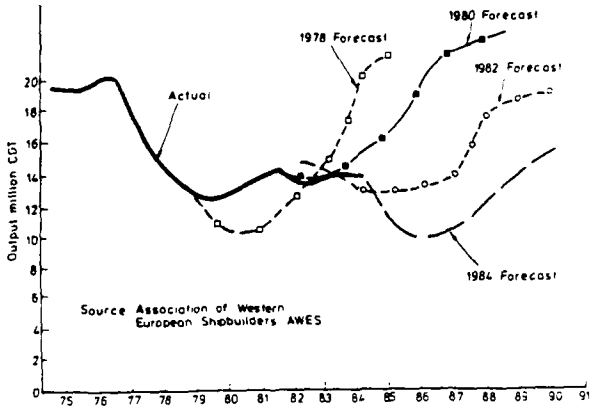


Fig. 6 - A COMPARISON OF FORECASTS OF WORLD SHIPBUILDING REQUIREMENTS 1978 TO 1984

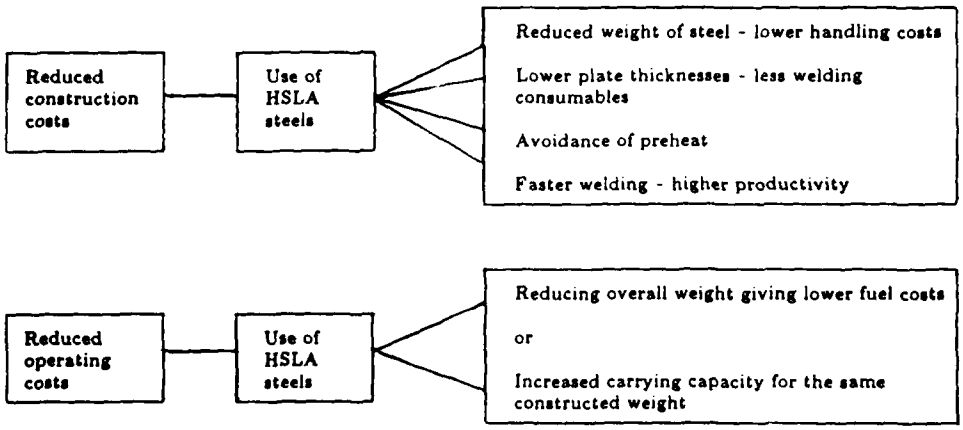


Fig. 7 - ADVANTAGES OF HSLA STEELS IN SHIPBUILDING

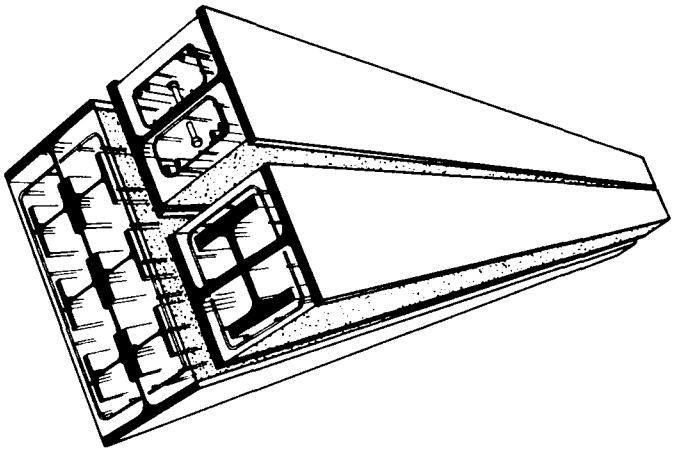

Fig. 9 - COMPOSITE STEEL CONCRETE
FIRE RESISTANT COLUMN

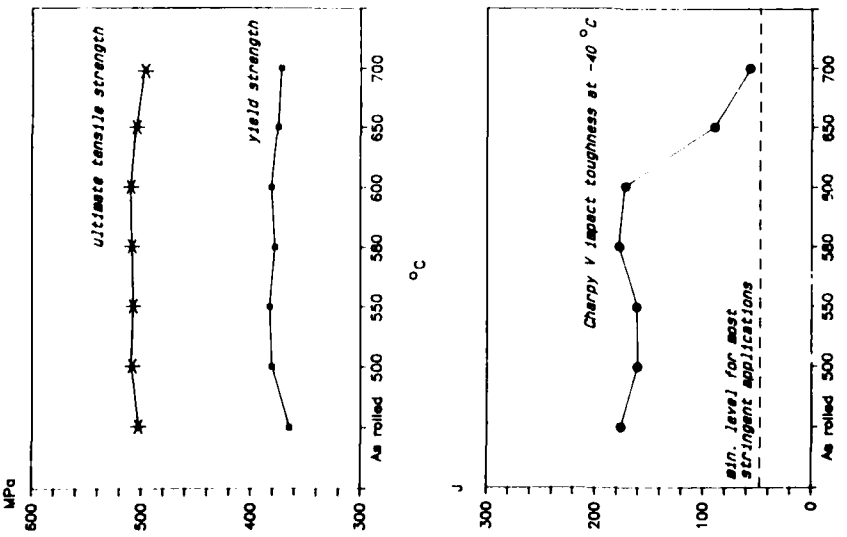


Fig. 8 - MECHANICAL PROPERTIES OF A THERMO-MECHANICALLY TREATED HSLA STEEL AFTER REHEATING AT DIFFERENT TEMPERATURES

| | |
|---|---|
| **Design codes** | Do they allow sufficient reduced thicknesses to compensate for increased initial cost? |
| **Fabrication** | Savings due to reduced volume of weld metal for reduced thickness<br><br>Savings due to lower transport and handling costs during fabrication<br><br>Savings due to higher quality implicit in HSLA steels giving reduced welding costs |
| **Operational savings** | Propulsion energy savings due to decreased weight<br>or<br>Payload increases due to lighter weight<br><br>Increased pumping capacity in linepipe since higher gas pressures can be used |

Fig. 10 - REASONS FOR USING HSLA STEELS

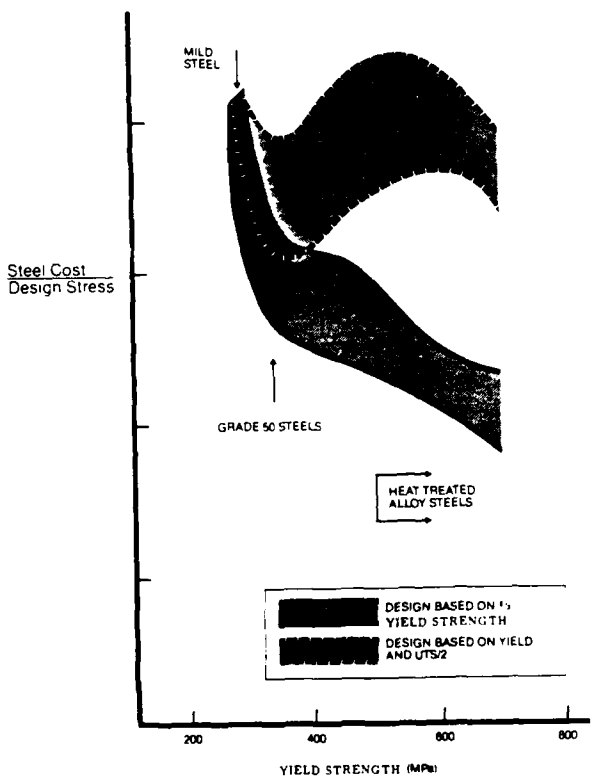


Fig. 11 - DESIGN COST ADVANTAGES FOR HSLA STEELS - STRUCTURAL USE

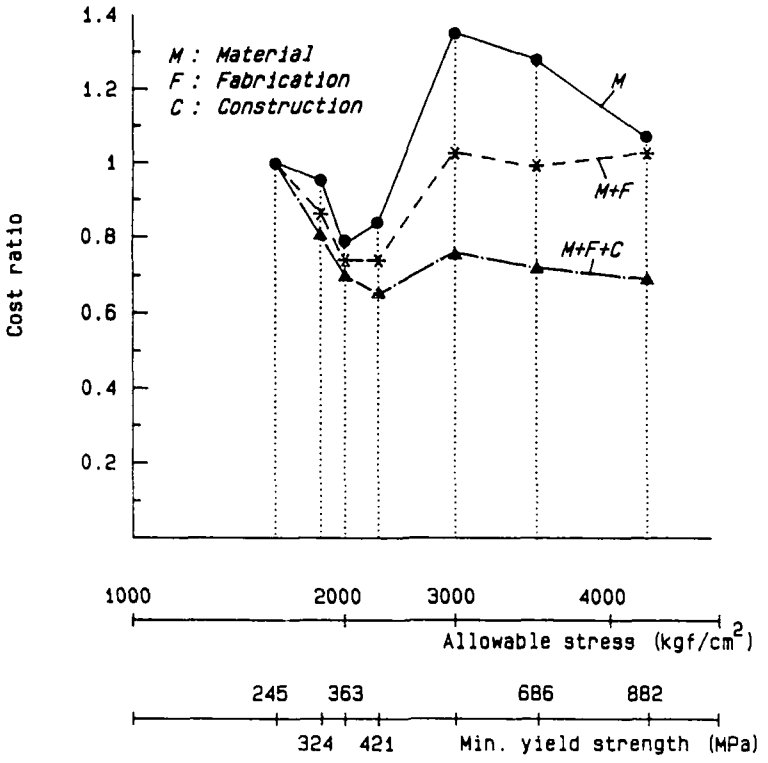


Fig. 12 - COST REDUCTIONS WITH INCREASING STRENGTH FOR A TYPICAL BRIDGE CONSTRUCTION

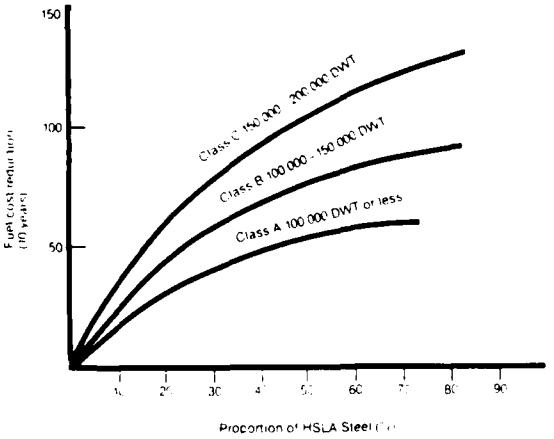


Fig. 13 - REDUCTION IN FUEL COSTS OF HSLA STEEL BASED SHIPS

# JUSTIFICATION FOR THE USE OF HSLA STEELS IN VARIOUS APPLICATIONS

**S. S. Hansen**
Bethlehem Steel Corporation
Bethlehem, Pennsylvania, USA

ABSTRACT

The benefits of HSLA steels to potential users in terms of more efficient designs, reduced production or fabrication costs and/or improved performance are reviewed. In addition to increased strength, other important engineering properties of HSLA steels are also considered. It is suggested that, because of the economic benefits possible through the use of HSLA steels, users carefully assess the cost/performance trade-offs on a case-by-case basis, emphasizing the design criteria that control the service performance of a component.

ALTHOUGH additions of the so-called microalloying elements (V, Nb and Ti) have been made to steels on an experimental basis for over sixty years, significant usage of "microalloyed" or "high-strength low-alloy" (HSLA) steels in various applications and product forms has only occurred since about 1960. Since then, there has been considerable research and development activity aimed at understanding the interrelationship between structure, properties and processing in these steels - much of this activity has been described in the proceedings of several international conferences [e.g. 1-5]. Concurrently, there has been continued growth in the usage of HSLA steels in a variety of product forms. For example, data on shipments of HSLA steels by American producers (AISI statistics) are provided in Figure 1 for various products. It is apparent that the marked increase in HSLA steel shipments in plate and heavy structural products began in the early 1960's (concurrent with the development of V/N-alloyed steels [6]). The growth in plate is particularly notable, increasing from about 5% of shipments in the 1960-62 timeframe to more than 20% today. In comparison, significant growth in HSLA hot- and cold-rolled sheet only began in the mid-1970's, coinciding with mandated automotive fuel economy requirements [7] and the resulting push by automakers for weight reduction [e.g. 8, 9]. Meanwhile, in some other steel product areas the trend to HSLA steels has not yet caught on. For example, while there is considerable ongoing research and development activity on bar/forgings, applications to date in the U.S.A. have been limited. Similarly, there are still other domestic market areas where HSLA steels are underutilized compared to Europe and/or Japan. A recent study by the International Iron and Steel Institute [10] suggests that significant additional penetration of HSLA steels is still possible in the U.S.A. in the areas of shipbuilding, off-shore structures, pressure vessels, sheet piling and reinforcing bars.

Although there are many technical, design or government-mandated reasons for adopting HSLA steels in various applications, it is clear that, in almost all cases, the driving force is economic, i.e. the use of HSLA steels to replace current grades saves money. To quote from Gordon Walter's rapporteur summary at Microalloying 75 [11], "Higher strength has no redeeming value unless it allows weight reduction on a cost-effective basis or enables designs to be completed that could not be done with lower strength steel." Although there are examples where the cost of HSLA steel (per ton) is less than that of current grades, more often (when HSLA steels replace mild steel), HSLA steels are more expensive than the current grade of choice. Consequently, potential users of these steels must look for economic benefits by considering fabrication and final system operating costs as well. Each application should be considered separately, assessing several areas of potential savings, e.g.,

- In some cases, the current component design or a redesign may allow the thickness of the HSLA product to be reduced relative to that of mild steel. If there is sufficient thickness reduction, the weight savings of

the final structure or component may itself compensate for the higher materials cost of HSLA steels. In some designs there may be a "multiplying" effect, where weight reduction of one component may allow weight reduction elsewhere in the final assembly.

- Sometimes, weight reduction in the vehicle design will allow either fuel savings or additional payload at the same fuel cost. In addition, lighter final structures mean reduced transportation and handling costs during the fabrication process.
- Using as-rolled steels to replace grades that were designed to be heat-treated at some point during the fabrication process reduces the customer's manufacturing cost by eliminating one or more processing steps.
- There are also examples where the improved weldability of HSLA steels compared to current grades can eliminate the need for preheat and/or weld cracking. The result can be a dramatic reduction in fabrication costs which often outweighs the higher initial cost of HSLA steels.

Of course, there may also be cases where the use of HSLA steels allows new designs to be undertaken that would not be possible with lower strength grades. In these cases, the result is a new product which offers a competitive advantage (i.e. improved performance).

The present paper considers several factors that can justify the use of HSLA steels in a variety of end applications. Examples will be presented covering various processes and product forms and it will be shown that while HSLA steels can offer considerable advantages to potential users, there are also properties other than strength that should be considered before these steels are put into full-scale production. This paper provides a brief overview of the specific examples; additional details are, of course, provided in the references.

## JUSTIFICATION FOR THE USE OF HSLA STEELS

WEIGHT REDUCTION - Among the factors which argue for the use of HSLA steels, it is perhaps the potential for weight reduction (by substituting HSLA steels for mild steel) that has received the most attention in the technical literature as well as in the popular press. Particular attention has been given to the weight reduction of U.S. automobiles since the mid-1970's. The 1973-74 Arab oil embargo and subsequent gasoline shortages in 1978-79 provided the impetus for several government-mandated energy conservation measures, among them the Corporate Average Fuel Economy (CAFE) standards for new automobiles. This standard mandated systematic increases in fuel economy from 7.6 km/l (18 mpg) in 1978 to 11.7 km/l (27.5 mpg) in 1985* and beyond [7]. Compared to an average value for the 1974 new car fleet of about 6 km/l (14 mpg), this goal represented an increase of almost 100% in fuel economy over an eight year period.

Several authors [e.g. 12-15] have reviewed the routes available to improved fuel economy in automobiles and their general consensus is that while improved aerodynamics, a more efficient drivetrain and better engines can all be of significant benefit, vehicle weight is the primary factor affecting fuel consumption. For example, data for most of the new 1988 models [16] (compared to results for 1974 vehicles [15]) for the EPA city/highway cycle are shown in Figure 2. The importance of "getting the weight out" has been well appreciated by the automotive industry, and through a combination of downsizing and materials substitution, the weight of the average domestically-produced automobile has been reduced from 1,705 kg (3,760 lb) in 1976 to 1,442 kg (3,178 lb) in 1987 [17]. This mandated weight reduction has had the desired impact - the average annual fuel consumption of all vehicles on the road in the U.S.A. has decreased by about 30% over the same time frame. Although cars have become smaller, an increase in the use of plastics (primarily in trim and finish applications), aluminum and especially HSLA steels (Figure 3) since 1973/74 has had a major impact on weight reduction. Today the average domestically-produced automobile contains more than 90 kg (200 lb) of HSLA steel [17, 18].

Over the past decade or so, much of this materials substitution was implemented to meet the CAFE requirements. More recently, however, the theme of "cost-effective" weight reduction has been promoted. On this basis (Figure 4), HSLA steels are the only material under consideration by the automobile industry that can actually provide a cost savings (for materials only) when substituted for mild steel [18]. Although HSLA steels cost more than mild steel on a per ton basis, if full advantage can be taken of their higher strength, material cost savings will be achieved. For example (Figure 5), when substituting a 550 MPa (80 ksi) HSLA grade for 200 MPa (29 ksi) mild steel, a weight reduction of about 30% (the exact number depends on relative prices) must be obtained to reduce the material cost [19]. Whether this degree of weight reduction can be achieved depends on the particular application being considered. For example, as shown in Figure 6 [20], the performance of any part, particularly when subjected to bending or torsion, depends on the component geometry as well as its yield strength. In those applications where yield strength controls the design (e.g. door beams

* This was later reduced by the EPA to 11 km/l (26 mpg) for 1986, 1987 and 1988 vehicles.

and bumpers), very efficient use of HSLA steels can be made and weight savings of 40-60% can be achieved by the use of a reduced thickness and higher strength (340-550 MPa [50-80 ksi]) grades substituting for mild steel. However, for other parts (e.g. outer body panels) which are also subjected to bending and/or buckling, stiffness is more important, and part geometry and the modulus of elasticity (identical for carbon and HSLA steels) controls materials selection. In these cases, the potential weight savings on direct substitution is considerably reduced, and HSLA steels may not be economical. In some cases, component redesign (e.g. the use of beads or ribs to increase panel stiffness) may improve the structural performance of the part and allow for more efficient use of the increased strength of HSLA steels.

Of course, the benefits of weight reduction in terms of reduced fuel consumption are not limited to automobiles. For example, HSLA steels are used successfully to reduce weight, and hence improve fuel economy, in trucks, rail cars, off-highway vehicles and even ships (Figure 7 [10]). Although there are concerns about the extent to which weight can be reduced in ships because of buckling and stiffness considerations, a range of 10 to 30% for HSLA steel usage is probably reasonable [21]. Alternatively, instead of fuel savings, the use of HSLA steels to reduce vehicle or vessel weight allows an increase in payload while keeping fuel costs the same, an important consideration for the transportation industry.

Finally, the idea of "iterative" weight reduction should be presented. An example of this redesign process as applied to off-highway vehicles is shown in Figure 8 [22]. Weight reduction in one component (in this case a tool attachment) can lead to a "multiplying" effect by allowing smaller engines, drive-trains, and body support structure. Although the amount of this "other" weight reduction depends significantly on the type of vehicle being considered, estimates for automobiles suggest that this additional weight savings is about 50% of the component weight reduction [23].

REDUCED CUSTOMER PRODUCTION COSTS/MORE EFFICIENT DESIGN - An area of interest to most steel fabricators is the possibility of reducing their in-house production costs. In a variety of applications the substitution of HSLA steels for medium carbon or alloy grades that would normally be quenched-and-tempered after a variety of operations has proved to be cost-effective. For example, consider the manufacture of crankshafts (Figure 9) by drop forging [24]; here the use of microalloyed steels to develop the required properties in the as-forged and cooled condition has resulted in the elimination of the quenching, tempering, straightening and stress relieving operations. Final part cost savings on the order of 10% for forged components like connecting rods and crankshafts have been achieved by the substitution of HSLA steels for heat-treated grades [25].

Another example involves the use of microalloyed steel wire rod for automotive fasteners to replace a heat-treated medium carbon steel (Figure 10). In this case, both spheroidize annealing (before drawing and cold heading of the conventional medium carbon wire rod) and subsequent quenching and tempering were eliminated [26].

A noteworthy effort to reduce fabrication costs is the ongoing move to HSLA steels in Navy shipbuilding to replace the heat-treated, high-alloy HY-80 and HY-100 grades [21]. In addition to the lower material cost of the Cu-bearing HSLA-80 and HSLA-100 grades, there are major benefits in terms of the improved weldability of the HSLA grades (Figure 11). For example, by moving to the lower carbon, more-weldable, HSLA-80 grade (to replace HY-80) the need for preheat is eliminated. The Navy estimates the cost of preheating at $0.09 to $0.18 per kg ($0.20 to $0.40 per pound). Considering anticipated Navy shipbuilding programs, the reduced material and fabrication costs translates into a potential reduction in Navy shipbuilding costs of about $0.2 to $1.0 billion over the next decade [21].

The use of HSLA steels in building and bridge construction provides a good example of reduced costs through more efficient design. In fact, the development of hot-rolled and normalized HSLA steels in the early 1960's allowed more cost-effective design of buildings and bridges, (hence the rapid growth of HSLA plate and heavy structural shipments in this time frame - Figure 1). Considering alternate designs for structures (Figure 12 [10]), it becomes apparent that, if the design strength is based on both yield and tensile strength, the most efficient design (in terms of material costs) is for steels with yield strengths of about 350 MPa ([50 ksi], usually produced to ASTM A572 and A588 specifications). More recent work, however, suggests that if fabrication and construction costs are also considered, there may be some cost advantage in moving to even higher strength levels [10]. This is obviously a situation that deserves further attention.

NEW DESIGNS - IMPROVED PERFORMANCE - Perhaps the classic example of how the use of HSLA steels can result in otherwise unachievable designs is in the development of HSLA steels for oil and gas pipelines [27,28]. In the transport of natural gas via a pipeline, some of the gas must be used to fuel compressor stations along the line. The amount of gas used as a fuel decreases with increasing operating pressure and increasing pipe diameter. The development of HSLA linepipe steels permitted the use of larger pipelines operating at pressures in excess of 112 bar (1600 psi) (Figure 13 [28]). Today HSLA linepipe grades with yield strengths up to 483 MPa (70 ksi), in thicknesses up to 25 mm (1 inch) are readily

available. Of course, in addition to higher strength in greater thicknesses, these HSLA grades also provide excellent toughness, good field weldability, resistance to ductile crack propagation, and in some cases, good resistance to aggressive (sour gas or $CO_2$) environments. This combination of properties makes linepipe steels the premium HSLA grades available today. Similar considerations are also being given to steels for offshore structures, particularly for application in colder, more hostile seas.

## OTHER CHARACTERISTICS OF HSLA STEELS

In the previous sections we have focused on some of the factors contributing to the increased use of HSLA steels in various applications. As such, we have accentuated the benefits of these steels in terms of weight reduction, design efficiency and reduced fabrication costs. However, some of the other engineering properties of HSLA steels that may impact on manufacturing or service performance must also be considered.

FORMABILITY - Generally speaking, increasing strength means reduced formability in all forming modes. Several authors [29-31] have defined the loss in stretch formability resulting from the increased strength level of HSLA steels; for example, forming limit diagrams for 350 and 550 MPa (50 and 80 ksi) steels compared to mild steel are shown in Figure 14* [30]. Similar strength effects are noted when assessing the sensitivity to edge failure (e.g. cracking during expansion of a sheared hole); however, in this case, control of inclusion volume fraction and shape may offset some of the formability loss at the higher strength levels [32]. Whether the formability of a particular HSLA steel is adequate depends on the particular application. In most cases, part redesign and/or minor modifications in the manufacturing process have successfully resolved initial forming difficulties encountered with HSLA steels.

NOTCH TOUGHNESS - Toughness is of significance in many structural applications, and in general, the combination of microalloying and controlled rolling** produces improved toughness compared to hot-rolled mild steel (Figure 15 [33]). Even better levels of toughness (e.g. to meet severe linepipe or Navy toughness requirements) can be achieved by judicious compositional modification (e.g. lower carbon and sulfur contents, nickel additions, etc.) and/or processing changes (e.g. more severe controlled rolling, accelerated cooling after rolling, etc.).

Ensuring an adequate level of toughness is of particular concern when an HSLA steel replaces a quenched-and-tempered (Q&T) product, e.g., as is being considered for some of the forging applications discussed earlier. In these cases, the conventional Q&T product is usually a medium-carbon steel and the thermomechanical treatment imparted by the standard forging operation is akin to hot-rolling. If a microalloyed steel at the same strength level is substituted without any modification in carbon level or forging practice, the result, illustrated in Figure 16, is usually reduced notch toughness [34]. With a reduced carbon content, controlled forging practices and accelerated cooling after rolling, some improvements in toughness are achievable. However, considering the available routes to higher strength in HSLA grades, the development of a Charpy transition temperature similar to the Q&T grades at yield strength levels of 700 MPa (100 ksi) or higher is unlikely. Whether the reduced toughness levels of these HSLA steels will suffice depends on the specific application, e.g. medium carbon HSLA forging steels have been judged to be adequate by Volvo for automobile connecting rods and steering knuckles, but not for truck front axle beams [35].

FATIGUE PROPERTIES - In many applications, fatigue strength is the important design parameter. The fatigue strength of steels generally increases with increasing tensile strength. Thus HSLA steels exhibit improved fatigue behavior compared to as-rolled mild steel. In addition, microalloyed steels exhibit hardening during cyclic testing while Q&T steels cyclically soften. Thus, a 550 MPa (80 ksi) yield strength HSLA steel has about the same strain-life fatigue behavior as a 700 MPa (100 ksi) yield strength Q&T product [36]. In most applications, fatigue strength does not limit the use of HSLA steels. However, in the presence of a welded joint, fatigue strength can be significantly reduced [e.g., 22, 34, 37]. Consider, for example, the use of HSLA steels for automotive wheel rims (Figure 17). While the fatigue strength increases continuously with increasing tensile strength for the base metal, in the presence of a notch (simulating a welded joint in a rim) there is a maximum in fatigue strength at a base metal tensile strength of about 585 MPa (85 ksi) [37]. Consequently, in conventional wheel rim production, there may be a limit to the strength level at which HSLA steels can be effectively utilized. In extreme cases, if the welded joint is in the high stress area, there may be no advantage gained by using HSLA steels (since the fatigue strength of the welded joint

---

* In many cases total elongation as measured in a tensile test provides a realistic rating of the relative formability of these steels.

** Controlled rolling uses lower rolling temperatures compared to conventional hot rolling. When combined with appropriate microalloying, the result is significant ferrite grain refinement, and hence improved toughness.

is similar to what would be achieved in mild steel). In these cases, component redesign to put the weld in a less critical spot relative to the operating stresses offers one way to make use of HSLA steels.

WELDABILITY - In various kinds of welding procedures, adequate weldability is usually defined in terms of a "maximum" carbon equivalent [e.g. 31, 38]. In terms of resistance spot welding in the automotive industry, HSLA sheet steels can be successfully joined with suitable adjustment of welding parameters. For example, HSLA steels require lower currents and a higher electrode force (Figure 18 [39]) than mild steel. Minimum nugget diameters, about 20-30% larger than for mild steel, are also usually specified for HSLA steels to eliminate "interface cracking" of the weld, and to provide for increased load transfer to match the higher strength of the HSLA grades. Most manufacturing engineers are now familiar with the parameters required to successfully spot weld HSLA steels, and inadequate weldability no longer appears to be a significant barrier to the increased use of HSLA sheet grades.

In arc welding of plate steels, we are concerned with cold-cracking in or near the heat-affected zone of a weld. To avoid cold-cracking, conventional steels are often pre-heated; the necessary preheat depends on factors such as strength level, composition, weld restraint level, plate thickness, welding heat input and weld metal hydrogen. There have been many successful efforts to develop preheat temperature guidelines based on these factors, and the state-of-the-art has been recently summarized by Yurioka [38]. Considering compositional factors, it is now well appreciated that the "Pcm" carbon equivalent allows a more realistic assessment of the weldability of low carbon steels compared to the conventional IIW carbon equivalent [40]. More recently, Yurioka et al. [41] proposed a "blended" carbon equivalent, CEN, which is similar to the Pcm formula at low carbon levels (<0.17%), and follows the IIW formula at higher carbon levels*. Many modern HSLA steels exhibit superior weldability to mild steel because of their lower carbon contents and lower carbon equivalents (Figure 19 [42]), and do not generally require any preheat to avoid cold-cracking, even in thicker plates. HSLA steels are also available with deliberate additions of Ti or various combinations of Ti, B, rare earth metals or Ca; these additions provide good toughness in the heat-affected zone, even when welding at high heat inputs [43-45].

MACHINABILITY - In forging applications, in particular, machining of the final part may contribute as much as 50-60% to the total cost of manufacture [46]. The machining properties of HSLA steels compared to Q&T steels at a similar strength (hardness) level, are therefore of importance with regard to the application of these grades. Research to date generally indicates that HSLA steels have at least similar, and sometimes better machinability than Q&T steels (Figure 20 [47]). Of course, standard routes to improved machinability (e.g. calcium treatment, higher sulfur contents, etc.) may also be applied to HSLA steels.

CORROSION RESISTANCE - The corrosion performance of HSLA steels in various environments is considered to be similar to that of mild or low-alloy steel [21,31]. Consequently, when the use of HSLA steels leads to a reduction in component thickness, reduced corrosion life may be a concern. However, with today's knowledge of corrosion prevention techniques and the availability of a variety of improved coatings, corrosion concerns are usually not a barrier to the application of HSLA steels.

## SUMMARY

This brief review demonstrates that HSLA steels can provide significant benefits to potential users in terms of more efficient designs, reduced production or fabrication costs and/or improved performance. At the same time many other important engineering properties of HSLA steels may also be improved or at least be similar to those of the low carbon or quenched-and-tempered grades currently in use. On the other hand, there may be some instances where the reduced formability or notch toughness of some HSLA steels (compared to current grades of choice) may limit applications. However, with the bottom-line gains that are achievable through the use of HSLA steels, it is important for potential users to carefully assess the cost/performance trade-offs on a case-by-case basis, with special emphasis on the design criteria that control the service performance of the component.

---

* These various carbon equivalent formulae are,

$$CE\ (IIW) = C + \frac{Mn}{6} + \frac{Cu + Ni}{15} + \frac{Cr + Mo + V}{5}$$

$$Pcm = C + \frac{Si}{30} + \frac{Mn}{20} + \frac{Cu}{20} + \frac{Ni}{60} + \frac{Cr}{20} + \frac{Mo}{15} + \frac{V}{10} + 5B$$

$$CEN = C + A(C)\cdot\left[\frac{Si}{24} + \frac{Mn}{6} + \frac{Cu}{15} + \frac{Ni}{20} + \frac{Cr + Mo + Nb + V}{5} + 5B\right],$$

where, $A(C) = 0.75 + 0.25 \tanh [20(C-0.12)]$

ACKNOWLEDGMENTS

The permission of Bethlehem Steel Corporation to publish this paper and valuable comments from B. L. Bramfitt, J. M. Chilton and J. G. Speer are gratefully acknowledged.

REFERENCES

1. "Microalloying 75, Proceedings", Union Carbide Corporation, New York, New York (1977).
2. "Thermomechanical Processing of Microalloyed Austenite", edited by A. J. DeArdo, G. A. Katz and P. J. Wray, The Metallurgical Society of AIME, Warrendale, Pennsylvania (1982).
3. "HSLA Steels: Technology and Applications", American Society for Metals, Metals Park, Ohio (1984).
4. "HSLA Steels: Metallurgy and Applications", edited by J. M. Gray, T. Ko, Zhang Shouhua, Wu Baorong and Xie Xishan, ASM International, Metals Park, Ohio (1986).
5. "Fundamentals of Microalloying Forging Steels", edited by G. Krauss and S. K. Banerji, The Metallurgical Society of AIME, Warrendale, Pennsylvania (1987).
6. Stephenson, E. T., G. M. Karchner and P. Stark, Trans ASM, 57, 208-219 (1964).
7. U. S. Congress, "Energy Policy and Conservation Act" (1975).
8. Pond, J. B., R. H. Eshelman and C. A. Gottesman, Automotive Industries, 37-47 (December 15, 1973).
9. Wrigley, A., "Wards Automotive Yearbook - 1975", 55-62 (1975).
10. "High Strength Low Alloy Steels", IISI Committee on Technology, Brussels, Belgium (1987).
11. Walter, G. H., Reference 1, 622-633 (1977).
12. LaPointe, C., SAE Paper No. 730791 (1973).
13. Huebner, G. J., Jr. and D. J. Gasser, SAE Paper No. 730518 (1973).
14. "Potential for Motor Vehicle Fuel Economy Improvement", DOT-EPA joint report (October, 1974).
15. Pierce, J. R., Scientific American, 232, 32-44 (1975).
16. Consumer Reports 53, 226-245 and 264-269 (1988).
17. "MVMA Motor Vehicle Facts and Figures - 1988", Motor Vehicle Manufacturers Association of the United States, Inc., Detroit, Michigan (1988).
18. Magee, C. L., SAE Paper No. 820147 (1982).
19. Younger, D. G., "Proceedings of Mechanical Working and Steel Processing Conference XII", p. 63-89, The Metallurgical Society of AIME, New York, New York (1974).
20. Younger, D. G., Metals Progress, 107, 43-47 (1975).
21. Montemarano, T. W., B. P. Sack, J. P. Gudas, M. G. Vassilaros, and H. H. Vanderveldt, Journal of Ship Production, 2, 145-162 (1986).
22. Tucker, L. E. and J. K. Dunn, Reference 1, 645-652 (1977).
23. Marshall, K. D., SAE Paper No. 700174 (1970).
24. Engineer, S., B. Huchtemann and V. Schuler, Reference 5, 19-37 (1987).
25. Chambers, A. R. and D. Whittaker, Metals Technology, 11, 323-333 (1984).
26. Namiki, K., K. Isokawa and T. Kato, Reference 5, 521-537 (1987).
27. Jones, B. L., Reference 3, 715-722 (1984).
28. Gray, J. M. and T. V. Bruno, "Trends in the Technology and Specification of Pipeline Steels", presented at the AISE Meeting, Houston, Texas (March 30, 1982).
29. Hecker, S. S., General Motors Corporation Report No. 1339, Detroit, Michigan (February 16, 1973).
30. Dinda, S., J. A. DiCello and A. S. Kaspar, Reference 1, 531-538 (1977).
31. Magee, C. L., R. G. Davies and P. Beardmore, Journal of Metals, 32 28-35 (November 1980).
32. Pradhan, R. R., "Proceedings of Mechanical Working and Steel Processing Conference XVII", p. 1-18, The Metallurgical Society of AIME, Warrendale, PA (1979).
33. Hansen, S. S., Reference 5, 155-174 (1987).
34. Babu, P. B., D. R. Gromer, D. J. Lingenfelser and G. P. Shandley, Reference 5, 389-423 (1987).
35. Gunnarson, S., H. Ravenshorst and C. M. Bergstrom, Reference 5, 325-338 (1987).
36. Landgraf, R. W., and A. M. Sherman, Reference 1, 498-502 (1977).
37. Irie, T., K. Tsunoyama, M. Shinozaki, T. Kato and N. Aoyagi, SAE Paper No. 880695 (1988).
38. Yurioka, N., "A Method for Determining Necessary Preheating Temperature in Steel Welding", paper presented at AISC Annual Conference, Miami, Florida (July, 1988).
39. Dinda, S., C. Belleau, and D. K. Kelley, Reference 3, 475-483 (1984).
40. Ito, Y. and K. Bessyo, Journal of Japan Welding Society, 37, 683-691 (1968).
41. Yurioka, N., H. Suzuki and S. Ohshita, Welding Journal, 62, 147s-153s (1983).
42. Suzuki, H., Trans ISIJ, 23, 189-204 (1983).
43. Kanazawa, S., A. Nakashima, K. Okamoto and K. Kaneya, Trans. ISIJ, 16, 486-495 (1976).
44. Kosazu, I., Reference 3, 593-607 (1984).
45. Itoh, K., H. Mimura, S. Matsuda, K. Yamamoto, Y. Ohno, Y. Okamura and Y. Kawashima, Reference 4, 669-673 (1986).
46. Tonshoff, H. S. and H. Winker, VDI-Z, 124, 481-485 (1982).
47. Bhattacharya, D., Reference 5, 475-490 (1987).

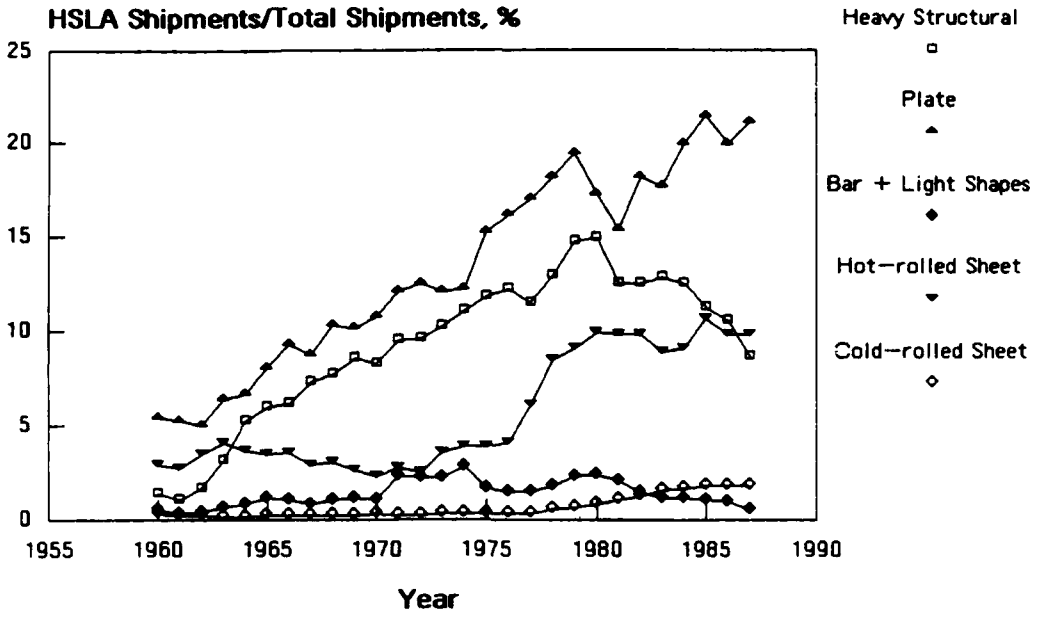


Figure 1. HSLA steel shipments for various products as a percentage of total AISI-reported shipments (1960 to 1987).

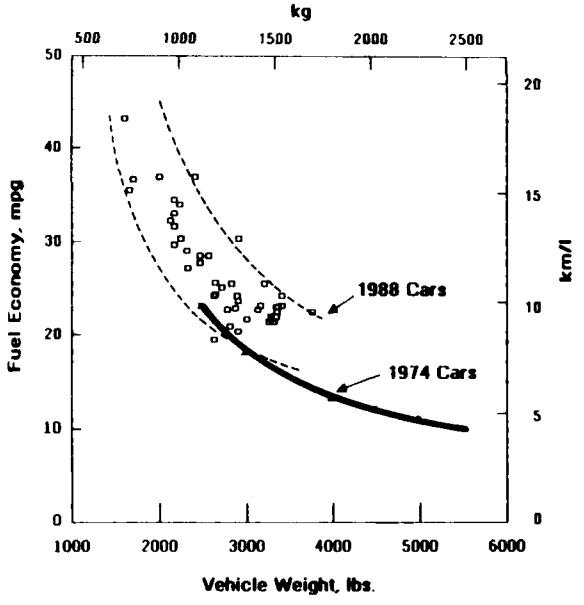


Figure 2. Effect of vehicle weight on fuel economy for combined city/highway cycle (from references 15, 16).

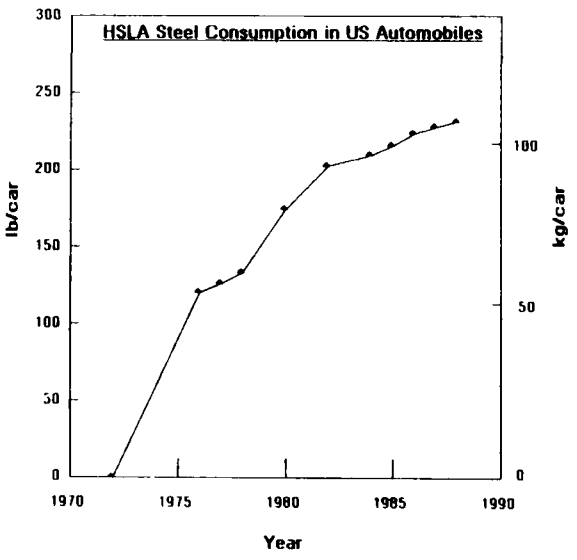


Figure 3. Trend in the use of HSLA steels in automobiles produced in U.S.A. (from references 17, 18).

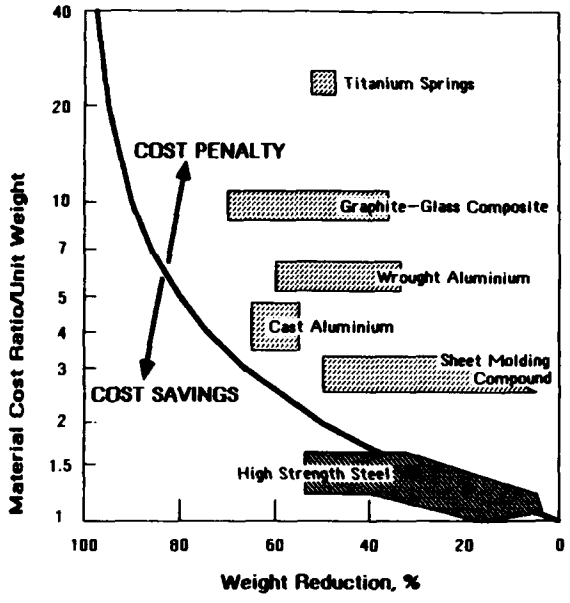


Figure 4. Material cost ratio as a function of weight reduction potential for various materials compared to mild steel as the base. Solid line is break-even line for materials cost.

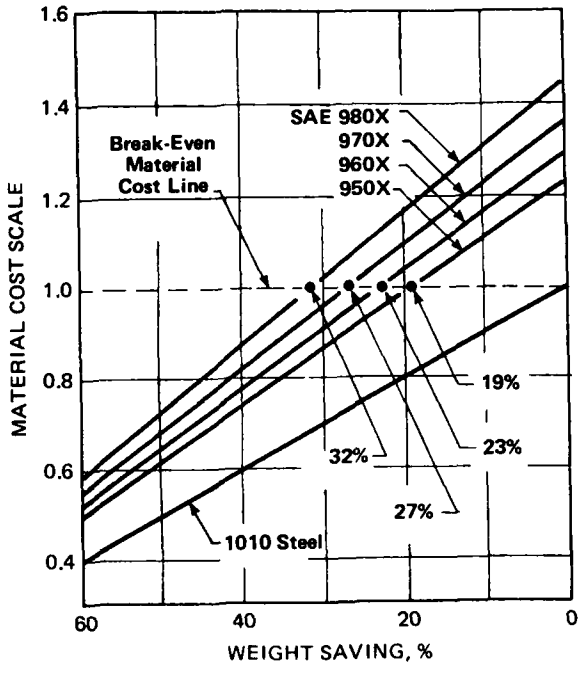


Figure 5. Weight savings required to break even when substituting 340 to 550 MPa (50 to 80 ksi) yield strength HSLA steels for mild steel, e.g. SAE 980X is an 80 ksi [550 MPa] grade (from reference 19).

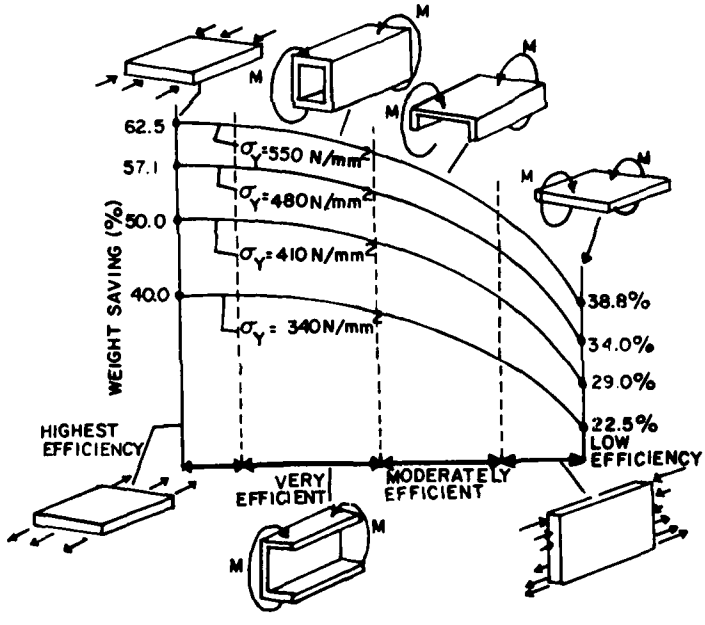


Figure 6. Potential weight savings for 340 to 550 MPa yield strength HSLA steels when substituted for 200 MPa yield strength mild steel in various structural components (from reference 20).

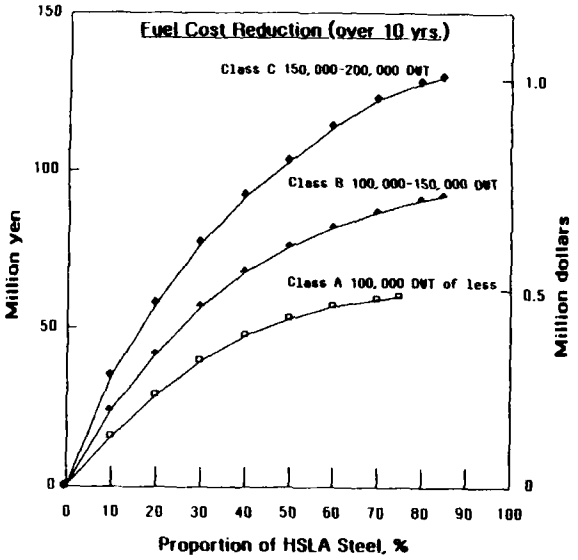


Figure 7. Reduction in the fuel costs of various class ships (over a 10 year period) as a function of the proportion of HSLA steels used in vessel construction (from reference 10).

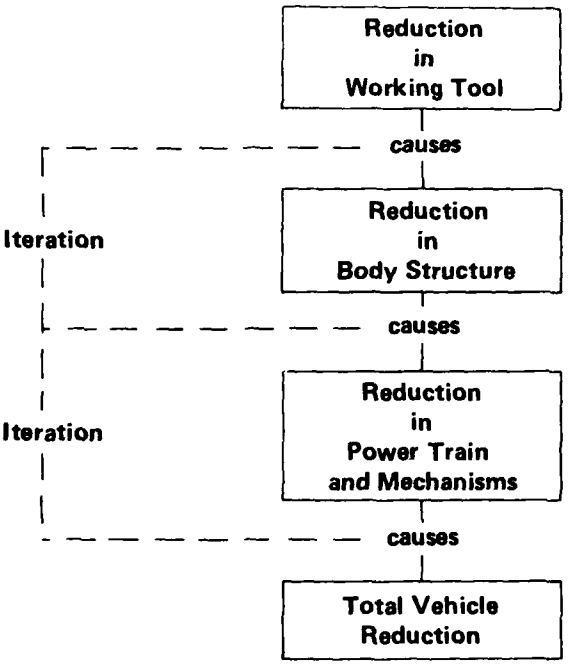


Figure 8. Iterative weight reduction model for redesign of off-highway vehicles (from reference 22).

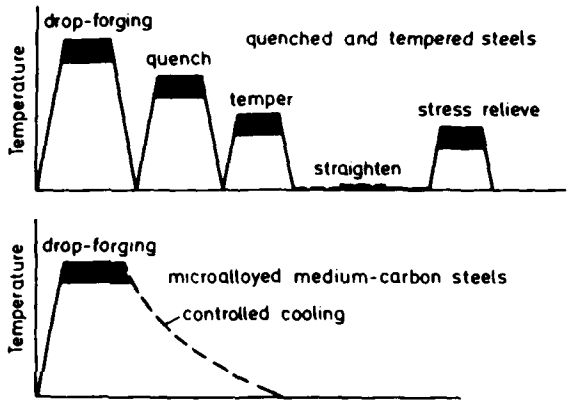


Figure 9. Required manufacturing steps for producing crankshafts from quenched and tempered and microalloyed medium carbon steels, respectively (from reference 24).

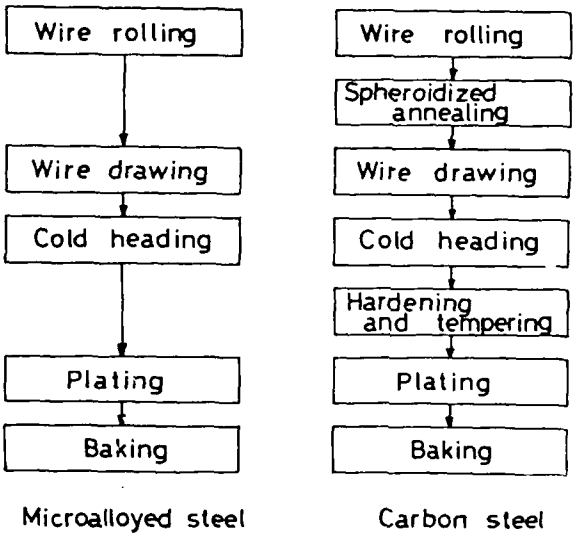


Figure 10. Manufacturing sequence for class 8.8 automotive bolts from microalloyed and carbon steels, respectively (from reference 26).

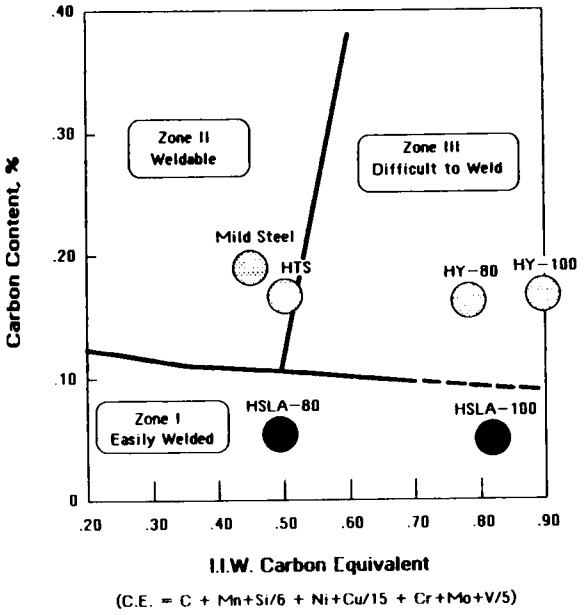


Figure 11. Cold-cracking susceptibility of various Navy shipbuilding steels as a function of carbon content and IIW carbon equivalent (from reference 21).

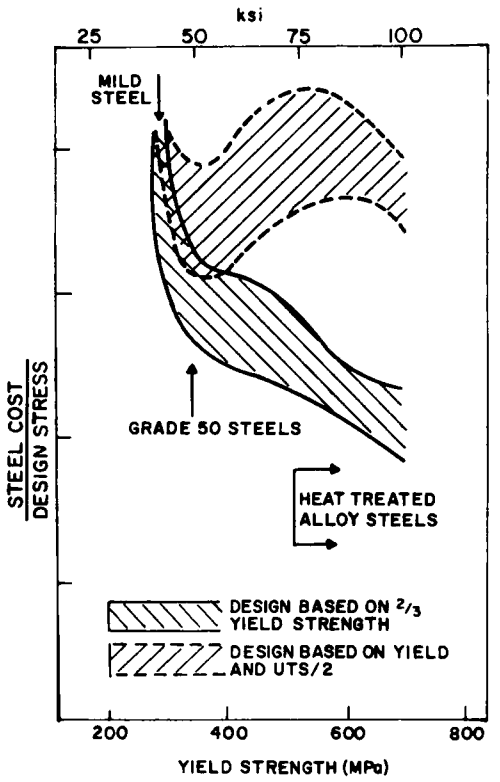


Figure 12. Relationship between steel cost per unit design stress and yield strength for structural designs based on either yield strength or yield and tensile strength (from reference 10).

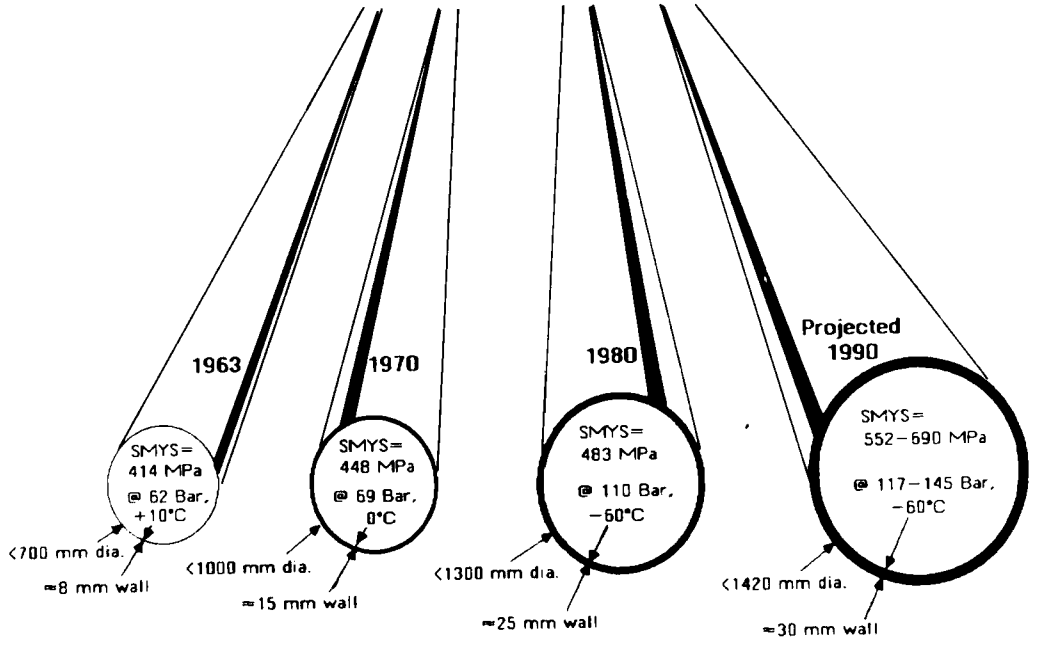


Figure 13. Trends in pipeline design requirements since 1963 (from reference 23).

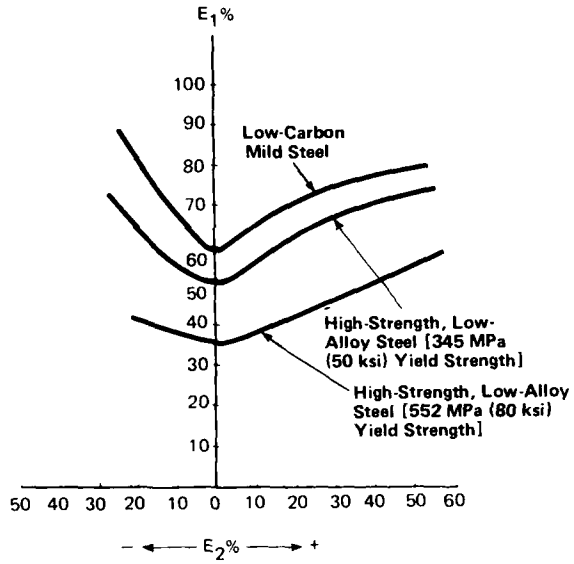


Figure 14. Forming limit diagrams for a low-carbon, and two HSLA, sheet steels at a thickness of 2.54 mm (0.10 inch) (from reference 30).

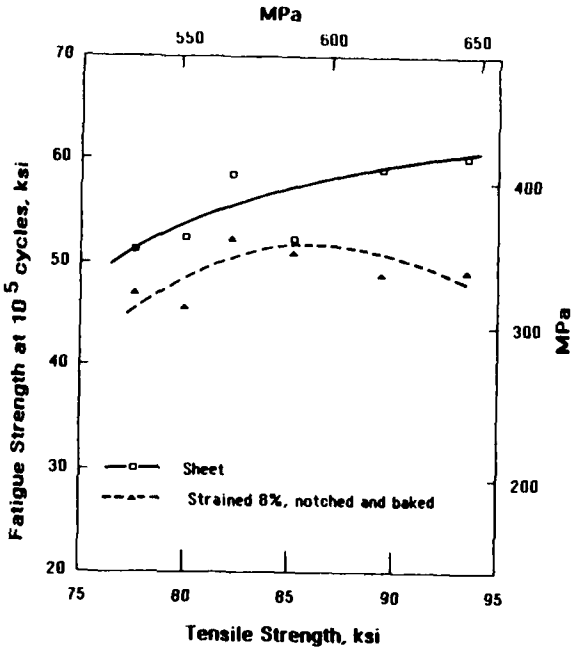


Figure 17. Effect of tensile strength on the fatigue strength of HSLA steels in the as-received and strained/notched/baked conditions; stress ratio (R) = -1 (from reference 37).

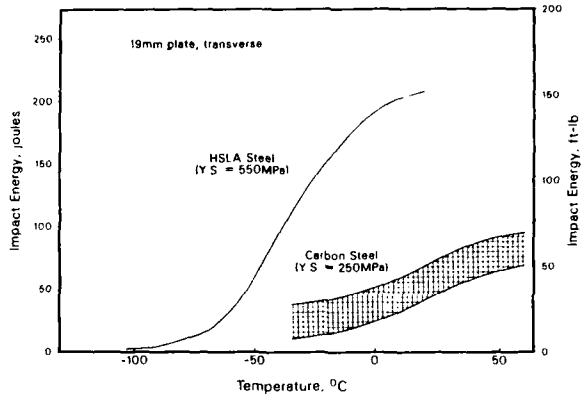


Figure 15. Comparison of Charpy curves for carbon and HSLA plate steels (from reference 33).

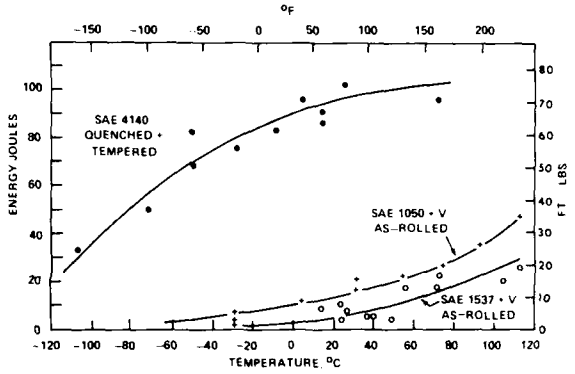


Figure 16. Comparison of Charpy curves for quenched and tempered and HSLA medium carbon forging grades (from reference 34).

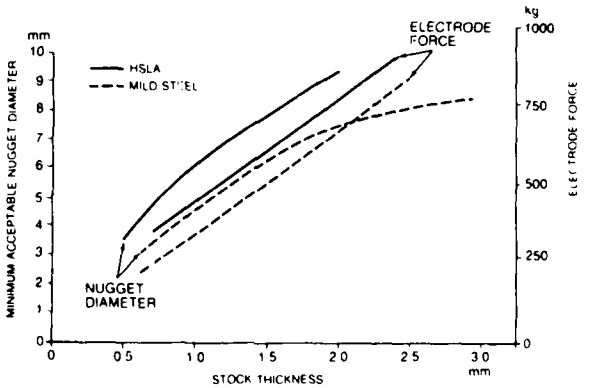


Figure 18. Comparison of required spot welding parameters for low carbon and HSLA sheet steels (from reference 39).

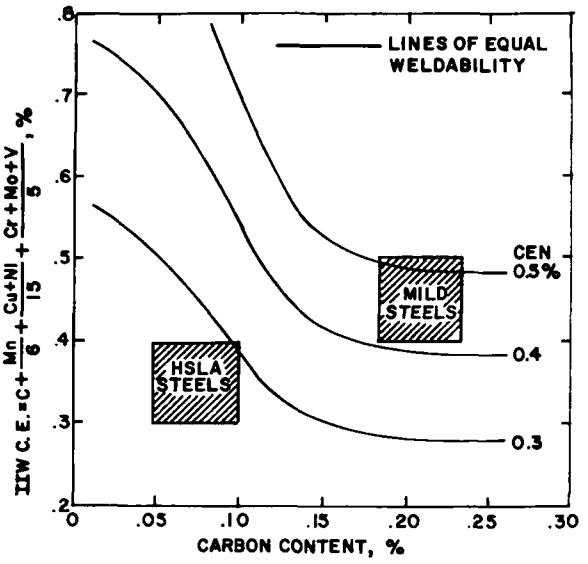


Figure 19. Weldability comparison of mild and HSLA steels. Lines at constant CEN represent the possible trade-off between IIW carbon equivalent and carbon content to maintain equal cold-cracking resistance in carbon and low-alloy steels (from reference 42).

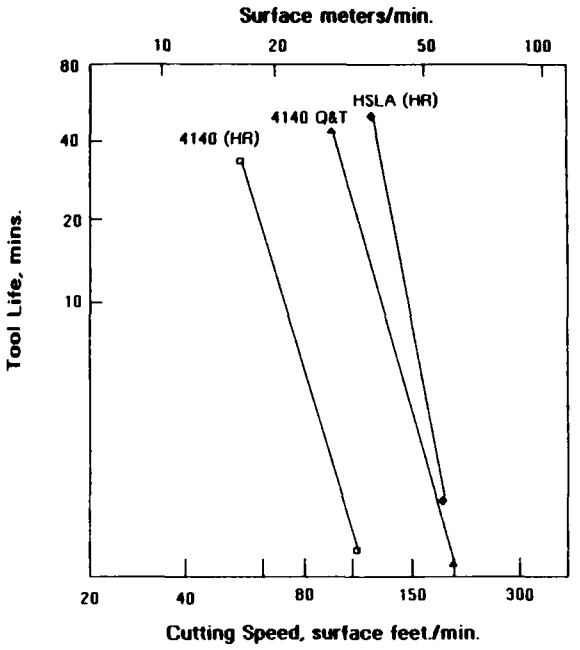


Figure 20. Taylor Tool Life vs. cutting speed curves for 4140 quenched and tempered and HSLA (1045+V) steels (from reference 47).

# DEVELOPMENT AND APPLICATION OF HIGH STRENGTH STEELS FOR COST AND WEIGHT REDUCTION

**D. J. Naylor**
British Steel Corporation
Swinden Laboratories
Rotherham, S60 3AR
South Yorkshire, Great Britain

ABSTRACT

The paper will review several developments of HSLA steels, including microalloyed steels, in the form of long (billet and bar derived) and flat (narrow strip) products.
These new materials have been made available through recent advances in modern steelmaking practices, e.g. improved cleanness (lower sulphur contents and inclusion shape control), close chemical composition control and thermomechanical treatments.
These developments have been stimulated in response to the demands of steel users for products with increased strength levels whilst maintaining or even improving the toughness at progressively lower temperatures, and also with acceptable formability, machinability or weldability and for use in increasingly more aggressive environments.
Several illustrations will be given of the development and applications of high strength steels which offer better 'value in use'. These include:
- Microalloyed steels for air cooled forgings, not requiring conventional heat treatment.
- High strength, tough and weldable steels for forged fittings and flanges
- Hot and cold rolled strip for automotive components.
- High strength, tough steels for more efficient gas cylinders.

The successful application of high strength steels for cost and weight reduction and more efficient material utilisation will also depend on design considerations and optimisation.
Another important aspect influencing the successful implementation of HSLA steels is the demonstration of 'fitness for purpose' to ensure safe and acceptable service performance. The contribution of fracture mechanics and strain controlled fatigue data to help achieve this objective will also be described and discussed.

DESPITE THE SIGNIFICANT CONTRACTION in the European steel industry during the past decade, there have been major improvements in plant and processing conditions. These have included continuous casting, ladle arc steelmaking, clean steel practices, inclusion modification, controlled rolling and other thermo-mechanical treatments. They have led to increased productivity and also to improved product quality. Combined with a better metallurgical understanding of the relationships between processing, microstructure and properties, it has therefore been possible to develop, at an economical cost, new steels for a wide range of applications. Over the same period, there have been growing demands from steel users for:

| | |
|---|---|
| weight saving: | to improve fuel consumption and provide more efficient components. |
| cost reduction: | to resist the challenge from alternative materials. |
| increased safety: | to provide greater resistance to damage without increasing weight or cost. |

These requirements can be satisfied by the use of higher strength steel. In many cases, the increased stength levels have to be achieved whilst maintaining, or even increasing, the toughness, at progressively lower temperatures. Futhermore, the higher strength steels must have acceptable formability, weldability and machinability, to ensure that the components can be fabricated economically. This paper provides several examples of the development and applications of high strength steels for cost and weight reduction.

The successful application of high strength steels for better "value-in-use" and more efficient material utilisation depends also on design considerations and optimisation. Weight saving, through the use of higher strength materials will depend upon how the structure or component is stressed. For all practical purposes, the elastic modulus of steels is fixed and the use of a higher strength steel simply provides the design engineer with the opportunity to stress the material to a higher elastic limit. The presence of non-uniform stress fields, such as in bending, limits this weight saving potential, which is clearly maximised under uniform axial loading conditions. Close attention to design detail to limit stress concentrations is therefore required.

Care must be taken, when modifying an existing design, to ensure that a reduced section thickness does not endanger the stability of the product due to buckling. Control of elastic displacement is also an important consideration which can often limit the use of higher strength steels in building construction and in moving part machinery.

The design engineer must also take into consideration the likely increase in the risk of fracture resulting from the higher operating stresses, as well as the need to evaluate any potential problems arising from fatigue loading or environmental susceptibility. Another important prerequisite, therefore, is the demonstration of fitness-for-purpose of higher strength steels to ensure a safe and acceptable in-service performance. The use of fracture mechanics and strain controlled fatigue data in these considerations will be described and discussed.

## LOW COST HIGH STRENGTH STEELS FOR AUTOMOTIVE FORGINGS

Over the past 15 years, the UK production of cars and commercial vehicles has fallen from over 2 million to about 1 million units/annum. Consequently, the home market demand for engineering steels in the form of billet and bar has also reduced by about 50%. Over the same period, there has been a growing demand from the automotive industry for lower cost components which, together with an increasing threat from alternative materials such as castings and composites, has represented a considerable challenge to the steelmaking and forging industries. In response, a new series of medium carbon microalloyed steels has been developed[1,2] with the objective of eliminating the cost of expensive heat treatments to achieve the specified properties. These steels attain the desired properties during controlled air cooling following forging.

A small addition of vanadium (typically 0.1%) to a medium carbon steel produces a 20% increase in tensile strength, Fig. 1, by the formation of a fine dispersion of vanadium carbo-nitride precipitates during air cooling. A German specification, 49MnVS3, was first utilised in the 1970's for this approach but it was apparent that this steel could not match effectively some of the high strength alloy steels used for automotive transmission components. Consequently trials were conducted at Swinden Laboratories on various C-Mn-V steels, which led to the achievement of increased strength levels compared with 49MnVS3. The composition of the new steel is selected from the range shown in Table 1, depending upon the specific properties required, equivalent ruling section and forging conditions. Controlled sulphur ranges are selected, depending on the machinability requirements. The full mechanical property specifications are also shown in Table 1, indicating the higher strength, higher toughness and ductility compared with 49MnVS3. The new steels satisfy the BS 970 280M01 specification and the superior properties compared with SG and austempered cast irons are illustrated in Fig. 2.

Table 1 - Microalloyed Forging Steel

(a) Chemical Composition, Wt. %

| C | Si | Mn | P | S | V |
|---|---|---|---|---|---|
| 0.30/ 0.50 | 0.15/ 0.35 | 1.0/ 1.5 | 0.035 max. | 0.10 max. | 0.04/ 0.20 |

(b) Mechanical Properties

| VANARD Grade | HB | Yield Strength N/mm² | Tensile Strength N/mm² | Charpy El. % | U Notch J |
|---|---|---|---|---|---|
| 850 | 223/277 | >540 | 770-930 | >18 | >20 |
| 925 | 248/302 | >600 | 850-1000 | >16 | >20 |
| 1000 | 269/331 | >650 | 930-1080 | >12 | >15 |
| 1100 | 293/352 | >700 | 1000-1160 | >8 | >10 |
| 49MnVS3 | 240/260 | >500 | 800-900 | >8 | >15 |

This development programme included a detailed evaluation of the effects of chemical composition and processing variables upon microstructure and mechanical properties. A minimum soaking temperature of 1100°C is necessary to realise the full strengthening potential of the vanadium addition. The ductility and toughness of microalloyed steels are improved by reducing the finish forging temperature, consistent with a refinement in the austenite grain size. However, the specified properties can be developed over a wide range of forging temperatures. Increasing the post forging cooling rate generally increases yield and tensile strength, due to grain and precipitate refinement and enhanced dispersion hardening. However, there is an optimum cooling rate, above which the strength is reduced, due to the formation of bainite and the suppression of precipitation. Bin cooling direct from the forge must be eliminated and the forgings should be cooled individually to 600°C, either on a conveyor or on a rack. Some forgers have installed special conveyor systems which have the facility to accelerate or retard the cooling rate as required.

Following the extensive testing of laboratory and production casts, it has been possible to establish rigorous multiple regression relationships between composition, processing conditions and properties. These equations facilitate the selection of the precise chemical composition needed to meet the desired properties and also enable recommendations to be made to the forging industry on the processing conditions that will give the most consistent property response. The excellent correlation between the predicted and measured tensile strength for several as-forged automotive components is shown in Fig. 3. It has also been demonstrated that these air cooled forgings exhibit more consistent properties than conventionally heat treated parts.

Unlike most heat treated carbon and low alloy steels, which soften during repeated loading, microalloyed carbon steels exhibit cyclic strain hardening, as shown in Fig. 4. This effectively compensates for the initial lower yield strength of the air cooled steels.

In addition to achieving the specified mechanical properties, it has also been necessary to satisfy potential users that microalloyed steel forgings can be finished and fabricated without problems. The surface hardening response of air cooled microalloyed steel, with induction hardening and nitriding, has been shown to be quite satisfactory. It has also been demonstrated that the machinability of these steels is at least as good as that of equivalent strength heat treated steels. However, in some instances, it may be necessary to optimise tool geometry and cutting conditions to maximise the benefits.

Because of their lower impact toughness compared with heat treated steels, the initial applications of the high strength microalloyed forging steels were restricted to non-shock loaded components, such as crankshafts and connecting rods. Before being introduced into production vehicle

manufacture, extensive product evaluation and rig testing were conducted to demonstrate that they had acceptable fatigue performance. The new steel is now being used by Austin Rover for the 1.3 litre Metro and Maestro engine crankshafts and by Ford Motor Company for the York diesel engine connecting rods. As confidence in these new materials has grown, trials have also been conducted on more safety-critical steering and suspension parts. Acceptable fatigue properties have been obtained on steering arms, which are now used on the Metro car, wheel spindles, knuckles and hubs. Following successful component fatigue tests, Rolls Royce have approved the use of microalloyed steels for drive couplings. Microalloyed steel steering knuckles have shown more than double the fatigue life of heat treated alloy steel. Front wheel hubs have been subjected to pendulum impact tests at -45°C without inducing fracture. Rear wheel hubs have also been subjected to curb impact testing without fracture occurring, whilst adjacent parts of the suspension were broken or damaged. These practical results clearly indicate the fitness for purpose of air cooled, microalloyed steels for many safety critical applications in the chassis. Other evaluations, which are currently in progress, include steering swivels, lifting arms, track roller shafts and gears.

The fracture toughness of air cooled, microalloyed steels have been determined with values between 50 and 85 MPa $\sqrt{m}$, compared with 80 to 120 MPa $\sqrt{m}$ for heat treated alloy steels. Consequently, the critical crack sizes are smaller than with conventionally heat treated low alloy steels. Therefore each application should be judged on its merits to determine whether these are tolerable.

There is much interest currently in attempts to improve the impact toughness of air cooled microalloyed steels for forging and bar applications. The use of lower finishing temperatures is known to refine the austenite grain size and enhance toughness, although this is often not practicable. Claims have been made that microalloyed steels with bainitic structures offer improved toughness[3,5]. A more cost effective prospect, however, is that offered by a small grain refining addition of titanium, which is best applied to continuously cast steels. Fig. 5 illustrates the improved properties that can be obtained.

Cost savings of up to 25% have been realised through the replacement of heat treated alloy steels by microalloyed steels. The new steels are being produced from continuously cast billet and in some cases, forgings have been manufactured directly from as-cast billet, representing further savings.

The success of this development, which has contributed to the retention and growth of traditional markets for steel forgings, has been dependent upon close collaboration between the steelmaker, forger and automobile manufacturer. The microalloyed steels referred to in this section are being marketed by United Engineering Steels, under the trade name of VANARD.

## HIGH STRENGTH, TOUGH AND WELDABLE FITTINGS AND FLANGES

As described in an earlier paper at this conference, there have been, in recent years, significant developments in the controlled rolling of plate for linepipe, such that much higher strength levels are now regularly specified, e g up to API X65. Until recently, this has not been matched by compatible developments in fittings manufactured from plate, forgings or rolled rings. Therefore, the fittings have been made from lower strength materials and consequently they are larger and heavier than if the strength was equivalent to that of the pipe.

For many years, HYPLUS 29 has been the standard steel for " high strength" fittings. HYPLUS 29 is a 0.22% C max., 1.6% Mn max., 0.2% V max. steel, with a minimum yield strength of 400 N/mm$^2$ in sections up to 60 mm and a minimum Charpy impact energy of 27J at -30°C. This is adequate for many applications but linepipe and fittings are increasingly required to cope with greater demands in terms of the gas/oil being carried, the pressure of operation and the environmental conditions. This has necessitated the development of an improved high strength steel for pipeline fittings. However, the increased strength has to be obtained together with higher impact energy levels at increasingly lower test temperatures and with adequate weldability. These requirements may be summarised as follows:

| | |
|---|---|
| Yield Strength | > 448 N/mm$^2$ |
| Tensile Strength | > 530 N/mm$^2$ |
| Impact Energy | > 50 J @ -46C |
| Section Size | < 150 mm |
| Carbon Equivalent | < 0.45 % |

A new series of low carbon microalloyed steels has been developed[6] to meet these objectives with compositions in the range: 0.10% C max., 1.5% Mn max., 0.015% P max., 0.005% S max., 0.20% Mo max., with additions of Nb and V. Steels within this composition range are also being used to meet the BS-224-490 and LF2 (mod) specifications.

The variation of yield strength with carbon equivalent value in these new CMnMoVNb steels is shown in Fig. 6, for normalised and water quenched and tempered conditions in 50 and 150 mm sections. This enables a composition to be selected for a given application.

The properties produced in a large water quenched and tempered 36 inch weld neck flange from a production cast made to the new analysis are shown in Table 2, with the specimen locations shown in Fig. 7. The end user has conducted a detailed welding assessment on this flange and has obtained satisfactory results with the maximum HAZ hardness of 279 HV.

Table 2 - Mechanical Properties of X65 Flange
(a) Tensile Results

| Direction | Position | 0.2% Proof Stress | Tensile Strength N/mm$^2$ | El. % | R of A % |
|---|---|---|---|---|---|
| Tangential | AT7 | 447 | 589 | 29 | 72 |
| | AT8 | 453 | 584 | 29 | 72 |
| | BT7 | 454 | 591 | 28 | 70 |
| | BT8 | 446 | 578 | 28 | 74 |
| | CT7 | 450 | 589 | 29 | 73 |
| | CT8 | 442 | 576 | 29 | 74 |
| Radial | AR | 473 | 607 | 26 | 68 |
| | AR1 | 497 | 622 | 23 | 69 |
| Axial | DX4 | 444 | 585 | 23 | 55 |
| | DX5 | 440 | 583 | 25 | 65 |
| Tangential Weld Neck | DT9 | 571 | 680 | 24 | 74 |
| Test Bar Longitudinal | | 525 | 642 | 24 | 73 |

(b) Charpy Impact Results

| Direction | Position | Impact Energy at 0°C J |
|---|---|---|
| Tangential | AT1 | 162 |
| | AT2 | 167 |
| | AT3 | 161 |
| | AT4 | 170 |
| | AT5 | 166 |
| | AT6 | 202 |
| | BT1 | 185 |
| | BT2 | 150 |
| | BT3 | 162 |
| | BT4 | 165 |
| | BT5 | 162 |
| | BT6 | 172 |
| | CT1 | 178 |
| | CT2 | 169 |
| | CT3 | 186 |
| | CT4 | 220 |
| | CT5 | 168 |
| | CT6 | 204 |
| Radial | AR1 | 120 118 60 |
| | AR2 | 118 100 90 |
| | AR3 | 90 65 91 |
| Axial | DX1 | 112 |
| | DX2 | 54 |
| | DX3 | 111 |

Excellent toughness values were obtained in the HAZ of welded fittings in the CMnVNb steel, as shown in Table 3.

Table 3 - Toughness of Welded and Stress Relieved Joint in New BS-224-490 Microalloyed Steel Forging

| Location | ImpactEnergy Charpy at 30°C J |
|---|---|
| Weld | 132 |
| Fusion line | 122 |
| Fusion line + 1 mm (plate) | 118 |
| Fusion line + 4 mm (plate) | 157 |
| Fusion line + 1 mm (forging) | 271 |
| Fusion line + 4 mm (forging) | 266 |
| Plate | 166 |
| Forging | 264 |

Acceptable results have also been obtained in HIC tests conducted in BP and NACE solutions.

It is axiomatic that the lighter, smaller section fittings, that can be designed in these higher strength steels, will also assist in the achievement of a good combination of properties from as lean a composition as possible. For instance, in 50 mm sections, the CMnMoVNb steel is capable of achieving X75 properties, in the water quenched and tempered condition.

Various organisations are tending to devise individual specifications for high strength fittings. These involve different restrictions on the main alloy and microalloying additions. These often appear to be quite arbitrary and the diversity of approach increases markedly the amount of development and product validation work required. Greater rationalisation of steel specifications would benefit both the steelmaker and end user and facilitate the development of steels for even more demanding applications.

There is a growing requirement for the steelmaker to "guarantee" acceptable properties in his product after forging, heat treatment, welding and post-weld stress relief. There is, therefore, a need for continuing collaboration between steelmaker, forger, fabricator and the end user on the preparation of the most appropriate and relevant specifications for high stregth, tough and weldable steels such that the maximum benefits can be gained from these new microalloyed steels.

## HIGH STRENGTH STEEL STRIP

The demand for higher strength low alloy (HSLA) steel strip, particularly in the automotive industry, has increased steadily over the past two decades. Down gauging becomes possible (provided stiffness is not a limiting factor), and the weight of components is reduced, leading to lighter vehicles, reduced pay load and improved fuel consumption. In addition, more stringent safety requirements for vehicles may be met more economically by using higher strength strip. However, in general, increasing strength leads to a reduction in formability/ductility and this has put pressure on the steel producer to improve the formability of high strength steels. Furthermore, the increasing complexity of design of components has necessitated tighter gauge tolerances and greater consistency of mechanical properties, particularly yield strength to control springback. Springback control together with ease of weldability is required to facilitate production or assembly of components in fully automated processes.

The principal strengthening mechanisms utilised in strip are:

- increasing carbon content - this has a very adverse effect on formability and weldability.
- grain refinement, through microalloying additions of niobium or titanium and control of soaking temperature, finish rolling temperature and cooling rate.
- solid solution strengthening, by phosphorus, nitrogen, silicon or manganese - used mainly in cold rolled gauges.
- transformation strengthening by the evolution of acicular ferrite, bainite or dual phase structures.
- dislocation strengthening by cold work, e.g. temper rolling, after annealing cold rolled strip. Partial annealing of cold rolled strip to develop a recovered structure also offers the potential of reasonable strength and formability.
- precipitation strengthening by vanadium, titanium or niobium. These elements are every effective in combination with the control of the rolling parameters, in providing a capability of a wide range of strengths in strip products.
- 'bake hardening', by strain ageing of the cold formed part during the stove painting process (at ~180°C). A bake hardening steel has the advantage of a relatively low strength ($<200$ N/mm$^2$) in the as-received condition, only achieving the desired strength in the finished component. However, the strength attainable is quite low, e.g. $<255$ N/mm$^2$.

The British Steel Corporation offers high strength steels, in wide and narrow strip form, under the trade names of Tenform and HYPRESS[7], respectively. The properties of these steels are summarised in Table 4.

Table 4 - Properties of BSC High Strength Steel Strip

| Grade | Minimum Yield Strength N/mm² | Minimum Tensile Strength N/mm² | Minimum Elongation % (50 mm GL) |
|---|---|---|---|
| Hot Rolled | | | |
| HYPRESS 20 | 300 | 400 | 28 |
| HYPRESS 23 | 350 | 430 | 25 |
| HYPRESS 26 | 400 | 460 | 22 |
| HYPRESS 29 | 450 | 510 | 21 |
| HYPRESS 35 | 550 | 600 | 17 |
| HYPRESS 40 | 620 | 680 | 18 |
| HYPRESS 45 | 700 | 750 | 15 |
| Mild Steel (HS4) | 170 | 280 | 25 |
| TENFORM XK300 | 300 | 400 | 26 |
| TENFORM XK350 | 350 | 430 | 23 |
| TENFORM XK400 | 400 | 460 | 20 |
| TENFORM XK450 | 450 | 500 | 20 |
| TENFORM XK300 | 300 | 400 | 28 |
| TENFORM XF350 | 350 | 430 | 25 |
| TENFORM XF450 | 450 | 500 | 22 |
| Cold Rolled | | | |
| HYPRESS 20 | 300 | 400 | 28 |
| HYPRESS 23 | 350 | 430 | 25 |
| HYPRESS 26 | 400 | 460 | 22 |
| HYPRESS 29 | 450 | 510 | 21 |
| TENFORM XJ300 | 300 | 400 | 24 |
| TENFORM XJ350 | 350 | 430 | 22 |
| TENFORM PK255 | 255 | 360 | 28 |
| TENFORM PK270 | 270 | 400 | 28 |

Formability is a particularly important parameter in the use of HSLA strip and the inclusion content of the steel has a major effect on the cold forming properties. This is illustrated in Fig. 8, which shows the effect of sulphur content on the hole expansion characteristics. In modern steelmaking practices, sulphur contents as low as 0.005% are achieved quite readily. However, even at this sulphur level, it may be necessary to add sulphide globularising agents, such as calcium, in order to reduce the adverse effect of elongated sulphides and maximise the formability of the steel.

There is currently interest in the use of CMn steel strip, produced under carefully controlled rolling, cooling and coiling conditions, for car wheel applications. Typical yield and tensile strength levels are 360 and 550 N/mm² respectively. These steels offer superior fatigue properties to mild steel and, as shown in Fig. 9, better formability than equivalent strength microalloyed steel.

HSLA steel strip finds extensive application in motor cars and trucks and examples include:

wheels, bumpers, brackets, clutch and brake parts, seat frames and slides, chassis and side frame members, suspension parts, roll over protection sections, door frames and hinges and other structural parts.

HSLA steels are also used in the construction industry for various cold formed sections for buildings, scaffolding parts and storage racks.

The rephosphorised, cold rolled steels are used for bonnets, boots, tailgates, dashboards, doors, sills, floors and underbody. Automotive manufacturers would prefer to produce many of these components from bake hardening steels, particularly the outer body parts where fidelity of form is more important. This is perceived to be the major growth opportunity for HSLA steels, which will probably also involve single sided electrozinc coating treatment.

Dual phase steels, which offer high strength levels and good stretch formability appear now to have a fairly limited range of practical applications in view of their high cost.

Depending on design, gauge reductions of up to 25% can be achieved by using high strength steels in place of mild steel. However, for many body applications, modulus is the limiting design feature and in these circumstances, down gauging must be accompanied by the use of appropriate stiffening features.

Component designers are seeking to predict the life of components from a knowledge of the loading spectrum and material properties, based on cyclic stress/strain and strain controlled fatigue data. There was a concern that the high strain fatigue resistance was inversely proportional to strength being related to the reduction in ductility. Fig.10 confirms that the elastic limit is proportional to strength (0.5xTS) and that the plastic fatigue properties are unaffected by strength. This should give added impetus to the adoption of higher strength steels for the construction of cars, trucks and highway vehicles.

HSLA steel strip can be adhesively bonded or welded readily, provided that the appropriate strength adhesives or consumable is used. Higher electrode forces and longer times are required for spot welding. Excessive localised heating should be avoided to prevent softening occurring in the HAZ.

## GAS CYLINDERS

High pressure gas containers are used in diverse applications, ranging from heavy industry, health care to sub-aqua diving. The need to maintain high standards of cylinder safety is paramount but there is also a requirement for the industrial gas companies to ensure high efficiency, cost effectiveness and convenience. Over the past 50 years, there has been a progressive improvement in the efficiency of seamless, steel cylinders, as shown in Fig. 12[8]. For instance, a 50 litre water capacity cylinder that would have weighed 210 kg in 1920 now weighs only 60 kg. The major changes have been accomplished through the use of more highly alloyed, higher strength steels, as shown in Table 5.

Table 5 - The Composition, Heat Treatment and Mechanical Properties of Seamless Steel Gas Cylinders

(a) Chemical Composition, Wt. %

| Steel | C | Si | Mn | P | S | Cr | Mo | Ni |
|---|---|---|---|---|---|---|---|---|
| Low C | 0.15-0.25 | 0.05-0.35 | 0.4-0.9 | 0.05 max. | 0.05 max. | | | |
| High C | 0.35-0.45 | 0.05-0.35 | 0.6-1.0 | 0.05 max. | 0.05 max. | | | |
| C-Mn | 0.40 max. | 0.10-0.35 | 1.3-1.7 | 0.05 max. | 0.05 max. | | | |
| Cr-Mo | 0.37 max. | 0.10-0.35 | 0.4-0.9 | 0.05 max. | 0.05 max. | 0.8-1.2 | 0.15-0.25 | 0.50 max. |

(b) Mechanical Properties

| Steel | Heat Treatment | Yield Stress* N/mm² | Tensile Stress N/mm² | El. % |
|---|---|---|---|---|
| Low C | N or N + T | 250 | 430-510 | 22 |
| High C | N or N + T | 310 | 570-680 | 19 |
| C-Mn | N or N + T | 445 | 650-760 | 20 |
| | Q + T | 755 | 890-1030 | 14 |
| Cr-Mo | Q + T | 755 | 890-1030 | 14 |

N - normalised
Q - quenched
T - tempered
* - max. design value
- min. actual value

Another way of improving the efficiency of gas cylinders is to increase the ratio of the stress (pressure) in the container to the strength of the material. Throughout the world there exists a vast number of specifications, standards and regulations for the design and manufacture of seamless cylinders and for the transportation of their contents. Recently, an international specification, ISO 4705, has been agreed and EEC directives relating to seamless and welded steel cylinders and seamless aluminium cylinders became effective.

Different design formulae are adopted in different countries to calculate the cylinder wall thickness from the operating or test pressure, yield strength, and cylinder diameter. A safety factor is also built into these relationships, expressed as a fraction of the yield strength. There is considerable debate about the value of this safety factor. Clearly the higher the factor, the thinner the wall but the lower the apparent safety margin. The cylinder wall is the thinnest region in the vessel and hence the most highly stressed. A cylinder, if it is to burst ( e.g. in an extreme fire), will normally rupture in the parallel portion. However, high stresses can be generated near the knuckle region, at the transition from the wall to the concave base. Recent advances in the use of finite element analysis techniques have led to the development of cylinders in which such stress concentrations are minimised.

It is anticipated that the trend to increased efficiency (i.e. gas carried per unit weight) of cylinders will continue. This will require even higher strength steel but without risk of catastrophic failure. Therefore such a development will entail a consideration of the factors governing the safe performance of gas containers - e.g. should a failure occur, it is desirable that the container should depressurise safely by a leak rather than by a burst. Attention is therefore focused on the role of defects in possible failures. A fracture mechanics philosophy is being adopted to identify steel compositions, heat treatments and design criteria that will provide the basis for a more efficient and safe gas container.

Work in the U.K., as part of a Government sponsored project[9], has been addressing itself to this issue. Arising from this project, it is likely that recommendations will be made to revise the appropriate British Standard (BS 5045) to allow a higher minimum yield strength, together with a higher design stress/yield stress ratio. Compared with BS 5045/1/1982, these steps should provide a very significant increase in efficiency.

One way to increase the strength of the heat treated, low alloy Cr-Mo steel used for gas cylinders is to adopt a lower tempering temperature. However, this will result in a reduction in toughness. An alternative approach is to use a more highly alloyed steel with a better tempering resistance, such that a higher strength can be obtained at conventional tempering temperatures, without loss of ductility and toughness. In order to assess whether the properties obtained by such practices are acceptable, prototype cylinders were produced initially in the conventional alloy steel, varying the strength levels by adjusting the tempering temperature. These were subjected to a comprehensive property and microstructural evaluation, which included fatigue and burst tests with and without the presence of artificial defects. Fracture toughness tests were also conducted and several models were formulated to predict the failure modes.

One of these models considers the failure of thin walled pressure vessels by both plastic instability and fracture. "Leak and Arrest" occurs when the failure hoop stress is equal to the part-through tensile instability stress. "Leak and Propagate" occurs when the critical stress of a through-wall crack is exceeded and propagation occurs. "Burst" occurs when the critical fracture stress of a part-through crack is exceeded and failure occurs without prior leakage. It is necessary in such an analysis to apply a correction to the hoop stress for both part-through and through-thickness defects due to bulging. The relevant stress ratios have been computed for different defect sizes (Depth D and Length L), expressed as a proportion of the wall thickness (t) and the boundaries between "Burst", "Leak and Arrest" and "Leak and Propagate" behaviour for four strength levels, achieved by varying the tempering temperature of a standard steel, are shown in Fig. 12. It is clear that only at the highest strength level examined in this work are burst type fractures likely. This was confirmed in the practical trials on the test cylinders.

The use of microalloy additions, such as vanadium, to increase the strength has been proposed[10] and it was also suggested that low sulphur contents and sulphide modification are necessary in order to achieve acceptable toughness at tensile strength levels in excess of 1030 N/mm². A series of laboratory casts has been produced by BSC to examine various options, including higher molybdenum and silicon contents and a vanadium addition. These have been processed to simulate gas cylinder production with the intention of achieving a minimum yield strength of 950 N/mm² in the quenched and tempered condition. The results of tensile and impact tests on these steels are given in Table 6.

Table 6 - Properties of Alternative High Strength Steels for Gas Cylinders

| Steel | 0.2% Proof Stress N/mm² | Tensile Strength N/mm² | El. % | R of A % | Charpy at -60°C J |
|---|---|---|---|---|---|
| 1% Cr-0.2% Mo (standard) | 788 | 909 | 20 | 70 | 133 |
| Standard | 851 | 951 | 18 | 68 | 104 |
| 1% Cr-0.35% Mo | 996 | 1093 | 18 | 67 | 104 |
| 1% Cr-0.2% Mo-0.1% V | 965 | 1032 | 17 | 63 | 59 |
| 1% Cr-0.2% Mo-1.0% Si | 985 | 1095 | 20 | 63 | 51 |

Certain disadvantages are noted with respect to the vanadium treated steels and the best strength - toughness relationships are obtained in the Cr-Mo steels. Further trials are being conducted on cylinders made from some of these alternative compositions to improve further the efficiency of gas containers, either by increasing the pressure of the gas and/or reducing the wall thickness.

This development demonstrates that through the co-ordinated approach of designers, steelmakers and component manufacturers, very significant advances can be made in material utilisation, reduced costs and ease of gas handling, through the use of high strength steel.

## SUMMARY

This paper has highlighted several applications of high strength steels where benefits have accrued through weight and/or cost reduction. These developments, most of which have involved microalloying additions, have all provided a metallurgical challenge with the need to maintain toughness, ductility, formability and weldability at an increased strength level. Many of these requirements have only been attainable with the advent of modern steelmaking practices and the production of low sulphur, clean steels with close chemistry control, controlled processing and consistent properties. The new high strength steels have provided economic benefits, ease of fabrication, reduced operating costs, improved safety standards and more efficient material utilisation. These developments have also helped to preserve and expand the market for steel against increasing pressure from competing materials.

The full potential of high strength steels is only realisable when there is close collaboration between steelmaker, component manufacturer, fabricator, designer and end user, with appropriate design modification and optimisation.

Further development and application of high strength steels will also depend to some extent on continuing capital investment in modern steel plant, e.g. accelerated cooling for plates, controlled rolling for bar products, continuous annealing for strip and also controlled processing facilities in the forge.

## ACKNOWLEDGEMENTS

The author wishes to thank Dr. R. Baker, Director of Research and Development, BSC for permission to publish this paper and his colleagues at Swinden Laboratories for input material for this paper

## REFERENCES

1. Thewlis, G. and Naylor, D.J., 'Advances in the Physical Metallurgy and Application of Steel', The Metals Society, Book 284, 1982, 863.
2. Reeder, A., Vasey, C.G., and Naylor, D.J., 'Fundamentals of Microalloying Forging Steel', AIME, 1987, 217.
3. Heitmann, W.E. and Babu, P.B., ibid, 55.
4. Tither, G., Cameron, T.B and Diesberg, D.E., ibid, 269.
5. Hara, H. and Kobayashi, M., Institute of Metals - Vanitec Award Paper 1987.
6. Thewlis, G., Vasey, C.G. and Naylor, D.J.. Third International Conference on 'Welding and Performance of Pipelines', Welding Institute, London, 1986, paper 15.
7. Edmonds, C., Balliger, N., White, B. and Welburn, R.W., IAVD Congress, 1984.
8. Irani, R.S., Metals & Materials, 1987, 3, (6),333
9. Irani, R.S. and Oldfield, F.K., Pressurised Transport Containers, I. Mech. E., April, 1985.
10. Rana, M.D. and Selines, R.J., European Patent, 1987, 0126461.
11. Kunishige, K. and Nagao, N., Sumitomo Search, 1985, 31, 53.

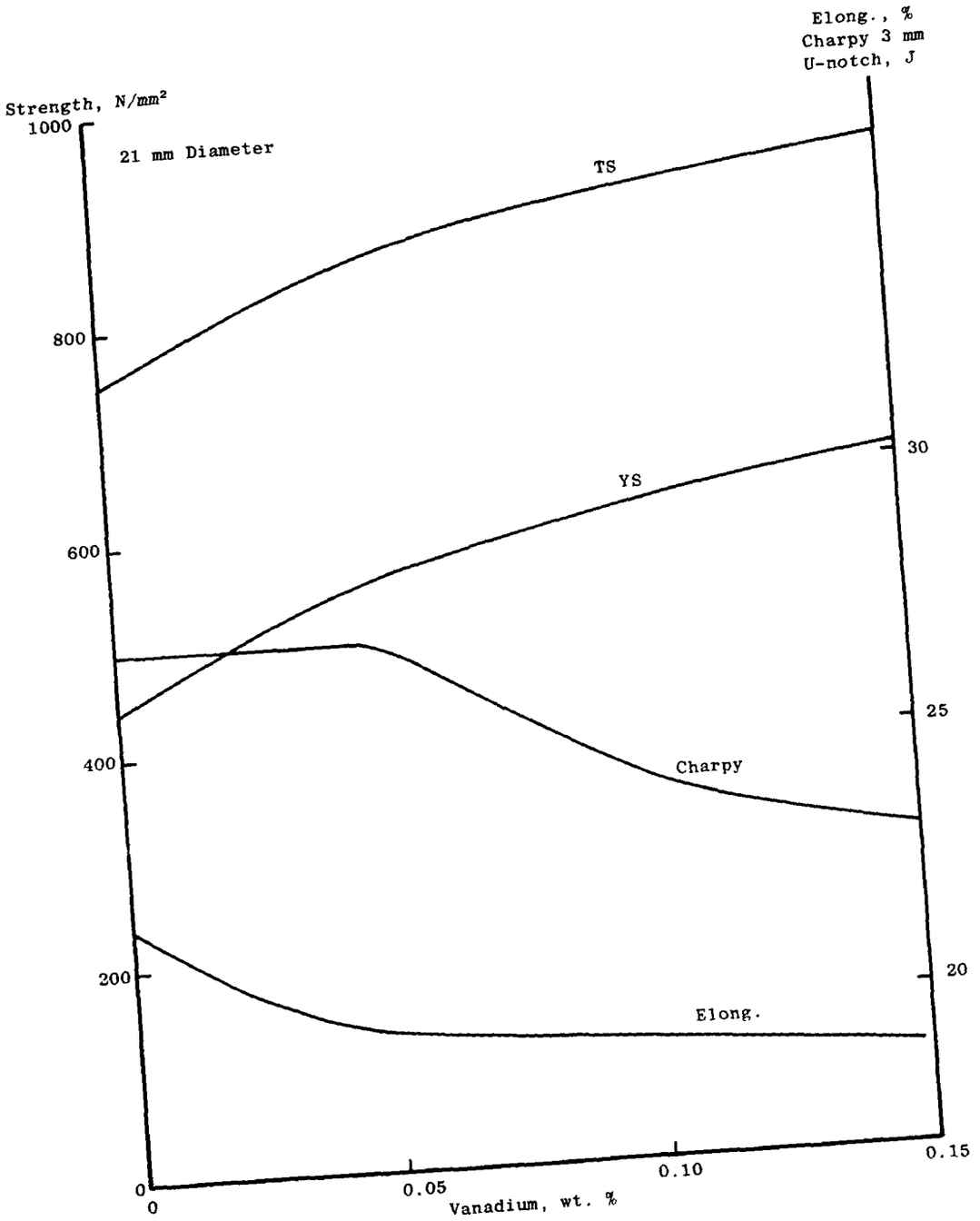


Fig. 1 - Effect of vanadium on strength, ductility and toughness of air cooled 0.45% C, 0.9% Mn steel

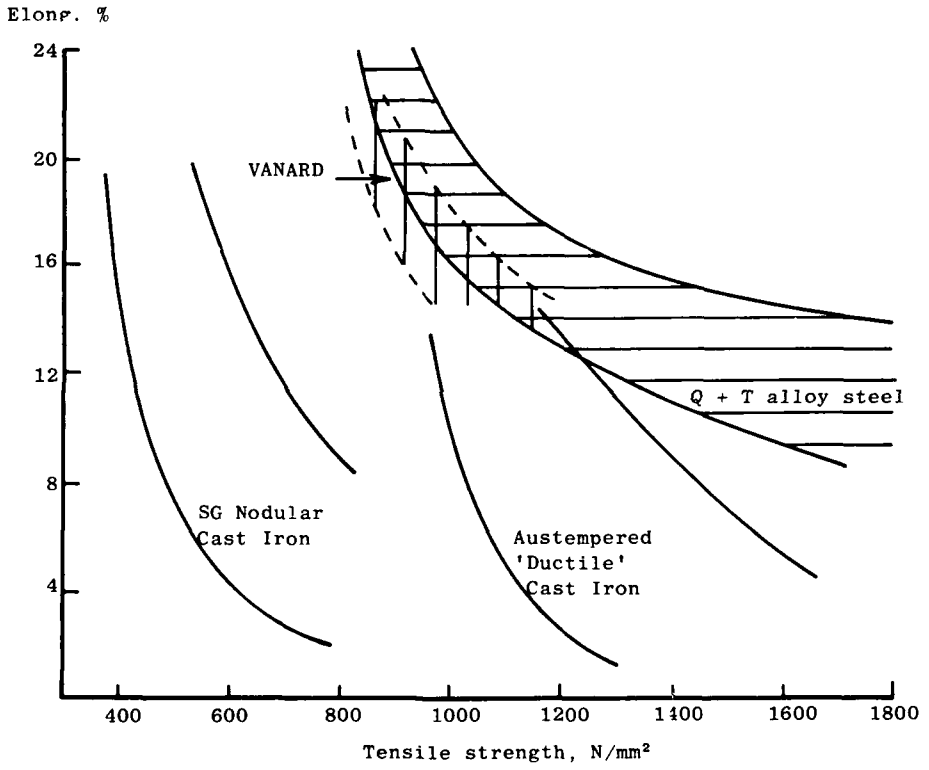


Fig. 2 - Comparison of properties for steel and cast iron

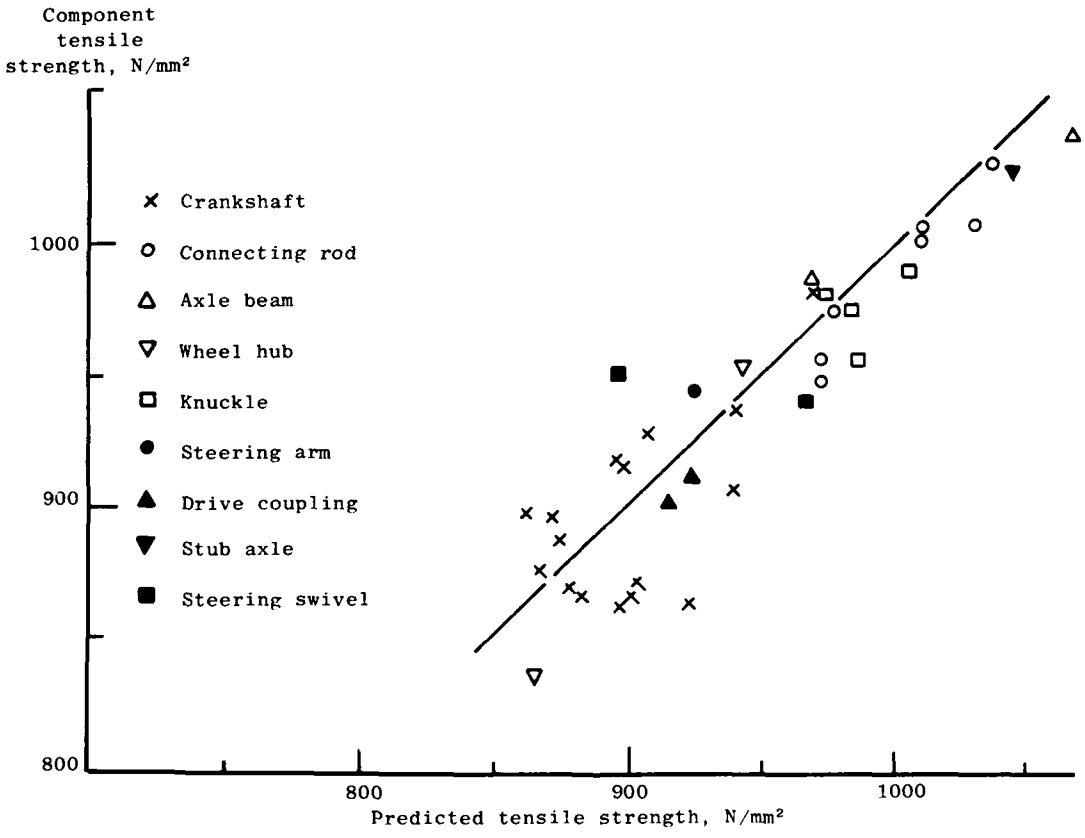


Fig. 3 - Comparison of actual and predicted properties of microalloyed steel forgings

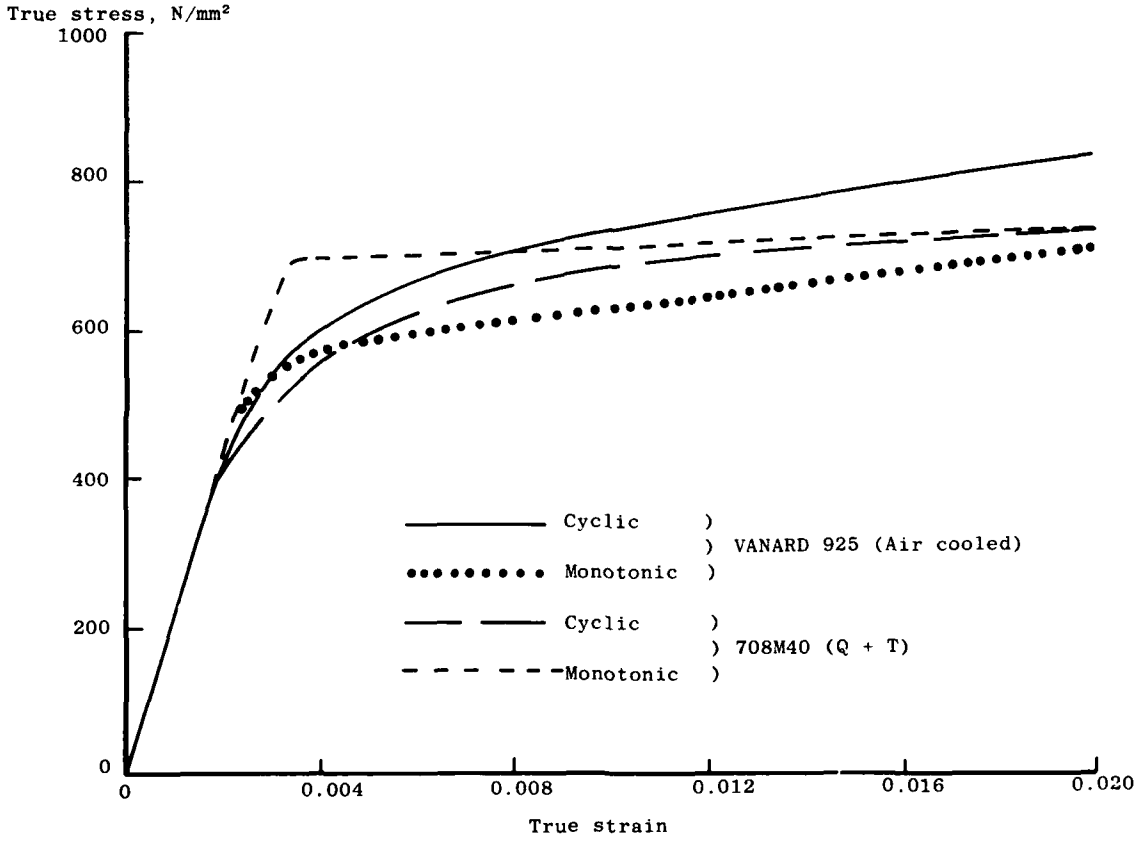


Fig. 4 - Comparison of monotonic and cyclic properties for VANARD 925

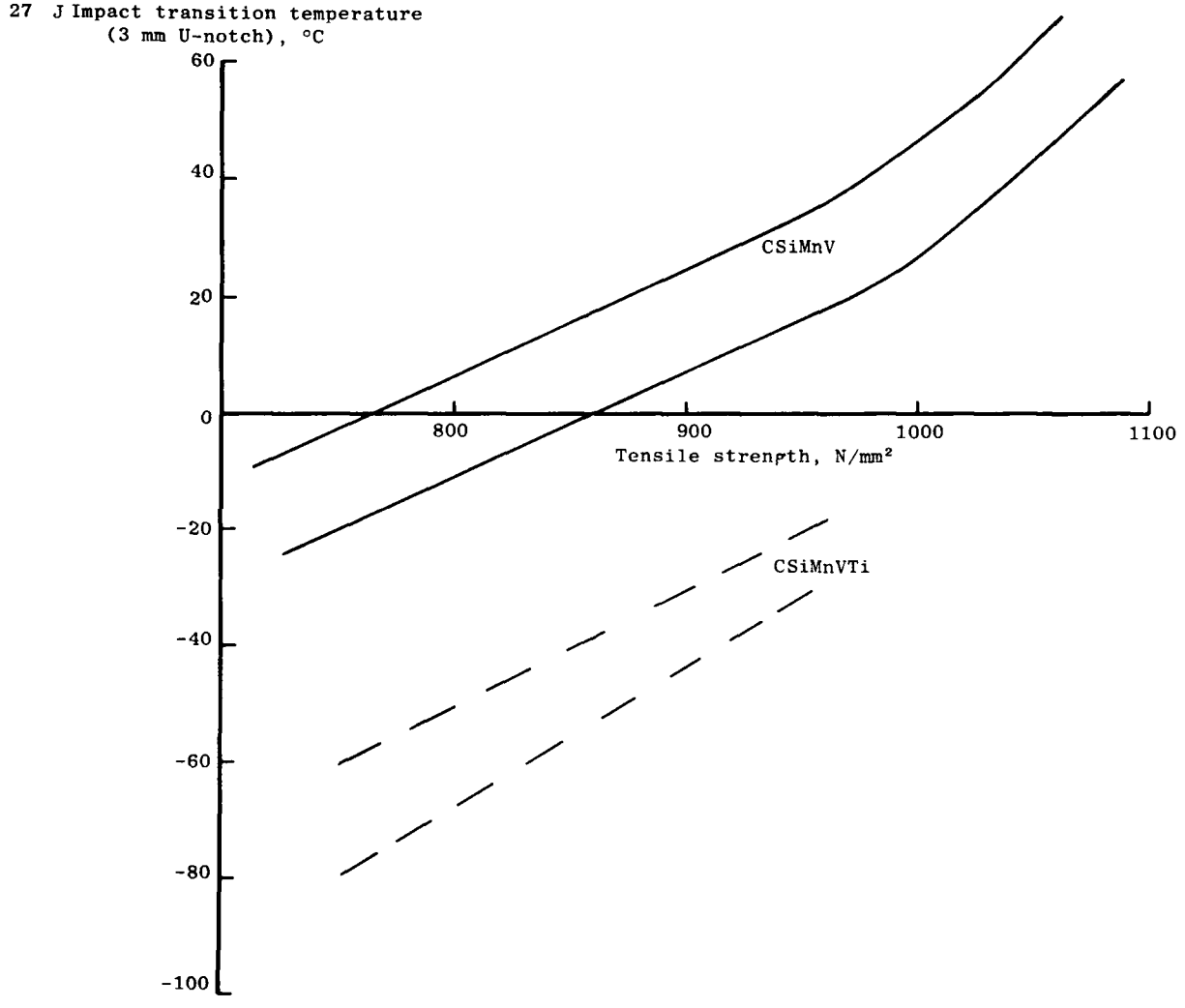


Fig. 5 - Improved toughness in titanium treated air cooled microalloyed steels

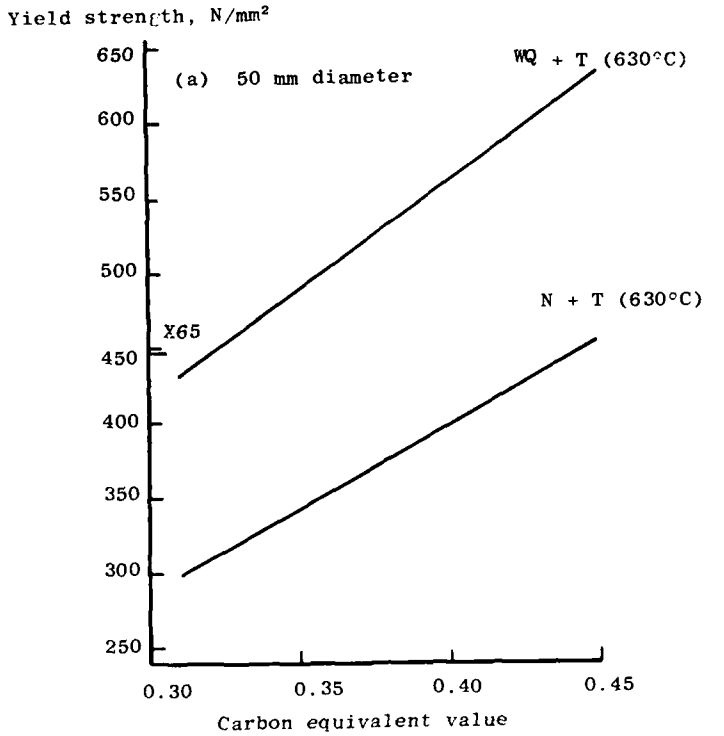


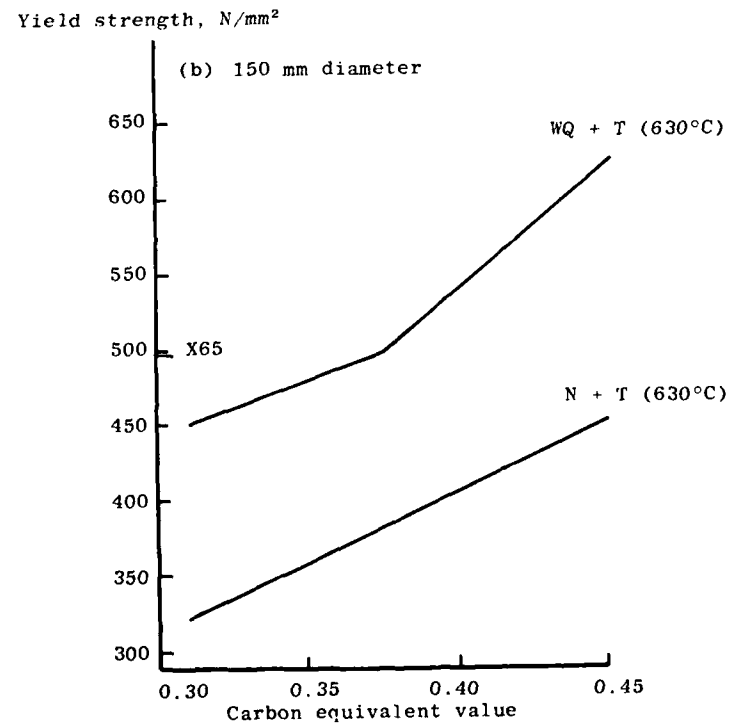


Fig. 6 - Effect of composition on yield strength of CMnMoVNb steels

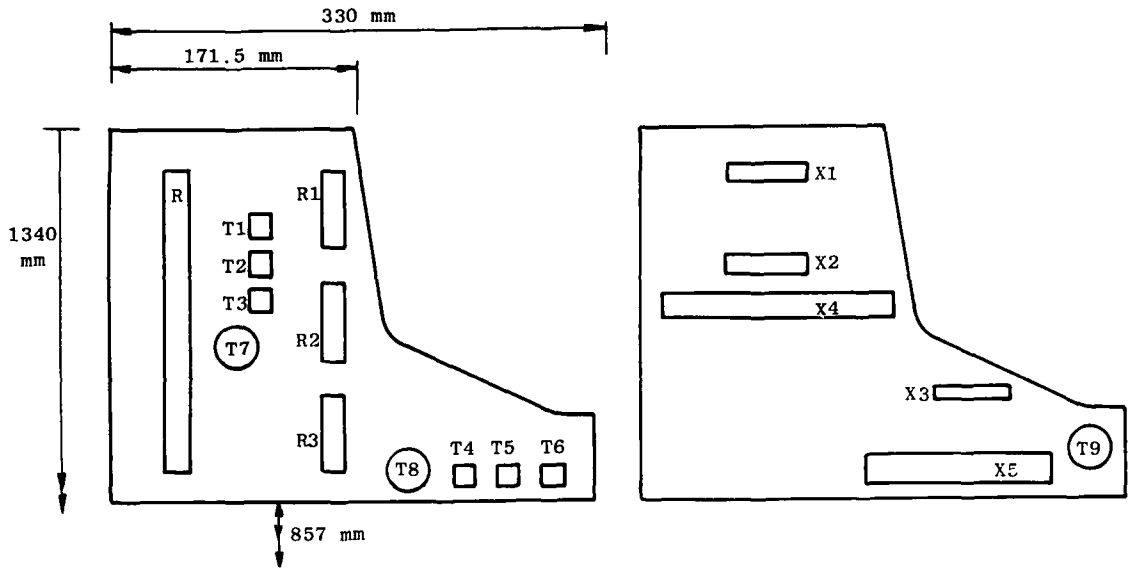


Fig. 7 - Test piece location in X65 flange

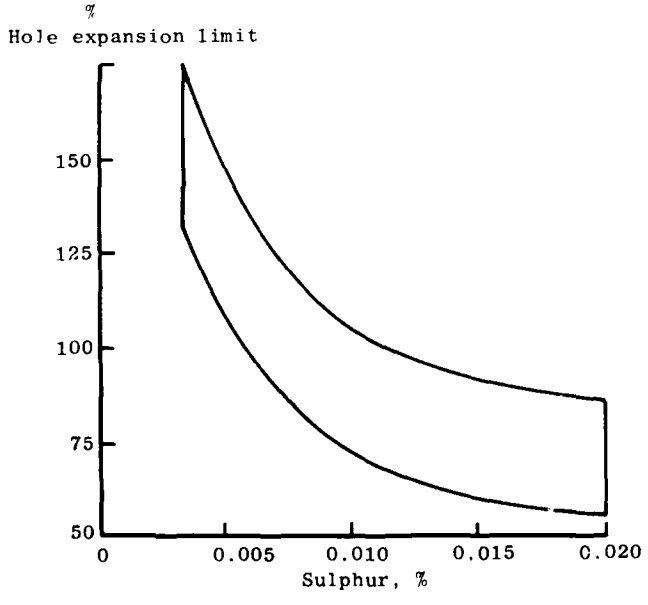


Fig.8 - Effect of sulphur content on the hole expansion properties of high strength steel strip

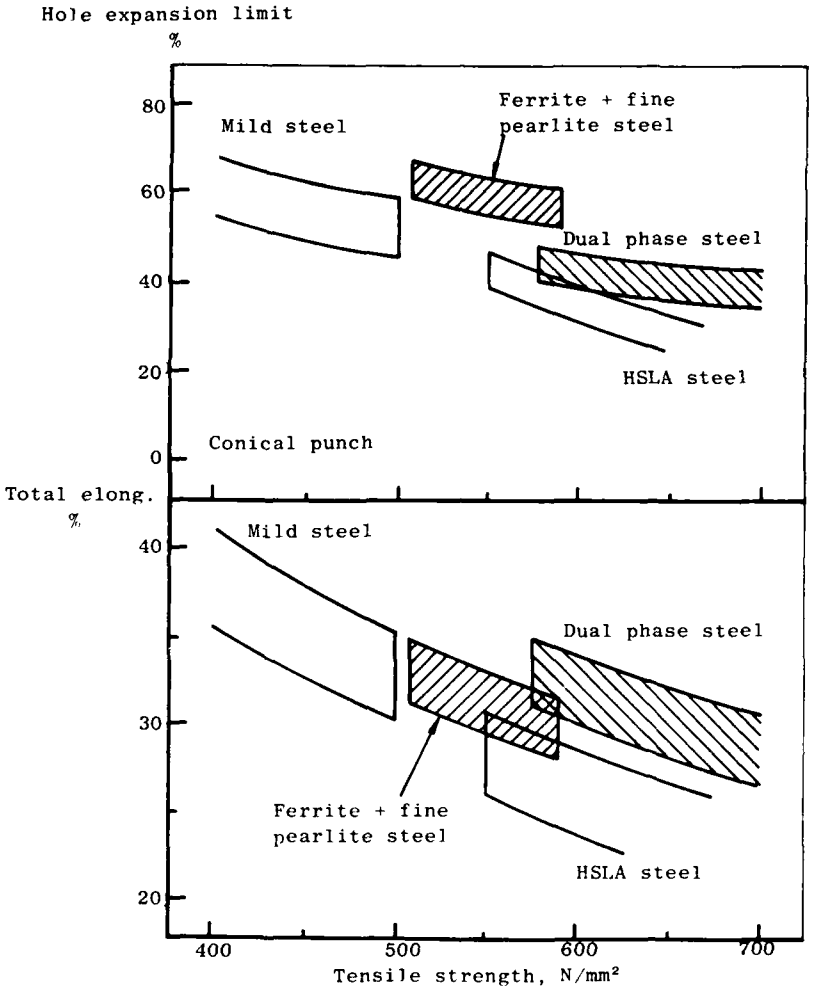


Fig. 9 - Formability of mild and HSLA steels[11]

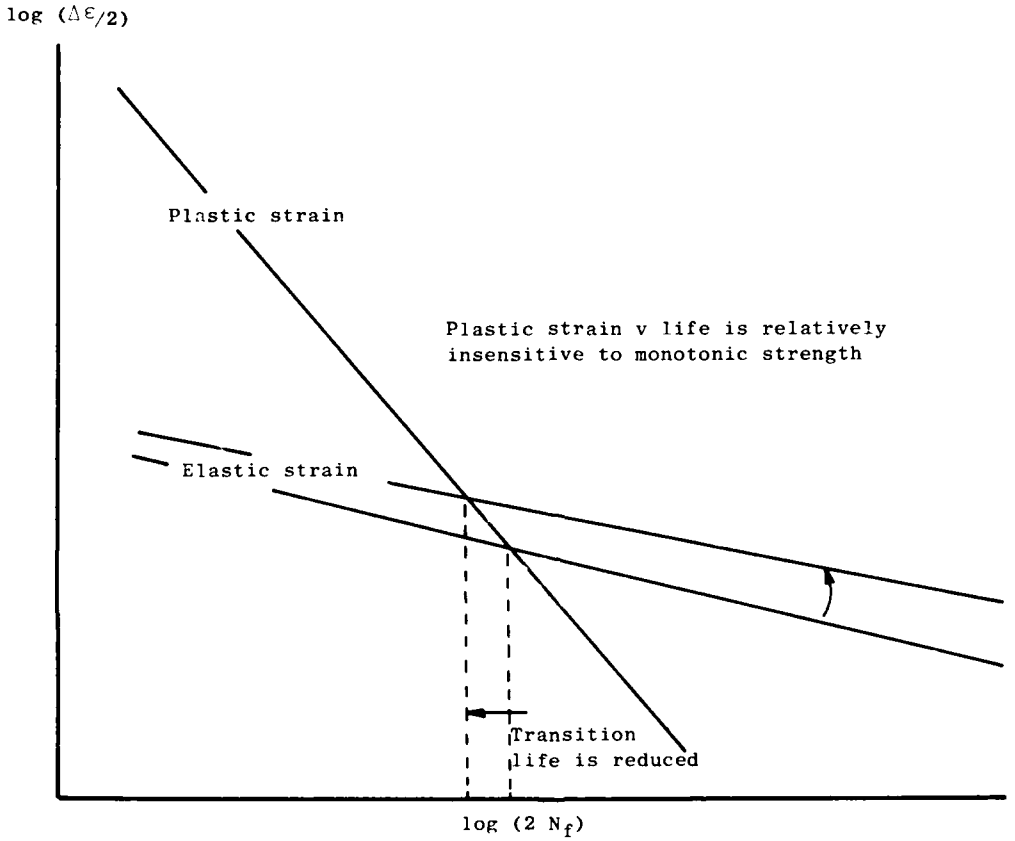


Fig. 10 - Effects of strength level on the strain-life properties of strip steels (Schematic)

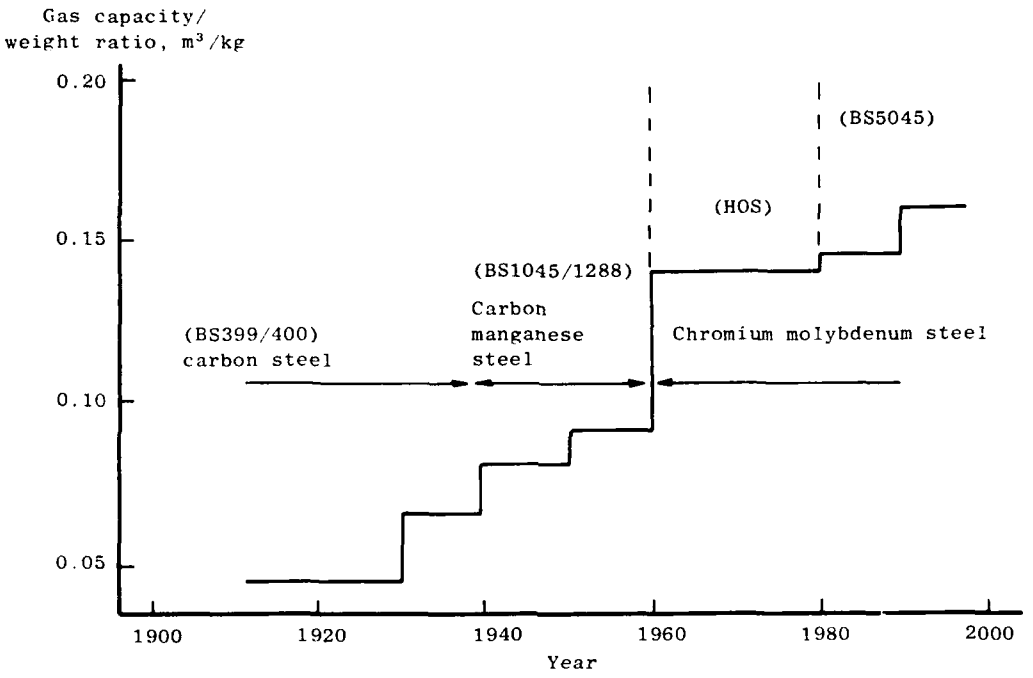


Fig. 11 - Progressive changes in the efficiency of seamless steel cylinders in the United Kingdom

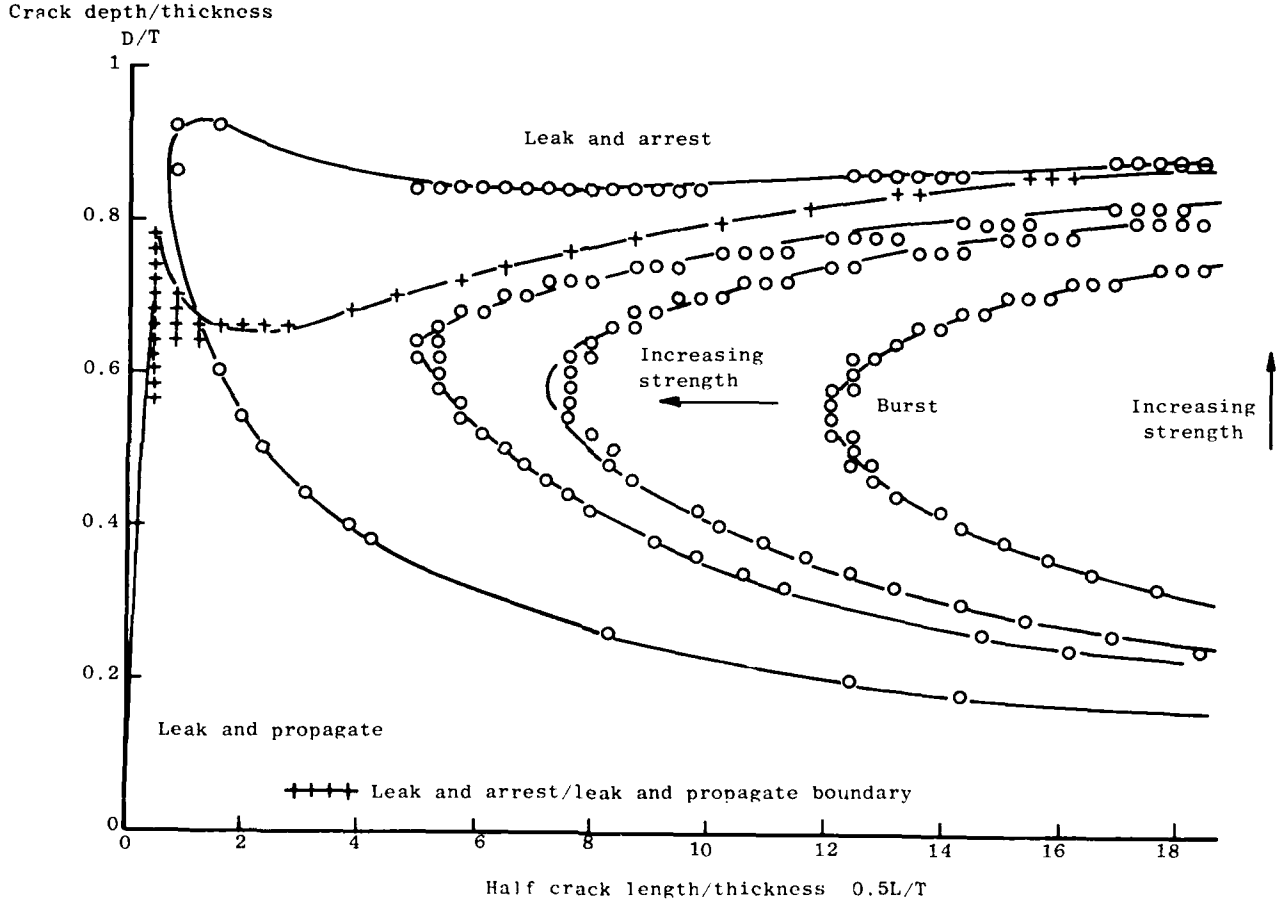


Fig. 12 - For prediction of failure mode in seamless gas cylinders at difference strength levels

# ALLOY DESIGN OPTIONS AND COMPOSITIONAL TRENDS FOR HLSA LINE PIPE

**J. Malcolm Gray**
Microalloying International, Inc.
Houston, Texas, USA

"ABSTRACT"

Compositional and manufacturing trends for high strength linepipe are reviewed.
Current technology reflects the evolutions in steelmaking, thermo-mechanical and alloy design that have occurred during the last thirty years. All steels are low in interstitials, namely nitrogen and carbon, and have impressive reductions in impurities achieved through ladle metallurgy. Inclusion shape control is widely practiced such that the steels have excellent notch toughness and resistance to $H_2S$ degradadation.
Carbon equivalents for the higher strength grades such as X-80 are at very low levels not considered feasible as recently as ten years ago. The resulting low HAZ hardnesses ensures high resistance to hydrogen assisted cold cracking and degradation by SSC mechanisms.

THE METALLURGY OF LINEPIPE STEELS has evolved since 1959 when microalloyed (HSLA) steels were first introduced into the pipelining arena.

The incentive for adopting microalloyed steels related to their improved weldability when compared with steels based on traditional high carbon-manganese formulations. In retrospect the steels were still very crude, being semi-killed and having impurity levels of sulfur and phosphorus around 0.025 percent which were typical of steelmaking and refining technology at that time.

Nevertheless the steels were enthusiastically received and the momentum led to their wide widespread adoption. In the ensuing thirty years the steels have evolved from their utiliutilitarian beginning to become sophisticated engineering materials that feature prominently in the major oil and gas arteries that span the continents as well as in offshore platforms, undersea pipelines and in other infrastructure related to petrocarbon recovery.

The rate of development of microalloyed steels has been stimulated by end user demands for higher strengths but more importantly by the need to simultaneously improve other properties that affect the integrity of the completed pipeline. The focus on specific properties has rotated with time as different priorities emerged with each major projects and with escalation of safety requirements imposed by regulating bodies.

End user demands and influences are summarized in the tabulation below:

- o Higher Strengths.
- o Better toughness at low temperatures (-60°C).
- o Improved weldability - Lower hardnesses and resistance to cold cracking.
- o Resistance to sour hydrocarbons.
- o Resistance to "frost heave" in permafrost conditions.
- o Improved ductile fracture resistance.
- o Economic pressures leading to demand for steel formulations and manufacturing routes that maintain the economics of microalloyed linepipe.

This exacting environment produced a fertile arena for applying microalloying concepts, and steelmakers and pipe manufacturers responded by developing new technologies such as those listed below:

- o Better steelmaking - Lower carbon and nitrogen contents and improved compositional control.

- o Advanced continuous casting practices-uniform cooling and in line (soft) reduction.
- o Ladle metallurgy. Lower gas contents and impurity levels and inclusion shape control treatments.
- o Thermomechanical processing.
- o Accelerated cooling after rolling.
- o Improved seam welding technology.

Linepipe manufacture is the most internationalized segment of the steel industry and all major producers with the exception of those in the Soviet Union are net exporters of product. Naturally the rate of technology development was not uniform and in the early 1970's Japanese, German, French and Italian mills assumed the ascendancy; all stimulated by heavy demand for advanced linepipe for Soviet and Middle Eastern construction.

During this conference we shall hear reports by several manufacturers who will describe the current state-of-the-art concerning linepipe manufacture and HSLA metallurgy. Internationalization of the industry created a very competitive market place as the New Industrialized Countries (NIC's) entered the picture. This and the vast centralized purchasing power of the Soviet Union has led to continuing cost pressures while specifications have advanced or become more sophisticated. The need to contain the costs of new projects in the Arctic and the introduction of novel design concepts will perpetuate this tendency.

While there will always be a hierarchy governing the technical capability of producers it is important to note that today international standards and expectations are generally at a uniformly high level. The state of development in the NIC's is described in the paper being presented by Bordignon at this conference. (1).

Historically the gas transmission pipeline industry has been based on straight-seam submerged arc welded linepipe but considerable progress has been made in adopting spiral seam product and in extending the ERW manufacturing technique to larger sizes. (2). Both of these products have been used extensively in critical applications in offshore lines and in other environmentally sensitive situations.

The organizers of this conference have asked us to prepare a review of metallurgical trends that have prevailed in the pipelining environment described above, and have further requested that the speakers adopt a tutorial approach in the presentation of their data.

## METALLURGICAL DEVELOPMENTS

The first microalloyed steels used in pipelines had a yield strength of 52 ksi (363 MPa) (X-52) (1). Today the predominant strength levels used for onshore pipelines are 60 to 70 ksi (420 to 489 MPa) (X-60 to X-70) with a move to X-80 appearing imminent. However existing technology could probably accommodate requests for X-100 linepipe (3) if the engineering and cost benefits can be verified and fears of increased susceptibility to stress corrosion cracking can be diffused. For offshore pipelines it is normal to use X-60 or X-65 Grade linepipe particularly if sour hydrocarbons are present. Higher strengths and thinner walls increase negative buoyancy which adds to the costs of installing the lines.

The demand for higher strengths and simultaneous improvement in toughness presents a dilemma for the metallurgist since these properties normally related by an inverse trend. However strengthening based on ferrite grain refinement satisfies the need to maintain toughness as strength increases and all processing developments described in the literature (4) are related to reducing ferrite grain diameter or refining the bainite microstructure of the final linepipe plate.

Grain refinement is usually achieved by arranging the rolling of austenite such that small austenite grains are produced that have a high level of stored energy Sv resulting from low temperature rolling in the "non-recrystallization" region. The magnitude of Sv is obtained from the relationship :

$$S_V = S_V\,(GB) + S_V\,(IPD)$$

$$S_V = 0.429N_{LR} + 2.571\,N_{LZ} - N_{LT} + \frac{N_{DB}}{Sine\,\phi}$$

where $S_V$ = total effective area per unit vol., $mm^2/mm^3$

$S_V\,(GB)$ = grain boundary contribution to $S_V$, $mm^2/mm^3$

$S_V\,(IPD)$ = intragranular planar defect contribution to $S_V$, $mm^2/mm^3$

$N_{LR}$, $N_{LZ}$, $N_{LT}$ = grain boundary intercept number per unit length

along rolling, thickness and transverse directions, respectively.

$N_{DB}$ = number of IPD per unit area, $mm/mm^2$

$\phi$ = angle between IPD and plate thickness direction

The temperature of transformation to ferrite is controlled either by alloying with manganese, nickel, boron or molybdenum used singly or in combination, or by increasing the cooling rate with water delivery that is applied via complex water delivery systems that are installed close to the plate mill exit. Of the two approaches water cooling results in higher ferrite nucleation rates, (5) plus superior weldability and economics, and this accounts for continued expansion in its use. Figure 1.

## CHEMICAL COMPOSITIONS

Typical chemical compositions of steels used today for producing yield strengths of X-65 to X-100 have been presented in a recent paper (5) and it is inappropriate to duplicate all tabulated data in that manuscript in the limited space available in these proceedings. The basic alloy designs for each strength level generally fit into the following compositional ranges.

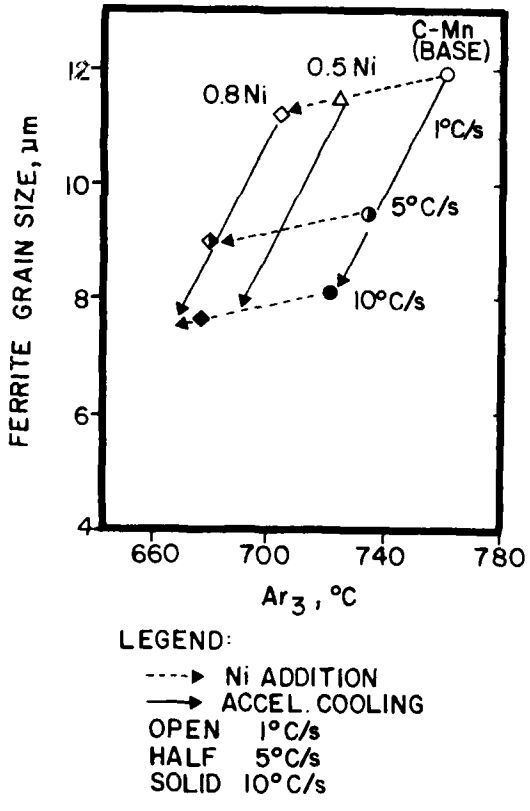


FIGURE 1. Effect of Interrupted Accelerated Cooling and Nickel Content on Grain Size of Ferrite Transformed from Deformed Austenite (4).

Copper and nickel may be added at the rates of 0.30 and 0.15 percent respectively when the steels are designed for sour service.

Carbon Contents - Carbon contents have moved steadily downward and desirable levels may be as low as 0.02 to 0.03 percent for steels based on acicular ferrite microstructures. The dramatic changes since 1975 can be judged by comparing the compositions in Table I with those published in the line- pipe papers in the proceedings of the conference "Microalloying 75". For convenience that data is summarized in Table II

TABLE I

Typical Chemical Compositions of Steels Used for Manufacture of X-52 to X-100 Linepipe

| | C | Mn | S | P | Nb | V | Mo | B | Ti |
|---|---|---|---|---|---|---|---|---|---|
| X-52/60 | 0.06/0.14 | 0.90/1.30 | <0.010 | 0.018 | 0.03 | - | - | - | - |
| X-65 | 0.05/0.11 | 1.10/1.50 | <0.005 | 0.015 | 0.03 | 0.04 | - | - | 0.015 |
| X-70 | 0.04/0.09 | 1.30/1.60 | <0.004 | 0.015 | 0.03 | 0.08 | * | * | 0.015 |
| X-80 | 0.02/0.05 | 1.50/0.05 | <0.002 | 0.010 | 0.05 | 0.08 | * | * | 0.015 |
| X-100 | 0.02/0.04 | 1.60/1.80 | <0.001 | 0.010 | 0.05 | 0.08 | 0.15/0.30 | * | |

*Optional

TABLE II

Summary of Chemical Compositions of X-52 to X-100 Steels used for Manufacture of Linepipe, Circa 1974/75.

| Company | Grade | Thickness | Carbon | Manganese | Silicon | Columbium | Vanadium | Molybdenum | Nickel | Chromium |
|---|---|---|---|---|---|---|---|---|---|---|
| Australian Iron & Steel | X65 | 10.2 mm | 0.17% | 1.30% | 0.25% | 0.045% | – | – | – | – |
| Usinor | X65 | 16 mm | 0.12% | 1.45% | 0.30% | 0.045% | – | 0.22% | – | – |
| IPSCO | X70 | 11.9 mm | 0.045% | 1.89% | 0.10% | 0.077% | – | 0.25% | – | – |
| U.S. Steel Corp. Research | X65 | 12.7 mm | 0.07% | 1.40% | 0.25% | 0.035% | – | 0.30% | – | – |
| Kawasaki Steel | X70 | 25 mm* | 0.06% | 1.70% | 0.25% | 0.04% | 0.03% | — | 0.30% | – |
| | | | 0.07% | 1.80% | 0.25% | 0.055% | – | – | – | 0.20% |
| | | | 0.05% | 1.80% | 0.25% | 0.06% | – | 0.10% | – | – |
| Nippon Kokan K.K. | X70 | 19 mm | 0.08% | 1.50% | 0.30% | 0.035% | 0.10% | – | – | – |
| Hoesch-Estel | X65 | 15.1 mm | 0.13% | 1.62% | 0.26% | 0.039% | 0.053% | – | – | – |
| Nippon Steel | X70 | 19 mm | 0.10% | 1.40% | 0.25% | 0.045% | 0.10% | – | 0.30% | – |
| | X70 | 20 mm | 0.08% | 1.75% | 0.11% | 0.047% | – | 0.25% | 0.20% | – |
| | X70 Q&T | 15 mm | 0.10% | 1.30% | 0.30% | 0.03% | – | – | 0.45% | – |
| Sumitomo Metal Industries | X65 | 19 mm | 0.09% | 1.39% | 0.33% | 0.018% | 0.08% | – | – | – |
| Italsider | X60/65 | 15 mm* | 0.14% | 1.50% | 0.30% | 0.04% | – | – | – | – |
| | X60/70 | 15 mm* | 0.13% | 1.50% | 0.30% | 0.035% | 0.07% | – | – | – |
| | X70 | 30 mm* | 0.06% | 1.65% | 0.35% | 0.05% | – | 0.35% | 0.30% | – |
| USSR Research | X65 Normalized | 40 mm* | 0.15% | 1.30% | 0.23% | – | 0.13%† | – | – | – |

*maximum thickness
†plus 0.028% nitrogen

SULFUR AND PHOSPHORUS - The trend in guaranteed sulfur and phosphorus contents during the past fifteen years is shown in Figure 2 (7.8).

The pressure to reduce sulfur contents first emerged in the early 1970's in connection with the need to improve ductile fracture arrest capability. Later demands for improved HIC (stepwise cracking resistance) reinforced this trend.

Today huge quantities of linepipe steel, totalling over 10 million tons/yr are produced with sulfur levels of 0.005 percent and below. To put this development into perspective it should be recalled that as recently as 10 years ago contents of twice these levels were not available on a uniform basis and even then they often attracted severe cost premiums when mandated by specifications.

Phosphorus increases activity of carbon and increases the hardening tendency in carbon segregated regions of continuously cast slabs. Thus, lower phosphorus levels are useful for educing the tendency for link-up of HIC cracks by stress assisted SSCC mechanism and it is usual to limit maximum contents to 0.008 to 0.010 maximum for sour service linepipe. These levels require application of hot metal dephosphorization treatments to reduce contents from the 0.015 to 0.018 percent maximum levels that are representative of todays iron ore sources and steelmaking technology.

NITROGEN - Nitrogen is very harmful to Charpy and BDWTT transition temperatures increasing both at the rate of 35°F/0.001N (9). It also detracts from attainment of high HAZ toughness levels and it increases the likelihood of sub-surface cracking during continuous casting. For these reasons optimum nitrogen levels have moved down to 0.003 to 0.004 percent during the past five years. At these concentrations supplemental treatment with 0.010 to 0.015 percent titanium which acts as a scavenger reduces "free" nitrogen to innocuous levels thereby reducing risk of HAZ degradation during welding and ensuring maximum toughness at low operating temperatures.

Attainment of these desirable nitrogen levels is far from universal amongst different steelmakers and problems still may be encountered particularly when Electric Arc Furnace steelmaking is combined with deep desulfurization and poor stream protection during casting.

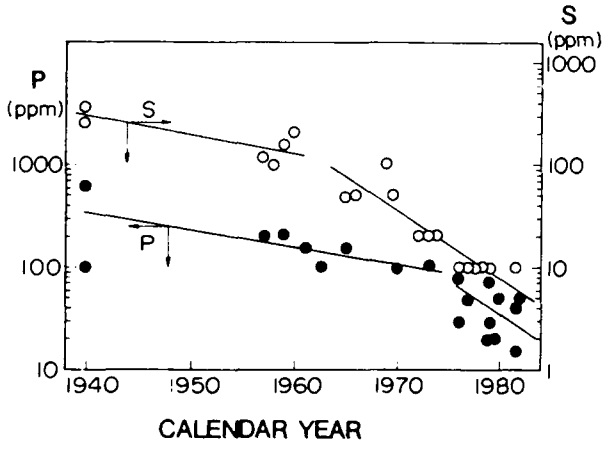


FIGURE 2. Trend of warranted sulfur and phosphorus level converter steels melted in Japan (7.8)

INCLUSION SHAPE CONTROL - Metallurgists have known for some time that globularization of inclusions is as important as desulfurization in improving Charpy V-notch shelf energy and reducing stepwise cracking. (Hyrogen Induced Cracking (HIC) in sour environments.) For this reason inclusion shape control with zirconium rare earths or calcium were introduced on a broad basis in the 1972 to 1977 period. Most high toughness pipe used to guard against ductile fracture propagation was produced by these means.

Rare earths tend to produce sub-surface oxysulfide stringers in ingot casting and result in nozzle blockage during continuous casting and zirconium suffers from other disadvantages. For this reason ladle metallurgy techniques have been perfected to reduce sulfur to very low levels and to allow optimized treatment with calcium which has emerged as the preferred globularizer. Typical ranges for residual calcium are in the 15 to 50 ppm range since high levels lead to renewed risk of problems caused by inclusion stringers and they may affect arc stability when field welding with the GMAW process.

WELDABILITY - The Microalloyed steels that first entered the linepipe market had carbon equivalents of 0.50 percent and above (10). This is considered a relatively high level today but in 1959 the steels were hailed for their superior weldability and resistance to hydrogen assisted cold cracking (11) compared with the simple carbon-manganese steels that they replaced.

Further improvements in steelmaking and alloy design have led to a steady decline in carbon contents as described earlier. For the X-70/80 Grades the microalloying strengthening processes will not operate efficiently at high carbon and nitrogen levels due to the effect of these interstitials in reducing solubility of carbonitrides. Therefore X-70/80 steels have carbon contents that do not purely reflect concerns for field weldability and one can argue that their field performance may often be superior to lower strength steels when all other factors are equal.

The trend toward improved weldability as a function of time and the simultaneous escalation of strength level are shown in Figure 3. The carbon contents and carbon equivalents are superimposed on the cracking risk diagram developed by Granville (12).

Most advanced linepipe steel manufactured today has low nitrogen contents and is alloyed with 0.010/0.015 percent titanium. The resulting low free nitrogen content reduces the risk of hydrogen assisted delayed cracking and furthermore greatly improves HAZ toughness values.

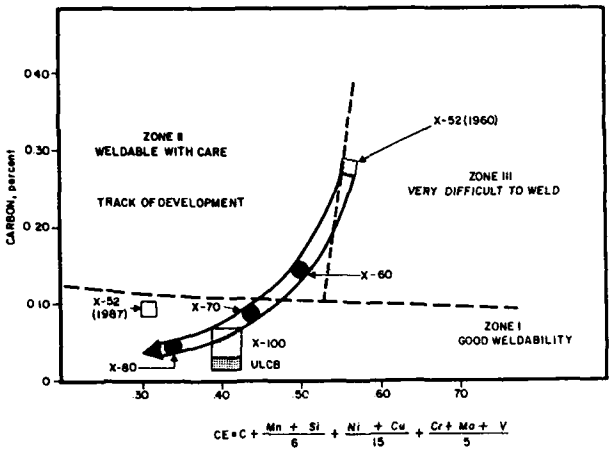


FIGURE 3. Path of Linepipe Development with respect to Graville's (12) Hydrogen Assisted Cracking Diagram.

CONCLUSION - Todays linepipe steels reflect thirty years of evolution during which period strength and toughness requirements have been increased. The trend in mechanical properties has been matched by improvements in steelmaking, ladle metallurgy, continuous casting and rolling. Second generation alloying approaches based on low carbon acicular ferrite and availability of accelerated cooling devices support the trend toward X-80 or even X-100 strength levels while maintaining the excellent weldability for which microalloyed steels are noted.

For sour service applications degradation by SSCC mechanisms limits useful yield strengths to the X-60/70 strength level but low carbon microalloying designs teamed with excellent impurity control result in sophisticated products that are highly resistant to $H_2S$ attack.

REFERENCES

1. P. Bordignon, "Trend in Development and Availability of HSLA Linepipe in Developing Countries"
This Conference.

2. H. Nishi, T. Ohtani, Y. Tomizawa, S. Watanabe, "ERW Pipes with Improved Service Performance" Pipe Technology, Rome, Italy 17/19 November, 1987. (p. 323).

3. H. Ueda, T. Tanaka, S. Suzuki, Y. Kakatsuka, T. Hashimoto, Y. Komizo, M. Tsukamoto, "Recent Development of High Grade Line Pipe up to X-100", ibid (p. 201).

4. Proceedings TMS/AIME Conference, "Thermemechanical Processing of Austenite" Ed. A.J. DeArdo, G.A. Ratz and P.J. Wray.

6. Proceedings, Microalloying '75 Conference, October 1-3, 1975, Washington, D.C., Copyright Union Carbide Corporation, 1977.

7. Yamada K. and T. Usui, "The Role of Hot Metal Pretreatment and the Converter Process for Clean Steel Production." Proceedings of Conference Inclusions and Residuals in Steel, Ottawa, Ontario, March 4-5, 1985, p.3.

8. Kozasu, I. and K. Tsukada, "The Metallurgical Design of Modern Line Pipe Steels." Proceedings of Conference Inclusions and Residuals in Steel, Ottawa, Ontario, March 4-5, 1985, p.119.

9. J.M. Gray "Strength - Toughness Relationships for Precipitation Hardening," Trans AIME 1972 v 3 p.1495.

10. Altenburger, C.L., "Columbium Treated, Mild Carbon Semi-killed Steel," AISI Regional Technical Meeting No. 59, Buffalo, N.Y. 1960. See Also U.S. Patent No. 3,101,822.

11. Barkow, A.G., "Columbium-Treated Steel in High Pressure Line Pipe Service." AISI Regional Technical Meeting No. 59, Buffalo, N.Y., 1960.

12. Graville, B.A. "Cold Cracking in Welds in HSLA Steels." Welding of HSLA (Microalloyed) Structural Steels, Published by ASM., AIM/ASM Conference, Rome, Italy, November 9-12, 1976.

# EXPERIENCE IN SUPPLY OF ARCTIC GRADE LINE PIPE FOR SOVIET CONSTRUCTION PROJECTS

**Peter A. Peters, Hans-Georg Hillenbrand**
Mannesmannröhren-Werke AG
4330 Mülheim a.d.
Ruhr, FRG

MANNESMANN HAS A LONG TRADITION of cooperative work with Russia in the field of pipelines. This is best documented by the fact that Siemens constructed a pipeline from Mannesmann pipes for the Caucasian copper mine works as early as 1889. In 1897 seamless pipes of 8" diameter were supplied to Russia. They were threaded pipes and were used in the construction of an oil transmission pipeline of over 850 km length. The pipes were joined together using couplings. The components were furnished by the works at Komotau and Rath. The pipeline between Baku and Batumi (Figure 1) has been in operation since 1906.

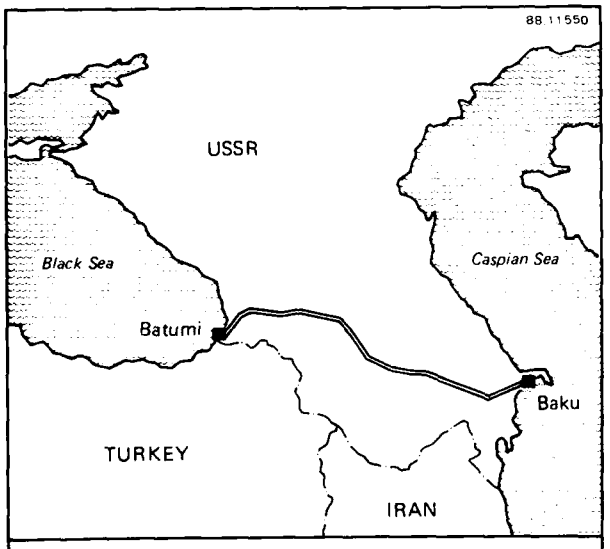


Figure 1

This speaks well for the quality of pipes from Mannesmann. It is of course also a proof of the careful laying operations and the subsequent maintenance of the pipeline.

The trade in pipes resumed after World War II. About 200,000 tonnes of pipes were supplied in 1962 before the business was practically brought to a standstill by the embargo in 1963.

The present paper only refers to the time period from 1970 till now. Moreover, it is only concerned with the large diameter line pipe for the transportation of sweet gas.

Figure 2 shows the length of pipe in kilometers supplied every year during the period 1970 to 1987.

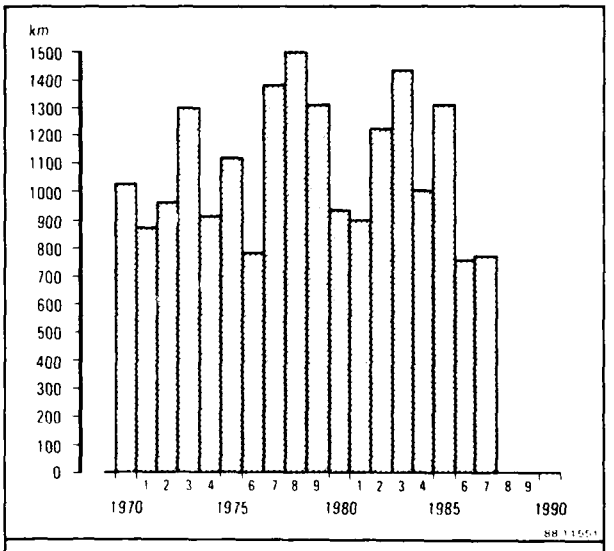


Figure 2

The yearly supplies varied between 750 km and 1500 km and the total length of the pipe supplied over the entire period is 20,000 km. Pipes with a diameter of 56" constituted a major portion of these supplies. The pipes were intended for use at an operating pressure of 75 bar. From 1980 onwards pipes have also been specified for an operating pressure of 100 bar. In the course of these 17 years, the line pipe specifications and also the production methods have been improved as the state-of-the art in technology has advanced. For example, the wall thickness of 56" diameter pipes has been reduced over the years from 17 mm through 15.7 mm to 14.5 mm, making use of the increase in minimum tensile strength values of the line pipe steels and the lowest design factors.

## REQUIREMENTS FOR LINE PIPE WITH A DIAMETER OF 56" (1420 MM)

Pipes made from conventionally rolled and normalized plates were only supplied during the years 1970 to 1974, as shown in Figure 3.

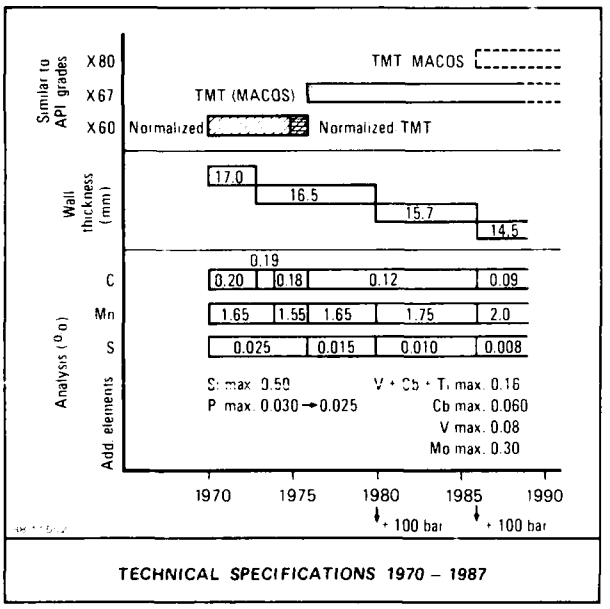


Figure 3

This was mainly due to high costs associated with thermomechanical processing of steel plate with thicknesses ≥ 16.5 mm as a result of reduced rolling mill efficiencies (efficiency reductions up to 60 %), compared to conventional rolling. From 1975 onwards, thermomechanically processed plates have been used for pipes with thinner walls in addition to conventionally rolled and normalized steel plates for pipes with wall thicknesses ≥ 19.5 mm. From 1976 onwards, the plates have only been produced by thermomechanical rolling, irrespective of the plate thickness. Since 1986 accelerated cooling has also been incorporated into the process of plate manufacture, whenever needed.

During the same period, the requirements of the Russian specifications have also been altered. The specified minimum yield strength has been increased from 412 N/mm² through 461 N/mm² (X 67) to 510 N/mm². The carbon content of the steel has been reduced from 0.20 % through 0.12 % maximum to 0.09 % maximum. The carbon equivalent as determined by the IIW formula has also been reduced from 0.50 to 0.44 maximum (Figures 3 and 4). Figure 3 shows further that manganese levels up to 2.0 % will be accepted nowadays. The maximum allowable sulphur contents have been lowered from 0.025 % to 0.008 %.

The concept of moving over towards higher operating pressures has often been discussed since 1980, but has not yet been materialized on a large scale.

The toughness and transition temperature requirements are also contained in Figure 4.

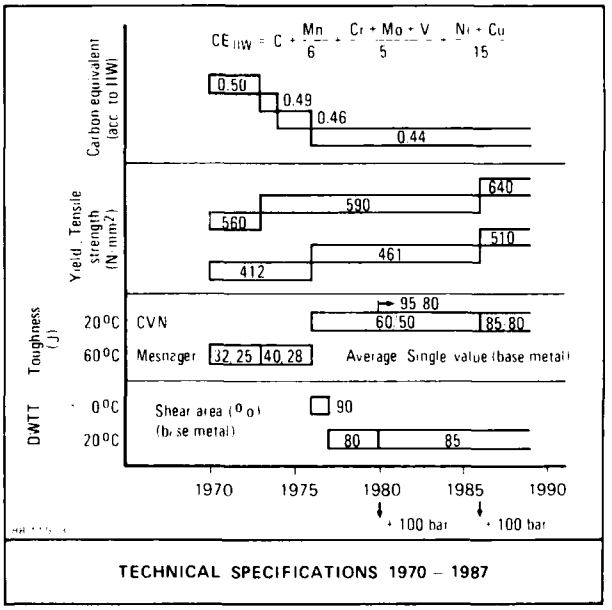


Figure 4

## STEEL DEVELOPMENTS

There was no scope to improve the strength levels of normalized steels beyond X 60. The reasons for this were the requirement for improved field weldability and the desire for increased toughness levels. This restricted the increase in the amount of alloying elements which would have been necessary to raise the mechanical strength. No additional improvement was possible in this field until a new rolling process known as thermo-mechanical treatment (TMT) was introduced on a commercial scale.

Figure 5 shows the developments that have taken place in line pipe steels, starting from the X 60 normalized steel, as supplied in the early 1970's.

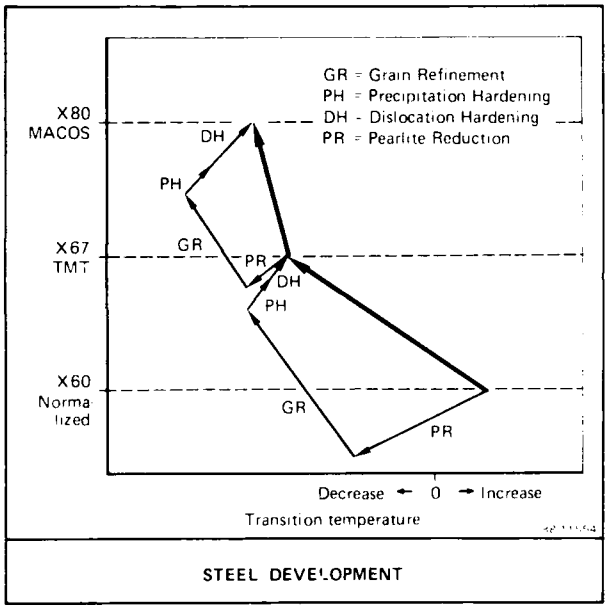


Figure 5

The chemical composition of this steel was about 0.2 % C, 1.55 % Mn, 0.12 % V, 0.03 % Nb and 0.02 % N.

The thermomechanically processed X 67 steel mentioned in the figure was microalloyed and contained only just 0.12 % C.

Thermomechanical rolling resulted in a significant reduction of the ferrite grain size. Grain refinement is the only method by which both strength and toughness can simultaneously be improved.

The loss of strength resulting from reduced pearlite contents could be offset by precipitation strengthening and dislocation strengthening.

Reduction of pearlite content, grain refining, dislocation hardening and precipitation hardening had contributed in combination to the development of X 67 steel with improved weldability and favourable transition temperatures.

Further increases in strength and toughness, which led to the development of X 80 steel, could only be attained by altering the steel matrix from ferrite-pearlite to ferrite-bainite microstructure. In comparison with the thermomechanically rolled X 67 steel, the X 80 steel has a reduced carbon content, reduced grain size and an increased dislocation density. These two steel grades also differ in their precipitation characteristics.

Figure 6 shows the actual changes that these developments have brought about in individual steel grades, for example, in the yield strength, transition temperature, impact energy, carbon content and carbon equivalent.

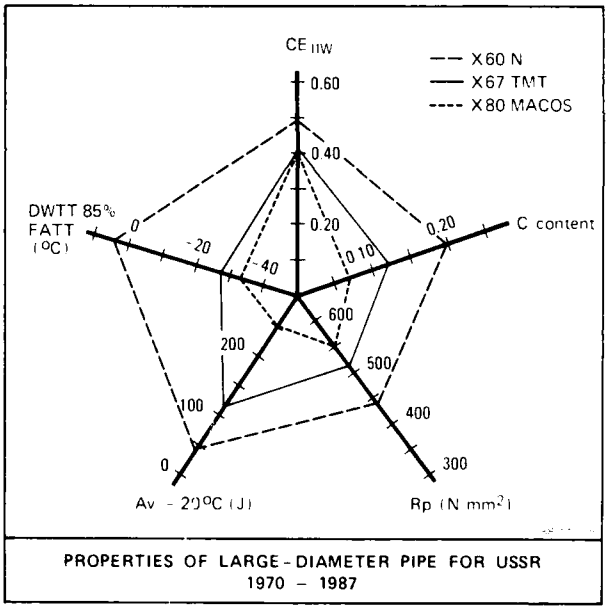


Figure 6

A comparison of the conventionally rolled and normalized X 60 steel with the thermomechanically processed and accelerated cooled X 80 steel shows that the yield strength has been improved by more than 120 N/mm². At the same time, the low impact energy values of about 50 J of the X 60 steel have been raised to greater than 120 J for the X 67 steel and approx. 210 J for the X 80 steel. The DWTT transition

temperature (85 % shear area), which is a major criterion for pipeline safety, is below - 30 °C for the X 80 steel. The field weldability is also an important property in the context of line pipe steels. One of the most governing factors on field weldability is the carbon content of the steel. It has been reduced from 0.2 % for the X 60 steel to 0.07 % for the X 80 steel. The carbon equivalent of the thermomechanically processed and accelerated cooled X 80 steel is almost the same as that of the thermo-mechanically processed X 67 steel, whose field weldability has already been proved by a large number of existing pipelines.

The developments in line pipe steels can be better illustrated by considering the improvements achieved in the microstructure. Figure 7 shows typical microstructures of the three types of line pipe steels discussed.

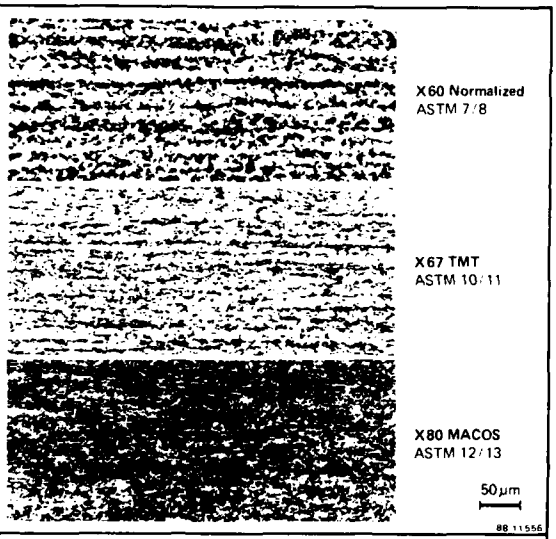


TYPICAL MICROSTRUCTURES OF NORMALIZED, TM – TREATED AND MACOS – STEELS

Figure 7

Banded ferrite and pearlite and coarse ferrite grain size (ASTM 7 - 8) are the characteristic features of conventionally rolled and normalized X 60 steels. The microstructure of X 67 steels is more uniform and the ferrite grains are finer (ASTM 10 - 11). The most uniform and extremely fine microstructure is attained by accelerated cooling that follows thermomechanical rolling, as shown for the X 80 steel. The improved properties of this steel are to be attributed to its ferritic-bainitic microstructure.

Grain refinement and increased dislocation density attained by accelerated cooling as well as modified recrystallization and precipitation characteristics attained by a combined addition of niobium and titanium at reduced nitrogen levels are the basic principles involved in the development of line pipe steels.

Figure 8 gives an idea of the actual grain size distribution in ferrite and bainite /1/.

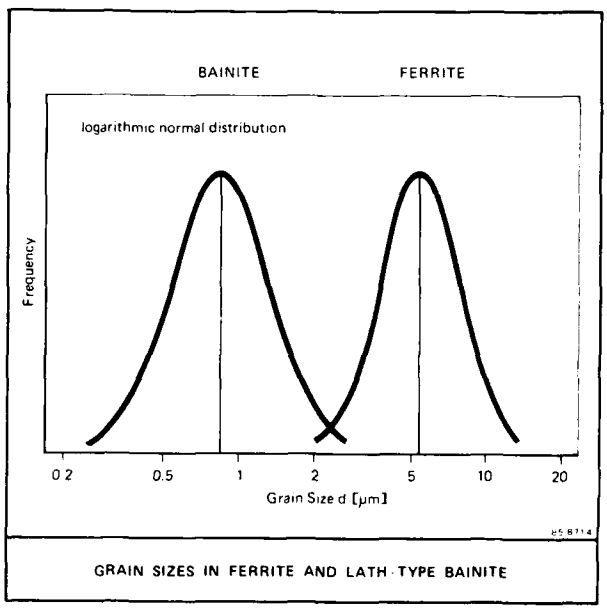


GRAIN SIZES IN FERRITE AND LATH-TYPE BAINITE

Figure 8

The measurement of bainite grain size is only possible in the electron microscope. Dark field technique was used, since only by this technique is a distinction between low and high angle grain boundaries possible. The average and the smallest grain diameters of ferrite in thermomechanically treated steels are 5 µm and 2 µm respectively. In contrast, the average grain diameter in bainite is < 1 µm and individual bainite laths with widths as low as 0.2 µm are found. The logarithmic values of grain sizes both in ferrite and bainite exhibit normal distributions.

Bainite has normally a higher dislocation density than ferrite. Measurement of dislocation densities requires extensive experimental work. It includes the measurement of specimen thickness at each area of dislocation density measurement. Then a set of high magnification micrographs are to be

taken from the same specimen area. Convergent beam diffraction technique is preferentially used to measure the specimen thickness, since this technique, among other things, enables one to make the most accurate measurements. The micrographs are subsequently analyzed by superimposing grids over them and counting the number of intersections between the grid lines and dislocations. These counts in conjunction with the specimen thickness measurements are then used to calculate the dislocation densities. Figure 9 shows, as an example, the results of two series of dislocation density measurements /1/.

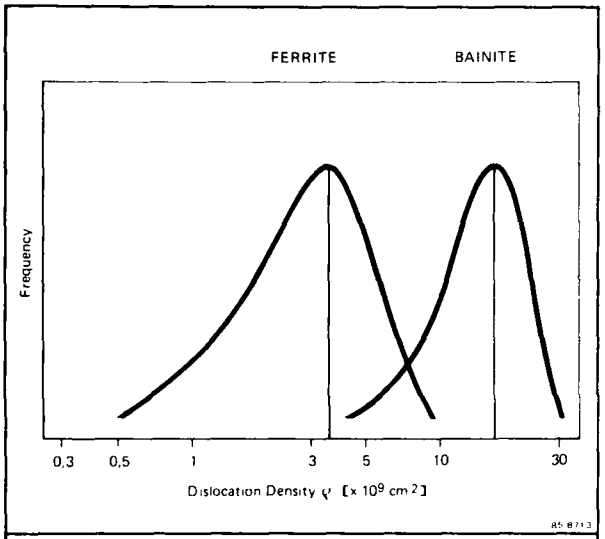


DISLOCATION DENSITIES IN FERRITE AND LATH-TYPE BAINITE

Figure 9

The ferritic specimen was thermomechanically rolled at a finish rolling temperature just above the $Ar_3$ temperature, which is responsible for the low dislocation density (3.7 x $10^9$ $cm^{-2}$) measured here. Markedly higher dislocation densities can also be obtained in ferrite if the finish rolling is carried out in the two phase region close to the $Ar_1$ temperature. The dislocation density of the bainitic specimen is 16.9 x $10^9$ $cm^{-2}$ and is also low, compared to the values normally found with bainitic structures. The lower dislocation density of the bainitic specimen here is to be attributed to a relatively low finish rolling temperature. Significantly higher dislocation densities have indeed been measured in other bainitic samples.

Grain size and dislocation density measurements were made as in the case of Figures 8 and 9, in order to derive the vectors of Figure 5.

## DEVELOPMENT OF THE MNNBTI STEEL

In the course of the development work, a large number of laboratory casts with varying chemical compositions were tested, which exhibited excellent property combinations even in the accelerated cooled condition.

Addition of 0.02 % titanium to a niobium microalloyed C-Mn steel with about 0.1 % C, 1.5 % Mn and 0.03 % Nb results in an enhanced grain refinement. The mechanism of grain refinement through titanium additions will be discussed later in some detail. The grain refinement coupled with a reduced carbon content of 0.08 % results in significantly higher toughness but slightly lower strength (Figure 10).

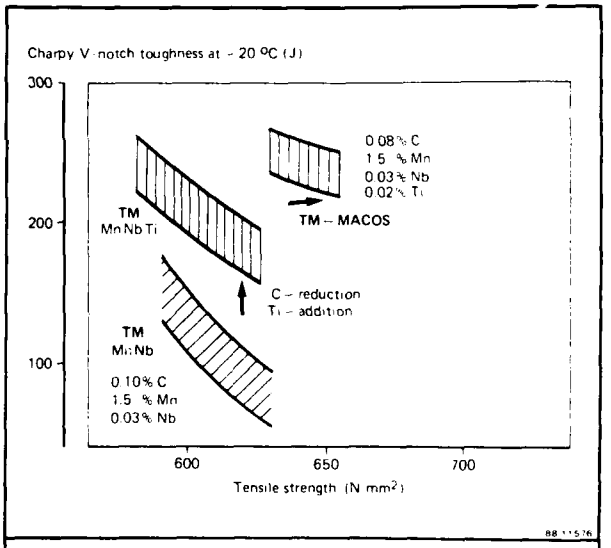


DEVELOPMENT OF MnNb-STEELS THROUGH ADDITIONAL MICRO-ALLOYING WITH TITANIUM AND THE USE OF TM-MACOS

Figure 10

Accelerated cooling of the plate after thermomechanical rolling leads to an increase in the strength by 50 $N/mm^2$ to 70 $N/mm^2$ without any detriment to the toughness.

The effect of microalloying elements on the mechanical and technological properties of thermo-mechanically processed line pipe steels is governed by the reactions of these

elements with carbon and nitrogen. Therefore, knowledge of these reactions will greatly assist in achieving the specific targets set in the development of materials. The prerequisite for the successful use of niobium and titanium was the availability of tonnage processes for producing steels with low nitrogen levels.

Energy-dispersive X-ray micro-analysis and measurement of lattice constants were carried out in order to determine the compositions of carbonitrides precipitated in the steels which had been microalloyed with niobium and titanium in various concentrations.

In the MnNb steels, a major fraction of the niobium reacts with nitrogen in the upper austenite region and gets tied up. Only a minor fraction of the niobium remains in solution that is free to form Nb (C, N) in the lower austenite or ferrite region to cause precipitation hardening.

In the MnNbTi steels, one takes advantage of the high affinity of titanium to nitrogen. At titanium-to-nitrogen ratios higher than the stoichiometric ratio, nearly all of the nitrogen combines with titanium at high temperatures to form nitrides or carbonitrides. These precipitates contain very little niobium or no niobium at all. The carbonitride precipitates, which are rich in nitrogen, inhibit grain growth in the upper austenite region. Practically, all of the niobium remains in solution. It lowers the recrystallization temperature and thereby leads to a smaller austenite grain size. Moreover, it is free to form carbon-rich carbonitrides at lower temperatures. The free niobium gives rise to the formation of fine precipitates in the lower austenite region and to an intensive hardening through coherent precipitation in the ferrite.

These microstructural changes are better understood by the results of electron microscopic investigations on the precipitates. Figure 11 shows, by way of an example, the results of energy-dispersive X-ray microanalyses of carbonitride precipitates in the MnNbTi steel /2/.

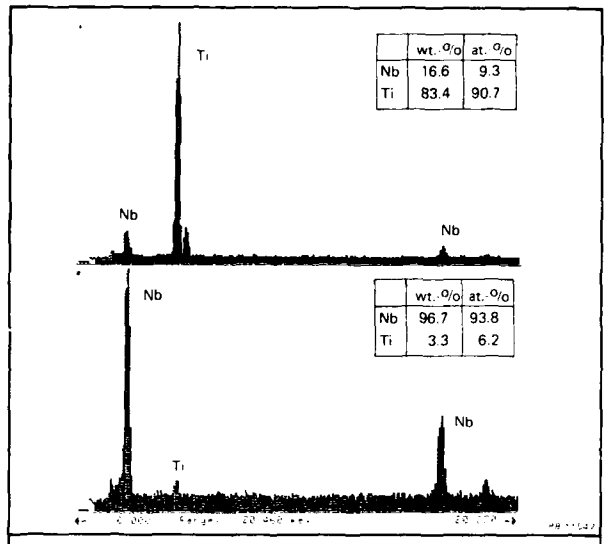


EDX – ANALYSIS OF CARBONITRIDES IN Mn Nb Ti – STEEL (TM – TREATED)

Figure 11

The spectrum given in the upper half of the figure shows the concentrations of metallic components in the cube-shaped carbonitride particles and reveals that they consist mainly of titanium, together with a small proportion of niobium. The lower half of the figure shows the metal content in rounded particles and suggests that they are composed almost wholly of niobium.

The chemical compositions of the non-coherent particles were determined by coupling the results of extensive microanalyses with the information obtained from the corresponding diffraction patterns.

Figure 12 shows the distribution of the lattice parameters of carbonitride particles found in a MnNb steel /2/. The data presented in the figure reveal that the precipitates are mainly NbN. The small fraction of titanium carbonitrides found is to be ascribed to the presence of titanium as a residual element in the steel. These carbonitrides are practically always present in steels, even when they are not alloyed with titanium.

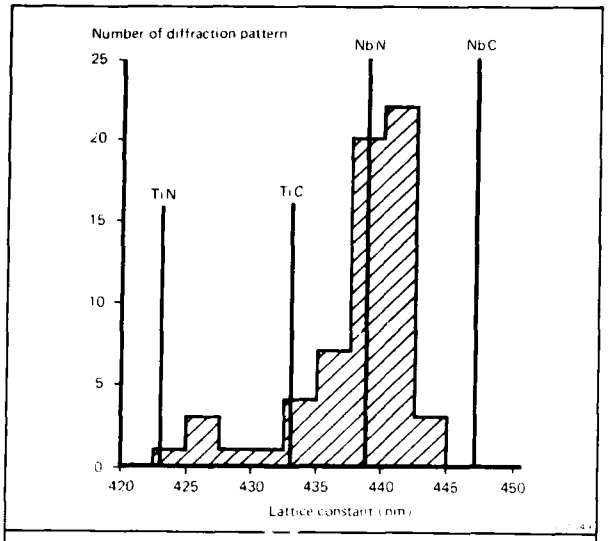


FREQUENCY DISTRIBUTION OF LATTICE CONSTANTS OF CARBONITRIDES (Mn Nb - STEEL, TM - TREATED)

Figure 12

The results obtained with MnNbTi steels differ markedly from these, as shown in Figure 13 /2/.

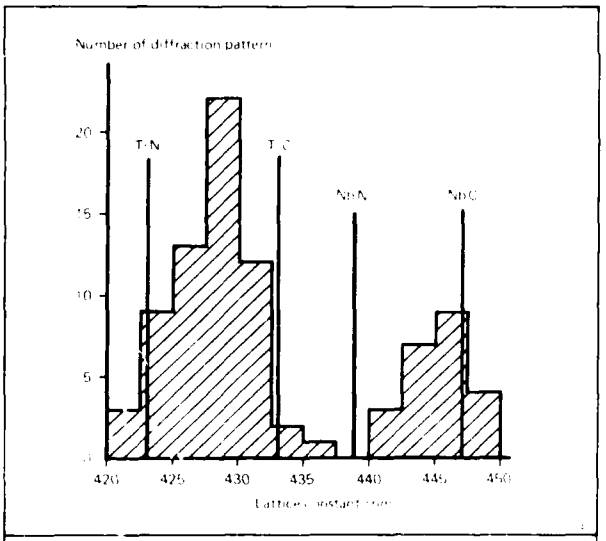


FREQUENCY DISTRIBUTION OF LATTICE CONSTANTS OF CARBONITRIDES (Mn Nb Ti - STEEL, TM - TREATED)

Figure 13

The histogram in this case exhibits two distinct maxima. The first of these two maxima corresponds to titanium carbonitrides that form at very high temperatures. The second one corresponds to niobium carbonitrides rich in carbon. They form during thermomechanical rolling in the lower austenite region.

Figure 14 shows the variation of tensile strength and toughness with the manganese content in MnNbTi steels.

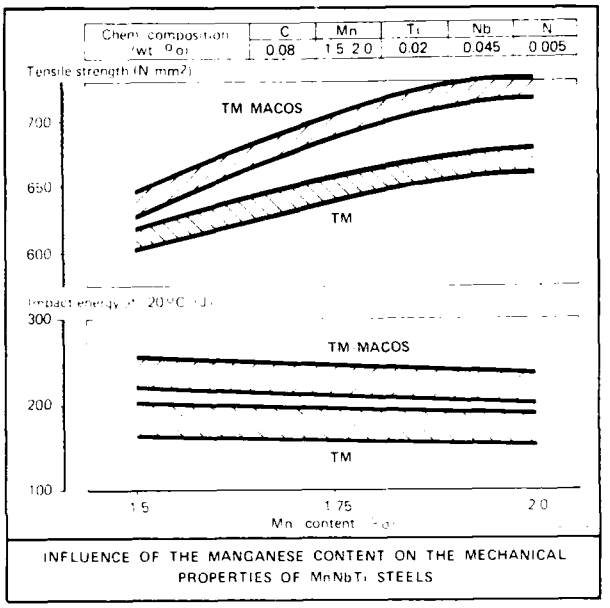


INFLUENCE OF THE MANGANESE CONTENT ON THE MECHANICAL PROPERTIES OF MnNbTi STEELS

Figure 14

With conventional manganese contents of about 1.5 % it is possible to attain tensile strengths $\geq$ 600 N/mm² through thermomechanical rolling. Accelerated cooling following the thermomechanical rolling results in an increase of the tensile strength to $\geq$ 650 N/mm² at manganese levels > 1.6 %. In order to attain tensile strengths $\geq$ 700 N/mm², manganese levels in excess of 1.8 % are needed and the thermomechanical rolling should be followed by accelerated cooling. The increased manganese contents have practically no adverse effect on the toughness of the MnNbTi steels. These results also show that the fine-grained bainitic microstructure obtained through thermomechanical rolling plus accelerated cooling results in more attractive properties than the ferrite-pearlite microstructures obtained through thermomechanical rolling involving work hardening of the ferrite.

## EFFECT OF ACCELERATED COOLING AFTER THERMOMECHANICAL ROLLING

Figure 15 illustrates that steels with strength levels up to X 100 can be produced economically through accelerated cooling of the plate following thermomechanical rolling /3/.

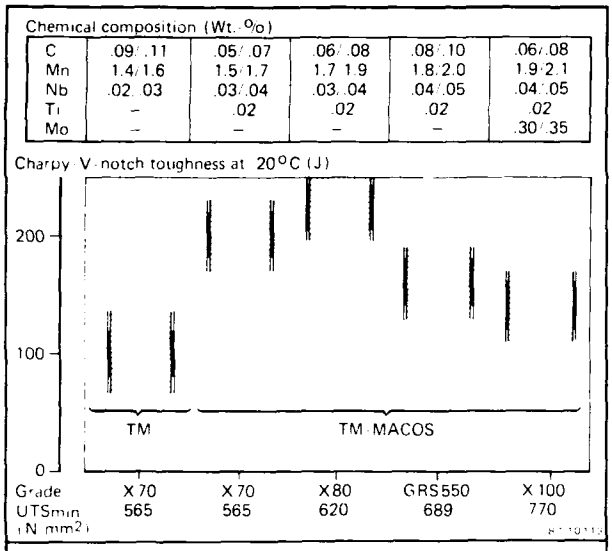


DEVELOPMENT OF ACC. COOLED STEELS (MACOS)

Figure 15

The cooling system is used to advantage, especially, in the production of very high strength steels with high toughness and good weldability. The starting point for the steels having improved strength is the optimized thermomechanically rolled X 70 (X 67) MnNb steel with Charpy V-notch impact energy values of about 100 J at -20 °C. The MnNb steel is used nowadays for plates up to 20 mm thickness. If a MnNbTi steel is used in conjunction with accelerated cooling, the same strength level is obtained but with improved Charpy V-notch impact energies of about 200 J. Increase of strength up to X 80 is possible with MnNbTi steels if the manganese content is raised to 1.7 % to 1.9 %. If these steels are subjected to accelerated cooling after thermomechanical rolling toughness values greater than 200 J can be achieved even at this high strength level.

To produce a GRS 550 steel plate, which has a higher tensile strength than X 80 steel, it is necessary to raise the carbon and manganese levels only marginally. Additional alloying with molybdenum enables strength levels as high as X 100 to be achieved, along with high toughness.

The nomogram in Figure 16 shows the influence of important processing variables on the mechanical properties of Mannesmann Cooled Steels (MACOS) /3/.

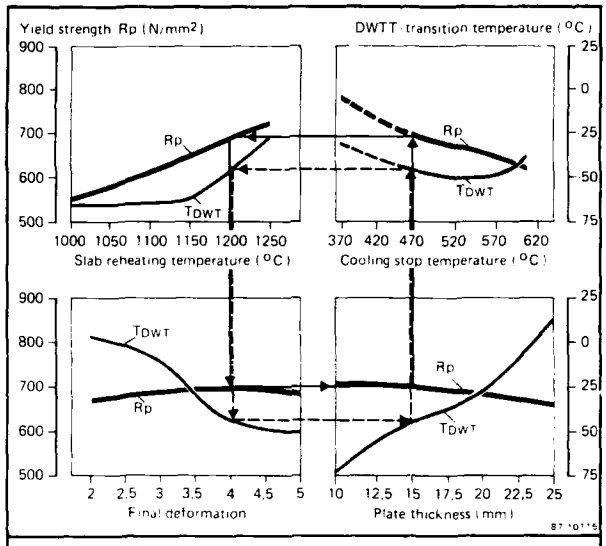


INFLUENCE OF ROLLING AND COOLING PARAMETERS ON THE MECHANICAL PROPERTIES OF A MnNbTi-STEEL

Figure 16

The results were obtained on a MnNbTi steel containing 0.09 % C, 1.94 % Mn, 0.056 % Nb, 0.021 % Ti and 0.0038 % N. The values of the four parameters used in the development of the nomogram are shown by arrows in the figure. They are: slab reheating temperature = 1200 °C, final reduction ratio = 4, plate thickness = 15 mm and cooling stop temperature = 470 °C.

In this study, the slab reheating temperature was varied between 1000 °C and 1250 °C. The nomogram shows that the yield strength increases with increasing slab reheating temperature, over the entire temperature range studied. The tensile strength, which is not expressly shown here for the sake of clarity, also increases in a similar way. The DWTT transition temperature remains constant at about -65 °C up to a slab reheating temperature of 1150 °C, above which it increases considerably.

The influence of finish rolling temperature on the mechanical properties is not shown here, since the finish rolling temperature was so

selected that it was always in the region of the $Ar_3$ temperature. It is well known that variations in finish rolling temperature between 740 °C and 830 °C do not exert any significant influence on the yield and tensile strength. Finish rolling temperatures far above the $Ar_3$ temperature result in a coarse austenite and consequently in a coarse bainite, but with an enhanced dislocation density. This has no noticeable effect on the mechanical strength of the steel but an adverse effect on the transition temperature. Optimum DWTT transition temperatures will be attained if the finish rolling temperature is in the region of the $Ar_3$ temperature.

The influence of reduction ratio during finish rolling on the mechanical strength is negligibly small in the temperature range below 900 °C. However, the final reduction ratio should not be too low, as otherwise low DWTT transition temperatures cannot be attained.

The yield strength decreases only slightly when the plate thickness increases, provided the rolling and cooling parameters are kept more or less constant. The fact that the DWTT transition temperature increases with increasing plate thickness is to be attributed to the effect of specimen geometry. The transition temperatures of thick plates can be improved by lowering the slab reheating temperature and increasing the final deformation ratio, as shown in the nomogram. But this results in a slightly lower strength of the plate.

The cooling stop temperature influences both strength and toughness. Lowering the cooling stop temperature from 600 °C to 470 °C leads to an increase in the yield and tensile strength of the plate. The yield strength increases by a greater amount than the tensile strength, which means that the yield-to-tensile strength ratio increases with decreasing cooling stop temperature. Cooling stop temperatures below 470 °C are not desired because they result in an increase of these volume fraction of M-A constituent, which has a detrimental effect on the toughness properties.

## MECHANICAL AND TECHNOLOGICAL PROPERTIES AND ECONOMIC CONSIDERATIONS

A comparison of the actual values of mechanical and technological properties (Figure 6) with the requirements of the specifications (Figure 4) shows that there was always a comfortable margin of safety between the two.

Figure 17 shows, by way of an example, the values of yield strength, tensile strength, yield-to-tensile strength ratio and Charpy V-notch impact toughness at -20 °C, determined in the course of production of approx. 50,000 tonnes of line pipe for an order.

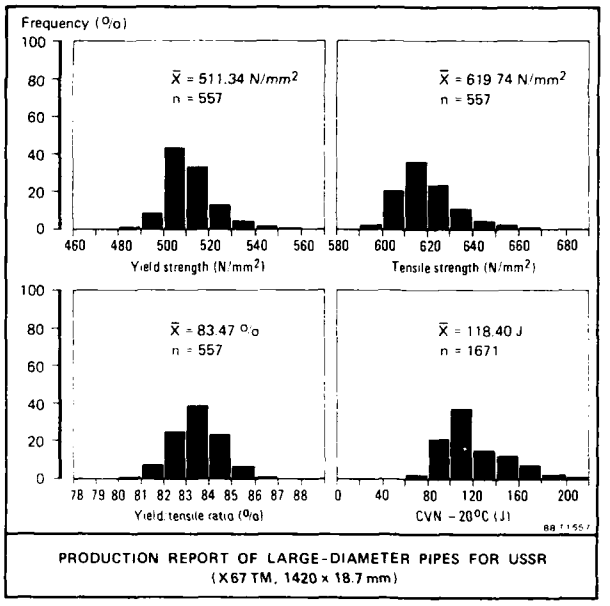


Figure 17

The histograms in the figure show that a consistent product was furnished in this case. The yield and tensile strengths were closely controlled and they are constantly above the specified minimum values. The yield-to-tensile strength ratios are relatively low. This is to be attributed to the steel composition chosen here. The Charpy V-notch impact energies of the specimens have a mean of about 120 J. The scatter towards very high values up to 200 J is to be ascribed to extremely low sulphur contents of some casts. These results are representative of the quality of all the line pipe shipments (weighing more than 10 million tonnes) made to the Soviet Union. If one looks now at the property requirements shown in Figures 3 and 4 one may not find them extraordinarily stringent. But, as per the standards of 1976 the jump in the yield strength from 412 N/mm² to 461 N/mm² with relatively heavy plates of thicknesses $\geq$ 16.5 mm was very big, because a minimum of 80 % shear area on

the fracture surfaces of the correctly tested DWTT specimens at -20 °C and relatively high Charpy V-notch impact energies were also demanded at the same time. The increased tensile strength, compared to the API specification for the same grade material, exacerbated the situation further. This can be better demonstrated by the steel chemistries used worldwide at that time. Owing to the state-of-the-art in thermomechanical processing at that time it was necessary for all the pipemakers to select steels alloyed with molybdenum for pipes of these dimensions. The molybdenum contents in the steels varied between 0.30 % and 0.60 % depending on the level of maturity attained by the individual plate mills in thermomechanical processing. The steels were additionally microalloyed with vanadium and niobium and increased nitrogen levels. The basic composition was approx. 0.08 % carbon and 1.5 % manganese. The enormous increase in the price of molybdenum forced us to resort to alternative methods that enabled molybdenum to be reduced or even avoided, as otherwise the production would have been absolutely uneconomical.

Thanks to a modified rolling technique, we were able to produce the 16.5 mm thick plate from steels not alloyed with molybdenum already in 1977. It was necessary to raise the niobium and vandium contents by small amounts and alloy the steel with about 0.15 % chromium. In the subsequent years, the non-molybdenum steels were also used for pipes with wall thicknesses $\leq$ 26 mm. The economic constraints caused by worldwide overcapacities and the resultant loss in profits also provided an incentive in the subsequent period to make use of the steadily increasing experience in thermomechanical rolling and to incorporate accelerated cooling into the production process to develop more economic steel compositions. Developments in secondary metallurgy, which permit steel compositions to be specified with narrower limits, optimization of continuous casting technique and balanced heating, rolling and cooling parameters during thermomechanical processing have all contributed to the successive reduction of the amount of alloying elements in the steel. Thus, it is possible nowadays to produce an 18.7 mm thick X 67 steel plate from a simple CMnNb steel without the addition of any other elements, as shown in Figure 17. Needless to say, these steels also consistently comply with the other requirements of the specification, for example, a minimum of 85 % shear area on the fracture surface of the DWTT specimen tested at -20 °C.

## ADDITIONAL FACTORS INFLUENCING THE PERFORMANCE OF PIPES DURING LAYING OPERATIONS IN THE ARCTIC REGIONS

Apart from the developments in steelmaking and plate manufacture, the developments in pipe forming, welding, nondestructive testing and coating have a strong influence on the quality of the final product, namely the line pipe. All these steps are so adjusted that the line pipe is produced economically and is fit for the intended service. In many regions, pipe laying is only possible in the winter. In view of the environmental temperatures between -55 °C and -60 °C existing in the northern regions, it is understandable that a series of tests are specified that enable one to assess the behaviour of line pipe at -55 °C or -60 °C. For example, the Mesnager specimens shall exhibit adequate toughness at -60 °C in order to ensure that there are no risks during handling, including also field bending. In the case of polyethylene mill-coated line pipe, the supplier is required to prove that the coating system does not deteriorate in the temperature range between +80 °C and -55 °C. Welding is mostly carried out at temperatures not below -45 °C. One can easily envisage that manual operations at these temperatures are fraught with problems. This is especially true for sensitive operations like girth welding in the field. Apart from field weldability, the geometrical tolerances of the pipe play a significant role under these unfavourable environmental conditions. Some relief to this situation is the joining of two or three pipe lengths by submerged-arc welding process in well equipped welding stations. The pipes must exhibit close dimensional tolerances so that the alignment operations are reduced to a minimum.

On many occassions, it has been confirmed by the Russians that the advantage of our shipments consists in the fact that once we accept a specification we will furnish line pipe to that specification with consistent quality, no matter how large the shipments may become later.

## SPECIAL RUSSIAN DEVELOPMENTS

Occurrence of long ruptures in large diameter transmission pipelines and the axiomatic necessity to solve these problems were the background to special Russian developments such as multi-layer pipe, quasi-monolithic pipe and crack arrestors. Moreover, owing to the state-of-the-art of Russian plate mills it was not possible for them to produce economically large tonnages of expensive thermomechanically processed steel plate needed for the line pipe.

The commor goal of all these developments is to improve the resistance of line pipe to long running cracks without adversely affecting the production efficiencies and without raising the cost of steelmaking and plate production. Two-layer spiralweld pipes and multi-layer pipes produced by joining several individual pups made by winding up hot rolled strip are known to exist. But these products could not compete with the monolithic pipe because of their instability and the lack of possibility to test them. Quasi-monolithic pipe (multi-layer pipe) made from rolled multi-layer plate that was produced by suspending plates in the casting mould and subsequent rolling were found to resist the development of long-running cracks in laboratory as well as full-scale burst tests. But this type of pipe is not economic.

A further step towards the improvement of pipeline safety was the development of multi-layer crack arrestors having diagonal slots in the inner layers or multi-layer hot rolled crack arrestor pups. It has been proved that these crack arrestors fulfil their function.

## FUTURE DEVELOPMENTS

We recognize from the above discussions and the published Russian work that in the future the manual operations are intended to be reduced more than in the past. This implies that human incompetence will be avoided and high efficiencies will be achieved through the use of gas metal arc welding with flux cored wires and above all through the use of flash butt welding. Apparently, the Russians are prepared to accept that certain demands such as high notch toughness and CTOD values in the weld metal and heat affected zone, which are usually specified in the western specifications, cannot be applied to the flash butt welds, as otherwise the construction of a number of pipelines cannot be completed within the planned period. They must also have thought over whether they should adopt the western fitness-for-purpose approach and thereby avoid flash welding or use other criteria for assessing the pipeline integrity. The recent publications indicate that they have decided on the new concept of using mechanised welding processes. The Russian research institutes have revised the requirements for girth welds.

The intention of incorporating crack arrestors into the pipeline system fits in well with the above concept concerning pipeline safety. In order to safeguard the important components such as compressors, slides and valves and thereby avoid failures and pipeline shutdowns the crack arrestors are intended to be incorporated in the locations of transition to smooth pipeline sections.

Considering the quality of the line pipe supplied by us and the service conditions known to us, we are of the opinion that there is no need to use such special safety measures with our line pipe. However, in view of the problematical environments in the upper northern regions it may be prudent to use crack arrestors to prevent failures in the important locations of the pipeline system. Moreover, third-party damage to an operating pipeline cannot always be excluded.

## SUMMARY

Mannesmann looks back on its ninety-year tradition in furnishing the Soviet Union with line pipe. About 20,000 km of line pipe, weighing approx. 10 million tonnes, was shipped to the Soviet Union in the period since 1970 alone.

From the very beginning, the specifications have been drawn up for line pipe intended for use in the Arctic regions. Later, the specifications became more and more stringent as the gas production moved to farther northern regions.

The steadily increasing demands have been complied with by changing over from normalized plate through thermomechanically processed plate to thermomechanically processed plus accelerated cooled plate. The developments in the alloy design (MnNbTi steel) in conjunction with the accelerated cooling technology (TM-

MACOS) have enabled the yield strength to be raised from 412 N/mm² to 510 N/mm². At the same time, the DWTT transition temperature has been lowered from 0 °C to -20 °C. The Charpy V-notch impact energy has been increased from 60 J at -20 °C to 95 J at -20 °C. These improvements are attributed in the paper to the microstructural changes, including the reduction of pearlite content, refinement in the grain size, increases in the dislocation densitiy and changes in the precipitation characteristics.

The development of steels with the tensile strength values of 700 N/mm² and 770 N/mm² is addressed.

Quoting molybdenum bearing steels as an example, it is shown how the economic constraints have led to changes in alloy design and faster developments in processing technology.

Russian developments such as multi-layer line pipe, quasi monolithic line pipe, crack arrestors and flash butt welding of girth welds are outlined.

## REFERENCES


/1/ W. M. Hof, M. K. Gräf, B. Hoh, H. G. Hillenbrand, P. A. Peters
**New High-strength Large-diameter Pipe Steels**
CSM Conference, HSLA Steels '85, Beijing (China)

/2/ M. K. Gräf, H. G. Hillenbrand, P. A. Peters
**Accelerated Cooling of Plate for High-strength Large-diameter pipe**
Conference on accelerated cooling of steels, Pittsburgh, August 19 - 21, 1985

/3/ H. G. Hillenbrand, W. M. Hof, B. Hoh
**Modern Line Pipe Steels and the Effect of Accelerated Cooling**
4th International Steel Rolling Conference, Deauville (France), June 1 - 3, 1987

# RECENT DEVELOPMENT OF LINE PIPE STEELS AT CHINA STEEL CORPORATION

**Shyi-Chin Wang, Shi-Rong Chen, Chuen-Taur Wu, Yeong-Tsuen Pan**
Research and Development Department
China Steel Corporation
Kaohsiung, Taiwan, R.O.C.

Abstract

During the last few years, a large scale of efforts has been made on the development of line pipe steels at China Steel Corporation. The development has been conducting through a series of works including laboratory research, on line trial and mass production.

At the stage of laboratory research, the effects of rolling schedules and chemical composition on the properties of steels are evaluated. According to the results, the chemical composition and rolling process are designed for API X65 and X70 steels. Tryout experiments were conducted both in pilot mill and production line with satisfied results.

The mass production of line pipe steels in the plate mill of China Steel Corporation has also been conducted. More than eighty thousand tons of API X52 has been manufactured during the last 2 years for a 30'' diameter 400 km long gas transmission pipe in Taiwan.

## Introduction

The pipes are the most economical means of the transpotation of natural gases and oils. The drive for a high transport efficiency has brought about a steady increase in the operation pressure of the transmission pipelines. To meet such a requirement, a great progress [1,2] has been made on the development of linepipe steels with high strength, high toughness and good weldability. Practical applications of the controlled rolling[3,4] and beneficical utilization of microalloying elements[4-6] such as niobium, vanadium and titalium have provided the groundwork for this progress. As a new fellow in steel industry, China Steel Corporation has also made great efforts on the development of thermomechanical treatment and microalloying technology to manufacture high strength low alloy steels. The high quality linepipe steels are conducted. During the last few years, API X52 grade steel was sucessfully manufactured in mass production, and the properties requirements of API X60, X70 were also fully achieved in pilot production.

In this paper, the laboratory studies of API X65 and X70 grade steels will firstly be described. The effects of chemical compositions and process parameters in the controlled rolling process on the mechanical properties will be discussed. Secondly, the progress in the pilot production of API X60, X65 and X70 steels will be briefly described. Finally, the results of mass production of API X52 steels in production line will be demonstrated.

## Procedures

The experimental material was melted in a vacuum induction furnace and casted in steel mold with dimensions of 300mm in width and 210mm in thickness. Each cast was 250 Kg in weight. The chemical composition of steels is listed in Table 1. The experimental steels can be devided into six groups, i.e., Mn and V series, to be used for the evaluation of the effects of Mn and V respectively; FRT and Re series, to be used for the study of the effects of Finish Rolling Temperature and Reduction at low temperaturer region respectively; L and F series, to be used for Laboratory and Field tryout rolling which is designed for API X65 and X70 and tested in laboratory and production line respectively.

All of the steels except the F series were rolled in the laboratory rolling mill. Before rolling, the steels were heated at 1175 C for 2 hours. During rolling, the temperature was measured using pyrometer. In the case of low finish rolling temperature lower than 770°C an thermal couple was embeded at the midthickness

of slab to measure the temperature. For the field tryout experiments, a commercial CC slab was selected and rectangular holes were sectioned. Two ingots from the laboratory were then embedded and welded on these holes and the slab was reheated and rolled in the plate mill. After rolling the laboratory material was cut out to evaluate the mechanical properties. The rolling schedule for all of the steels is listed in Table 2.

For tensile and impact tests, the specimens were sectioned from both of the transverse and longitudinal directions of plate. The tensile specimens were in full thickness, 25mm wide in reduced area and 50mm in gauge length. For impact test, standard 10 x 10 x 55mm Charpy V-notch specimens were machined. The impact energy and shear fracture area ratio were measured.

## Results and Discussion

The microstructure of Mn series steels is shown in Figure 1. From the microstructure it can be seen that as the Mn content is increased the grain size of ferrite is decreased and the morphology of second phase is being modified from pearlite to degenerate pearlite. In steel Mn3, see in Figure 1, some Bainite/Martensite islands can also be found.

Figure 2 shows the effect of Mn content on the mechanical properties of steels. It can be seen that the strength increases with the increasing of Mn content. This can possibly result from a combined effect of solid solution hardening, grain refinement and second phase hardening as the amount of Mn is increased. When the Mn content is high, e.g. Mn3 with 1.66 Mn, the Lüders strain is being eliminated and thus results in an apparent drop of yield strength. In this steel, the formation of bainite and martensite islands introduces free dislocations in the neighborhood which may result in a continuous yielding behavior and thus a lower yield strength. As shown in Figure 2, when the steel Mn3 was heated at 550°C for one hour, the Lüders strain is recovered and the yield strength is increased.

Increasing the Mn content has resulted in the grain refinement and thus better impact toughness. However, when the Mn content is too high such as that of steel Mn3, the upper shelf energy is decreased seriously. It was also found that the amount of separation on the fracture surface of steel Mn3 was much more than that of steels Mn1 and Mn2. This resulted in a reduced upper shelf energy[7] of Mn3 steel. As shown in Figure 3, when steel Mn3 was heated at 650°C for one hour then rapidly cooled, the separation on fracture surface can greatly be eliminated and the upper shelf energy can be increased.

The effects of V content on the mechanical properties are shown in Figure 4. Because of the precipitation hardening effect of Vanadium carbides, the strength of steel is increased with the increasing V content. In the V series steels, a small amount of Ti was added such that the vanadium precipitate is primarily to be VC which gives smaller strengthening effects than that of VN[8,9]. Although the precipitation hardening is detrimental to the toughness of steel[10], the results showed smaller or negligible effects of V content on the toughness.

The effects of Finish Rolling Temperature (FRT) on the grain size and mechanical properties are shown in Figure 5. A discontinuous point of mechanical properties can be found around 770°C which is very close to the calculated Ar3 temperature[11] and therefore this temperature can be considered to be the Ar3 temperature of the steel used. The lower the FRT, the smaller the grain size was found. At FRT higher than the Ar3 temperature the yield strength is inversely propotional to the FRT due to the grain refinement effect. But the tensile strength follows the opposite trend to the yield strength. According to the quantitative metallography it is possible to estimate the strength contribution from precipitation hardening. The calculated results according to

$$EQ^{(12)}: \sigma_{ppt} = YS - (\sigma_o + \sigma_{ss} + kd^{-\frac{1}{2}})$$

$$\sigma_o = 6.5 kg/mm^2, \quad \sigma_{ss} = 3.25\,(Mn\%) + 8.4(Si\%)$$

$$k = 1.81 kg/mm^{-3/2}$$

are listed in Table 3. As shown in this table at temperature above Ar3 the precipitation hardening effect decreases with the decreasing FRT. The microhardness of ferrite matrix is listed in Table 3. These results reveal that at lower FRT, the ferrite strength is lower. From these results it can be seen that lowering the FRT, the effects of precipitation hardening are reduced and thus the tensile strength of steel is decreased.

Because of the grain refinement and less precipitation hardening effect with lower FRT, see in Figure 5, the total elongation and 50% FATT are improved as the FRT is lowered. However, when FRT is lower than Ar3 temperature, both of the tensile and yield strengths are increased significantly without a serious change in impact toughness. Accompanied with the increase in strength of steel, the ductility is decreased.

The effects of total reduction at low temperature austenite phase region on the ferrite grain size and mechanical properties can be realized from Figure 6. It can be seen that the

greater the amount of reduction, the finer the grain size of ferrite. This grain refinement effect becomes less pronounced for reduction above 70%. Higher amount of reduction at the low temperature austenite phase region enhances the strain induced precipitation in austenite phase(13) such that the available amount of Nb and V becomes smaller to precipitate in ferrite phase, therefore, the tensile strength is decreased. Figure 6 also shows that the yield strength increases with the increasing reduction initially due to the grain refinement effect. But in the case of reduction above 70% the grain refinement diminishes and, consequently, the less precipitation hardening effect causes the decrease in yield strength. From this figure, the beneficial effects of higher reduction in the low temperature austenite region to the total elongation and FATT can also be visualized.

Based on the above results, the chemical composition and the rolling process for APIx60, x65 and x70 were designed. The confirmation test was first conducted in a laboratory rolling mill. The results are listed in Table 4. The tensile properties of steels 13 and 18 with thickness 13 and 18mm can all satisfy the API x60 specifications. The 50% FATT of Charpy V-notch impact test for these specimens is lower than -80°C and the upper shelf energy is around 20kg-M in longitudinal direction. The composition of steel 13B is similar to that of steel 13 but without Ti-addition. Because the free N content available for the VN formation in ferrite phase after rolling to achieve the precipitation hardening effect is higher for the Ti-free steel. It can be found that the tensile strength of steel 13B is higher than that of steel 13 and can meet the API x70 specifications. The toughness of steel 13C is poorer than that of steel 13 some extent. The composition of steel 13C is also similar to that of steel 13, however, the total amount of reduction in two-phase region was about 35% and the finish rolling temperature is around 700°C which is lower than that of steel 13, 70°C. The tensile properties show that two-phase rolling results in an increase in strength which achieves the requirements for API x70. The Charpy test results show that after rolling in two phase region the absorbed energy of steel decreases, the amount of separation on the frature surface increases and the FATT is not greatly influenced.

The enlargement of the results from the laboratory scale to the mass production is accomplished first by evaluating the mechanical properties of steels after on-line rolling. For this purpose, two experimental test ingots were embedded and welded on the rectangular holes of a commercial CC slab and then rolled on the production line. The results are listed in Table 5. It was found that steel plates thus rolled on the production line possess similar strength but poorer toughness than that of laboratory products. For example, the composition of steel F1 is close to that of steel 13. The difference in yield and tensile strengths are within 1kg/mm$^2$ between these two steels. The 50% FATT of steel F1 is -40°C which is about 40°C high than that of steel 13. The poorer toughness of steel F1 is possibly due to a high slab reheating temperature which results in both of the coarse and mixed grains in the steel plates. The composition of steel F2 is similar to that of steel F1 except that carbon content is 0.047% higher. The test results revealed that carbon increases the strength and impairs the toughness significantly.

The final stage of work on the development of linepipe steels was completed by rolling commercial API slabs on the production line. Some of the results are listed in Table 6. The process conditions of steels A and B are about the same except that steel A was reheated at 1250°C and steel B, at 1100°C. It can be seen that at low reheating temperature practice of steel B improves the toughness significantly without loosing the strength.

The plate mill at CSC has already rolled API x52 linepipe steel over 80,000 tons during the last 2 years. Although the requirements on mechanical properties for API x52 are much lower than that for API x70, however, the requirements on the surface and internal quality, flatness and dimensional tolerance are strict. At the beginning many plates were rejected because of the internal defects. Great efforts have been performed in the steel making, refining and continuous casting process to improve the internal quality of slabs. Finally, the total production yield of this steel was over 90%. From this experience CSC gains great confidence to meet more strict challenge on the production of high grade linepipe steels.

## Conclusions

The development of high grade line pipe steels at CSC is progressing step by step. The basic effects of composition and rolling process on the properties have been extensively studied in the laboratory. The composition and rolling process for API x60, x65 and x70 are designed. The confirmation tests are conducted both in laboratory and production line. The results are encouraging and the success in mass production of API x52 has come to the experience of manufacturing x60, x65 even x70 line pipe steels.

## Reference

1. M. A. Civallero, C. Parrini and N. Pizziment, Microalloying 75, union carbide corporation, New York,451-469 (1977).
2. A. P. Coldren and J. L. Mihelich, Molybdenum

Co. 14-28 (1981).
3. T. Tanaka, Inter. Met. Rev. 4, 185-212 (1981).
4. A. M. Sage, Metals Technol. 8, 94-102 (1981).
5. R. Roussev, Trans. ISIJ. 13, 105-110 (1973).
6. D. P. Dunne, T. Chandra and S. Misra, HSLA Steels Metallurgy and Applications, AMS, 207-212 (1983).
7. B. L. Bramfitt and A. R. Marder, Metall. Trans. 8A, 1263-1273 (1977).
8. R. K. Amin, M. Korchynsky and F. B. Pickering, Metals Technol. 8, 250-262 (1981).
9. N. K. Balliger and R. W. K. Honeycombe, Metall. Trans. 11A, 421-429 (180).
10. K. J. Irvine, F. B. Pickering and T. Gladman, JISI. 205, 161-182 (1967).
11. C. Ouchi, T. Sampei and I Kozasu, Tans. ISIJ. 22, 214-222 (1982).
12. E. A. Almond and R. S. Irani, Metals Technol. 8, 339-351 (1981).
13. J. J. Jones and I. Weiss, Met. Science, 13, 238-245 (1979)

Table 1. The chemical compositions of experimental steels.

| Steel | C | Si | Mn | P | S | Nb | V | Ti | Al | Cu | Ni | Nppm |
|---|---|---|---|---|---|---|---|---|---|---|---|---|
| Mn1 | .075 | .29 | 1.18 | .011 | .007 | .037 | .070 | .014 | .022 | .16 | .07 | 28 |
| Mn2 | .078 | .30 | 1.39 | .015 | .005 | .034 | .074 | .017 | .026 | .16 | .08 | 25 |
| Mn3 | .083 | .28 | 1.66 | .009 | .004 | .034 | .080 | .015 | .026 | .24 | .20 | 28 |
| V1 | .100 | .24 | 1.42 | .012 | .005 | .043 | .036 | .017 | .030 | .18 | .18 | 52 |
| V2 | .078 | .30 | 1.39 | .015 | .005 | .034 | .074 | .017 | .015 | .16 | .08 | 52 |
| V3 | .084 | .24 | 1.40 | .010 | .012 | .042 | .108 | .019 | .027 | .19 | .18 | 65 |
| V4 | .097 | .25 | 1.39 | .012 | .005 | .042 | .130 | .014 | .027 | .18 | .19 | 60 |
| FRT | .080 | .30 | 1.23 | .014 | .007 | .030 | .075 | .007 | .030 | .15 | .15 | 33 |
| Re | .081 | .22 | 1.24 | .010 | .011 | .033 | .091 | .020 | .017 | .20 | .20 | 52 |
| 13 | .095 | .24 | 1.45 | .007 | .007 | .045 | .095 | .012 | .020 | .22 | .19 | 56 |
| 18 | .100 | .28 | 1.49 | .008 | .007 | .047 | .096 | .013 | .021 | .21 | .20 | 56 |
| 13B | .101 | .30 | 1.45 | .011 | .009 | .040 | .093 | --- | .025 | .18 | .18 | 54 |
| 13C | .107 | .29 | 1.40 | .009 | .008 | .037 | .090 | .018 | .030 | .18 | .16 | 47 |
| F1 | .083 | .24 | 1.44 | .010 | .009 | .048 | .097 | .013 | .027 | .19 | .16 | 50 |
| F2 | .130 | .24 | 1.45 | .011 | .009 | .047 | .098 | .024 | .031 | .19 | .16 | 66 |

Table 2. The rolling parameters of experimental steels

| Steel | RHT °C | initial t (mm) | holding t (mm) | finish t (mm) | FRT °C |
|---|---|---|---|---|---|
| MnX | 1175 | 210 | 40 | 12 | 800 |
| VX | 1175 | 210 | 40 | 12 | 800 |
| FRT1 | 1175 | 50 | 27 | 12 | 908 |
| FRT2 | 1175 | 50 | 27 | 12 | 870 |
| FRT3 | 1175 | 50 | 27 | 12 | 843 |
| FRT4 | 1175 | 50 | 27 | 12 | 810 |
| FRT5 | 1175 | 50 | 27 | 12 | 770 |
| FRT6 | 1175 | 50 | 27 | 12 | 760 |
| Re1 | 1175 | 150 | 27 | 12 | 775 |
| Re2 | 1175 | 150 | 33 | 12 | 774 |
| Re3 | 1175 | 150 | 40 | 12 | 785 |
| Re4 | 1175 | 150 | 50 | 12 | 790 |
| 13 | 1175 | 210 | 40 | 13 | 770 |
| 18 | 1175 | 210 | 55 | 18 | 775 |
| 13B | 1175 | 210 | 40 | 13 | 810 |
| 13C | 1175 | 210 | 40 | 13 | 700 |
| FX | 1250 | 210 | 40 | 13 | 770 |

Table 3. The contribution of precipitation hardening on the yield strength and the microhardness of ferrite matrix (10P).

| Steel | YS | $\sigma_0$ | $kd^{-\frac{1}{2}}$ | $\sigma_{ss}$ | $\sigma_{ppt}$ | Hv |
|---|---|---|---|---|---|---|
| FRT1 | 42.9 | 6.5 | 16.1 | 8.2 | 12.1 | 219 |
| FRT2 | 43.3 | 6.5 | 17.5 | 8.2 | 11.1 | 205 |
| FRT3 | 43.5 | 6.5 | 19.2 | 8.2 | 9.6 | 195 |
| FRT4 | 44.5 | 6.5 | 20.6 | 8.2 | 9.2 | 190 |
| FRT5 | 46.5 | 6.5 | 21.0 | 8.2 | 10.8 | --- |
| FRT6 | 49.0 | 6.5 | 21.7 | 8.2 | 12.6 | --- |

Table 4. The mechanical properties of tryout product in laboratory.

| Steel | YS | TS | YS/TS | EL | Impact Absorbed Energy (Kg-M) | | | | FATT |
|---|---|---|---|---|---|---|---|---|---|
| | kg/mm² | kg/mm² | | % | -20°C | -40°C | -60°C | -80°C | °C |
| 13 | 51.1 | 57.6 | .89 | 40.4 | 24.0 | 21.0 | 21.2 | 15.9 | <-80 |
| 18 | 51.7 | 58.3 | .89 | 43.3 | 19.4 | 17.3 | 14.6 | 11.9 | <-80 |
| 13B | 55.9 | 63.2 | .88 | 40.3 | 15.1 | 12.5 | 11.5 | 7.9 | -75 |
| 13C | 55.0 | 63.6 | .86 | 38.6 | 13.3 | 10.8 | 9.6 | 8.6 | <-80 |

Table 5. The mechanical properties of experimental steels F1 and F2 rolled in the production line.

| Steel | YS | TS | YS/TS | EL | Impact Absorbed Energy (Kg-M) | | | | FATT |
|---|---|---|---|---|---|---|---|---|---|
| | kg/mm² | kg/mm² | | % | -20°C | -40°C | -60°C | -80°C | °C |
| F1 | 50.3 | 58.4 | .86 | 39.5 | 15.4 | 11.8 | 2.4 | 1.2 | -40 |
| F2 | 52.3 | 63.5 | .82 | 34.3 | 9.6 | 4.5 | 2.4 | 1.1 | -30 |

Table 6. The composition, rolling process and mechanical properties of steels manufactured in the production line.

| Steel | CEQ | Nb | V | RHT | Hodling | Finish | FRT | YS | TS | EL | Charpy | DWTT |
|---|---|---|---|---|---|---|---|---|---|---|---|---|
| | % | % | % | °C | t (mm) | t (mm) | °C | Kg/mm² | Kg/mm² | % | 50%FATT | 50%FATT |
| A | .37 | .04 | .08 | 1250 | 48 | 16 | 770 | 47.6 | 58.4 | 46.2 | -35 | -10 |
| B | .37 | .04 | .08 | 1100 | 48 | 16 | 770 | 46.6 | 57.1 | 47.6 | -80 | -50 |

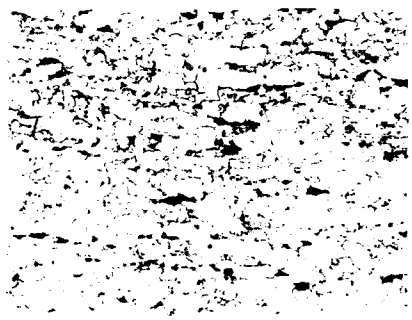

Mn1

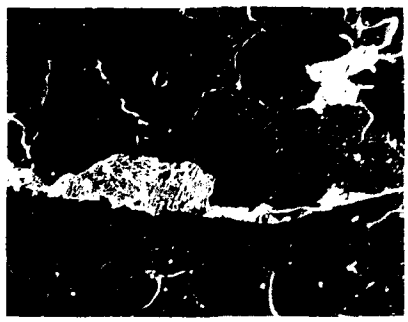

Mn1

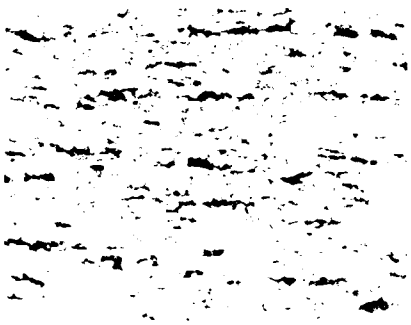

Mn2

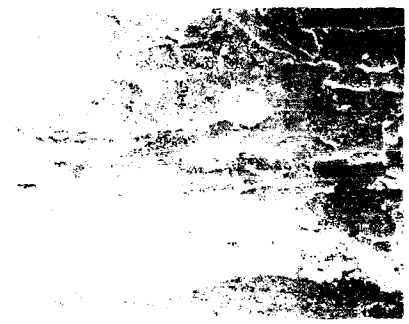

Mn2

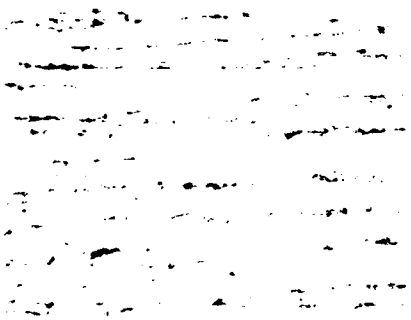

Mn3

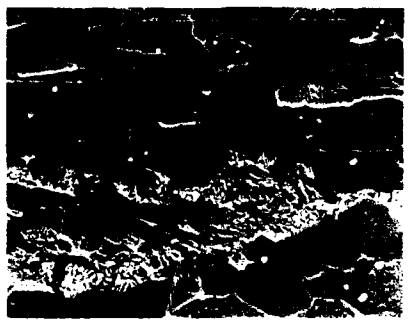

Mn3

100μm

10μm

Figure 1 The microstructure of Mn series steels.

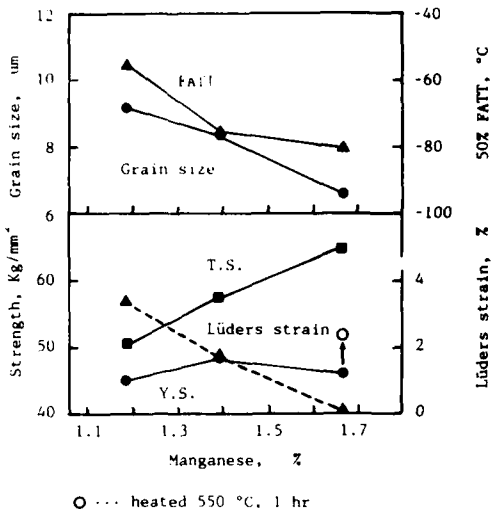


Figure 2 Effect of Mn content on the mechanical properties of steels.

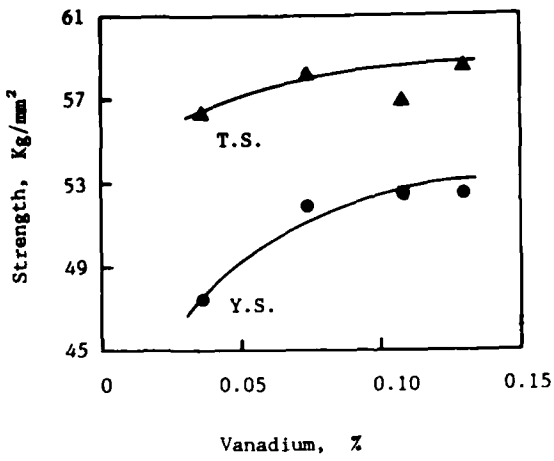


Figure 4 Effect of V content on the strength of steels.

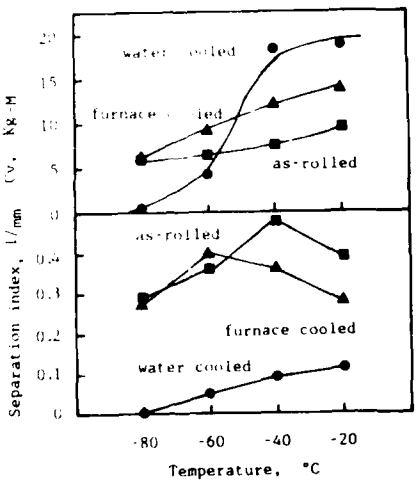


Figure 3 The Charpy impact absorbed energy and separation index of steel Mn3 as a function of test temperature.

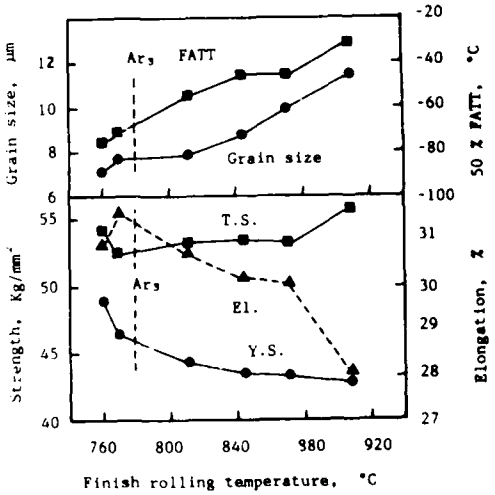


Figure 5 Effect of finish rolling temperature on the grain size and mechanical properties of steels.

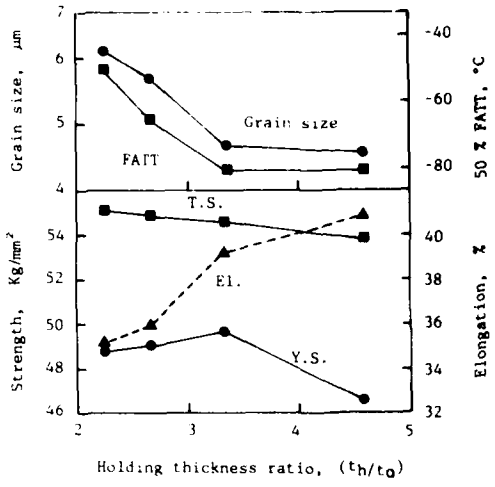


Figure 6 Effect of holding thickness ratio on the grain size and mechanical properties of steels.

# INDUSTRIAL DATA ON THE FIRST API X80 LINE PIPE PRODUCED IN LATIN AMERICA

**V. Lazzari, S. Machado, C. Silva, O. Neto, J. Moreira**
COSIPA Works
São Paulo, Brasil

ABSTRACT

The world-wide trend in HSLA line pipe steels is to increase the steel strength and toughness requirements allied to thickness reduction of pipe wall, for the same outside diameter.

Grade X80 requirements can be met with several chemical compositions and production processes. The objective of this development was to test Nb-V-Cr-Ni and Nb-Mo-Ti steels in controlled rolled plates, 9.53 mm thicknes for 22" OD pipes.

The alloy design aimed at Ceq ≤ 0,44% and 50% FATT under -60°C through a poligonal ferrite microstructure containing martensite - austenite (MA) islands as the dispersed phase.

This article describes the experiment results obtained under industrial scale for production of X80 UOE pipes.

IT IS WELL-KNOWN that there has been, since the last decade, a strong trend in the pipe steel consuming in the direction of steels with higher strength and superior toughness and weldability characteristics. For Grade X80 these requirements would be difficult to obtain with a ferrite-perlite steel. In addition typical loss in yield strength after pipe production would make mandactory the use of an alloy design that in order to guarantee X80 strength level in the pipe product could seriously affect toughness and weldability properties as well as create production problems in the pipe plant.

In order to improve the above-mentioned steel characteristics, it was used low C ( ≤ 0,10%) and specific microalloyings combined with controlled rolling to get a microstucture consisting essentially of poligonal ferrite plus martensite-austenite (MA) constituent islands that promote a continuous stress-strain curve. Therefore, the pipe production in the U-O-E process would be facilitaded (low yield

strength increase after pipe manufacturing process).

## INDUSTRIAL PRODUCTION OF PLATES X80

The steelmaking procedures used for API X80 were the same as those for Grade X70 with high toughness, that is, the utilization of RIC process (Refining by Calcium Injection) developed by COMPANHIA SIDERÚRGICA PAULISTA-COSIPA which acts in the quantity and morphology inclusions, combining low level of sulfur and oxygen.

Table I shows the chemical compositions obtained where the requirements $C \leq 0,10\%$ and $Ceq \leq 0,44\%$ are met.

The controlled rolling schedule used for the plates is shown below:

- Reheating temperature = 1100°C
- Total thickness reduction = 95%
- Total finishing reduction in the non-recrystallization region = 67%
- Finish rolling temperature = 740°C

It was used low reheating temperature to avoid intensive grain growth and also mixed grains in the final product. Strong reduction aimed at the first stage of controlled rolling improved a grain refining through recrystallization. The second stage was carryed out above and below the austenite-ferrite transformation temperature to obtain higher strength and a lower ductile-to brittle transition temperature.

## RESULTS AND DISCUSSION

Average tensile and toughness properties for plates produced from two heats are shown in Table II.

Based on a work by Glodowski and Thompson (1) it could be anticipated from the 2% yield strength results of the plates produced that X80 strength level could be achieved after pipe production.

Pipe production followed its normal process with 1% cold expansion. The API specimens were taken from the same equivalent position as those from the plate product.

Table III shows the results obtained in pipes with the Nb-V-Cr-Ni steel showing strength levels higher than the Nb-Mo-Ti steel. The good relationship between $YS_{2\%}$ plate x $YS_{0,5\%}$ pipe was confirmed in this experience, Figure 1.

In Figure 2 it can be observed that in spite of Nb-V-Cr-Ni steel having presented higher strength, the Nb-Mo-Ti steel exhibited higher mechanical hardening during pipe forming. This fact is due to the different stress strain curve. The Nb-Mo-Ti showed a continuous curve and the Nb-V-Cr-Ni steel presented a small sharp knee stress-strain curve. Therefore, the Nb-Mo-Ti alloy design is prefered by the pipe manufacturer as its higher work hardening allows X80 pipe production from plate product with lower yield strength, facilitating pipe forming.

TABLE I

CHEMICAL COMPOSITION OF STEEL

| Steel | C | Mn | Si | P | S** | Al | Nb | V | Cr | Ni | Mo | Ti | N | Ceq* |
|---|---|---|---|---|---|---|---|---|---|---|---|---|---|---|
| 1 | .09 | 1.56 | .37 | .014 | .003 | .022 | .044 | .066 | .20 | .22 | - | - | 0.007 | .42 |
| 2 | .08 | 1.53 | .21 | .017 | .005 | .026 | .026 | - | - | - | .34 | .016 | 0.004 | .40 |

* IIW formula

** Sulfide shape control

TABLE II

MECHANICAL PROPERTIES FOR PLATES

| STEEL | Y.S. (MPa) | T.S. (MPa) | EL (%) | DWTT (-20°C) | CVN(-20°C) (J/cm²) |
|---|---|---|---|---|---|
| 1 | 565 | 703 | 28 | 100% | 102 |
| 2 | 488 | 663 | 31 | 100% | 174 |

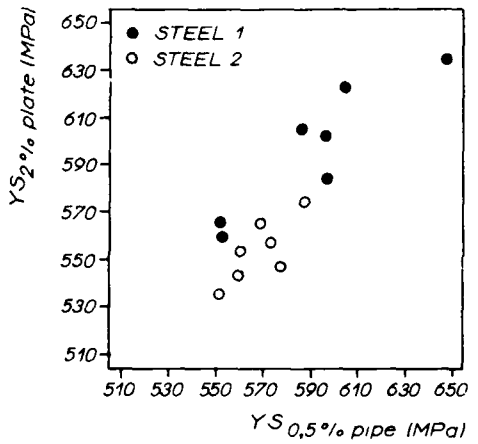


FIG 1 - RELATIONSHIP BETWEEN $YS_{2\%\ plate} \times YS_{0,5\%\ pipe}$

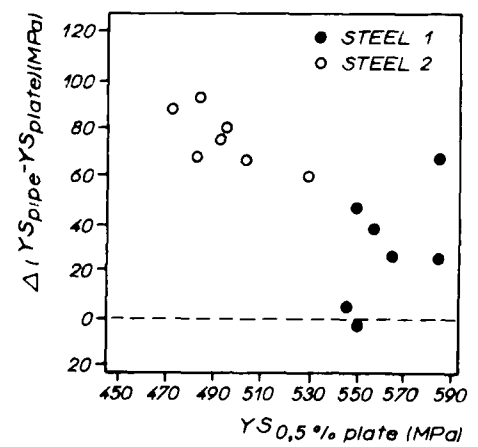


FIG 2 - RELATIONSHIP BETWEEN $\Delta\,|\,YS_{pipe} - YS_{plate}\,| \times YS_{plate}$

TABLE III

MECHANICAL PROPERTIES FOR PIPES

| STEEL | Y.S. (MPa) | T.S. (MPa) | EL (%) | DWTT (-20°C) | CVN(-20°C) (J/cm²) |
|---|---|---|---|---|---|
| 1 | 590 | 721 | 26 | 100% | 87 |
| 2 | 564 | 694 | 30 | 100% | 123 |

In fact, both plate and pipe production occurred without overload in the equipment.

Impact results in transverse specimens are shown in the transition curves, Figure 3 and 4, for plate and pipe from both steels. It is observed that Nb-Mo-Ti steel shows superior toughness property than Nb-Cr-V-Ni steel both in plates and pipes. It can be noted that the transition temperature is very low, probably under -100°C. These results are similar to those presented by other authors (2,4,14) as regards absorved energy and transition temperature, and for the carbon levels under consideration.

## MICROSTRUCTURES

The microstructural analysis was done by optical and transmission (TEM) microscope.

Nb-V-Cr-Ni STEEL - The observed microstructure shows presence of elongated ferrite grains with MA islands distributed at random as it can be seen in Figure 5 (MA black regions).

The average ferrite grain size was 5.79 $\mu$m and the MA volumetric fraction 13.4%. It was noted dislocation arrangements inside the ferrite grains (see Figure 6), interacting with existing precipitates, which are especially fine, Figure 7.

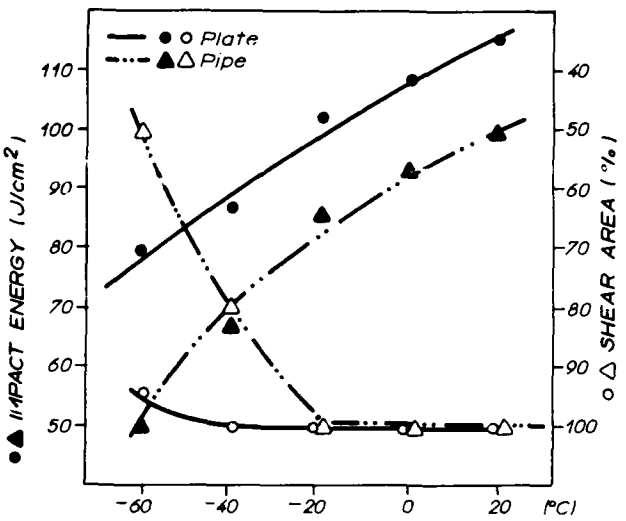


FIG:3 - TRANSITION CURVES - TRANSVERSE SPECIMENS (STEEL 1)

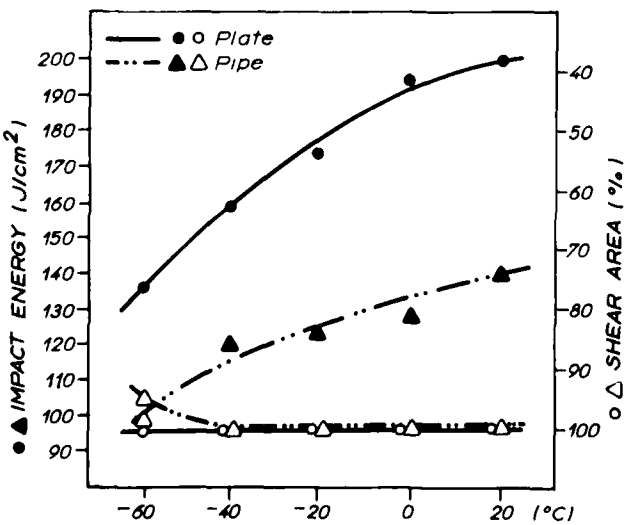


FIG:4 - TRANSITION CURVES - TRANSVERSE SPECIMENS (STEEL 2)

The identification analysis of these precipitates showed the presence of NbC, NbN, VC and VN, of which NbC and VC were the finest ones. Also chromium carbides and aluminates were identified These sizes of main precipitates are as follow:

| Precipitate | Size Range of the Precipitates |
|---|---|
| NbC, VC | 10 - 40 nm |
| NbN, VN | 25 - 60 nm |
| (Cr, C) | 200 - 400 nm |

An optical photomicrograph is shown in Figure 8.

Nb-Mo-Ti STEEL - The observed microstructure was identical to the one obtained in the Nb-V-Cr-Ni steel, see Figure 9 and 10. The average ferrite grain size was 6.35 $\mu$m and the MA volumetric fraction 16.7%.

It was also observed the presence of NbTi and TiN (cubic precipitates) besides NbN, NbC, AlN and $Mo_2C$.

This carbide distribution can be seen by TEM replica in the light field of Figure 11. The precipitate sizes observed are as follows.

| Precipitate | Size Range of the Precipitates |
|---|---|
| TiN | 200 - 500 nm |
| NbTi | 25 - 200 nm |
| Nb (C,N) | 50 nm |
| $Mo_2C$ | 150 - 500 nm |

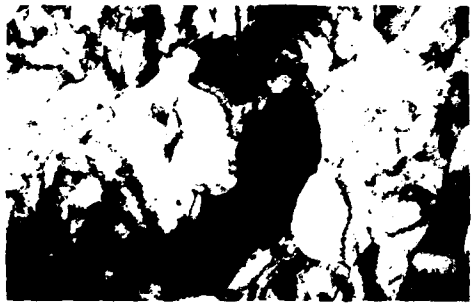

Fig. 5: Microstructure showing elongated ferrite grains and MA islands in the black regions (4000 x)

Fig. 6: Dislocation arrangements inside the ferrite grains (15000 x)

Fig. 7: Transmission electron micrograph, light field replica with fine precipi tates (10000 x)

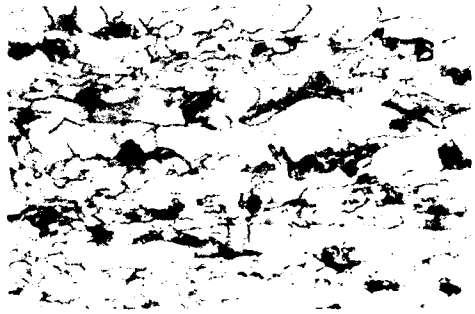

Fig. 8: Optical micrograph showing microstructure of Nb-V-Cr-Ni steel (775 x)

Fig. 9: Microstructure showing elongated ferrite grains and MA islands in the black regions (4000 x)

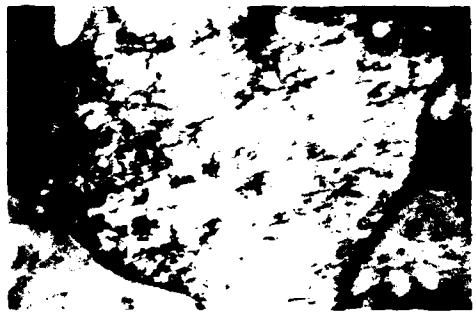

Fig. 10: Dislocation arrangements inside the ferrite grains (15000 x)

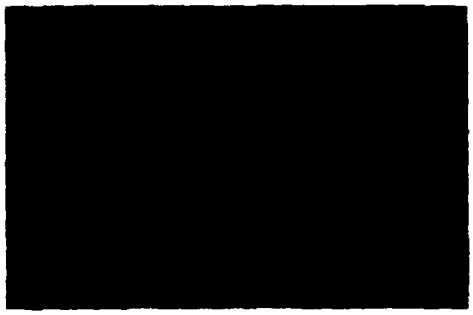

Fig. 11: Transmission electron micrograph, light field replica with fine precipitates (10000 x)

Fig. 12: Optical micrograph showing microstructure of Nb-Mo-Ti steel (775 x)

Figure 12 shows the optical photomicrograph of the obtained structure in Nb-Mo-Ti steel. As it can be observed the ferrite grain and precipitate sizes in the Nb-V-Cr-Ni steel were smaller than those in the Nb-Mo-Ti steel, which were processed under the same conditions.

## WELDING RESULTS

Welding - The investigations was made on a pilot scale and the seam welds were made with a single pass on each side by two wires SAW process. Groove preparation and seam welding conditions are shown in Table IV.

The flux/wire combination used was according to AWS A 5.17 F72 EM 12 K classification. Therefore, as the present results were the first ones in Brazil to develop X80 steel grade adequate welding consumables for this grade are not easily available yet. Thus, in this section comments are not made about weld metal properties.

The tensile results were identical to the plate and the fracture location was in the base metal.

Hardness Profile Across Welded Joint - The variation in hardness across welded samples of Nb-V-Cr-Ni and Nb-Mo-Ti are shown in Figure 13. It can be observed that both steels have HAZ hardness similar to that of parent metal.

Impact Properties - The weldment toughness is shown in Figures 14 and 15 as a function of test temperature for notches at the weld metal, fusion line and 1,3,5 mm far from the fusion line. Independently of notch location in the welded joint, Nb-Mo-Ti steel presented better results than Nb-V-Cr-Ni steel, as was with plate properties.

Hardness - To examine the HAZ hardenability, the maximum hardness test was made in accordance with JIS 23101. The SMAW process was used for this purpose. Typical results indicated that the Nb-V-Cr-Ni and Nb-Mo-Ti had a maximum of 245 and 207 HV 10 respectively.

TABLE IV

WELDING PROCEDURES - SAW

| | LEAD | | TRAIL | | WELDING SPEED (cm/min) | HEAT INPUT (kj/cm) | GROOVE PREPARATION |
|---|---|---|---|---|---|---|---|
| | (A) | (V) | (A) | (V) | | | |
| BACKING | 550 | 34 | 500 | 36 | 150 | 15 | 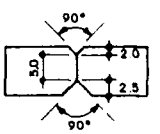 |
| FINAL | 600 | 34 | 550 | 36 | 150 | 16 | |

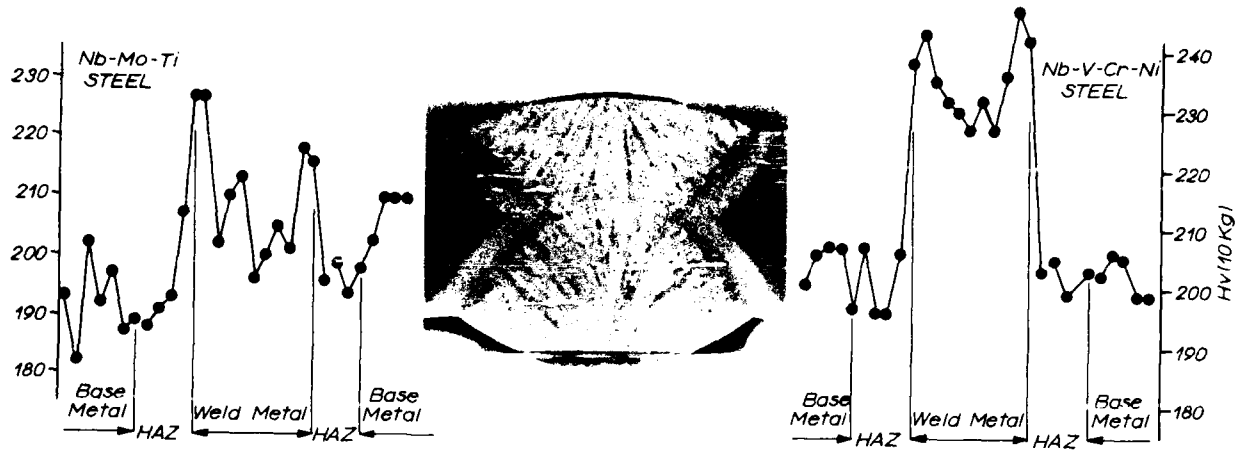


FIG. 13 - PROFILE OF HARDNESS ACROSS WELDED JOINT IN BOTH STEELS

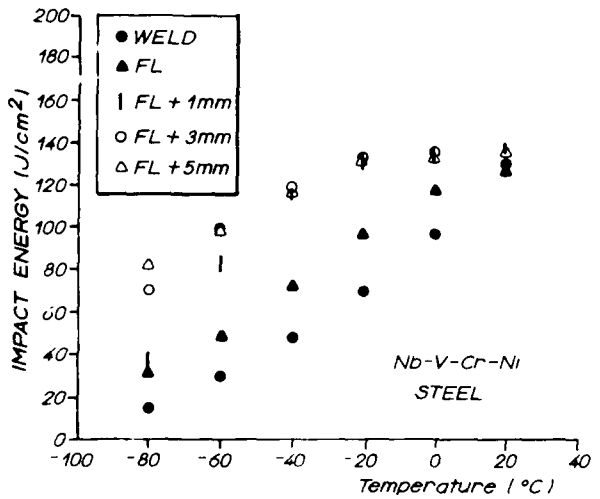


FIG 14 - TRANSITION CURVES - TRANSVERSE SPECIMENS IN THE WELDED JOINT FOR Nb-V-Cr-Ni STEEL.

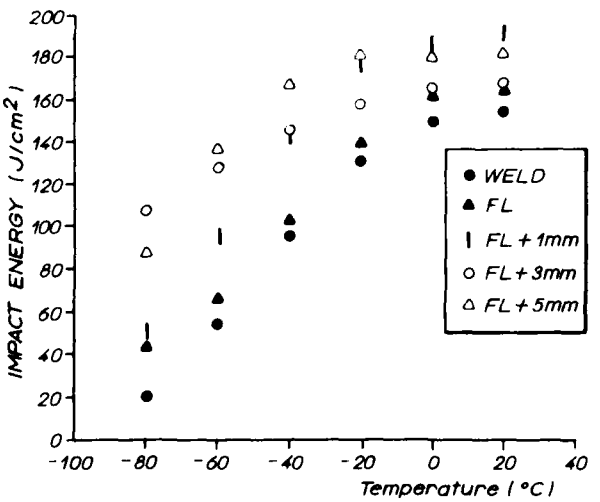


FIG. 15 - TRANSITION CURVES - TRANSVERSE SPECIMENS IN THE WELDED JOINT FOR Nb-Mo-Ti STEEL

## CONCLUSION

Based on the industrial results obtained in COSIPA, the following conclusions can be drawn:

1) It was obtained plates for the production of API X80 pipes through controlled rolling process with good mechanical properties and weldability besides good performance in the plate-and-pipe production lines.

2) The materials with a yield strength recovery after pipe production facilitated the pipe forming by using plates with lower yield strength.

3) The present work has marked the introduction of a new stage of product development in the direction of high grade and modern API steels produced by controlled rolling.

4) For attending plate specifications for API pipe production which are getting stricter and stricter COSIPA continues research and development of these materials.

REFERENCES


1. Glodowski, R.J. and J.N. Thompson. Mech. Work and Steel Proc. XI, Metal Society of Aime, 59 (1973).

2. C. Shiga and K. Amano, T. Hatomura, Y. Saito, K. Hirose, T. Choji, p. 127, "Steels for Line Pipe and Pipeline Fittings", London, England (1981).

3. H.N.Lander, J.W.Morrow, A.P. Coldron, "Steels for Line Pipe and Pipeline Fittings", London, England (1981).

4. Pontremoli, M. and P. Bufalini, A. Aprile, C. Janone, 7, Metals Technology, 504 (1984).

5. Nintz, B. Metals Technology, 7, 265 (1984).

6. N. Pizzimenti and A. de Vito, P. Bufalini, M.Pontremoli, "International Symposium of Niobium, p. 803, San Francisco, USA (1981).

7. Sage, M.A. Metals Technology, 6, 224 (1983).

8. Nara, Y. and T. Kyogoku, T. Yamura, I. Takeuchi. Metals Technology, 8, 322 (1983).

9. P. Bufalini, and G. Buzzichelli, M. Pontremolli, A. Aprile, C. Janone, A. Pozzi, "HSLA Metallurgy and Applications", p. 457, Beijing, China (1985).

10. M. Grumbach, "Microalloying 75", p. 348, Washington D.C., USA (1975).

11. T. Tanaka, "Microalloying 75", p. 350, Washington D.C., USA (1975).

12. T. Yamaguchi and T.Osuka, T.Taira, N. Ywasaki, "Microalloying 75", p. 415, Washington D.C., USA (1975).

# FRACTURE CONTROL IN NATURAL GAS AND $CO_2$ PIPELINES

**A. B. Rothwell**
NOVA Corporation of Alberta
Calgary, Alberta, Canada

ABSTRACT

Traditionally, fracture control plans for pipelines transporting compressible fluids have centred around the establishment of the necessary toughness properties for the pipeline materials. It is becoming increasingly apparent that the approach to fracture control for major, long-distance transmission systems must be much more integrated in nature, encompassing not only materials design and specification, but also the construction and operational phases. The most important feature of effective design against fracture remains the prevention of the initiation of ruptures, but this can only be accomplished with a full appreciation of the prevalent causes of failure. These include mechanical damage, during both installation and operation, corrosion, and displacement-controlled longitudinal strains which may be difficult or impossible to design against. As a result, the prevention of rupture also involves the design and quality assurance of cathodic protection and coating systems, construction surveillance and operating practices. In addition, in-service monitoring may form an integral part of an overall fracture control plan, particularly in regions of unstable or unpredictable terrain.

Recognizing that total prevention of rupture over the lifetime of a pipeline may not be achievable, a great deal of research has been carried out, and is still continuing, on the material properties required to arrest a running fracture. For methane pipelines of modest diameter operating under conventional service conditions, any of a number of existing models will give a reliable estimate of "arrest toughness", and mill specifications can be framed to give the required performance. Higher operating pressures and hoop stresses not only reveal inadequacies in the existing models, but call into question traditional ways of measuring fracture propagation resistance. Carbon dioxide and natural gas containing large fractions of higher hydrocarbons present particular difficulties and, at present, the use of crack-arrestors often represents the most suitable approach to fracture limitation for systems involving these fluids.

THE EVOLUTION OF THE gas transmission industry's formal approach to fracture control can be traced back some thirty years, to the occurrence of several long, brittle failures. The longest of these occurred in 1960 during gas testing of an NPS 30 (762 mm OD) pipeline, and extended some 13 km (8 miles). Industry-sponsored research in response to this problem resulted in the development of the Battelle drop-weight tear test, and to its virtually universal use as a means of specifying line pipe which will not support brittle fracture under the pipeline operating conditions. Beginning in the late sixties, several relatively long ductile failures also occurred, and a number of research programs were initiated which were aimed at identifying material requirements for the arrest of ductile fracture. Research in this area is still continuing, but the early outcome was the concept of an "arrest toughness", specified initially in terms of Charpy impact energy,

which could be used to reduce the probability of long ductile fractures to an acceptable level. At the same time, it was widely realized that the key element of fracture control lay in the prevention of initiation. Again, models were developed which allowed a desired tolerance to defects to be achieved by the specification of a minimum level of Charpy energy. Thus, by the seventies, the concept of a comprehensive fracture control plan had been established[1]. Typically, it was based on: (a) The specification of a high minimum shear area in the DWTT, to ensure freedom from brittle fracture propagation; (b) The specification of a minimum Charpy energy at the design temperature corresponding to a critical through-wall defect size for failure initiation which was some high fraction of the maximum attainable (typically 80 - 90%); (c) The consideration of anticipated Charpy toughness distributions in relation to the arrest toughness to ensure that, on a statistical basis, ductile fracture lengths could be limited to a desired maximum. In some cases, this would lead to the specification of an all-heat average Charpy requirement, to a higher minimum requirement, overriding the value specified for initiation resistance, or to some other means of ensuring the presence of the desired proportion of "arrest" pipe in the pipeline as constructed.

This approach is still appropriate for many conventional pipelines. In recent years, however, considerable changes have taken place in an attempt to optimize the economics of major, long-distance transmission systems. In particular, some of the changing design aspects which impact fracture control include larger diameters, new, higher-strength materials, thicker walls, higher pressures and lower temperatures, together with the transmission of gases containing substantial proportions of higher hydrocarbons. Long-distance pipeline transportation of carbon dioxide in the supercritical state for enhanced oil recovery projects has also become commonplace. The effect of these factors has not only been a great escalation in the toughness levels required, but also to call into question the existing predictive models for fracture arrest and even the way in which fracture resistance is determined. As a result, since the late seventies, use has also been made of crack-arrestors to ensure the limitation of fracture length; considerable advances have been made in their design in recent years.

At the same time as these developments have been occurring, increased operating experience with conventional pipelines designed with a rational fracture control plan has indicated the importance of detailed consideration of the causes of failure. In such pipelines, service failures initiating from material deficiencies have been extremely rare, as have been propagating fractures. Mechanical damage, whether caused during construction or in service, corrosion and, in some areas, stress corrosion have been the most important factors, with ground movement, either due to subsidence or slope stability problems, presenting a special hazard because of the difficulty of designing a priori against it. The focus of the industry's concerns for operating integrity has thus shifted somewhat, towards factors more directly related to these causes of failure.

The remainder of the present paper will concentrate on the factors controlling the initiation of rupture in the context of the principal causes of failure which have just been indicated, and on the measures available for the control of fracture length. Brief attention will also be given to the analysis of risk and economics.

## FRACTURE INITIATION

THROUGH-WALL FLAWS - In design against fracture initiation, a key consideration is whether a defect which penetrates the pipe wall, by whatever mechanism, will initiate rupture or merely leak; under most circumstances the latter will have much less serious consequences. Through-wall flaws initiate rupture under conditions which are generally described with good accuracy by an equation developed for the American Gas Association by Battelle Columbus Laboratories in the early seventies[2]. The flaw length sustainable, at any given stress, increases with increasing Charpy energy, but is ultimately limited by the flow stress and geometry of the pipe. As the flow-stress-limited defect length is approached, very large increases in Charpy energy produce insignificant gains in defect tolerance, so that many pipeline operators have chosen as a baseline toughness requirement a Charpy energy corresponding to a critical defect length 80 or 90% of the maximum value. In this way, most of the benefit of improved toughness, relative to initiation from through-wall flaws, can be secured, while

Charpy requirements are limited to readily attainable and physically meaningful levels.

Figure 1 shows the results of applying this philosophy to a number of hypothetical design cases involving pressures ranging from the currently conventional range for natural gas transmission service (7 000 - 10 000 kPa [1000 - 1435 psig]) up to 14 893 kPa (2160 psig), which probably represents the current upper limit for suitable valves and fittings. It is clear that increasing design pressure, diameter and strength level lead to significant increases in the required Charpy energy. To place these requirements in context, currently-specified minimum Charpy values for large-diameter pipe typically range from 40 - 68 J (30 - 50 ft lbf). Nevertheless, considering worldwide pipe-mill capabilities, even the highest requirements appear to be readily obtainable, although probably at some incremental cost. The actual critical flaw lengths associated with these toughness levels range from 95 mm (3.75 in) for NPS 36, Grade 550 (X80) pipe operating at 7 446 kPa (1080 psig) to 230 mm (9.06 in) for NPS 56, Grade 483 (X70) pipe operating at 14 893 kPa (2160 psig).

MECHANICAL DAMAGE - It has been recognized for many years that the most prevalent cause of reportable service failures in North America is that classified as "outside force" (53.5% of all service failures between 1970 and 1984)[3]. Within that category, mechanical damage accounts for three-quarters of the incidents, and thus represents by far the most important single cause of failure.

A considerable amount of research has been carried out aimed at assessing the effects of mechanical damage on failure conditions. Fairly recently, work has been completed which allows the failure stress to be related to material toughness and to the geometry of mechanical damage consisting of a gouge in a dent[4]. Note that ungouged dents are of little significance for the initiation of rupture, while plain gouges can be dealt with using a surface flaw equation analogous to that discussed above for through-wall flaws. The failure curve is shown in Figure 2, and allows

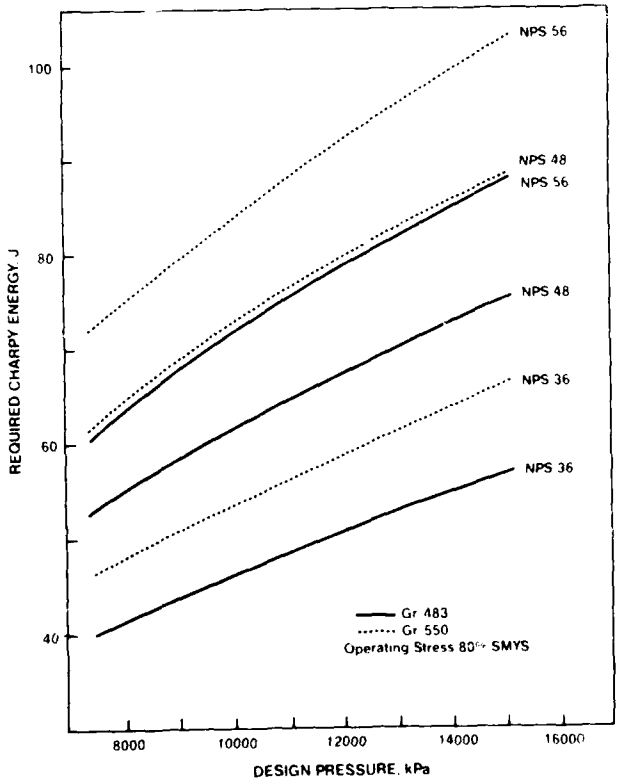


Fig. 1 Required Charpy Energy to Give Critical Through-wall Defect Length Equal to 90% of Maximum.

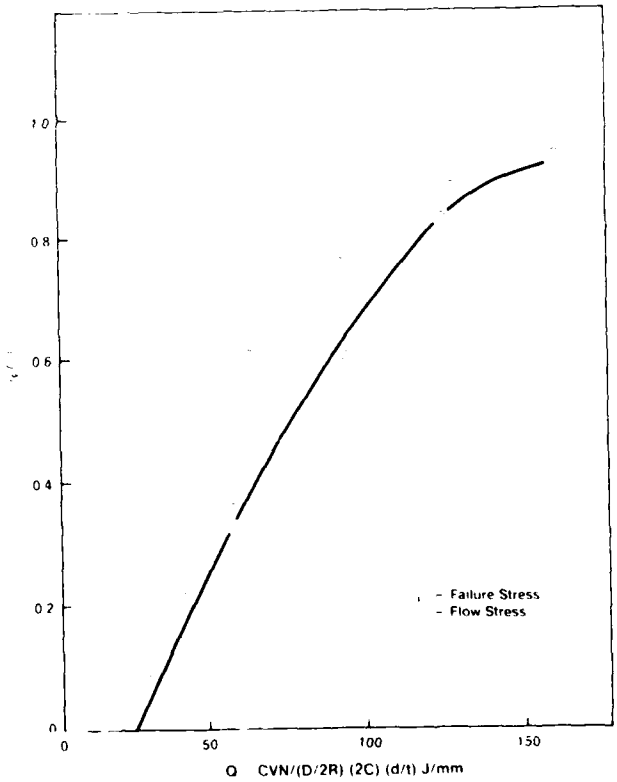


Fig. 2 Failure Stress From Dent and Gouge Defects as a Function of 'Q' Parameter (After Maxey)

a critical value of the parameter Q, derived from the material toughness and damage geometry, to be determined for a given ratio of service stress to flow stress. In order to relate critical gouge length to required Charpy energy, however, it is clearly necessary to make some assumptions concerning the depth of both gouge and dent. Maxey has suggested that a gouge depth 10% of the pipe wall and a dent depth 5% of the pipe diameter are appropriate limiting values[5]. With these assumptions, it is possible to calculate the critical gouge length which will cause failure at the maximum operating pressure, when the Charpy energy is that determined by the 90% maximum through-wall flaw criterion previously described. When the same design cases used to develop Figure 1 were analyzed in this way, it was found that critical gouge lengths were some 25 - 40% lower than the critical through-wall flaw length in the absence of damage. The resulting critical flaw sizes, in some cases, could be considered insufficient, particularly for the smaller pipe sizes which are intrinsically more susceptible to damage. On the basis of Figure 2, it is also possible to determine the Charpy energy corresponding to a critical gouge length equal to the critical through-wall defect length in undamaged pipe. As Figure 3 shows, significant increases would be required.

Clearly, this criterion for gouge length is an arbitrary one, and a consideration of actual flaw sizes, and of the susceptibility of some of the larger and thicker pipe sizes to damage, may suggest that there is little justification for the adoption as a specification minimum of some of the more extreme toughness values appearing in Figure 3. In practice, it is preferable to consider the effect of toughness on damage tolerance on a case-by-case basis so that the benefits of increasing the specified minimum Charpy energy can be assessed in relation to any incremental costs.

TIME-DEPENDENT FAILURE - The fracture criteria so far referred to describe the conditions of failure when the pressure on a pipe containing a defect is continuously increased until failure occurs, or when critical damage is inflicted on a pressurized pipe. In reality, some important mechanisms of failure involve the slow growth of a defect under sustained loading. In some instances, fluctuating loads may also be significant. Work in progress on failure under such conditions aims at modelling flaw growth and developing revised failure criteria[6]. Figure 4

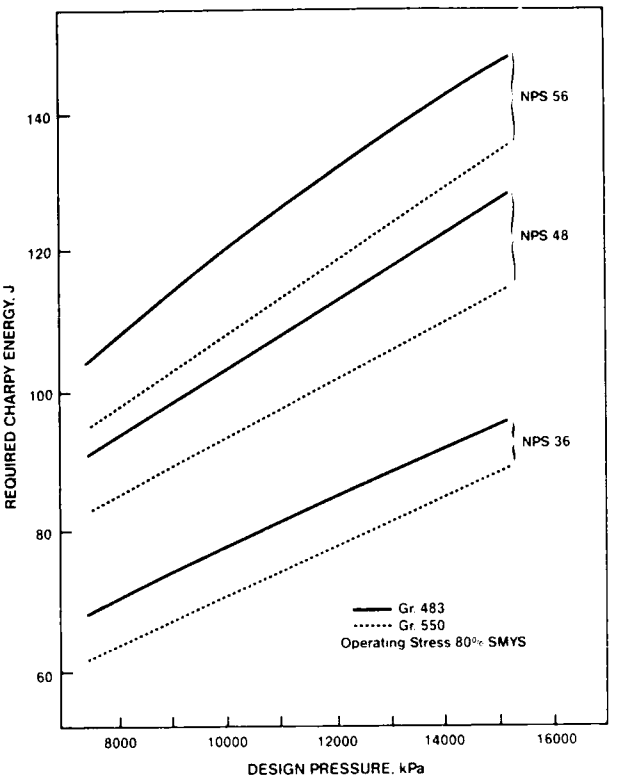


Fig. 3 Required Charpy Energy For Failure From 5% Dent, 10% Gouge at Same Defect Length as Critical Through-wall Defect Length, Fig. 1.

illustrates the results of a full-scale test on an NPS 22 pipe containing an axial, through-wall flaw, initially 63.5 mm (2.5 in) long. The test procedure was to raise the pressure by a small increment and monitor the crack extension. The pressure was held constant until no further crack extension occurred, and then a further pressure increment was applied. Crack extension began at a pressure well below that corresponding to the SMYS of the pipe material, and the final failure pressure was significantly lower than would have been predicted using the time-independent methodology referred to earlier for through-wall flaws. The model under development for flaw behaviour under sustained loading successfully predicted the pressure both at the onset of stable crack growth and at failure. Continuing work is aimed at extending the model to axial surface flaws, a configuration of more practical significance for pipeline operations, and to higher-strength steels more suitable for high

pressure systems; when completed, this work should provide a better vehicle for assessing the integrity of a pipeline known to contain defects, as well as allowing hydrostatic retest programs to be planned in such a way as to minimize the potential for damage.

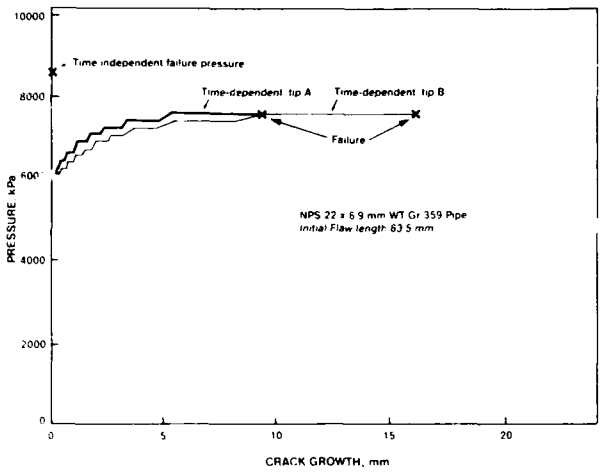


Fig. 4 Time-dependent Growth to Failure of a Through-wall Flaw in a Vessel Test (After Leis)

HYDROGEN-ASSISTED CRACKING - Hydrogen stress cracking has been known as a source of pipeline failures for many years, but it was initially only observed in conjunction with hard spots arising from inadvertent rapid cooling during production of skelp with much higher carbon contents than modern pipeline steels[7]. Hardness values well over 400 HV throughout the pipe thickness were not uncommon in such regions. Hydrogen liberated at coating holidays by the action of cathodic protection potentials more negative than -1170 mV vs. $Cu/CuSO_4$ provides a source of atomic hydrogen in the steel which, combined with the applied stress, can then lead to cracking at the hard spot.

In the last few years, several service failures of a related nature have taken place in modern pipeline steels which are not susceptible to the presence of hard spots[8]. Typical steels which have been involved contain only about 0.09% carbon, and bulk hardnesses are generally in the range 200 - 250 HV. The key factor in the initiation of these failures has been the presence of mechanical damage in the form of gouges, in some cases with minor denting. A disturbing feature has been the relatively minor nature of the damage, and the restricted extent of any associated strain hardening. The highest hardnesses measured have been around 315 HV, in very localized regions immediately below the gouge. Important contributory factors appear to be relatively high local tensile residual stresses associated with the damage, and strain-aging of the pipe material at the service temperature. In the cases which have occurred on the NOVA system, the damage was caused during construction; final failure occurred from five to ten years later. This emphasizes the prime importance of attentive inspection at all phases of construction, as well as of proper attention to coating integrity.

STRESS-CORROSION CRACKING AND GENERAL CORROSION - External stress-corrosion cracking (SCC) has been recognized as a potential source of failure for over twenty years[9]. The great majority of such failures has taken place in the U.S.A., whose pipeline infrastructure is by far the most extensive and also, on average, the oldest in the world. More recently, however, significant SCC failures have taken place in other countries, most notably in Australia[10] and, recently, in Canada.

Many of the controlling parameters associated with SCC are now well established[11], at least for the "classical" SCC phenomenon which has been extensively studied in the U.S.A. and elsewhere. It is clear that the predominant electrolyte involved is a carbonate-bicarbonate solution, and that cracking occurs when CP potential decays into a relatively narrow range (typically quoted as -600 to -750 mV) and is held there for long periods as a result of locally defective coating conditions. For any given combination of material and operating conditions, there is a threshold stress below which cracking will not take place. SCC growth rates appear to increase with temperature, so that the most severe problems have often been experienced immediately downstream of compressor stations. Surface condition of the pipe is an important factor; mill-scaled surfaces appear particularly susceptible to SCC, while grit-blasting greatly improves SCC resistance.

SCC, when it occurs, is generally a serious problem, since cracks rarely occur singly. In addition, as a result of multiple crack linkage, cracks generally develop high aspect ratios by the time the pipe wall is penetrated, so that they are apt to cause ruptures rather than leaks. Often, long, continuous sections of pipelines are found to be affected; in a recent investigation, over

50% of nearly 300 sites investigated on a single pipeline were found to show SCC indications. Rehabilitation of a line known to contain SCC is difficult and costly, since in-line inspection for axial cracks is still in a developmental stage. Since the range of soil types, pH, electrolyte characteristics and pipe material which have been associated with SCC is now extremely extensive, mitigation of this failure mechanism must be a concern in the fracture control plan for many, if not most, long-distance pipelines. Since it is economically (and, for higher pressures, technically) impractical to design such systems at stresses which are reliably below the SCC threshold, the use of high integrity, plant-applied coatings represents the only effective defense. Apart from the improved performance of the coatings themselves, the associated surface preparation is also of considerable benefit.

External corrosion has been a continuing source of pipeline integrity problems (about 7% of all reportable service incidents in the U.S.A. between 1970 and 1984)[3]. Again, many factors are involved, including groundwater chemistry, bacterial effects, and cathodic protection practices, but the single most important factor is, once again, coating integrity. Here, too, for the planning of major, new pipelines, only the specification of high integrity, plant-applied coatings, coupled with careful inspection both in-plant and during construction, represent an adequate response.

SOIL MOVEMENT - A significant number of pipeline failures has been associated with soil movement. The site-specific design of modern pipelines will involve the consideration of allowable longitudinal strains in both the tensile and compressive directions. In the former case, the fracture resistance of girth welds will generally be the limiting factor, while buckling resistance is the major concern in the latter. Extremely complex and costly mitigative measures have been proposed for specific pipelines, particularly in regions where frost-heave and thaw-settlement may be encountered. As the available technology advances, it is becoming clear that it may be appropriate to pay more attention to in-service monitoring rather than to attempt, at the design stage, to allow for all the displacements which may occur over the life of the pipeline. Remote monitoring techniques using satellite communications, intelligent, position-sensing pigs and other advanced techniques may be applied, together with traditional strain-monitoring and high level modelling of pipe-soil interactions, to determine when intervention is necessary to preserve the integrity of the pipeline.

## FRACTURE PROPAGATION

DUCTILE FRACTURE PROPAGATION AND ARREST - As has been mentioned, research on the propagation and arrest of ductile fracture in gas pipelines began some twenty years ago, and is still continuing. Such research is both extremely expensive and technically challenging, since the validation of any model requires large-scale testing involving realistic pressurizing fluids. Over this period, many methodologies have been proposed to determine the necessary toughness level for fracture arrest. Figure 5 shows the results of calculations using five of these approaches[1,12], some of which involve detailed consideration of the interaction between the driving force provided by the gas and the fracture resistance of the pipe, while others

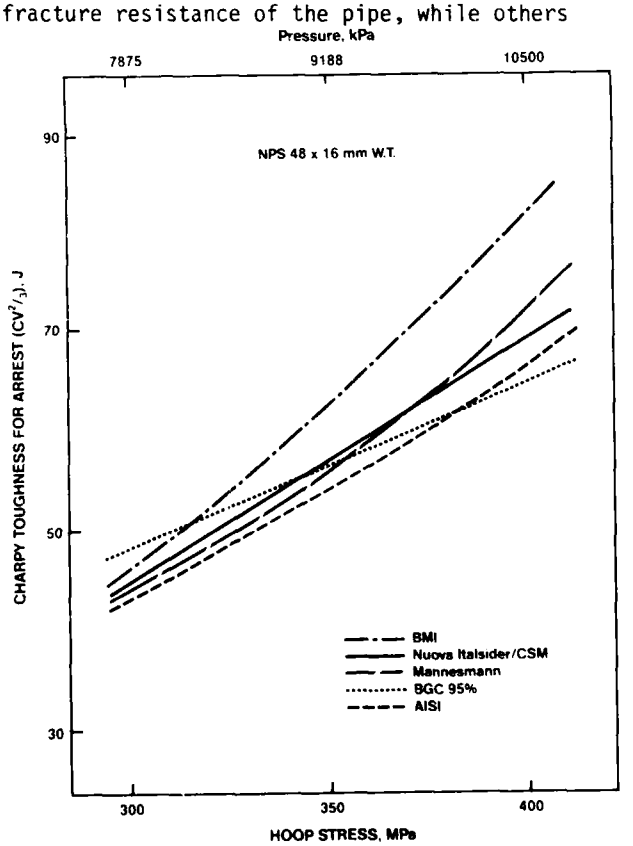


Fig. 5 Arrest Toughness ($^2/_3$ Charpy - V Energy) As a Function of Hoop Stress for Five Different Prediction Methods

are purely statistically-based. Though the latter may be adequate for predicting the behaviour of many pipelines transmitting nearly pure methane, only those models which explicitly consider gas behaviour can be used for more complex natural gas mixtures or for $CO_2$.

As the example in Figure 5 shows, a wide range of alternative approaches yield similar results at relatively low hoop stress. Significant divergences begin to be observed as hoop stress increases. It is noteworthy that, at least up to the stress levels shown (approximately corresponding to Grade 483 (X70) pipe operating at 80% SMYS or Grade 550 (X80) at 72% SMYS) the Battelle "long-form" model[2] provides the most conservative predictions.

The model is a useful one to consider in some detail, since it is simple enough to allow the logical structure to be followed quite readily but complete enough to allow certain complexities, particularly in terms of gas composition, to be addressed. In addition, the basic equations, while including some empirical factors and simplifications, are strongly based on the physical phenomena involved. The model essentially depends on three relationships. First, a "fracture arrest stress" (and corresponding pressure) is calculated, based on the material flow stress, pipe geometry and toughness. Initially, Charpy shelf energy was used as the measure of toughness, but obviously the model can accommodate other approaches, as will be discussed later. Second, the variation of fracture velocity with the ratio between crack-tip pressure and arrest pressure is developed. Finally, the variation of crack-tip pressure as a function of initial pressure and the appropriate expansion wave velocity is determined. For gases which closely approximate perfect gas behaviour such as pure methane under typical transmission pipeline conditions, theoretical equations predict very closely the observed decompression behaviour. Generally speaking, as the proportion of higher hydrocarbons increases, and at higher pressures and lower temperatures, decompression behaviour deviates progressively from perfect gas behaviour. Various computer-based models exist which allow the accurate prediction of the behaviour of "rich" gases. Because of the particular decompression behaviour of $CO_2$ from the supercritical range, it must be treated separately, and this is discussed below.

The way in which the interaction between gas decompression and fracture is handled is most easily understood by means of the

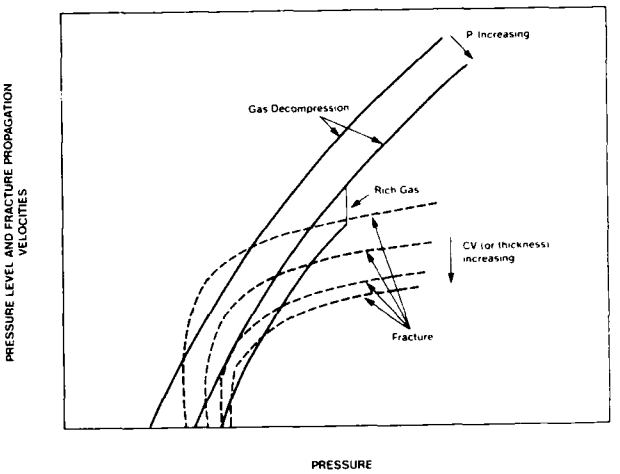


Fig. 6 Effect of Initial Pressure and Rich Gas on Fracture Arrest Toughness According to Battelle Model - Schematic

graphical presentation shown schematically in Figure 6, in which curves expressing the variation of fracture velocity and pressure-wave velocity with pressure level appear. As fracture first begins to propagate, decompression wave velocity is higher than fracture velocity, and the crack-tip pressure progressively falls as the decompression front runs ahead of the fracture. However, if an intersection occurs between the decompression velocity curve and the appropriate fracture velocity curve, the related pressure level and the fracture will ultimately travel at the same speed, and the fracture would theoretically propagate indefinitely at that speed. If, on the other hand, no intersection exists, the crack-tip pressure will fall below the arrest pressure, and no further propagation can occur. The dividing line between propagation and arrest is thus represented by tangency between the two types of curve, and the "arrest toughness" is determined accordingly. In reality, as can be readily understood, the process of pressure decay takes a finite time, during which the fracture continues to propagate, so that the effective arrest toughness is a function of the desired arrest length. Maxey found empirically that a distance of around 10 m (33 ft) was necessary to arrest a fracture at the theoretical arrest toughness[2]. Greater distances may be needed close to the origin, or where very large changes in toughness occur from pipe to pipe.

Figure 6 also illustrates the effect of increasing gas pressure on the predicted

| | Grade 483 (X70) | | | | | | | | | Grade 550 (X80) | | |
|---|---|---|---|---|---|---|---|---|---|---|---|---|
| Pressure, kPa (psig) | 7446 | (1080) | 7446 | | 8687 | (1260) | 9928 | (1440) | | 7446 | 8687 | 9928 |
| Temperature, °C (°F) | 20 | (68) | 4 | (39) | 4 | | 4 | | | 4 | 4 | 4 |
| Diameter, NPS | | | | | | | | | | | | |
| 36 | | | | | | | 155 | (114) | | | | |
| 42 | | | | | | | 170 | (125) | | | | 210 (155) |
| 48 | | | | | 155 | (114) | 190 | (140) | | | 185 (136) | |
| 56 | 150 | (111) | 160 | (118) | 170 | (125) | | | | 190 (140) | | |

toughness required for arrest; a higher initial pressure leads to higher crack-tip pressures at any fracture velocity, and hence to higher arrest toughness. The effect of rich gas is also indicated: at some stage of the decompression process, the phase boundary is intersected, liquid dropout occurs, and a constant pressure region is encountered in the decompression curve. As mentioned above, this effect is intensified by high initial pressures and low initial temperatures, and usually results in increased toughness requirements for fracture arrest, as is indicated in Figure 6. It should also be noted that, other design factors being equal, the arrest pressure (the intercept of the fracture velocity curve on the pressure axis) decreases with decreasing thickness. Using higher strength materials at a constant design factor, while usually attractive from an economic point of view, thus demands increased toughness. The quantitative effect of some of these variables, as well as that of increasing diameter, can be illustrated by reference to the above table, which gives arrest toughness in joules (ft-lbs) for a typical, rich gas composition and for a constant, 80% design factor.

An additional observation which may be made is that the Charpy requirements predicted are extremely high for all of these designs. An extensive program of full-scale burst tests carried out in Canada revealed that the practical situation is even more severe, as Figure 7 indicates[13]. It was found that actual arrest toughness values were some 30% higher than the predictions of the Battelle model which, at the time these tests were conducted, was the most conservative of the existing approaches. Burst tests carried out elsewhere on materials up to Grade 550, and at pressures up to 18 000 kPa (2610 psig)[14], have confirmed this general trend, and have called into question the ability of a single, small-scale notched bend test, such as the Charpy test, adequately to reflect the fracture resistance of large-diameter pipes which, today, may be produced in many different ways.

As a result of the above difficulties, considerable efforts have been made, and are still continuing, aimed at identifying mechanical tests which are representative of the true fracture resistance of a complete range of pipeline materials, and at developing models which give a more complete representation of fracture behaviour. An ideal fracture propagation model would allow the prediction of fracture velocity, point by point, for any propagation event. The High Strength Line Pipe Research Committee of the Iron and Steel Institute of Japan has developed a methodology which aims at achieving this result[15]. The form of the three fundamental equations is essentially the same as in the Battelle approach, but the constants were redetermined by regression on data from a series of burst tests on NPS 48, 18.3 mm (.72 in) WT, Gr. 483 (X70) pipe. The primary measure of fracture resistance adopted was the energy absorbed in the statically-precracked drop-weight tear test (DWTT). For the most part, the method was quite successful in reproducing the point-by-point fracture propagation behaviour of the tests from which the coefficients were determined. It remains to be demonstrated that this approach can be extended to a wider range of test conditions.

A similar approach can be pursued using the original Battelle equations, which have been extremely successful in describing fracture velocity and discriminating between arrest and propagation under "conventional" pipeline conditions similar to those for which they were developed. Figure 8 shows an example from the Canadian tests, involving a NPS 56, 13.7 mm (.54 in) WT, Gr. 483 (X70) test section. Though the gas was rich, test conditions were such (7446 kPa (1080 psig), 19°C (66°F)) that there was no significant discontinuity in its decompression behaviour. Two observations are apparent. First, Charpy shelf energy seriously underpredicts fracture velocity, while the relationship between predicted and observed fracture length is inconsistent. In addition, this method allows

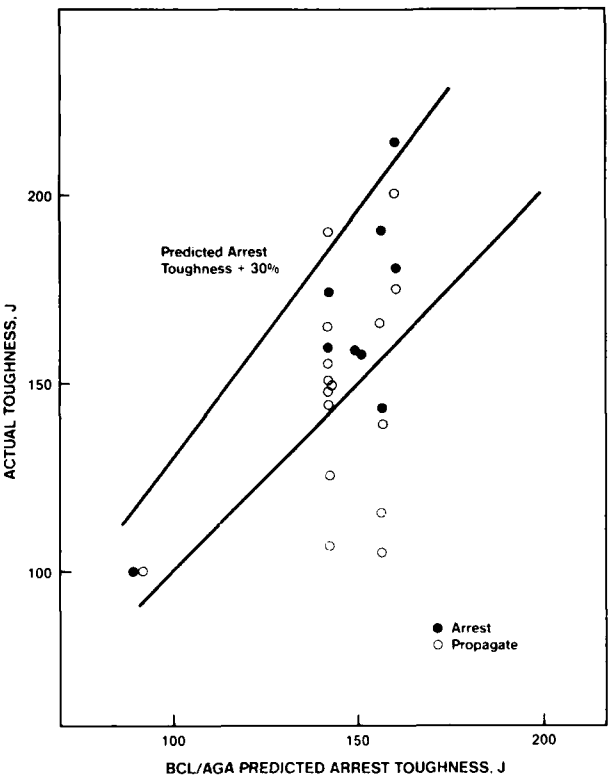


Fig. 7 Comparison of Observed and Predicted Burst Test Results; NPS 48 and 56, Gr. 483 Containing Rich Gas at Pressures up to 8687 kPa

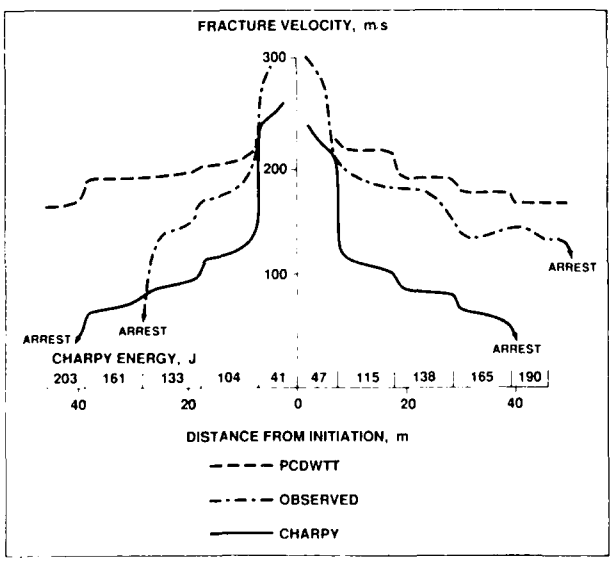


Fig. 8 Fracture Velocity Predictions Based on PCDWTT and Charpy Energy Using the Battelle Model

continued propagation at velocities significantly below about 80 m/s (250 ft/s), which is not observed in practice in on-land tests of this type. On the other hand, the use of precracked DWTT energy overpredicts fracture velocity, and no fracture arrest is predicted. This example is illustrative of the difficulty of extending the use of a model outside the range for which it was developed.

In reality, it may be that the search for a single, simple notch-bend test which will represent the material's response to the fracture event for all geometries, steel types and levels of driving force is doomed to failure. Much of the research effort in this area has centered around the idea that fracture surface separations, typical of many high strength line pipe steels, account in some way for the inability of the Charpy test to predict fracture behaviour, and that links can be found between appearance of these separations and specific skelp production techniques. On the other hand, DWTT developments have concentrated on the hypothesis of "excess initiation energy" in ostensibly high toughness steels, and on devising methods to eliminate it. The precracked DWTT is one example of this effort, though it has not gained widespread popularity as a result of difficulties of standardization. While this work may well prove to be valuable, it now seems apparent that the only approaches offering some hope of a universal understanding of fracture propagation and arrest are those which involve a detailed consideration of the deformation processes which accompany fracture, and the way in which they relate to measurable material properties. At the least, the way in which the material responds to the opening of the "flaps" behind the fracture front, directing a zone of intense plastic deformation to the area immediately ahead of the crack tip, and the way in which the final, local necking and separation take place in this zone, need to be explicitly considered. It should certainly be no surprise that these two phenomena may vary in different ways with material characteristics and geometry, and that a single, simple test may not be adequate to represent both aspects of the material response. Work is continuing in a number of laboratories aimed at resolving some of these issues.

Despite the difficulties enumerated above, it is still often possible to define, for specific project conditions, some value of a material property or properties which will give a very high probability of arrest (which we

shall continue to refer to as "arrest toughness"). It may not be logical, however, for demanding designs, to take this value as a specification minimum. It is generally more appropriate, in the context of an overall analysis of risk and economics, to decide what is an appropriate maximum length for fracture, at an appropriate level of probability. This maximum length may be quite short, for a pipeline which traverses regions of high population density, or longer (but possibly, for logistic reasons, at a higher probability level) for pipelines in remote areas. Extensive Monte Carlo simulations have been used to determine what fraction of "arrest pipe" is needed as a function of maximum fracture length, but relatively simple closed-form statistical calculations are also effective[1]. Figure 9 shows this relationship for a number of probability levels; it is clear that, if maximum fracture lengths of several hundred metres can be tolerated, a relatively low percentage of "arrest pipe" is needed. If, on the other hand, fracture must be contained within a few pipe joints, very few "propagate pipes" can be accepted. Specifications and mill inspection schemes can be devised on a statistical basis to meet these requirements in a reliable and economical manner.

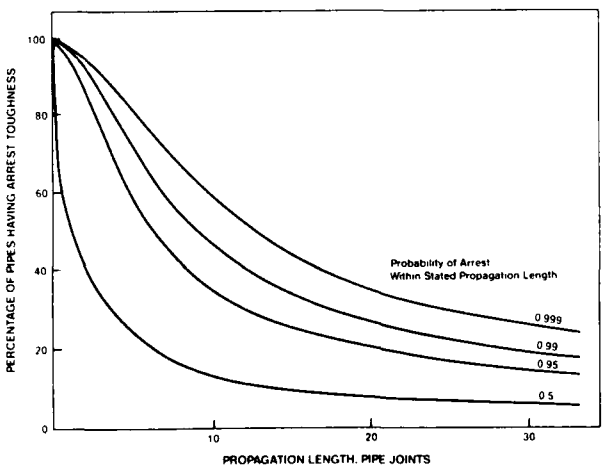


Fig. 9 Relationship Between Propagation Length and Percentage of Arrest Pipe in the Pipeline

FRACTURE ARREST IN $CO_2$ PIPELINES - The analysis of fracture arrest requirements in $CO_2$ pipelines is simpler than in natural gas pipelines but, unfortunately, for typical operating conditions their achievement is more difficult. $CO_2$ pipelines are generally designed, for economic and operational reasons, to operate in the high pressure, supercritical range. The operating point shown in the pressure-enthalpy diagram of Figure 10 represents the maximum pressure and temperature for a typical design; unlike rich natural gas, $CO_2$ presents increasingly severe fracture arrest conditions as the temperature increases. On initiation of rupture, decompression will take place along a line of constant entropy until the phase boundary is encountered, as shown. Pressure then remains essentially constant at the saturation pressure, (about 7000 kPa [1000 psi] in the current case), throughout the subsequent fracture event. This theoretical behaviour has been confirmed by experimental determinations of $CO_2$ decompression behaviour from typical pipeline conditions.

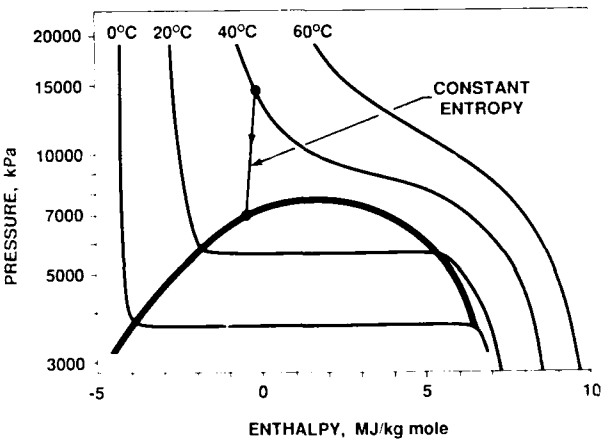


Fig. 10 Pressure - Enthalpy Diagram for Pure $CO_2$

Since the fracture propagation phenomenon takes place essentially at constant pressure, it follows that, in order for arrest to occur, the arrest pressure determined by the pipe geometry, flow stress and toughness must be higher than the saturation pressure. As Figure 11 illustrates, using the Battelle equation for arrest stress, this may be difficult to accomplish. The case examined is that of an NPS 16 $CO_2$ pipeline operating at 72% SMYS; initial conditions were 14 031 kPa (2035 psi) and 40°C (104°F), as in Figure 10. Saturation pressure on isentropic decompression is thus about 7000 kPa (1000 psi); an arrest pressure corresponding to this level cannot be achieved at any toughness level in Gr. 414 (X60) pipe. Only by increasing the wall thickness can arrest pressures over 7 000 kPa

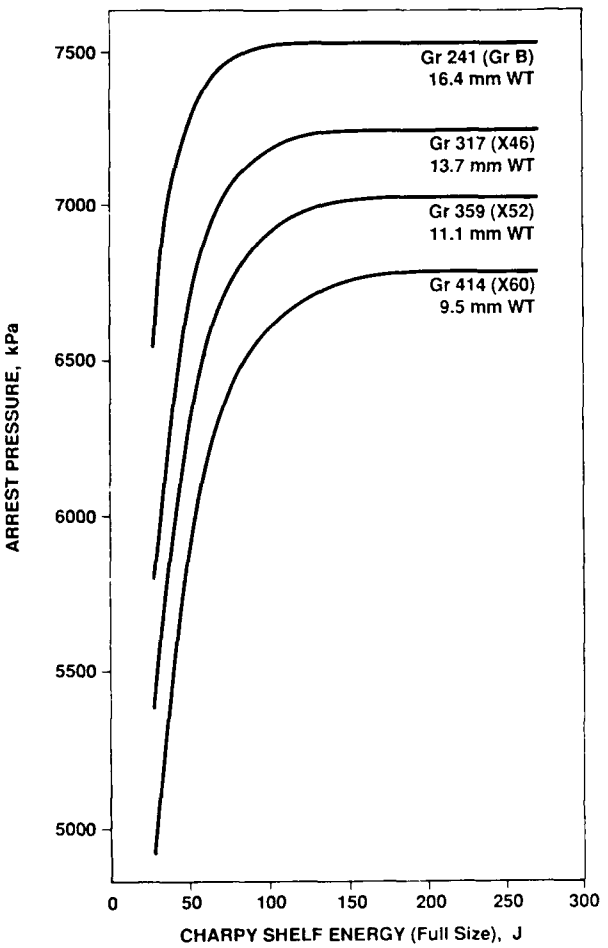


Fig. 11 Arrest Pressure as a Function of Charpy Energy for a Supercritical $CO_2$ Pipeline

be achieved and then, except at the lowest strength levels, only at relatively high Charpy toughness. It will thus often be preferable, from an economic point of view, to use an alternative approach to fracture control, involving crack-arrestors: these will be discussed in the following section.

CRACK-ARRESTOR DESIGN - As a result of the extremely high fracture resistance predicted to ensure arrest in advanced, high pressure natural gas pipelines and in supercritical $CO_2$ pipelines, as well as of the conceptual difficulties involved even in specifying and measuring the required properties, a good deal of attention has been devoted to the design of independent crack-arrestors. Various types of arrestor have been installed on a number of high pressure natural gas lines, as well as on $CO_2$ lines. Specific types studied (not all of which have been applied) include "in-line" arrestors having heavier walls, higher toughness, or both, loose and grouted steel sleeves, multi-layer pipe, steel wire cables, and glass-reinforced composite sleeves[12]. A concept currently under development for the Gas Research Institute in the U.S.A. is the glass-reinforced composite "clock-spring" arrestor which can be wound onto the pipe without requiring a loose end, and is thus both inexpensive and easy to install[16]. Burst tests on pipe up to NPS 30, with high crack-driving force provided by gas mixtures containing a large proportion of $CO_2$, have demonstrated its effectiveness.

The most comprehensive study of the design principles for sleeve-type arrestors was carried out by Wilkowski et al. for the AGA[17]. The necessary arrestor length, as a function of pipe diameter, is linearly related to the velocity of the incoming fracture, which can be estimated from diagrams similar to that shown in Figure 6; the slope of this relationship depends on radial clearance. Grouted sleeves were found to behave as if they had a radial clearance of 1.9%; clock-spring arrestors so far appear to perform similarly to steel sleeves with a clearance in the range 3.5 - 4.3%. Figure 12 shows the slope of the arrest/propagate boundary as a function of radial clearance; the required ratio of arrestor length to pipe diameter (L/D in Figure 12) can thus be determined. This analysis is on sound theoretical ground, since L/D and radial clearance together determine the

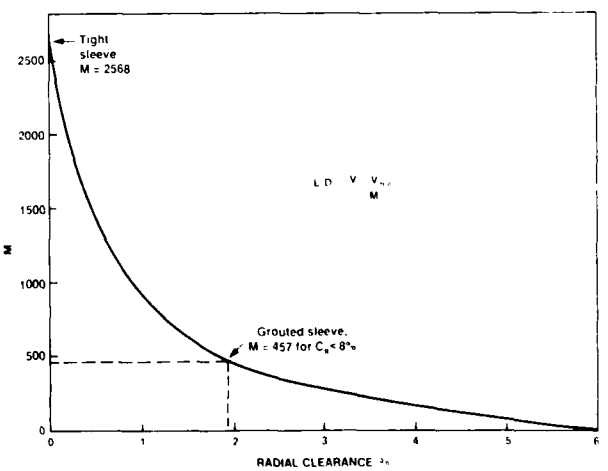


Fig. 12 Slope of the Arrest/Propagate Boundary as a Function of Radial Clearance for Sleeve Arrestors (After Wilkowski)

maximum crack opening angle; the latter parameter has been increasingly seen as a fundamental reflection of fracture resistance which may be particularly useful for pipelines.

Arrestor thickness has been determined simply by ensuring that it provides the same ultimate load as the equivalent length of pipe wall. This may be difficult to justify theoretically, but has been validated by numerous model- and full-scale tests on different arrestor designs.

ECONOMIC ANALYSIS - While the choice of economic factors as the primary determinant of a desired maximum fracture length may, at first sight, appear inappropriate, this often provides the only logical basis for the selection of mitigative procedures. Once a rupture has occurred, gas will be lost, service may be interrupted, a safety hazard may have been created and replacement pipe will have to be installed. All these factors are consequences of the initiation event itself; what remains is a consideration of whether, and in what way, their impact is related to fracture length, whether any additional hazards are introduced as fracture length increases and what is the most effective way of ensuring that the cost of long fractures is minimized. In order to carry out an economic analysis of this type, many assumptions are necessary. First, any rupture event will lead to a fixed cost component, which is related to the mobilization and labour costs of a repair crew and the cost of a minimum length of replacement pipe. Similarly, it is assumed that any rupture will lead to a certain minimum outage time, with additional outage time related to incremental length. For the purposes of an illustrative calculation, a minimum replacement length of 75 m (250 ft) and a minimum outage time of 3 days, with repair rates for incremental lengths of 200 m/day (650 ft/day), have been used. A rupture frequency of $1/10^4$ km/yr (1/6200 miles/yr) and a design life of 20 years represent other important input parameters. The system considered involves 2167 km (1350 miles) of NPS 48 and 56 pipe; the tariff regime is such that an abatement to shippers of $\$3.5 \times 10^6$/day would be applicable for outages exceeding 3 days. The latter figure has a very large effect on costs and on optimum fracture lengths, and will vary greatly from project to project. In addition, it has been assumed that an arrest toughness can be specified, and that sufficient "arrest pipe" to ensure a maximum fracture length of 650 m (2133 ft) at a 0.95 probability can be obtained without incremental cost, while additional arrest pipe would carry a 10% cost premium. Installed cost of arrestors was taken as $2000 each. Figure 13 shows the results of the analysis. With the given assumptions, it can be seen that the optimum solution is to rely on pipe toughness, at an estimated total incremental cost of some $\$66 \times 10^6$ and a maximum fracture length of 250 m (820 ft).

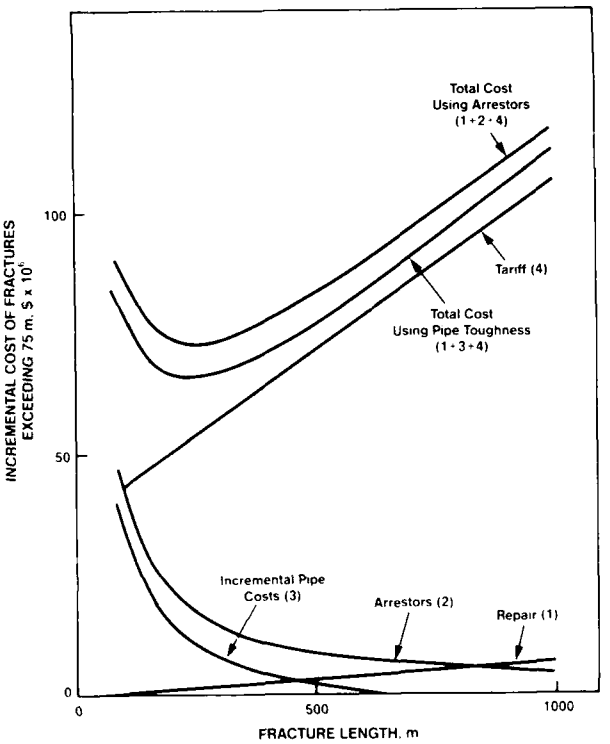


Fig.13 Incremental Cost of Fractures Exceeding 75 m in Length Over the Lifetime of a Hypothetical Long-Distance Pipeline

Clearly, higher incremental pipe costs or lower arrestor costs could change the relative merits of the two approaches. Similarly, if the probability of containing fracture within the specified length must be greater than 0.95, additional arrest pipe will be needed and again, crack arrestors may be favoured. The fundamental assumptions behind such an analysis are so many, and their influence so great, that no general inferences should be drawn from the example shown. In particular, the tariff costs are dominant in the present case, and tend to force the optimum towards relatively short lengths. Nevertheless, such examples can be useful in illustrating the logical framework within which the preferred approach to the

limitation of fracture length can be determined.

## ANALYSIS OF RISK

The analysis of risk has increasingly become a formalized process over the last twenty years, and has addressed both individual and societal risk as well as financial risk associated with gas transmission pipelines. The British Gas Corporation, mainly as a result of very specific legislative requirements, has carried out one of the most thorough analyses of individual and societal risk, and has concluded that the levels of risk associated with the BGC transmission system are very low relative to other common sources[18]. In particular, they are one or more orders of magnitude lower than the societal risks associated with most other forms of transportation, and also an order of magnitude lower than standards proposed in the U.K. for chemical process plants.

One of the techniques of risk analysis which appears to have direct application in the development of fracture control strategies and pipeline integrity studies is fault-tree analysis[19]. This approach breaks down the cause of a given "top event" (e.g., a specific system failure) through a number of logical "and" or "or" gates. Frequencies and probabilities can be assigned to the various subresultant and basic events and combined through the different logic gates by simple probability calculations. For the evaluation of very complex fault-trees, extensive computer software packages have been developed, but simple fault-trees are readily evaluated by hand. One of the most promising applications in the field of fracture control appears to be in the analysis of the sensitivity of specific failure events to a range of causal factors. Figure 14 illustrates part of a fault tree which could be used to determine the expected frequency of a specific, undesired failure event (fractures longer than L metres) as a function of all the possible causal factors. The evaluation of such fault-trees can be extremely helpful in determining the relative value of mitigative practices aimed at individual causal factors; in addition, in the present case, it may be useful in defining the appropriate probability level at which to enter diagrams such as that in Figure 9. One difficulty associated with the use of such techniques is the determination of appropriate input values. While unreliability and

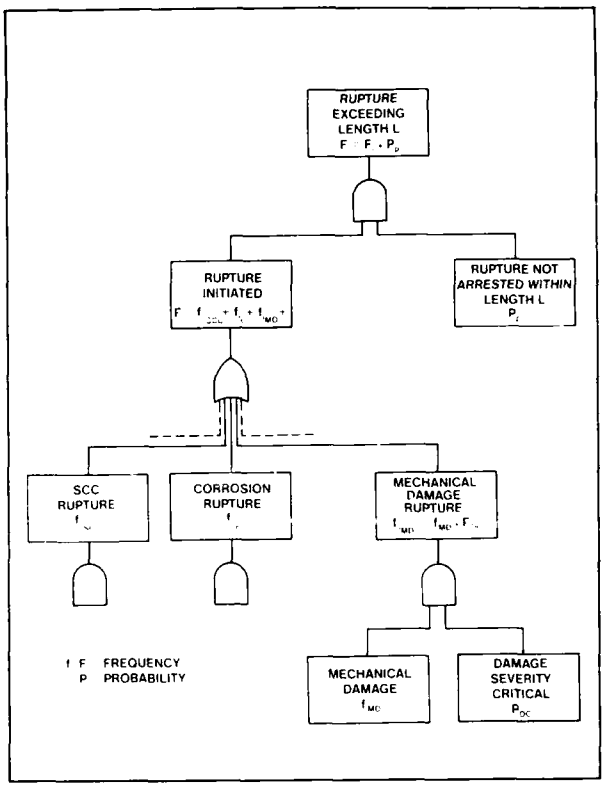


Fig. 14 Partial Fault-tree Illustrating a Possible Approach to Assessing Sensitivity of a Given Failure Event to Causal Factors

unavailability statistics are available for a surprising range of equipment used in the oil and gas industry, failure statistics for pipelines are in general drawn from populations which are highly heterogeneous both geographically and in time (and hence, in technology). As an example, corrosion failure frequencies heavily biased by statistics for uncoated or inadequately coated lines, or lines without CP, would be an inappropriate input for a modern pipeline using a high integrity coating and well-designed CP. Conversely, because technology development is a continuing process, the failure statistics for systems typical of current design practice are (happily) limited. A good deal of judgement is therefore required in order to achieve useful results at the design stage. Past experience may be much more applicable, on the other hand, to the integrity assessment and rehabilitation of existing systems.

## CONCLUSIONS

Comprehensive fracture control plans for major, high pressure pipelines involve a consideration of the most prevalent causes of failure as well as of the means of restricting the length of any rupture which is initiated. Methods are available to determine suitable values of material toughness to minimize the incidence of ruptures; the required toughness increases significantly with increasing pressure and pipe diameter. Mechanical damage is an important source of failure whose mitigation may dictate further increases in toughness. For a number of other important failure mechanisms, the only practical approach is an emphasis on high integrity coating and on attentive inspection at all stages of construction. The length of any ruptures which are initiated can be restricted, in principle, either by the specification of appropriate material toughness or by the use of independent crack arrestors. The specification of arrest toughness on the basis of existing models may be difficult for large-diameter, high-strength pipelines operating at high pressures and for pipelines containing rich gas or $CO_2$; for such systems, the use of optimally-designed crack-arrestors may represent the only viable option. A number of statistical, economic and risk analysis techniques can be used to advantage to determine the most appropriate approach for the mitigation of the consequences of ruptures in the design of new pipelines, and for the planning of integrity assessment and rehabilitation programs on existing systems.

## REFERENCES


1. Rothwell, A. B. and G. Fearnehough, Proc. International Seminar on Fracture in Gas Pipelines, Moscow, 1984, p. 135. CBMM, Sao Paulo, (1984).
2. Maxey, W. A., Proc. 5th Symposium on Line Pipe Research, p. J-1. AGA, Arlington, Va., (1974).
3. Eiber, R. J., D. J. Jones and G. S. Kramer, Proc. 7th Symposium on Line Pipe Research, p. 2-1. AGA, Arlington, Va., (1986).
4. Maxey, W. A., Ibid, p. 14-1.
5. Maxey, W. A., Proc. 6th Symposium on Line Pipe Research, p. H-1. AGA, Arlington, Va., (1979).
6. Leis, B. N., D. P. Goetz, P. M. Scott and F. W. Brust, Proc. 7th Symposium on Line Pipe Research, p. 16-1. AGA, Arlington, Va., (1986).
7. Groeneveld, T. P., Proc. 4th Symposium on Line Pipe Research, p. E-1. AGA, New York, N.Y., (1969).
8. Kiefner, J. F. and R. J. Eiber, Proc. 7th Symposium on Line Pipe Research, p. 1-1. AGA, Arlington, Va., (1986).
9. Fessler, R. R., Proc. 4th Symposium on Line Pipe Research, p. F-1. AGA, New York, N.Y., (1969).
10. Baker, T., G. G. Rochfort and R. N. Parkins, Proc. 7th Symposium on Line Pipe Research, p. 27-1. AGA, Arlington, Va., (1986).
11. Beavers, J. A. and R. N. Parkins, Ibid, p. 25-1.
12. Wiedenhoff, W. W. and G. Vogt., Ibid, p. 18-1.
13. Rothwell, A. B., "Inclusions and Residuals in Steel: Effects on Fabrication and Service Behaviour", ed. J. D. Boyd and C. S. Champion, p. 141. Supply and Services Canada, Ottawa, (1985).
14. European Pipeline Research Group, Proc. 7th Symposium on Line Pipe Research, p. 20-1. AGA, Arlington, Va., (1986).
15. Sugie, E., M. Matsuoka, T. Akiyama, H. Mimura and Y. Kawaguchi, Trans ASME, J. Pressure Vessel Technology, 104, 338-343 (1982).
16. Fawley, N.C. Private Communication. NCF Industries Inc., Long Beach, Ca.
17. Wilkowski, G., P. Scott and W. Maxey, AGA/PRC Line Pipe Supervisory Committee Report 134, 1983.
18. Townsend, N. A. and G. D. Fearnehough, Proc. 7th Symposium on Line Pipe Research, p. 3-1. AGA, Arlington, Va., (1986).
19. Fussell, J. B. "Generic Techniques in Systems Reliability Assessment", Ed. E. J. Henley and J. W. Lynn. Noordhoff, Amsterdam, (1976).

# TRENDS IN DEVELOPMENT AND AVAILABILITY OF HSLA LINE PIPE STEELS IN DEVELOPING COUNTRIES

**Pascoal J. P. Bordignon**
Companhia Brasileira de Metalurgia e Mineração
São Paulo, SP. Brazil

ABSTRACT

Development and large scale production of traditional high grade line pipe steels have recently been established in a group of developing countries that have had investments on modernization and expansion of their steel industry. The present paper summarizes the developments which have occurred in those countries, specially in Brazil, in the subject area of HSLA steels for submerged arc welded - SAW pipes. As the development of line pipe steels is very related to the development stage of the steel industry considerations are also made about some of the equipments available in the steel mills.

THE APPLICATION OF MICROALLOYING in large industrial scale dates back to the late fifties (1) but it was during the seventies that the technology of microalloying became a reality in a wide number of steel products. As shown in figure 1 (2) the highest rates of development of microalloying technology occurred between 1970 and 1980. During that period accurate controlled rolling practices were established in steel mills located in developed countries with tradition in the steel industry, specially Japan, West Germany, Italy and France.

In very simple terms, microalloying combined with controlled rolling, or controlled thermomechanical processing, is the necessary condition for the production of high grade line pipe steels. Thus, and as a natural consequence, large scale production of line pipe steels has been concentrated on those developed countries, where the industrial technology was developed and where investments were made to allow production of clean steels and processing under very high separating forces during rolling. During the eighties the line pipe steel product area has experienced a period of metallurgical sophistication and super tough grades up to X80 strength level are produced from steels containing very low levels of almost everything (C, P, S, and N). This achievement is mainly related to sophistication during production of liquid steel (developments in hot metal treatment, combined blowing, secondary refining - RHOB) and, to a certain extent, introduction of accelerated cooling of plates.

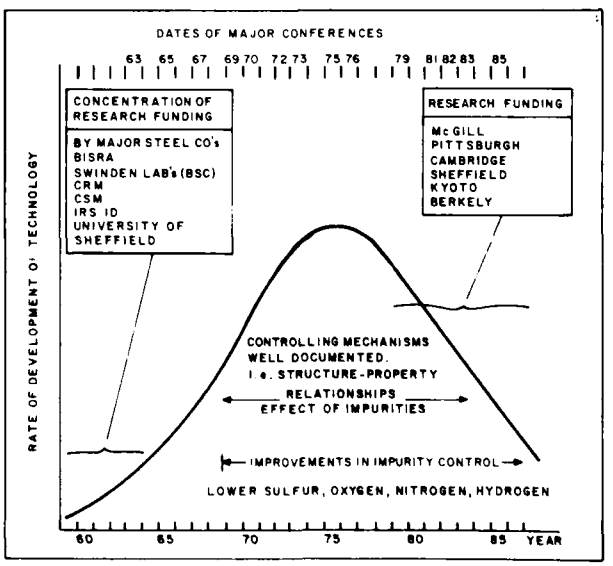


Figure 1- First Microalloying (HSLA) Life Cycle

Until recently, developing countries, or new industrialized countries - NIC, could not be

quoted among producers of good quality line pipe steels. The situation however is changing as some developing countries have been making large investments to expand and modernize their steel industry. Availability of raw material, low labor cost, well equipped steel mills, foreign technical assistance and well qualified personnel are conditions that have lead some developing areas to the position of competitive producers of line pipe microalloyed grades. Steel grades are still limited to conventional ferrite pearlite type but it can be expected that in the near future, as steel plant modernization continues, developing countries will also be producing the sophisticated "low everything" steels. Developing countries with larger potential in the microalloyed line pipe steels product area are Brazil, South Korea, Mexico and Taiwan. Venezuela, Argentina, China and a few others will certainly join the group of high grade line pipe producers in a not too distant future.

## IS THE WORLD STARTING TO HAVE A CHANGE IN THE GEOGRAPHY OF STEELMAKING?

Large tonnage steel making has for a long time been a tradition of a group of developed countries, specially USA, Japan and West Germany. URSS has maintained its position of the largest world steel producer. However, it is also the largest importing country for high grade line pipe steels. As figure 2 shows there is a tendency towards decrease in steel production in important traditional steelmaking areas (3,4). Those areas, have reached a high level of economic growth and intensive infrastructure building is something of the past, which is equivalent to a decrease in the need for steel. High labor cost and strict regulations on pollution control are also inhibiting factors for expansion of steel production in developed countries.

Developing countries, on the other hand, have growing needs for steel. Labor cost is low and, in some cases, there is large availability of raw materials. Brazil, for instance, has one of the lowest production cost of steel in the world, figure 3 (5). As a result, a group of developing countries is becoming important steel producer, figure 4 (3,4). It can be expected that these countries will give continuation to the expansion in their steel industry, although many of them have at present serious economical problems, significantly affecting the geography of steelmaking. Parallel to the increase in steel production capacity intensive modernization of existing steel works as well as construction of new plants with recent technology have occurred generating the necessary conditions for the production of microalloyed line pipe steels.

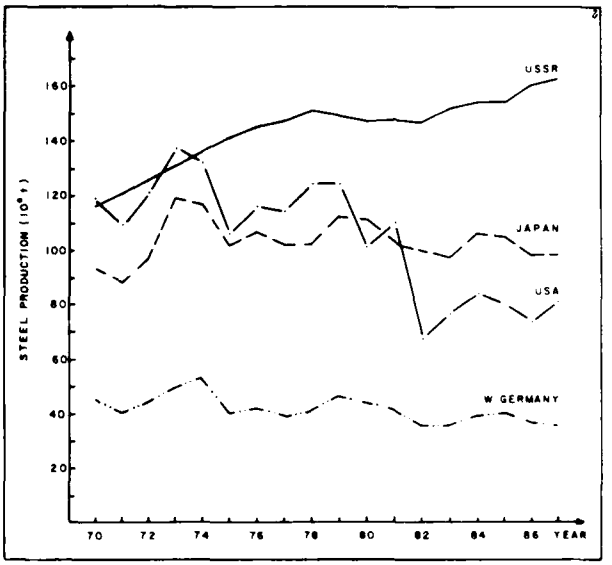


Figure 2 - Raw Steel Production by Traditional Large Steel Producers

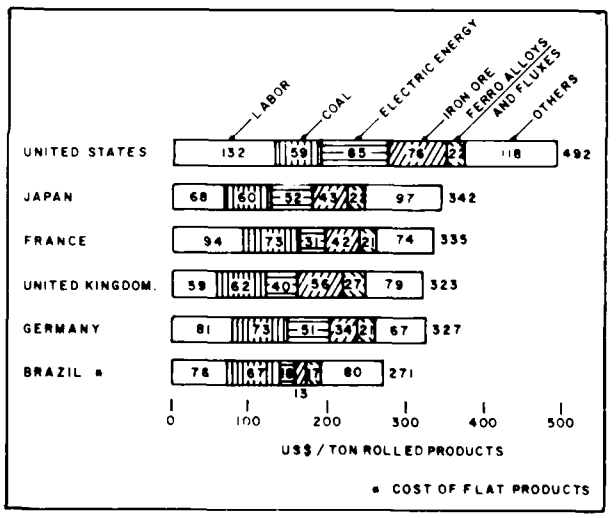


Figure 3 - Production Costs in Some Selected Countries Considering 90% Utilization Ratio.

## HSLA LINE PIPE STEELS IN DEVELOPING COUNTRIES.

The lines that follow briefly describe about the development of microalloyed SAW line pipe steels in a group of developing countries. Mention is also made, in some cases, to the stage of development of the steel industry. This might be the first document trying to summarize the subject in such a large geographical area and there is not much

published information available. Thus, there might be unintentional omission to some existing work.

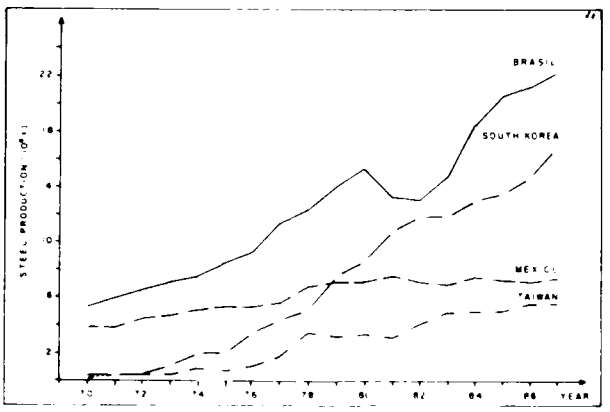


Figure 4 - Raw Steel Production in a Group of Developing Countries

BRAZIL - In the last seventeen years steel production in Brazil increased from 5.4 mt to 22.2 mt in 1987, and the country is now the 7th largest steel producer in the world. During the expansion programmes the local steel industry was equipped with advanced and efficient technologies and the country reached a high degree of competitiveness. From the position of steel importer in the mid seventies Brazil evoluted to a large exporter of steel products in the eighties, figure 5 (6). In September 1986 the objectives of the 2nd National Steel Plan were announced by the government. That plan establishes an increase in production capacity from 26 m tpy, in 1987, to 50 m tpy in the year 2000. It is to be developed through further expansion and modernization of existing plants and construction of new steel mills in different areas of the country. During that expansion program accelerated cooling for plate product is to be incorporated to one or two steel mills in Brazil. Work is already in progress to introduce combined blowing in BOF steelmaking at USIMINAS, a large line pipe steel producer in Brazil.

The steel companies in Brazil producing and processing microalloyed line pipe steels are Usinas Siderurgicas de Minas Gerais - USIMINAS, Companhia Siderurgica Paulista - COSIPA and, to a lesser extent, Companhia Siderurgica Nacional - CSN, with present raw steel production capacities of 3.9; 3.5 and 4.6 m tpy, respectively. All these companies operate hot metal treatment and sulphide shape control. USIMINAS and COSIPA are equipped with vacuum degassing RH units and USIMINAS has electromagnetic stirring also. Plate mills are located in USIMINAS and COSIPA which have powerful, about 6000 t separating force, 4100 mm wide rolling mills.These plants also have facilities for heat treatment of plates. CSN, on the other hand, has a modern 7 stand hot strip mill with production capacity of 3.2 m tpy and produces coils with maximum weight of 40 ton. Additional information about steel plant facilities and achievements in Brazil are available in good recent publications (5,7,8).

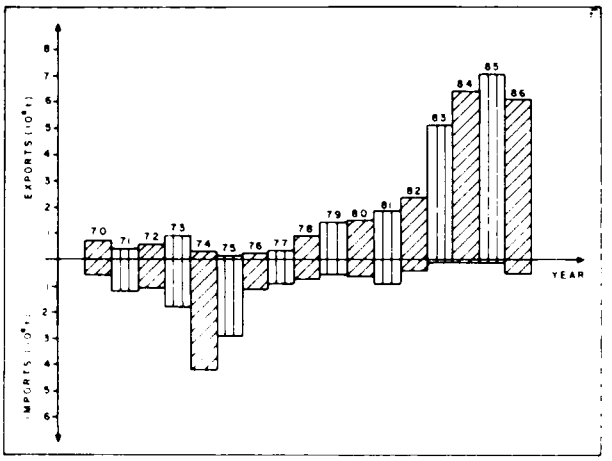


Figure 5 - Imports and Exports of Steel Products

In Brazil, production of plates for pipes on a commercial scale and meeting standard API 5LX was started in 1978 by the two steel plants equipped with plate mills - USIMINAS and COSIPA. Steel grades developed by that time were X52 and X60. Typical X60 grade alloy design comprised 0.15% C; 1.24% Mn; 0.22% Si; 0.010% P; 0.010% S; 0.035% Nb and 0.055% V for plates produced at USIMINAS (9). Similar steel was being produced by COSIPA. Exports of API steels started in 1979 when CONFAB (the Brazilian SAW pipe producer) produced 43 thousand tons of X52 pipes for Mexico. The plates were provided by USIMINAS.

The development and production of these two grades marked the beginning of the application of controlled rolling practices in Brazil. These practices had been assimilated through technical training and the visits of Brazilian metallurgists to steel plants in Japan and Europe.

Also in 1978, production of microalloyed steels by continuous casting started. USIMINAS, after having conducted extensive studies of the

TABLE I - TYPICAL CHEMICAL COMPOSITION AND MECHANICAL PROPERTIES OF API STEELS PRODUCED IN BRAZIL

a. CHEMICAL COMPOSITION

| STEEL | THICKNESS (mm) | CHEMICAL COMPOSITION | | | | | | | | | | |
|---|---|---|---|---|---|---|---|---|---|---|---|---|
| | | C | Mn | P | S | Si | Al | Nb | V | Cu | Ni | Ti |
| (1) X52 | 15.88 | 0.15 | 1.10 | 0.017 | 0.008 | 0.25 | 0.032 | 0.03 | - | - | - | - |
| (1) X60 | 19.05 | 0.14 | 1.30 | 0.018 | 0.006 | 0.22 | 0.035 | 0.03 | 0.06 | - | - | - |
| (1-2) X60 | 20.62 | 0.10 | 0.91 | 0.020 | 0.003 | 0.20 | 0.034 | 0.03 | 0.043 | 0.31 | 0.15 | 0.022 |
| (1) X65 | 9.53 | 0.11 | 1.40 | 0.018 | 0.005 | 0.25 | 0.029 | 0.03 | 0.040 | - | - | 0.03 |
| (2-3) X65 | 10.31 | 0.12 | 0.85 | 0.015 | 0.001 | 0.24 | 0.021 | 0.036 | 0.032 | 0.30 | 0.15 | 0.011 |
| (3) X70 | 14.27 | 0.10 | 1.58 | 0.015 | 0.004 | 0.27 | 0.022 | 0.033 | 0.072 | - | - | - |

b. MECHANICAL PROPERTIES

| STEEL | THICKNESS (mm) | MECHANICAL PROPERTIES | | | | |
|---|---|---|---|---|---|---|
| | | Rp (MPa) | Rm (MPa) | A (%) | C V N -20 C (J) | DWTT -20 C % F.F. |
| (1) X52 | 15.88 | 420 | 540 | 40 | 60 | 100 |
| (1) X60 | 19.05 | 510 | 610 | 37 | 72 | 100 |
| (1-2) X60 | 20.62 | 490 | 570 | 41 | 144 | 100 |
| (1) X65 | 9.53 | 570 | 640 | 33 | 88 | 100 |
| (2-3) X65 | 10.31 | 550 | 599 | 35 | 75 | 100 |
| (3) X70 | 14.27 | 610 | 696 | 32 | 101 | 100 |

NOTES: 1. PRODUCTS FROM USIMINAS
2. HIC RESISTANT STEEL
3. PRODUCTS FROM COSIPA

quality of continuously cast steel (10-11), produced since 1976, started casting a vanadium microalloyed structural grade - SAR 50 (12). The experience gained in these studies,and by being alert to the necessary measures recommended for continuous casting of microalloyed steels, resulted in good quality indices for SAR 50 continuously cast slab. At about the same time production of X52 and X60 grades by continuous casting was initiated (13), and this also maintained good quality indices. In addition to the application of controlled rolling and continuous casting to microalloyed API steels in 1978, an important point was the success of efforts in the direction of low sulfur steels. Although 0.010%S is the typical figure mentioned above for X60 steel sulfur contents of 0.005%-0.008% were being obtained by USIMINAS and COSIPA (13-14).

During subsequent years, production of API steels at USIMINAS and COSIPA increased substantially. Considering that API steel is one major consumer of microalloys in the product mix of USIMINAS, the above statement can be illustrated by figure 6 where the evolution of special ferroalloys consumption during the period 1978 - 1986 is shown (9,15).Contemporaneously with the increase in production, quality improvement occurred with the installation of units for sulfide shape control at USIMINAS and COSIPA. The ladle injection system at COSIPA began operation in 1980. That system was developed by COSIPA and a local research institute. At present, two of those units are in operation at COSIPA.

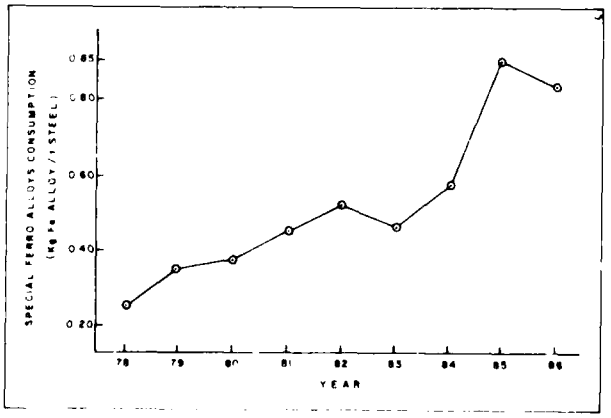


Figure 6 - Evolution of Special Ferroalloys Consumption at USIMINAS (FeNb+FeV+FeTi+FeCr)

The experience accumulated in the production of API steels in the late seventies accelerated the development of grades X65 and X70. Since 1981 those grades have been in normal production at COSIPA. USIMINAS started producing X65 grade in 1980 and X70 in 1983(16). These API steels have alloy designs based on the standard combination of niobium and vanadium , and exhibit fine ferrite-pearlite microstructures. Typical chemical compositions and mechanical properties are given in table I (17,8). Since the development of higher grade API steels in Brazil their commercial production has been significantly increasing, as shown in figure 7 (17). API steels produced in Brazil have been consumed in several projects, local and abroad. Some of them are mentioned in table II (17).

TABLE II - SOME APPLICATIONS OF BRAZILIAN API STEELS

| DESTINATION | GRADE | PIPE DIAMETER (inches) |
|---|---|---|
| Oil line between California and Texas | X70 | 30 |
| Gas line Reynosa-Escalon, Mexico | X52 | 24 |
| Gas line - underwater-Campos Basin, Brazil | X60 | 24 |
| Oil line, Golf of Campeche - Bocas, Mexico | X60 | 36 |
| Gas line Neuquém-Pachêco, Argentina | X52 | 30 |
| Gas line, Melbourne-Ballarat, Australia | X65 | 30 |
| Gas line-underwater-Bombayn, India | X60 | 20 |
| Gas line Neuquém-Bahia Blanca, Argentina | X60 | 30 |
| Gas line, Harzira-Jagdishpur, India | .60 | 18 and 36 |
| Gas line, V. Redonda-S. Paulo, Brazil | X65 | 22 |

In the mid of present decade CSN put into operation its modern hot strip mill which can produce, as previously mentioned, 3.2 m tpy of products, in width and thickness up to 1575 mm and 12.7 mm, respectively. Development of API steels up to X60 grade has been carryed out (18).

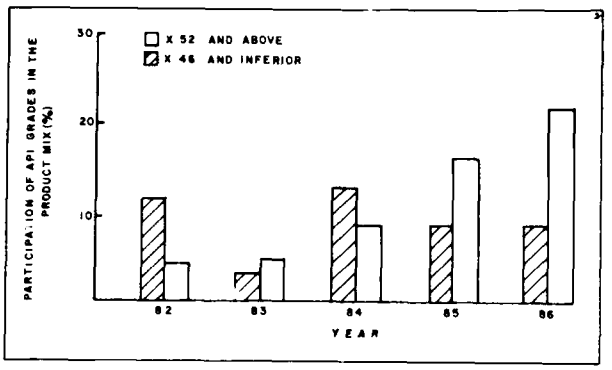


Figure 7 - Participation of API Steels in USIMINAS Product Mix

HIC resistant steels have been developed since about 1984 (19). To date HIC resistant grades up to X65 are available in USIMINAS (20) and also in COSIPA. Typical chemical composition is also shown in table I. The steels follow the recommended measures for HIC resistance, low S, low Mn, Cu addition and Ti treatment and meet BP conditions. HIC resistant steels under NACE solution have not been developed yet.

At present, a second generation of API HSLA steels is under development both at USIMINAS and COSIPA. Those two companies have been investigating steels with microstructure comprising lower temperature transformation products. USIMINAS has published the initial results obtained in industrial trials, table III (17). In that table it is observed a further move in the direction of lower carbon contents. COSIPA has started development to obtain X80 grade and a move to lower carbon content is expected in order to meet higher toughness requirements. Further information about this development is presented by COSIPA in this conference.

USIMINAS is participating with CONFAB and CBMM of an international program on the development of superior steels processed under relaxed controlled rolling regime. An industrial heat was produced and chemical composition and mechanical properties are shown in table IV. With the alloy design selected, independently of the severity of the rolling schedule applied very high toughness properties are obtained. At present, a detailed pipe weldability program is being concluded at CONFAB and results are to be published soon.

It is also important to mention that Brazilian API steels are marketed either in the form of plate or in the form of pipes. SAW pipes in Brazil are produced by Confab Industrial SA. The SAW pipe division of that company was established in 1974 and produces pipes in diameters up to 48 inches. CONFAB also produces spiral and ERW pipes and has been giving an important contribution to the development of line pipe steels in Brazil. The company is very much involved in new developments with the Brazilian steel companies.

The production of API steels meeting strict quality requirements has added Brazil to the list of the few countries which export such products. It is now expected that Brazil will start the stage of sophistication of the API grades.

SOUTH KOREA - South Korea, as well as Brazil, are two of the world's fastest growing steelmaking countries, after China, figure 4. Raw steel production in South Korea increased from only 480 thousand tonnes in 1970 to 16.8 mt in 1987. Pohang Iron and Steel Co. - POSCO is the largest and most important steel company in South Korea with a total raw steel production capacity of 11.8 m tpy, in two works - 9.1 m tpy in Pohang Works and 2.7 m tpy in Kwangyang Works (21). The later is a very modern steel plant, producing hot strip products, which started operation in 1987. Pohang works is also a modern steel plant that had its start up in 1973 (22). At that time Pohang works could produce 1 m tpy (23). Successive expansions boosted production capacity to present 9.1 m tpy level and modern equipments have been installed.

Although raw materials for steelmaking are mostly imported from overseas very efficient steel mills and low labor cost will certainly keep the South Korea position of a growing and strong steel industry complex. Productivity at Pohang Steel Co. is rated at 760 ton/man/year (24) and total cost of producing steel products is 39% lower than that of Japan (25). It is predicted that crude steel productior will rise by an average 6.5% until 1990 and then 3.9% annually between 1991 and 2000 (21). Exports of steel products are predicted to rise by an average 4.7% until 1990 and then fall to an average of 1.1% annually by the end of the century. In 1987 South Korea exported about 44% of its flat products production. However, it is also expected that local demand of steel products will be above production capacity by the year 2000 (21).

POSCO, in Pohang Works, has steelmaking facilities to produce superclean steel grades. Hot metal treatment, RH degassing as well as ladle furnace and electromagnetic stirring in continuous casting are available (22,26,27). The processing equipments are impressive also.

TABLE III - CHEMICAL COMPOSITION AND MECHANICAL PROPERTIES OF ACICULAR FERRITE X 70 STEEL PLATES

a. CHEMICAL COMPOSITION

| | CHEMICAL COMPOSITION | | | | | | | | |
|---|---|---|---|---|---|---|---|---|---|
| THIC-KNESS (mm) | C | Mn | Si | P | S | Al | Nb | V | Mo |
| 14.00 | 0.07 | 1.74 | 0.26 | 0.023 | 0.006 | 0.035 | 0.038 | 0.062 | 0.20 |
| 12.00 | 0.05 | 1.65 | 0.26 | 0.015 | 0.005 | 0.038 | 0.041 | 0.061 | 0.25 |
| 9.50 | 0.07 | 1.63 | 0.22 | 0.018 | 0.003 | 0.033 | 0.041 | 0.062 | 0.20 |

b. MECHANICAL PROPERTIES

| | MECHANICAL PROPERTIES | | | | | | |
|---|---|---|---|---|---|---|---|
| THIC-KNESS (mm) | Rp (MPa) | Rm (MPa) | A (%) | Rp / Rm (%) | CVN (-20 C) J /cm2 | DWTT (-20 C) (%) | HV10 |
| 14.00 | 520 | 750 | 21 | 69 | 80 | 100 | 235 |
| 12.00 | 540 | 720 | 20 | 75 | 130 | 100 | 235 |
| 9.50 | 560 | 710 | 21 | 79 | 135 | 100 | 230 |

There are two plate mills with maximum separating forces of 4000 ton (prod. cap. of 0.4 m tpy) and 7000 ton (prod. cap. of 1.4 m tpy) capable of producing plates with maximum widths of 3000 mm and 4500 mm, respectively. There are two hot strip mills, one of them with 3 continuous and 1 reversing type roughers plus a finishing train of 4 high x 7 stands. This mill has a production capacity of 3.3 m tpy.

The development of line pipe steels at Pohang works was initiated in 1975 and progressed under steps as follows (28):

1978 - Development of controlled rolling and cooling technology.

1983 - Development of sulphide shape control technology

1983 - Improvement on microalloying technology for grain refining.

As a result, line pipe steel grades up to X70 strength level are commercially produced. Not only NbV microalloyed line pipe grades with ferrite + pearlite microstructure (plus Ti treatment) have been developed. Investigations have been made also on acicular ferrite grades

of which first results were published in 1984 (29). Exports of line pipe steel by POSCO have already started.

It can be expected that POSCO will experience further progresses in the area of line pipe steels. Modern and sophisticated equipments are available and by November this year on-line accelerated cooling is to start operation in number 2 plate mill (28). In addition, very modern research and development facilities with well qualifyed metallurgists are available to support new products development. The research and development centre (Research Insitutte of Industrial Science and Technology - RIST), with about 400 employees, has, among other facilities, modern electronic microscopes and powerful pilot rolling mills, one of them with a pilot unit for simulation of accelerated cooling of plates.

TAIWAN - Taiwan, in sequence to Brazil and South Korea, is classified as the third developing area that has become a major steel exporter and have a dominant steel export power for the rest of the century (25). Steel production in Taiwan has been increasing since 1977, as shown in figure 4, specially due to expansions in its most important company China Steel Corportation - CSC. CSC started operation not long ago, 1977, with a production capacity of about 1.5 m tpy. In a second stage the production capacity of the plant was increased to 3.25 m tpy and in April this year the third expansion stage is to be completed, lifting CSC installed capacity to 5.65 m tpy. A fourth expansion is planned to increase installed capacity to 8 m tpy (30). As a natural consequence of the recent expansions CSC is a steel works with up to date technology in steelmaking and processing, capable of developing high quality line pipe steels. The plant is 100% operated by continuous casting. Hot metal treatment, combined blowing, vacuum degassing, ladle injection technology, high quality metallurgical expertise and excellent research facilities are available. The plate mill has a production capacity of 400,000 tpy and the hot strip mill has been modernized to produce 3.7 m tpy.Concentration on the development of line pipe steels in CSC has occurred during the last five years and has aleady reached the X70 grade. The subject, however, is not discussed further in this session as it is to be presented in detail in S.C. Wang et. al., technical contribution to this conference (31).

MEXICO - Mexico, as an oil producing country, is a regular consumer of HSLA line pipe steels from both local supply and imports. The evolution of Mexican steel production is shown in figure 4 where it is seen a significant increase during the seventies. Since 1979 steel production has stabilized at the level of 7 m tpy which is about the quantity absorbed by the local market (32). Steel production capacity is 9.16 m tpy (33). Large tonnage steelmaking is concentrated in three steel companies - Altos Hornos de Mexico SA - AHMSA; HYLSA SA and Siderurgica Lazaro Cardenas - Las Truchas SA, SICARTSA with production capacities of 3.2; 1.85 and 1.25 m tpy, respectively.

Production of HSLA line pipe steels is concentrated at AHMSA where the X42 and X52 grades were initially produced between 1963-1965 (34). At that time the API grades were semi-killed C-Mn steels. In 1968/1969 the first microalloyed steels were produced, using either vanadium or niobium, depending on product thickness (X52 - $t \geq 12.5$ mm = vanadium strengthened; $t <$ 12.5 mm = microalloyed with niobium).

The company has produced up to grade X65 under maximum thickness and of 21mm and 3050mm, respectively. The API up to grade X65 are also produced in [illegible] mi for ERW pipes( 1473 mm max [illegible]). ypic[illegible] ch[illegible]nical compositions and mec[illegible]al properties o[illegible] line pipe steels produced . AHMSA are shown in table V (35). In that table it is noticed that HIC resistant steels have been developed also. Hot metal treatment and CaSi injection technology (wire feed) are available in the plant for production of clean steels with sulphide shape control. AHMSA 2 stands plate mill and the hot strip mill can produce annually 960,000 t and 1.7 mt, respectively. The plant has a modernization plan that includes botton blowing, vacuum degassing and upgrading of the hot strip mill. The rehabilitation of the hot strip mill will not expand production capacity and is to be completed in 1990 (36).

A major impact on the line pipe steels product area will certainly occur when SICARTSA II project is concluded. That project includes installation of a new 1.5 m tpy plate mill. However, delays have been occurring and there is a chance that the plate mill will not be operating in the next few years (37). A new pipe mill (Productora Mexicana de Tuberia SA - Protumsa) for the production of large diamenter pipe - OD up to 48 in - with production capacity of 300,000 tpy has already been in operation in the SICARTSA area for about two years (38).

Mexico has become an exporting country of HSLA line pipe steels and recently was supplying to the Loma de la Lata - Buenos Aires X60 gas line in Argentina. That line comprises pipes of 24, 30 and 36 in OD. Steel plates were

TABLE IV - PROCESSING CONDITION AND MECHANICAL PROPERTIES OF SPECIAL GRADE API STEEL

| 0.05C 1.66Mn 0.005S 0.022Ti 0.10Nb 0.31Cr | | | | | | | |
|---|---|---|---|---|---|---|---|
| ROLLING CONDITION | | MECHANICAL PROPERTIES | | | | | |
| | | | | | CHARPY TEST | | |
| REDUCTION | FINISH TEMP. C | Rp (MPa) | Rm (MPa) | A (%) (50.8mm) | CVN 20 C (J) | FATT ( C) | DWTT 85% FATT ( C) |
| 2.8t<900 C | 780 | 455 | 550 | 48 | 221 | ND | ND |
| 2.9t<910 C | 800 | 464 | 540 | 50 | 240 | < -80 | -46 |
| 2.9t<800 C | 740 | 474 | 560 | 46 | 255 | < -80 | -46 |
| 4.3t<810 C | 730 | 490 | 571 | 41 | 217 | < -80 | -55 |

NOTES: t = 16.5 mm
REHEATING TEMPERATURE = 1180 C

TABLE V - TYPICAL CHEMICAL COMPOSITION AND MECHANICAL PROPERTIES OF HSLA STEELS FOR WELDED PIPE PRODUCED IN MEXICO (AHMSA)

| | CHEMICAL COMPOSITION (2) | | | | | | | MECHANICAL PROPERTIES | | | | |
|---|---|---|---|---|---|---|---|---|---|---|---|---|
| STEEL | C | Mn | P | S | Si | Nb | V | Rp (MPa) | Rm (MPa) | A (%) | CVN C | CVN J |
| (1) X52HIC | 0.08 | 1.0 | 0.014 | 0.005 | 0.25 | 0.012 | 0.045 | 427 | 552 | 38 | -15 | 75 |
| X52 | 0.15 | 1.1 | 0.015 | 0.015 | 0.10 | 0.025 | - | | | | | |
| X56 | 0.12 | 1.3 | 0.015 | 0.015 | 0.20 | 0.025 | - | | | | | |
| (1) X60HIC | 0.08 | 1.0 | 0.014 | 0.005 | 0.25 | 0.035 | 0.060 | 483 | 586 | 39 | -15 | 85 |
| X60 | 0.12 | 1.2 | 0.015 | 0.010 | 0.20 | 0.025 | 0.05 | | | | | |
| X65 | 0.12 | 1.3 | 0.015 | 0.010 | 0.25 | 0.025 | 0.05 | 503 | 593 | 35 | 0 | 79 |

NOTE: (1) Ca treated; Cu = 0.30; Ni = 0.24; processed in the plate mill only.
Other grades processed in the hot strip mill also.
(2) Al = 0.04

supplied by AHMSA,(maximum pipe diameter from AHMSA plates is 36 in). API steels have also been exported to Malaysia, China, Colombia and India.

VENEZUELA AND ARGENTINA - Venezuela and Argentina, countries that reached the level of 3.5 mt of raw steel produced in 1985, have already started the development of HSLA line pipe steels for SAW pipes.

In Venezuela, Siderurgica del Orinoco - SIDOR is the steel company producing HSLA flat products. The plant, with a total raw steel production capacity of 4.8 m tpy, has been developing line pipe steels processed in the hot strip mill. Plates are produced out of the roughing stands of that mill. Vanadium microalloyed grades up to X60 strength level have been produced. In order to improve toughness properties a program has been initiated to produce API steels microalloyed with niobium. Due to the use of direct reduction product as raw material in steelmaking (electric arc furnaces) production of clean steels is not a difficult task at SIDOR. Sulphide shape control is carryed out through calcium treatment by wire injection in the argon stirring stations.

In Argentina, production of steel for welded API grades is by Sociedad Mixta Siderurgia Argentina - SOMISA, which has a raw steel production capacity of 4.6 m tpy. SOMISA started production of microalloyed steels in 1974. In the late seventies production of API X52 started, for products with thickness between 4.75 mm and 9.5 mm, processed in the hot strip mill (SOMISA is not equipped with a plate mill yet) (39). The initial production of API grades was microalloyed with titanium and as the company succeeded in developing low sulphur steels there was a move to niobium microalloying. Although with power limitation in the hot strip mill the company has developed up to X60 grade in thickness up to 9.50 mm . The rolling mill has 4 roughing and 6 finishing stands. Maximum product thickness and width are 12.7 mm and 1506 mm, respectively. The chemical compositions for the range of thicknesses produced are shown in table VI (40). At present,low sulphur steels contain about 0.005%S. Hot metal treatment is available and Ca injection is being installed. Several measures in the plant have been or are being taken to improve product quality and those include quality of refractories used, change in type of nozzles used in the continuous casting plant, system to avoid contamination of the heat with slag, insulations in the HSM, automation for the cooling system and diferential coiling temperature (40). Further significant progress in the development of HSLA steels for welded pipe at SOMISA is expected after the installation of a plate mill which was commissioned by that company.

INDIA - In the last 10 years steel production in India has been situated between 10 and 12 m tpy (12.6 m ton in 1987). The local demand for steel product, at present about 15 m tpy, is expected to increase to 25 m tpy by the end of the century (41). Steel Authority of India Ltd.- SAIL is the largest steel company with a production of 7 m tpy of final products in eight steel works. SAIL has an expansion plan to increase final products output to 15 m tpy and to modernize its steel works (60% of SAIL steel production is via open hearth process).

In addition to being the largest steel company in India it is in SAIL that development of line pipe steels has been concentrated, specially in its Rourkela Steel Plant - RSP where hot metal treatment, secondary refining under vacuum and a modernized (1980) hot strip mill are available (42-43). RSP also has plants for ERW (1960) and spiral welded (1976) pipe production.

Development of X60 grade and trial for the production of X70 dates to the early eighties and were published by RSP in 1984 and in 1986 (42-43). The two grades X60 and X70 are NbV and NbMo microalloyed, respectively. Sulphide shape control is done by misch metal additions in the ingot mould. Typical chemical composition and mechanical properties for X60 grade are shown in table VII.

The X60 grade developed by RSP already found commercial application in the local market. RSP supplied 22000 ton of that steel to the Gas Authority of India Ltd after being successful in a competition with several international suppliers (43).

The Tata Iron and Steel Co has also been working in the area of microalloyed steels. With the operation of a new melting shop equipped with secondary refining which allows production of low sulphur steels that company will certainly start the production of high strength line pipe steels (44).

ALGERIA AND INDONESIA - Algeria and Indonesia do not produce large quantities of steel but have started to develop HSLA steels, processed in the hot strip mill, for welded pipe.

In Algeria, Societe Nationale de Siderurgie - El Hadjar steel works has a production capacity of 2.2 m tpy. Plant facilities include both BOF and Electric Arc Steelmaking, continuous casting and a plant for spiral welded pipe. Line pipe steel development for spiral pipes

TABLE VI - API HSLA STEELS FOR WELDED PIPE PRODUCED BY SOMISA

| GRADE | THICKNESS | C | Mn | P(max) | S(max) | Si | Al (max) | Nb |
|---|---|---|---|---|---|---|---|---|
| (1) X52 | 4.75 - 5.50 | 0.07 - 0.11 | 0.45 - 0.75 | 0.025 | 0.015 | 0.15 - 0.30 | 0.02 | 0.02 - 0.04 |
| | 5.51 - 6.35 | 0.08 - 0.13 | 0.60 - 0.90 | 0.025 | 0.015 | 0.15 - 0.30 | 0.03 | 0.02 - 0.04 |
| (2) X52 | 4.75 - 6.35 | 0.10 - 0.15 | 0.60 - 0.90 | 0.025 | 0.015 | 0.15 - 0.30 | 0.03 | 0.02 - 0.04 |
| | 6.35 | 0.06 - 0.10 | 0.90 - 1.10 | 0.025 | 0.015 | 0.15 - 0.30 | 0.045 | 0.02 - 0.04 |
| | 6.36 - 9.50 | 0.12 - 0.16 | 0.90 - 1.15 | 0.025 | 0.015 | 0.15 - 0.35 | 0.02 | 0.025 - 0.045 |
| | 12.50 | 0.12 - 0.16 | 0.95 - 1.20 | 0.025 | 0.015 | 0.15 - 0.35 | 0.02 | 0.03 - 0.05 |
| (3) X60 | 7.90 - 9.50 | 0.08 - 0.11 | 1.15 - 1.35 | 0.020 | 0.010 | 0.20 - 0.35 | 0.02/ 0.05 | 0.03 - 0.05 |

NOTES: 1. Min. Tensile Strength 455 MPa
2. Min. Tensile Strength 495 MPa
3. X60/X65; Ti = 0.02 - 0.04

TABLE VII - CHEMICAL COMPOSITION AND AVERAGE MECHANICAL PROPERTIES OF GRADE X60 DEVELOPED AT ROURKELA STEEL PLANT

| CHEMICAL COMPOSITION | | | | | | MECHANICAL PROPERTIES (t = 9.5mm) | | | |
|---|---|---|---|---|---|---|---|---|---|
| C | Mn | Si | Nb(1) | V(1) | Al | Rp (MPa) | Rm (MPa) | A (%) | C V N O C (J)(transverse) |
| 0.06 | 1.15 | 0.30 | 0.03 | 0.05 | 0.025 | 539 | 608 | 35 | 100 |
| 0.10 | 1.30 | 0.40 | 0.05 | 0.08 | 0.040 | | | | |

NOTE: (1) Nb + V $\leq$ 0.10%

has reached grade X60 and trials for the development of X70 have been made.

P.T. Krakatau Steel in Indonesia, 1.5 m tpy production capacity by electric arc steelmaking and continuous casting, put in operation, beginning of 1984, a modern 1 m tpy hot strip mill. In that same year production of API steels started and at the end of that year the company was producing Nb microalloyed X56 grade to meet an order of 5600 t, product thickness of 14.3 mm. Most of the production of API HSLA steel at Krakatau steel has been X52 grade for ERW pipe (45). Further progress on the development of API grades at Krakatau steel can be expected in the near future.

CHINA - China already produces some quantities of HSLA API steels for welded pipes and the country will certainly become a regular producer of high grade API steels in the future.

Steel production in China has been continuously increasing. The country has become the fourth world major steel producer and in 1987 raw steel production reached 55.3 m ton. There are plans to reach 80 m tpy by the end of the century (46).

Not only steel production is increasing but also steel mills are being modernized aiming at increasing productivity and upgrading the product mix. In China there are 14 steel companies with production capacity above 1 m tpy. The largest is Anshan Iron and Steel Co. with a production capacity of 7.2 m tpy. Anshan produces large quantities of HSLA steels but has not concentrated on the API grades for SAW pipe yet due to plant facilities available at present. The company however is to expand to 10 m tpy by the early 1990s and to 15 m tpy by the end of century (47). In the expansion plan it is included new steelmaking facilities and installation of a plate mill which is to start up in 1991 (48-49). Anshan steel works has a good R and D infrastructure and has been doing several developments in the area of HSLA Steels. Recently, Prof. Y. Cao - an expert from Anshan, published a review paper on the subject which includes processing of line pipe steels (50). Thus, when the equipment is available Anshan will certainly become a strong producer of microalloyed steel for SAW pipes.

Second in size is Wuhan Iron and Steel Co - WISCO with a production capacity of 4 m tpy. WISCO has a modern 1700 mm hot strip mill and its melting facilities include hot metal treatment, combined blowing, vacuum degassing (51) and sulphide shape control. WISCO has developed API steels processed in the hot strip mill. WISCO is to expand its production to 7 m tpy.

Baoshan Iron and Steel Works is a modern 3 m tpy steel company that started operation in 1985 producing semi-products. Construction of phase II is underway and a new 4.2 m tpy hot strip mill will start operation in the near future.

Shoudu Iron and Steel works, locatd in Beijing, is an efficient steel works - 2 m tpy with- its product mix concentrated on long products. However, tne company has commissioned a heavy plate mill from the spanish steel company Ensidesa (52). The plate mill is expeced to start operation in Shoudu in 1989.

The above are just a few examples that indicate that China can and certainly will reach a position of significant producer of high grade microalloyed steels, including API steels for SAW pipes. In addition to the investments which are being made on expansion, modernization and new facilities the importance of HSLA steels is well assimilated by the technical community. For instance, in 1985 the Chinese Society of Metals organized in Beijing an international conference on the subject, " HSLA steels 85" and a second similar event is already being organized to take place in 1990.

## CONCLUSION

The world is experiencing changes in the geography of steelmaking and those changes are starting to affect the geography of production of API steels for SAW pipes too.

A group of developing countries has reached a stage in its steel industry where production of traditional high grade line pipe steels has become one more item in the normal product mix of the steel mills. The sophisticated grades, such as very low carbon bainitic grades, have their production still limited to the traditional producers, but possibly not for a long time from now.

There are also potential new comers that will certainly spread even more the production of high grade API steels in a not too distant future.

Line pipe stels have long been the locomotive for the understanting and development of the metallurgy of microalloyed steels. Thus, it is a natural consequence that as microalloying becomes international, and as the adequate equipment is available, production of line pipe steels becomes international too.

## REFERENCES

(1) Stuart, H; Heisterkamp,F. Tendencias En El Uso de Ferroniobio En La Siderurgia Mundial. In: Ferroaleaciones 82. Proceedings, Santiago, ILAFA, 1982.

(2) Gray, J. M. and Ko, T. Conference Summary and Closing Remarks. In: HSLA Steels - Metallurgy and Applications. Proceedings, ASM International, 1986.

(3) Estadisticas de Produccion Siderurgica de America Latina. Siderurgia Latinoamericana - ILAFA, 331, Nov. 1987.

(4) World 1987 Cutput Second Highest Ever. Metal Bulletin no. 7255, 28 Jan. 1988.

(5) Soares, R.C.. The Present Stage of the Technical Capability of the Brazilian Iron and Steel Industry and Perspectives for Future Developments. Metalurgia International, 1 (1) October 1987.

(6) Anuario Estatistico da Industria Siderurgica Brasileira. Rio de Janeiro, IBS, 1975; 1983 - 1987.

(7) Leal, F.L. Technological Development of the Brazilian Steel Industry. Materials and Society 11(4) 1987.

(8) Bordignon, P. J. P., Schiesari, J. R. P., Oliveira, E.Q.. Experience in The Metallurgical Design and Production of HSLA Steels in a Developing Country - Brazil. ibid 2; pp. 407-421.

(9) Andrade, S.L.; Oliveira, J.I.; Hanan, I. Desenvolvimentos Recentes de Chapas Grossas na USIMINAS. In: Seminario de Laminação de Planos e Não Planos. Proceedings. Pp. 111-26. ABM/COPLAM, Ipatinga, 1982.

(10) Fontes R.S. and Pereira, L. O.. Qualidade do Material Produzido no Lingotamento Continuo da USIMINAS. Metalurgia, ABM, 33(238) pp. 573-7, 1977.

(11) Fontes, R. S.; Damiao W. C., Pereira, L. O., Horta, M.R.. Principais Tipos de Defeitos em Placas de Lingotamento Continuo. Metalrugia ABM, 34(251) pp. 721-8, 1978.

(12) Fontes, R.S., Taiss, E.J.M.; Miyashita, T. Chapas Grossas de Alta Resistencia Originadas do Lingotamento Continuo. Metalurgia ABM, 35(259) pp. 429-33, 1979.

(13) Fontes, R.S.; Miyashita, T.; Guidoni,V.; Braga, N.C.; Cardoso, A.D.; Puntigan, F.W.; Mangualde, A.; Castro, L.C.. Chapas Grossas para Tubos com Especificacoes Extras. Metalurgia ABM, 36(273) pp.517-21, 1980.

(14) Alarcon, O.E.. Desenvolvimento da Technologia de Fabricacao dos Acos de Baixa Liga e Alta Resistencia (acos BLAR) com Niobio. Siderurgia Latinoamericana ILAFA, (226) pp. 61-73, 1979.

(15) Andrade, S.L.. USIMINAS, 1986 - Personal Communication.

(16) Ferreira, I.S.. USIMINAS,1985 - Personal Communication.

(17) Guimaraes, N.C; Coelho, M.R; Ratnapuli, R.C.; Pereira, J.E.A.. Producao de Chapas Grossas na USIMINAS Destinadas a Fabricacao de Tubos de Grandes Diametros. In: II Encontro de Technologia e Utilizacao dos Acos Nacionais. Proceedings. ABM. COPPE-URFJ - Rio de Janeiro, 18-22, May 1987, pp. 189-205.

(18) Brito, R.M; Scal, M.W; Germano, R.L.; Caetano, F.D.; Souza, O.A; Candido, M.C.. Aplicacao de Conceitos de Tratamentos Termomecanicos no Desenvolvimento de Acos para Atendimento a Norma API. Metalurgia ABM, 41(335) pp. 569-74,1985.

(19) Miranda,F.J.F.; Ratnapuli,R.C.; Miyashita, T.; Avaliacao de Susceptibilidade de Acos API da USIMINAS à Trincas Induzidas por Hidrogenio em Meios Contendo H2S e Água . In: XXXIX Congresso Anual - ABM. Proceedings, Belo Horizonte - July 1984, pp.279-294.

(20) Miranda, F.J.F; Sathler, L.; Gomes, J.A.P.. Estudo da Nucleação e Propagação de Trincas Induzidas pelo Hidrogênio em Meios Aquosos Contendo H2S. In: XLII Congresso Anual - ABM. Proceedings, Salvador, October 1987, pp. 579-591.

(21) Rapid Growth Leaves Room For Two-Way Trade. Metal Bulletin Monthly, May 1987, pp. 49-52.

(22) Baik, D.K.. Improvement in the Product Yield in Iron and Steelmaking. SEAISI Kuala Lumpur Conference, 21-25 May, 1986.

(23) Mc. Manaus, G. Steel in the Third World. Iron Age, 5 July, 1985, pp. 23-31.

(24) Soares, R.C.. Perspectivas Tecnológicas para a Indústria Siderúrgica Brasileira. Metalurgia ABM, 43(357) pp. 490-511, 1987.

(25) Tanaka, F.J.. Production, Technology and Structural Adjustment Aspects of the International Iron and Steel Industry. SEAISI Conference, Bangkok, 18-20 May, 1987.

(26) Steel Times News. Steel Times 215(9) pp. 428,1987.

(27) POSCO Steel Products. Pohang Iron and Steel Company Ltd. Conpany publication.

(28) Lee,W.P.. Pohang Iron and Steel Company Ltd. Private Communication, 1987.

(29) Kim,T.U.; Kim,Y.G.; Kim,J.E.; Oh,S.I. Development of a Low Carbon - Manganese HSLA Steel For Arctic Linepipe Applications. In: High Strength Low Alloy Steels. Proceedings. D.P. Dunne and T. Chandra, Univ. of Wollongong, Wollongong, 1984, pp. 236-238.

(30) Metal Bulletin News. Metal Bulletin no. 7267, Thursday, 10 March 1988, pp.27.

(31) Wang, S.; Chen,S.; Wu,C.: Pan,Y.. Recent Development of Line Pipe Steels in Taiwan, Republic of China. Microalloying 88 - World Materials Congress, Chicago, 24-30, September 1988.

(32) Latin American Iron and Steel in Figures - 1987, ILAFA Publication, 1987.

(33) Santos, E.B.. La Siderurgia Mexicana en 1986-87 Y Sus Perspectivas. Siderurgia Latinoamericana - ILAFA, (331) pp. 42-46. November 1987.

(34) De Leon,C.V.D.. Altos Hornos de Mexico S.A. Private Communication, 1988.

(35) Villanueva,R.A. Tratamentos Termomecanicos de los Aceros. Siderurgia Latinoamericana - ILAFA, (315). July 1986 pp. 2-26.

(36) Metal Bulletin News. Metal Bulletin no. 7270, 21 March 1988, pp. 23.

(37) Metal Bulletin News. Metal Bulletin no. 7260. 15 February 1988, pp.26.

(38) Latin American Producers Gear Up for Growth. Metal Bulletin Monthly (203) November 1987, pp. 38-40.

(39) Zuliani, J.L. and Fiorino, H.. Producion de Aceros Microaleados en SOMISA. Siderurgia Latinoamericana - ILAFA (327). July 1987, pp.54-58.

(40) Zuliani, J.L.. Sociedad Mixta Siderurgia Argentina - SOMISA. Private Communication, 1987.

(41) Metal Bulletin News. Metal Bulletin no. 7226. 12 October 1987, pp.45.

(42) Patnaik, B.B.; Singh, K.S.; Tudekar, S.G.. Manufacture and Processing of Microalloyed Steels (SAILMA) at Rourkela Steel Plant. ibid 29, pp. 45-50.

(43) Mishra, S.; Chaudhuri, S.K.; Datta, R.; Saxema, A.K.; Ray,S.. Development of Thermomechanically Processed High Strength Linepipe Steels. First Indo-US Workshop on Iron and Steel Technology. January 1986.

(44) Mitra,A.N.;Maheshwari, M.D.; Mukherjee,T.; Irani, J.J.. A Family of High Strength Structural Steels - Developments at Tata Steel. Ibid 29, pp. 38-44.

(45) Soesilanto, I.. p.t. Krakatau Steel, Private Communication - 1987.

(46) Zhou, C. Prospects of the Chinese Iron and Steel Industry. Ibid 2, pp. 3-6.

(47) Metal News. Chinese Journal of Metal Science and Technology 3(4) 1987. pp 237.

(48) Metal Bulletin News. Metal Bulletin no. 7266, 7 March 1988, pp. 23.

(49) Metal Bulletin News. Metal Bulletin no. 7287 - 23 May 1988 pp. 47.

(50) Cao, Y.. Controlled Rolling and Accelerated Cooling of HSLA and MA Steels. Chinese Journal of Metal Science and Technology 3(2) 1987. pp. 63-73.

(51) Lu Da. The Developing Iron and Steel Industry of China. Metalurgia International 1(1) 1987, pp. 20-23.

(52) Metal Bulletin News. Metal Bulletin no. 7277, 18 April 1988, pp.23.

# INDUCTION BENDING OF HIGH STRENGTH LINE PIPE FOR SEVERE SERVICE APPLICATION

**Charles H. Moore**
Associated Piping & Engineering Company
Clearfield, Utah, USA

Abstract

Induction bending has progressed considerably since its inception, allowing for succession to a more sophisticated method for manufacturing elbows. With a key aspect of the process being the finite, hot-deformation band, derived for dimensional control and aesthetic formability, it has also been refined and developed as a metallurgical tool for developing superior microstructure and mechanical properties.

Additionally, the need for dimensional improvements has been recognized. For pipe bends with large diameter-to-wall ratios and small radii, bending forces can produce an ovality or flattening in excess of 2 1/2 per cent, typically unacceptable for pigging applications. In extreme cases, wrinkling of the intrados will occur. Avoiding productivity losses, an increase in wall thickness, which effectively stiffens the section, and an increase in bending temperature, which allows for improved material flow, have been used as solutions. However, excessive temperatures in the austenite phase can result in degradation of mechanical properties in high-strength, microalloyed, line pipe steels except when properly designed for such thermal cycles. And if a post-bend tempering treatment is applied to obtain properties in the bends, it inevitably leads to degradation of low-temperature toughness in the as-deposited, longitudinal seam, as found in the straight portion of the bend.

The fundamental considerations relating to induction bending and bendability are presented along with results from evaluations on induction bends. It is shown that dimensional and metallurgical balances can be obtained while focusing on typical pipeline requirements for high-strength, severe service application.

RAPID INDUCEMENT TO AUSTENITE in microalloyed, carbon-steel pipes during induction bending

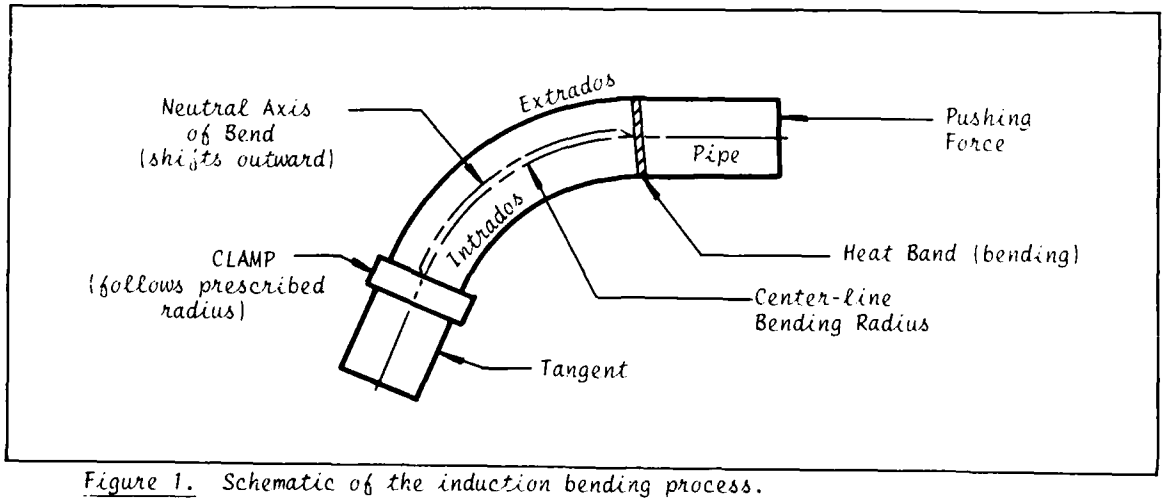


Figure 1. Schematic of the induction bending process.

provides the opportunity for studying the short-term kinetics of this transformation and its interaction with solute elements and compounds, and the affect on decomposition products and properties. Since the thermomechanical (TM) cycles are intentionally varied between quadrants to improve steel flow according to forming requirements, attention must be given to the compositions, manufacturing histories, process controls, and hence final microstructures of the parent and weld metals. Accordingly, productivity improvements can be implemented from the research, deleting energy-consuming and costly post-bend treatments such as normalizing or quenching plus tempering.

## INDUCTION BENDING

Inducing a rather narrow, hot, annular band in the pipe restricts the yielding to this location during bending, which assists in restraining roundness by confining the volume of material that is forced to pivot. The allegory has often been the simple bending of a soda straw on a small radius: the bent portion will flatten severely at the intrados and extrados, primarily due to the failure to limit the width of the annular deformation band to about the thickness of the wall.

Regarding Figure 1, the front tangent is clamped to follow the bending radius as the pipe is pushed from the rear. Application of the pushing force, which develops a bending moment, also causes a slight compressing of the overall length being bent and an outward shift of the neutral axis, which helps reduce thinning at the extrados. Net material flow is at the intrados, mostly toward the inside diameter, and is typically the most significant strain. These are all influenced by the bending radius, which affect on various strains is shown in Figure 2. Disregarding other consequences, ovaling forces can be minimized through temperature increases at the 'doses as the bending radius is decreased, augmenting flow demand with lower

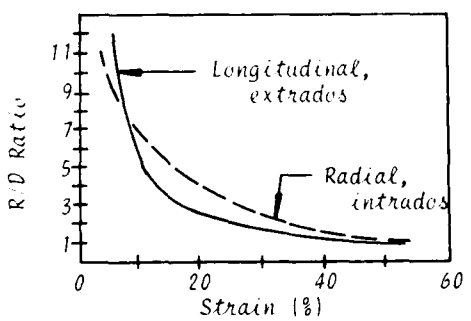


*Figure 2. Influence of the bending radius, expressed as R/D, on two significant strains.*

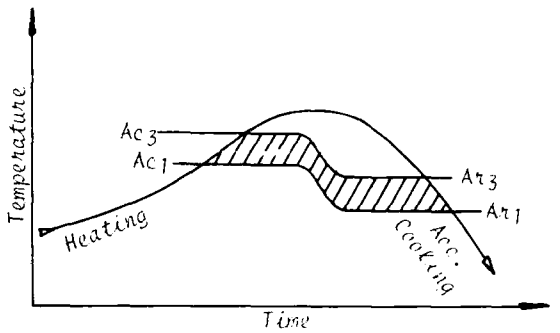


*Figure 3. Induction bending thermal cycle for high-strength severe service bends: austenitized less than 1 minute.*

yield strengths, reducing bending moment. There is little demand for strain in the neutral axis, which is customarily considered to be at the top and bottom quadrants.

These upsets, which are ultimately triaxial, occur in the austenite phase at a constant rate, subsequently fixed by the annular water-spray delivered by the induction coil. This thermal cycle is represented in Figure 3.

## SEVERE SERVICE CRITERIA

With the need to transmit sour hydrocarbons under pressure through hostile environments, it is necessary to use parent and weld metals that are compatible with the intended installation and service conditions. As well as high strength and good weldability, the steels must have resistance to one or more forms of hydrogen cracking and a notch-ductility that will oppose, under stress, crack initiation or propagation at the minimum handling or service temperature, typically defined as -46°C (-50°F) for arctic environments.

Recent studies [1, 2, 3] indicate various controls for negating the affects of hydrogen-induced cracking (HIC) and sulfide stress cracking (SSC), which also incorporates a hydrogen damage mechanism.

HIC resistance is possible by minimizing hydrogen ion entry to the steel matrix through the use of a protective film: for a pH greater than 5, additions of copper, nickel or chromium will suppress hydrogen penetration when the film is properly formed and maintained. Resistance is also possible by limiting the quantity of hydrogen ion traps, as well as optimizing their shape (spherical) and distribution, to minimize localized stress from $H_2$ formation. It is therefore significant to have fewer sulfide inclusions by controlling sulphur to less than .005 to .003 per cent, to employ inclusion shape

control in rolled plates by the use of even lower sulphur content or the use of calcium or rare-earth metal additions, and to have low levels of manganese segregation and segregated (banded) structures.

It is also important to confine hydrogen traps when lowering sensitivity to SSC; yet susceptibility also involves other parameters such as applied stress, hardness (per cent carbon and/or microstructure) and $H_2S$ concentration. For good resistance to SSC, high-strength pipe steels require low phosphorous, low volume fractions of nonmetallic inclusions, and of a spherical shape to reduce local stress intensity, and hardness less than about 248 HV10 (237 HB equivalent).

Notch-ductility is typically improved when the morphology of the microstructure is enhanced to resist HIC and SSC. It is also important that the as-manufactured microstructure be a result of fine grain practice and of a low carbon level, allowing transformation to more ductile constituents. This philosophy, which reduces hardenability and hence strength, is adequately compensated by microalloying the C-Mn steels that are rolled into plate for use in high strength line pipe.

Although these design criteria generally apply to the longitudinal weld seam too, microalloying may not be sufficient or may be injurious, depending on the subsequent heat treatment: re-austenitization followed by accelerated cooling, as employed during the induction bending of these steels; and tempering as needed, which can result in excessive precipitation of carbides or carbonitrides from the weld seam in the tangent (straight) portion of the bend, often resulting in a severe loss of low-temperature notch-ductility.

## BENDABILITY

It is essential that both the parent steel and weld seam of the pipe to be induction bent have good bendability; that is, that each be compatible with intended bending and/or post-bending treatments, applied in view of size and metallurgical design, for producing the desired dimensional and metallurgical responses. High-strength steel pipe, whether nonexpanded or expanded, is typically received in the following conditions:

parent (wrought): (a) control rolled (CR), or
(b) CR + accelerated cooled (AC);

weld (cast): (a) as-deposited x submerged arc (SAW) employing consumables of peculiar chemistries, or
(b) fusing of parent x electric resistance (ERW) without consumables, followed by re-austenitizing and cooling.

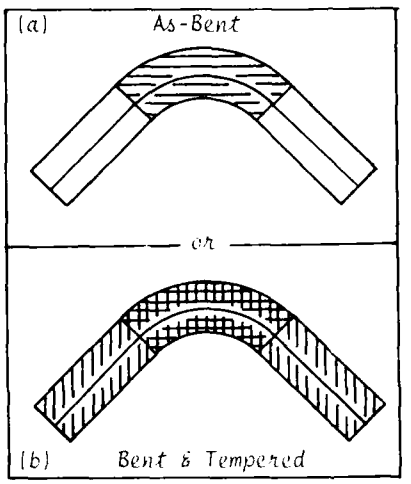


*Figure 4. Illustration of two thermal treatments for severe service induction bends.*

Most line pipe is designed for direct installation in the field, satisfying engineering criteria in the as-manufactured condition. Nevertheless, this can preclude metallurgical adaptability to the thermal cycles utilized for induction bends, particularly notch ductility for severe environments. Several thermal treatments likely to be encountered in a finished bend are shown in Figure 4.

The peculiar TM cycles chosen for a bend are themselves a function of the service criteria. the chemistries of the pipe, the TM history of the parent steel and the thermal history of the weld seam, the difficulty in bend geometry, and post-bend tempering, if necessary.

Post-bend tempering may be applied for the purposes of adjusting roundness, hardness, strength or toughness in the bend. It may even be used for the adjustment of a property in the tangent portion of the bend, which in most cases would be the toughness of the weld seam, to be discussed later. The difficulty of the geometry can be expressed as:

$$\text{Diff} = (D/w)/(R/D) = D^2/wR$$

where D = pipe bend outside diameter,
w = pipe bend wall thickness, and
R = center-line radius applied in bending,

which is also shown graphically in Figure 5. Bends with Diff = 15 to 20 require starting pipe with a design capable of responding to the more demanding TM cycles.

PARENT - This wrought steel should have low to very low carbon to adequately depress the hardness and the impact transition temperature, and broaden the range for preferred austenite decomposition products. Lower carbon typically necessitates an increase in manganese and various microalloying additions to ensure

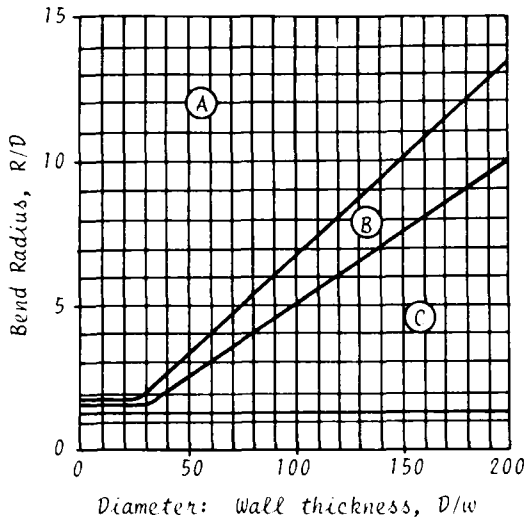


Figure 5. Relative difficulty for induction bending, as a function of its geometry: A = safe, B = difficult, and C = questionable.

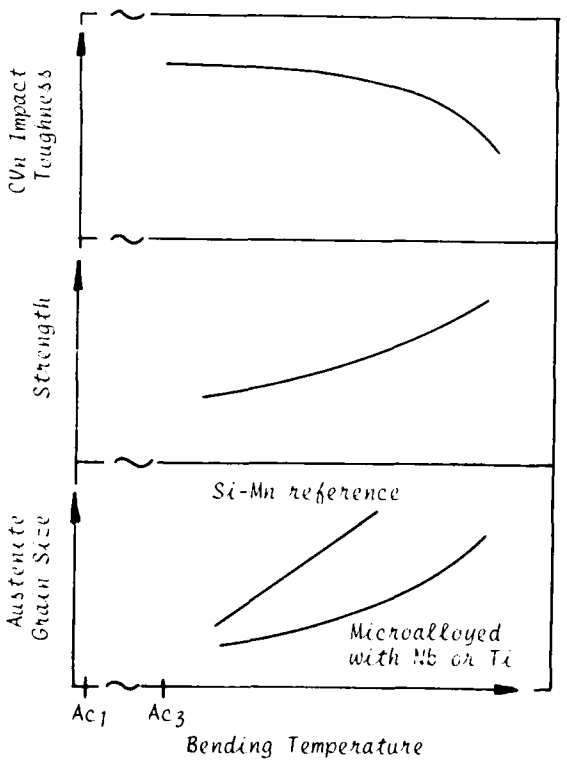


Figure 6. The effect of induction bending temperature on several properties of microalloyed pipe steels.

adequate strength throughout the wall thickness. Additions of aluminum, niobium and titanium produce fine austenite grains upon reheating, with subsequent recrystallization and growth inhibited by these elements during forming [4, 5]. Control of the austenite grain structure is lost when these compounds dissolve, thereby allowing rapid grain coarsening. Dissolution, primarily a function of temperature and carbonitride precipitate composition, will affect decomposition products and degrade properties according to the quantity and size of the coarsened grains, exemplified in Figure 6.

The composition of the wrought steel may be partially described by its carbon equivalent, $Ceq = C + Mn/6 + (Cr + Mo + V)/5 + (Ni + Cu)/15$, which helps quantify the adequacy of the steel in producing the desired mechanical properties. Figure 7 shows such a relationship [6], which may be adjusted by factors such as elements not so described, inclusion morphology, austenite conditioning or cooling rate.

WELD - The primary concern in the weld seam is its response to one or more types of heat treatments in developing satisfactory, low-temperature toughness. By retarding transformation from low-carbon, fine-grain austenite to a microstructure of acicular ferrite, bainite or even martensite, adequate toughness can be available, even after tempering. Such transformation may be suppressed by optimizing oxygen, Ceq and cooling rate for each thermal cycle applied to the seam [7].

Figure 8 shows an example of the affects on toughness, in a low-carbon deposited weld, of various heat treat conditions used for induction bends when alloyed with nickel and deposited with fluxes having different oxygen potentials. These data suggest that when post-bend tempering is planned, an optimum Ni-O composition will assist in producing severe service toughness while meeting the one per cent nickel maximum also required by NACE Standard MR-01-75 [8]. The resultant microstructures will respond favorably to tempering: acicular ferrite and bainite as-deposited and martensite as-bent (accelerated cooled), which help offset the deleterious effects of carbide and carbonitride precipitates coincident with tempering [9, 10, 11, 12].

For bends suitable for supply without tempering, transformation to martensite would be inappropriate, which has led to the development of very-low carbon steels with less orthodox microalloying philosophies.

## RESULTS

In the wake of much research, Figure 9 shows quantitative results of an intentional balance between parent steel and weld seam for induction bends of difficult geometry for high-strength, severe service applications. These 610 mm OD x 12.7 mm NW x 3D radius x 90° arc,

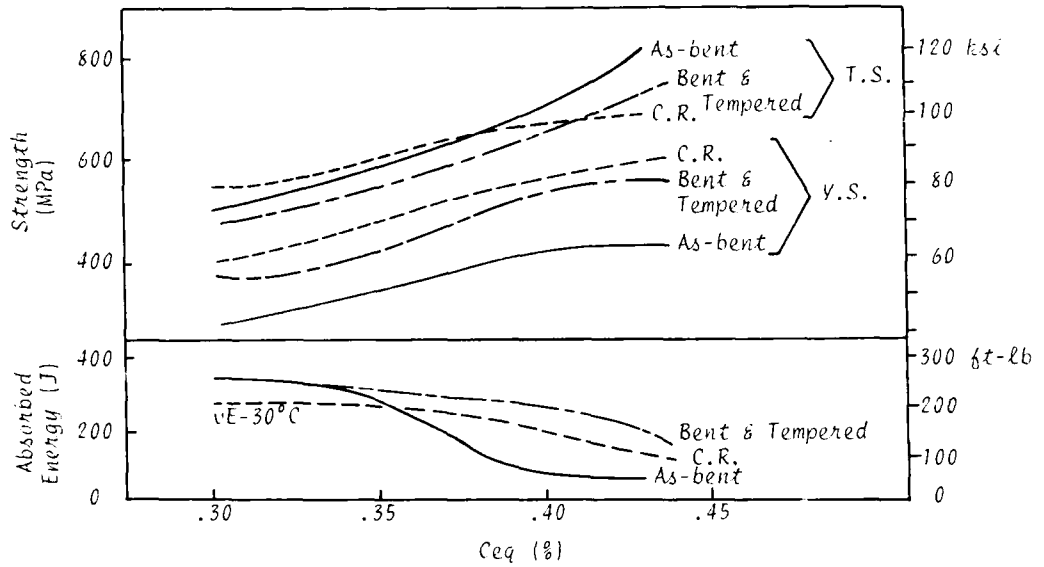


Figure 7. Relationship between carbon equivalent, Ceq, and mechanical properties. After Yamura, Hashimoto, et al. [6].

448 MPa (24" OD x .500" NW x 3D x 90°, X65) bends, with Diff = 16, were formed from straight-seam DSAW, cold expanded pipe.

The parent steel was aluminum deoxidized and calcium treated, with sulphur = .001 to .002 per cent and phosphorous = .012 per cent, and then continuous cast and control rolled. The welds, deposited while submerged under a highly basic flux to control the oxygen

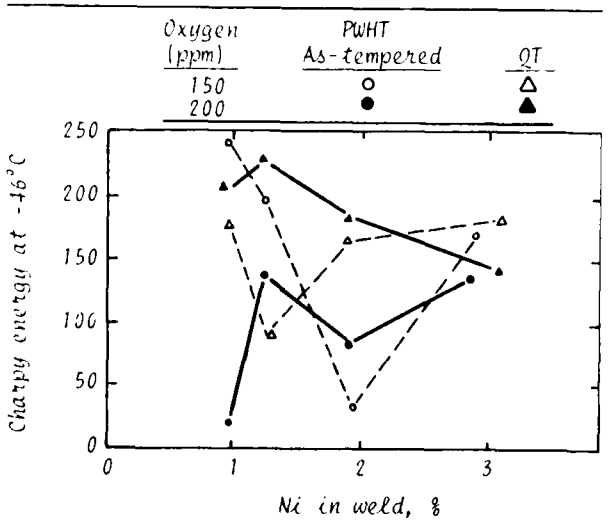


Figure 8. Effect of oxygen content on PWHT weld metal toughness for high Ni deposits. After Croft and Hipley [9].

concentration, were also very low in sulphur and phosphorous, yet notably gained a good portion of carbide formers by dilution from the parent. The double seam annotated DSAW 1 was used with the parent steel shown, and had a different nickel content for each pass. The other seam, DSAW 2, was used with an otherwise equivalent parent steel that was alloyed with 1/4 per cent copper plus 1/8 per cent nickel for improved HIC resistance and .07 per cent vanadium in place of molybdenum (both carbide formers). Note the compatibility of both weld seams for the thermal cycles employed, irregardless of precipitates coincident with tempering that would otherwise endanger toughness.

Careful process controls were employed to balance the high temperatures necessary for acceptable roundness and acceptable metallurgical properties, such as parent toughness at the extrados. One can imagine the control "window" upon careful study of the figure, noting the intrados supported a higher temperature where material flow was in greatest demand. Ovality and flattening were 3.1 per cent and 1.8 per cent maximums, respectively, and 2.1 per cent and 1.0 per cent maximums when applying mechanical constraint.

## CONCLUSION

With cooperation between the manufacturers of the plate, the welding consumables, the pipe and the induction bends, it is possible to make bendable linepipe for forming elbows for high-strength, severe service: acceptable dimensional and metallurgical properties from demanding TM cycles.

| | C | Mn | Si | Mo | V | Nb | Ni | O |
|---|---|---|---|---|---|---|---|---|
| Parent, % | .10 | 1.50 | .23 | .14 | - | .02 | .02 | - |
| DSAW 1, % | .09 | 1.47 | .25 | .07 | - | .02 | * | 190 ppm |
| DSAW 2, % | .09 | 1.43 | .24 | .01 | .04 | .02 | .86 | 200 ppm |

* inside pass, 0.89%; outside, 2.0%.

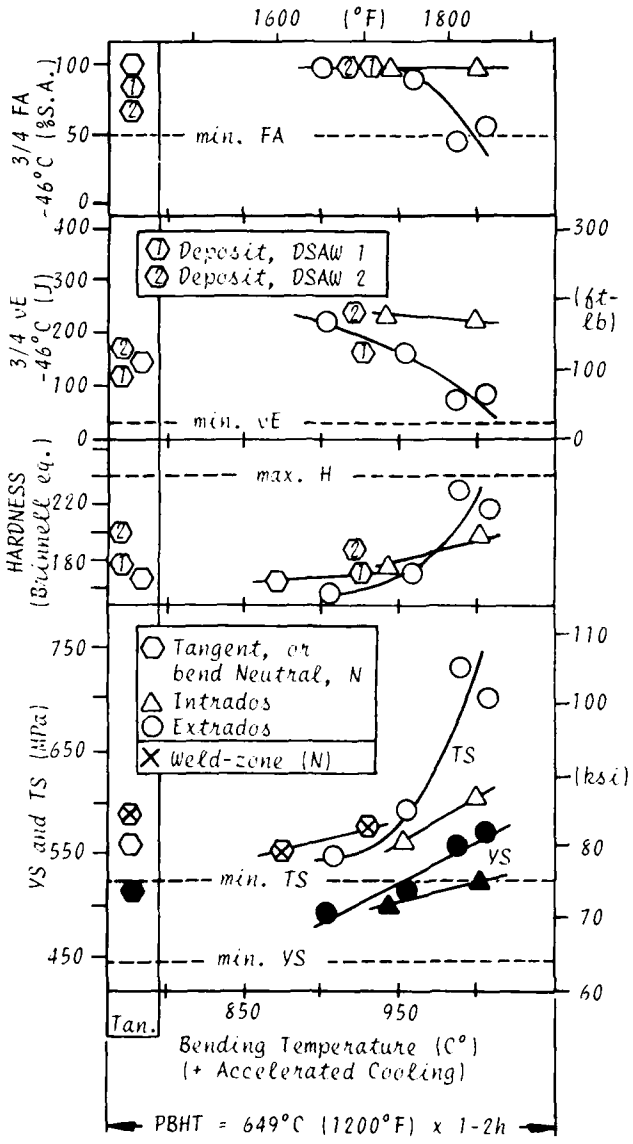


*Figure 9. Properties of tangent and bend versus thermal cycles employed, showing intended compatabilities of parent and weld metals.*

## REFERENCES


[1] Jones, C.L., P. Rodgerson and A. Brown, "Mechanism of Hydrogen Induced Cracking in Pipeline Steels", from the International Conference on Technology and Applications of HSLA Steels, October 1983, Philadelphia.

[2] Pressouyre, G.M., R. Blondeau and L. Cadiou, "HSLA Steels With Improved Hydrogen Sulfide Cracking Resistance", ibid, Ref. [1].

[3] Hill, R.T., "Specification and Fabrication of Steels For Use in Sour Hydrocarbon Pipelines", from the International Conference on HSLA Steels '85, November 1985, Beijing, China.

[4] Watanabe, H., Y.E. Smith and R.D. Pehlke, "Precipitation Kinetics of Niobium Carbonitride in Austenite of High-Strength Low-Alloy Steels", reprinted from Hot Deformation of Austenite.

[5] Gray, J.M. and A. J. DeArdo, "Austenite Conditioning Alternatives For Microalloyed Steel Products", ibid. Ref. [3].

[6] Yamura, T., T. Hashimoto, Y. Komizo, T. Sawamura, I. Hoshi and H. Nakate, "Development of Heavy Wall High Strength Bent Pipe For Arctic Usage", from the International Conference on Welding in Energy Related Projects, Toronto, September 20-21, 1983.

[7] Gray, J.M., R.T. Hill and C.H. Moore, "Metallurgical Implications of Induction Bending", from the Advanced Pipe Fabricating Technology Conference, New Orleans, April 18-19, 1988.

[8] National Association of Corrosion Engineers, Technical Practices Committee, Standard MR-01-75, "Material Requirements: Sulfide Stress Cracking Resistant Metallic Materials for Oil Field Equipment", January 1984, USA.

[9] Croft, N.H. and R.L. Hipley, "Microstructure and Properties of Heat Treated Weldments", from the International Conference on The Effects of Residual, Impurity, and Microalloying Elements on Weldability and Weld Properties, London, 15-17 November 1983.

[10] Croft, N.H., J.M. Gray and A. J. DeArdo, "Submerged Arc Weld Metal Toughness In Microalloyed Linepipe Steels - The Effects of Post-Weld Heat Treatment", from the International Conference on HSLA Steels, Philadelphia, October, 1983.

[11] Akao, K., K. Uma, K. Hirabayashi, T. Taira, O. Hirano, J. Takehara and T. Murata, "Development of Large-Diameter UOE Pipes for High Strength Bent Pipes Fabricated By Induction-Hot-Bending Process", from the OMAE Conference, New Orleans, 1986.

[12] Taira, T. and C.H. Moore, "Induction Bending of Large Diameter, Welded, High-Strength and Duplex S.S. Linepipes For Arctic Environments", from the Pipe Technology International Conference, Rome, 17/19 November 1987.

# EXPERIENCES WITH STRUCTURAL STEELS IN THE OFFSHORE INDUSTRY

**Mamdouh M. Salama, Marvin L. Peterson, William H. Thomason**
Conoco Inc.
Ponca City, Oklahoma, USA

ABSTRACT

In general, the offshore petroleum industry has had good experience with structural steels. This can be attributed to the conscious cooperation between domestic international steel suppliers and those involved in offshore design, fabrication, certification and operation. This involvement of all interested parties has resulted in major advances in the steel making process and the introduction of new technology steels that meet the demand for higher strength, good through thickness (Z-direction) properties, higher toughness, and improved weldability. This paper reviews offshore industry experiences highlighting successes and discussing the cause and the effect of the few problems on the steel technology. The paper will also provide some insight on the current concerns of the offshore industry with structural steels as it moves to develop offshore facilities in deepwater and arctic conditions.

OVER THE LAST TWO DECADES, technology employed by the offshore petroleum industry has seen dramatic changes to allow exploration and production in environments that were considered prohibitive twenty years ago. This technology development which has revolutionized the offshore petroleum activities is the result of a conscious cooperation between all those involved in offshore exploration and development. Figure 1 provides a historical and projected water depth for offshore exploration and production activities(1). This exponential increase in water depth was a major motive for the offshore industry to develop new concepts such as Tension Leg Platforms and to strive to reduce the weight of both these new concepts and the conventional fixed jackets. The weight reduction of conventional offshore structures was achieved by eliminating uncertainties and reducing conservatism. It is, therefore, not surprising nowadays to see much lighter jackets, with as much as 25 percent reduction in the weight of the structural steel, as compared to similar designs of a few years ago(2). The combination of structural optimization, weight reduction, increased water depth, and the operation in harsher environments made offshore operators more conscious of the need for large quantities of structural steels with improved quality, strength, toughness and weldability. Responding to this need, major steelmakers invested heavily in new plants and facilities to modify the process route. This resulted is several major changes in the steelmaking processes which included the close control of the blast furnace to the supply of desulfurized iron, the wide spread use of continuous casting of thick slab for rolling to plate, the introduction of vacuum arc degassing, vacuum degassing, argon stirring and injection techniques, and the almost exclusive use of basic oxygen steelmaking (3). In addition, extensive research and development programs were initiated by some steel and operating companies which resulted in the major improvement of conventional steels and the commercial application of new steels such as controlled rolled accelerated cooled, and low alloy quench and tempered (Q&T) steels.

Advances in offshore structural steels are intended to achieve higher strength, increased toughness, improved weldability, and resistance to lamellar tearing. This is in addition to improved fatigue and corrosion resistance. In order to achieve these goals it was important to reduce impurities such as sulphur, nitrogen and phosphorous in the steelmaking process of conventional steels. A major challenge was, however, to also reduce the carbon content, the carbon equivalent, and the alloy content to improve the weldability while maintaining strength. The development of the controlled rolled accelerated cooled steels was one of the steel industry's answers to this challenge.

This paper reviews offshore industry experiences highlighting the successes and

discussing the cause and the effect of the few problems on the steel technology. The paper will also provide some insight on the current concerns of the offshore industry with structural steels as it moves to develop offshore facilities in deepwater and arctic conditions.

## STEEL SELECTION FOR OFFSHORE STRUCTURES

Although the offshore industry has had good experience with structural steel, failures have been reported on drilling and production structures that were build in the 1950s and 60s (4,5,6). Early structures were fabricated from API 5L B pipe or conventional structural steels such as ASTM A7 and ASTM A36. Failure analysis studies on several salvaged structures have shown that low notch toughness, laminations in the steel, lamellar tearing and poor weldability were major contributors to the failures. Figures 2 and 3 illustrate some of these problems. In order to avoid these problems in future structures, the offshore industry and major steel companies initiated extensive research programs to develop and qualify high quality structural steels. These developments included the reducing of sulfur to levels below 0.01 weight percent, reducing carbon content, increasing manganese, reducing carbon equivalent, understanding the interaction between chemical compositions, reducing of impurities and nonmetallic inclusions, controlling grain size by using low temperature rolling, using selected microalloying elements, etc.

The types of structural steels used by the offshore industry includes: killed fine grain normalized, controlled rolled, quench and tempered, controlled rolled and accelerated cooled (referred to as TMCP), and precipitation hardened steels. The newer steels differ in their approach to achieve high toughness and improve weldability while maintaining the strength. Table 1 provides a summary of the primary strengthening mechanisms for various steel types. Figure 4 illustrates the effect of different strengthening mechanisms on the fracture toughness of steel. Figure 5 gives the general relationship between the yield strength and the weldability, as measured by the carbon equivalent, of the different steels. Conventional steels refer to normalized, controlled rolled and quench and tempered steels. The TMCP, precipitation hardened, and new lean alloy quenched and tempered steels are considered new technology steels.

## INDUSTRY STANDARDS FOR OFFSHORE STRUCTURAL STEEL

During the mid-1960s, several in-service and structural fabrication problems that were attributed to inadequate, undefined, or inconsistent steel properties were encountered by several of the major U.S. Gulf of Mexico operators. These problems illustrated that the common (ASTM) structural steels produced by domestic mills often did not meet the design/service need for the offshore industry. Conventional structural steel standards such as ASTM did not generally address properties such as weldability, lamellar tear, laminations, and toughness. As a result, during the late 1960s several operators began to develop their own steel specifications for the purpose of obtaining better quality steels.

As in the case with the steel suppliers who, under the continuous demand from offshore operators for better quality steel, made a conscious effort to make major advances in steelmaking; the standards writing and certifying authorities were engaged in preparing new standards. The effort to write custom made specifications for the offshore industry was started in 1967-68 by the American Petroleum Institute (API). This effort was followed by government sponsored efforts in countries across the Atlantic such as the UK and Norway. The success of these extensive specification writing efforts required the commitment and cooperation of offshore operators, steel suppliers, and governmental agencies.

The API effort to develop steel plate and other specifications for offshore tubular structural applications took advantage of specifications that were developed in the early 1970s by several oil companies. These specifications were used by API as a basis for developing the first API Specification 2H, which was issued in January 1974. Later editions included specific requirements for notch toughness, and supplemental requirements for notch toughness at lower temperature, lower nitrogen, ultrasonic testing to identify laminations, Z-direction testing, individual plate testing, low sulphur, and preproduction qualification. The fifth edition of API 2H was approved in 1987 and issued in the summer of 1988.

API's approach to standards is based on the use of specifications, recommended practice (RP) documents and bulletins. Specifications are used to identify a product, e.g. steel plate, while an RP is used to identify a method or practice such as RP 2X--Recommended Practice for Ultrasonic Examination of Offshore Structural Fabrication. Bulletins are used to convey technical or other information on a particular subject. The need to prepare such documents starts with the identification of an available technology being used by some of the major operators. Then the appropriate API committee forms a task group to develop the necessary information and prepare an acceptable draft document. This document with all supporting information is presented to the appropriate subcommittee, and if accepted will be voted by letter ballot by all voting members. Generally, all 'negative' ballots are resolved before the document is printed. Therefore, the API standards reflect the consensus of the industry which in the case of structural steel specifications includes offshore operators, fabricators, and steel companies. Specifications such as API 2H, 2W and 2Y are currently available. The API 2W in a new specification which addresses the new (TMCP) steels.

## USERS' PHILOSOPHY ON STEEL SPECIFICATIONS

Traditionally, for large offshore projects the operator will most likely purchase the steel and free issue it to the fabricator. This steel is purchased based on steel specifications that are developed by the operator. In general, there are two basic approaches to developing these specifications.

One approach is to write a comprehensive, purpose-written specification which includes information on the required steelmaking, chemistry, mechanical properties, weldability data, tolerances, inspection, marking, statistical data reporting and delivery conditions which are usually tailored for the specific project requirements. This type of specification is a stand alone document which reflects the operator's philosophy and past experience, and includes all relevant parts of the industry accepted standards and recommended practice.

Another approach is to adopt an industry standard, which generally represents a minimum performance specification, as a baseline specification and then add a list of special requirements and exceptions to the standard specification. These requirements, generally, include additional limitations on chemical composition, higher toughness, weldability evaluation, reduced tolerances and increased frequency of testing.

Although both approaches have been used and both can, in principle, provide acceptable materials, the first approach may be necessary and more suitable for purchase of steel for critical applications. The stand alone specification is likely to be more consistent because the chance of conflict between the special requirements and the industry standard can be eliminated. Although it may be expected that the first approach will result in increased steel cost, actual data show that for large steel orders no increase in cost has been observed.

The above argument does not imply that industry standards are unnecessary but it reflects the reality that most national standards provide minimum requirements. Also, they are often based on a compromise between the members of the specification writing committee which may be dominated or influenced by full time professional employees of the special interest groups. Most committees are made up of producers, consumers and independents. For example, a steel specification committee is often made up of producers (steel companies), consumers (oil companies) and independents (usually consultants). Therefore, the standards may not reflect the capability of the state-of-the-art steel mills. It is interesting to compare the API 2H: 1974 and 1986 specifications with the composition of typical offshore structural steels produced in the early 1970s and those produced now. Such a comparison is provided in Table 2. It is clear from Table 2 that even the 1986 API specification does not totally reflect current steelmaking capabilities, and that within the last decade major improvements in steel weldability, toughness and lamellar tear resistance were achieved through dramatic reduction in elements such as sulphur and carbon. In several cases, by the time the specification was ready for publication it represented an out-dated technology.

A major difference between an industry standard and an oil company specification is that the company standard will reflect specific design, fabrication and operating requirements. Therefore, the company specification may include requirements for higher toughness, good weldability, Z-direction properties, limits on impurities and alloying elements, higher frequency of testing, special mechanical tests, and limits on the minimum and maximum values of both yield and tensile strength. Requirements such as matching weld metal properties, compensating for potential deterioration of HAZ properties when using specific welding process, minimizing the number of welding procedures and their qualifications, limiting deterioration due to strain aging, and other considerations can only be reflected in a purpose written specification.

## RECENT ADVANCES IN OFFSHORE STRUCTURAL STEEL

Most offshore structures have been built using normalized carbon-manganese steel. However, advances in computer control and rolling capacity led to the development of a new class of steels, namely TMCP (Thermo-Mechanical Control Process) steels, with higher strength, high fracture toughness, improved weldability and lower cost. The TMCP involves both controlled rolling and controlled (accelerated) cooling using either controlled water sprays or direct quenching. Figure 6 provides a schematic diagram of the conventional, controlled rolled, and TMCP processes. The TMCP produces a very fine grain steel (ASTM 10-12) and, thus, achieves the desired properties by a combination of carefully selected chemical composition and accurate control of the manufacturing process from slab reheating to postrolling cooling. TMCP steels are characterized by low carbon content (usually less than 0.10 weight percent) which makes the steel less susceptible to hardness increase due to high cooling rates (between 800°C and 500°C) during welding. It is, therefore, expected that TMCP steels can be welded with little or no preheat which can result in lower fabrication cost (7).

Users must realize that TMCP is a "generic" term that refers to a family of steels manufactured to proprietary processes, procedures, and chemical compositions. Steel suppliers may refer to TMCP steels using proprietary names such as OLAC (On-Line Accelerated Cooling), MACS (Multipurpose Accelerated Cooling System), CLC, DAC, KONTCOOL, etc. Although TMCP steels contain a small amount of alloy additions, the interactions are quite complex and some of the information may be considered proprietary. The formation of particular phases or precipitates depends not only on the absolute amount of the

elements but also on the interaction effect with other elements, the processing variables, and, in some cases, the sequence in process or addition of elements. As an example, the ratio of Ti to N must be carefully controlled to promote the desired amount of TiN formation. Excess Ti may form TiC, which is detrimental to toughness.

When TMCP steel was first introduced two types of problems were reported (8). The first is that residual stresses which remain in the TMCP steel plate tend to be higher than those in a conventional normalized steel plate. Therefore, greater distortions can occur during flame cutting and welding. This problem which was rather serious during early stages of the developments of TMCP steels has been resolved through improvements of cooling processes. Some distortions are still experienced when flame cutting long strips from large steel plate. The second problem is related to reduction in strength in some regions of the heat affected zone (HAZ) of weldments. For thin plates, this problem can be accommodated by appropriate selection of welding process and procedures. For thick plates, above 50 mm thickness, the problem can be minimized with appropriate microalloying additions, process-variable control, and welding processes. This may, however, result in an increase in the steel or fabrication cost.

TMCP steels have been used successfully for a number of major offshore structures and pipeline projects (8). In addition to the use of TMCP steels for mobile arctic drilling rigs, the first documented successful use of TMCP steel for a major offshore structure was for Norsk Hydro's Oseberg jacket in the North Sea. About 65,000 tons of CLC steel were supplied by Nippon Steel Corporation (9). The specified minimum yield strength of the steel varied between 355 $N/mm^2$ for plate thickness equal to or less than 25 mm, and 310 $N/mm^2$ for plate thickness between 75 and 120 mm. Other uses of TMCP steels for major projects include Conoco's Jolliet TLWP and Shell's Bullwinkle jacket which successfully utilized both normalized and TMCP steels. Although all published information do not suggest any problem with TMCP steels, a new user must be careful because of the limited experience and the tendency of most users and suppliers to only report success stories. This concern will be discussed later.

Another type of steel that has been used by the US Navy as a substitute to the HY 80 grade is a precipitation hardened steel which is similar to ASTM A710. Unlike the traditional carbon steel, which is strengthened by pearlite and, therefore, requires certain level of carbon, A710 uses copper to form a finely dispersed copper precipitate in conventional ferrite microstructure. This is a very effective strengthening mechanism which allows the carbon content to be reduced to exceptionally low levels which results in improved weldability. A drawback of this steel is that it relies upon a higher level of alloy addition and requires a heat treatment making the cost higher than (about twice) microalloyed steels. This issue has been recognized by the Japanese steel companies who are currently active in combining the technologies of both the TMCP and precipitation hardened steel to produce high strength steel (above 80 ksi yield) at low cost.

## INDUSTRY CONCERNS

Although the offshore industry has extensive experience with structural steels, there are still several areas where debate on the optimum steel chemistry and steel making process continues within the industry (both steel suppliers and users). It is, sometimes, difficult for the users to understand the real cause of the difference of opinion between the steel suppliers. Is it due to variation in experience and available data, or due to variation in available steel making facilities? However, the underlying fact is that modern structural steel making is becoming a very complex and highly scientific process. Full understanding of all the intricate interactions is of paramount importance to establish the optimum chemistry and process for high quality steel. The application of stringent quality control during steel production cannot be overemphasized. Recognizing this issue and because of several failures, most users specify higher frequency of testing for critical applications. This may minimize potential problems but cannot eliminate all of them. Mill quality control is the only reliable approach.

The steel companies are still debating which is the best approach to eliminate the risk of lamellar tearing. Some suggest that the best approach is to reduce the sulfur level to below 0.008 percent while others argue that a better approach is through the modification of the sulfide shape. The latter approach relies on the addition of calcium or rare earth metals to form spheroidal calcium or rare earth sulfides. This approach usually results in both the elimination the risk of lamellar tearing and improvement of the transverse impact properties (3). Most users prefer the implementation of both approaches.

In order to improve weldability and reduce HAZ hardness, carbon contents have been dropped from a previous range of 0.16 to 0.24 percent to a range of 0.07 to 0.15 percent, and carbon equivalents (IIW) are now often below 0.4. In order to meet the strength requirement for normalized steel, the reduction of carbon is compensated for by an increase in solid solution hardening elements such as manganese, silicon, nickel, copper, niobium and vanadium. In addition, stringent control of residual elements such as Bi, Sb, Sn, N, As, and P is imposed to eliminate the potential of embrittlement by grain boundary segregation and deterioration of HAZ toughness. This is the reason that the company purpose written specification specifies

limits and requests reporting on more elements than industry standards as illustrated in Table 2.

Another concern to users is segregation arising from the use of continuous casting, i.e. centerline segregation. The extent of segregation depends on composition, ladle superheat, the condition of the continuous casting equipment (roll gap, roll alignment, roll bending, roll wear), and slab heating times and temperatures. The benefits of using electromagnetic stirring to redistribute the centerline segregation band is being questioned because all that is done is to spread the potentially harmful zone over a greater portion of the central region. The approach preferred by users is to minimize segregation in the first place by ensuring the proper condition of the continuous casting equipment, and by minimizing the use of elements known to segregate easily during solidification. These elements include C, Mn, S and P. Users also specify minimum slab soaking time and temperature to reduce centerline segregation. However, requirements for testing of centerline properties may be a more effective method of control.

With the introduction of ultra clean low carbon steels such as TMCP steels, a concern has been developed regarding the susceptibility to develop local brittle zones (LBZ) in the HAZ. This is an issue which is being addressed in several fronts. LBZ refers to areas in the HAZ where fracture toughness deterioration is greatest. The HAZ can be subdivided as shown in in Figure 7 based on the peak temperature reached and thermal cycles. It is known that HAZ areas with reduced fracture toughness due to welding are: 1) the subcritical HAZ (SCHAZ), 2) the intercritical HAZ (ICHAZ), and 3) the coarse grain (CG) regions. In most steels LBZ are associated with the CG regions (10). Evaluation of wide plate tests suggest that fractures are likely to initiate from the CG areas where grain size is greater than 80 microns (ASTM 4) (11). The CG regions consist of the unaltered CGHAZ, the IRCG, and the SRCG (defined in Figure 7).

The questions are: 1) What is the connection between the steel chemistry, steel making practice, and the presence of LBZs? 2) What is the significance of LBZs to service performance? Although the answer is still being debated, most industry experts agree that the presence of LBZs is neither a new problem nor confined to TMCP steels (10-13). However, the possibility is greater that the ultraclean low carbon steels such as TMCP steels may exhibit significantly greater tendencies toward grain coarsening during welding. It is generally accepted that LBZ resulting from high heat input welding (>1.5 kJ/mm) are more likely to be detrimental than LBZ from low heat input processes. Several offshore operators take the problem seriously and extensively evaluate the HAZ toughness of candidate steels prior to purchase. In response to this need API developed the recommended practice API RP 2Z (14).

Figures 8 and 9 show the influence of cooling time between 800 and 500°C, and the peak temperature on CVN fracture toughness of both normalized and TMCP steels with the chemical composition given in table 3. Both steels show a drop in toughness after being subjected to the intercritical temperature. Although this normalized steel has a relatively very low carbon, TMCP steels appear to be more sensitive to cooling rate and peak temperature.

As stated above, the presence of LBZs is neither a new problem nor limited to TMCP steels. Also no structural failure has ever been reported due to LBZs. It is, therefore, justifiable to ask: Do LBZs really have any structural significance to justify this concern? The answer to this question is still being evaluated within the offshore industry and no consensus has been reached. The view of the authors is that the offshore industry should not ignore LBZs in structures fabricated from any steel.

Unlike normalized steel in which the HAZ yield strength is usually higher than the base plate, the HAZ yield strength of TMCP steels tends to be lower than the base plate, especially with higher heat input welding processes. Since local strain will tend to concentrate in the lower strength region, a fatigue crack will tend to propagate within that region. As a result, the crack front may sample more LBZs in TMCP steels than it would in normalized steel. Therefore, extrapolating the industry experience with normalized steels to TMCP steels may not be appropriate. Realizing that CG region will always exist in structural steels, but its size and properties depends on both the steel and the welding process, it is necessary to identify what would be an acceptable size. Most materials experts in the offshore industry believe that LBZs will have a minimal influence on toughness if it represents less than 10 percent of the crack front. Recent results by Fairchild (13) appears to confirm this number. Figure 10 shows that as long as the percent of the CG regions sampled by the crack front of CTOD specimens is less than 7 percent, no low toughness values were measured.

Although the offshore industry has been using advanced fracture mechanics analysis methods and testing, such as CTOD, $J_R$, $R_6$ and wide plate, to assess structural integrity and establish fracture control requirements, design codes still rely on Charpy energy and transition temperature concepts as the main criteria. Use of Charpy criteria is based on experience with normalized steels and their application for new technology steels may be inappropriate. Factors such as strain aging, the slope of the transition curve, the relationship between the specified Charpy transition temperature energy and nil ductility temperature (NDT), etc., must all be addressed before applying the current code criteria. For example current codes specify 30 to 40 joules as a measure for the transition temperature (TR). This can be valid for normalized steel because the 50 percent shear

TR, and the NDT are similar to the 35 J TR. However, for TMCP steel the 50 percent shear TR will correspond to a greater than 150 J TR, and the NDT will correspond to the upper shelf energy.

Due to geoeconomic restrictions, offshore operators may find themselves forced to build structures using both normalized and TMCP steels from various sources. Welding qualifications become very critical to ensure a low hardness for the HAZ of the normalized steel and a minimum deterioration in strength, toughness, and grain size for the HAZ of the TMCP steels. Also, TMCP steels were developed to reduce fabrication costs by eliminating the need for preheat. Although, this is true, the cost of fabrication is also greatly influenced by the deposition rate which usually requires high heat input for high deposition rates. The use of high heat input welding processes, unless very carefully controlled, can be detrimental to TMCP steels not specifically designed for high heat input welding.

## CONCLUDING REMARKS

Traditionally, the steel companies placed their primary emphasis on developing new steels with improved properties, while fabricators were involved in developing improved fabrication technology and higher production welding processes. Historically, fabricators have not supported significant technology development, and due to business reduction in recent years, they have lost valuable expertise in many cases. Realizing that this situation cannot be expected to change for some time to come, it is necessary for steel companies to devote some of their development budget to welding technology to bring it to a level consistent with the current level of steel technology. A select few of the offshore oil producers actively conduct research and encourage steel producers, welding consumable manufactures, and welding equipment manufactures to develop and produce improved products. In order to fully utilize the properties of new technology steels, additional research efforts must be directed toward welding consumables and welding processes.

Future offshore exploration and development will probably concentrate in deepwater and the Arctic. This offers the petroleum industry, the fabricators, and the steel companies several challenges. The problem of HAZ toughness when using high deposition rate welding needs to be addressed. Steels that can be easily welded underwater would be attractive when repair is necessary. Also, most tendons for deepwater TLPs are being designed to be neutrally buoyant which means that sizes in the order of 45 inches in diameter and 1.5 inch wall thickness are expected. The offshore industry is concerned that facilities to produce these size tubulars in long lengths are quite limited and may not currently exist. Methods other than the U-O process will produce an inferior product at a much higher cost.

In order to insure that solutions to these problems are developed, the offshore operators should continue their research and encourage fabricators, steel manufacturers, and companies involved with welding to concentrate on addressing these problems.

## ACKNOWLEDGMENT

The authors wish to express their thanks to the management of Conoco Inc. for permission to publish this paper.

## REFERENCES

1. Salama, M. M., "Lightweight Materials for Deepwater Offshore Structures", Proc. of the 18th Annual Offshore Technology Conference, paper OTC 5185, V. 2, 297-304, (1986).

2. Hoenmans, P. J., "Technology the Key to Living with $15 Oil", Oil & Gas Journal, V. 7, No. 86, 56, February 15, 1988.

3. Walker, E. F., "Steel Quality, Weldability and Toughness", in Steel in Marine Structures, edited by C. Noordhoek and J. de Back, 49-69, Elsevier Science Publishers (1987).

4. Peterson, M. L., "Evaluation and Selection of Steel for Welded Offshore Drilling and Production Structures", Proc. of 1st Annual Offshore Technology Conference, Paper No. OTC 1075, V. 2, 59-64 (1969).

5. Carter, R. M., Marshall, P. W., Swanson, T. M., and Thomas, P. D., "Materials Problems in Offshore Platforms", Proc. of 1st Annual Offshore Technology Conference, Paper No. OTC 1043 (1969).

6. Peterson, M. L., "Steel Selection for Offshore Structures", J. of Petroleum Technology, V. 27, 274-282 (1975).

7. Peterson, M. L., "TMCP Steels for Offshore Structures", Proc. of 19th Annual Offshore Technology Conference, Paper No. OTC 5552, V. 4, 21-28 (1987).

8. Masubuchi, K., and Katoh, K., Uses of Thermo-Mechanical Control Process (TMCP) Steels for Ships and Offshore Structures and Welding Considerations", Proc. of the 6th International Conference on Offshore Mechanics and Arctic Engineering, V. 3, 137-144, (Salama, M. M., et al. editors), ASME (1987).

9. Harneshaug, I. S., Valland, G., Gundersen, K., and Roland, M., "HAZ Fracture

Toughness in Low Carbon, Controlled Rolled and Accelerated Cooled Steel Used in North Sea Offshore Platform Structures", Proc. of the 7th International Conference on Offshore Mechanics and Arctic Engineering, V. 3, 181-189, (Salama, M. M., et al. editors), ASME (1988).

10. Fairchild, D. P., Theisen, J. D., and Royer, C. P., "Philosophy and Technique for Assessing HAZ Toughness of Structural Steels Prior to Steel Production", ibid, 247-255 (1988).

11. de Koning, A. C., Harston, J. D., Nayler, K. D., and Ohm, R. K., "Feeling Free Despite LBZ", Proc. of the 7th International Conference on Offshore Mechanics and Arctic Engineering, V. 3, 161-179, (Salama, M. M., et al. editors), ASME (1988).

12. Webster S. E. and E. F. Walker, "The Significance of Local Brittle Zones to the Integrity of Large Welded Structures", ibid, 395-403 (1988).

13. Fairchild, D. P., "Fracture-Toughness Testing of Weld Heat Affected Zones in Structural Steel", presented in ASTM symposium on Fatigue and Fracture Testing of Weldments, April 25, 1988, Nevada, to be published in ASTM STP (1988).

14. API RP 2Z, "Recommended Practice for Preproduction Qualification for Steel Plates for Offshore Structures", 1st edition, May 1, 1987.

15. API 2H, "Specification for Carbon Manganese Steel Plate for Offshore Platform Tubular Joints," 5th edition, July 1, 1988.

Table 1. Primary Strengthening Mechanisms for Various Steel Types

| Strengthening Mechanism | Steel Type | | | | |
|---|---|---|---|---|---|
| | Normalized | Controlled-Rolled | Quench and Tempered | Accelerated-Cooled | Precipitation-Hardened |
| Reduction in Grain Size | x | x | x | x | x |
| Increase in Solid Solution | x | | | | |
| Increase in Dislocation Density | | x | | x | |
| Formation of Martensite or Bainite | | | x | x | |
| Precipitation Hardening | | | | | x |

Table 2. Comparison Between the API Required (Ladle) and Typical Chemical Composition of Offshore Structural Steel

| Element | API-2H (15) | | Typical-1972 | Typical-1986 | |
|---|---|---|---|---|---|
| | 1974 | 1986 | | U.S. Mill | Foreign Mill |
| Carbon | 0.18 | 0.18, max. | 0.17 | 0.15 | 0.12 |
| Manganese | 0.90-1.35 | 1.15-1.6 | 1.30 | 1.34 | 1.44 |
| Phosphorus | 0.04 | 0.04, max. | 0.025 | 0.015 | 0.009 |
| Sulfur | 0.035 | 0.02, max. | 0.02 | 0.006 | 0.001 |
| Silicon | 0.15-0.3 | 0.15-0.40 | 0.40 | 0.30 | 0.38 |
| Columbium | NS | 0.01-0.05 | 0.05 | 0.05 | 0.20 |
| Aluminum, total | NS | 0.02-0.05 | 0.03 | 0.040 | 0.035 |
| Nickel | | NS | NR | 0.17 | 0.18 |
| Chromium | | NS | NR | 0.08 | 0.009 |
| Molybdenum | | NS | NR | 0.056 | 0.001 |
| Vanadium | | NS | NR | 0.002 | 0.001 |
| Copper | | NS | NR | 0.032 | 0.[illegible] |
| As | | NS | NR | NR | 0.003 |
| Sn | | NS | NR | NR | 0.001 |
| Sb | | NS | NR | NR | 0.000 |
| CE, max | | 0.43 | 0.41 | 0.40 | 0.38 |
| Minimum Yield (ksi) | 42 | 50 | 42 | 50 | 50 |

NS : Not Specified
NR : Not Reported

$$\text{IIW Carbon Equivalent (CE)} = C + \frac{Mn}{6} + \frac{Cr + Mo + V}{5} + \frac{Ni + Cu}{15}$$

Table 3. The Chemical Composition of the Investigated Steels

| | Chemical Compositions Wt% (ppm) | | | | | | | | | | | | | | | |
|---|---|---|---|---|---|---|---|---|---|---|---|---|---|---|---|---|
| | C | Si | Mn | P | S | Cu | Ni | Cr | Mo | V | Ti | Nb | Al | N | O | H |
| Normalized Steel | 0.11 | 0.45 | 1.32 | 0.005 | 0.002 | 0.21 | 0.15 | 0.05 | 0.02 | 0.01 | 0.004 | 0.017 | 0.027 | 0.007 | 26 | <0.5 |
| TMCP Steel (plate) | 0.09 | 0.18 | 1.49 | 0.004 | 0.001 | 0.12 | 0.38 | 0.02 | 0.01 | 0.01 | 0.008 | 0.011 | 0.027 | 0.005 | 60 | 1.5 |
| TMCP Steel (pipe) | 0.08 | 0.10 | 1.57 | 0.005 | 0.002 | 0.21 | 0.25 | 0.03 | 0.01 | 0.01 | 0.011 | 0.011 | 0.001 | 0.002 | 23 | |

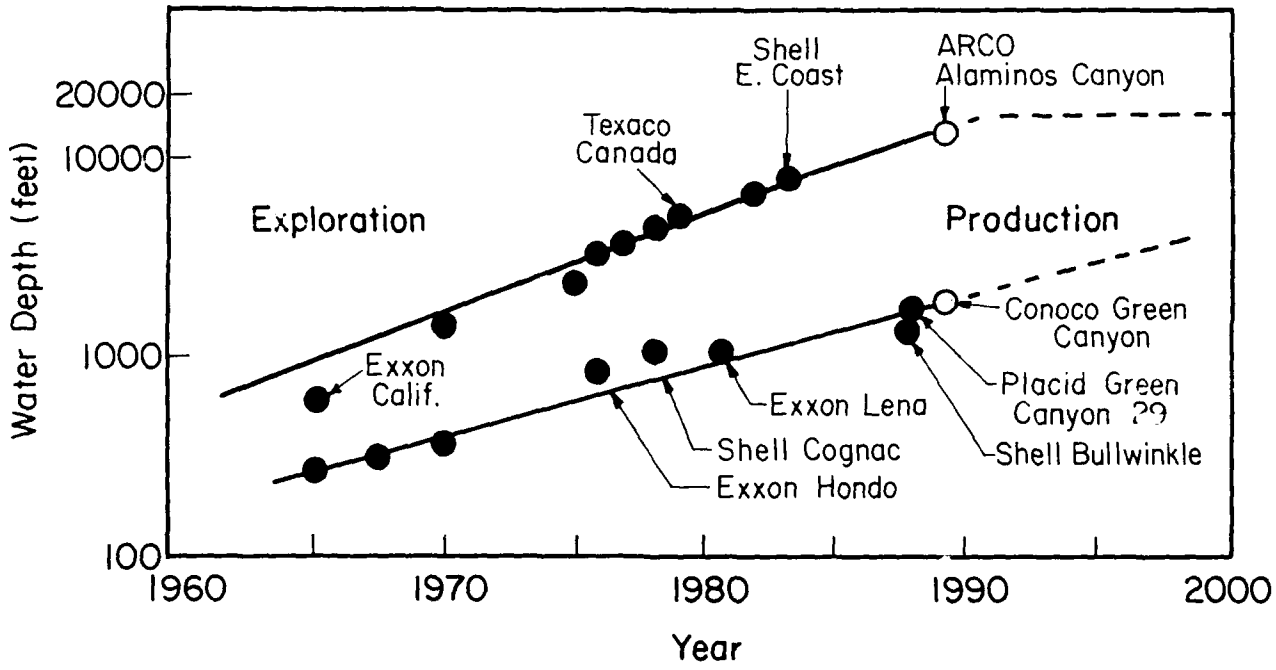


Fig. 1 - Historical and projected water depth for exploration and production activities.

Fig. 2 - Example of brittle fracture in an offshore platform jacket-log (Top) and a lamellar tear failure in a large laboratory test sample with the inset showing the crack propagation pattern (bottom).

Fig. 3A - Example of lamination in steel plate exposed by flame cut.

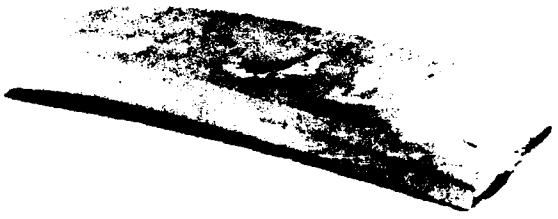

Fig. 3B - Field failure influenced by lamination.

Fig. 3C - Cross section of weld failure because of hard HAZ.

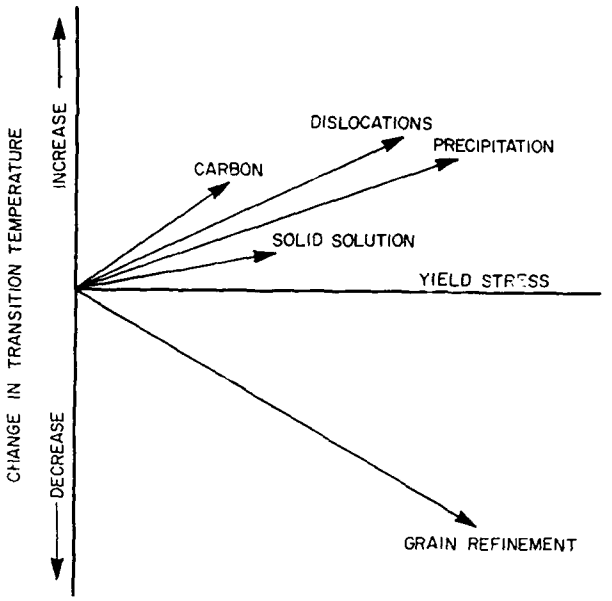


Fig. 4 - The effect of different strengthening mechanisms on transition temperature.

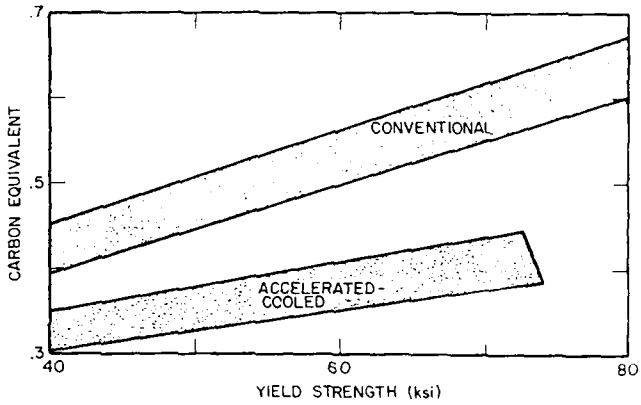


Fig. 5 - General relationship between yield strength and carbon equivalent.

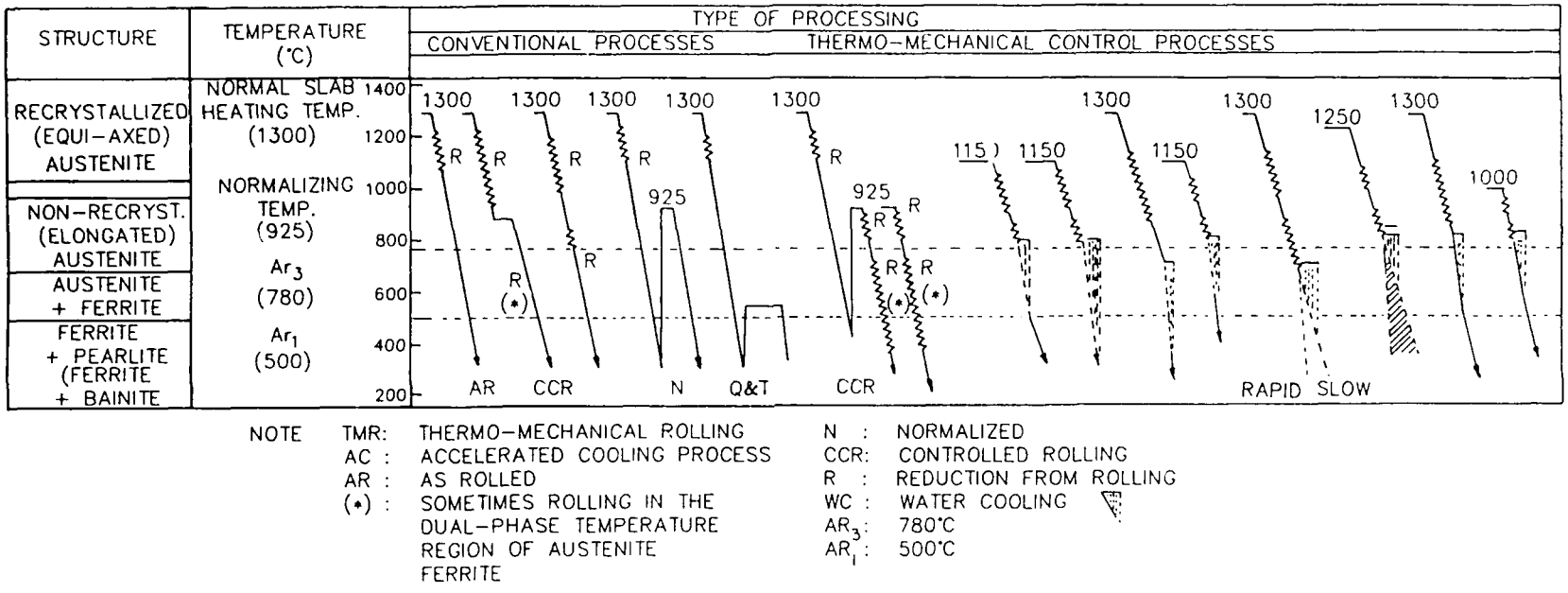


NOTE
TMR: THERMO-MECHANICAL ROLLING
AC : ACCELERATED COOLING PROCESS
AR : AS ROLLED
(*) : SOMETIMES ROLLING IN THE DUAL-PHASE TEMPERATURE REGION OF AUSTENITE FERRITE
N : NORMALIZED
CCR: CONTROLLED ROLLING
R : REDUCTION FROM ROLLING
WC : WATER COOLING
$AR_3$: 780°C
$AR_1$: 500°C

Fig. 6 - Schematic diagrams of TMCP and conventional process for rolling and cooling of steel plate.

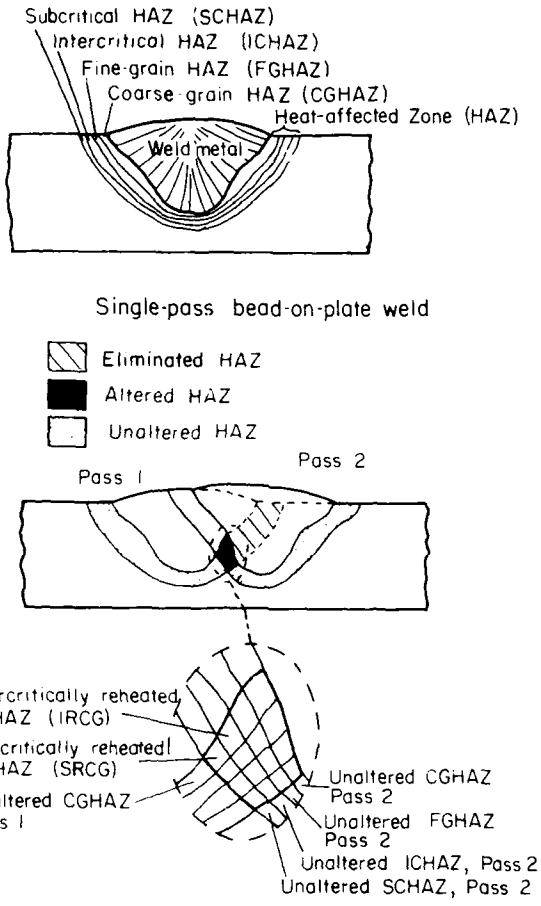


Fig. 7 - The HAZ regions.

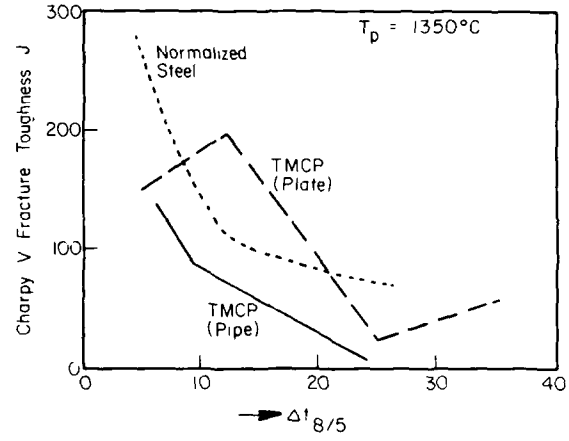


Fig. 8 - The influence of the cooling time ($\Delta t$ 8/5) on the notch toughness of the weld HAZ thermal simulated specimens. The test temperature was -22°C for the normalized steel and -40°C for the TMCP steels.

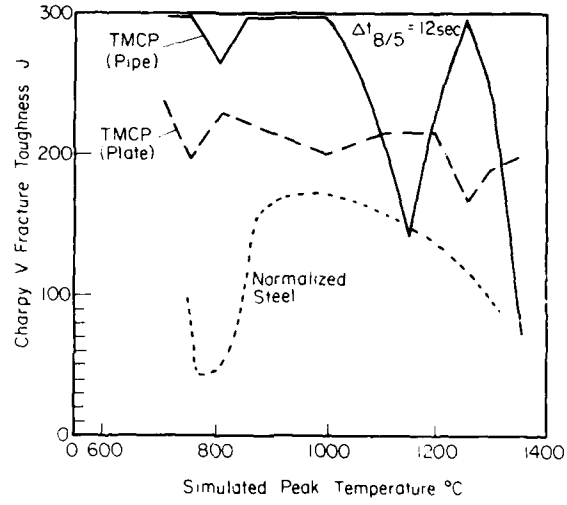


Fig. 9 - The influence of the peak temperature ($T_p$) on the Charpy V notch toughness of the weld HAZ termal simulated specimens. The test temperature was -22°C for normalized steel and -40°C for TMCP steels.

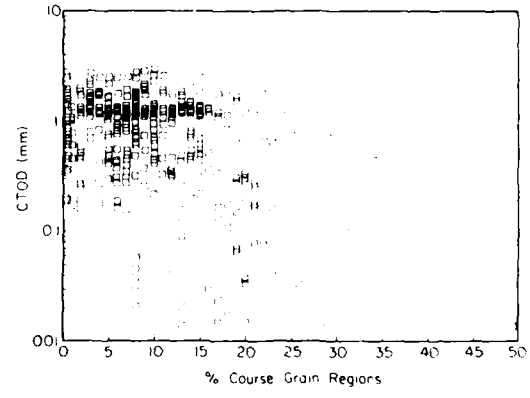


Fig. 10 - CTOD vs. percent coarse grain regions for all steels. (13)

# DEVELOPMENT IN MICROALLOYING AND PROCESSING OF HSLA STEELS FOR OFFSHORE STRUCTURES

**Mikifumi Katakami**
Oita R&D Lab.
Nippon Steel Corp.
Oita, Japan

**Naomiti Mori**
Joining Technology Lab.
Nippon Steel Corp.
Sagamihara, Japan

**Toshiaki Haze**
Plate, Bar, Shape & Rod Lab.
Nippon Steel Corp.
Sagamihara, Japan

**Kametaro Ito**
Plate Technical Div.
Nippon Steel Corp.
Tokyo, Japan

ABSTRACT

Recent developments of the use of microalloying elements and processing technology to produce HSLA steels for offshore structures are presented. (1) HAZ toughness is improved by new mechanisms which utilize Ti oxide or TiN-MnS-$Fe_{23}(CB)_6$ as ferrite nucleation site within austenite grain to produce finer microstructure. High carbon matensite formed in the intercritically heated grain coarsened region acts as a crack initiation site and should be minimized by proper choice of microalloying elements. (2) Good weld metal toughness is obtained when acicular ferrite structure is introduced by proper choice of Mn content and microalloying elements. New carbon equivalent parameter, CEN, to evaluate proper hardenability is also shown. (3) Effects of microalloying elements to produce finer austenite and resultant finer microstructure are reviewed. Recent progress of estimation for recrystallization and transformation of microalloying element(s) containing steels is introduced. Accelerated cooling technology for finer microstructure and strengthened ferrite is stressed to obtain good toughness and strength with low carbon equivalent. (4) Processing technique to control impurities and desired microalloying elements is practiced by the aid of processing computer. (5) Finally, products for offshore structures recently developed by microalloying technology are presented.

NOMENCLATURE

| | |
|---|---|
| TMCP | thermo-mechanical control process |
| CR | controlled rolling |
| $\gamma$ | austenite |
| $\alpha$ | ferrite |
| M* | high carbon martensite |
| HAZ | weld heat-affected zone |
| IFP | intra-granular ferrite plate |
| LBZ | local brittle zone |
| vTrs | fracture appearance transition temperature by Charpy V-notch test |
| CTOD | crack tip opening displacement |

INTRODUCTION

Microalloying has advanced into a highly sophisticated technology in line with the development of steels for offshore structures that demand the most comprehensive and severe steel properties among steel structures. The properties required of steels and welding materials used to develop, produce, store and transport energy cover a wide spectrum as follows:

(1) Strength, ductility and toughness of base metal and welded joint
(2) Unsusceptibility to weld cracking (including lamellar tearing)
(3) Internal soundness (base metal, heat-affected zone and weld metal)
(4) Fatigue strength (including corrosion fatigue behavior)
(5) Corrosion resistance (including resistance to hydrogen induced cracking, hydrogen sulfide cracking and stress corrosion cracking)

An active exploration of offshore oil fields have gradually moved from warm seas to subarctic and arctic seas, and large offshore structures have been built from the standpoint of economy. Structures installed and operated in subarctic and arctic seas must be absolutely safe to ensure environmental protection and operational stability. Brittle fracture is catastrophic and its prevention is of the utmost importance. This type of fracture initiates and propagates from a latent defect or extended fatigue crack in welds with high stress concentrations. Besides proper design and fabrication methods, steels and welding materials are especially required to be capable of preventing the occurrence of cracks in welds and inhibiting the initiation and propagation of brittle fracture. It becomes more difficult to meet these requirements as steel plates increase in strength and thickness. To solve the technological problems involved, many theoretical and practical research and development efforts have been made on a wide range of subjects, and

the results achieved have been applied to the construction of structures. Of these efforts, the development of TMCP steels and corresponding high-toughness welding materials has been epochal and has provided means for the total solution of the problems noted above.

The development of TMCP steels has not depended on the development of a new rolling process alone. The TMCP steels have also been made possible by basic research to clarify rational criteria for the respective steel properties and to elucidate factors governing the toughness of the base metal, weld metal and heat-affected zone and by development of highly advanced refining and rolling techniques. Above all, the results of studies conducted on the effects of microalloying elements on the properties of the TMCP steels and on the behavior of the TMCP steels in the refining, casting, rolling, heat treating and welding steps have made the TMCP steels commercially successful.

Based on the above recognition, this report reviews the progress of technology for the microalloying and processing of HSLA steels and describes the future problems of HSLA steels by focusing attention on

(a) the effects of microalloying elements on
    notch toughness of weld heat-affected zone,
    notch toughness of weld metal,
    susceptibility to weld cracking,
    notch toughness and strength of base metal
(b) developments in processing of TMCP steels
(c) results of manufacturing microalloyed steel plates for offshore structures by application of TMCP technology.

In this paper the recent technical data of Nippon Steel Corporation are mainly quoted to assure the consistency of technical ideas presented, paying attention to the pioneering works throughout the world.

## BRIEF HISTORICAL REVIEW OF APPLICATION OF MICROALLOYING ELEMENTS TO STEEL PLATE MANUFACTURING

Brittle fractures frequently occurred in entirely welded ships in World War II. The subsequent investigations into these failures brought about the concept of toughness. In 1958, toughness and strength were found to be improved by the grain refinement of ferrite.[1,2] Nowadays, three decades later since then, grain refining is still regarded as the only economical means that can improve both strength and toughness at the same time. Therefore, most of the studies on both controlled rolling technology and the microalloying technology have been related to the grain refinement.

Controlled rolling appeared in the 1950s as technology for manufacturing 40 kgf/mm$^2$ strength shipbuilding steels with improved toughness. In 1958, the controlled rolling technology for carbon-manganese steel started its progress with aluminum addition and manganese/carbon ratio increase, among other techniques[3].

High-strength steel produced by the addition of niobium, a microalloying element that still occupies the most important position in the controlled rolling technology, was developed in the United States in 1958[4]. The study on the effect of Nb followed successively[5,6]. Microalloying elements advanced literally together with the controlled rolling technology.

In the 1960s, the role of microalloying elements in the controlled rolling technology was made clearer, and new steels and manufacturing processes were developed. For example, strengthening by niobium and vanadium is due to the fine precipitation in ferrite[7,8], increasing the manganese content of niobium-microalloyed steel lowers the $Ar_3$ transformation temperature and increases the content of niobium carbonitrides that contribute to the strength increase[9], and the addition of niobium inhibits the recrystallization of austenite[10~13].

In 1963, Japan developed its first niobium-microalloyed semi-killed steel with a yield point of 36 kgf/mm$^2$, independently of Europe[14]. The controlled rolling technology aimed at increasing strength and toughness by utilizing microalloying elements made remarkable progress in 1969 when Japan's three steelmakers jointly received an order for supplying steel plates to produce low-temperature service API 5LX65 line pipe for installation in Alaska. The backbone of the present controlled rolling technology was established in this period.

In the 1970s, the efforts to obtain high strength and toughness with a lower carbon equivalent culminated in the development of extralow-carbon-high-manganese-molybdenum-niobium acicular ferrite steel[15] and extralow-carbon-high-manganese-niobium bainite steel[16]. In the last half of the 1970s, application of accelerated cooling technology to steel plates was earnestly tackled and the accelerated cooling technology accomplished a major qualitative change into the present TMCP technology.

The major histrical topics are shown in Table 1.

Table 1 CR and TMCP Technology Developments

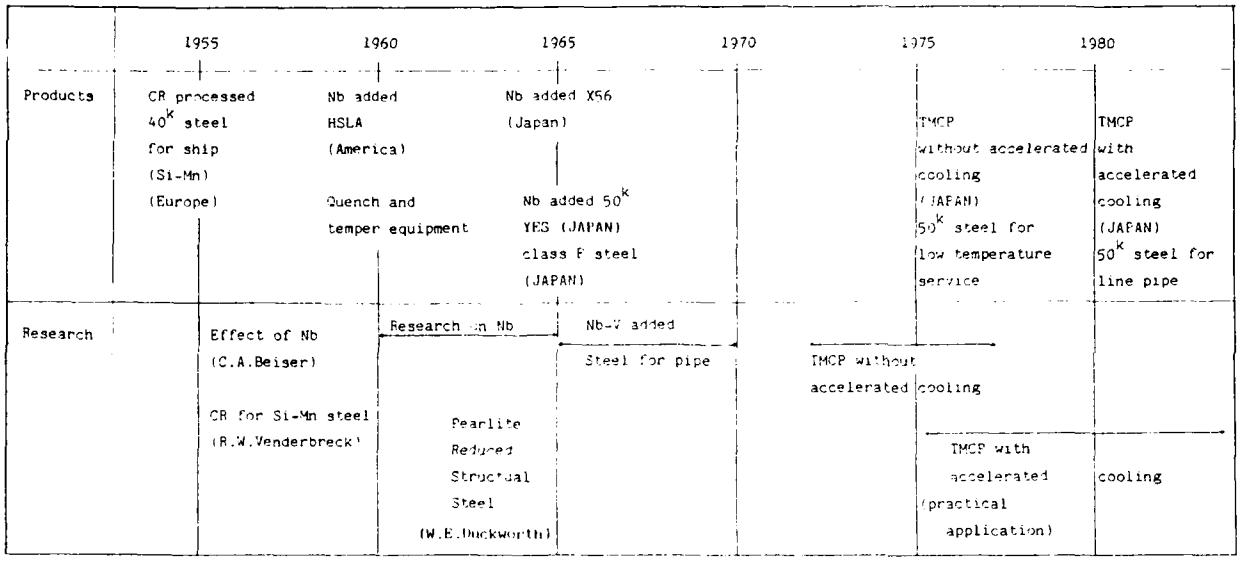


When the production of steel plates for offshore structures is designed, the strength and toughness of welded joints are factors of equal importance as those of base metal. Because of the heat input by welding and of the resultant transformation, the toughness of welded joints usually becomes the most critical. An essential prerequisite in this respect is to select the contents of microalloying elements within permissible limits while considering the strength and toughness of the base metal.

## RESULTS OF FUNDAMENTAL RESEARCH ON THE EFFECTS OF MICROALLOYING ELEMENTS ON THE NOTCH TOUGHNESS OF WELDED JOINTS

### NOTCH TOUGHNESS OF WELD HEAT-AFFECTED ZONE

Many studies have been published on improvement in the notch toughness of the weld heat-affected zone. The basic idea to get the refined microstructures for better HAZ toughness has two aspects. The first is to retard the austenite grain growth before transformation by microalloying. The second is to utilize the ferrite nucleation site within the austenite grain and get the fine IFP structures. The results of research on titanium nitride (Ti-N) steel, as an example of the first, and titanium-boron (Ti-B) steel and titanium oxide (Ti-O) steel, as examples of the second are described below. In case of Ti-N steel, the effect of the second phase on the HAZ toughness is focused.

#### Ti-N Steel

Kanazawa et al.[17] clarified that the formation of upper bainite, exhibited ZW in Fig. 1, brought from coarse-grained austenite is responsible for the embrittlement of high-heat input welded joints, such as one-side single-pass submerged arc welded joints, that are used in shipbuilding, among other applications. They succeeded in improving the notch toughness of such welds by preventing the grain coarsening of austenite and promoting the transformation of austenite to finer ferrite. Fig. 1 shows those effects of Ti addition. Since then, it has become general practice to add titanium for improving the notch toughness of the HAZ. Multiple-pass welds in offshore structures have a complicated microstructures compared to those of single-pass welds. The microscopic local brittle zone[18] of the HAZ exerts a particularly large effect on the CTOD of welded joints, and some steps must be taken against the adverse effect of the LBZ. Systematic investigations clarified the effects of microalloying elements on the LBZ[19~23].

The microstructures and thermal histories of HAZ portions in a welded joint are schematically illustrated in Fig. 2. The grain-coarsened zones A to D formed after heating by bead 1 to high temperatures are reheated by bead 2 and change into various microstructures. As can be seen from the thermal history curves, zone D is closest to bead 2 and thus is reheated to the highest temperature and is not altered into the grain-refined structure. Zones C, B and A decrease in reheating temperature in proportion to the distance from the fusion line and microstructures change into a grain-refined ferrite structure, a second phase containing grain-coarsened structure and tempered grain-coarsened structure, respectively, depending on the reheating temperature involved. This way, the HAZ of the welded joint varies in microstructure and hence in notch toughness from position to position. The experiments using a thermal cycle simulator showed that the particular zone where the temperature rose to the two phase region, $Ac_1$ to $Ac_3$, became very brittle. Fig. 3 shows that when the peak temperature of the second cycle ($T_{p2}$) is 800 C, the CTOD value is the lowest. This portion corresponds to the

second phase containing grain-corsened zone (B) in Fig. 2[22].

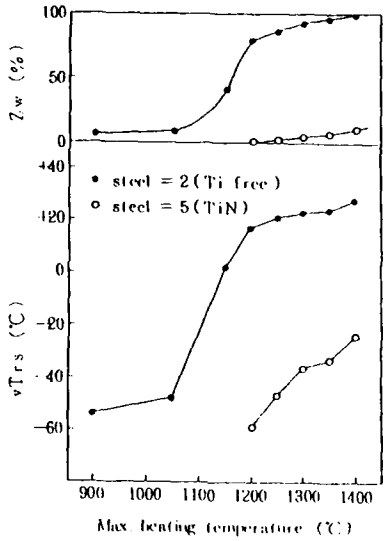


Fig. 1. Change of microstructure and vTrs with max. heating temperature examined by thermal cycle simulator.[17]

chemical composition, wt%

| steel | C | Si | Mn | sol.Al | Ti |
|---|---|---|---|---|---|
| 2 | 0.13 | 0.19 | 1.31 | 0.006 | - |
| 5 | 0.13 | 0.19 | 1.32 | 0.007 | 0.019 |

The precise study by scanning electron microscopy, transmission electron microscopy, and Auger electron spectroscopy revealed that the second phase was high carbon martensite[20].

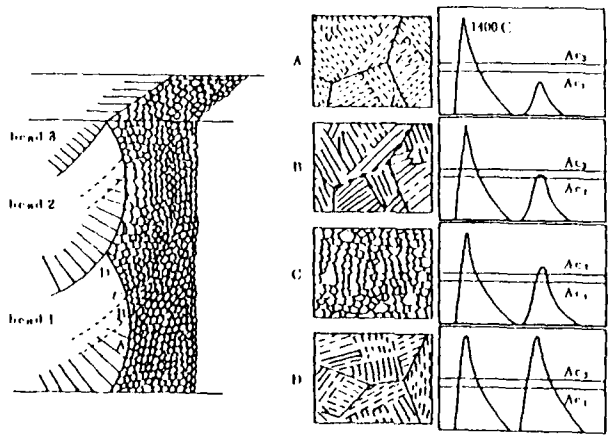


A: subcritically reheated grain-coarsened zone
B: intercritically reheated grain-coarsened zone
C: supercritically reheated grain-coarsened zone
D: grain-coarsened zone

Fig.2. Schematic illustration of the heat-affected zone of a multi-pass welding.

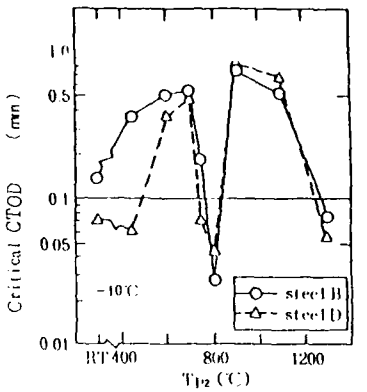


Fig. 3. Distribution of CTOD value of HAZ along the fusion line: simulated HAZ, double thermal cycle (Tp1=1400℃, dt8/5=20sec.[22])

chemical composition, wt%

| steel | C | Si | Mn | Cu | Ni | Nb | Al | Ti |
|---|---|---|---|---|---|---|---|---|
| B | 0.11 | 0.37 | 1.50 | 0.22 | 0.21 | 0.027 | 0.027 | 0.006 |
| D | 0.18 | 0.35 | 1.46 | - | - | - | 0.032 | 0.007 |

When the portion near the crack origin and right beneath the fracture surface in the fractured CTOD test specimen was examined, as shown in Photo. 1, the crack initiated at the interface between the matrix and the second phase, high carbon martensite.

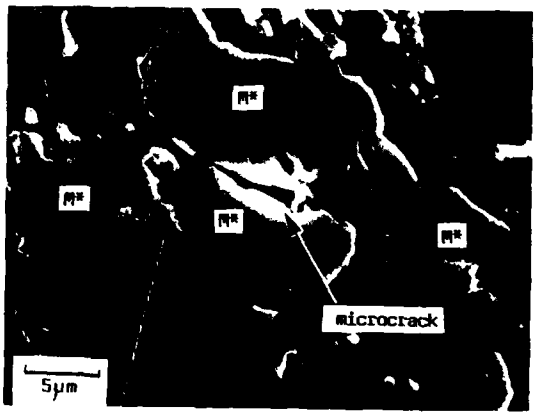


Photo. 1. SEM micrograph of microcrack formed at the interface between high carbon martensite (M*) and ferrite matrix.
steel: 0.11%C-0.37%Si-1.50%Mn-0.22%Cu-0.21%Ni-0.027%Nb

When the portion near the crack origin in the fracture surface was observed, a massive second phase was found at the center and a cleavage crack was seen running from the vicinity of the second phase, as shown in Photo. 2. Thus it is concluded that M* plays a major role on the notch toughness in the second phase containing grain-coarsened zone.

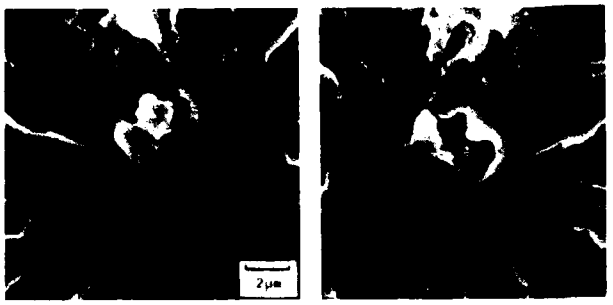


Photo. 2. SEM micrographs of second phase at crack initiation site.
steel: 0.14%C-0.36%Si-1.47%Mn-0.21%Cu-0.19%Ni-0.026%Nb-0.04%V-0.033%Al-0.007%Ti

The maximum size of high carbon martensite has a good relation with the critical fructure stress as shown in Fig. 4.

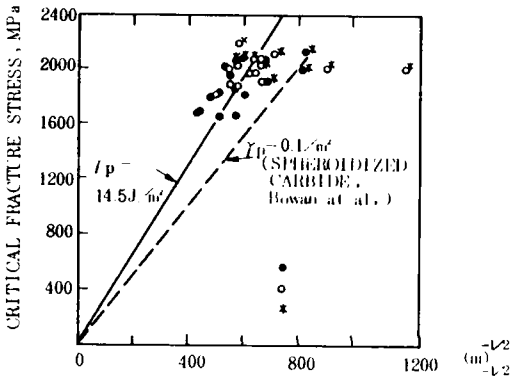


Fig. 4. Relationship between maximum size of high carbon martensite and critical fracture stress.[21]
steel: 0.10%C-0.22%Si-1.53%Mn-0.28%Mo-0.03%Al-0.01%Ti-0.003%N

The maximum size of M* is correlated to the amount of M*[21]. Decreasing the amount of M* is thus effective in improving the LBZ in the HAZ of the Ti-N steel. In reality, a good correlation was established between the amount of M* and the value of critical CTOD ($\delta_C$) for initiation of failure[20]. The effects of microalloying elements on the embrittlement of HSLA steel by M* were investigated by the simulated HAZ CTOD test. The results was summarized in Fig. 5 by a parameter $r_M$. The larger the value of $r_M$, the smaller the value of $\delta_C$ is. As evident from Fig. 5, the alloying elements can be classified into four groups according to the intensity of their effect on the deterioration of $\delta_C$. That is, the alloying elements are ordered as follows: N, B · Cr, Mo, Nb, V · C, Si · Mn, Cu, Ni. Carbonitride formers, such as Cr, Mo, Nb and V exert a strong effect on the deterioration of $\delta_C$.

When the HSLA steel is intercritically re-heated, portions containing many carbide particles first transform to austenite selectively and form M* on cooling. Since carbonitride formers are concentrated in these portions, they increase the hardenability of the local portions and facilitate the formation of M*, thereby exerting a particularly strong effect on the deterioration of $\delta_C$. Therefore, the microalloying elements, most of which are carbonitride former, should be added in as small amounts as possible. A good example of microalloying use by small amount is the only 0.01% Nb containing steel[19].

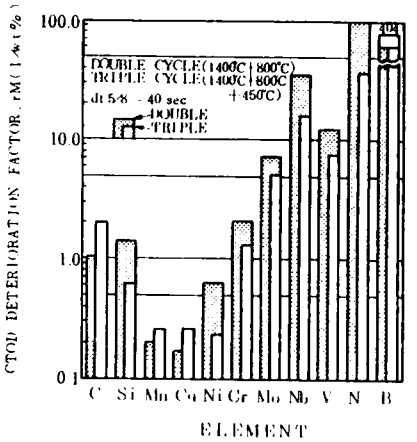


Fig. 5. CTOD deterioration factors for alloying elements: simulated HAZ (double and triple thermal cycles).[22]

chemical composition, wt%

| | C | Si | Mn | Cu | Ni | Cr | Mo | Nb | V | Al | N | B |
|---|---|---|---|---|---|---|---|---|---|---|---|---|
| base | 0.10 | 0.25 | 1.50 | - | - | - | - | - | - | 0.03 | 0.003 | - |
| range | 0.08 | 0.10 | 1.00 | 0.00 | 0.00 | 0.00 | 0.00 | 0.00 | 0.00 | - | 0.002 | 0.000 |
| | 0.14 | 0.40 | 1.60 | 0.60 | 0.60 | 0.60 | 0.30 | 0.04 | 0.06 | - | 0.008 | 0.002 |

Ti-B Steel

Titanium-boron (Ti-B) steel was developed especially for welding with high heat input[24,25]. Photo. 3 shows the microstructure of the HAZ of the Ti-B steel, simulated with a heat input of 130kJ/cm on a weld thermal cycle simulator. The microstructure is characterized by the formation of IFP.

When the IFP transformation nuclei were examined, they were found to be TiN-MnS-$Fe_{23}(CB)_6$ complex precipitates, as shown in Photo. 4.

The precipitation temperature of the precipitates in the Ti-B steel is shown in Fig. 6. The precipitation of $Fe_{23}(CB)_6$ as nuclei for the formation of IFP is shown to proceed in the vicinity of 650 °C. The dissolved boron is thought to be effective in retarding the growth of ferrite formed at the austenite grain boundaries. The notch toughness of the HAZ in high-heat input welded joints of the Ti-B steel is higher than that of the conventional steel for these reasons. The Charpy impact test results of weld thermal cycle simulated test specimens of the Ti-B steel are compared with those of the conventional Ti-N steel in Fig. 7. The notch toughness of the Ti-B steel is significantly improved.

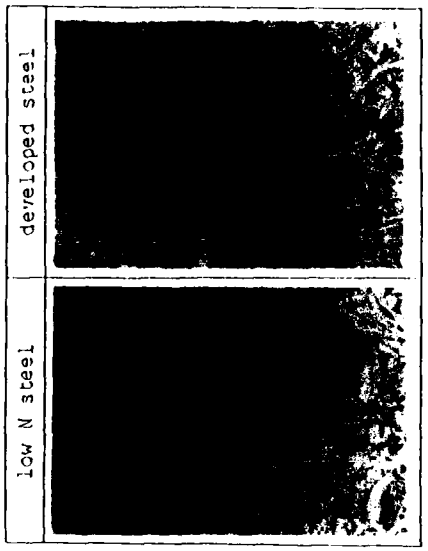


Photo. 3. Microstructure of simulated HAZ with equivalent heat input of 130 kJ/cm.

chemical composition, wt%

| steel | C | Si | Mn | Al | Ti | B | N |
|---|---|---|---|---|---|---|---|
| developed | 0.08 | 0.26 | 1.38 | 0.055 | 0.007 | 0.0011 | 0.0021 |
| low N | 0.09 | 0.27 | 1.35 | 0.031 | - | - | 0.0022 |

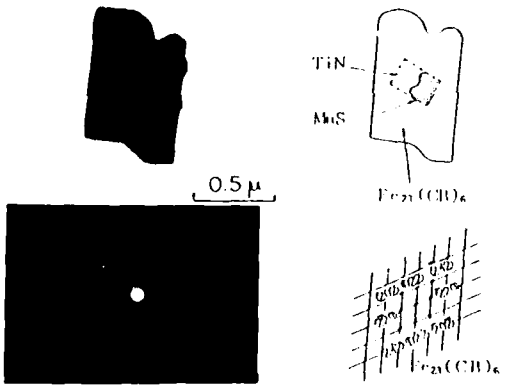


Photo. 4. TiN-MnS-$Fe_{23}(CB)_6$ complex precipitate.[24]

steel: 0.08%C-0.26%Si-1.38%Mn-0.055%Al-0.007%Ti-0.0011%B-0.0021%N

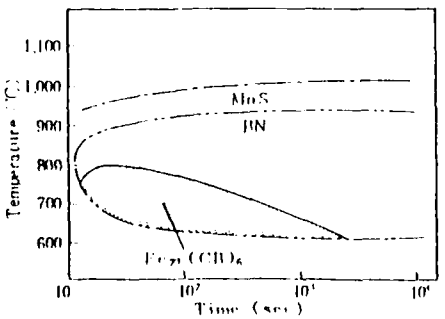


Fig. 6. Precipitation temperature of $Fe_{23}(CB)_6$, BN and Mns.[24]

steel: same as shown in Photo. 4

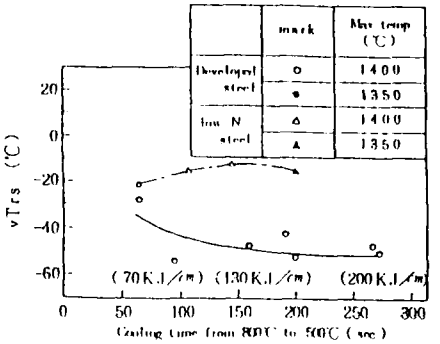


Fig. 7. Charpy impact test results of weld thermal cycle simulated HAZ specimens.[24]

steels: same as shown in Photo. 3

Ti-O Steel

The titanium oxide (Ti-O) steel is similar to the Ti-B steel in that a fine ferrite microstructure is produced from the formation of IFP within austenite grains. It is also characteristic in that titanium oxide is utilized as transformation nuclei and that aluminum is made substantially free to reduce the amount of aluminum oxide and increase the amount of titanium oxide[26,27]. As IFP increases in volume, the better toughness is obtained, as shown in Fig. 8. An X-ray diffraction analysis of IFP nuclei in the Ti-O steel is shown in Photo. 5. $Ti_2O_3$ is recognized. It is 2 to 3 μm in size and is often identified as a complex precipitate containing MnS and $Al_2O_3$ or MnO when examined in detail.

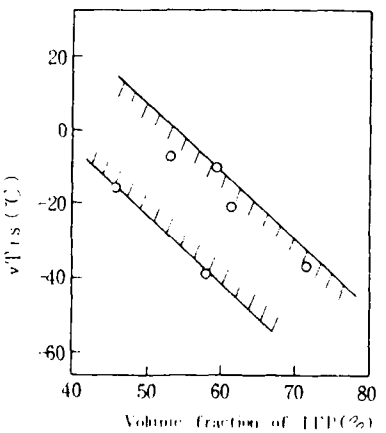


Fig. 8. Relationship between volume fraction of IFP and Charpy V-notch transition temperature in simulated HAZ.[26]

steel: 0.08%C-1.5%Mn-0.013%Nb-0.003%Al-0.012%Ti-0.0023%N

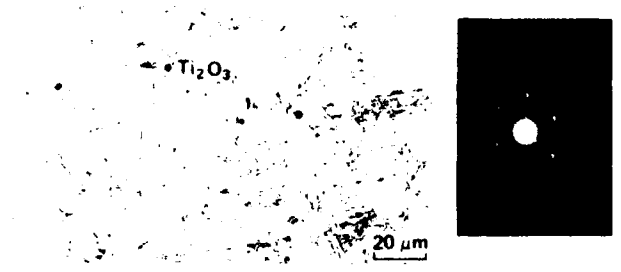


Photo. 5. IFP initiated from titanium oxide particles in specimen quenched from 600 °C during cooling in simulated weld thermal cycle test.

The continuous cooling transformation curves of the Ti-O steel are given in Fig. 9. The temperature range over which IFP is formed is considerably wide and the rate of cooling from 800 to 500 °C is 0.3 to 50 °C/s, a range that corresponds to welding with high heat input.

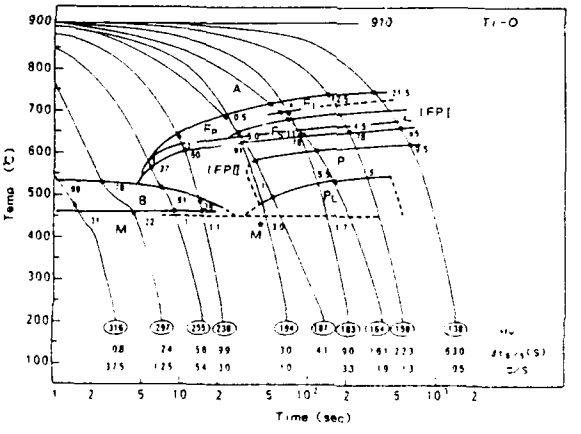


Fig. 9. Continuous cooling transformation diagram of Ti-O steel.[27]
steel: 0.08%C-0.20%Si-1.39%Mn-0.002%Al-0.012%Ti-0.0015%N

In exploiting the effectiveness of the $Ti_2O_3$, Al content must be decreased to a small, as shown in Fig. 10.

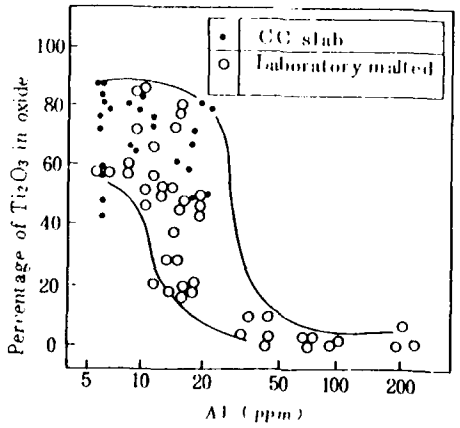


Fig.10. Effect of Al content on the precentage of $Ti_2O_3$ in all oxides.[26]

Since IFP nucleates from $Ti_2O_3$, an oxide of high melting point, the Ti-O steel gives superior notch toughness at the higher peak temperature compared to Ti-N steel as shown in Fig. 11. In addition, the M* should be avoided even in Ti-B and Ti-O steels.

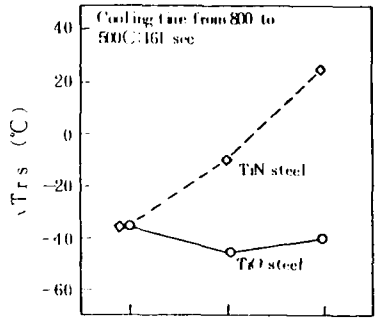


Chemical composition (wt%)

| Steel | C | Si | Mn | P | S | Al | Ti | N |
|---|---|---|---|---|---|---|---|---|
| TiO | 0.08 | 0.20 | 1.4 | 0.01 | 0.001 | 0.002 | 0.012 | 0.0020 |
| TiN | 0.08 | 0.20 | 1.4 | 0.01 | 0.001 | 0.020 | 0.018 | 0.0050 |

Fig. 11. Change in Charpy V-notch transition temperature of simulated HAZ with peak temperature.[26]

Summary Of This Section

The findings obtained are summarized as follows:
(a) The addition of titanium, which refines the austenite grain size, is effective in improving the notch toughness of the HAZ.
(b) The formation of IFP in coarsened austenite grains refines the transformed grain size and improves the notch toughness of the HAZ. Among the particles that nucleate IFP are $Ti_2O_3$ in the Ti-O steel and TiN-MnS-$Fe_{23}(CB)_6$ in the Ti-B steel.
(c) The amount of M* in the second phase containing grain coarsened zone is one of the largest factors that decrease the notch toughness of the HAZ. Since the amount of M* tends to increase with increasing additions of carbonitride formers, the additions of niobium and other carbonitride formers should be preferably minimized.

## NOTCH TOUGHNESS OF WELD METAL

The notch toughness of ferritic weld metal greatly depends on the microstructure produced. To obtain a weld metal microstructure conducive to high notch toughness, it is necessary to select appropriate welding materials by considering welding processes, welding conditions, chemical composition and other factors involved.

Figure 12 shows the relationship between the manganese content of weld metal and the vTrs of welded joints. The structures obtained are also exhibited in the figure[28]. As the manganese content of weld metal increases, the

microstructure of weld metal changes from a mixture of grain boundary ferrite and acicular ferrite to acicular ferrite alone and then to a mixture of acicular ferrite and upper bainite and finally becomes an upper bainite. The notch toughness of the weld metal is highest in the manganese content range where prior austenite grains transform to acicular ferrite and the amount of grain boundary ferrite at the prior austenite grain boundaries is reduced. It is important to secure appropriate hardenability and obtain a desirable acicular ferrite structure at these cooling rates. When welds are made with high heat input, therefore, weld metal of higher hardenability is required. The dilution of weld metal by base metal must also be taken into account. The percentage of dilution is about 50% in submerged arc welded joints. If the base plate has a low manganese content, welds must be made by using an electrode wire of high manganese content to secure the desired hardenability of the weld metal deposited.

Appropriate hardenability is not enough to yield an acicular ferrite microstructure and acicular ferrite requires nuclei for transformation. When titanium and boron are added to the welding material, the acicular ferrite microstructure can be obtained over a considerably wide range of welding conditions[29]. The mecha nism of Ti and B is same to that of Ti-B steel.

At present, Mn-Ti-B welding materials are widely used for the welding of offshore structures as materials for making submerged arc and shield metal arc welds with superior low-temperature notch toughness.

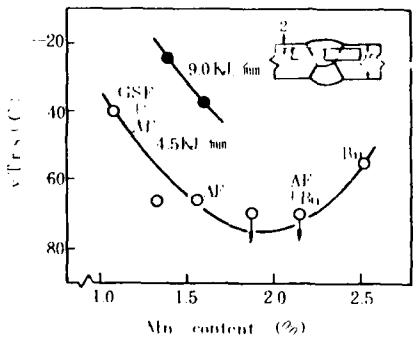


Fig. 12. Effect of manganese content on fracture appearance transition temperature.[28]
AF: acicular ferrite
Bu: upper bainite
GSF: grain boundary ferrite
weld metal: 0.1%C-0.25%Si-0.02%Ti-0.004%Al-0.013%Nb-0.02%V-0.0035%B

Figure 13 shows the effect of the niobium and vanadium contents on the notch toughness and tensile strength of weld metal on the conditions favorable to the formation of acicular ferrite. As niobium and vanadium contents increase, the tensile strength increases but the notch toughness changes little. If dilution is taken into account, the niobium and vanadium contained in the base plate pose no problems to the notch toughness of the weld metal.

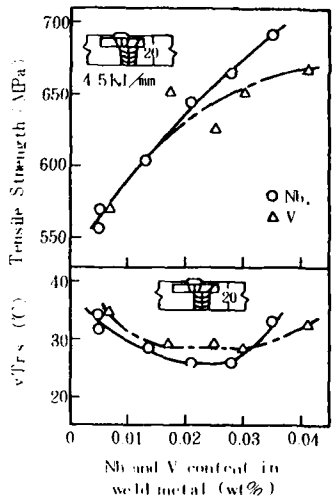


Fig. 13. Effect of niobium and vanadium contents on fracture appearance transition temperature and tensile strength.[28]
weld metal: 0.11%C-0.25%Si-1.30%Mn-0.004%Al-0.20%Ti-0.0035%B

Summary Of This Section

As discussed above, the following measures are effective in improving the tensile strength and notch toughness of ferritic weld metal:
(a) The base composition, particulary Mn content, and microalloying elements are adjusted to an optimum level so that the microstructure is composed of acicular ferrite.
(b) Niobium and vanadium increase the tensile strength of weld metal with little or no notch toughness deterioration when added up to a certain level.

## SUSCEPTIBILITY TO WELD CRACKING

A general mode of fracture in structures is such that a fatigue crack initiates from a weld defect in a welded joint and propagates for a certain critical length before it results in a brittle fracture. The typical example is the failure of the Alexander L. Kielland[30]. Therefore, weld cracks that initiate fatigue cracks and particularly weld cracks with sharp notches must be absolutely avoided. Weld cracking may be cold cracking that arises from the hardened microstructure of the HAZ and from the presence of hydrogen; hot cracking or cracks in the weld metal; or lamellar tearing or terrace-like cracks in the base metal.

Hot cracking is influenced by welding materials to a large extent. This problem can be practically prevented if over current is avoided and welding is not performed at a very high speed.

Lamellar tearing became a serious problem with the welding of offshore structures and many steps were undertaken against lamellar tearing. Lamellar tearing mainly depends on the nonmetallic inclusions and segregation present in the steel plate[31]. Processes are already established for desulfurizing the hot metal and for controlling the inclusions and segregation

in the molten steel[32]. Advanced countries can now supply steel plates that do not develop lamellar tearing and lamellar tearing is not a serious problem any longer.

Whether or not cold weld cracking occurs depends on the combination of steel plates and welding proceuures to be used. If this combination is inappropriate, the total cost of steel and welding becomes too high for the economy of weldments. It is necessary to accurately evaluate the cold weld cracking susceptibility of steel plates, to clarify welding procedures that meet the evaluated susceptibility and to make a comprehensive judgement on the cost involved.

The cold weld cracking susceptibility of steel is evaluated by the carbon equivalent and the International Institute of Welding (IIW) carbon equivalent formula is used throughout the world[33]. This concept of carbon equivalent was first proposed by Dearden[34].

Increased use of microalloying element coupled with the decrease in the use of carbon, triggered the formulation of the new carbon equivalent parameter Pcm[35 ~ 37].

Yurioka et al.[38] have proposed a new parameter, CEN, that can be used to evaluate the weldability of both old and new types of steels.

$$CEN = C + A(C)\left(\frac{Si}{24} + \frac{Mn}{6} + \frac{Ni}{20} + \frac{Cu}{15} + \frac{Cr+Mo+Nb+V}{5} + 5B\right) \quad (1)$$

$$A(C) = 0.75 + 0.25 \tanh\{20(C - 0.12)\} \quad (2)$$

CEN approaches Ceq (IIW) as the carbon content increases and approaches Pcm as the carbon content decreases. CEN was adopted by Canadian Standards Associations in 1986.

Decreasing the carbon content is particularly effective in decreasing the cold weld cracking susceptibility. If the same level of steel plate strength is to be achieved, the carbon content should be decreased and the microalloying elements sould be added instead from the standpoint of cold weld cracking. The microalloying elements, however, should be used in such quantities that the notch toughness of the HAZ is not impaired. The beneficial use of microalloying element is clearly shown in Fig. 14.

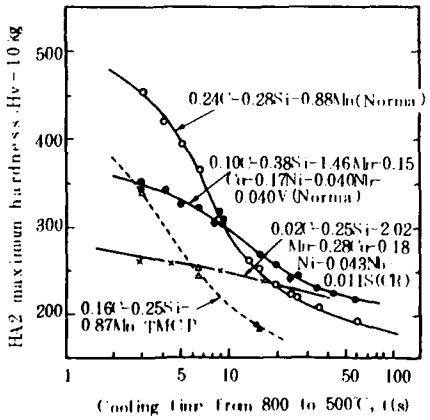


Fig. 14. Effect of cooling time on the HAZ maximum hardness for various type of steels.

Summary Of This Section

To summarize, the cold weld cracking susceptibility of steel plates can be improved if desired strength is secured by decreasing the carbon content and adding microalloying elements to such a degree that the notch toughness of the HAZ is not impaired.

## COMBINED EFFECTS OF MICROALLOYING ELEMENTS AND TMCP IN IMPROVING STRENGTH AND NOTCH TOUGHNESS OF BASE PLATES

Many reports have been published that present the results of studies conducted to improve the yield point and notch toughness of the base plate by the grain refinement of niobium- or vanadium-microalloyed, aluminum-killed steel through controlled rolling. Research and development work in this field in Japan was mainly carried out concerning line pipe steel. These efforts were then combined with the development of accelerated cooling technology and were reviewed and incorporated into the TMCP technology.

This chapter describes the methods of improving the strength and notch toughness of base plates when microalloyed plates steel for offshore structures are manufactured by the TMCP technology.

The changes in the microstructure of steel during reheating, controlled rolling and accelerated cooling are schematically illustrated in Fig. 15.

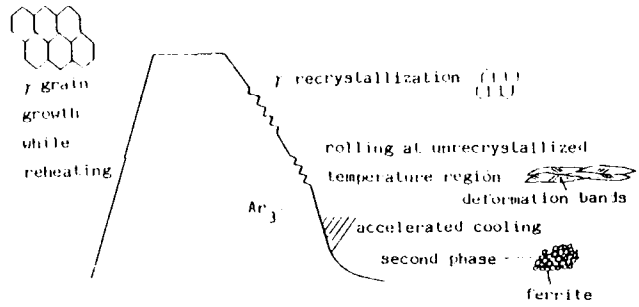


Fig. 15 microstructure change during plate manufacturing.

The simultaneous achievement of toughness improvement and strength increase are performed by grain refinement. Referring Fig. 15 the key factors to produce fine grain are

a) restraining of austenite grain growth while reheating
b) retardation of recrystallization
c) increase in ferrite nucleation site
d) retardation of ferrite grain growth

The effects of microalloying elements and accelerated cooling for each factor are reviewed.

## Effects of Microalloying

Since the preferred formation sites of ferrite during transformation are austenite grain boundaries, austenite before transformation should be preferably fine-grained. Nitrides or carbonitrides of titanium, niobium or aluminum are effective in restraining the growth of austenite grains during the slab reheating[39,40]. Of the nitrides and carbonitrides, titanium nitride has the highest thermal stability and is most effective to restrain the grain growth. The experimental results of Kobayashi et al. are shown in Fig. 16.

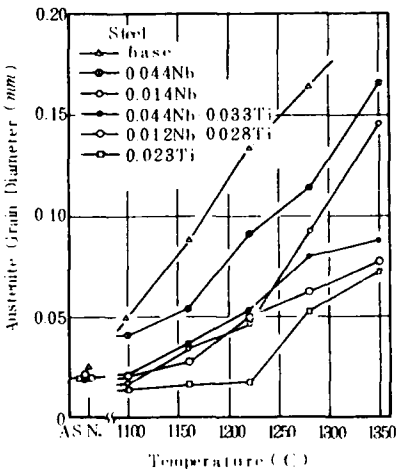


Fig. 16. Variation of austenite grain size with temperature when steel is heated for 5 s. As N: As normalized at 950°C for 15 h.[39]
steel, wt%: C;0.04/0.07 Si;0.34/0.37 Mn;1.73/1.77 Al;0.025/0.046

The grain refinement of austenite during rolling is effected by rolling strain, delayed recrystallization and retardation of recrystallized grain growth[41~58]. Niobium, vanadium, titanium and molybdenum are effective in this grain refinement of austenite.

In Fig. 17, the effect of niobium, vanadium and molybdenum on the recrystallization of austenite is described. Of the three microalloying elements, niobium is most effective in the delayed recrystallization.

Rolling in the unrecrystallized region forms elongated austenite and deformation bands within austenite grains[57]. Since the deformation bands effectively act as ferrite formation sites, a grain-refined transformation microstructure is obtained. Rolling in the unrecrystallized region is thus an important element of the controlled rolling technology. The addition of niobium and vanadium expands the unrecrystalized temperature region toward the high end and promotes the aforementioned effectiveness of niobium and vanadium. Niobium is more effective than vanadium in this respect. Fig. 18 shows the effect of Nb, Ti, V and B on the recrystal-

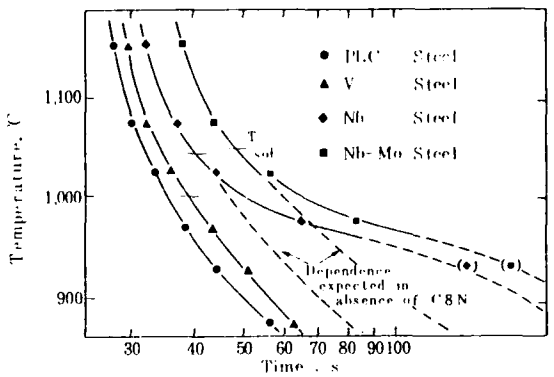


Fig. 17. Effect of alloying elements on the recrystallization behaviour.[44]
chemical composition, wt%

| steel | C | Si | Mn | Al | Nb | V | Mo |
|---|---|---|---|---|---|---|---|
| Pl.C | 0.06 | 0.24 | 1.43 | 0.025 | - | - | - |
| V | 0.05 | 0.25 | 1.20 | 0.030 | - | 0.115 | - |
| Nb | 0.05 | 0.27 | 1.25 | 0.030 | 0.035 | - | - |
| Nb-MO | 0.06 | 0.21 | 1.33 | 0.025 | 0.040 | - | 0.30 |

lization stop temperature. Recrystallization and precipitate formation are thermally activated processes. Therefore, as the temperature decreases, the growth of the grain and precipitates becomes slower. In this respect, the decrease in $Ar_3$ is preferable to realize the low temperature rolling. Low temperature rolling also increases the deformation bands.

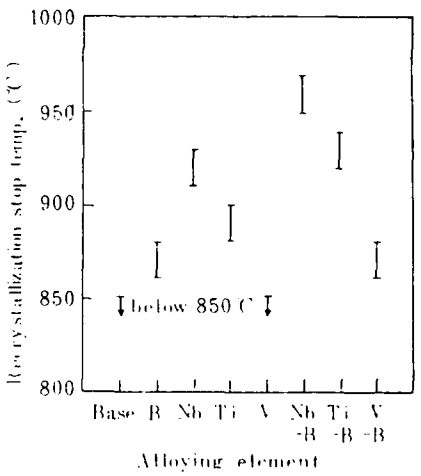


Fig. 18. Effect of alloying element on recrystallization stop temperature.[58]
steel: 0.03%C-0.15%Si-1.5%Mn-0.025%Al
Nb; 0.05%, Ti; 0.02%, V; 0.08%, B; 0.001%

Remarkable progress has been recognized in the prediction of the recrystallization behavior of austenite in recent years. Figure 19 shows the results of calculations made to determine the strain necessary for the recrystallization of austenite in niobium-microalloyed steel by incorporating about 30 factors[59]. The calculated values closely agree with the observed values.

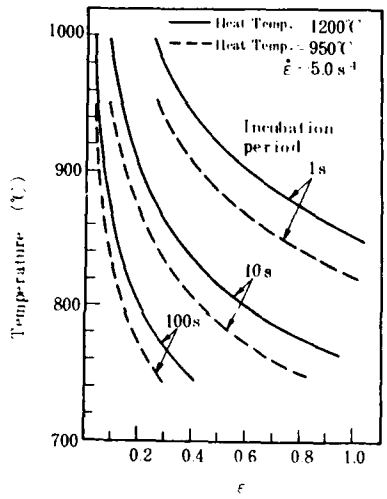


Fig. 19. Calculated critical conditions of austenite recrystallization.[59]
steel: 0.07%C-0.23%Si-1.33%Mn-0.46%Cu-0.79%Ni-0.037%Al-0.01%Nb

When austenite transforms to ferrite after controlled rolling, the smaller the grain size of austenite before transformation, the finer the microstructure after transformation. In this case, carbonitrides are effective in producing finer ferrite grains. The effects of niobium and vanadium on the grain size of austenite and ferrite are shown in Fig. 20[50].

Fine precipitates of nitrides or carbide are widely recognized to have a prominent effect on strength increase[60,61].

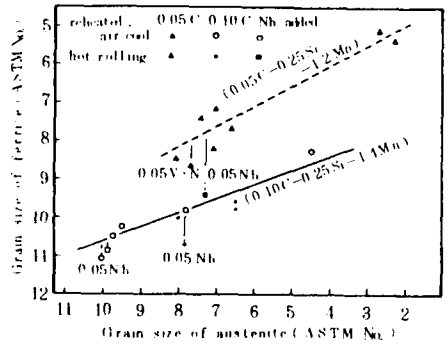


Fig.20. Relationship between austenite grain size before transformation and ferrite grain size after transformation and effects of niobium and vanadium additions on austenite and ferrite grain size.[50]

Effects Of Accelerated Cooling

Accelerated cooling retards the growth of ferrite and makes the grain size of ferrite finer than air cooling[62]. The effect of cooling rate on ferrite grain size is shown in Fig. 21. It is evident that the ferrite grain size decreases with increasing cooling rate.

The transformation behavior of ferrite is estimated as vigorously as the recrystallization of austenite is. Transformation percentage and grain size of ferrite in carbon-manganese steel and niobium-microalloyed steel was found to be in good agreement with experimental data. The calculated and observed volume fractions of ferrite are compared in Fig. 22[59].

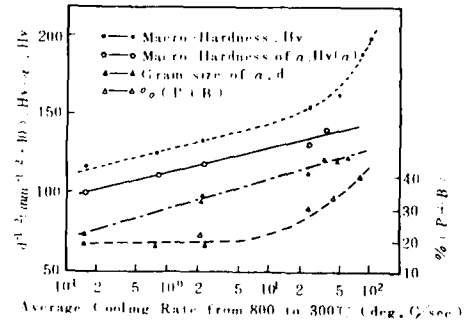


Fig. 21. Change in hardness, grain size and microstructure with cooling rate.[62]
steel: 0.15%C-0.17%Si-0.66%Mn

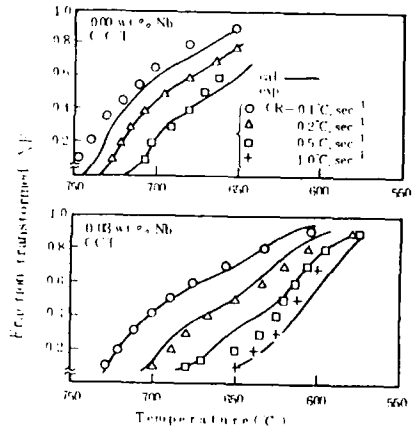


Fig. 22. Comparison of progress of transformation between experimental data and calculated results.[59]
steel: 0.1%C-0.20%Si-1.4%Mn

Accelerated cooling strengthens ferrite and hence increases the strength of the steel as shown in Fig. 21. In addition, a second phase formed as a result of accelerated cooling, pearlite or bainite, is finely dispersed between ferrite grains to increase the strength of the steel without impairing the notch toughness of the steel.

The accelerated cooling technology has thus made it possible to obtain the same level of strength as that of conventional controlled rolled steels with a lower value of carbon equivalent than in the conventional steels. Moreover, toughness of accelerated cooling processed steels can be improved than that of conventional normalized steels when optimised conditions of controlled rolling and accelerated cooling are combined. These examples are shown in Figs. 23 and 24. The decrease in carbon equivalent directly improves the cold weld

cracking susceptibility. Accelerated cooling technology is also quite useful in this respect.

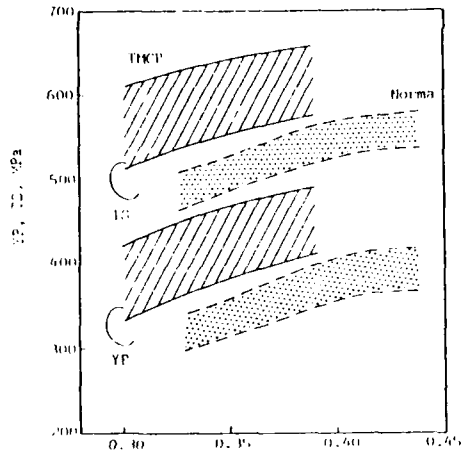


Ceq = C + Mn/6 + (Cr + Mo + V)/5 + (Ni + Cu)/15,%

Fig. 23 Relationship between Ceq and strength for TMCP steels and normalized steels. (plate thickness 12 ~ 50 mm, HT 50 class)

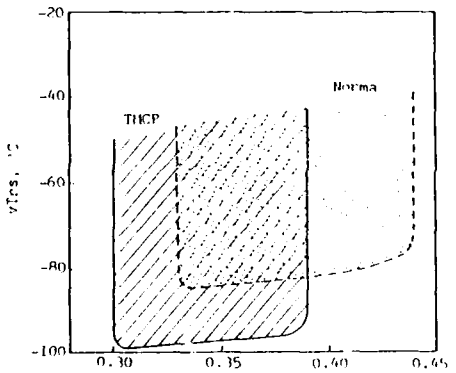


Ceq = C + Mn/6 + (Cr + Mo + V)/5 + (Ni + Cu)/15,%

Fig.24 Relationship between Ceq and vTrs for TMCP steels and normalized steels. (plate thickness 12 ~ 50 mm, HT 50 class)

Further, accelerated cooling makes best use of microalloying element to increase the strength of base metal when steel plates are used with stress-relief heat treatment. Fig. 25 shows the typical example of Ti and Nb addition on the strength of steel after stress relief. High tensile strength is assured when accelerated cooling stop temperature is below 530 °C in this figure. The strength increase is due to Nb and Ti precipitation.

The effects of microalloying elements and accelerated cooling on the grain refinement of base metal and HAZ are summarized in Fig. 26.

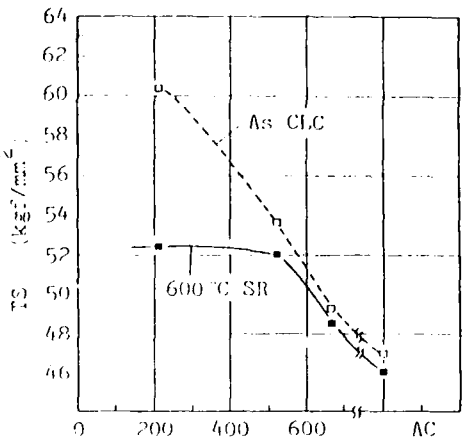


Fig. 25 Effect of accelerated cooling stop temperature on the strength of Nb-Ti containing steel after stress relief. (30 mm in thickness, 0.7 $m^3/min \cdot m^2$)
steel: 0.10%C-0.24%Si-1.48%Mn-0.013% Nb-0.020%Ti-0.041%Al

Summary Of This Section

The effects of microalloying elements on the strength and notch toughness of base plates are summarized as described below.

For grain refinement to improve toughness and strength,

(a) The addition of titanium is effective in restraining the growth of austenite grains during slab reheating.

(b) To refine the austenite grains during rolling, the addition of Nb, V and Ti are effective in expanding the unrecrystallization temperature region of austenite and retarding the growth of austenite grains. Among these, Nb has a prominent effect.

(c) Decrease in $Ar_3$ by the addition of Nb, V and Ti increases deformation bands and maintains the effective size of precipitates, allowing rolling at the low temperature,

(d) Accelerated cooling after rolling refines and strengthens ferrite grains.

## DEVELOPMENTS IN PROCESSING OF HSLA STEELS

When microalloying elements are added to steels, their effectiveness varies with steel plate manufacturing process conditions, for example, alloy types, addition methods and plate manufacturing conditions. Process techniques must be thus developed to make effective use of microalloying elements. In recent years, latest processes for manufacturing steel plates for offshore structures, including the TMCP, have been introduced. Principal process techniques that greatly affect the effectiveness of microalloying elements are summarized in Table 2.

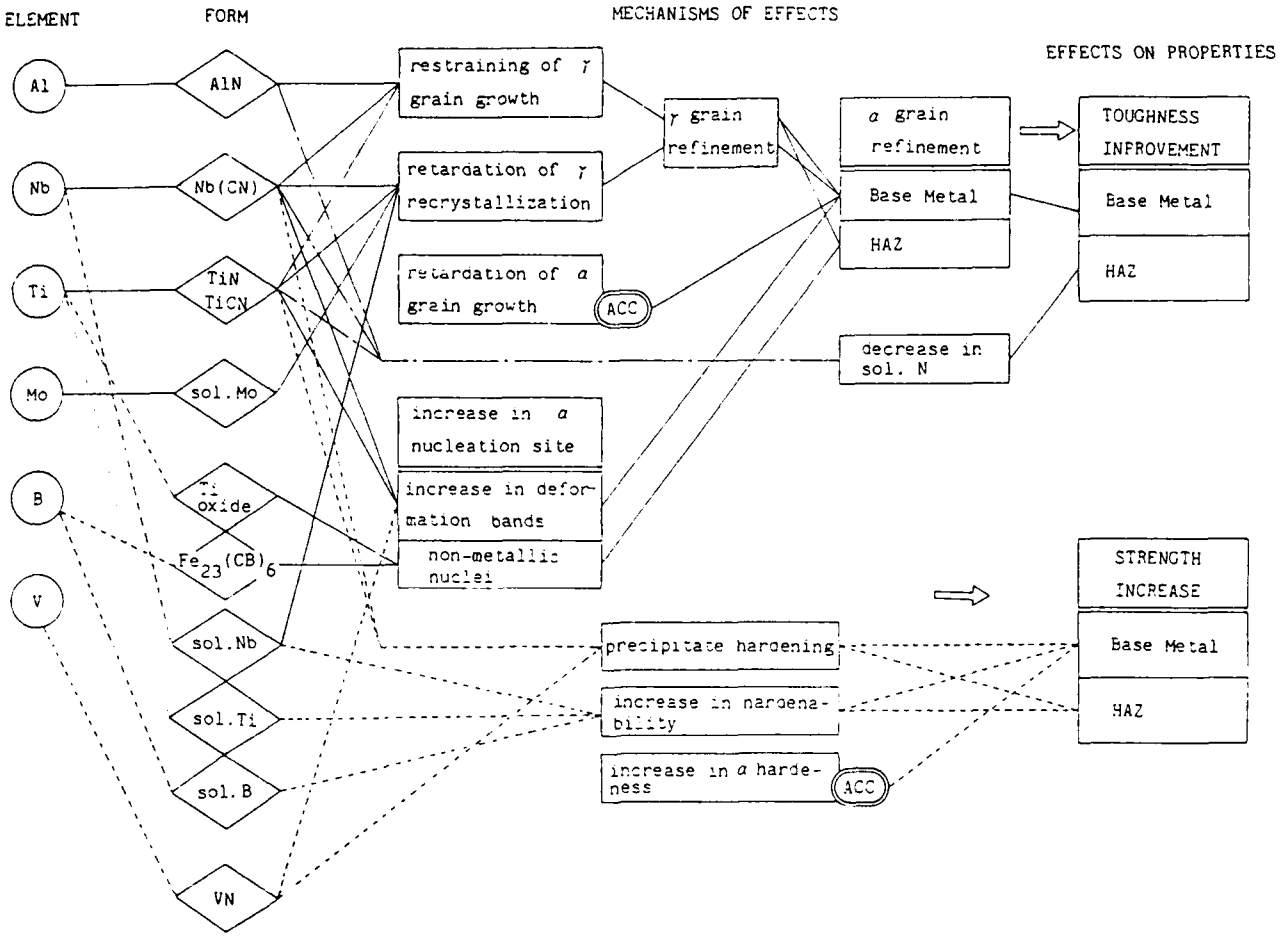


Fig. 26. Effects of microalloying elements and accelerated cooling (ACC) on toughness improvement and strength increase.

Sulfur, phosphorus, oxygen and nitrogen content control techniques are important as they are aimed at achieving the benefits of these alloying elements in various forms. A typical modern steel plate production process is shown in Fig. 27 together with the aim contents of these elements. The process is a combination of hot metal pretreatment, LD converter steelmaking and vacuum degassing. The contents of microalloying elements must be precisely controlled for both property control and economy. Technology is established whereby titanium, niobium, vanadium, calcium and other microalloying elements, which are frequently utilized in steel plates for offshore structures, are added to the molten steel being vacuum degassed. The contents of these microalloying elements can be controlled within narrow limits by this technology.

Figure 28 shows the layout and general view of typical accelerated cooling control equipment (commonly called the continuous on-line control system and abbreviated CLC). The accelerated cooling system embodies the long-standing dream of metallurgists to control the transformed microstructure of the steel plate by controlling the rate of cooling after rolling.

Table2. Main process techniques to make effective use of microalloying elements.

| Technology | Process |
|---|---|
| Control of Impurities (S, P, O, N) | ◦ purification of pig-iron<br>◦ optimum operation of LD converter<br>◦ vacuum degassing |
| Control of amount of microalloying elements | ◦ utilization of computer<br>◦ vacuum degassing process |
| Decrease in center segregation of continuous cast slab | ◦ Electronic stirring of molten steel<br>◦ Rolling of slab by serial rolling stand<br>◦ Pressured casting |
| Precise temperature control of heating furnace | ◦ computer control |
| Controled rolling and accelerated cooling | ◦ Controlled rolling with large reduction<br>◦ computer control for temperature control<br>◦ accelerated cooling |

Fig. 10 - CTOD vs. percent coarse grain regions for all steels. (13)



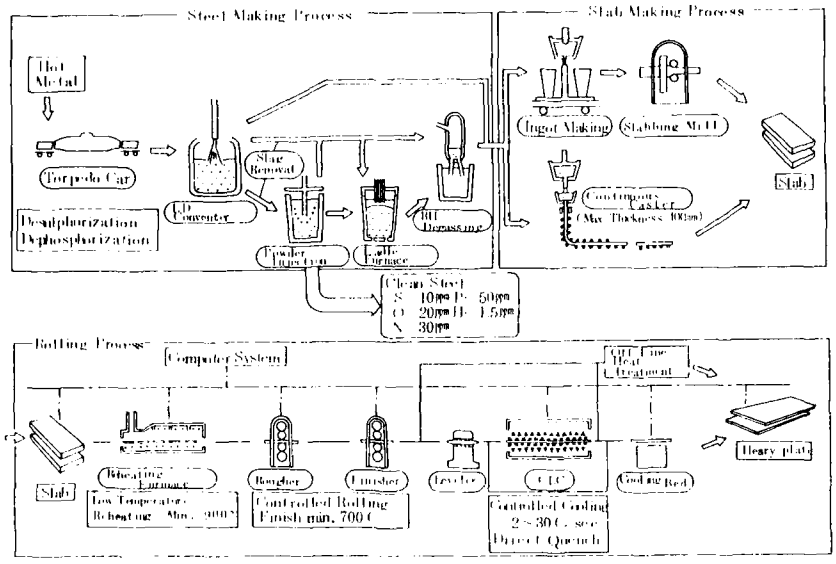


Fig. 27. Typical integrated plate production process.

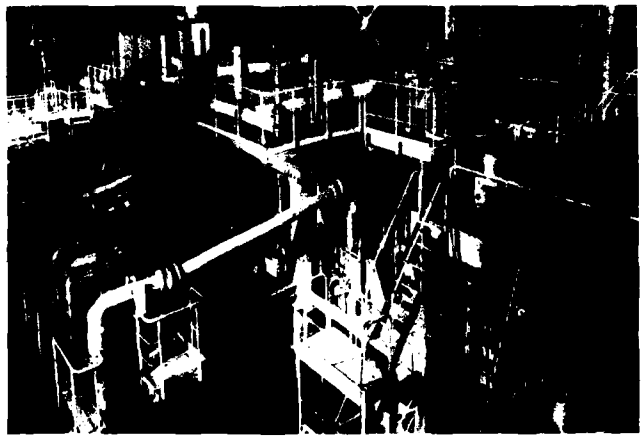

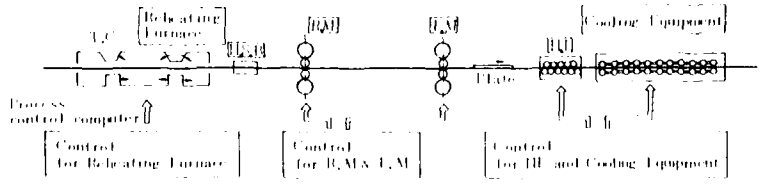


Fig. 28. General view and lay-out of cooling equipment for CLC process.

## RESULTS OF MANUFACTURING MICROALLOYED STEEL PLATES FOR OFFSHORE STRUCTURES BY APPLICATION OF TMCP TECHNOLOGY

The effects of microalloying elements on the properties of steel plates for offshore structures and typical manufacturing processes have been described in the preceding chapters. Of the new processes, accelerated cooling technology was a major breakthrough and dramatically improved the properties of this class of steel plates. The typical properties of steel plates for offshore structures manufactured by the TMCP are shown below.

Table 3 lists the chemical compositions of nine representative types of plate steels developed or produced by the TMCP. Steels A to C are microalloyed with titanium and niobium, have a yield point of 355 MPa and are produced for fixed-type platforms in the North Sea. Steels D and E are microalloyed with titanium and boron, have a yield point of 355 MPa, are intended for welding with high heat input and are produced for arctic semisubmersible drilling rigs. Steels F and G are titanium-microalloyed, 355 MPa yield point grades developed for Charpy impact test temperatures of -60°C and -75°C, respectively. Steel H is a 420-MPa yield point grade produced by the use of titanium oxide to improve the notch toughness of the HAZ. Steel I is a titanium and niobium-microalloyed, 450-MPa yield point grade developed by large additions of nickel and copper to increase tensile strength and notch toughness. The main mechanical properties of base metal and welded joints of these plates are given in Tables 4 and 5. The combination of the TMCP and microalloying technologies provide steel plates with a low carbon content and helps to meet the strength and toughness requirements of base metal and welded joints. The HAZ CTOD values of steels A, B, C and H are shown in Figs. 29 and 30. Satisfactory results are obtained.

Table 3. Chemical compositions of the developed steels.

| Steel | Type | Thickness (mm) | Chemical composition (wt%) C | Si | Mn | P | S | Cu | Ni | Nb | Ti | Al | B | Ceq (IIW) |
|---|---|---|---|---|---|---|---|---|---|---|---|---|---|---|
| A | Ti,Nb added YP355MPa | 38 | 0.08 | 0.26 | 1.46 | 0.009 | 0.003 | - | - | - | 0.007 | 0.043 | - | 0.32 |
| B | for -40°C | 49 | 0.09 | 0.17 | 1.43 | 0.005 | 0.001 | 0.31 | 0.47 | 0.007 | 0.007 | 0.025 | - | 0.36 |
| C | Ti-B added YP355MPa for high heat input welding | 100 | 0.08 | 0.21 | 1.47 | 0.003 | 0.001 | 0.24 | 0.43 | 0.004 | 0.006 | 0.031 | - | 0.37 |
| D | | 32 | 0.08 | 0.36 | 1.38 | 0.007 | 0.001 | - | - | - | 0.007 | 0.055 | 0.0010 | 0.31 |
| E | | 46 | 0.09 | 0.26 | 1.45 | 0.007 | 0.002 | - | - | - | 0.007 | 0.054 | 0.0010 | 0.33 |
| F | Ti added YP355 MPa for -60°C | 50 | 0.07 | 0.27 | 1.40 | 0.005 | 0.002 | 0.31 | 0.36 | - | 0.011 | 0.030 | - | 0.35 |
| G | Ti added YP355 MPa for -75°C | 75 | 0.07 | 0.35 | 1.30 | 0.007 | 0.002 | 0.47 | 0.52 | - | 0.008 | 0.037 | - | 0.37 |
| H | Ti-O YP420MPa for -40°C | 50 | 0.09 | 0.17 | 1.54 | 0.004 | 0.002 | 0.21 | 0.34 | 0.013 | 0.014 | 0.003 | - | 0.37 |
| I | High Cu,Ti-Nb YP450MPa -60°C | 80 | 0.06 | 0.20 | 1.42 | 0.005 | 0.002 | 0.30 | 0.73 | 0.010 | 0.010 | 0.030 | - | 0.41 |

Table 4 Mechanical properties of the developed steels.

| Steel | Type | Thick-ness (mm) | Base Metal: Tensile test Location | YP (MPa) | TS (MPa) | El (%) | Charpy impact test Location | Temp. (°C) | vE (J) | vTrs (°C) | Weld Joint: Charpy impact test Groove Type | H.I. (kJ/mm) | Location | Temp. (°C) | vE (Ave/min) (J) | Crack prevention temp. of y-groove test |
|---|---|---|---|---|---|---|---|---|---|---|---|---|---|---|---|---|
| A | Ti,Nb added YP355MPa for -40°C | 38 | 1/4t T | 403 | 511 | 36 | 1/4t T | -40 | 186 | | SAW K | 5 | 1/2t Fusion-Line | -40 | | ≤ 25°C |
| B | | 49 | 1/2t T* | 411 | 510 | 29 | 1/2t T | -40 | 221 | -80 | SAW K | 5 | | -40 | 235 213 | ≤ 25°C |
| C | | 100 | 1/2t T | 369 | 480 | 33 | 1/2t T | -40 | 290 | -85 | SAW K | 5 | | -40 | 230 192 | ≤ 25°C |
| D | Ti-B added YP355MPa for high heat input welding | 32 | 1/2t T | 391 | 522 | 35 | 1/2t T | -60 | 203 | -85 | SAW X | 11.1 | | -60 | 110 51 | ≤ 0°C |
| E | | 40 | 1/2 T | 399 | 533 | 29 | 1/2t T | -60 | 246 | -90 | SAW X | 21.8 | | -60 | 115 78 | ≤ 0°C |
| F | Ti added YP355 MPa for -60°C | 50 | 1/2 T | 369 | 509 | 30 | 1/2t T | -60 | 215 | -84 | SAW K | 7 | | -60 | 200 178 | ≤ 20°C |
| G | Ti added YP355 MPa for -75°C | 75 | 1/2t T | 401 | 506 | 34 | 1/2t T | -80 | 225 | -104 | SAW X | 5 | | -75 | 133 85 | ≤ 20°C |
| H | Ti-O YP420MPa for -40°C | 50 | 1/2 T | 457 | 558 | 32 | 1/2 T | -60 | 334 | -40 | SAW K | 5 | | -40 | 114 63 | 75°C |
| I | High Cu,Ti-Nb YP45MPa -60°C | 80 | 1/2t T | 479 | 580 | 28 | 1/2t T | -60 | 135 | -80 | SAW K | 7 | | -60 | 210 185 | 25°C |

* transverse direction

Table 5. Mechanical properties of the developed steels.

| Steel | Type | Thick-ness (mm) | PWHT: PWHT Temp. (°C) | Tensile test Location | YP (MPa) | TS (Mpa) | El (%) | Charpy impact test Location | Temp. (°C) | vE (J) | vTrs (°C) |
|---|---|---|---|---|---|---|---|---|---|---|---|
| B | Ti,Nb added YP355MPa for -40°C | 49 | 575 | 1/2t | 391 | 484 | 31 | 1/2t | -40 | 246 | -80 |
| C | | 100 | 575 | | 356 | 483 | 35 | | -40 | 319 | -80 |
| F | Ti added YP355 MPa for -60°C | 50 | 580 | | 383 | 494 | 31 | | -60 | 191 | -93 |
| G | Ti added YP355 MPa for -75°C | 75 | 580 | 1/4t | 394 | 501 | 39 | | -75 | 307 | -112 |
| H | Ti-O YP420MPa for -40°C | 50 | 575 | 1/2t | 435 | 541 | 35 | | -60 | 192 | -80 |
| I | High Cu,Ti-Nb YP450MPa -60°C | 80 | 580 | 1/2t | 465 | 567 | 27 | | -60 | 154 | -67 |

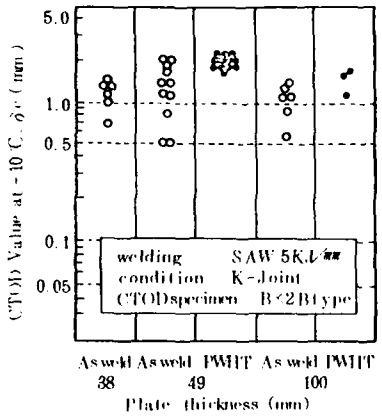


Fig. 29. Test results of steels for offshore structures with yield point of 355-MPa class.[23]

chemical composition, wt%

| thickness | C | Si | Mn | Cu | Ni | Nb | Ti | Al |
|---|---|---|---|---|---|---|---|---|
| 38 | 0.08 | 0.26 | 1.42 | - | - | - | 0.007 | 0.043 |
| 49 | 0.09 | 0.17 | 1.43 | 0.25 | 0.27 | 0.007 | 0.007 | 0.025 |
| 100 | 0.08 | 0.21 | 1.47 | 0.24 | 0.40 | 0.009 | 0.006 | 0.031 |

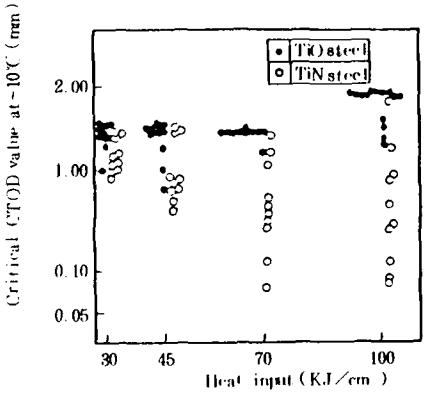


Fig. 30. Critical CTOD values for various heat levels of welding.[26]

chemical composition, wt%

| steel | C | Si | Mn | Cu | Ni | Nb | Al | Ti |
|---|---|---|---|---|---|---|---|---|
| Ti-O | 0.082 | 0.17 | 1.54 | 0.22 | 0.24 | 0.013 | 0.003 | 0.014 |
| Ti-N | 0.085 | 0.23 | 1.52 | 0.25 | 0.26 | 0.012 | 0.027 | 0.011 |

As discussed above, the TMCP technology and auxiliary techniques have helped Nippon Steel Corporation to develop and produce 355-MPa and 450-MPa yield point steel plates for offshore structures as shown in Fig. 31.

Plate steels with higher strength and lower temperature service are under development to meet future requirements.

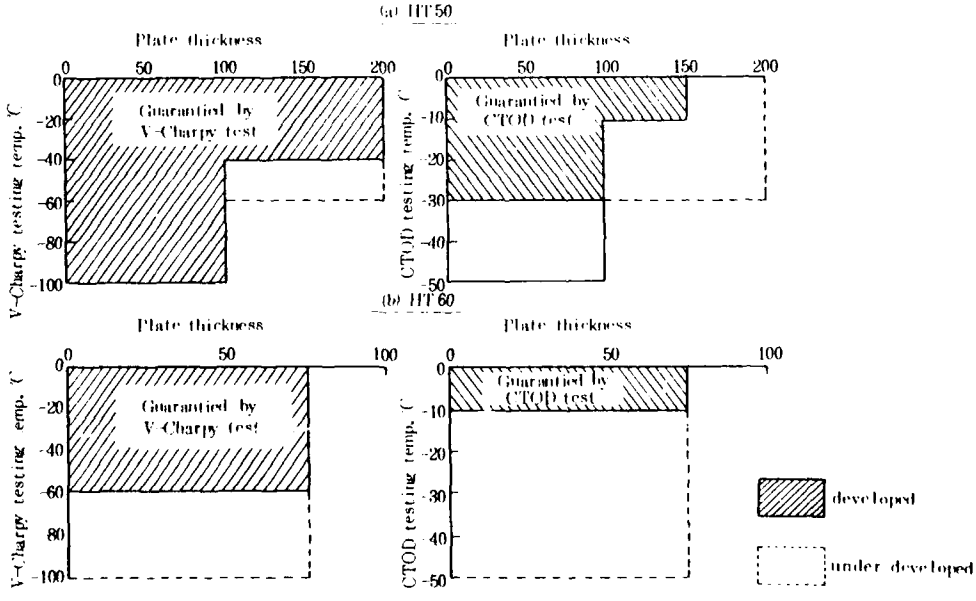


Fig. 31. Example of series of steel plates used for offshore structure specified notch toughness of HAZ. (welding heat input 75 KJ/cm)

## FUTURE DEVELOPMENTS

The use of microalloying elements in coordination with plate manufacturing processes will be an important point in developing new steel plates for HSLA steels that are expected to operate in environments of ever increasing severity. Subjects of future research and development in this respect are as follows:
(a) Better understanding of microalloying elements on formation of high carbon martensite in HAZ
(b) Promotion of development of steel plate that contains IFP, formed from oxide nuclei, in HAZ
(c) Promotion of research on effective utilization of microalloying elements in TMCP technology, rolling and cooling steps in particular
(d) Development of higher strength steel for lower temperature service through application of combination of TMCP and microalloying
(e) Development of steel for welding with high heat input and with high HAZ notch toughness through application of combination of TMCP and microalloying
(f) Development of sophisticated metallurgy to predict an optimum design of chemical composition and production process for required properties.

## CONCLUSIONS

The manufacturing technology and properties of steel plates for arctic offshore structures have been overviewed with attention mainly focused on the microalloying elements and TMCP technology. The TMCP technology is extremely effective in securing the desired strength and toughness of base metal and welded joints, and titanium and niobium are added as principal microalloying elements to improve the strength and toughness of base metal and welded joints. These benefits are accomplished by various steelmaking process techniques.

To develop steel plates for offshore structures to be built for service in punishing subarctic and arctic seas, it will be necessary to utilize the combination of TMCP and microalloying for achieving higher strength and better toughness and to develop economical processes for manufacturing such steel plates.

## REFERENCES


1. N. J. Petch: Phil. Mag., vol. 3 (1958) P.1089.
2. J. Heslop and N. J. Petch: Phil. Mag., vol. 3 (1958) P.1128.
3. R. W. Vanderbreck: Weld. J., vol. 37 (1958) P.114S.
4. Great Lake Steel Corp.: vol.116 (1960) Apr. 11, P.102.
5. C. A. Beiser: Preprint, 138, Annual Convention ASM, Chicago, Nov. 1959 (1959).
6. F. W. Staraat: J. Met., vol. 10 (1958) P.799.
7. W. B. Morrison: JISI, vol. 201 (1964) P.317.
8. E. T. Stephensen, G. H. Carchner and P. Stark: Trans ASM, vol. 57 (1964) P.208.
9. W. E. Duckworth, R. Philips and J. A. Chapman: JISI, vol. 203 (1965) P.1108.
10. H. Sekine, T. Maruyama, Sekiguchi, and Ohno: Tetsu to Hagane, vol. 56 (1970) P.569.
11. R. Philips, W. E. Duckworth and P. E. L. Copley: JISI, vol. 202 (1964) P.593.
12. Omori: Nihon Kinzoku Gakkaishi, vol. 30 (1966) P.1664.
13. J. J. Irani, D. Burton, J. D. Jones and A. B. Rothwell: ISI Spec. Rept., vol. 104 (1967) P.10.
14. Goda, Gondoh. Kimura, Hiyoshi, Yonai and Masumoto: Patent (JAPAN) Tokugansho 38-2228 (1963).
15. Y. E. Smith, A. P. Coldren and R. L. Cryderman: Toward Improved Ductility and Toughness (1972) P.119.
16. H. Nakasugi, H. Matsuda and H. Tamehiro: Proc. Intntl. Conf. on Steel Rolling (1980) P.1028.
17. S. Kanazawa, A Nakashima, H. Mimura, K. Yamato, K. Okamoto, Y. Hagiwara: "Development of new steels for high heat input welding", IIW (1976) IX-952-76.
18. C. Thaulow, A.J.Paau and A.Gunleiksrud: Metal Construction,vol. 17, No.2 (1985) P.94R.
19. K. Uchino, Y. Ohno, S. Aihara, T. Haze, Y. Hagiwara, K. Horii, Y. Kawashima, Y. Tomita, R. Chijiiwa: "Development of 50 kgf/mm$^2$ class steel for offshore structural use with superior HAZ critical CTOD" Fifth Int. Conference on OMAE, Tokyo, vol.2 (1986), P.373.
20. T. Haze, S. Aihara: "Metallurgical Factors Controlling HAZ Toughness In HT 50 Steels", IIW (1986), Doc. XI-1423-86.
21. S. Aihara and T. Haze: "Influence of high-carbon martensitic island on crack-tip opening displacement value of weld heat-affected zone in HSLA steels", 1988 TMS annual Meeting, Jan. 25 (1988).
22. T. Haze and S. Aihara: "Influence of toughness and size of local brittle zone on HAZ toughness of HSLA steels, Seventh Int. Conference on OMAE, Houston, Feb. 7 (1988 .
23. T. Haze, S. Aihara and H. Mabuchi: CIM Conf. on Accelerated Cooling of Rolled Steel (1987.8.23), Winnipeg/Canada.
24. Ohno, Okamura, Uchino, Yamamoto, Matsuda, Ikeda and Sato: Seitetsukenkyu, vol. 326 (1987) P.45.
25. Y. Ohno, Y. Okamura, K. Uchino, S. Yano and S. Matsuda: "Development of Low Temperature Use Steel for Large Heat Input Welding" Wollongong, Australia, 20-24 August 1984 , 129-133.
26. R. Chijiiwa, H. Tamehiro, M. Hirai, H. Matsuda and H. Mimura: presented at the 7th Intntl. Conf. and Exhibit on Offshore Mechanics and Arctic Engineering Feb. 7-12 (1988).
27. K. Yamamoto, S. Matsuda, T. Haze and R. Chijiiwa: "Newly Developed Ti-Oxide Bearing Steel Having High HAZ Toughness: Symposium on Residual and Unspecified Elements in Steel, ASTM, Nov. 1987.
28. Y. Horii, S. Ohkita, M. Wakabayashi, M. Namura: "Development of Welding Materials for Low Temperature Service", Int. Trends in Welding Research, ASM, Tennessee, May,

1986.
29. N. Mori, H. Honma, S. Ohkita and M. Wakabayashi: J. of the Japan Welding Soc., 50 (1981) 2, P.174.
30. A. Naess, J. Hargensen, B. Lian, T. Moan and T. Simonsen: "Investigation of the AlexanderL. Kielland Failure-Metallurgical and Fracture Analysis", Offshore Technology Conference, (1982) OTC4236, Houston, USA.
31. S. Kanazawa, K. Kawamura, K. Yamato, T. Haze, T. Inoue, T. Nuibe and T. Fukuda: IIW Doc. IX-873-74, (1974).
32. Y. Ohno, S. Yano, Y. Okamura: Int. Conf. of Trends in Steels and Consumables for Welding, Nov. (1978) London, The Welding Institute.
33. I. L. Comittee of JWES: IIW Doc. IX-1152-80, (1980).
34. J. Dearden and H. O'Neill: Trans. Inst. Weld, 3 (1940), P.203.
35. AWS D1, 1-86: Appendix O "Guideline on Alternative methods for determing preheat", AWS, (1988).
36. British Standard BS5135, (1984) "Process of arc welding of carbon and manganese steels".
37. Y. Itoh and K. Bessho: J. of Japan Welding Soc., vol. 37 (1968), P.983.
38. N. Yurioka, S. Ohsita and H. Tamehiro: Symposium "Pipiline welding in the 80's", Australian Welding Research Association, (1981).
39. H. Kobayashi and H. Kasamatsu: Tetsu to Hagane, vol. 67, No. 11 (1981) P.1990.
40. T. Gladman and F. B. Pickering: JISI, June (1967) P.653.
41. M. Nishida, T. Kato, N. Ohashi and T. Mori: Tetsu to Hagane, vol. 63 (1977) P.1116.
42. K. Matsumoto, K. Tsukada, S. Yamamoto and C. Ouchi: Tetsu to Hagane, vol. 74, No. 1 (1988) P.107.
43. D. J. Towle and T. Gladman: Met. Sci., vol. 13 (1979) P.246.
44. J. J. Jonas and M. G. Akben: Metals Forum, vol. 4 (1981) P.92.
45. I. Kozasu, C. Ouchi, T. Sampei and T. Okita: Microalloying 75 (1977) P.120.
46. R. W. K. Honeycombe: Scandinavian Journal of Metallurgy, vol. 8 (1979) P.21.
47. R. A. Petkovic, M. J. Luton and J. J. Jonas: Canadian Metallurgical Quarterly, vol. 14, No. 2 (1975) P.137.
48. H. Weiss, A. Gittons, G. G. Brown and W. J. McG. Tegart: ISIJ, vol. 211 (1973) P.703.
49. H. Sekine and T. Maruyama: Tetsu to Hagane, vol. 59 (1973) P.A45.
50. H. Sekine and T. Maruyama: Tetsu to Hagane, vol. 58 (1972) P.1424.
51. J. J. Jonas and A. B. Rothwell: I. S. I. Spec. Rept. vol. 108 (1968) P.78.
52. T. Tanaka and T. Tabata: Tetsu to Hagane, vol. 64, No. 9 (1978) P.1353.
53. J. Irvine and T. N. Baker: Metal Science, March - April '1979) P.228.
54. F. Heisterkamp and L. Meyer: Thyssenforschung (1971) P.44.
55. T. Tanaka, T. Hanamura, T. Tabata: Kawatesugiho, vol. 6 (1974) P.522.
56. C. Ouchi, T. Sampei, T. Okita and I. Kozasu: Hot Deformation of Austenite, J. B. Ballance Edited AIME (1976) P.316.
57. I. Kozasu: Trans ISIJ, 12 (1972) P.241.
58. H. Tamehiro, M. Murata, R. Habu and M. Nagumo: Trans ISIJ, vol. 27 (1978) P.120.
59. A. Yoshie, M. Fujioka, H. Morikawa and Y. Ono: to be presented in the THERMEC'88.
60. M. Tanino and K. Aoki: Trans ISIJ, vol. 8, No. 5 (1968) P.337.
61. M. Tanino, T. Nishida, K. Ooka and K. Yoshikawa:Nihon Kinzoku Gakkaishi, vol. 29, No. 7 (1965) P.734.
62. Y. Onoe, H. Morikawa, Y. Sogo and K. Nakajima: TMS-AIME Annual Meeting, Atlanta, GA, March 6 - 10, 1983.

# WELDABILITY OF STEELS FOR OFFSHORE STRUCTURES

**P.H.M. Hart**
The Welding Institute
Abington Hall
Abington, Cambridge CB1 6AL, UK

## INTRODUCTION

The use of offshore structures for the recovery of hydrocarbons can be traced back for at least 40 years and certainly prior to the first introduction of microalloyed steel. The demands on the weldability of steel imposed by the early offshore developments, which were in locations of relatively easy climate, for example the Gulf of Mexico and the Middle East, were very small. However, when offshore hydrocarbon production extended to the higher latitudes of the North Sea, with its inclement climate, the demands on the weldability of the steel increased significantly. Indeed, in the last 20 years or so of successful production of oil and gas from the North Sea, and more recently other hostile areas such as the Arctic ocean, the development of steel for construction of offshore structures particularly of the fixed type has become increasingly weldability-led. During this time span the aspects of weldability receiving the attention of steel producers, designers, fabricators and users, have shown notable changes in emphasis. The paper will consider these changes together with the current state of weldability of steels for offshore structures and finally will examine future needs. The principal aspects of weldability in relation to fixed offshore structures which have been, and need to be addressed are lamellar tearing, hydrogen cracking, heat affected zone (HAZ) and weld metal toughness and HAZ hardening behaviour. Other aspects of weldabiity such as HAZ liquation cracking, or solidification cracking will not be considered since they have not been significant problems. Moreover the topic of local HAZ corrosion, not commonly referred to as weldability, will also not be covered as general experience is not indicative of a problem provided cathodic protection systems are operative. Before discussing the principal items of weldability mentioned, brief attention to change in steel compositions is necessary.

## TRENDS IN OFFSHORE STEEL COMPOSITION AND MANUFACTURE

In considering the weldability of steels for offshore structures and the changes that have occurred, it is essential to note the trends in steel composition and production methods that have also taken place since the link between weldability and composition in particular is very strong. While the trends in composition will also need to be assessed in relation to each weldability topic, general trends can be outlined here.

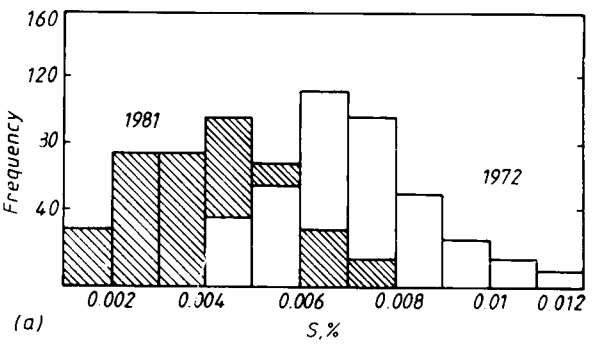


(a)

| | S | P | N | O | H |
|---|---|---|---|---|---|
| 1984 | 20 | 150 | 100 | | 2 |
| 1990 | 10 | 15 | 35 | 20 | |
| Long term | 45 | | | | |

(b)

Fig 1: Trends in impurity elements in microalloyed C:Mn steels (a) after Kirkwood (62), (b) after Fitzgerald (63).

The early offshore steels were no different to structural steels of those times, ie they were generally semi killed C:Mn materials with, by today's standards, high levels of carbon (~ 0.20%) and impurities, particularly sulphur, say 0.03% as a typical value. Through the years since early offshore developments took place we can see carbon and carbon equivalent (CE) (unless otherwise specifically mentioned the most widely used IIW formula is referred to ie

$$CE = C + \frac{Mn}{6} + \frac{Cr + Mo + V}{5} + \frac{Ni + Cu}{15}$$

levels have fallen dramatically. A significant step in this direction was taken in the early days of microalloying by the use of Nb additions in normalised steels, although microalloying additions were often initially viewed as a means of obtaining increased product strength without raising steel carbon content. Additions of typically 0.03 to 0.06%Nb became a common ingredient in normalised steels of around the 350 $N/mm^2$ yield strength level so typical for fixed offshore platform construction. The use of such Nb additions allowed small reductions in carbon and CE to take place helping steel producers to meet ever increasingly stringent maximum CE levels in steel specifications. Recent years have seen the introduction of continuous casting, which has brought another variable into the weldability arena, and the increasing use of accelerated cooling, which has allowed yet further reductions in plate carbon and CE levels while maintaining or improving mechanical properties.

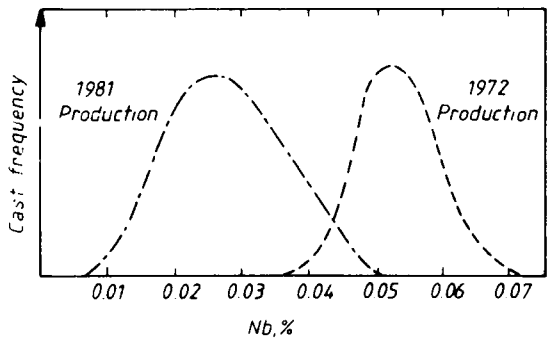


Fig 2: Changes in niobium level in the production of C:Mn:Si:Nb:Al steels (after Kirkwood (62)).

There have been many changes in the compositions of offshore steels during the last 20 years and these have been predominantly in relation to steadily increasing property requirements, particularly weldability development. There has been and still is a continuous evolution of these steels, but the principal compositional trends and changes can be identified as:

1. A reduction in carbon content to typically 0.10% for normalised steels, and lower for controlled rolled and accelerated cooled material.

2. Reductions in impurity elements particularly sulphur, phosphorus and nitrogen, see Fig 1, and oxygen levels.

3. Steady reduction in Nb levels. Fig 2 indicates the trend in earlier years while since 1980 maximum levels have further fallen as specifications calling for 0.025%(1) and even 0.020%(2) have been increasingly appearing.

4. Additions of Ni and Cu typically at approximately 0.2% each although some producers replace the Cu with Ni.

5. Ti treatment.

6. Ca treatment.

7. Reduction in CE level largely through the reduction of carbon content. Figure 3 gives some indication of the trend and to some extent this is continuing, particularly of course, through the use of accelerated cooling.

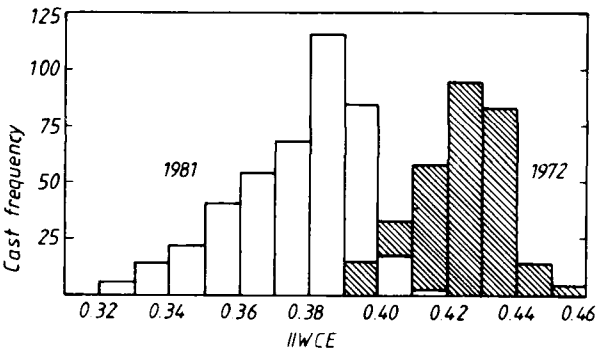


Fig 3: Changes in carbon equivalent level in production of C:Mn:Si:Nb:Al steels (after Kirkwood (62)).

A feature of steel processing which has changed very remarkably during the past 20 years is the wide spread introduction and use of continuous casting. The relevance of this change to a consideration of steel composition is the marked influence on variations in composition through a plate thickness arising from the generic problem of centreline segregation. The local increases in C, Mn, Nb and phosphorus in particular can be quite marked conferring different and generally deteriorated weldability on local regions of steel plate (3). Developments in continuous casting techniques have provided a significant improvement in respect of this aspect but while the dark etching feature so typical of the continuous cast plates in the 70s and early 80s (Fig 4) is

less obvious today, the problem can still be a cause of deterioration in weldability.

Fig 4: Appearance of dark etching centre line segregation.

## LAMELLAR TEARING

During the 1960s and early 1970s lamellar tearing was a major problem for structural steel fabricators, occurring in those joints experiencing the through-thickness strain that puts them at risk. For the offshore industry with its high level of ultrasonic inspection, lamellar tearing was occasionally a devastating problem because of a severe impact on construction times which were necessarily particularly constrained by the need to meet completion for launch during suitable weather windows. Extensive research in the late 60s and early 70s demonstrated the disastrous effect that type II MnS inclusions had on through-thickness ductility (4). The development of lamellar tearing resistant plate that followed largely depended upon the obvious benefit of reduced sulphur levels. Since another oil industry cracking problem, that of hydrogen induced, pressure, stepwise or blister cracking was also becoming endemic in wet/sour environments at the same time, and was also found to be improved by a reduction in sulphur levels, the incentive for the steel industry to introduce clean steel was very considerable. Gradually the steel industry responded, and of course today's steel of the necessary extra low sulphur level, of about 0.005% and below to provide resistance to the problem of lamellar tearing, even in highly restrained joints, is now widely available. To all intents and purposes lamellar tearing is now only an historical problem and no longer appears as an item on a modern list of weldability aspects of concern in steel for offshore structures.

However, while a low sulphur level undoubtedly brings with it many other advantages for the properties of steel and welded joints, it seems as if the presence of sulphides may also sometimes have beneficial roles to play (5) and their reduction has not always been viewed as universally beneficial in respect of weldability. One aspect of weldability where an adverse affect from cleaner steels is sometimes attributed is in the field of HAZ hydrogen cracking and hardening.

## HYDROGEN CRACKING

As an aspect of weldability the problem of under bead, hard zone, cold, delayed, restraint, or simply HAZ hydrogen cracking can probably claim to have been the longest and most widely studied problem in welding ferritic steels. In terms of its role as the most common cracking problem and the dominant contributory part it can exert in initiating catastrophic brittle fracture and fatigue failures, this extensive study is understandable. As the various names by which this form of cracking is sometimes described imply, many factors are involved in its occurrence, but simply expressed it occurs under the combined simultaneous presence of:-

Sufficient hydrogen
Hard HAZ microstructures
Tensile stresses
Temperatures near to normal ambient (20°C)

The role played by the steel in this list concerns the effort to avoid the formation of the necessary predominantly martensitic microstructure in the HAZ. For very many years, as a generalisation, it has been known that the risk of HAZ hydrogen cracking can be reduced by limiting those elements in the steel which increase the tendency to form hard predominantly martensitic microstructures in the heat affected zone. For a long time too, the major elements of concern have been grouped together to include their influence relative to that of carbon, in a carbon equivalent formula of which the most widely used is the IIW

$$\left(C + \frac{Mn}{6} + \frac{Cr + Mo + V}{5} + \frac{Ni + Cu}{15}\right)$$

Hence, in a general sense, steel development for improved resistance to HAZ hydrogen cracking has been aimed at lowering the CE value of the steel composition. The formula clearly shows that a reduction in carbon content is the most effective means of lowering the CE value. However,

reductions in carbon have to be achieved while maintaining plate yield strengths of the order of 350N/mm$^2$ and it is in that area that major steel developments have taken place, as described in Section 2.

What is the effect of the changes in steel composition considered in section 2 on HAZ hydrogen cracking behaviour? Certainly during the last five to eight years there have been a number of reports and publications claiming that many of these trends in composition and processing have had an adverse effect on some aspect of weldability particularly hydrogen cracking and HAZ hardening behaviour (6,7). Even a few years ago, however, in a study of several modern offshore steels, Boothby found no evidence for an adverse influence of modern against older steels. He did however find that there was no improvement and possibly some deterioration in resistance to cracking as the carbon equivalent decreased from 0.43 - 0.36.

Over the last few years at the Welding Institute several modern structural steels covering the CE range 0.30 - 0.45 have been examined. The results of these studies are presented in Fig 5 together with the data from Boothby's study. In any such compilation of data the inherent scatter in welded hydrogen cracking tests must be recognised and taken into account. Moreover even in one laboratory the reproducibility of the two parameters in the figure could, at best, be of the order of ± 0.5 secs and ± 0.15 CE. Bearing this in mind, the trend in the figure can clearly be seen, over the wide range of CE for which data are presented, to be for a reduction in the risk of cracking as the CE level is decreased. In general this is supported by industrial fabrication experience for such steels.

At the same time, some of the changes in composition, particularly the increased cleanliness, can give rise to a greater than expected HAZ hardening characteristic - see next section - and certainly as the carbon decreases there is a trend for cracking to occur at lower HAZ hardness levels, ie for critical hardness levels to decrease, compared to the experience with the higher carbon steels of the 60s and early 70s (8-10). For example in a steel with 0.18% C and a CE of 0.44 the critical hardness may be about 420 HV, while in a 0.07%C, 0.30 CE steel cracking may occur at HAZ hardness nearly as low as 300 HV. Collectively these features of increased hardening and lower critical hardness, especially when present together, can mean some locally increased tendency for cracking behaviour and that may account for some of the scatter in the diagram. Of course it is almost certain that the scatter can be reduced by the derivation of a better descriptive compositional parameter than CE, and future work at The Welding Institute will be exploring this aspect. However, as recent studies and their formulae (11,12) have indicated, the complexities of the

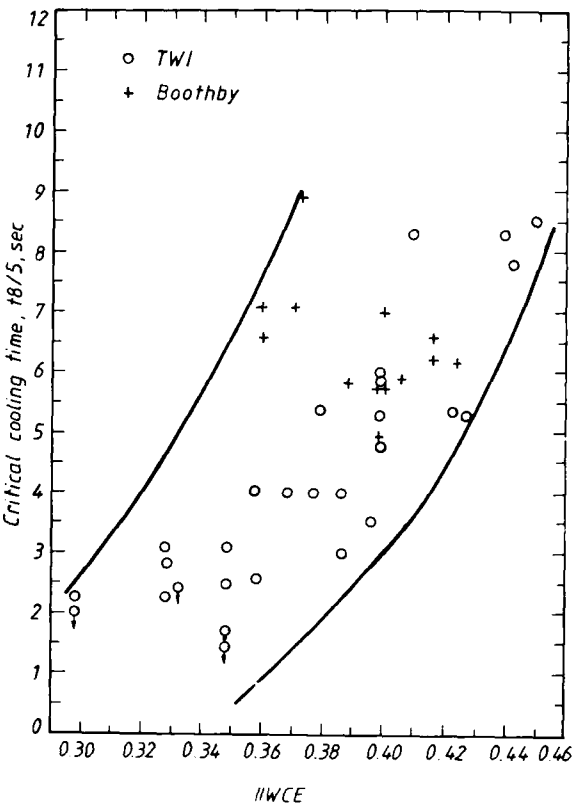


Fig 5: Current CTS results on modern C:Mn steels. Critical cooling time for weld hydrogen level of ~ 10-12 ml/100 g deposited metal.

subject are such that further investigations are most unlikely to lead to a simple parameter if a significant reduction in scatter is to be sought. The principal message however is clear, that overall, the present trend in steel composition is beneficial for the problem of HAZ hydrogen cracking.

Hydrogen embrittlement and cracking is not exclusive to the HAZ and can also occur in weld metal. In general, in the past, welding procedures to avoid HAZ cracking were adequate to protect the weld metal. However, the downward trend in CE, while improving the resistance of the HAZ to hydrogen cracking and lowering the protection it needs, has not helped the weld metal. In practice there are now several fabrication situations where weld metal hydrogen cracking is more likely than HAZ cracking, and this is particularly so at higher heat inputs, for example with submerged arc welding, which significantly softens the HAZ while having relatively little effect on weld metal hardness. The form of weld metal cracking most commonly

observed is transverse and angled at approximately 45° to the weld surface, Fig 6. It can be very difficult to detect, particularly because of its orientation, unless appropriate ultrasonic inspection techniques are used (13). Despite significant reductions in consumable moisture content, the problem still occurs intermittently, sometimes with very major impact on production schedules and costs. To allow full economic advantage of the low risk of HAZ hydrogen cracking offered by today's low CE steels, further work is required both to carefully define the need for and level of preheat as a function of hydrogen level and welding procedure to prevent weld metal hydrogen cracking, and to obtain even lower weld hydrogen levels from improved consumables.

## HAZ HARDENING

There is little doubt that under some circumstances the cleanliness of a steel ie the number of oxide and sulphide particles present, can influence the HAZ austenite to ferrite transformation in such a way that a reduction in numbers of these particles can result in an increased hardening and hence HAZ hydrogen cracking tendency (14). Bearing in mind the established influence of second phase particles, particular oxides (15-17) but recently sulphides (18), on austenite decomposition in weld metals , an effect in the HAZ is not metallurgically surprising. The reported variability in HAZs is clearly in large part linked to the lack of correlation between weight percent of oxygen and sulphur and the metallurgically important parameter of numbers of particles (19). The absence of an effect in a few specific studies (14,20, 21) in certain steel compositions may be linked to other factors not yet identified.

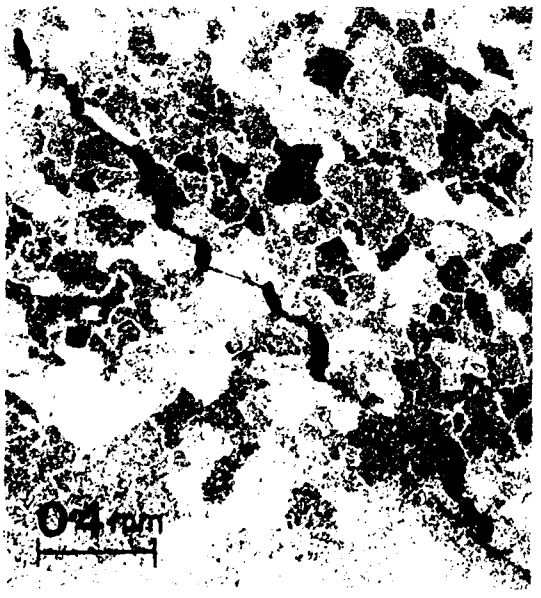


Fig 6: Example of 45° or 'chevron' cracking in C:Mn submerged arc weld metal.

In practical terms this effect of cleanliness on HAZ hardening and hydrogen cracking is generally only small but individual cases have occasionally reported large effects with major fabrication difficulties, eg (22). In general it seems that practical difficulties only arise when a change in steel cleanliness coincides with the use of previously satisfactory procedures which had a very small margin of safety in respect of meeting HAZ hardness requirements or avoiding HAZ hydrogen cracking. Moreover the reported incidence of problems was greatest only during the several years of transition from less clean to today's very clean steels. Now, with many years experience of welding clean steels, this aspect is far less, if at all, a practical problem especially when balanced against the vast array of improved properties associated with cleaner steels.

Of course with the trend to reduce carbon contents, maximum hardness levels obtainable in HAZs are lower as a direct effect of carbon on martensitic hardness. However, the rate of softening of modern steels with increased heat input may not always be as great when compared with older steels, particularly if compared using just the simple CE IIW formula. Part of the reason for this may be related to the influence of other elements not included in the formula, such as boron, and their interactions with changes in nitrogen and aluminium levels (5,12,23), while part of it may be the need to use more specifically designed compositional parameters eg those recently proposed by Nippon Steel or Mannesmann (12,24) for describing HAZ hardening behaviour in carbon manganese microalloyed steels.

## WELD METAL TOUGHNESS

In the early 70s weld metal deposited by most of the processes used in offshore platform construction, principally manual metal arc and submerged arc, produced relatively inferior as-welded levels of toughness, sometimes requiring costly post weld heat treatment (PWHT) to provide adequate fracture resistance, particularly for the critical node regions (25). Extensive study of factors influencing weld metal toughness which was taking place in the late 70s and early 80s highlighted the role of oxygen level and inclusions on weld metal microstructure development and toughness. Continued study demonstrated the interaction of steel composition with weld metals particularly for the high dilution submerged arc process, which is widely used for the manufacture of tubulars for platforms. These studies (26-29) showed that weld metal toughness was very strongly influ-

enced by aluminium content, Fig 7, when using basic fluxes, which are widely employed for obtaining the required toughness levels. Indeed it is now well established that in general the optimum aluminium level decreases with decreasing weld metal oxygen level and hence the tolerance to aluminium, which can be derived from parent steel by dilution, is lower with the lower oxygen level of basic fluxes. Practical problems in obtaining required weld metal toughness levels were experienced in several projects when plate aluminium levels rose significantly above about 0.04%. Similar problems have been reported and observed in line pipe manufacture (30). However, in general, at the present time, weld metal toughness is not a major problem for this fabrication type (for minimum design temperatures of -10°C) largely because of the successful consumable development, and, particularly in relation to the use of self shielded consumables, the knowledge gained in respect of procedural requirements to obtain adequate toughness (31). Lower design temperatures and a possible increased usage of gas shielded tubular wires are likely to require further development however.

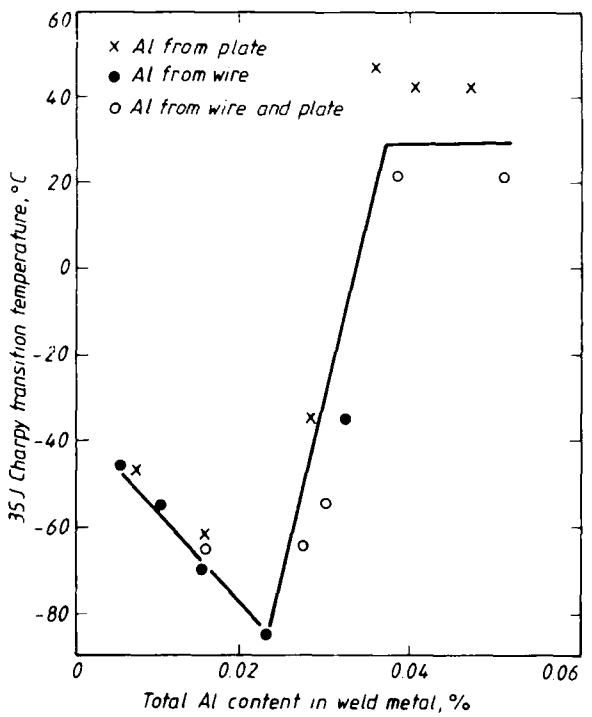


Fig 7: Effect of weld metal Al content on charpy hydrogen in submerged arc welds made with a basic flux (26).

## HAZ TOUGHNESS

Concern over the problem of brittle fracture in offshore structures operating in the North Sea, perhaps highlighted by the failure of the "Seagem" in 1965 and the gathering pace of development in the late 1960s and early 1970s, prompted extensive European studies of HAZ toughness in offshore steels (32,33). Those studies generally found adequate levels of toughness provided heat inputs were within the range 1.5 to 4.0 kJ/mm. However, in the 80s an increasing incidence of low levels of HAZ toughness, particularly CTOD fracture toughness, were experienced. Moreover the experience was not confined exclusively to the high temperature grain coarsened region in the as-welded condition. These findings introduced a period of intense study of HAZ toughness, and in the last five years have possibly provided the dominant driving force for steel development for this market.

Extensive studies of the effect of many factors on HAZ CTOD fracture toughness including steel composition, welding procedure, peak temperature on reheating, the proportion and size of brittle regions in multipass welds etc, have been carried out (34-38). To a large extent, but not exclusively, as sometimes misleadingly simplified, the problem has been found to be one of initiation of cleavage fracture from the intercritically reheated grain coarsened (ICGC) HAZ region, at least in the as-welded condition. In the post-weld heat treated condition initiation is usually from grain coarsened HAZ which may or may not have been sub-critically reheated (SCGC).

These regions are quite small and hence have given rise to the term "local brittle zones" (LBZ). However it should be recalled that both HAZ fracture toughness testing in the past and failure analysis have shown fracture can initiate from small local zones of poor toughness and in that sense LBZs are not a new phenomena. Nor indeed, as recent work has shown, are they especially associated with modern steels (39). Moreover recent wideplate testing (40) indicates they can be structurally significant when welded joints, with crack tips located in such regions are highly stressed at minimum design temperatures. That the recent history of offshore structures is essentially free of brittle fractures is largely considered to be a reflection of the low probability of a simultaneous occurrence of all factors necessary to produce a fracture, ie high load at low temperature in a cracked joint such that the crack tip is in a region of low toughness, rather than an indication that low CTOD values have no structural relevance at all (41,42). However, the subject is highly complex since concern relates to multipass welds mainly, with the attendant multiplicity of thermal cycles and micro-

structural regions, and to an understanding of properties in both the as-welded and post-weld heat treated conditions. Hence it is very important that studies are, in the large part, conducted on multipass welds which need to be carefully monitored in respect of their consistent production of microstructural regions of concern eg ICGC HAZ, and which require a post-testing examination of the fracture initiation region and of regions sampled by fatigue crack tips. Two recently published specifications recognise this and provide helpful guidance in this difficult area (43,44).

From the studies that have been carried out, and are still in progress, it seems that the basic factors influencing HAZ toughness are the principle factors which influence cleavage fracture in ferritic materials, ie effective grain size, yield strength, and extent and size of microcrack initiators. Thus toughness is improved by:

Lowering the matrix hardness or yield strength
Reducing the effective grain size

Reducing the size and extent of microcrack initiators eg carbides, M-A (martensite-austenite) and inclusions.

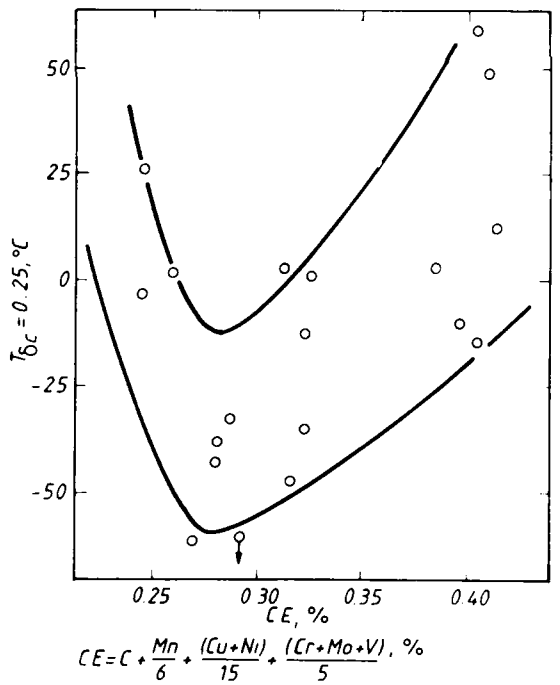


Fig 8: Effect of carbon equivalent on HAZ CTOD fracture toughness (after Nakaniski et al (45)).

In general it is found therefore that toughness is deteriorated by increasing heat input, arising largely as a result of coarsened microstructures, ie a larger effective colony size as the austenite grain size increases and larger M-A and carbide phases. Compositional factors leading to a decreased hardness, often expressed as decreasing carbon equivalent, have also been found to increase toughness, over the range applicable to C:Mn microalloyed steels. However, as the work of Nakanishi shows (45) such relationships, Fig 8, are rarely linear, and if the carbon equivalent, or perhaps carbon, drops too low in this family of steels, toughness can deteriorate again, since the effective grain size starts to increase. While niobium microalloying is clearly advantageous for development of excellent plate properties, many studies (37,46-48) over the years have indicated that decreasing niobium levels, at least for medium to high heat inputs, is yet another way to improve HAZ toughness. This largely arises from a reduced HAZ hardness or yield strength at lower niobium levels. In the effort to obtain improved HAZ toughness, with so many factors influencing it, each possible improvement contribution is likely to be used and so typical niobium levels are still falling today with 0.010 to 0.015% becoming increasingly common, particularly in accelerated cooled plates. The extent to which these lower levels of Nb are just a reflection of improved toughness is unclear, since with improved plate processing, especially accelerated cooling, the required Nb levels to attain present plate properties are also falling. Hence it is likely that the observed trends in Nb level reflect many factors, of which improved HAZ toughness is just one.

As mentioned above one of the regions of low toughness is the ICGC HAZ and studies have shown the low toughness to be due to the detrimental effect of small areas of "island martensite" or M-A formed from original high carbon austenite regions and then acting as crack initiators. Factors influencing M-A formation have been investigated (37), and work at the Welding Institute (49) has shown that M-A is not always formed in modern steels, pearlite sometimes being the type of microphase developed (Fig 9). There is some indication that although an ICGC HAZ microstructure containing pearlite may be of lower toughness than its corresponding SCGC HAZ microstructure, pearlite is nevertheless less harmful than M-A. Further study is needed to confirm this and to determine the alloying features which contribute to its formation rather than to the formation of M-A.

To some extent the centreline segregation aspect of continuous casting has aggravated the HAZ toughness problem by locally raising microstructural hardness. In addition Metz et al (50) have associated reduced Charpy toughness after

PWHT, especially at mid thickness of concast plates, with segregation and increased phosphorus levels. A possibly related aspect which has come to light is the significant tendency for low toughness after PWHT to be associated with the formation of intergranular fracture facets (51,52). The most likely cause of this is from the locally enhanced phosphorus levels, producing some type of temper embrittlement, although further study of this is required.

## FUTURE TRENDS AND REQUIREMENTS

There can be little doubt that fabricators and users will continue to demand material of even better weldability than the present day, already substantially improved materials are offering.

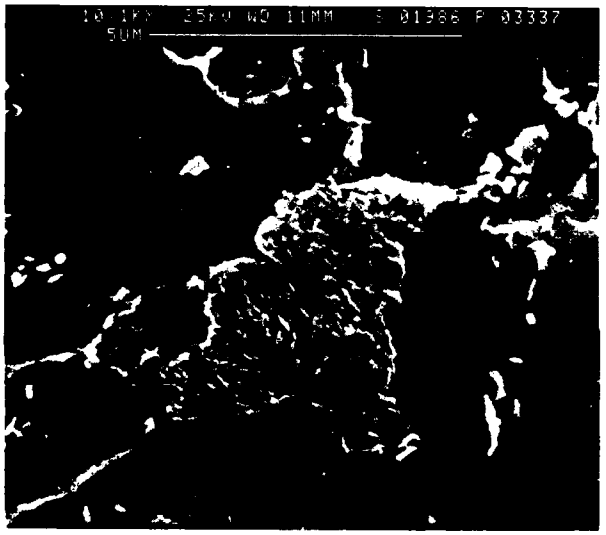


Fig 9: SEM micrograph of pearlite in ICGC HAZ (after Sparkes (49).

Greater ease in avoiding cracking and producing soft and ductile HAZs will be required together with a great consistency of properties through a plate, from plate to plate, and from heat to heat. A need to obtain adequate toughness both at higher heat input welding conditions and at lower minimum design temperatures can also be envisaged.

How will these demands be met and are current trends in the right direction? At least in a general sense further improvement can be obtained by lower carbon and carbon equivalent levels, and it seems that there will be further use of the cheapest "alloying element" - water - through the wider and more effective use of accelerated cooling techniques to maintain parent material strength and toughness levels while allowing this trend to lower carbon and CE levels to continue. This will benefit avoiding HAZ cracking, meeting HAZ hardness requirements and HAZ toughness. However, as indicated earlier in Fig 8, we cannot expect lowering CE to continue improving toughness regardless, since if the hardenability is too low coarse microstructures develop with a consequent reduction in toughness. There is an additional factor which may limit the extent to which continued reduction of CE levels will always lead to improved HAZ fracture behaviour and that relates to the possibility of developing softened HAZ regions. Recent wideplate studies of high strength steels (53) indicate that these can show unexpectedly low strains to fracture and this has been attributed to the development of undermatching strength regions in the HAZ. With very low CE C:Mn steels of approximately 350 $N/mm^2$ yield strength, corresponding low strength HAZ regions may develop, (54) especially at high welding heat inputs. A point to note is that this behaviour may not be apparent just from CTOD fracture toughness testing and could require wideplate testing to identify it. However, useful improvements in HAZ toughness, especially for North Sea design temperatures, have already been obtained and this softening aspect may be some way off yet, in terms of lower CE, for the 350 $N/mm^2$ strength steels.

Impurity levels are already low in this class of steel but at least in respect of HAZ toughness benefit can be expected by further reductions both in nominal phosphorus levels and especially in the extent of segregation, so as to reduce the incidence of intergranular fracture in the centre segregation region of continuous cast plate materials after post weld heat treatment. No adverse effect of reduced phosphorus level is envisaged, however far it is taken, except for a small penalty in plate strength.

The same cannot be said in respect of nitrogen since continued reduction as with CE may not always result in improved HAZ toughness, as continued reduction in nitrogen may also be associated with adverse side effects, eg a reduction in austenite grain growth resistance in the high temperature HAZ arising from fewer or less optimum sized nitrides. As is the case with TiN steels, where an optimum non-zero nitrogen level exists, (55) so even for Al treated steels too low a nitrogen level could be a disadvantage.

An element which has received relatively little attention, at least in this class of steel, is silicon. Haze and Aihara (37) indicate that, for the ICGCHAZ its detrimental effect is similar to that of carbon, while Kinaka et al (56) indicate optimum levels may be as low as around 0.15%. Certainly further research into this element seems warranted especially where the loss of strength at such low levels can be

accommodated by the use of less embrittling elements. According to Haze and Aihara, these could be Mn, Cu or Ni all having a CTOD deterioration factor significantly less than that of Si.

Just as in their own way the introduction of microalloying, controlled rolling and accelerated cooling can, with hindsight, be seen as step changes in our development of more weldable steels, the next step change is probably just appearing on the commercial horizon. To aid the current weldability topics of HAZ hydrogen cracking, hardening and toughness, the common metallurgical requirement is for the development of HAZ microstructures of low but adequate yield strength, yet of fine grain size. Reduced CE (or Pcm or CEN or any parameter chosen to assess alloying) is beneficial for reducing hardening but this does little for the production of a fine ferrite grain size. Many years ago efforts were made to reduce the damaging austenite grain growth that occurs in the high temperature HAZ by the use of TiN particles (57) and hence develop a fine transformed microstructure. Experience to date some, 10-15 years on from the earlier developments, still meets with only mixed success either in terms of significant control of austenite or ferrite grain size. This is because production of the required TiN particles, and maintenence of them through subsequent steel processing, including welding, has proved very difficult although improved control is being obtained.

Weld metal microstructures from modern consumables can develop fine grain ferrite structures over a wide range of practical cooling rates and this is achieved by using the inherent oxide particles to provide Particle Microstructural Control (PMC). These fine microstructures are developed not by reducing the austenite grain growth but by promoting nucleation of intragranular decomposition of austenite to ferrite using fine second phase particles, which are generally, but not exclusively, oxides (48,58,59). This PMC technology is now beginning to be applied to produce fine grained ferrite in the HAZ of parent steels where the use of stable oxides in particular eg titinium oxide allows easier processing of the steel after casting than was the case for the TiN approach. The potential benefits of this next step change are very substantial but the technological requirements of consistently producing an even distribution of fine second phase particles are very daunting. Nevertheless there are reports of such steel having been produced on a commercial scale (35) and research in this area is definitely gathering pace.

Other ways of producing fine grained soft transformed microstructures may be found yet it is interesting to note that recent studies (60, 61) have shown that vanadium appears to be able to promote intragranular nucleation and fill development of finer microstructures. Whether this feature can be utilised to improve HAZ toughness, while maintaining required plate mechanical properties without additional alloying, remains to be seen.

## SUMMARY AND CONCLUDING REMARKS

Over the history of steel construction for offshore oil and gas production, weldability of the steel has changed from a near non-requirement to a primary property specification, as important as the steel strength and toughness. To meet this changing situation, major developments have taken place in steel making, steel compositions and steel processing techniques. Early developments were particularly focused on the problems of lamellar tearing and HAZ hydrogen cracking and produced substantial reductions in sulphur and carbon levels in particular. The improvement in cleanliness has been so extensive and widespread that lamellar tearing is no longer a fabrication problem in this industry. The reduction in carbon, and carbon equivalent, brought about by microalloying, improved processing of normalised steels, and more recently accelerated cooling, have, together with improved consumables, led to a significant overall reduction in the potential for HAZ hydrogen cracking, despite any adverse effect on hardenability from the increased cleanliness. However, the full economic advantage, in terms of absence of preheat, offered by very low CE steels, for the avoidance of HAZ hydrogen cracking, cannot always be utilised since preheat is sometimes still required to protect the weld metal from hydrogen cracking especially in thick section joints.

In the present decade, development of improved weldability has probably been primarily focused on understanding the causes of low HAZ CTOD fracture toughness and developing steels with improved behaviour in respect of this aspect. Research to date has indicated significant benefits can be obtained by reduced carbon and carbon equivalent as well as decreases in HAZ hardness from lowered microalloyed content, largely Nb. Accelerated cooling of plates has been particularly beneficial in allowing these reduced carbon and alloy levels to take place while maintaining or improving plate mechanical properties. Reductions of impurities, particularly phosphorus, are continuing and, with the possible exception of a need to optimise nitrogen, are universally beneficial. Further reductions in the degree of segregation in continuous cast plate will improve HAZ toughness and hence the use of this economic production route.

Attainment of adequate HAZ toughness for the most arduous operating temperatures or Arctic regions and under high heat input high productivity welding conditions, will require

further developments, of which the use of controlled second phase particles, particularly oxides, giving particle microstructural control (PMC) to produce fine transformed ferritic HAZ microstructures is probably the most promising. This high level technology will be difficult to implement but it can be expected to also provide benefits in other areas of weldability including HAZ hydrogen cracking and hardening behaviour as well as aiding achievement of good HAZ and weld metal toughness of joints made by the principally single pass, autogenous electron beam and laser welding processes.

**ACKNOWLEDGEMENTS**

The author gratefully acknowledges helpful comment from Drs T G Gooch and P L Harrison.

**REFERENCES**

1. Norsk Standard, NS 12 603, "Structural Steel for Offshore Applications".

2. Lefebvre, G. and Dufrane, J.J. Int. Seminar on "Modern High Strength Steel in Marine Structures, Delft, Oct. 1987.

3. Yurioka, N. International Conf. on Welding Research, Boston, July 1984.

4. Farrar, J.C. and Dolby R.E., "Lamellar Tearing in Welded Steel Construction". The Welding Institute, 1972.

5. Hart, P.H.M., Met. Con., 18 610-616, 1986.

6. Boniszewski, T. and Keeler, T., Met. Con. October 1984.

7. Walker, R., "Welding Specs - a Call for Realism". Offshore Engineer, February 1984.

8. Watkinson, F. and Bodger, P., Weld. Res. Intnl. 5, 34-62, 1975.

9. Boothby, P.J., Met. Con. 17, 508-513 and 612 - 620, 1985.

10. Hart, P.H.M., Matharu, I. and Jones, A.R., OMAE, Houston, 1988.

11. Cottrell, C.C.M., Met. Con. 16 740-44 (1984).

12. Yurioka, N., Okumra, M., Kasuya, T. and Cotton, H.J.P., Met. Con. 19 217-223, 1987.

13. Hart, P.H.M. and Mudge, P.J. Background to new guidance on structural steel and steel constructions standards in offshore structures, HMSO 1986.

14. Hart, P.H.M. Welding in the World, 23 230-237, 1985.

15. Ito, Y. and Nakaniski, M., Sumitomo Search No 15 27-47, May 1976.

16. Cochrane, R.C. and Kirkwood, P.R. Trends in Steel and Welding consumables for welding. Int. Conf. London Nov. 1978.

17. Abson, D.J., Dolby, R.E. and Hart, P.H.M. ibid.

18. Oham, M. and Homma, M. Improvement of EB Weld Metal toughness in Steels. Int. Conf. on Applications of Electron and Laser beam welding, Hartford USA, Sept. 1987.

19. Hart, P.H.M. Low Sulphur levels in C-Mn steels and their effect on HAZ hardenability and hydrogen cracking. Int. Conf. Trend in steel and consumables for Welding, London Nov. 1978, The Welding Institute.

20. Duren, C., 3R International March 1982 (also IIW Doc IX-B-12-82.)

21. Okamura, M., Yurioka, N., Kasaya, T. IIW Doc IX-1459-87.

22. Smith, N. and Bagnall, B. I. Brit. Weld. J., 15 63-69 1968.

23. Habu, R., Migata, M., Sekino, S., Goda, S., Trans. ISI J 18 492-501 1978.

24. Duren, C., IIW Doc IX-1358-85 1985.

25. Cotton, H.C. Welded Steel for Offshore Construction Proc. I. Mec. E. 193 1979.

26. Terashima H. and Hart, P.H.M. Int. Conf. on The effect of residual impurity and micro-alloying element on weldability and weld properties. London Nov. 1983.

27. Devillers, L., ibid.

28. Oldland, b., Australian Welding Research 13 1-8 1984.

29. Suzuki, M. IIW Doc IX-1854-85 1985.

30. Thewlis, G., Int. Conf. Welding and Performance of Pipelines, London, Nov. 1986.

31. Rodgers, K.I. and Lockhead, I.C. Weld. J. 66 49-59 1987.

32. Pisarski, H.G. and Harrison, P.D. Paper 2 European Offshore steel research seminar, Cambridge, England, Nov. 1978.

33. Eide G.H. Fracture Mechanics of Assessing the Safety against Brittle Fracture in Offshore Installations. Welding Institute Seminar - COD fact or fiction, Sheffield, April 1980.

34. Bateson, P.H. Webster C.E. and Walker, E.F., OMAE Houston, Feb. 1988.

35. Harneshaug, I.S., Valland, G., Gunderson, H. and Roland, M., ibid.

36. Thaulow, C. and Paauw, A.J., ibid.

37. Haze, T. and Aihara, S. ibid.

38. Satoh, H. and Toyada, M. ibid.

39. de Koning, A.C., and Harston, J.D. and Nayler, K.D., and Ohm, R.H., ibid.

40. Webster, S.E. and Walker, E.F. ibid.

41. Fairchild, D.P., TMS Denver Conference. Welding Metallurgy of Structural Steels, Feb 1986.

42. Royer, C. P., ibid.

43. EEMUA publication 150 Steel specification for fixed offshore structures. 1987.

44. API Recommended Practice 2Z 1987.

45. Nakaniski, M., Komizo, Y. and Fukada, Y. The Sumitomo Search, 22-34, Nov. 1986.

46. Dolby, R.E. Weld. J. 58 225-238 1979.

47. Hannerz, N.E., Int. Conf., Welding of HSLA Microalloyed Structural Steels, ASMA, Rome, Nov. 1976.

48. Yamamoto H, Matsuda, S., Haze, T., Chijiiwa R., and Mimura, H., Symposium on Residual and Unspecified elements in steel, ASTM, Nov. 1987.

49. Sparkes, D.I., The Welding Institute Report 352/1987.

50. Metz, R., Coleman, S., and Denney, A., HSLA Steels Technology and Applications, ASM Philadelphia Oct. 1983.

51. Thaulow, C., Paauw, A.J., Guleikstud, A. and Naess, O.I., Met. Con. 17 94-99, 1985.

52. Pisarski, H.G., Harrison, P.L., and Nayler, K.D., OMAE Feb. 1988.

53. Denys, R.M. International Seminar on Modern High Strength Steel in Marine Structures, Delft Oct. 1987.

54. Kozasu, I. HSLA Steels Technology and Applications, ASM Philadelphia, Oct. 1983.

55. Bessyo, K., Ozawa, H., Nakano, N., and Nakaniski, M., 2nd Int. Conf. on Offshore Welded Structures, London Nov. 1982.

56. Kinaka, R., Okumura, T., Terashima, H., Minagawa, S., Nakano, Y. and Matsumoto, S., Kawasaki, Tech. report No 17, Oct, 56-63 1987.

57. Kanazawa, S., Trans. ISIJ 16 486-495 1976.

58. Nakaniski, M., and Komizo, Y. IIW Doc IX-1281-83.

59. Deshimasu, S., Hirai, I., Amano, H., Ueda, S., Uemura, T., Tsutota, H., Kawasaki Steel Tech. Report 34-40 Oct. 1987.

60. Gooch, T.G. and Hart, P.H.M., Int. Conf. Trends in Welding Research, Gatlinburg, USA, May 1986 ASM.

61. Lau, T.W., Wang, C.R. and North, T. To be published in Mat. Sci. and Tech.

62. Kirkwood, P.R., TAIS Denver Conference, Welding Metallurgy of Structural Steels, Feb, 1986.

63. Fitzgerald, F. Proc. 3rd Int. Conf. on Clean Steels, IOM, Balatonfured, Hungary, June 1986.

# DEVELOPMENTS IN THE WELDABILITY AND TOUGHNESS OF STEELS FOR OFFSHORE STRUCTURES

**A. D. Batte, P. R. Kirkwood**
*British Gas Engineering Research Station*
Newcastle on Tyne, UK

ABSTRACT

The economic achievement of improved combinations of strength, toughness and weldability in offshore structural steels has been an important aspect of ongoing research and development during the last decade. Recent interest has concentrated largely on the heat affected zone (HAZ) and its microstructure; in particular the dependence of weldability and toughness on weld heat input, preheat and post weld heat treatment. Significant improvements in weldability have been achieved over the years through reductions in carbon equivalent, but a consequence of this trend has been a shift in balance from carbon-dominated to alloy element-dominated strengthening mechanisms in the steel, and the resultant undermining of the basis for the original relationships between carbon equivalent and weldability. The increased use of crack tip opening displacement (CTOD) testing in recent years has focussed attention on the occasional occurrence of very low CTOD values in heat affected zones, particularly if the crack samples a sufficiently large region of coarse grains adjacent to the fusion boundary, known as a local brittle zone (LBZ). Recent and ongoing research is directed towards characterising the extent to which such zones occur and establishing their influence on the behaviour of the welded fabrication as a whole.

THE DEVELOPMENT OF THE OIL AND GAS FIELDS in the North Sea commenced with exploratory drilling and the first gas discoveries in the mid-1960's, and was followed by the development of the first major production facilities in the early 1970's. The direct involvement of British Gas in these early and dramatic days of North Sea exploitation was comparatively minor, although the company had been active in exploration and had for many years held interests in several oil and gas fields in the UK sector. However, a significant change in the company's involvement was heralded by the decisions taken in the latter part of the 1970's to develop the depleted gas field at Rough as a storage facility and the Morecambe gas field on a variable loading pattern to meet seasonal fluctuations in demand[1,2]. Consequently, in the early 1980's British Gas rapidly achieved the status of a major offshore operator; some 100,000 tonnes of offshore structural steel were purchased in the space of a few years, to construct eight new steel offshore fixed platforms.

The involvement of British Gas as a user of offshore structural steel is still continuing. Work has commenced on two new platforms to be placed on the South Morecambe field and conceptual designs for development of the North Morecambe field are being evaluated. Against this background the present paper examines the implications of some of the changes in steelmaking and steel processing technology which have taken place to meet the stringent design and commercial requirements of platform construction in the UK Continental Shelf. The particular viewpoint of the steel user is developed by examining two interrelated areas which are of continuing concern, namely the control of the heat affected zone (HAZ) microstructure and its influence on weldability and toughness properties.

## STRUCTURAL STEEL DEVELOPMENT

DESIGN AND CONSTRUCTION REQUIREMENTS - In common with those of many other offshore platforms in UK waters, the fixed platforms owned and operated by British Gas utilise a steel jacket manufactured from tubular steel

members. The platform design must include consideration of the air and sea temperatures, the wave loading associated with wind speeds of up to 200 km/h (120 mph) and the working life of up to 40 years.

The most basic requirements for satisfactory behaviour of the tubular structure are that it should possess adequate static strength, particularly in the joint regions, together with resistance to brittle fracture[3-6]. The prevention of brittle fracture initiation has traditionally been ensured by specifying a minimum Charpy impact energy in the longitudinal, and later in the transverse, orientations. However, the increasing use of fracture mechanics analyses to assess fitness for purpose and acceptable defect sizes, particularly in the weld zones, has placed increased emphasis on measurement of crack tip opening displacement (CTOD).

Fatigue resistance is also an important design requirement. Although more than 80% of the structure does not see a significant fatigue loading[6] the highly stressed node regions require particular attention. The results of extensive fatigue testing programmes[7], both on laboratory test specimens and on full-scale welded tubular joints, indicate that for cyclic endurances above about $10^4$ cycles the fatigue strength of welded joints is largely independent of the tensile strength of the parent material, but is instead controlled by the joint profile and the loading of the member.

In addition to these basic mechanical design requirements there are several specific metallurgical requirements for offshore structural steels, especially homogeneity, weldability and formability[3-6,8-10]. Homogeneity in this context describes freedom from harmful segregation, laminations, internal cracks and unfavourable inclusion distributions, as well as isotropy of mechanical properties. The need for formability relates to the requirement to form a large proportion of structural steel plates into tubular or conical sections; in the early years this usually meant that hot forming was necessary and that the specified properties must be achieved entirely through the normalising heat treatment carried out on completion of hot forming. Today most fabricators have adequate cold forming capacity even for the thickest plates being fabricated, and controlled rolling is now becoming more widely uses for plates up to about 40 mm (1.5 in) thick.

It is essential that all the steel for offshore structures must be readily weldable. Two aspects of weldability which have been of considerable importance in the evolution of structural steel specifications are resistance to heat affected zone hydrogen cracking and resistance to lamellar tearing. Heat affected zone hydrogen cracking is linked to the carbon equivalent* of the material; lower carbon equivalent values generally lead to improved resistance to hydrogen cracking, and careful control of carbon equivalent has thus been of major importance. Lamellar tearing, which can occur due to the build-up of stress in the through-thickness direction in the node regions of a fabricated structure[1], is generally controlled by minimising the extent of elongated manganese sulphide inclusions.

These considerations have led over the years to the development of specifications for normalised (air cooled) steels with a nominal yield strength of ~345 $N/mm^2$ (50 ksi), corresponding in the British Standard BS 4360[12] to the Grade 50 strength level. The same specified strength levels are also required after post-weld heat treatment in material greater than 50 mm (2 in) thick. Clearly the design and manufacturing requirements for offshore structural steels necessitate careful control of the balance between strength, toughness and weldability, taking into account the economic constraints and the requirements for large tonnages of material.

STRUCTURAL STEEL METALLURGY - The metallurgical evolution of microalloyed steels in general and offshore structural steels in particular during the last three decades is an immense subject area. Since many excellent and detailed reviews of all aspects of structural steel development have been published during this time[3-6,8-10,13-27], the present paper will not attempt to present a comprehensive picture but will instead highlight one or two specific aspects which are of particular interest to the user.

The significant advances in steelmaking technology have come about as steelmakers worldwide have invested heavily in new plant and facilities in order to meet the requirement for large quantities of high quality steel at an economic price[4,10,14,18,28-36]. Major changes include the introduction of basic oxygen steelmaking (BOS), improvements in the accuracy of process technology and reductions in sulphur through the use of ladle steelmaking. In the early years the quest was for sulphur levels below 0.015% and the consistent achievement of such levels was difficult, but with combinations of preliminary hot metal desulphurisation, BOS furnace desulphurisation and secondary refining, achievable sulphur levels have dropped dramatically[37] (Figure 1) and sulphur levels less than 0.002% can now be achieved if required for particularly onerous applications. Similarly, phosphorus levels can now be reduced to less than ~0.005% by combinations of hot

*In this paper carbon equivalent is defined by:

$$CE = C + \frac{Mn}{6} + \frac{Cr + Mo + V}{5} + \frac{Cu + Ni}{15}$$

metal pretreatment, BOS furnace treatment and secondary refining. There have also been significant improvements in the control of the process itself, such that the reliability and controlled quality of the end product have significantly improved and the steelmakers now have the ability to produce large tonnages of molten steel to tight chemical specifications, with minimal rejection rates.

Of perhaps even more importance than the changes in molten steel production technology have been the changes in casting process, particularly the introduction of continuous casting. In the early 1970's the majority of steel plates were ingot cast, but by the late 1970's continuous casting probably accounted for more than 80% of UK plate production for offshore construction. As the achievable thickness of continuously cast slabs increased towards 300 mm (12 in), so the production of heavier individual plates, up to ~35 tonnes, has become possible. Centreline segregation, particularly of carbon, niobium, sulphur, phosphorus and manganese, were problems in the earlier years. However, careful control of pouring temperatures and solidification patterns, including the use of electromagnetic stirring, have enabled the control of segregation to tolerable levels. Clearly, general improvements in steel cleanness, together with the reduction in sulphur and phosphorus levels, have helped to minimise the consequences of segregation in the final plate product.

One clear trend during the last two decades has been the progressive reduction in carbon equivalent in order to improve weldability. For many years this was largely achieved by improving the effective use of plate rolling and heat treatment schedules, enabling reductions in the microalloying element additions. However, whilst these developments have yielded significant benefits in improved weldability without significant loss of strength, there is a limit to what can be achieved if the steel is to be normalised after rolling. The introduction of thermomechanical controlled rolling processes in recent years has enabled the achievement of the same yield strength at a significantly lower carbon equivalent or of higher strength levels without sacrificing weldability, (Figure 2). The most recent developments include accelerated cooling immediately after controlled rolling stops, improving still further the achievable combinations of weldability and strength[35,38-43].

It is interesting to note that the level of niobium has been tending to fall in structural steel plates during the last decade; a comparison of steels produced in 1972 and 1981[37] illustrates that the niobium level has halved from <0.06% to <0.03% (Figure 3). It appears that part of this change has been as a result of more efficient use of niobium, along with closer control of the plate rolling schedules, achieving the same degree of grain size control with less alloying additions. However, there has also been a tendency to specify reduced niobium because of its suggested adverse influence on HAZ toughness[16,44,45]; as will be discussed in more detail later, niobium is not always detrimental[37,46] and the combined effects of niobium and other elements on HAZ grain size control and toughness may be more complex than they first appear.

Titanium, like niobium, exhibits a strong affinity for several of the elements present in steel, and consequently can give rise to a wide variety of different effects. The principal influences are those involving nitrogen and carbon, either alone or in combination with other elements. Comparison of the solubility characteristics[47] of the various carbide and nitride forming elements (Figure 4) indicates that titanium and niobium can both be particularly effective in maintaining grain size control up to the melting point. If the titanium level is kept just below 0.02%, precipitation occurs after solidification and the particles are extremely small. Titanium was not used in earlier years, apparently because of problems with obtaining and retaining uniform additions throughout the ingot[26,35,48]. Nevertheless steels containing titanium, often in combination with niobium and vanadium, are now finding applications in a number of areas[26,29,30,35,41,42,49-51] particularly where HAZ microstructure control during welding is important, as will be described in a later section.

The trends towards increased steel cleanness and reduced levels of oxygen and nitrogen have enabled increased use of boron as an alloying element in steels[26-28,32,52-54]. Significant changes in this respect have been the improved control of steelmaking practice which has enabled reproducible results from boron additions, and the greater emphasis on finding alternatives to other increasingly scarce microalloying additions. Small additions (up to 15 ppm) of boron can significantly increase the hardenability of the steel, provided that the boron remains active during cooling of the solid steel, having been protected from combining with nitrogen and precipitating at grain boundaries. Boron, like titanium, can have a significant influence on the development of the parent metal microstructure during plate processing, and can also have an important effect on HAZ microstructure and properties during welding.

## AREAS OF ON GOING DEVELOPMENT; THE STRUCTURE AND PROPERTIES OF HEAT AFFECTED ZONES

The preceding section illustrates briefly that, compared with the original offshore structural steels used in the North

Sea, considerable improvements have been made in the combinations of strength, toughness and weldability which can now be achieved on a routine production basis. Notwithstanding this apparently healthy situation, there is still scope for further improvements which can be of direct benefit to the constructors and operators of offshore platforms. Current interest is principally focussed on the HAZ microstructure and its influence on weldability and toughness.

WELDABILITY - RESISTANCE TO HYDROGEN INDUCED HAZ CRACKING - As was indicated earlier, weldability has traditionally been linked to carbon equivalent, and much steelmaking development has therefore been directed towards decreasing the amounts of those elements which contribute to carbon equivalent. The relationship between weldability, or more specifically the resistance of the steel to hydrogen assisted cracking, and carbon equivalent is embodied in the procedures for safe welding contained in the British Standard BS 5135[55], the principal reference document for offshore fabrication in the UK sector.

Difficulties experienced by various offshore fabricators[22] have suggested that these guidelines and procedures may not be satisfactory for normalised structural steels with carbon equivalents below about 0.40. Experimental work has confirmed that the anticipated improvements in weldability with reducing carbon equivalent are not always realised and, for the time being at least, it has been recommended[56] that procedures for avoiding HAZ hydrogen cracking are based on a carbon equivalent of 0.40 minimum (or the actual value if it is higher).

It has been suggested[57] that the inconsistent weldability response of normalised C-Mn steel may be linked to the low sulphur content, particularly in some of the more modern steels. Despite some conflicting reports in the literature[41,57,58], it appears that low sulphur per se does not have a systematic effect on weldability[59] (Figure 5). However, it may in some circumstances modify the inclusion morphology and distribution, and consequently change both the austenite transformation characteristics and the availability of sites for formation of molecular hydrogen. In a recent re-examination[37] of some earlier work completed by British Gas[60,61], it was seen that steels with greater than 0.10% sulphur were less hardenable (giving lower hardnesses for a given cooling rate) than those with 0.002% to 0.009% sulphur. These differences were probably due to differences in the volume fraction of fine inclusions, but nevertheless they did not result in systematic differences in HAZ hydrogen cracking response.

It would appear that the observed inadequacies of the BS 5135 guidelines in defining safe welding conditions for low carbon equivalent materials are linked to the changes which have taken place over the years in steel chemistry and to their effects on the HAZ hardness level at which cracking occurs; this hardness level is lower in steels with lower carbon equivalent[61,62]. The guidelines were originally derived using data from steels that contained generally higher carbon and niobium contents than are in use today, with little or no aluminium, and that were in some cases semi-killed. In these older steels weldability, hardness and steel transformation characteristics were all dominated by the carbon-based and niobium-based strengthening mechanisms, with comparatively small contributions from other sources. In the more recent steels, however, both carbon and niobium contents have generally been reduced, and other metallurgical influences such as grain size (microalloying, aluminium/nitrogen ratios etc) and steel cleanness (inclusion distribution) are able to exert much greater effect in determining transformation characteristics and susceptibility to HAZ hydrogen cracking[37,63]. These influences control the degree of grain boundary pinning at high temperature, the extent of microalloy precipitation and solid solution strengthening during subsequent cooling, and the nucleation and growth characteristics of the transformation product. In this situation it is hardly surprising that the simple IIW carbon equivalent, or any other carbon equivalent formula, is not sufficiently accurate to predict the behaviour of such steels.

A further complication in the prediction of safe welding procedures to avoid HAZ hydrogen cracking has arisen with the introduction of boron-containing steels. Boron in small quantities, particularly in conjunction with niobium or molybdenum, significantly retards polygonal ferrite nucleation at the austenite boundaries during cooling of the HAZ, allowing reduced transformation temperatures and the development of tougher bainitic microstructures[26,52]. This increases the hardness of the microstructure and is usually countered in practice by reducing the carbon levels. Boron is not included in the IIW carbon equivalent formula, but has been incorporated in the $P_{cm}$ carbon equivalent developed in Japan[64]; however it appears that the original factor of 5 was insufficient to account for the effect of boron at these lower carbon levels, and a higher factor of 23 has now been applied [54] to the 'effective' boron content (the uncombined boron, which is in turn dependent on the amounts of nitrogen and titanium present in the steel). It is possible that at very low carbon and boron levels the factor should be even higher.

The experiences with the low carbon equivalent normalised steels, particularly the recently developed compositions, suggest that

it may be even more difficult to derive simple guidelines for the safe welding of the newer thermomechanically processed and accelerated cooled steels. It is clear that developing a comprehensive quantitative understanding of the weldability of these types of steels will be an ongoing problem for some time to come.

TOUGHNESS - CONTROL OF THE HAZ MICROSTRUCTURE - Carbon content and cooling rate - The overall toughness of the HAZ is dependent on the relative yield strengths and microstructure of the different regions in the zone and by their spatial relationship to one another. In a multipass weld, which may also be subject to post weld heat treatment, the complexities of HAZ microstructure [47,65] are immediately apparent (Figure 6). One area which is often dominant in controlling toughness is the unrefined course grained region immediately adjacent to the fusion boundary[16,18,19,37,66,67]. The microstructure in this region is primarily dependent on the chemistry, steel cleanness, austenite grain size and cooling rate through the transformation range; the first two parameters are fixed by the plate manufacturing route, and the last two are largely dependent on the weld thermal cycle. Within the range of welding processes and procedures used in offshore construction, austenite grain sizes can vary from ~30μm to ~200μm (0.001 to 0.008 in); this effect can be of considerable importance in controlling the development of the rest of the microstructure and its resultant toughness.

The microstructural constituents of the coarse grained HAZs in C-Mn steels range from polygonal and Widmanstatten ferrites at the slowest cooling rates in high heat input welds, though coarse upper bainite, lower bainite, lower bainite and auto-tempered martensite to untempered martensite at the fastest cooling rates in low heat input welds[60] (Figure 7). It is clear that in addition to chemical composition the transformation temperature, and hence the cooling rate through the critical 800-400°C temperature range, is of major importance in determining the HAZ microstructure and toughness.

The combined influence of chemical composition and transformation temperature on HAZ microstructure and toughness is illustrated in Figure 8. The pair of diagrams should be considered as schematic rather than quantitative, although they have been extensively based on results obtained by Rothwell and Bonomo[68] and Bufalini et al[69] over a decade ago and still earlier by Pickering and Clark[70]. In Figure 8a lines have been constructed corresponding to the mean transformation temperature below which a marked improvement in impact transition temperature was observed[68], the mean temperature of transition from upper to lower bainite and the martensite start (Ms) temperature[69,70], each determined from dilatometric and microstructural studies on a range of steels with different carbon contents. A final line corresponds to the transformation temperature below which Bufalini et al[69] began to observe toughness deterioration. These lines delineate zones of carbon content and transformation temperature within which each of the microstructural constituents predominates, and where major changes in toughness behaviour occur.

Figure 8b schematically shows sections through Figure 8a at three carbon contents to illustrate more clearly the corresponding relationship between transformation temperature and toughness. Considering first the high carbon (0.21%) situation, good toughness cannot really be obtained at slow cooling rates which result in transformation above about 500°C, when the coarse grained HAZ microstructure is dominated by upper bainite, coarse side plates and occasionally polygonal ferrite. At faster cooling rates a gradual transition to lower bainite takes place. Unfortunately lower bainite is usually of even poorer toughness in high carbon systems, and not until the transformation temperature is depressed below ~420°C, the Ms temperature, does toughness begin to improve. However at this carbon content the improvement is unlikely to be significant in the context of the toughness levels necessary in modern offshore steels.

In the low carbon (0.07%) steels the situation is quite different. At transformation temperatures above about 530°C the coarse grained HAZ microstructure is dominated by polygonal and side plate ferrite, with decreasing amounts of upper bainite as the temperature decreases and approaches Ms which, at this carbon level, is approximately 480°C. The optimum toughness is achieved with transformation temperatures below Ms, probably in the range 400-460°C, the predominant microstructural constituent then being auto-tempered martensite. Thus with low carbon systems good toughness can be achieved over a wide range of transformation temperatures, although it may be necessary to add reasonable quantities of manganese and other microalloying elements (nickel, copper and niobium) to ensure that sufficiently low transformation temperatures are achieved during welding.

Perhaps the most interesting sequence of behaviour is that at the intermediate carbon level (0.14%). Above approximately 460°C the coarse grained HAZ is dominated by upper bainite; below that temperature lower bainite begins to form, possibly also mixed with Type III (Ohmori[71] classification) bainite. These are considerably tougher than upper bainite at this carbon level, and toughness improves dramatically. Below the Ms temperature of 430°C, auto-tempered martensite is observed in combination with a lower bainite and toughness continues to improve. However below

about 410°C the opportunity for auto-tempering is reduced and hard, untempered martensite is considerably less tough. Hence, while extremely good toughness is possible in steels with intermediate carbon levels, it can only by achieved over a narrow transformation temperature range, which can severely restrict the useful heat input range during welding.

Microalloying Elements - Having described the effects of carbon content on HAZ microstructure and toughness, it is now appropriate to examine the specific roles of the microalloying elements. Carbide and nitride forming elements such as niobium, vanadium and titanium can have a variety of influences on HAZ microstructure, depending on the plate composition and weld thermal cycle under consideration. Although the effects of these elements on HAZ microstructure are qualitatively similar, their differing solubilities as carbide, carbo-nitride or nitride result in some important differences. Niobium and titanium carbo-nitride precipitates can both exert a significant restraint on austenite grain growth, particularly in low heat input welds, although the available nitrogen level may be more important than carbon content in determining the alloy carbo-nitride solubility, and the available nitrogen is in turn linked to the aluminium/nitrogen ratio. The amount of alloy carbide taken into solution in the austenite will determine the extent to which intragranular precipitation will occur during cooling, and the size and distribution of these precipitates will be influenced by the cooling rate and transformation product. Alternatively, the alloy elements may remain in solution, increasing the hardenability and lowering the transformation temperature; titanium in particular is known to significantly modify the coarseness of intragranular ferrite sideplates[26,36,41,58].

While niobium has been widely used for many years to achieve improved grain refinement, the use of titanium has been comparatively recent. It appears that close control of the ingot cooling rate and the slab reheating/cooling cycle are necessary[26,47] in order to obtain a uniform dispersion of sufficiently fine titanium carbo-nitride particles for effective grain boundary pinning. Fine dispersions of titanium oxides can also be used to pin austenite grain boundaries in the HAZ; in some recently developed steels a fine dispersion of oxides has been used[36,43] to pin the austenite grain size and to promote the initiation of intragranular ferrite plates, giving rise both to good toughness and to good HAZ hydrogen cracking resistance.

The complexities of the interactions between alloy elements, aluminium and nitrogen in determining HAZ grain size is illustrated by the results of some recently reported work conducted at British Gas[37]. When a series of offshore steels was subjected to weld thermal simulation, higher niobium levels led to a smaller prior austenite grain size, as expected (Figure 9). There was also an indication from these results that higher aluminium/nitrogen ratios, at low niobium levels, were associated with larger grain sizes, suggesting that in such steels it may become necessary to specify an upper limit to aluminium/nitrogen ratio as well as a lower limit. More obviously however, the addition of 0.026% titanium resulted in a significant decrease in grain size, compared with the trend shown by the rest of the group of steels studied.

These comments serve to indicate the complexity of grain size and microstructure control through the use of microalloying additions, especially when several elements are used in conjunction. They also highlight the importance of close understanding between the steelmaker and the welding metallurgist, so that the steel composition can be tailored to suit the expected range of weld thermal cycles during fabrication. Unlike poor weldability, which can be overcome by use of low hydrogen electrodes or high preheat temperatures, low toughness cannot be ameliorated.

TOUGHNESS - THE PROPERTIES AND SIGNIFICANCE OF LOCAL BRITTLE ZONES - One consequence of the strong influence of microstructure is that there are zones of different toughness in every multipass weld. The dominance of grain size in determining toughness was indicated in the previous sections; hence it is not unexpected that zones of low toughness (LBZs) correspond to the zones of unrefined coarse grained HAZ adjacent to the fusion line.

Heat treatment of the deposited weld beads and HAZ by the subsequent weld thermal cycles can also have a significant influence on HAZ microstructure and toughness. The intercritically reheated region (that part of the parent metal or the preceding weld HAZ which is subjected to a thermal cycle peaking between ~700 and ~900°C) is known to be an area of possible poor toughness, particularly if the chemical composition is such that the partial transformation results in islands of carbon-rich austenite that can re-transform to high carbon twinned martensite on cooling[72,73], similar to those found previously in submerged arc weld metal[74]. The islands of brittle martensite, surrounded by local areas of high transformation stress, can significantly reduce the toughness of the material (Figure 10).

Where HAZ CTOD requirements are incorporated in a steel purchase specification or a fabrication weld qualification procedure, they usually call for sets of three specimens to be tested at 0°C (for subsea service) or -10°C (for topside service, in the UK North

Sea). Test results are all expected to exceed typically 0.25 mm (0.01 in), the actual value depending on the details of the design.

The observations of low toughness in CTOD specimens which sample the coarse grained heat affected zone are not new[16]. However, it appears that the frequency with which occasional low toughness values were obtained increased significantly in the early 1980's. Three factors may have been responsible for this; a reduction in toughness of the steels being tested, the increased use of CTOD testing on a routine basis, or changes in the CTOD testing procedure.

Detailed re-examination of the test results from a large number of sources indicates that there is no evidence that the newer steels, which generally contain less carbon, sulphur and niobium, are inherently less tough than their earlier counterparts. It is certainly true that there is an increased awareness of low toughness values resulting from increased use of CTOD testing on a routine basis. However, the most significant factor appears to be the increased use of asymmetric V or K weld preparations with reduced overlap of subsequent weld thermal cycles and increased proportions of unrefined HAZ microstructure resulting in a higher proportion of tests which accurately sample the coarse grained region.

The problem for the steel user is how to handle the low CTOD values, some of which have been less than 0.05 mm (0.002 in). In an attempt to answer the question experimentally, the relationship between CTOD test results and large scale wide plate test results has been examined in several studies[72,75-78].

The results of such a study have been published recently[75]. A steel which was known to give rise to low CTOD values, despite being acceptable when tested using Charpy specimens, was subjected to a series of wide plate tests at -10°C. For both CTOD and wide plate tests the welding procedure was deliberately adjusted to give large regions of coarse grained HAZ, corresponding to 10-30% of the weld interface. In total, some 20% of the CTOD test results were below 0.1 mm (0.004 in) and 10 of the 20 wide plate tests fractured (Table 1). In this material low CTOD values occurred when the pre-crack sampled coarse grained material with grain size above ~80 μm (0.003 in), and low strain (<0.5%) fractures in the wide plate tests occurred when the pre-cracks intercepted this coarse grained microstructure in continuous lengths exceeding 30 mm (1.2 in, 20% of the crack length). However, even in the lowest fracture strain specimen, in which the pre-crack intercepted an 80 mm (3 in) length of coarse grained microstructure, the failure stress was 340 N/mm$^2$ (49.3 ksi), equivalent to more than 95% of the yield strength of the parent plate.

Other recently completed studies[76-88] are also helping to build up a general picture of the significance of LBZ size and shape on toughness measured in different types of test specimen. The bending stress and high degree of constraint ensure that the CTOD test is sensitive to the presence of LBZs, particularly if the zone is more than 5 mm (0.2 in) long (Figure 11) and is intersected by more than ~10% of the precrack length. With surface notched CTOD specimens the probability of this occurring may be reduced, and in shallow notched CTOD specimens the reduced constraint often results in higher measured toughness; this is even more evident in tensile-loaded wide plate specimens. In Charpy tests the blunt notch tends to result in an averaged energy value over a range of microstructures; this energy may not be significantly reduced by the presence of a brittle zone unless it is particularly large.

Although in many respects the test results are beginning to provide some answers, it is still not easy to relate them to the behaviour of an offshore structure, and they do not yet provide a satisfactory basis for acceptance or rejection of a steel plate product or weld fabrication procedure which demonstates occasional low CTOD values. Indeed they suggest that occasional low values will always be observed in some steels, provided that enough tests are conducted. It may eventually be possible to assess the significance of the results on a probabilistic basis[79], but while it is easy to advance qualitative arguments and the absence of service failures is reassuring, the derivation of a quantitative probabilistic design analysis appears very difficult. Meanwhile, the whole subject of LBZ significance is an important ongoing international research activity.

In the absence of clear guidelines on how to assess the significance of the low CTOD values which result from LBZs, the steelmaker and user are forced to concentrate on completely eliminating their occurrence. While much of the steelmaker's effort has rightly been directed towards grain refinement of the coarse grained HAZ for the relevant range of welding conditions, it is important to remember that grain size is not the only determinant of toughness. The results of some work completed recently[89] serve to illustrate the importance of intragranular microstructure as well as grain size. Detailed microstructural examinations and CTOD tests at -10°C were carried out on two low carbon (~0.10%) steels. The first, which contained 0.045% Nb, gave CTOD values below 0.05 mm (0.002 in) when the fatigue crack sampled the region adjacent to the fusion line; the coarse grained microstructure consisted largely of coarse upper bainite. The second steel, which contained less than 0.02% Nb but included 0.013% Ti, also contained areas of coarse

grains with an upper bainite microstructure, but no CTOD values below 0.27 mm (0.01 in) were obtained. It appeared that the changed balance of niobium and titanium, in conjunction with the particular carbon, nitrogen and aluminium levels in the steel in question, modified the form of the upper bainite to reduce the inherent cleavage fracture resistance, without significantly changing the grain size.

These and other similar results indicate that coarse grains are not always detrimental to toughness, but that the microstructure within the grains is of major importance. They also reinforce the argument that very close cooperation between the steel supplier and user is needed in order to achieve the desired weld properties during fabrication.

## OVERVIEW AND CONCLUDING REMARKS

The history of structural steel development during the last two decades can be linked to one central theme; the requirement to produce improved combinations of strength, toughness and weldability in large tonnages at an economic price. It is interesting to note how the different strands of development illustrated in the preceding sections contribute to the overall goal.

Developments in steelmaking and plate processing technology have clearly been devoted towards making more efficient use of microalloying elements and hence reducing the carbon equivalent without loss of strength; this has been particularly evident in the general reduction of carbon and niobium levels. Considerable improvements have also occurred in steel cleanness and segregation. While developments in the steelmaking technology of the normalised product have probably now reached the stage where little further improvement in useful properties can be achieved, thermomechanical processing techniques offer the immediate benefit of a significant reduction in carbon equivalent without loss of strength. Thermomechanically processed plate steels are still somewhat in their infancy, but their potential is clearly evident.

The trend towards lower carbon contents has provided greater freedom to avoid weldability problems, but at the expense of a change in the balance between carbon-dependent and microalloy-dependent hardening processes, such that the original relationships between weldability and carbon equivalent, embodied in standards such as BS 5135, are no longer universally accurate for materials with low carbon equivalent. Further understanding of this subject, particularly for the newer thermomechanically processed and high strength steels, is clearly important.

The dominant effect of prior austenite grain size in controlling coarse grained HAZ toughness is evidently important, and continued moves towards improved grain size control over a wider range of welding conditions are enabling the development of more tolerant steels. Grain size is not necessarily a primary influence, but frequently has an indirect influence through control of the transformation temperature and the intragranular microstructure. The influence of titanium, the most recent of the carbide/nitride formers to be exploited in structural steels, is most interesting in this respect. In addition, the use of titanium oxide dispersions to control both grain size and intragranular ferrite nucleation is a significant indicator of possible future developments. One message is clear, however; there are no simple answers regarding the influence of particular elements on grain size or toughness, and there are many apparently conflicting statements in the literature.

The significance of coarse grained areas in the HAZ of a multipass weld is also an area of ongoing concern. As indicated above, coarse grains may or may not have poor toughness per se; but even if they do have poor toughness, the significance of a local region of poor toughness in terms of structural integrity is far from clear. The results of wide plate tests are beginning to suggest that in some situations low CTOD values do not imply inadequate structural integrity, but changes in the CTOD test procedures have increased the probability that occasional low CTOD values will be obtained, and the problems of how to handle them at the design and weld procedure qualification stages have not been resolved. Experience qualitatively supports the argument that the problem is a very rare one in service, but quantitative probabilistic analyses are still in their infancy. An improvement in the present level of understanding of this problem is clearly necessary.

The comments above should not be taken to imply that the user's requirements of strength, toughness and weldability cannot be achieved by the steelmaker. Clearly many thousands of tonnes of satisfactory steel have been manufactured during the last two decades and the service experience has largely been exemplary. Nevertheless, there is still scope for improvement so as to facilitate economies in construction, and there are important needs for steel structures to operate in colder, deeper waters than hitherto. Given the improvements which have taken place in metallurgical, processing and fabrication technology during the last two decades, it is not unreasonable to expect that the new challenges will be met in the decades to come.

## ACKNOWLEDGEMENTS

The authors wish to thank British Gas plc for permission to publish this paper and their many colleagues at the Engineering Research Station

for their valued help in its preparation.

REFERENCES

1. Brown C H, paper presented at 124th AGM of Inst Gas Engineers, Harrogate, (1987). Communication 1325.

2. Gibbon R B, paper presented at 124th AGM of Inst Gas Engineers, Harrogate, (1987). Communication 1326.

3. Garland J G and P R Kirkwood, Proc Financial Times/Petroleum Times, International Offshore Technology Conference, London, (1974).

4. Cotton H C, Proc I Mech E 193, 193-206, (1979).

5. Harrison J D, Welding Institute Research Report 153, (1981).

6. Carter R M, P W Marshall, P D Thomas and T M Swanson, Offshore Technology Conference Paper OTC 1043 (1969).

7. UK Offshore Steels Research Project. Papers presented in Conference on 'Fatigue in Offshore Structural Steels', London, February 1981, and UKORSP II Technical Meeting, London, (1985). UKORSP Project Secretariat, Matsu, Harwell.

8. Adrian H, M Haneke and C Strassburger. 3R International 16, 686-695, (1977).

9. Wintermark H S, Proc ASME Conf on 'Structural Integrity Technology', Washington, 89-96, (1979).

10. Barr R R, Proc 2nd Welding Institute Int Conf on 'Offshore Welded Structures', London, Paper 61, (1982).

11. Farrar, J C M and R E Dolby, "Lamellar Tearing in Welded Steel Fabrication", The Welding Institute, (1972).

12. "Weldable Structural Steels", British Standard BS.4360: 1979.

13. Chapman J A, A Clark and P R Kirkwood. Welding Inst Conf on 'Welding in Offshore Structures', Newcastle, Paper 6, (1974).

14. Preston R R, IOM Conf 'Low Carbon Structural Steels for the Eighties', Plymouth, (1977).

15. Cotton H C, Phil Trans Roy Soc, A 282, 53-64, (1975).

16. Dolby R E, Weld J Res Supplement, 225-S to 238-S, (1979).

17. Kirkwood P R, paper presented at 124th Annual Conf of Inst Gas Engineers, Harrogate, (1987), Communication 1334.

18. Walker E F, "Steel in Marine Structures", 49-69, eds C Noordhoek and J de Back, publ Elsevier Science Publishers, Amsterdam (1987).

19. Grong O and O M Akselsen, Met Constr, 18, 557- 562, (1986).

20. Woodhead J H and S R Keown, Proc ASM Int Conf on 'HSLA Steels; Metallurgy and Applications', Beijing, 15-28, (1987).

21. Roberts J E, Proc Royal Society Rosenhain Conference on 'The Contribution of Physical Metallurgy to Engineering Practice', 277-287, 1976.

22. Dolby R E, paper presented at Welding Inst Conference, 'Towards Rational and Economic Fabrication of Offshore Structures - Overcoming the Obstacles', London, (1984).

23. Dufrane J-J, "Steel in Marine Structures", 617-613, eds C Noordhoek and J de Back, publ Elsevier Applied Science, Amsterdam (1987).

24. de Konig A C, Met Constr, 17, 727-734, (1985).

25. Pickering F B, Proc ASM Conf on 'HSLA Steels, Technology and Applications', Philadelphia, 1-31, (1983).

26. Roberts W, Proc ASM Conf on 'HSLA Steels, Technology and Applications', Philadelphia, 33-65, (1983).

27. Kozasu I, Proc ASM Conf on 'HSLA Steels, Technology and Applications', Philadelphia, 593-607, (1983).

28. Meyer L, C Strassburger and C Schneider, Proc ASM Int Conf on 'HSLA Steels, Technology and Applications', 29-44, (1985).

29. Williams J G, C R Killmore, I D Williams and J A Wood, Proc ASM Int Conf on 'HSLA Steels, Metallurgy and Applications', Beijing, 567-578, (1985).

30. Tomita Y, R Yamaba, K Okamoto, S Aihara, T Haze and K Ito, Proc ASM Int Conf on 'HSLA Steels, Metallurgy and Applications', Beijing, 641-650, (1985).

31. Ikeda K, Y Kurogi, Y Ohno and Y Okamura. Nippon Steel Technical Report No 24, 25-33, (1984).

32. Kozasu I, Proc AIME Int Symposium on 'Welding Metallurgy of Structural Steel', Denver, 63-77, (1987).

33. Lieurade H P and H Lecoq, "Steel in Marine Structures", 605-615, eds C Noordhoek and J de Back, publ Elsevier Applied Science, Amsterdam, (1987).

34. Yano S, K Itoh, M Katakami, H Nakamura and T Kusunoki, Proc AIME Int Symposium on 'Welding Metallurgy of Structural Steel', Denver, 581-613, (1987).

35. Someya R, M Fujimoto, I Seta, H Kimura and M Nakanishi, Sumitomo Search No 32, 30-431, (1986).

36. Chijiiwa R, H Tamehiro, M Hirai, H Matsuda and H Mimura, Proc ASM 7th Int Conf on 'Offshore Mechanics and Arctic Engineering', Houston, Vol 5, 165-172, (1988).

37. Kirkwood P R, Proc AIME Int Symposium on 'Welding Metallurgy of Structural Steels', Denver, 21-44, (1987).

38. Ouchi C, Proc Conf on "High Strength Low Alloy Steels", Wollongong, 17-27, (1984).

39. Saito Y, M Tanaka, T Sekine and H Nishizaka. Proc Conf on 'High Strength Low Alloy Steels', Wollongong, 28-32, (1984).

40. Muesgen N, H Baumgardt, H de Boer and W Janzen. Offshore Technology Conference, Houston Paper OTC 5072, (1985).

41. Suzuki H, Trans ISIJ 23, 189-203, (1983).

42. Suzuki H, Proc 2nd Welding Inst Conf on 'Offshore Welding Structures', London, Paper 16, (1982).

43. Harneshaug I S, G Valland, K Gundersen and M Roland. Proc 7th ASME Int Conf on 'Offshore Mechanics and Arctic Engineering', Houston, Vol 3, 181-189, (1988).

44. Hannerz N E, Welding J 54, 162, (1975).

45. Bordignon P J P, SEAISI Quarterly, 55-68, (1986).

46. "Heat Affected Zone Toughness. A Viewpoint on the Role of Microalloying Elements". Publ Companhia Brasileria de Metalurgia e Mineracao, (1980).

47. Easterling K, "Introduction to the Physical Metallurgy of Welding", Butterworths Monographs in Metals, publ Butterworths and Co Ltd, (1983).

48. George T J and N F Kennon. J Aust Inst Met, 17, 73-80, (1972).

49. Killmore C R, G R Harris and J G Williams, Proc Conf on 'High Strength Low Alloy Steels', Wollongong, 57-63, (1984).

50. Chatterjee S, M K Banerjee, A K Seal, S Mishra and V Ramaswamy, Proc Conf on 'High Strength Low Alloy Steels', Wollongong, 51-56, (1984).

51. Bessyo K, H Ozawa, N Nakano and M Nakanishi, Proc 2nd Welding Inst Conf on 'Offshore Welded Structures', London, Paper 11, (1982).

52. Brownrigg A, A-J Chong, G Glover and E E Banks, Welding Inst Conf on 'The Effect of Residual, Impurity and Microalloying Elements on Weldability and Weld Properties', London, Paper 23, (1983).

53. Banks E, Proc Conf on 'High Strength Low Alloy Steels', Wollongong, 256-260, (1984).

54. Baba Z, M Nakanishi, T Hashimoto, Y Komizo, I Takeuchi and Y Ando. Proc Welding Inst Conf on 'Welding and Performance of Pipelines', London, Paper 36, (1986).

55. "Process of Arc Welding for C and C-Mn Steels", British Standard BS.5135: 1984.

56. "Department of Energy: Offshore Installations; Guidance on Design and Construction", 3rd Edition and Subsequent Amendments, HMSO Publication, (1984).

57. Hart P H M, paper presented at Welding Institute Conf, 'Trends in Steels and Consumables for Welding', London, (1978).

58. Threadgill P L, Proc ASME Int Symposium on 'Welding Metallurgy of Structural Steels', Denver, 567-579, (1987).

59. Batte A D, paper presented at Welding 7th Institute Seminar on 'Quantifying Weldability', Coventry, (1985).

60. Boothby P J and P Rodgerson. Paper presented at Welding Institute Conf, 'Towards Rational and Economic Fabrication of Offshore Structures - Overcoming the Obstacles', London, (1984).

61. Boothby P J, Met Const 17, 508R-513R and 612-619R, (1985).

62. Hart P H M and I S Matharu, Proc ASME 7th Int Conf on 'Offshore Mechanics and Arctic Engineering', Houston, Vol 3, 111-120, (1988).

63. Kirkwood P R, Proc AIME Int Conf 'Niobium 81', San Francisco, 761-802, (1981).

64. Ito Y, and K Bessyo, paper presented to the Annual IIW Meeting, Kyoto. IIW Doc

IX-631-69, (1969).

65. "Steel Specification for Fixed Offshore Structures", (Adapted from BS4360: 1986). EEMUA Publication No 150, (1987).

66. Pisarski H G and J D Harrison, Met Const, 18, 748-753, (1986).

67. Pisarksi H G and J D Harrison, paper presented at European Offshore Steels Conference, Cambridge, (1978).

68. Rothwell A B and F Bonomo, paper presented at AWS 57th Annual Meeting, St Louis, (1976).

69. Bufalini P, F Bonomo and C Parrini, BTF-Maggio, 337, (1977).

70. Pickering F B and B R Clark, BISRA Conf on 'Properties of Martensite and Bainite', ISI Special Report 93, 143, 1965).

71. Ohmori Y, H Ohtani and T Kunitake, Trans ISIJ 11, 250-259, (1971).

72. Satoh K and M Toyoda, Proc ASME 7th Int Conf on 'Offshore Mechanics and Arctic Engineering', Houston, Vol 3, 495-502, (1988).

73. Haze T and S Aihara, Proc ASME 7th Int Conf on 'Offshore Mechanics and Arctic Engineering', Houston, Vol 3, 515-523, (1988).

74. Garland J G and P R Kirkwood. Met Const, 1, 275-283 and 320-330, (1975).

75. Webster S E and E F Walker, Proc ASME 7th Int Conf on 'Offshore Mechanics and Arctic Engineering', Houston, Vol 3, 395-403, (1988).

76. Pisarksi H G and J Kudoh, Proc AIME Int Symposium on 'Welding Metallurgy of Structural Steels', Denver, 263-275, (1987).

77. Denys R and H I McHenry, Proc ASME 7th Int Conf on 'Offshore Mechanics and Arctic Engineering', Houston, Vol 3, 379-385, (1988).

78. Watanabe I, H Kagawa and Y Matsuda, Proc ASME 7th Int Conf on 'Offshore Mechanics and Arctic Engineering', Houston, Vol 3, 387-39 (1988).

79. Fairchild D P, Proc AIME Int Symposium on 'Welding Metallurgy of Structural Steels', Denver, 303-318, (1987).

80. Royer C P, Proc AIME Int Symposium on 'Welding Metallurgy of Structural Steels', Denver, 255-262, (1987).

81. Koo J Y and A Ozekcin, Proc AIME Int Symposium on 'Welding Metallurgy of Structural Steels'. Denver, 119-135, (1987)).

82. de Konig A C, J Harston, K D Naylor and R K Ohon, Proc 7th ASM Int Conf on 'Offshore Mechanics and Arctic Engineering', Houston, Vol 3, 161-70, (1988).

83. Thaulow C and A J Paauw, Proc ASME 7th Int, Conf on 'Offshore Mechanics and Arctic Engineering', Houston, Vol 3, 275-286, (1988).

84. Wastberg S, Proc ASME 7th Int Conf on Offshore Mechanics and Arctic Engineering', Houston, Vol 3, 287-295, (1988).

85. Hanus F E, Proc ASME 7th Int Conf on 'Offshore Mechanics and Arctic Engineering', Houston, Vol 3, 509-513, (1988).

86. Devillers L, D Kaplan and E Maar, Proc ASME 7th Int Conf on 'Offshore Mechanics and Arctic Engineering', Houston, Vol 3, 525-530, (1988).

87. Denys R M, Proc ASME 7th Int Conf on 'Offshore Mechanics and Arctic Engineering', Houston, 405-413, (1988).

88. Kohler G, R Whitfield and C Chipperfield. J Theoretical and Applied Fracture Mechanics 6 39-44, (1986).

89. Wintermark H S, paper presented at Int Conf on Offshore and Marine Technology, Gothenburg, (1985).

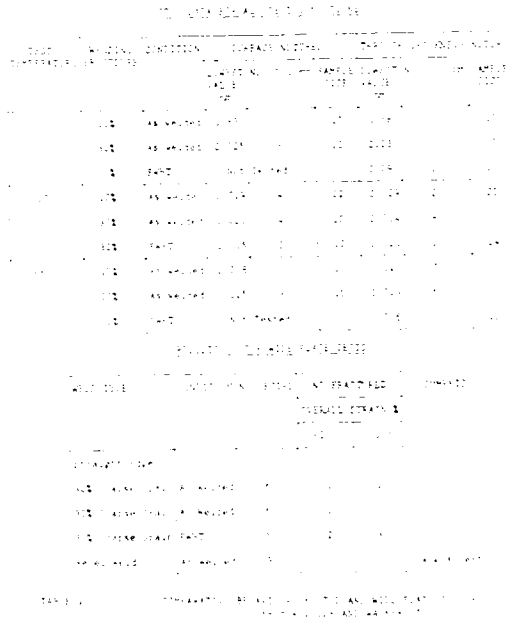

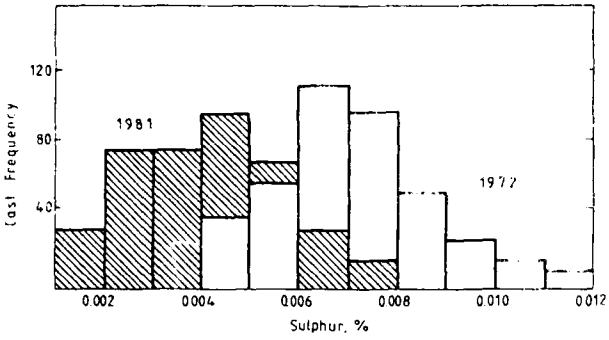


Figure 1 Change in sulphur levels in production casts of C-Si-Mn-Nb-Al offshore structural steels (from Kirkwood[37]).

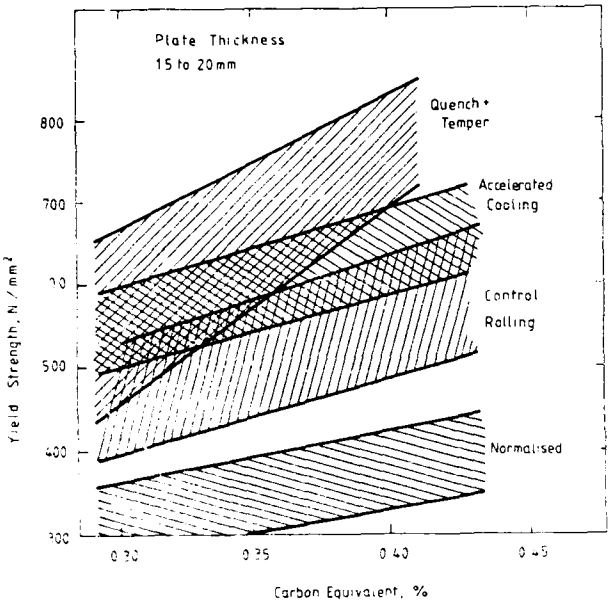


Figure 2 Effect of composition and plate manufacturing process on strength (from Lieurade and Lecoq [35]).

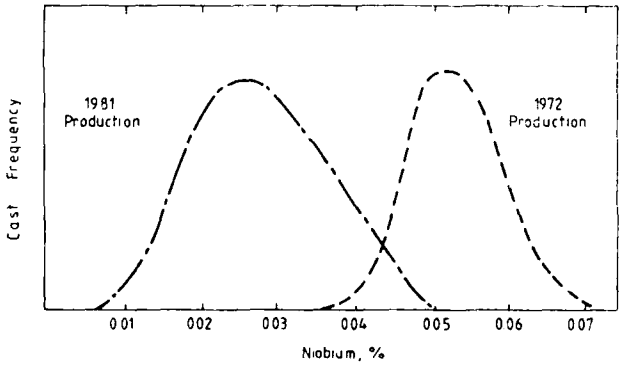


Figure 3 Change in niobium levels in production casts of C-Si-Mn-Nb-Al offshore structural steels (from Kirkwood[37]).

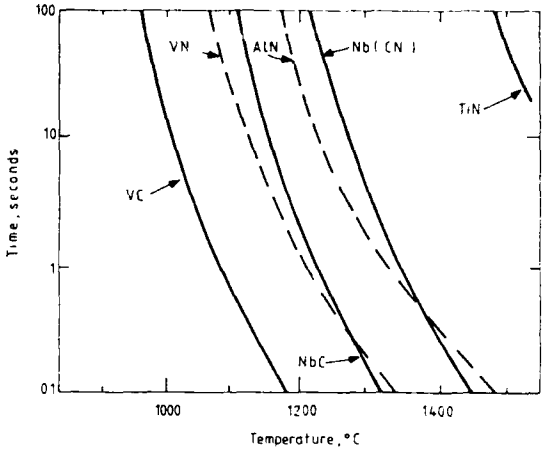


Figure 4 Precipitate dissolution characteristics of carbides and nitrides (from Easterling [47]).

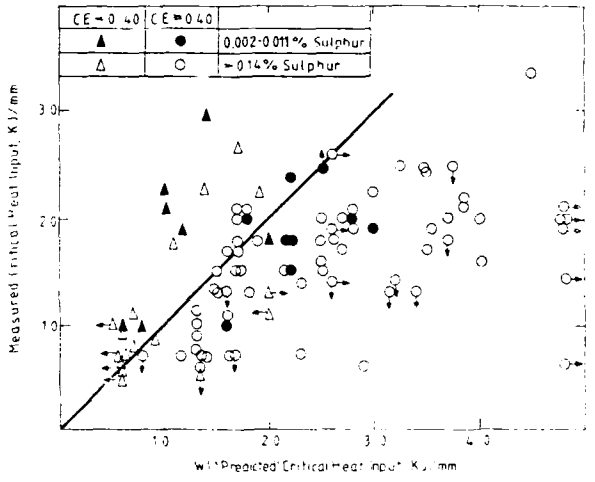


Figure 5 Effect of sulphur and carbon equivalent on weldability (from Batte [59]).

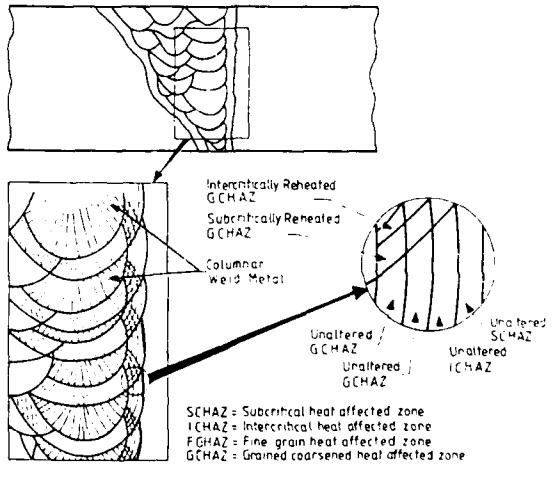


Figure 6 Multipass weld HAZ microstructures (from EEMUA [65]).

| C | Si | Mn | P | S | Mo | Cu | Nb | Ni | Cr | Al | V | $N_2$ | Ti | CE |
|---|---|---|---|---|---|---|---|---|---|---|---|---|---|---|
| 0.14 | 0.39 | 1.50 | 0.018 | 0.006 | 0.012 | 0.027 | 0.032 | 0.027 | 0.007 | 0.041 | <0.002 | 0.0040 | <0002 | 0.40 |

Peak Austenitising
Temperature 1300°C

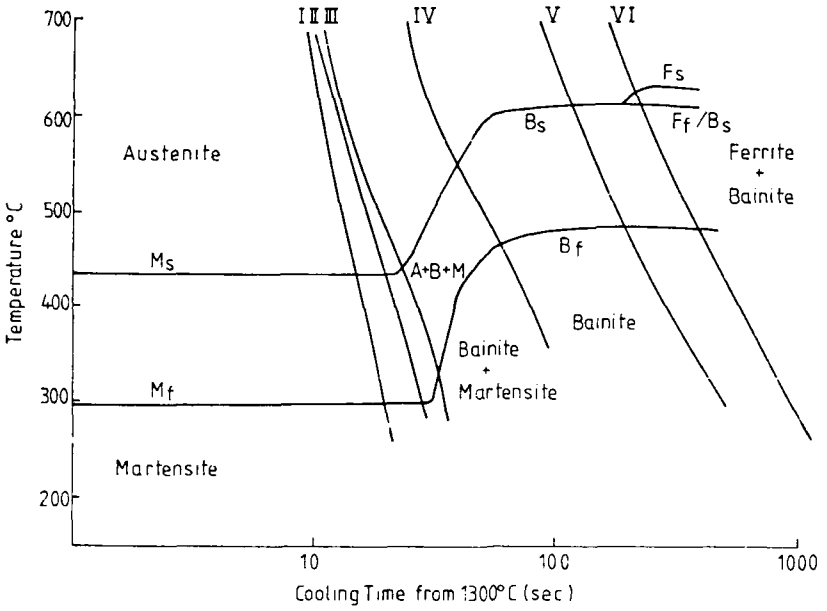


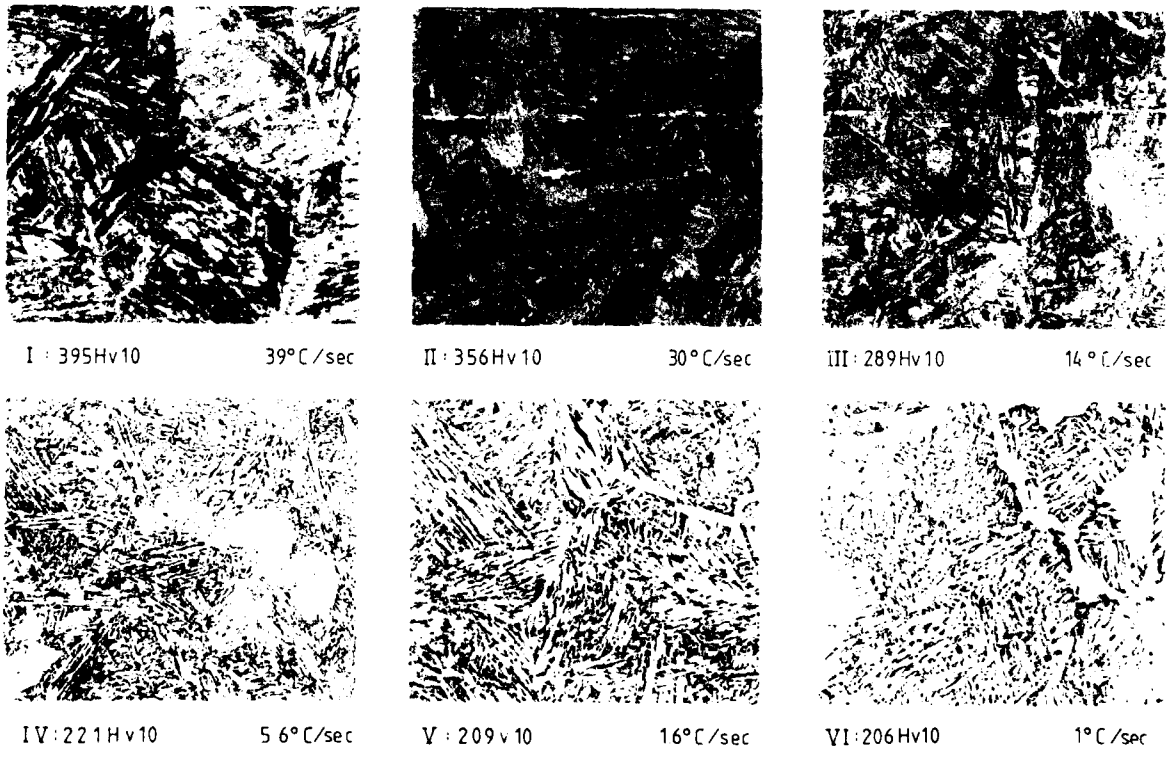


Figure 7 Continuous cooling transformation diagram and corresponding micrographs (from Boothby and Rodgerson [60]).

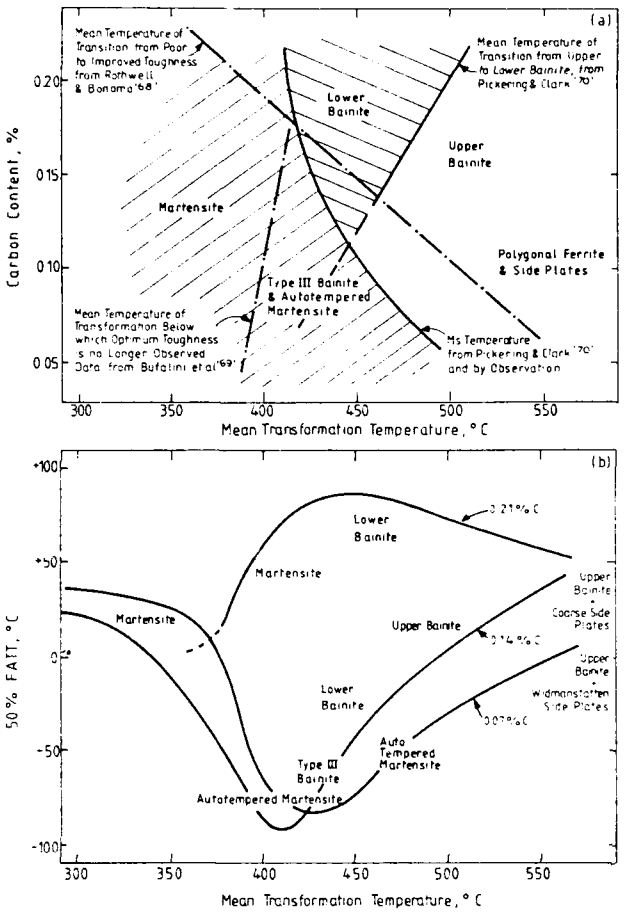


Figure 8 Influence of carbon content and transformation temperature on HAZ microstructure and toughness.

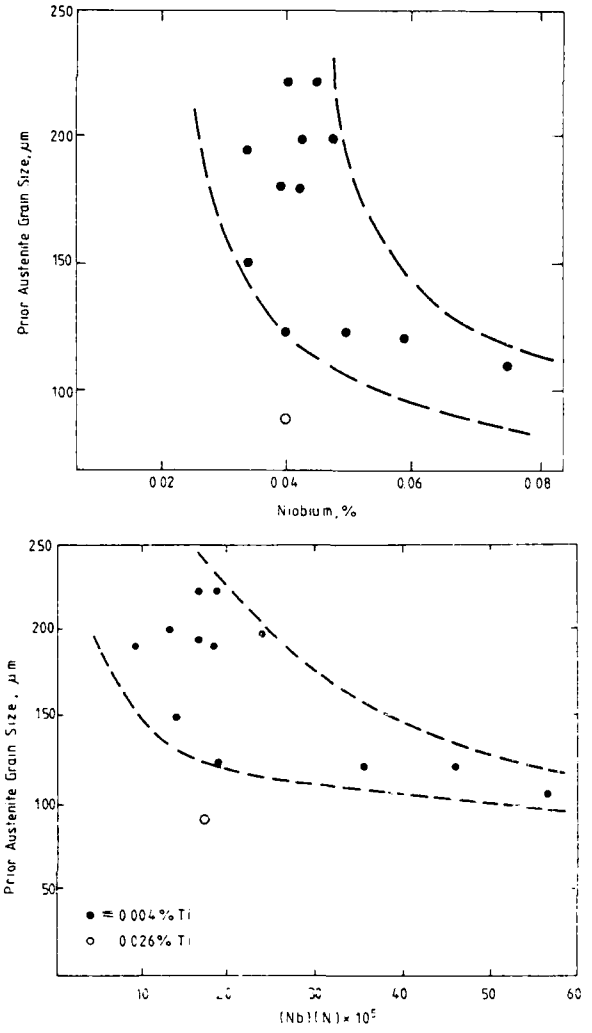


Figure 9 Effect of titanium, niobium and nitrogen on prior austenite grain size (from Kirkwood [37]).

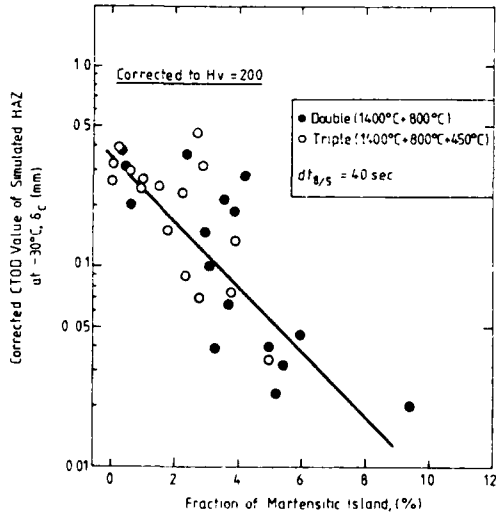


Figure 10 Influence of martensite islands on toughness (from Haze and Aihara [73]).

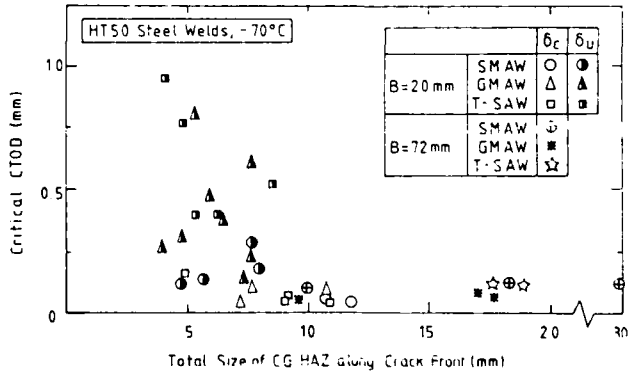


Figure 11 Effect of LBZ length on toughness (from Satoh and Toyoda [72]).

# FACTORS INFLUENCING FRACTURE TOUGHNESS OF STEEL WELD METAL FABRICATION

**S. R. Bala, K. G. Leewis**
Welding Institute of Canada
Oakville, Ontario, Canada

**T. H. North**
WIC/NSERC Chair, University of Toronto
Toronto, Ontario, Canada

ABSTRACT

This paper reviews Canadian research on the fabrication of structures which operate in low-temperature, Arctic environments. The main emphasis is on the metallurgical factors controlling HAZ and multipass weld metal fracture toughness.

The integrity of steel welded structures can be preserved by proper design to avoid fracture initiation. As long as components possess adequate strength and fracture toughness, the latter expressed in terms of $K_{IC}$ or more appropriately as developed by Welding Institute (UK) crack tip opening displacement (CTOD) values, a pre-existing flaw of subcritical size may be tolerated without the risk of developing an unstable fracture under operating levels of stress. The risk of fracture developing in a welded construction depends on and will be determined by properties of the microstructures locally surrounding the tips of the defects. The conditions for fracture initiation are a defect, a tensile stress normal to the defect and a susceptible microstructure at the defect tip. Welding contributes to all three factors, since welds contain buried defects, welding introduces yield stress magnitude tensile residual stresses and the weldment toughness is usually inferior to the parent steel.

In CTOD testing there is a transition in toughness with temperature. This transition temperature is strongly influenced by strain rate and thickness. High strain rates and higher thicknesses increase transition temperature values. Traditional CVN tests with blunt notch and arbitrary strain rates cannot provide a direct measure of fracture toughness. Also, because of thickness limitations and increased plastic strain levels, the LEFM approach to $K_{IC}$ is also not feasible. Thus, CTOD tests and analyses as developed by TWI have been extensively used when characterising fracture toughness.

Since there is a CTOD toughness transition with temperature, the toughness requirements for structures operating in Arctic environments, such as the Beaufort Sea, are necessarily demanding and the specifications are more stringent than those for less severe environments such as the North Sea.

From the fabricator's point of view, it would be ideal to weld at the highest heat input possible, consistent with defect-free welds (in order to increase joint completion rates). However, higher heat inputs lead to coarse grain formation adjacent to the fusion boundary, and precipitation of carbonitrides of microalloying elements (especially Nb) which adversely affect HAZ toughness properties. Post-weld heat treatment instead of improving HAZ toughness, as occurs in C-Mn steels, can cause further deterioration through increased precipitation hardening effects. As a result, worldwide steel development has involved i) the use of Ti (to promote TiN formation which restricts grain growth in the HAZ), ii) the use of lower carbon levels to counter its known adverse effects on toughness and weldability properties, and iii) minimal use of microalloying additions by adding Cu, Ni, B, etc. Steels based on Cu-B additions have been developed in Japan and by Canadian researchers (1) and those based on V-B additions by Lukens steel in the U.S.A.

The severe requirements of Canadian offshore and Arctic applications have been satisfied by the development of high quality steels which have good weldability, corrosion resistance and fracture toughness properties (in both parent and HAZ regions). Similarly, considerable research on welding procedure/weld metal property requirements has been carried out to confirm methods of fabricating structures capable of the most onerous field applications.

This paper examines some Canadian research on the metallurgical factors controlling HAZ and weld metal toughness properties.

## STEELS

Steel strength is markedly dependent on carbon content. However, high carbon steels have poor weldability and inadequate fracture toughness properties. HSLA steels were developed with lower carbon contents, to meet the onerous weldability and toughness demands of applications such as linepipe construction in the Canadian Arctic. The lower strength values (due to removal of carbon) were counteracted by additions of nickel, copper and so on.

These steels have minimum yield strengths of 300 $MN/m^2$ and maximum carbon equivalent values (CE) of 0.43. Thicker plates (75 mm thick) are normalized and thinner sections are produced by TMCP (controlled-rolling) treatments. Niobium is particularly effective in controlling austenite grain size during rolling. Both niobium and vanadium also improve strength due to precipitation hardening. The fracture toughness of these steels is further improved by having reduced sulphur contents and/or sulphide-shape control processing. Typical steels developed for Arctic and Canadian offshore applications are Algoma LT60, A710, BS 4360, Gr 50 or 55, Kawasaki Macs EH 36 ACC and DQT, etc.

The excellent toughness in these steels is reduced somewhat after cold forming (bending), e.g., in offshore platforms the tubulars are fabricated by bending plates 25-100 mm thick into cylinders and welding the longitudinal seams. This decrease in toughness properties does not appear until more than 30% plastic strain occurs on the tension surfaces of the tubular members (2). The fracture toughness of welded joints will consequently be affected by strain ageing, and if the plate thickness exceeds 38 mm, by the stress-relieving treatment after welding.

## HEAT AFFECTED ZONE TOUGHNESS PROPERTIES

The heat affected zone toughness properties in HSLA steels depend on the complex interplay of microstructure, grain size, particle (carbonitride, nitride) dissolution and reprecipitation, and plate chemistry. It is well known that niobium and vanadium carbonitrides dissolve during the heating cycle of fusion welding, and reprecipitate if the cooling rate is slow enough (3, 4, 5). It follows that the effect of any microalloying addition (such as niobium) on HAZ toughness properties depends markedly on the heat input used (on the thermal cycle enabling particle solution, possible reprecipitation and subsequent hardening), and on the effect of soluble niobium on the phase transformations occurring during cooling after welding. In HSLA steels alloyed with niobium only, the cooling time is the dominant factor (6). At short cooling times (6 to 16 seconds for the 800°C/500°C temperature range) niobium has a beneficial influence on HAZ toughness. However, in higher heat input (slower cooling rate) welding situations niobium has a detrimental effect on toughness values.

The situation is more complicated when different combinations of microalloying elements are present in the steel. The effect of titanium, titanium plus niobium, and titanium plus vanadium additions on the HAZ toughness properties of linepipe steel were evaluated by McCutcheon (7). When welding at 2 kJ/mm heat input, niobium additions to titanium bearing steel decreased toughness values as a result of significant solute strengthening. Vanadium in combination with titanium improved HAZ toughness values, and vanadium additions to a 0.05% niobium bearing steel produced a slight fall-off in toughness properties. Precipitate dissolution and reprecipitation during the weld thermal cycle are also affected when different combinations of microalloying elements are present. Suzuki and Weatherly (5) observed that in steels containing titanium plus niobium, niobium-rich precipitates dissolved and titanium-rich particles reprecipitated later in the heating cycle. This reprecipitation effect explained the finer HAZ grain sizes in TiNb-containing steels.

Recent Japanese results have suggested a relation between the effect of any addition, say niobium, on toughness and the primary agent present in the steel for grain size control (8). Quite different results were produced when similar niobium contents were added to plates containing TiN and $Ti_2O_3$ particles as the grain refining agents. Niobium had a detrimental effect on the fracture toughness of steel containing TiN particles (due to Nb microsegregation around TiN precipitates, increased hardenability and suppression of acicular ferrite formation). However, there was negligible influence of niobium additions on the toughness of plate containing a dispersion of $Ti_2O_3$ particles.

The Welding Institute of Canada has been carrying out an extensive research program evaluating the fracture toughness properties of HAZ regions in constructional steels (9, 10). This research program evaluated the influence of different combinations of microalloying elements (Nb, V, Ti) on the fracture toughness of the coarse grained HAZ region of single pass deposits (see Table 1 for the plate chemistries used). When welding at a range of heat inputs (3 kJ/mm to 6 kJ/mm) HAZ toughness results indicated that:

1) Steel microalloyed with titanium only (0.014%) produced the highest toughness values at all heat input levels.
2) the poorest HAZ toughness values were exhibited by steel containing a combination of 0.027% Nb, 0.082%V and 0.016%Ti (at all heat input levels).

TABLE 1

Steel Compositions

| Code | C | Mn | Si | V | Nb | Ti | Al | N | P | S | O |
|---|---|---|---|---|---|---|---|---|---|---|---|
| 50 | .11 | 1.33 | .26 | .082 | .027 | .016 | .058 | .010 | .004 | .005 | .057 |
| 51 | .12 | 1.36 | .28 | .080 | <.005 | .014 | .049 | .008 | .003 | .005 | .060 |
| 52 | .11 | 1.35 | .27 | <.003 | .026 | .015 | .054 | .009 | .004 | .005 | .067 |
| 53 | .11 | 1.35 | .26 | <.003 | <.005 | .014 | .055 | .009 | .004 | .005 | .057 |
| 55 | .11 | 1.34 | .56 | <.003 | <.005 | .014 | .049 | .009 | .004 | .006 | - |
| 56 | .077 | 1.44 | .56 | <.003 | <.005 | .015 | .050 | .009 | .004 | .006 | - |
| 58 | .13 | 1.41 | .29 | .093 | <.005 | <.002 | .053 | .008 | .004 | .004 | .068 |
| 59 | .13 | 1.52 | .29 | <.003 | .029 | <.002 | .052 | .009 | .004 | .004 | .065 |

3) increasing silicon content (from 0.26% to 0.56%), and decreasing carbon content (from 0.11% to 0.077%) in HSLA steel microalloyed with titanium alone impaired HAZ toughness properties.

4) increasing heat input from 3 kJ/mm to 6 kJ/mm had a particularly detrimental effect on the HAZ toughness of steel containing 0.08%V and 0.015%Ti. This occurred due to replacement of the acicular ferrite-like microstructure by coarse, equiaxed ferrite.

5) steel containing 0.093%V alone had excellent toughness when welded at 6 kJ/mm. However, when welded at 3 kJ/mm HAZ toughness properties were impaired since higher hardness values counteracted the beneficial influence of the acicular ferrite-like microstructure in the HAZ.

6) The combination of titanium plus niobium (0.012%Ti 0.026%Nb) produced much poorer toughness properties than titanium alone (due to increased sideplate ferrite formation, and lower acicular ferrite contents in the HAZ microstructure). These results are shown graphically in Figures 1 to 3.

No relation between the 0.1 mm CTOD transition temperature and grain boundary (polygonal) ferrite content, sideplate ferrite content or any combination of microstructural constituents was apparent. Yamamato (8) indicated that the point of fracture initiation occurs when sideplate ferrite cracks and therefore any factor promoting decreased sideplate ferrite content (such as acicular ferrite formation) improved HAZ toughness values. In our work, the optimum HAZ toughness values were generally associated with microstructures containing an acicular ferrite-like microstructure. However, no simple monotonic relation existed between the content of the acicular ferrite-like microstructure and CTOD fracture toughness properties. Luo and Embury (11) have also indicated that coarse ferrite in the HAZ micro-

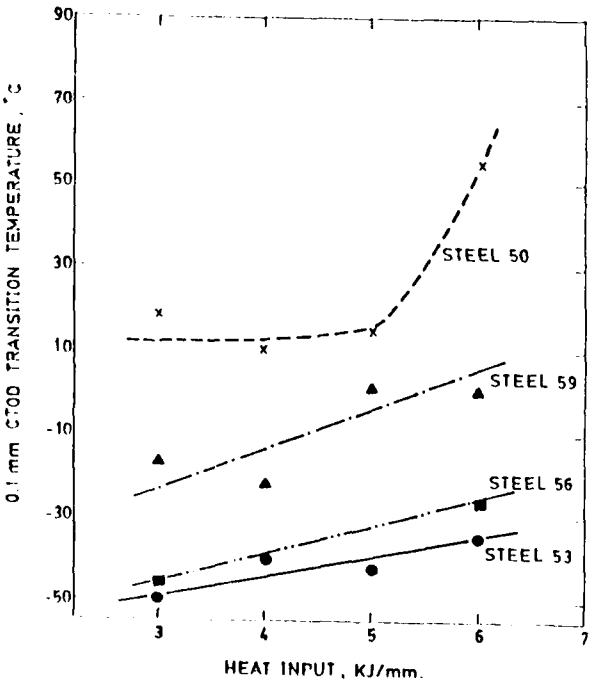


Figure 1. 0.1 mm CTOD transition temperature/-heat input relations for Steel 50 (NbVTi), Steel 53 (Ti), Steel 56 (C, Ti) and Steel 59 (Nb).

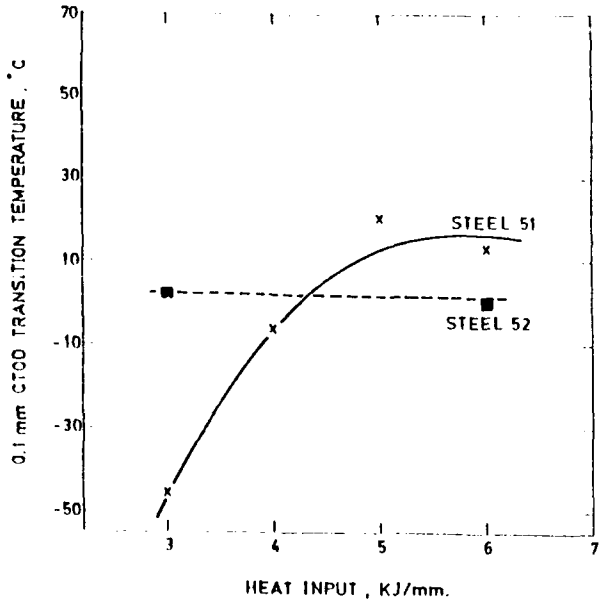


Figure 2. 0.1 mm CTOD transition temperature/-heat input relations for Steel 51 (VTi) and Steel 52 (NbTi).

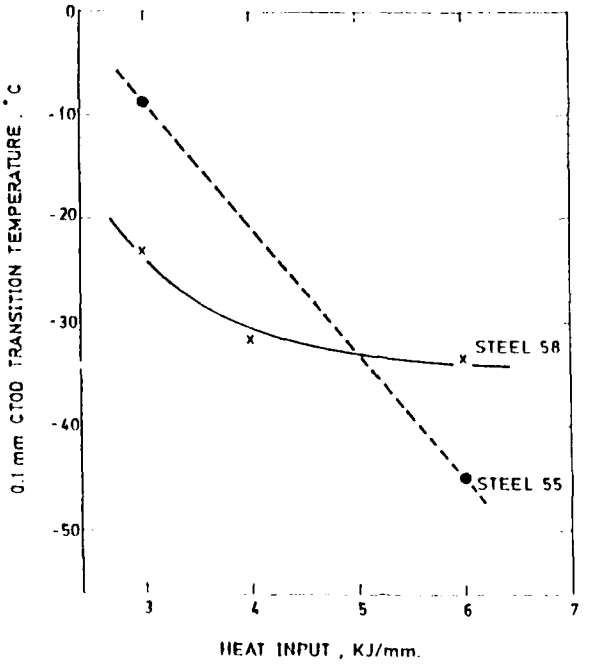


Figure 3. 0.1 mm CTOD transition temperature/ heat input relations for Steel 55 (Si, Ti) and Steel 58 (V).

structure acts as a nucleus for cleavage fracture, and that higher contents of coarse ferrite lower the cleavage fracture stress. In their work the coarse ferrite content was evaluated by point counting and summating the contents of grain boundary ferrite, ferrite sideplates and intergranular polygonal ferrite. Since yield stress decreased more rapidly than cleavage fracture stress (as coarse ferrite content increased) the transition temperature was lower at high coarse ferrite contents. This explained the lower transition temperatures they observed in the welds deposited at 10 kJ/mm c.f. 2 kJ/mm.

It is apparent that the interplay between HAZ microstructure and toughness properties is extremely complex and that the fracture toughness depends on the combined effects of both coarse ferrite and acicular ferrite-like constituents.

The research described above emphasized the factors controlling the toughness of the coarse grained HAZ region in single pass welds. However, other regions in the HAZ of multipass welds are equally important, viz., the subcritical and intercritically reheated regions in the HAZ microstructure. This problem area has been evaluated in detail in recent work by Thaulow et al (12), and consequently will not be dealt with in the present paper.

## WELD METAL TOUGHNESS PROPERTIES

Weld metal microstructure (acicular ferrite content) has a controlling influence on the fracture toughness properties of HSLA deposits. Knott et al (13) have shown that the cleavage crack path preferentially follows grain boundary ferrite regions and acicular ferrite acts as a barrier to crack propagation. It is generally agreed that intergrannular acicular ferrite is nucleated by weld metal oxide inclusions, and the inclusion content is dependent on the oxygen potential of the flux, electrode coating or gas shielding system employed. However, the ideal inclusion composition(s), and particle size or particle distributions promoting acicular ferrite formation are still a subject of debate. This is to be expected considering the multivariable nature of the deposit microstructure/-inclusion/ toughness relationship. For example, it is difficult to vary deposit oxygen content without changing weld metal composition, inclusion chemistry, size and distribution simultaneously.

In a multipass welding situation, the combined effects of cooling time between 800°C and 500°C (dependent on heat input, joint thickness, preheat and interpass temperature), number of weld beads and welding position complicate the situation. Weld metal toughness properties generally increase in the order of vertical-up, overhead, horizontal and flat positions. These differences in toughness properties have been

attributed to heat input variations, to different numbers of weld beads, the differing proportions of refined and unrefined weld metal, and so on. Also, weld metal nitrogen content (particularly in shielded-metal-arc welding) increases as arc length is increased, and changes in welding position can affect both arc voltage and deposit values. The fracture toughness properties of Ti-B containing welding consumables will be markedly reduced if nitrogen content is increased (the beneficial role of boron in controlling the austenite/ferrite transformation will be prevented). Bearing in mind that dynamic strain ageing lowers the toughness properties of the root region in comparison to final pass material, it is apparent that research on the toughness properties of multipass welds is an extremely complex undertaking.

Bala et al (14) carried out a detailed research program aimed at evaluating the fracture toughness properties of multipass welds in 20 mm thick plate. A wide range of proprietary flux-cored welding consumables were used (5 rutile type, 6 basic type, 4 metal-cored electrodes and 1 innershield electrode). All welds were made in the vertical-up position, using a heat input of 2 kJ/mm, 75% Ar 25% $CO_2$ shielding gas, and an interpass temperature of 150°C. Full-thickness CTOD fracture toughness specimens were cut with the notches on the weld centreline. For any element, the wide range of deposit chemistries produced were used to relate chemistry and toughness properties. Bearing in mind the considerable limitations of this approach (a monotonic relation between the element considered and deposit toughness properties is assumed) some general comments can be made:

1) the lowest 0.1 mm and 0.2 mm CTOD transition temperature values for rutile, basic, metal cored and flux-cored welding consumables were,

| | 0.1 mm CTOD | 0.2 mm CTOD |
|---|---|---|
| Basic-Cored Electrodes 50°C | -50°C | - |
| Rutile-Cored Electrodes 30°C | -50°C | - |
| Metal-Cored Electrodes 3°C | -25°C | - |
| Innershield Electrodes 10°C | -33°C | - |

2) the highest toughness values were produced by weld metals having the lowest carbon contents (0.07%), see Figure 4.

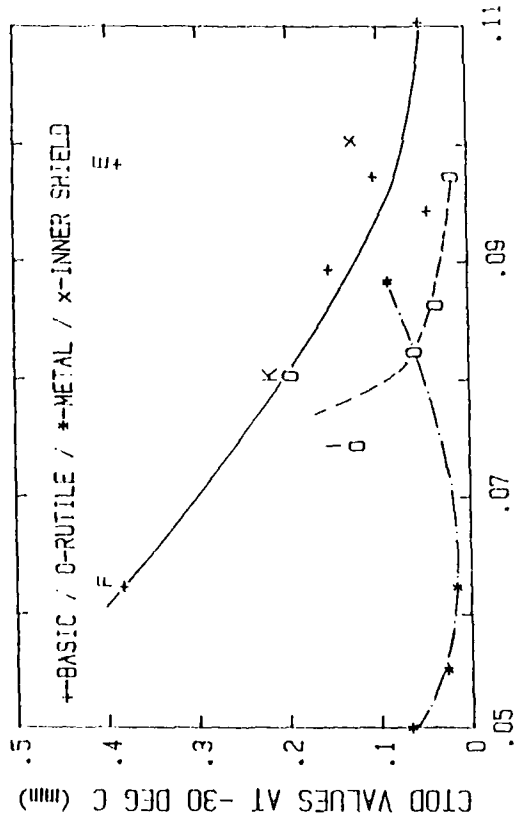


Figure 4. CTOD values at -30°C versus carbon content of the welds in 20 mm thick plates.

3) optimum toughness values in rutile and in basic-cored electrode deposits were produced when the silicon content was 0.4% (see Figure 5). At higher silicon contents the increased hardenability contribution was not counteracted by any weld microstructural improvement.

4) increased nickel content to 2.4% improved the toughness of deposits made using basic-cored electrodes (see Figure 6). Increasing nickel content had little influence on the toughness of metal-cored weld deposits.

## CONCLUSIONS

This paper has provided a limited review of some of the research presently being carried out on Canadian Offshore fabrication problems. This work is continuing at WIC, and throughout Canada, in order to meet the technological challenges of structures operating in low-temperature Arctic environments.

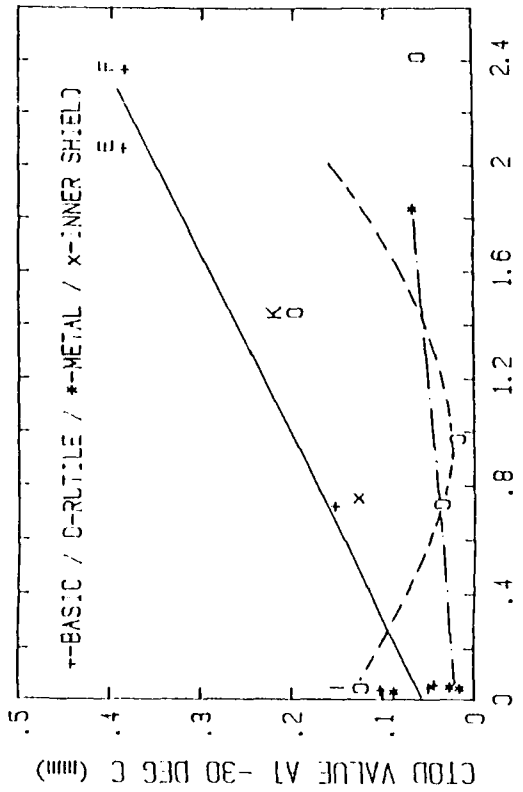


Figure 6. CTOD values at -30°C versus nickel content of the welds in 20 mm thick plates.

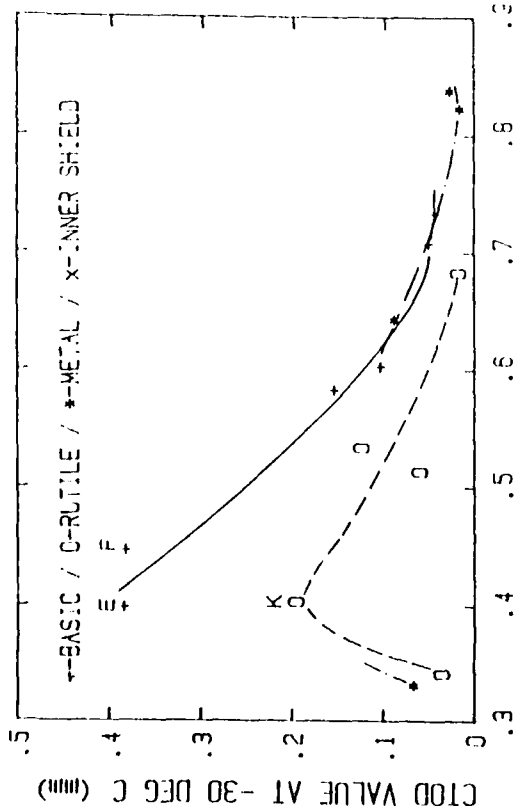


Figure 5. CTOD values at -30°C versus silicon content of the welds in 20 mm thick plates.

REFERENCES


1) N.Krishnadev, Personnel communication. Laval University, Quebec.

2) S.R. Bala, S. Pond, "Weldability and Formability of Two Candidate Steels for Offshore Structures and Arctic Vessels", AMCA Report No. 1-183-014/F (1983).

3) I. Hvrinak, Zvanacski Spravy, 1, (3), (1974).

4) R.E. Dolby, Metal Construction, 4, (2), 1972.

5) S. Suzuki, G.C. Weatherly, ASM Conference, Characterization of Precipitates and Grain Growth in Simulated HAZ Thermal Cycles of Ti-Nb Bearing Steel Weldments, Beijing, China (1985).

6) B. Graville, A.B. Rothwell, Metal Construction, 9, (1), (1977).

7) D.B. McCutcheon, J.T. McGrath, M.J. Godden, G.E. Ruddle, J.D. Embury. ASTM-STP-792, Conf. Micon-82, Optimization of Processing Properties and Service Performance Through Microstructure Control, Houston (1982).

8) K. Yamamato, S. Matsuda, H. Toshiaki, R. Chijiiwa, H. Mimura. Unpublished research, Nippon Steel Corporation (1982).

9) T. Lau, G.R. Wang, T.H. North. To be published, Materials Science and Technology, The Institute of Metals, U.K. (1988).

10) G.R. Wang, T.H. North, K.G. Leewis. To be published, Welding Journal, U.S.A. (1988).

11) L.G. Luo, J.D. Embury. The Relationship Between COD Transition Temperature and HAZ Structures in HSLA Steel. Internal Report, Department of Materials Science and Engineering, McMaster University, Hamilton, Ontario (1987).

12) C. Thaulow, A.J. Paaluw, K.G. Uttormsen, Welding Journal, 66, (9), (1987).

13) J.H.Tweed, J.F. Knott, Metal Science, 17, 45 (1983).

14) S.R. Bala, S. Santyr, "Evaluation of Flux-Cored Arc Welding Consumables for Offshore and Arctic Structure Fabrication", AMCA Report No. 7-184-096/F (1986).

# FRACTURE MECHANICS TESTING OF HSLA STEELS FOR OFFSHORE APPLICATIONS

**C. Thaulow, O. M. Akselsen, M. Hauge, B. Melve, A. J. Paauw, G. Rörvik, J. K. Solberg, J. Troset**
SINTEF
7034 Trondheim
Norway

## INTRODUCTION

During the last 5 years SINTEF has taken an active part in the evaluation of low fracture toughness results from the testing of HAZ of modern low-carbon structural steels.

The new classes of structural steels for offshore application are characterized by a reduction of sulphur and strict control with chemical elements such as phosphorus, niobium and nitrogen. This should primarily serve an increased weldability. However, during welding procedure testing of the first platform to be built of low-carbon steel in Norway, very low CTOD values were found in the HAZ. This was of great surprise, since the HAZ toughness was considered to be of no problem.

At an early stage, during the fabrication of the platform, SINTEF was engaged by the Norwegian Petroleum Directorate (NPD) to evaluate the reasons and consequences of the low HAZ fracture toughness. Until now more than 15 low-carbon microalloyed steels, delivered for application in offshore structures, have been tested in accordance with the test procedures developed for NPD /1,2,3/. A summary of the experience from these tests is under preparation /4/. The tests included weld thermal simulation and bead-in-groove CTOD testing. The low fracture toughness was correlated with brittle zones in the HAZ.

The investigations performed in the NPD projects were limited, and an industry-sponsored program was therefore initiated in order to examine the HAZ toughness and the significance of the low toughness in more detail. The investigations included the HAZ microstructures, weld thermal simulation Charpy toughness, fracture toughness and crack arrest toughness.

This paper summarizes the experience from the various examinations and compares the "older" CMn steels (with typically 0.18 % C) with new low-carbon steels.

## MATERIALS

Three low-carbon microalloyed and one CMn steel have been examined in the normalized condition. The chemical composition and mechanical properties of the base materials are outlined in Table 1 and 2. The low-carbon microalloyed steels were delivered from three different steelworks, and their chemical compositions are rather similar, except for different levels of nitrogen and impurities. Steel D is a CMn steel of higher cleanliness than the traditional grades: It was included in the program as a reference steel.

## WELD THERMAL SIMULATION TESTING

Experience in the past has revealed that it may be difficult to hit the brittle zones during CTOD testing of weldments. The fatigue crack tip has to be positioned close to the brittle zones and a certain fraction of the crack tip has to be affected by these zones before low CTOD values are recorded. The problem of notch positioning can be avoided by the use of weld thermal simulation testing. The aim of these investigations was to establish the relationships between the HAZ toughness, microstructures and the weld thermal cycles on the basis of Charpy testing of simulated HAZs.

The weld thermal simulation testing program, Table 3, was designed to cover the most interesting areas of the HAZ, Fig. 1.

The grain-coarsened HAZ toughness is unfavourably affected by an increase in cooling time, Fig. 2, mainly because of the formation of grain boundary ferrite and the more predominant ferrite sideplates, Fig. 3. The impact properties reach a low value when the fraction of these unfavourable microstructures exceeds about 50 vol%. At volume fractions below 10 %, i.e. as a result of fast cooling rates, no correlation is evident. The low toughness of steel A at fast cooling rates, Fig. 2, is explained on the basis of phosphorus

embrittlement, and for steel D on the basis of formation of high-carbon lath martensite.

A correlation has been established between the cooling rates and the austenite grain size of the grain-coarsened HAZ, Fig. 4. The effect is most pronounced at slow cooling rates and is probably due to impurity drag effects by phosphorus at the grain boundaries during grain growth. Post-weld heat treatment (PWHT) of the grain-coarsened HAZ was favourable for steel C and D, Fig. 5. Concerning steel A, i.e. the steel with the highest phosphorus content, temper embrittlement was, as expected, most pronounced at the slowest cooling rate. Steel B appears to be susceptible for PWHT for all investigated cooling rates, resulting in intergranular fracture and an increase in the transition temperature. The potential harmful effect of phosphorus after PWHT is outlined in Fig. 6, but there are many unanswered questions with respect to the detailed deterioration mechanisms.

It has been suggested that small amounts of free nitrogen might be critically important to embrittlement of the grain-coarsened HAZ /2/. The free nitrogen content was analysed in a limited number of specimens, but no direct correlation with the toughness could be established.

The deterioration of the grain-coarsened HAZ impact properties after a second weld thermal cycle, Fig. 7, is mainly associated with an increased volume fraction of high carbon plate martensite.

The partly transformed HAZ toughness is mainly determined by the formation of high-carbon plate martensite islands. Toughness improves with increased cooling time, Fig. 8, and after PWHT, Fig. 5.

## FRACTURE MECHANICS TESTING

The aim of this study was to determine the HAZ fracture toughness properties of real weldments in the four steels investigated. At present there exists no generally accepted standards for fracture mechanics testing of weldments /5-7/, therefore different specimen geometries and notch depths have been applied in order to examine the effect of surface vs. through-thickness notching.

Many of our findings have recently been published, /8/, and therefore only a brief summary will be presented in the present paper.

Low heat input (Shielded Manual Arc Welding - SMAW) and high heat input (Submerged Arc Welding - SAW) butt welds were prepared with a K groove in 50 mm thick plates. In addition, the cap layer was simulated with bead-in-groove CTOD testing of single weld layers.

Both the CTOD testing with a shallow surface notch (a/W=0.06) of bead-in-groove and butt weldments revealed the lowest toughness for the CMn steel, steel D in Fig. 9 and 10. The HAZ CTOD values from surface notched specimens, with a/W=0.3, were generally high. The lowest value for the SMAW specimens was 0.24 mm for steel A and, for the SAW specimens, steel B with 0.37 mm. The CMn steel had a toughness level at least as high as the low-carbon micro-alloyed steels. But in the case of through-thickness notching, the CMn steel showed the lowest values for both SMAW (0.14 mm) and SAW (0.18 mm).

From the weld thermal simulation testing one should expect that all four steels had defined areas with brittle microstructures, and it is therefore somewhat surprising that only the CMn steel showed some tendency to low CTOD values. This behaviour is explained by the fact that the initiation of the brittle fracture depends upon both the existence of a brittle microstructure and the detailed notch positioning. The best control with these parameters was obtained in the CTOD bead-in-groove test, and brittle fracture initiation was experienced for all four steels with this testing technique. The lower values for the CMn steel, Fig. 9, can be explained by the simulation test results where this steel is most prone to brittleness, Fig. 7 and 8. In real weldment testing, the size and shape of the embrittled areas will vary and notch positioning will be difficult. The CMn steel will have the largest volumes with embrittled microstructure, and therefore the highest probability of revealing low fracture toughness.

From the weld thermal simulation testing it is evident that only a part of what is defined as grain-coarsened zone has low Charpy energy, Fig. 8, and that the extension of the brittle volume will depend on factors such as steel quality and heat input/cooling time. This is consistent with fractographic observations of the CTOD specimens and indicates that only a narrow region of the grain-coarsened zone, close to the fusion line, will be brittle (in addition to the partly transformed zone). Hence, careful notch positioning, very close to the fusion line and at a location where the brittle zone has a maximum width, gives the optimum conditions for low CTOD values. This trend has also been confirmed in another investigation, Fig. 11 /9,10/.

## CRACK ARREST TESTING

The CTOD bead-in-groove tests in this investigation, and previous projects /2/, have shown that brittle fracture can initiate in the HAZ and propagate in a quite brittle manner through the base material of these tough low-carbon microalloyed steels, Fig. 12. Hence, it has been questioned if the high CTOD crack initiation level has been obtained at the expense of a low crack arrest toughness. The aim with the present crack arrest testing was to determine the base material crack arrest properties in accordance with the small scale testing method proposed by ASTM /11/.

Experience from other projects indicated that a large number of duplicate specimens might be necessary in order to obtain satisfactory results, hence the number of steels to be tested had to be restricted. Three steels were tested, steel 1 and 8 from previous investigations /1,2/, and steel B from the present project. Steel 1 and B are low-carbon microalloyed steels: Steel 1 with high phosphorus (0.021%) and niobium (0.041%) contents and steel B with low phosphorus (0.007%) and niobium (0.020%) contents. Steel 8 is a typical CMn steel.

It was of interest to test the material in both the thickness direction (normal to the plate, as in the CTOD bead-in-groove specimens) and in the plate direction (the traditional test geometry), hence two specimen geometries were selected, Fig. 13. The DUP specimen (duplex specimen with a brittle start section electron beam welded to the test section) for the direction normal to the plate and the MRL specimen (weld embrittled start zone) in the plate direction. A total number of 60 specimens were prepared, 10 duplicates for each steel/specimen geometry.

The test temperature was initially set at $-10^0$C, but was later reduced to $-30^0$C for most of the tests.

As expected a number of difficulties were experienced when applying the ASTM standard on the high toughness, moderate yield strength structural steels. The ASTM recommendations were originally developed for pressure vessel steels, and the test geometries and validity requirements were specified on this basis. These limitations will not be discussed here.

Valid plain strain crack arrest toughness was only obtained for four specimens, Table 4. Ignoring the validity requirements specified in /11/, the average crack arrest toughness for the specimens with a brittle fracture arrest in the test material are presented in Table 5. The results clearly indicate that the low-carbon microalloyed steels, steel 1 and B, have better crack arrest properties than the older CMn steel. This is further demonstrated in Table 6, where the average crack jump lengths are correlated with the average of the stored energy at crack initiation. Steel B has the highest stored energy and the shortest crack jumps, indicating that this steel absorbs the most energy during crack propagation.

The results are promising with respect to the future application of the low-carbon steels. The applied testing technique should now be further developed in order to increase the number of valid plain strain crack arrest toughness results to a statistically satisfactory level. The tests, so far, have concentrated on the base material toughness, but the crack arrest properties in the HAZ and weld metal should also be examined. In the CTOD testing of steel A it was often observed that the crack propagation followed a preferred path along the fusion line, and similar evidence for unstable crack propagation along the HAZ has recently also been reported in wide plate testing /12/. The future acceptance criteria of local brittle zones will probably include the evaluation of the crack arrest properties of: 1) the material surrounding the brittle microstructure and 2) as the next barrier the general crack arrest properties of the base material and the weldment. It has recently been proposed that these evaluations can be bases upon the NDT temperature from Pellini Drop Weight Test /13/, but since this test is highly empirical and restricted to base material testing of plates with moderate thickness, it is thought that further developmens of dynamic fracture mechanics based tests will be more favourable /10/. The necessary developments are now being investigated in the research project at SINTEF designated CAOS (Crack Arrest Offshore Steel) /14/.

## COMPARISON OF THE STEELS

The weld thermal simulation Charpy toughness of the grain-coarsened zone was low for all steels, but the lowest values were always observed for the CMn steel, Fig. 14. This is in accordance with the results from previous tests, Fig. 15, where the CMn steel, steel 8, represents the lower-bound values.

The trend established in the weld thermal simulation testing was in general confirmed by the CTOD bead-in-groove testing and the CTOD weldment testing. The lowest CTOD values were obtained from the CMn steel. It is remarkable that no low HAZ CTOD values were recorded during the comprehensive fracture toughness testing of the CMn class of offshore steels 10-15 years ago. A critical point in the through-thickness CTOD testing is the positioning of the notch tip with respect to the embrittled microstructure, and since brittleness in the weld metal was a problem, restrictions were put upon the positioning procedure in order not to hit weld metal. With a somewhat curved fusion line, the result may have been that a major part of the fatigue crack tip is positioned in the base material.

The base material crack arrest toughness of the low-carbon microalloyed steel with the lowest phosphorus and niobium content was better than a low-carbon steel with higher contents of these elements, and substantially better than the CMn steel. This might indicate that steel B and C have better crack arrest properties than steel A. In addition, steel A showed a tendency for brittle crack propagation along the fusion line in the through-thickness CTOD tests.

The overall conclusion is rather positive and optimistic with respect to the fracture toughness of the low-carbon microalloyed steels. The new class of steels has obviously better fracture toughness than the CMn steels, but low CTOD values are frequently recorded, and the significance of these low values is

questioned. There is a need to explain why there have been no major brittle fracture accidents in the offshore structures fabricated with CMn steel and to present recommendations on how to treat low HAZ CTOD values in the future. The absence of accidents can, as a first attempt, be explained on the basis of the low probability of having a fatigue crack positioned at a location where the local brittle zone has both a maximum volume and local constraint just at the moment when high stresses are experienced /8,12/. This aspect should be further explored on the basis of probabilistic analysis. Probabilistic fracture mechanics analysis can now indicate where fatigue cracks will develop and how they will grow /15/. Hence, it should be possible to map the fatigue crack tip with respect to location and crack tip stresses. The next step will then be to model the HAZ with respect to the parameters of significance for brittle fracture initiation (and arrest), and evaluate them in a probabilistic manner. To do this, a research proposal "APPLICATION OF PROBABILISTIC FRACTURE MECHANICS IN THE EVALUATION OF LOCAL BRITTLE ZONES IN OFFSHORE STRUCTURES" will be presented in the near future. The aim will partly be to answer why there has been no major brittle fracture accidents offshore, and partly to propose a probabilistic based defect analysis procedure.

With respect to fracture mechanics testing, there is a need for relevant and simple weldment testing procedures /5,6,7/. Recently, API has published a recommended practice bases on EXXON's typical test requirements /16/, to be used in prequalification tests of steels and welding procedures. Other tests, such as the combination of CTOD bead-in-groove and weld simulation testing, may be effective in identifying the brittle microstructures and the extent of such brittleness (only a fraction of the grain-coarsened HAZ will be brittle) and thereby rank the steels /3/. The tendency to HAZ brittleness in the low-carbon steels varies, Fig. 15, and steelworks are continually changing their production procedures and chemical composition in order to minimize the HAZ embrittlement. The latest development aimed to obtain high HAZ toughness by introducing titanium as a deoxidation element. Such developments can be evaluated by using the testing procedures described in reference /3/ while different welding procedures could be based on the procedure given in reference /16/.

## CONCLUSION

The HAZ toughness of three low-carbon and one CMn steel have been examined and compared. The examinations included the HAZ microstructures, weld thermal Charpy simulation testing, CTOD testing of bead-in-groove and butt weldments and base material crack arrest testing.

- The weld thermal simulation Charpy toughness of the grain-coarsed HAZ was low for all steels, but the lowest values were always observed for the CMn steel.
- The lowest CTOD values in bead-in-groove and butt weldment testing were obtained for the CMn steel.
- The base material crack arrest properties for the low-carbon steel with the lowest content of phosphorus and niobium were better than for a low-carbon steel with higher contents of these elements, and substantially better than the CMn steel.
- The significance of the low HAZ CTOD values frequently observed is discussed with reference to probabilistic fracture mechanics and testing procedures.

## ACKNOWLEDGEMENT

These results are part of a project sponsored by Nippon Steel Corporation, Fabrique de Fer de Charleroi s.a., AG der Dillinger Hüttenwerke, A/S Norsk Jernverk, Chevron, Norsk Hydro, Statoil, ESSO, ELF and Mobil.

Financial support, technical discussions and kind permission to publish the results are highly acknowledged.

## REFERENCES

/1/ Thaulow, C. , A. J. Paauw, Å. Gunleiksrud and O. J. Næss, "Heat affected zone toughness of a low-carbon microalloyed steel", Metal Construction, 17, 94R-99R, (1985)

/2/ Thaulow, C. , A. J. Paauw and K. Guttormsen, "The heat affected zone toughness of low-carbon microalloyed steels", The Welding Journal, 9, 266s-279s, (1987)

/3/ Thaulow, C. , "Fracture mechanics testing of weldments", to be published in Engineering Fracture Mechanics.

/4/ Thaulow, C. and A. J. Paauw, "Materials characterization with respect to HAZ local brittle zones", to be presented on WELDTECH'88, London November 1988

/5/ Squirell, S. J. , H. G. Pisarski and M. G. Dawes, "$K_{IC}$, CTOD and J tests of weldments", Third ASTM Int. Symp. on Nonlinear Fracture Mechanics, Knoxville October 1986

/6/ Satoh, K. and M. Toyoda, "Guidelines for fracture mechanics testing of WM/HAZ", IIW Doc. X-1113-86, (1986)

/7/ Andersson, H. , C. Debel, C. Thaulow and K. Wallin, "Evaluation of standards for fracture mechanics testing", SINTEF Report STF16 A86138, Trondheim-Norway, (1986)

/8/ Thaulow C. and A. J. Paauw, "Effects of notch depth and orientation with respect to fracture toughness of the HAZ of structural steels", OMAE'88 Seventh Int. Conf. on Offshore Mechanics and Artic Engineering, Houston-Texas February 1988, Proceedings Vol. 3, 275-286, (1988)

/9/ Paauw, A. J. , C. Thaulow, G. Rørvik, B. Lian, Å. Gunleiksrud and T. Simonsen, "The HAZ fracture toughness of low-carbon microalloyed steel for plate thickness from 30mm to 160mm", SIMS'87 Third Int. ECSC Offshore Conference on Steel in Marine Structures, Delft-The Netherlands June 1987, Proceedings, 657-669, (1987)

/10/ Thaulow, C. , A. J. Paauw and G. Rørvik, "Fracture mechanics testing of weld metal for low-carbon microalloyed steels", TMS Symposium on Welding Metallurgy of Structural Steels, Denver-Colorado February 1987, Proceedings, 277-301, (1987)

/11/ Proposed ASTM test method for crack-arrest fracture toughness of ferritic materials, ASTM 1984

/12/ Webster, S. E. and E. F. Walker, "The significance of local brittle zones to the integrity of large welded structures" OMAE'88, Houston-Texas February 1988, Proceedings Vol. 3, 395-404, (1988)

/13/ Koning de, A. C. , J. D. Harston and K. D. Naylor, "Feeling free despite LBZ", OMAE'88, Houston-Texas February 1988, Proceedings Vol. 3, 161-180, (1988)

/14/ Crack-Arrest Testing of Offshore Steel (CAOS), Project proposal, SINTEF, 1987

/15/ Kirkemo, F. ,"Applications of probabilistic fracture mechanics to offshore structures", Appl. Mech. Rev., 41, 61-85, (1988)

/16/ Royer, C. P. , D. P. Fairchild and J. D. Theisen, "Philosophy and technique for assuring HAZ toughness of structural steels prior to fabrication", OMAE'88, Houston-Texas February 1988, Proceedings Vol.3. 247-256, (1988)

Table 1 : Steel chemical composition in wt.%.

| Steel No | C | Si | Mn | P | S | Cr | Ni | Mo | Cu | Al | Ti | Nb | V | B | N | O | Ca | As | Sn | Pb | Bi | Sb |
|---|---|---|---|---|---|---|---|---|---|---|---|---|---|---|---|---|---|---|---|---|---|---|
| A | 0.09 | 0.41 | 1.51 | 0.018 | 0.003 | 0.02 | 0.18 | 0.01 | 0.19 | 0.051 | 0.001 | 0.037 | 0.01 | 0.0002 | 0.008 | 0.0049 | 0.0024 | 0.006 | 0.004 | 0.0002 | <0.0001 | 0.0005 |
| B | 0.10 | 0.41 | 1.32 | 0.007 | 0.003 | 0.06 | 0.17 | 0.02 | 0.23 | 0.024 | 0.002 | 0.020 | 0.01 | 0.0004 | 0.008 | 0.0050 | 0.0016 | 0.028 | 0.016 | 0.0020 | <0.0001 | 0.0020 |
| C | 0.11 | 0.37 | 1.51 | 0.005 | 0.002 | 0.02 | 0.21 | 0.01 | 0.21 | 0.024 | 0.006 | 0.039 | 0.01 | 0.0003 | 0.002 | 0.0052 | 0.0036 | 0.007 | 0.003 | 0.0005 | <0.0001 | 0.0016 |
| D | 0.12 | 0.37 | 1.47 | 0.005 | 0.002 | 0.02 | 0.02 | 0.01 | 0.01 | 0.027 | 0.006 | 0.002 | 0.01 | 0.0003 | 0.002 | 0.0040 | 0.0040 | 0.009 | 0.003 | 0.0002 | <0.0001 | 0.0019 |

Table 2 : Mechanical properties (certificate values).

| Steel No | Yield strength MPa | Tensile strength MPa | Elongation % | Reduction of area % | Impact energy at -40°C 1) J |
|---|---|---|---|---|---|
| A | 377 | 495 | 32 | | 227 |
| B | 353 | 498 | 29 | 76 | 238 |
| C | 377 | 501 | 34 | | 233 |
| D | 332 | 522 | 32 | | 162 |

1) Charpy V-notch specimens in the transverse direction. Average of three specimens

Table 3 : Weld thermal simulation and heat treatment programmes applied for a detailed characterization of the HAZ impact properties.

| Cooling time 1) ($\Delta t_{8/5}$) s | Charpy V-notch testing at -40°C | | | | ITT 3) |
|---|---|---|---|---|---|
| | Single cycle | | Double cycle | | Single cycle |
| | $T_p$ °C | PWHT 2) for $T_p$ °C | $(T_p)_1$ °C | $(T_p)_2$ °C | $T_p$ °C |
| 5 | 600 - 1350 | 1350 | 1350<br>1000<br>750 | 600 - 1100<br>600 - 950<br>300 - 700 | 1350 4)<br>1000<br>750<br>600 |
| 12 | 600 - 1350 | 1350 | 1350<br>1000<br>750 | 600 - 1100<br>600 - 950<br>300 - 700 | 1350<br>1000<br>750<br>600 |
| 24 | 1350 | | | | |
| 35 | | | | | 1350<br>1000<br>750<br>600 |
| 50 | 1350 | | | | |

1) Corresponding to Rosenthal's temperature cycle for thick plates
2) Heat treatment performed at 300°C, 400°C, 500°C, 600°C and 700°C for 1 hour
3) Impact transition temperature (ITT) for both as-simulated and PWHT at 580°C for 1 hour
4) Including PWHT at 400°C for all steels, and PWHT at 600°C for steel B only

Table 4 : Plane strain crack-arrest toughness values at -30°C.

| Steel No. | $K_{Ia}$ 1) MPa.m$^{1/2}$ |
|---|---|
| 1 | 79.2<br>80.2 |
| 8 | 69.5 |
| F | 85.4 |

1) Temperature : -30°C

Table 5 : Crack-arrest toughness $K_a$ at different temperatures with number of duplicate specimens (N).

| | $K_a$ (MPa.m$^{1/2}$) and number of duplicates (N) | | | | | | | |
|---|---|---|---|---|---|---|---|---|
| Temperature | -10°C | | -30°C | | | | -50°C | |
| Specimen type | DUP | N | DUP | N | MRL | N | DUP | N |
| Steel 1 | | | 85 | 1 | 81 | 6 | | |
| Steel 8 | 82 | 2 | 76 | 6 | 1) | | | |
| Steel F | | | 85 | 1 | 110 | 7 | 112 | 2 |

1) Total failure

Table 6 : Average of $K_0$ versus arrest-length ($a_a$) for MRL specimens at -30°C with number of duplicate specimens (N).

| Steel No. | $K_0$ MPa.m$^{1/2}$ | $a_a$ mm | N |
|---|---|---|---|
| 1 | 218 | 150 | 7 |
| 8 | 204 | 168 | 5 |
| F | 224 | 129 | 7 |

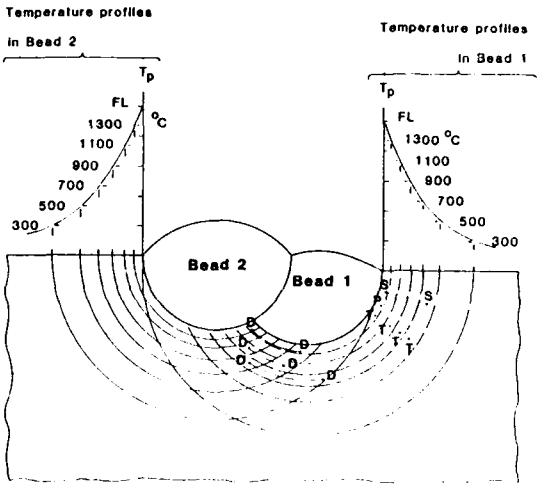


S : Single cycle : Different $T_p$ for $\Delta t_{8/5}$ = 5, 12 and 35s

T : Single cycle : Transition curves for $\Delta t_{8/5}$ = 5, 12 and 35s both as simulated and after PWHT (580°C/1hr)

P : Single cycle : Different temperatures for PWHT (100°C - 500°C)

D : Double cycle : For $(T_p)_1$ = 1350°C, 1000°C and 770°C and $(\Delta t_{8/5})_1$ = 5 and 12s, different $(T_p)_2$ for $(\Delta t_{8/5})_2$ = 5 and 12s.

Fig. 1 : Schematical illustration of the weld thermal simulation parameters related to the position in the real weld.

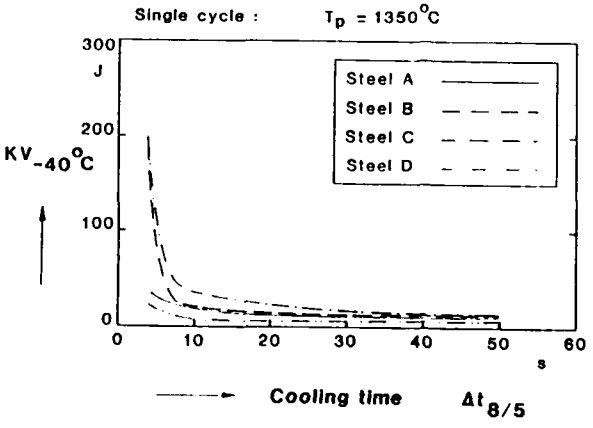


Fig. 2 : Effects of the cooling time ($\Delta t_{8/5}$) on the Charpy V-notch toughness at -40°C of the grain-coarsened HAZ ($T_p$ = 1350°C).

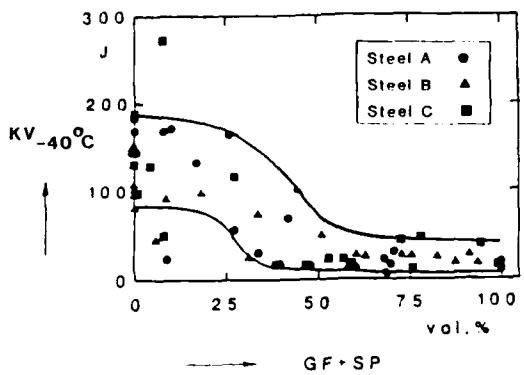


Fig. 3 : Effects of the grain-boundary ferrite and ferrite sideplates on the Charpy V-notch toughness at -40°C.

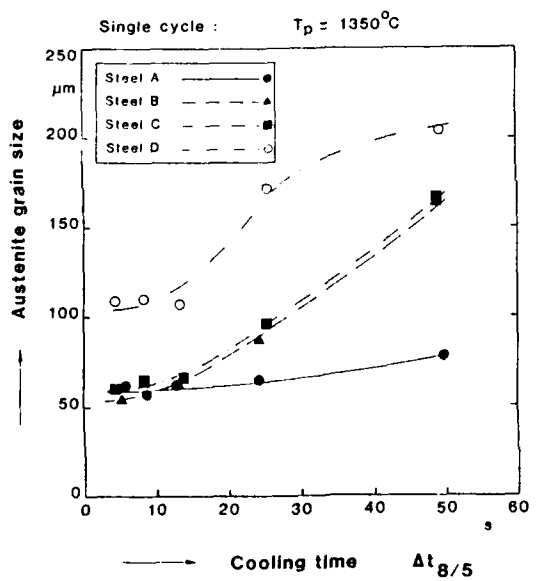


Fig. 4 : Effects of the cooling time ($\Delta t_{8/5}$) on the austenite grain-size ($T_p$ = 1350°C).

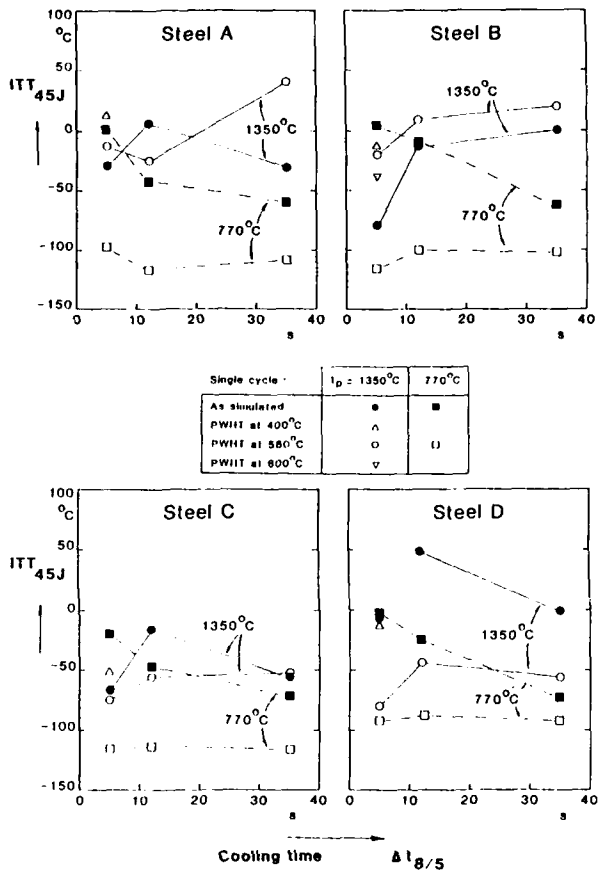


Fig. 5 : Effects of the cooling time ($\Delta t_{8/5}$) on the impact transition temperature (ITT) for KV = 45J.

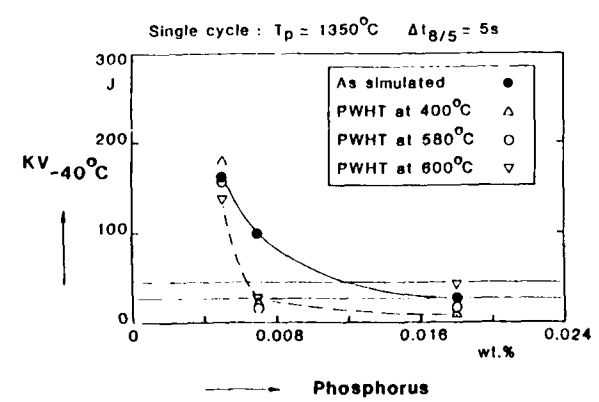


Fig. 6 : Effects of the phosphorus content on the Charpy V-notch toughness at -40°C of the grain-coarsened HAZ with $T_p$ = 1350°C and $\Delta t_{8/5}$ = 5s.

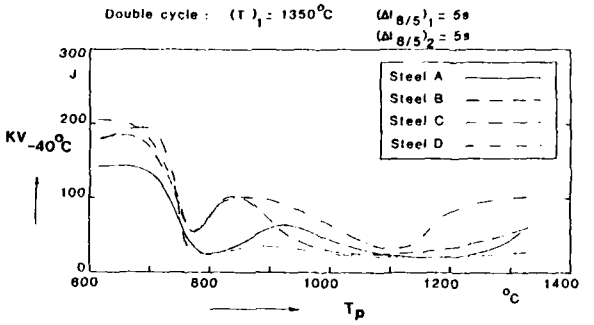


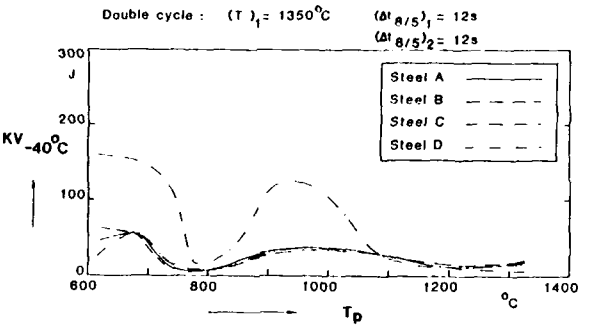


Fig. 7 : Double weld thermal simulation : Effects of the peak temperature of the second cycle on the Charpy V-notch toughness at -40°C for the initial grain-coarsened HAZ ( $T_p$ = 1350°C of the first cycle). The cooling time ( $\Delta t_{8/5}$) was 5s and 12s.

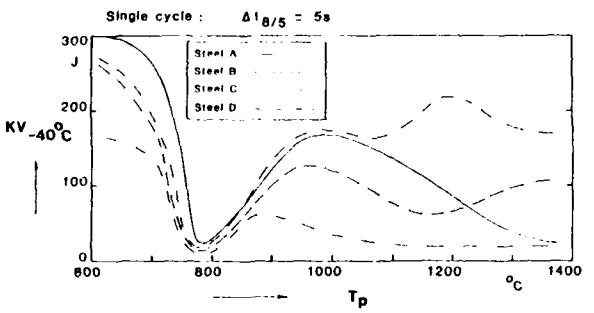


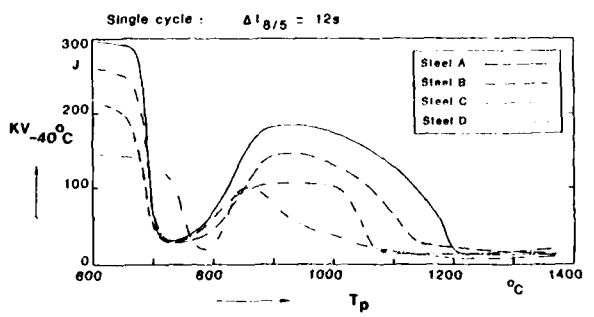


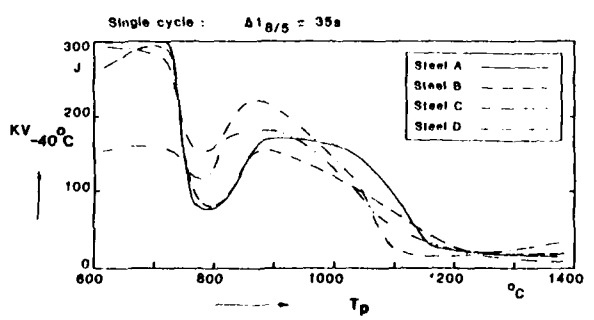


Fig. 8 : Effects of the peak temperature ($T_p$) on the Charpy V-notch toughness at -40°C for the cooling times of 5s, 12s and 35s.

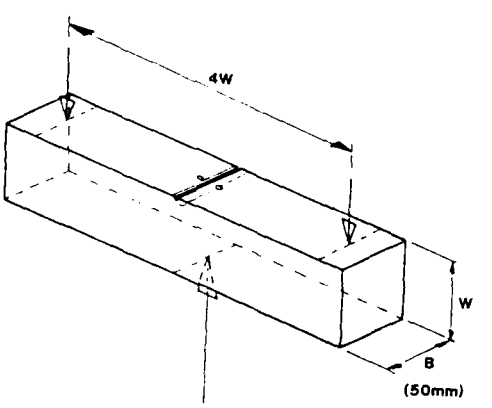


( a )

Fig. 9 ... continue on next page

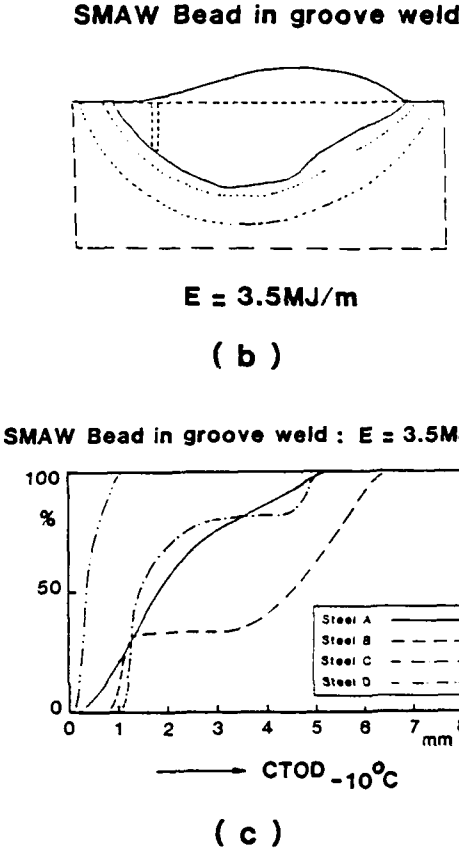


Fig. 9 : Bead-in-groove testing with an electro discharged machined (EDM) notch :
(a) The CTOD specimen.
(b) The weld bead geometry.
(c) Cummulative presentation of the CTOD results expressed as percentage of duplicate specimens.

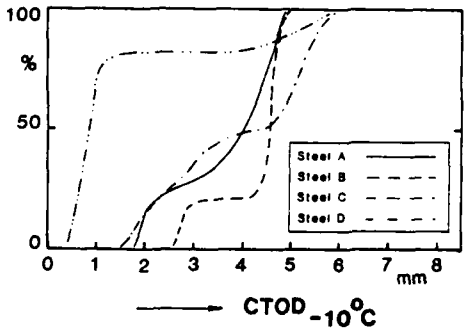


Fig. 10 : Cummulative presentation of the CTOD results from shallow surface notched specimens (a/W = 0.06) from butt weldments, expressed as percentage of duplicate specimens.

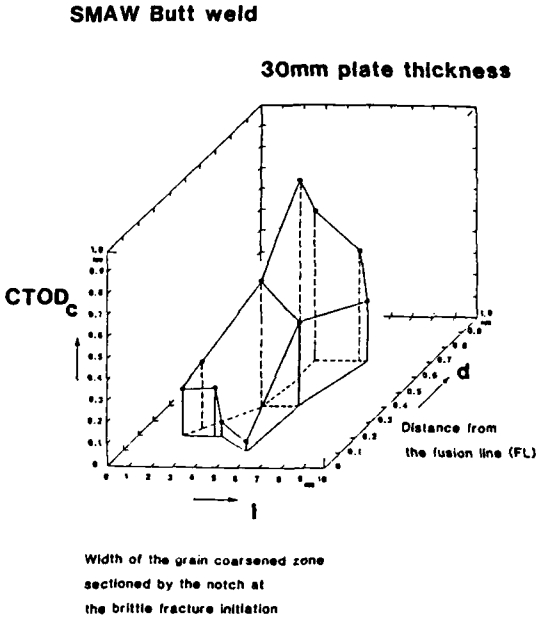


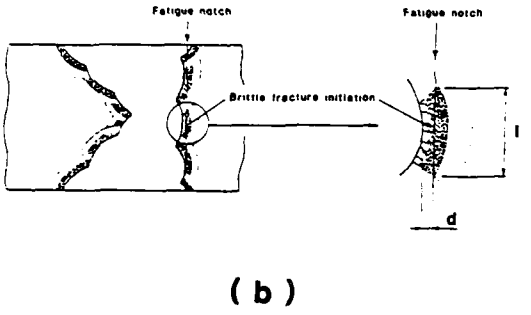


Fig. 11 : Evaluation of parameters influencing upon the initiation of brittle fracture in the grain-coarsened HAZ /9, 10/ :
(a) Relationship between the length of the grain-coarsened HAZ, the distance to the fusion line and the CTOD values for 30mm thick specimens with through thickness notching.
(b) Definition of the parameters used in (a).

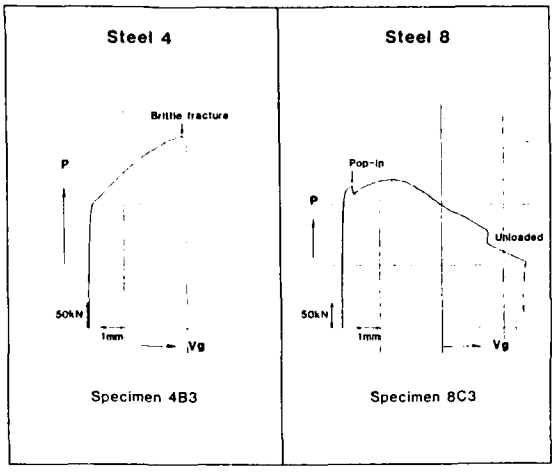


Fig. 12 : Examples of load/clip-gauge records from bead-in-groove specimens of a low-carbon microalloyed steel (Steel 4) and a CMn steel (Steel 8) /12/.

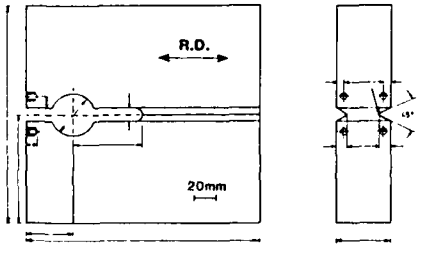


( a )

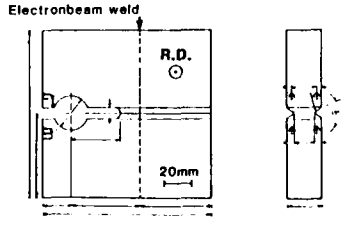


( b )

Fig. 13 : Dimensions of the crack-arrest specimens :
(a) MRL specimen.
(b) DUP specimen.

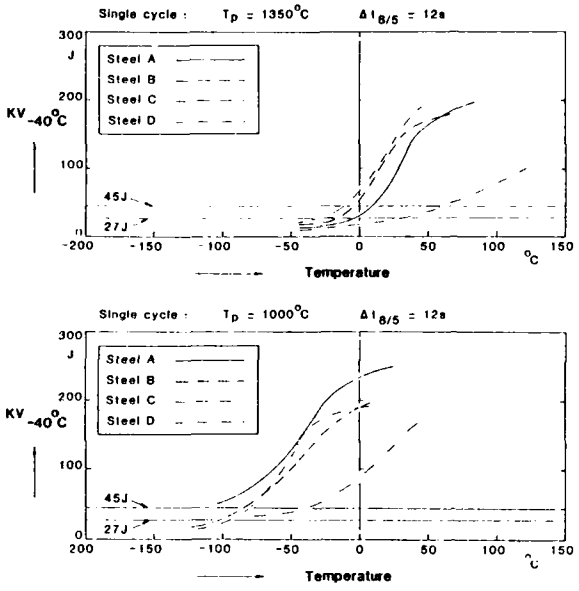


Fig. 14 : Charpy V-notch transition curves of the single cycle weld thermal simulation of the grain-coarsened HAZ (upper figure) and the grain-refined HAZ (lower figure).

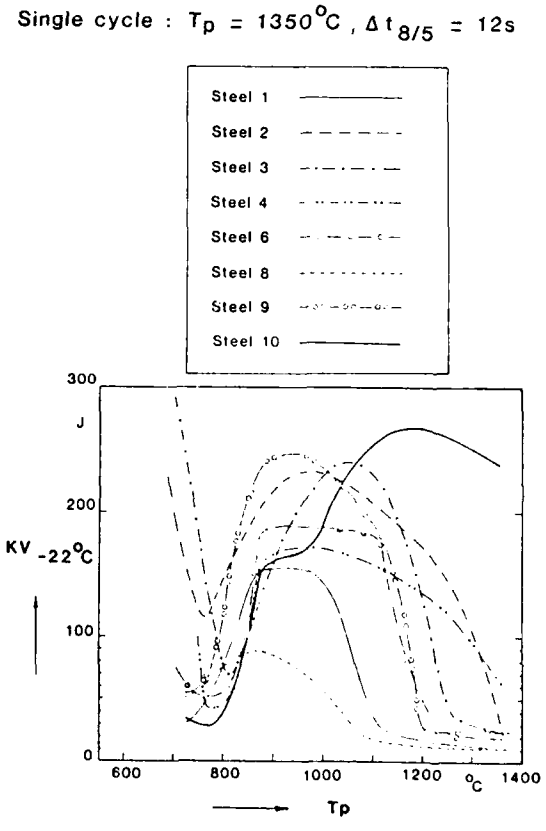


Fig. 15 : Effects of the peak temperature ($T_p$) on the Charpy V-notch toughness at -22°C of weld thermal simulated specimens. Steel 8 is a CMn steel while the other steels are low-carbon microalloyed steels /2/.

# APPLICATION OF TMCP STEELS FOR SHIPBUILDING AND OFFSHORE STRUCTURES

**H. J. Kim**
Welding and Materials Research Institute
Hyundai Heavy Industries Co., Ltd.
Ulsan, Korea

**W. Y. Choo**
Research Institute of Industrial
Science & Technology
Pohang, Korea

ABSTRACT

The type of high tensile steels used for general shipbuilding has been changed from conventional steels to TMCP steel as the latter provides an appreciable improvement in productivity through the broad application of high heat input welding processes and the less restriction in welding workmanship. However, the softening behavior occurring in the HAZ of high heat input welded joint becomes severe with increasing heat input and thus can limit the maximum heat input applied. For offshore application, on the other hand, the appreciation of TMCP steel has not been widely accepted and further evaluations are needed for its favorable usage. Most importantly, based on the studies on HAZ toughness related with local brittle zone, it is discussed that the maximum heat input for TMCP steel can be increased substantially over that specified for conventional steels.

THE QUALITY AND COMPOSITION of structural steel plates used in heavy industries have changed considerably over the last decade, almost entirely in response to demands laid down by fabricators and operators. In the shipbuilding industries, as an integral part of the energy saving measures, the use of high tensile steel ($HT_{}$ steel) having a yield strength over 32 $kg/mm^2$ is gaining wider acceptance to reduce overall weight of ship. At the same time, shipbuilders have modified the high heat input welding procedures to be more practical in shipbuilding and have tried to expand their application to reduce production cost. As a consequence, shipbuilders have looked for HT steel plates which can be welded with high heat input welding processes.

On the other hand, the situation in offshore industries is quite different because of the difference in operating condition. Along with the progress in ocean development, offshore structures have been designed under more severe conditions for operation in deep waters subject to higher waves or in polar region. To cope with these severe conditions, the steel plates for offshore structures have to have an excellent toughness not only in the base metal but in the weld heat affected zone (HAZ), and thus to insure the security of offshore structures from brittle fracture. This has led to an specification requiring prequalification of steel plate and severe limitations in welding practice. Eventually steel makers were requested to perform the crack tip opening desplacement (CTOD) test on the HAZ as a part of prequalification of their steels.

In short, the structural steels needs for shipbuilding and offshore structures are not the same in terms of the user's requirements, i.e. shipbuilders consider its capability for high heat input welding processes but offshore fabricators concern its resistance against brittle fracture in the welded joint.

The scope of this paper is to illustrate from industrial viewpoint how those requirements have been accomodated by the application of advanced steel grades, particularly by that of thermo-mechanical control process (TMCP) steels. The first part of this paper will describe the TMCP technology compared with those of conventional processes and will demonstrate the possible advantages obtained by using TMCP steels. In the second part, steel plates including TMCP steel developed for high heat input welding will be evaluated for selecting a better material in shipbuilding.

In the last part, the capability of TMCP steels for offshore structures will be discussed based on its superior resistance to brittle fracture.

## Characteristic of TMCP steel

The definition of TMCP has not been well established yet, but it is understood to employ such techniques as (a) rolling process in the non-recrystallized austenite region, (b) rolling process in two phase ( $\alpha + \gamma$ ) region, (c) lower heating temperature of slab and (d) accelerated cooling after controlled rolling. Because the most striking improvement in strength and toughness can be obtained through a combined process of accelerated cooling and controlled rolling, the accelerated cooled type TMCP (hereinafter referred to as TMCP) has been applied very widely for manufacturing various grades of steels.

Fig.1 compares the manufacturing process of TMCP steel with those of conventional steels. TMCP with water cooling is simply an improved version of controlled rolling (CR) wherein slab preheating and rolling conditions are controlled more strictly than the conventional CR practice. As shown in this figure, the TMCP consists of the two step controlled rolling, in which the first rolling is performed in the recrystallized region and the second one in the non-recrystallized region of austenite, and the accelerated cooling in the transformation ( $\gamma \rightarrow \alpha$ ) region. The purpose of controlled rolling which makes up the first half of the TMCP is to obtain a fine microstructure which can reserve good toughness, and that of accelerated cooling which makes up the second half is to introduce hard phases into ferrite matrix and thus to increase the strength of steel plate(1). The

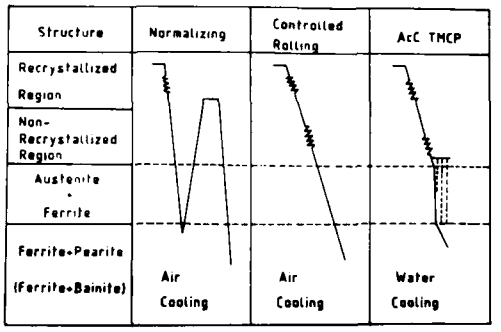


Fig.1 Schematic drawing of manufacturing processes of high tensile steel plates.

microstructural difference between the air-cooled normalized and the accelerated-cooled TMCP steels is presented in Fig.2. The second phase observed in the normalized steel has a typical lamellar structure of pearlite while that in TMCP steel is likely a single phase of bainite and is distributed in a very fine scale. By utilizing this strengthening effect of accelerated cooling the TMCP makes it possible to decrease the carbon equivalent to less than that of conventional steels resulting in the improvement of weldability.

## Application of TMCP Steels for Shipbuilding

### High Tensile Steels for Shipbuilding

The employment of high tensile (HT) steel plate for shipbuilding has been initiated in the 1960's in Japan, and increased substantially for last ten years to meet the growing


(a) (b)

Fig.2 Microstructure of high tensile steels manufactured (a) by normalizing treatment and (b) by TMCP. P:Pearlite, B:Bainite

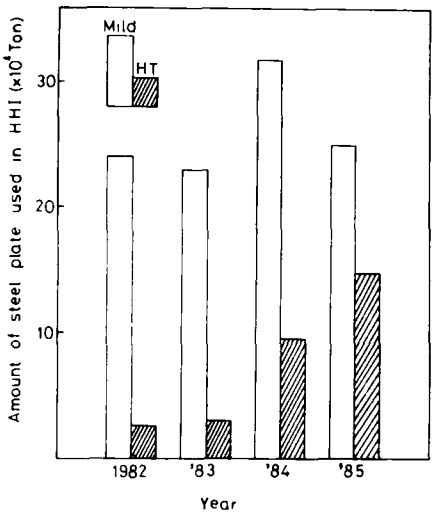


Fig.3 Amount of mild and high tensile steel plates used for shipbuilding

demand for large-sized vessels. This resulted in a considerable weight reduction of hull structure.

In the present rules of the Ship Classification Societies, two grades of HT steel are specified depending on yield strength level, i.e. HT steel with a yield strength of 32 kg/mm$^2$ (hereinafter referred to as HT32) and HT steel of 36 kg/mm$^2$ (HT36). In this company, the HT steel has begun to use since 1980 and its usage increased very repidly year as shown in Fig.3. However most of the HT steel used were HT32 plates and the HT36 plates have scarcely been used. A part of the reason for this is the relatively poor weldability of the conventional HT36 steels since they have a relatively high carbon equivalent and contain microalloy elements such as Nb and V and thus require preheating to prevent cold cracking and a restricted welding heat input for satisfying the required HAZ toughness. Due to these problems, the introduction of TMCP steels was highlighted in the shipbuilding industries and it contributed significantly to the greater use of HT steels, particularly HT36 steel(2). Under this circumstances, even higher tensile steel with yield strength of 40 kg/mm$^2$ (HT40) has been developed very recently by applying TMCP and is now being used in Japan for fabricating ship strength decks and other important hull strength members(3).

## Steels for High Heat Input Welding

In the normalized steels, the carbon equivalent (Ceq.) value becomes higher with the strength level as listed in Table 1. As a consequence, HT steels are more sensitive to heat cycles than the mild steel with higher susceptibility to weld cracking at HAZ in low heat input welding and with lower impact toughness in the HAZ associated with high heat input welding.

Although the weld cracking problem was able to be managed mostly by using low hydrogen type welding consumables, the HAZ embrittlement occurring in the high heat input welded joint could not be solved since it is caused by the austenite grain growth during welded thermal cycle. Hence, the application of high heat input welding processes such as one-side submerged arc welding (SAW) and electro-gas or slag welding processes were restricted severely in welding conventional HT steels.

In an effort to develop steel plate that can withstand high heat input several kinds

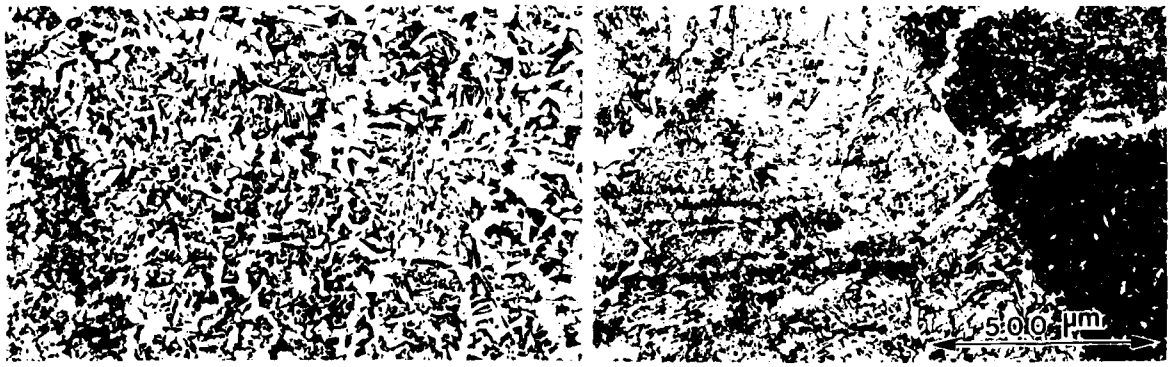


(a) (b)

Fig.4 Microstructures of HAZ near fusion boundaries in (a) Ti-treated and (b) non Ti-treated steels.

Table 1 Typical carbon equivalent (Ceq.) of steel plate produced by normalizing treatment

| Steel grade | min. Y.S. ($kg/mm^2$) | min. Cv, at $-40^{\circ}C$, ($kgf \cdot m$) | Ceq.* |
|---|---|---|---|
| E | 24 | 2.8 | 0.27 |
| EH32 | 32 | 3.5 | 0.37 |
| EH36 | 36 | 3.5 | 0.41 |

$$^{*}Ceq. = C + \frac{Mn}{6} + \frac{Cr+Mo+V}{5} + \frac{Ni+Cu}{15}$$

of HT steels have been developed by adding various alloying elements which are known to be effective in suppressing the grain growth of in gathering impure elements such as N(4-7) . Addition of Ti was the most popular method adopted for this purpose(4-6). Metallurgical basis for Ti addition is to form finely distributed TiN precipitates which are stable at high temperatures and thus to suppress the grain growth in the HAZ near fusion boundary as well as to promote formation of ferrite by acting as nuclei of -transformation. Fig.4 (a) and (b) show HAZ microstructures of Ti-treated (Ceq. = 0.41) and non-Ti treated steels (Ceq. = 0.38) respectively. The welding was done on the 15.5mm thick plate with electro-gas welding process. As expected, not only the width of coarse grained region but also the size of prior austenite grains revealed along the fusion boundaries are much smaller in the Ti-treated steel than those in the non-Ti treated (conventional) steel. Such differences in HAZ microstructure would influence the impact toughness property of HAZ. The result of Charpy impact test made on the both welded joints are shown in Fig.5. The impact properties in the HAZ of Ti-treated steel meets the required value for the hull structural plate of DH grade while in the case of the non Ti-treated steel plate the resultant HAZ impact values are below than that required.

With such a favorable result, even higher heat input was applied on a Ti-treated steel plate to find out the maximum heat input applicable. Fig.6 shows the result of Charpy impact tests performed on the electro-gas welded joint of 24mm thick Ti-treated steel plate (Ceq. = 0.41). The applied heat input was 160 KJ/cm. As shown in this figure, this welded joint satisfies no longer the required value specified for the base plate of DH grade.

This result and that shown in Fig.5 demonstrate that Ti-treatment of steels is quite effective in raising the maximum heat input but still has a clear limit at about 100 KJ/cm. Besides, it is also kept in mind that since Ti-treatment does not affect the carbon equivalent of steel plate, this treatment can not relieve the various restrictions applied on the welding workmanship of HT steels. This fact is quite important since the productivity of shipbuilding is largely limited by those restrictions on welding workmanship(2).

Concerning the limited function of Ti-treatment, it has been claimed(8,9) that a part of TiN precipitates dissolve in the area adjacent to the fusion boundary heated at a temperature close to the melting point so that it can not act as a pinning site or as a nucleation site. Futhermore, it was reported (10) that Ti and free N produced as a result of dissociation of TiN exhibit a deleterious effect on HAZ toughness. Another thing to mention here is that a formation of upper bainite or side plate ferrite can not be prevented in the HAZ of both steels unless the carbon equivalent of steel plate lowers sufficently. Therefore, the steel plate for high heat input welding would better be designed in a way to lower its carbon equivalent and thus to suppress the formation of upper bainite. The adoption of TMCP made it possible and thus can secure the HAZ toughness even in the non Ti-treated condition.

Actually, when TMCP steel was used as a base metal, higher heat inputs over 100 KJ/cm could be applied. Fig.7 shows the result of Charpy impact test performed on the 25mm thick TMCP steel plate (Ceq. = 0.32) welded with heat input of 173 KJ/cm. It is understood from this result that such a high heat input is still applicable for TMCP steel. With further increasing heat input, it was found that the weld metal toughness drops to a larger extent than the HAZ toughness. In other words, the practical limitation in welding heat input for TMCP steel is set by the limitation of the weld metal toughness but not by its HAZ toughness. Therefore, the maximum heat input for TMCP steel can be further increased in future by the development of welding consumables.

As described above, it is quite clear that there are various advantages in fabricating ship structures where conventional steel plates are replaced with TMCP steels in terms of wide application of high heat input welding processes and less limitation on the welding workmanship. However, it is worth mentioning here that there are several things to be considered in fabricating TMCP steel. One of those is the strength reduction of welded joint. It is mainly because the strength increased by accelerated cooling process is lost either by weld thermal cycles having slow cooling rate or by post weld heat treatment (PWHT).

HAZ Softening

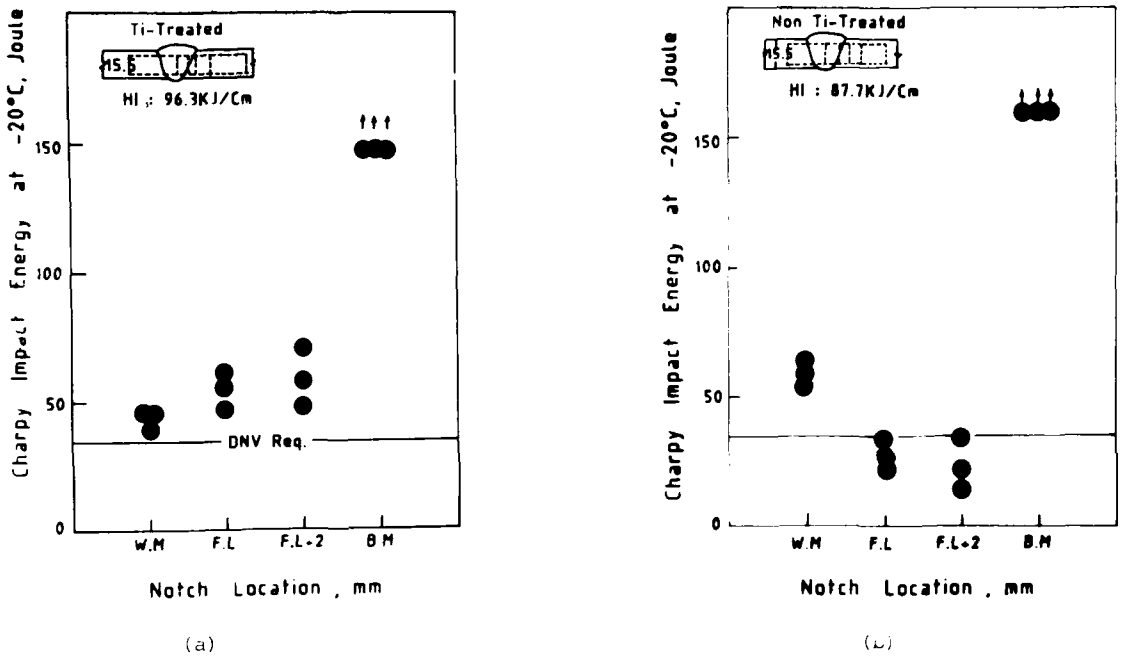


Fig.5 Variation of Charpy impact energy in the electro-gas welded joint of (a) Ti-treated and (b) non Ti-treated steels.

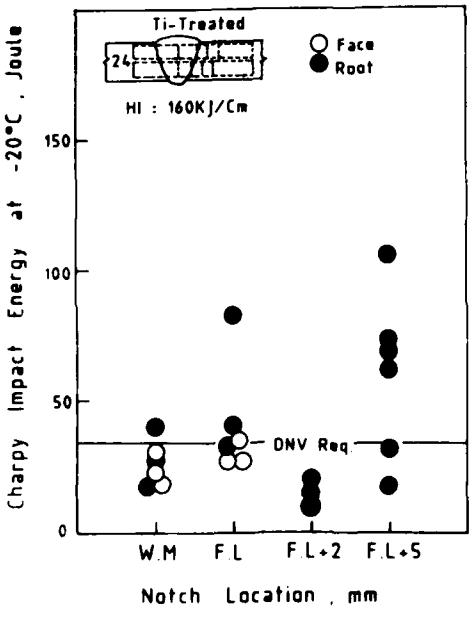


Fig.6 Variation of Charpy impact energy in the electro-gas welded joint of Ti-treated steel with heat input of 160 KJ/cm.

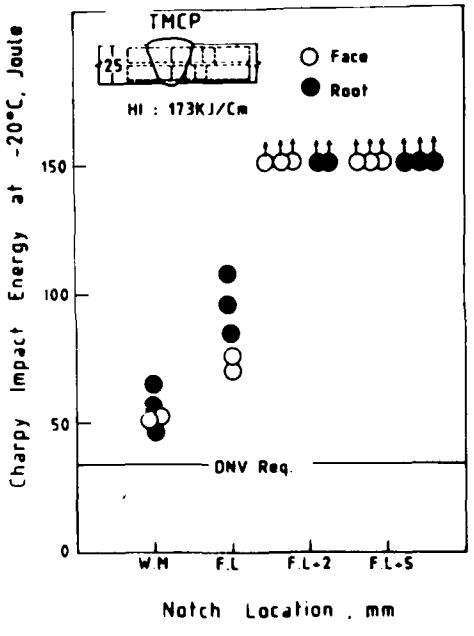


Fig.7 Variation of Charpy impact energy in the electro-gas welded joint of TMCP steel with heat input of 173 KJ/cm.

When a high heat input welding is applied on the TMCP steel plates, softening in HAZ occurs since the strengthening effect of the accelerated cooling is diminished by the slow cooling rate involved in the weld thermal cycle. Fig.8 shows an example of the hardness profiles accross the HAZs of the TMCP and the normalized steels. The normalized steel shows higher hardness values in its HAZ while the TMCP steel shows lower hardness values. This softening certainly increases as the welding heat input increases or as the carbon equivalent of base metal decreases.

The degree of softening, which can be represented with the minimum hardness value measured in HAZ, is plotted as a function of heat input in Fig.9. As a result of softening in HAZ, the transverse tensile strength of TMCP steel welded joint decreases with the increase of welding heat input as shown in Fig.10. It was also noted from the broken tensile specimens that fracture always occurred within the HAZ as shown in the inserted photograph of Fig.10. This result demonstrates a important role of HAZ softening in determining the tensile strength of TMCP steel welded joint. Therefore, since the degree of softening increases as the carbon equivalent decreases at a given strength level, the lower limit of carbon equivalent should be specified considering the maximum heat input used in the shipbuilding industries in order to preserve the base metal strength even after the high heat input welding.

If post weld heat treatment (PWHT) is applied, further softening is anticipated. Fig.11 shows the result of hardness measurements before and after PWHT at 580°C for 30 minutes. This result clearly shows the additional softening occurring in the HAZ as well as in the base metal. In order to emphasize the significance of HAZ softening, the tensile strengths of TMCP steel welded joint were compared with those of normalized steel in the as-welded and in the PWHT condition. A significant reduction in tensile strength is shown in the TMCP steel welded joint but a little change in the normalized steel. Since the strength obtained in the PWHT condition falls below the specified strength of 50 kg/mm$^2$, the application of PWHT on the TMCP steel structure should be limited unless the PWHT temperature lowers substantially.

## Application of TMCP Steels for Offshore Structure

In the offshore industries, a combination of increased use of fracture mechanics by design engineers and the identification of local brittle zones (LBZ) in the HAZ by metallurgist has required quantitative toughness analysis in those regions. For this purpose, some oil companies have developed HAZ toughness evaluation programs (prequalification tests) which were published in 1987 as API Recommended Practice 2Z, and also specified the minimum CTOD values. The typical CTOD values required are 0.15-0.35mm at -10°C, depending on the specific project.

Traditionally, offshore structural steels have been delievered in the normalized condition and thus have a high carbon equivalent.

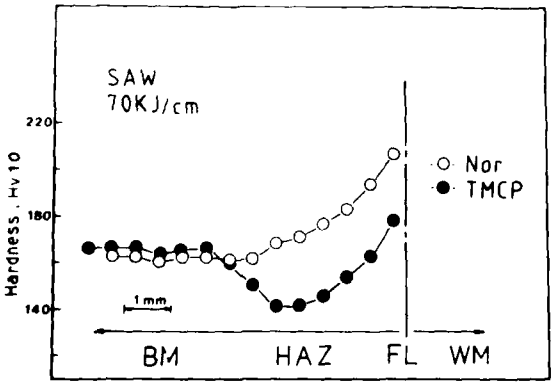


Fig.8 Hardness profiles in the HAZs of normalized and TMCP steels welded with heat input of 70 KJ/cm.

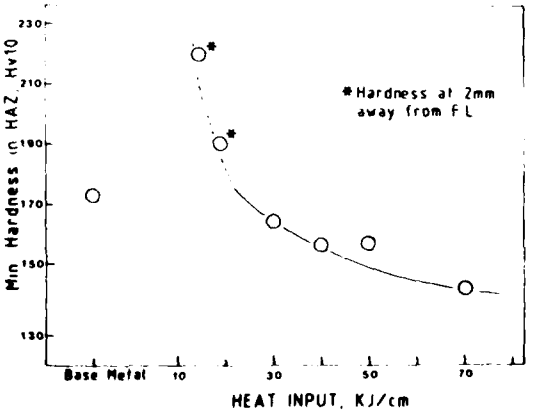


Fig.9 Variation of minimum hardness in HAZ of TMCP steel with welding heat input.

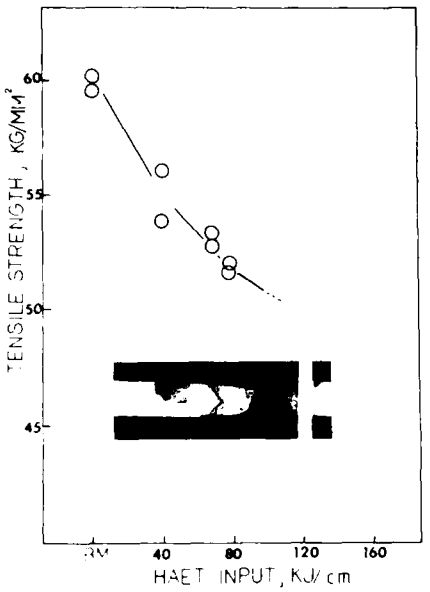


Fig.10 Effect of welding heat input on the transverse tensile strength of TMCP steel welded joint.

However, as the TMCP has been found to be very effective in improving weldability of steels through the reduction of carbon equivalent, the TMCP steel was eventually specified in API specification 2W for offshore structures in 1987.

In this institute, the CTOD property of TMCP steel welded joint was studied and compared with those of normalized steels. The steels selected were API 2H Gr.50 of TMCP type and BS 4360 Gr.50D delievered in normalized condition, and their carbon equivalents were calculated as 0.31 and 0.41% respectively. The thickness of both plates were 45mm. The groove was made in K shape and the welding was performed either by shielded metal arc welding (SMAW) with low heat input of 15 KJ/cm or by submerged arc welding (SAW) with high heat input of 50 KJ/cm. Machined notches were made to locate fatigue crack tip along the coarse grained region of HAZ. The CTOD tests at four different temperatures, ie -10, -40, -60 and -80°C, were performed in accordance with BS 5762, and their results are shown in Fig.13. From this figures, it is noted that TMCP steel exhibits better HAZ toughness than the normalized steel regardless of heat input level and that TMCP steel appears to be less sensitive to the welding heat input. More significantly, all of the normalized steel specimens tested exhibited brittle fracture mode in their fracture surface, only five out of 17 TMCP steel specimens did. Through a careful examination of sectioned specimens, it was found that the brittle fracture in these specimens always initiated from the coarse grained region of HAZ, so called local brittle

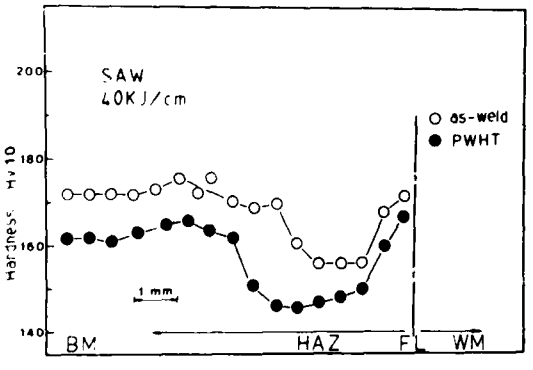


Fig.11 Effect of PWHT on softening of TMCP steel welded joint.

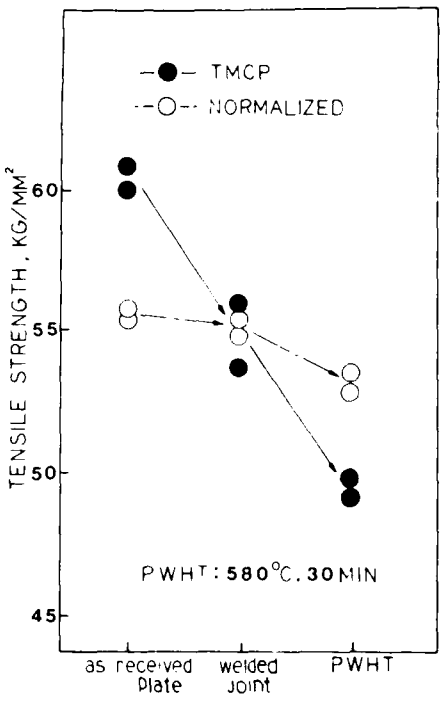


Fig.12 Effect of manufacturing processes on the tensile strength of welded joint.

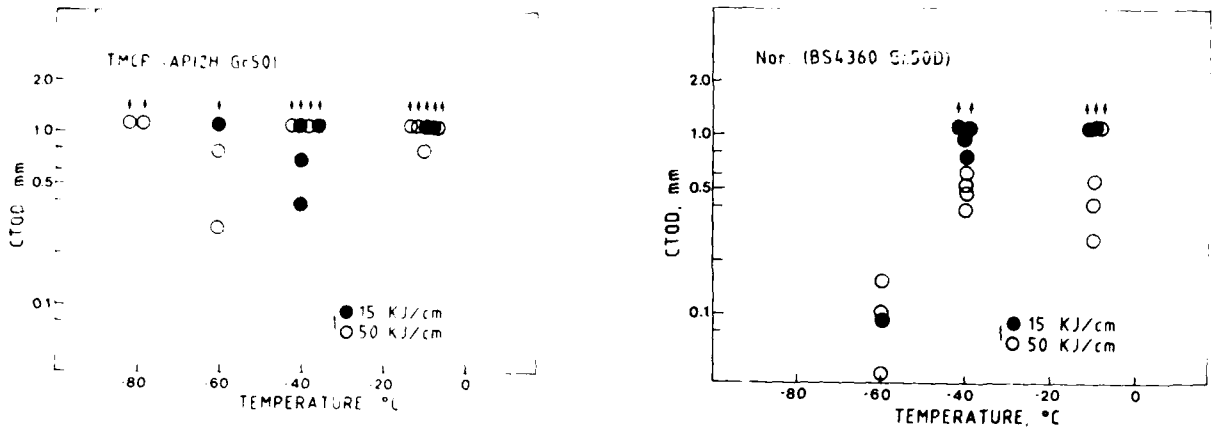


Fig.13 CTOD test results of the HAZ in as-welded condition. (a) TMCP and (b) Normalized steels

zone (LBZ).

When the CTOD value is evaluated, the notch position is most important with respect to the coarse grained HAZ. Fig.14 shows the relationship between the CTOD value and the fraction of coarse grained region located along the fatigue crack front. It shows that the CTOD value drops substantially when the fraction of coarse grained HAZ exceeds a certain amount, ie about 5% in the case of normalized steel and about 15% in the TMCP steel. This result along with the CTOD test result (Fig.13) indicates that TMCP steel is more resistant to LBZ than the normalized steel in the case of 50 KJ/cm.

Recently perhaps reconnizing the TMCP steel as more LBZ-resistant steel than the normalized steel, several oil companies have come to specify TMCP steel to be used exclusively for the primary structure. However, they did not consider to alleviate the various restriction imposed on the welding practice, for example maximum heat input of about 50 KJ/cm and preheating temperature requirement of AWS D1.1, which have been applied to normalized steel. From the fabricators point of view, the current heat input restriction, normally 15-50 KJ/cm, could be modified into a broader range reflecting the excellent CTOD properties obtained in this heat input range. In addition the preheating temperature could be lowered significantly considering the low carbon equivalent of TMCP steel so that the advantage of TMCP steel could be fully utilized and favored in the offshore industries as has been accomplished in the shipbuilding industries.

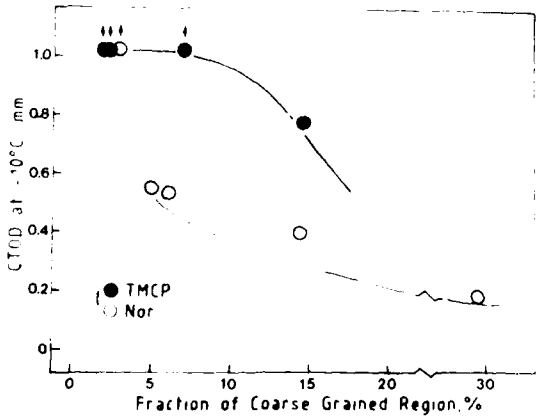


Fig.14 Variation of CTOD value at -10°C with the fraction of coarse grained region.

## Concluding Remark

After the introduction of TMCP steels in early 1980's, it has been recognized to possess a good combination of mechanical properties and weldability, and they have been applied very widly by replacing conventional steels. In shipbuilding industries, particularly TMCP steel plays very important role not only in escalating the use of high tensile steels which can reduce hull weight but also in saving the fabrication cost through the less restriction on the welding practice. The maximum heat input, for example , can be raised up to the working limit of welding consumables without having any problems in HAZ toughness. However, the drawback

of TMCP may be the appreciable strength reduction of the high heat input welded joint and the limitation of PWHT.

In offshore industries, however, the TMCP steel has not been appreciated as much as that in the shipbuilding industries. The main reason for this seems to be the conservative attitude of oil companies in selecting steel materials for their structures. However, under the recent change in offshore structures , i.e. the steel plate becomes thicker and the HAZ toughness is of the most important concern, there is a movement to use TMCP steel preferentially for the primary structure. It is further expected that, through more systematic studies on HAZ toughness record related with LBZ and on the accumulating supply, the use of TMCP steel will be stimulated more intensively and come to be favored in the offshore industries as well.

## Reference


(1) I. Kozasu, "Welding Metallurgy of Structural Steel", ed. J.Y.Koo, pub. AIME, p.63 (1987)

(2) H. Kitada, NK Technical Bulletin, p.53 (1986)

(3) H. Kitada, Y. Yajima and S. Noda, Transaction of the West-Japan Society of Naval Architects, No.74, August (1987)

(4) S. Kanazawa et al., Tetsu-to-Hagane, 61 (11), p.2589(1975)

(5) Y. Kazamatsu et al., Tetsu-to-Hagane, 65(8), p.1232 (1979)

(6) P.L. Threadgill, Welding Institute Research Bulletin, 22(7), p.189(1981)

(7) M. Nakanishi et al., IIW Doc. IX-1281-83 (1983)

(8) I. Watanabe and M. Suzuki, Metal Construction, 16(5), p.311(1984)

(9) S. Mukae, K. Nishio and M. Katoh, IIW Doc. IX-1426-86 (1986)

(10) M.Suzaki, K.Tsukada and I.Watanabe, Int. Conf. on Offshore Welded Structure, paper #16, London, Nov. (1982)

(11) D.P.Fairchild, J.D.Theisen and C.P.Royer, Proc. of 7th Int. Conf. on OMAE, Vol.III, p.247(1988)

# ADVANCED TMCP STEEL PLATES FOR OFFSHORE STRUCTURES

**K. Ohnishi, S. Suzuki, A. Inami, R. Someya, S. Sugisawa**
Sumitomo Metal Industries, Ltd.
Kasima Gun
Ibaraki Prefecture, Japan

**J. Furusawa**
Sumitomo Metal Industries, Ltd.
Amagasaki City
Hyogo Prefecture, Japan

ABSTRACT

Exploitation of new offshore resources requires high strength steel with good weldability. Low Pcm steel, transformation strengthened by an accelerated cooling process, has been meeting this requirement aided by the use of the full potential of microalloying elements. In this process it is very beneficial to use niobium (Nb), a small amount of which strengthens the base plates and prevents the weld heat affected zone (HAZ) from softening, through precipitation of Nb(C,N) or lowering transformation temperature. Niobium also toughens the base plates by refining grains. On the other hand, the combination of microalloying elements (boron (B), titanium (Ti), and so on) can improve the HAZ toughness. Thus by combining the effect of microalloying elements and the accelerated cooling method appropriately we have developed steel characterized by Nb-Ti-B microalloying, reduced aluminum (Al) and balanced nitrogen (N). This steel can match the requirements of high-heat-input welding as applied to offshore structure used in low temperature.

RECENT EXPLOITATION OF OIL AND GAS tends to be moving into the regions and environments which are very hard on steel structures. This is why steel with sufficient toughness at low temperatures, such as -60°C, are required. On the other hand, the steel, whose properties are not damaged by high-heat-input welding, are required in order to increase welding efficiency. But up to this time, heat-input has been restricted in welding steel used in low-temperature because grain coarsening, which occurred through high-heat-input, deteriorates the welded joint toughness [1].

Therefore, we investigated the effect of microalloying elements in the high-heat-input welded joint and have developed a new type of steel which had high toughness in the welded joint even with high-heat-input.

## THE METHOD OF IMPROVING THE HAZ TOUGHNESS IN HIGH-HEAT-INPUT WELDING

The method of improving the HAZ toughness in high-heat-input welding can be summarized into as follows:

1. improvement of the matrix toughness;
2. prevention of microcracks (prevention of producing M-A constituents);
3. control of the microstructure;
   a. suppression of bainite and/or martensite transformation;
   b. refinement of the microstructure.

We gave detailed consideration to these three points.

IMPROVEMENT OF THE MATRIX TOUGHNESS - Effective ways to improve the matrix toughness are to decrease carbon equivalent (Ceq.= C+Mn/6 +(Cu+Ni)/15+(Cr+Mo+V)/5) and to eliminate residual elements. The recent development of the Thermo-Mechanical Control Process (TMCP) enables the production of high tensile strength steel with a low Ceq. [2][3].

Unfortunately, however, a high-heat-input welding tends to soften the welded joint strength of the TMCP steel. The addition of niobium had been considered to prevent softening of TMCP steels in welding. Fig.1 illustrates the influence of niobium content on the strength of the welded joints and that of the weld metals. A small amount of niobium in base metal can prevent the weld metal from softening, since the niobium, which dissolves into weld metal, holds the strength of the welded joints through precipitation of Nb(C,N).

Large amounts of niobium, however, tend to deteriorate toughness of the welded joints. Then a small amount of niobium, less than 0.020%, was microalloyed to put its strengthening-and-toughening effect into a practical

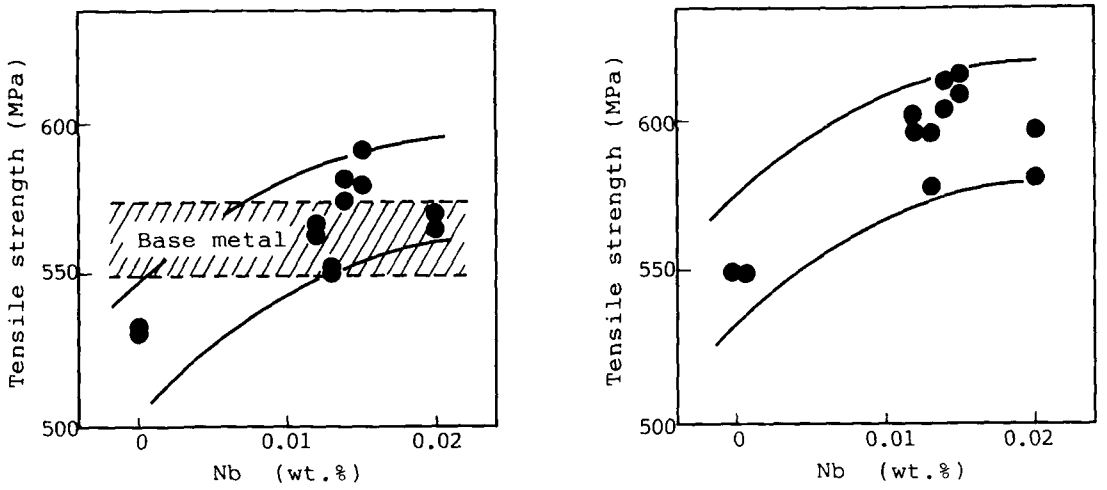


(1) Butt-weld transverse tensile test

(2) All-weld-metal tensile test

Fig.1 The Influence of Nb content in base metal on tensile strength of butt-weld-joints and all-weld-metals
Base metal : 0.11C-0.3Si-1.4Mn
Weld joint : SAW high-heat-input welding

use in the TMCP. The addition of a large quantity of niobium generally induces some deterioration in the toughness of the weld [4]. On the contrary, we found that a small amount of niobium, up to 0.020%, hardly affects the toughness of the weld metal and the HAZ at all, as shown in Fig.2.

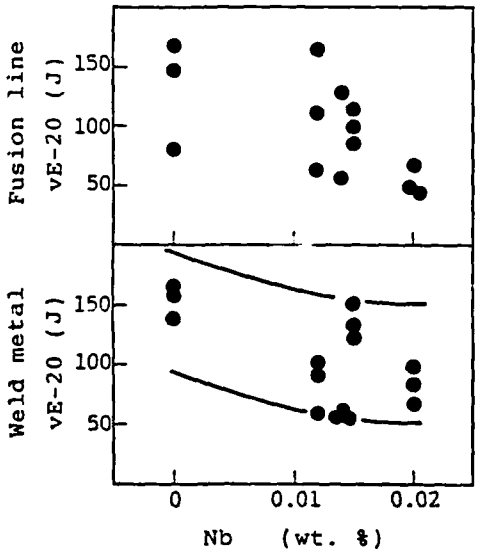


Fig.2 The Influence of Nb content in base metal on Charpy absorbed energy of weld metal and fusion line
Base metal : 0.11C-0.3Si-1.4Mn
Weld joint : SAW high-heat-input welding

Another effective method to improve the matrix toughness is to reduce the nitrogen because nitrogen in solid solution deteriorates the toughness of the matrix. Reduction of soluble nitrogen can be achieved by two means: one is to reduce the total nitrogen content and the other is to add some strong nitrogen-scavengers, e.g. Al, Ti, B, Zr and so on. This point will be discussed later.

PREVENTION OF MICROCRACKS - Increase of the hardeningability of steel has a general trend of producing M-A constituents [5] in HAZ. M-A constituents can easily create Griffith cracks between the M-A constituent and matrix ferrite and damage the toughness of the HAZ. Accordingly it is important to optimize the hardeningability of the steel and to decrease the amount of M-A constituents.

CONTROL OF THE MICROSTRUCTURE - Suppression of bainite and/or martensite transformation and refinement of the microstructure are very effective in improving the HAZ toughness.

Fig.3 shows the effect of changing the microstructure and the influence of soluble nitrogen on the toughness of the fusion line in the high-heat-input (13kj/mm) welded joints[6]. As mentioned before reduction of soluble nitrogen results in the improvement of the HAZ toughness, but this trend is dependent on the microstructure, as shown in Fig.3.

The vTs value of the HAZ, composed of a large quantity of bainite, can not be lowered below -40°C even if soluble nitrogen is reduced to zero. It is consequently recognized that the microstructure in the HAZ should be composed of ferrite-pearlite in order to obtain sufficient toughness at -60°C.

In addition to this, it is unquestionable that the refinement of the HAZ microstructure always achieves high toughness.

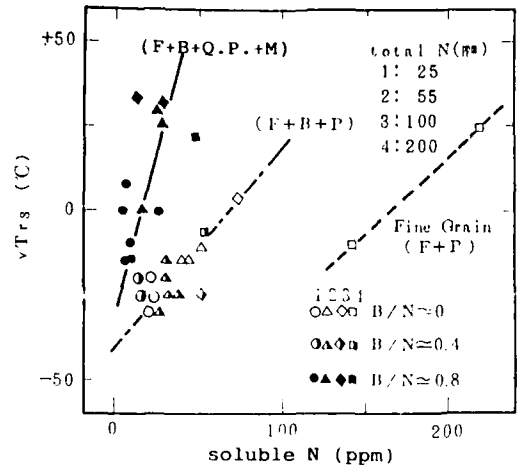


Fig.3 The Influence of soluble N and microstructures on the toughness of the fusion line
Note F: ferrite P: pearlite
B: bainite M: martensite
Q.P.: quasi-pearlite
B/N : weight ratio of B to N

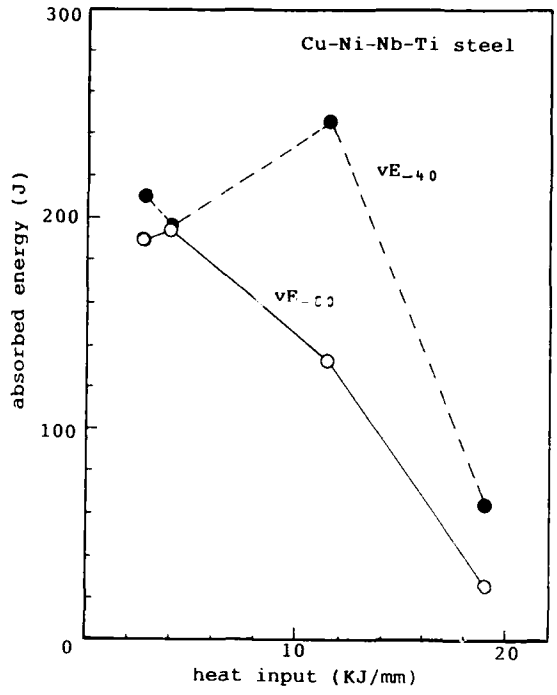


Fig.4 The Influence of heat-input on the toughness of the welded joint HAZ, which indicates the most inferior toughness

## DEVELOPMENT OF CU-NI-NB-TI STEEL

Taking into consideration of the three HAZ-toughness-improving measures mentioned before, we had developed Cu-Ni-Nb-Ti steel [7], of which the chemical composition is shown in Table 1. A small amount of niobium, the effect of which is promoted by an accelerated cooling method (one sort of TMCP), toughens the base metal and prevents the weld metal from softening. On the other hand, a small amount of titanium toughens the welded joints: Finely-dispersed TiN, which is very stable nitride at a high temperature, can prevent the austenite grain from coarsening during heating in the weld thermal cycle through the Zener pinning effect [8]. Finely-dispersed TiN can become the nucleation site of pro-eutectoid ferrite during cooling, and the reduction of soluble nitrogen by titanium addition also contributes to the improvement of the HAZ toughness [9][10][11].

Table 1 Chemical Composition (wt %)

| C | Si | Mn | P | S | Cu | Ni | Nb | Ti | Sol. Al | N | Ceq* | $P_{cm}$** |
|---|---|---|---|---|---|---|---|---|---|---|---|---|
| 0.08 | 0.22 | 1.33 | 0.013 | 0.002 | 0.17 | 0.24 | 0.015 | 0.017 | 0.023 | 0.0020 | 0.33 | 0.17 |

* $Ceq = C + \frac{Mn}{6} + \frac{Cu+Ni}{15} + \frac{Cr+Mo+V}{5}$

** $P_{cm} = C + \frac{Si}{30} + \frac{Mn}{20} + \frac{Cu}{20} + \frac{Ni}{60} + \frac{Cr}{20} + \frac{Mo}{15} + \frac{V}{10} + 5B$

Table 2 Properties of the Base Metal

| Thickness (mm) | Tensile test | | | | Charpy impact test | | |
|---|---|---|---|---|---|---|---|
| | Direction | YS(MPa) | TS(MPa) | El(%) | Direction | $vE_{-60}$ (J) | vTs(°C) |
| 30 | T | 449 | 509 | 36.6 | L | 307 | -112 |

T : Transverse L : Longitudinal

The Cu-Ni-Nb-Ti steel indicates very high toughness at -60°C in the base metal, as shown in Table 2. But the Cu-Ni-Nb-Ti steel can not keep its HAZ toughness above 10kj/mm heat-input welding, whereas it indicates very high toughness in the HAZ at -60°C up to 10kj/mm heat-input welding, as shown in Fig.4. This is presumed as: at high-heat-input welding, TiN, kept for a long time near the peak temperature on the fusion line, is partly dissolved [12]. This results in some grain coarsening, and the increase of nitrogen in the solid solution can not be combined easily during cooling of the welded thermal cycle because of the relatively low diffusion rate of titanium.

If large-heat-input welding is applied, we therefore have to find another element, instead of titanium, to promote the nucleation of ferrite and prevent the bainite or martensite transformation.

Boron is one of the best candidates for this purpose because boron has high diffusion rate in austenite and is a strong nitrogen-scavenger. Only BN, amongst many other nitrides, can precipitate from austenite during the cooling of the weld thermal cycle, and become the nucleation site of ferrite.

Consequently, for new steel, which has sufficient toughness in high-heat-input welding, we studied the utilization of boron.

## STUDY ON THE IMPROVEMENT OF THE HAZ TOUGHNESS AT HIGH-HEAT-INPUT WELDING

From the above considerations the utilization of boron with titanium, aluminum and nitrogen, which are thought to affect the kinetics of boron-nitride formation, was examined to control microstructure of the HAZ and to improve its toughness in a high-heat-input welding.

EXPERIMENTAL PROCEDURE - Table 3 shows chemical compositions of the investigated steel. After the investigated steel is refined in the electric furnace in a vacuum, slabs are hot-forged to 100mm thickness. Reheated slabs are then rolled to 30mm thickness before accelerated cooling.

The HAZ toughness is examined through the process of the synthetic thermal cycles. In order to evaluate the fusion line the maximum heating temperature was fixed at 1350°C. Cooling time from 800°C to 500°C (indicated as t800-500) was varied from 9 to 150 seconds.

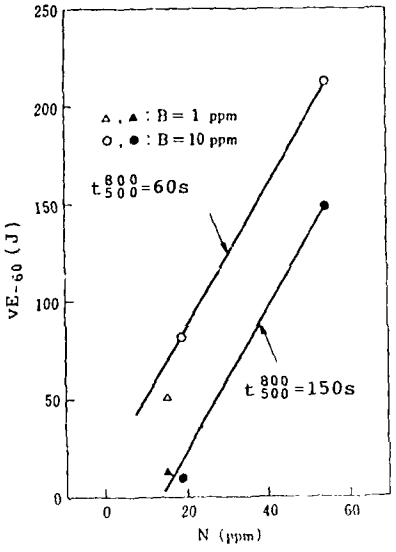


Fig.5 The Influence of N and B content on the toughness of the simulated HAZ (maximum heating temperature : 1350°C)

The cooling times of 9, 60 and 150 seconds correspond to the thermal cycles at fusion lines of 1.5, 10 and 25kj/mm heat-input welded joints of 30mm thick plate respectively.

EXPERIMENTAL RESULTS

The Influence of Nitrogen with Boron on the HAZ Toughness- It is well known that the increase of the nitrogen content results in the deterioration of the HAZ toughness because of the increase of nitrogen in solid solution. But when the steel contains boron, the experimental test results of the influence of nitrogen on the simulated HAZ toughness, Figure 5, showed the reverse trend. Fig.5 also shows the effect of boron addition on the simulated HAZ toughness, and a noticeable improvement of the toughness was observed by the small amount of boron addition.

Small boron-nitride precipitates in the simulated-HAZ samples was observed by electron microscope in the boron-bearing steel. Boron-nitrides were supposed to promote the ferrite formation during the austenite-ferrite transformation in the HAZ and to have contributed to decrease nitrogen in solid solution, and to improve the toughness of the HAZ.

Table 3 The Range of Chemical Composition of the Investigated Steel

| C | Si | Mn | Ni | Ti | sol.Al | B | N |
|---|---|---|---|---|---|---|---|
| 0.06 | 0.15 | 1.40 | 0.40 | 0.01 | 0.001 ~ 0.060 | 0.0001 ~ 0.0034 | 0.0008 ~ 0.0070 |

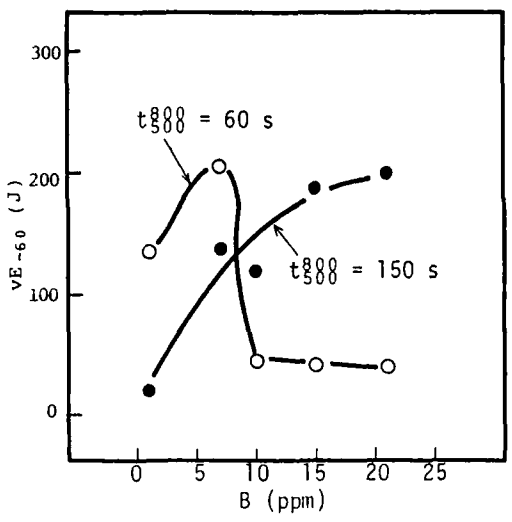


(a) 0.030Al-50ppmN

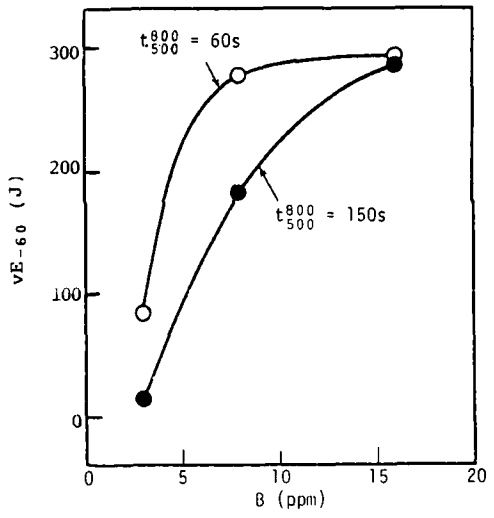


(b) 0.007Al-50ppmN

Fig.6 The Influence of Boron content on the toughness of the simulated HAZ (maximum heating temperature : 1350°C)

However, there must be the optimum amount of nitrogen to promote the mechanism as mentioned above, and too much nitrogen content might deteriorate the toughness.

The Influence of Aluminum with Boron on the HAZ Toughness - Fig.6 shows the influence of boron contents on the simulate HAZ toughness at two levels of the aluminum contents: 0.030 wt%-Al and 0.007wt%-Al. As shown in Fig.6, the influence of boron has remarkably different trends between with 0.030%-Al and 0.007%-Al.

When the steel contained 0.030%-Al the excessive amount of boron addition of more than 10ppm extremely deteriorated the toughness at the relatively high cooling rate (t800-500= 60sec.), although it improved the toughness at the low cooling rate (t800-500=150sec.).

This can be interpreted by the interaction among boron, aluminum and nitrogen; that is, aluminum is thought to hinder some how the formation of boron-nitride and the more excessive boron strongly hardens the HAZ structure when the cooling rate is relatively faster.

On the other hand lowering aluminum promotes the formation of boron-nitride by increasing nitrogen in solid solution. And even at relatively high cooling rate the HAZ toughness was greately improved by increasing boron up to 15ppm when the aluminum content was rearly trace, as shown in Fig.6(b).

The Influence of Titarium with Boron on the HAZ Toughness - From the above experiments we concluded that low Al-medium N-B steel has a trend to improve the HAZ toughness. In this experiment, the content of titanium was kept at constant value of 0.010%. Because it is generally recognized that a small amount of titanium does not impair HAZ toughness but improves it.

Titanium is one of the strong nitride-formers, and almost all titanium combines with nitrogen if the total content of titanium is small compared with the required amount in equilibrium to form nitride. Therefore, titanium was added to control the initial nitrogen content in solid solution at the peak temperature during cooling.

## DISCUSSION

To confirm the above experimental results, we investigated the balance of nitrogen in the simulated HAZ under high-heat-input welding comparing the actual analyzed values of nitride with values calculated by solubility limit in equilibrium. In calculating we hypothesized that the values, extracted independently from Fe-Ti-N, Fe-Al-N and Fe-B-N systems as shown below [13][14][15], were available for Fe-Ti-Al-B-N system.

$$\log[Al][N] = -8960/T + 2.70 \quad (1)$$

$$\log[B][N] = -13970/T + 5.24 \quad (2)$$

$$\log[Ti][N] = -16192/T + 4.72 \quad (3)$$

Fig.7 and Fig.8 show the difference between the value of (Ti as TiN)/total Ti and (B as BN) /total B, calculated with a solubility limit in equilibrium of 1350°C, and the analyzed value in the simulated HAZ, which had a cooling time of 800°C to 500°C in 60 seconds.

In the case of TiN, the calculated values coincident with the analyzed ones very well. In the case of BN, the calculated values are completely different from the analyzed ones. The latter comparison indicates that almost all boron exists as soluble boron when kept at a high temperature for a long time, as in the instance of high-heat-input welding. However boron precipitated as BN during cooling before austenite-ferrite transformation.

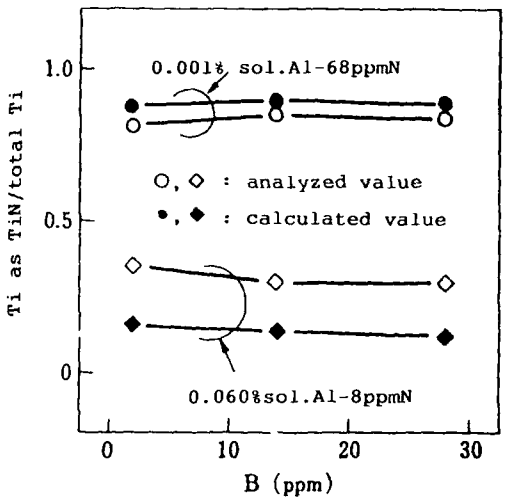


Fig.7 The Influence of sol.Al, B and N content on the ratio of (Ti as TiN) to total Ti in the simulated HAZ
maximum heating temperature : 1350°C
t800-500 : 60 sec.

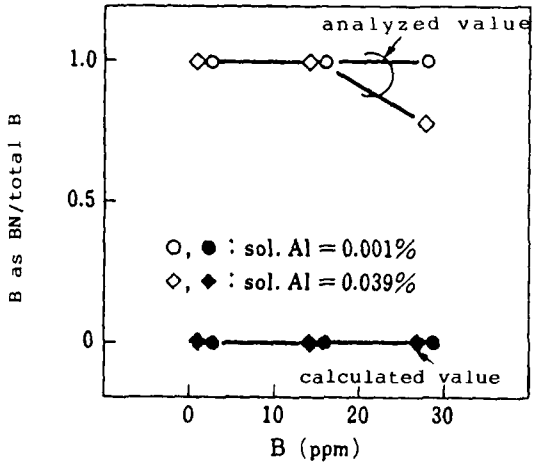


Fig.8 The Influence of sol.Al and B on the ratio of (B as BN) to total B in the simulated HAZ
maximum heating temperature : 1350°C
t800-500 : 60 sec.
N content : 60ppm

Fig.8 also shows that in medium (0.039%) Al-high B steel some amount of the boron remains in solid solution. Soluble boron tends to accelerate bainite and/or martensite transformation, and results in deterioration of the HAZ toughness. This confirms that lowering the amount of aluminum is very effective to diminish the detrimental effect of soluble boron.

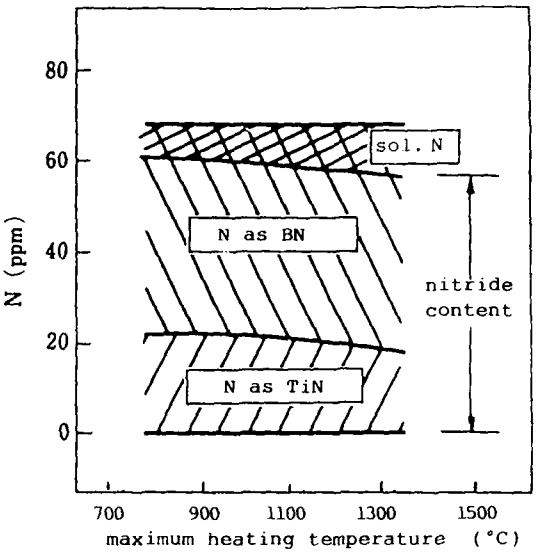


Fig.9 The Influence of the maximum heating temperature on the amount of sol.N in the simulated HAZ
sol.Al : 0.001%
B : 28ppm
N : 68ppm

Fig.9 shows the influence of the maximum heating temperature on the amount of soluble nitrogen in the simulated HAZ. As a result of the precipitation of TiN and BN, soluble nitrogen is reduced to below 10ppm at various heating temperature. This is why low Al-high B steel indicates sufficient toughness in the all regions of the HAZ.

From the above investigation we confirmed, controlling the amounts aluminum, boron and nitrogen in titanium treated steel, that the increase of TiN and BN can toughen the welded joints significantly.

## DEVELOPMENT OF A NEW TYPE OF STEEL FOR OFFSHORE USE

From the above-mentioned experimental study we have developed a new type of steel which preserves its strength and low-temperature toughness even at a high-heat-input welding. The chemical composition of this steel, the properties of the base metal and the properties of the welded joint are shown in table 4, 5 and 6 respectively.

This steel is characterized by Nb-Ti-B microalloying, reduced aluminum and balanced nitrogen content. An accelerated cooling process was applied to maintain the specified strength with a sufficient toughness for 38mm-thick of YS 500MPa steel plate.

The test results showed that the base metal and the HAZ have very high values of Charpy impact absorbed energy at -60°C.

Table 4 Chemical Composition (wt %)

| C | Si | Mn | P | S | Nb | Ti | B | Sol. Al | N | Ceq* | $P_{cm}$** |
|---|---|---|---|---|---|---|---|---|---|---|---|
| 0.08 | 0.14 | 1.50 | 0.009 | 0.002 | 0.007 | 0.009 | 0.0015 | 0.004 | 0.0044 | 0.33 | 0.17 |

$$*Ceq = C + \frac{Mn}{6} + \frac{Cu+Ni}{15} + \frac{Cr+Mo+V}{5}$$

$$**P_{cm} = C + \frac{Si}{30} + \frac{Mn}{20} + \frac{Cu}{20} + \frac{Ni}{60} + \frac{Cr}{20} + \frac{Mo}{15} + \frac{V}{10} + 5B$$

Table 5 Properties of the Base Metal

| Thickness (mm) | Thickness position | Tensile test | | | | Charpy impact test | | | NRL test |
|---|---|---|---|---|---|---|---|---|---|
| | | Direction | YS(MPa) | TS(MPa) | El(%) | Direction | $vE_{-60}$ (J) | vTs(°C) | NDTT(°C) |
| 38 | 1/4t | Transverse | 402 | 527 | 28.5 | Longitu-dinal | 276 | -80 | -70 |

Table 6 Properties of the Welded Joint

| Thickness (mm) | Welding method | Heat input (KJ/mm) | Charpy impact test | | | |
|---|---|---|---|---|---|---|
| | | | TS(MPa) | Notch position | $vE_{-40}$ (J) | $vE_{-60}$ (J) |
| 38 | SAW | 5 | 547 | Fusion line | 273 | 231 |
| | | | | HAZ 1mm | 294 | 264 |
| | | | | HAZ 3mm | 294 | 256 |
| | EGW (electrogas arc welding) | 20 | 528 | Fusion line | 165 | 174 |
| | | | | HAZ 1mm | 267 | 222 |
| | | | | HAZ 3mm | 294 | 166 |

Compared with conventional steel (such as Cu-Ni-Nb-Ti steel as shown in Fig.4) this new steel has superior HAZ toughness even in 20kj/mm heat-input welding.

This results from the refined ferrite--pearlite microstructure in the HAZ of this type of steel, as shown in Fig.10. As far as welded joint strength is concerned, this steel meets the requirement of TS 500MPa class steel, even in high-heat-input welding, due to the effect of niobium, as shown in Fig.11.

Furthermore, the CTOD behavior of this steel was examined because excellent CTOD characteristics in HAZ have become increasingly demanded in steel for offshore structure to secure against brittle fracture.

In the CTOD characteristics of HAZ the occurrence of a local brittle zone (LBZ) is recognized as something which deteriorates fracture toughness. Here the LBZ is defined as the coarse grain region which is reheated in the ferrite-austenite region by the subsequent weld, but not reheated more than 450°C by the following weld. Recent investigations [16][17][18] have pointed out the noticeable influence of the M-A constituent precipitation and the grain size in HAZ.

The HAZ microstructure of this steel is controlled by the profitable selection of microalloying elements, as mentioned before. This steel is, therefore, expected to have excellent CTOD characteristics in HAZ. Then we examined the CTOD properties of this steel with a small-sized specimen in which the weld thermal histories had been simulated corresponding to 1kj/mm and 10kj/mm heat-input.

Test results of three thermal cycles, e.g. reheating up to 1350°C, 1350°C + 800°C and 1350°C + 800°C + 450°C, are shown in Fig.12 to provide comparisons with conventional steel. The deteriorated CTOD characteristics of this steel, thermal cycled with 1350°C + 800°C, are recovered through the subsequent 450°C reheating as occurres in conventional steel. But the feature of this steel is to show excellent CTOD characteristics in high-heat-input welding, although even in relatively low-heat-input welding this steel shows better CTOD than conventional steels do.

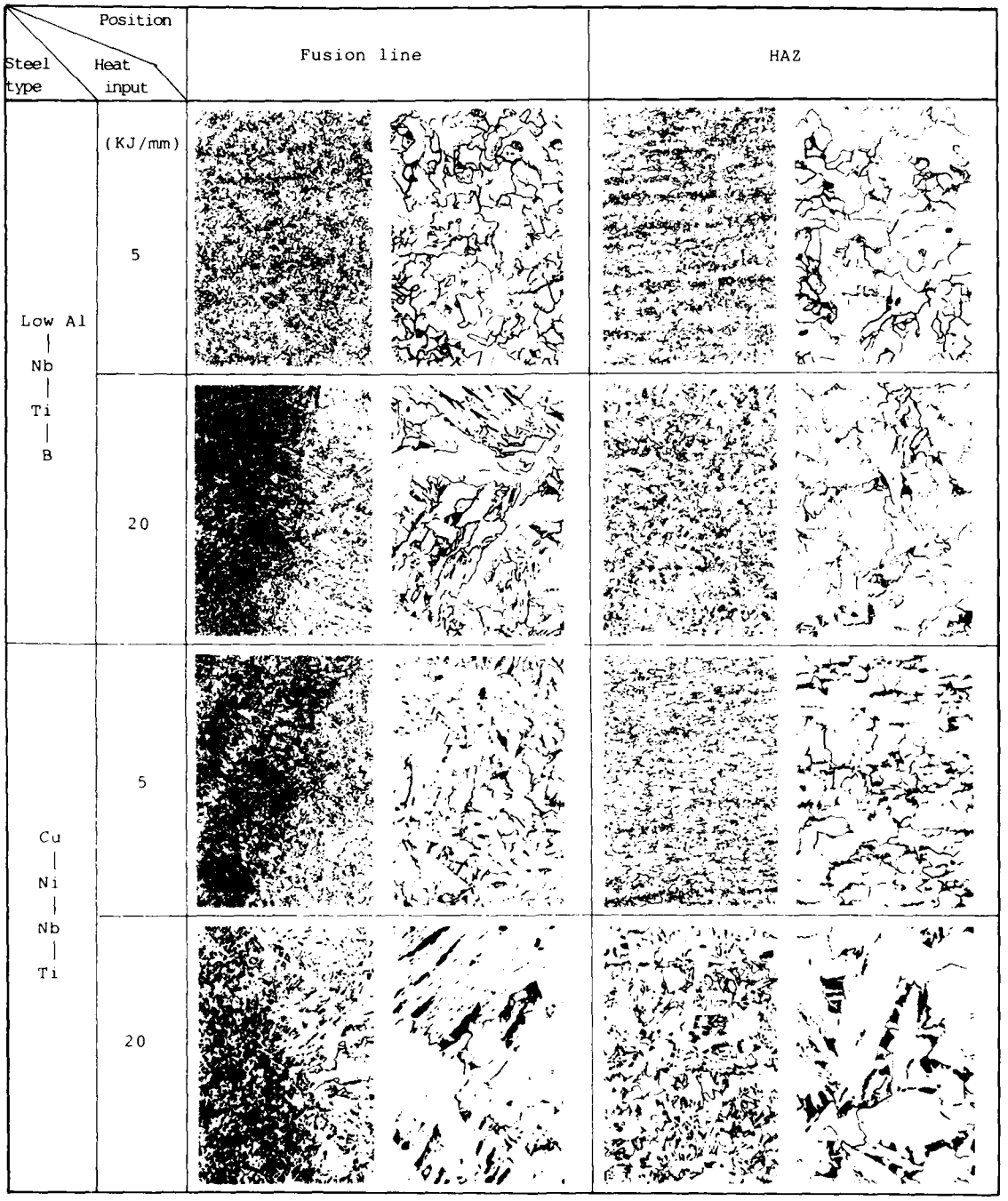


Fig.10 Comparison of the welded joint microstructures between Cu-Ni-Nb-Ti steel and low Al Nb-Ti-B steel

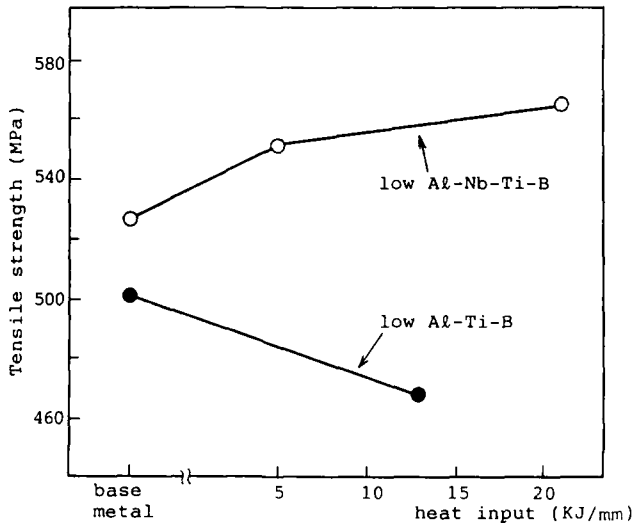


Fig.11 Change of the welded joint strength according to the heat input

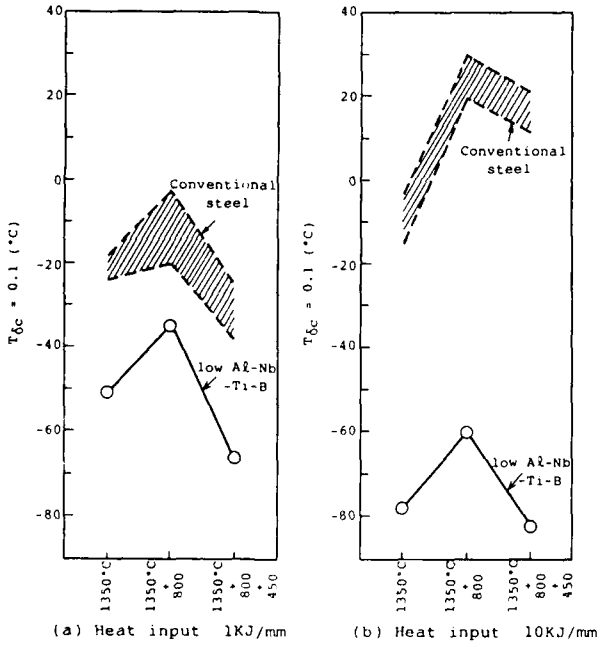


Fig.12 Comparison of CTOD characterictic of LBZ between conventional steel and low Al-Nb-Ti-B steel

## CONCLUSION

Systematic investigation of the influence of microalloying elements, which include niobium, titanium, boron, nitrogen and aluminum, on the properties of high-heat-input welded joints showed that:

A small amount of niobium, less than 0.010%, is beneficial in maintaining the strength of the welded joints without noticeable deterioration of toughness;

Titanium can control the available nitrogen level needed for an adequate amount of BN precipitation, in addition to its usefulness in the suppression of the HAZ austenite grain growth;

Boron plays quite an important role in the microstructure control of the HAZ. Boron can combine with nitrogen during the cooling process at the welding owing to its high diffusion rate. The formed BN precipitates extremely well and promotes the formation of ferrite. This results in improving the HAZ toughness, even though in high-heat-input welding, where TiN loses its effect of toughening the HAZ;

The nitrogen content should be balanced to produce adequate amounts of TiN and BN which co-operate to toughen the HAZ;

Lowering the amount of aluminum reduces the amount of nitrogen fixed as AlN, promotes the combining of nitrogen with boron during cooling process, even at relatively fast cooling rate, and this results in keeping the HAZ toughness at various cooling rates.

From the above experimental results we have developed a new type of steel for offshore use. This steel shows sufficient toughness at -60°C not only in the base metal but in all positions in the HAZ even at 20kj/mm high-heat-input. In addition to that, it is confirmed that this steel has excellent CTOD characteristics under a wide range of welding conditions.

## REFERENCES

[1] E.F.Nippes, W.F.Savage and R.J.Allio: Welding. Journal., 1957,vol.36, p.513s.

[2] H.Takeuchi, K.Bessyo, and T.Hashimoto: The Sumitomo Search, 1986, vol.32, p.8.

[3] Japan Ship Building Society: Symposium on Application of TMCP Steel for Welded Structure, 1983.

[4] N.E.Hannerz: "Welding of HSLA Structural Steels" Proceedings of International Conference, 1976, Rome Italy, edited by A.B Rothwell and J.M.Gray, ASM, p.365.
1983.

[5] A.P.Coldren and R.L.Cryderman: Symposium Steel Strengthening Mechanism, Zurich 1969, p.17.

[6] H.Ohtani, S.Watanabe, Y.Kawaguchi and Y.Yamaguchi: Tetsu to hagane, 1978, vol.64, p.107.

[ 7] N.Nakano, K.Bessyo, Y.Iida, I.Seta and Y.Kamada: The Fifth International Symposium & Exhibit on OMAE, 1986, vol.2, p.354.
[8] C.Zener: Trans.AIME., 1948, vol.175, p.45.
[9] R.Someya, M.Fujimoto, I.Seta, H.Kimura and M.Nakanishi: The Sumitomo Search, 1986, vol.32, p.30.
[ 10] H.Tamura: Journal of the Japan Welding Society, 1966, vol.35, p.29.
[ 11] S.Kanazawa, A.Nakashima, K.Okamoto and K.Kanaya: Transaction of Iron and Steel Institute of Japan, 1976, vol.16, p.486.
[12] S.Suzuki, G.C.Weatherly and D.C.Houghton: Acta Metallurgica, 1987, vol.35, p.341.
[13] H.Nakamura and M.Fukagawa: Journal of the Materials Science Society of Japan, 1964, vol. 1. p.273.
[ 14] R.W.Fountain and J.Chipman: Trans Metal Society, AIME, 1962, vol.224, p.559.
[ 15] H.Sawamura and T.Mori: Hetsu to Hagane, 1957, vol.43, p.31.
[ 16] M.Toyosada, N.Nohara, T.Ohtsuka and Y.Hagiwara: IIW Doc.X-1104-86.
[17] T.Haze and S.Aihara: IIW Doc.X-1423-86.
[18] M.Nakanishi, Y.Komizo and Y.Fukada: The Sumitomo Search, 1986, vol.33, p.22.

# EXTENSIVE USE OF HIGH STRENGTH STEEL PLATES PRODUCED BY TMCP IN CONSTRUCTION OF SHIPS AND OFFSHORE STRUCTURES

**Chiaki Shiga, Yoshifumi Nakano**
Kawasaki Steel Corporation
Chiba, Japan

**Keniti Amano, Eiji Kobayashi**
Kawasaki Steel Corporation
Kurashiki, Japan

**Hiroshi Yajima, Akinobu Kawamura**
Mitsubishi Heavy Industries, Ltd.
Nagasaki, Japan

**Takuo Nawata**
Mitsubishi Heavy Industries, Ltd.
Hiroshima, Japan

Abstract

High strength steel plates have been used in Japan to build merchant ships for the past two decades. The main purpose of using high strength steel plates exists in the reduction of weight of ship structures which realizes high performance of ships such as low consumption of fuel. The high strength steel plates for ship hull structure had the yield strength of 315 MPa in the early days. In recent years, however, the yield strength was increased to 390 MPa. This trend in using higher strength steel plates owes to the progress in technologies of steel plate manufacturing and ship design and construction. Significant progress in manufacturing technique includes the development of thermo-mechanical control process (TMCP). The TMCP technique significantly contributes to the increase in strength of steel plates, improvement of weldability and toughness of welded joints and reduction of consumption of resources.

The TMCP has been applied to the production of steel plates to increase yield strength further without deteriorating weldability and toughness of welded joints made by high heat input welding. The 390 MPa yield strength steel plates and their welded joints made with heat input ranging from 15 to 27 kJ/mm are studied using ordinary mechanical tests as well as small and large scale fracture mechanics tests to prove their good performance in actual use. With these kinds of test, the 390 MPa yield strength steel plates have been successfully applied to very large merchant ships such as bulk carriers.

High strength steel plates which are weldable with heat input as large as 20 kJ/mm are also required in building mobile offshore drilling units such as semi-submersible rigs and caisson rigs. The development and qualification test of 415 and 450 MPa yield strength steel plates have been performed to fulfill those requirements. The use of TMCP technique is again essential to produce these steel plates. The qualification tests including mechanical and fracture mechanics tests prove that they can be applied to the construction of mobile offshore drilling units to be operated in the Arctic region.

The merits of using high strength steel plates produced by TMCP in the actual design and construction of ships are also discussed.

## 1. Introduction

The TMCP of Kawasaki Steel's version is named MACS (Multi-purpose accelerated cooling system), in which controlled rolling is followed by accelerated cooling. Benefits of MACS plates are summarized in Table 1. Taking advantage of benefits obtained by MACS, new plates with higher strength, lower temperature toughness and

Table 1 Summary of benefits of TMCP plates

| Benefits of TMCP (MACS) plates | |
|---|---|
| **For welded joints** | |
| (1) Decreased Ceq or Pcm | a) Improvement of HAZ toughness, especially in large heat input welding<br>b) Low susceptibility to weld cracking<br>c) Low susceptibility to SSCC |
| **For Parent metal** | |
| (2) Reduction of pearlite and bainite band microstructure | a) Low susceptibility to HIC. |
| (3) Fine grained microstructure | a) Increase in low temperature toughness, especially crack arrestability |
| **For Productivity** | |
| (4) Omission of heat treatment in on-line production | a) High productivity |

heavier thickness have been developed. More than a half million tons of MACS plates have been produced for ships, mobile offshore drilling units and fixed type offshore structures such as jackets, and large diameter linepipes[1),2),7)].

Shipbuilders require steel plates which have excellent heat affected zone (HAZ) toughness when welded with high heat input. Large ships have many portions which are constructed with plates of large size at ship yards. Shipbuilders want to decrease the number of welding passes. They also want to use one-side welding because they do not want to turn over large pannel plates. For 30mm thick plates, for example, one-side one-pass welding is used.

Mobile offshore drilling units such as semi-submersible rigs and caisson-retained islands used in the North Sea and the Arctic region need steel plates with good toughness at low temperatures. For these structures whose minimum service temperature is -50°C, a ship rule such as ABS rule requires the 2mm V-notched Charpy absorbed energy of 45J at -80°C for a special application structure. The steel plate for this purpose requires Ni content of more than 1.0% when produced by normalizing process. As a result, the plate is expensive and does not have good weldability. The MACS process, on the other hand, can reduce carbon equivalent (Ceq) sufficiently to attain excellent low temperature toughness with the Ni content of less than 0.5%.

This paper describes fundamental concept of strengthening and improvement of HAZ toughness in high heat input welding and examples of newly developed high strength steel plates. The test results of HAZ toughness of actual welded joints made with high heat inputs are mainly described for a YP400MPa grade for ships and a YP460MPa grade for mobile offshore drilling units which are highest grades in both structural steels used so far.

## 2. Strengthening and improvement of toughness by ACC

Figure 1 shows a schematic drawing representing the difference between MACS and conventional processes. The MACS-ACC is suitable for plates thinner than 75mm and the MACS-DQT, for over 75mm in thickness. The MACS plates described in this paper are thinner than 40mm and were produced by MACS-ACC which gives a mean cooling rate of about 10°C/s. Controlled rolling was followed by accelerated cooling. The finish-rolling temperature was 800°C for AH and DH grade plates in ship rules and $Ar_3$ temperature for mobile offshore drilling units.

The yield strength (YS) and tensile strength (TS) obtained by ACC, CR and normalizing for steels with various Ceq values is shown in Fig. 2. The figure indicates that the ACC process increases YS by about 100MPa comparing with the normalizing process.

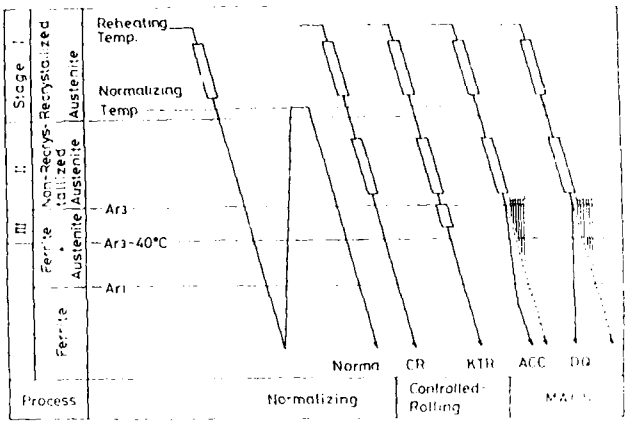


Fig.1 Schematic drawings of normalizing, controlled rolling (CR,KTR) and MACS process (ACC,DQ)

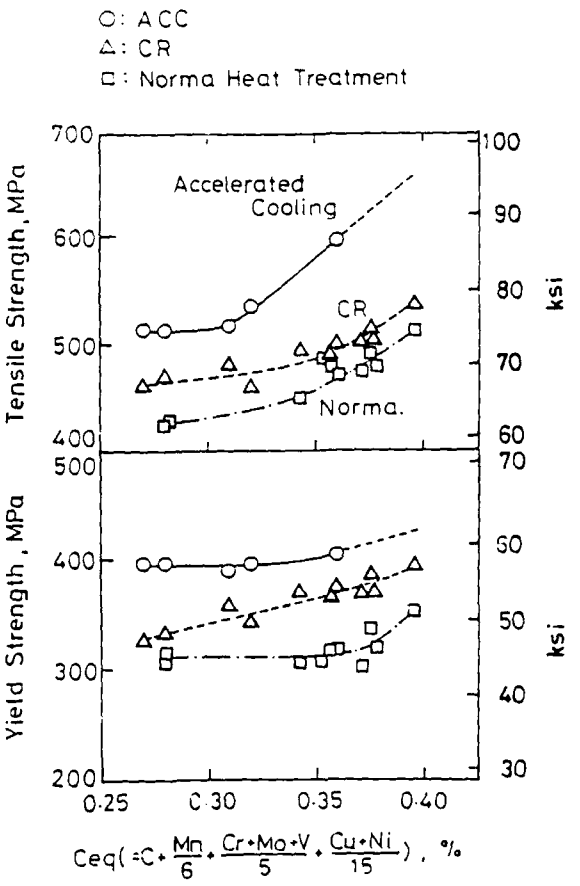


Fig.2 Relation between carbon equivalent and tensile properties for Si-Mn steel plates obtained by ACC, CR and normalizing (Norma)

Figure 3 shows the relation between Ceq of steel and HAZ toughness. This relation was obtained using synthetic HAZ. The cooling time from 800°C to 500°C in the thermal cycle was 230 sec, which is corresponding to the heat input of 20kJ/mm. The decrease of Ceq is useful to improve HAZ toughness. This improvement results from the change in HAZ microstructure from bainite to ferrite, which is realized by the reduction of Ceq.

The improvement of HAZ toughness through tempering effect of the subsequent welding passes can not be obtained in the case of one pass or two pass welding. Therefore, improvement of HAZ toughness through the reduction of Ceq and microalloying elements in steel is very important. The ACC process is useful not only for development of higher strength steel but also for improvement of weldability of ordinary steels through reduction of Ceq.

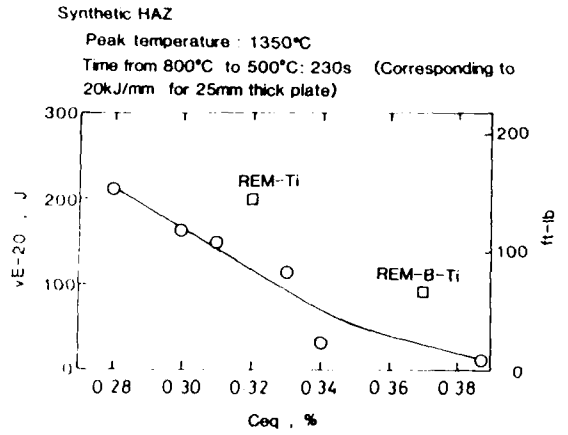


Fig.3 Effect of carbon equivalent of steel on synthetic HAZ toughness, CVN absorbed energy at -20°C (vE-20)

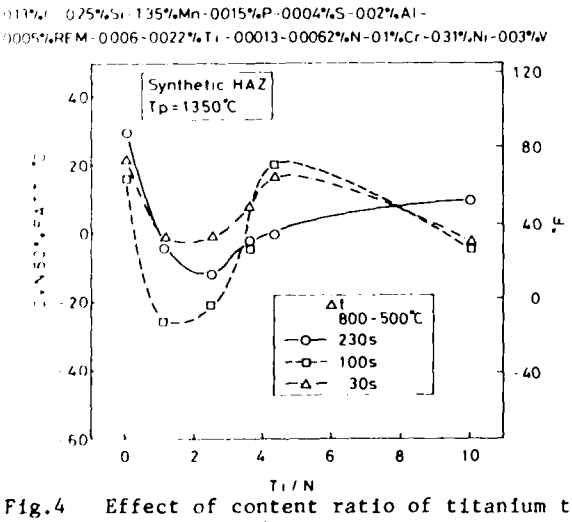


Fig.4 Effect of content ratio of titanium to nitrogen, Ti/N, on synthetic HAZ toughness, CVN 50% FATT

3. Improvement of HAZ toughness

In addition to the reduction of Ceq mentioned above, the addition of Ti and rare earth element which mainly consists of Ce and is called REM is effective in improving HAZ toughness in high heat input welding. Figure 4 shows the effect of the ratio of Ti to N, Ti/N, on HAZ toughness. The HAZ toughness (CVN 50% FATT) is excellent in the region of Ti/N ranging from 2 to 3.5 when the heat input is between 3 and 20kJ/mm. This preferable region is related to the small size of TiN precipitate, which is smaller than 0.04μm in diameter. Small precipitates of TiN inhibit γ grains from coarsening in HAZ.

The REM forms REM-oxisulfides as indicated by REM(O,S), which inhibit γ grains from coarsening when exposed to thermal cycle of high temperature and work as nuclei of ferrites inside γ grains during cooling after welding. The TiN precipitates are resolved and have little effect as inhibiters when heated up to 1400°C. On the other hand, the REM(O,S)'s are not resolved, so that they are effective even at that temperature. Figure 5 schematically illustrates the effects of TiN and REM(O,S) on microstructure of HAZ exposed to high temperatures in welding.

The reduction of impurities such as N, S and P improves HAZ toughness in high heat input welding. Especially soluble N in matrix and N resolved from TiN during welding deteriorate not only HAZ but also weld metal because of dilution of N from HAZ. In case of Ti-B bearing weld metal, weld metal toughness is more deteriorated by diluted N which decreases acicular ferrite in the microstructure of weld metal because diluted N combines with soluble B to form BN precipitates. Therefore, nitrogen content of modern plates is usually reduced to below 40ppm.

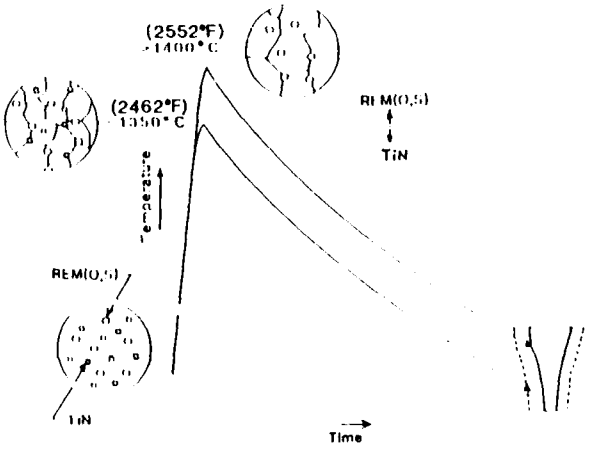


Fig.5 Schematic model showing the effect of TiN and REM(O,S) on the size of austenite grain in HAZ

4. HAZ softening in high heat input welded joint

From the view point of HAZ toughness improvement, the reduction of Ceq is preferable as mentioned above, but it is accompanied by HAZ softening.

Figure 6 shows the relationship between Ceq of steel and tensile strength of welded joint. The relation was obtained by performing tensile test of actual welded joints. The specimen was of NK U2A. The steel plates had various Ceq values and were welded with heat input ranging from 15 to 25 kJ/mm. To obtain the required tensile strength of welded joints, the reduction of Ceq must be limited.

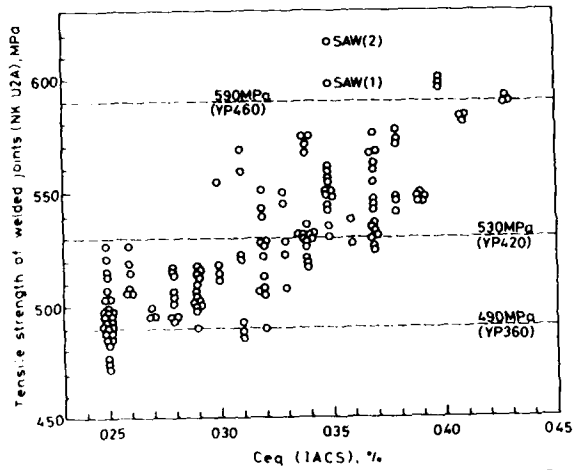


Fig.6 Relation between tensile strength of welded joints and Ceq of steel plates. The specimen size of welded joints follows NK U2A of NK rule.

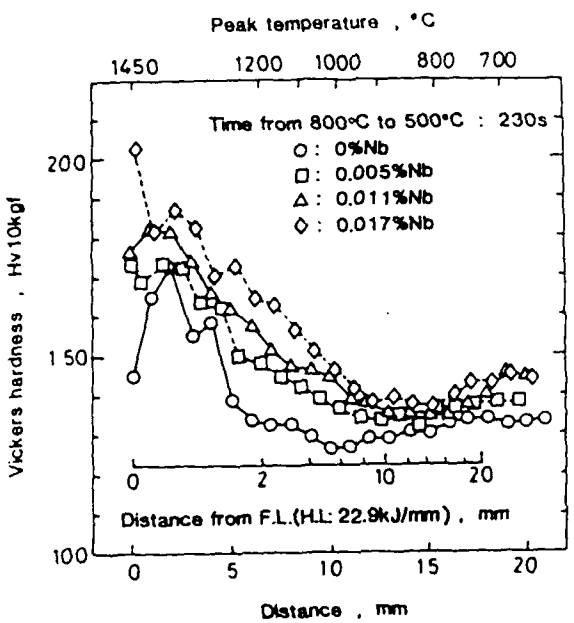


Fig.7 Vickers' hardness distribution over the distance from the simulated fusion lines of steel plates produced by MACS-ACC.

Figure 7 shows the effect of the addition of a small amount of Nb on hardness distribution in HAZ. The addition of 0.005% Nb is effective to prevent HAZ softening. The addition of Nb has often been disliked in the HAZ toughness aspect. However, a small amount of Nb, which does not exceed 0.015% for high heat input welding and 0.03% for low heat input welding, does not deteriorate HAZ toughness as shown in Fig. 8 and furthermore it is useful for strengthening in ACC process.

In the normalizing process, Nb in steel does not raise strength because of formation of coherent Nb(C,N) precipitates. In the ACC process, on the other hand, it raises strength because of formation of bainitic structure which results from soluble Nb. It is well known that soluble Nb is effective in refining grain size of ferrite and bainite through formation of deformation bands during controlled rolling. Therefore, a small amount of Nb is indispensable for producing good low temperature toughness steel plates for high heat input welding.

Figure 9 shows the relation between Ceq of steel and weld cracking susceptibility obtained using CTS test with the heat input of 0.5 kJ/mm. When Ceq is above 0.38%, weld cracking easily occurs. Therefore, Ceq should not be above 0.38%.

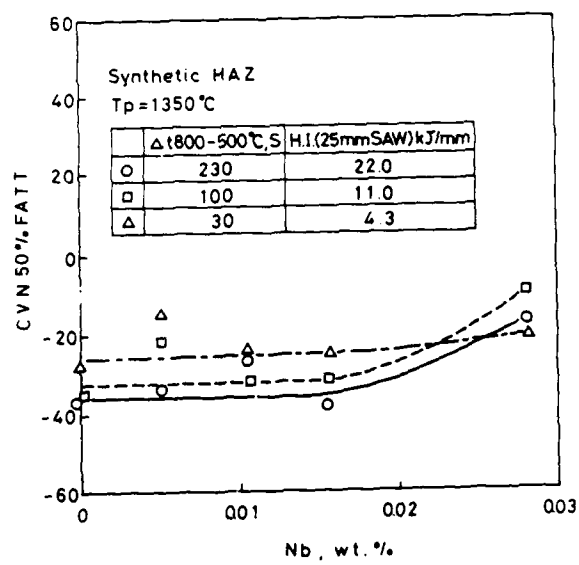


Fig.8 Effect of Nb content on synthetic HAZ toughness

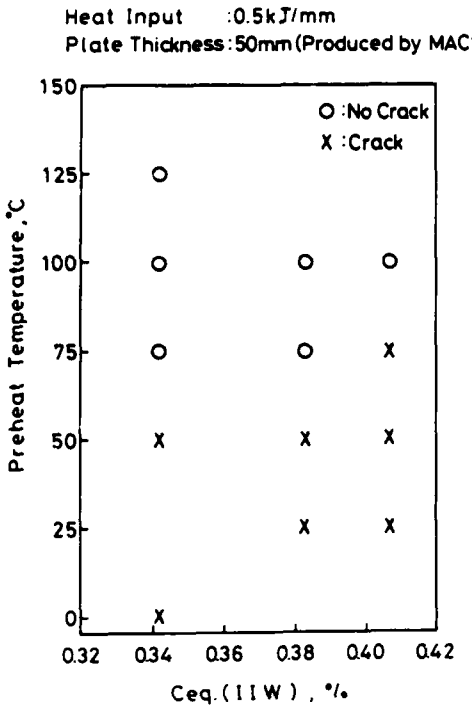


Fig.9 Relation between preheat temperature to prevent weld cracking determined by CTS test and Ceq of steel plate

5. Newly developed, high strength and low temperature toughness steel plates

Examples of newly developed steel plates for ships and mobile offshore drilling units are shown in Table 2. Three grades of steel plates, YP320MPa, YP360MPa and YP400MPa, have been developed and used for ships, and four grades, YP320MPa, YP360MPa, YP420MPa and YP460MPa, for mobile offshore drilling units.

This paper describes the mechanical properties of A and E class YP400MPa grade steel plates (Y40A and Y40E) for ships and those of YP470MPa grade steel plate (Y47S) for mobile offshore drilling units as examples. The chemical compositions of the steel plates are shown in Table 3. They are characterized by low Ceq, Nb-REM-Ti bearing and low impurities of P, S and N. The contents of REM and Ti are 60ppm and 0.007%, respectively. The mechanical properties of these plates are shown in Table 4.

Table 2 List of newly developed TMCP (MACS) plates for ships and mobile offshore drilling units

**MACS plates**

| | | | | | | | |
|---|---|---|---|---|---|---|---|
| for ships | Grade (MPa) | YP320 | YP360 | YP400 | | | |
| | Test Temp.* | 0°C | −20°C | | | | |
| | Thick. | 40mm | | | | | |
| for mobile drilling units | Grade (MPa) | YP320 | YP360 | | YP420 | YP460 | |
| | Test Temp.* | 0°C | −20°C | −40°C | −60°C | −80°C | |
| | Thick. | 40mm | | | | | |

*: Charpy impact testing temp.

Table 3 Chemical compositions of AH40, EH40 and EH47 modify grade steel plates

(wt%)

| Steel | C | Si | Mn | P | S | Al | Cu | Ni | Nb | N | Ceq* | Pcm** |
|---|---|---|---|---|---|---|---|---|---|---|---|---|
| A | 015 | 034 | 1.18 | 0012 | 0002 | 0033 | — | — | 0015 | 00035 | 035 | 022 |
| E | 009 | 034 | 141 | 0012 | 0002 | 0035 | — | — | 0016 | 00035 | 033 | 017 |
| S | 0095 | 029 | 134 | 0007 | 0002 | 0027 | 026 | 027 | 0018 | 00031 | 035 | 019 |

REM-Ti Treatment

$$* \quad Ceq = C + \frac{Mn}{6} + \frac{Cu+Ni}{15} + \frac{Cr+Mo+V}{5}$$

$$** \quad Pcm = C + \frac{Si}{30} + \frac{Mn+Cr+Cu}{20} + \frac{Ni}{60} + \frac{Mo}{15} + \frac{V}{10} + 5B$$

Table 4 Mechanical properties of AH40, EH40 and EH47 modify grade steel plates

| Plate | Grade | Steel | Thickness (mm) | YS (MPa) | TS (MPa) | El (%) | $vE_{-40}$ (J) | $vE_{-60}$ (J) | $vE_{-80}$ (J) |
|---|---|---|---|---|---|---|---|---|---|
| Y40A | AH40 | A | 30 | 436 | 564 | 30 | 263 | 196 | 137 |
| Y40E | EH40 | E | 25 | 441 | 549 | 31 | 314 | 307 | 309 |
| Y47S | EH47mod. | S | 30 | 510 | 637 | 25 | — | 234 | 222 |

(Longitudinal Direction)

The steel was refined by an LD converter and continuously cast into slabs, which were controlled-rolled to 30mm in thickness, followed by accelerated cooling in the MACS facility.

Figure 10 plots crack arrest toughness, Kca, obtained by ESSO test vs. temperature. The relationship for the less than 0.5% Ni bearing steel plates made by normalizing is indicated by a hatched zone. The Kca values of Y40E and Y47S are higher than those of the normalized plates. Good crack arrestability is one of the characteristics of MACS plates.

The following crack arrest toughness has been reported as a requirement to the steel plates for ship hull structure[8]:

$$Kca > 400\sim600 kgf\sqrt{mm}/mm^2 \quad (124\sim186 MPa\sqrt{m})$$

As the Kca value of Y40A plate is more than $600 kgf\sqrt{mm}/mm^2$ at -20°C, is has sufficient crack arrestability as a crack arrester.

The crack arrest toughness required to the steel plates for mobile offshore drilling units are still to be determined. If the same crack arrest toughness requirement is applied, however, it is satisfied at -68°C. Thus, it is concluded that this plate can be used as a crack arrester in the Arctic region.

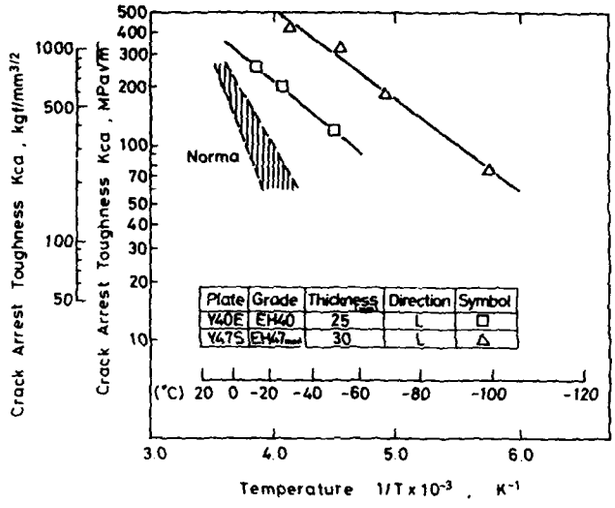


Fig.10 Temperature dependence of Kca for EH40 and EH47 modify grade steel plates

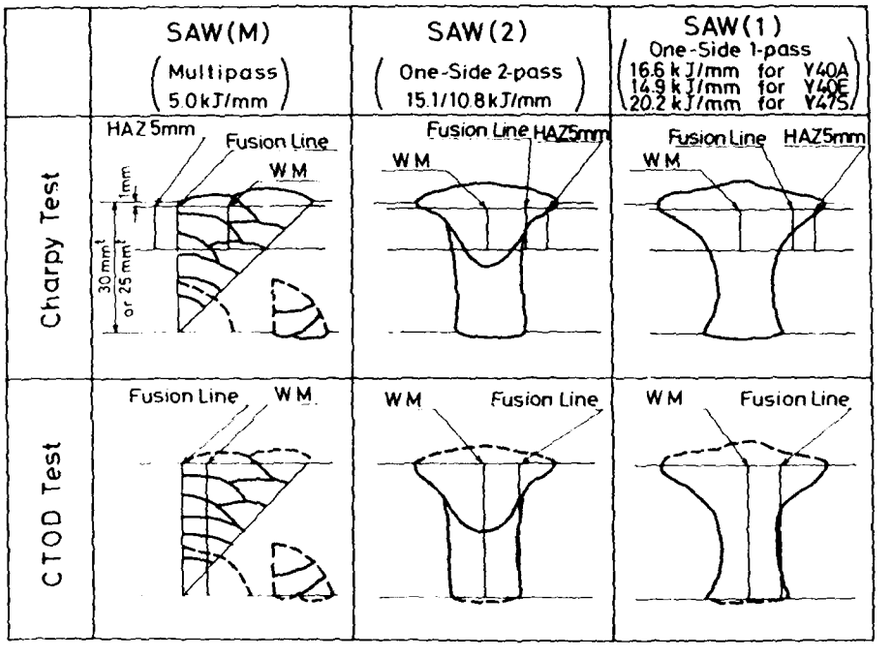


Fig.11 Schematic drawings of welded joints and notch positions of CVN impact and CTOD test specimens

The welded joints of Y40A, Y40E and Y47S steel plates were made using various kinds of submerged arc welding(SAW). Multi-pass SAW was applied to Y47S plate with heat input of 5kJ/mm, one-side two-pass SAW for Y40A, Y40E and Y47S plates with heat inputs of 15.1 and 10.8 kJ/mm, and one-side one-pass SAW for Y40A plate with 16.6kJ/mm, Y40E plate with 14.9kJ/mm and Y47S plate with 20.2kJ/mm.

Schematic drawings of welded joints and notch positions in Charpy and CTOD test specimens are shown in Fig. 11. Figure 12 shows the CVN absorbed energy at either 0°C or -20°C for the notch positions of weld metal (WM), fusion line (FL) and heat affected zones of 1, 3 and 5mm apart from FL. The test temperature was 0°C for Y40A welded joint and -20°C for Y40E. All the welded joints of these plates have sufficient absorbed energy values to meet the requirements for DH and EH grades as specified in the rules for ship null structures.

Figure 13 shows the CVN absorbed energy values at -40 and -60°C for all notch positions of Y47S welded joint made by one-side two-pass SAW. The CVN absorbed energy at -60°C for fusion line is more than 42J. Furthermore the welded joint of this plate gives the CVN absorbed energy of more than 42J at -80°C if multi-pass SAW is applied with the heat input of 5kJ/mm as shown in Fig. 14.

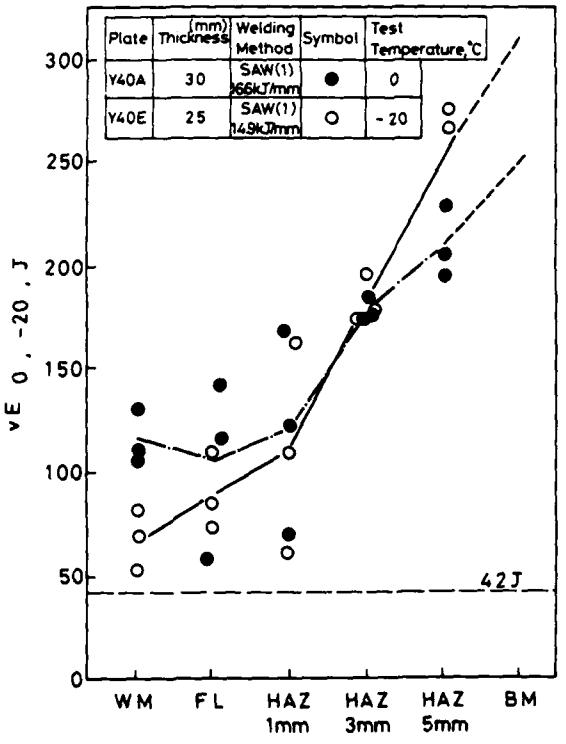


Fig.12 CVN impact absorbed energy value obtained at 0°C and -20°C for the welded joints of Y40A and Y40E plates made by one-side one-pass SAW

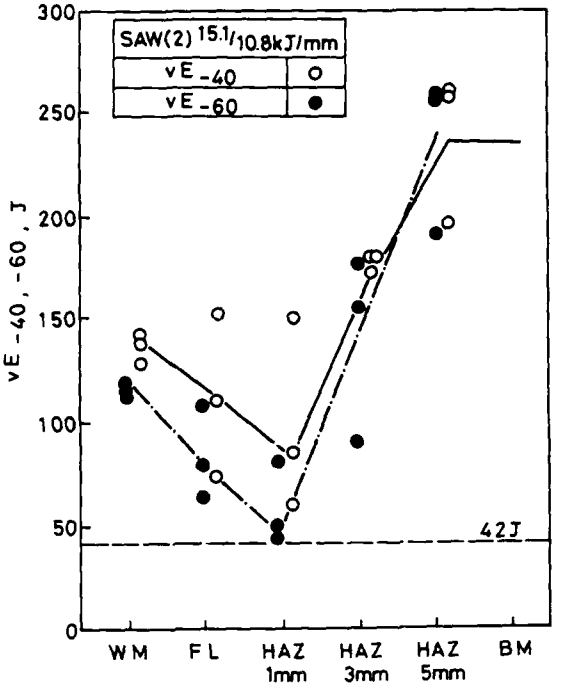


Fig.13 CVN impact absorbed energy values obtained at -40°C and -60°C for the welded joints of Y47S plate made by one-side two-pass SAW

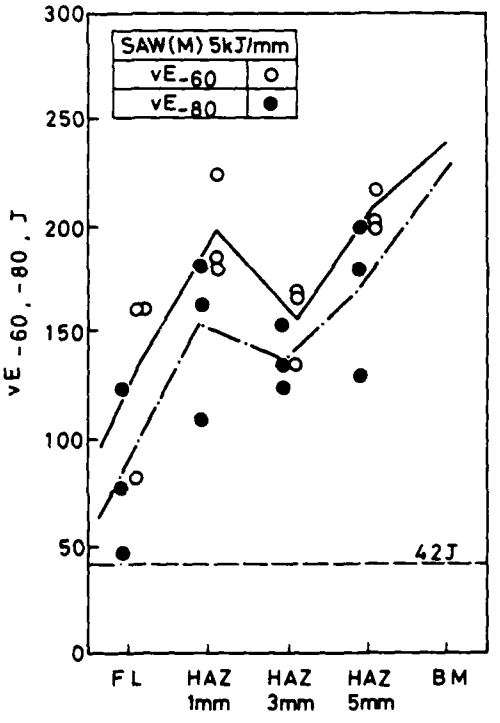


Fig.14 CVN impact absorbed energy valued obtained at -60°C and -80°C for the welded joints of Y47S plate made by multi-pass SAW

Figure 15 shows the temperature dependence of CTOD of the one-side two-pass SAW joint of Y47S. A calculation with the assumption that the design stress is $0.8\sigma_{YO}$ ($\sigma_{YO}$: specified yield strength), the stress concentration factor is 2, the welding residual stress is as large as $\sigma_{YO}$, and the surface defect is 0.25t deep and 2.5t long where t is thickness gives the required CTOD value of 0.1mm at service temperture. If this CTOD requirement is applied, it is concluded that the one-side two-pass SAW joint of Y47S can be used at -30°C.

The ABS rule classifies structures into three classes, depending on which Charpy test temperature is determined 0 to 30°C lower than service temperature. In the case of a special application structure, for example, the material must be tested at -60°C if the service temperature is -30°C. At each test temperature the absorbed energy must be higher than 42J.

Figure 16 summarizes the welding conditions for Y47S steel plate and the fitness as offshore structures on the basis of the criteria mentioned above. In the figure, the mark of circle indicates that the criteria are satisfied. One-side one-pass SAW can be applied to the structure whose service temperature is -10°C, one-side two-pass SAW is for -30°C, and multi-pass SAW is for -50°C.

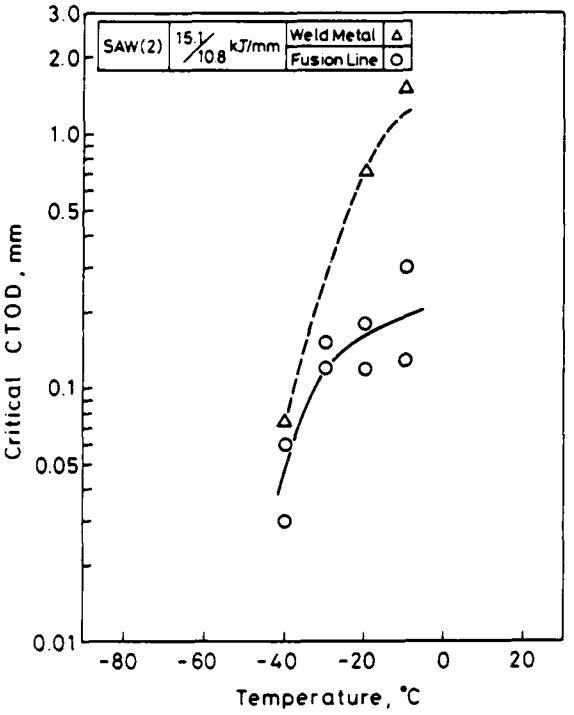


Fig.15 Temperature dependence of CTOD for the welded joint of Y47S plate made by one-side two-pass SAW

| Welding Method | Offshore structure | | |
|---|---|---|---|
| | For Arctic Ocean (Service Temp: -50°C) | For Behring Sea (Service Temp: -30°C) | For North Sea (Service Temp: -10°C) |
| SAW(1pass) (20.2kJ/mm) | $vE_{-80°C}$ X | $vE_{-60°C}$ X | $vE_{-40°C}$ O |
| | $\delta_{c\,-50°C}$ X | $\delta_{c\,-30°C}$ X | $\delta_{c\,-10°C}$ O |
| SAW(2passes) (15.1/10.8kJ/mm) | $vE_{-80°C}$ X | $vE_{-60°C}$ O | $vE_{-40°C}$ O |
| | $\delta_{c\,-50°C}$ X | $\delta_{c\,-30°C}$ O | $\delta_{c\,-10°C}$ O |
| SAW(Multi pass) (50kJ/mm) | $vE_{-80°C}$ O | $vE_{-60°C}$ O | $vE_{-40°C}$ O |
| | $\delta_{c\,-50°C}$ O | $\delta_{c\,-30°C}$ O | $\delta_{c\,-10°C}$ O |

Fig.16 The fitness diagram of Y47S plate made according to criteria of CVN absorbed energy of 42J and CTOD of 0.1mm

A softened zone exists in the welded joint made by one-side one-pass SAW. The minimum hardness in the softened zone drops by 35 in Hv number for the weight of 10kgf in comparison to the base plate, while the tensile strength of the welded joint is 610MPa. Even if a local softened zone exists, the tensile strength of the whole welded joint satisfies the aiming value when the strengths of both base plate and weld metal are appropriate. The tensile strengths of the whole welded joints made by one-side one-pass and one-side two-pass SAW are shown in Fig. 6.

The maximum hardness test according to JIS Z3101 and the Y groove restraint weld cracking test according to JIS Z3158 were carried out. The maximum hardness values for the bead lengths of 10 and 50mm were 329 and 284 in Hv, respectively, even though welding was performed at 0°C without preheating. Weld cracks on root face and cross section were not observed in the Y groove restraint weld cracking test. Thus, preheating-free welding is possible for these steel plates.

## 6. Conclusions

The reduction of carbon equivalent, the addition of small amounts of Nb, rare earth element and Ti, the reduction of impurities such as N, S and P and also the use of advanced TMCP technique have made it possible to develop high strength steel plates of YP400MPa for ships and those of YP460MPa for mobile offshore drilling units used in the Arctic region. Preheat-free welding and high heat input welding can be used for these newly developed steel plates.

The main results obtained follow:

1. The reduction of carbon equivalent in steel is effective not only to decrease the susceptibility to weld cracking, but also to improve HAZ toughness, especially in the use of high heat input welding.
2. The addition of a small amount of Nb is useful for grain-refinement of base plate and inhibiting softening of HAZ of the high heat input welded joint. The Nb content of not more than 0.02% does not deteriorate HAZ toughness of the high heat input welded joint, while that of less than 0.03% is allowed for the low heat input welding.
3. The additions of rare earth element and Ti and the reduction of impurities such as N, S and P improve HAZ toughness of the high heat input welded joint.
4. The preferable ratio of Ti to N exists in the region of 2 to 3.5.
5. A YP400MPa steel plate was developed for ships, which can be welded by one-side one-pass SAW with the heat input of 20kJ/mm.
6. A YP460MPa steel plate was developed for mobile offshore drilling units to be used in the Arctic region. One-side one-pass SAW, one-side two-pass SAW with the heat input of 15kJ/mm and multi-pass SAW with the heat input of 5kJ/mm can be used for service temperatures of not lower than -10°C, -30°C and -50°C, respectively.
7. The steel plates of YP400MPa and YP460MPa had good crack arrestability which is a characteristic property of the TMCP steel plates.

## References


1) C. Shiga, et al., "Ferrite-Fine Bainite Line Pipe of X70 and X80 grades for Low Temperature Service," Proceedings of Int. Conf. on "Steels for line pipe and pipeline fittings," The Metals Society, London, 1981, pp.127-135
2) C. Shiga, K. Amano, T. Enami, et al., "Applications of Multipurpose Accelerated Cooling System (MACS) to the Production of HSLA Steel Plate," Proceedings of Int. Conf. on Technology and Applications of High Strength Low Alloy (HSLA) Steels, AMS, Philadelphia, 1983, pp.643-654
3) C. Shiga, K. Amano, Y. Hirai and Y. Sannomiya, "Tensile Strength 490MPa Grade Controlled-Rolled and Accelerated-Cooled Steel Plate for Arctic Use," Proceedings of Int. Conf. on Offshore Mechanics and Arctic Engineering, ASME, Vol.III, 1984, pp.368-376
4) M. Koda, K. Amano, Y. Nakano, C. Shiga, et al., "Development of 420MPa Yield Strength Steel Plate for Arctic Offshore Structures," Proceedings of Int. Conf. on Offshore Mechanics and Arctic Engineering, ASME, Vol.III, 1987, pp.45-52
5) K. Amano, C. Shiga, Y. Hirai, et al., "New High Strength Steel Plate for Ice-Breaking Ships Designed to Operate in Low Ambient Temperature," Proceedings of 5th Int. Conf. on Offshore Mechanics and Arctic Engineering, ASME, vol II, 1986, pp.338-345
6) J. Matsuyama, F. Kawabata, N. Nishiyama, C. Shiga, et al., "Development of SAW Consumables with High Toughness and Low Hardenability for Sour Service Offshore UOE Line Pipe" '88-Annual Assembly of International Institute of Welding, Doc. XII, pp.1065-88
7) Y. Nakano, K. Amano, J. Kudo, et al., "Preheat- and PWHT-free, 150mm Thick API 2W Grade 60 Steel Plate for Offshore Structures." Proceedings of 7th Int. Conf. on Offshore Mecanics and Arctic Engineering, ASME. vol.III, 1988, pp.89-94
8) H. Yajima, M. Tada, K. Kajimoto, A. Kawamura, S. Noda and T. Nawata, "Extensive Application of TMCP-manufactured High Tensile Steel Plates to Ship Hulls and Offshore Structures," Mitsubishi Juko Giho, vol.23, 1986, pp.383-392

# HIGH STRENGTH PLATE STEELS FOR DEFENCE APPLICATIONS

**R. H. Phillips**
Materials Research Laboratories
Department of Defence
Melbourne, Victoria, Australia

**J. G. Williams**
BHP Steel International Group
Slab & Plate Products Division
Wollongong, NSW, Australia

**J. E. Croll**
Bunge Industrial Steels Pty Ltd.
Wollongong, NSW. Australia

ABSTRACT

A number of developments which have taken place in Australia with regard to high strength alloy and low-alloy steels for defence applications such as naval surface ship and submarine construction, and armour plate, are presented with particular emphasis on production experience, mechanical properties and weldability.
The developments have utilised, either singly or in combination, (i) stringent TMCP schedules coupled with separate ageing treatments; (ii) conventional Q&T heat treatment cycles applied to hot rolled plate product; (iii) controlled additions of Nb, V and Ti for grain refinement and precipitation hardening; and (iv) additions of Cu and Ni for matrix toughness and intermetallic precipitation hardening.

TRADITIONALLY, HY-80 and HY-100 steel plate grades conforming to MIL-S-16216 specification have been used for highly stressed areas of decks, steerage surfaces and hulls of surface ships, as well as pressure hulls and pressure tight bulkheads of conventional submarines. The high cost associated with welding these materials, particularly in relation to stringent preheat requirements has in recent times focussed attention on the development of more weldable compositions without compromising on strength or toughness. The efforts made in the USA in the last few years to permit the usage of Q&T ASTM A710 conforming steels as a more weldable alternative to HY-80 have been particularly successful. At present, the use of this steel (known as HSLA-80) has been restricted to "non critical" applications (ie. precluding crack arrest structures, ballistic plating etc.) and generally confined to plate thicknesses in the range of 6-19mm (1/4 to 3/4in) thus covering the ship classes of small surface combatants and selected areas of underwater vessels and carriers.

Much of the impetus behind new grade development stems from the advances in several key steelmaking technology areas over the last decade. This paper will describe the utilisation in Australia of modern steelmaking (BHP) and heat treatment (BIS) facilities to achieve enhanced properties in conventional HY-80/HY-100 Q&T grades and also a thermomechanically processed (TMCP) and aged HSLA-80 grade which has achieved significant alloy savings over the hitherto quenched and tempered ASTM A710 type grades. It will also be shown that these same advances in steelmaking, plate processing and heat treatment capabilities have enabled the production of high hardness armour plate with very good low temperature toughness and room temperature formability and excellent ballistic properties.

## PROPERTY REQUIREMENTS

In order to qualify HY-80 and HY-100 steel plate for use in highly critical naval structural applications, such as the pressure hulls of submarines, the US Naval Sea Systems Command (NAVSEA) have specified that the steels meet several tiers of mechanical test requirements. These specifications have also been adopted by the Australian Navy for similar applications. The mechanical test specifications include tensile strength, elongation and reduction-of- area requirements, as well as stringent toughness and shock resistance requirements. These latter requirements are set out below:

CHARPY IMPACT TESTS - Standard test specimens are taken 3mm below the plate surface with the notch perpendicular to the plate surface and parallel to the rolling direction. Tests to AS 1544 Part 2 or ASTM E23-83 are carried out at temperatures of -18°C (0°F)

and -84°C (-120°F). The minimum acceptance levels for HY-80 and HY-100 are listed in Table 1.

DYNAMIC TEAR TESTS - The location and notch orientation of dynamic tear tests is the same as used for the Charpy tests (described above). Tests are conducted at -40°C (-40°F). Minimum acceptance levels are listed in Table 1.

EXPLOSION BULGE TESTS - The ultimate qualification test, which measures the resistance to cracking under shock loading is the explosion bulge test. This test was originally developed by Hartbower and Pellini as a means of evaluating and assuring adequate performance of candidate steel plate and welding consumables in the construction of naval vessels(1,2). For this qualification test, two crack starter and four un-notched explosion tests are required and testing is conducted at -18°C (0°F). The test procedure and acceptance criteria are described in MIL-S-2149 (1983). It is presently considered that of the two tests, the crack starter test provides the more useful information, as in this case, the resistance of the material to the extension of a pre-existing crack under explosive loading conditions is more positively measured.

The philosophy behind these three tiers of toughness testing is that as well as being self consistent, the specified property requirements constitute three distinct strata in the level of assurance of achieving adequate base plate (and ultimately weld metal) crack toughness under shock loading conditions.

The Charpy test is relatively cheap and provides a useful first approximation to explosion bulge performance. The dynamic tear test is a significantly larger scale test, sampling over six times the material of the Charpy, is still relatively inexpensive to conduct, and is considered to be a somewhat more useful indicator of explosion bulge performance. The ultimate qualification test is the explosion bulge test. This test is very expensive to conduct, however it provides the most useful indicator of material performance.

At present, HSLA-80 (A710) type steels are not permitted in critical submarine applications. However, they are extensively used in the construction of naval surface combatants in the USA.

The mechanical test requirements for HSLA-80 (A710) including Charpy and dynamic tear, for use in the hulls of naval surface combatants, are identical to the requirements for HY-80 with the notable exception that the explosion bulge test is not required. The thickness of HSLA-80 plate in surface combatants rarely exceeds 20mm, with most requirements falling in the 10mm to 15mm thickness range.

One important question to be addressed in future is whether the Charpy and dynamic tear benchmark values listed in Table 1, are reliable indicators of explosion bulge performance for other grades of high strength steel suitable for naval structural applications, such as HSLA-80. In this respect, an important consideration may turn out to be the shape of the Charpy or dynamic tear curve ie. whether it shows shallow or steep transitional behaviour.

## FABRICATION ADVANTAGES OF HSLA-80 (A710 TYPE) COMPARED TO HY-80

In the naval construction arena there is a powerful economic driving force to replace HY-80 with HSLA-80 type steels. This is presently manifested in the construction of naval surface combatants in the USA where substantial substitution of HSLA-80 for HY-80 has already occurred.

Although HSLA-80 may be potentially cheaper to produce than HY-80 because of its lower alloy content the major cost reductions are achieved in fabrication savings. The most important of these are listed below:

i) no necessity to preheat HSLA-80.

ii) lower level of welding skill required, which affords the opportunity to reduce labour costs.

iii) greatly reduced inspection and repair cost.

iv) no requirement for time consuming grinding off of attachments.

v) no requirement for cleaning weld bead surfaces prior to depositing subsequent weld passes.

vi) decreased surface preparation.

In addition a much wider variety of product forms can be economically produced with HSLA-80, and flame forming and straightening is permissible with HSLA-80 but not with HY-80. Finally, high productivity welding processes such as high frequency welding can be used to produce inexpensive product forms such as T stiffeners.

Table 1 - Minimum NAVSEA Impact Requirements for HY-80 and HY-100

| Test Temperature | | Charpy | | | | Dynamic Tear | | | |
|---|---|---|---|---|---|---|---|---|---|
| | | HY-80 | | HY-100 | | HY-80 | | HY-100 | |
| °C | °F | J | (Ft-lb) | J | (Ft-lb) | J | (Ft-lb) | J | (Ft-lb) |
| -18 | 0 | 81 | (60) | 81 | (60) | - | | - | |
| -84 | -120 | 47 | (35) | 60 | (45) | - | | - | |
| -40 | - 40 | | | | | 610 | (450) | 680 | (500) |

## STEEL ALLOY DESIGN

In satisfying the abovementioned property requirements, steel chemical composition should be optimally selected with due recognition of processing capabilities. For instance, there may be scope for reducing the hardenability and therefore alloy content of conventional Q&T grades when more efficient quenching devices are used. Alternatively, utilisation of suitable TMCP techniques may permit the achievement of required properties so as to obviate the need for those alloy additions which promote quench hardenability such as Cr and Mo. Some principles of alloy design for HY-80/HY-100 and HSLA-80 as produced in Australia are discussed below:

HY-80/HY-100 - The chemical composition of HY-80/HY-100 is comparatively tightly specified by the relevant military specification, MIL-S-16216(3), and is based on a low Mn-Ni-Cr-Mo steel type; Ni primarily being added for low temperature toughness, with Cr and Mo conferring a high level of quench hardenability. No microalloying additions of Nb, V, Ti or B are allowed.

While the fundamental approach to alloy design with the HY-80/HY-100 steels has not changed, some major developments have occurred over the last 25 years with regard to specific composition limits. As shown in Table 2, these have been largely confined to tightening the allowable concentrations of:

i) trace elements such as Sn, Sb and As,
ii) tramp elements such as P and S, and
iii) controlling the range of C content.

These changes themselves reflect the significant advances in steelmaking technology that has occurred internationally during this time especially with respect to the achievement of much lower P and S contents.

MIL-S-16216 allows slightly different ranges for C, Ni, Cr and Mo contents to accommodate increasing plate thickness and to assist in obtaining the higher strength values of HY-100 relative to HY-80. On the other hand, there are attractions in terms of the ability to supply small item lots with maximum flexibility, if both HY-80 and HY-100 grades can be sourced from the one heat in as large a range of plate thicknesses as possible. Our experience has been that due to the close and consistent control of all elements as a result of efficient tonnage vacuum degassing, it has been possible to develop an internal specification with a single, more restrictive set of alloy ranges than is allowed in MIL-S-16216, such that both HY-80 and HY-100 grades can be sourced in plate thicknesses from 6 to 50mm (1/4 to 2") from a single heat. A typical chemical composition is shown in Table 3.

As will be described subsequently, micro Ti treatment of the traditional HY-80/100 grade has recently been investigated to explore the potential for reduced weld preheat which has been achieved in C Mn and HSLA steels by virtue of the reduced HAZ hardenability and peak hardness levels derived from a fine dispersion of stable TiN precipitates(4).

HSLA-80 - The alloy design of conventional ASTM A710 type steels is based on the ε-Cu age hardening "Nicuage" steels of the late 60's and a typical composition is shown in Table 4. The

Table 2 - Chemical Composition Refinements of HY-80 Specification(3)
Ladle Analysis - Mass Percent

| MIL-S-16216 Revision: | G | H | J | K |
|---|---|---|---|---|
| Dated: | 27 February 1963 | 15 March 1972 | 16 August 1982 | 19 June 1987 |
| Carbon | 0.18 max | 0.12/0.18 | 0.12/0.18 | 0.12/0.18 |
| Phosphorus | 0.025 max | 0.025 max | 0.020 max | 0.015 max |
| Sulphur | 0.025 max | 0.025 max | 0.002/0.020 | 0.008 max |
| Phosphorus + Sulphur | 0.045 max | 0.040 max | 0.035 max | (3) |
| Arsenic | NS (2) | NS | 0.025 max | 0.025 max |
| Tin | NS | NS | 0.030 max | 0.030 max |
| Antimony | NS | NS | 0.035 max | 0.025 max |

(1) The chemical limits are for 25mm (1") thick HY-80 plate.
(2) NS = Not Specified
(3) No limit specified, although plates with S contents less than or equal to 0.002 should be specially identified.

Table 3 - Typical Chemical Composition of HY-80/HY-100 (mass %)

| C | P | Mn | Si | S | Ni | Cr | Mo | Cu | Al | CEQ(IIW) |
|---|---|---|---|---|---|---|---|---|---|---|
| .15 | .014 | .26 | .23 | .003 | 2.65 | 1.55 | .38 | .010 | .050 | .756 |

Table 4 - Chemical Composition (mass %)

| Steel | C | Mn | Si | S | Ni | Cu | Cr | Mo | Al | Ti | Nb | CEQ(IIW) |
|---|---|---|---|---|---|---|---|---|---|---|---|---|
| ASTM A710 Class 3 (Q&T) | .05 | .50 | .25 | .005 | .90 | 1.15 | .70 | .25 | .02 | - | .040 | .46 |
| BHP HSLA-80 (TMCP) | .05 | 1.40 | .25 | .003 | .85 | 1.0 | - | - | .02 | .015 | .020 | .41 |

Table 5 - Typical Chemical Composition of High Hardness Armour Plate (mass %)

| C | P | Mn | Si | S | Cr | Mo | Al | Ti | B | CEQ(IIW) |
|---|---|---|---|---|---|---|---|---|---|---|
| .28 | .015 | .54 | .28 | .003 | .94 | .16 | .036 | .036 | .0015 | .592 |

steel exhibits good quench hardenability, largely due to Ni, Cr, Mo additions, so that it has been well suited to production via the quench and ageing process route especially for rather heavy plates. However, a more appropriate low alloy modified alternative has been developed by BHP for plates of up to about 28mm (1-1/8"). This steel can be produced in the TMCP + aged condition with the following main compositional/processing differences:

i) Cr and Mo additions have been eliminated since high hardenability is not needed in these thin plates when TMCP is applied. The elimination of these elements provides for further weldability improvements over HY-80 (reduction in Pcm carbon equivalent from .29 to .20) and other measured benefits to steelmaking such as improved hot ductility during continuous casting and lower production costs.

ii) A higher Mn addition partly to compensate the strength reduction arising from elimination of Cr and Mo and also to improve "control rollability" and promote ferrite grain refinement due to reduced $\gamma$-$\alpha$ transformation temperatures.

iii) The application of TMCP involving controlled rolling to finish temperatures just above the $Ar_3$ and subsequent accelerated cooling to about 550°C to suppress Cu "auto" ageing in the as rolled condition.

iv) Micro Ti treatment and reduced Nb content for enhanced HAZ toughness(4).

ARMOUR PLATE - The important material characteristics for homogeneous quenched and tempered steel armour plate include a high hardness level of 500 HB nominal; good low temperature toughness and through-thickness ductility to prevent shattering, spalling or plug formation on impact of the projectile; and fabrication performance in terms of weldability and formability compatible with the other requirements.

MIL-A-46100C(5) specifies basic chemical composition limits for steel armour plate with a hardness of 477-534 HB, and supports these with longitudinal and transverse Charpy V-notch impact tests at -40°C (-40°F) and room temperature bend tests.

Alloy design for high hardness armour plate manufactured by BIS involves a consideration of:

i) C contents which are sufficiently high to achieve the desired hardness level, but not so high as to seriously effect ductility, formability and weldability. Optimum levels are .27/.30 C.

ii) Controlled Cr, Mo and B additions to achieve through hardening. Actual concentrations depend on the severity of quench employed.

iii) Steelmaking practices aimed at producing low sulphur contents, with or without non-metallic inclusion shape control.

A typical chemical composition is shown in Table 5.

## STEEL MANUFACTURING ASPECTS

The advances made in several steelmaking technology areas over the last decade have not only provided the stimulus for new grade development but have also made possible significant improvements in the characteristics of older steels such as HY-80/HY-100. Capital investment in the Australian steel industry over this period has ensured that such property enhancements are available by utilisation of the following steel production facilities:

HOT METAL & STEEL LADLE DESULPHURISATION - Low sulphur levels (ie. < 0.005% S) with or without inclusion shape controlling additions of Ca are an important pre-requisite for high Charpy energy values, especially in the transverse to rolling direction, and also for good through thickness ductility. Such sulphur levels are assured at BHP by the employment of hot metal desulphurisation and steel ladle injection of calcium compounds which also guarantees conversion of $Al_2O_3$ clusters to globular particles(6). In addition to these property improvements, the ballistic properties and performance of plates in special tests such as the explosion bulge test (EBT) are enhanced by clean steelmaking practice.

TONNAGE VACUUM DEGASSING TREATMENT - RH vacuum degassing at low vacuums such as 0.5 torr is applied at BHP in the production of high strength defence steels to achieve reductions in gas contents such as $H_2$, $N_2$, $O_2$, some removal of non metallic inclusions and close control needed over alloy additions, especially microalloys such as B and Ti.

CONTINUOUS CASTING OF SLABS - The recently commissioned No.2 Caster at BHP provides for the production of improved steel cleanness, excellent surface quality and internal homogeneity by virtue of the following attributes:

i) large capacity (48 tonne) tundish and automatic mould level control,

ii) air tight ladle to tundish shrouding system and fully sealed tundish with inert gas flushing capability,

iii) improved centreline segregation control with closely spaced split rolls, internally water cooled rolls and bearings for reduced roll bending,

iv) air mist cooling for uniform cooling control across the strand width,

v) variable machine taper and in-roll variable cycle electromagnetic stirring (EMS).

THERMOMECHANICALLY CONTROLLED PROCESSING (TMCP) - Strict TMCP rolling schedules are necessary to achieve the low temperature toughness levels needed for HSLA-80 type steel to obviate the need for reaustenitising heat treatments. At BHP, optimum toughness is achieved by ensuring that austenite is recrystallised to a suitable fine grain size during high temperature roughing and an appropriate level of non recrystallising austenite deformation is completed just above the $Ar_3$ temperature(4). In the case of HSLA-80, key aspects of the TMCP practice are highlighted schematically in Figure 1 and briefly described below:

Disciplined Rough Rolling Practice - The main objective in the rough rolling stage is to ensure a fine recrystallised grain size prior to the commencement of finish rolling in the non recrystallising region. The high Cu addition is thought to contribute to more sluggish recrystallisation behaviour than for plain Nb steels(7) and the strategy adopted at BHP has been to perform the roughing reduction at rather high temperatures in conjunction with sufficiently heavy individual pass reductions to limit the possible formation of mixed austenite grain size. The micro Ti treatment is effective in achieving this goal and in restricting the subsequent growth of recrystallised grains.

Non-Recrystallising Austenite Deformation - Rather heavy total reduction levels in the austenite non-recrystallising temperature regime have been found to be beneficial for the enhanced low temperature toughness of HSLA-80. The objective is to multiply ferrite nucleation sites in order to secure Charpy transition temperatures below about -120°C in the as rolled condition. Such low transition temperatures must be achieved to compensate for the embrittling effect of the subsequent Cu age hardening treatment.

Controlled Cooling - Maximum Cu age hardening capability requires that the extent of auto-ageing after finish rolling be restricted. To prevent wasteful premature precipitation of ε-Cu, an accelerated plate cooling practice after finish rolling has been employed in which the plate is passed through a water spray bank until the mean temperature is about 550°C. Modest cooling rates of only ~2-3°C/sec have been achieved in 25mm thick plates with this practice and have proved sufficient to ensure comfortable achievement of strength properties.

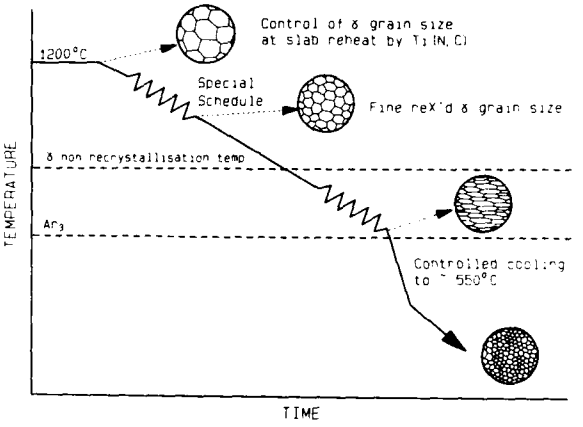


Fig.1 - Schematic outline of TMCP process for HSLA-80 plates

EFFICIENT QUENCHING & TEMPERING (Q&T) FACILITIES - The #2 plate heat treatment plant operated by BIS was commissioned in 1984, and represents the latest technology in independent quenching and tempering capability. This plant is capable of heat treating plate in the thickness range 5-100mm (3/16-4"), to a maximum plate width of 3200mm (126"), and a maximum plate length of 15 metres (590"). This size range embraces all current local defence requirements for high strength steel plate, and in particular satisfies all needs for Q&T plate for the New Construction Submarine (NCSM) Project.

A special feature of the continuous roller quench unit in this plant is the high intensity curtain water header which enables the production of high strength grades from comparatively lean (ie. low alloy) steel compositions, thereby lowering carbon equivalent values and improving weldability. Total water flow rates of up to 30,000 litres/minute (6,600 gallons/minute) during quenching together with the design of the quench rollers, ensure a metallurgically efficient quenching

operation. For example, the cooling rate over the temperature range 800-300°C at the mid-thickness position of a 25mm (1") thick plate has been determined to be approximately 40°C/second (70°F/second)(8).

## STEEL PROPERTIES

Mechanical properties, weldability and other aspects of fabrication and service of quenched and tempered HY-80/HY-100, TMCP + aged HSLA-80 and armour plate are discussed below:

HY-80/HY-100 - The mechanical properties of normally produced HY-80 and HY-100 plates as well as the test results obtained on the special Ti treated material are described in the following sections.

Strength and Charpy Impact Tests - Typical tensile and Charpy V-notch impact test data for HY-80/HY-100 plates are shown in Table 6. Note the very low longitudinal to transverse Charpy upper shelf energy ratios of about 1.1.

The distributions of Charpy impact energy values for both HY-80 and HY-100 plates, shown in Figure 2, again highlight the exceptionally good low temperature toughness of this material due to the combined effects of clean steel and efficient quenching facilities.

Dynamic Tear Tests - Similarly the results of dynamic tear tests carried out on HY-80 and HY-100 plates (refer Figure 3) are extremely good, and provide a good guide to the ultimate performance in the explosion bulge test.

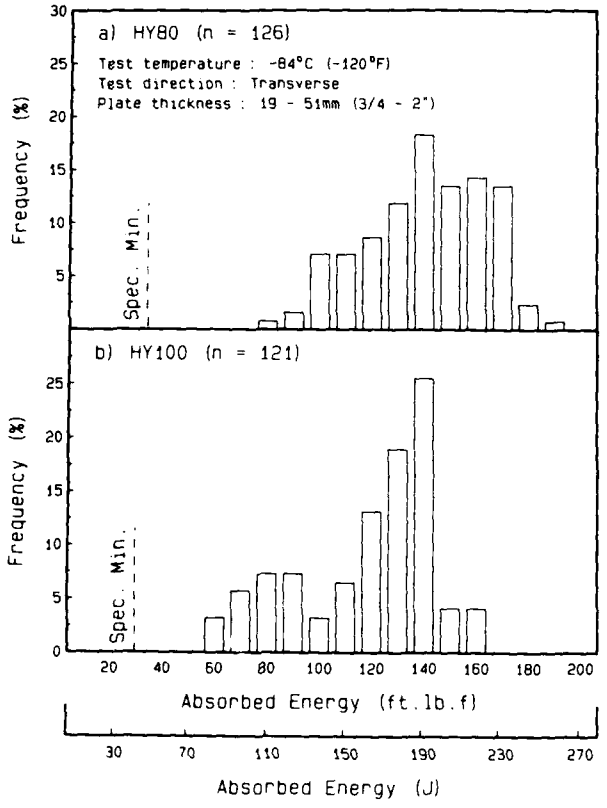


Fig.2 - Charpy V-notch impact energy of HY-80 and HY-100 plates

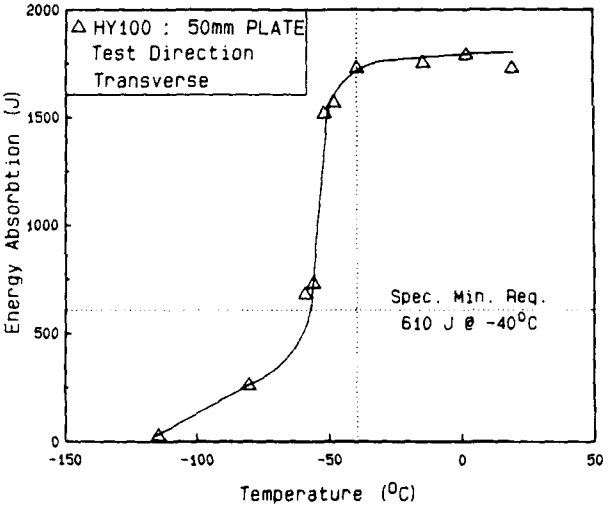


Fig.3 - Dynamic tear test transition for HY-100

Table 6 - Typical Tensile & Charpy V-notch Impact Test Data for HY-80/HY-100 Plates

| Grade | Plate Thickness (mm) | Tensile Properties 0.2%PS (MPa) | TS (MPa) | El (%) | Charpy Impact Energy Temp (C) | Long (J) | Trans (J) |
|---|---|---|---|---|---|---|---|
| HY-80 | 9.5 | 644 | 762 | 32 | - | - | - |
| HY-80 | 50 | 616 | 731 | 25 | +20 | 216 | 207 |
| | | | | | -18 | 214 | 203 |
| | | | | | -40 | 209 | 193 |
| | | | | | -84 | 184 | 164 |
| HY-100 | 25 | 745 | 828 | 24 | +20 | 203 | 168 |
| | | | | | -18 | 199 | 168 |
| | | | | | -40 | 198 | 163 |
| | | | | | -84 | 187 | 138 |

Explosion Bulge Tests - Explosion bulge tests (EBTs) have been performed in accordance with the provisions of NAVSHIPS 0900-005-5000 and NAVSEA 0900-LP-005-5000. Parent plate samples and welded assemblies, with and without crack starter weld beads, have been tested at -18°C (0°F) with excellent results.

The manual metal arc welded samples of 50mm (2") thick HY-80 plates shown in Figure 4 have thinned 29.9 and 25.7% respectively after five blasts, easily satisfying the specification requirement of 16% thinning. This demonstrates the very good crack arrest ability of this material under explosive loading conditions.


Fig.4 - Profiles of two explosion bulge tests of fully MMA welded HY-80 plates after 5 blasts

Weldability - Special investigations were carried out to assess the potential improvements to HAZ microstructure and properties which might result from a micro Ti addition to continuously cast HY-80/HY-100 steel. Such improvements have been widely exploited in recent years in HSLA steel plates by virtue of the controlling influence of fine TiN precipitates on the extent of austenite grain growth adjacent to the fusion line(4). The results of this work are summarised briefly below:

i) Microstructure - The effects of Ti treatment on HAZ microstructure was demonstrated in a series of bead-on-plate welds using a GMA welding process on 50mm thick plate at various heat inputs in the range of 1.0-6.0kJ/mm. The HAZ microstructures for both Ti and non Ti bearing steels consisted of untempered martensite despite major differences in the austenite grain size and the width of the grain coarsened regions (Figure 5). Typical photomicrographs at the higher heat input level of 4kJ/mm are shown in Figure 6.

ii) Hardness - HAZ peak hardness measurements and hardness traverses across the HAZ were also performed on the bead on plate welds over the range of heat input. The results are summarised in Figure 7 and indicate that no advantage of Ti with respect to hardenability in the grain coarsened region was apparent. In fact somewhat higher hardnesses were observed in the grain coarsened HAZ microstructure for the Ti treated steel, probably due to the slightly higher carbon equivalent. Since the grain coarsened HAZ microstructure for this steel type was completely martensitic over the range of heat inputs examined, the commonly exploited benefits of TiN precipitates on reduced HAZ hardenability (and hence hardness) in low CEQ steels do not appear to be achievable. Consequently, reduced susceptibility to cold cracking and relaxation of preheat requirements which has been reported elsewhere for Ti treated HSLA steels(4) is unlikely to apply to highly hardenable steels such as conventional HY-80/HY-100. This was also evidenced in the results of controlled thermal severity (CTS) tests performed on Ti treated and non Ti treated HY-80 as indicated in Table 7 where both steels reported similar cracking resistance at preheat temperatures over the range of 20°C to 100°C.

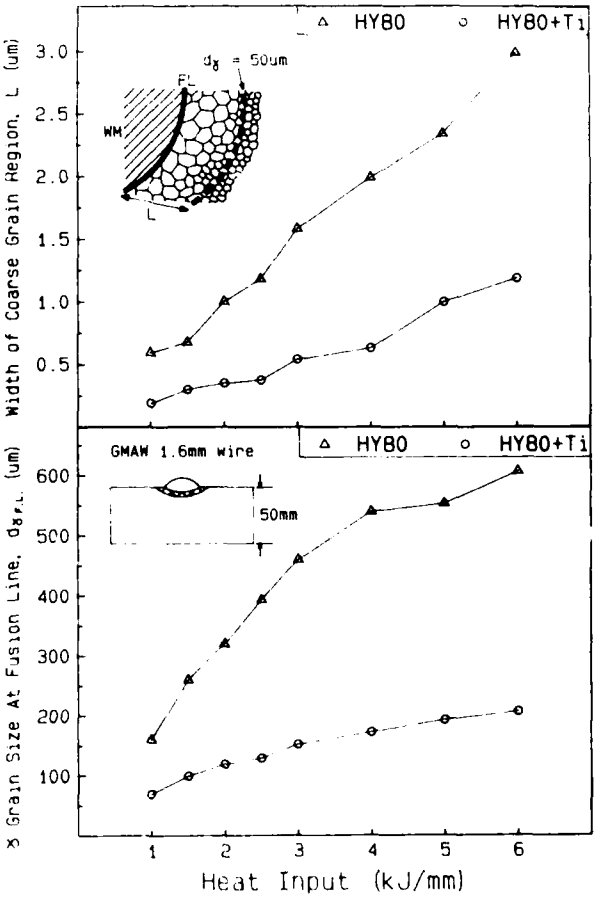


Fig.5 - Effect of Ti on the austenite grain size at the fusion line and the width of the coarse grain region (HY-80 plate)

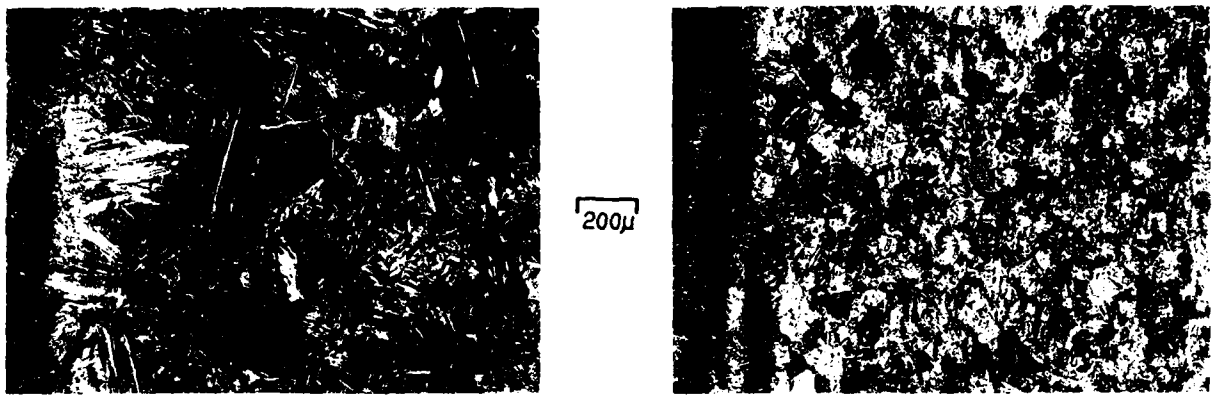


HY-80 HY-80 + Ti

Fig.6 - Effect of Ti on the HAZ microstructure of HY-80 plate (4kJ/mm bead on plate weld)

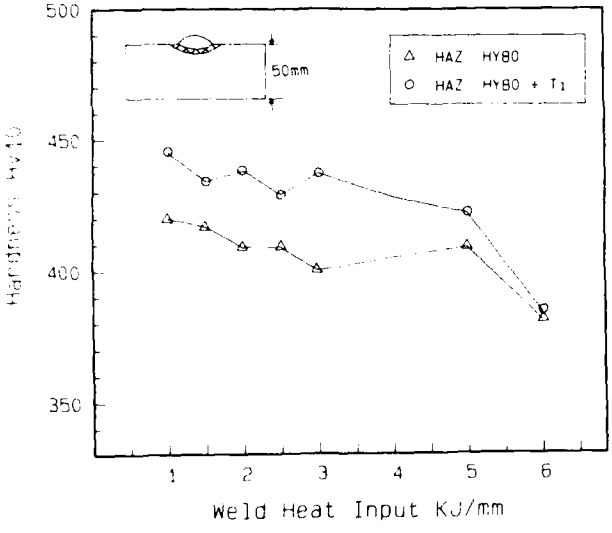


Fig.7 - Maximum HAZ hardness in GMAW bead on plate welds for HY-80 plate

Table 7 - Controlled Thermal Severity (CTS) Test Results (50mm Plate Thickness)

| Test | | CTS (% Leg Length Cracked) | | | |
|---|---|---|---|---|---|
| Steel Type | | HY-80 | | HY-80 + Ti | |
| Heat Input (kJ/mm) | | 1.6 | 2.2 | 1.6 | 2.2 |
| Preheat Temp | 20°C | 19 | 18 | 18 | 18 |
| | 60°C | 11 | 15 | 7 | 10 |
| | 100°C | 6 | 7 | 4 | 8 |

iii) Toughness - The strong grain refining influence of TiN precipitates on the austenite grain size in the HAZ would be anticipated to have some beneficial effect on toughness as measured by Charpy V specimens. However, this was not apparent in tests performed on the HAZ of multipass submerged arc welds (heat input 4kJ/mm) described in Table 8.

HSLA-80 - The mechanical properties of the newly developed TMCP + aged HSLA-80 grade are described below for plate thicknesses in the range of 12-25mm.

Table 8 - HAZ Charpy V-Notch Impact Properties (50mm Plate, K-weld Prep, 4 kJ/mm Heat Input)

| Steel | Specimen | Test Temperature 0°C | | | | | | -84°C | | | | | |
|---|---|---|---|---|---|---|---|---|---|---|---|---|---|
| Type | Location | Cv En (J) | | | % Fib | | | Cv En (J) | | | % Fib | | |
| HY-80 | Top Surface | 165 | 200 | 264 | 100 | 100 | 100 | 197 | 204 | 272 | 100 | 100 | 100 |
| | Bottom Surface | 110 | 168 | 264 | 100 | 100 | 100 | 54* | 109 | 217 | 15 | 100 | 100 |
| HY-80 | Top Surface | 166 | 186 | 298 | 100 | 100 | 100 | 246 | 261 | 261 | 100 | 100 | 100 |
| (+ Ti) | Bottom Surface | 116 | 148 | 247 | 100 | 100 | 100 | 46* | 54* | 207 | 20 | 20 | 65 |

* Weld metal notch location

Strength - Typical tensile properties established in production trial plates are summarised in Figure 8 for both the as rolled (TMCP) condition and TMCP + aged 550°C condition for various plate thicknesses. For normal air cooling of plates after TMCP, the yield strength after ageing was marginal at the heavier plate thicknesses ie. ~25mm. The application of a modified TMCP schedule and controlled cooling after TMCP produced a significant improvement in yield strength of 20-25mm thick plates by virtue of a microstructural refinement and reduced "auto" ageing. The yield strength increment derived from the ageing treatment, was typically in the order of 100 MPa for the range of thicknesses investigated such that the HY-80 yield strength requirement of 550 MPa minimum was comfortably achieved. These results suggest some scope for further reductions in steel alloy levels so as to further enhance weldability. Alternatively "overageing" might be considered as a means for reducing the deterioration of toughness properties associated with the age hardening process, particularly in the thicker plates, as discussed below.

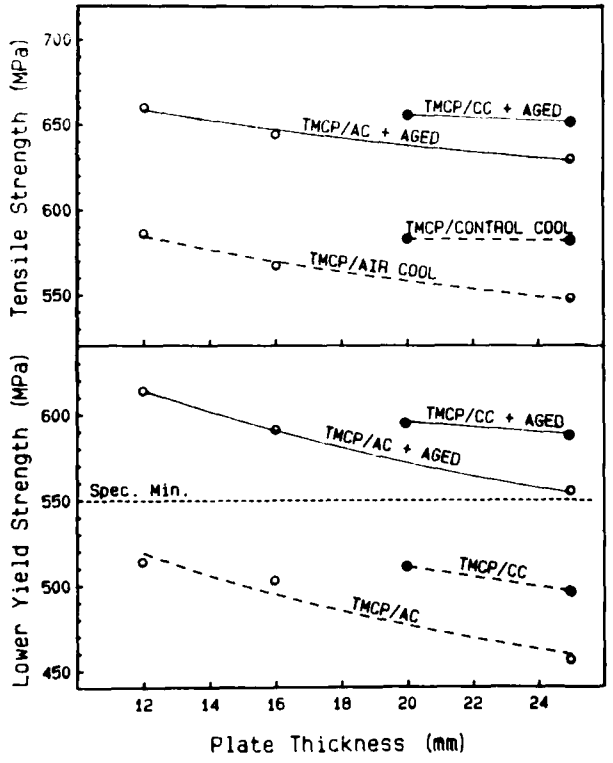


Fig.8 - Influence of plate thickness and TMCP on tensile properties of HSLA 80 (Ageing Temp: 550°C)

Toughness - The toughness properties of production trial plates as measured in Charpy V-notch test are summarised in Figures 9 & 10 for plates in both the as TMCP and TMCP + aged 550°C condition. The ageing treatment of 1/2 hr at 550°C was chosen to achieve the peak strengthening increment from $\epsilon$-Cu precipitation and, by inference, the maximum likely upward shift in Charpy transition temperature. From Figure 9 it is evident that "peak ageing" can deteriorate the Charpy 50% FATT by up to about 30°C. This is of significance especially in the case of thicker plates eg. 25mm where the 50% FATT in the peak aged condition has in fact been raised to the vicinity of the specified test temperature for HY-80 ie. -85°C. In order to increase the safety margin for satisfying this specification requirement, "overageing" of the $\epsilon$-Cu precipitates has been found to be useful for reducing the upward shift in Charpy transition temperature whilst still comfortably achieving the strength requirements. The influence of ageing treatments on strength and toughness is highlighted in Figure 10 for a 25mm thick plate. For instance, an "overageing" treatment such as 1/2 hr at 610°C can reduce the upward shift in Cv transition temperature to only 15°C and simultaneously satisfy the yield strength requirement of 550 MPa although by a reduced margin.

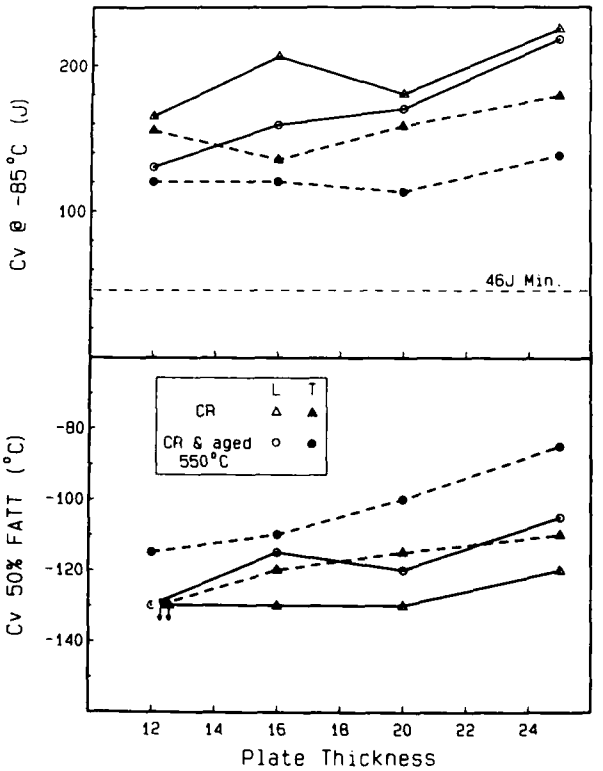


Fig.9 - Effect of Ageing on Charpy V-notch energy at -85°c and 50% FATT for various plate thicknesses of HSLA-80

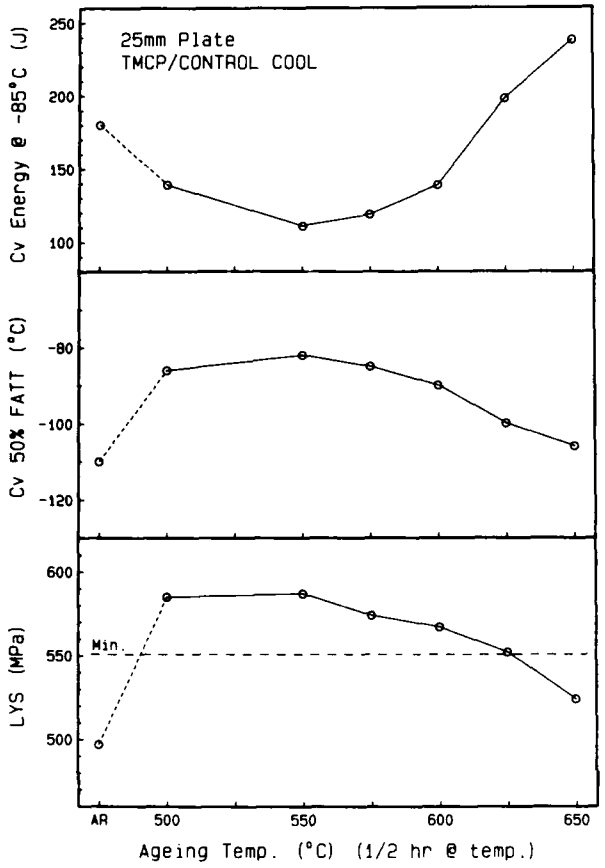


Fig.10 - Effect of Ageing Treatment on Charpy V-notch and tensile properties of 25mm HSLA-80 plate

Dynamic tear test transition curves were also performed on 20 and 25mm plates and results are presented in Figure 11. Both plates met the specification requirement of 610 J at -40°C with the "overageing" treatment (610°C) again proving beneficial in improving the performance of the 25mm plate.

Weldability - The following weldability investigations have confirmed the excellent potential of HSLA-80 for fabrication economy due mainly to the low carbon equivalent (CEQ (IIW) = 0.40, Pcm = 0.20), low carbon content and micro Ti treatment.

i) Bead on Plate Tests - Bead on plate tests were performed on 36mm thick HSLA-80 plate utilising the gas metal arc GMA welding process for 1.0, 1.5 and 2.5kJ/mm heat inputs and submerged arc (SAW) welding process for 2.5, 4.0 and 6.0kJ/mm heat inputs. All tests were performed without preheat. Peak hardnesses and hardness traverses from the fusion line across the HAZ were determined in both as welded condition and also after a subsequent ageing treatment of 30 mins at 500°C to investigate possible age hardening effects. The results are presented in Figures 12-14 and briefly summarised below:

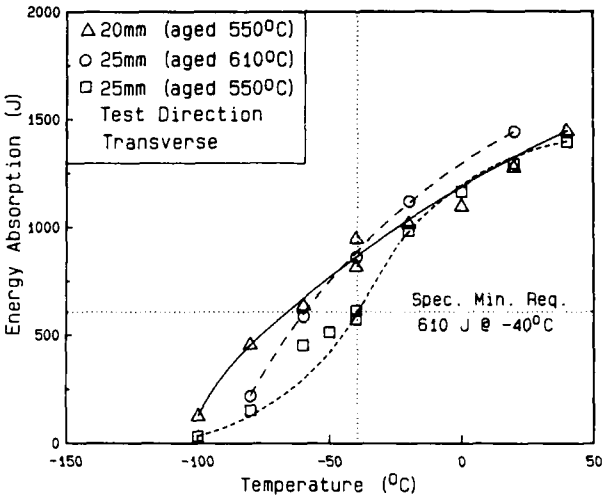


Fig.11 - Dynamic Tear Test Transitions for HSLA-80 plates

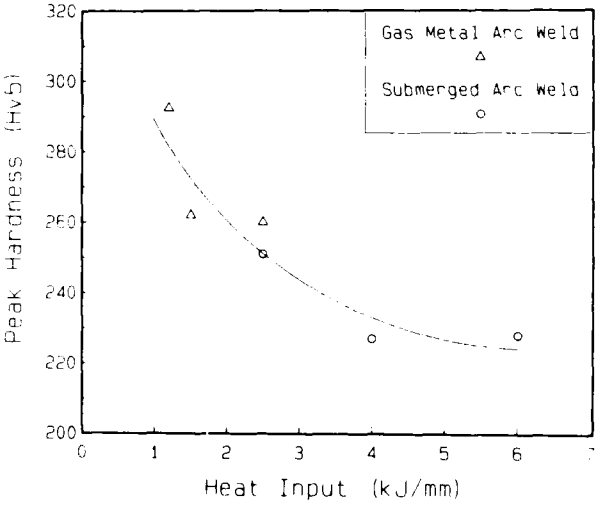


Fig.12 - Peak Hardness for varying heat inputs for GMAW/SAW bead on plate welds of HSLA-80

a) The peak hardness in the as welded condition was below 300 Hv for the lowest heat input weld of 1kJ/mm (see Figure 12). These values may be compared with the results of HY-80 in Figure 7 where the peak hardness under similar conditions was in the vicinity of 420-450 Hv.

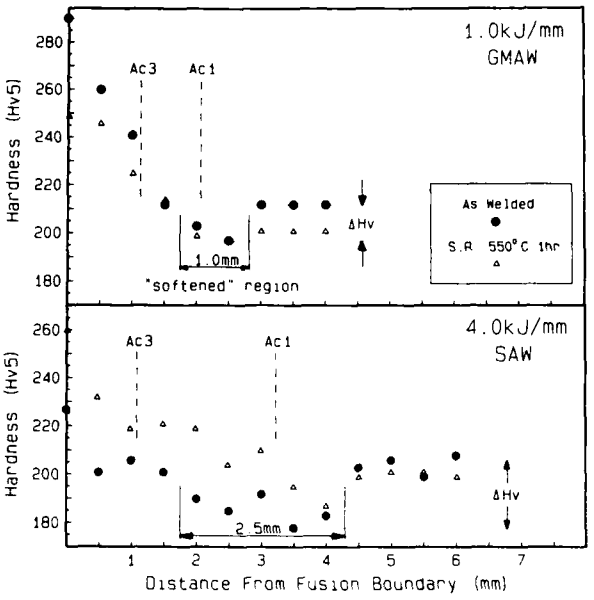


Fig.13 - Hardness traverse across HAZ of bead on plate welds of 36mm HSLA-80 plate

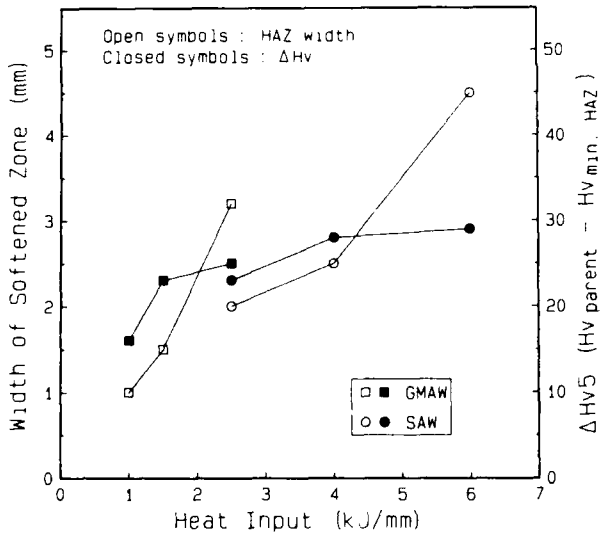


Fig.14 - Influence of Heat input on width of softened zone and amount of softening (Δ Hv) for 36mm HSLA-80 plate

b) A "softened" region occurred in the intercritical and subcritical HAZ, the width of which was dependent on the welding process and heat input level (Figures 13 & 14). The degree of softening was up to 30 Hv. The effect of the 550°C ageing treatment was to produce an increase in hardness in the supercritical and intercritical HAZ. The extent of this hardness increase was dependent on the heat input level and ranged from about zero for 1kJ/mm up to about 40 Hv for the 6kJ/mm weld. This secondary hardening effect was attributable to reprecipitation of ε-Cu which had been taken into solution in the weld thermal cycle. Such hardening should advantageously offset the extent of "softening" in multipass welding.

c) As mentioned earlier micro Ti treatment in steels of relatively low hardenability contributes to reduced HAZ hardenability and hence hardness by virtue of austenite grain size control in the weld thermal cycle. Measurements of the austenite grain size at the fusion line and the width of the coarse grain region for the various heat input levels are presented in Figure 15 and clearly demonstrate the efficacy of the micro Ti treatment in this steel.

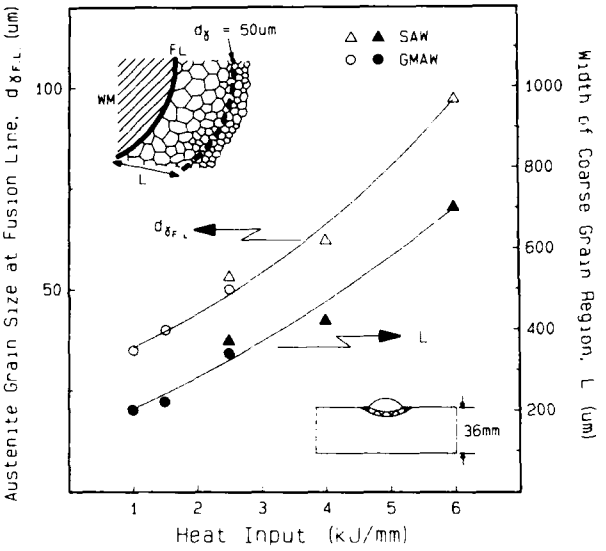


Fig.15 - Austenite grain size at fusion line and width of coarse grain region in bead on plate welds on HSLA-80 plate

ii) Weld Zone Toughness - The weld zone toughness of HSLA-80 was tested in a weld procedure shown in Figure 16. The planar HAZ hereby produced allows the sampling by a CTOD specimen of a large intersection of coarse grain HAZ/fusion line which should represent the most brittle zone. The good low temperature toughness was demonstrated by the 0.2mm CTOD transition temperature of about -50°C for the coarse grain/fusion line HAZ region.

iii) Delayed Cracking Test - Controlled thermal severity (CTS) tests (Table 9) were carried out on 36mm thick plate with hydrogen controlled electrodes in conjunction with no preheat. The steel exhibited excellent resistance to delayed cold cracking (0%

cracking) presumably reflecting the low maximum hardnesses achieved in the HAZ by virtue of the low CEQ and micro Ti treatment as well as the restricted width of the coarse grain region (hardened zone).

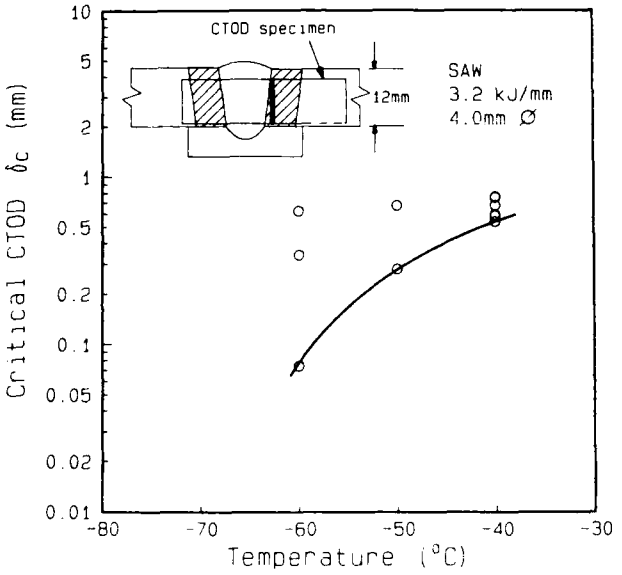


Fig.16 - CTOD transition in Fusion line/Coarse grain HAZ of HSLA-80 plate

Table 9 - Controlled Thermal Severity (CTS) Tests for HSLA-80 (36mm Plate) Ambient Preheat (20°), E10018M - 40mm electrodes - 4ml/100gm av $H_2$

| Arc Energy (kJ/mm) | 1.0 | 1.6 | 2.2 |
|---|---|---|---|
| % Cracking | 0 | 0 | 0 |
| Peak Hardness $Hv_5$ | 299 | 283 | 283 |
| Ave Peak Hardness | 291 | 280 | 272 |

ARMOUR PLATE - Australian-produced Q&T armour plate in the thickness range 6-38mm (1/4-1.5") has been subjected to laboratory tests to assess mechanical properties, including through-thickness ductility, bend test performance and ballistic properties. Results of these tests are summarised in the following sections.

Toughness - The Charpy impact test requirement for armour plate complying with MIL-A-46100C is for the absorbed energy to be not less than 10 ft.lb.f (13.5 J) for the transverse orientation, and 12 ft.lb.f (16.3 J) for the longitudinal orientation, when full size (10 x 10mm) specimens are tested at -40°F (-40°C). The results shown in Table 10 clearly demonstrate that despite the high hardness of this material, typically 495-515 HB, the toughness as measured in the Charpy impact test is quite good and comfortably meets the MIL specification requirement. This is further evidence of the beneficial effects of the clean steelmaking practices employed and the high quench rates achieved in the continuous roller quench unit.

Table 10 - Average Charpy V-notch Impact Test Data - High Hardness Armour Plate

| Plate Thick (mm) | Specimen Size (mm) | Charpy Energy at -40°C Long (J) | Charpy Energy at -40°C Trans (J) | 50% Fibrous Transition Temperature (°C) |
|---|---|---|---|---|
| 6 | 10 x 5 | 19 | 12 | -40 |
| 10 | 10 x 7.5 | 24 | 16 | -32 |
| 12 | 10 x 10 | 29 | 24 | -28 |
| 25 | 10 x 10 | 27 | 26 | -28 |
| 35 | 10 x 10 | 26 | 24 | -30 |

Through-thickness reduction of area values of 28.8 and 30.5% RAz have been obtained on a 35mm (1.375") thick plate, also indicating the inherently good through-thickness ductility resulting from the particular combination of steel composition and processing route.

Bend Test - The bend test requirement in MIL-A-46100C is for 90 included angle bends to be conducted in accordance with ASTM E290, with the axis of the bend perpendicular to the plate rolling direction (ie. transverse bends). Transverse bends are less severe than those for which the bend axis is parallel to the rolling direction. Minimum inside bend radius is 4 x plate thickness for plates up to and including 5/16" (8mm) thick, and 6 x plate thickness for thicker plates to 1/2" (12mm). Tests are not required on thicker plates.

Test results on this material are summarised in Table 11, and reflect both good ductility and a fabrication potential which belies the high hardnesses involved.

Ballistic Tests - To date the high hardness armour plate has been tested exclusively against the requirements of an Australian Standard for bullet resistant material, AS2343(9). The highest severity requirements of this standard call for the test panel to withstand three impacts from ammunition fired at 90° obliquity from one of two rifles, designated R1 and R2:

i) R1 category is M193 5.56mm (.219 calibre) ammunition fired at a velocity of 980 m/sec (3215 ft/sec).

ii) R2 category is NATO 7.62mm (.300 calibre) ammunition fired at a velocity of 853 m/sec (2800 ft/sec).

It has been shown that 8mm thick 500 HB Q&T plate will easily meet the requirements of the R2 category, while 10mm thick plate will consistently pass the R1 and R2 categories.

Table 11 - Bend Test Performance - High Hardness Armour Plate

| Plate Thickness (mm) | Spec Requirement Transverse Bends (Angle @ Radius) | Bend Test Results - Pass | |
|---|---|---|---|
| | | Longitudinal Bends | Transverse Bends |
| 6 | 90 @ 4.0t rad (1) | 180 @ 4.0t rad | 180 @ 4.0t rad |
| 8 | 90 @ 4.0t rad | - | 180 @ 2.0t rad |
| 10 | 90 @ 6.0t rad | - | 180 @ 3.0t rad |
| 12 | 90 @ 6.0t rad | 180 @ 2.0t rad | 180 @ 2.0t rad |
| 16 | NR (2) | 180 @ 1.6t rad | 180 @ 1.6t rad |
| 19 | NR | 180 @ 1.4t rad | 180 @ 1.4t rad |
| 38 | NR | 180 @ 2.0t rad | 180 @ 2.0t rad |

(1) 90 bend, with minimum inside radius equal to 4.0 times the plate thickness (t)
(2) NR = No Requirement in MIL-A-46100C

## CONCLUDING REMARKS

In addition to focussing on production experience and properties of conventionally produced Q&T HY-80/HY-100 steels and armour plate, this paper has presented an overview of recent developments directed towards defence requirements for special plate grades, which are on-going within the Australian steel industry. These include the development of a micro-titanium treated HY-80/HY-100 modification, and a new HSLA-80 grade. Both developments rely heavily on the use and availability of modern steelmaking, plate processing and heat treatment facilities.

## REFERENCES


(1) C E Hartbower and W S Pellini, Weld J., Res. Sup. 1951, 30, 307-318.
(2) C E Hartbower and W S Pellini, Weld J., Res. Sup. 1951, 30, 499-511.
(3) MIL-S-16216 "Steel Plate, Alloy, Structural High Yield Strength (HY-80 and HY-100)".
(4) J G Williams, C R Killmore, J F Barrett and A K Church, Int. Symposium on Processing, Microstructure and Properties of HSLA Steels, Pittsburgh, USA. Nov 1987.
(5) MIL-A-46100C "Armour Plate, Steel, Wrought, High Hardness", 13 June 1983.
(6) I D Simpson and R Serge, Proc. Clean Steel 3 Conference, Institute of Metals, 1987, 85.
(7) T Abe, M Kurihara, H Tagawa and K Tsukada, Trans ISIJ, Vol 27, 1987, 478.
(8) J E Croll, "Production & Usage of QT Steel Plate in Australia", Proc. of HSLA Steels Conf., Wollongong, August 1984.
(9) AS2343, Part 2 "Bullet-Resistant Panels for Interior Use Part 2 - Opaque Panels", 1984.

# PROPERTIES AND PROSPECTS OF APPLICATION OF A HSLA STEEL (WDL-60) WITH LOW SUSCEPTIBILITY TO WELD CRACK

**Chen Xiao**
Iron & Steel Research Institute
Wuhan Iron & Steel Company
Wuhan, P. R.China

Abstract
This paper introduces the properties and applications of a HSLA steel with low susceptibility to weld crack researched and developed by the Wuhan Iron and Steel Company in recent years. This steel was verified as being excellent in weldability and low- temperature toughness,and producing no cracks in t≤50mm plates without preheating or with slightly preheating (~75°C) before welding. The plates have been applied to the manufacture of spherical tanks with 2.94MPa pressure,separated oil vessels under 7.84MPa pulsative high pressure,and low-temperature spherical vessels with 1000M volume and 2.16MPa pressure, showing good properties and gaining obvious economic benefit.

IN VIEW OF THE FACT that many malignant accidents happened at large welded steel structures,especially high pressure vessels in recent ten years,WISCO has developed a new-type HSLA steel (WDL-60) with low susceptibility to weld cracd in order to simplify welding process, save material, working - hour and energy and enhance the reliability of the steel structures.

This newly developed steel was designed with low carbon content (≤0.09%), reasonaboe utilization of Ni, Cr, V, Mo, B alloying and micro-alloying elements[1], strict control of carbon equivalent value(Ceq≤0.42) as well as weld crack susceptibility composition (Pcm≤0.20), andwas processed with quench and high-temperature heat treatment, so that the optimum microstructure, hence, the excellent weldability and low temperature toughness could be obtained. The main technical standards are as follcws: YP≥ 490MPa, TS=600-740MPa,δ≥17%, vE(-40°C)≥ 47J,bend test, d=3t, 180°, good.

At the same time,new-type welding materials matched to WDL-60 steel and forging pieces were developed.The large amount of experiments and the results of manufacture and applications show that WDL-60 steel is an ideal material for large pressure messels, hydraulic power station pressure pipes,off shore structures,great span bridges and heavy engineering machinery used under severe conditions,and so,has broad application prospect.

## INDUSTRIAL TRIAL

To determine the chemical composition of WDL-60 steel,the laboratary work on 50KW vacuum induction furnace and 500kg electric arc furnace was completed first to investigate the effects of alloying and microalloying elements Ni, Cr, Mo, V, Ti,B, N, Al on the mechanical properties and weld simulated heat circulation through orthogonal design and regressive analysis.The optimum heat-tueatment process was determined by property testing and mean square regression.

The industrial trial was carried out on 50 ton converter--continuous casting--2800 plate rolling mill--heat treatment oven production line in WISCO. The physical[2] and mechanical[3] testing, stress-corrosion[4] and welding experiments[5] as well as microstructure and mechanism analysis[2] were accomplished by WISCO.and co-operative universities, research institutes and manufacture plants.

1. Chemical Composition

Table 1-Chemical Composition

| C | Si | Mn | P | S | Ni | Cr | Mo | V | B | Pcm | Ceq |
|---|---|---|---|---|---|---|---|---|---|---|---|
| 0.068 | 0.22 | 1.11 | 0.017 | 0.006 | / | 0.25 | 0.17 | 0.036 | 0.0025 | 0.17 | 0.36 |
| 0.08 | 0.22 | 1.36 | 0.024 | 0.004 | / | 0.21 | 0.21 | 0.040 | 0.003 | 0.20 | 0.41 |
| 0.064 | 0.24 | 1.31 | 0.022 | 0.006 | 0.385 | 0.186 | 0.20 | 0.042 | 0.0011 | 0.18 | 0.39 |
| 0.059 | 0.27 | 1.45 | 0.022 | 0.008 | 0.436 | 0.198 | 0.19 | 0.045 | 0.0014 | 0.18 | 0.41 |

$Ceq=C+Si/24+Mn/6+Ni/40+Cr/5+Mo/4+V/14$

$Pcm=C+Si/30+Mn/20+Cr/20+Ni/60+Mo/15+V/10+5B$

2. Mechanical Properties

Table 2-Mechanical Properties

| Plate thickness | Sampling location and direction | | Tensile test YP(MPa) | Tensile test TS(MPa) | Tensile test $\delta_5$(%) | Impact test -40°C VE (J) | Bend test d=3t 180° |
|---|---|---|---|---|---|---|---|
| 24 | 1/2t | L | 510 510 | 608 598 | 26 25 | 270 220 262 | good |
| | | T | 529 529 | 647 617 | 25 24 | 175 203 220 | |
| 36 | 1/4t | L | 588 608 | 676 676 | 20 20 | 224 216 184 | good |
| | | T | 568 568 | 647 637 | 22 23 | 166 147 168 | |
| 50 | 1/4t | L | 598 598 | 666 676 | 21 22 | 172 159 162 | good |
| | | T | 568 627 | 686 696 | 18 19 | 109 117 137 | |

3. Toughness Testing

3.1 Impact Test with Instrument

- All the specimens were taken from the 1/4 thickness position in the plate section. The testing results are shown in Fig.1

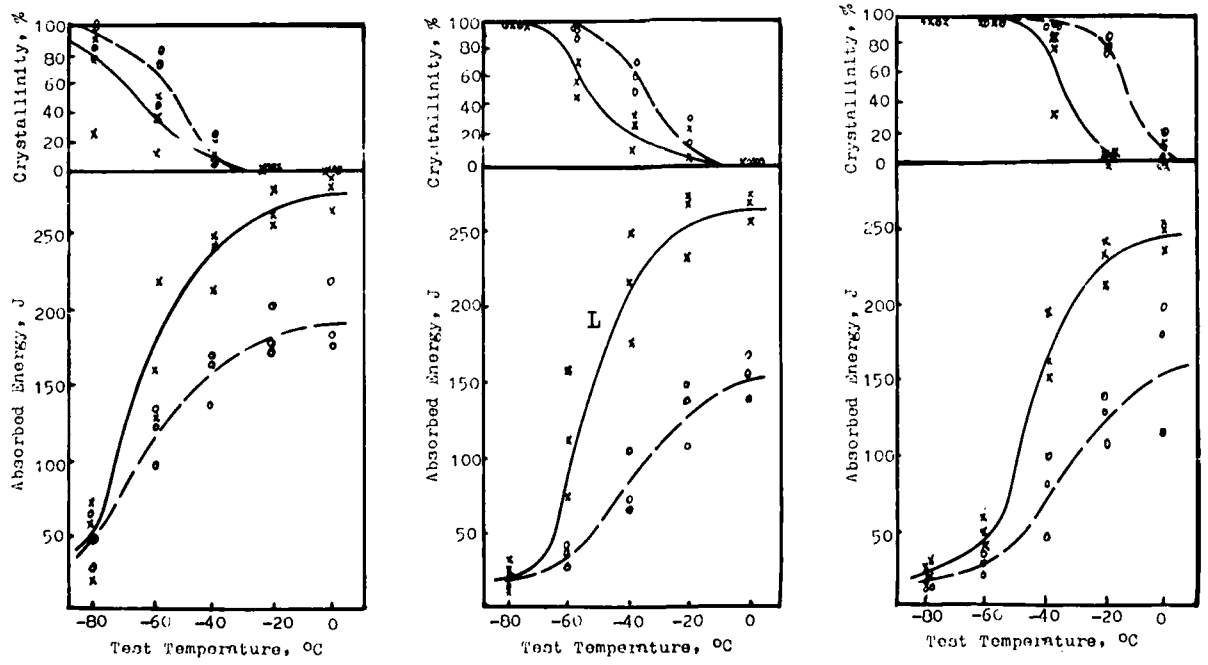


Fig.1 2mm V Notch Charpy Impact Test Results

3.2 Ductility - Brittleness Transition Temperature assessed by Various Methods and Criteria.

Table 3 - Ductility - Brittleness Transition Temperature

| Plate thickness | Specimen orientation | ITT (°C) | FATT (°C) | $VT_{47J}$ (°C) | $VT_{0.38}$ (°C) | -40°C VE (J) (average) |
|---|---|---|---|---|---|---|
| 24 | L | -80 | -80 | -80 | -80 | 251 |
| | T | -72 | -76 | -80 | -80 | 187 |
| 36 | L | -80 | -80 | -80 | -80 | 208 |
| | T | -64 | -47 | -80 | -80 | 161 |
| 50 | L | -66 | -64 | -80 | -80 | 165 |
| | T | -46 | -40 | -60 | -76 | 122 |

Note: ITT - Impact Transition Temperature by 50% Maximum shelf energy

FATT - Fracture Appearance Transition Temperature by 50% brittle grain fracture.

$VT_{47J}$ - ITT by 47J impact energy.

$VT_{0.38}$ - ITT by specimen bottom side-expansion value 0.38mm.

3.3 Drop Weight Test - According to ASTM-E208 standard, P2 type specimen were adopted to determine the Nil-Ductility Transition (NDT) temperature. The results are shown in Table 4.

Table 4- Results of NRL Drop Weight Test

| Plate thickness (mm) | Specimen orientation | Specimen type | Impact energy (J) | NDT temp. (°C) |
|---|---|---|---|---|
| 24 | L | $P_2$ | 402 | -55 |
| | T | $P_2$ | 402 | -50 |
| 36 | L | $P_2$ | 402 | -55 |
| | T | $P_2$ | 402 | -50 |
| 50 | L | $P_2$ | 402 | -50 |
| | T | $P_2$ | 402 | -45 |

3.4 Crack Tip Opening Displacement Test - The COD characteristic values $\delta_i$ and $\delta_{0.05}$ are illustrated in Table 5.

Table 5 - COD Test Results

| Plate thickness (mm) | Specimen orientation | Specimen size B×W×L (mm) | a/w | Testing temperature (°C) | COD charact. value $\delta_i$ (mm) | COD charact. value $\delta_{0.05}$ (mm) |
|---|---|---|---|---|---|---|
| 24 | TL | 20×24×116 | 0.45 | room temp. | 0.114 | 0.171 |
| 36 | TL | 26×31.2×145 | 0.40 | room temp. | 0.152 | 0.186 |
| | | | | -40 | 0.146 | 0.181 |
| | | | | -80 | 0.138 | 0.180 |
| 50 | TL | 26×31.2×145 | 0.40 | room temp. | 0.167 | 0.202 |

3.5 J Integral Test - The results of the J Integral Test shown in Table 6.

Table 6 - Results of J Integral Test

| Plate thickness(mm) | Specimen Position & orientation | J Integral Charact. Value (N/mm) | | |
|---|---|---|---|---|
| | | Ji | $J_{0.05}$ | $J_{0.02}$ |
| 36 | t/4 LT | 120.4 | 188.1 | 391.0 |
| | t/4 TL | 113.8 | 150.7 | 261.6 |
| 50 | t/4 LT | 122.9 | 177.5 | 341.2 |
| | t/4 TL | 112.0 | 143.7 | 238.8 |

3.6 Fatigue Crack Propagation Rate da/dN

Table 7 - Results of da/dN Tests

| Specimen size B×W×L(mm) | Regressive Equation |
|---|---|
| 20×24×116 | $da/dN=3.7287\times10^{-10}(\Delta K)^{2.798}$ |

Note: a - 0.25~0.60 mm
Ratio of stresses - 0.1
Frequency - 50Hz

4. Special Tests

4.1 Z-Direction Tensile Test

Table 8 - Results of Z-Direction Tensile Test

| Plate thickness (mm) | Specimen size (mm) | Z-direction Tensile TS(MPa) | Z-direction $\psi_z$% | Standard $\psi_z$ (%) |
|---|---|---|---|---|
| 50 | $d_o$=10 $L_o$=1.5$d_o$ | 676 ~696 | 42 ~53 | ≥35 |

4.2 Strain Aging Charpy Impact Test - At the strain rate of 5%, the aging treatment (250°C×1hr. - AC) was given and the test pieces used for the impact test were taken. Then, the strain aging Charpy impact test was conducted.

Table 9 - Results of Strain Aging Charpy Impact Test

| Plate thickness(mm) | Specimen orientation | Impact Test -40°CVEA(J) matrix | Impact Test -40°CVEA(J) aged | Susceptibility index results |
|---|---|---|---|---|
| 36 | T | 148<br>109<br>119 | 132<br>89<br>97 | 0.15 |
| 50 | T | 98<br>115<br>90 | 119<br>60<br>66 | 0.19 |

4.3 Fatigue Test - The test results are shown in Table 10.

From the results of toughness tests and some special tests described above, it can be seen that WDL-60 steel has excellent low temperature toughness, with high impact energy at -60°C (Fig 1), very low ductility-brittleness transition temperature from -60°C to -80°C

Table 10 - Fatigue Test Results

| Plate thickness (mm) | Stress condition | Smooth specimen without notch $\sigma_{0.15}$ (MPa) | 45°×2mm notched specimen $\sigma_{0.15}$ (MPa) |
|---|---|---|---|
| 36 | tensile-tensile | No brittle fracture | 235 |
| 50 | tensile-tensile | No brittle fracture | 235 |

Note: Frequency f=170Hz
Stresses Ratio=0.15

by most of testing methods (Table 3) and NDT temperature from -45°C to -55°C by Drop Weight Test (Table 4); at the same time, this steel has good fracture resistance with COD characteristic value $\delta_i$ from 0.114 to 0.167 mm, J-integral characteristic value Ji from 112.0 to 122.9 (Tables 5 and 6), and excellent fatigue resistance, without any brittle fracture for smooth specimen under high frequency fatigue, even for 45°×2mm notched specimen, with a yield stress of 235MPa (Table 10). Furthermore, WDL-60 steel can satisfy large engineering steel structure's Z-direction requirements, namely, $\psi_z \geq 35\%$ during Z-direction tensile (Table 8) and it also has low susceptibility index (0.15-0.19) to strain aging (Table 9).

5. The Effect of Stress-Relief Heat Treatment on Properties

5.1 The Effect of SR Treatment on Mechanical Properties (Fig 2)

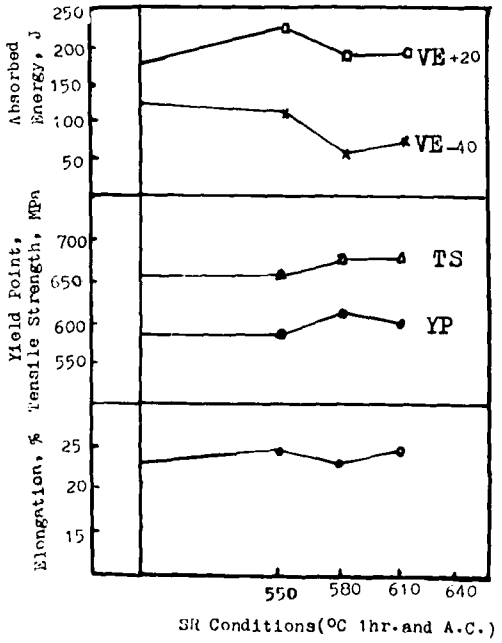


Fig.2 Effect of SR Treatment on Mechanical Properties

5.2 The Effect of SR Treatment on NDT Temperature

Table 11 - Results of NRL Drop Weight Test

| SR Process | Without SR QT state | SR 550°C×5hr | SR 580°C×5hr | SR 610°C×5hr |
|---|---|---|---|---|
| NDT Temp. | -50°C | -35°C | -40°C | -45°C |

5.3 The Effect of SR Treatment on COD & J-integral Characteristic Values

Table 12 - Results of COD & J-integral Test

| Characteristic Values | Without SR QT state | SR Treatment | | |
|---|---|---|---|---|
| | | 550°C×5hr | 580°C×5hr | 610°C×5hr |
| $\delta_i$ (mm) | 0.113 | 0.127 | 0.116 | 0.127 |
| $\delta_{0.05}$ (mm) | 0.155 | 0.188 | 0.163 | 0.174 |
| $J_i$ (N/mm) | 113.8 | 118.7 | 108.7 | 118.5 |
| $J_{0.05}$ (N/mm) | 150.7 | 167.5 | 145.0 | 155.0 |
| $J_{0.2}$ (N/mm) | 255.7 | 314 | 254.3 | 264.9 |

It can be seen from Fig.2 and Table 11 & 12 that after stress-relief heat treatment under the temperature of 550°C～610°C for 5hr, WDL-60 steel keeps good strength, plasticity and toughness as well as fracture resistance similar to those of the steel without SR treatment, only with a slight rise in NDT temperature.

6. Stress Corrosion Resistance

6.1 Constant Stress Tension Test (Table 13)

6.2 Simple Supporting Beam Test (Table 13)

6.3 Constant Displacement WOL Test (Table 13)

Table 13 - Results of $\sigma_{th}$, $S_c$ & WOL Test

| Specimen position | Plate thickness | YP (MPa) | $\sigma_{th}$ (720hr) | $S_c$ (MPa) | $K_{1scc}$ (MN/m$^{3/2}$) | $K_{1scc}$/YP (mm$^{1/2}$) |
|---|---|---|---|---|---|---|
| Matrix | 24 | 549 | / | 1360 | 52.7 | 3.04 |
| Matrix | 36 | 588 | 0.69YP | 970 | 46.8 | 2.52 |
| Welded joints | 36 | 549 | 0.61YP | / | 53.9 | 3.11 |
| Standard | / | ≥490 | ≥0.45YP | ≥830 | / | ≥1.51 |

WDL-60 steel plate and welded joints were tested in $H_2S$ solution by contant stress tension, simple supporting beam and WOL methods according to NACE standard, and showed higher $\sigma_{th}$, $S_c$ and $K_{1scc}$/YP values than the standards, and good $H_2S$ stress corrosion resistance.

7. Weldability

7.1 Cold crack Suseptibility Test

7.1.1 Maximum Hardness Test (Table 14)

Table 14 - Results of Maximum Hardness Test

| Plate thickness (mm) | Specimen thickness(mm) | Maximum Hardness | |
|---|---|---|---|
| | | Room temp. welding | Preheat 50°C welding |
| 36 | 20 | 320 Hv | 280 Hv |

7.1.2 Y-slit Restraint Cracking Test

- In accordance with JIS Z3158, Y Slit Restraint Cracking Test was conducted. The test results are shown in Table 15.

Table 15 - Results of Y Slit Restraint Cracking Test

| Preheating Temp.(°C) | 25 (room temp.) | 50 |
|---|---|---|
| Cross Section crack rate | 0 | 0 |
| Rcot crack rate | 0 | 0 |

Note: Welding seam diffusible hydrogen content equals to 1.46ml/100g

7.1.3 Window-type Restraint Cracking - Window-type restraint cracking tests with angular distortion are used to test the cracking of the weld toe in butt-welded joints which are produced under angular distortion and in which a large

bending moment is induced as a result of welding.

Table 16 - Results of Wendow-type Restraint Cracking Test

| Restraint Plate size (mm) | Specimen plate size (mm) | preheating temperature (°C) | Heat input (KJ/cm) | Interpass temp. (°C) | Holding time after welding | test methods cut X-ray piece |
|---|---|---|---|---|---|---|
| 1200×1200×50 | 500×180×36 | 50 | 17-25 | 150-200 | 48 | No crack |

7.1.4 Tensile Restraint Crack (TRC) Test (Fig.3)

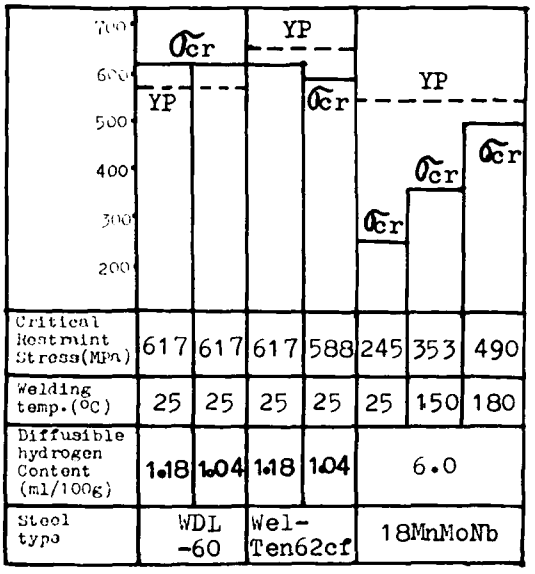


Fig.3 The effect of different processes on the critical restraint stress

The above experimental results show that WDL-60 steel $Hv_{max} < 330$ (Table 14), has low hardenability. Root cracks can be avoid completely when extra low hydrogen electrode with $[H] < 1.5ml/100g$ are adopted (Table 15). Window shape restraint tests also show that no cracks occur (Table 16). This experiment simulated large steel structure restraint conditions and welding processes on the spot. TRC test can be used to in vestigate the effects of restraint stress, welding seam diffusive hydrogen content and welding techniques etc. on the cold crack suseptibility quantitatively, and the critical restraint stress $\sigma_{cr}$ is taken as the criterion. Fig.3 indicates that the $\sigma_{cr}$ of WDL-60 steel is higher than yield point. From what is mentioned above it can be seen that this steel has excellent cold crack resistance.

7.2 Hot Crack Susceptibility Test

Varestraint test with TIG welding simulated to hand-welding (17.5KJ/cm) and submerged arc welding (40.5KJ/cm) was adopted. The results show that the solidification crack critical stresses $\varepsilon_{min}$ of this steel simulated to hand-welding and submerged arc welding are 1.15% and no crack respectively. The corresponding HAZ liquified crack critical strain $\varepsilon_{min}$ for hand-welding is 2.54% and no crack for submerged arc welding. This illustrates that this steel has very good hot crack resistance.

7.3 Reheating Crack Susceptibility Test

- The high temperature slow tensile test recommended by IIW and the implant method were adopted. The results show that when the SR temperature is higher than 600°C, there is a certain degree of reheating crack susceptibility. However, when SR temperature decreased to 580°C, the reheating crack susceptibility decreased remarkably, or even no crack produced. In fact, in the explosion test of WDL-60 steel simulative pressure vessel, the end covers and connected pipes were SR treated under 600°Cx2hr after welding, the welding seam surface were examined by 100% color-painting test, and no cracks were found. During the exploding, the real pressure exceeded the theoretical estimate, the original exploding point was not on the SR treated connection, but was on the matrix of the pipe. This shows that WDL-60 steel has no bad results after 600°C SR treatment.

7.4 Welding process Estimation Test

- According to "The Pressure Vessel Safety Test Standard" published by the Labor Ministry of the People's Republic of Chna, the hand welding process of WDL-60 steel was verified. The welding positions are classified as downhand welding, vertical welding and horizontal welding. The groove shape was of unsymmetrical X shape. Welding heat input was 17～25KJ/cm without preheating and the temperatures between layers were 150～200°C.

7.4.1 Jin Zhou Heavy Machine Plant Welding Process Estimate - The test results are shown in Table 17.

Table 17 - Results of Tensile, Bend and Hardness Test on Welded Joint

| Tensile test | | Bend test | | | Impact test | | | Hardness test |
|---|---|---|---|---|---|---|---|---|
| | | Bend radius R=1.5t | | Bend angle 100° | -40°C,vE(J) Notch position | | | |
| YP (MPa) | TS (MPa) | Face | root | side | Weld metal | Fusion line | HAZ | HAZ,$Hv_{max}$ (10kg) |
| 490 | 678 | good | good | good | 219 | 151 | 80 | 289 |
| 519 | 671 | | | | 70 | 153 | 229 | |
| | | | | | 66 | 94 | 179 | |

7.4.2 Lan Zhou Petroleum Chemistry machinery Plant Welding Process Estimate

Table 18 - Results of Tensile and Bend Test on Welded Joint

| Welding position | Heat input KJ/cm | Treatment | Tensile test | | $\delta_5$(%) | Bend test | | |
|---|---|---|---|---|---|---|---|---|
| | | | YP(MPa) | TS(MPa) | | Bend radius R=1.5t | Bend angle 100° | |
| | | | | | | Face | Root | Side |
| Downhand | 17~19 | As welded | 598 | 686 | 23 | / | / | / |
| | | SR | 588 | 647 | 25 | good | good | good |
| Vertical | 40 | SR | / | 632 | / | good | good | good |
| Horizontal | 30 | SR | / | 647 | / | good | good | good |

7.4.3 Charpy Impact Test for Butt Welded Joints of Various Welding Position - Charpy impact test results are shown in Fig.4 - a,b,c,d.

It can be seen from the results in Table 17 and 18 that the strength and plasticity are higher than those of the standard and the cold bending in three positions are also up to standard. The results in Fig.4 shows that the -40°C low temperature impact energy in three positions are higher than 47J defined by the standard. Thus, WDL-60 steel can adapt to the welding process and satisfy the property requirement, especially the low temperature toughness requirement.

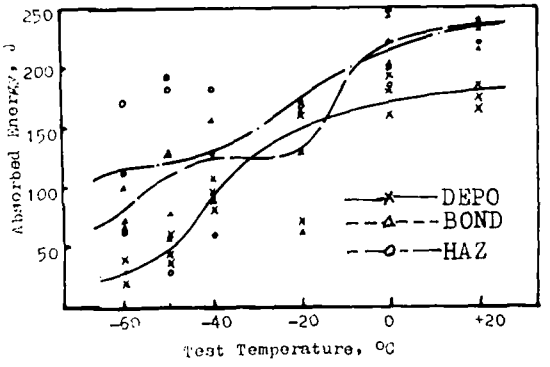


Fig.4-a 2mm V Notch Charpy Impact Test Results of Welded Joint (Downhand welding)

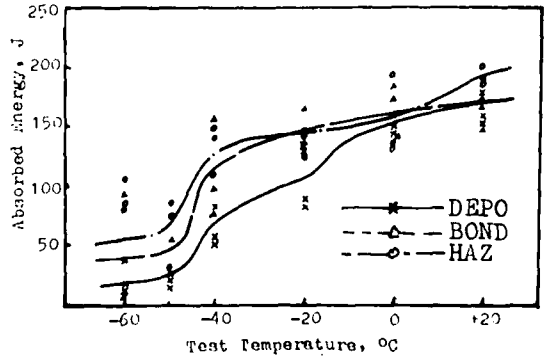


Fig.4-b 2mm V Notch Charpy Impact Test Results of Welded Joint after SR Treatment (Downhand welding)

8. Microstructure Analysis

8.1 Quenching state: After water-quench the microstructure of WDL-60 steel was lath martensite and bainite in various amount with the change of plate thickness, as shown in Fig.5. Under the transmission electron-microscope, this kind of bainite could be identified as type I bainite(BI) and type Ⅲ bainite($B_{Ⅲ}$), while neither type Ⅱ bainite($B_{Ⅱ}$) nor filmy and granular pearlite and sorbite was found in the film specimen (Fig.6).

8.2 Quench and high-temperature temper state:

The microstructure analysis revealed various structure changes during precipitation, recovery and recrystallization through high temperature temper treatment in the quenched WDL-60 steel.

In the process of precipitation,

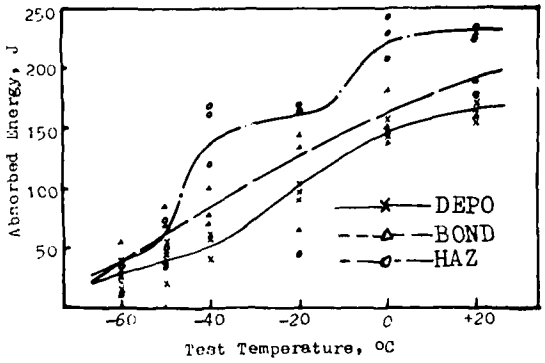


Fig.4-c 2mm V Notch Charpy Impact Test Results of Welded Joint after SR Treatment (Vertical welding)

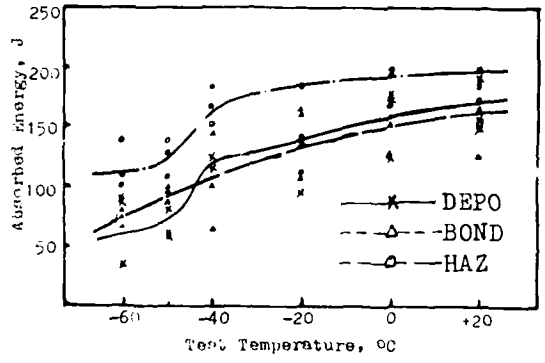


Fig.4-d 2mm V Notch Charpy Impact Test Results of Welded Joint after SR Treatment ( Horizontal position welding )

because of the high density of dislocation (about $10^{11}\sim10^{12}$/cm ) and the inner twin in the martensite lath, which can form the nuclei of the second phase precipitation just like the martensite lath boundaries, the carbide can precipitate either on the martensite boundaries or in the martensite lath, as shown in Fig.7. But in the bainite lath, there are very few saturated carbon atoms, nor dislocations and twins as the nuclei of precipitation, therefore, very few carbide particles can be seen in the bainite lath. Residual austenite between BI and martensite lath transformed into sorbite in a quite small micro-zone.

During recovery, the dislocation twists are untied, and offset to each other. Those laths with small angle boundaries merge into broad laths, even a bunch of laths merge into one lath. This process leads to most carbide precipitating on the bunch boundaries, as shown in Fig.8.

With the transition of large angle boundaries, recrystallization starts and polygonal ferrite gradually comes into

Fig.5 Quenching microstructure photograph 630X

Fig.6 Precipitation after quench under eletron-microscope (Film specimen) 30000X

Fig. 7 Precipitation after quench under electron-microscope (Film specimen) 31500X

being, in which the density of dislocation further decreases; and the second phase particles originally segregated on the lath boundaries and on the bunch boundaries, tend to distribute homogeneously, as shown in Fig.10. When the temper temperature increases, especially to ($\alpha+\gamma$) interstitial zone , martensite islands and recrystallized ferrite will occur (Fig.11).

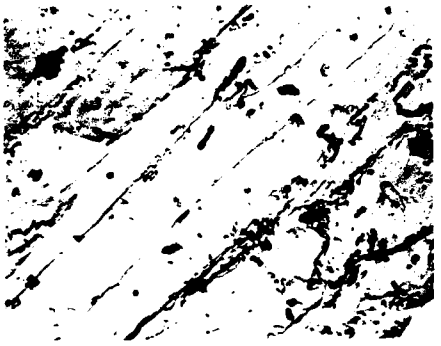

Fig.8 Precipitation after quench under electronmicroscope (Extracted duplication) 4000X

Fig.9 Recovery structure after quench (Extracted duplication) 5600X

Fig.10 Recrystallization after quench (Extracted duplication) 4000X

8.3 The Optimum Combination of Strength and Toughness.

The large amount of experimental results show that under reasonable quench and temper process of WDL-60 steel, the optimum combination of strength and toughness corresponds to the microstructure obtained from the last stage of recovery during the tempering treatment. Even the microstructure obtained from the preliminary stage of recrystallization can still keep good balance of strength and toughness.

Fig.11 Recrystallization after quench (Film specimen) 18000X

THE APPLICATION OF WDL-60 STEEL

1. Large Spherical Tank

WDL-60 steel has been applied by Jinzhou Heary Machinery Plant and Lanzhou Petroleum Chemistry Machinery Plant to the manufacture of large spherical vessels, such as, oxygen spherical vessels with volumes of 200M$^3$ and 400M$^3$, designing pressure 2.94MPa and the shell thickness 30 & 38 mm; ethylene spherical vessel of 1000M$^3$ valume, -40°C temperatur , 2.16MPa pressure & 38 mm shell thickne. ; gas tank with 2000M$^3$ volume, 1.67MPa pressure & 36 mm shell thickness. Through the manufacture and installation, for example, cutting, groove-working, cold-forming, welding and repairing as well as final constructing WDL-60 steel shows excellent process properties and the performance of spherical vessels is very good.

2. High Pressure Oil Seperate Vessels

WDL-60 steel was also adopted by Hunan Electric Power Equipment Plant to make pulsative high pressure oil separate vessels with 7.84MPa pressure, 40 times/min pulsative frequency and 24mm hull thickness. A group of four vessels were used to make up a powerful high pressure pump which was purchased by Hangzhou Power Station to send the dust pulp to a place 26.5km far away. This kind of vessels had been made of 16MnR steel plate of 30mm and produced cracks in less than 400hr. Since WDL-60 steel was adopted, the vessels have been working for more than 6000hr without any cracks. According to the estimate based on the fatigue testing curve, the oil separate vessels made of WDL-60 steel will work 5～10 years.

3. High water Fall-Difference Power Station Pressure Pipes, off shore struc-

tures, Liquified Gas Ship, Great Span Bridge and High Stress and Load Engineering Machinery Applications Prospect:

WDL-60 steel has been verified by the domestic departments concerned, and is considered to be excellent in low temperature toughness and weldability, and can be compared with the advanced products of similar grades in the world.[6~14] Thus, the application of WDL-60 steel in above fields has broad prospect.

## CONCLUSIONS

1. WDL-60 steel is a HSLA steel with low susceptibility to hot, cold and reheating weld crack which has excellent weldability without preheating or with slight preheating under 75°C mainly due to low carbon, low carbon equivalent (Ceq) micro alloying and welding crack susceptibility composition (Pcm) control.
2. This steel has good low temperature toughness based on the reasonable heat treatment process and obtained fine microstructure proved by various toughness tests and welding process estimate experiments.
3. This steel was applied to large spherical vessels and pulsative high pressure oil separate vessels. The performance of above vessels is good.

Because of the comprehensive properties, the welding process was simplified, the manufacture period was shortened, the plate thickness was decreased, the welder's working conditions were improved, the quality and reliability of large steel structure was enhanced, the service life of the vessels will be prolonged, the economic benefit and social benefit are obvious. The application prospect is quite broad.

## ACKNOWLEDGEMENT

This research project was accomplished by the WISCO with the collaboration of the following twelve other units in China, such as Centrol Institute for Iron & Steel Reseach, Hefei General Machinery Reseach Inst. , BeiJing Polytechnic University, Metal Research Inst. of Chinese Academy of Sciences, Tinzhou Heavy Machinery Plant, Lanzhou Petroleum Chemistry Machinery Plant, Shanghai Electric Power Equipment Manufacture Plant and so on.

The author of this paper is particularly grateful to the relevant scientific and technical workers of the units mentioned above.

## REFERENCES

1. Chen Xiao; Zheng Lin et al., "Research on Microalloying Elements and Process of WDL-60 Steel"(WISCO).
2. Yu Zhao-kun; Chen Qian-ti; Tu Yun-shen et al., Research on the Phisical Properties & Microstructure of WDL-60 Steel. (CISRI& WISCO)
3. Gu Xian-shan; Wu Guo-yun et al., Research on the Mechanical Properties of WDL-60 Steel. (HGMRI & WISCO)
4. Yao Xi Meng et al., Research on Stress Corrosion Property of WDL-60 Steel. (BPU)
5. Wang Yong Da; Mei An Jing; Qian Bai Nian et al., Research on Weldability and Toughness of Welded Joint of WDL-60 Steel. (CISRI, WISCO & MRICAS)
6. Pickering F.B. in "Microalloying 75", New York, NY, Union Carbide Corp., 1987, 9 - 31.
7. Korchynsky M., conf. org., "HSLA-Steels - Technology and Applications" Metals Park, Ohio, ASM, 1984.
8. G.E.Kampschaefer, Jr. and R.J.Jesseman, "Use of Microalloyed Steels in Heavy Construction"
9. I.G.Hamilton, "The Use of Microalloyed Steels in the Manufacture of Thick Pressure Vessels"
10. W.P.Carter "Microalloyed Steels for Storage Tanks and Pressure Vessels Operating at Low Temperatures"
11. T.Gladman, D.Dulieu, and Ian D. McIvor, "Structure-Property Relationships in Microalloyed Steels".
12. Kobe Steel-Making Tech., 1979, Vol.29, No 2, 101
13. Kawasaki Steel-Making Tech., 1980, Vol.12, No 1, 154--163
14. Simitomo Metal, 1979, Vol.31, No 4 97--117

# PROPERTIES AND MICROSTRUCTURES OF COPPER PRECIPITATION AGED PLATE STEELS

**A. D. Wilson, E. G. Hamburg**
Lukens Steel Company
Coatesville, Pennsylvania, USA

**D. J. Colvin, S. W. Thompson, G. Krauss**
Colorado School of Mines
Golden, Colorado, USA

Abstract

The properties, microstructures and alloy design considerations for low-carbon, copper-bearing, precipitation-aged plate steels are presented. Four chemistries based upon the A710/HSLA-80 system with modified levels of Mn, Mo, Ni and Cu were investigated. Commercial heats with plate thicknesses up to 8 inches (203 mm) provided the sample material for this investigation. The transformation behavior is characterized by continuous cooling transformation diagrams established with a computerized, closed-loop, thermomechanical system. Depending on alloy content, proeutectoid ferrite, granular bainite, and martensite were found to be the dominant microstructures over wide ranges of cooling rates. The effects of ageing and plate thickness on strength and toughness are documented. In the most hardenable steel, slight increases in carbon content (0.04 pct to 0.06 pct) were found to significantly increase strength. Structural refinement via double austenitizing or controlled rolling prior to heat treatment improved toughness.

LOW-CARBON, COPPER-BEARING, precipitation-aged plate steels have been attracting increasing interest and applications. These steels have evolved from IN-787, which was developed in the late 1960's by the International Nickel Company[1]. Steels with a nominal composition 1 pct Cu, 0.8 pct Ni, 0.7 pct Cr, 0.2 pct Mo, and a small amount of Nb have been designated as A710 for structural applications and A736 for pressure vessel applications over 10 years ago by ASTM. This type of steel has been used in a variety of applications including offshore platforms, arctic linepipe valves, mining equipment, and dredging equipment. However, a significant recent application of these steels is as a replacement for HY-80 (MIL-S-16216) steels by the U.S. Navy. The military specification for the military form of this steel is MIL-S-24645 and the steel is commonly referred to as "HSLA-80". In all applications of this steel, the high strength (80 ksi, 552 MPa min. yield strength) and excellent toughness are critical to its application. However, of greatest importance is the excellent weldability of the low-carbon alloy.

Copper-bearing, precipitation-aged steels were originally developed for use in the rolled and aged condition. Controlled rolling provides higher strength and toughness in thicker plates[2]. When the ASTM specifications were developed, three classes of steel were identified: Class 1 plates are produced by rolling and ageing, Class 2 by normalizing and ageing, and Class 3 by austenitizing, water quenching, and ageing (Q&A). Currently, thinner plates, less than 5/16 inches (7.9 mm), are produced as Class 1 or Class 2 for U.S. Navy applications. All thicker plates are produced by Class 3 Q&A methods. The major tonnage of steel used in Naval or commercial applications has been in the Q&A treatment. All of the results reported in this paper will be on Q&A alloys.

The successful application of HSLA-80/A710 steels has led to further study of strength/toughness/thickness interrelationships. Recently, a modified A710 steel with higher Mn (1.4 pct) and Mo (0.45 pct) content (A710 Modified) was developed, which exhibited improved strength/toughness/thickness properties[3]. In conjunction with the U.S. Navy, a new grade of steel known as HSLA-100 with higher amounts of Ni, Cu, Mn, and Mo than those of the HSLA-80/A710 was developed[4]. A steel with a chemistry intermediate to HSLA-80 and HSLA-100 has also been developed[5]. This intermediate composition (HSLA-80/100 modified) has higher levels of Mn, Mo, and Ni than the HSLA-80 steel, but less than the 3.5 pct Ni found in HSLA-100. This intermediate chemistry was developed to provide 80 ksi (552 MPa) minimum yield strength in thicker plates and 100 ksi (690 MPa) minimum yield

for thin plates with a leaner chemistry than HSLA-100. In the following sections, the alloy design considerations, the properties, and the microstructures of these copper-bearing, precipitation-aged steels are presented. All plates for evaluation of these four alloys were produced from commercial heats with the heat chemistries presented in Table I.

## ALLOY DESIGN CONSIDERATIONS

The original alloy development program responsible for the A710 grade of steel identified the importance of key alloying elements[2]. Since that time, a need to improve the strength and toughness levels for thicker plates has led to further developments in this alloy system. As introduced above, these developments have led to an improved understanding of the influence of increased alloy additions on the behavior of this family of steels. Detailed below are the metallurgical contributions of each of the important alloying elements.

- Carbon: In the original A710 specification, C was limited to 0.07 pct. This low-carbon content leads to improved weldability of this grade of steel as is indicated by the Graville diagram[6] shown in Figure 1. It has been demonstrated that these alloys can be welded with little or no preheat[7,8]. Lower carbon contents also lead to improved toughness. At these low-carbon levels, small changes in C content can affect strength dramatically.
- Copper: The addition of copper increases strength in these low-carbon steels by precipitation of copper-rich particles during ageing. Copper also improves hardenability and decreases the tempering rate of bainitic and martensitic regions during high-temperature ageing.
- Nickel: Nickel was originally added in amounts greater than 0.7 pct to prevent the hot shortness normally associated with copper-containing steels[9]. Nickel dramatically increases the hardenability and promotes higher toughness.
- Chromium and Molybdenum: Both of these alloying elements were originally added to retard Cu-precipitation during cooling from the austenite range. These elements are very important in influencing the transformation kinetics of these steels, and particularly they increase bainitic hardenability by delaying the onset of proeutectoid ferrite formation. Both elements are important in retarding tempering during the ageing treatment.
- Niobium: This alloying element provides grain refinement during hot rolling and subsequent austenitizing treatments.

The influence of these alloying elements on the bainite start ($B_S$) temperature is determined by the Steven and Haynes formula[10].

$$B_S\ (^oC) = 830 - 270\ (\text{pct C}) - 90\ (\text{pct Mn}) - 37\ (\text{pct Ni}) - 70\ (\text{pct Cr}) - 83\ (\text{pct Mo}) \quad (1)$$

The martensite start ($M_S$) temperature as a function of composition is given by the Andrew's product formula[11]:

$$M_S\ (^oC) = 512 - 453\ (\text{pct C}) - 16.9\ (\text{pct Ni}) + 15\ (\text{pct Cr}) - 9.5\ (\text{pct Mo}) + 217\ (\text{pct C})^2 - 71.5\ (\text{pct C}^*\ \text{pct Mn}) - 67.6\ (\text{pct C}^*\ \text{pct Cr}) \quad (2)$$

Increased alloying therefore promotes structural refinement by lowering the $B_S$ and $M_S$ temperatures. Others have found the Steven and Haynes formula useful in studies of ultra low carbon bainitic steels[12]. The carbon equivalent values are also dependent on the amounts of alloying elements. The Graville diagram is based upon the carbon equivalent (CE) formula as shown in Figure 1. The calculated $B_S$, $M_S$ and CE values are summarized in Table II for the five commercial heats of steel evaluated in this program. Of prime importance to the microstructural development is the effect of alloying elements on the location of the proeutectoid ferrite C-curve. Hence, the austenite transformation behavior is best described by continuous cooling transformation (CCT) diagrams.

## CONTINUOUS COOLING TRANSFORMATION BEHAVIOR

To better understand the response of characteristics of austenite decomposition, CCT diagrams were developed for three of the alloys: HSLA-80, A710 Modified and HSLA-100 with 0.06 pct C. These diagrams are useful for understanding the transformation response of these alloys to water quenching of various plate thicknesses from austenitizing temperatures. The CCT work was performed on a Gleeble 1500 machine. The specimens used in the study were 0.25 inches (6.35 mm) round and 4.0 inches (101.6 mm) in length. Hollow specimens were cooled at the fastest rates by quenching in helium. Radial contraction was measured at the midspan diameter of each test specimen as a function of temperature. Specimens were heated by electric resistance

Table I - Chemistries of Mill Production Heats and Chemistry Specification
(weight percent)

| | C | Mn | P | S | Cu | Ni | Cr | Mo | Si | Nb |
|---|---|---|---|---|---|---|---|---|---|---|
| HSLA-80 | .05 | .50 | .009 | .002 | 1.12 | .88 | .71 | .20 | .28 | .035 |
| A710 Modified | .06 | 1.45 | .012 | .002 | 1.25 | .97 | .72 | .45 | .35 | .040 |
| HSLA-100 | | | | | | | | | | |
| Heat #1 | .04 | .86 | .008 | .002 | 1.58 | 3.55 | .57 | .60 | .27 | .033 |
| Heat #2 | .06 | .83 | .010 | .002 | 1.66 | 3.48 | .58 | .59 | .37 | .028 |
| HSLA-80/100 Modified | .05 | 1.00 | .009 | .001 | 1.23 | 1.77 | .61 | .51 | .34 | .037 |
| MIL-S-24645 HSLA-80 | | | | | | | | | | |
| - Min. | | .40 | | | 1.00 | .70 | .60 | .15 | | .02* |
| - Max. | .07 | .70 | .025 | .010* | 1.30 | 1.00 | .90 | .25 | .40 | .06 |
| Interim HSLA-100 | | | | | | | | | | |
| - Min. | | .75 | | | 1.45 | 3.45 | .45 | .55 | | .02 |
| - Max. | .06 | 1.05 | .015 | .006 | 1.75 | 3.65 | .75 | .65 | .40 | .06 |

* For A710 0.025 pct max. S and 0.02 pct min. Nb only.

Table II - Experimental and Calculated Critical Temperature

| | $M_S$[a] °F (°C) | $B_S$[b] °F (°C) | CE[c] | $A_{C1}$[d] °F (°C) | $A_{C3}$[d] °F (°C) |
|---|---|---|---|---|---|
| HSLA-80 | 894 (479) | 1242 (672) | .42 | 1319 (715) | 1589 (865) |
| A710 Modified | 871 (466) | 1038 (559) | .51 | 1274 (690) | 1580 (860) |
| HSLA-100 | | | | | |
| Heat #1 | 811 (438) | 968 (520) | .66 | | |
| Heat #2 | 793 (423) | 968 (520) | .70 | 1256 (680) | 1517 (825) |
| HSLA-80/100 Modified | 856 (458) | 1067 (575) | .53 | - | - |

(a) Calculated from Equation 2
(b) Calculated from Equation 1
(c) Calculated from Figure 1
(d) Experimentally determined by P. Coldren at AMAX Research Laboratories using 2°C/min. heating rate.

**Influence of Carbon Level and Carbon Equivalent on Susceptibility to HAZ Cracking of Plate Steels. (from Graville)**

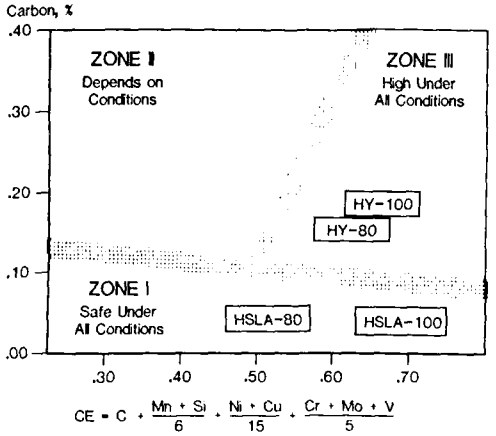


Figure 1 - Weldability of Steel As A Function of Carbon Content and Carbon Equivalent from Graville[6]

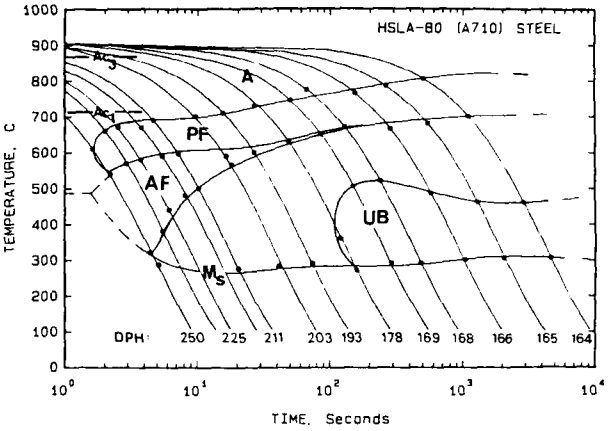


Figure 2 - Continuous Cooling Transformation Diagram for HSLA-80; A = Austenite, PF = Proeutectoid Ferrite, AF = Acicular Ferrite, UB = Upper Bainite, $M_S$ = Martensite Start

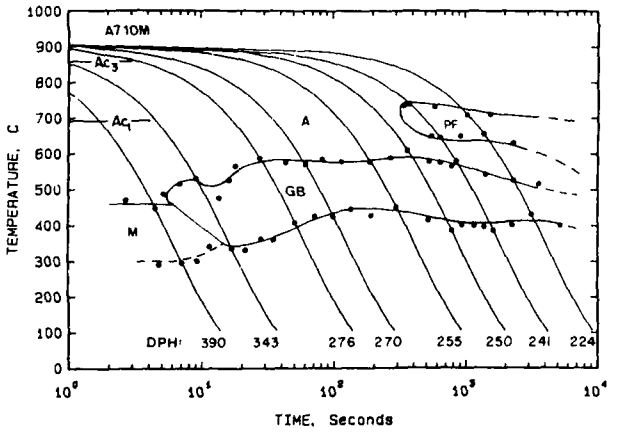


Figure 3 - Continuous Cooling Transformation Diagram for A710 Modified; M = Martensite, GB = Granular Bainite

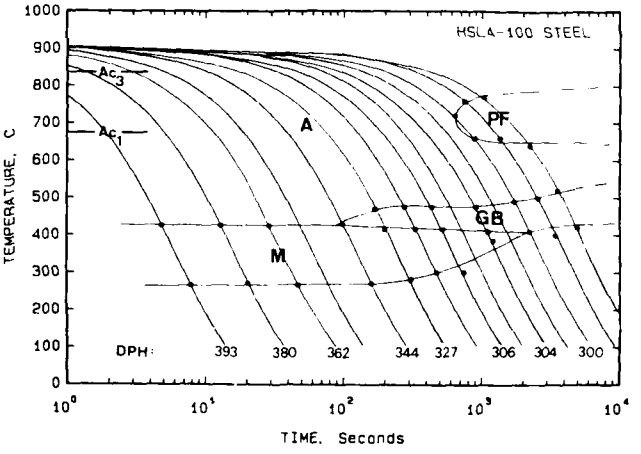


Figure 4 - Continuous Cooling Transformation Diagram for HSLA-100

heating and the temperature was monitored with thermocouples welded to the specimen midspan. Each sample was cooled exponentially similar to the Newtonian formula for natural cooling[13,14,15]. The cooling time over the temperature interval of 1472°F (800°C) to 935°F (500°C) was used to determine cooling rate. Specimens were austenitized at 1660°F (905°C), which is the austenitizing temperature used for the mill heat treatment of these alloys. Table II presents the critical temperatures associated with these alloys. The CCT diagram was outlined by the transformation start and finish temperatures for each transformation as determined by dilatometry. These temperatures were established by evaluating inflection points from the radial contraction/temperature record. Diamond pyramid hardness values were also determined at the end of the cooling cycle.

Results of the CCT diagram studies are summarized in Figures 2 to 4. The experimentally determined $M_S$ and $B_S$ temperatures compare well with the calculated values. Furthermore, the location of the proeutectoid ferrite C-curve reflects the alloy content of each steel. The HSLA-80 CCT diagram (Figure 2) consists of proeutectoid ferrite, acicular ferrite, martensite, and upper bainite. This CCT diagram agrees well with information reported by others [16]. The CCT diagram for A710 Modified steel (Figure 3) shows an extensive bainitic region. At very fast and very slow cooling rates, martensite and proeutectoid ferrite form, respectively. The granular bainite formed in the A710 Modified steel is discussed in the next section. The extensive bainitic region also correlates well with the fact that fully bainitic microstructures have been found in plates produced from this alloy up to 8 inches in thickness[4]. A preliminary CCT diagram of the HSLA-80/100 modified steel exhibits behavior similar to the A710 Modified, but with a larger martensite region. The HSLA-100 CCT diagram (Figure 4) shows an extensive martensitic region, so even thick plates exhibit a martensitic microstructure. At much slower cooling rates, granular bainite and proeutectoid ferrite form. These observations also agree with results from mill-produced materials[17]. The only other CCT diagram available on comparable steels was produced by Speich and Scoonover[16] on an HSLA-80 steel with a slightly lower carbon content. Their work aided in the interpretation of the results of the current study.

## MICROSTRUCTURAL CHARACTERISTICS

As discussed in the previous section, a range of microstructural constituents have been found in this family of low-carbon steels. In HSLA-80, proeutectoid ferrite is the primary microstructural component. Much smaller amounts of acicular ferrite and martensite are part of the commercially produced microstructure. Examples of these microconstituents are shown in Figure 5. Areas that resemble granular bainite, to be discussed in the next section, have also been observed in mill-quenched HSLA-80 plates. Microsegregation within this alloy may lead to local areas enriched in Mn and Mo which may transform to bainite or martensite.

In the case of A710 Modified, the dominant microconstituent at intermediate cooling rates is "granular" bainite. The term granular bainite was first used by Habraken and Economopoulos[18]. The typical appearance of granular bainite is shown in Figure 6. Figure 6(a) is a light micrograph and Figure 6(b) is a montage of TEM micrographs. Granular bainite consists of packets of ferrite laths with non-cementite, interlath, second-phase particles. These particles were identified with the TEM as retained austenite or a combination of retained austenite and martensite[19]. The presence of retained austenite at room temperature indicates that the bainite finish temperature does not represent 100 pct transformation of the parent austenite. These microstructures are sometimes incorrectly identified as upper bainite which consists of ferrite and cementite. The volume fraction of these second-phase particles is about 0.15. Approximately one-half of the volume fraction of the second-phase particles is austenite and the other half martensite[19]. The large particles were found to be mostly martensitic, but are frequently surrounded by films of austenite. No cementite was identified in as-quenched steel. Subsequent to ageing, the microstructure showed little change in the volume fractions of martensite or austenite; however, some interlath cementite was found[19]. This observation indicates that most of the austenite is extremely stable with respect to transformation during the high-temperature ageing treatments. Granular bainite forms in austenite grains as similarly oriented ferrite laths[19]. The interlath pools of austenite are most likely enriched in carbon.

The dominant phase in thin and intermediate thickness plates of the HSLA-100 steel (0.06 pct C) is martensite. Granular bainite forms at much slower cooling rates (thicker plates). The martensite laths in this steel are too fine to be resolved in a light microscope and prior austenite grain boundaries are not easily distinguished with a nital etch. This observation is demonstrated in Figure 7(a). The granular bainites that are found in the HSLA-100 at slower cooling rates are very similar to those found in the A710 Modified. However, the martensitic microstructure tends to be much finer than the coarser granular bainite. The effect of C-content on the microstructures of 2 inch (51 mm) thick plates is clearly shown in Figure 7. The HSLA-100 with 0.04 pct C is primarily bainite (Figure 7(b)) compared to the principally martensitic microstructure of the

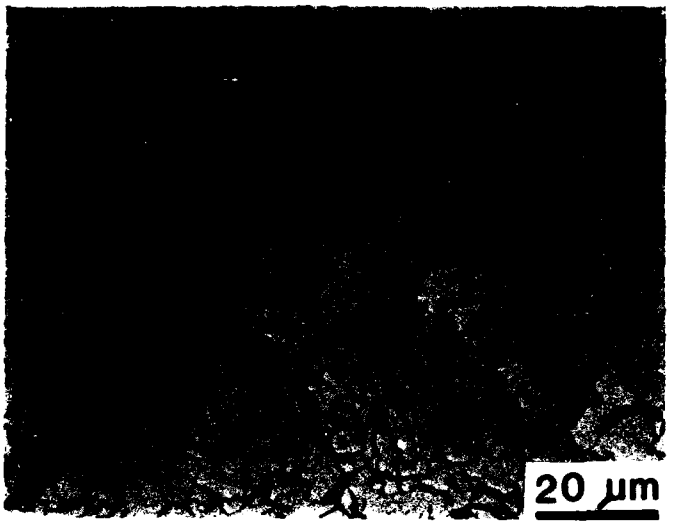


Figure 5 - Typical Microstructure of 1 Inch (25 mm) Thick HSLA-80/A710 Showing Proeutectoid and Acicular Ferrite. Some Granular Bainite Also Shown. (Nital-Picral Etch)

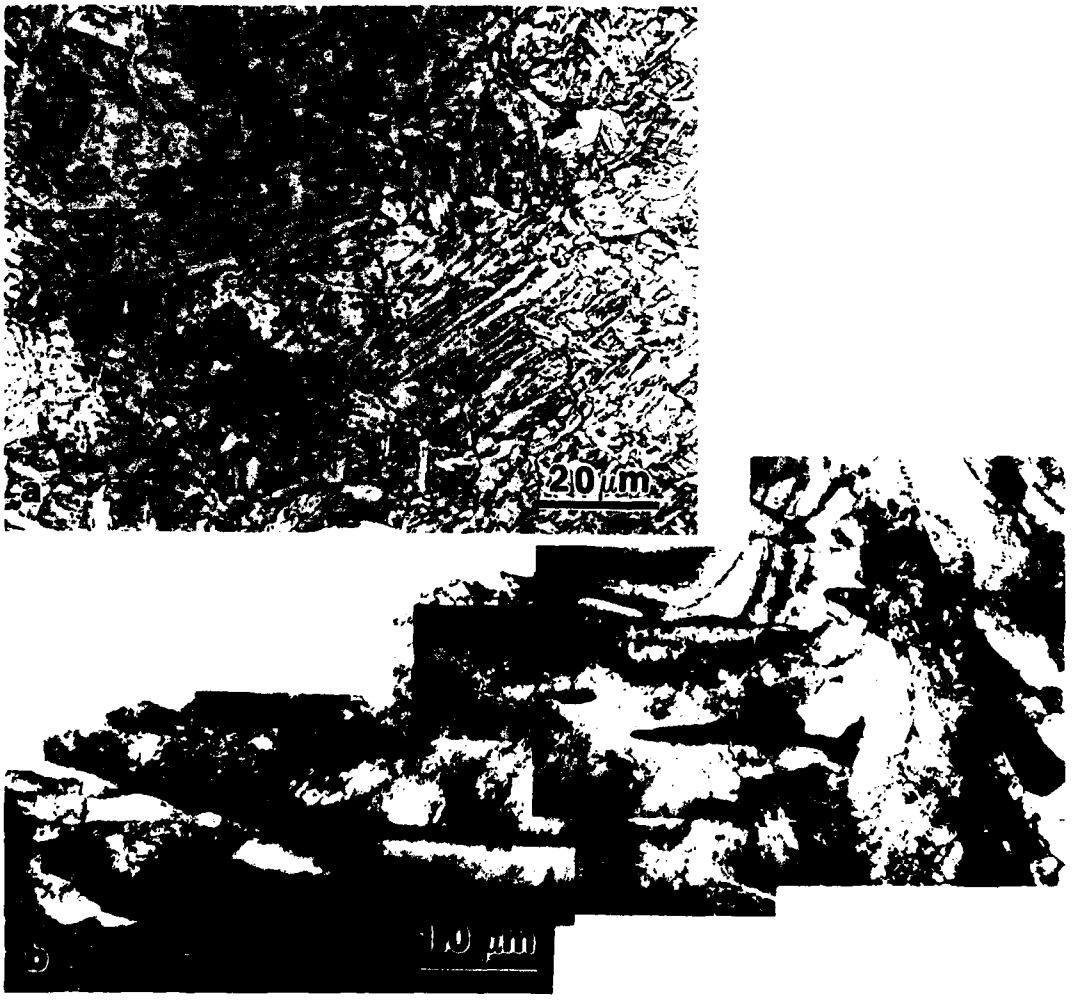


Figure 6 - Typical Microstructure of A710 Modified Exhibiting Granular Bainite: (a) Light Micrograph, (b) Montage of TEM Micrographs.

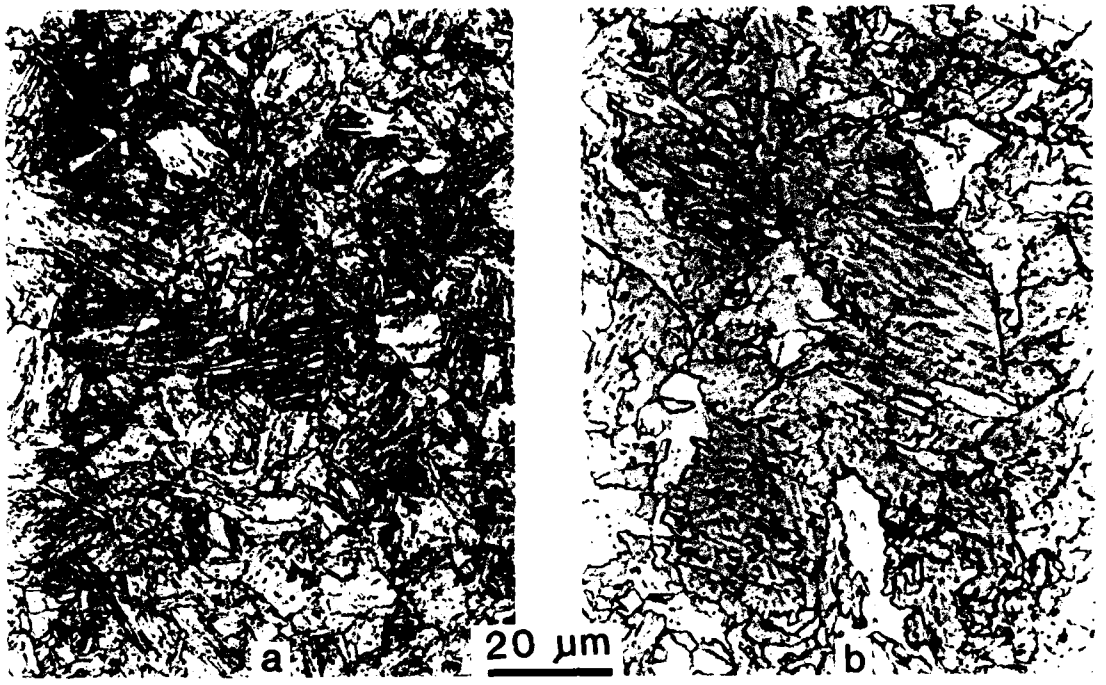


Figure 7 - Typical Microstructures 2 Inch (51 mm) Thick HSLA-100 Steel. (Nital Etch) (a) 0.06 pct C Steel. (b) 0.04 pct C Steel.

0.06 pct steel (Figure 7(a)).

In summary, by changing the levels of Mn, Mo and Ni, the positions of each transformation region can be altered, giving rise to different austenite trans-formation characteristics. For a wide range of cooling rates, the HSLA-80 steel microstructure is dominated by proeutectoid ferrite. Similarly, the microstructures of A710 Modified steel and the HSLA-100 steel (0.06 pct C) are dominated by granular bainite and martensite, respectively.

Copper precipitates which form in these steels have also been examined. The copper precipitates which are evident in the TEM are epsilon-Cu. After ageing, typical precipitate sizes range from 2 to 25 nm in diameter. These precipitates are found at dislocations within the ferrite grains (Figure 8(a)), at ferrite lath boundaries (Figure 8(b)) and are associated with sub-boundaries (Figures 8(c)and 8(d)).

## AGEING BEHAVIOR

A detailed study of the ageing response of 1-1/8 inch to 1-1/4 inch (29 and 32 mm) plates was conducted[17]. Plates, mill austenitized and water quenched, were subsequently aged in the laboratory. Mechanical properties were determined from samples of these steels in the as-quenched condition and from samples aged at 500°F (260°C) to 1250°F (677°C). All samples were water quenched after ageing. HSLA-80, A710 Modified, HSLA-80/100 Modified, and HSLA-100 steels (0.04 pct and 0.06 pct C) were investigated. Figures 9 and 10 show the effect of ageing on the yield strength and ultimate tensile strength of some of these steels. Peak yield strengths for these steels occurred in samples that were aged at 850 to 950°F (454 to 510°C). CVN toughness properties are also shown in Figures 11 and 12. Minima in energy absorbed at -120°F (-84°C) and the 50 pct FATT correlated with the peak yield strengths. Figure 13 presents a summary of the yield strength/FATT relationships of the four steels. Comparisons can be made directly between the strength and toughness properties of different steels. For example, at a yield strength of 110 ksi (758 MPa), the FATT of the A710 Modified is about -70°F (-57°C) while the FATT of the HSLA-100 is -160°F (-107°C). The enhanced toughness of the HSLA-100 composition correlates with the higher nickel content and may be related to the presence of tempered martensite in comparison to granular bainite.

The yield strength of the HSLA-100 decreases rapidly when it is aged above 1150°F (621°C). Despite this lower strength level, the FATT does not improve at a similar rate (i.e., the slope of the curve in Figure 13 changes dramatically between 1150 and 1250°F (621 and 677°C)). A rapid decrease in strength between 1150°F (621°C) and 1250°F (677° C) is undesirable for production processing because

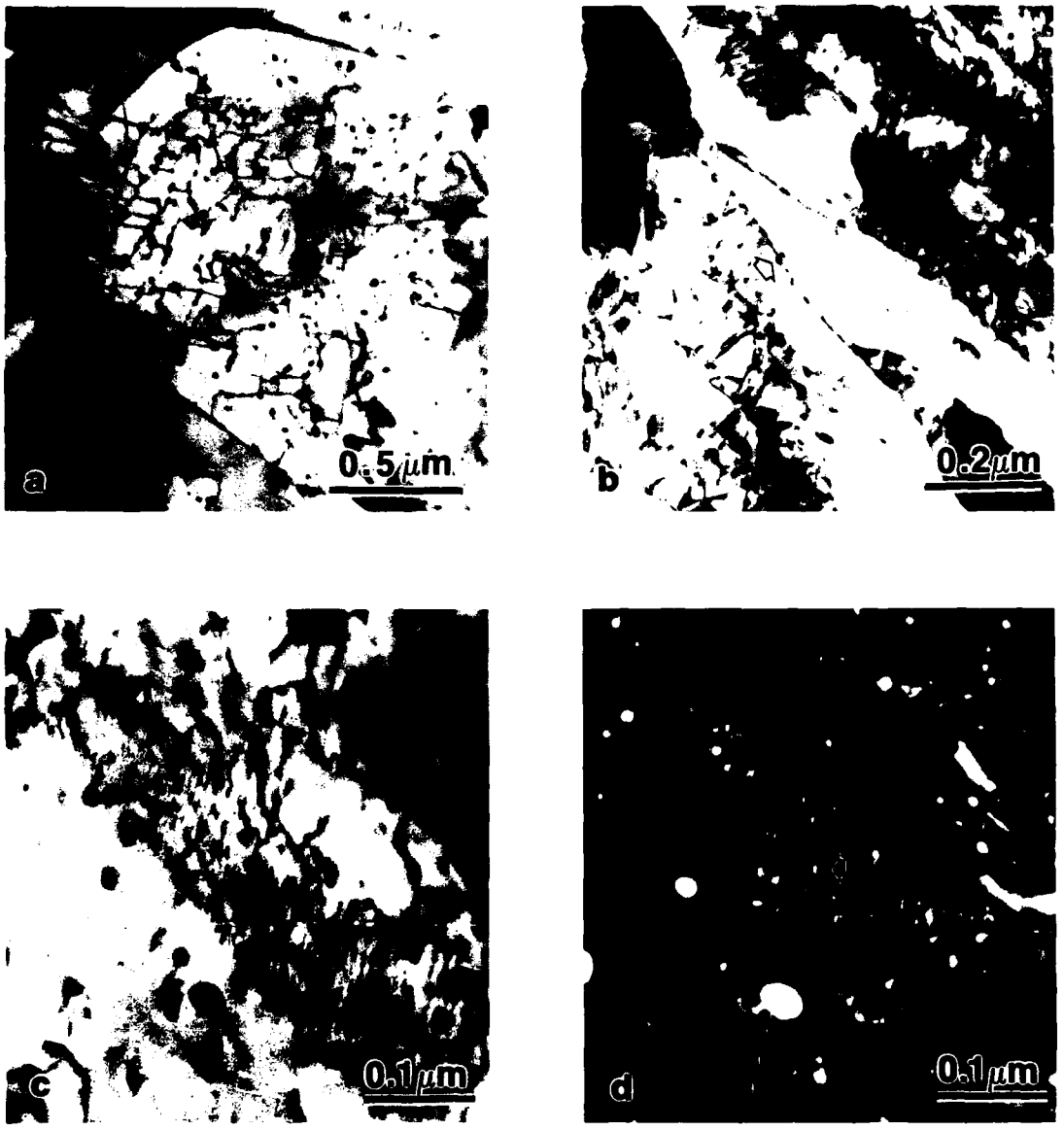


Figure 8 - Precipitates in These Alloy Steels: (a) Epilson-Cu at Dislocations, (b) Epsilon-Cu at Lath Boundaries, (c) Bright Field and (d) Dark Field Epilson-Cu at Sub-Boundaries.

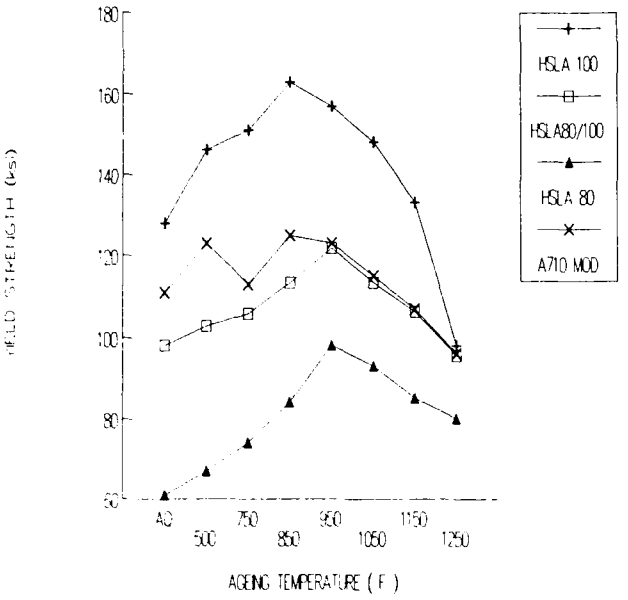


Figure 9 - Yield Strength of HSLA Steels As A Function of the Ageing Temperature

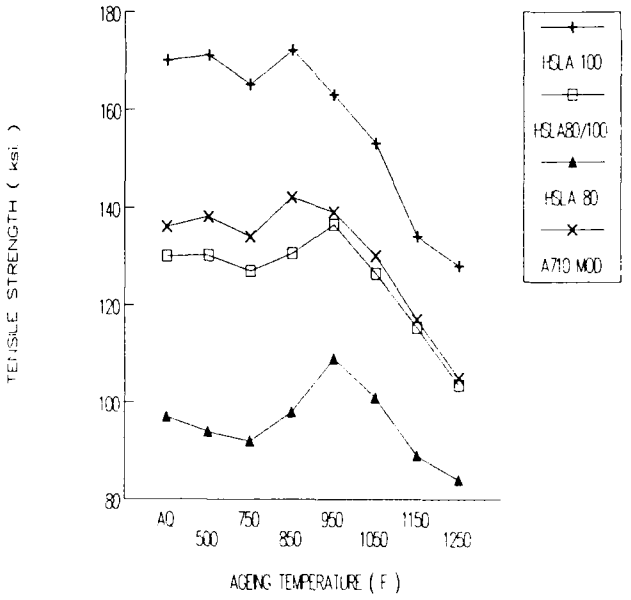


Figure 10 - Tensile Strength of HSLA Steels As A Function of the Ageing Temperature

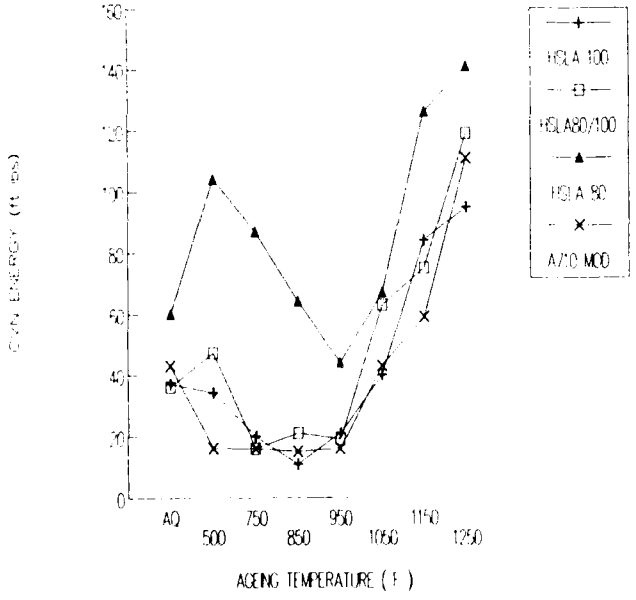


Figure 11 - Charpy V-Notch Energy at -120° F (-84° C) of HSLA Steels As A Function of the Ageing Temperature

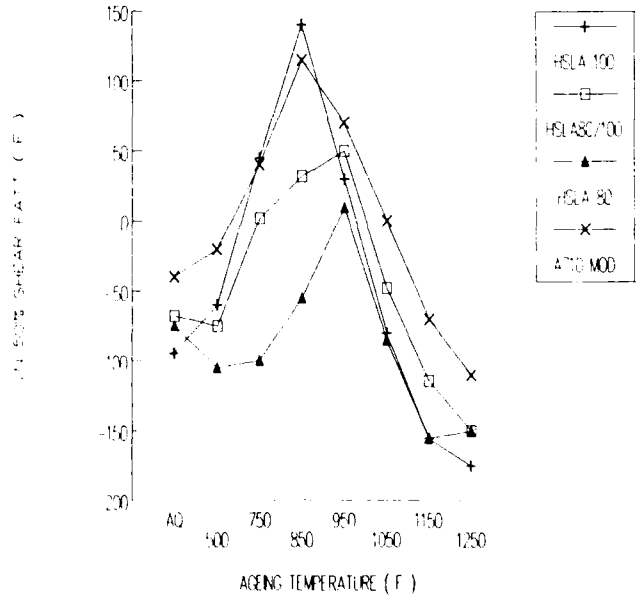


Figure 12 - Charpy V-Notch 50% Shear Fracture Appearance Transition Temperature of HSLA Steels As A Function of the Ageing Temperature

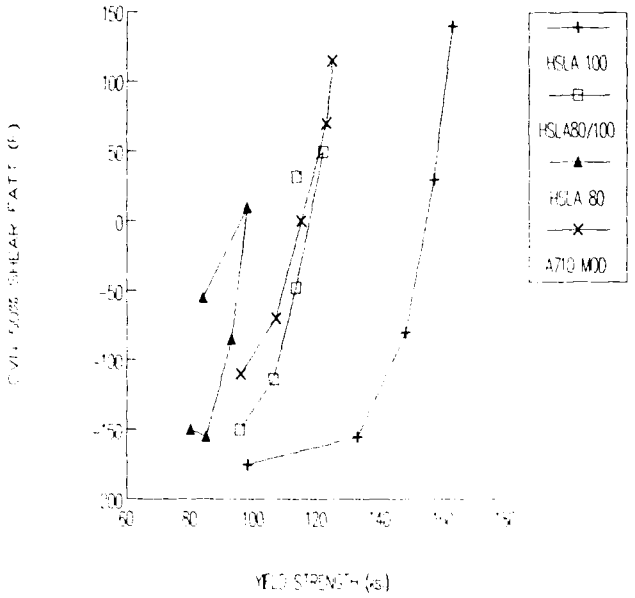


Figure 13 - Yield Strength-Toughness Relationship for HSLA Steels Aged Between 850° F (454° C) and 1250° F (677° C)

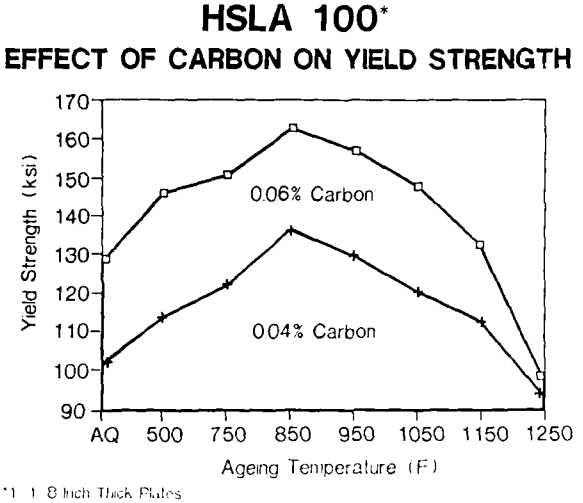


Figure 14 - Yield Strength of 0.04% C Compared to 0.06% HSLA-100 As A Function of the Ageing Temperature

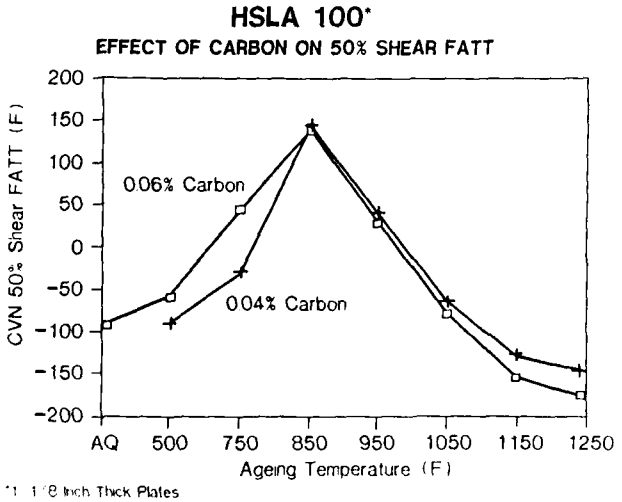


Figure 15 - Fracture Appearance Transition Temperature of 0.04% C Compared to 0.06% HSLA-100 As A Function of the Ageing Temperature

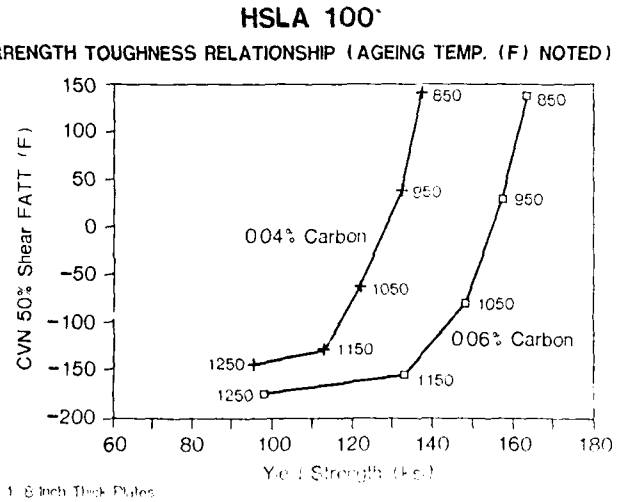


Figure 16 - The Yield Strength-Toughness Relationship of 0.04% C HSLA-100 Compared to 0.06% C HSLA-100

of the variability of strength that can occur in the product. This is particularly a concern when trying to meet the required range of yield strength allowed in this product of 100 ksi (690 MPa) to 115 ksi (793 MPa).

Carbon content also has a strong effect on the strength of HSLA-100. The first production heat contained 0.04 pct C while the second production heat contained 0.06 pct C. Comparing the yield strengths of the two heats shows a substantial carbon strengthening effect for this plate thickness, on the order of 30 ksi (207 MPa), at all ageing temperatures up to 1150°F (621°C), shown in Figure 14. Figure 15 shows the influence on toughness behavior. When a strength-toughness plot is prepared (Figure 16), the improved performance of the higher carbon steel is demonstrated. In other words, at any given yield strength, the 0.06 pct C steel has superior toughness to the 0.04 pct C steel. At these generally low levels of carbon, small increases in carbon content have a large effect on hardenability. The presence of martensite compared to a mixture of martensite and bainite lowers the FATT. In addition, for a given yield strength, the 0.06 pct C steel is always aged at a higher temperature. Hence it is to be expected that the higher C steel has coarser copper precipitates and a coarser dislocation substructure which is more conducive to improved ductility and toughness. The potential deficiency of the greater carbide content in the microstructure of the higher carbon steel is outweighed by these phenomena.

## PRODUCTION EXPERIENCE

HSLA-80 has been the most widely produced alloy from this family of steels. Figure 17 shows the range of strength and CVN impact properties that have been achieved in HSLA-80/A710 Grade A, Class 3 steel. It was very easy to achieve 80 ksi (552 MPa) minimum yield strength and the CVN toughness levels at -120°F (-84°C) in this steel. Furthermore, if more stringent toughness requirements are required, such as dynamic tear testing, controlled rolling prior to the reaustenitizing, quenching and ageing has been found to be beneficial[17]. This is further demonstrated by the dynamic tear testing of mill plates, Figure 18. Controlled rolling can be done with a number of schedules that normally result in lower finishing temperatures during the hot rolling cycle. Because of the limited hardenability in the A710 steel, the plate thickness is normally restricted to 1-1/4 inch (32 mm) for very high toughness applications. However, when only modest toughness and lower levels of yield strength are required, this steel has been produced in thicknesses up to 5 inches (127 mm).

Only one commercial heat has been produced with the A710 Modified chemistry, and plates from 1/2 inch (12.7 mm) up to 8 inches (203.20 mm) in thickness were produced. A 100 ksi (690 MPa) minimum yield strength up to 2 inches (51 mm) and 80 ksi (552 MPa) yield strength up to 8 inches (203 mm) was achieved with a modest toughness level. A summary of the properties of the plates produced from this heat of steel is given in Figure 19.

The higher hardenability of the HSLA-100 steel indicates that it is able to achieve much higher levels of strength than the HSLA-80 and A710 Modified steels. Plates from 1/2 inch (12 mm) up to 3-3/4 inches (95 mm) in thickness were produced from the 0.06 pct C steel discussed previously. A summary of the properties obtained from this heat are shown in Figure 20. High levels of toughness were achieved in this steel with 100 ksi (690 MPa) minimum yield strength throughout this range of thicknesses. The ageing temperature required to stay within the yield strength specification range was between 1180°F (582°C) and 1240°F (671°C). However, the high ageing temperatures for the thinner plates is very close to the $Ac_1$ temperature, 1256°F (680°C). This observation indicates that the 1-1/2 inch (30 mm) plate thickness is the practical lower limit for this chemistry to avoid reaustenitization, which causes considerable scatter in testing. A leaner chemistry, such as the HSLA-80/100 modified is appropriate for the plate thickness less than 1-1/2 inches (30 mm). Figure 21 shows the dynamic tear (DT) testing results at -40°F (-40°C) for this steel. Upper shelf DT results were achieved in all plates up to 3 inches in thickness. At 3-3/4 inches (95 mm), one value was not on the upper shelf.

These steels also benefit from multiple austenizating and quenching treatments prior to ageing. Typical results are presented in Table III. The primary improvement, shown in Table III, is in the CVN toughness in the transition region. Through multiple austenitization treatments, the presence of isolated large austenite grains is minimized. This feature is demonstrated in the 0.04 pct C HSLA-100 steel shown in Figure 22.

The improved hardenability in going from HSLA-80 to A710 Modified, HSLA-80/100 modified and HSLA-100 steels is shown in Figure 23. In this Figure, mill quenched plates of 1-1/4 inches (31.1 mm) thickness are compared. As shown in Figure 23, the dominant microstructural constituents are proeutectoid ferrite, granular bainite, granular bainite and martensite for HSLA-80, A710 Modified, HSLA-80/100 modified and HSLA-100 (0.06 pct C) steels, respectively.

A significant concern in the use of any of these steels is the weldability. It has been well established that these steels are highly weldable[7,8,20,21]. However, it also has been established that they are susceptible to stress relief cracking[20,22-24]. Upon welding of these steels, copper precipitates dissolve in the heat affected zones. With subsequent stress relief, reprecipitation of copper

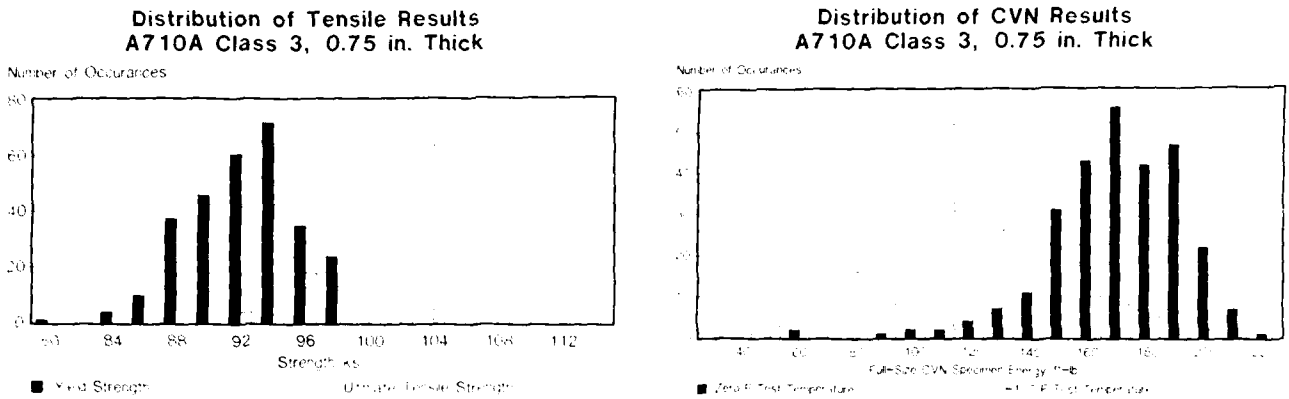


Figure 17 - Distribution of Properties in 0.75" (19 mm) Thick HSLA-80/A710 Grade A, Class 3 Plates

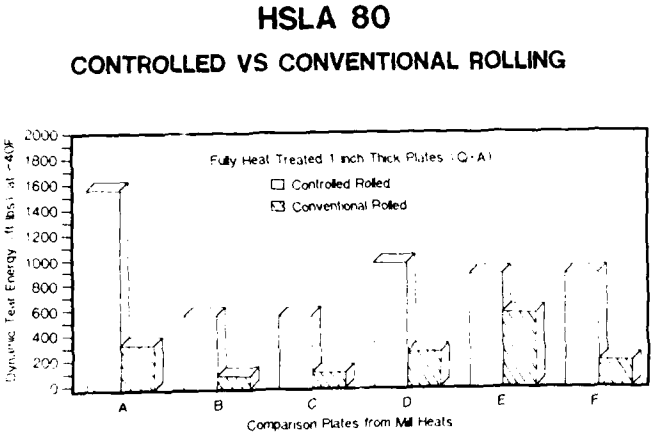


Figure 18 - Comparison of DT Toughness at -40°F (-40°C) of HSLA-80 Plates Produced Using Either Controlled Rolling or Conventional Rolling Prior to Re-Austenitizing, Water Quenching and Ageing

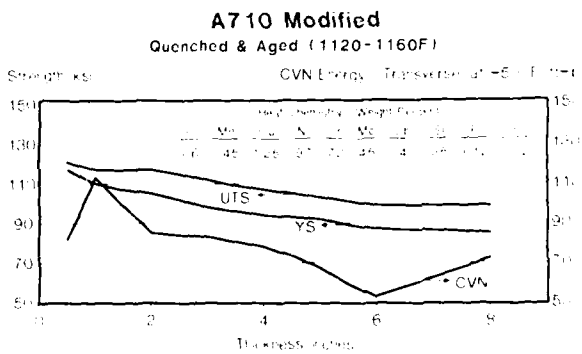


Figure 19 - Summary of Results for A710 Modified Plates of 1/2"-8" (13-203 mm) Thickness

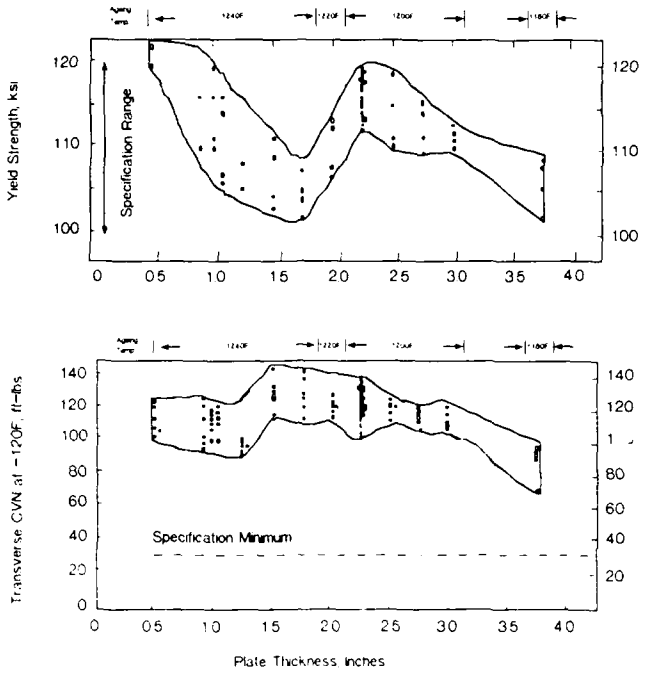


Figure 20 - Distribution of Mechanical Properties of HSLA-100 Plates from 0.06 pct C Heat in Thickness from 1/2" (12 mm) to 3-3/4" (95 mm)

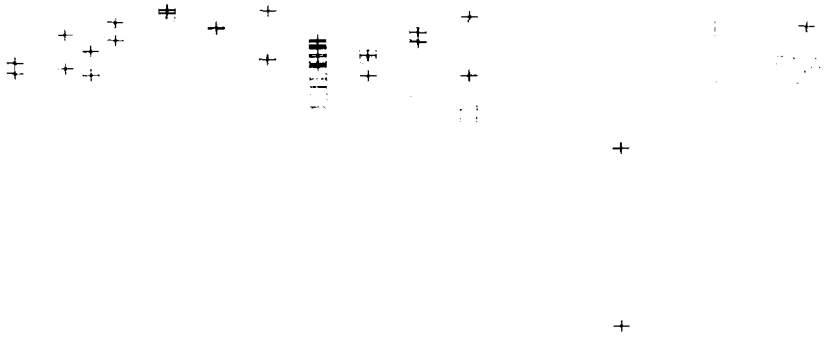

Figure 21 - Distribution of Dynamic Tear Results for 0.06 pct C Heat of HSLA-100 for A Range of Plate Thicknesses

Table III - Effects of Multiple Austenization on 2 inch (51 mm) Plates[a]

| | Number of Austenizations | Yield Strength[b] ksi (MPa) | Ave./Min.[c] CVN in ft.lbs. (J) 0°F (-18°C) | -120°F (-84°C) |
|---|---|---|---|---|
| A710 Modified | 1 | 90.9 (627) | 156/142 (212/193) | 60/45 (81/61) |
| 1240°F (671°C) Age | 2 | 92.8 (640) | 183/162 (248/220) | 116/92 (157/125) |
| HSLA-100 | 1 | 107.9 (744) | 179/161 (243/218) | 87/22 (118/30) |
| 1189°F (638°C) Age | 2 | 112.7 (777) | 175/167 (237/226) | 113/98 (153/133) |

(a) Produced in mill; each austenitize followed by water quench
(b) Average of 4 tests
(c) Average and minimum values for 6 CVN tests

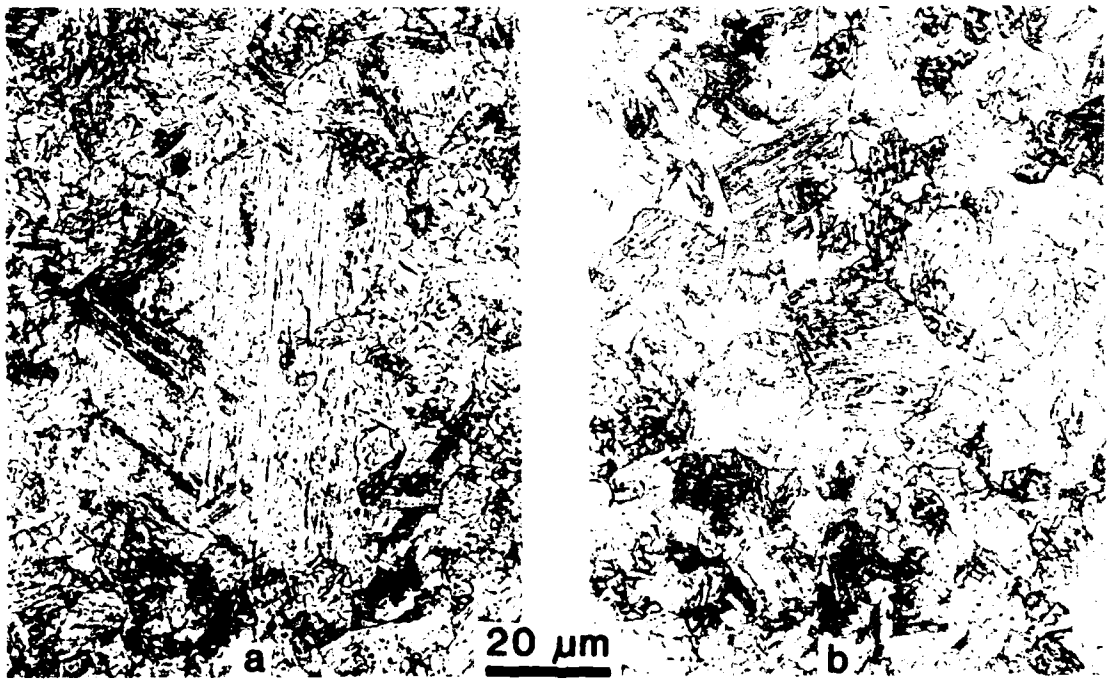


Figure 22 - Photomicrographs Showing the Influence of Double Austenization on Bainite Packet Size. (a) Shows Large Bainite Packet in Single Austenitized 2" HSLA-100 Plate Compared to (b) After Double Austenization

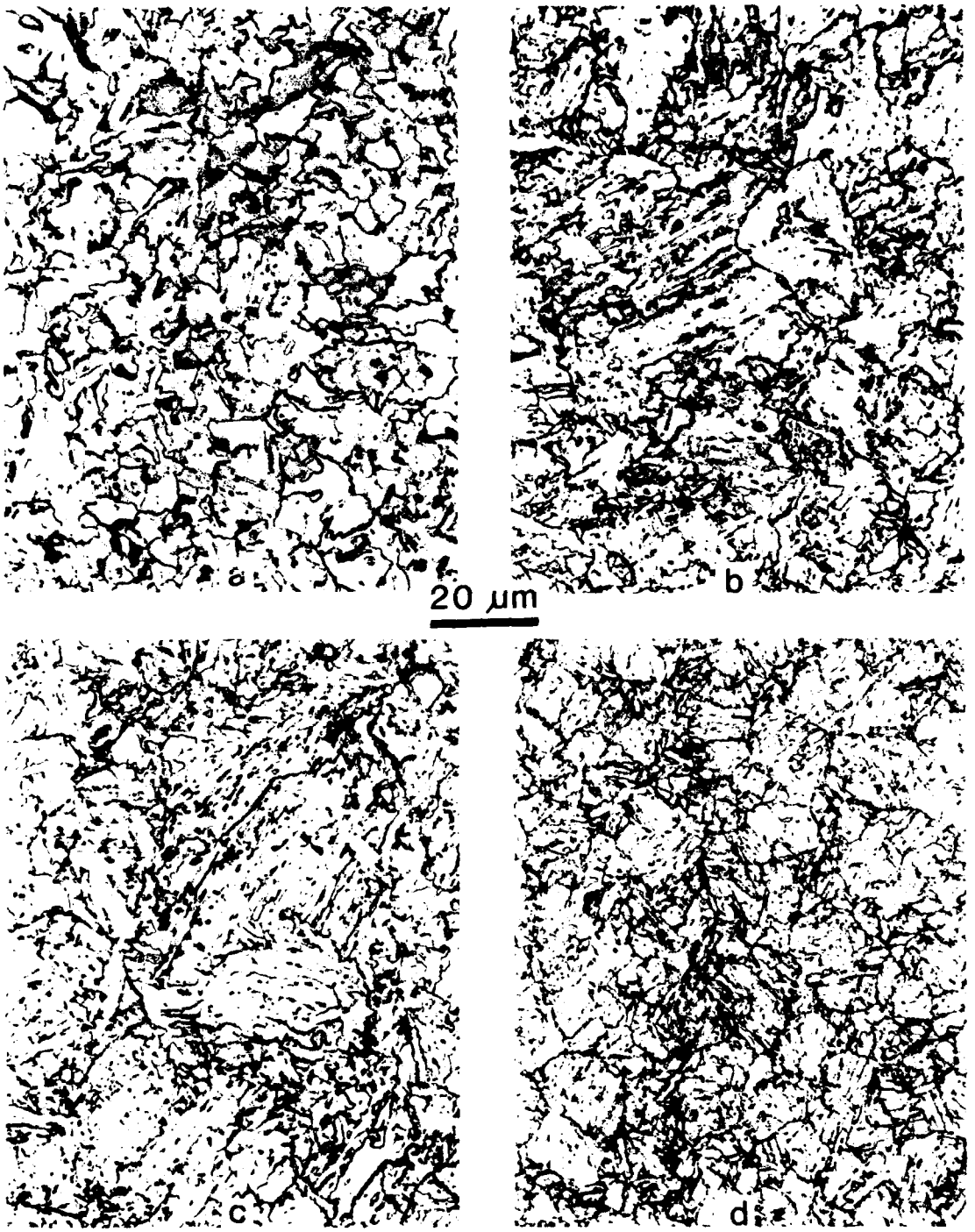


Figure 23 - Typical Microstructures from 1-1/4" (32 mm) Plates of All Four Chemistries: (a) HSLA-80, (b) A710 Modified, (c) HSLA-80/100 Modified and (d) HSLA-100 (Nital-Picral Etch)

particles occurs, which hinders the normal creep processes within grains that are required to give adequate stress relieving response. Further work is continuing on the mechanism for this phenomena in this family of steels.

## SUMMARY

The influence of various alloying elements on the properties and microstructures of low-carbon copper-bearing, precipitation aged plate steels has been presented. The importance of maintaining a bainitic and/or martensitic microstructure in promoting high strength levels has been demonstrated. By varying the levels of Mn, Mo, and Ni, the position of each transformation region is altered giving rise to different austenite transformation characteristics. Through use of these various alloying elements, the strength and toughness of these alloys can be matched to the thickness and particular application. Granular bainite has been found in both the A710 Modified and HSLA-100 steels. This microconstituent has retained austenite and martensite as the second phase interlath particles, rather than the cementite found in the conventional upper bainite. Carbon content has been found to play a very important role in the hardenability and strength of HSLA-100 steel even at the very low levels present. Use of double austenitizing and controlled rolling prior to further heat treatment have been found to lead to overall structural refinement and improved toughness in these steels.

These results indicate that there is further potential for alloy design and improved strength/toughness properties in this alloy system. Through microstructural control via alloying, low-temperature transformation products (i.e., granular bainite and martensite) can be maintained in very thick plates. The strengthening contribution from the copper precipitates, together with solid solution strengthening and structural refinements from processing may lead to stronger and tougher alloys. These enhancements will be examined in the future.

## ACKNOWLEDGMENTS

The authors would like to appreciatively acknowledge the contributions of J. R. Lohr and L. P. Kerr to the various phases of the research program; to C. R. Roper for consultation on microstructures; to H. D. Swarr for assistance in production of mill plates; and to E. J. Czyryca of the David Taylor Research Center, the program manager for the Navy HSLA steel development program. The guidance and suggestions of J. H. Bucher are also gratefully noted. The contributions of D. J. Colvin, S. W. Thompson, and G. Krauss were made possible by the Advanced Steel Processing and Products Research Center at the Colorado School of Mines.

## REFERENCES

1. "In-787, A Precipitation Hardening Alloy Steel", The International Nickel Company, Inc., New York, 1978.

2. R. A. DePaul and A. L. Kitchin, Met. Trans., 1, pp 389-393, Feb. 1970.

3. A. D. Wilson, E. G. Hamburg and J. H. Bucher, Journal of Ship Production, Vol. 3, No. 2, May 1987, pp 114-115.

4. A. P. Coldren and T. B. Cox, "Development of 100 ksi Yield Strength HSLA Steel", DTNSRDC/SME-CR-07-87, June 24, 1987.

5. E. G. Hamburg, C. R. Roper and A. D. Wilson, "Development of An Intermediate Composition for Navy HSLA-80/100 Steels", Lukens Steel, Coatesville, PA, RQR 88-1, Feb. 1988.

6. B. A. Graville, "Cold Cracking in Welds in HSLA Steels", Welding of HSLA (Microalloyed) Structural Steels, ASM, Rome, Italy, Nov. 9-12, 1976.

7. L. G. Kuidahl, Welding Journal, 64, No. 7, pp 42-48, July 1985.

8. J. C. West, Journal of Ship Production, 3, No. 2, pp 111-118, May 1987.

9. P. P. Hydrean, A. L. Kitchin and F. W. Schaller, Met Trans., 2, pp 2541-2548, Sept. 1971.

10. W. Steven and A. G. Haynes, "Atlas of Continuous Cooling Transformation Diagrams", ASM, Metals Park, OH, p 228, 1980.

11. K. W. Andrews, JISI, pp 721-727, July 1965.

12. C. I Garcia and A. J. DeArdo, "Study of the $B_S$ Temperature in A Molybdenum Containing Ultra Low Carbon Bainitic Steel for Heavy Plate Applications", DTNSRDC/SME-CR-22-86, Dec. 1986.

13. S. Biagiotti, Stone and Webster Inc., private communication, 1987.

14. H. W. Cias, "Austenite Transformation Kinetics in Ferrous Alloys", Climax Molybdenum Co., Greenwich, CT, 1977, pp 5-22, pp 55-57.

15. "Atlas of Continuous Cooling Transformation Diagrams", ASM, Metals Park, OH, 1980, p 224.

16. G. R. Speich and T. M. Scoonover, "Continuous-Cooling-Transformation Behavior of HSLA-100 (A710) Steel",

presented TMS AIME Symposium on Processing, Microstructure and Properties of HSLA Steels, Nov. 1987, Pittsburgh, PA.

17. E. G. Hamburg and A. D. Wilson, "Production and Properties of Copper, Age Hardened Steels", presented same as Ref. 16.

18. L. J. Habraken and M. Economopaulas, "Transformation Hardenability in Steels", Climax Molybdenum Co., Ann Arbor, MI, 1967, p 81.

19. S. W. Thompson, D. J. Colvin and G. Krauss, "On the Bainitic Structure Formed in A Modified A710 Steel", accepted for publication Scripta Met.

20. A. D. Wilson, unpublished research, Lukens Steel Co., 1988.

21. R. Wong and E. J. Czyryca, private communication, DTRC, Annapolis, MD, 1988.

22. C. D. Lundin and R. Menon, "Postweld Heat Treatment Cracking in HSLA Steels", presented AWS Convention, Chicago, IL, Mar. 1987.

23. A. W. Pense, et. al., "Heat Affected Zone and Weldment Studies on A710 Steel", report to PVRC, Lehigh University, Jan. 1988.

24. J. P. Balaguer, E. F. Nippes and Z. Wong, "Heat Affected Zone Transformation in Copper Containing HSLA Steels", presented AWS Convention, New Orleans, LA, April 1988.

# THE EFFECT OF WELDING AND FABRICATION OPERATIONS ON THE TOUGHNESS OF A710 STEEL

**Walter Bolliger**
Giovanola Freres SA
Monthey, Switzerland

**Rajan Varughese**
Bell Laboratories
Murray Hill, New Jersey, USA

**Eric Kaufmann, Wei-Fang Qin, Alan W. Pense, Robert D. Stout**
ATLSS Center
Lehigh University
Bethlehem, Pennsylvania, USA

Abstract

ASTM A710 microalloyed precipitation strengthened steel provides to potential users a constructional material of high strength and toughness combined with excellent fabrication weldability. Of importance to its application are the properties of its weldments, particularly the toughness, its response mechanical forming, and the effects of heat treatment after forming or welding on its properties. The study reported here was designed to provide data in these areas.

The A710 steel studied was 32 mm thick Grade A Class 3 and had a yield strength of 602 MPa and a tensile strength of 673 MPa. The transverse orientation 47 J Charpy impact transition temperature of the plate was -145C. Cold plastic strain of 5% increased the transition temperature to -113C. Aging at 370C for 10 hours did not increase the transition temperature further. Stress relief treatments of 2 and 10 hours at 620C decreased the transition temperature to -127C or below.

The course grained heat affected zone of A710 weldments had a lower toughness than the base metal, an effect that was greater at higher welding heat inputs. For heat inputs of 2KJ/mm, the as-welded 47J transition temperature in the heat affected zone was -78C. High heat input welds, 5.3 KJ/mm, resulted in heat affected zones with a 47J transition temperature of -33C. Weld metals used for the study, typical of those used in construction, were adequate in strength but had transition temperatures above those of the heat affected zone in the same weldment.

Post weld heat treatment at 620C did not consistently improve heat affected zone toughness over the as-welded condition and 2 hour heat treatment cycles increased heat affected zone transition temperatures. Similar treatments had little effect on base plate toughness. The A710 showed potential for stress relief cracking in the modified Lehigh restraint test, the effect being greatest above 600C but observable at 482C. These latter two effects suggest that post-weld heat treatment should not be used on this steel for metallurgical reasons.

THE USE OF MICROALLOYED STEELS for constructional and pressure vessel applications has a long history, going back to the 1940's when critical material shortages made the utilization of only small amounts of alloys in steel products mandatory. In the 1950's, a number of companies also introduced construction steels that contained, along with Mn and other alloys, V, Ti, and Nb. Most of these steels are now covered by ASTM specifications A588 and A572 and may also be considered early microalloyed steels, although they were not identified as such. However, it was in the 1970's that the microalloyed steels with low carbon content, high Mn levels and microalloy carbide and nitride formers really became identified as construction materials with high strength, good weldability and good low temperature toughness. These materials allow control of grain size and microstructure such that, either as-rolled or specially processed, steels with good combinations of properties are now available for a number of applications.

The use of Cu in amounts over 0.2% to strengthen structural steels also has a long history, starting at least in the 1940's, when it was used in some ship steels. Structural steels clearly using Cu for precipitation strengthening, forerunners to the current ASTM A710 grades, were actually introduced in the 1960's, but generated little interest at that time. However, engineering needs change, and there is now a considerable interest in the combination of properties that Cu bearing steels of the ASTM A710 type provide.

Of special interest is the very low carbon content, below 0.07%, that virtually prohibits hard, crack sensitive heat affected zones on welding, making preheat for welding unnecessary. Because of the choice of alloys present and the strengthening mechanism, strength can be very high and transition temperatures, low. This combination makes it especially attractive for special ship steels but there are also structural and pressure vessel applications where one or more of its characteristics may be useful.

It was for these reasons that the Pressure Vessel Research Committee and the Center for Advanced Technology for Large Structural Systems at Lehigh University initiated a program in 1985 to study the strength, toughness and fabrication characteristics of the A710 steel as a complement to its then nearly completed study of conventional and new microalloyed steels. The prior studies [1,2,3,4,5,6] covered the effects of heat treatment, forming operations and welding on the strength and toughness of A572, A588, and A737 Grades B and C steels. A parallel investigation of A808 steel has just been started and a similar study on A710 appeared a natural extension of this program. As in the previous work, the effects of fabrication operations, i.e., cold forming and welding, were given emphasis, as were the effects of heat treatments following these operations. The philosophy followed was that base metal properties are relatively easy to document, but changes in these properties, especially toughness, during fabrication operations are often unknown and should be the focus of the investigation.

## MATERIALS AND PROCEDURES

MATERIALS-The base material was a 32mm thick plate of A710 Grade A Class 3 steel. The composition properties of the plate are given in table 1 along with the specified properties for the grade. During the weldability program, two weld metals were used to produce the test weldments. The welds were used primarily to create joints to measure heat affected zone properties but were intended to be adequate in strength for the base plate. The major weld metal types used were AWS 5.20 70T-1 and 5.29 E91 T1-K2. Their typical chemical and mechanical properties are given in table 1. In the stress relief cracking studies, two additional weld metals were used to develop the restraint necessary for the test specimen, E110 T5-K4 and E8018-C1. They were selected for their nomiral strength level, and their compositions and properties were not assessed.

MECHANICAL PROPERTIES MEASURED-The test program consisted primarily of Charpy impact tests performed in the transverse (TL) orientation to the rolling direction of the plates. This was the philosophy followed in the previous studies so that "worst case" or conservative data would be produced. Strength properties were a secondary consideration and were not measured for all conditions of testing. All tension and Charpy impact tests were perfomed in accordance with ASTM Specification E370. The impact specimens were standard size. The tension test specimens had a diameter of 6.4 mm and a gage length of 25.4.

STRAIN AGING STUDY-The strain aging study was performed by tensile prestraining of bars 70 mm wide 13 mm thick and 457 mm long. This prestraining specimen is seen in figure 1. The bar was cut from approximately the quarter thickness position of the plate. Prestraining was done in a universal testing machine using scribe marks on the bar surface to control strain. The uniform strain gage length was 241 mm and approximately 16 standard Charpy V-notch specimens were prepared for each condition of test. Specimens were both strained and tested in the TL orientation. The conditions tested are given below.

1. As received.
2. Stress relieved 2 hr at 620C.
3. Stress relieved 10 hr at 620C.
4. Plastically strained 5%.
5. Strained and aged at 370C for 10 hr.
6. Strained, aged and stress relieved 2 hr at 620C.
7. Strained, aged and stress relieved 10 hr at 620C.

WELD HEAT AFFECTED ZONE STUDY-The heat affected zone study utilized weldments made on full thickness base metal using the flux cored arc process with varying weld heat inputs. The weld preparation was a single bevel on one side of the groove so that, after welding, a straight heat affected zone was produced on the unbevelled side of the joint. The joint preparation used and specimen locations are shown in figure 2. The shielding gas used was CO2. A multipass weld was deposited in the groove at a sufficient angle, usually 30 degrees, to the surface of the plate to produce good sidewall fusion on the unbevelled side. There was a 4 mm root gap and a backing plate was used to provide root fusion. The variations in heat input were produced by changing arc amperage and travel speed. Wire diameters of 1.6 mm were used for heat inputs up to 2.0 KJ/mm. For higher heat inputs, wire diameters of 2.4 mm were used. One weld, at 4.0 KJ/mm, was made with the submerged arc process using an AWS 5.23 EM2 electrode.

The Charpy impact specimens for testing were taken from the quarter thickness positions in the plate in the coarse grained heat affected zone as shown in figure 2 and were notched within one mm of the fusion line. The plates were welded such that the specimens were in the TL orientation to the plate rolling direction. The specimens were notched transverse to the plate thickness and each specimen was etched prior to notching so as to locate the notch as precisely

as possible.

Early tests made from plates welded with the relatively lower toughness AWS 5.20 70T-1 weld metal showed lower HAZ toughness values than expected and substantial test data scatter. Individual specimens were metallographically studied to determine if the fracture path had incorporated a large amount of weld metal. In some cases this was true, but for many specimens, it was not. Additional tests made with the higher toughness AWS 5.29 E91 T1-K2 weld metal and using more accurate notch placement reduced the test scatter to some degree but by no means eliminated it. Moreover, the HAZ test results were not significantly changed. Eventually it was concluded that more scatter than normally encountered is a characteristic of this steel.

STRESS RELIEF CRACKING STUDY-The stress relief cracking study performed on the A710 steel used a modified Lehigh restraint specimen. This specimen is seen in figure 3. The specimen has an open slot in which the weld is made such that one end of the weld is free to contract transversely on solidification and subsequent cooling while the other is constrained by the width of the plate. The weld is deposited in the machined groove above the slot such that it does not penetrate through the land, leaving a notch in the root area. This root notch, in conjunction with the transverse constraint in the specimen, produces cracking in the weld heat affected zone in susceptible materials. Welding is from the open end toward the restrained (keyhole) end.

After welding, the specimen is given the stress relief treatments desired by charging in a preheated furnace and is cut transverse to the weld along a line 25 mm from the center of the keyhole, i.e., at the highly restrained end. The section is polished and etched to reveal the size and location of cracks. This test can also be used to reveal hydrogen induced cold cracking but A710 is very resistant to this phenomenon. The height of the crack at the 25 mm location is used as a measure of cracking potential. Tests show that the crack is highest at the 25 mm location and decreases toward the less restrained end. Thus the 25 mm crack height is a good parameter to characterize the cracking behavior.

Welding in this part of the study was done using an AWS E110 T5-K4 flux cored electrode. with CO2 shielding at a heat input of 2 KJ/mm. This electrode overmatched plate strength and increased cracking potential. To study weld metal strength effects, a weld matching one of the test conditions was also made at the same heat input with the shielded metal arc process and a lower strength E8018-C1 electrode.

METALLOGRAPHY-Light microscopy was used to examine all of the stress relief cracking samples for determination of crack height. Many of the heat affected zone samples were examined by light and scanning electron microscopy for microstructure identification.

## RESULTS AND DISCUSSION

BASE AND WELD METAL PROPERTIES-The data of table 1 illustrate the excellent combination of strength and toughness that the A710 Grade A Class 3 material can provide and also the influence of stress relief (post weld heat treatments) on its properties. For the material used in this investigation, strength properties were well above the minimums required and treatments at 620C for up to 10 hours did not decrease them below this level. Similarly, both weld metals met the minimum strength requirements for the base metal as welded. Based on the response of weld metal 1, they would be expected to do so for treatments of up to 8 hours at 620C.

The biggest disparity between the base and weld metals is in toughness. The base metal has a very low transition temperature, -145C, and maintains it after stress relief treatments of up to 10 hours at 620C. Weld metal 1, a typical structural weld filler metal, has a transition temperature over 150C higher than the base metal and weld metal 2, which would normally be considered a filler of good toughness, has a transition temperature 87C higher. This is not attributable to any deficiency on the part of these fillers but rather the unusually low transition temperature of the A710 Grade A Class 3 plate. The strength and toughness of the weld deposit is somewhat dependent on the heat input used in welding and table 3 shows that high heat input can increase the transition temperature of weld metal 2 by as much as 40C.

STRAIN AGING STUDY-The results of the study of the effects of straining, aging and stress relief are shown in table 2 and figure 4. As noted before, stress relief treatments alone have little effect, resulting in small decreases in transition temperature. Plastic strain of 5%, with or without aging at 370C, produces a 32C increase in transition temperature. About half of this is recovered by stress relief treatments at 620C. The increase in transition temperature on straining similar to the 25C observed in most other microalloyed steels[1]. The residual shift after stress relief is reduced to about 15C. In the light of its initially good toughness, strain aging must be considered a minor effect for this steel.

WELDING HEAT AFFECTED ZONE STUDY-Weld heat affected zones in the A710 material studied here have a clear tendency to lower toughness than the original plate, as is evident from the data of table 3 and figure 5. An upward shift in transition temperature is evident even at low heat inputs, where it might be expected to be minimal, and increases with increasing heat input. The minimum transition temperature shift observed in as-welded material is 67C and the maximum is 112C. These shifts are substantial, exceeding those observed in other microalloyed steels, where they were typically no more than 30 to 40C and often much less[1].

To provide a comparison to this work, table 4 is a listing of weldment data taken from the open literature and private sources for both A710 Grade 1, Classes 2 and 3 and HSLA-80, a version of this material of interest to the U. S. Navy. The A710 studies listed on table 4 show a similar, but smaller, shift in HAZ transition temperature on welding. They also appear to show a dependance of the transition temperature on heat input, as noted in the current work, and on plate thickness. These points are illustrated in figure 6 where the extent of the shift decreases with increasing plate thickness and increases with increasing heat input. The studies on HSLA-80 listed in table 4 do not show such a dependence. The shifts, which range from 11C to 44C, appear definite but fairly random, averaging about 28C.

If the transition temperature shifts are a direct result of the effect of welding heat on the base metal, a dependence on heat input might be expected. Indeed, a study of simulated heat affected zones in HSLA-80[7] has shown just such an effect and the data from the study are listed in table 5. Transition temperature shifts observed ranged from 50C to 114C for heat inputs of 1 to 4 KJ/mm, about the range in the current work. The authors of the study attributed these shifts to a change in microstructure with increased heat input from fine packet martensite to coarse bainite. These observations were supported with microhardness measurements.

In the current work, a coarsening in microstructure was observed with increasing heat input but hardness changed little and in all cases corresponded with the range for higher heat input welds in the HSLA-80 study, about 250 VHN. In the low heat input heat affected zones in the A710 work reported here, the structure appeared to be acicular ferrite. In the higher heat input welds, the structure was bainite. Grain size increases in the heat affected zone alone can account for some of the transition temperature increases, but changes in fine structure unit sizes, reported in the HSLA-80 work, must also play a role. This is a subject of continuing study at Lehigh University.

The effects of post weld heat treatment on the toughness of the weld heat affected zones are also shown in table 3 and figure 5. Post weld heat treatment at 620C for 10 hours results in a modest benefit in toughness in two out of three conditions studied but short time treatments increase transition temperature. This mixed effect has been observed in some other microalloyed steels[5,8] and is undoubtedly a result of coarsening and precipitation processes that occur during the post weld heat treatment.

Preliminary microstructure studies on the A710 heat affected zone samples show that the microstructure coarsens by what appears to be a recovery process after 2 hours at 620C, but new grain boundaries resulting in a finer structure appear after 10 hours. These observations do not include TEM studies of precipitate behavior and thus must be considered incomplete.

STRESS RELIEF CRACKING STUDIES-The results of stress relief cracking tests using the modified Lehigh restraint specimen are listed in table 6 and shown in figure 7. The potential for reheat cracking in this steel has been reported previously[9] and this work confirms the effect. The temperature range of cracking extends from about 500C to over 600C and can occur for times as short as 15 minutes. Some of the cracking reported for the higher temperature treatments may have occurred during heating of the specimen to the temperature of the heat treatment furnace. Complete cracking in the test corresponds to crack heights of about 2.5 mm and thus some of the cracks reported here are substantial.

A large number of stress relief or reheat cracking tests were performed at Lehigh University in the 1960's on low alloy quenched and tempered steels using a similar specimen[10]. In comparing the results seen in figure 7 with the previous work, the A710 appears to be neither the least nor most sensitive material Lehigh has tested. It is more sensitive to cracking than A517J steel for which little cracking was reported in service but less than A517F, which was reported to have a high cracking sensitivity. Potential for reheat cracking was found to exist in a number of low alloy steels, especially those with precipitation processes occurring in their weld heat affected zones during post weld heat treatment. For most of the steels, post weld heat treatment could still be applied successfully if proper attention was given to control of weld discontinuities. For the more sensitive steels, it was recommended that they should be used in the as-welded condition, with post weld heat treatment to be applied only after careful consideration of all the factors involved. Since A710 steel relied on precipitation processes for most of its strength, it is perhaps not surprising that it is also susceptible to reheat cracking.

## EVALUATION AND SUMMARY

The studies performed on A710 Grade A Class 3 steel show it to be a material of high strength and very high toughness. Fabrication operations, both straining (with or without aging) and welding (with or without post weld heat treatment), will result in an upward shift in transition temperature. This will be small after straining and aging, but can be substantial after welding. However, the increase in transition temperature on welding must be placed in the context of the use of the steel. With an initial transition temperature of -145C, an increase of 110C in the heat affected zone from

high heat input welding, 5.3 KJ/mm, still results in a transition temperature of -33C. For most structural applications, this is well below what would be required. Moreover, it is also well below that of the relatively tough weld metal from the same weldment, which was -18C.

Lower heat input welding, for example 2 KJ/mm, results in heat affected zone transition temperatures close to -60C, a level superior to most other structural materials at this or any strength level. Welding at 4 KJ/mm, a common industry practice, results in a heat affected zone transition temperature of -55C, which is still a very satisfactory level. Thus the loss in transition temperature on welding, while substantial, may not be so significant.

The effects of post weld heat treatment on the A710 studied here suggest that the material can best be used in the as-welded condition. Post weld heat treatment must be applied for relatively long times to have any beneficial effects on heat affected zone toughness, and even then, improvement is modest. In addition, potential for stress relief cracking exists, and this may preclude weld heat treatment for joints whose design might promote cracking, such as those incorporating partial penetration welds. Because of the high toughness of the steel, its low tendency for hydrogen induced cold cracking and its moderate heat affected zone hardness at normal heat inputs, many of the reasons for post weld heat treatment are obviated. Thus post weld heat treatment may not be necessary in most cases and is not desirable from the metallurgical viewpoint.

## ACKNOWLEDGEMENT

The authors would like to acknowledge the technical and financial support of the Pressure Vessel Research Committee and the Lehigh NSF Center for Advanced Technology for Large Structural Systems for this work. The continued interest and personal involvement of the members of the Thermal and Mechanical Effects Subcommittee of the Materials and Fabrication Division of PVRC has been a great encouragement and continuing resource to Lehigh University in this investigation.

## REFERENCES

1. Herman, W. A., et al, "The Strain Aging Behavior of Microalloyed Steels", WRC Bulletin No. 322, April 1987.
2. Aadland, J. A., et al, "The Fracture Behavior of ASTM A737 Grade B and Grade C Microalloyed Pressure Vessel Steels", WRC Bulletin No. 322, April 1987.
3. Aurrecoechea, J. C., et al, "The Fracture Behavior of ASTM A737 Grade B and Grade C Microalloyed Steel Weldments", WRC Bulletin No. 322, April 1987.
4. Shinohe, N., et al, "Long Time Stress Relief Effects in ASTM A737 Grade B and Grade C Microalloyed Steel" WRC Bulletin No. 322, April 1987.
5. Robino, C. V., et al, "The Fracture Behavior of A588 Grade A and A572 Grade 50 Weldments", WRC Bulletin No. 330, January 1988.
6. Pense, A. W., "Mechanical Property Characterization of A588 Steel Plates and Weldments", WRC Bulletin No. 332, April 1988.
7. McGrath, J. T., et al, "Microstructure and Property Relationships in the HAZ of HSLA-80 Steel", IIW Doc. IX-517-88, Canada Centre for Mineral and Energy Technology. February, 1988.
8. Konkol, P. J., "Effect of Long-Time Postweld Heat Treatment on the Properties of Constructional-Steel Weldments" WRC Bulletin No. 330, January 1988.
9. Lundin, C. D., and Menon, R., "Postweld Heat Treatment Cracking in HSLA Steels", AWS 87th Annual Meeting, Chicago, Il., March 1987.
10. de Barbadillo, J. J., et al, "The Creep Rupture Properties of Pressure Vessel Steels - Part II", The Welding Journal, V45, No. 7, July 1966.

## LIST OF TABLES



## LIST OF FIGURES

Toughness in A710 Weldments.
7. Results of Stress Relief Cracking Tests on A710 Grade A Class 3 Plate.

Table 1. Composition and Mechanical Properties of the A710 Grade A Class 3 Plate and Weld Metals Used in the Weldment Study

A. Chemical Composition (Wt %)

| Material | C | Mn | P | S | Si | Ni | Cr | Mo | Cu | Al | V | Nb |
|---|---|---|---|---|---|---|---|---|---|---|---|---|
| A170 Plate | .05 | .53 | .008 | .003 | .24 | .98 | .72 | .21 | 1.13 | .027 | | .008 |
| Weld Metal 1 | .07 | 1.45 | - | - | .48 | - | - | - | - | - | | |
| Weld Metal 2 | .06 | 1.13 | .006 | .011 | .37 | 1.78 | .03 | .02 | .02 | - | .02 | |

B Mechanical Properties

| Material and Heat Treatment | Yield Str., MPa | Tensile Str., MPa | Elong. % | Red. of Area % | 47 J Trans. Temp., C |
|---|---|---|---|---|---|
| A710 Plate | 602 | 673 | 29.9 | 78.3 | -145 |
| SR 2hr 620C | 573 | 640 | 29.9 | 79.4 | -147 |
| SR 10hr 620C | 542 | 610 | 30.0 | 78.5 | -148 |
| (ASTM Spec. | 515 | 585 | 20 | - | - |
| Weld Metal 1[1] | 535 | 615 | 26 | - | +8 |
| SR 8hr 620C | 515 | 609 | 26 | - | - |
| Weld Metal 2 | 595 | 665 | 23 | - | -58 |

1. As welded, flux cored electrode, AWS 5.20 E70 T1, typical composition and properties. Transition temperature measured as welded at 2 KJ/mm.

2. As welded, flux cored electrode, AWS 5.29 E91 T1-K2, typical properties. Transition temperature measured as welded at 1.8 KJ/mm

Table 2. Results of the Strain Aging Study on A710 Grade A Class 3 Plate

| Condition | 47J Transition Temperature, C | Shift in Transition Temperature, C |
|---|---|---|
| As received plate | -145 | - |
| Stress relieved 2hr 620C | -147 | -2 |
| Stress relieved 10hr 620C | -148 | -3 |
| Prestrained | | |
| As strained 5% | -113 | 32 |
| Strained and aged 10hr 370C | -113 | 32 |
| Strained, aged, stress relieved | | |
| Stress relieved 2hr 620C | -131 | 14 |
| Stress relieved 10hr 620C | -127 | 18 |

Table 3. Summarized Charpy Impact Test Results Foor Heat Affected Zone and Weld Metal Studies on A710 Grade A Class 3 Weldments

| Material | Heat Input KJ/mm | Post Weld Heat Treat. 620C, hr | 47 J Trans. Temp., C | Shift in Trans Temp[1], C |
|---|---|---|---|---|
| Base Plate | none | none | -145 | none |
| | none | 2 | -147 | -2 |
| | none | 10 | -148 | -3 |
| Heat Affected Zone | 1.8 | none | -78 | 67 |
| | 1.8 | 2 | -60 | 85 |
| | 1.8 | 10 | -97 | 48 |
| | 2.0 | none | -78 | 67 |
| | 2.0 | 2 | -59 | 86 |
| | 2.0 | 10 | -75 | 70 |
| | 4.0 | none | -55 | 90 |
| | 4.0[2] | none | -55 | 90 |
| | 5.3 | none | -33 | 112 |
| | 5.3 | 10 | -44 | 101 |
| Weld Metal 1 | 2.0 | none | 8 | - |
| Weld Metal 2 | 1.8 | none | -58 | - |
| | 5.3 | none | -18 | - |

1. Shift from base metal without stress relief.

2. Test of SAW weld HAZ in same base plate

Table 4. Shifts in Transition Temperature Between Plate and Heat Affected Zone for As-Welded A710 grade A and HSLA-80 Steels.

| Plate Type, Number and Thickness, mm | | Welding Process | Heat input KJ/mm | Shift in Transition Temperature, C |
|---|---|---|---|---|
| A710 (1) | 9.5 | SAW | 1.0 | 3 |
| | | | 2.0 | 24 |
| | | | 3.0 | 40 |
| A710 (2) | 19.1 | FCAW | 3.0 | 24 |
| A710 (3) | 19.1 | SAW | 2.0 | 27 |
| | | | 3.0 | 26 |
| | | | 4.9 | 85 |
| A710 (4) | 57.2 | SMAW | 1.8 | 16 |
| | | | 1.8 | 11 |
| A710 (5) | 63.5 | SAW | 3.0 | 10 |
| | | | 4.9 | 34 |
| HSLA-80 (1) | 15.8 | SAW | 1.3 | 27 |
| | | SMAW | 1.7 | 25 |
| | | SMAW | 3.3 | 26 |
| | | SAW | 3.9 | 25 |
| HSLA-80 (2) | 15.8 | GMAW | 2.0 | 11 |
| HSLA-80 (3) | 19.1 | SAW | 1.2 | 42 |
| | | FCAW | 1.2 | 29 |
| | | SMAW | 1.8 | 44 |
| | | SMAW | 3.9 | 26 |

Table 5. Shifts in Simulated Heat Affected Zone Transition Temperature for Various Heat Inputs in HSLA Steel[1]

| Simulated Heat Input, KJ/mm | Cooling Time $T_{800-500}$, S | Hardness DPH | Shift[2] in Transition Temperature, C |
|---|---|---|---|
| 1 | 5 | 316 | - |
| 2 | 11 | 288 | 50 |
| 3 | 25 | 275 | 87 |
| 4 | 45 | 247 | 114 |

1. From reference 7

2. Basis for comparison is 1 KJ/mm heat input samples. Plate thickness not specified but estimated from cooling rates to be about 25 mm

Table 6. Results of Stress Relief Cracking Tests Using the Modified Lehigh Restraint Specimen on A710 Grade A Class 3 Plate[1]

| Post Weld Heat Treatment Conditions | | Total Crack Height |
|---|---|---|
| Temperature, C | Duration, hr | mm |
| 482 | 2 | 0.10 |
| 510 | 2 | 0.00 |
| | 10 | 1.02 |
| 537 | 2 | 0.51 |
| 565 | 2 | 0.00 |
| 593 | 2 | 0.00 |
| | 10 | 0.20 |
| 607 | 0.25 | 0.76 |
| | 2 | 0.51[2] |
| | 2 | 1.27[3] |

1. E110 T5-K4 flux cored filler metal used to overmatch the strength of the plate for most welds.

2. Lower strength E8018-C1 shielded metal arc electrode used.

3. Two cracks at weld root, one on each side.

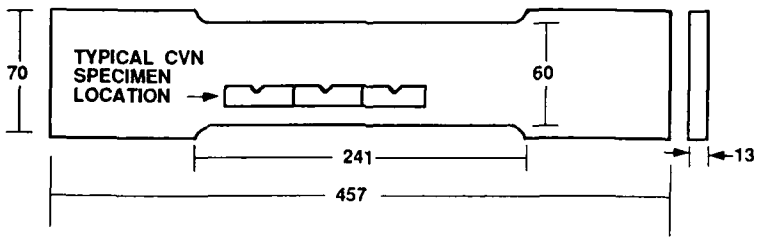


Fig. 1. Specimen configuration used in the strain aging study.

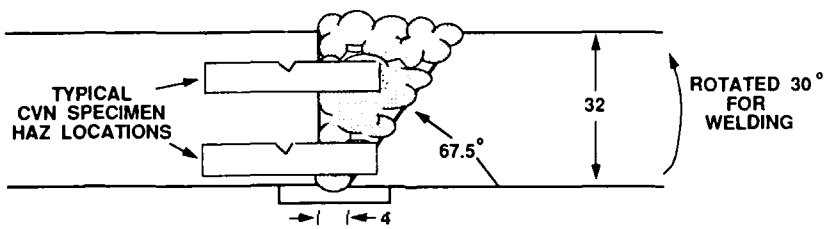


Fig. 2. Weldment configuration and specimen location for the heat affected zone study.

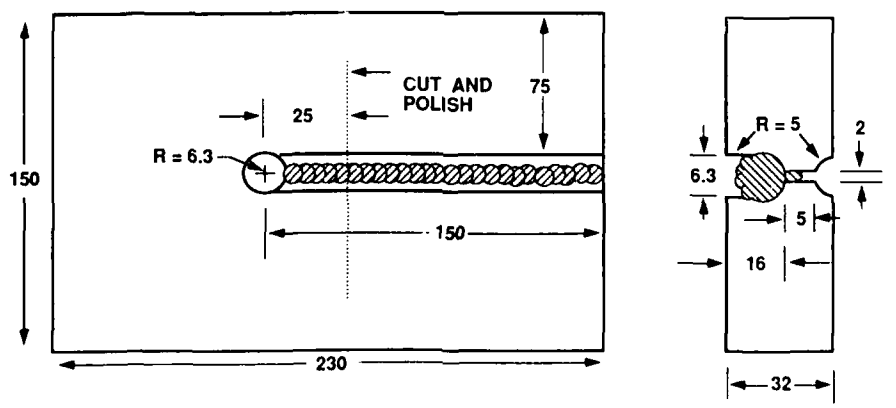


Fig. 3. Modified Lehigh Restraint Specimen for stress relief cracking tests.

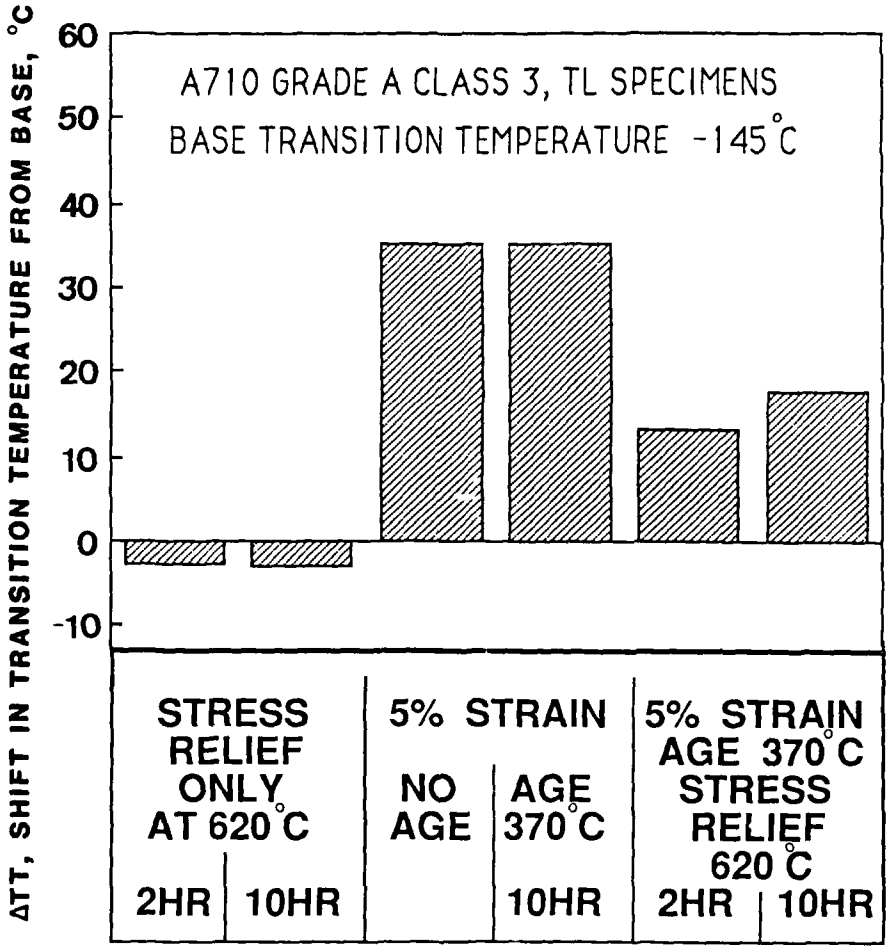


Fig. 4. Results of strain aging tests on A710 Grade A Class 3 plate.

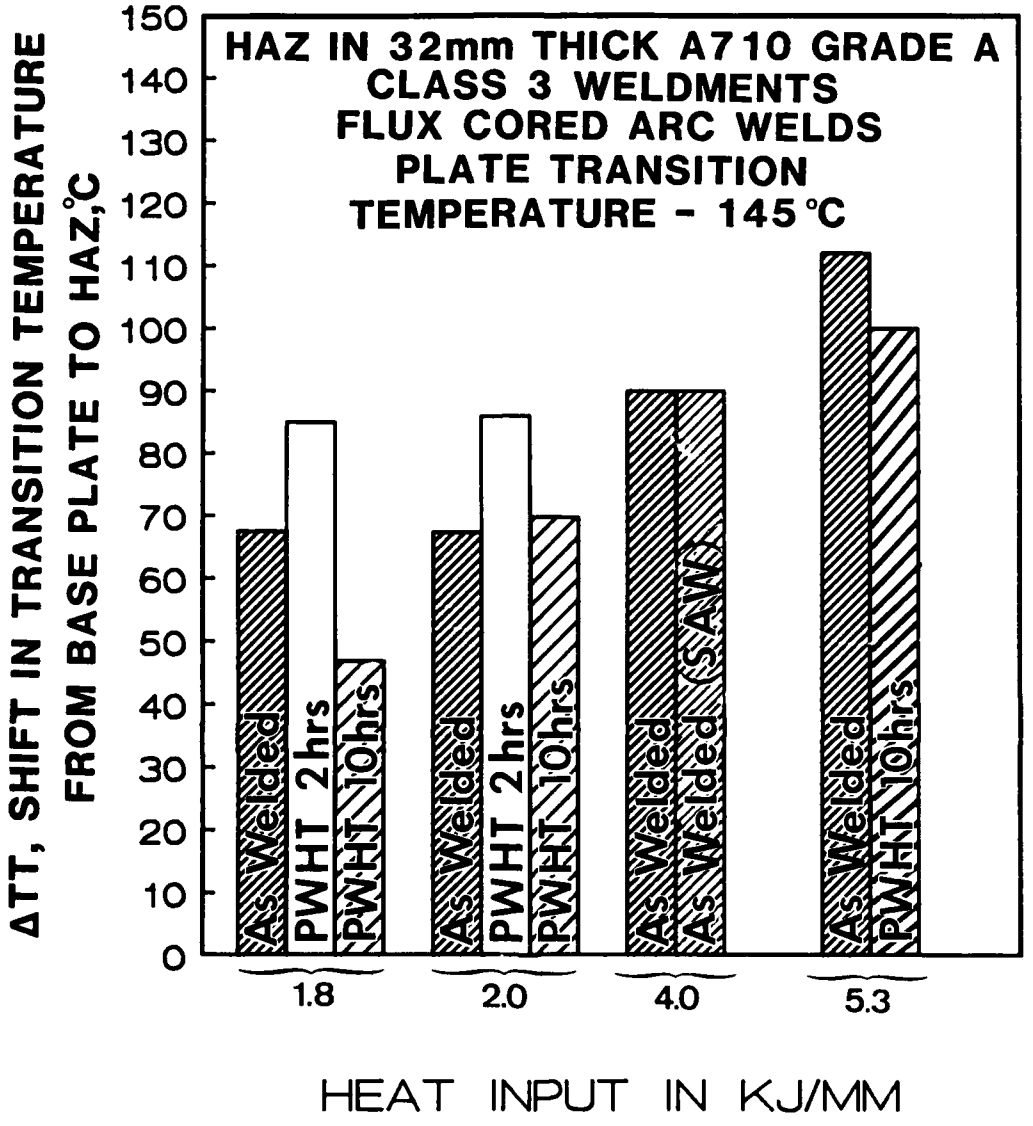


Fig. 5. Results of heat affected zone tests on A710 Grade A Class 3 weldments.

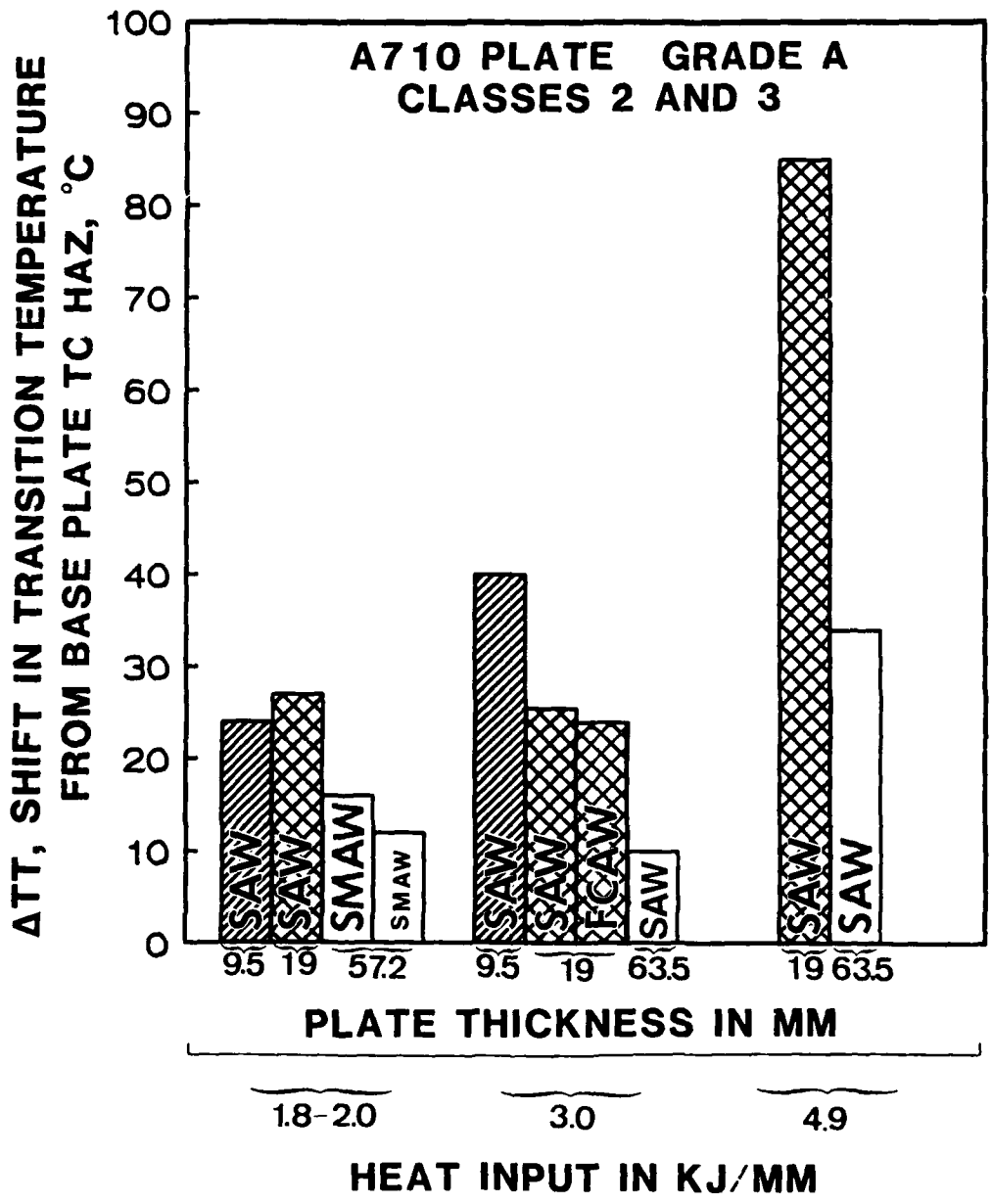


Fig. 6. Literature data on the effect of heat input and plate thickness on HAZ toughness in A710 weldments.

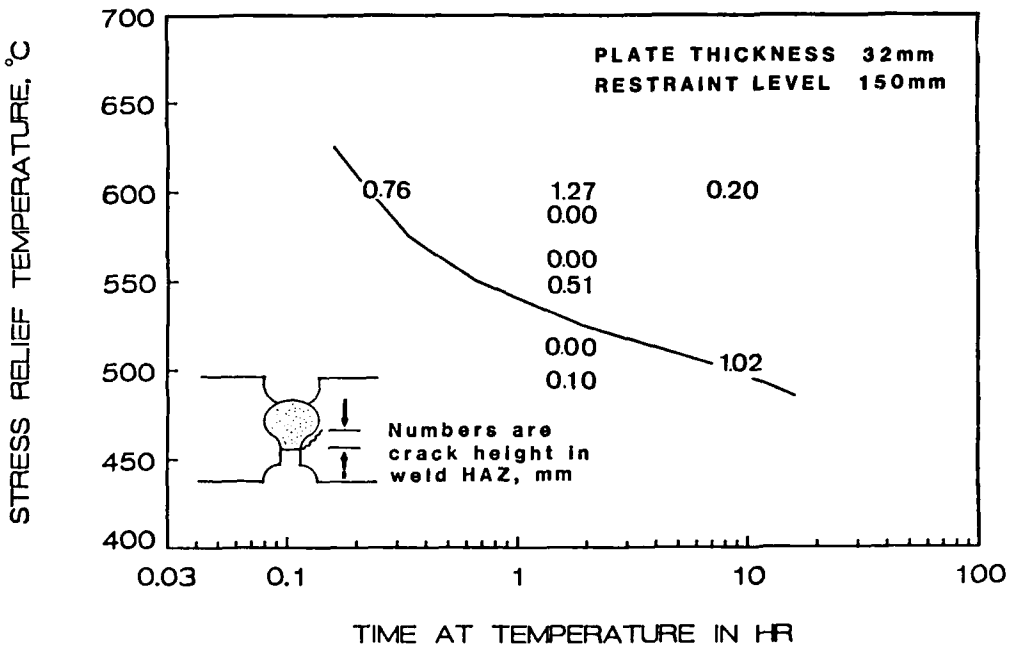


Fig. 7. Results of stress relief cracking tests on A710 Grade A Class 3 plate.

# STRUCTURE AND PROPERTIES OF ULCB PLATE STEELS FOR HEAVY SECTION APPLICATIONS

**C. I. Garcia, A. J. DeArdo**
Basic Metals Processing Research Institute
Department of Materials Science and Engineering
University of Pittsburgh
Pittsburgh, Pennsylvania, USA

STRUCTURE AND PROPERTIES OF ULCB PLATE STEELS FOR HEAVY SECTION APPLICATIONS

by

C.I. Garcia and A.J. DeArdo

Basic Metals Processing Research Institute
Department of Materials Science and Engineering
University of Pittsburgh

## ABSTRACT

Traditionally, steels used in heavy-section applications have been heat treated low-alloy steels. These normalized or quenched and tempered steels derive their strengths from their carbon contents. While carbon is a very efficient and cost-effective element for increasing strength in ferrite-pearlite or tempered martensitic structures, it is also, unfortunately, associated with poor notch toughness. Furthermore, it is well-recognized that both the weldability and weldment properties become increasingly deteriorated with carbon content, especially at high hardenability levels or carbon equivalent values. It is this difficulty in welding these traditional steels which leads to high fabrication costs. A new family of steels has recently been developed which can be used in the as-hot rolled condition, and which contain very low carbon levels. These new steels are the ultra-low carbon bainitic (ULCB) steels, and they derive their strength from dislocation and solid solution hardening. The ULCB steels exhibit excellent low temperature toughness which is a result of good austenite conditioning during hot rolling. The weldability and weldment properties of the ULCB steels are expected to be very good because of their low carbon content. The ULCB steels have been developed as candidates to possibly replace the HTS and HY steels currently used in U.S. Navy ship and submarine construction. This paper reviews the influence of composition on the Bs temperature and yield strength, and the influence of austenite conditioning on resistance to fracture.

**FOR SEVERAL DECADES**, two types of plate steels were available to the U.S. Navy for ship construction: The HTS steels and the HY steels[1]. The HTS steels are ferrite-pearlite steels of moderate strength (350 MPa) whereas the HY steels are used in the tempered martensite condition and exhibit high strength (560 MPa and 690 MPa). The HTS steels are C-Mn steels which rely on carbon for strength. The HY steels also rely on carbon for strength, and also contain alloying elements required for adequate hardenability. Both the HTS and the HY steels exhibit base plate properties which are adequate for their intended purposes. However, the HY steels suffer from poor weldability which is caused by both the high carbon content and high carbon equivalent values. It is well known that both the overall weldability and weldment toughness are inversely related to the carbon equivalent value, especially at high carbon contents. For this reason the weldability of HY steels has been and continues to be rather poor, Figure 1.

While the base plate properties are important when discussing the merits of a given plate steel, a potentially more important consideration may be the toughness of the heat-affected-zone (HAZ) in multi-pass welding operations. Recent work has revealed the importance of HAZ composition and microstructure on HAZ toughness, especially at low temperatures[2]. This study revealed the critical importance of the amount and size of martensite-austenite islands on the HAZ toughness, Figure 2. Hence, base plate steels which have high carbon and alloy contents have the potential for low HAZ toughness.

Both Figures 1 and 2 suggest the critical importance of low carbon contents in improving the weldability and weldment toughness in base plates. In an effort to reduce the welding costs and fabrication times, a series of new low-carbon steels have been developed. These new steels rely on strengthening mechanisms which are largely independent of carbon content, unlike the older heat treated ferrite-pearlite or martensitic plate steels. At the present time there are two versions of these new low carbon steels available. One family is known as HSLA-80 or -100 which is a copper precipitation strengthened steel. The second family is the ultra-low carbon bainitic (ULCB) steel. The ULCB steels derive their strengths from dislocation substructure and solid solution strengthening.

The present study summarizes a portion of the results of a research program being conducted at the Basic Metals Processing Research Institute of the University of Pittsburgh on the development of ULCB steels for ship and submarine construction. This paper will discuss the influences of austenite conditioning and alloy composition on base plate properties of 25 mm (1 in) thick hot rolled plates.

## EXPERIMENTAL PROCEDURE

The chemical composition (in wt%) of the steels used in this study is shown in Table I. Steels Nos. 1, 2 and 3 were vacuum melted, the other steels shown in Table I were air

induction melted. The ingot weight and size was 225 Kg (500 lbs) and 200 mm x 200 mm x 675 mm (8 in x 8 in x 27 in), respectively.

**MATERIALS PROCESSING** - To evaluate the influence of reheating temperature and thermomechanical processing on the microstructural conditioning of the austenite, steels 1, 2, 3 and 4 were subjected to the thermomechanical treatment illustrated in Figure 3. For all the steels used in this study, the amount of deformation during roughing and final rolling was maintained constant such that the final plate thickness was always the same, 25 mm (1 in).

The other steels (5, 6 and 7) were processed using optimum controlled-rolling practices such as the one illustrated in Figure 3c.

The effect of tempering treatments on the mechanical properties of the as-hot rolled ULCB steels was also investigated. The steel samples were tempered for one hour in the temperature range of 500-675°C (1022-1247°F) and then air cooled to room temperature.

**MECHANICAL PROPERTIES** - The mechanical properties of all the steels in both the as-hot rolled and tempered conditions were determined using standard procedures. The tensile properties were determined in sub-size flat tensile specimens with a 25.4 mm (1 in) gage length. The specimens were cut transverse to the rolling direction. In addition, impact properties were obtained from full size Charpy V-notch specimens. The notch of the specimens was perpendicular to the rolling plane (T-L orientation).

**MICROSTRUCTURAL PARAMETERS** - The overall microstructure of the steels after both reheating and thermomechanical processing was evaluated using standard metallographic procedures. In addition, the stereological parameters of the non-metallic inclusions present in the steels were determined using a computer controlled Bioquant System IV image analyzer.

## RESULTS AND DISCUSSION

All of the steels used in this study were designed to achieve a fully bainitic structure in the as-hot rolled condition in 25 mm (1 in.) thick plates. As expected, the reheating temperature and thermomechanical treatment used have a strong influence on the final microstructure and consequently on the final properties for a given steel composition.

**EFFECT OF REHEATING TEMPERATURE** - The effect of reheating temperature on the austenite grain size is illustrated in Figure 4. This figure shows the typical microstructural response of as-cast ULCB steels with Ti (steel 1) and without Ti additions (steel 2) after reheating at 1150°C and 1250°C for 1 hour. A comparison of the optical micrographs shown in Figure 4 reveals that the average grain size of the Ti-bearing steels is finer than the average grain size in the steels without Ti additions for a given reheating temperature. For example, the average austenite grain size in the Ti-bearing steel was 30 $\mu$m after reheating at 1150°C and 33 $\mu$m after reheating at 1250°C, whereas the Ti-free steel showed grain sizes of 35 and 220 $\mu$m at the same temperatures. However, a close examination of the grain size distribution of the ULCB steel with Ti additions shows a non-uniform distribution (see Figs. 4a and 4b). In the case of the ULCB steel without Ti additions, the grain size distribution was large but uniform at the high reheating temperatures (i.e. 1250°C), see Figure 4d. The importance of having a uniform grain size distribution prior to thermomechanical processing (TMP) is essential, since the proper response of austenite to TMP is strongly related to the uniformity of the as-reheated grain size prior to roughing. The influence of the metallurgical condition of the as-reheated structure to thermomechanical processing (e.g. Figure 3c) is illustrated in Figure 5.

The microstructure of the austenite in the Ti-free steel (steel 2) after reheating to 1250°C, rough rolling and then reheating to 950°C is shown in Figure 5a. After the controlled rolling finishing passes (schedule 3C), a uniform pancaked austenite microstructure results, Fig. 5b. By comparison, Fig. 5c shows the final austenite microstructure in the Ti-bearing steel. The heterogeneous final austenite microstructure exhibited in Fig. 5c is caused by the non-uniform microstructure which resulted from the initial reheating at 1250°C in this steel, Fig. 4a.

Figures 4 and 5 illustrate an important principle which is central to attaining proper TMP; neither roughing nor finishing rolling can eliminate heterogeneities in grain sizes which originate in the initial as-reheated austenite microstructure. It is well-recognized in ferrite-pearlite steels that the final, transformed microstructure is a reflection of final, rolled austenite microstructure and heterogeneities in the microstructure of the final rolled austenite will cause similar non-uniformities in the final transformed microstructure. The presence of mixed grain sizes in ferrite-pearlite steels has been shown to be responsible for a deterioration in resistance to low temperature brittle fracture[3]. In bainitic steels, the resistance to brittle fracture is controlled to a large extent by the size, shape and uniformity of the final, rolled austenite microstructure. Good resistance to low temperature toughness is promoted by the presence of a uniform distribution of fine austenite grains. This relationship will be discussed below.

**INFLUENCE OF COMPOSITION ON STRENGTH** - The tensile properties of steels No. 1 through 7 are shown in Table II. The results indicate that the strength of ULCB steels can be controlled and optimized by a careful control of the composition. That is, the steel composition controls the Bs temperature which in turn controls the strength of ULCB steels. The relationship between the measured strength and the measured Bs temperature is illustrated in Figure 6. Figure 6, shows a linear relationship between the measured strength and the measured Bs temperature. A comparison of the results obtained in the present investigation (Figure 6) with the data from Pickering[4] and Coldren[5] is shown in Figure 7. In addition, in this figure are shown tensile strength values calculated using Pickering's equation[3] for some of the steels used in this study. A comparison of the results between the measured and calculated strength values of the ULCB steels shows a large difference in strength for a given Bs temperature. There are two possible explanations for the large difference observed. First, the Bs temperature used in the Pickering study corresponded to the temperature at 50% transformation whereas the Bs used in the present study corresponded to the 15% transformation temperature. Second, the carbon content used in the Pickering study was near 0.1%, or approximately 5 times higher than that used in the present study.

In Figure 7 is also shown a comparison of the results obtained by Coldren et. al.[4] and the results of the present study. The Bs temperature used in both experiments was defined at 15% transformation. It is clear that the two studies have observed different temperature dependences of the yield strength. For example, Coldren et. al. found that the Y.S. increased by 1.89 MPa/°C whereas the present study found an increase of 3.39 MPa/°C. The difference in behavior observed in the two studies is most likely caused by differences in the way in which the Bs temperatures were varied. In the Coldren et. al. study, the Bs temperature was varied principally by altering the cooling rate. In the present study, the changes in Bs temperatures were obtained through variations in steel composition, hence, the larger increases in strength observed in the ULCB steels for a given Bs temperature are most likely due to solid solution effects.

In summary, it has been shown that bainitic steels can exhibit yield strengths in the range of 700-900 MPa (100-130 ksi) in 25 mm (1 in) thick hot rolled plates. Since the strength of these steels varies with the Bs temperature, the strength

observed in these steel can be simply related to their composition.

**INFLUENCE OF MO AND B ON YIELD STRENGTH** - The effect of increasing Mo additions to ULCB steels is illustrated in Table III. As expected, the yield and tensile strength increased with higher Mo contents. From the results shown in Table III, it is important to notice that the combined effect of Mo and B appears to affect only the yield strength of the steels. The ultimate tensile strength does not seem to be markedly affected by the presence or absence of B. The correlation between the yield and tensile strength behavior observed in the ULCB steels with the presence or absence of B for a given Mo content is shown in Figure 8. This figure also shows the excellent linear relationship between the measured Bs temperature and the measured strength of the steels.

**INFLUENCE OF THERMOMECHANICAL PROCESSING ON THE NOTCH TOUGHNESS OF ULCB STEELS** - It is well known that the strength of bainitic steels varies inversely with the Bs temperature. Furthermore, the Bs temperature is also known to vary linearly with composition. However, in most of the early work published in the literature, the parent phase was in the fully recrystallized condition prior to transformation. This resulted in an inverse relationship between strength and resistance to brittle fracture[6]. The results of the present study have shown that austenite conditioning can have a dramatic effect on the Bs temperature and, therefore, also on strength, Table IV. However, the major influence of austenite conditioning was in improving the resistance to brittle fracture. The impact toughness behavior of ULCB steels is shown in Figure 9. The results from this figure clearly show the excellent combination of strength and toughness exhibited by the ULCB steels in the as-hot rolled condition. The steels shown in Figure 9 surpassed the impact energy of 47 Joules (35 ft-lbs) at -85°C (-120°F) that is required by the U.S. Navy for ship construction applications.

The beneficial effects of a well designed and processed steel in terms of the overall package of mechanical properties are shown in Table V. This table shows the effects of austenite conditioning (i.e. $S_v$, the effective interfacial area per unit volume), the total projected inclusion length per unit area ($\Sigma b$) and yield strength on the fracture appearance transition temperature ($FATT_{50\%}$) and on the upper-shelf energy (USE) of the ULCB steels investigated in this program. The effectiveness of austenite conditioning is usually described by the parameter $S_v$[7], which encompasses internal surface/volume effects originating from grain boundaries, deformation bands and incoherent twins. The $S_v$ shown in Table V has been calculated from the equivalent grain diameter $D_\gamma$ and includes only contributions from grain boundaries. In general, well conditioned austenite is described by $S_v$ values in excess of about 150 $mm^{-1}$.

As expected, the results shown in Table V clearly indicate that the overall package of properties exhibited by bainitic steels can be dramatically improved by proper austenite conditioning. For example, a comparison between steels 1 and 4 with similar yield strength, reveals that steel 1 which has an average austenite grain size of 87.3 $\mu$m had a $FATT_{50\%}$ of 0°C, whereas steel 4 with an austenite grain size of 33.2 $\mu$m had a $FATT_{50\%}$ of -68°C. This represents an improvement of -68°C in low temperature impact toughness due to the microstructural refinement of austenite.

Another microstructural feature which is known to influence both ductile and brittle fracture is the non-metallic inclusions or steel cleanliness. In general, the resistance to both ductile and brittle fracture is improved with increased steel cleanliness. The cleanliness of a given steel can be assessed in several ways, including the parameter $\Sigma b$, or total projected length[8]. A good assessment of the influences of cleanliness and austenite grain size on the USE and the FATT is shown in Table V for steels 1, 4 and 7.

## EFFECT OF TEMPERING TEMPERATURE ON STRENGTH AND TOUGHNESS

As hot rolled plates are often tempered or aged after rolling. For example, tempering may be intentionally used to improve the base plate properties of a given steel. On the other hand, tempering may be unintentional, e.g. during the stress-relief annealing of weldments. In either event, it is important to know how the base plates will respond to tempering.

The behavior of as-rolled ULCB steels to aging treatments is presented in Figure 10. The results from this figure show that ULCB steels have basically a two stage response to tempering treatments. In the first stage, the ULCB steels appear to be fairly insensitive to tempering treatment when tempered below about 550°C. The second stage results in overall softening. During low temperature tempering, the yield strength increases slightly with higher temperature. However, the overall strength level in this stage is controlled by the Mo content. During the softening stage of tempering, the strength does not appear to be strongly influenced by the Mo level. Furthermore, the transition between the two stages of tempering appears to be inversely related to the Mo content. For example, the transition for steel 6 (3.05 Mo) is near 550°C whereas it is near 580°C for steel 4 (1.76 Mo). The behavior shown in Figure 10 is indicative of complex strengthening mechanisms involving dislocation, precipitation and solid solution hardening.

The major contribution of the tempering treatments was in the impact toughness behavior of ULCB steels. Figure 11 clearly shows the beneficial effect of tempering on the impact toughness of the steels. The results from Figure 11 illustrate that tempering not only increases the USE of the steel but also simultaneously increases the resistance to brittle fracture. The significant gain in impact toughness is realized without a decrease in strength due to tempering treatments. The above behavior can be explained in terms of two concomitant and offsetting events that take place during tempering. That is, the loss in strength due to dislocation annihilation and rearrangement is most likely balanced by the increase in strength due to the precipitation reactions. The increase in impact toughness is due to subgrain formation and elimination of stresses introduced during the bainitic transformation reaction.

## CONCLUSIONS

1. The strength of as-rolled ultra-low carbon bainitic steels can be controlled by the proper combination of alloy design and thermomechanical processing. The strength is controlled by the Bs temperature.
2. The strength of steels with a high Bs temperature is strongly sensitive to austenite conditioning, whereas the strength of steels with a low Bs temperature is less dependent on processing conditions.
3. The excellent impact toughness properties of the as-rolled ULCB steels were attained through proper microstructural refinement of the parent phase austenite.
4. Tempering of the as-rolled ULCB steels produces an additional increase in the impact toughness of the steels, without a significant decrease in strength.

## ACKNOWLEDGMENTS

The authors wish to thank Molycorp Incorporated a subsidiary of Unocal for providing the support for this study.

In addition, we would like to thank United States Steel, Division of U.S.X. Corporation for supplying the materials.

## REFERENCES

T.W. Montemarano, B.P. Sack, J.P. Gudas, M.G. Vassilaros and H.H. Vanderveldt, *Journal of Ship Production*, 2, No. 3, pp. 145-162 (August, 1986)

T. Haze and S. Achara, *Proceedings of Seventh International Conference on Offshore Mechanics and Arctic Engineering*, 7-12 February, 1988, Houston, Texas

H. Abrams and G.J. Roe, *Proceedings of MiCon 78: Optimization of Processing, Properties and Service Performance Through Microstructural Control*, ASTM STP 672, 3-5 April, 1978, Houston, Texas

F.B. Pickering, *Symposium: Transformation and Hardenability in Steels*, Climax Molybdenum Company of Michigan, Ann Arbor, Michigan, pp. 109-129 (1967)

A.P. Coldren, R.L. Cryderman and M. Semchyshen, *Symposium: Steel Strengthening Mechanisms*, Climax Molybdenum Company, Zurich, pp. 17-44 (1969)

K.J. Irvine and F.B. Pickering, *Journal of the Iron and Steel Institute*, 201, p. 518 (1963)

G.R. Speich, L.J. Cuddy, C.R. Gordon and A.J. DeArdo, *Phase Transformations in Ferrous Alloys*, A. Marder and J. Goldstein, Eds., TMS-AIME, Warrendale, PA (1984)

T.J. Baker and J.A. Charles, *Journal of the Iron and Steel Institute*, 210, p. 680 (1972)

**TABLE I, COMPOSITION (WT%) OF STEELS INVESTIGATED**

| # | STEEL | C | Mn | P | S | Cr | Ni | Mo | Nb | N | Ti | B |
|---|---|---|---|---|---|---|---|---|---|---|---|---|
| 1 | | .021 | .94 | .005 | .004 | -- | 1.41 | 1.49 | .052 | .006 | .016 | .001 |
| 2 | | .017 | 1.01 | .006 | .004 | -- | 3.15 | 3.02 | .055 | .001 | .013 | .0011 |
| 3 | | .018 | .51 | .002 | .003 | -- | 3.05 | 1.53 | .053 | .006 | .020 | .002 |
| 4 | | .024 | .95 | .002 | .002 | .48 | 3.54 | 1.76 | .050 | .009 | -- | -- |
| 5 | | .026 | .92 | .003 | .003 | .42 | 3.58 | 2.59 | .053 | .008 | -- | -- |
| 6 | | .027 | .95 | .008 | .002 | .45 | 3.63 | 3.05 | .055 | .007 | -- | -- |
| 7 | | .026 | 1.01 | .007 | .002 | .49 | 3.58 | 1.70 | .052 | .006 | -- | -- |

**TABLE II, TENSILE PROPERTIES OF STEELS INVESTIGATED**

| # | STEEL | YS MPa(ksi) | UTS MPa(ski) | $e_f^{(a)}$ % | RA % |
|---|---|---|---|---|---|
| 1 | | 750(109) | 883(128) | 18.3 | 63.2 |
| 2 | | 945(137) | 1073(156) | 15.7 | 65.1 |
| 3 | | 670(97) | 807(117) | 23.5 | 66.0 |
| 4 | | 752(109) | 924(134) | 19.2 | 61.8 |
| 5 | | 779(113) | 972(141) | 15.9 | 58.2 |
| 6 | | 834(121) | 1027(149) | 16.0 | 61.3 |
| 7 | | 745(108) | 917(133) | 18.3 | 67.4 |

(a) 25.4 mm (1 in) gage length

**TABLE III, INFLUENCE OF Mo AND B ON TENSILE PROPERTIES**

| # STEEL | YS MPa(ksi) | UTS MPa(ksi) | $e_l^{(a)}$ % | RA % |
|---|---|---|---|---|
| 1 | 750(109) | 883(128) | 18.3 | 63.2 |
| 2 | 903(131) | 979(142) | 16.0 | 60.7 |
| 5 | 800(116) | 986(143) | 16.1 | 55.6 |
| 6 | 834(121) | 1027(149) | 15.8 | 60.5 |
| 7 | 745(108) | 917(133) | 18.3 | 67.3 |

(a) 25.4 mm (1 in) gage length

**TABLE IV, INFLUENCE OF AUSTENITE DEFORMATION BELOW RECRYSTALLIZATION TEMPERATURE ON Bs TEMPERATURE**

| | Bs Temperature (°C) at Indicated Deformation | | | | |
|---|---|---|---|---|---|
| # STEEL | 0% | 20% | 50% | $Bs_{(20\%)}-Bs_{(0\%)}$ | $Bs_{(50\%)}- Bs_{(0\%)}$ |
| 1 | 590 | 608 | 614 | 18 | 24 |
| 4 | 540 | 553 | 552 | 13 | 12 |
| 5 | 504 | 497 | 493 | -7 | -11 |
| 7 | 564 | 562 | 569 | -2 | 5 |

**TABLE V, COMPARISON OF QUANTITATIVE PARAMETERS OF AUSTENITE GRAIN SIZE AND INCLUSIONS WITH MECHANICAL PROPERTIES OF STEELS TESTED**

| # STEEL | YS MPa(ksi) | $S_V$ $mm^{-1}$ | $\Sigma b$ $\mu m/mm^2$ | USE J(ft-lb) | $FATT_{(50\%)}$ °C |
|---|---|---|---|---|---|
| 1 | 750(109) | 69 | 1054 | 80(59) | 0 |
| 2 | 945(137) | 93 | 432 | 83(61) | -15 |
| 3 | 690(100) | 114 | 676 | 111(82) | -50 |
| 4 | 752(109) | 179 | 390 | 127(94) | -68 |
| 5 | 800(116) | 256 | 1416 | 81(60) | -55 |
| 6 | 834(121) | 209 | 339 | 115(85) | -48 |
| 7 | 745(108) | 221 | 243 | 153(113) | -75 |

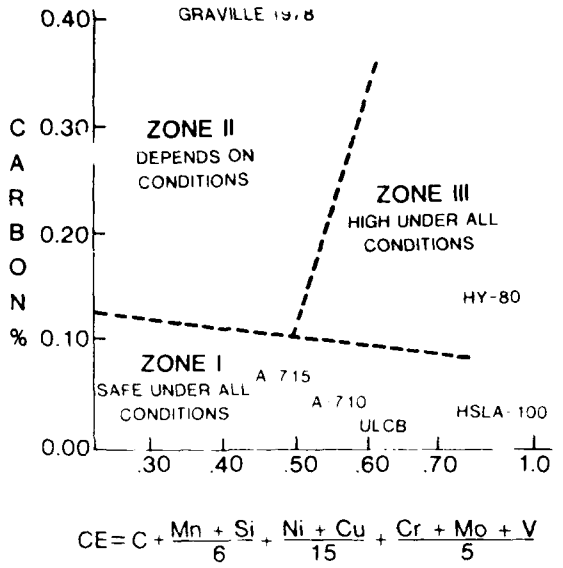


**Figure 1. Susceptibility to heat affected zone cracking.**

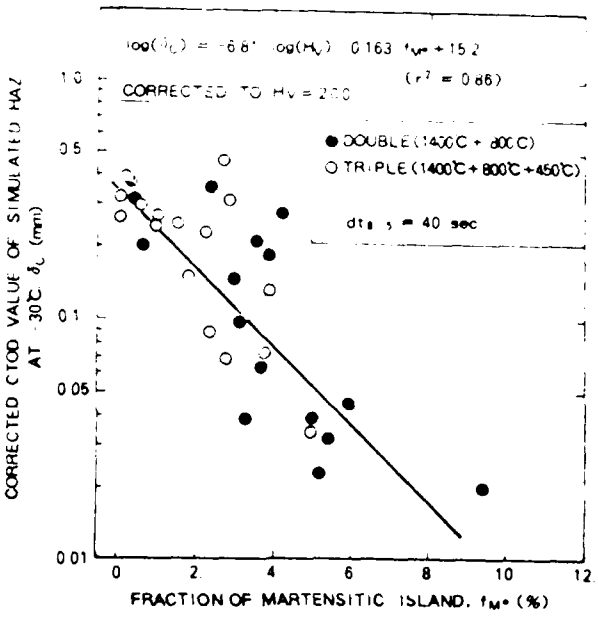


**Figure 2. Relation between CTOD value and fraction of martensitic islands of simulated HAZ[2].**

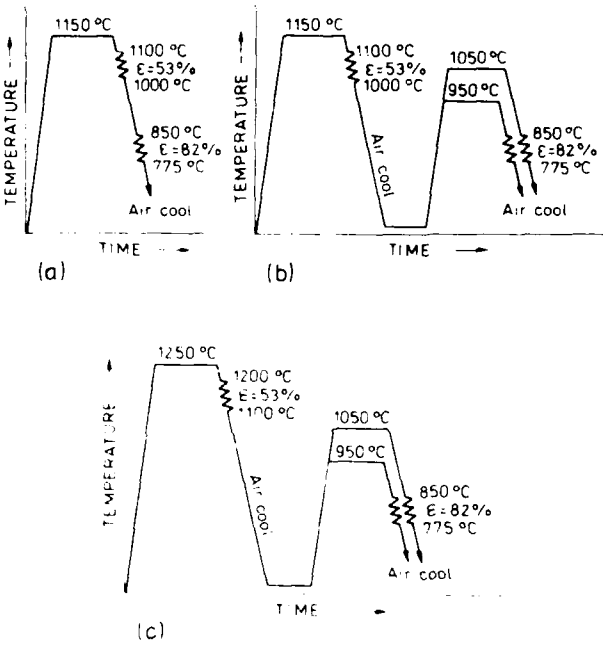


**Figure 3. TMP of ULCB steels.**


Figure 4. Optical micrographs of as-cast ULCB steels: a) Ti-bearing steel reheated at 1150°C, b) reheated at 1250°C, c) without Ti, reheated at 1150°C and d) reheated at 1250°C.

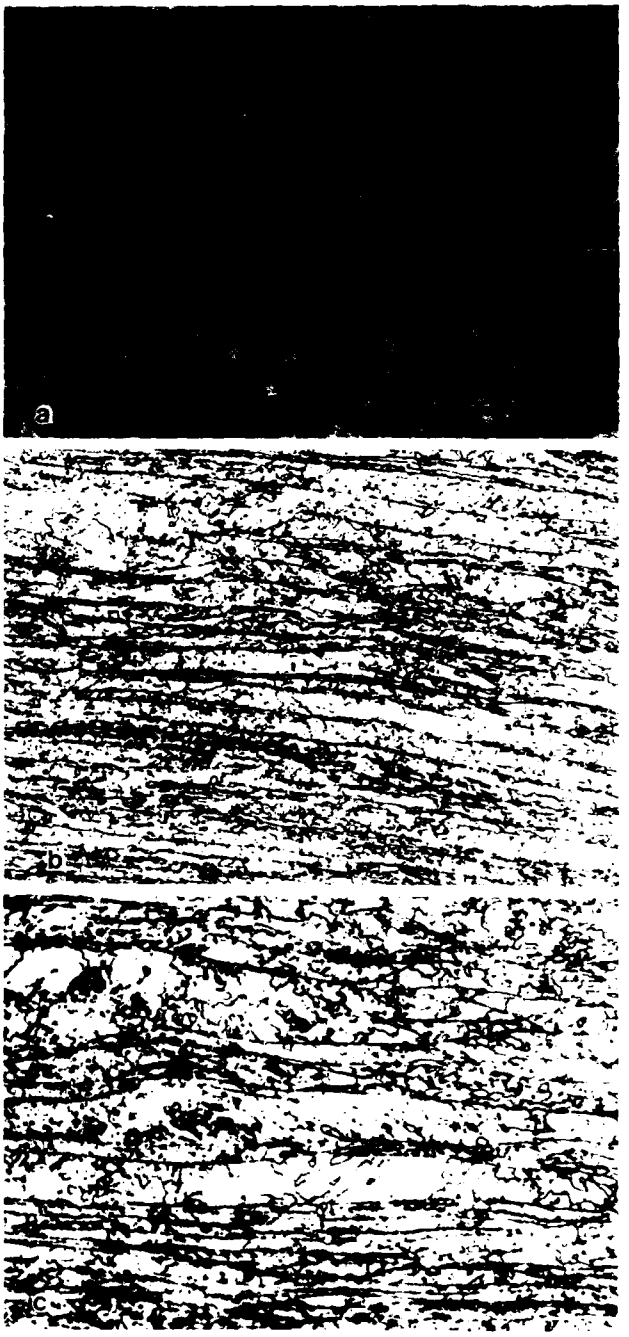


Figure 5. Optical micrographs of ULCB steels after reheating and final rolling: a) as-reheated at 950°C prior to final rolling (steel 4), b) uniform microstructure of well conditioned austenite, and c) microstructure of non-uniform austenite grains.

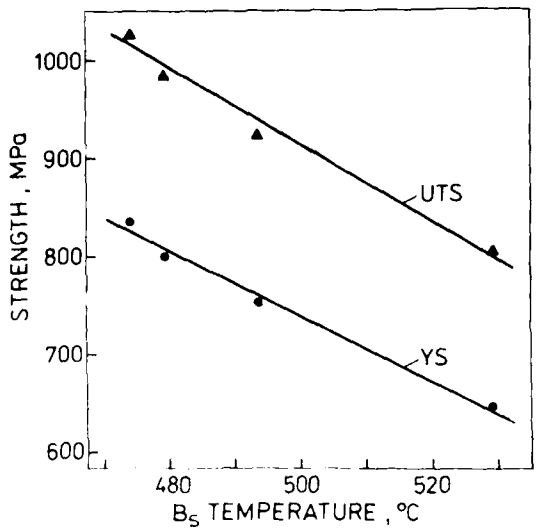


Figure 6. Relationship between measured Bs temperature and measured strength of ULCB steels.

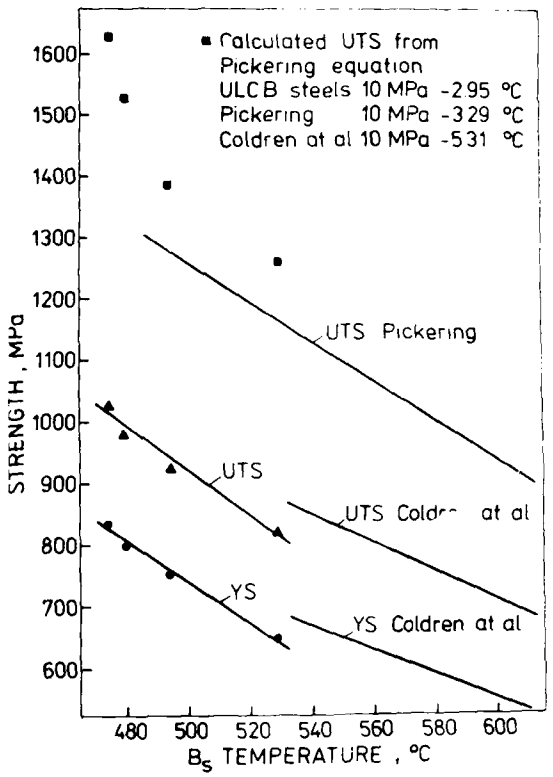


Figure 7. Comparison of measured versus calculated strength values for a given Bs temperature.

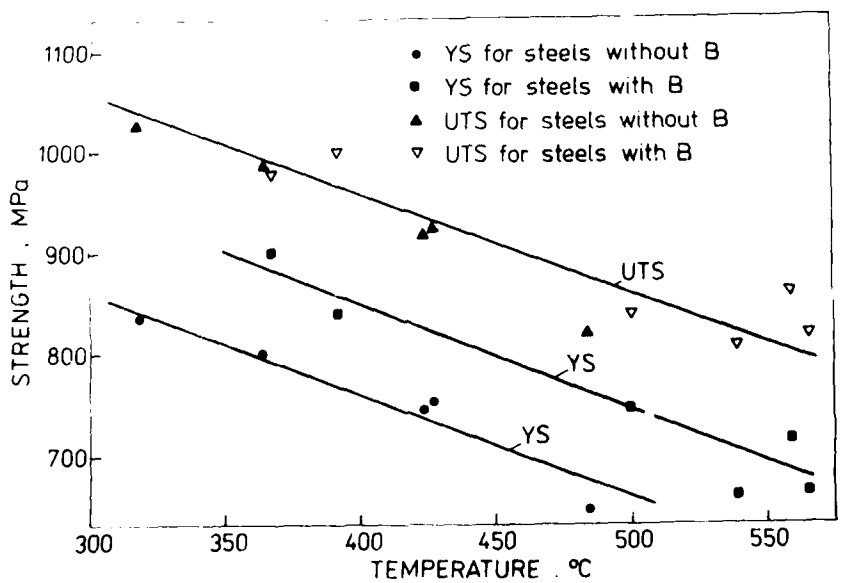


Figure 8. Influence of B on the strength of ULCB steels.

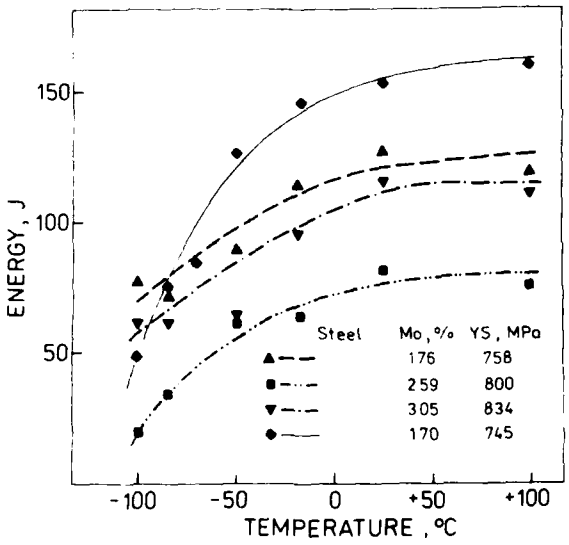


Figure 9. Impact toughness of as-hot rolled ULCB steels.

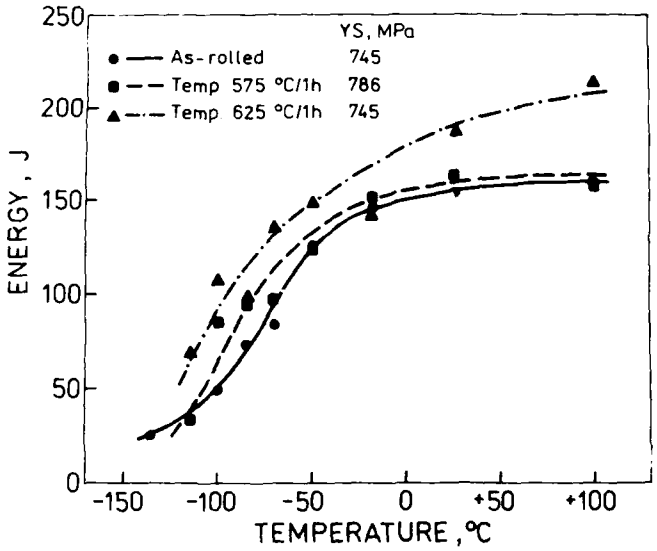


Figure 11. Comparison of impact toughness between as-hot rolled and as-tempered ULCB steels.

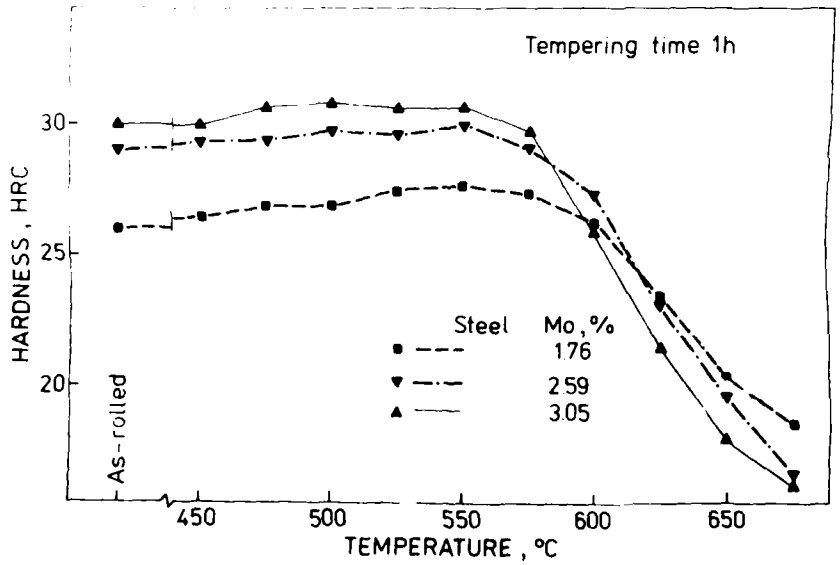


Figure 10. Tempering behavior of ULCB steels.

# THE BEHAVIOR OF V-N HSLA STEEL IN MANUFACTURE OF SPHERICAL PRESSURE VESSEL

**W. Y. Zhou, Z. Q. Lu, G. M. Cao**
Chinese Society of Metals
Beijing, P.R.China

ABSTRACT

Performance of 15MnVN steel after cold forming, its weldability and properties resulting from heat treatment after welding for relieving residual stress were comprehensively and systematically studied. Reliability of gas storing spherical pressure vessel made of this steel was analysed. The experimental result show up the influences of the manufacture process during cold forming, welding and heat treatment on mechanical properties and micro-structure of the steel and welded joints, as well as the degree of influence to which changes in properties would give on the manufacture of the spherical vessel and safety in service. Methods to avoid embrittlement and to improve reliability for application are proposed by the authors.

The V-N ferrite high strength low alloy steel (15MnVN),which was developed in the 1970s, with it's $\sigma_s \geq 441$MPa (45Kg·f/mm$^2$), $\sigma_b \geq 592$MPa (60Kg·f/mm$^2$) in the normalized condition, has been used in manufacture of gas storing spherical pressure vessel under a pressure of 2.94MPa 30Kg·f/cm$^2$). Because of its higher strength than the C-Mn series of steel commonly used in our country, the thickness of the vessel wall made of this steel plate can therefore be reduced. According to designning calculation, the wall thickness of a pherical vessel with diameter 9.2m may be reduced from 50mm to 42mm. Due to the reduce of the wall thickness, 16% of material may be saved and the productivity raised greatly. The 15MnVN steel has a better ductility and toughness, and the brittleness transformation temperature is lower. In a large number of tests on the properties of the steel, weldability and low temperature simulative explosion, it was shown that the 15MnVN steel can satisfy the service requirements on the gas storing spherical pressure vessel, but the yield stress and impact toughness of this steel were lowered during the manufacture of the sphere shell due to the cold forging formation. On welding, a marked tendency to cold cracking appered for the higher carbon equivalent. If a great heat in-put was applied, the coarse grained region in HAZ would be more brittle. A slight brittleness occured near the fusion line of welds when relieving residual stress after welding.

15MnVN steel is a C-Mn type high strength low alloy fine grained steel, it is strengthed and fine grained by the precipitation of such alloying elements as nitrogen, vanadium, aluminium. The typical chemical composition and mechanical properties are listed in table 1 and 2.

In order to test the reliability of spherical pressure vessel made of 15MnVN steel, the characteristics of the steel after cold forging and its weldability, as well as the influences of heat treatment for relieving residual stress after welding on the performance of the welded joints were researched by Central Research Institute of Building and Construction of M.M.I.

## 1. The Influence of Cold Forming on the Characteristics of 15MnVN Steel

The cold forming process has been widely applied in fabricating the shell of gas storing spherical vessel. For various volumes of spheres, the diameters of sphere range from 4.6 to 12.3m. The cold forming process may cause plastic deformation in steel. G.M.CAO etc investigated the influences of the cold forming and strain aging on the characteristics of 15MnVN steel. Because the value of the plastic deformation rate ($\varepsilon$) varies with the radius of curvature and thickness of the shell it can therefore be calculated using the following formula:

$$\varepsilon = \frac{75s}{R}\left(1 - \frac{R}{R_d}\right)\%$$

where, $R_d$- Original radius of curvature of gravity center layer;
R - Designed radius;
s - Thickness of plate.

None of the values of so calculated for a sphere of 4.6-12.3m in diameter, made of plate 24-50mm in thickness exceeded 1.1%, but in fact, the distribution of the actual deformation rates ($\varepsilon$) in different locations of the plate are heterogeneous during the cold forming of the sphere shell. The degree of heterogeneity changes depending on the method of forming and dimensions of the sphere section. According to the authors' practical measurements of $\varepsilon$ on equatorial zone on the sphere of 9.2m diameter in 44mm plate thickness deformed by cold forming,a maximum deformation rate of 1.1% was demonstrated at the external surface of the shell, much higher than the calculated value (0.7%), and its location was at the central region of the external surface along the long side direction. But a minimum deformation rate was found to be only 0.15% at the edge of the external surface of the shell along the short side direction. It can be seen that the distribution law of deformation rates at external surface of sphere shell (as shown in Fig.1) would be: the most heaviily de-

formed at the center and becoming less and less deformed towards the edge. The deformation on the internal surface of sphere shell was all of a compressively strained nature except the central region showing a strain under tension. With a deformation distribution curve along the long edge of the plate that showed a low deformation rate at the center which gradually became higher when being farther away from it. On all cases, the absolute value of deformation rate on internal surface was smaller than that on the external and was determined as -0.75% max. The curve of deformation rates measured and the polar temperature zone shows a distribution and type of deformation basically similar to those of the quatorial zone with strain under tension at the external surface while strain under compression at the internal surface and the absolute values of the two types being basically the same, e.g. The maximum 0.75% and the minimum 0.15%. Obviously the deformation rate of a sphere shell in diameter of less than 9.2m should be larger than that of the sphere in 9.2m diameter. Besides the measured values may possibly be larger than the calculated ones. Guided by this analysis, the sample with compressive deformation rates of 0.5%, 1.5% and 2.5% were selected to tensile tests and the samples with tensile deformation rates pf 1%, 3%, 5% to impact tests, drop weight tests and aging tests at 250°C for 1 h. In addition, samples were taken by machining for impact tests from both the internal and external surface layers which had been undergone tensile or compressive deformation respectively.

The test results are shown as the curves in Fig.2. It indicates that no obvious changes are seen on $\delta$, $\Psi$, $\sigma_b$ values within the tested range for compressive cold forming and that an influence of the compressive deformation on $\sigma_s$ did exist. When the compressive deformation rate increases, the $\sigma_s$ value decreases gradually from 485MPa to 355MPa at a point corresponding to the deformation rate of -1.5%, a drop of 27%.

To verify the above test results, samples were machin-taken from the central region of internal surface at polar temperature zone of the sphere shell. The results from those samples showed obvious dropping of $\sigma_s$ from 500MPa at the initial condition to 441 MPa, a decrease by 12%.

For samples deformed by tension and compression, the decrease of impact toughness at room temperature was more obvious when at the deformation rate of 1% (see Fig.3) and did not change much as the deformation rate further increased. Only after an aging at 250°C for 1 h, did the increase of tensile or compressive deformation rate cause a declining trend of impact toughness (see Fig.4).

The influence of tensile or compressive deformation on the hardness is completely the same as on impact toughness (see Fig.5).

The results of drop weight tests suggested that when the deformation rate was 1% in 36mm thickness of sphere shell, the non-toughness transition temperature NDT was increased by 5°C from the original 30°C at the initial state.

From the above experiments it can be seen that the $\sigma_s$, $C_v$ and NDT show remarkable decrease when the deformation rate of sphere shell is in the range of 0.5 -1.5%. Such decreases will then become less as the deformation rate increased continuously.

The actually measured deformation rates on the sphere shell 9.2 m in diameter and 44 mm in plate thickness were in the range of 0.1 - 1.1%, but would be so high as to be beyond this range if the sphere diameter was smaller than 9.2 m. Since it has been proved that cold deformation, especially when under compression within the range of 0.1-1.5%, tends to lower the toughness and yield stress of the steel, it is therefore necessary to maintain a uniform distribution of deformation of the sphere shell during the cold forming process so as to help minimize the maximum deformation rate of the spherical shell.

The reasons about the embrittlement of steel by cold deformation is commonly considered as the result of increase in dislocation density by deformation and aging,which has lowered down the level of energy to initiate and expand cracking. The plastic relax ability of metal elastic stress is decreased by aging in the case of the cracks expansion.

2. The Tendency of Cracking of 15MnVN Steel in Welding

The tendency of cracking in welding is usualy related directly to the alloyed elements and their contents in steel, expressed as carbon Equivalent (Ceq %) and recently also as cracking sensitive index number (Pcm %). The calculation formula is given below:

$$Ceq(\%)\ (IIW) = C + \frac{Mn}{6} + \frac{Ni+Cu}{15} + \frac{Cr+Mo+V}{5}$$

$$Pcm(\%) = C + \frac{Si}{30} + \frac{Mn+Cu+Cr}{20} + \frac{Ni}{60} + \frac{Mo}{15} + \frac{V}{10} + 5B$$

According to the chemical composition designed (see table 1), the Ceq(%) of 15MnVN steel is high ($Ceq_{max.}$=0.52%), which can be assumed to heve a strong tendency to cracking in welding. A highest hardness test (Fig.6), Y-groove cracking restraint test (Fig.7) and inplant test (Fig.8) were conducted to estimate the cold cracking tendency of 15MnVN steel by the authors under the condition of constant hydrogen diffusion and constant heat input during welding. The test results are listed in table 3.[2,3]

From the results of the highest hardness test in HAZ it is shown that the maximum hardness of HAZ under the applied welding condition has been 400(Hv) or so. Even if preheated to 175°C, the hardness value of HAZ can still be as high as 382 Hv.

From the results of Y-groove cracking restaint tests, it can be seen that the welding cracking rate of 15MnVN steel is high and the preheating temperature should reach 175°C to avoid the appearance of welding cracking.[4]

The results of inplant tests show that the 15MnVN steel has a comparatively low critical stress beyond which cracks would possibly occur.

but this critical stress increases as the preheating temperature raises. If extra low-hydrogen electrodes are applied in welding, it's critical cracking stress, compared with the ordinary low hydrogen electrodes, could be raised from 294MPa to 441MPa when t8/5 is equal to 6.5 sec at a preheating temperature of 100°C. Another group (3 and 7) of test data show that the critical cracking stress can be increased from 441MPa to 578MPa when t8/5 is equal to 7.3-7.8 sec at a preheating temperature of 150°C.

From the results of all the tests presented above, it has been demonstrated that the welding cracking sensitivity of the 15MnVN steel is high, it is therefore necessary to adopt high preheating temperature such as 150-200°C[4] to avoid welding cracking. If the ultralow-hydrogen electrodes are applied, the resistance to cracking in welding will be better.

3. The Characteristics of Coarse Grained Zone in HAZ

Usually the toughness of the coarse grained zone in HAZ is rather low during the welding of HSLA steel. The zone is therefore a weak link of the joints. The 15MnVN steel, though strengthened through precipitation of alloying elements, being good at toughness and with a brittleness transition temperature lower than -80°C and a non-toughness transition temperature NDT between -45°C and -60°C, exhibits remarkable embrittlement in the heat affected transition zone when great input of energy is applied in welding.

Y. Tian etc[5] (Qinghua University) have determined the influence of variance of cooling time from temperature of 800°C to 500°C ($\Delta t8/5$) on the toughness of the steel using a method of simulated heating cycle. The simulated specimens were machined from the 15MnVN steel containing 0.18% carbon. Then the microstructure of overheat zone was subjected to a simulated heating to the peak temperature of 1350°C on Gleebe-1500 apparatus at six different cooling rates. The $\Delta t8/5$ were $2_s$, $6_s$, $18_s$, $30_s$, $40_s$ and $60_s$ respectively. Impact tests were performed at room temperature and -40°C. The test results are shown in Fig.9.

From Fig.9, it is demonstrated that only the samples with $\Delta t8/5 \leq 2_s$ had fairly high impact toughness, its impact energy being 51.3j (5.23 Kg·m) Once the $\Delta t8/5$ increased ( $6_s$), the toughness would decrease so severely that the impact energy even at room temperature was already below 9.8j(1Kg.f.m), and an obvious embrittlement tendency was shown in the over-heated zone. The impact toughness was only slightly improved as $\Delta t8/5$ continued to increase. The reason of the embrittlement tendency can be found from the exmination on the microstructure of the over-heated zone by means of optical micro-scope and electron transmission (as shown in table 4). When $\Delta t8/5 < 2_s$, the specimens were under a rapid cooling condition. Only plate-like martensite in the sole form appeared and no upper bainite was separated inside the grains, nor was there a second phase separated in grain boundary. The above mentioned martensite was of low-carbon and had fairly good toughness. As $\Delta t8/5$ increased, upper bainite began to appear inside the grains while at the boundaries was formed a net-shaped prior eutectoid ferrite, accomparied by occurance of brittle phase of M-A texture. In this case, cracks might readily be initiated on the interphase of the prior eutectoid ferrite and M-A phase when subjected to external force. Further increase of $\Delta t8/5$ brought about a coarsening of upper bainite as well as M-A phase at the boundaries, leading to easy fracture as a result of intergranular cleavage fracture when affected by thermal stress in welding. When $\Delta t8/5$ was up to $30_s$, the upper bainite got so fully developed and M-A phase became so large in cross section as to cause cleavage fracture to occur even at room temperature.

Y. Zhang etc of Central Research Institute of Building and Construction of M.M.I. performed a series of simulated heating tests on 15MnVN steel with 0.20% C at peak temperatures of 1350°C and 1250°C for cooling time of $5_s$, $8.5_s$, $12.5_s$, $20_s$ and $40_s$ respectively and then carried out impact tests at different temperatures and metallographical analysis, the results are shown in Fig.10 and the photos.

From the curves in Fig.10, it is shown that the values of impact toughness and its changing trend, when $\Delta t8/5 = 20_s$, are similar to the test results obtained by Y. Tian, namely, when $\Delta t8/5 < 5_s$, impact toughness was at its maximum, corresponding to a structure with martensite as matrix inside the grains and side platelike bainite and small amount of acicular ferrite spreading on it (see Photo 1). In the case of $\Delta t8/5 = 8.5_s$, the metallographical structure was similar to that in the cas of $\Delta t8/5 = 5_s$ but the impact toughness decreased sharply. When $\Delta t8/5 = 12.5_s$. the impact toughness remained about the same as when $\Delta t8/5 = 8.5_s$ but there appeared granular bainite mixing with martenisite and acicular ferrite with prior eutectoid ferrite existing at boundaries (see Photo 2). The structure corresponding to $\Delta t8/5 = 20_s$ was similar to that for $12.5_s$, merely except that prior eutectoid ferrite had now been coarser and the while low temperature impact toughness remained unchanged, the room temperature impact toughness was increased instead. Further until $\Delta t8/5 = 40_s$, the prior eutectoid ferrite got much coarser and became continuous. At this time, granular bainite and acicular ferrite constituted major part of a grain with only a little of fine pearlite as the remainder. Some of the M-A phase in the granular bainite had dissolved (see Photo 4) and hence the impact toughness at room temperature was increased considerably. Obviously dissolution of the M-A phase should be considered to be a reason for the increase in impact toughness. Within this cooling time of $\Delta t8/5$, the phenomenon of impact toughness increasing does not fully conform to the test results by Y.Tian. But under the condition of test at low temperature, the changing trend of impact toughness vs $\Delta t8/5$ is in consistence with the curves shown in Y.Tian's experiment. Reasons for the discrepan-

cy between the two may be deemed as the differences in chemical composition of the steels they used and in the conditions of cooling cycle applied in each own simulated heating tests.

Although the impact toughness of the simulatively heated sample from the coarse grained zone in HAZ of 15 MnVN is low, what was seen on the actual welded joints was quite different from this. Z.Q.Lu etc[7] (Central Research Institute of Building and Construction of M.M.I.) made welding tests on specimens at a preheating temperature of 165°C using an in-put energy of 20-60 Kj/cm. Impact test specimens were cut-taken from within HAZ of the welded joints and subjected to impact test. The results of toughness obtained were on the whole higher than those from simulated thermal tests (see Fig.7). At different rates of coolint embrittlement transition temperature (with 34 J/cm$^2$ as the critical point) of the coarse grained zone in HAZ was at its minimum when $\Delta t8/5=8.5_S$, and began to show an increase when $\Delta t8/5=21_S$, then to be turning down after $\Delta t8/5=35_S$ (see Fig.8). This indicates that even though the impact toughness of the coarse grained zone in HAZ at the welded joint is higher than that from simulated thermal specimens, the changing tendancy of embrittlement transition temperature vs $\Delta t8/5$ is well in line with the simulated thermal test.

Metallographic analysis on the coarse grained zone in HAZ at the welded joints suggests that when $\Delta t8/5=8.5_S$, the single heated structure of over heated zone was substancially consisted of platelike martensite as the matrix with acicular ferrite distributed on it, both taking up 90% of the entirety. Meanwhile, the martensite had undergone self-tempered and carbides separated (see Photo 4). It could obviously be concluded that large amount of ferrite and self-tempering of martensite be the main reason for a lower embrittlement-transition temperature. In the case of $\Delta t8/5=21-26_S$, heating would produced a structure of granular bainite mixed with acicular ferrite, accounting for 80% totally and 17% occupied by granular bainite along (see Photo 5). It is quite clearly that existance of granular bainite in large amount constituted a major cause for the increase of embrittlement transition temperature. As for $\Delta t8/5=35_S$, very possibly due to the proportion of 17% taken up by the granular bainite shifting down to that of about 8%, the embrittlement transition temperature dropped again with toughness improved.

The regularity of slight improvement on toughness vs increasing of $\Delta t8/5$ is in consistensy with the results of simulated thermal tests by Y.Zhang. The corresponding changes in the micro structure was dissolution of and less proportion by the granular martensite. And this again was the cause for toughness to improve.

Normally the impact toughness of coarse grained zone in HAZ of the real joints is higher than that of simulatively heated specimens. Because the simulatively heated specimen was heated at the peak temperature of 1350°C, its microstructure after cooling was a uniform one developed from a single heating process. In fact, when the impact specimen was machined from the HAZ of a real joint, the fracture path from the apex of V-notch to the bottom of the specimen should cover both the single heated structure formed in the previous weld run and the heated structure formed in the subsequent weld run. So the microstructure of the examined area through which the fracture passed was not uniform. The toughness of single heated structure of the coarse grained zone in HAZ of a real joint was higher than that of the simulatively heated specimen and the hardness of the former, lower than that of the latter because of that the next weld run had a tempering effect on the previous run. As a results granular carbides were separated from low carbon martensite and the toughness improved.

Further study on the real joints would recommend that the double heated structure of the over-heated zone in HAZ be devided into three types. The first type of structure is one which shows a coarsening effect of the original over-heated structure because it had been over-heated for a second time at high temperature by the second weld run (Photo 7). The second type of structure is of equiaxial fine grained ferrite and scattered sorbite (Photo 8) produced by a moderately high temperature in the second weld run. In the third type of structure,the original granular bainite has dissolved by a lowly high temperature and the tempered martensite, acicular ferrite and the small amount of sorbite are all remained (Photo 9). Therefore the second and third types of structure exhibit higher toughness and lower hardness than the first one. The microstructure of the second heated zone in over heated region in HAZ varies wildly with changes in in-put energy and cooling rate. But generally speaking, toughness of the second heated structure is higher than the primary one at the hardness of the former is lower than that of the latter. Thus in general, the impact energy of over-heated zone in HAZ of a real joint involving the primary and the second heated structure is higher than that of the simulatively single heated specimen.

Though the values of impact toughness test with simulatively heated specimen tend to be lower than that of the real joint, such a research method is quite simple and economic for investigating the regularity of structure formation and changes in properties of steel under the infuence of different heating cycles.

## 4. The Influence of Heat-treatment after Welding on the Characteristics of HAZ

Many researchers at home and abroad have presented the tendency of reheat cracking initiated in HAZ of welded joint on HSLA steel when heat-treatmented after welding (PWHT). It is generally considered that the cracks would readly be initiated by the hardening effect through precipitation of carbides of alloying elements during heat-treatment or by stress relaxing in HAZ during the reheating process, namely by the

creep embrittlement as a result of the decrease in residual stress with the change of time.[8] It is a common view that Nb-B steel is susceptible to reheat cracking while V-N steel is not. But it has been proved in practice that the toughness of HAZ at welded joints on 15MnVN steel decreased in stress relieving after welding. A series of experiments were performed to investigate the level of embrittlement for the steel. J.L. Wang etc (Northeast Industrial College)carried out experiments using simulated heating method to evaluate the tendency for 15MnVN steel to be reheat embrittle. In their experiments, coarse grained structure was first made to appear the HAZ in welding on the specimens by imitating the heating-cooling cycle in welding process. The simulated peak temperature was chosen 100°C below the maximum temperature in the HAZ in the actual welding process, which means to be heated to 1250°C, A time of $20_s$ for cooling from 800°C to 500°C ($\Delta t8/5$) was selected as the cooling rate. These heating parameters corresponded to welding in-put energy of 24-28 Kj/cm.

Then impact specimens were machined from the simulatively heated specimens after being reheated at five different temperatures of 520°C, 550 °C, 580°C, 610°C and 650°C. The results of the impact tests are shown in Fig.8. It is indicated in Fig.8 that the impact toughness at various heating temperatures were close to those of the as welded specimens. Only one group of tests at temperature of 0°C had apparently low values of toughness. The results of impact tests performed by S.H. Hou[10] on HAZ of the actual welded joints specimens which had been undergone re-heating at the same temperature did demonstrate the existance of an embrittlement temperature range. After annealing treatment of the actual welded joints at different temperatures, the impact toughness of HAZ decreased slightly with the increase of annealing temperature from 520°C, but the magnitude of decrease was small (shown in Fig.9). The regularity seen in the vickers hardness test was consistent to that of the impact tests, that is, the hardness after annealing was higher than as welded. In spite of this, the results of tensile and bend tests showed that the tensile strength of the joints was only 4-30 MPa lower than that of the as welded one and the results of bend test were all acceptable.

The single heated microstructure examination of HAZ in real welded joints shows that after stress relief annealing at embrittlement temperature, the M-A islands in granular bainite had been dissociated into ferrite and cementite, while the acicular ferrite and side platelike ferrite remained in their original appearance. Generally speaking, the toughness of such structure should be improved. So only dissociation of granular bainite and separation of cementite are not enough for being explained as the reason for the reheat embrittlement. Neither the mechanism of creep-relaxing which is currently thought as a result of hardening through precipitation of carbon-nitrides in the over heated zone during annealing followed by intergranular sliding, nor the theory of initiation of embrittlement along grain boundaries due to re-precipitation of trace impurity elements, has now been made clear enough to serve as a main cause of re-heating embrittlement for 15MnVN steel. All still need to be investigated in more details.

## 5. Conclusions

From above mentioned results of the tests by the authors, conclusions can be made is follows:

6.1. The properties of 15MnVN steel were apparently decreased after cold forming process. The $\sigma_s$ of the specimen with a deformation rate of 1.5%, was reduced by 27%. The impact toughness at room temperature decreased by 21% and 15.8% respectively when tensile and compressive deformation rate was about 1%. The non-ductility transition temperature (NDT) of plate in thickness of 36mm with a deformation rate of 1% was increased from -30°C in the original state to -25°C.

These changes in mechanical properties are significant and the corresponding deformation rates are within the range of the measured values of the deformation rates on the sphere shell, still these can satisfy the requirements of application. If the forming process is further improved to have the deformation rates distributed, more evenly, this will facilitate raising the safety in service.

6.2. Because of the high Ceq of 15MnVN steel, the resistance to cracking in welding was poor, the hardness value (Hv) of HAZ maximum hardness tests was higher than 350. The Y-groove restraint cracking tests in room temperature showed a cracking rate of 100%. Therefore it is necessary to use high preheat temperature, say, 150-200°C adopt suitable welding process with welding materials as appropriate, then the cold cracks in welding can be avoided.

6.3. The impact toughness of over-heat zone in HAZ of 15MnVN steel was low. Not only in simulatively heated specimens, byt also in real welding joints, the toughness was all decreased with the change of $\Delta t8/5$ within a certain range. The separation of upper bainite, granular bainite and the separation and coarsening of the netty prior eutectoid ferrite in the microstructure can be explain as the reason for embrittlement. With an in-put energy set at a suitably small amount and a cooling speed properly controlled, the impact toughness that conforms to the application requirement can be obtained. The submerged arc welding having a great in-put energy would lower the toughness in over-heat zone of HAZ. This is a problem for 15MnVN steel, which may be solved by better design of composition.

6.4. The over heated zone in HAZ of real welded joint of the 15MnVN steel showed a tency to embrittlement within a certain range of temperature when heat treated after welding. The embrittlement transition temperature of the over heated zone was raised by 19°C compared with

that in the as welded state. Embrittlement can be avoided by proper selection of a temperature for heat treatment.

To sum up, the 15MnVN steel, when used in the manufacture of pressure vessel for storing gas, is entirelly acceptable in such aspects as the properties after manufacture, weldability and so on. The vessel can be used at the temperature of $-40^{\circ}C$. Nowadays the 15MnVN steel has widely been used in the manufacture of spherical pressure vessel for storing gas in many companies such as Benxi, Maanshan, and Baoshan etc.

Photo 1 $\Delta t8/5=5s$ 500X

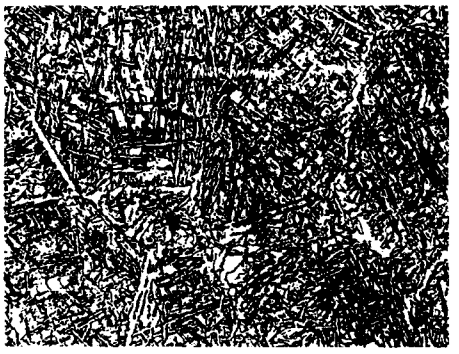

Photo 2 $\Delta t8/5=12.5s$ 500X

Photo 3 $\Delta t8/5=40_S$ 500X

Photos 1-3 Single heated microstructure of coarse grained zone in HAZ on simulated heating[6]

REFERENCES


[1] J.M. Cao, W.H. Li and J.W. Shang
Petroleum Engineering Construction 13-6 (1987)

[2] W.W. Chang et al.
The Evaluation of 15MnVN Steel Coldcracking Sensitivity by Tuplant Method, 1983.6

[3] W.W. Chang et al.
The Measured Data of Sensitivity of Welding Cold cracking in HSLA Steel, 1985.10

[4] Z.Q. Lu, W.H. Li et al.
The Basic Welding Data Handbook of 15MnVN Steel, 1985.10

[5] Y. Tian, L.J. Zhuang and Z.C. Luo
The Fifth National Symposium of China Welding Society of CMES, (1986) 2-25

[6] Y. Zhang, R.Y. Huang and X.Y. Chen
The 5th Nat. Sym. of Chi. Wel. Soc. of CMES (1986) 2-46

[7] Z.Q. Lu, X.L. Qu and H.Z. Yin
The 5th Nat. Sym. of Chi. Wel. Soc. of CMES (1986) 2-47

[8] G.M. Xiao
The Toughness and Toughen of Metal, 1979.2

[9] J.L. Wang, Q.S. Wang et al.
The Simulated Heating Investigation of Heat Treatment after Welding in 15MnVN Steel, 1986.5

[10] S.H. Hou, R.N. Zhao and L.G. Lin
The 5th Nat. Sym. of Chi. Wel. Soc. of CMES (1986) 2-54

[11] K.T. Wang et al.
The Investigation on Manufacture of Storing Gas Sphere Pressure Vessel Made of 15MnVN Steel, 1985.

Table 1. Chemical Composition of 15MnVN Steel[4]

| | Thickness (mm) | Chemical Composition % | | | | | | | Ceq | Pcm |
|---|---|---|---|---|---|---|---|---|---|---|
| | | C | Si | Mn | P | S | V | N | | |
| Normal value | | 0.12-0.23 | 0.20-0.60 | 1.30-1.70 | 0.045 | 0.05 | 0.1-0.2 | 0.01-0.02 | | |
| Typical value | 20 | 0.18 | 0.40 | 1.67 | 0.018 | 0.003 | 0.13 | 0.0215 | 0.48 | 0.3 |
| | 36 | 0.20 | 0.37 | 1.61 | 0.017 | 0.032 | 0.19 | 0.016 | 0.51 | 0.3 |
| | 50 | 0.16 | 0.40 | 1.43 | 0.018 | 0.009 | 0.14 | 0.02 | 0.43 | 0.5 |

Table 2. Mechanical Properties of 15MnVN Steel[4]

| | Thickness (mm) | Provided condition | $\sigma_s$ MPa (Kg.f/mm$^2$) | $\sigma_b$ MPa (Kg.f/mm$^2$) | $\delta_5$ % | Bending 180° | Cv[J/cm$^2$ (Kg.M/cm$^2$)] 20°C | Cv[J/cm$^2$ (Kg.M/cm$^2$)] -40°C |
|---|---|---|---|---|---|---|---|---|
| Normal value | 10 | Rolled or normalized | 441 (45) | 588 (60) | 17 | d=2a | 58.8 (6) | 29.4 (3) |
| | 11-25 | Normalized | 421.4 (43) | 568.4 (58) | 18 | d=3a | | |
| | 26-38 | Ditto | 411.6 (42) | 548.8 (56) | 17 | | | |
| | 40-50 | Ditto | 392 (40) | 529.2 (54) | 17 | | | |
| Typical value | 20 | Ditto | 539 (55) | 676.2 (69) | 24 | acc. | | 114.7 (11.7) |
| | 36 | Ditto | 455.7 (46.5) | 617.4 (63.0) | 25.5 | acc. | 100 (10.2) | 69.6 (7.1) |
| | 50 | Ditto | 431.2 (44) | 588 (60) | 27.0 | acc. | 224.4 (22.9) | 129.7 (13.8) |

Table 3. The Sensitivity Testing for Cold Cracking in Welding of 15MnVN Steel[2,3,4]

| No. | Electrode | [H]* (ml/100g) | Input energy (KJ/cm) | $\Delta t_{8/5}$ (s) | $T_o$** (°C) | Hv10 | Cracking rate*** (%) | | $\sigma_{cr.}$**** (MPa) |
|---|---|---|---|---|---|---|---|---|---|
| | | | | | | | Surface | Section | |
| 1 | Low Hydrogen | 3.34 | 16-17 | 5 | 20 | 468 | 100 | 100 | 200.9 |
| 2 | " | " | " | 6.5 | 100 | 399 | 84 | 94 | 294 |
| 3 | " | " | " | 7.3 | 150 | 394 | 0 | 26 | 411 |
| 4 | " | " | " | 8 | 175 | 382 | 0 | 0 | 568.4 |
| 5 | " | " | " | 5 | 20 | | | | 421.4 |
| 6 | " | " | " | 6.5 | 100 | | | | 441 |
| 7 | " | " | " | 7.8 | 150 | | | | 578 |

Notes: * The diffusive hydrogen content of weld metal was measured by glycerine method. The electrode was baked at 400°C for 1 h.
** Preheat temperature.
*** Y-groove cracking restraint test.
**** The critical stress of inplant test.
The plate thickness of 36 mm was used.
The chemical composition of steel is as follows: C-0.19%, Mn-1.37%, Si-0.36%, P-0.018%, V-0.22%, N-0.013% and S-0.026%.

Table 4. The Structure and Properties of Smulative Overheated Zone in the Different Δt8/5[5]

| Mark | Δt8/5 (s) | Austenitic grain diameter (μ) | Width of boundary ferrite (μ) | $Hv_5$ | $V_E$(15°C) J (Kg.m) | Structure inside grain | Case of grain boundary | Facture form |
|---|---|---|---|---|---|---|---|---|
| $C_1$ | 2 | 90 | 0 | 445 | 51.3 (5.23) | Platelike martensite | No separarion | All through grain |
| $C_2$ | 6 | 92 | 0.7 | 427 | 16.6 (1.69) | Platelike M & upper bainite | A little fine boundary ferrite & M-A | Through & along grain |
| $C_3$ | 40 | 110 | 5 | 327 | 7.74 (0.79) | Upper B.& acicular ferrite | Net shaped boundary ferrite & M-A | Through & much along grain |

Table 5. The Tensile Strength after Annealing at Different Temperature[10]

| Annealing temperature (°C) | Tensile strength (MPa) | Fracture location |
|---|---|---|
| As welded | 577 | Parent plate |
| 520 | 562 | " |
| 550 | 573 | " |
| 580 | 549 | " |
| 610 | 552 | " |
| 650 | 547 | " |

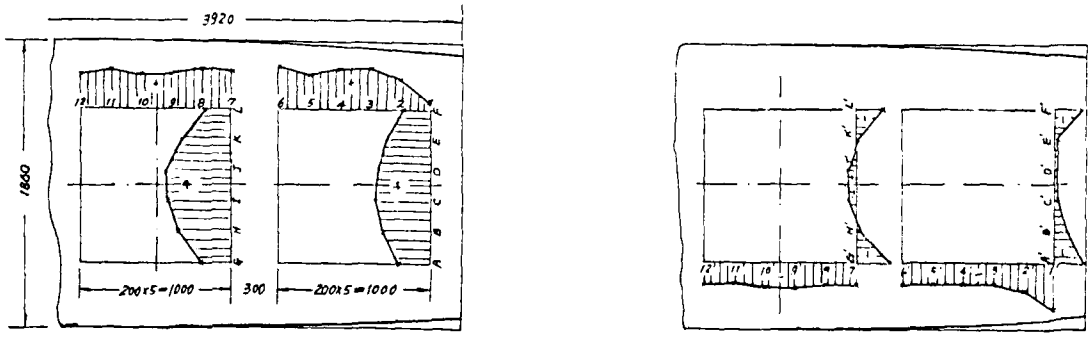


a. external surface b. internal surface

Fig.1 Distribution of deformation rates measured at sphere shell after cold forming[1]

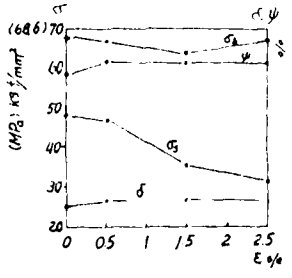


Fig.2 The influence of compressive deformation on properties of the sample[1]

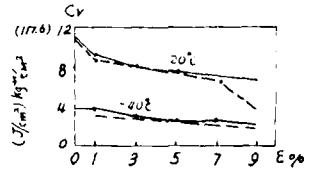


Fig.3 The influence of tensile and compressive deformation on impact toughness of the sample[1]
——Strain under tension;
---Strain under compression.

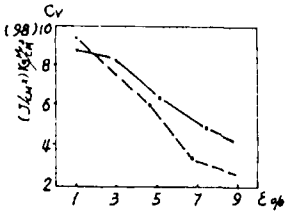


Fig.4 The influence of strain aging on impact thoughness of the sample[1]
—— Strain under tension;
--- Strain under compression.

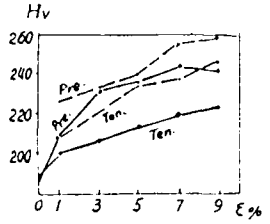


Fig.5 The influence of tensile and compressive deformation on Hardness of the sample[1]
—— Not Aged; --- Aged

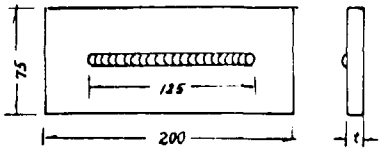


Fig.6 Specimen for highest hardness test in HAZ

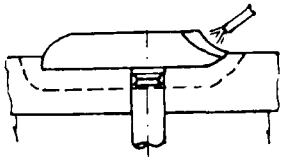

Fig.7 Sketch of inplant test

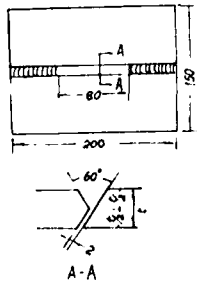


Fig.8 Specimen for Y-groove restrained cracking test.

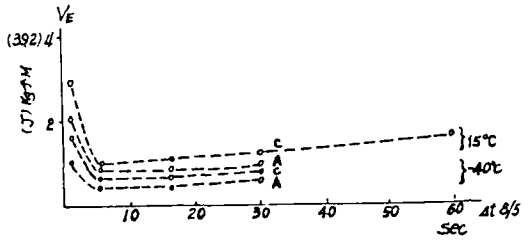


Fig.9 Relation between Δt8/5 and impact toughness in simulated heating tests.[5]

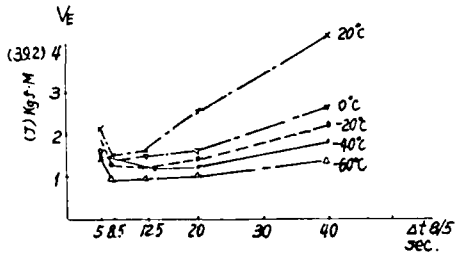


Fig.10 Relation between Δt8/5 and impact toughness in simulated heating.[6]

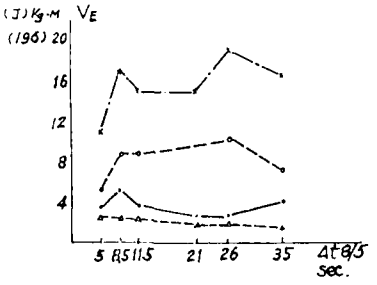


Fig.11 Relation between Δt8/5 and impact toughness of over-heated zone in real joints[7]

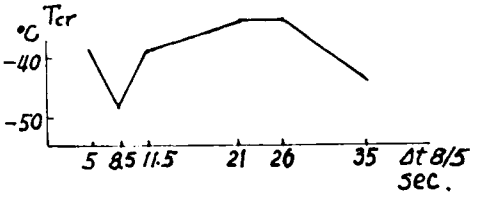


Fig.12 Relation between Δt8/5 and brittleness transformation temperature of over-heated zone in HZA of real joints [7]

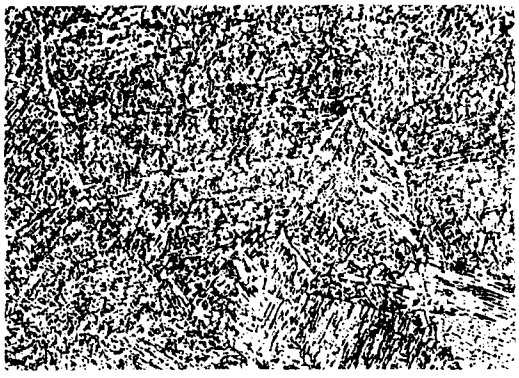

Photo 4 Δt8/5=8.5s 400X

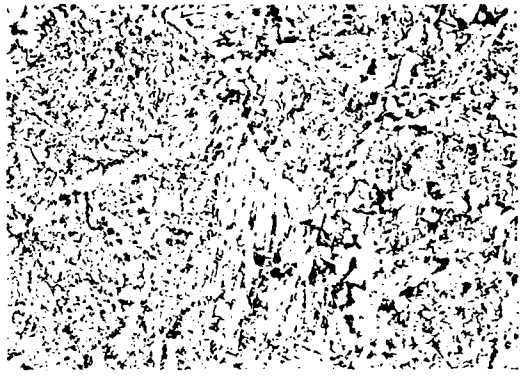

Photo 7 400X

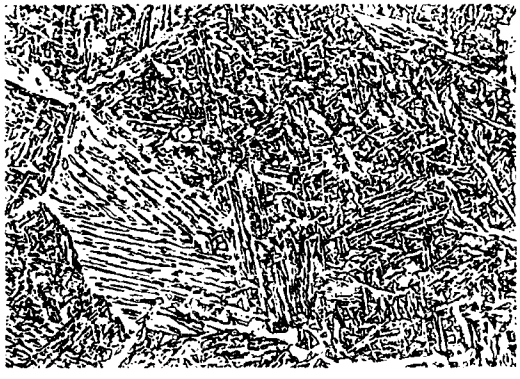

Photo 5 Δt8/5=21s 400X

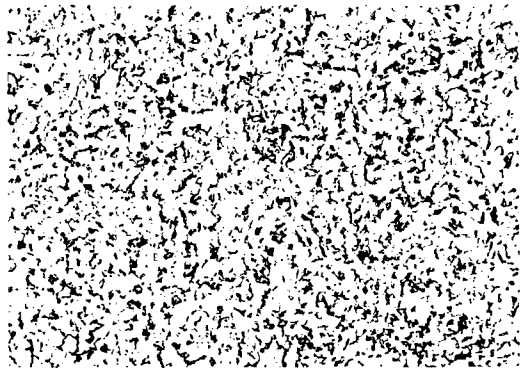

Photo 8 400X

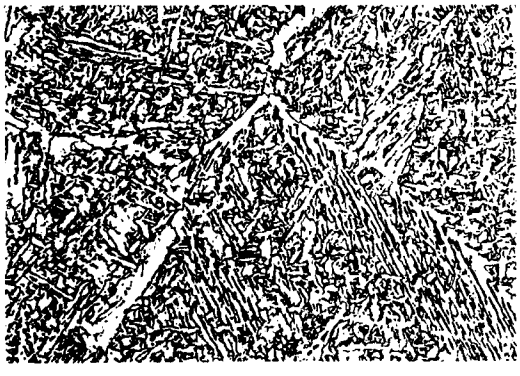

Photo 6 Δt8/5=35s 400X

Photo 9 400X

Photos 4-6 Single-heated microstructure of over-heated zone of real joints[7]

Photos 7-9 Double heated structure over-heated zone in HAZ of real joints[7]

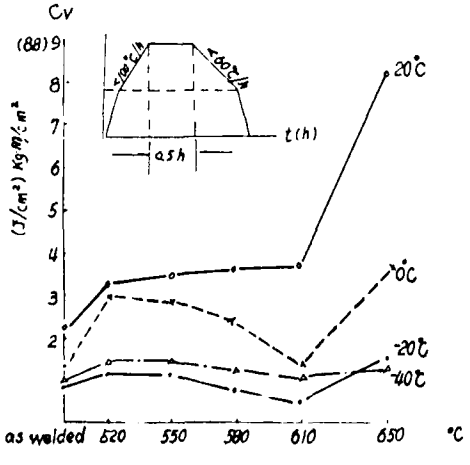


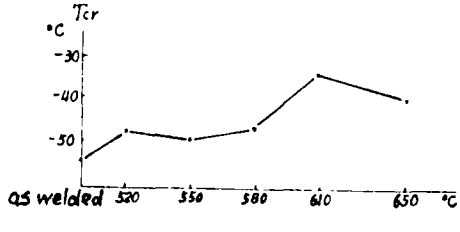


Fig.14 Relation between annealing temperature of real joints and brittleness transformation temperature[10]

Fig.13 Relation between annealing temperature and toughness of simulatively heated specimen[9]

# HIGH STRENGTH STEELS IN AUTOMOBILES—PAST DIFFICULTIES TO FUTURE CHALLENGE

**R. G. Davies**
Ford Motor Company
Dearborn, Michigan 48121-2053 USA

Weight reduction through the use of high strength steels (HSS) is a cost effective way to reduce fuel consumption. This paper briefly reviews the three basic types of HSS-conventional (grain size, precipitate strngthened, recovery annealed/ martensitic and duel-phase. The major problems encountered in their application to stamped automotive components have been associated with reduced ductility (lower forming limit curves and higher edge cracking tendency), shape control (springback and side-wall curl) and spot welding difficulties. These problems have been exacerbated by the use of coatings (zinc/zinc alloy) for corrosion protection. The advent of the "world-wide" automobile company makes it difficult to predict what the future holds for HSS; depending on the country of origin there may be less use of and/or different types of HSS. Whatever the mix of steels in the car there will be an increased need for consistent steels; consistent in mechanical properties, thickness and coating weights.

It is just over 10 years ago that there was the first extensive use of cold-rolled gage high strength steels (HSS) in automobiles. This usage was in response to the gasoline shortage and the subsequent government fuel economy regulations. Fuel consumption as shown in Fig. 1 decreases with decreasing weight of the vehicle; improvements in engines and other power train components move the curve downward but do not negate the influence of weight reduction. Over the last 10 years the average weihgt of a U.S. automobile has been reduced by about 360 kg (800 lbs), mainly as a result of vehicle downsizing and more efficient packaging but with important contributions from the use of lightweight materials such as HSS, plastics and cast aluminum.

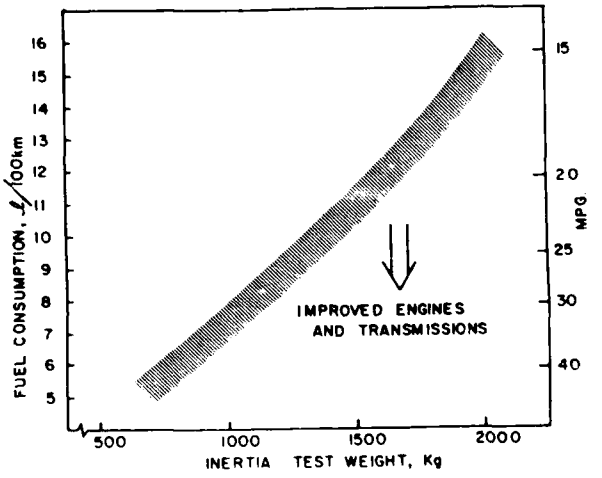


Fig. 1 Fuel consumption as a function of vehicle inertia weight

The intent of this paper is to review what has been learned about the properties of HSS and the difficulties encountered in their application to automobiles. An attempted will then be made to predict what the future holds for the usage of these materials in the light of a rapidly changing automobile industry.

## TYPES OF HSS

For the purpose of this paper HSS will be defined as steels whose yield strengths are in excess of 25 MPa (40 ksi) and thus tensile strengths greater than 360 MPa (52 ksi). As a comparison, the yield strength of cold-rolled low-carbon steel is usually in the range 165 to 234 MPa (24 to 34 ksi).

HSS can be divided into three basic groups depending on the types of strengthening mechan-

isms employed. The three groups of steels are often referred to as: 1. recovery annealed/ martensitic-these are strengthened by the presence of dislocation substructures, 2. dual-phase steels whose strength depends upon the percentage of martensite in the structure(1) and 3. conventional HSS. The relationship of these steels to one another can best be visualized by plotting the tensile strength as a function of total elongation as shown in Fig.2(2); tensile strength is chosen as it a good measure of fatigue(3) and crush resistance(4,5) while total elongation is a reasonable indication of formability.

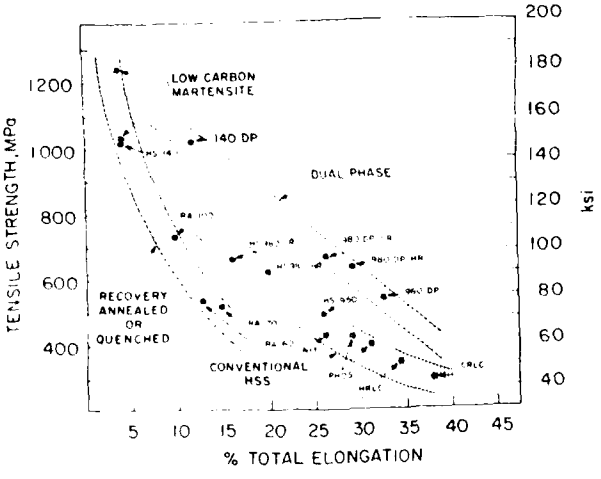


Fig. 2 Tensile strength versus total elongation for the three basic types of HSS.(2)

The conventional HSS utiliz one or more of the following basic strengthening mechanisms: solid solution strengthening by P, Si or Mn, grain refinement and precipitation hardening by Nb, V or Ti carbides or carbo-nitrides (6-8). Fig. 3 shows the contributions to the yield strength of these mechanisms for a typical hot-rolled HSS containing approximately 1% Mn, 0.5% Si and various amounts of Nb and V. It can be seen that Nb, through its grain refining action, is the most efficient microalloying element (6). In cold-rolled gage HSS, which have been annealed at 640-700°C, most of the strengthening is from the grain size reduction and solid solution elements; the act of annealing has coarsened the precipitates so that they contribute little to the strength. The majority of conventional HSS, both hot and cold-rolled gages, rely upon Nb alone or a mixture of Nb and V as their micro-alloy strengthening element. Ti has not been widely used for strengthening, even though its carbide is the most stable, because the mechnical properties have been very inconsistent especially in the cold-rolled gages.

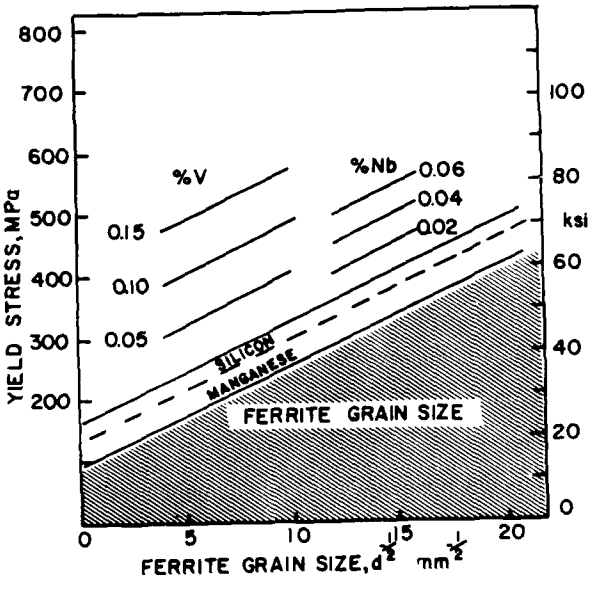


Fig. 3 Variation in yield strength with grain size and Nb and V content, for a typical hot-rolled HSS containing approx. 0.1%C, 1%Mn and 0.5%Si.(8)

## PAST EXPERIENCE

The past 10 years have been a time of learning for both the users and the producers of HSS (particularly the cold-rolled gages). The users-in this case the automobile industry-have had to learn how to design and produce components in a material with lower ductility than low carbon steel; forming problems are discussed below. The steel industry has made tremendous progress in its ability to produce HSS with constant properties from coil to coil and from beginning to end of a given coil. Two steel companies have insta-led continuous annealing lines which are ideal for producing high wuality HSS. The lack of consistency of the properties of HSS hindered the application of these steels and, to a certain extent, still does to this day. There are still people around the industry who remember "when we had a 950 steel with a 75 ksi yield"; the steel producers must continue their education program to show the progress that they have made in all facets of steel making.

The difficulaite encountered in the production of HSS components are briefly reviewed in the following sections.

a. INTRINSIC FORMABILITY - HSS have reduced formability compared to low carbon steels as revealed by the forming limit diagram (FLD) in Fig. 4(9); if the forming strain encountered during a stamping operation remain below the line then failure (severe necking or fracture) will not occur. It can be seen that the higher the strength of the steel the less is the available strain; the exception to this is the dual-phase steel which has the same tensile strength as the HSLA 80 but considerably better formability. The FLD is sensitive to the thickness of the steel such that the formability decreases with decreasing thickness. In addition, the lower strain harding exponent (n value) of the HSS will result in increased strain localization(10) and an increased propensity for splits and thinning.

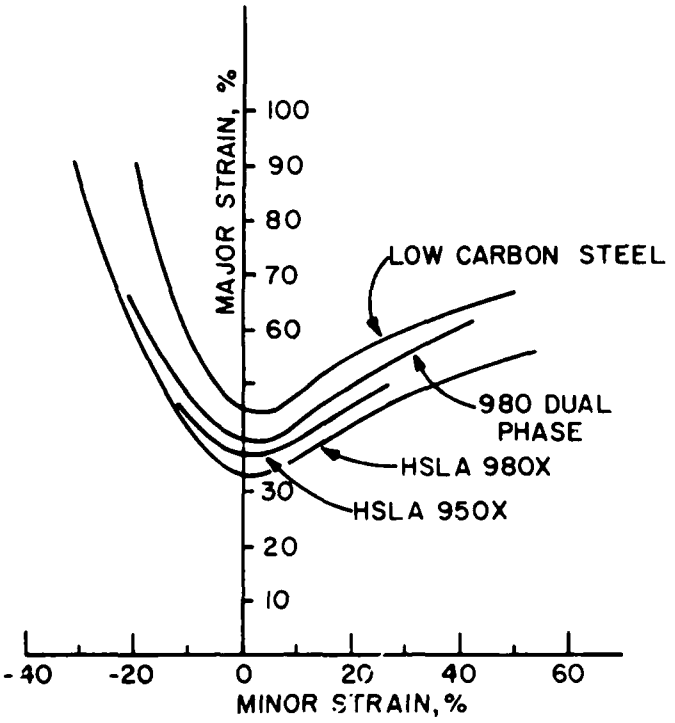


Fig. 4 Forming limit diagram for various HSS.(9)

It is worth noting that a specific measure of the FLD is used for the in-plant evaluation of formability. This measure is the limiting dome height (LDH) and is essentially the minimum value of the FLD. In the majority of stampings the minor strain is in the range -10 to +10% and thus the LDH value is a good indicator of press performance. The major use of the LDH value is in statistical process control and thus it assists in deciding the origin of stamping defects. For example, if excessive splitting is being encountered then the LDH test can indicate whether the material is deficient or whether the press needs adjustment. Knowing the source of the problem allows a solution to be found quicker.

b. EDGE CRACKING - Edge cracking, which is observed when a sampled hole is expanded into a sheared edge is subsequently stretched, is also a measure of the materials ductility. Hole expansion, which is a measure of the strain to fracture at an edge, is dependent upon the cleanliness of the steel (number and shape of the sulfide inclusions), the type of HSS and the quality of the sheared edge(11). Inclusion shape control is accomplished by the addition of rare-earth elements, Ti or Zr and results in rounded, globular sulfides rather than the common elongated Mn sulfides(12). Figure 5 shows the influence of both tensile strength and sulfide shape control upon the hole expansion; the lower curve is for steels without shape control. It can be seen in this figure that the edge carcking resistance decreases rapidly with increasing tensile strength and, at a given tensile strength, is improved by inclusion shape control.

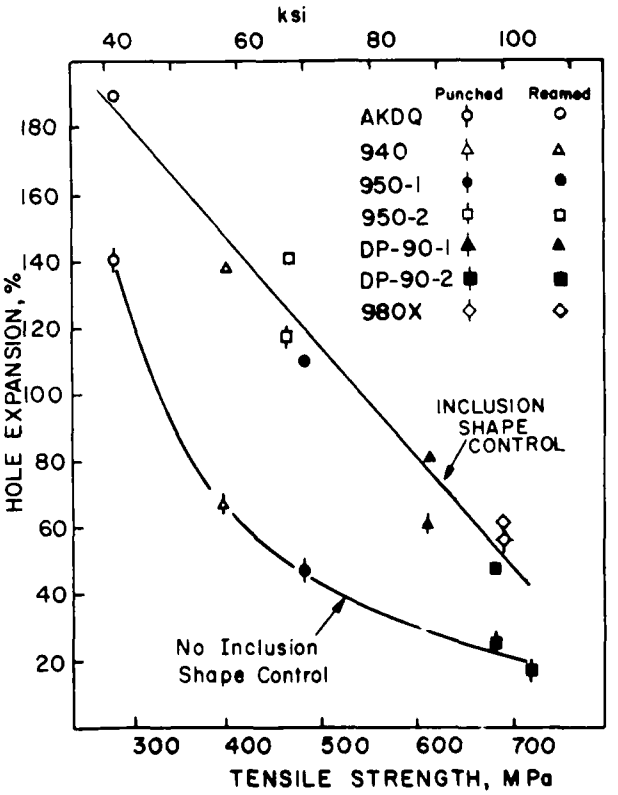


Fig. 5 Hole expansion as a function of tensile strength; the lower curve is for alloys without inluusion shape control while the upper curve is for steels with inclusion shape control and/or good quality edges.(11)

The hole expansion data for the high alloy dual-phase steel (1.5%Mn-0.6%Si), which has rare-earth additions (DP-90-2), is considerably less than for a conventional HSS of comparable tensile strength. This ease of edge cracking is thought to be due to the brittle nature of the high carbon martensite islands in this structure. However, the lean alloy dual-phase steel (0.6% Mn, DP-90-1) which contains tempered martensite, behaves similarly to the conventional HSS.

In stamping plants it is not unusual to find that certain regions of the sheared edge of a few HSS components are being flame annealed prior to edge stretching. The annealing improves the "quality" of the edge by removing the cold-work put in by the action of the shear. Such an annealing step is both time consuming and expensive but often it is the only way a part can be made. Edge cracking is still a serious problem in the plant.

c. SPRINGBACK - Springback, which is the difference in configuration of the component between when it is in the die and when it is taken out, is a problem with all materials. For a simple bend operation like forming a bracket or a U-channel, it is found that springback is a function of die-gap, bend radius and material thickness and strength(13). For constant die conditions the springback is, as shown in Fig. 6, proportional to the yield strength. Springback is thus an intrinsic property of the material and cannot be modified by manipulating the metallurgical structure. However, various die techniques such as the "double-bend"(14,15) can be used to minimize or eliminate springback.

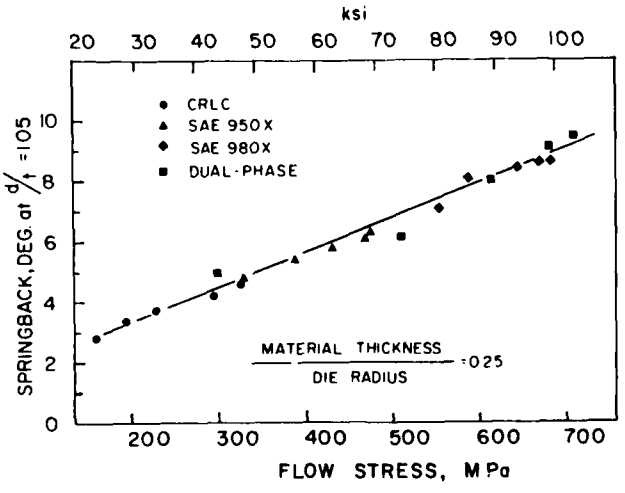


Fig. 6 Springback as a function of flow stress for various cold-rolled gage steels(13)

As springback is dependant upon the strength of the material then the consistency of the strength becomes very important. Variations in the strength from coil to coil lead to variations in springback which influences part fit-up and quality. Since springback can often be compensated for in the dies, consistent mechanical properties are often more important in determining quality parts than the absolute magnitude of the properties.

d. SIDE-WALL CURL - When a hat shaped section is formed by a punch pulling the steel over a radius into a die cavity it is seen that, in addition to springback, the side-walls are curved; this is referred to as side-wall curl. "Curl" increases with increasing tensile strength and decreasing thickness of the material (see Fig. 7) and is in general minimized by a large die radius (16,17). The majority of hat-section and similar structural components were traditionally made of low-carbon steel of about 1.6mm thick and curl was not a problem. However, with the substitution of thinner gage HSS, such components now exhibit "curl" which leads to assembly difficulties.

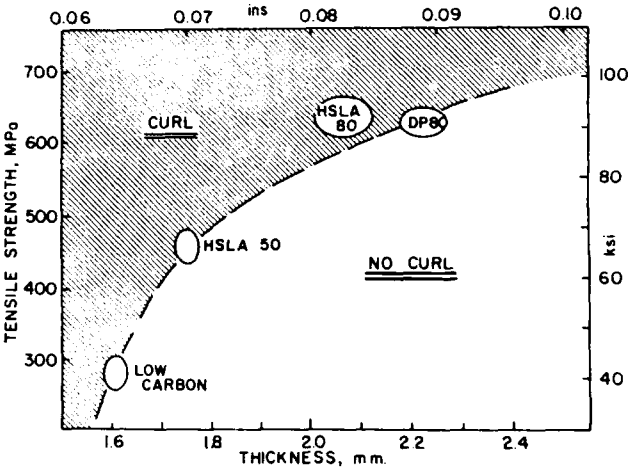


Fig. 7 Plot of material thickness versus tensile strength showing the region where "curl" can be expected.(16)

Side-wall curl is consequence of the non-uniform distribution of residual stresses through the thickness of the sheet caused by the action of pulling over a radius. Since plastic deformation can eliminate residual stresses, then the stretching of the side-wall as a final forming stemp will remove the "curl". Indeed it is found(16) that, independent of material and the initial valur of "curl", a 1% plastic strain removes the "curl". This method of part shape control is often used in the stamping plant where hat-shaped sections are made in multi-stage presses.

e. SPOT WELDING - In addition to the above mentioned forming problems, the use of HSS leads to spot welding difficulties; spot welding is the major mode of assembly of sheet metal components in the automobile industry. HSS result in a change in the magnitude of the current and the current range, when compared to low-carbon steels. Each steel producer/steel mill obtains a given set of mechanical properties by alloying additions that are best suited to their specific situation. As different elements change the welding current by differing amounts, then materials interchangabillty from spot welding considerations is difficult.

f. GALVANIZED STEEL - There has been a large increase over the last six or seven years in the number of components that are zinc or zinc alloy coated. It is snticipated that in three ot five years time all components will be galvanized, independent of whether they are made of low-carbon or HSS. The presence of the zinc or zinc alloy coating results in a whole new set of forming problems.

The formability of galvanized steel depends on the properties both of the substrate and the coating. During the hot-dipping process the formability of the substrate material may be degraded; the electrogalvanizing process does not change, in any real way, the properties of the substrate. However, independent of the substrate, the coating does reduce the formability. The pure zinc coatings tend to gall more than the alloy coatings and yet, being softer and more ductile they do not crack and flake off as readily as the alloy coatings. The flaking and spalling is most severe under forming conditions that involve compressive stresses in the plane of the sheet. In addition, each coating will react with and hold lubricants differently; this is true even for one type of coating, for example, electogalvanized steels made on lines with different cell geometries will have distinctly different surface characteristics. The surface topography influences both friction (galling tendency) and lubrication through its ability to retain oil.

In prototype development many new and difficult to form parts are initially formed on zinc-based soft tooling. This tooling reacts much differently with the galvanized steel than does the production hardened steel tooling. Thus a part may form readily in the soft tooling but present many problems in production.

The spot welding of galvanized steel has been a serious problem in the assembly plants; there is a drastic reduction in welding tip life. The material factors that influence weldability are type of coating and its thickness. Each of the coatings has different surface roughnesses, electrical resistance, thermal conductivities and melting temperatures; these factors will alter the heat balance, and therefore the quality of the weld and the electrode life. The hot-dipped galvanized steels are the most difficult to weld while the alloyed coatings present the least problems. The thinner the coating, for a given coating type, the longer is the electrode life. Thus, electrodeposited zinc, which tends to be thinner and more uniform than hot-dipped zinc, leads to less severe electrode tip degradation.

## THE PRESENT

From the above it can be seen that there are many obstacles and difficulties associated with the downgaging of automotive components with HSS, and that the increased usage of zinc/zinc alloy coatings is compounding these problems. In spite of these problems the average, the average 1988 automobile contains approximately 100-134 kg (225-300 lbs.) of HSS; this represents about 8-10% of the dry weight of the vehicle.

The vast majority of the HSS used are of the 950 grade with a yield strength of 345 Mpa (50 ksi); these are conventional type HSS which rely on grain size control for most of their strength. Contrary to what was predicted(18) 6-10 years ago, there is very little use made of the more ductile dual-phase steels even though there are now two high capacity continuous annealing lines in operation. There are at least tow reasons for the lack of interest in the dual-phase steels: 1). historical-there is a great reluctance to change materials especially when forming difficulties have been overcome and the components are performing well, and 2). the issue of repairability of damaged components. Vehicles that have been damaged in an accident are often repaired by heating the component, or structure, with a blow-torch to red heat and then beating back into shape. Repairability was evaluated by heating specimens to 550-700C for 2-5 mins.; it was found that conventional HSS retained their mechanical properties while both the water quenched low-alloy dual-phase steels, and the recovery annealed/martensitic steels exhibited serious degradation. Thus when a component may be repaired, instead of replaced, following an accident, care must be exercised in selecting the proper HSS.

The US steel industry has made great strides over the last ten years in producing more consistent HSS steels both by the addition of new equipment-continuous annealing lines-and by upgrading of the controls of the batch annealing furnaces. In addition, the ladle metallurgy stations now coming into greater use will allow the production of lower sulfur, cleaner steels with greater edge cracking resistance. Bake-hardenable steels, with improved dent resistance(19), are also now available and are finding use in such components as hoods.

Over the last 10 years the automobile industry has met the government mandated fuel economy standards through a combination of processes-downsizing, aerodynamic styling, increased

engine/transmission efficiencies and the use of lightweight materials (Al castings, plastics and thinner gage HSS). Fuel economy is still important but there is not the "pressure" on the industry that the fuel crises of the 1970's produced.

## THE FUTURE AND HSS

a. STEEL INDUSTRY - It is anticipated that there will be further improvements in the production of steels with tighter controls of both mechanical properties, gage and coating weight of hot dipped galvanized steels. Gage control is very important for the influence it has upon the binder restraining force in the stamping(20); if the material is too thich then the restraining force increases and this can lead to splits in the stamping.

From the ladle metallurgy/vacuum degassing stations there will be very low carbon steels ( 0.02%C) with improved formability which will aid in parts integration. Such steels can be strengthened with solid solution elements as P and Si to give highly formable, higher strength materials. If the problems of "surface quality" can be overcome, then P containing steels could find extensive use for outer-body panels. In addition, good carbon control will lead to better bake-hardenable steels.

b. AUTOMOBILE INDUSTRY - The nature of the US automobile industry has been changing over the last 6-8 years; there has been a large reduction in production capacity, as imports now have about a 30% share of the market, and a concentrated effort to improve quality and productivity. Increasing productivity will have both a positive and a negative impact on the use of HSS. The trend to more integration of components into a single stamping will require more formable steels, and thus mitigate against the use of HSS. Of course, the other alternative for component integration, composites, leads to a total loss of the business for the steel industry.

There is a trend in the automobile industry to produce high performance derivatives of certain car lines to satisfy a certain segment of the market. These vehicles have, in general, a higher loading upon suspension components and it is found that HSS are required to minimize the weight. Such a suspension system may contain approximately 75 kg (170 lbs) of HSS; most of this represents increased usage of HSS. In addition, with the decreasing cost and increasing speed of computers, the FEA (finite element analysis) of more complex components becomes feasible. To do a FEA the engineer needs to know the minimu properties of the material. HRLC (hot-rolled low-carbon) steel is a rather variable material and therefore there is a trend for the design engineer to specify a lower strength HSS (yield strength 300 MPa (43 ksi)). This material has adequate formability with controlled mechanical properties.

The major change that is taking place in the automobile industry is the designing of a vehicle for world-wide production. For example, small cars may be designed in Japan for production in both the US and Europe; other "world" vehicles are being designed in Europe and the US. Such vehicles are not only being engineered in these countries but production feasibility is being established as well. Thus the home country for a vehicle will be responsible for specifying the materials to be used and, as is well known, different philosohies as regards to the usage of HSS and to the types of protective coatings. The US and Japan both use significant amounts of HSS but US steel tends to be of a higher yield strength variety; Europe, on the other hand, does not use large amounts of HSS. The overall impact of this change in the way business is done may be a reduction in the amount of HSS used in automobiles.

## SUMMARY

It is clear that the problems associated with the use of HSS-springback, side-wall curl and reduced ductility-will never go away as they are intrinsic to the material. However, process modifications can be made so as to minimize these problems. Another factor that can contribute to the successful application of HSS is consistent material-consistent in mechanical properties, thickness and, when used, coating weight. The steel industry has to get the word out to the engineers of the great strides that they have made in the last ten years in producing consistent steels.

With the advent of the "world automobile industry" the outlook for HSS is not so clear; some replacement car lines may use less HSS than at present while others will use different types of steels. It will be a challenge to the steel industry to tie-in with this new way of doing business. The last ten years have seen great changes in the types of sheet steels used in the automobile; the next ten years will probably produce similar changes.

## REFERENCES


1. Davies, R.G., Met. Trans. 9A, 671-79 (1978)
2. Davies, R.G. and C.L. Magee, J. Metals 31, no. 11, 17-23 (1979)
3. Magee, C.L., R.G. Davies and P. Beardmore, J. Metals 32, no. 11, 28-35 (1980)
4. Magee, C.L. and P.H. Thornton, SAE Preprint No.780434, Feb. (1978)
5. Thornton, P.H. and C.L.Magee, Trans. ASME 99, 114-20 (1977)
6. Korchynsky, M. and H. Stuart, Symposium on Low Alloy High Strength Steels, pp. 17-27, Ges. Electromet.mbtt, Duesseldorf, Germany (1970)
7. Gray, J.M. and R.B.G. Yeo, Trans. ASM 61, 225-69 (1968)
8. Gladman, T., D. Dulieu and I.D.McIvor, Proceedings of Microalloying 75, pp. 32-55, Union Carbide, N.Y. (1975)
9. Rashid, M.S., SAE Preprint No. 770211, Feb. (1977)
10. Keeler, S.P., Machinery 74, May (1968)
11. Davies, R.G., J. of Applied Metalworking 2, 293-99 (1983)
12. Luyckx. L., J.R. Bell, A. McLean and M. Korchynsky, Met. Trans. 1, 3341-50 (1970)
13. Davies, R.G., J. of Applied Metalworking 1, 45-52 (1981)
14. Liu, Y.C., J.S. Patent 4,373,371
15. Davies, R.G. and Y.C. Liu, J. of Applied Metalworking 3, 142-47 (1984)
16. Davies, R.G., J. of Applied Metalworking 3, 120-26 (1984)
17. Chu, C.C., Proceedings IDDRG, pp. 227-30, ASM Int., Metals Park, Ohio, USA (1988)
18. Davies, R.G., "Metallurgy of Continuous-Annealed Sheet Steel", pp. 35-47, AIME, N.Y. (1982)
19. Kokubo, I., S. Momura, M. Miyahara, K. Komero and K. Kawamoto, Kobe Steel, private communication.
20. Selkirk, J. F., Proceedings IDDRG, pp. 1-7, ASM Int., Metals Park, Ohio, USA (1988)

# THE PAST, PRESENT AND FUTURE OF HIGH-STRENGTH SHEET STEELS IN THE AUTOMOBILE

**Moinuddin S. Rashid, Chongmin Kim**
General Motors Research Laboratories
Warren, Michigan, USA

ABSTRACT

High-strength low-alloy(HSLA) steels took center stage of the automotive materials scene in the early seventies, when the U. S. car industry sought ways to simultaneously improve automotive fuel economy and comply with new federal environmental and safety requirements. Lower formability of these steels compared with plain-carbon steels led to the evolution of dual-phase steels, such as GM980X, which had far better formability and machinability than conventional high-strength steels at the same strength level. Successful applications of GM980X steel followed; parts made with the steel were considerably lighter and usually cost about the same as their plain-carbon steel counterparts, even though the material cost more. In production runs with HSLA and dual-phase steels, valuable lessons were learned on steel quality, property requirements and forming methods. However, the present usage of high-strength steels, dual-phase steels in particular, is considerably below predicted levels, but the usage is expected to grow. Stamping plants are now more comfortable in using higher-strength steels and are trying new forming technologies. Steel companies are now capable of producing quality high-strength steels with closely controlled properties.

## THE PAST

EMERGENCE OF HIGH-STRENGTH LOW-ALLOY(HSLA) STEELS - High-strength sheet steels were drawn onto automotive center stage in the early seventies, when fuel price increased sharply and new federal safety and emission laws were enacted. The higher fuel cost increased the sale of small, more fuel-efficient cars, and forced car manufacturers to reduce vehicle weight, whereas compliance with the new safety and emission standards tended to negate vehicle weight reduction. The least disruptive solution to meeting these diametrically opposite trends for vehicle weight was the substitution of lighter-gage high-strength steel components for plain-carbon steel components.

High-strength sheet steel was favored over aluminum and plastics, because it was assumed that the same dies and rules of thumb used for forming plain-carbon steels would also be applicable for making high-strength steel parts. Microalloyed HSLA steels[1], which had just been introduced, seemed the most attractive substitute for plain carbon steels. These steels derived their high strength from thermomechanically processing steels of essentially plain-carbon steel to which a few hundredths of a percent of a microalloying element such as V, Nb or Ti had been added. Initially, only two grades of steel were produced, SAE950X, which had typically a yield strength of 50 ksi(350 MPa) and a tensile strength of 65 ksi(450 MPa), and SAE980X, with a yield strength of 80 ksi(550 MPa) and a tensile strength of 95 ksi(655 MPa). The former was preferred in Japan, while the U. S. automotive companies chose to work more with the higher-strength steel in strength-limited parts. This was an exciting period for metallurgists and engineers alike, who had to grasp and satisfy the fast changing needs of the automotive industry, with no time for systematic introduction of new materials and processes.

PRODUCTION PROBLEMS WITH HSLA STEELS - It was realized very quickly in forming parts such as bumpers, bumper reinforcements and brackets that high-strength steels behaved quite differently from mild steels in the stamping press. The high-strength steels had lower formability, which made it difficult to produce parts with the same complexity and quality that were common with plain-carbon steels without altering the die design. Rules of thumb valid for forming mild steel had to be reexamined.

Die and/or part design changes were required, which created turmoil and apprehension in the automotive industry.

The higher strength produced greater elastic springback when HSLA steels were formed. The problem was further compounded by variations in the steels' mechanical properties and chemical composition, which produced varying amounts of springback. Even though the magnitude of property variation relative to the strength level in high-strength steels was not much different from that for plain carbon steels, the lower strength and greater ductility of the latter steels rendered them more forgiving. Furthermore, the HSLA steels had low r-values, did not draw as easily as plain-carbon steels, and also developed large degrees of side wall curl.

Yet, several production parts such as brackets and bumper reinforcements were made with HSLA steels[2]. However, when the need for HSLA steels was not imperative, production problems caused some users to revert back to mild steel, thereby slowing down the introduction of high-strength steels.

These problems brought about the realization that tighter process control was needed in high-strength steel manufacture. This led to vigorous implementation of modern steel making practice, sophisticated instrumentation for inspection and stricter quality control measures at the U. S. steel mills. However, the reduced formability of HSLA steels remained an issue. In order to use high-strength steels successfully for automotive weight reduction, stamping methods had to be modified, part complexity reduced, or steel formability improved. This provided adequate motivation which led to the development of dual-phase steels[3].

EVOLUTION OF DUAL-PHASE STEELS - The development of dual-phase steels was the single most significant achievement in sheet steel development of the 1970's. Originally, these steels were developed to have the same tensile strength as the SAE980X steels(650 MPa minimum tensile strength) but with ductility equal to or better than that of the SAE950X steels(i. e., about 30 % total elongation in a 2 in. gage length). Moreover, to keep the cost down, these steels had basically the same chemical composition as that of plain-carbon steel. Developments occurred simultaneoulsy in the United States and Japan. Essentially, three different types of dual-phase steels evolved.

GM980X, which was developed at General Motors Research Laboratories, is produced by intercritically annealing and slow cooling a steel containing about 0.1 % C, 1.5 % Mn, and up to 0.1 % V as an optional microalloying element[3]. Typically, GM980X has a yield strength of 50 ksi(350 MPa), no yield point elongation, a high work hardening rate, n-value(work hardening exponent) of 0.25, and tensile strength of 90 ksi(650 MPa), Figure 1. Most importantly, the ductility of GM980X was far better than that of prior HSLA steels with similar tensile strength. The higher work hardening rate and ductility promised improved formability, as was experienced.

GM980X was also produced in galvanized form[4]. A modified hot-dip galvanizing cycle was used not only to galvanize the steel but also to produce the dual-phase microstructure and mechanical properties. The modification consisted of a suitable combination of zinc pot temperature, sheet steel immersion time in the pot, and cooling rate. With an ever increasing requirement of corrosion protection, especially for thinner-gage steel parts, this simple and elegant production method was another plus for the steel.

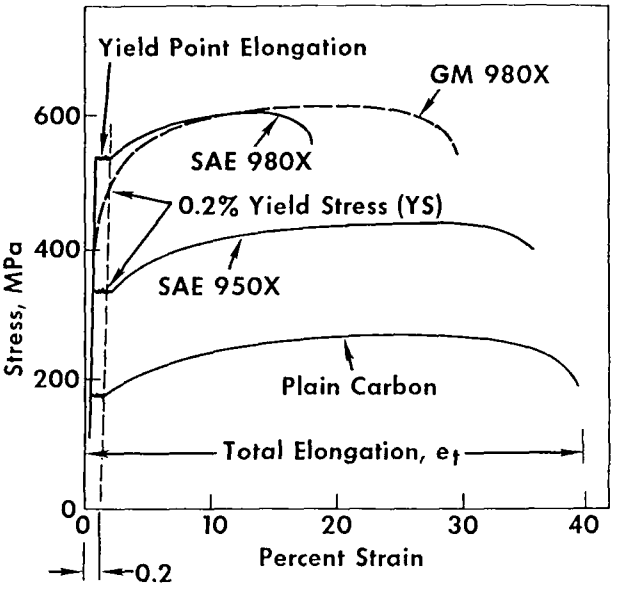


Figure 1. Schematic stress-strain curves for GM980X, SAE980X, SAE950X and plain-carbon steels.

Since continuous annealing lines were not plentiful in the U. S., an alternative method was found for developing GM980X type properties in steels that could be produced "as-rolled" directly off the hot rolling mill rather than by continuous annealing. The as-rolled dual-phase steels were pioneered by Climax Molybdenum Company, who thermomechanically processed steels containing typically 0.06 C, 0.9 % Mn, 1.35 % Si, 0.45 % Cr and 0.35 % Mo in the intercritical temperature range on the hot-rolling mill[5]. The mechanical properties of these steels were generally similar to those of GM980X, even though GM980X had somewhat greater total elongation in tension.

Development of the third type of dual-phase steels occurred in the United States and Japan, but commercialization of the steels has been most active in Japan. This type of dual-phase steel is produced by continuous annealing steels

with less than 0.1 % C and 1.0 % Mn, quenching the steels, and then tempering them to develop the desired combination of strength and ductility[6]. All three types of dual-phase steels, while possessing high tensile strength, exhibited considerably greater ductility and work hardening rate than traditional steels of the same strength levels.

The microstructure of GM980X steel consists of about 5 to 10 % martensite, 10 to 15 % untransformed austenite, and the balance, ferrite[3]. The other two types of dual-phase steels consist of about 75 to 80 % ferrite, with the balance being martensite. The former microstructure appears to be more conducive to improved ductility at the same strength level. This has been attributed, in part, to the more ductile ferrite and the untransformed austenite.

Several versions of dual-phase steels, with similar C, Mn and Si contents but with varying amounts of microalloying elements were produced all over the world to meet the GM980X specification. In addition to substitution of V with Nb, additions of Cr or Mo were utilized to produce dual-phase steels. Several of these steels were made in production quantities and used in production automobiles.

PRODUCTION USE OF DUAL-PHASE STEELS - Forming trials with dual-phase steels were far more successful than with HSLA steels of the same strength level. Almost 80 million GM980X components have been built into General Motors' production automobiles thus far. For example, the steering coupling reinforcement shown in Figure 2 has been produced using hot-dip galvanized GM980X steel since 1975[7]. Previously, the part used to be made by forming plain carbon steel, carburizing to obtain the required strength and durability, and then plating for corrosion protection. The heat treatment and plating steps were eliminated when GM980X was used, with accompanying improvements in productivity and part quality and at lower cost. This part is still in production today.

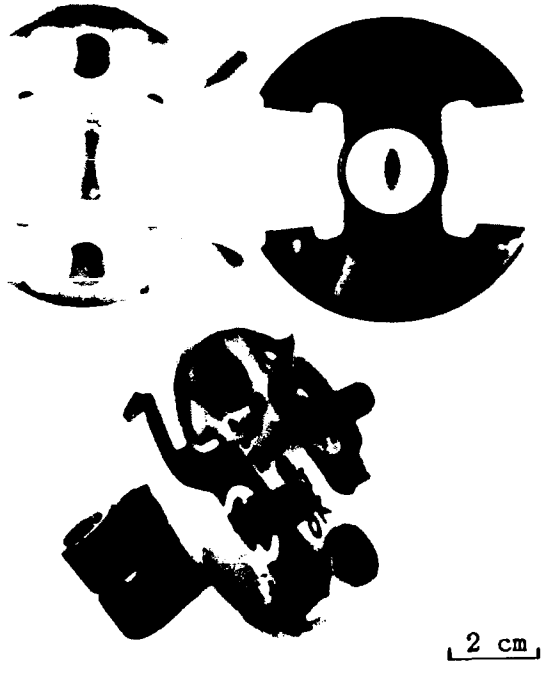


Figure 2. Steering coupling reinforcements made with hot-dip galvanized GM980X dual-phase steel. The two individual and the assembled component are shown.

Other GM980X components produced thus far include bumper face bars, bumper reinforcements, wheel rims and discs, an independent rear suspension control arm, an alternator fan, and an overrunning clutch hub[8, 9]. In addition, several other parts were successfully developed using GM980X, although they were not released for production; they include a stabilizer bar, a water pump pulley, an air cleaner plate, a styled wheel disc, a complete bumper jack, a wiper linkage mechanism, a torque converter housing, a door beam and assorted brackets. All these components were made on production tools which were designed for the much lower-strength, plain carbon steel. The consumption of GM980X dual-phase steel in General Motors reached a peak of about 20,000 tons in one year.

In each preceeding application, weight savings of 25 to 33 % were realized at no extra cost over the plain carbon steel production component. In some instances there was actual cost reduction, even though the dual-phase steel was more expensive than plain carbon steel.

Experimenting with new manufacturing methods led to a pleasant discovery that, in addition to superior formability, GM980X with its unique microstructure also had superior machinability[9]. The clutch hub, shown in Figure 3, required a high-quality surface on the broached splines. The existing manufacturing method involved stamping a plain-carbon sheet steel cup and finish-machining the cup walls, on which the splines were broached. The surface quality of the broached, plain-carbon steel parts was poor, Figure 3A. Galling occurred, and the broach life was unacceptably low. GM980X easily formed the cup. The steel work-hardened to more than 23 HRC, enabling high quality broaching of the splines, Figure 3B. In addition, GM980X produced small chips which did not adhere to the tool and were far easier to clean than mild steel chips. Most importantly, the broach life increased twenty-fold.

LESSONS LEARNED - Much was learned in these production runs about forming high-strength steel. The dies had to be designed for the unique characteristics of the steel, namely, high strength, high work hardening rate and good formability. Forming loads were not much higher compared with plain-carbon steels because of the reduced steel thickness. The high work

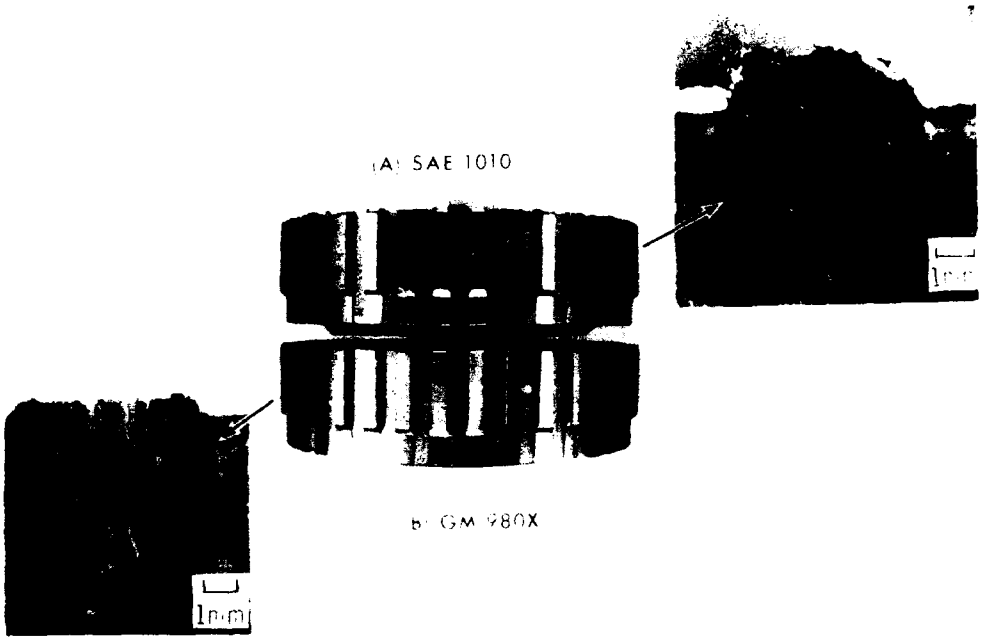


Figure 3. Photographs showing splines in the (A) SAE1010 clutch hub and (B) GM980X dual-phase steel hub. Note the burr and galling at the root of the spline in the SAE1010 hub.

hardening rate reflected good formability, but because of the low(50 ksi, or 350 MPa) yield strength, a suitable amount of plastic strain was required to develop higher strength in the part. The forming sequence had to be such that it would create sufficient strain in those areas of the formed part where the part design called for a strength level higher than 50 ksi. For example, in components such as bumpers and bumper reinforcements which have large, flat or generously curved areas, conventional forming imparts very little strain. For higher strength at these locations, the die would have to be designed such that these areas are strained at least 5 % during forming.

While the high work hardening rate of dual-phase steels improved formability, it also had an unwanted side effect, namely, low ductility of sheared edges, which sometimes caused microcracks to form at these edges, and poor punched hole stretchability[10]. Proper setting of shear gaps, well dressed shear tools and, as a last resort, a shaving tool or reaming the hole, solved the problem.

Lessons were also learned on steel quality requirements. Many of the same problems that hindered the wide-spread use of HSLA steels, namely, variations in composition and mechanical properties also hampered implementation of ingot-cast GM980X and as-rolled dual-phase steels. However, this is not as serious a problem for the low-C low-Mn dual-phase steels currently being produced in modern continuous lines.

The lack of modern steel making and processing technologies were partly responsible for variations in dual-phase steel properties in the 1970's and early 80's. Modern continuous casting and ladle refining technologies had not yet been not widely implemented in the North American steel industry. When ingot cast, the dual-phase steel exhibited a considerable degree of composition segregation due to its relatively high manganese content. This added to the mechanical property variations in the finished steel. Cleanliness of the steel was also a problem. Without ladle refinement to remove sulfur and other undesired elements, the steel microstructure would contain large stringers of manganese sulfide and other inclusions, which contributed to reduced edge ductility.

Lessons were also learned about the preferred mode of interactions among all groups involved in the manufacture of stamped parts. For effective implementation of a new steel, a new process, or a new application, close collaboration is needed among the steel metallurgist, the die designer, the part designer, and the manufacturing engineer. The team should cooperatively identify the most effective and economical forming process and undertake necessary developmental work to "make the steel work" for the part. The new combination of steel and process must be implemented systematically and progressively. The steel supplier must persevere together with the steel user, continuously providing technical support. It is most unfortunate that such collaboration has not always been practiced effectively. As we all know, the need for this "early involvement" of supplier and user has been emphasized publicly by concerned managers in the automotive and steel industries in recent years.

PREDICTIONS OF HIGH-STRENGTH STEEL USAGE - The preceeding production successes invoked steel mill projections of up to one million tons of GM980X per year by 1985, in spite of the fact that GM980X utilization had not been without problems. As recently as 1980, there prevailed an expectation that dual-phase steels would account for about half of the sheet steel content in the automobile body by the end of the decade[11]. It was also predicted that the proportion of high-strength steels would increase by 50 to 150%, to 135 to 270 kg, or about 30 to 50 % of total sheet steels used in an average passenger car by 1990[11]. A recent survey[12] shows, however, that an average 1988 model U. S. passenger car contained a total of about 755 kg of sheet steel, only 14 %, or 105 kg, of which was high-strength steels. Also, there is relatively little dual-phase steel presently used in the automotive industry. The reasons for this are mostly non-technical or too controversial to discuss here.

## THE PRESENT

CURRENT APPLICATIONS - As just mentioned, high-strength steels account for about 14% of the body-in-white of an average 1988 year U. S. passenger car, the most rapid growth in their usage having occurred during 1978-82, Figure 4[12]. It must be noted, however, that, even though the growth rate of high-strength steel usage has slowed down since 1982, continued growth occurred while the weight of the body-in-white underwent a sizable reduction. It is important to note that this increase occurred during a period when gasoline price was predicted to go up, but on the contrary, was quite stable or even went down.

Components currently being made with conventional high-strength steels are mostly strength-limited parts having relatively simple geometries, for example, rail-shaped parts such as door beams, wheels, bumper reinforcements, and an assortments of brackets and mounts. Dual-phase steel parts currently in production include steering coupling reinforcements, an alternator fan, and a wheel spider.

GM980X dual-phase steel is currently being used to make steering coupling reinforcements at GM Saginaw Division and alternator fans in GM Delco-Remy Division. Roughly five million steering coupling reinforcements are produced annually using about 600 tons of hot-dip galvanized GM980X steel. The alternator fan application accounts for another 600 tons. Dual-phase steel wheels are produced in the U. S. for a Japanese automotive company. The steel is a high-alloy, hot-rolled type, imported from Japan. The mechanical properties of the steel meet the GM980X specification.

A noteworthy feature regarding the wheel spider application is that the supplier of the dual-phase steel has been able to meet the tensile strength tolerance of +5 ksi, imposed by

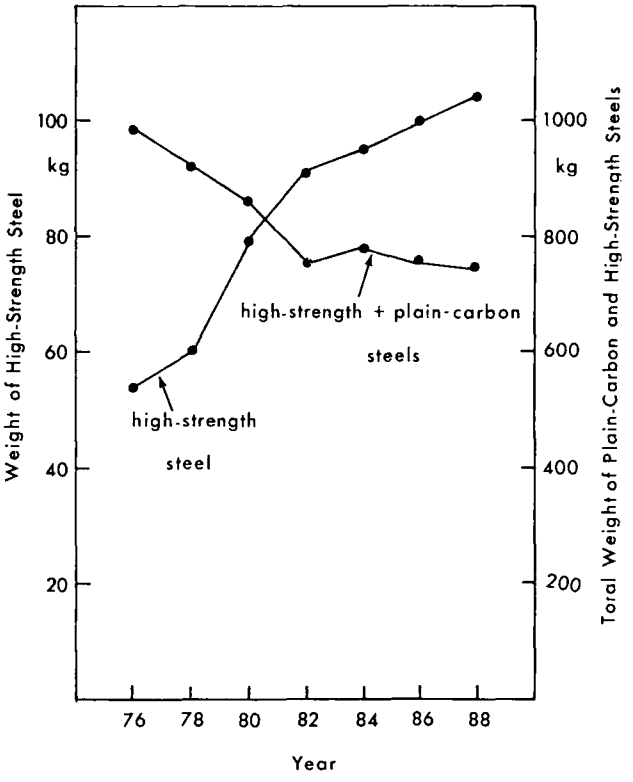


Figure 4. High-strength steel content in the average U. S. passenger car in the past decade[12].

the steel user. Annual consumption of the steel is estimated at 2000 tons. If all steel companies could produce high-strength steels to such a tight mechanical property specification, the usage of these steels would be increased substantially.

It is expected that, with experience being accumulated and advances being made in forming technology, HSLA steels will find more applications in more complex shaped components, and that dual-phase steel usage will grow in stiffness- as well as strength-limited parts. The increase in high-strength steel usage will certainly be accelerated further, should there be another oil crisis in the future.

DEVELOPMENTS IN SHEET STEEL PRODUCTION TECHNOLOGY - The demand from automotive companies for tighter control of mechanical properties of high-strength steels has resulted in sweeping changes at U. S. steel producers in their manufacturing technologies and quality control measures. For example, the steel companies have implemented measures for producing clean, ladle-refined steel. Now commonplace is continuous casting technology, which has markedly improved steel composition uniformity and yield compared with ingot casting technology. Continuous annealing lines have been installed, which enable a large variety of sheet steel to be produced with closely controlled mechanical properties. Savings in

energy and time for heat treatment are also significant advantages with the continuous annealing line compared with the batch annealing method. There are currently only two major U. S. steel companies which have modern continuous annealing lines, but the number is expected to increase. The past decade has also saw extensive use of computers in steel mills to control all phases of steel production and to moniter steel properties and quality.

Past problems arising from variability of mechanical properties and gage thickness of high-strength steels have decreased significantly, as steel companies have implemented measures for statistical process control in all phases of steel production. The result of such efforts can be observed in the recent reduction of gage tolerance for sheet steels imposed by the automotive companies. Until recently, General Motors specified the full AISI tolerance. GM is currently imposing a half tolerance, but already some suppliers are meeting quarter tolerance. Research work at General Motors[13] has shown that seemingly minor variations in forming parameters such as steel sheet gage and blank size exert major influences on the quality of stamped components. Therefore, The reduction in gage tolerance, together with more consistent mechanical properties, will undoubtedly contribute to decreased stamping reject rates and improved, overall quality of stamped components.

DEVELOPMENTS IN SHEET STEEL FORMING TECHNOLOGY - Increasing number of stamping plants are now using transfer presses and stretch-draw operations to form high-strength as well as plain-carbon steels. Whereas the low r-value(drawability) of high-strength steels has often limited the steels' applications, the stretchability is much less of a problem, especially for dual-phase steels. Frequently, however, there may be a viable, alternative forming method for these steels. Consider a process in which the initial step bulges(stretches) the steel blank roughly to the part shape, and following steps introduce the design part shape to the bulged blank using mainly bending and low amounts of stretching, drawing and compressive strains. Forming methods of such variation can open new possibilities for wider application of high-strength steels. The stretch-draw operation will also markedly reduce the degree of elastic springback in the final formed part compared with traditional forming methods. Further popularity of transfer presses at stamping plants is expected to contribute to greater usage of high-strength steels.

The past decade has also seen significant progress in computer assisted techniques for analyzing forming strains, designing and optimizing part shape and forming method. GM Research Laboratories has developed a 3-dimensional finite-element code, named GMFORM. Although not fully developed, simplified versions of the code are already in use. Another development at GM worthy of mention is a computer assisted routine, which simultaneously optimizes the part design and material[14]. Even though this routine has been applied only to simple, channel-shaped components, extended application to complex parts is expected in the near future.

STEEL USER-SUPPLIER PARTNERSHIP - The awareness of the need for early involvement of steel companies in production of automotive components has resulted in the creation of the Auto-Steel Partnership Program(ASPP)[15]. This program stresses full cooperation between the automotive and steel industries in order to enable both industries to remain efficient and competitive in the world market. The ASPP committees consist of representatives from major U. S. automotive and steel companies who handle a variety of important issues such as quality control standards and corrosion tests for galvanized steels. The need for close partnership between the automotive and steel industries is also being emphasized in Europe and Japan[16, 17].

## THE FUTURE

In spite of the rather slow inroads that high-strength steels have made into the automobile body during the past two decades, stamping plants today are far more comfortable in using high-strength steels than at any time in history and are more receptive to trying new steels to replace low-strength steels. The technology of producing parts with SAE950 grade steels is now fairly mature, and future efforts will be directed largely toward using more higher-strength steels. Although current usage of high-strength steels is mostly for strength-limited parts, usage of the steels for stiffness-limited parts is expected in the future.

Predicting the future of HSLA sheet steels in the automobile is quite difficult to do. The amount of high-strength steels used in the automobile body will also depend on the degree of success of competing materials such as aluminum and plastics in replacing steel components. It appears reasonable, however, to say that each material will eventually find its own, deserving level of use, and that high-strength steels will account for a greater portion of the automobile body-in-white than the present level. If asked to make a specific forecast, the authors make the following speculation, realizing fully that the dependability of such prediction is as good as that of a Michigan weather forecast on a given day: 1) The usage of high-strength steels will continue to grow for the next ten years, albeit at a slow rate, to 20 to 25 % of the body-in-white weight. 2) Dual-phase steels will account for about one quarter of the total weight of high-strength steels.

ACKNOWLEDGEMENT

The authors thank Mr. J. E. Hunter for reviewing this manuscript.

REFERENCES

1. F. B. Pickering, Microalloying 75, Symposium Proceedings, 1975, p. 9.

2. F. L. Green, Microalloying 75, Symposium Proceedings, 1975, p. 634.

3. M. S. Rashid, Annual Review of Materials Science, Vol. 11, 1981, p. 245.

4. J. H. Bucher and E. G. Hamburg, SAE Transactions, Vol. 86, No. 1, 1977, p. 730.

5. A. P. Coldren and G. Tither, Journal of Metals, Vol. 30, No. 4, 1978, p. 6.

6. Structure and Properties of Dual-Phase Steels, AIME Conference Proceedings, R. A. Kot and J. W. Morris, Eds., 1979.

7. D. D. Rogers and D. A. Wilkinson, HSLA Steels - Technology and Applications, Conference Proceedings, ASM, 1984, p. 459.

8. M. S. Rashid, SAE Technical Paper 770211, 1977.

9. C. Kim, M. S. Rashid and W. J. Riffe, SAE Technical Paper 840011, 1984.

10. R. G. Davies, Journal of Applied Metal Working, Vol. 2, No. 4, 1983, p. 293.

11. C. L. Magee and R. G. Davies, Alloys for the Eighties, Symposium Proceedings, Climax Molybdenum Company of Michigan, 1980.

12. Metal Working News, Vol. 15, No. 672, Feb. 1988, p. 28.

13. J. Siekirk, Journal of Applied Metal Working, Vol. 4, No. 3, 1986, p. 262.

14. C. Ni, R. J. Yang and J. Zuzelski, SAE Technical Paper #880916, 1988.

15. M. A. Rumel, American Iron and Steel Institute Media Briefing, Feb. 29, 1988.

16. G. M. Davies and S. J. A. Thompson, Steel Times, Vol. 216, No. 4, 1988, p. 180.

17. H. Matsubara, Steel times, Vol. 216, No. 4, 1988, p. 194.

# MANUFACTURING CONDITION AND AUTOMOTIVE USE OF BAKE HARDENABLE STEEL SHEETS

**Kazumasa Yamazaki, Takashi Horita**
Nippon Steel Corporation
Tokai-shi, Aichi, Japan

**Yuuji Umehara, Tadaaki Morishita**
Toyota Motor Corporation
Toyota-shi, Aichi, Japan

ABSTRACT

Bake hardenable steel satisfies the contrary requirements of formability and dent resistance. It has been commercially used since early 1980's, and now accounts for the major portion of the high strength steel used for car bodies.

Bake hardenability is closely related to strain aging. A yield point elongation greater than 0.2% produces a forming defect of stretcher strain. From this point of view no more than 5 kgf/mm$^2$ (49MPa) of bake hardenability is practical. Reduction of gauge was achieved by 0.05mm to 0.1mm for moderate drawing panels such as hoods and doors by using 35kgf/mm$^2$ (343MPa) bake hardenable steel together with various improvements in die design and stamping technologies. Bake hardenability is also effective for parts which need higher deformation starting strength when dynamically loaded. So bake hardenable steels are applied also to structural parts such as members.

Bake hardenable steels help reduce the weight of car bodies.

## INTRODUCTION

Deterioration of panel stiffness and dent susceptibility is an obstacle to the downgauging. The use of high strength steel makes it possible for dent resistance of the panel to be kept unchanged even when its gauge is reduced. But the thinner steel with a higher yield strength can easily cause geometrical surface defects. "Surface warp" emerged as the most critical defect to be solved for successful application of high strength steel. Bake hardenable steel is particularly suited for solving the problem, because it has low yield strength for good shape fixability when stamped and has high yield strength after stamping for good dent resistance.

This concept was unsuccessfully tried to put into practice during the 1960's and the 1970's.(1)(2)(3) Because at that time, rimmed steel was mainly used, in which nitrogen could not be controlled. A forming defect of stretcher strain could not be avoided without the control of dissolved elements. After the 1973 oil crisis, the use of high strength steel in car body production accelerated due to the growing demand for fuel-efficient cars. A great deal of research has been carried out on high strength steel. The concept of bake hardening has become the center of attention again. After a lot of research works on manufacturing and application of bake hardenable steel, it has been commercially used since beginning of the 1980's. The reason its commercial application has been made possible in recent times is that aluminum killed steel and vacuum degassed steel are available at reasonable cost. The use of aluminum killed steel can eliminate a forming problem of stretcher strain and dissolved carbon content can be controlled by vacuum degassing or continuous annealing process. Various improvements were also made in die design and stamping technologies.

This paper describes the current status of bake hardenable steels used in car body production in Japan from the manufacturing and application points of view.

## USE OF BAKE HARDENABLE HIGH STRENGTH STEEL FOR CAR BODIES

High strength steel now accounts for about 30-40% of the total weight of car bodies. The changes in the ratio of high strength steel to cold rolled steel sheet production at Nippon Steel are shown in Figure 1. The use of high strength steel has been increasing steadily year by year. Figure 2 shows the ratio of production of each grade of high strength steel to the total production in 1986 at Nippon Steel Nagoya works, and typical applications. High

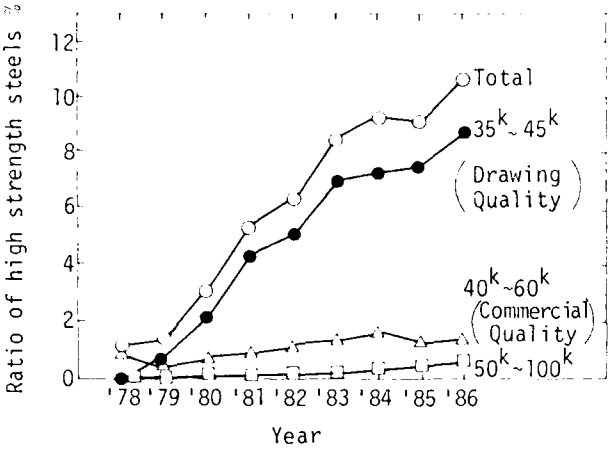


Fig. 1 The changes in the ratio of high strength steel to cold rolled steel sheet production at Nippon Steel

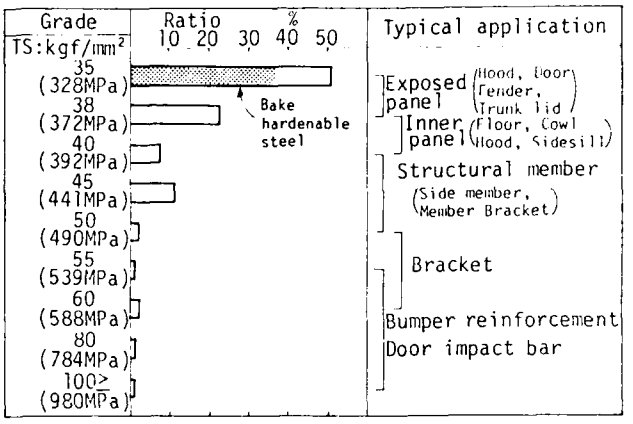


Fig. 2 The ratio of production of each grade of high strength steel to the total production and typical application

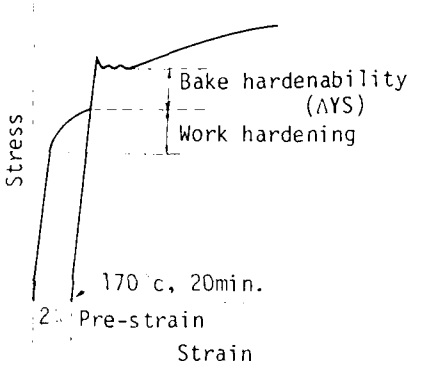


Fig. 3 Schematic stress-strain curve showing the evaluation of bake hardenability

strength steels with tensile strength below 40 kgf/mm² (392MPa) are largely used. These high strength steels are applied to exposed panels moderately drawn such as hoods, doors, and trunk lids, and to inner panels such as floors, cowls and side sills. High strength steels with tensile strength above 40 kgf/mm² (392MPa) are applied to structural parts such as members. And high strength steels with the tensile strength above 60 kgf/mm² (588MPa) are applied to reinforcements such as bumpers and door impact bars.

Bake hardenable steels account for about 45% of the high strength steels at Toyota Motor. Bake hardenable steels are mainly applied to the exposed panels because of the advantage in reduction of gauge and dent resistance. The other application of bake hardenable steel is for members which need higher resistance against a impact load.

## METALLURGICAL FACTORS IN THE MANUFACTURING OF BAKE HARDENABLE STEELS

Bake hardenability is measured as the difference between the flow stress at 2% tensile strain and the yield stress after heat treatment for 20 minutes at 170°C as shown in Figure 3.

Bake hardening is a kind of strain aging and it is caused by dissolved nitrogen and carbon. When nitrogen is used to produce bake hardening, a forming defect of stretcher strain emerges frequently because of its diffusion coefficient several times larger than that of carbon at ambient temperature.(4) Nitrogen produces larger yield point elongation than carbon when the concentration of dissolved nitrogen is equal to that of dissolved carbon. It is considered that nitrogen has larger pinning force of dislocation than carbon at ambient temperature. Today bake hardenable steels are produced from aluminum killed steel, in which nitrogen can be easily precipitated as AlN. Therefore the manufacturing method of bake hardenable steels is nothing but the control of dissolved carbon.

### Effect of dissolved elements and grain size

Figure 4 shows the effect of solute elements and grain size on the bake hardenability of aluminum killed steels with 0.015-0.041% carbon.(5) Though the figure uses the total quantity of carbon and nitrogen as an index for concentration of solute elements, only the carbon was dissolved when (C+N)<15 ppm. Bake hardenability depends upon the grain size as well as the concentration of dissolved carbon and nitrogen. Figure 5 shows the effect of grain size and dissolved elements on bake hardenability more clearly.(5) As the concentration of dissolved carbon becomes very high, the increase in bake hardenability

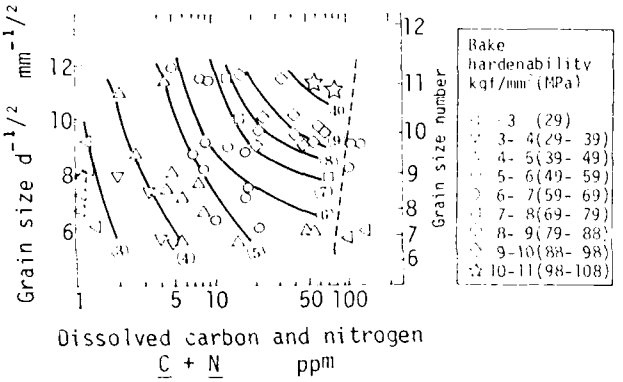


Fig. 4 Effect of grain size and dissolved elements on bake hardenability of aluminum killed steels

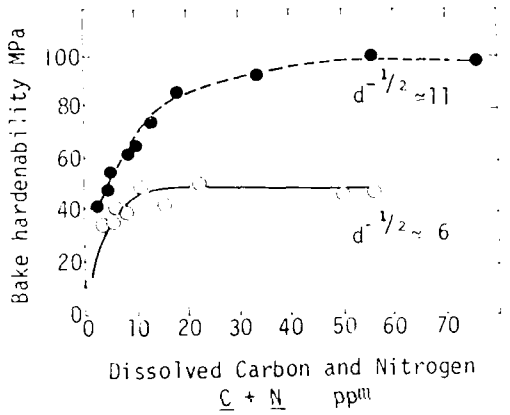


Fig. 5 Effect of grain size and dissolved elements on bake hardenability

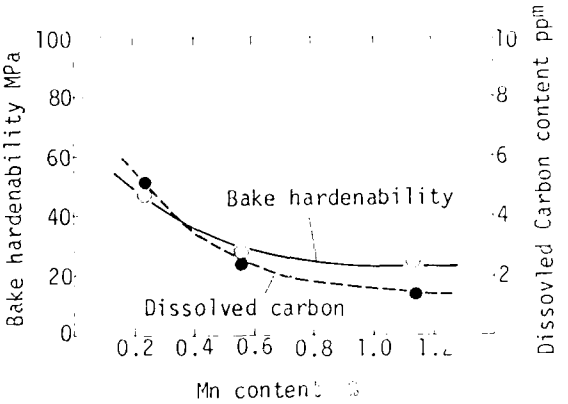


Fig. 6 Effect of Mn content on bake hardenability and dissolved carbon content

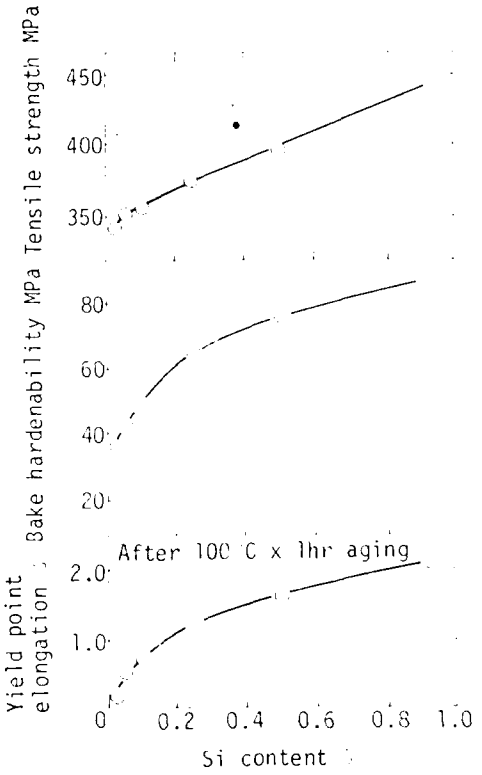


Fig. 7 Effect of Si content on bake hardenability, yield point elongation and tensile strength

reaches a saturation point. The grain size appears to determine the maximum bake hardenability attainable. The smaller the grain size becomes, the higher the bake hardenability. But a maximum of 10 kgf/mm² (98MPa) of bake hardenability is obtainable because the grain size could be reduced practically to as small as eleven in grain size number. The reason why bake hardenability depends on the grain size is not clear, but it is inferred that the influence of dissolved carbon on bake hardenability differs depending on the location of carbon. Different effect of dissolved carbon was reported on the bake hardenability depending on its location, at grain boundary and inside grain.(6)(7)

Effect of manganese

Figure 6 shows the effect of manganese content on the bake hardenability.(5) Manganese reduces the bake hardenability.(5)(8) It has an affinity for carbon and forms a dipole with carbon.(9) Dissolving of manganese into cementite accelerates the precipitation of cementites(10), which reduces dissolved carbon content resulting in lower bake hardenability. Manganese has another disadvantage because it reduces plastic strain ratio.

Effect of silicon

Figure 7 shows the effect of silicon content on the bake hardenability. Silicon enhances the bake hardenability.(5)(8) It is

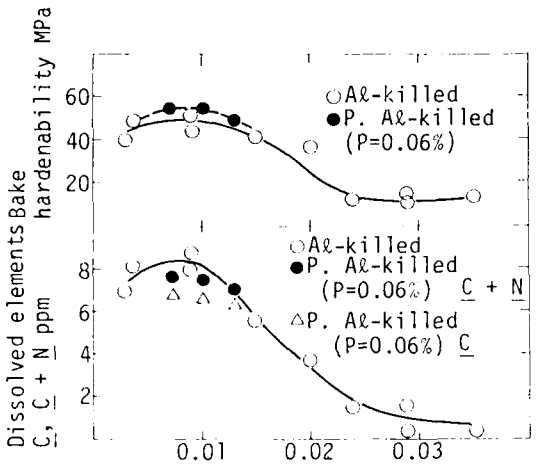


Fig. 8 Effect of carbon content on bake hardenability and dissolved carbon and nitrogen contents

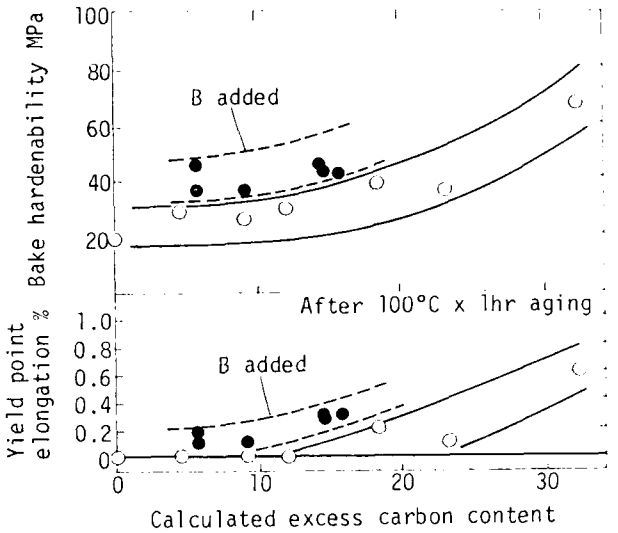


Fig. 9 Bake hardenability of titanium-plus niobium-bearing ultra-low carbon steel with deep drawing quality

repulsive to carbon. Silicon delays the precipitation of cementites because it enhances the activity of carbon around the cementites. Therefore higher bake hardenability is obtained as silicon content increases. But silicon causes higher yield point elongation as compared with its strengthening ability as shown in Figure 7. Silicon is not used for bake hardenable steel as long as steel can be strengthened by other elements.

Effect of phosphorus

Figure 8 shows the effect of carbon content on bake hardenability and dissolved (C+N) content both of low carbon aluminum killed steel and rephosphorized aluminum killed steel.(5) Though (C+N) content does not change by addition of phosphorus, rephosphorized aluminum killed steel shows a little higher bake hardenability. The reason is that rephosphorization reduces the grain size, 8.0 to 9.0 in grain size number in the case shown in Figure 8. Thus the phosphorus contributes to increase in bake hardenability by reducing the grain size. Phosphorus has advantage that addition of it does not deteriorate the plastic strain ratio. So it is used mainly as the strengthening element of bake hardenable high strength steel of drawing quality. But more than 0.1% phosphorus causes strain induced brittleness.

Bake hardenable steel of deep drawing quality

Bake hardenable steel of deep drawing quality is produced from ultra-low carbon steel containing both titanium and niobium.(11) In this steel, all nitrogen is combined with titanium and carbon is incompletely combined with niobium. There remains a small quantity of dissolved carbon unlike the titanium-bearing ultra-low carbon steel in which the titanium is contained to combine all of carbon and nitrogen in it. Titanium- plus-niobium-bearing steel suffers no deterioration of formability when carbon is incompletely combined. Figure 9 shows the bake hardenability of this steel. Boron enhances the bake hardenability of this steel as shown in Figure 9. The reason is not clear, but it is inferred that boron that has affinity for carbon and exists mainly on the grain boundary, attracts the carbon into the grain boundary that is considered a more effective location for carbon existence in bake hardenability than inside the grain.

Relationship between bake hardenability and yield point elongation

Since the bake hardenable steel is applied to exposed panels, it is required to produce no forming defect of stretcher strain. Bake hardenability is closely related to aging at ambient temperature since bake hardening is a kind of strain aging phenomenon. Figure 10 a) is a result of experiment that steels with yield point elongation of 1.5% are formed in various strain conditions to see the surface defects produced. It shows stretcher strain appears when formed lightly and changes to a surface defect called inhomogenious surface roughness is caused as strain is increased further. Both surface defects deteriorates the panel quality after painting. According to Figure 10 b), yield point elongation has to be less than 0.2% for the steel to be used for exposed panels.

Figure 11 shows the relationship between the bake hardenability and the yield point elongation after aging at 100 °C for an

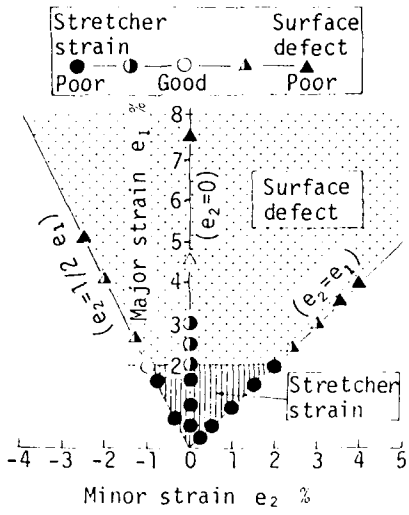


a) Occurrence region of stretcher strain and surface defect on the forming diagram
(Sample A)

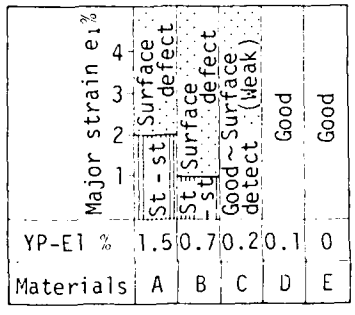


b) Occurrence of stretcher strain and surface defect
(Major strain is equal to minor strain)

Fig. 10 Occurrence of stretcher strain and surface defect

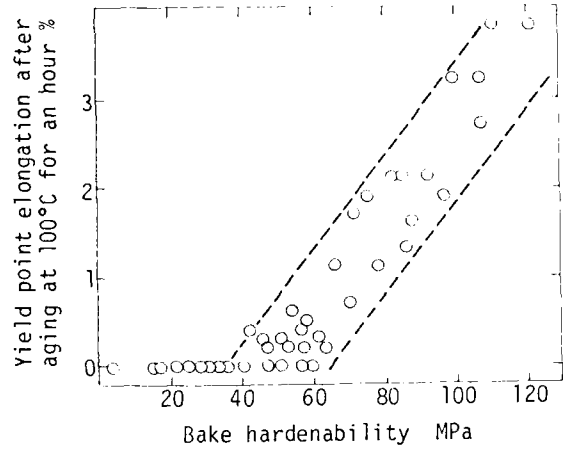


Fig. 11 Relationship between bake hardenability and aging at ambient temperature

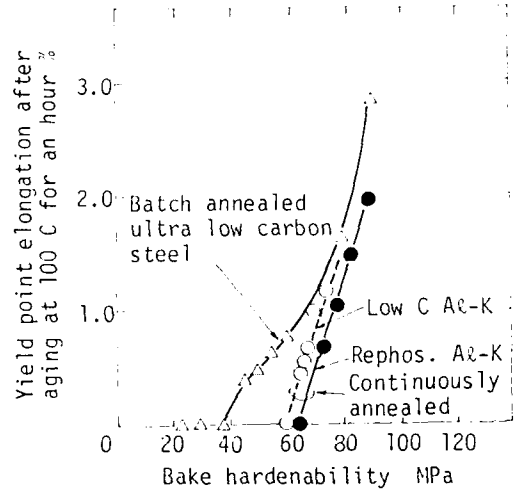


Fig. 12 Effect of annealing condition and carbon content on the relation between bake hardenability and yield point elongation

hour.(12) Since 0.2% yield point elongation is acceptable, no more than 5kgf/mm² (49MPa) of bake hardenability on average is practical.

In order to study about the factors behind the variation of the data in Figure 11, three kind of bake hardenable steels were investigated concerning the relation between bake hardenabily and yield point elongation after aging.(13) According to Figure 12, batch annealed ultra-low carbon aluminum killed steel ( C: 10 to 50 ppm ) shows yield point elongation when bake hardenability is more than 4 kgf/mm²(39MPa), while continuously annealed low carbon steel ( C: 0.04% ) has no yield point elongation until bake hardenability reaches 6 kgf/mm²(59MPa). It is thought as follows. The continuously annealed low carbon steel can be easily induced more dislocations, which suppresses the yield point elongation, than the batch annealed ultra-low cardon steel when they are temper-rolled. It is because the former has smaller grain size and a larger number of finely dispersed cementites resulted from its annealing process. Batch annealling process is not so favourable for producing bake hardenable steel, because carbon content must be reduced to 0.01% level, which makes it difficult to suppress yield point elongation. In continuous annealing process dissolved carbon is controllable even when 0.04% level of carbon is contented.(14)

Production of bake hardenable steels

To control the concentration of carbon, following methods are employed: decreasing carbon content(15), increasing the cooling rate by utilizing the open coil annealing process(16), coasening the cementite by

Table 1 Bake hardenable steels in production at Nippon Steel

| Grade | Annealing | Chemical compositions % | | | | | | | Mechanical properties | | | | | | |
|---|---|---|---|---|---|---|---|---|---|---|---|---|---|---|---|
| | | C | Si | Mn | S | P | Ti | Nb | YS kgf/mm² | TS kgf/mm² | El % | $\bar{n}$ | $\bar{r}$ | WH kgf/mm² | BH kgf/mm² |
| HSS 35BH (DQ) | Batch | 0.017 | 0.01 | 0.23 | 0.010 | 0.072 | - | - | 23 | 36 | 40 | 0.21 | 1.7 | 2.4 | 5.4 |
| | CAL | 0.04 | 0.01 | 0.20 | 0.009 | 0.027 | - | - | 22 | 36 | 43 | 0.21 | 1.5 | 3.0 | 7.0 |
| DQ-BH | Batch | 0.008 | 0.01 | 0.22 | 0.009 | 0.012 | - | - | 17 | 31 | 45 | 0.23 | 1.8 | 2.5 | 5.3 |
| DDQ-BH | Batch | 0.003 | 0.02 | 0.15 | 0.007 | 0.009 | 0.009 | 0.018 | 15 | 29 | 48 | 0.24 | 2.0 | 3.3 | 4.4 |

Gauge: 0.7mm

supercritical annealing or high coiling temperature after hot rolling(15), and appliying continuous annealing process.

Bake hardenable steel with the tensile strength of 35 kgf/mm²(343MPa) is produced commercially at Nippon Steel by combining either vacuum degassed low carbon steel (C:0.01%) with batch annealing process, or conventional low carbon (C:0.04%) with continuous annealing process. The level of 5 kgf/mm² (49MPa) of bake hardenablity is obtained by controlling the content of dissolved carbon at 6 to 8 ppm. As the strengthening elements phosphrus is mainly used. Because silicon is apt to produce yield point elongation, and manganese reduces bake hardenability. Phosphorus shows no deterioration of bake hardenability and plastic strain ratio.

Table 1 lists the bake hardenable steels which Nippon Steel produces(12). Bake hardenable mild steels are also produced commercially and applied to back door for example.

## APPLICATION OF BAKE HARDENABLE STEEL TO CAR BODIES

The gauge of exposed panels is determined by dent resistance and panel stiffness. The reduction of gauge by applying high strength steel is made possible only in the case that the panel gauge is determined by dent resistance. Panel stiffness is pure elastic deformation, while dent resistance is elastic-plastic deformation depends on the yield strength. From the stand point of dent resistance, higher yield strength after forming and baking is desired. But, lower yield strength is better for stamping formability and shape fixability. Therefore the main subject is what degree of yield strength is to be commercially acceptable from both points of shape fixability and dent resistance.

### Dent resistance

Dent resistance and stiffness are important panel qualities to determine the gauge. In case dent resistance is critical, downgauging is made possible by using a steel with high yield strength. Figure 13 shows the relation between dent resistance and panel yield strength for a door panel formed by 400 ton stamping machine at Nagoya R&D Lab. The panel yield strength was measured by the specimen taken from the panel after being stamped. Therefore it represents actual yield strength against which weight is loaded to measure dent depth. The figure indicates about 5 kgf/mm² (49MPa) of increase in panel yield strength enables downgauging from 0.8mm to 0.7mm for that panel. Depth of dent varies depending on dimensions, shape and curveture of panels(17) and different criteria are employed on allowable dent depth for each of the panels. Although relation is different depending on the panels between increase in panel yield strength and reduction of gauge achievable, it is thought in general that panel yield strength is needed to increase by 7 kgf/mm²(69MPa) for the downgauge of 0.05mm to 0.1mm. Because maximum 5 kgf/mm² (49MPa) of bake hardenability is commercially practical as mentioned previously, increase of more than 2 kgf/mm² (19MPa) is necessary in the yield strength before stamping.

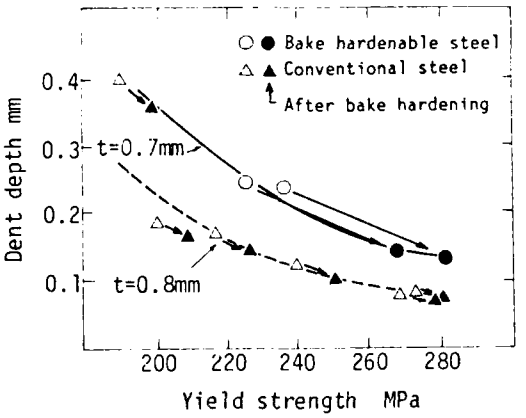


Fig. 13 Effect of bake hardening on dent depth

Bake hardenable high strength steel with tensile strength of 35 kgf/mm² (343MPa) was develoved to meet these requirements. It has yield strength from 20 to 23 kgf/mm²(196 to 225 MPa), 2 to 3 kgf/mm²(20 to 29MPa) up from conventional mild steel for the exposed panel of moderate drawing, and over 5 kgf/mm²(49MPa) of bake hardenability.

Surface warp

Figure 14 shows the typical forming defects by high strength steel used for exposed panels.(18) Surface warp becomes one of the major defects of shape unfixing. Figure 15 shows surface profiles around the hollow for door handle, which were formed from mild steel

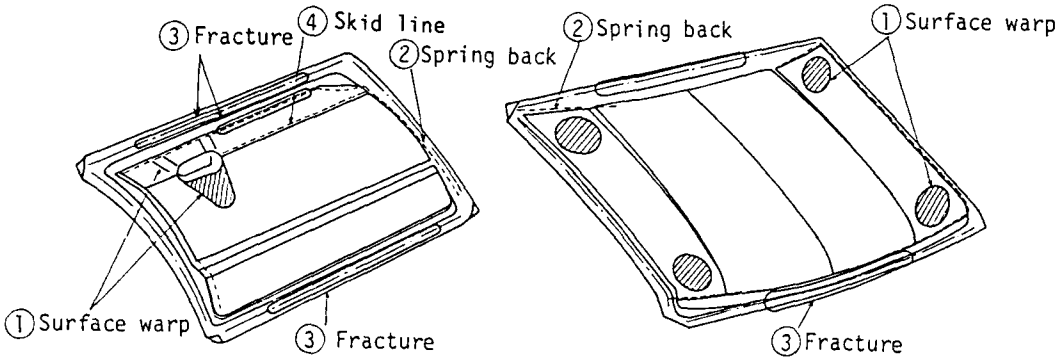


Fig. 14 Typical forming defects of exposed panels

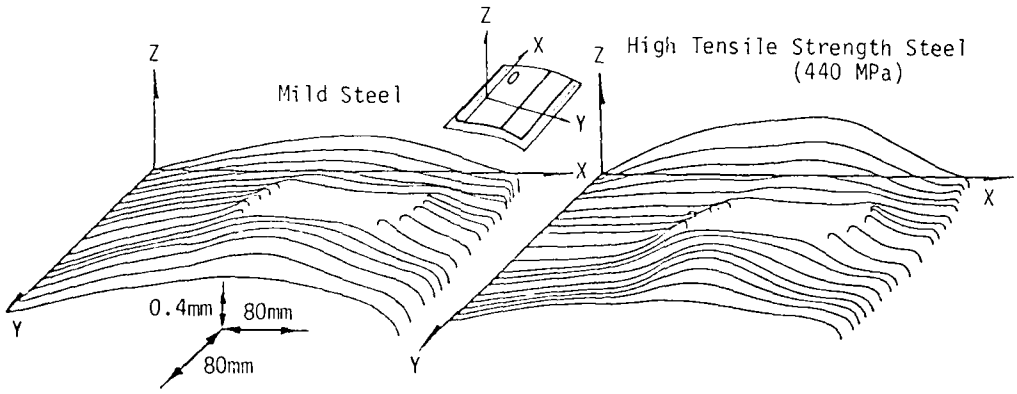


Fig. 15 Phase of surface warp around door handle hollow

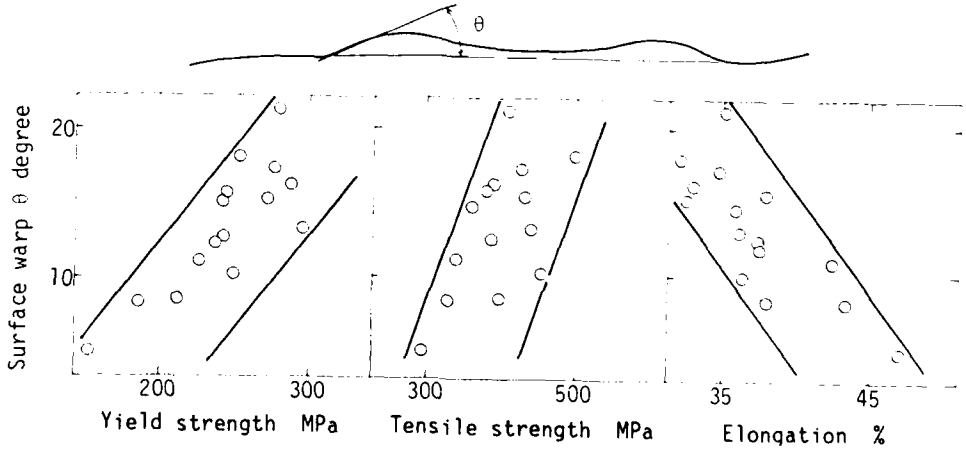


Fig. 16 Relation between surface warp and major mechanical properties

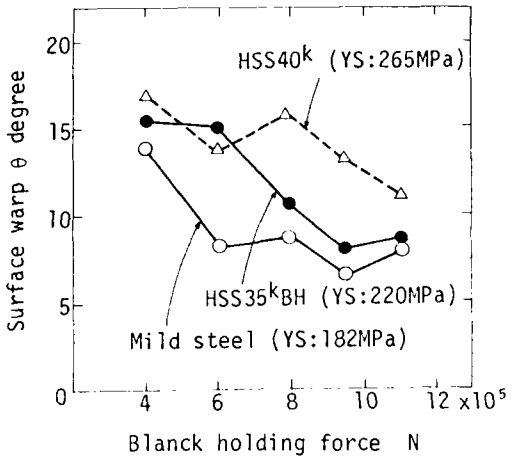


Fig. 17 An example of diminishing surface warp around a hollow for door handle by changing forming condition

and high strength steel with the tensile strength of 45 kgf/mm² (440MPa).(19) It indicates the high strength steel produces larger surface warp than mild steel when formed under the same stamping condition. The relationship between surface warp and mechanical properties was investigated as shown in Figure 16.(19)(20)

Panel quality could be deteriorated in terms of surface warp when mild steel was replaced by 35 kgf/mm²(343MPa) bake hardenable high strength steel because the latter is designed to have higher yield strength than the former as mentioned above. Improvements were made in die design and stamping technology to use the steel with higher yield strength than before. They were focussed on the methods to uniform stress distribution and to minimize localized elastic deformation. An example is shown in Figure 17. High blank holding force can reduce the surface warp. Die design was modified to curb draw-in of flange and to allow uniform strain distribution over the panel.

The 35 kgf/mm²(343MPa) bake hardenable high strength steel is produced to add phosphorus to low carbon or ultra-low carbon aluminum killed steel. Application of aluminum killed steel can improve formability which otherwise deteriorates with increased strength because it has much better formability than rimmed steel which had been used for exposed panel. Moreover, strengthening by phosphorus does not sacrifice drawability. Other production variables are also controlled to improve mechanical properties such as elongation, strain hardening coefficient and aging. The 35 kgf/mm²(343MPa) bake hardenable high strength steel produced today is capable to stand severe stamping condition necessary for prevention of surface warp.

As the results, no more than 23 kgf/mm² (225MPa) of yield strength is acceptable for the exposed panels 35 kgf/mm² (343MPa) bake hardenable high strength steel is applied to. Figrure 18 shows an example of the application of bake hardenable steels to automobile parts at Toyota Motor.

Effect of bake hardenability on structural parts

The increase of yield strength by bake hardenability was also desired to be effective against impact loading. Box-shaped parts illustrated in Figure 19 were examined to clarify the effect of bake hardenability on structural parts. They were loaded dynamically by a weight with the velocity of about 35 km/h. And deformation starting load Ps and absorbed energy Ea were measured as shown in Figure 19. The relationship between deformation starting

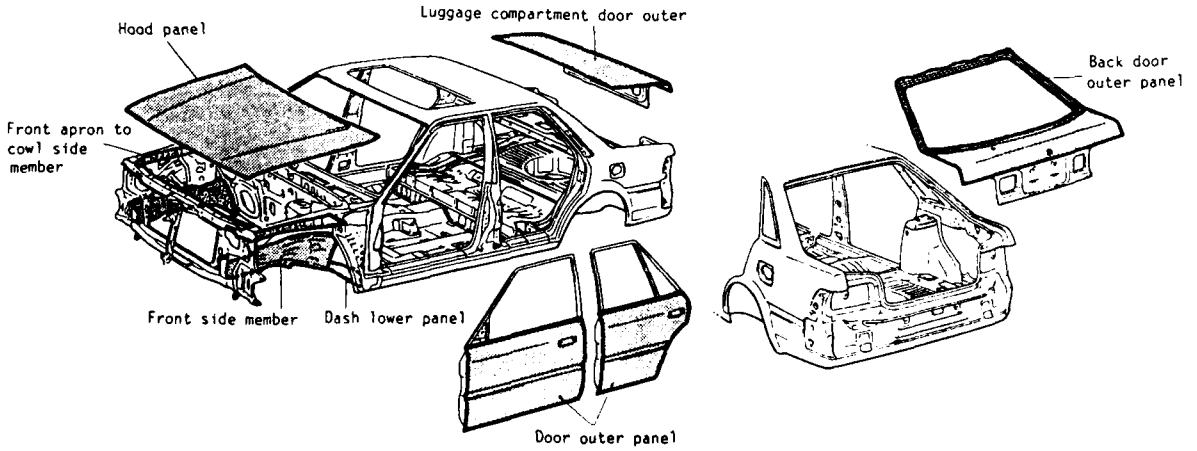


Figure 18 Application of bake hardenable steel to automobile parts

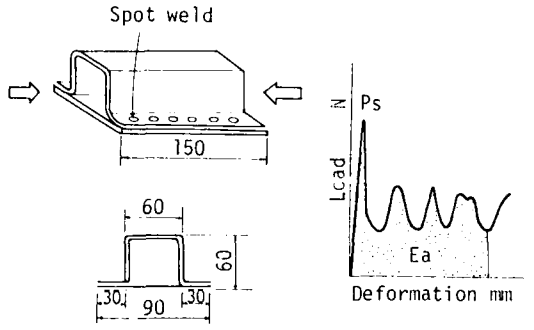


(a) The shape and dimension of crush test structure (b) A load-deformation curve

Fig. 19 Bax-shaped structure and load-deformation curve of crush test

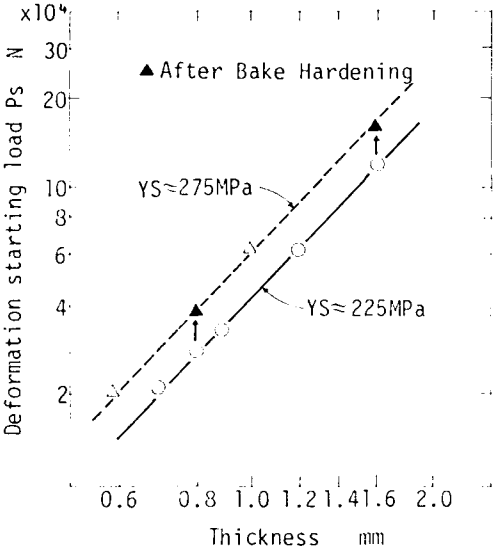


Fig. 20 Relationship between deformation starting load and panel thickness

load Ps and sheet thickness is shown in Figure 20. As previously known, Ps bears the relation with the flow stress at 2 % strain $\sigma_2$ and the sheet thickness t as following equation(21):

$$Ps = K_1 \sigma_2^{0.6} t^{2.0} \quad (1)$$

It was also found in this investigation that deformation starting load was in proportion to $t^{2.0}$. And the increase of deformation starting load by bake hardening was clearly noticed. From this result use of bake hardenable steel had the same effect of reducing gauge by 0.1 to 0.2 mm. But the advantage on the absorbed energy Ea was not recognized. As previously known the absorbed energy is closely correlated with the tensile strength $\sigma_B$ and sheet thickness as the following equation(21):

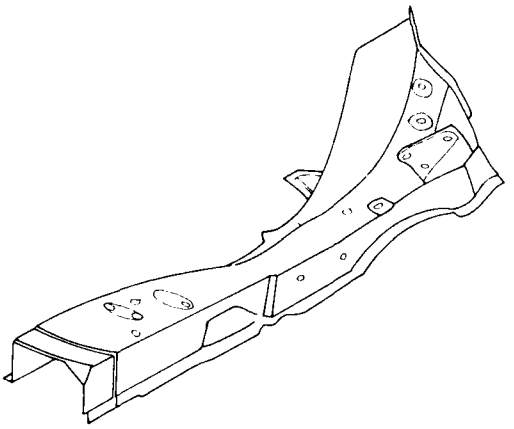

Fig. 21 Front side member-an example for application of bake hardenable steel to the structural part

$$Ea = K_2 \sigma_B^{0.6} t^{2.0} \quad (2)$$

Since the increase of tensile strength by bake hardening is only 1 to 2 kgf/mm² (10 to 20MPa) in the case of 5 kgf/mm² (49MPa) of bake hardenability, it does not contribute to increase in absorbed energy.

In stamping structural parts as well as panels it is difficult to obtain good shape fixability when the steel with higher yield strength is used. For these reasons bake hardenable steels are applied to the structural parts which need high deformation starting strength such as front side member as shown in Figure 21. Examples of the application of bake hardenable steel to structural parts are also shown in Figure 18.

## CONCLUSIONS

Bake hardenable steels has entered main stream of auto production. Several kinds of bake hardenable steel are now in production at Nippon Steel. Metallurgical factors affecting bake hardenability were clarified. The results of research and improvements in steel making technologies made it possible to control the concentration of dissolved carbon at 6 to 8 ppm which produces 5 kgf/mm² (49MPa) of bake hardenability without causing stretcher strain. Today, 20 to 23 kgf/mm² (196 to 225MPa) of yield strength is thought the most appropriate for meeting contrary requirements, formability and shape fixability. Reduction of gauge was achieved by 0.05 to 0.1mm for panels of moderate drawing such as doors and hoods by using 35 kgf/mm² (343MPa) bake hardenable high strength steel which was developed for this usage. Improvements in die design and stamping technologies are also attributable to successful application of the steel.

Bake hardenable steels are also applied to the structural parts such as members in order

to obtain high deformation starting strength.

Bake hardenable steels are successfully used for reducing the weight of car bodies.

REFERENCES


(1) R.D.Butler, J.F.Wallace:Recent Developments in Annealing, I.S.I. Special Report 79, (1963),p131
(2) B.S.Levy: SAE Preprint 720017 (1972)
(3) S.R.Goodman, P.R.Mould: SAE Preprint 790168 (1979)
(4) W.R.Thomas, G.M.Leak: Phil. Mag., 45(1954) p986
(5) S.Hanai, N.Takemoto, Y.Tokunaga, Y.Mizuyama :Trans.I.S.I.Japan, vol.24 (1984) p17
(6) M.Kinoshita, A.Nishimoto: Tetsu-to-Hagane vol.73, no.13 (1987) S1264
(7) M.Kinoshita, A.Nishimoto: Current Advances in Materials and Processes (Report of the I.S.I.J. Meeting) vol.1 (1988) 950
(8) M.Takahashi, A.Okamoto: Tetsu-to-Hagane vol.66 (1980) S367
(9) H.Abe, T.Suzuki, S.Okada: Trans. Japan Inst. Metals vol.25, no.4 (1984) p215
(10)A.S.Keh, W.C.Leslie: Mater.Sci.Res. 1(1963) p208
(11)M.Yamada, Y.Tokunaga, K.Ito: Seitetsu Kenkyu, no.322 (1986) p90
(12)M.Oka, H.Takechi: "Formability and Metallurgical Structure" (Proceeding of the Fall Meeting of the Metallurgical Society) (1986) p83
(13)O.Akisue, S.Ueda, T.Yamada, K.Yamazaki: Tetsu-to-Hagane vol.67 (1981) S462
(14)K.Katoh, K.Koyama, K.Kawasaki: "Technology of Continuously Annealed Cold-Rolled Sheet Steel" (Proceeding of TMS-AIME Fall Meeting) (1984) p79
(15)A.Okamoto, M.Takahashi, T.Hino, S.Nakai: Tetsu-to-Hagane, vol.68 (1982) p1369
(16)S.Nomura, M.Miyahara, Y.Yutori, K.Kameno, I.Kokubo: Tetsu-to-Hagane, vol.68 (1982) p1283
(17)S.Nomura: J.of the Japan Soc. for Technology of Plasticity, vol.24, no.275 (1983) p1244
(18)Y.Umehara, M.Iwasaki: Press Gijutsu,vol.20, 8 (1982) p55
(19)Y.Umehara: Memoires Scientifiques Revue Metallurgie, (1980) p287
(20)H.Ishigaki, Y.Umehara, I.Okamoto: Proc.10th I.D.D.R.G. Congress, Warwick (1978) p53
(21)H.Takechi: SAE Preprint 865053 (1986)

# HOW TO IMPROVE MECHANICAL PROPERTIES OF HIGH STRENGTH STEELS FOR THE AUTOMOTIVE INDUSTRY

**Wolfgang Bleck**
Thyssen Stahl Aktiengesellschaf
Oberhausen, FRG

**Antonio Massip**
Thyssen Stahl Aktiengesellschaf
Duisburg, FRG

**Lutz Meyer**
Thyssen Stahl Aktiengesellschaf
Friedrichsfeld, FRG

**Wolfgang Müschenborn**
Thyssen Stahl Aktiengesellschaf
Dinslaken, FRG

ABSTRACT

The development of high-strength steels with highly uniform properties for use in the automotive industry has become increasingly important.Product and market developments are discussed. Multi-alloying concepts for hot strip steels with Ti, Nb, V, and Zr or Ca are presented. A new Strength-Temperature-Alloy Diagram is introduced, which quantifies the relation between YS, chemical composition, and rolling temperature. Together with coiling temperature control, this permits a reduction of scatter. These techniques can also be applied to the development of normalizing-rolled steels.
The degree of dispersion hardening of microalloyed cold-rolled steels depends both on the degree of cold-reduction and on the annealing cycle and is always lower than in hot strip. Up to a YS of about 350 N/mm² the use of rephosphorized steels is more advantageous, but the specific effect of alloying with P differs according to the steel type and the annealing cycle. Careful consideration of these effects has allowed the production of hot-dip galvanized strip with a min. YS of 260 N/mm² and a standard deviation nearly equivalent to that of DDQ.

IN RESPONSE TO THE INCREASING DEMAND of the automotive industry for HSLA Steels, Thyssen Stahl AG has developed a complete range of hot and cold rolled products paying special attention to reducing the spread of both mechanical and geometrical properties[1,2].

After having satisfactorily solved the problem of optimizing strength and formability through micro-alloying, transformation hardening, dual- and multi-phase structures, extreme desulfurization and other techniques which are now state-of-the-art[3,4], we believe that uniformizing properties is the most important outstanding task in steel development. This has become an acute question because of the introduction in the automotive industry of highly automatized production lines which do not tolerate large variations of properties.

This paper reports on research directed to better understanding how alloy design and production factors can be optimized to increase uniformity of mechanical properties. Although closely connected with this goal, geometrical properties are not considered here. Examples are given of thermomechanically treated hot strip, normalizing-rolled hot strip and high strength cold strip, uncoated and galvanized.

## 1. Products and markets - a Thyssen view

PRODUCTS - Thyssen Stahl AG offers a large variety of high-strength low-alloy steels for cold forming (Fig. 1).

Hot-rolled steels with a minimum YS up to 550 N/mm² are conventional ferritic-pearlitic, thermomechanically (TM) treated strip, and follow closely the German standard SEW 092[5]. For the higher minimum YS up to 750 N/mm² no official standard exists. These steels have structures which vary from a mixture of polygonal ferrite and low-carbon bainite to 100% low-carbon bainite.

SEW 092 also includes normalized steels with a minimum YS up to 500 N/mm² and permits normalizing-rolling as an

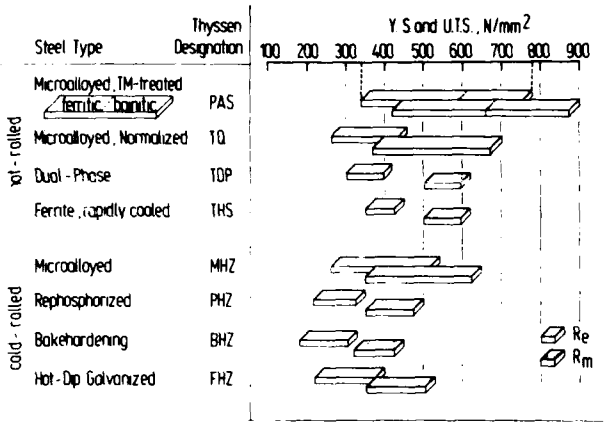


Fig. 1 - High strength steels for cold forming

alternative. This is a difficult task in the hot-strip mill, which has been achieved for the lower range of YS up to and including 380 N/mm² min YS.

Two other types of high-strength steels are also offered for special applications such as wheel disks, namely hot-rolled dual-phase steels and very rapidly cooled steels with a structure of very fine ferrite and degenerated pearlite.

Standard microalloyed cold rolled steels covered in SEW 093[6] (min. YS up to 420 N/mm²) have been available for about 15 years. Other grades with a min. YS up to 500 N/mm² are also produced. Bake-hardening and rephosphorized steels with a min. YS up to 300 N/mm² are standard (SEW 093) and offer enhanced formability. New developments are good formable, non-aging, hot-dip galvanized sheet based on rephosphorized or microalloyed steels.

MARKETS - Market development was different in the last 5 years for hot and cold rolled steels. Hot rolled steels were introduced about 20 years ago and specially in truck construction the advantages which they offer in reducing weight were quickly recognized and put into practice. In the Federal Republic of Germany most truck frames are made today from micro-alloyed HSLA steels either TM treated or normalized (or normalizing rolled). Fig. 2 reflects the typical situation of a mature market: little or no net growth at a relatively high absolute level. But the proportion of the higher strength steels is growing steadily. This is due to increasing experience in fabrication and to the positive results obtained with these materials.

On the other hand, we observe for cold-rolled steels a strong increase in total volume caused by the recent introduction of these steels in light trucks

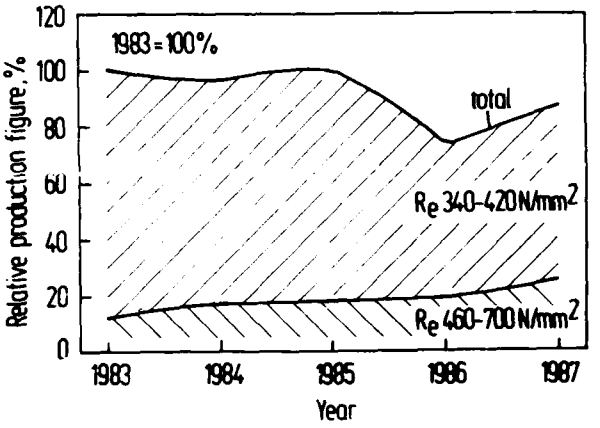


Fig. 2 - Development of production figures for thermomechanically hot-rolled steel

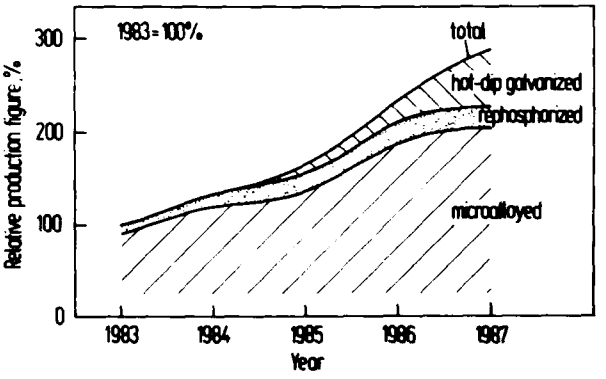


Fig. 3 - Development of production figures for high-strength cold-rolled steel

and in automobiles (Fig. 3). Since 1983 cold rolled microalloyed steels are being used more and more for such parts as pillars and suspensions. In the newest automobiles up to 30% of the weight of the white body are being covered with HSLA steels with YS greater than 260 N/mm². Most recently even parts which involve difficult forming operations are being pressed from high strength steels, and this is the reason for the rising production of rephosphorized and the newer hot-dip galvanized steels. There is also a large increase in the use for outer panels of steels with a YS of about 220 N/mm² and an UTS greater than 350 N/mm², but this will not be discussed here.

## 2. High-strength low-alloy thermomechanically treated steels

High-strength hot-rolled steel strip can be made with microalloying additions of Nb, V , Ti or a combination of these elements, each of which may have particular advantages according to

the alloy design specifications. Ti, for example, is low-priced, binds up N, so that effectively non-aging steels result, and can be added in higher concentrations to give extremely high levels or dispersion hardening This makes it possible to produce steels having a range of minimum yield strength between 340 and 700 N/mm², depending on the Ti content. In addition sulfide shape control is also possible with Ti.

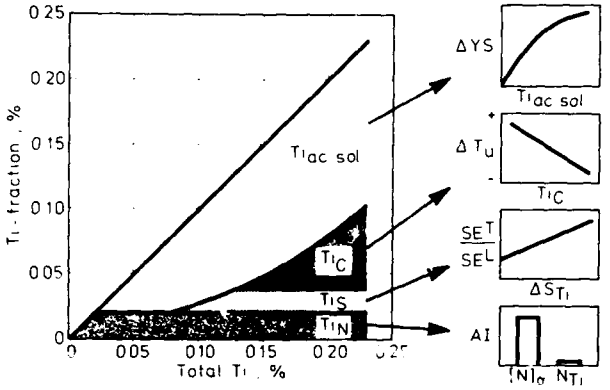


Fig. 4 - Various effects of Ti in TM-treated low-C hot strip steel

Fig.4 shows for a series of thermo-mechanically treated hot strip steels the amount of Ti bound up in different compounds as the Ti content is gradually increased[7]. Until all N is bound up, TiN is formed. Excess Ti above the stoichiometric composition with N appears at first as transformation-induced coherent precipitates, which are responsible for dispersion hardening. This fraction can be separated chemically through selective filtration after boiling 2h in (1+1)HCl[8] [for a similar method see [9]]. Depending on the ratio Ti/Mn, formation of $Ti_4C_2S_2$ begins and is complete at Ti/Mn > 0.125[7,8]. At still higher Ti contents strain-induced TiC may be precipitated during rolling, but this depends on the degree of supersaturation at rolling temperature[10].In particular for bainitic steels, the transition temperature is improved as strain-induced TiC precipitation increases[7].

The multiplicity of effects which is characteristic for Ti may be advantageous for some applications, but on the other hand, if all of this potential is applied, some serious disadvantages may result. For example, variations in the N and S contents may reduce the Ti available for precipitation hardening

$$Ti_{av} = Ti_{total} - 3.4N - 3S - TiC_{strain\text{-}induced}.$$

As a result, large variations in YS and UTS can occur. This can be seen from Fig. 5, which shows the relationship between acid-soluble (Ti+Nb) and strength properties for a steel with a large Ti and a small Nb content. A difference of 0.01% in $Ti_{acid\text{-}soluble}$, which may be provoked by a change of

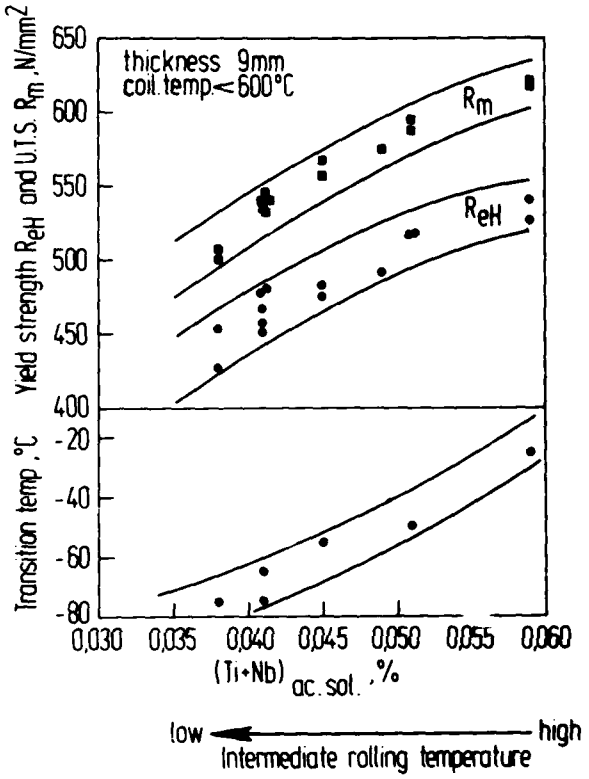


Fig. 5 - Influence of the acid-soluble fraction of micro-alloying elements on mechanical properties

0.003% in S or N, will alter strength by about 35 N/mm². For this reason we prefer to achieve sulfide shape control either through small additions of Zr or through Ca treatment. Larger Zr additions could also bind up all of N, but this is not practicable with continuous casting.

In the above equation the last term corresponds to the strain-induced carbides, which precipitate during rolling and are incoherent after transformation, so that they do not contribute to precipitation hardening, but greatly improve toughness at low temperatures through grain refinement. We support this function through addition of small amounts of Nb.

We have found that under certain conditions we can estimate the amount of strain-induced carbides in hot strip from the ladle analysis and the rolling

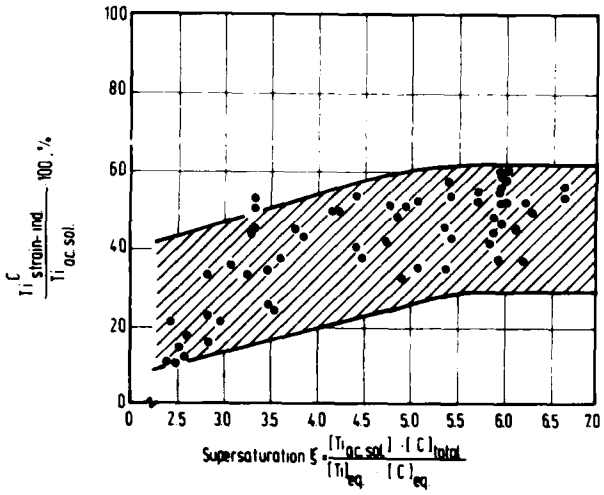


Fig. 6 - Percentage of strain-induced TiC precipitation as a function of supersaturation at intermediate rolling temperature

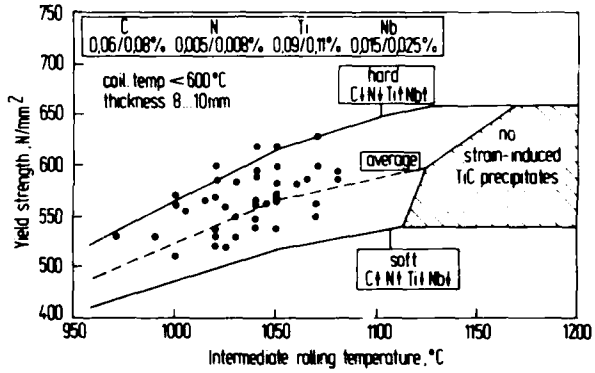


Fig. 7 - Calculated yield strength as a function of intermediate rolling temperature

temperature at the last intermediate stand before entering the finishing train. The solubility limit for TiC is reached at about this point of the rolling process. No strain-induced precipitation can take place before this point, all of it takes place afterwards, and the amount depends on the degree of supersaturation (Fig. 6). This treatment assumes that total deformation, strain rate and temperature at and after the last intermediate stand has reached a steady state in which all relevant parameters are constant. That this is not exactly the case is shown by the broad scatter band in the figure in which the ordinate of the points has been determined through chemical analysis using the following equation:

$$Ti_{strain-induced} = Ti_{total} - 3.4N - Ti_{acid-soluble}.$$

It assumes that all N is bound up by Ti and that S has been eliminated or bound up by other means.

The empirical data collected in Fig. 6 can now be used to calculate the amount of strain induced carbides and therefore the acid soluble content. For this we use the center line of the scatter band in Fig. 6. We can now read the expected YS from a diagram like Fig. 5. In this case we use the *lower* bound of the scatter band, because we need a safety factor to make sure that the somewhat colder edges of the strip also reach the required minimum YS.

Fig. 7 shows the results of this procedure, which we call a Strength-Temperature-Alloy Diagram for a steel with a minimum YS of 500 N/mm². It relates the rolling temperature the last intermediate stand before entering the finishing train to the YS which is to be expected from the hardest and the weakest possible combination of elements within the alloy specification. Since four elements are significantly involved, the probability of reaching such an extreme combination is small, so that the variations of strength due to changes in chemical composition should be contained within the indicated limits. As can be seen, this is indeed the case except for the systematic displacement to higher strengths due to the safety factor discussed above. For the production run documented in this figure, the coiling temperatures were held essentially constant at a level which assures maximum dispersion hardening.

A STAD can be used to determine the optimum rolling temperature at the intermediate stand and also to investigate the effects of changes in chemical composition, but it is not appropiate for control purposes, since the possibilities of regulating the rolling temperatures in the hot strip mill are very limited. Fine tuning of the strength properties to reduce scatter can be more effectively achieved by changing the coiling temperature. Fig. 8 shows how dispersion hardening is reduced with increasing coiling temperature so that the CT can be adjusted to compensate for variations in chemical composition.

To determine how these measures are reflected in production practice, the mechanical properties of a random sample of eight coils from four different melts were examined at five different positions along the strip length, Fig. 9. We can see that consistency of properties over the length of the strips is very good in a given direction, but there is

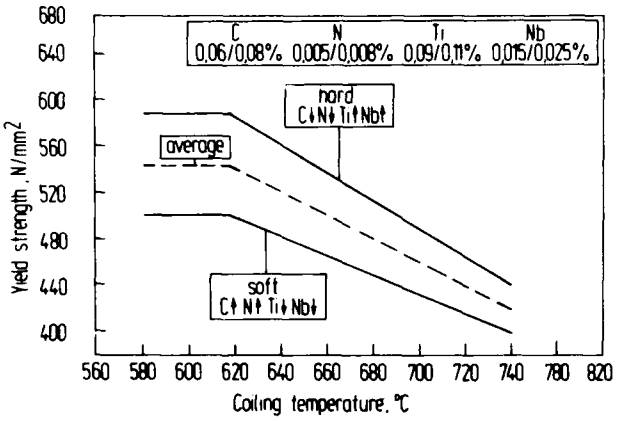


Fig. 8 - Calculated yield strength as a function of coiling temperature

also a systematic difference between longitudinal and transverse YS due to rolling texture. This can be reduced using higher rolling temperatures, but cannot be totally eliminated, which, of course, increases total scatter. Nevertheless, these are highly satisfactory results, if we consider that for higher strength steels, the shape of the STAD is such, that a change in rolling temperature has a much greater effect on mechanical properties than for lower strength steels.

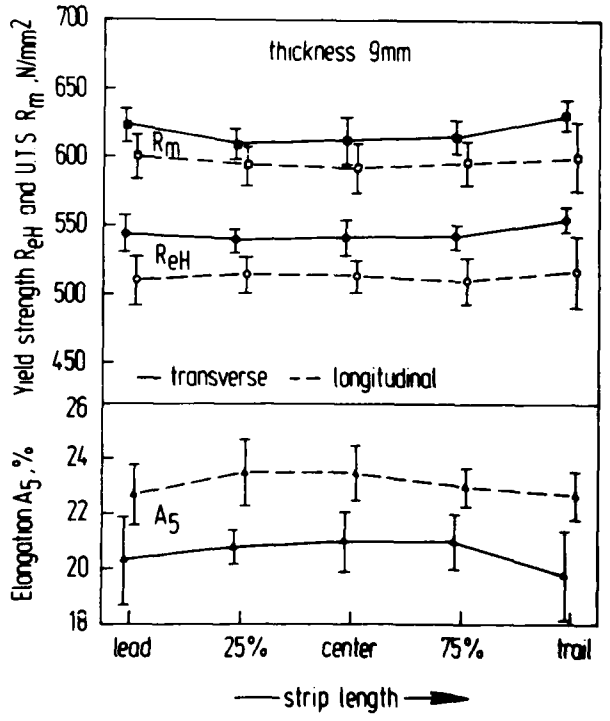


Fig. 9 - Distribution of mechanical properties of thermomechanically hot-rolled steel over strip length

## 3. Normalizing-rolled steels.

The conventional normalizing anneal of HSLA steels can be replaced under specific conditions by an appropiate hot rolling scheme. One advantage of normalizing-rolled steels is that they may be heat-treated at any time, as in repair work, without any great changes in properties. Another is that surface quality in the as-rolled state is much better than after normalizing. Such steels can also be processed directly from the coil.

Normalizing-rolled steels are characterized in a German specification[11] as having a YS in the as-rolled condition which does not differ more than by 60 N/mm² from the YS in the normalized state. This is a difficult condition to meet, especially if account has to be taken of differing degrees of N fixation in the two states. We avoid this problem by adding Ti in slightly overstoichiometric quantities and obtain therefore also a limited amount of dispersion hardening. In addition very small amounts of Nb and some V are added in such proportions that grain size and dispersion hardening of the two states are essentially the same.

With this alloying concept the lines in the STAD are nearly horizontal in the interval of practical rolling temperatures and the limited dispersion hardening in the as-rolled state corresponds very well with the degree of dispersion hardening in the normalized state. Fig. 10 shows a statistical eval-

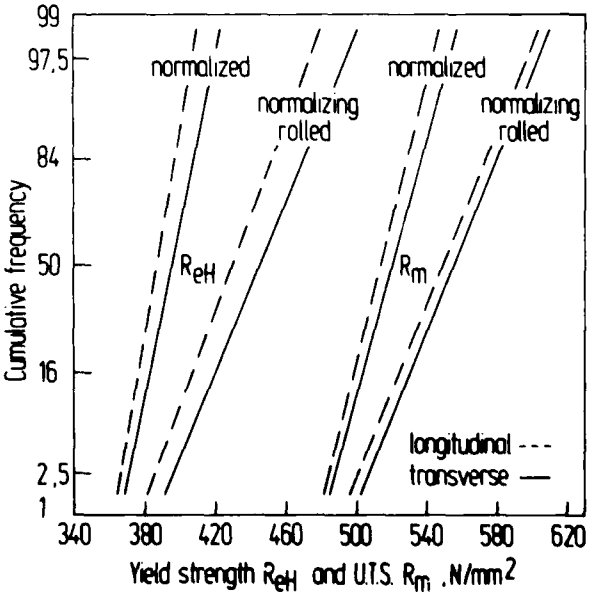


Fig. 10 - Distribution of strength properties for normalizing-rolled steels and subsequently normalized steels

uation of a production run of about 10 000 t of normalizing-rolled steel with a minimum YS of 355 N/mm² in thicknesses between 6 and 8 mm. As can be seen, scatter is greater for the as-rolled state. The difference of the means of YS and UTS between normalized and normalizing-rolled steels is 50 and 32 N/mm² respectively. In a further development of this technique, it was found that after increasing rolling temperatures and simultaneously reducing the cooling rate on the run-out table, the difference in the grain sizes of the two states was considerably reduced. Since the latter measure leads to higher CT, a certain amount of dispersion hardening is eliminated in the coil. This makes it possible to reduce the differences in properties drastically, even to the extent that YS and UTS of the normalized state lie *above* the values for the as-rolled state, Fig. 11.

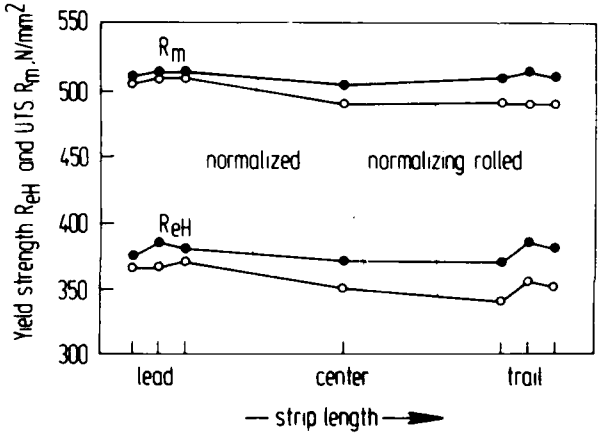


Fig. 11 - Comparison of the strength properties of a normalizing-rolled steel and subsequently normalized steel

## 4. Cold-rolled steels

Besides the factors which have already been discussed - chemical composition and control of rolling and coiling temperatures - other important parameters have to be considered in the production of cold-rolled high-strength steels. They are, first of all, the degree of cold reduction and annealing temperature.

Cold-rolled microalloyed steels have a much lower degree of dispersion hardening than hot rolled steels. The reason for this is the coarsening of the coherent precipitates during annealing. Using the annealing process during continuous hot-dip galvanizing as an example, we can see from Fig. 12 that

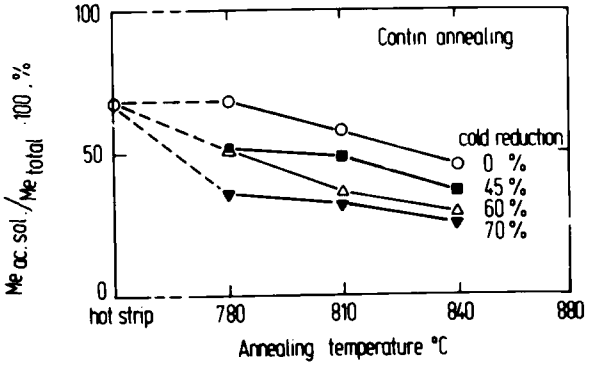


Fig. 12 - Reduction of acid-soluble micro-alloying elements

the content of acid-soluble microalloying elements decreases as the annealing temperature increases[12]. This is a direct consequence of the reduction of the amount of very fine precipitates through coarsening, since only these fine precipitates are acid-soluble. Cold reduction also affects precipitation hardening, because a higher dislocation density accelerates diffusion and particle coarsening. The strengthening effect of microalloying elements in cold-rolled steels depends, therefore, only to a small degree on dispersion hardening and is based instead on the extremely strong grain-refining effect, which is nearly independent of the degree of cold-reduction.

However, the degree of cold-reduction has great importance in how it affects the degree of recrystallisation of microalloyed steels. Depending on the specific steel composition of HSLA-steels, recrystallization kinetics may create strength variations in the annealed condition. This is demonstrated by a HSLA/ Ti+Nb steel (0.06% C, 0.90% Mn, 0.02% Nb, 0.08% Ti), which exhibits a very sluggish recrystallization (Fig. 13). Both under batch-annealing and continuous-annealing conditions, different strength levels can be realized, depending on the selected temperature. Strength levels above the as hot-rolled condition indicate, that recrystallisation has been substantially retarded. Even in the case of high annealing temperatures, cold-reductions above 30% are necessary to produce significant recrystallisation effects. Only an exact knowledge of the interaction between cold-reduction and annealing cycle can provide procedures for a successful production. In the manufacture of high-strength, highly formable continuous

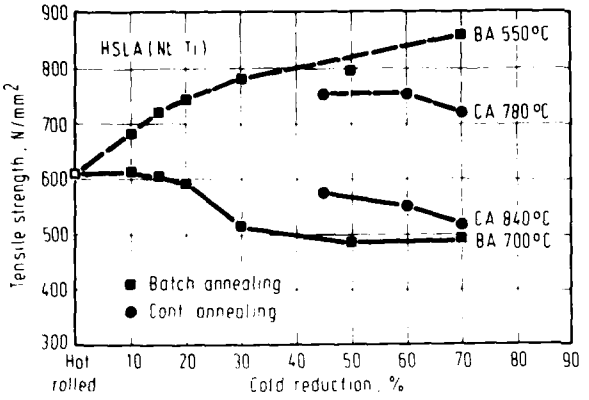


Fig. 13 - Influence of cold reduction and annealing cycle on tensile strength of cold-rolled HSLA steel

hot-dip galvanized steels, for example, there are limits to the process parameters which must be controlled, if we are to achieve a given combination of properties. With increasing Nb-content strength increases and recrystallisation temperature also, as can be seen from the right boundary of the shaded field in Fig. 14[13]. On the other hand, at extremely high annealing temperatures a reduction of dispersion hardening results which above 800° C is unacceptably high. Both of these boundaries, specially the one between the fully recrystallized and the partially recrystallized fields, can be moved by changing the degree of cold-reduction.

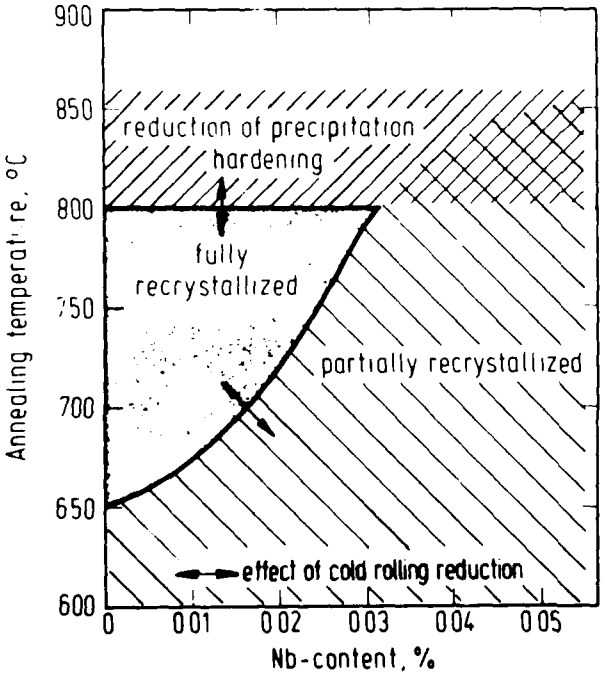


Fig. 14 - Limits for continuous annealing of Nb-microalloyed steels

Because of these problems, we use rephosphorized steels for the production of continuous hot-dip galvanized steels

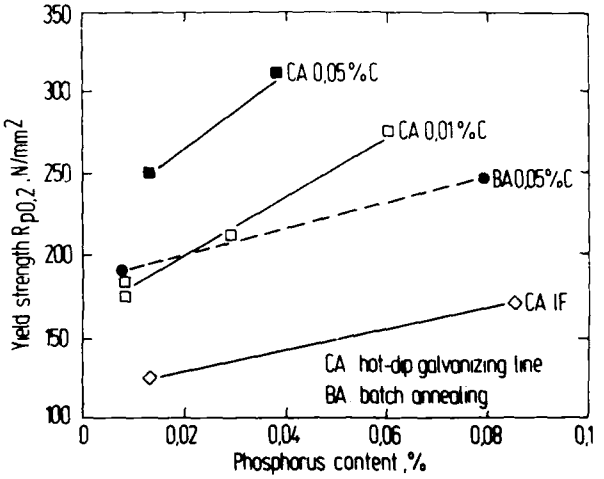


Fig. 15 - Influence of P-content on yield strength of cold-rolled strip

with a minimum YS up to 350 N/mm². These steels were originally developed for batch annealing so that a considerable amount of know-how was available. Nevertheless, we found that the hardening effect of phosphorus differs not only between batch annealing and continuous annealing but also for different grades of steels (Fig.15). For example, it is found that batch annealed cold-rolled strip undergoes a yield strength increase of about 7.5 N/mm² for every 0.01% of added P. A comparable value is determined following annealing in a continuous furnace comprising in-line overageing. However, the yield strength increase is greater following hot-dip galvanizing and subsequent overageing in a batch annealing furnace. We suspect that this is attributable to an interaction of P and C which leads to a finer precipitation distribution of carbides. The solid solution hardening effect of P in continuous annealed IF-steel is comparable to batch annealed steels, which is consistent with this explanation.

Using this physical-metallurgical information it is possible to achieve a more efficient control of the manufacturing process to reduce the scatter of properties. This is necessary in order to increase the use of these steels beyond the level reached up to now. High-strength, continuously hot-dip galvanized steels are used in cars not only to reduce weight but also because of their superior corrosion resistance. Besides a high level of surface quality, fabricators are demanding much narrower

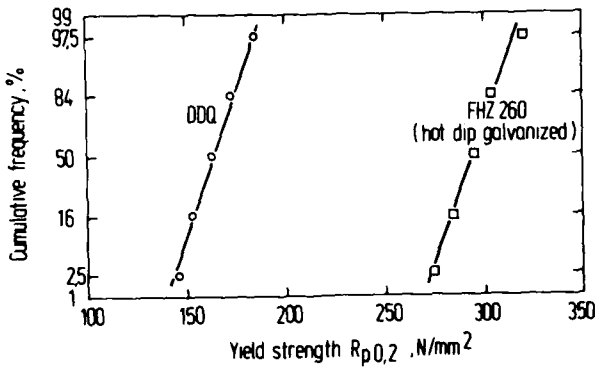


Fig. 16 - Yield strength distribution of mild steel DDQ and of hot dip galvanized high strength steel FHZ 260

limits for mechanical properties than heretofore. The hot-dip galvanized steel which at present is most used in Europe has a minimum YS of 260 N/mm² and can be produced after an optimizing phase with a standard deviation of the YS which is nearly equal to the standard deviation of DDQ steels (Fig.16).

## CONCLUSIONS

1. With multi-alloying in Ti steels it is possible to reduce the alloying functions of Ti, so that scatter of properties is diminished.
2. The development of Strength-Temperature-Alloy Diagrams allows the selection of the optimum rolling temperature for a steel of given composition. Small variations in composition can be compensated by changing the coiling temperature to adjust dispersion hardening.
3. Both the degree of cold-rolling and the annealing temperature affect the degree of recrystallisation and the loss of dispersion hardening through particle coarsening. Control of these two factors reduces scatter.
4. Adapting the P-addition to the annealing process and the steel type permits the production of hot-dip galvanized sheet with a minimum YS of 260 N/mm² and a standard deviation nearly equivalent to that of DDQ.

## REFERENCES


1. Bleck, W., Bode, R. and O. Maid, Thyssen Technische Berichte 18, 167-176 (1986).
2. Massip, A., and U. Schriever, Thyssen Technische Berichte 18, 207-222 (1986)
3. L.Meyer, Thyssen Technische Berichte 14 48-65 (1982).
4. Haastert, H.P., Metzing, J. and J. Wolf, Thyssen Technische Berichte 14, 1-10 (1982).
5. Stahleisen Werkstoffblatt 092,VDEh, Düsseldorf, W. Germany (1982).
6. Stahleisen Werkstoffblatt 093, VDEh, Düsseldorf, W. Germany (1987).
7. Massip, A. and L. Meyer, Stahl und Eisen, 106, 115-124 (1986).
8. Massip, A. and L. Meyer , Proceedings of the 4th International Conference " Residuals and trace elements in iron and steel ",p.275-278, Ljubljana, Yugoslavia (1986).
9. Kawamura, K., Watanabe, S., Uchida, T., and T. Suzuki, Tetsu-to-Hagané, 60, 656 Lecture 318 (1974).
10. Massip, A. and L. Meyer, Revue de Métallurgie-CIT, 84, 317-325 (1987).
11. VdTÜV-Merkblatt 1263, March 1976.
12. Bleck, W., Müschenborn, W. and L. Meyer Steel Research, 59 to be published (1988).
13. Bleck, W. and H.T. Junius,in "Annealing Processes - Recovery, Recrystallisation and Grain Growth", editors N. Hansen, D.Juul Jensen, T. Leffers, B. Ralph, published by Risø National Laboratory, Denmark.

# HIGH-STRENGTH COLD-ROLLED SHEET FOR AUTOMOBILES

**Kennet Olsson, Karl-Inge Nilsson**
*Swedish Steel Strip Products*
S-781 84 Borlänge, Sweden

ABSTRACT

A range of niobium microalloyed high-strength steel grades for production of cold-rolled continuously annealed steel sheet has been developed. The steel grades involved are ultra low carbon rephosphorized steels, precipitation-strengthe ned steels, and dual phase steels. The ultra low carbon rephosphorized steels are superior in deepdrawing and stretchforming which means they can easily replace mild steels. The precipitation- strengthened steels have the advantage of very uniform mechanical properties and excellent bendability. With the dual-phase steels very high strength levels can be achieved. All grades have special applications in the automotive industry from outer body panels to bumper reinforcements and door impact beams.

HIGH-STRENGTH COLD-ROLLED steel sheet is used for automotive application mainly because weight reduction is important for reduction of fuel consumption. At the same time as the weight of a component can be reduced its strength is increased which makes it possible to meet tougher safety standards.

When a mild steel grade is replaced by a high-strength steel grade formability and weldability of the high-strength steel must be good enough to make the part. The new way to increase formability and weldability of high-strength steel sheet is to produce the sheet by continuous annealing. An excellent annealing temperature control and a short annealing time makes it possible to produce high-strength steel sheet with very uniform mechanical properties and leaner alloying contents which improves weldability (1-7).

At SSAB microalloying with niobium has been used for development of ultra low carbon rephosphorized steels, precipitation strengthened steels, and dual-phase steels.

In the ultra low carbon rephosphorized steels niobium is used to stabilize carbon as niobium carbides. These steels have excellent deep drawability (8-10). Yield strength levels of produced steel grades are 220 MPa and 260 MPa. These grades can be used for exposed and nonexposed components when formability demands are almost equal to the level of mild DDQ steel.

In order to increase the yield strength to a minimum value ranging from 280 MPa up to 420 MPa niobium is used for precipitation-strengthening and grain refinement. These steels are excellent in uniformity compared to conventional batch-annealed steels which makes them very useful in the forming of beams and other structural members where variations in springback has been a great problem in the past.

To reach the yield strength level 550 MPa niobium microalloying is used for precipitation-strengthening and grain refinement in combination with a dual-phase microstructure. This steel has been developed for safety components like door impact beams and bumpers. Bendability has been reported to be improved by the microalloying compared to nonmicroalloyed grades of the same strength level (11).

This paper describes the relationsships between processing, microstructure, and mechanical properties for the different types of microalloyed high-strength cold-rolled steel sheet produced at SSAB. Results are reported from both laboratory annealing experiments and full-scale commercial production.

## MANUFACTURING PARAMETERS

The processing which is schematically shown in Fig. 1 involves steelmaking, hot-rolling, cold-rolling, and continuous annealing in a water-quenching type NKK CAL.

CHEMICAL COMPOSITION - The chemical base composition is shown in Table 1.

*DOCOL 220 RP-X and DOCOL 260 RP-X are re*phosphorized steels with ultra low carbon content which is achieved by RH degassing. The higher yield strength in the grade DOCOL 260 RP-X is obtained by an increased solid solution

Table 1 - Chemical Base Composition in Weight-%

| Grade | C | Si | Mn | P | S | Al | Nb |
|---|---|---|---|---|---|---|---|
| DOCOL 220 RP-X | 0.003 | 0.01 | 0.15 | 0.070 | 0.010 | 0.040 | 0.025 |
| DOCOL 260 RP-X | 0.003 | 0.01 | 0.30 | 0.090 | 0.010 | 0.040 | 0.025 |
| DOCOL 280 YP | 0.05 | 0.01 | 0.40 | 0.010 | 0.010 | 0.050 | 0.020 |
| DOCOL 350 YP | 0.05 | 0.20 | 0.40 | 0.010 | 0.010 | 0.050 | 0.030 |
| DOCOL 420 YP | 0.05 | 0.40 | 1.00 | 0.010 | 0.010 | 0.050 | 0.040 |
| DOCOL 550 YP | 0.12 | 0.50 | 1.50 | 0.010 | 0.002 | 0.050 | 0.030 |

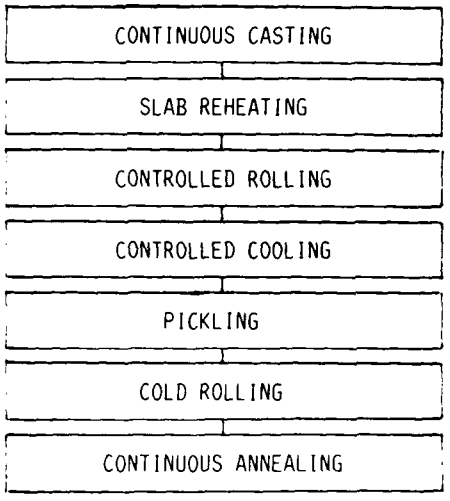


Figure 1 - Manufacturing steps for continuously annealed steel sheet.

hardening by manganese and phosphorus. Nb microalloying is used for stabilizing of C.

DOCOL 280 YP, DOCOL 350 YP, and DOCOL 420 YP are low carbon aluminium or silicon-aluminium killed steels which are grain refined and precipitation hardened by niobium microalloying. Silicon and manganese are used for solid solution hardening in addition to the precipitation hardening effect by niobium.

DOCOL 550 YP is a silicon-aluminium killed and niobium microalloyed steel with increased contents of carbon and manganese. This steel is a dual-phase steel which is precipitation hardened by niobium precipitates to increase the yield strength and refine the grain size. The increased manganese content is intended for further grain refinement and increased hardenability to cause a dual-phase microstructure of precipitation hardened ferrite and martensite. Sulphur content is kept low for increased formability in bending.

HOT-ROLLING - Hot rolling temperatures are listed in Table 2. The DOCOL RP-X grades are reheated at 1250°C, followed by high finishing and coiling temperatures which is favourable for precipitation of aluminium nitrides and niobium carbides. The stabilizing of nitrogen and carbon is important for the deep drawability. The hot-band thickness is between 4.2 mm and 4.5 mm depending on steel grade for a final cold-rolled thickness of 1.50 mm.

In the case of the DOCOL YP grades, reheating at 1250°C is necessary to be sure that all niobium precipitations in the cast slabs are dissolved. The finishing temperature interval 830-900°C is intended to be as low as possible in the austenite region to nucleate a ferrite grain size after recrystallization which is as fine as possible. The coiling temperature 600°C is found to be most effective for precipitation of niobium carbonitrides. For a final cold-rolled thickness of 1.50 mm, the hot-bands are rolled to a thickness between 3.4 mm and 3.6 mm depending on strength level.

COLD-ROLLING - After removal of the oxide scale the hot-bands are cold-rolled in a five-stand tandem mill with a six-high final stand. Cold reductions are listed in Table 3. The difference in cold reduction between the different grades depends on a difference in hot-band strength. The cold reduction should be as high as possible because the $\bar{r}$-value of the DOCOL RP-X grades and the final grain size of the DOCOL YP grades (3) after recrystallization are strongly dependant on this parameter.

Table 2 - Hot-Rolling Temperatures

| Grade | Reheating temp. (°C) | Finishig temp. (°C) | Coiling temp. (°C) |
|---|---|---|---|
| DOCOL RP-X | 1250 | 860-940 | 730 |
| DOCOL YP | 1250 | 830-900 | 600 |

Table 3 - Cold Reductions

| Grade | Cold reduction (%) | Cold rolled thickness (mm) |
|---|---|---|
| DOCOL 220 RP-X | 67 | 1.50 |
| DOCOL 260 RP-X | 64 | 1.50 |
| DOCOL 280 YP | 58 | 1.50 |
| DOCOL 350 YP | 58 | 1.50 |
| DOCOL 420 YP | 57 | 1.50 |
| DOCOL 550 YP | 57 | 1.50 |

Table 4 - Continuous Annealing Temperatures

| Grade | Annealing temp. ($^{o}$C) | Quenching temp. ($^{o}$C) | Overaging temp. ($^{o}$C) |
|---|---|---|---|
| DOCOL RP-X | 830 | 530 | 200 |
| DOCOL 280 YP | 750 | 570 | 400 |
| DOCOL 350 YP | 750 | 570 | 400 |
| DOCOL 420 YP | 750 | 570 | 400 |
| DOCOL 550 YP | 800 | 780-800 | 300 |

CONTINUOUS ANNEALING - Typical continuous annealing temperatures are shown in Table 4. The annealing temperature is high for the DOCOL RP-X grades, 830$^{o}$C, because a high annealing temperature results in a high r-value. As almost all carbon is stabilized by niobium the overaging temperature can be kept low, 200$^{o}$C, for these grades.

The precipitation strengthened steels DOCOL 280 YP, DOCOL 350 YP, and DOCOL 420 YP are typically annealed at 750$^{o}$C/2 min. to get a recrystallized ferrite after cold-rolling. The annealing is followed by air-cooling down to 570$^{o}$C, water-quenching, and overaging at 400$^{o}$C/2 min. The overaging treatment is used to precipitate solute carbon from the ferrite matrix which increases the aging resistance.

In the case of the dual-phase steel DOCOL 550 YP annealing is typically performed at 800$^{o}$C/2 min. to create a dual-phase microstructure of ferrite and austenite. The austenite is transformed to martensite during water-quenching from a temperature as near the annealing temperature as possible. The overaging treatment is 300$^{o}$C/2 min. At this temperature the solute carbon in the ferrite is decreased and the martensite becomes softer which increases both ductility and bendability (11).

The two different thermal profiles used for laboratory simulation of the continuous annealing process are schematically shown i Fig. 2. The important parameters are annealing temperature, $T_A$, quenching temperature, $T_Q$, and overaging temperature, $T_{OA}$.

The temperatures n the full scale continuous annealing line have been determined from the laboratory annealing results. The air cooling between annealing temperature and water-quenching temperature is in full scale annealing replaced by gas-jet cooling with almost the same cooling rate.

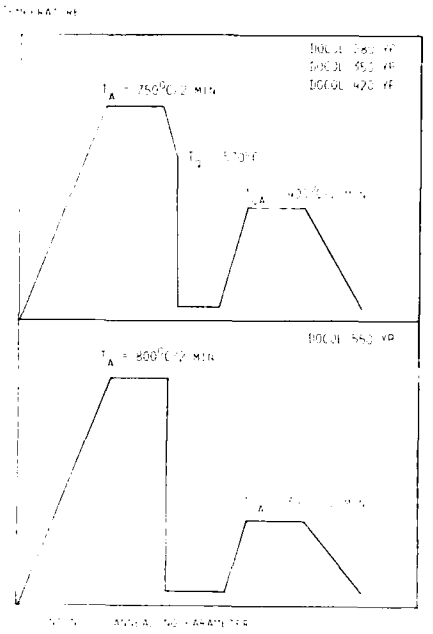

Figure 2 - Thermal profiles for laboratory simulation of continuous annealing.

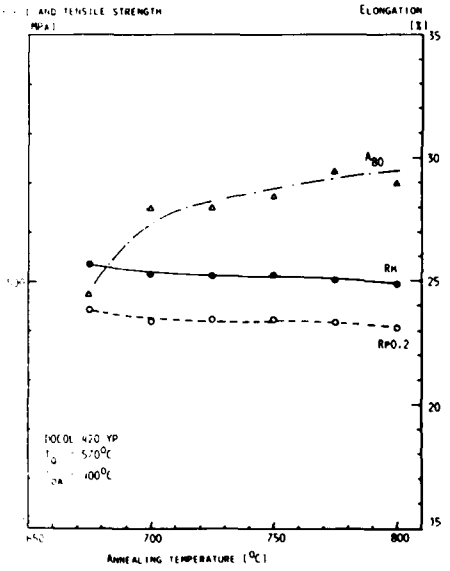


Figure 3 - Mechanical properties after laboratory simulated continuous annealing of DOCOL 420 YP.

## MICROSTRUCTURE AND MECHANICAL PROPERTIES

LABORATORY SIMULATION OF CONTINUOUS ANNEALING - As shown in Fig 3. for the ferritic-pearlitic steel DOCOL 420 YP yield and tensile strengths are only slightly decraesing with increasing annealing temperature after annealing between 675$^{o}$C and 800$^{o}$C for 2 minutes. Elongation values are increasing with increasing annealing temperature, especially in the interval 675-725$^{o}$C. The corresponding microstructure indicates that the recrystallization is not complete at temperatures up to 700$^{o}$C which is the explanation to low ductility. The carbon rich phase changes from spheroidized cementite

at 675°C to grain boundary situated pearlite at 800°C. The pearlite is formed during air cooling from the ferrite-austenite region down to the quenching temperature 570°C. The ferrite grain size is not changed dramatically even after annealing at 800°C which explains why the yield strength is quite insensitive to the annealing temperature. The slight decrease in strength which is observed ought to be connected with a decrease in precipitation hardening at higher annealing temperature. The most favourable annealing temperature for this ferritic-pearlitic steel seems to be around 750°C because ductility becomes too low at lower annealing temperatures due to an incomplete recrystallization.

In the case of the dual-phase steel DOCOL 550 YP both yield and tensile strengths are increasing with increasing annealing temperature after annealing between 725°C and 850°C for 2 minutes, see Fig. 4. Ductility decreases in the same temperature interval depending on an increased amount of martensite. The martensite fraction increases from 30% at the annealing temperature 725°C to 96% at 850°C annealing temperature. The most favourable annealing temperature range seems to be between 750°C and 800°C because yield and tensile strengths become too low at lower annealing temperature and ductility is deteriorated at higher annealing temperature.

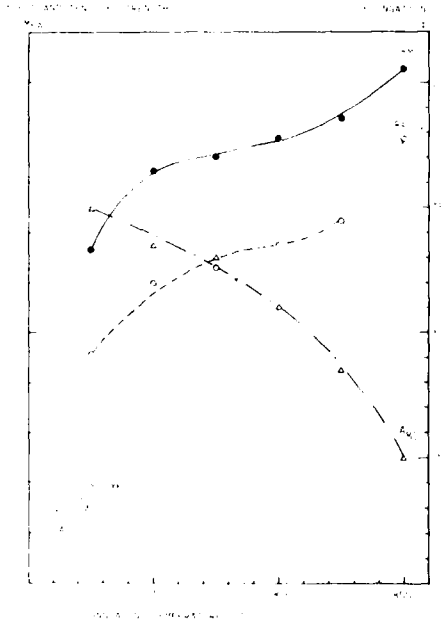

Figure 4 - Mechanical properties after laboratory simulated continuous annealing of DOCOL 550 YP.

FULL SCALE CONTINUOUS ANNEALING - The microstructure after continuous annealing of the DOCOL RP-X grades is ferrite with a high amount of preferable (111) recrystallization texture. The ferrite grain size is about 10 um.

The precipitation-strengthened steel grades DOCOL 280 YP, DOCOL 350 YP, and DOCOL 420 YP are annealed within the ferrite-austenite region which results in a microstructure of ferrite and pearlite. The ferrite grain size is about 6-8 um. In the steel DOCOL 550 YP, which is annealed and quenched from a high temperature, the microstructure is ferrite and about 30% martensite. The martensite is dark because of a tempering temperature of about 300°C. The ferrite grain size is about 8 um.

Typical microstructures are exemplified in Fig. 5 for the grades DOCOL 220 RP-X, DOCOL 350 YP, and DOCOL 550 YP.

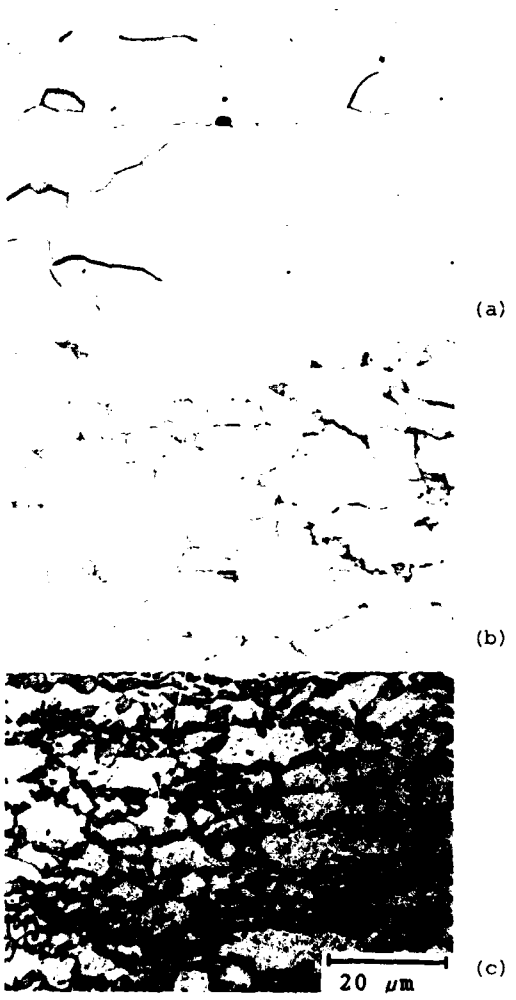


Figure 5 - Microstructure after full scale continuous annealing. (a) DOCOL 220 RP-X, (b) DOCOL 350 YP, and (c) DOCOL 550 YP.

Table 5 - Typical Mechanical Properties

| Grade | Yield strength (MPa) | Tensile strength (MPa) | Elongation (%,80 mm) | n | r |
|---|---|---|---|---|---|
| Mild DDQ | 190 | 311 | 43 | 0.23 | 1.8 |
| DOCOL 220 RP-X | 250 | 370 | 37 | 0.23 | 2.0 |
| DOCOL 260 RP-X | 280 | 400 | 35 | 0.23 | 1.8 |

Typical mechanical properties for DOCOL RP-X are shown in Table 5. The properties of conventional low carbon continuously annealed mild DDQ steel are given as a reference. It can be concluded that in spite of much higher yield and tensile strengths, both n-values and r-values of DOCOL RP-X are comparable to those of the mild DDQ steel. This means that mild DDQ steel can be repaced by these high-strength grades without pressforming problems.

Fig. 6 shows mechanical properties for the DOCOL YP grades. Elongation values are decreasing with increasing strength which means that the highest strength levels can not be used for difficult pressforming operations.

However, in the applications which DOCOL YP grades are used for variations in springback is the main problem which means that consistent mechanical properties is very important. The uniformity in mechanical properties which is possible to obtain by the continuous annealing process is shown in Table 6. The tensile testing specimens were taken from the first and last end of five coils of the grade DOCOL 350 YP in the thickness 1.60 mm. The total weight of the coils, which were from the same heat, was 100 tons.

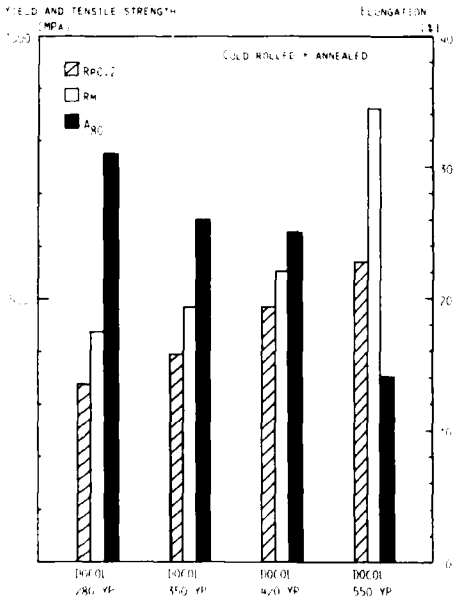


*Figure 6 - Mechanical properties after continuous annealing.*

Table 6 - Uniformity of DOCOL 350 YP

| Coil no | Yield strength (MPa) | Tensile strength (MPa) | Elongation (%, 80 mm) |
|---|---|---|---|
| 1 | 380 | 486 | 25 |
| | 383 | 478 | 24 |
| 2 | 374 | 473 | 28 |
| | 382 | 479 | 26 |
| 3 | 380 | 480 | 26 |
| | 381 | 479 | 26 |
| 4 | 382 | 483 | 26 |
| | 381 | 479 | 25 |
| 5 | 381 | 482 | 26 |
| | 387 | 478 | 30 |
| Mean value | 381 | 480 | 26 |
| Standard deviation | ±3 | ±4 | ±2 |

Depending on a spread in chemical composition between different heats the spread in yield strength is increased to a total value of maximum 60 MPa for DOCOL RP-X and maximum 70 MPa for DOCOL YP between several coils from several heats.

## WORK HARDENING AND BAKE HARDENING

In order to increase the yield strength further it is easy to obtain bake hardening properties in ultra low carbon grades if niobium is used as stabilizing addition. Bake hardenability increases if the annealing temperature is increased to a temperature over 830°C to cause a partial dissolution of the niobium carbides. r-value is still high because the recrystallization texture is fully developed before the dissolution of niobium carbides starts (8). In the DOCOL RP-X grades it is possible to increase the yield strength by about 30-40 MPa through 2% prestrain plus baking at 170°C for 2 min. Without predeformation there is no increase in yield strength by baking which means that the steel is free from aging in non-pressformed condition.

In the ferritic-pearlitic grades DOCOL 280 YP, DOCOL 350 YP, and DOCOL 420 YP, the increase in yield strength which is possible to obtain by 2% predeformation plus baking at 170°C for 20 min. is limited to about 70 MPa.

The work hardening and bake hardening properties for the dual phase steel grade DOCOL 550 YP are illustrated in Fig. 7. From a yield strength level of 570 MPa the steel has work hardened by an amount of 160 MPa after 2% predeformation. If the steel is baked at 170°C for 20 min. the yield strength is further increased by about 70 MPa. This means that the yield strength of this steel grade can be increased to about

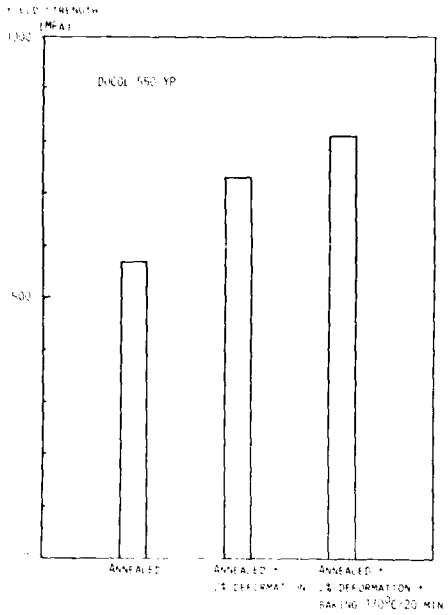


Figure 7 - Work hardening and bake hardening properties of DOCOL 550 YP.

800 MPa after press forming and baking at a temperature which is common in the automotive industry for drying of the paint coating. The reason for the high work hardenability is the fast generation of dislocations around martensite islands caused by the hardness difference between the hard martensite and the soft ferrite. The increase in yield strength by bake hardening is caused by a decoration of dislocations by solute carbon.

## FORMABILITY AND WELDABILITY

Table 7 shows some results from laboratory formability tests for different steel grades. MDF is the maximum draw ratio defined by the maximum diameter of a round blanket which can be deepdrawn to a cup without cracks, divided with the punch diameter 100 mm. H/d is the maximum dome height which can be obtained in stretching divided with the punch diameter 100 mm. The sheet thickness, t, was 0.7-1.0 mm in the MDF and H/d tests.

It can be concluded from Table 7 that DOCOL 220 RP-X is even better than a conventional mild DDQ grade in deepdrawing and stretchforming. This conclusion is in good correlation with the high $\bar{r}$- and n-values obtained in this grade.

The DOCOL YP grades have a limited deepdrawability and stretchformability which also corresponds to lower $\bar{r}$-values than in DOCOL RP-X grades. One important conclusion from Table 7 is that in spite of a much higher strength in DOCOL 550 YP, the MDF value is almost at the same level as in DOCOL 350 YP. This follows from the fact that the $\bar{r}$-value is about 1.0 in both grades.

Table 7 - Deepdrawability, stretchformability, and bendability

| Grade | MDF | H/d | Bend mandrel diameter $180^{\circ}$ |
|---|---|---|---|
| Mild DDQ | 2.19 | 0.35 | 0 x t |
| DOCOL 220 RP-X | 2.24 | 0.36 | 0 x t |
| DOCOL 350 YP | 2.03 | 0.33 | 0 x t |
| DOCOL 550 YP | 1.99 | 0.31 | 0 x t |

All grades mentioned in this paper can be bent $180^{\circ}$ with a very small bending radius. One exception is DOCOL 550 YP where the bend mandrel diameter must be limited to 1.0 x t as a result of the high strength level.

Both DOCOL RP-X and DOCOL YP grades can be easily welded with conventional welding methods. The continuous annealing technology makes it possible to decrease alloying contents compared to conventional batch annealing which improves the welding properties.

## APPLICATIONS

The DOCOL RP-X grades have typical applications in both outer panels and non-exposed parts. The great advantage is that an increased strength can be obtained without decreasing formability. This type of steel can be used to replace mild DDQ steel even in very difficult pressforming operations. The limitation is that the highest minimum yield strength which is produced today is 260 MPa.

Higher yield strengths are often needed for different parts like side members, cross members, seat reinforcements, and other types of inner reinforcements. In these applications an excellent bendability and a high consistency in mechanical properties for minimum variations in springback are important. The DOCOL YP grades with minimum yield strength 280 MPa, 350 MPa, and 420 MPa are very suitable for these types of applications.

The highest demands on yield strength are found in safety details like bumper reinforcements and door impact beams. DOCOL 550 YP has been developed to meet these demands.

Some examples of pressformed components can be seen in Fig. 8.

## SUMMARY AND CONCLUSIONS

Continuously annealed high-strength cold-rolled steel sheets microalloyed with niobium are successfully produced in full scale. The following key conclusions can be pointed out from laboratory experiments and full scale production experience:

1. Ultra low carbon steels solution hardened with phosphorus are excellent in both deepdrawing and stretchforming operations. Minimum yield strength is 220-260 MPa.

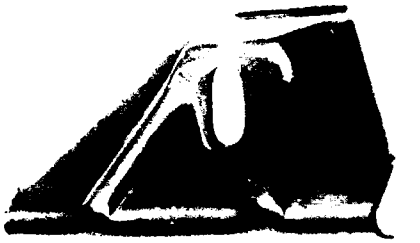

25 mm (a)

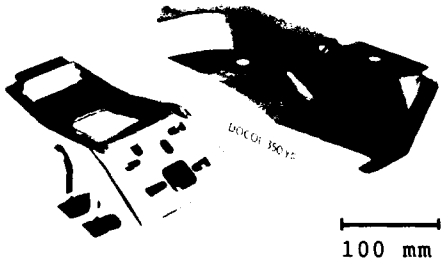

100 mm (b)

Figure 8 - Pressformed components in (a) DOCOL 220 RP-X and (b) DOCOL 350 YP.

2. Precipitation-strengthened steels with very uniform mechanical properties are produced as a result of a very close temperature control in the annealing process. Uniform mechanical properties are important for minimizing of springback problems in forming operations. Minimum yield strength is 280-420 MPa.
3. Different strengthening mechanisms can be used at the same time to produce high strength steel sheet depending on a flexible annealing technique. Solid solution hardening, precipitation hardening, and martensite transformation hardening has been used to produce a steel grade with minimum yield strength 550 MPa.
4. The yield strength can be further increased by work hardening and bake hardening. For the dual phase steel DOCOL 550 YP the increase in yield strength can be more than 200 MPa at 2% predeformation.
5. Low alloying contents can be used because of the short annealing time which improves weldability.

ACKNOWLEDGEMENT

The authors are very grateful to N. Hägglöf who performed the laboratory annealing experiments.

REFERENCES

1. Davis, R. G., "Metallurgy of Continuous-Annealed Sheet Steel", p. 35, The Metallurgical Society, Dallas, Texas (1982).
2. Mould, P. R., "Metallurgy of Continuous-Annealed Sheet Steel", p. 3, The Metallurgical Society, Dallas, Texas (1982).
3. Pradhan, R. R., "Metallurgy of Continuous-Annealed Sheet Steel", p. 203, The Metallurgical Society, Dallas, Texas (1982).
4. Pradhan, R. R., Scand. J. Metall. 13, 298-307 (1984).
5. Pradhan, R. R. and E. P. Melcher, SAE Technical Paper Series 84 0008 .
6. Pradhan, R. R., J. J. Battisti, and E. D. Melcher, Iron & Steelmaker, 25-30 (February 1987).
7. Brun, G. G. H. and M. J. M. Munier, "HSLA Steels: Metallurgy and Applications", p. 941, The Chinese Society of Metals and China Science and Technology Excange Center, Beijing, China, (1985).
8. Irie, T., S. Satoh, A. Yasuda, and O. Hashimoto, "Metallurgy of Continuous-Annealed Sheet Steel", p. 155, The Metallurgical Society, Dallas, Texas (1982)
9. Irie, T., S. Satoh, I. Takahashi, and O. Hashimoto, Kawasaki Steel Technical Report, 14-22 (March 1981).
10. Klosawa, M., S. Satoh, T. Obara, K. Tsunoyama, and T. Irie, Int. J. of Vehicle Design, IAVD Congress on Vehicle Design and Components, B 95-B 109 (1986).
11. Kinoshita, M. and K. Osawa, "HSLA Steels: Metallurgy and Applicatons", p. 833, The Chinese Society of Metals and China Science and Technology Exchange Center, Beijing, China (1985).

# INFLUENCE OF TM-ROLLING PARAMETERS ON PROPERTIES OF MICROALLOYED COLD ROLLED STEELS

**Ludwing G. E. Vollrath**
Verein Deutscher Ingenieure
(VDI)
Dusseldorf, FRG

**R. Hackl, Kh. G. Schmitt-Thomas**
Tech. Universität München
München, FRG

**D. Daub**
Hoesch Hohenlimburg
AG, FRG

**Summary**

The study on hand is to clarify to what extent the control of the hot-rolling parameters (finishing temperature, final deformation degree, coiling temperature) of thermomechanically treated niobium-microalloyed fine grain structural steel will allow an optimization of mechanical characteristics. To this end, the impact of the hot-rolling parameters on the precipitation and recrystallization behaviour of the hot strip in a subsequent heat treatment was studied. In respect of controlled rolling parameters (finishing temperature $T_F$, final deformation degree $\varepsilon_F$ and coiling temperature $T_C$) it was found that, with a cold deformation of the hot strip by 20 % and subsequent recrystallization annealing at 550, 600 and 650°C, the loss in strength of the cold strip induced by microstructure recovery and recrystallization processes can be clearly compensated in part by precipitation hardening effected by niobium as the microalloying element. The study shows the feasibility and restrictions of strength enhancement in the subsequent heat treatment.

**Introduction**

Today's hot-rolled strips feature a high surface quality so that suitable hot-rolled products are often substituted for conventional cold-strip grades. However, there still are numerous applications which require cold-rolled products, i.e. with the surface quality of the cold strip.

With microalloyed fine-grain structural steels, such a cold strip is subjected to recrystallization annealing after cold deformation as a rule. This, however, results in a substantial loss of all those mechanical properties which were achieved by the thermomechanical process.

The study on hand focusses on recrystallization annealing of cold worked hot strip material, which is performed in a temperature range in which niobium carbonitrides are precipitated, in order to clarify whether or not a combination of microstructure recovery, recrystallization and precipitation hardening processes will take place which, in their sum total, will compensate or even overcompensate the softening effects of the recrystallization processes. If so, this would allow to adjust associated process parameters appropriately for optimum strength characteristics.

The test method used differs from conventional production of cold strips from niobium-microalloyed fine-grain steels and involves modification of process parameters. Cold coiling of the strip ($T_C < 500$°C after hot-rolling) is applied to prevent complete precipitation hardening, thus retaining a residual aging potential. After cold rolling, such a material is subjected to a subsequent heat treatment which achieves a overlapping of recovery, recrystallization and precipitation hardening. The recovery-induced softening setting in rapidly is counteracted by the formation of further niobium precipitates in the ferrite during this heat treatment of the cold strip (1, 2, 3).

Hot-rolling parameters (finishing temperature, final deformation degree) are varied in order to modify initial conditions in such a way as to obtain optimum properties with as good a combination of high strength and high ductility as possible after this treatment combining cold rolling and subsequent annealing.

Such materials will be attractive for industry, since cold rolling plus thermal after-treatment will allow to preset or "standardize" a condition which cannot be achieved except by additional upgrading of carbon steels. Yield strengths of c. 650 N/mm² and tensile strengths of c. 700 N/mm² at elongations (A5) of c. 18 % and over can be achieved with such a procedure.

**Thermomechanical Treatment**

In principle, thermomechanical rolling means a procedure involving targeted setting and matching of temperatures and deformation conditions throughout the whole process. The outcome is a favourable combination of materials properties already achieved in the as-rolled condition which, as a rule, dispenses with any subsequent heat treatment of the hot strip.

The term of thermomechanically rolled steels emerged in the development of microalloyed fine-grain steels. Thermomechanical rolling allows to use sophisticated automatic process control for targeted setting and monitoring of rolling temperatures, deformation degress and cooling rates after hot-rolling so that defined and reproducible materials conditions can be set to obtain after cooling of the rolled product in coil.

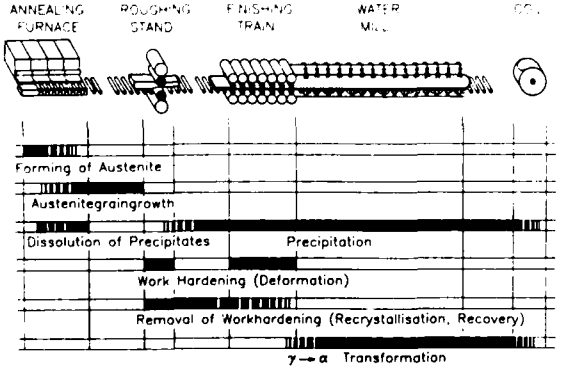


Fig. 1: TM-Production of hot strip (4)

Figure 1 gives an overview on the most important processes occurring in the hot strip during thermomechanical production (4,5). These metallurgical processes take place concurrently from austenitizing of the material in the pusher furnace via hot deformation to subsequent cooling in the cooling section and coil. They overlap in time and influence each other. The mode of action of microalloying elements (like Nb, Ti and V) and application of suitable deformation technology allow to effect tailored conditions in term. of grain refinement, agehardening and transfer of the substructure of the hot-deformed austenite to the transformation structure (6, 7).

**Production of Hot Strip**

Figure 2 shows the chemical composition of the alloy used. Al-killed continuous-cast slabs from a single smelting charge were available for application in the hot-rolling mill. The chemical composition of this low-ferrite steel shows strongly reduced contents of sulphur and phosphorus and has no microalloying elements other than niobium.

| | C | Si | Mn | P | S | Al | Nb | Ni | Cu | Cr | Ni |
|---|---|---|---|---|---|---|---|---|---|---|---|
| A,B,C,D, E,F,G | 0,09 | 0,03 | 0,72 | 0,011 | 0,002 | 0,049 | 0,046 | 0,008 | 0,02 | 0,02 | 0,02 |

Fig. 2: Hot strip composition (in weight percent)

The material was thermomechanically rolled on the medium-strip rolling mill of the Hoesch Hohenlimburg AG company. This medium-strip rolling mill comprises a reversing preroll stand and 2 two-high and 7 four-high roll stands in the continuous working section, and is equipped with a process automation system. The laminar cooling section is equipped with 50 individually controlled elements and is also integrated with the computer system thus allowing necessary control actions to be performed anytime and anywhere in the line. Seven different hot-rolling variations were set for the production of hot strips A - G (cf. fig. 3).

| Hot Strip | Dimension (mm) | Annealing Temp. $T_{Ann}$ (°C) | Annealing Time | Finishing Temp. $T_F$ (°C) | Final Deform. $\varepsilon_F$ (%) | Coiling Temp. $T_C$ (°C) |
|---|---|---|---|---|---|---|
| A | 390x3.5 | 1290 | 3h40' | 850 | 20 | 490 |
| B | 390x3.5 | 1290 | 3h50' | 900 | 12 | 490 |
| C | 390x3.5 | 1290 | 3h55' | 900 | 20 | 490 |
| D | 390x3.5 | 1290 | 3h50' | 900 | 20 | 590 |
| E | 390x3.5 | 1290 | 3h50' | 950 | 12 | 540 |
| F | 390x3.5 | 1290 | 3h50' | 930 | 12 | 490 |
| G | 390x3.5 | 1290 | 3h55' | 930 | 20 | 490 |

Fig. 3: Hot rolling parameters of test material

Finishing temperature, final deformation degree after the last rolling pass, and coiling temperature were varied while maintaining the other hot-rolling parameters constant to a large extent. A lowered coil temperature of 490°C was revealed by earlier studies to be optimal for further processing of the hot strip (1,8,9).
Rapid cooling of the strip down to this temperature level results in partial suppression of the formation of niobium precipitates in the ferrite - a fact which can be used as residual aging potential in recovery annealing after cold rolling.

The hot strips A - G described in fig. 3 were subjected to cold deformation by 20 % in total in two rolling passes after thermomechanical treatment. Subsequent recrystallization treatment was effected in a bell furnace. Figure 4 shows a schematic representation of the total production of the cold strip though it should be mentioned that a skin pass roll reducing the strip by 1,2 % was included after the heat treatment.

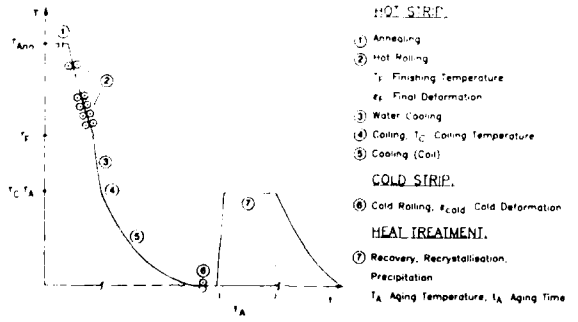


Fig. 4: Time-Temperature-Diagram of TM-treatment

## Hot Strip Microstructure and Mechanical Properties

Figure 5 gives an overview on the grain sizes of the hot strips. Hot strip A exhibits a very fine grain effected by the low finishing temperature of 850°C.
All grain sizes of hot strips B - G are in the fine grain range and classify as sizes 11 and 12 according to ASTM standard E 79-52. The grain size of hot strip A classifies as 13.

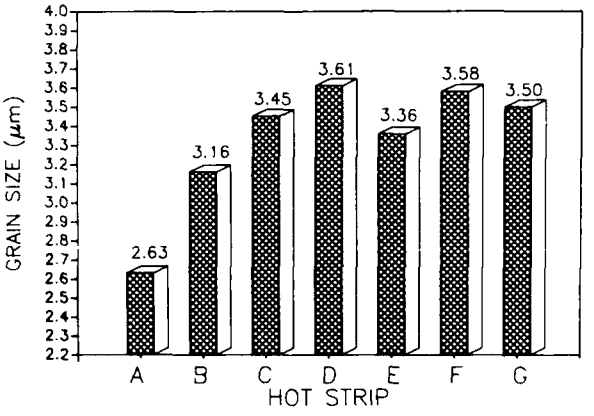


Fig. 5: Grain size of hot strip

The mechanical properties of the various hot strips are approximately the same. Mechanical testing yielded the following data:

| | |
|---|---|
| Tensile strength Rm: | 550 - 750 N/mm² |
| Yield point Re: | 460 - 480 N/mm² |
| Elongation A5: | 29 - 30 % |

In order to study the precipitation behaviour of the hot strips, they were aged in a salt pot furnace at temperature levels of 550, 600, and 650°C and at dwell times between 0 and 10,000 min. Hardness measurements (HV20) were performed at regular intervals. The results are shown in figures 6 a-e. The low coiling temperature was found produce strength enhancement in subsequent heat treatment owing to the formation of niobium carbonitride precipitates which influence recrystallization retardation and inhibit dislocation movement.

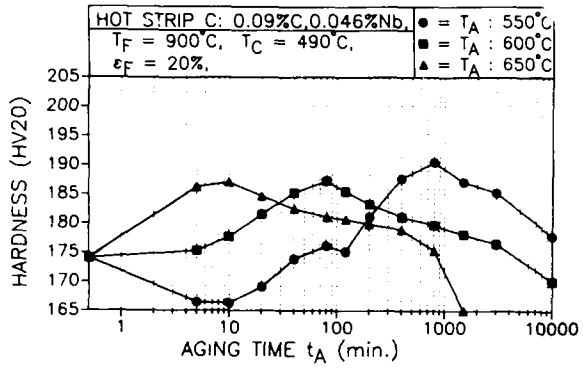


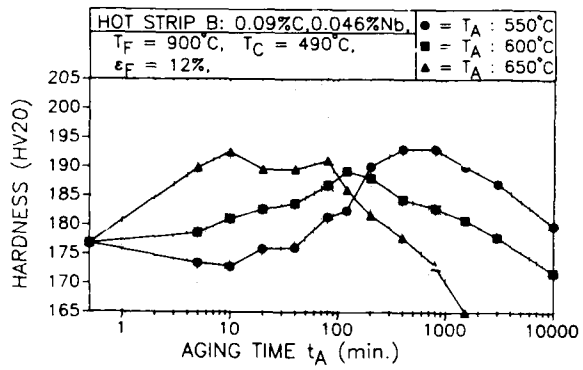


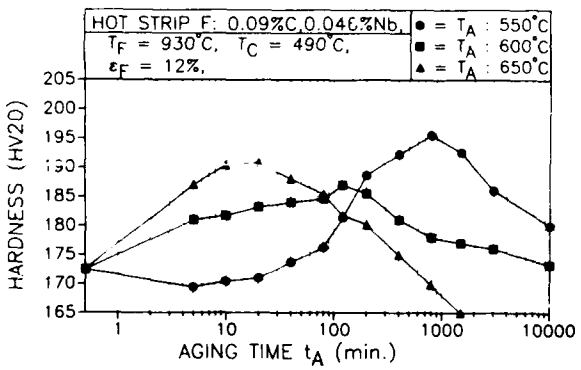


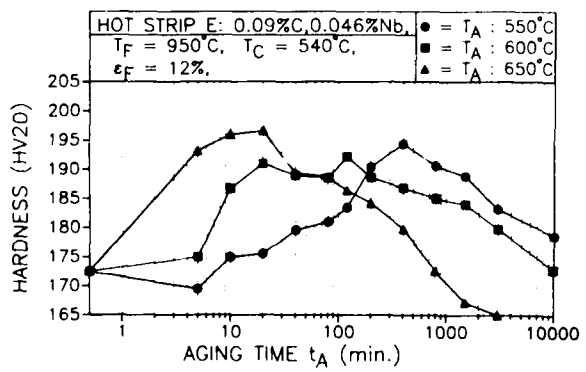


Fig. 6 a-d: Hardness changes of hot strip during aging

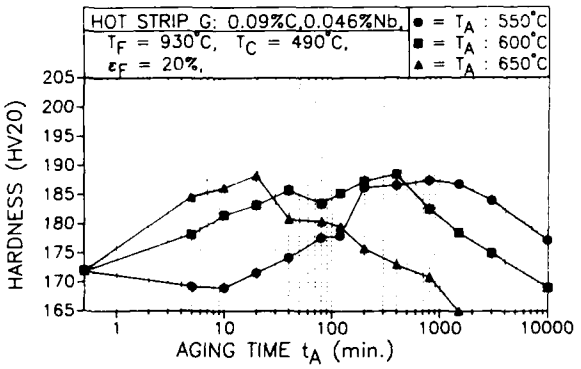


Fig. 6 e: Hardness changes of hot strip during aging

The hot strip with a higher coiling temperature of 590°C (hot strip D) showed hardly any tendency to precipitation hardening; neither did not strip A with its low finishing temperature.

## Properties of the Cold Strip

Precipitation in niobium-microalloyed low-pearlite steels occurs at the same temperatures as recrystallization does. Hence, the hot strip was cold-deformed by 20 % and isothermally annealed in order to study the interaction between carbonitride precipitation and recrystallization and its impact on mechanical properties.

Figure 7 shows the mechanical characteristics of the 20 % cold-deformed strip with and without thermal after-treatment. It was found that, in dependence from the hot rolling parameters, a 12 h industrial heat treatment in a bell furnace partially resulted in a clear increase in tensile strength. In each of the cold-rolled conditions, the yield point values were found to decrease due to recovery and recrystallization processes induced by heat treatment, whereas tensile strength and elongation exhibited higher values after heat treatment.

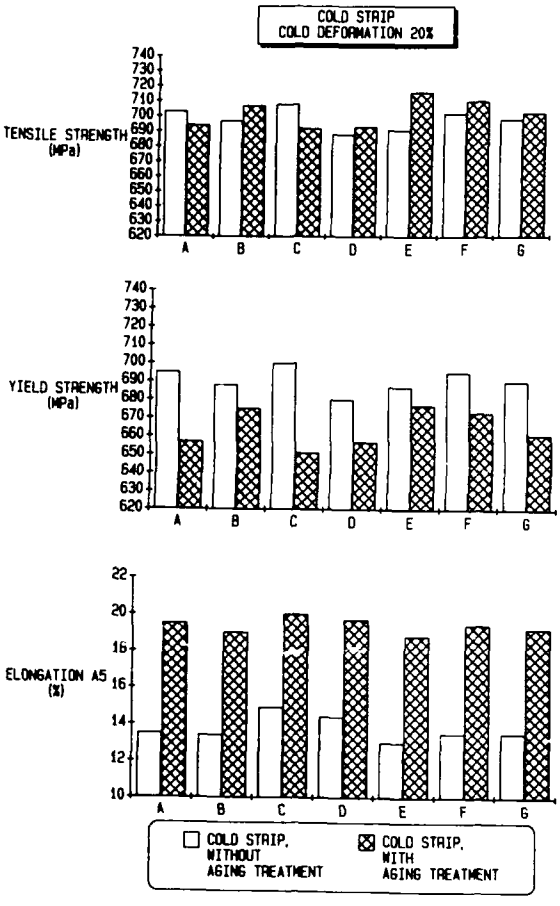


Fig. 7: Mechanical properties of cold strip

Figure 7 reveals, when taking the difference of tensile strength increases in the course of heat treatment in absolute terms, the highest strengths were found in the hot strips with the lowest degree of deformation in the last rolling pass of 12 % (hot strips E, D and F). Higher finishing temperatures combined with a low deformation degree of 12 % in the last rolling pass (hot strip E) were found to possess the greatest precipitation potential for a subsequent heat treatment of the cold strip. The absolute values for the increase of elongation A5 for these conditions were remarkable, too.

At a 20 % deformation in the last roll stand, nor or only slight strength increases of the aged cold strip were found. In the case of low finishing temperatures (hot strip A and C) the strength of the 20 %-deformed niobium-microalloyed material will decrease after thermal treatment.

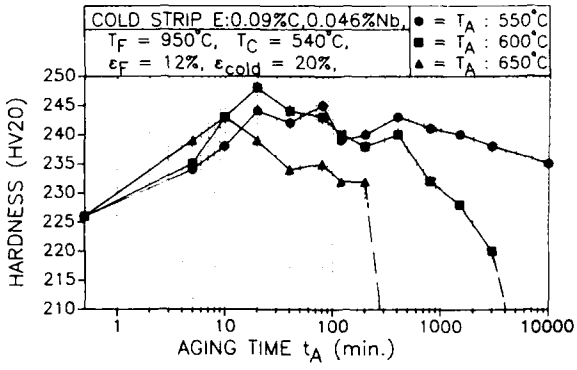


Fig. 8: Hardness changes of cold strip E during isothermal heat treatment

Figure 8 depicts the influence of an isothermal heat treatment on the hardness of strip E. It is shown, that annealing at 550°C will led to higher hardness values than the cold strip condition over the whole range of reported annealing time (up to 10.000 min.). Even annealing at 650°C showed an increase in hardness upto an annealing time of 200 min.

## Conclusions

The results of these studies on the influence of the hot-rolling parameters (finishing temperature, final deformation degree, coiling temperature) of niobium-microalloyed low-pearlite structural steel show that optimization of hot-rolling parameters will allow to produce a microalloyed fine-grain structural steel which will feature tensile strength values after cold rolling and subsequent recrystallization annealing, which will be higher than those of the cold-rolled non-aged condition.

These favourable tensile strength values were due to precipitation hardening via Niobium carbonitrides counteracting and overcompensating the effects of recovery and recrystallisation. These heat-treated cold-strip conditions show markedly greater toughness values thus indicating a enhanced safety reserve of the material .

## References


1. L. Vollrath: PhD Diss., Techn. Universität München, 1983
2. L. Vollrath and Kh.G. Schmitt-Thomas: HSLA-Steels '85, Metallurgy and Applications, J.M. Gray et al. (Eds), Proc. intern. conf. Beijng, 1985, p. 599
3. Chr. Oehler: PhD Diss., Techn. Universität München, 1988
4. R. Kasper, L. Peichl and O. Pawelski: Stahl und Eisen 101, 1981, 12, p. 722
5. L. Meyer: VDI-Berichte Nr. 428, 1981, p. 36
6. L. Meyer: Thyssen Techn. Berichte, 1986, 1, p. 12
7. L. Meyer: Stahl und Eisen 101, 1981, 7, p. 483
8. Kh.G. Schmitt-Thomas and L. Vollrath: Arch. Eisenhüttenwesen, 1982, 53, p. 443
9. Kh.G. Schmitt-Thomas and L. Vollrath: Arch. Eisenhüttenwesen, 1982, 53, p. 403

# MICROALLOYED STEELS FOR AUTOMOBILES— DEVELOPMENTS AT TATA STEEL

**M. D. Maheshwari, A. N. Mitra, T. Mukherjee, J. J. Irani**
The Tata Iron & Steel Co. Ltd.
Jamshedpur-831001, India

## 1) INTRODUCTION

*In response to drastic increases in oil prices over the past decade and a half, auto manufacturers worldwide have made significant progress in producing low cost, fuel efficient vehicles. Two main avenues were identified in successful attainment of these objectives:*

*i) Reduction of the weight of vehicles - Apart from downsizing, this has been achieved through improvement of power train efficiency and use of higher strength steels. The trend of vehicle weight reduction in U.S. passenger cars is indicated in Fig. 1. (1) Analysis of the cost of various materials as a function of their weight reduction potential, clearly suggests that microalloyed steels have the best cost advantage as compared to other materials.*

*ii) Energy saving - Addition of microalloying elements to various medium carbon and low alloy forging quality steels has eliminated the need for heat treatment of various components used in automobiles without affecting their toughness, fatigue behaviour machinability, etc.*

*In India the automobile industry has been growing at a fair rate. Actual production of cars and two wheelers in 1985 and in 1987, along with the projected trends for 1990 are indicated in Fig. 2. (2) Not unexpectedly, has the cost of production of vehicles risen. An example of the trend of rise in the cost of chassis for buses is indicated in Fig. 3. (2)*

*Considering the enormous potential of HSLA steels, TATA STEEL had taken the initiative a decade ago to develop various grades of microalloyed steels for diverse applications (3-5). More recently, however, efforts have been directed, in specifically developing microalloyed steels for the automobile industry both for weight reduction as well as for energy saving. Some of these steels have already been commercialized, whereas, others are in an advanced stage of being commercially produced. This paper discusses the developmental efforts undertaken at TATA STEEL in the development and production of microalloyed steels for the automobile industry.*

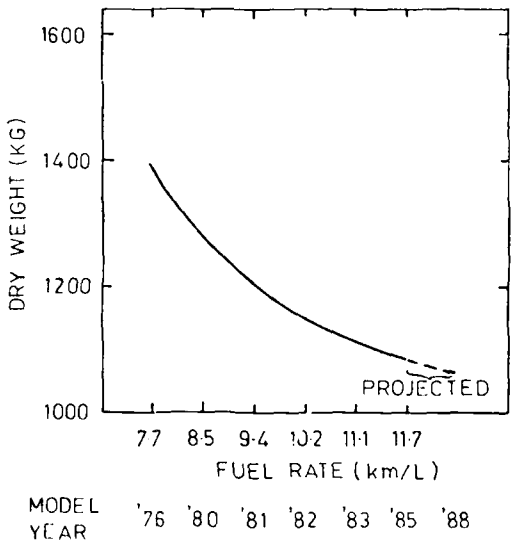


FIG.-1 CAR WEIGHT AND FUEL ECONOMY TRENDS IN U. S. (1)

CAST NO.: M06627

COMPOSITION : C = 0·07 % , Mo = 0·45 % , P = 0·024 % ,
S = 0·021 % , Si = ·106 % , V = 0·10 %

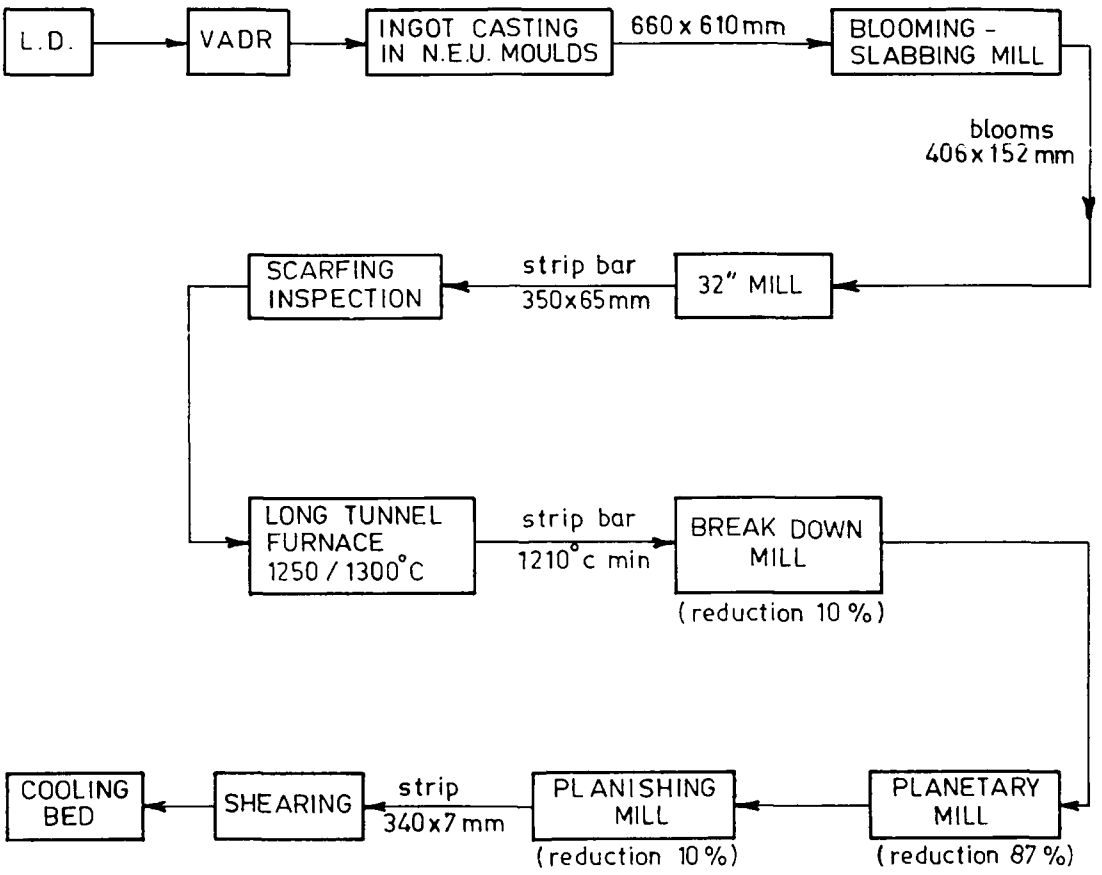


FIG. 4 SCHEMATIC PROCESS ROUTE FOR THE PRODUCTION OF LONG MEMBERS FOR TRUCK CHASSIS.

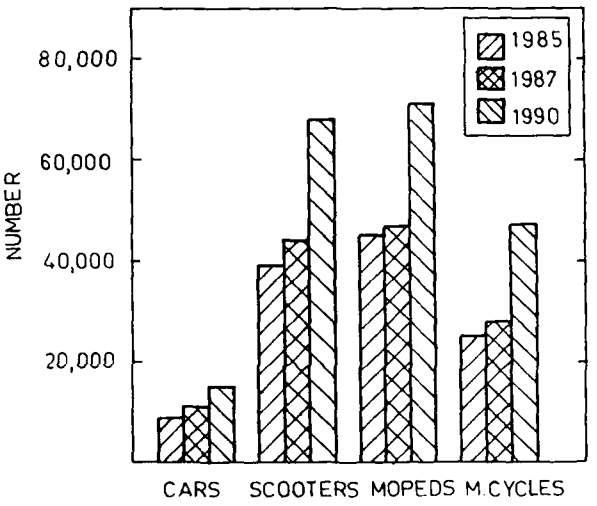


FIG.-2 PRODUCTION TRENDS OF CARS AND TWO WHEELERS IN INDIA (2)

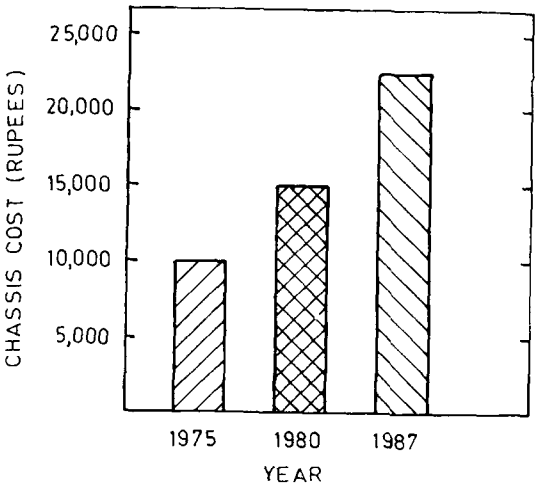


FIG.-3 CHASSIS COST FOR BUSES (RUPEES) (2)

## 2. FACILITIES

*Microalloyed steels are produced from two different routes: (a) open hearth furnace and (b) LD- VAD route for applications necessitating low levels of inclusions and other residuals. As yet, since there is not bloom or slab caster in the Company, liquid steel from the two different routes are cast into either narrow-end-up or wide-end-up ingots. The ingots are soaked in soaking pits at a temperature 1250-1300°C and rolled into blooms or slabs in one of the two blooming-slabbing mills of the Company. The blooms/ slabs are inspected, dressed and then rolled into finished products in one or more of the finishing mills within the Company or outside.*

## 3. DEVELOPMENT AND COMMERCIALIZATION

### 3.1 Flat Products

***CHASSIS MEMBERS FOR TRUCKS:*** *The total demand for these members in India is about 60,000 t.p.a., and almost all of it is currently imported. Grades of steel commonly used for these members are indicated in Table 1.*

*Commercial trials were carried out for producing the E-28 grade. The details of the cast involved and the route chosen for the production of this grade are schematically indicated in Fig. 4. Obviously the fine balance of properties, a combination of high yield strength and high elongation/ductility, had to be met through controlled finishing temperatures and reductions given in the last stages of deformation. Preliminary trial production resulted in yield strengths far exceeding the minimum stipulated requirements, and cracking of long members formed out of these strips. Microstructures of these failed strips indicated mixed grain size and also incomplete recrystallization. On investigation it was found that in some cases the finishing temperatures were lower than 800°C. In order to lower the yield point and consequently improve formability, the following steps were taken in the subsequent trials:*

*a. Temperatures in zones 3 & 4 of the Tunnel furnace were maintained at 1250°C and 1300°C respectively, instead of 1200°C and 1250°C.*

CHEMICAL COMPOSITION

| | E 28 | E 34 | E 38 | E 42 |
|---|---|---|---|---|
| % CARBON | 0.12 | 0.1 max | 0.10 max | 0.10 max |
| % PHOSPHOROUS/ SULPHUR | 0.03 | 0.03 max | 0.03 max | 0.03 max |
| % NIOBIUM | -- | 0.06 max | 0.06 max | 0.06 max |
| % MANGANESE | 0.80 | 0.70 max | 1.00 max | 1.20 max |
| % ALUMINIUM | -- | 0.02 min | 0.02 min | 0.02 min |
| % SILICON | -- | Trace | Trace | Trace |

TENSILE PROPERTIES

| | E 28 | E 34 | E 38 | E 42 |
|---|---|---|---|---|
| YIELD STRENGTH ($kg/mm^2$) | 28 min | 34-40 | 38 min | 42 min |
| TENSILE STRENGTH ($kg/mm^2$) | 38 min | 40-50 | 45-57 | 49-61 |
| % ELONGATION (Lo = 5.65 /So) | 27 min | 27 min | 25 min | 23 min |

TABLE - 1: GRADES OF STEEL FOR CHASSIS MEMBERS

*b. Slabs were adequately soaked in the furnace. No slab was drawn from the furnace until it had reached a temperature of 1210°C minimum.*

*c. Flow of cooling water in the Planetary and Planishing Mill stands were decreased.*

*d. Reduction at the Planishing Mill was reduced from a level of 18/20% previously, to a level of 10%.*

*It was observed that with these steps, the finishing temperatures were in the range of approximately 850°C as compared to 760/780°C in the earlier trials. Samples were collected from each slab and their properties assessed. These are indicated in Table. 2. It was found that the properties of the long members were quite consistent - yield strength varied between 34 and 37 kg/mm² and elongation varied from 27 to 30%. Samples tested for bend revealed that they could withstand a bend of 0.5 t, which reflected the good formability of the members. ASTM grain size was found to be in the range of 7 to 7½. These strips could be successfully formed into chassis members without cracking.*

***PROPELLER SHAFT:*** *These tubes used to be manufactured in the Tubes Division of the Company from conventional plain carbon steel strips through the ERW process followed by cold drawing. To meet the desired physical properties, a minimum carbon equivalent of 0.24% had to be maintained. Reduction of carbon equivalent to improve weldability and ductility was successfully attempted through microalloying. The chemical composition and physical properties, of conventional plain carbon and microalloyed propeller shaft tubes, are indicated in Table 3.*

| MATERIAL | CHEMICAL COMPOSITION | TYPICAL PHYSICAL PROPERTIES | OTHER FEATURES |
|---|---|---|---|
| PLAIN CARBON | C% 0.18/0.23 | Y.S. - 40 Kgf/mm² | Coarse structure with minor amount of pearlite at grain boundaries. |
| | | U.T.S, 52 Kgf/mm² | |
| | Mn% 0.35/0.50 | Elongation, % - 10 | Hardness of HAZ - 160/190 VPN. |
| | Carbon - 0.24 min equivalent | | |
| MICRO ALLOYED | C% 0.12 max. | Y.S. - 48 Kgf/mm² | Fine ferritic structure. |
| | Mn% 0.70 max. | U.T.S - 55 Kgf/mm² | Hardness of HAZ - 150/170 VPN |
| | Micro-alloying elements - 0.10% max. | | |
| | Carbon - 0.20 max. equivalent,% | Elongation - % -12 | |

TABLE - 3: CHEMICAL COMPOSITION AND PHYSICAL PROPERTIES OF PROPELLER SHAFT TUBES

| COIL NO. | THICKNESS (mm) | YIELD STRENGTH (kg/mm²) | TENSILE STRENGTH (kg/mm²) | BEND TEST | ELONGN (%) |
|---|---|---|---|---|---|
| 1 L | 7.17 | 36.14 | 44.54 | -- | 28.57 |
| 1 T | 7.21 | 36.58 | 45.80 | OK(0.5T) | 27.05 |
| 2 L | 7.09 | 34.10 | 44.07 | -- | 29.91 |
| 2 T | 7.00 | 37.02 | 44.90 | OK(0.5T) | 29.71 |
| 3 T | -- | -- | -- | OK(0.4T) | -- |

TABLE - 2: PROPERTIES OF E 28 CHASSIS MENMBERS ROLLED AT AHMEDABAD ADVANCED MILLS, NAVSARI

### *3.2 Forging Quality Steels*

*The development of microalloyed forging quality steels for the automobile industry is relatively more recent, compared to the concept of microalloying in structural steels. In the latter, the idea is to increase strength of the steel through grain refinement or to lower the carbon equivalent (to improve the formability/weldability) for the same strength level. The concept of addition of microalloying elements to medium carbon and low alloy forging quality steels is grain refinement and for the purpose of eliminating costly heat treatment of the finished products rather than weight reduction. This concept is, however, finding a very rapid growth rate in recent years all over the world (6,7). Reputed auto manufacturers in different continents have accepted the usefulness of addition of microalloying elements in conventional forging quality steels. It has been reported that (8) crank shafts forged by Gerlach Werke for Volkswagen, Audi, and Daimler-Benz automobiles have been entirely converted from hardened and tempered steels to microalloyed steels within a decade. Microalloyed 49MnVS3 is also being increasingly used for truck crank shafts, 37% in 1982. (8).*

*A wide variety of medium and plain carbon, and low alloy forging quality steels, is used by different auto manufacturers in the production of different parts/components, e.g., crank shafts, connecting rods, steering arms, steering levers, axle shafts, steering worms, hubs, etc. These parts/components are usually forged out of basic steel bars/rods supplied by steel makers, followed by heat treatment and machining. Out of several grades, three popular grades were identified for microalloying trials, viz., C-45, 20MnCr1 and SAE 1541.*

The Steel Company supplies 125mm dia C-45 steel, used as raw material for manufacture of front hubs of trucks, after two stages of forging and heat treatment consisting of quenching and tempering. Niobium treated C-45 steel was supplied with the objective of eliminating/reducing the final heat treatment. The results of the trial were as follows:

**Chemical Composition**

%C - 0.52, %Si - 0.23, %Mn - 0.81, %S - 0.04

**Mechanical Properties**

| | U.T.S. Kg/mm$^2$ | Y.S. Kg/mm$^2$ | Elong. % | R.A. % | Impact/ Charpy Mkg/cm$^2$ |
|---|---|---|---|---|---|
| As Rolled 125mm dia | 72.5 | 40.7 | 17.0 | 30.5 | 1.25/ 2.25 |
| As Rolled to 60mm square | 69.0 | 37.1 | 18.0 | 43.8 | 1.50 2.10/ |
| As forged to hub | 71.73 | — | 17.5/ 19 | 41/ 43 | 1.0/ 3.75 |

Though the mechanical properties were fully met, the impact properties of the Hubs were inconsistent and generally on the lower side. However, on normalizing the impact properties improved significantly to 4-6Mkg/cm$^2$, and the auto manufacturer decided to manufacturer the front hub with normalizing treatment only instead of the costly quenching and tempering route.

125mm dia. 20MnCr5 grade of steel is supplied for manufacturer of truck crown wheels following forging, case carburising, and oil quenching and tempering. Since separate heat treatment was carried out following the carburising treatment, an attempt was made to replace the conventional steel by microalloyed steel, which would enable direct quenching after carburising at a temperature higher (970$^0$C) than the normal 910-920$^0$C. Separate trials were carried out with Niobium and Titanium added steels, the results of which are indicated below:

**A. Chemistry**

| | Specified | Nb-treated | Ti-treated |
|---|---|---|---|
| %C | 0.17-0.22 | 0.18 | 0.17 |
| %Mn | 1.00-1.40 | 1.18 | 1.20 |
| %Si | 0.10-0.35 | 0.27 | 0.23 |
| %S | 0.02-0.035 | 0.022 | 0.023 |
| %P | 0.035 max | 0.020 | 0.020 |
| %Cr | 1.00-1.30 | 1.08 | 1.10 |

**B. Tensile Properties**

(Forged down from 125 to 60 mm dia. and normalized)

| | | | |
|---|---|---|---|
| UTS(kg/mm$^2$) | 74 (max) | 65.8 | 66.7 |
| Y.S.(kg/mm$^2$) | — | 47.2 | 45.2 |
| Elongation% | — | 15.0 | 16.0 |

**C. Treatment**

| | | | |
|---|---|---|---|
| Carburising | 910-920$^0$C separate Q&T | 970-980$^0$C direct Q&T | 970-980$^0$C direct Q&T |

**D. Properties after heat treatment Jominy Hardenability**

| | | | |
|---|---|---|---|
| J5 | 36.48 Rc | 40.5 Rc | 42 Rc |
| J30 | 34 Rc(max) | 25 Rc | 24 Rc |
| ASTM Grain Size | 5 - 8 | 7 - 8 | 7 - 8 |

Based on the satisfactory results obtained, the auto manufacturer decided to go in for large scale commercial trials in producing crown wheels out of microalloyed 20MnCr5 steel.

100mm$^2$ billets of SAE-1541 composition is supplied for the manufacturer of steering arms of tractors. The component after final heat treatment should have high yield strength (520 kg/mm$^2$), and yet, high elongation (14% mimum) and RA (35% minimum values) to withstand cold splicing. Niobium treated steel was supplied with the objective of eliminating the costly quenching and tempering treatment. The results of the trials are as follows:

**Chemical Composition**

%C - 0.37, %Mn - 1.43, %S - 0.021,
%P - 0.02, %Nb - 0.043, %Al - 0.018

**Processing**

100mm sq - rolled to 50mm dia - Forged (1200 - 1050$^0$C)

**Mechanical Properties**

Y.S. Kg/mm$^2$ - 52.9,
U.T.S. Kg/mm$^2$ - 80.5,
%Elongation - 16, %RA - 40.5,
Hardness - 240 HV

With the final properties having been achieved successfully, the tractor manufacturer has expressed a desire to go in for large scale trials with the SAE 1541 Niobium steel.

***CONCLUSION:*** *In India the automobile industry is growing at an accelerated rate than ever before. The cost of petroleum in the country is amongst the highest in the world. In these contexts, it is all the more imperative for the auto manufacturers in the country to produce not only fuel efficient vehicles but also to bring down the cost of the vehicles. Microalloying can serve the dual purpose of reducing the weight of the vehicles and the cost of various parts/components through elimination/reduction of the heat process(es) involved. Examples cited in the paper clearly indicate the initiative taken, both by the Steel Company and some of the auto manufacturers in the country, in this regard. It is expected that microalloyed steels will find wide scale usage in the country within the next decade.*

## *REFERENCES*


1. *B. J. Clarsen and K.C.W. Glasgow: Proc. Int. Conf. on High Strength Low Alloy Steel, University of Wollongong, Australia, 1984, 282*

2. *Annual Review, Economic Times of India, 1987.*

3. *M. D. Maheshwari, S. C. Mohanty, A. N. Mitra and T. Mukherjee: Trans. IIM, 1982 35 (6), 633.*

4. *M. D. Maheshwari, A. N. Mitra, T. Mukherjee and J. J. Irani: Proc. Int. Conf. on High Strength Low Alloy Steels, University of Wollongong, Australia, 1984, 38.*

5. *R. Jha, M. D. Maheshwari, T. Mukherjee and J. J. Irani: ibid, 151.*

6. *M. Nakamura and H. Maeda, SEASI Quarterly, April 1983, 81.*

7. *M. D. Maheshwari, S. K. Mondal, S. C. Gupta and T. Mukherjee, Tool and Alloy Steels, Feb. 1983, 69.*

8. *J. Stoeter and J. Kneller: Metal Progress March, 1985, 61.*

# PRODUCTION, PROPERTIES AND APPLICATION OF HSLA STEELS IN CRANE AND VEHICLE CONSTRUCTION

**J. Degenkolbe, B. Müsgen, U. Schriever**
Thyssen Stahl AG
Kaiser-Wilhelm-Str. 100
D-4100 Duisburg 11, FRG

ABSTRACT

The present paper describes the application of HSLA steels in crane and vehicle construction. After a survey of the steel grades used, a report is given on metallurgical progress, and modern rolling and heat treatment methods are presented. For normalised, TM-rolled and QT steels, the strength and toughness properties, as well as the forming and welding characteristics are explained. Finally examples are given from various areas of application.

HSLA STEELS are used extensively in modern vehicle construction and, thanks to their good characteristics, they have proven themselves superbly. The commercial vehicles used in the different sectors of material handling and transport, e.g. trucks, tankers, mobile cranes, dumper trucks or track-bound heavy goods vehicles, have to satisfy specific requirements according to their intended use.

HSLA steels are frequently used for especially important components of the structure. Thus they are used for longitudinal and transverse girders on trucks, rear axle bridges, frames, supports and struts, crane booms, wheel disks, structural pipes and tanker vessels (1)(2). By utilising the specific advantage of these steels, namely high strength combined with excellent workability, it is possible to make structures which display not only a high load-bearing capacity, but also a favourable ratio of play load to dead load.

A look at the historical development of weldable structural steels shows that, since the introduction of the steel St 52 about 50 years ago, special alloys, rolling techniques and heat treatments have been used to develop steels which today cover an extraordinarily broad range of application with their spectrum of properties. This has been made possible by the consistent application of the wellknown strengthening mechanisms (3)(4).

## STEEL GRADES FOR COMMERCIAL VEHICLE CONSTRUCTION

The grades of steel used in the construction of commercial vehicles have to display various chemical compositions and they have to be produced by optimised manufacturing procedures in order to ensure the best possible ratio cost-effectiveness for the intended application. For this reason, use is made of variously alloyed steels which have been normalised, normalising rolled, thermomechanically rolled or quenched and tempered. Such steels display excellent formability and are extremely suitable for welding (5)(6)(7).

Figure 1 shows the usual grades of steel with a minimum yield strength range of 210 to 960 N/mm², their alloying concept and the plate thickness ranges normally used.

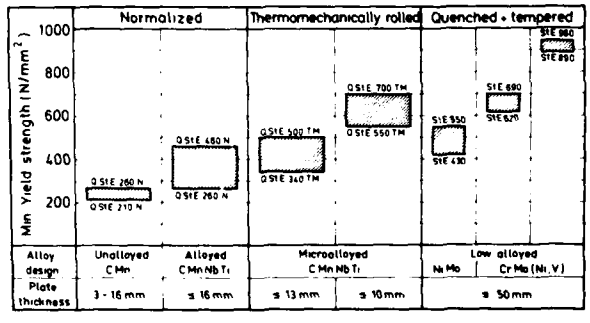


Fig. 1 - Plate and strip for the construction of commercial vehicles

For the minimum yield strength range of 210 to 460 N/mm², use is made of unalloyed or alloyed steels with low carbon contents and a fine-grain structure. They are supplied in normalised or normalising rolled condition in the form of flat products with thicknesses of up to 16 mm.

For the minimum yield strength range of 340 to 700 N/mm², there are micro-alloyed, thermomechanically rolled fine-grain structural steels.

Because of their reduced carbon content, they have a very low perlite or carbide fraction in a fine-grain microstructure.

Quenched and tempered fine-grain structural steels, especially in greater plate thicknesses, satisfy the most rigorous requirements concerning strength and ductility characteristics. These are steels whose chemical composition and production process are adjusted in such a way that minimum yield strengths in the range of 450 to 960 N/mm² are achieved.

Figure 2 shows typical chemical compositions for important steel grades used for the construction of commercial vehicles. With increasing strength it is possible to make savings in material and fabrication costs by means of reduced thickness. Often, structures only become possible through the use of HSLA steels. By reducing the deadweight of the structure the operating costs of transport vehicles are lowered.

| Steel grade | Minimum Yield strength N/mm² | Tensile strength N/mm² | Treatment | Typical chemical composition [%] | | | | | | |
|---|---|---|---|---|---|---|---|---|---|---|
| | | | | C | Si | Mn | Cr | Mo | Nb | Ti |
| QStE 240 N | 240 | 370 - 450 | N | 0.07 | - | 0.45 | - | - | - | 0.015 |
| QStE 380 N | 380 | 500 - 640 | | 0.14 | 0.30 | 1.20 | - | - | - | 0.15 |
| QStE 550 TM | 550 | 600 - 750 | TMR | 0.07 | 0.30 | 1.00 | - | - | 0.02 | 0.10 |
| StE 690 | 690 | 790 - 940 | QT | 0.17 | 0.60 | 0.80 | 0.80 | 0.30 | - | - |

Fig. 2 - Typical composition of HSLA steels for the construction of commercial vehicles

MODERN PRODUCTION PROCEDURES FOR HSLA STEELS

PRODUCTION OF STEEL - The production of high-quality steels for the construction of commercial vehicles requires many years' experience and modern production facilities. Figure 3 shows the usual steel making process. The steels are produced predominantly in oxygen converters. Combined blowing using the Thyssen Blowing Metallurgy process constitutes an improvement in the familiar top-blowing process (8). With a downstream ladle metallurgy including vacuum treatment, it has become possible to adjust the narrow composition limits, to modify the inclusions, to lower the hydrogen content and to homogenize the heat. The result are improved steel properties (9). The steel is subjected mainly to continous casting, and in some cases to ingot casting (10).

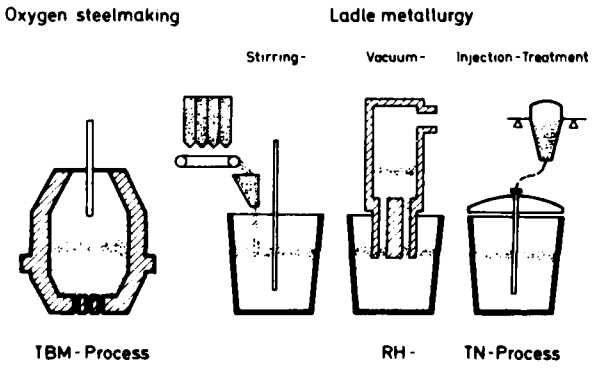


Fig. 3 - Steel making process

ROLLING AND HEAT TREATMENT - The development of the rolling technique is shown in Figure 4. Conventional rolling is characterized by high rolling temperatures with correspondingly low deformation resistance in the material. The coarse ferritic-perlitic structure which sets in must be refined after rolling by normalisation for demanding applications. With normalising rolling, the finish-rolling takes place in the normalising temperature range. The fine-grain structure produced has properties equivalent to those of a normalised structure. The advantage of normalising rolling is the better surface condition of the rolled material not subjected to heat treatment. This process is beneficial for the environment thanks to the simplification of production (11)(12)(13)(14)(15).

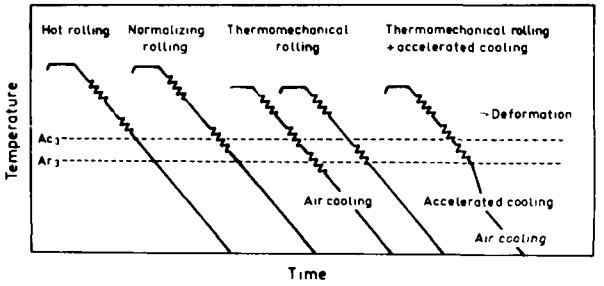


Fig. 4 - Development of rolling technique

Thermomechanical rolling entails a whole package of rolling operations (15). To achieve high strength with simultaneous good toughness characteristics, it is necessary to control the temperature and to maintain certain deformation conditions. Thermomechanically rolled plates display a ferritic-perlitic structure with some bainite. The production conditions and the availability of carbide-forming or carbide-nitride-forming micro-alloying elements result in an extraordinarily fine structure. In operational practice, the control of the final rolling temperature is used primarily to adjust the required yield strength. The final rolling temperature can be lowered to around $Ar_3$ to increase the yield strength, and so during the rolling small fractions of ferrite can already form in the structure. The strainhardening of such a ferrite fraction hardly impairs the toughness of the steel (14)(16).

In the further development of TM-treated steels, accelerated cooling plays a special role. At the end of the rolling process cooling water is directed onto both surfaces of the plate which is thus cooled rapidly. Cooling takes place at around 15 K/s down to temperatures of

about 550°C. The effects of the rolling and cooling conditions with accelerated cooling can be summarised as follows. The yield strength and tensile strength are raised by about 50 N/mm² as against thermomechanical rolling. The toughness is not impaired. This is achieved by shifting the structural transformation from ferrite/perlite to ferrite/bainite and by the production of a finer ferrite grain.

The yield strength increasing effect from accelerated cooling can also be used to reduce the alloy content. With a given yield strength, it is possible to make a steel with a leaner composition (15)(17).

For steels with yield strengths above 460 N/mm², thermomechanical rolling is only possible in a limited thickness range. Thus, where very high standards are set for strength and ductility quenched and tempered steels are used, especially for thick plates. Conventional quenching and tempering of plates begins with a through heating to temperatures in the austenite area. Then comes a rapid quenching using pressurised water, and this transforms the microstructure into martensite or bainite (18)(19). During the subsequent tempering, a microstructure forms which displays an extremely fine-grain substructure with finely dispersed precipitated carbides. With direct quenching, the plate is treated with pressurised water immediately after rolling at the fastest possible cooling rate.

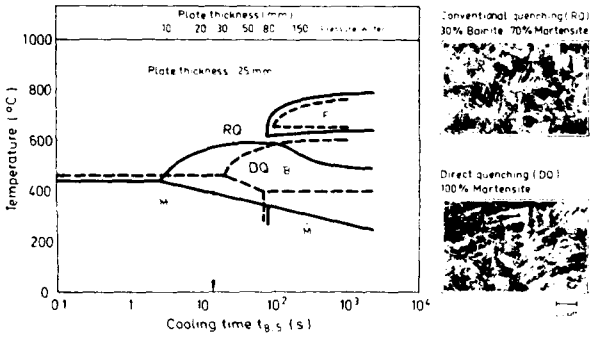


Fig. 5 - Influence of direct quenching on transformation characteristics

The improvement in the hardenability achieved with direct quenching can be illustrated with reference to Figure 5 for a CrMo-alloyed QT steel with 690 N/mm² minimum yield strength. Compared with conventional quenching the structural transformation during direct quenching starts after longer cooling times and/or at lower temperatures. Thus, for example, a 25 mm plate can be hardened through from the rolling temperature martensitically, while with hardening after reheating it partly transforms in the bainite stage.

## PROPERTIES OF HSLA STEELS FOR COMMERCIAL VEHICLE CONSTRUCTION

At the beginning a report was given of the mechanical characteristics achievable with the individual steel grades. Now a number of selected examples will be taken to illustrate the material properties achieved in actual production operations. At the same time the tendency in the development of the material will be described and hence the efficiency of normalised, thermomechanically rolled and quenched and tempered steels in commercial vehicle construction will be documented.

STRENGTH AND TOUGHNESS PROPERTIES - HSLA steels cover a wide range of applications for vehicle constructions. Figure 6 shows the relation between the yield strength and the transition temperature $T_{27}$ for unalloyed carbon-manganese steels, normalised and thermomechanically rolled microalloyed steels with ferritic-perlitic structure and quenched and tempered steels. The yield strength has values of between 210 and 960 N/mm², according to type of steel and treatment condition. With a lowering of the carbon content, a fine-grain structure and special metallurgical measures, very good toughness characteristics are achieved. The transition temperature $T_{27}$ is in the range between -20°C and -110°C (1)(20).

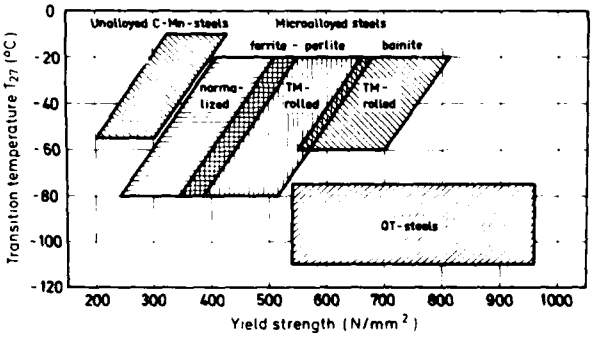


Fig. 6 - Characteristic properties of HSLA steels for commercial vehicle construction

The characteristic feature of quenched and tempered structural steels is the high yield strength, as compared with that of normalised steels. The tempering temperature plays a major role as a control factor in this connection. Figure 7 shows the relation between the yield strength and the notched bar impact energy at -60°C test temperature. In order to achieve a yield strength of about 900 N/mm² it is necessary, for example, to temper a quenched steel plate containing nickel, chromium, molybdenum and vanadium at about 670°C. The related impact energy at -60°C test temperature was about 70 Joules (18).

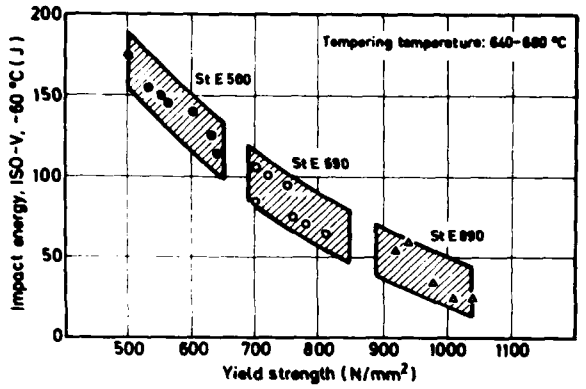


Fig. 7 - Yield strength and transition temperature of QT steels

In the construction of mobile cranes in particular, the limitation of axle loads to 10 or 14 t in relation to the total weigth and efficiency of the cranes play a major role (21)(22)(23). In crane construction, therefore, steels with very high minimum yield strengths are demanded in order to achieve high load-bearing capacities with low dead load. The use of quenched and tempered steels with, for example, 960 N/mm² minimum yield strength thus offers not only technical advantages, but also economic ones, and especially with cranes subjected to heavy loads.

To improve further the properties of plate of quenched and tempered steels, the application of direct quenching from the rolling temperature appears promising, in addition to alloying measures. The research results in Figure 8 show that direct quenching with subsequent tempering can raise the yield strengths on average by 130 N/mm², as compared with those achieved with conventional quenching. With an unchanged yield strength, the carbon equivalent can be improved by around 0.05% (18).

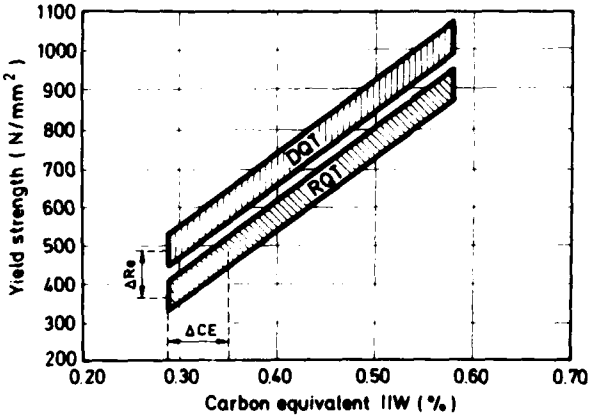


Fig. 8 - Comparison between reheat quenching and direct quenching

BRITTLE FRACTURE SAFETY - In the case of components of cold-formed steels, as used in the construction of commercial vehicles, a considerable forming capacity and a high level of brittle fracture safety under critical conditions are required.

Component tests were conducted under practical conditions on U sections similar to longitudinal girders of microalloyed hot strip with a minimum yield strength of 420 N/mm². Brittle fracture in notched sections only occurs at a temperature of -50°C to -70°C (1). Unnotched sections remain crack-free and are ductile down to -100°C, in spite of a rough cutting edge.

Similarly good results were obtained on bainitic thermomechanically rolled steels with 850 N/mm² yield strength (Figure 9). The brittle fracture behaviour of a longitudinal truck girder of TM steel was excellent.

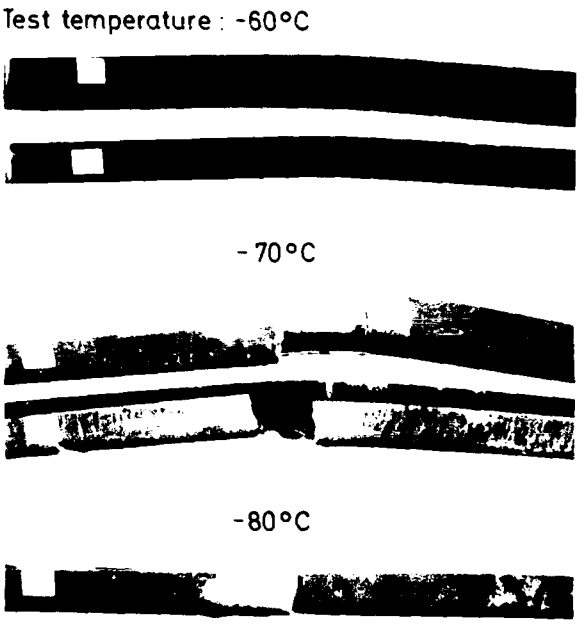


Fig. 9 - Unnotched girders, 73 x 305 x 1400 mm, 6,4 mm thick. Distance between supports: 1200 mm Load: 0.3 t from 1.3 m height.

The brittle fracture behaviour of quenched and tempered fine-grain structural steels was investigated by means of the Pellini drop weight test (18). This is to check whether the brittle fracture in a welding bead spreads to one of the two lateral surfaces of the specimens, or whether it is stopped before that happens. Figure 10 shows NDT temperatures of various steels in the form of scatter bands determined on various plate thicknesses. The results show that these steels display very good toughness properties, despite their high yield strength.

| Steel grade | Alloying elements | Yield strength N/mm² | Plate thickness mm | NDT - temperature, °C -20 -40 -60 -80 -100 -120 |
|---|---|---|---|---|
| StE 460 | MoNi | 505 | 20 - 25 | Pellini test piece |
| StE 500 | MoNi | 510 - 610 | 15 - 35 | |
| StE 690 | CrMoZr, NiCrMoB | 720 - 800 | 20 - 75 | |
| StE 890 | NiCrMoV | 920 - 1050 | 15 - 35 | |

Fig. 10 - NDT temperatures of quenched and tempered steels

FATIGUE STRENGTH - The resistance of the steels under discussion to cyclic load is of great importance for vehicles. Of special interest is the fatigue strength of welded joints, which is below that of the base metal because of the high notch effect at the transitions between weld and base metal. Post-treatment of these transitions by shot peening or TIG dressing can give a more favourable configuration to the critical transition areas. Recent research results shown in Figure 11 reveal that, under optimized post-treatment conditions, the welded joints can achieve the fatigue strength of the base metal (24)(25)(26).

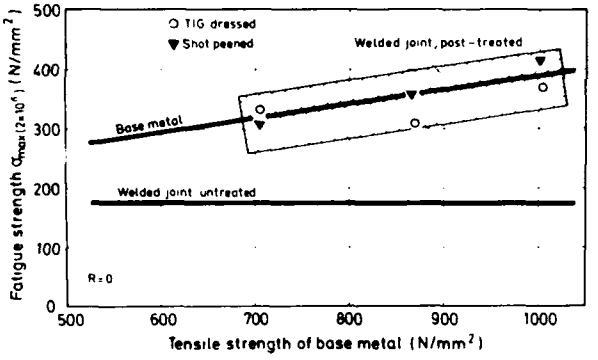


Fig. 11 - Improvement of fatigue behaviour of butt-welded joints

WELDABILITY - A high level of weldability is an important requirement in steels used in vehicle construction. With thermomechanically rolled steels, it is less the question of maximum hardness or embrittlement in the heat affected zone which play the mayor part. Rather it is a question of limiting the heat input, because of the softening zone which arises during welding in the heat affected zone. Figure 12 shows the tensile strength of welded joints of 6 mm thick TM steel with a minimum yield strength of 700 N/mm² as a function of the cooling time between 800 and 500°C. For the steels investigated, an upper limit for the cooling time of 15 s is recommended (27), in order to remain above the required tensile strength.

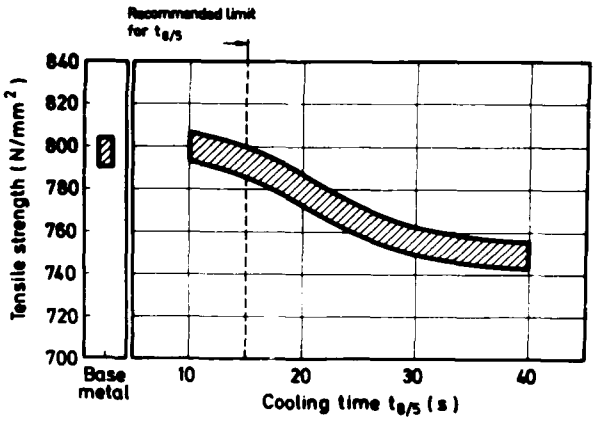


Fig. 12 - Tensile strength of welded joints as a function of welding conditions

The influence of the welding conditions on the toughness of the heat affected zone of quenched and tempered structural steels is shown in Figure 13, with reference to the example of a CrMo-alloyed steel with a minimum yield strength of 690 N/mm². It can be seen that it is necessary to limit the heat input upwards for an HAZ ductility comparable with that of the base metal. The heat input applied during welding depends on the welding procedure, plate thickness, preheating temperature, weld preparation and the requirements imposed on the structures.

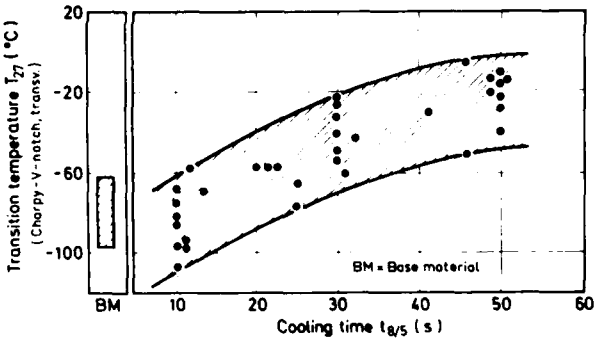


Fig. 13 - Influence of the welding conditions on the ductility of the heat affected zone

FORMABILITY - HSLA steels for the construction of commercial vehicles tend to be cold-formed. The normalised steels discussed and the thermomechanically rolled steels are suitable for use in forming processes with high requirements regarding cold-forming behaviour in longitudinal and transverse direction. Their good cold-forming behaviour is brought about with the help of an optimized sulphide shape control by the addition of certain alloying elements. As a proof for the cold-forming behaviour of TM-rolled steels the excellent formability of QStE 700 TM in bending specimens should be mentioned. Even after the application of an artificial notch to simulate cutting edges during processing the material deformed without cracking. Hot

forming is generally not acceptable here, because the TM condition is then no longer present (27).

Quenched and tempered structural steels are generally also fabricated by cold-forming, i.e. at temperatures below the maximum allowable stress relieving temperature. The strain hardening effect and the loss of ductility through cold deformation can be partly repaired by stress relieving. Hot forming above 600°C makes it necessary to perform a fresh quenching and tempering which corresponds to the treatment in the production route. It can be seen that the fabrication technology is of fundamental importance for the practical suitability of products made from these steels (28).

Figure 14 also shows that, with an increasing yield strength, a larger bending radius has to be provided to ensure crack-free forming. In Figure 15 the allowable limit of the mandrel diameter for crack-free bending, related to the plate thickness, is plotted against the minimum yield strength.

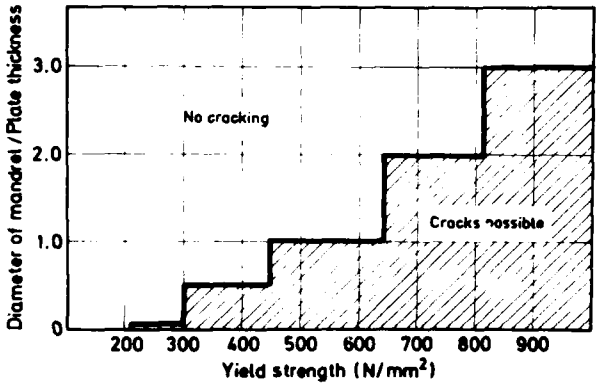


Fig. 14 - Characterization of the formability in the bending test

WEAR RESISTANCE - The behaviour under wear-inducing conditions is important for steels in commercial vehicles. Figure 15 shows the wear resistance of TM-rolled steels and quenched and tempered steels as compared with the steel St 37-3. The results show that both conventional cold formable steels as well as bainitic TM steels perform in an excellent fashion in the laboratory peening test. By lowering the tempering temperature, it is possible to increase the hardness level of quenched and tempered steels, and hence to improve their wear behaviour yet further as against conventional structural steels (29).

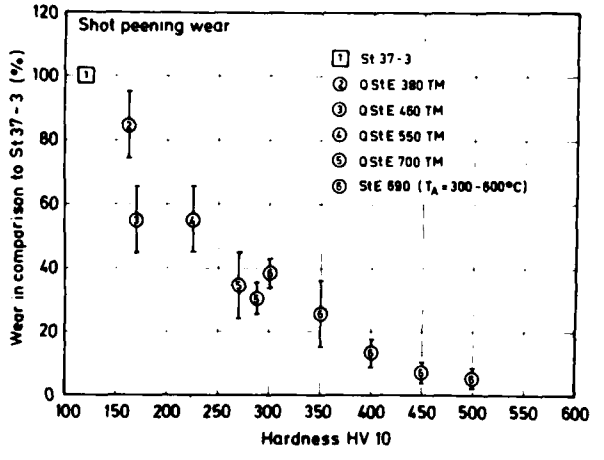


Fig. 15 - Relation between hardness and wear behaviour of HSLA steels

## APPLICATIONS

The range of applications for normalised, thermomechanically rolled and quenched and tempered fine-grain structural steels encompasses a wide spectrum of components, some with complicated shape, e.g. cross-girders bent at right-angles, front axle elements and complete vehicle frames. Whole vehicles, e.g. garbage municipal trucks and truck trailers, are manufactured from perlite-reduced TM steels, whereas quenched and tempered steels are given preference for the construction of mobile cranes, road tankers and other particularly critical applications.

## REFERENCES


(1) Meyer, K., Fickel, H.-P. and D. Stender, Thyssen Techn. Ber. 11, H. 1, 86-93 (1979)

(2) Herr, D. and B. Müsgen, Thyssen Techn. Ber. 11, H. 1, 77-85 (1979)

(3) Degenkolbe, J. and D. Uwer, Thyssen Techn. Ber. 14, H. 1, 29-46 (1982)

(4) Meyer, L., Thyssen Techn. Ber. 14, H. 1, 48-65 (1982)

(5) Stahl-Eisen-Werkstoffblatt 092, Warmgewalzte Feinkornstähle zum Kaltumformen, VDEh (1975)

(6) Euronorm 137, Bleche und Breitflachstahl aus vergüteten schweißgeeigneten Feinkornbaustählen (1983)

(7) Baumgardt, H., de Boer, H., Müsgen, B. and U. Schriever, Stahl u. Eisen 105, Nr. 13, 709-716 (1985)

(8) Haastert, H.-P. and E. Höffken, Thyssen Techn. Ber. 17, H. 1, 1-10 (1985)

(9) Haastert, H.-P., Mehlan, D., Richter, H. and R.W. Simon, Stahl u. Eisen 105, Nr. 11, 617-622 (1985)

(10) Schauwinhold, D., Stahl u. Eisen 102, Nr. 21, 1077-1082 (1982)

(11) Lessels, J., High Strength Low Alloy Steels International Iron and Steel Institute Committee on Technology (1987)

(12) Müsgen, B., Thyssen Techn. Ber. 14, H. 1, 66-78 (1982)

(13) Baumgardt, H., Rohde, M. and L. Schulz, Thyssen Techn. Ber. 14, H. 2, 126-135 (1982)

(14) de Boer, H., Beenken, H., Branscheid, P., Floßdorf, F.-J., Haumann, W., Hof, W. and H. Litzke, Stahl u. Eisen 105, Nr. 22, 1297-1305 (1985)

(15) Degenkolbe, J., Mahn, J., Musgen, B. and J. Tschersich, Influence of Accelerated Cooling of Plate from Rolling Temperature on the Properties of Microalloyed Steel, Presented at the TMS-AIME Conf. on "Accelerated Cooling of Steels", Pittsburgh, Pa. (1985)
(16) Straßburger, C. and L. Meyer, Thyssenforsch. 3, H. 1/2, 2-7 (1971)
(17) Degenkolbe, J., Mahn, J., Müsgen, B. and J. Tschersich, Thyssen Techn. Ber. 19, H. 1, 41-55 (1987)
(18) Müsgen, B., Metal Constr. 17, Nr. 8, 495-500 (1985)
(19) Lotter, U., Müsgen, B. and H. Pircher, Thyssen Techn. Ber. 16, H. 1, 13-23 (1984)
(20) Gorges, G., Straßburger, C. and B. Pretnar, Merkblatt 498 der Beratungsstelle für Stahlverwendung, Düsseldorf (1978)
(21) Brenner, M., Oerlikon-Schweißmitteilungen 32, Nr. 1, 11-15 (1974)
(22) Gerster, P., Stahl u. Eisen 104, Nr. 2, 91-94 (1984)
(23) Uwer, D. and H. Dißelmeyer, IIW-Doc. No. IX-1433-86 (1986)
(24) Müsgen, B., Stahl u. Eisen 103, Nr. 5, 225-230 (1983)
(25) Hoffmann, K. and B. Müsgen, DVM Vortrags- und Diskussionstagung, Bad Nauheim, April 3-4 (1985)
(26) Hoffmann, K. and B. Müsgen, Proceed. "Steel in Marine Structures", 3rd International ECSC Offshore Conference, Delft, The Netherlands, June 15-18 (1987)
(27) Massip, A., Meyer, L. and G. Stich, Stahl u. Eisen 106, Nr. 3, 115-121 (1986)
(28) Müsgen, B. and J. Degenkolbe, Bänder Bleche Rohre 19, H. 2, 56-62 (1978)
(29) Pircher, H. and H. Lendowski, Thyssen Techn. Inform. "Werkstoffe für Verschleißbeanspruchung", Duisburg, 4-11 (1978)

# DIRECTION OF DEVELOPMENT OF MICROALLOYED FORGING STEELS FOR MOTOR CAR INDUSTRY

**Alain Guimier, Philippe Charlier***

*Formerly: ASCOMETAL-Hagondange
LeBronze Industriel
Bobigny, France

Renault
Boulogne Billancourt, France

RENAULT began to take close interest in microalloyed steels for bar products for mechanical engineering applications in 1976-77 in conjunction with SAFE (Société des Aciers Fins de l'Est - located in HAGONDANGE and now part of the ASCOMETAL Group (1). Since that date, a certain number of microalloyed steel parts have been manufactured or are in development. In parallel, better knowledge of the usage and implementation characteristics of these steels has been acquired. In 1988, the growth conditions for these steels are favourable for different reasons which will be explained in this report. Such a growth will make the most, not only of the main feature of these steels, which is to obtain a high tensile strength in the 'as forged' condition, but also of "complementary" and original characteristics to which we shall return.

## 1 - PRESENT SITUATION OF MICROALLOYED STEELS AT ASCOMETAL

ASCOMETAL is in a position to manufacture a wide range of microalloyed steels; "classic" steels of MV (Manganese-Vanadium) type, steels intended for threaded fasteners (UGITOS speciality - ASCOMETAL's FOS plant) and steels METASAFE (see table 1).

| | C | Si | Mn | Cu | Ni | Nb+V |
|---|---|---|---|---|---|---|
| METASAFE 800 | 0.22 | 0.15 | 1.5 | | | 0.19 |
| METASAFE 1000 | 0.43 | 0.15 | 1.5 | | | 0.16 |
| METASAFE 1200 | 0.21 | 0.55 | 1.5 | 1.4 | 1.5 | 0.13 |

TABLE 1. Average analytic composition (in %) of the principal METASAFE steels in terms of target tensile strengths.

A brief reminder should be made of the metallurgical principles on which the manufacture of these steels is based. Their main characteristic is to present a tensile stress, in the 'as forged' or 'as hot rolled' condition, practically independent of heating and cooling conditions. Depending on the tensile stress level, these steels contain variable contents of carbon, manganese, copper, nickel; they all contain the same types of microalloying elements (aluminium, niobium an vanadium). Their main roles are as follows:

- Precipitation hardening of the ferritic matrix.
- Resistance to enlargement of the austenitic grain and refining of the ferritic grain (especially Al and Nb).
- Control of hardenability (V and Nb) on which the microstructure obtained after hot forming greatly depends (lowering of the transformation temperature is especially favourable to a reduction in the interlamellar space of the perlite, which allows and increase in strengnt for categories with ferrito-perlitic structure; at UGITOS, research on the contrary aims to obtain a bainitic microstructure for low carbon content steels intended for threaded fasteners).

Besides the effects of microalloying elements, the following metallurgical principles are used:

- Hardening of the ferrite by the presence of elements in solid solution; this is chiefly manganese (see table 1), but also silicon.
- Additions of copper (METASAFE 1200 steels) which permit supplementary hardening both by an effect of solid solution and by structural hardening. It is to be noted that the complementary addition of nickel is necessary to avoid

phenomena of embrittlement due to the copper alone.

- Carbon plays a fondamental role since it determines the "basic" hardness of the matrix (see table 1). Depending on the category of METASAFE it varies between 0.15% and 0.45%.

In the beginning of the eighties a certain amount of knowledge was available regarding the implementability and the usage characteristics of these steels (2):

- Hot forming does not raise any particular problem.

- Machinability is, with given tensile strength and given contents of elements to improve machinability, at least as good as for quenched and tempered steels.

- Nitridibility, and in particular ionitridibility, is good (3).

- Fatigue resistance is comparable with that of steels quenched and tempered at the same hardness level.

- Impact strenght remains appreciably lower than that of steels quenched and tempered for the same level of hardness.

Research over the last few years has principally been directed towards the possibilities of improving impact strength and knowledge of the cold forming behaviour of these steels.

As regards impact strength, there expected from analytic compositions; on niobium, enable a fine grain to be obtained by thermomechanical treatment, hence a distinctly steel. In the field of bar products, these treatments are however difficult to implement on account of the heterogeneousness of the deformations, both on hot rolling and on hot forging, producing grains of very different size depending on the zones. For forgings, the research into optimum forming conditions would from this point of view require probably very difficult final development work. As regards rolled bars, cooling tests in a flat jet of water have recently taken place in Hagondange and examination of the samples is in progress; the metallurgical goal is to obtain transformation of the austenite of the steel at a fairly low and uniform temperature through the cross-section. Tests common ASCOMETAL/RENAULT/ENSMA (Ecole Nationale Supérieure de Mecanique et

Thermal hardening at 600°C enables a ferro-perlitic structure with very fine grains to be obtained, corresponding to a doubling of the impact strength level (see table 2) for an identical tensile stress value (1000 MPa).

| METASAFE 1000 | Rough rolled condition | Post isothermal hardening |
|---|---|---|
| Tensile stress (MPa) | 1000 | 1000 |
| Impact Strength (Mesnager daJ/cm²) | 5 | 10 |

TABLE 2. Improvement in impact strength by isothermal hardening at 600°C on a METASAFE 1000 type steel.

Other tests likewise carried out within the framework of the common research program have demonstrated that interesting results could be obtained by cooling in pulsed air.

Thus, controlled cooling on rolling for applications of parts machined from bar, or on forging (e.g. by fluidized bed for carrying out isothermal hardening), make it possible to envisage an improvement in impact strength properties of microalloyed steels at constant tensile strength without appreciable modification to their present analytical composition.

In another respect, it has been and demonstrated that the cold forming of parts made from 0.2% carbon microalloyed steels could be industrially envisaged (4).

## 2 - REVIVAL OF INTEREST IN THE USE OF MICROALLOYED STEELS IN THE FRENCH MOTOR CAR INDISTRY AND IN PARTICULAR AT RENAULT

Although metallurgically there has been no spectacular improvement in the characteristics of these steels over the past few years, there is at present some revival of interest.

Besides better knowledge of their properties, another determining factor is the interest of certain "complementary" and original properties of these steels. Thus, at RENAULT, there are of course cases of applications where it is the elimination of the quench and temper treatment which is decisive (case of reaction rods and swivel axle spindle carriers, see § 3 hereafter), but in several examples, it is the "complementary" characteristics that were decisive:

* Weldability

It is possible to considerably diminish the carbon content of these steels so as to give them good weldability without reducing the tensile strenght (compensation for loss of strength resulting from the drop in carbon content by an increase in manganese and/or copper and microalloying elements contents). The main example of the use of this good weldability is the rear antisway bar made from METASAFE F1200.

* Lesser sensitivity to quench cracking.

The possible drop in carbon content permitting good weldability as a rule enables the part to become less sensitive to thermal shock; this is the factor which was decisive for the production launching of swivel axle spindle carrier plates made from METASAFE 700 instead of an AF70 steel for which the minimum tensile strenght of 700 MPa can only be obtained with a high carbon content, of approximately 0.55%; with this carbon content, the cooling water of the automatic hot forging presses is responsible for the transitory appearance of incompatible quench cracking which can only be 100% eliminated by expensive part-by-part inspection.

* Cold formability of microalloyed steels with carbon contents lying between 0.1 and 0.2%.

These steels present cold formability which is likewise at the origin of other developments in the field of threaded fasteners (microalloyed steels type 20M5 and 10M7 and for the manufacture of swivel axle spindles (METASAFE 800 type steel).

For these applications, hardening of the steel by solid solution and by precipitation is completed by the work-hardening effect.

* Disappearance of the necessity for straightening operations indispensable for parts undergoing quench and temper treatment: example of manufacture of prototype anti-sway bars with very accurate geometry.

## 3 - EXAMPLES OF MANUFACTURE AND DEVELOPMENT OF PARTS MADE FROM MICROALLOYED STEELS AT RENAULT

### 3.1 History

The first tests on using parts made from microalloyed steels at RENAULT in conjunction with the SAFE involved a reference part which was a swivel axle spindle carrier: this was a swivel axle spindle carrier for the R12 and R18 made from 20MC5 (then 20MB5 quenched and tempered to give 900-1100 MPa), which revealed to be the ideal component for such testing. It is a safety-related part for which three important quality criteria are taken into account: hardness, fatigue resistance and impact strength. Different batches of parts were manufactured by SAFE from METASAFE 900 and METASAFE 1000 (including a version with improved machinability) and laboratory tested. If the hardness and endurance aspect proved to be satisfactory, the impact strength gave rise to some reserves taking into account the results of testing the steering arm on a vertical drop test rig: the parts made from quenched and tempered steel in fact allowed significant deformation of the steering arm without fracture while the parts made from microalloyed steels broke at lower deformation levels. Although this test was relatively severe, it left an unfavourable impression for that type of part without however brushing aside the possibility of employing microalloyed grades for differently stressed parts. Other factors likewise curbed the development of the use of such steels at RENAULT at that time:

- Insufficient knowledge of product usage characteristics.
- Sales price considered as unattractive (problem of commercial policy).

Parallel start-up of post forging direct treatment on conventional grades which were beginning to give interesting results.

The graph in figure 1, where the impact strength and the tensile stress are correlated, situates the potential utilizations of microalloyed steels on automotive parts: to be noted is the "comfortable" situation of quenched and tempered steels compared with microalloyed steels.

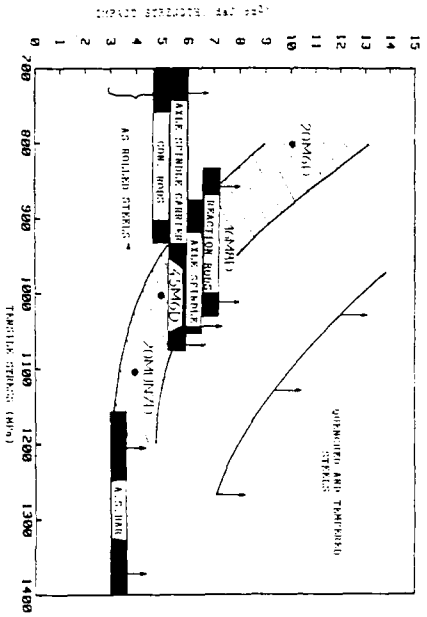

Fig 1 : Potential use of microalloyed steels.

The tensile strength properties of the different families of parts liable to be concerned by microalloyed steels are shown with the minimum impact strength requirements of the specification: reaction rods, swivel axle spindles, swivel axle spindle carriers, anti-sway bars and rods. The possibilities for use of these parts are detailed in the following paragraph.

3.2 Pratical exemples

3.2.1 R9-R11 rear anti-sway bars made from METASAFE 1200

This bar is the first industrial application of microalloyed steels in RENAULT products. It plays an active part in the quality of the vehicle's suspension and its roadholding. It is a part subjected to heavy torsional and flexural fatigue stresses. Its resistance demands a tensile strength of 1200 MPa and a minimum yield strength of 1050 MPa.

The part consists of a rectilinear bar with both ends welded to a yoke bolted to the rear suspension arms (see figure 2).

Fig 2. Anti-sway bar made from METASAFE F1200

The major manufacturing difficulty lies in the existence of two welds which are themselves also fatigue stressed. With be the conventional arrangement using quenched and tempered steel, post welding heat treatment of the entire bar was necessary, which called for a straightening operation and which raised the problem of the yokes. An arrangement using weldable, therefore low carbon steel, with elevated properties, was therefore sought after. Preservation of strength in the welded zones called for either the use of a highly alloyed quenched and tempered steel of the 18 CND6 kind, or the choice of a microalloyed steel, METASAFE 1200. Both arrangements were successfully tested and enabled the target endurance levels to be obtained (see figure 3). The microalloyed steel was decided upon because of economic criteria.

Since 1981, more than 4 million anti-sway bars have thus been manufactured with total reliability.

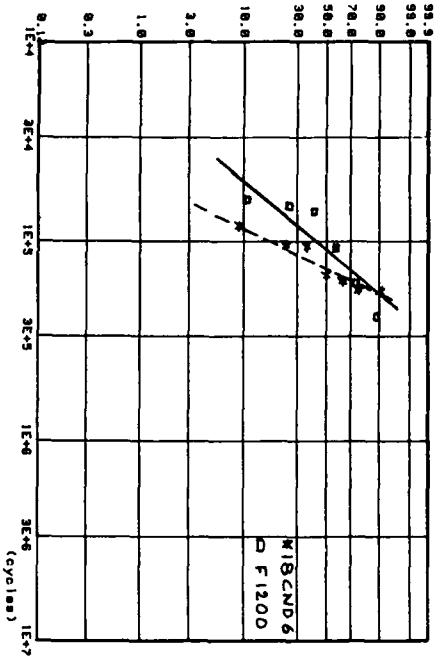


Fig 3. Fatigue life of anti-sway bars made from microalloyed or QT steels.

3.3.2 R4 rear swivel axle spindle made from METASAFE 800

The rear swivel axle spindle, press fitted in the suspension arm, is the spindle around which the roadwheel turns. It is subject to heavy fatigue stresses and must in addition be capable of supporting shocks without sudden fracture when the roadwheel strikes an obstacle. These essential requirements lead to the choice of a steel with minimum tensile strength of 870 MPa with localized induction hardening treatment of the press fitting zone (see figure 4).

Fig 4. Axle spindle made from METASAFE 800 and induction treated

The part is cold extruded. The initial arrangement consisted of 20MC5 post extrusion quenched and tempered steel. For economic reasons, it was then manufactured from METASAFE 800 microalloyed steel. This steel, with bainito-ferritic structure, behaves well on cold extrusion and induced work-hardening enables the required strength level to be attained.

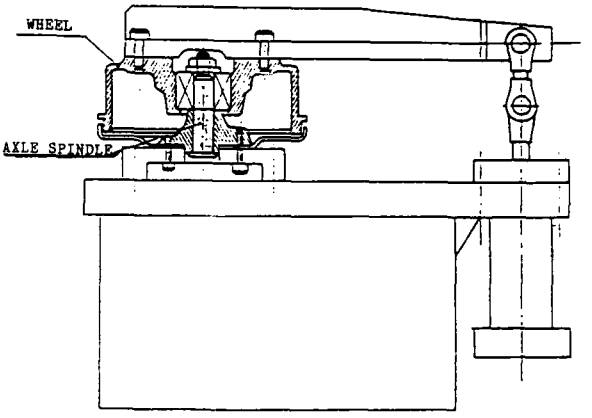


Fig 5. rig for fatigue testing of spindle

Tested on the rig shown in figure 5, the swivel axle spindle did not break after $10^7$ cycles at the nocinal stipulated load. Submitted to an overlead of 30%, its fatigue life, although slightly less than that of quenched and tempered steel, remains longer than 750,000 cycles at B10 (see figure 6).

Finally, its behaviour during impact testing is very satisfactory; even with a strong force, the part bends without breaking, just like the part made from 20MC5, thanks to induction hardening treatment of the flange.

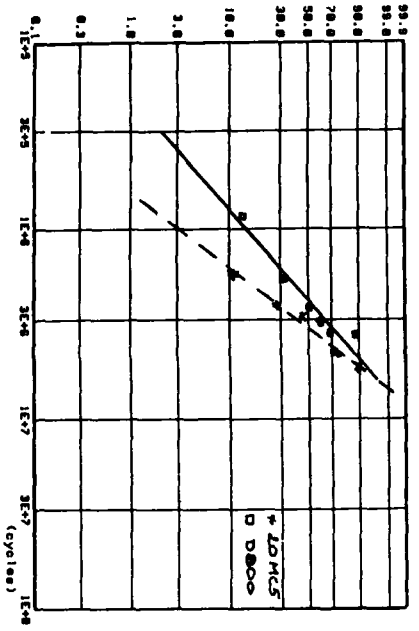

Fig 6. Fatigue life comparison between axle spindles made from microalloyed or QT steels.

3.2.3 R4-R25 reaction rods (see figure 7).

The reaction rod forms a wishbone with the front lower suspension arm of the R4 and with the upper arm of the R25. This part is submitted to compressive and flexural fatigue stresses. It must be capable of supporting impacts on the road-wheel without bending. In another respect, the mounting lug is cold formed. The METASAFE 800 arrangement is a good compromise between these various requirements and is economic in comparison with quenched and hardened arrangements.

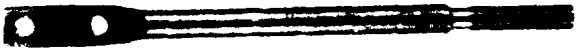

Fig 7. Reaction Rod made from METASAFE 800

3.2.4 R21 rear swivel axle spindle carrier plate

This part (see figure 8) is made from AF 70 S carbon steel with a tensile stress of 700 MPa. It is hot forged on a high-rate horizontal forging machine. Water cooling of tooling gave rise to a few quench craks which required a severe inspection procedure to be set up.

The use of a microalloyed steel, METASAFE 700, with improved machinability enabled the same mechanical properties to be obtained, while eliminating risks of quench cracking, on account of its low carbon content.

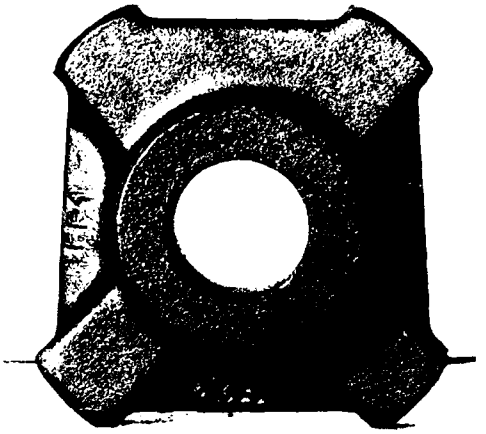

Fig 8. Swivel axle spindle carrier plate hot forged with METASAFE 700.

3.3 Parts under development

3.3.1 Rear swivel axle spindle: "nail-shaped" swivel axle spindle

This part, obtained by cold forming , is at present made from quenched and tempered 20MC5 steel. The required hardness can be obtained by combination of the effect of microalloying elements and cold forming. Figure 9 illustrates a comparison of hardnesses obtained according to the two processes. In spite of the slightly lower hardnesses, the METASAFE D800 arrangement meets the requirements of endurance and impact testing analogue to the description given in § 3.3.2. Type approval of the part for the entire

RENAULT medium range is under way.

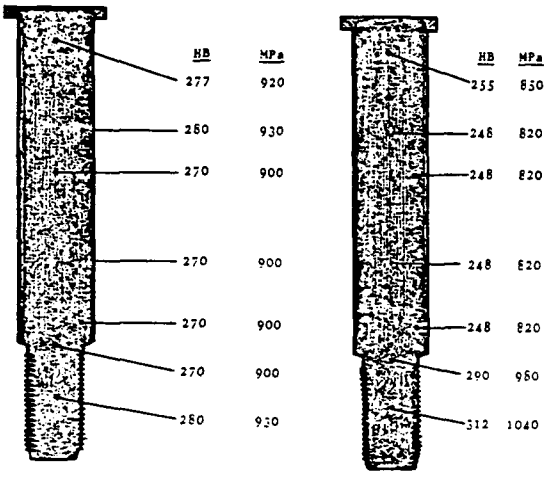


Fig 9. Comparaison of hardneses of cold form axles pindles
left. Quenched and tempered steel
right. Microalloyed steel.

3.3.2 Swivel axle spindle carrier

Contrary to other car manufacturers, RENAULT does not as yet use microalloyed steels for the manufacture of its swivel axle spindle carriers. The employment of annealed carbon steels or steels that have merely undergone a post forging controlled cooling cycle enables the necessary mechanical properties to be obtained (600 to 700 MPa).

However, for manufacturing more heavily stressed axle assemblies, increased hardness is becoming necessary and arrangements made from microalloyed steels are being tested in competition with quenched and tempered steels.

CONCLUSION

At present, we are withnessing real growth in the used of microalloyed steels for bar products in mechanical engineering.

ASCOMETAL was one of the first iron & steel metallurgists to launch this type of product and is continuing to actively participate in their growth on a European scale, and in particular with RENAULT.

At RENAULT, as with the other main users, growth is to be witnessed that is often connected with the original characteristics of microalloyed steels outside of their main feature, which is that which enables high tensile stress to be obtained without quenching and tempering heat treatment. The classic applications as substitution for quenched and tempered steels remain of course a reality as demonstrated by the industrial production start-up of reaction rods and Design Office testing on the manufacture of swivel axle spindle carriers for new vehicles.

References

1. BACKER L, CHARLIER P, CRIQUI B et EL HAIK R. in "HSLA Steels Technology and Applications (ASM-Metals Park, Ohio, 1984), 1025-10

2. BACKER L, CHARLIER P, HECHELSKI R : Séminaire sur les modifications des exigences de qualité dans la demande d'acier - ONU-TURIN (ITALIE) Juin 82

3. MONGIS J, PEYRE JP, TOURNIER C : traitement thermique 1984,n 3, 71/75

4. CHARLIER P: mise en forme à froid des aciers à dispersoïdes en produits longs : Ecole d'Ete "Matériaux. Mise en forme. Pièces formées". Ile d'Oléron 21.25/09/87 (recueil des communications à paraître).

# EVALUATION OF MEDIUM CARBON MICROALLOYED STEELS FOR CONNECTING ROD APPLICATIONS

**Debanshu Bhattacharya, Richard S. Cline**
Inland Steel Company
East Chicago, Indiana, USA

**Gary A. Garitson**
Cummins Engine Company
Columbus, Indiana, USA

## ABSTRACT

A joint program between Inland Steel Company and Cummins Engine Company has evaluated the use of medium carbon microalloyed steels for diesel engine connecting rods. Two medium carbon, microalloyed compositions were investigated, one of which also contained a machinability enhancing additive. Tensile properties, microstructures, machinability, and fatigue performance were evaluated and compared to the currently used quenched and tempered AISI 15B41.

The mechanical properties of the forged connecting rods show that comparable tensile strengths can be obtained using the air-cooled microalloyed steels compared to the quenched and tempered AISI 15B41. Machinability was evaluated using the Inland drill test since drilling is often the rate controlling machining operation in connecting rod manufacturing. Results of these tests show that the microalloyed connecting rods exhibit both lower drill force and lower drill torque indicating better machinability than the quenched and tempered 15B41. The fatigue properties of the rod forgings were evaluated by full component testing. An alternating load was applied around a compressive mean. Fatigue strength was found to be comparable between the microalloyed steel rods and those made from the AISI 15B41 material.

## INTRODUCTION

A joint program was undertaken between Inland Steel Company and Cummins Engine Company to evaluate microalloyed steels for connecting rod applications. This program is part of a larger program at Cummins Engine to investigate ways of reducing the overall cost of diesel engines. The microalloyed steels could contribute to this effort by eliminating the cost of heat treatment and perhaps by improved machinability compared to the quenched and tempered AISI 15B41 currently used for this part. The program was planned such that Inland Steel was to develop and supply the microalloyed steels, Modern Drop Forge would forge the connecting rods, and the forged connecting rods would be evaluated by Inland Steel Research and Cummins Engine Company.

## EXPERIMENTAL PROCEDURE

MATERIALS - The steels selected for the program were AISI 10V45, 15V37 Modified, and the currently used AISI 15B41 H. The AISI 10V45 was produced as an electric furnace heat and rolled from the 7 x 7 inch cast billet to 2-9/16 inch round at the Indiana Harbor Works of Inland Steel Company. The 15V37 Modified was produced as 300-lb air-melted heats at Inland Steel Research Laboratories and cast into 6-1/2 x 6-1/2 inch x 18 inch molds. These ingots were then forged into 2-9/16 inch round. The nominal chemical compositions of all the steels in the program are given in Table I.

TABLE I

Nominal Chemical Compositions

| | C | Mn | P | S | Si | V | Ca | Al | B |
|---|---|---|---|---|---|---|---|---|---|
| 10V45 | 0.43/0.50 | 0.60/0.90 | 0.04 max | 0.045 max | 0.15/0.30 | 0.08/0.15 | - | - | - |
| 15V37 Mod | 0.32/0.39 | 1.0/1.5 | 0.04 max | 0.5/0.6 | 0.08/0.15 | 0.08/0.15 | 0.002/0.004 | 0.03 max | - |
| 15B41 H | 0.35/0.45 | 1.25/1.75 | 0.04 max | 0.05 max | 0.15/0.30 | - | - | - | 0.0005/0.003 |

PROCESSING - Connecting rods were forged from the microalloyed bars by Modern Drop Forge. The bars were induction heated to 2350-2400 degrees Fahrenheit, forged and air-cooled. Current production connecting rods were made from 15B41, forged similarly, but were quenched and tempered following the forging operation.

The connecting rod forgings from all three compositions were machined by Cummins Engine Company into standard rods, using established manufacturing practices.

TESTING - To examine the through section hardening, connecting rods forged from all three steels were sectioned longitudinally at the mid-thickness plane, surface ground, and the HRC hardness measured at 0.375 inch intervals.

The microstructure was examined on cross-sections cut from the I-beam section of the connecting rods, and the prior austenitic grain size was determined using the 20 cm circle intercept method. Volume fraction pearlite was determined by using standard point count techniques.

The as-forged tensile properties were determined using standard ASTM tensile specimens obtained from the bolt boss area of the connecting rods.

Since drilling is probably the most important and often the rate controlling machining operation during manufacturing, the drill test developed at Inland was used to assess machinability. The details of the test have been reported previously (1); only the salient features will be mentioned here. A multiple spindle drill press with infinitely variable feed rates and equipped with dynamometers to measure the drill force and drill torque was used. In this work, a constant feed and speed of .008 ipr and 1000 rpm were used with a fixed 1 in hole depth and M7 (HSS) drill material. To avoid variability from the manufacturer's drill points, all drills were ground in-house to a specially designed point before testing. Samples for drill tests were cut from the cap-section of the connecting rods. Each sample was of sufficient size for six drill tests with four different drills. Four connecting rods were used to yield a total of 24 drill tests. The average measured drill force and drill torque and calculated resultant force were then used to assess drillability. In addition, chip morphology and chip thickness were also observed to evaluate chip disposability.

Machined connecting rods from all three materials were fatigued tested by Cummins Engine Company. Axial fatigue tests were conducted on the full component rods. Tests rods, for the purpose of this evaluation, were held constant around a compressive mean. Lubrication was provided to the bearing shells and pin bushing to simulate engine operating conditions.

## RESULTS AND DISCUSSION

CROSS-SECTIONAL HARDNESS - The hardening responses of the steels are illustrated in Figure 1. Comparing the two microalloyed steel cross-sections, it can be seen, as expected, that the AISI 10V45 developed a higher overall hardness. The hardness pattern in both microalloyed connecting rods is quite similar with the highest hardness being developed in the I-beam section with the softer areas in the region surrounding the crankshaft bearing area. This results from the slower cooling due to the larger mass.

As shown in Fig. 1-C, the hardness pattern of the 15B41 is similar to that of the microalloyed steels. The hardness is

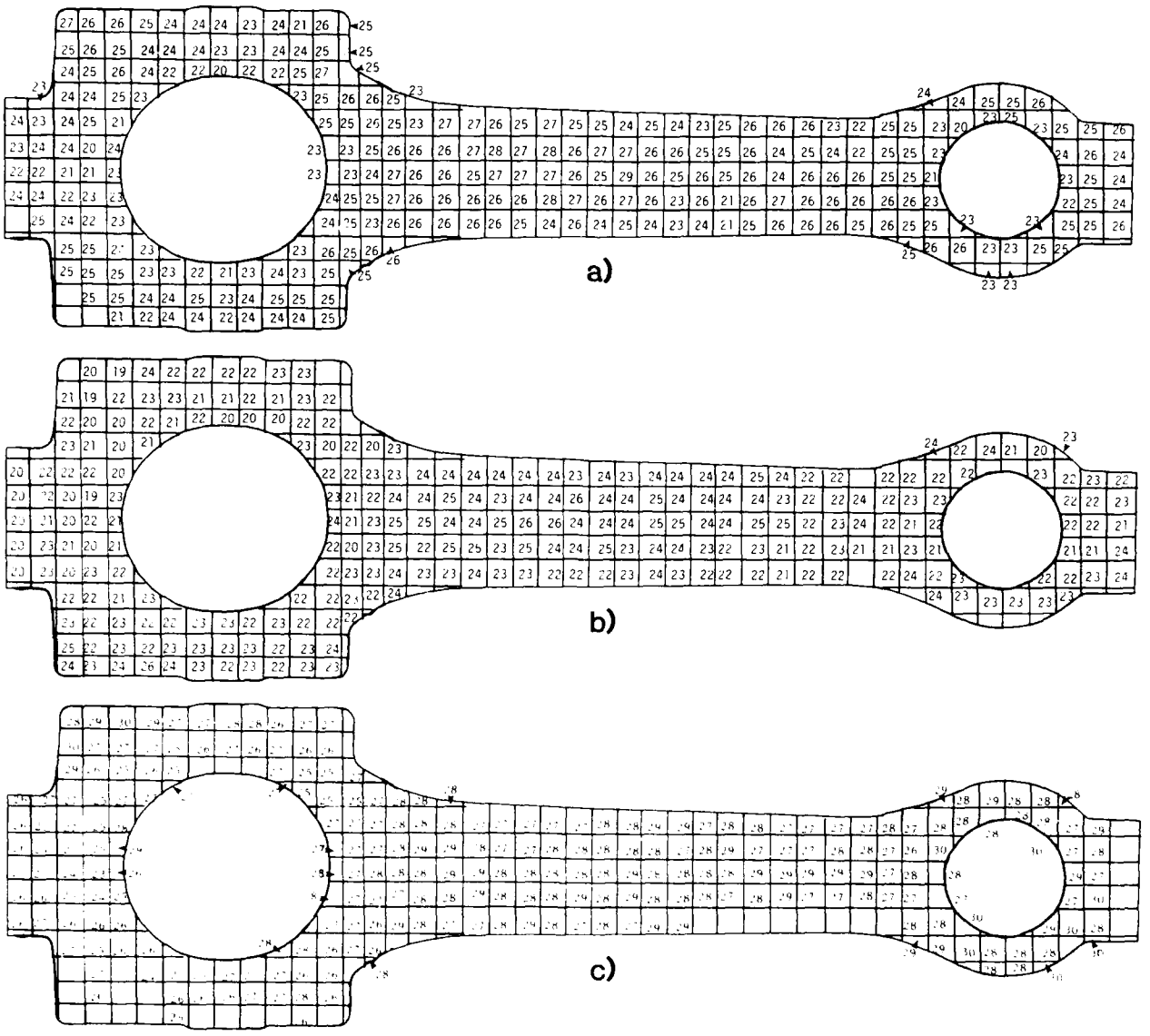


Figure 1 Hardness Profile at Mid-Cross Section of Connecting Rods HRC
a) 10V45, b) 15V37 Modified, c) 15B41H

slightly higher overall with the thinner sections exhibiting the higher hardnesses due to the faster quenching rate.

MICROSTRUCTURE - Typical microstructures of the three materials are shown in Figure 2. As expected, the 15B41 shows a tempered martensitic structure, while the microalloyed steels consist of a ferrite-pearlite structure. Austenitic grain size and pearlite volume fraction are given in Table II.

TENSILE PROPERTIES - Properties obtained from the forged connecting rods are given in Table III. These data show that an equivalent tensile strength can be obtained using the microalloyed steels compared to the current quenched and tempered product. However, the yield strengths and the ductilities are considerably lower for the microalloyed steels. Comparing the microalloyed steels, the 10V45 produces slightly higher tensile strength, but the 15V37 has a higher yield to tensile ratio. This steel also has

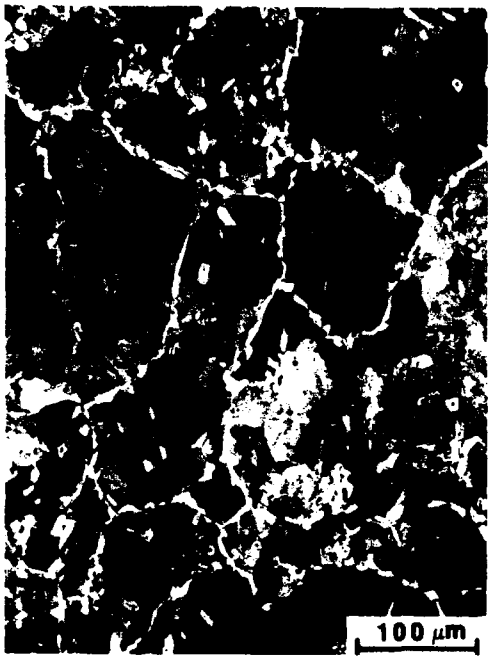


a) 10V45


b) 15V37 Modified


c) 15B41H

Figure 2 Typical Microstructures of the Connecting Rods Obtained from a Transverse Section of the I-Beam Region.

TABLE II

MICROSTRUCTURAL PARAMETERS

| | Austenitic Grain Size | | Volume Fraction Pearlite |
|---|---|---|---|
| Steel/Code | ASTM | μm | % |
| 10V45 | 1.7 | 172.1 | 94.5 |
| 15V37 Mod | 2.3 | 140.9 | 93.5 |
| 15B41H (Q&T) | 8.5 | 16.3 | ---- |

considerably higher ductility compared to the 10V45 because of the lower carbon content.

The tensile properties, Table III, are on the conservative side with respect to estimating the fatigue behavior of the connecting rod. This is because the tensile specimens were taken from the bolt boss area of the rod forging, which has lower hardness (see hardness distribution, Figure 1) than the I-beam section. Since the majority of fatigue failures occur in the I-beam section, the higher harnesses there should contribute positively to fatigue performance.

TABLE III

TENSILE PROPERTIES OF CONNECTING RODS

| Steel/Code | Y.S. (ksi) | T.S. (ksi) | YS/TS | $E_T$ (%) | Red in Area % |
|---|---|---|---|---|---|
| 10V45 | 86.0 | 133.8 | 0.64 | 10.2 | 17.5 |
| 15V37 Mod | 86.4 | 126.8 | 0.68 | 13.0 | 33.3 |
| 15B41/Q and T | 120.2 | 134.3 | 0.89 | 18.3 | 63.1 |

MACHINABILITY - The results of the drill test are given in Table IV, which includes the measured drill force and drill torque and the resultant force ($F_R$) calculated from the drill force (T) and torque (M), using the formula

$$F_R = \sqrt{\frac{T^2}{2} + \frac{2M^2}{D}} \qquad (1)$$

where D is the drill diameter.

Results are presented both for hot rolled bars and from forged connecting rods. Connecting rods of the material currently used, quenched and tempered 15B41, is used for comparison to microalloyed air-cooled connecting rods. However, hot-rolled bars of this grade could not be obtained, and hence quenched and tempered 4140 is used for comparison to the microalloyed as hot rolled bars. Resultant force for connecting rods are shown graphically in Figure 3.

These results clearly show the superior machinability of the microalloyed grades as compared to the quenched and tempered steels. In both cases of hot rolled bars and forged connecting rods, it is clear that both microalloyed grades show significantly lower drill force, drill torque and resultant force. This indicates better machinability than the corresponding quenched and tempered grades. This result is similar to earlier results on hot rolled 10V45 as compared to quenched and tempered 4140. (2)

Between the two microalloyed steel investigated, 15V37-modified shows somewhat better machinability than the 10V45, which can be explained both on the basis of lower carbon and higher sulfur for the 15XX steels than for the 10V45 steel. In terms of chip disposability, no significant differences were observed among the various grades.

TABLE IV

DRILLABILITY OF HOT ROLLED STEEL BARS AND FORGED CONNECTING RODS

| Hot Rolled Bars: | Drill Force (N) | Drill Torque (N-M) | Resultant Force (N) |
|---|---|---|---|
| Hot Rolled Bars: | | | |
| 10V45 | 1494 | 6.3 | 1517 |
| 15V37 Mod. | 1341 | 5.4 | 1327 |
| 4140/QT* | 1890 | 7.7 | 1882 |
| Forged Connecting Rods: | | | |
| 10V45 | 1673 | 5.5 | 1451 |
| 15V37 Mod. | 1357 | 5.4 | 1324 |
| 15B41/QT | 2235 | 5.6 | 1600 |

* For comparison only

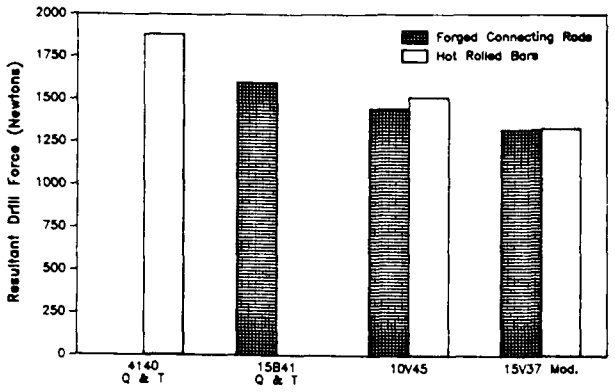


Figure 3 Comparison of the Resultant Drill Forces of the Steels Tested

In addition to the above laboratory test results, no machining difficulties were experienced during the manufacture of the sample rods on the production line. No adjustments were made in machining parameters to take advantage of potential machinability improvements with the microalloyed grades.

FATIGUE - The results of the component fatigue tests are shown graphically in Figures 4 and 5. The results have been "normalized" with current production rods being a base of 1.0.

These results show both grades of microalloyed steel to have greater mean fatigue strength than the current heat treated grade. Within the two microalloyed grades, the 10V45 had a slightly higher mean fatigue strength than the 15V37 modified.

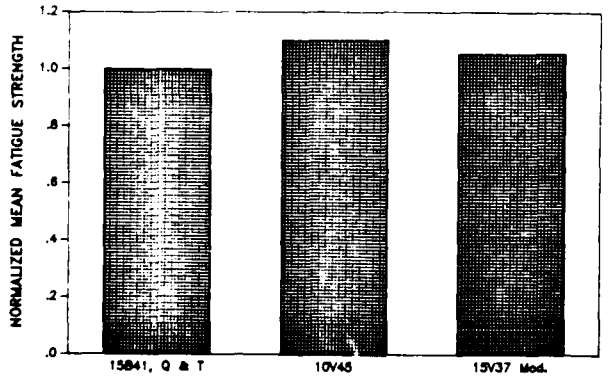


Figure 4 Comparison of the Normalized Mean Fatigue Strength of Forged Connecting Rods

In terms of distribution of data, both the current 15B41 and microalloyed 10V45 had narrow distributions, while the 15V37 modified had a broader band. This indicates that the 15V37 modified would have a statistically lower minimum fatigue strength (mean minus 3 times standard deviation).

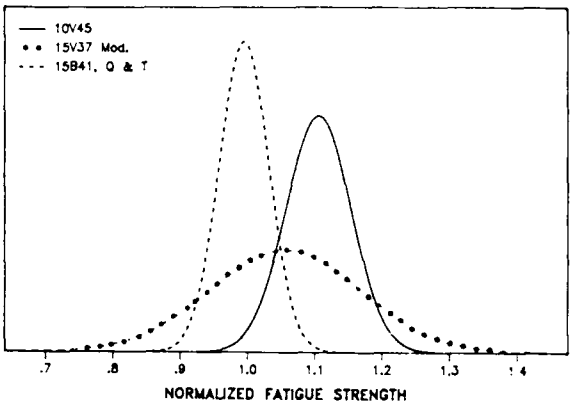


Figure 5 Comparison of the Distribution of the Normalized Fatigue Strength of Forged Connecting Rods

In analyzing the fatigue data, it should be pointed out that the 10V45 and 15B41 were mill-production heats, while the 15V37 modified were air-melted laboratory heats consisting of five separate ingots. This introduced additional variables in chemistry and material cleanliness which could negatively impact fatigue properties.

## SUMMARY AND CONCLUSIONS

Two air-cooled microalloyed compositions and one heat treated steel grade were evaluated for connected rod applications. Comparison of the results show:

1. Similar hardness patterns were observed for all three steels with the thinner regions of the I-beam section exhibiting the higher hardness.

2. Comparable tensile strengths can be obtained with air-cooled microalloyed steels. However, yield strength and ductility are lower for microalloyed than for the heat treated grade.

3. Machinability of the microalloyed steels is superior.

4. Both microalloyed steels had higher mean fatigue strengths than the quenched and tempered grade of comparable tensile strengths.

This evaluation has shown that microalloyed steels meet the functional requirements for connecting rod forgings. Further, microalloyed steels offer cost reduction potential through the elimination of one or more heat treatments following the forging operation. Improved machinability also reduces the cost of manufacture through increased tool life and/or higher productivity. Therefore, microalloyed steels of the compositions evaluated in this study can be recommended for connecting rod applications at Cummins Engine Company.

## ACKNOWLEDGEMENTS

The authors wish to acknowledge the cooperation of Modern Drop Forge Company, the contributions of Fred Neitzel and Craig Curtis of Inland Steel Company and those of Mike Oliphant and Matt Lewis of Cummins Engine Company.

## REFERENCES

1. Yaguchi, H., Mechanical Working and Steel Processing Conference, AIME, p. 223, October 1986.

2. Bhattacharya, D., Fundamentals of Microalloying Forging Steels, AIME, p. 475, July 1987.

# HIGH STRENGTH STEELS FOR OFF-HIGHWAY VEHICLES AND MINING EQUIPMENT

**G. Tither**
Niobium Products Company Inc.
Pittsburgh, Pennsylvania, USA

ABSTRACT

Various microalloyed steels, as produced in Europe, are described. Limitations of the mechanical properties with respect to plate thickness and alloy content are discussed for commercial normalized, thermo-mechanical controlled-rolled (TMCR) and quenched and tempered steels. Some industrial applications of microalloyed steels such as for mobile cranes, earthmoving equipment, mining roof support systems and ventilation systems are presented.

IMPROVEMENT IN EFFICIENCY is the basic reason for substituting higher strength steels for lower strength steel. In this context, efficiency can be defined as the benefits accrued due to weight saving, a higher inherent material strength and the use of thinner section sizes where volume production is critical.

A saving in component weight will increase the fuel efficiency of any mobile unit and if, as in the case of earthmoving equipment such as dump trucks, this can also be coupled with a dimensional saving in the body sections, an increase in volume transported will result. A higher inherent material strength will allow increased lifting capacity for a given section size which when combined into the body and chassis components of mobile cranes, for example, produces a faster, more fuel efficient, higher grade crane. A reduction in component section size by using high strength steel, as in the case of hydraulic roof supports now being used in many coal mines, maximizes the automatic cutter depth permitting more coal to be extracted from a given seam. All these uses of high strength steel can be simply translated into a saving in cost and therefore improved profitability.

It would be a huge task to describe all pieces of off-highway vehicles and mining equipment showing every application where high strength steel is used or could be used. The present paper will therefore present and briefly discuss a representative list of steels commercially produced in Europe and pinpoint several applications where they are being used. It should be remembered that equivalent steels are readily available in the USA, such as BethStar 80, T1 etc., together with many other grades of microalloyed high strength steels.

## COMMERCIAL HIGH STRENGTH STEELS

Remarkable progress has been made in recent years in understanding the metallurgy of microalloyed high strength steels. This progress has been thoroughly monitored at several international conferences.[1-4] Whilst these conferences have discussed at length the advances made in the physical metallurgy of microalloyed steels, little space was given to commercial applications, the exception being the large tonnage markets of linepipe and offshore. Of course these steels can be, and are being, used for other applications. Microalloyed steels in the normalized, thermo-mechanically controlled-rolled and quenched and tempered conditions are being effectively utilized in off-highway vehicles and other industries.

What has greatly assisted in making these steels attractive has been the accompanying progress made in primary and secondary steelmaking processes. Microalloyed steels have found increasing application due to the introduction of desulphurization and inclusion shape control, vacuum degassing and continuous casting. Confidence in the use of high strength steels has grown because of the benefits incurred from these secondary processes. These benefits mainly include:-

a. sulphur levels below 0.002%;
b. inclusion shape control;
c. hydrogen levels below 2 ppm;
d. nitrogen levels below 0.008%;
e. low levels of phosphorous, oxygen and the harmful residuals As, Sn, Sb, Bi and Pb;

f. accurate chemistry range control;
g. improved product yield, cost savings and other benefits.

In summary, these benefits serve to improve the toughness and weldability and produce an overall higher quality steel with improved product yield. The high strength, microalloyed steels can therefore now meet more stringent requirements, and previous restrictions to their use (as seen by the designer and the fabricator) should now play a minor role in the choice of steel.

The development of improved mechanical properties in the majority of commercial steels is based on well-established principles:-

a. a relatively low carbon content for improved weldability and notch toughness;
b. grain refinement to improve toughness and increase yield strength;
c. precipitation strengthening either during cooling after finish-rolling or from a normalizing treatment, or during an aging treatment after quenching;
d. solid solution hardening, although this technique is limited in that it results in impaired toughness.
e. benefits due to improved secondary processing as described earlier.

Grain refinement and precipitation strengthening are achieved by the addition of microalloying elements such as niobium, vanadium and titanium.

NORMALIZED STEELS - Normalized microalloyed steel is the workhorse of body construction for off-highway vehicles. Its usefulness is dictated by the strength required in a given section size. For plate thicknesses up to 63 mm it is possible to achieve yield strength levels of up to 420 N/mm$^2$ with good toughness using a 0.10%C-1.5%Mn-0.03%Nb steel.[5] A Nb-steel with a higher carbon equivalent value (CEV) of 0.49% max. is produced by Svenskt Stål (OX 542) which guarantees a minimum yield strength of 390 N/mm$^2$ in plate thicknesses up to 60 mm with a minimum Charpy V-notch (CVN) impact energy value of 27 Joules at -60°C. Similar niobium-containing steels are produced by other European steelmakers and a representative listing is presented in Table 1 (compositions) and Table 2 (mechanical properties).

While normalized vanadium-containing steels are commercially available which will meet a minimum yield strength of 500 N/mm$^2$, the plate thickness is generally restricted to about 16 mm. Yield strength levels greater than 480 N/mm$^2$ are guaranteed in plate thicknesses up to 35 mm in a V-Ni steel - see Grade WSTE (Table 2). Several other companies produce V and V-Ni steels, but to somewhat lower yield strength levels - see Tables 1 and 2.

Vanadium-niobium normalized steels have been developed in order to derive the individual benefits from both alloy additions. Most steel producers offer this type of steel, but the guaranteed minimum yield strength is heavily dependent on section thickness. For example, a V-Nb steel produced to meet a minimum yield strength of 460 N/mm$^2$ at 16 mm thickness is guaranteed to meet only 420 N/mm$^2$ at 80 mm thickness.

For all practical purposes current technology permits the commercial production of normalized steels with a minimum yield strength of 460 N/mm$^2$, but falling to 420 N/mm$^2$ at a plate thickness of 80 mm. However, good toughness with minimum CVN impact values of 60 J at -40°C in 75 mm thick plate can be achieved at these high strength levels.

THERMO-MECHANICAL CONTROLLED-ROLLED (TMCR) STEELS - The good combinations of strength and toughness achievable in normalized steels can be further improved by TMCR. Commercially, yield strengths up to 550 N/mm$^2$ combined with sub-zero impact transition temperatures can be obtained.

Although the property goals for TMCR steels have been set by the stringent requirements of the pipeline industry, application of these steels is by no means limited to this industry and TMCR steels are readily available and being used for general structural purposes, shipbuilding, mining machinery and earthmoving equipment. The main objective of TMCR is to produce a fine ferrite grain size giving improved strength and toughness properties. Niobium is the most common microalloy addition made to TMCR steels because of its strong influence on retarding austenite recrystallization and inhibiting subsequent grain growth by the precipitation of Nb(C,N) particles in the austenite phase. The result is that by lowering the slab reheating temperature, rolling is started from a finer-grained austenite which is maintained throughout the rolling schedule to the final plate and as the rolling temperature falls the austenite grains become more elongated and internally deformed. The increase in austenite grain boundary area, plus the introduction of deformation bands within the austenite, result in an increase in ferrite nucleation sites and a consequential fine-grained ferrite structure. The principles involved in TMCR relative to rolling practice and alloy design have been well-documented, both from a theoretical and a practical viewpoint.[1-4,6-7]

Other elements such as vanadium, titanium and molybdenum are also added to TMCR steels. Titanium behaves in much the same way as niobium in that precipitation of TiN or TiC particles (if low reheat temperatures are used) in the austenite is highly effective for grain refinement. Vanadium, on the other hand, is an effective precipitation-strengthener provided the finish-rolling temperature is not too low, say 800°C. The somewhat higher finishing temperature ensures that some vanadium remains in solution in the austenite and precipitates as V(C,N) during the austenite-to-ferrite transformation thereby strengthening the subsequent room temperature ferrite structure.

The majority of the higher strength TMCR steels produced in Europe at the present time contain both niobium and vanadium. A minimum yield strength level of 550 N/mm$^2$ with an excellent fracture appearance transition

temperature (FATT) of -80°C in the transverse direction is available in plate thickness up to, and including, 40 mm. It is claimed that yield strengths up to 700 N/mm² can be achieved in plate thicknesses up to 30 mm.[8]

A representative listing of the chemical compositions and mechanical properties of some of the TMCR microalloyed steels currently produced in Europe is presented in Table 3. As in the case of normalized steels, the mechanical properties of TMCR steels deteriorate as plate thickness increases, hence there is a limit on the potential applications for these steels. However, most, if not all, possible high strength component applications for off-highway vehicles and mining equipment should be within the scope of TMCR steels. Also of importance is that a given strength level can be obtained in TMCR steels at a much lower CEV than that possible in normalized steels,[9] see Figure 1, thereby making them more readily weldable.

QUENCHED AND TEMPERED STEELS - The effective way to manufacture higher strength structural steel plates with yield strengths of 550 N/mm² and above, in thicknesses of 30 mm and above, is by quenching and tempering. Except for a few exceptions,[10] to produce steels with yield strength values above 620 N/mm² with good toughness it is necessary to quench and temper even in thinner gauges.

The development of commercial quenched and tempered (QT) steels has taken two distinct paths:-

a. steels containing austenite grain refining and precipitation strengthening additions such as Nb, V and Ti;
b. steels containing only elements added for hardenability.

The microalloyed steels are generally limited to plate thicknesses ≤50 mm because of the reduced hardenability effect of a finer austenite grain size, although alloying to offset this reduction can raise the thickness to 80 mm.[11] QT steels containing additions of Ni, Cr, Mo and Mn can be designed to have sufficient hardenability to transform to martensite and lower bainite in plate thicknesses up to 150 mm and above. The level of alloying for both routes depends on the cooling rate and hence the quenching unit.

The microalloyed QT steels have lower CEV and hence better weldability. The metallurgical design for commercial QT steels has been dependent on the efficiency of individual steelmakers' quenching units. It is significant to note that the companies that utilize an efficient roller-quench unit have followed the microalloying route while those that possess a platten-quench unit (which gives a slower cooling rate) have tended to follow the 'alloying' route.

The chemical compositions of some of the reheated, quenched and tempered microalloyed steels produced in Europe are given in Table 4 and their mechanical properties in Table 5. It should be noted that the highest minimum yield strength quoted is 690 N/mm² and is only available from the two companies using the efficient high cooling rate roller-quench unit. These two companies also supply the thicker plates. A small addition of boron is made to the higher strength steels to effect through-hardenability.

Relating theory to practice, Figure 2 shows how the desired microstructures and hence mechanical properties of BSC's RQT steels are eventually achieved.[12] The higher cooling rates possible on the roller-quench mean that a low temperature transformation product is obtained even in plates of leaner composition. The continuous cooling curves for 12.7, 25 and 38 mm thick plates of RQT501 and 701 show that at all plate thicknesses the required microstructure can be achieved. The steels exhibit a uniform microstructure, and hence properties, throughout the plate thickness as illustrated by the hardness profiles in Figure 3. In the microalloyed QT steels the $M_S$ temperature is relatively high and the martensitic microstructure experiences significant autotempering ensuring freedom from cracking during quenching and heat-affected zone (HAZ) cracking during welding. Transverse CVN impact test results show that these microalloyed QT steels have very high shelf energies of 250-300 Joules due to the combination of low carbon and very low sulphur contents. Low impact transition temperatures of around -75°C are also recorded.[11]

Some of the higher alloyed Ni-Cr-Mo QT steels also contain microalloy additions such as the N-A-XTRA steels (0.12%Zr max.), the SUPERELSO steels (0.09%V) and the DSE steels (0.06%V), Table 6. In this category of steels there are two (OX 1002 and XABO 90) that achieve a minimum yield strength of 890 N/mm². The XABO 90 steel contains up to 0.10%V and can achieve this high strength level in plates up to 50 mm thick with a guaranteed minimum CVN impact energy value of 27 Joules at -40°C. The mechanical properties of the alloyed QT steels that contain microalloying additions are given in Table 7.

## OFF-HIGHWAY APPLICATIONS

The market for high strength, microalloyed steels in applications such as earthmoving equipment, excavators, industrial machinery, cranes etc. is dependent on the design criteria of individual companies and the size of equipment manufactured. Most companies use a 355 N/mm² yield strength steel for such parts as booms, dippers, chassis and general structural parts or panels. The major limitation to using higher strength steel is the fact that full advantage cannot be taken of the yield strength of the steel because the design is generally dictated by the fatigue of the welded joint. This, however, has not prevented the use of higher strength steels since various procedures can be adopted to overcome this problem. These will be discussed later where appropriate.

CRANES - For many years high strength steels have been used in the construction of cranes and other types of lifting gear. The strength levels used obviously depend on the type of crane and

the design philosophy. Manufacturers who design for long life, and for cranes that are subject to fatigue conditions, tend to use as-rolled or normalized V-Nb steel of 355 N/mm² minimum yield strength as their maximum strength material. The advantages of post-weld treatments to improve the fatigue life are well appreciated in most cases, but it is claimed that they are very difficult to implement and control. Using this design criterion, the only likely application for higher strength steel in the near future would be on a jib.

The area where higher strength microalloyed steel is rapidly becoming more established is for mobile cranes. A reduction in weight can greatly improve the performance and efficiency of a mobile unit. Steels with yield strength levels up to 690 N/mm² are rapidly replacing the lower yield strength (355 N/mm²) steels for most of the structural parts. This is being brought about because customers are requesting low temperature toughness properties coupled with weight saving. Weight saving is not only important with respect to fuel efficiency and performance but also because certain countries specify maximum axle weights for such vehicles. Therefore to remain competitive higher strength steels are being increasingly used.

Examples where microalloyed QT steel is being used in mobile cranes are shown in Figures 4-7. The AT400 (Figure 4) is produced by Grove Manufacturing Company in the USA and utilizes Grade T1 for many parts including the 70 ft telescopic boom and 43 ft telescopic swingaway. The vehicle weighs under 40,000 lbs with single axle loads below 20,000 lbs thereby making it 'roadable' throughout North America. The AT400 lightweight mobile crane can reach a maximum speed of 90 kph and still maintains over a 10 tonne pick-and-carry capacity.

The mobile cranes produced by Grove Coles Ltd. in the UK (Figures 5-7) are constructed mainly of roller-quenched and tempered, microalloyed steels. All grades of BSC's RQT steels (501, 601, 701) are used with all the booms being made from RQT701 (0.06%Nb-0.04%Ti). The majority of plates are 12, 16 and 20 mm thick, although RQT701 is purchased up to 30 mm thickness. Figure 6 shows the largest AT crane, the 1400, which has a lifting capacity of 125 tonnes. The most modern AT crane is the 1100 (100 tonne lifting capacity) which is manufactured on either a 4 or 5 axle chassis to suit individual roading regulations. These 70 kph mobile cranes all use a substantial amount of microalloyed high strength steel. It is estimated that a weight saving of about 30% is achieved when using RQT701 (690 N/mm² YS) as compared with a 355 N/mm² YS steel.

Other steels with strength levels intermediate of the normalized 355 grade and RQT701 are utilized in mobile cranes. Examples include BethStar 80, which is a controlled rolled steel of 550 N/mm² minimum yield strength,[13] and DOMEX 640XP, which is a controlled processed steel produced on a hot strip mill.[14] BethStar 80 is a low carbon steel containing 0.10%V and 0.06%Nb and has a CEV of only 0.40%. DOMEX 640XP is also a low carbon steel with about 0.14%V and 0.035%Nb and has excellent cold formability.

It should be noted that mobile cranes are generally designed for static loading conditions and so no fatigue conditions are experienced. The practice is to 'undermatch' the strength of the weld and high strength electrodes are only used if necessary, depending on the design.

For the future, the requirement is for a steel with a yield strength of 890-960 N/mm² with 14% minimum elongation. Such steels already exist e.g. OX 1002 (Svenskt Stål) and XABO 90 (Thyssen Stahl). XABO 90 (Ni-Cr-Mo, 0.10%V steel) has already been used for heavy duty cranes with a load capacity of 1000 tonnes.[15]

EARTHMOVING EQUIPMENT - Equipment used in the construction industry is subjected to both severe climatic conditions and a variety of different materials to be moved. In Canada and the Soviet Union, for example, vehicles may have to be used in temperatures as low as -40°C. Materials as diverse as soft soil or hard rock may have to be moved. Off-highway construction equipment includes crawler tractors, scrapers, loaders, bulldozers, dump trucks, haulers etc., all of which need good impact resistance at low temperatures, good fatigue properties and good weldability.

Earthmoving equipment invariably undergoes continual vibration while moving over undulating terrain and hence materials with good fatigue life are specified. Since the fatigue life of a structure is dependent on the fatigue life of the welded joint, the weight saving advantage of high strength steel in some applications cannot be fully gained. Consequently, there is a reluctance to use microalloyed steels unless the structure can be designed whereby the welded joints are not subjected to stress situations.

The maximum yield strength steel that manufacturers tend to use for general constructional purposes is normally restricted to 355 N/mm². In the UK this steel is typically supplied to BS 4360 : Grades 50B or 50C, both of which are nominally 0.04%Nb-0.08%V normalized steel (can be supplied in the as-rolled condition). The backhoe loader (a tractor-type vehicle with bucket at the front and digger at the rear) shown in Figure 8 is typical of such equipment. In 1987 J. C. Bamford (UK), the major manufacturer of backhoe loaders, produced over 7,000 units. They are using increasing tonnages of Grade 50B for the loader bucket and digger bucket frames. A Nb-V steel (Grade 50C) is also used in the construction of roll over protective cages (ROP's). Higher strength steel is unlikely to be used for this application since too thin a section would result and the tubes would start to buckle within the web. The strength of booms, tippers and loader arms is important when lifting dead weights and these are obvious candidates for microalloyed steel. A C-Mn-Si steel (no microalloy addition) is mainly used for the structure, so further scope remains for the production of an overall lighter unit by introducing the Nb-V steel.

Small tonnages (about 50 tonnes/year) of roller-quenched and tempered steel with a yield strength of 690 N/mm² (i.e. RQT701 or OX 812) are used on the backhoe loader. Small sections of 25mm plate are being placed in vulnerable collision areas such as the corners of buckets. This is a new application and if no problems are experienced the use of microalloyed QT steel will be greatly increased.

Caterpillar have recently started to manufacture backhoe loaders in the UK and whereas they also use large tonnages of Nb-V as-rolled or normalized steel (BS 4360 : Grade 50B), some 2,500 tonnes of microalloyed RQT701 is also consumed for the cutting edges on the backhoe bucket and the front loader bucket. The Nb-Ti QT steel is delivered as plate and then manufactured into a cutting edge section. A new application for microalloyed QT steel under evaluation at the present time is for rock buckets, to be manufactured in the UK.

The market for forklift trucks has improved considerably since 1980 and sales in the UK reached 3,000 units in 1986. The mast sections of the truck are now being produced from 460 N/mm² yield strength steel. The steel sections are rolled from steel with the following composition (wt.%):-

| C | Si | Mn | V |
|---|---|---|---|
| 0.23/0.30 | 0.15/0.30 | 1.0/1.3 | 0.05/0.08 |

The rough terrain forklift truck has a strong future in Europe because of its versatility in application, performing tasks which would normally be undertaken by self-erecting tower cranes.

Off-highway haulage trucks, Figure 9, are constructed mainly of high strength steel. This is simply to reduce weight and improve the payload-to-empty-weight ratio. High strength low alloy steel plate and sections are used for fabricated structural members such as frames and dump bodies. The latter application usually requires good dent and abrasion resistance. Quenched and tempered steels meeting ASTM Specification A514 are typically used and include low carbon 0.03/0.08%V-0.01/0.03%Ti steels or titanium-only steels (≈0.08%Ti). These steels are heat-treated to meet a minimum yield strength requirement of 620 N/mm² in section sizes above 63mm thickness, and 690 N/mm² in thinner product. Similar steels (RQT grades) containing small additions of Nb (±Ti) are produced in the UK for similar applications.

As an alternative to quenched and tempered low alloy steel, controlled-rolled microalloyed steel grades are becoming increasingly popular due to their lower production and alloying costs. As noted in Table 3, TMCP steels exhibiting minimum yield strength values of 550 N/mm² are readily available.

Also commercially available are controlled-processed hot strip mill grades such as DOMEX 640XP,[14] as mentioned in the previous section. The steel has a very low sulphur content (0.002%) for good formability and is produced in strip up to 8mm thickness. A typical chemical composition is (wt.%):-

| C | Mn | Nb | V | S | P |
|---|---|---|---|---|---|
| 0.10 | 1.60 | 0.035 | 0.14 | 0.002 | 0.015 |

with a minimum yield strength of 640 N/mm². DOMEX 640XP is used for the front wall and the 'ribs' in the body of dump trucks.

As mentioned earlier, dent resistance is an important property, particularly in earthmoving equipment subjected to conditions where rock or ore, for example, are dropped into the body. Although an obvious move to counteract denting would be to increase the section thickness, the desire for weight reduction obviously favours the use of higher strength steels. Results of dent resistance studies have been published by Nilsson[14] and are summarized in Figure 10. The superiority of the higher yield strength steel (655 N/mm²) is obvious and it can be seen that the dent resistance of a 3mm thick sheet of DOMEX 640XP is almost the same as that of a 5mm thick sheet of 380 N/mm² yield strength.

A more recent development has been that of higher strength bainitic grades produced on the hot strip mill.[16] The typical chemical compositions for two bainitic grades are (wt.%):-

| Min. YS | C | Mn | Nb | Ti | B | N | Mo |
|---|---|---|---|---|---|---|---|
| 700 N/mm² : | 0.08 | 1.30 | 0.05 | 0.18 | 0.003 | 0.006 | - |
| | C | Mn | Nb | Ti | B | N | Mo |
| 750 N/mm² : | 0.08 | 1.75 | 0.05 | 0.24 | 0.003 | 0.006 | 0.15 |

The steel chemistry is designed to combine the strengthening effects due to grain refinement, dislocation substructure and precipitation. Niobium, titanium, boron and molybdenum are instrumental in providing these effects. Applications include truck frames, cross members and others parts of dump trucks, mobile cranes and earthmoving equipment.

## MINING EQUIPMENT

Traditional applications of high strength steels in the mining industry include lift arms, buckets, skips, mining cages, roof support arches etc. More recently (since 1983) they have found application in hydraulic roof support systems, Figure 11, which are now being used in all major coal producing countries. Microalloyed 0.03%Nb-0.06%V steel plate processed to meet a minimum yield strength of 355 N/mm² is mainly used for the body structure. Higher strength steels (microalloyed QT steels) are used for the base, the canopy, tops and cantilever sections. The roof support system shown in Figure [illegible] utilizes RQT501, 601 and 701 for section sizes up to 40mm thickness and OX 812 for parts of greater thickness. The most popular section size used is 40mm t, followed by 20-25mm t.

The use of higher strength steels maximizes

the height between the base and the canopy by allowing a reduction in their section thickness thereby maximizing the automatic cutter depth and permitting a greater amount of coal to be cut from the seam. This is particularly important in shallow seams where just a small increase in blade depth can markedly increase the amount of coal extracted and make the operation much more efficient. The extra space also allows for better ventilation and easier access. Components were redesigned to incorporate high strength steels, and parts are designed up to the yield strength in order to obtain the best possible weight advantage and reduction in section thickness.

It is estimated that in the UK alone some 50,000 tonnes of microalloyed Nb-V steel to BS 4360 : 50B (minimum yield strength 355 N/mm$^2$) are currently consumed in the construction of roof support systems. The market for the microalloyed QT steels is around 15,000 tonnes, but the potential is for double this figure. These roof support systems are also only being used in coal mining at present and efforts are being made to extend their use to the mining of other minerals and deposits. The potential for microalloyed steels is therefore extremely promising.

High strength steels are finding increasing use for impellers and structural parts of fans, blowers and ventilation equipment in many industries, including mining. The main application is for impellers in fans, simply as a means of saving weight. The steels used in the impeller shown in Figure 12 (3000mm dia. impeller with a tip speed of 160m/sec.) are RQT501 or RQT701. These steels are required to maintain good mechanical properties up to 400°C. The microalloyed RQT steels comply with the necessary requirements:

RQT501: 360 N/mm$^2$ YS at 400°C and CVN 41 J at -40°C
RQT701: 610 N/mm$^2$ YS at 400°C and CVN 27 J at -45°C

Mild steel is still being used for impellers and therefore scope exists for increasing the tonnage of higher strength microalloyed steel for this application.

Higher strength steel in critically high-stressed components allows rotating equipment to be made lighter so that rotation is easier and the overall efficiency of the structure is significantly increased. From a different aspect, a larger rotor system could be assembled with a similar weight to that of a smaller rotor assembly constructed from lower strength steel and would give a better performance as a result of its increased size. The diameter of such rotors varies between 2.0 and 4.5m and the thickness of the plates used is 10-60mm with the majority of plates being up to 30mm thickness.

Aerofoil blades are also beginning to be produced from microalloyed QT steels. These blades are 20mm thick when made with mild steel. When RQT701 is used the blade thickness can be dramatically reduced to 6-8mm, thereby offering a significant weight saving.

In much the same way as surface earthmoving equipment benefits from the use of high strength steel, so too does mining equipment used below ground. In the example shown in Figure 13 the lift arms of the loader are made from OX 812 (0.05%V-0.002%B QT steel). In addition to reducing vehicle weight, the use of higher strength steel permits the haulage of a greater weight of rock/ore.

## SUMMARY AND DISCUSSION

The increasing use of microalloyed steel for some off-highway and mining applications has been discussed. Technological progress over recent years has made higher strength steels more acceptable to these and other industries. Depending on strength requirements and section thickness, microalloyed steels are available in the normalized, controlled-rolled or quenched and tempered conditions.

The use of microalloyed steels has been prompted by the desire to reduce vehicle or equipment weight. It should again be noted that by substituting a steel of 690 N/mm$^2$ YS for a steel of 355 N/mm$^2$ YS in the construction of mobile cranes, a weight saving of around 30% is possible. A more comprehensive assessment of the value of substituting higher strength steel for low strength steel has been made by Doennecke and Shelton.[17] They calculated that a mining truck operator with 20 trucks on an 80% availability base could save over $210,000 per year by using high strength steel for body and chassis members. By using a microalloyed QT steel of 690 N/mm$^2$ YS it was possible to reduce the weight of a haulage truck of 83,000 kg (empty) by 17% to 69,000 kg, thereby increasing the payload by some 17,500,000 kg per year. The economics of using higher strength steel are therefore obvious, as illustrated in Figure 14 which shows production figures relative to vehicle weight. The advantages of using microalloyed steel for roof support systems and impellers and blades in ventillation equipment have also been discussed. The marketplace for high strength steels for roof support systems is especially encouraging since only coal mines have so far been converted. Ventillation equipment is also taking advantage of microalloyed steel and much more efficient fans are now being manufactured. Faster rotational speeds are possible for similar size fans or a larger rotor system can be installed at a similar weight to that of a smaller unit made from lower strength steel.

However, each industry has its own individual problems associated with the use of higher strength microalloyed steels. The more common problems are springback and fatigue of welded joints. Springback is solved by experience - plates are 'over-formed' so that the plate edges return to a position that facilitates welding, the extent of over-forming being determined by trial and error. A secondary problem is that the first plate of a batch is typically used as a gauge to estimate how much the rest of the batch should be strained. Any inconsistency in plate

properties within a batch results in a variation in the percentage overstrain and obvious production problems. However, improvements in secondary steelmaking procedures and controlled processing have now minimized this problem and steelmakers are now capable of producing uniform and consistent mechanical properties for any particular grade of high strength, microalloyed steel.

Fatigue of welded joints has been a major drawback to the more extensive use of high strength steels since the stability of many structures is dictated by this property. In unwelded steels the fatigue strength increases as the tensile strength of a steel increases and this is because fatigue crack initiation takes longer in higher strength steels. Crack propagation, however, is independent of the mechanical properties and microstructure of the steel, and consequently using a higher strength steel rather than a lower strength steel will not improve the fatigue life of a structure unless weld defects can be eliminated. The elimination of weld defects will give a longer crack initiation period which will extend the fatigue life. Microalloyed steels could therefore be used to greater advantage if some type of post-weld improvement treatment is applied.

Weld improvement techniques such as peening, TIG-dressing and grinding, together with improvement in weld geometry, greatly reduce or eliminate defects or (in the case of peening) introduce a surface layer of compressive stresses which dramatically reduce crack propagation and significantly improve the fatigue life of higher strength steel joints.[18,19] As an example, it has been shown on welded joints of a 690 $N/mm^2$ yield strength steel that the fatigue strength could be increased by nearly 100% to about 350 $N/mm^2$ through the introduction of compressive stresses by shot peening,[20] Figure 15. The problem of weld fatigue could also be greatly reduced or eliminated by simply redesigning a structure whereby the welded joints are not subjected to high stresses. It should also be noted that the use of welding electrodes with improved fluidity has given a notable increase (up to 85%) in the fatigue life of welded joints in microalloyed steels.[21]

To conclude, the benefits of substituting microalloyed high strength steels for lower strength steels are being increasingly appreciated by industry. The off-highway and mining industries are no exception and many parts are now made from microalloyed steels. The potential for increased usage of these steels is most promising. Problems associated with springback and fatigue of welded joints can be, and have been, overcome.

## ACKNOWLEDGEMENTS

The author would like to thank Grove Coles Ltd. (UK), J. C. Bamford Ltd. (Rocester, UK), Dowty Mining Equipment Ltd. (Ashchurch, UK), James Howden & Company (Glasgow, UK) and Swedish Steel Ltd. (Lye, UK) for providing the photographs used in this paper.

## REFERENCES

1. "Strong Tough Structural Steels", ISI Publication 104, The Iron and Steel Institute, London (1967).

2. Proceedings Int. Conf., Microalloying '75, Washington D.C., USA, 1-3 October 1975.

3. Proceedings Int. Conf., Technology and Applications of HSLA Steels, ASM, Philadelphia, PA, USA, 1-3 October 1983.

4. Proceedings Int. Conf., HSLA Steels: Metallurgy and Applications, Beijing, China, 4-8 November 1985.

5. BSC Plates "Offshore" Brochure, Commercial Division-Plates, Motherwell, Scotland.

6. Proceedings Conf., Controlled Processing of High Strength Low Alloy Steels, York, UK, September 1976.

7. Proceedings Int. Conf., The Science and Technology of Flat Rolled Products, The Iron and Steel Institute of Japan, Tokyo, 28 September - 4 October 1980.

8. Dillinger Hüttenwerke, Technical Information Sheet No. 802E, 1981 and private communication, Chaussy, L-M.

9. LaFrance, M. et al, "Les outils et technologies moderne de production des aciers", Journées Franco-Belges du Soudage, Brussels, March 1987.

10. Svenskt Stål Aktiebolag, Domnarvet, Sweden, private communication.

11. BSC General Steels Publication, "RQT501T high strength steel plate for special structural applications", Commercial Division-Plates, Motherwell, Scotland, 1987.

12. BSC General Steels Publication, "RQT Plate", ibid, 1986.

13. Metal Progress, June 1982, p. 23.

14. Nilsson, T., Proceedings Int. Conf., Technology and Application of HSLA Steels, ASM, Philadelphia, PA, USA, 1-3 October 1983, p. 253.

15. Uwer, D. and Disselmeyer, H., IIW Doc. IX-1433-86, Thyssen Stahl AG.

16. Massip, A., Meyer, L. and Stich, G., Stahl und Eisen, 106, No. 3, 1986, p. 115.

17. Doennecke, H. C. and Shelton, J.A., "Materials for the construction of haulage equipment for the mining industry", Climax Molybdenum Company Symposium, Materials for the Mining Industry, Vail, Colorado, July, 1974.

18. Proceedings 2nd Int. Conf., Steel in Marine Structures, ECSC/IRSID, Paris, France, 5-8 October 1981.

19. Proceedings 3rd Int. ECSC Offshore Conf., Steel in Marine Structures (SIMS '87), Delft, The Netherlands, 15-18 June 1987.

20. Muesgen, B., Baumgardt, H., de Boer, H. and Janzon, W., "High-strength steels with improved toughness and weldability for the fabrication of offshore structures", paper presented at 17th Annual Offshore Technology Conf., Houston, Texas, USA, 6-9 May 1985.

21. Kobayashi, K. et al, "Improvements in the fatigue strength of fillet welded joint by use of the new welding electrode", IIW Doc. XIII-828-77.

Table 1 - Chemical Composition of a Representative Sample of Higher Strength Normalized Steels Produced in Europe

| Steel | Producer | Steel Composition, wt.% | | | | | | | | | | |
|---|---|---|---|---|---|---|---|---|---|---|---|---|
| | | C max. | Mn max. | Si max. | P max. | S max. | Nb max. | V | Ni | Cr max. | Mo max. | Cu |
| USITEN 420-II | USINOR | 0.22 | 1.6 | 0.55 | 0.035 | 0.030 | - | - | 0.5/0.7 | 0.2 | 0.1 | 0.3max. |
| USITEN 460-I | USINOR | 0.20 | 1.7 | 0.50 | 0.035 | 0.030 | 0.045 | 0.07/0.13 | ≤0.2 | 0.2 | 0.1 | 0.3max. |
| USITEN 460-II | USINOR | 0.18 | 1.7 | 0.40 | 0.035 | 0.030 | 0.045 | 0.09/0.15 | 0.5/0.7 | 0.2 | 0.1 | 0.3max. |
| FG 43 T | THYSSEN | 0.18 | 1.7 | 0.5 | 0.030 | 0.030 | - | 0.10/0.18 | 0.7 max. | - | - | - |
| FG 47 CT | THYSSEN | 0.15 | 1.5 | 0.5 | 0.030 | 0.030 | - | 0.08/0.18 | 0.5/0.7 | - | - | 0.5/0.7 |
| FG 51 T | THYSSEN | 0.21 | 1.7 | 0.5 | 0.030 | 0.030 | - | 0.10/0.20 | 0.4/0.7 | - | - | - |
| DILLINAL 55/43E | DILLINGER | 0.18 | 1.7 | 0.5 | 0.025 | 0.015 | - | 0.10/0.18 | 0.7 max. | - | - | - |
| DILLINAL 58/47E | DILLINGER | 0.20 | 1.7 | 0.5 | 0.025 | 0.015 | - | 0.10/0.20 | 0.7 max. | - | - | - |
| HYPLUS 29 | BSC | 0.22 | 1.6 | 0.5 | 0.05 | 0.03 | - | 0.20 max. | - | - | - | - |
| BS 4360 : 55E | BSC | 0.22 | 1.6 | 0.6 | 0.04 | 0.04 | 0.10 | 0.20 max. | - | - | - | - |
| WSTE 500 | CREUSOT-LOIRE | 0.18 | 1.6 | - | 0.015 | 0.010 | - | 0.10 max. | 0.3/0.7 | - | - | - |

Table 2 - Mechanical Properties of a Representative Sample of Higher Strength Normalized Steels Produced in Europe

| Steel | Minimum Yield Strength ($N/mm^2$) | | Minimum Ultimate Tensile Strength ($N/mm^2$) | | Minimum Charpy V-Notch Impact Energy (Joules) | | | |
|---|---|---|---|---|---|---|---|---|
| | Plate Thickness | | Plate Thickness | | 0°C | | -50°C | |
| | ≤16mm | 50<t≤80mm | ≤16mm | 50<t≤80mm | Long. | Trans. | Long. | Trans. |
| USITEN 420-II | 420 | - | 550 | - | 56 | 44 | 28 | 21 |
| USITEN 460-I | 460 | - | 590 | - | 48 | 36 | - | - |
| USITEN 460-II | - | 420 | - | 570 | 48 | 36 | 28 | 16 |
| FG 43 T | 420 | - | 530 | - | - | - | 27 | 27[a] |
| FG 47 CT | 460 | - | 560 | - | - | - | 27 | 27[a] |
| FG 51 T | 500 | - | 610 | - | - | 31 | 27[b] | - |
| DILLINAL 55/43E | 420 | 380 | 530 | 530 | 90 | 70 | 30 | 27 |
| DILLINAL 58/47E | 460 | 420 | 560 | 560 | 90 | 70 | 30 | 27 |
| HYPLUS 29 | 450 | 400[d] | 570 | 570 | 54 | - | 27[c] | - |
| BS 4360 : 55E | 450 | 415[d] | 550 | 550 | - | 61[a] | - | 27 |
| WSTE 500 | 480 | 450 | 610 | 610 | ≥44[a] | - | - | - |

[a] -20°C [b] -40°C [c] -30°C [d] >40≤63mm

Table 3 - Compositions and Mechanical Properties of Representative TMCR Steels Produced in Europe

| Steel | Producer | Steel Composition, wt.%[a] | | | | | | | Yield Strength ($N/mm^2$)[b] | Tensile Strength ($N/mm^2$)[b] | El.% min.[b] | CVN Impact Energy (J) at -40°C | |
|---|---|---|---|---|---|---|---|---|---|---|---|---|---|
| | | C | Si | Mn | S | P | Nb | V | | | | Long. | Trans. |
| DK 80 | DILLINGER | 0.18 | 0.6 | 1.6 | 0.025 | 0.040 | 0.05 | 0.15 | 550 | 655 | 18 | 140 | 110 |
| CR550 | BSC | 0.18 | 0.5 | 1.6 | 0.008 | 0.025 | 0.06 | 0.12 | 550 | - | 18 | - | - |
| Nb-steel | BSC | 0.11 | 0.28 | 1.33 | 0.002 | 0.015 | 0.027 | - | 400 | 514 | 27 | 194 | 125 |
| Fe E460 | ARBED | 0.20 | 0.55 | 1.70 | 0.025 | 0.035 | 0.06 | 0.10 | 460 | 560 | 17 | 28[c] | 28[d] |
| Nb+V Steel I | USINOR | 0.11 | 0.25 | 1.42 | 0.003 | - | - | 0.03 | 515 | 600 | - | - | 147[d] |
| Nb+V Steel II | USINOR | 0.11 | 0.35 | 1.55 | 0.007 | 0.025 | 0.07 | 0.10 | 550 | 700 | - | - | e |

[a] DK 80, CR550 and Fe E460 are maximum values, Nb and Nb+V Steel I are actual values.

[b] DK 80, CR550 and Fe E460 are minimum values for plates $\leqslant$19 mm thick, remainder are actual values with the Nb-steel from $\leqslant$23.5 mm thick plate.

[c] -50°C.

[d] -20°C.

[e] Transverse FATT of -100°C.

Table 4 - Compositions of Microalloyed Reheated QT Steels

| Steel | Producer | Steel Composition, wt.%, maximum | | | | | | | | | | | | |
|---|---|---|---|---|---|---|---|---|---|---|---|---|---|---|
| | | C | Si | Mn | S | P | Cr | Mo | Ni | V | Nb | Cu | Ti | B |
| ASA 64 T | ITALSIDER | 0.20 | 0.50 | 1.5 | 0.035 | 0.030 | 0.60 | 0.15 | 0.30 | 0.10 | - | - | - | - |
| ASA 68 T | ITALSIDER | 0.20 | 0.50 | 1.5 | 0.035 | 0.030 | 0.60 | 0.15 | 0.50 | 0.10 | - | - | - | - |
| RQT501 | BSC | 0.16 | 0.50 | 1.5 | 0.015 | 0.035 | - | [a] | - | [b] | - | - | - | - |
| RQT501T | BSC | 0.16 | 0.50 | 1.5 | 0.005 | 0.020 | - | 0.25[c] | 0.70[d] | 0.08[c] | - | - | - | - |
| RQT601 | BSC | 0.20 | 0.50 | 1.5 | 0.015 | 0.035 | [e] | [e] | [e] | - | 0.06 | - | 0.04 | 0.003 |
| RQT701 | BSC | 0.20 | 0.50 | 1.5 | 0.015 | 0.035 | [e] | [e] | [e] | - | 0.06 | - | 0.04 | 0.003 |
| Shoralism 450 | FABRIQUE DE FER | 0.10 | 0.50 | 1.6 | 0.005 | 0.015 | 0.15 | - | 0.50 | - | 0.03 | 0.35 | - | - |
| OX 602 | SVENSKT STÅL | 0.20 | 0.55 | 1.7 | 0.030 | 0.030 | - | - | - | 0.10 | - | - | [f] | - |
| OX 702 | SVENSKT STÅL | 0.20 | 0.70 | 1.7 | 0.030 | 0.030 | - | - | - | - | - | - | - | 0.005 |
| OX 812 | SVENSKT STÅL | 0.20 | 0.70 | 1.7 | 0.010 | 0.030 | - | 0.70 | - | - | - | - | - | 0.005 |

[a] May be added to 0.20%Mo max. and in plate thickness up to 50mm.

[b] Added to 0.08%V max. in plate thickness up to 50mm.

[c] Not added in plate thicknesses below 15mm.

[d] Only added in plate thicknesses between 50-80mm.

[e] Not normally used, but may be added up to 0.20% max.

[f] Added, but quantity unknown.

Table 5 - Mechanical Properties of Microalloyed Reheated QT Steels

| Steel | Producer | Gauge (mm) max. or range | Minimum Yield Strength ($N/mm^2$) | Tensile Strength ($N/mm^2$) | El.% min. | Minimum CVN Impact Energy (J) at -40°C | |
|---|---|---|---|---|---|---|---|
| | | | | | | Long. | Trans. |
| ASA 64 T | ITALSIDER | 50 | 490 | - | - | 35[a] | - |
| ASA 68 T | ITALSIDER | 30 | 540 | - | - | - | - |
| RQT501 | BSC | 50 | 470 | 560-710 | 21 | 41 | 70 |
| RQT501T | BSC | 50-80 | 430 | 530-700 | 20 | - | 70 |
| RQT601 | BSC | 40 | 620 | 690-850 | 19 | 27[b] | - |
| RQT701 | BSC | 40 | 690 | 790-930 | 19 | 27[b] | - |
| Shoralism 450 | FABRIQUE DE FER | 30 | 450 | ≥550 | 20 | - | 35 |
| OX 602 | SVENSKT STÅL | 50 | 500 | 610-770 | 20 | - | 40 |
| | | 64 | 480 | 610-770 | 20 | - | 40 |
| OX 702 | SVENSKT STÅL | 25 | 600 | 700-850 | 18 | - | 40 |
| OX 812 | SVENSKT STÅL | 64 | 690 | 780-930 | 20 | - | 40 |
| | | 75 | 620 | 690-930 | 20 | - | 40 |

[a] -20°C

[b] -45°C

Table 6 - Compositions of Alloyed QT High Strength Structural Steels Produced in Europe

| Steel | Producer | Steel Composition, wt.% (max. except where range is given)[a] | | | | | | | | | | |
|---|---|---|---|---|---|---|---|---|---|---|---|---|
| | | C | Si | Mn | P | S | Ni | Cr | Mo | B | V | Other |
| N-A-XTRA 96[b] | THYSSEN | 0.18 | 0.6 | 0.8 | 0.025 | 0.025 | - | 0.7 | 0.2 | - | - | 0.12Zr |
| N-A-XTRA 63[b] | THYSSEN | 0.18 | 0.6 | 0.8 | 0.025 | 0.025 | - | 0.8 | 0.3 | - | - | 0.12Zr |
| N-A-XTRA 70[b] | THYSSEN | 0.18 | 0.6 | 0.8 | 0.025 | 0.025 | - | 0.8 | 0.3 | - | - | 0.12Zr |
| XABO 90[b] | THYSSEN | 0.18 | 0.5 | 1.2 | 0.025 | 0.020 | 2.0 | 0.8 | 0.6 | - | 0.10 | - |
| T1 | THYSSEN | 0.10/0.20 | 0.35 | 0.6/1.0 | 0.025 | 0.025 | 0.2/1.0 | 0.4/0.85 | 0.4/0.6 | ≥0.0005 | 0.03/0.08 | 0.15/0.50 Cu |
| SUPERELSO 500[c] | CREUSOT-MARREL | 0.15 | 0.50 | 1.0/1.6 | 0.015 | 0.008 | 0.85 | 0.85 | 0.35 | - | 0.09 | 0.40Cu |
| SUPERELSO 600[d] | CREUSOT-MARREL | 0.14 | 0.40 | 1.0/1.6 | 0.015 | 0.008 | 0.75 | 1.05 | 0.35 | - | 0.09 | - |
| SUPERELSO 702[c] | CREUSOT-MARREL | 0.14 | 0.30 | 0.9 | 0.010 | 0.004 | 1.5 | 0.7 | 0.55 | 0.003 | 0.05 | - |
| DSE 500 | DILLINGER | 0.18 | 0.2/0.6 | 0.6/1.6 | 0.025 | 0.025 | 0.6 | 1.0 | 0.6 | 0.003[e] | 0.06[e] | - |
| DSE 550 | DILLINGER | | | | | | | | | | | |
| DSE 600 | DILLINGER | | | | | | | | | | | |
| DSE 690 | DILLINGER | | | | | | | | | | | |
| ASA 75 T | ITALSIDER | 0.20 | 0.8 | 1.5 | 0.030 | 0.035 | 0.5 | 0.75 | 0.30 | - | - | 0.15Zr |
| QT445B | BSC | 0.15/0.21 | 0.9 | 0.8/1.1 | 0.030 | 0.030 | - | 0.5/0.8 | 0.25/0.60 | 0.0025 | - | 0.15Zr |

[a] The N-A-XTRA analyses except for %C are typical values

[b] For plate thicknesses up to 50mm

[c] For plate thicknesses up to 100mm

[d] For plate thicknesses up to 80mm

[e] Added when required.

Table 7 - Mechanical Properties of Alloyed QT High Strength Structural Steels Produced in Europe

| Steel | Producer | Gauge (mm) max. | Minimum Yield Strength ($N/mm^2$) | Tensile Strength ($N/mm^2$) | El.% min. (50mm) | CVN Impact Energy (J) at -40°C[a] | |
|---|---|---|---|---|---|---|---|
| | | | | | | Long. | Trans. |
| N-A-XTRA 56 | THYSSEN | 50 | 550 | 670-820 | 18 | 40 | 31 |
| N-A-XTRA 63 | THYSSEN | 50 | 620 | 740-890 | 17 | 40 | 31 |
| N-A-XTRA 70 | THYSSEN | 50 | 690 | 790-840 | 16 | 40 | 31 |
| XABO 90 | THYSSEN | 50 | 890 | 940-1100 | 16 | 31 | 27 |
| T1 | THYSSEN | 63 | 690 | 760-900 | 16 | 27 | 20[b] |
| SUPERELSO 500 | CREUSOT-MARREL | 100 | 500 | 600-750 | 18 | 50 | 45 |
| SUPERELSO 600 | CREUSOT-MARREL | 80 | 600 | 700-850 | 17 | 50[c] | - |
| SUPERELSO 702 | CREUSOT-MARREL | 100 | 700 | 820-940 | 16 | - | 60[c] |
| DSE 500 | DILLINGER | 60 | 500 | 600-770 | 17 | 40 | 30 |
| DSE 550 | DILLINGER | 60 | 550 | 650-820 | 16 | 40 | 30 |
| DSE 620 | DILLINGER | 60 | 620 | 720-890 | 15 | 40 | 30 |
| DSE 690 | DILLINGER | 60 | 690 | 770-940 | 14 | 40 | 30 |
| ASA 75 T | ITALSIDER | 30 | 620 | - | - | 35[c] | - |
| QT445B | BSC | 51 | 695 | 800 | 18 | 20[b] | 27[d] |
| | | 63 | 618 | 730 | 18 | - | - |

[a] Minimum values, average of 3 specimens

[b] -46°C

[c] -20°C

[d] -15°C

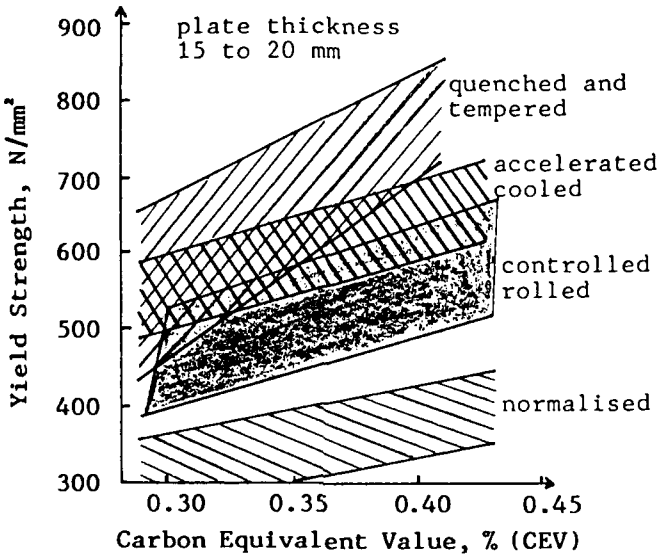


$$CEV = C + \frac{Mn}{6} + \frac{Cr + Mo + V}{5} + \frac{Ni + Cu}{15}$$

Fig. 1 - The effect of CEV on the yield strength of various grades of structural steels after different processing routes[9]

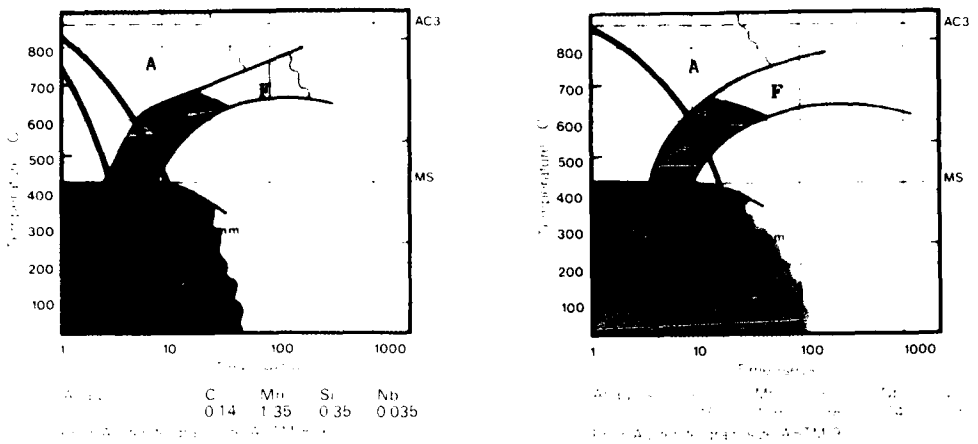


(a) RQT501

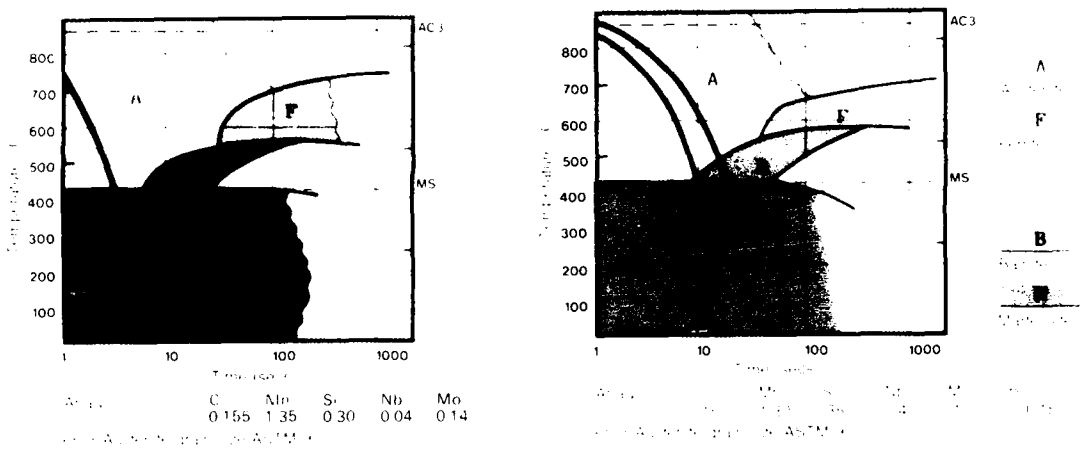


(b) RQT701

Fig. 2 - Continuous Cooling Transformation (CCT) Curves for (a) RQT501 and (b) RQT701[12] (Courtesy of British Steel Corporation)

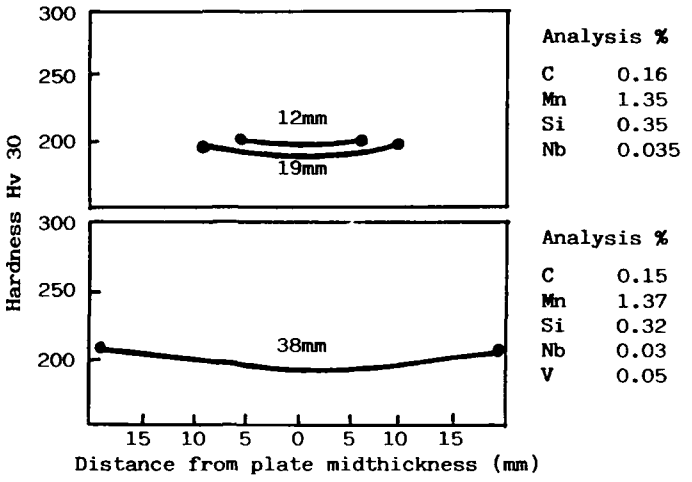


(a) RQT501

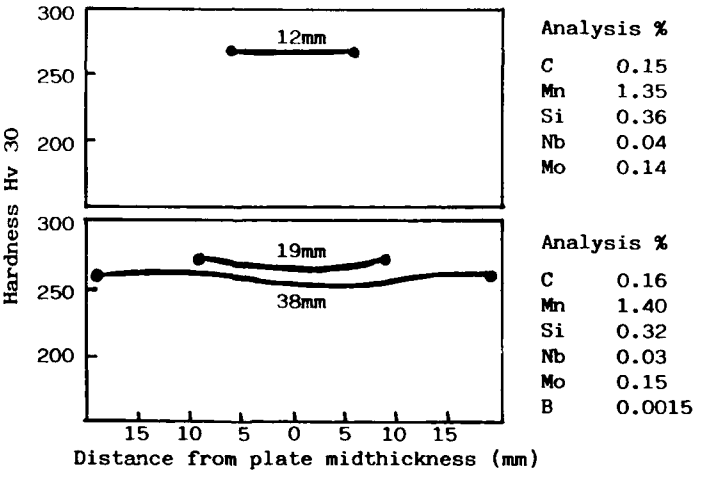


(b) RQT701

Fig. 3 - Typical through hardening performance of (a) RQT501 and (b) RQT701 (tempered condition)[12] (Courtesy of British Steel Corporation)

Fig. 4 - The AT400 lightweight mobile crane weighing less than 18 tonnes with a maximum speed of 90 kph (50 mph)

Fig. 5 - Mobile crane AT865

Fig. 6 - AT1400 - the largest mobile crane, having a lifting capacity of 125 tonnes

Fig. 7 - The AT1100 mobile crane - 100 tonne lifting capacity available on either a 4 or 5 axle chassis

Figures 4-7 Courtesy of Grove Coles Ltd., UK

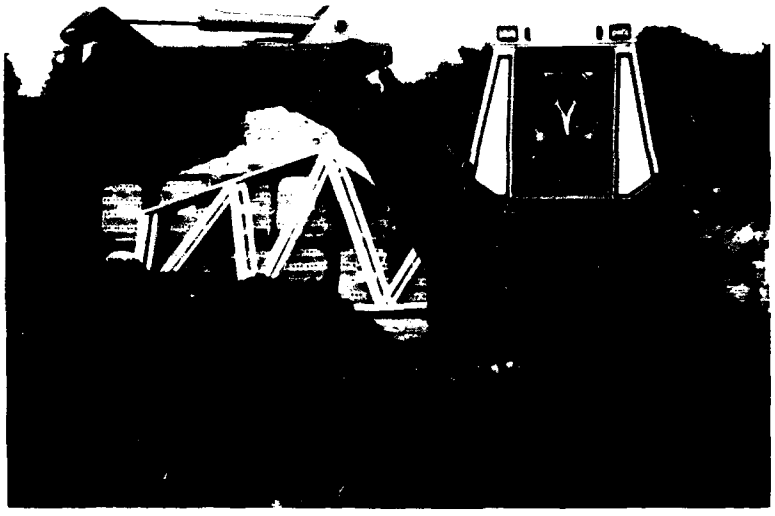

Fig. 8 - Backhoe loader using Nb-V steel for structural frame and other parts (Courtesy of J. C. Bamford Ltd., UK)

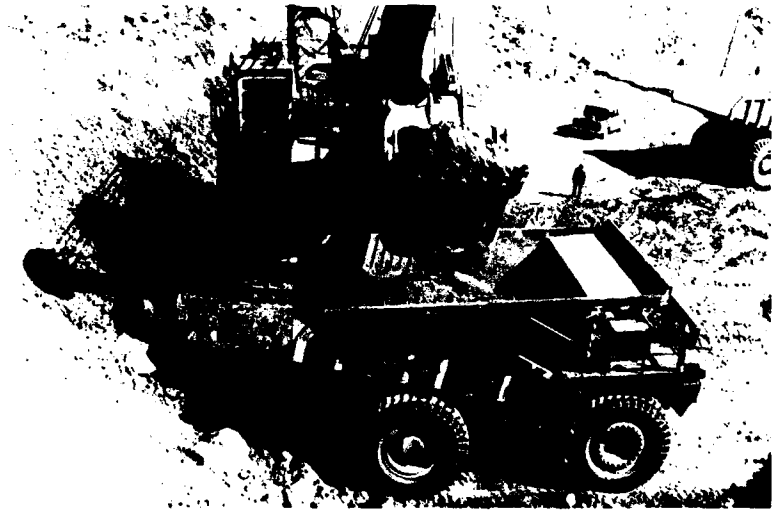

Fig. 9 - Off-highway haulage truck fabricated mainly of high strength QT microalloyed steel

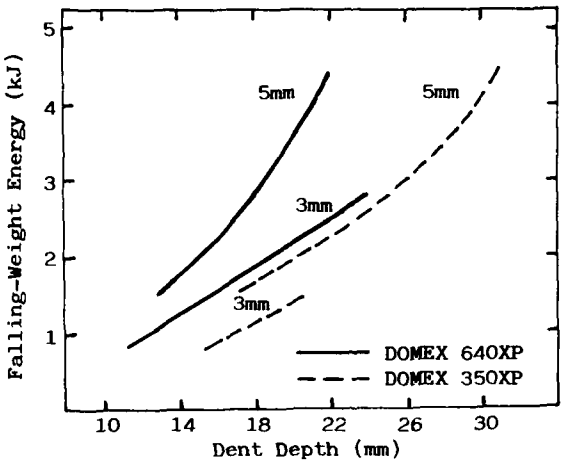


Fig. 10 - Dent resistance measurements of DOMEX 640XP (yield strength 655 N/mm$^2$) and DOMEX 350XP (yield strength 380 N/mm$^2$) in 3 and 5mm thickness[14]

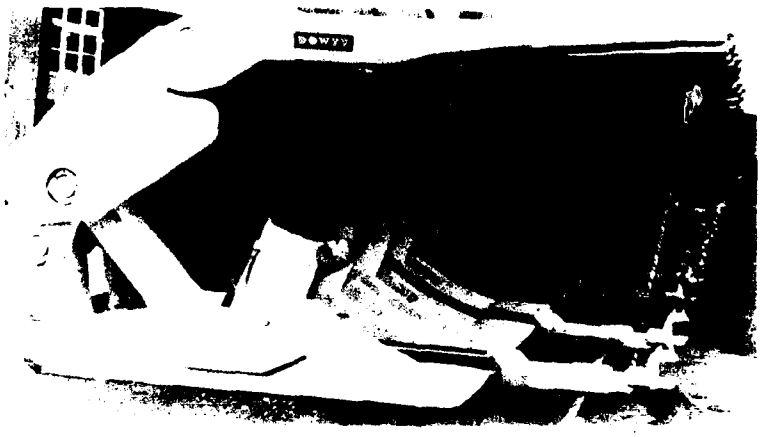


Fig. 11 - Hydraulic roof support system (Courtesy of Dowty Mining Equipment Ltd., UK)

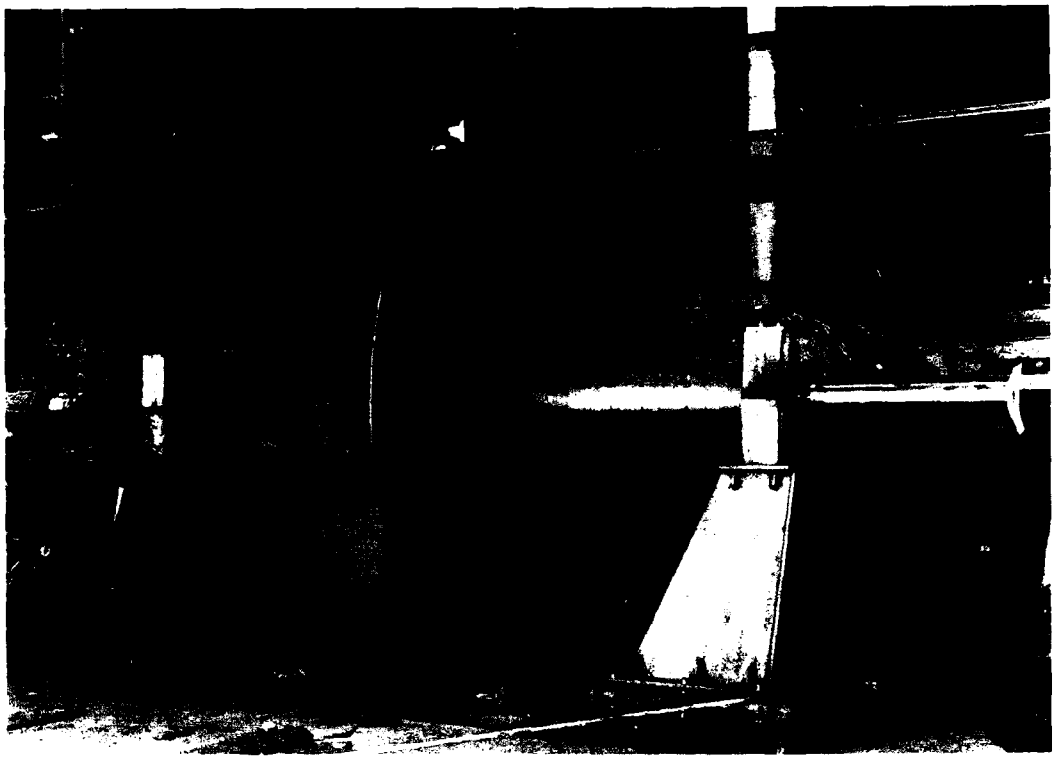

Fig. 12 - Impeller (3000mm dia.) fabricated using high strength microalloyed steel (Courtesy of James Howden & Company, UK)

Fig. 13 - Mining loader, lift arms fabricated from V-B QT steel (Courtesy of Swedish Steel Ltd., UK)

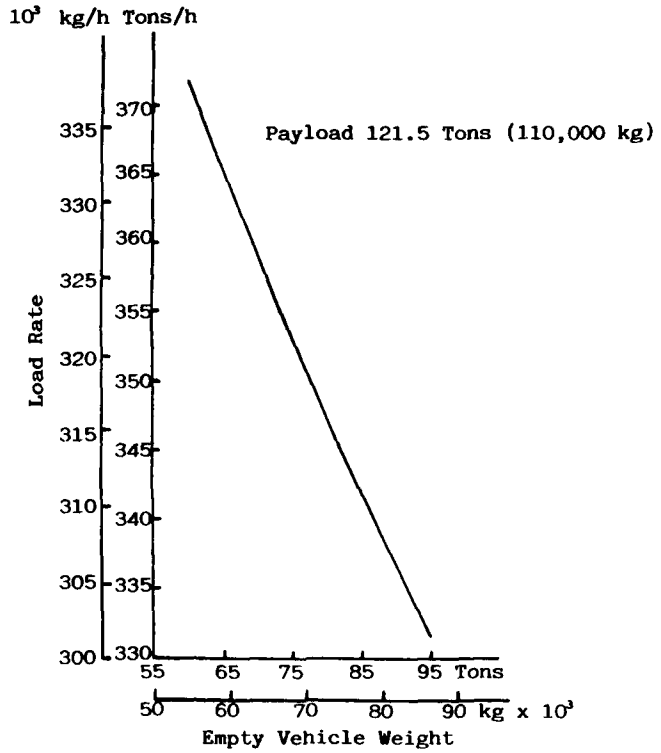


Fig. 14 - Load rate vs. empty vehicle weight[17]

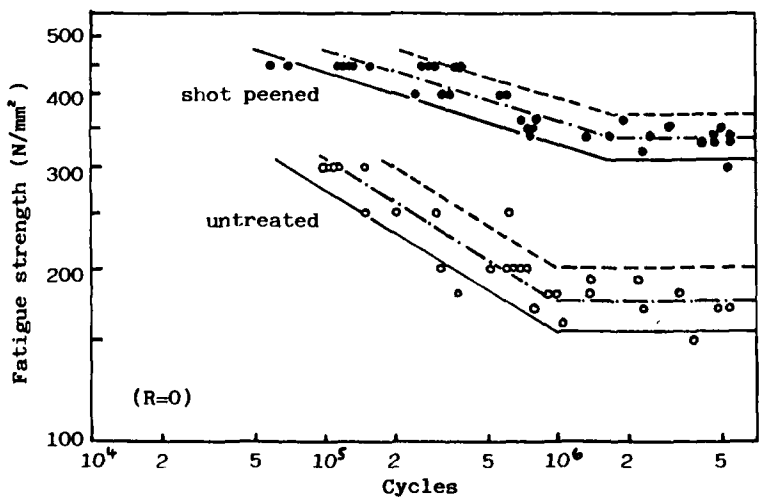


Fig. 15 - Improvement of fatigue strength of welded joints of StE 690[20]

# APPLICATION OF HSLA STEELS FOR CONSTRUCTION OF RAILROAD TANK CARS

**D. H. Stone, W. S. Pellini***
Association of American Railroads
Chicago, Illinois, USA

Abstract

This paper explains the evolution of modern weldable steels of primary interest to tank cars. The basis for initial selection of candidate steels for welding tests and mechanical properties characterization, is described in terms of weldability and fracture analysis factors.

Simplified explanations of welding metallurgy and weldability principles are presented -- in the interest of readers who are not familiar with these specialized aspects of modern weldable steels.

The engineering factors that will be examined are the AAR Tank Car Committee for selection of the new tank car steels are defined, including the role of design considerations.

The report consolidates various papers that were evolved for planning purposes by the Steel Task Force of the AAR Tank Car Safety and Test Project.

An important feature of this comprehensive report is the documentation of the complete use of modern technological practices for the selection of new steels for tank cars. As such, it should satisfy the common interest of users, fabricators, and regulatory agencies for tank cars.

THE CONTINUED EVOLUTION of improved weldable steels during the period of 1950 to 1985 was determined by a combination of metallurgical research and weldability experience defined the objectives for the next step of improvement. Metallurgical research which normally advances on a broad front, could then be focused to questions of welding metallurgy.

During the period of 1950 to 1979, the primary development cycles involved the C-Mn alloy system. By 1979 metallurgical research evolved the radically new Cb(Nb) microalloy system. The weldability advantages of micro-alloyed steels resulted in rapid use for welded structures.

By 1975 it became evident that the microalloyed steels were ideal for controlled rolling. Controlled rolling had been applied to C-Mn steels, with modest results as compared to normalizing heat treatment. The microalloyed steels could be controlled rolled to develop low temperature fracture properties equivalent to or better than obtained by normalizing. This finding stimulated the installation of large rolling mills that could mass produce steels of superior weldability and fracture properties. The subject of controlled rolled microalloyed steels is described in an AAR report, Reference (1).

The metallurgical literature defines steels in generic terms that describe the allow system, composition, processing, heat treatment, microstructure and mechanical properties. The usual engineering reference for steels is the American Society for Testing and Materials (ASTM) specification system for standard-grade steels. The engineering selection and procurement of steels is made in terms of a numerical designation, for example ASTM A-

*Deceased

516 Grade 70.

This paper is concerned with the evolution and applications of standard grade steels. Therefore, extensive use is made of the standard grade designation system. Reader assistance is provided by Table 1 which describes the compositions and tensile properties, for the standard grades that are discussed in this paper.

Weldability factors are not cited in the ASTM specifications. This aspect is expected to be considered by the design and fabrication industry. In past practice it was assumed that welding factors would be properly considered by the welding engineers responsible for fabrication. Modern design procedures require consideration of weldability during the design phase. Therefore, the design field must develop a reasonable understanding of weldability factors. The mixture of old and new steels in the ASTM specifications permits selection of steels that feature adequate weldability for the requirements of specific structures. The designer should select the best steel for the structure of interest.

Adequate weldability implies that the structure can be fabricated with a high degree of assurance that cracks are not developed in heat affected zone regions (HAZ) of welds. The cracks may escape detection, particularly if located in regions of complex weld connections.

The evolution of weldable steels has been focused in major part on the development of new steels of decreased sensitivity to fabrication cracking. The cracks are typically located in the heat-affected-zone (HAZ) of small welds. the superior weldability of modern steels minimizes requirements for exact control of welding procedures. Therefore, crack-free structures can be produced with a high degree of assurance.

Weldability research, coupled with improved understanding of welding metallurgy, has resulted in simplified methods for calculation of weldability parameters. These "weldability rating" numbers are calculated from the chemical composition of the steel. The %C is the primary factor in the calculations. The following weldability parameters are used extensively in the international steel literature.

Carbon Equivalent (CE%)

$$CE\% = C + \frac{Mn}{6} + \frac{Si}{6} + \frac{Cr}{5} + \frac{Mo}{5} + \frac{V}{5} + \frac{Cu}{15} + \frac{Ni}{15}$$

Parameter of Cracking Sensitivity for Base Metal ($P_{CM}$%)

$$PCM\% = C + \frac{Mn}{10} + \frac{Si}{30} + \frac{Cr}{20} + \frac{Mo}{15} + \frac{V}{10} + \frac{Ni}{60}$$

The % of the alloys, divided by the cited factors, are added to the % C to define added effects of the alloys in enhancing the primary effect of %C on HAZ cracking susceptibility.

The CE % parameter is used in combination with the % C (% C - CE%) to fully define the HAZ hardness that is developed for the case of small welds. Small welds are the primary sites of HAZ cracking. Decreasing the HAZ hardness, by decreasing the %C-CE% of the steel, decreases the sensitivity to HAZ cracking. Therefore, the significance of this parameter is most easily understood.

The $P_{CM}$% parameter was developed by empirical correlation with the results of weldability tests for HAZ cracking. It is a test-experience in fabrication. Decreasing $P_{CM}$% values correlate with decreased experience of HAZ cracking for particular types of structures and weld connections. Lower values of $P_{CM}$% are required to provide assurance of crack-free structures for complex structures, as compared to structures of simple configuration.

This paper describes the $P_{CM}$% values that are relatable to the simple configuration of tank car structures. The $P_{CM}$% values for steels in present service, which have experienced HAZ cracking -- are compared to the $P_{CM}$% values of the new steels which indicate sensitivity to HAZ cracking.

The table 1 listing of presently used tank car steels and new steels that are considered in the AAR project for future use -- includes the CE% and $P_{CM}$% parameters for the steels. This is the important weldability description of the steel which is not provided by the ASTM standard grade specifications. The modern practice in the international steel literature includes citing CE% and $P_{CM}$% parameters. The specification user should routinely calculate the CE% and $P_{CM}$% parameter values for any standard grade steel that is considered for welding fabrication.

By understanding the significance of the CE% and $P_{CM}$% parameters, it is possible to estimate the

TABLE 1

STEELS CITED IN REPORT

| | % Max. Ladle & Product Analysis | | | | | | | | | Tensile (Min.) ksi(MPa) | |
|---|---|---|---|---|---|---|---|---|---|---|---|
| | C | Mn | Si | Ni | Cr | Mo | Cu | V | Cb | Y.S. | T.S. |
| A-515(L) | .31 | 1.20 | .40 | - | - | - | - | - | - | 38(260) | 70(485) |
| (P) | .31 | 1.30 | .45 | - | - | - | - | - | - | | |
| A-516(L) | .28 | 1.20 | .40 | - | - | - | - | - | - | 38(260) | 70(485) |
| (P) | .28 | 1.30 | .45 | - | - | - | - | - | - | | |
| TC-128B(L) | .25 | 1.35 | .40 | .25 | .25 | .08 | .35 | .08 | - | 50(345) | 81(560) |
| A-612(P) | .29 | 1.46 | .50 | " | " | " | " | .06 | - | | |
| *A-633D (L) | .20 | 1.35 | .50 | .25 | .25 | .08 | .35 | .05 | - | 50(345) | 70(485) |
| PVQ (P) | .24 | 1.46 | .56 | " | " | " | " | .06 | - | | |
| *A-737B (L) | .18 | 1.60 | .50 | - | - | - | - | - | .05 | 50(345) | 70(485) |
| Low C (P) | .22 | 1.72 | .55 | - | - | - | - | - | .05 | | |
| *A-808 (L) S* | .12 | 1.65 | .50 | - | - | - | - | .10 | .10 | 50(345) | 70(485) |
| PVQ (P) | .15 | 1.77 | .56 | - | - | - | - | .11 | .10 | | |

| A-808 Plate Samples | | | | | | | | | | | | |
|---|---|---|---|---|---|---|---|---|---|---|---|---|
| | C | Mn | Si | Ni | Cr | Mo | Cu | V | Cb | S | Y.S. | T.S. |
| Mill A (CR) | .12 | 1.31 | .37 | .19 | - | - | - | .026 | .027 | .013 | 63(434) | 79(545) |
| Mill A (CR) | .11 | 1.33 | .38 | .28 | - | - | - | .028 | .026 | .013 | 63(434) | 78(538) |
| Mill B (HCR) | .08 | 1.43 | .28 | - | - | - | - | - | .030 | .003 | 57(393) | 69(476) |
| Mill B (HCR) | .06 | 1.46 | .25 | .20 | - | - | .26 | .039 | .044 | .003 | 70(482) | 79(545) |

*New-Project Steels S* A-808 restricted S= 0.010% (Max.)

TABLE 1 (continued)

STEELS CITED IN REPORT

WELDABILITY REFERENCE BASED ON TYPICAL PRODUCTION ESTIMATE

| STEEL | %C | CE% | $P_{CM}$% |
|---|---|---|---|
| A-515 | .26 | .42 | .32 |
| A-516 | .24 | .45 | .31 |
| TC-128B | .25 | .57 | .36 |
| A-633D | .20 | .53 | .30 |
| A-737(HC) | .18 | .46 | .27 |
| A-808 | .12 | .42 | .21 |

A-808 PLATE SAMPLES

WELDABILITY REFERENCE BASED ON PLATE COMPOSITION

| | %C | CE% | $P_{CM}$% |
|---|---|---|---|
| Mill A (CR) | .12 | .42 | .22 |
| Mill A (CR) | .11 | .42 | .20 |
| Mill B (HCR) | .08 | .37 | .16 |
| Mill B (HCR) | .06 | .38 | .15 |

weldability of a steel within close limits. The international steel literature routinely cites these parameters, with the expectation that serious readers have developed this degree of proficiency.

The AAR Tank Car Steel Project was developed by weldability and fracture analyses of:

(1) Old tank car steels.
(2) Presently used tank car steels
(3) New steels which would be selected for future use.

This method of analysis provides a numerical basis for comparison of the past fabrication and service experience for tank cars with the expected improvements for the new steels.

The weldability analysis graphs that has been developed for this purpose, provide a chronological description of the improvements in weldability for standard grade steels. The analyses cover the period of 1950 to 1955. The major steps int he evolution of weldable

steels are cited in the reference graphs.

## GENERAL DESCRIPTION OF THE AAR PROJECT FOR SELECTION OF NEW TANK CAR STEELS

During the past fifteen years the Association of American Railroads (AAR), in cooperation with the tank car industry (RPI), has conducted extensive studies for improvement of tank cars. Tank cars never fail in normal service. Failures by ductile tearing or brittle fracture have been experienced only for the case of severe accidents, such as derailment.

A review of brittle fracture experience, reference (2), for the sixteen year period of 1956 to 1980 indicates a very low incident rate. Only 19 cases of extensive brittle fracture were recorded for pressure cars involved in accidents. Of the 1345 pressure cars that were impacted in accidents, brittle fracture resulted for only 0.6% of the impact points. This is remarkable performance record, considering that the tank cars were constructed using as-rolled C-Mn steels that were fracture sensitive at service temperatures.

The role of weldability for the cited 19 cases of brittle fracture was analyzed in reference (2). Fracture initiation of 3 of the 19 cases resulted from the presence of HAZ fabrication cracks or hard HAZ due to inadequate post weld heat treatment (PWHT) after modification or repair welding. It should be recognized that, unlike stationary pressure vessels, tank car vessels are subjected to deformation loading in cases of accidents. Therefore, elimination of hard HAZ regions is a special requirement for tank cars.

In 1983 a complete head fracture was experienced for pressure tank car during humping operations in the Canadian National Railroad, Toronto yard. The tank car was fabricated in 1980 using TC-128B steel. Failure analysis, reference (3), defined the fracture initiation crack-source as illustrated in Figure 1. The fabrication crack was developed at the toe of a small fillet weld, which was the last pass for the weld connection tot he head. The hardness of the (HAZ) was equivalent to the maximum hardness that could be developed for the 0.25% C composition of the steel.

This case is of special interest because it was documented that proper

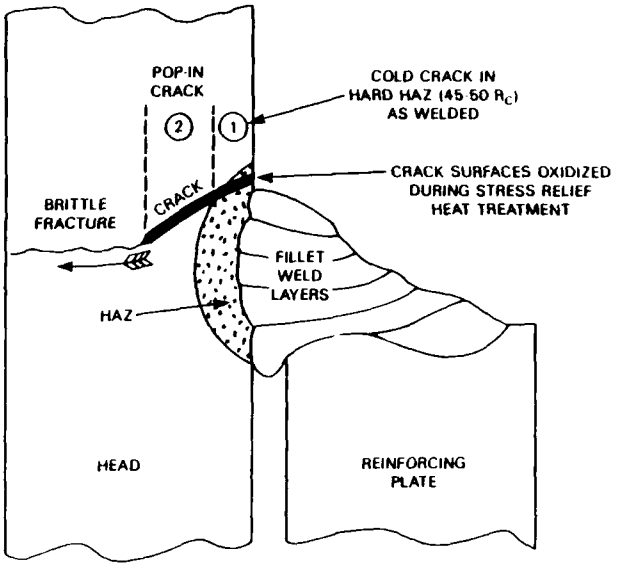


Figure 1 Description of 0.3 in. (7.6mm) Deep Weld Toe Crack Which Initiated the Head Fracture. Cross Section View.

welding procedures, including preheat, had been used for the weld. The basic problem was identified as the high %C-CE% of the steel which resulted in high HAZ hardness for the case of small welds.

While this case was isolated incident, it has resulted in placing regulatory demands for increased inspection for crack detection. These demands include possible requirements for certification of crack-free condition for specific types of tank cars.

Inspection to ensure the total absence of small fabrication cracks is not technologically feasible. If attempted, it would be very expensive. Moreover, such inspection does not provide protection against the development of HAZ cracks due to acc dent impact -- if hard HAZ regions are present. There is no practical way to guarantee the total absence of hard HAZ regions, for the case of field modifications or repairs. It is not possible to make significant hardness tests for the small HAZ regions.

This partial description of the certification problem indicates the importance of selecting new steels that inherently result in low hardness (ductile) HAZ for small welds. Crack-free structures can be certified by the weldability of the steel. The degree of inspection that is required can be minimized with considerable econom c benefit. These

objectives are essential aspects of weldability ratings for the steels.

The rationale for selecting specific candidate standard grade steels was discussed with the principal plate metallurgists of the U.S. Steel, Lukens, Bethlehem, Stelco and Algoma Steel Companies. The steel representatives contributed important information to the AAR Project.

It was not realistic to order special heats for the purpose of the Project because of excessive cost. Moreover, it was desirable to use steel samples from normal production sources. The steel companies which normally produce tank car steels, agreed to furnish plate samples for the new steels at no cost to the Project. The test plates are taken from current production of the steels. The U.S.Steel, Algoma, Stelco, Lukens, Bethlehem and Kawasaki Steel Companies are contributing specific steels, depending on their production schedules. Each of the steel companies has agreed to provide the microalloyed, controlled-rolled A-808 steel. The Project steels are listed in Table 1.

Analytical comparison implies numerical comparison of weldability factors and fracture properties expressed in fracture mechanics terms. Failure analyses for the old and presently used steels can be related exactly to weldability factors and fracture properties. The improved weldability and fracture properties of the new steels can be translated analytically to define the degree of assurance for prevention of service failures in the future.

## EVOLUTION OF WELDABLE STEELS AND APPLICATIONS TO TANK CARS

WELDABILITY FACTORS - Tank car steels are selected from standard grade steels. The description of specific steel grades that have been used for tank cars, or may be used in the future, serves as a reference to the evolution of weldable steels. Table 1 presents the chemical compositions and tensile properties for the standard grade steels discussed in this report.

The Table 1 listing of Project steels includes the A-808 microalloyed steel of Cb(Nb)+V type which is controlled rolled to CR practice. Figure 2 describes the rolling temperatures for conventional as-rolled steels, controlled rolled CR steels, and intensively controlled

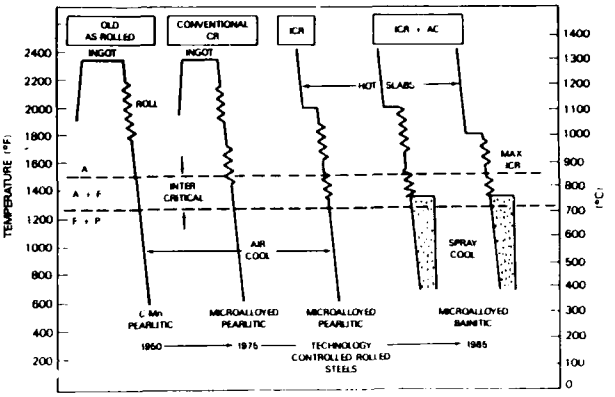


Figure 2 Comparison of the Conventional As-Rolled Practice and the New Controlled Rolling Practices.

rolled (ICR) steels. If accelerated cooling (AC) is used for ICR steels, the designation is ICR+AC.

The A-808 specification may be satisfied by CR or ICR controlled rolling. The U.S.A. and Canadian sources for the A-808 Project steel samples (five steel companies) use the Figure 2 defined CR practice. If a probable Japanese source (Kawasaki Steel Co.) for the A-808 steel is included, it is expected to be produced to the Figure 2 defined ICR practice. The project does not include ICR+AC steels because there is presently no ASTM grade for this type.

The following discussions describe the hardness level in the relative terms of high or low. This simplified description is more easily understood, as compared to citing specific hardness numbers.

The %C-%CE is based on the estimated typical composition, not on the maximum permissible cited in the specification. For the purposes of this report, it is not realistic to reference the almost-never produced maximum composition. After the reader becomes familiar with the significance of the %CE-CE% parameter, he may routinely use the reference to specification limits -- with the realization that the %C-CE% will be indicated for the high side of production range.

Figure 3 describes the evolution of weldable steels in terms of the typical %C-CE% combination for specific standard grade steels. Figure 4 defines the decrease in HAZ hardness level for Project steels with decreased %C. The effect of high CE% is to increase the HAZ hardness to the limit defined by the band for maximum attainable hardness.

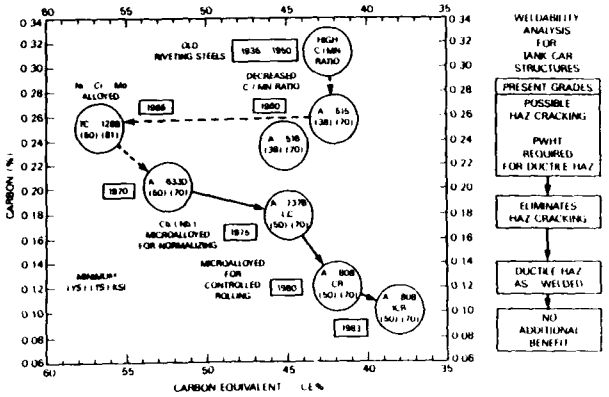


Figure 1 Evolution of Standard Grade Weldable Steels as Defined by the %C-CE% Weldability Rating. The Weldability Analysis Comments [illegible] Interpretation.

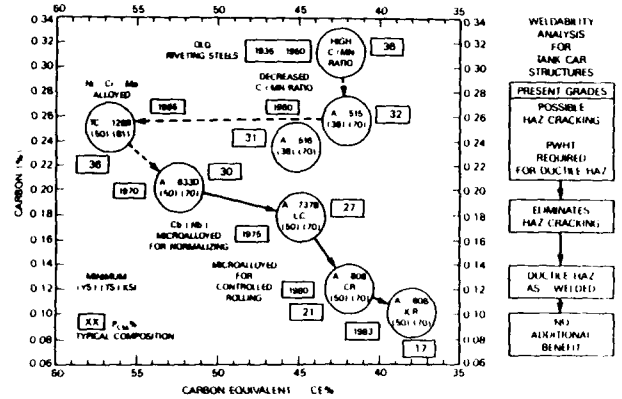


[illegible]

Low CE% reduces the hardness to a level that is below but near the maximum hardness band.

As a first approximation, Figure 3 may be interpreted to represent a rapid decrease in the HAZ hardness for small welds, with decreased carbon content. Therefore, the %C scale of Figure 3 serves as the primary reference for hardness level. For the same %C content, the CE% scale indicates that higher hardness will be developed if the CE% is high.

Figure 3 is interpreted to signify that the evolution of the steels involved:

(1) A desirable first step (1960) for reducing the HAZ hardness level by decreasing the %C.

(2) An undesirable second step (1965) with respect to weldability by increasing the alloy content which resulted in increased CE% for the TC-128B steel. The alloy additions were made for the purpose of improving the fracture properties.

(3) All following steps (1970, 1975, 1980, 1983) were aimed at reducing the %C and the CE%. This had the intended effect of continuously improving the weldability by continuous reduction of the hardness level for the HAZ of small welds.

The Figure 3 weldability analysis interpretations presented on the side of the figure, explain the practical significance of the 1979 to 1983 reductions in the %C-CE% combination.

By following this sequence of steel evolution, the reader can develop a significant understanding for the meaning of a cited %C-CE% combination. For example, it is desirable to decrease the %C as much as possible and aim for CE% values that are in the range of 0.45 to 0.40%.

It is noted that the 1970 step marked the end of the improvement for C-Mn steels. The desired minimum levels of tensile properties could not be retained by decrease of the typical carbon content significantly below 0.20%C. The first microalloyed steels (1975) which are used in normalized condition, provided a decreased typical carbon content to 0.18%C, with retention of tensile properties.

Controlled rolling permits the largest reduction of typical carbon content to the 0.12 to 0.10%C level, with retention of tensile properties. This is a special feature of the CR and ICR controlled rolled steels.

The Figure 3 weldability analysis interpretations are based on the fact that tank car structures feature relatively low levels of weld restraint stresses. Therefore, HAZ cracking is expected only for high combinations of %C-CE%. The presently used A-516(70), A-515(70), and TC-128B steels have developed such cracking for small welds. The incidence rate is low.

The A-633D and A-737 Project steels are indicated to preclude HAZ cracking because of the decreased %C-CE%. However, the HAZ hardness is considered sufficiently high to result in HAZ cracking if subjected to accident impact. Therefore, post weld heat treatment (PWHT) is necessary to develop softer (ductile) HAZ for small welds.

The A-808 steel (CR) features a %C level that can only result in soft (ductile) HAZ for small welds. This steel is indicated to preclude HAZ cracking in fabrication and accident

impact. It does not require PWHT for the purpose of softening the HAZ.

Figure 5 presents the Figure 3 plot with the added feature of the $P_{CM}$% factor. This HAZ crack sensitivity parameter indicates that the steel should feature significantly less than $P_{CM}$=0.30% for the purpose of precluding HAZ cracking for tank car structures.

The Figure 3 and 5 plots clearly indicate that the advances in steel technology since 1965 have resulted in reducing the %C-CE% and the $P_{CM}$% parameters. These advances have been made to the point of "saturation" because additional benefits related to weldability are not expected for the case of the simple structure features of tank car vessels. Complex structures such as offshore platforms may benefit from the lowest attainable %C-CE% and $P_{CM}$%

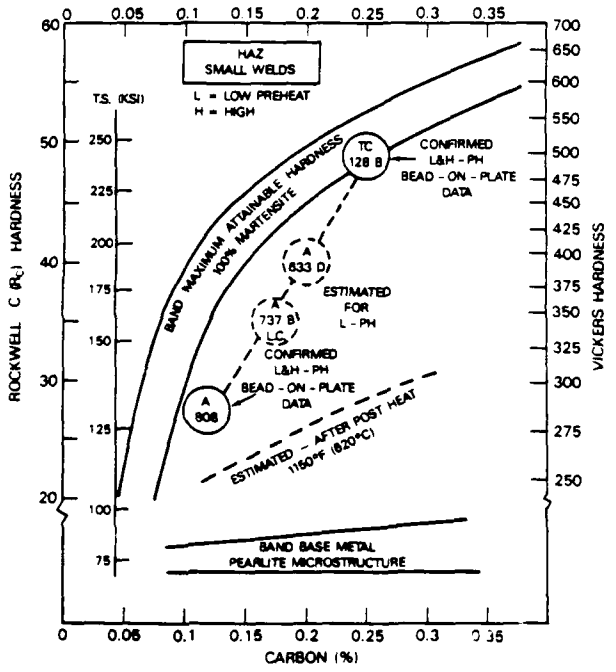


Figure 5 Comparison of the Estimated HAZ Hardness for the Project Steels.

Retention of yield and tensile strength properties becomes difficult as the %C is decreased. The strength factor establishes the lowest attainable %C level. Increasing the %Mn and adding the Ni and Cu permits attaining 0.06 to 0.08%C levels for CR and ICR steels. However, the steel mills are forced to produce the steels with a very small "spread" between the minimum specified tensile properties and the actual production values. Limits must be placed on the plate thickness in order to retain a practical "spread." It is "spread" of tensile strength properties that limits the lowest %C which can be used in the interest of improving weldability.

FRACTURE PROPERTIES FACTORS - The evolution of weldable steels that is described in Figure 3 is used as a reference for fracture properties. The 1965 development of TC-128B (A-612 type) steel provided a significant improvement in low temperature fracture properties as compared to the A-516(70) normalized steel. This was due to the Ni, Cr, Mo alloy additions. The following developments of new steels featured fracture properties equivalent to or better than the normalized TC-128B steel. The AAR project is intended to develop comparative data.

Because of its novel features, the A-808 steel has been examined in terms of available data. Figure 6 presents an analysis based on Charpy V ($C_V$) properties. The band for normalized TC-128B is used as a reference. The A-808 specification for steels of 0.010%S(max.) cites the $C_V$ values noted in Figure 6. These values indicate confidence by the steel industry for producing A-808 (CR) steel featuring the estimated band properties.

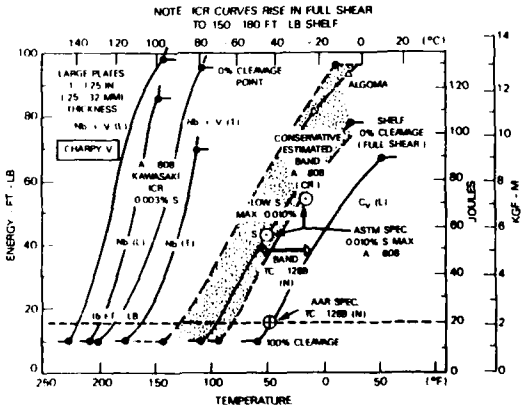


Figure 6 Comparison of (Charpy V ($C_V$) Fracture Energy Transition Curves for A-808 CR and ICR Controlled Rolled Steels. The Band for Normalized TC-128B Steel is Used as Reference.

The data for Japanese produced A-808 steels rolled by ICR practices is also presented in Figure 6. These steels feature very low 0.003%S. It appears that the combination of ICR plus very low %S as results in a large shift for the $C_V$ curves to lower temperatures, and high shelf values. The shifts were compared on the basis of the transition from 0% cleavage fracture (full shear), to

100% cleavage which indicates a completely brittle condition.

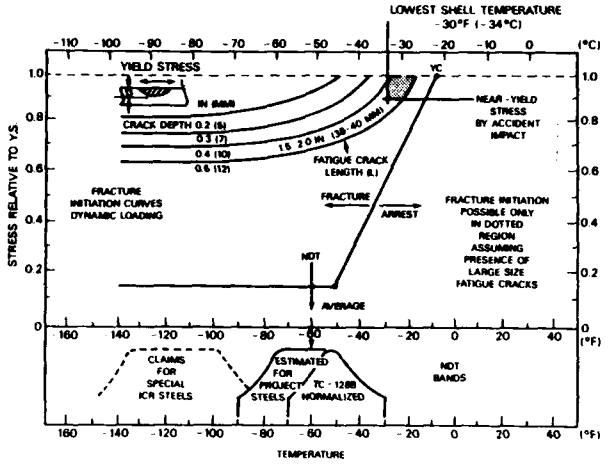


Figure 7 Slide-Graph Fracture Analysis for the New Project Steels.

The Figure 6 $C_V$ data have been analyzed in terms of the requirement for precluding the development of brittle fracture in the case of tank car accidents. The lowest anticipated service temperature (LAST) for the shell is -30°F(-34°C). The brittle fracture rate for the case of old and presently used as-rolled steels is 0.4%. These steels feature $C_V$ 15 ft.-lb. (20J) temperatures in order of 30°F (-1°C). It was concluded, reference (2), that use of normalized TC-128B steel which has a 15 ft.-lb.(20J) maximum temperature of -50°F (-46°) would reduce brittle fracture rates to 0.1%. This low value is based on the pessimistic assumption that the accident temperatures were close to the -30°F (-34°C) LAST.

Steels which feature a $C_V$ band that is significantly better than the normalized TC-128B band, are expected to reduce the brittle fracture rate to zero. Therefore, the estimated $C_V$ band for the A-808 (CR) steel of 0.010%S (max.) type implies that brittle fracture is not possible for all service temperatures equal to or higher than -30°F(-34°C). The very low $C_V$ transition curves of the 0.003% ICR type of A-808 steel are not required for the purpose of fracture prevention at lowest service temperatures.

Fracture analysis that does not require comparison with service experience may be made analytically by the use of the AAR slide-graph procedure. Figure 7 presents a slide-graph analysis which includes the A-633D, A-737L.C. and A-808 (CR-0.010%S) steels. The NDT band for these steels is estimated to be located at slightly lower temperatures than the TC-128B band. The Project data should define the exact location of this band. For purpose of preliminary analysis the average NDT temperature is conservatively estimated as -60°F(-15°C).

The slide-graph analysis indicates that at the -30°F) (-34°C) LAST it is necessary to develop near-yield-stress impact loading at sites of large cracks -- in order to develop a brittle fracture. At higher temperatures the steels are fracture-safe. Figure 6 cites that large fatigue cracks must be present for fracture at -30°F(-34°C). Fabrication cracks are not expected for the new steels, because of their superior weldability properties.

There is a very low probability that the crack stress loading conditions are developed at LAST temperatures. The slide graph analysis indicates near-zero probability for the development of brittle fracture for the new steels.

The very low NDT temperatures that are claimed for the A-808 type ICR(0.003%S) steels are not required for the purpose of preventing brittle fracture at near-LAST temperatures. The range of NDT temperatures of A-808(CR) steel is expected to satisfy fracture prevention requirements. Therefore, decreasing the NDT temperature by ICR controlled rolling of this steel does not provide additional benefits.

## CONCLUSIONS

The development of new types of weldable steel since 1970 provides three primary options for the selection of improved tank car steels. These options are defined by the following listing of astm standard grade steels. All of these steels are specified to the minimum tensile properties of 50 ksi (345 MPa) yield strength and 70 ksi (485 MPa) tensile strength.

(1) A-633D -- This steel is a lower %C version of the presently used A-612 (TC-128B) steel of C-Mn plus Ni-Cr-Mo-V alloy type. It is produced as a normalized steels.

(2) A-737B(LC.) -- This steel is representative of the first generation Cb(Nb) microalloyed steels. It is produced as a normalized steel because equivalent properties cannot

be developed by controlled rolling.

(3) A-808 -- This steel is representative of the second generation (Cb(Nb) plus V microalloyed, controlled rolled steels. While not specifically stated, the ASTM specification is intended to represent controlled rolled steels. This steel may be produced by CR or ICR rolling practices. For low temperature service the steel should be produced to the specification of 0.010%S (max.).

These primary options were defined by preliminary weldability analysis and fracture analysis. The weldability analyses were made by reference to the parameters %C-CE% and $P_{CM}$% parameters. A generalized interpretation of the weldability significance of specific parameter values is provided in this paper for readers who are not expert in the subject of weldability ratings.

The fracture analyses were made on the basis of design objectives for assured prevention of brittle fracture in cases of accident, at the LAST of -30°F(-34°C). The fracture properties of the three steel options that were first selected by weldability analysis, were estimated from available data.

Sample plates of the three new steel options and the presently used TC-128B (A-612 type) steel, have been procured for the purpose of weldability testing and mechanical properties determinations. These steels are cited as the AAR Project steels. The test program includes mechanical properties tests, weldability tests, and qualification type welding tests. Therefore, complete data documentation will be available for comparison of presently used and new steels.

There is a high degree of confidence that the Project data will confirm the general predictions of the preliminary weldability analyses and fracture analyses presented in this paper.

The purpose of the Project tests is to generate specific data required for final selection of the best option(s) for future use as AAR certified tank car steels. The final selection(s) will be made by the Steel Task Force of the AAR Tank Car Committee.

The general conclusions which can be made at this time were evolved entirely by preliminary weldability analysis and fracture analysis. As such, the conclusions are intended to indicate the probable bases for final selection by the Tank Car Committee.

The general conclusions are:
(1) The new standard grade steels that have been developed since 1970 are expected to satisfy near-term and long-term requirements for improved tank car steels.
(2) The normalized C-Mn type A-633D steel and the normalized microalloyed A-737B(L.C.) steels are expected to satisfy near-term requirements. These steels require post-weld-heat treatment (PWHT) for this purpose.
(3) The controlled rolled, microalloyed A-808(CR) steel of 0.010%S(max.) type is expected to satisfy long-term requirements. This steel does not require PWHT, because ductile (soft) HAZ are developed as-welded. This is a distinct advantage for the case of modifications and field-welded repairs.

A major reason for preference of the microalloyed A-808 CR steel is the fact that controlled-rolled steels are expected to replace normalized steels, as the primary source of plate products. The direct processing of CR steels eliminates the need for normalizing heat treatment, which is a more expensive batch operation. Lower cost and better availability in the future are important factors for the CR steels.

The CR steels are considered equivalent to the ICR steels, with respect to satisfying weldability and fracture properties requirements. Therefore, the case that may be made for use of ICR steels rests entirely on the economic factors of relative cost and relative availability. These are steel market considerations that are subject to change. The tank car fabrication industry normally considers these factors in procurement of tank car steels.

It is emphasized that the AAR-RPI Project does not include microalloyed steels of the ICR plus SC (Accelerated Cooling) type, described in Figure 2. also, that the Second Phase investigation described in Appendix C does not include ICR+AC type steels. The use of AC practice by the Japanese steel companies results in partial transformation to bainitic microstructures. Therefore, the AC steels represent a different and complex category of steel which is not covered by ASTM specifications.

The reader is advised that Japanese ICR+AC steels may be of

interest primarily for production of thick plates featuring relatively high tensile properties. Since the applications for tank cars are for plates of less than 1.0 in. (25 mm) thickness, the ICR+AC (bainitic) steels are not of interest to the Project.

## REFERENCES


1. W. S. Pellini, "Feasibility Analysis for Tank Car Application of New Microalloyed and Controlled-Rolled Steels - Description of Fracture Properties and Comparisons with Steels in Present Use," AAR Report no. 543, April 1983.
2. Phillips, E. A., and W. S. Pellini, "Phase 03 Report on the Behavior of Pressure Tank Car Steels in Accidents," RPI-AAR Tank Car Safety Project, Report no. RA-03-6-48, June 1983.
3. W.S. Pellini, "Engineering Significance of Failure Analysis Information for Tank Car UTLX 98646 Which Developed a Head Fracture During Humping-Switching Operations at the Toronto Yards of the Canadian National Railroad," AAR Report no. WP-113, January 1985.
4. K. Thorn, "Investigation of the Head Failure from Tank Car UTLX 98646," Welding Institute of Canada, May 8, 1984. Prepared for Canadian Transport Commission.
5. A. Ruitta, Personal Communication.
6. W.S. Pellini, "Guidelines for Fracture Mechanics Analysis of Pressure Tank Car Structural Integrity Factors," AAR Report no. R-586, January 1985.
7. W. S. Pellini, "Guidelines for Fracture-Safe and Fatigue-Reliable Design of Steel Structures," the Welding Institute, Cambridge, CBI-6AL, England, 1983.

# PRODUCTION AND APPLICATIONS OF HIGH STRENGTH STEEL SECTIONS

**A. Frantz, J. B. Schleich**
ARBED-Recherches
Esch-Alzette, Luxembourg

ABSTRACT

During the last years, competition with concrete as well as the pull of modern steel construction, resulted at ARBED in new advanced techniques for the cost-effective production of improved high strength low-alloy steels (HSLA).

In comparison to steels with lower yield point, HSLA steels present many economic advantages contributing to improve competition of structural steelwork.

Increasing requirements in construction steelwork ask for an impressive scope of mechanical and technological properties: high yield point, good weldability and excellent toughness.

In this paper are presented steelmaking, thermomechanical rolling, properties and applications of the following 2 ARBED steel grades:
- Fe E 460 - Fritenar (yield point 460 MPa min.)
- ASTM A 572 Grade 50 - Fritenar (yield point 345 MPa min.), developed for Jumbo columns

Concerning the applications results of tests performed at different universities are high-lighted, as well as the successfull use of Fe E 460 - Fritenar in buildings, park-houses and bridges.

1. INTRODUCTION - During the last years, competition with concrete, as well as the pull of modern steel construction, resulted at ARBED in new advanced techniques for the cost-effective production of improved high strength low alloy (HSLA) steel products [1, 2, 3].

In comparison to steels with lower yield strength, HSLA steels have many advantages contributing to improve the competitivity of structural steelwork:
- Higher loads and or lighter structures are possible
- Reduced transport and handling costs
- Reduced machining costs
- Lower assembly costs
- Reduced number of steel members
- Reduced building time

Increasing requirements in constructional steelwork ask for an impressive scope of mechanical and technological properties to be offered by HSLA steel sections:
- High yield strength
- Good resistance to brittle fracture
- Excellent weldability
- Unchanged properties after stress-relieving
- Resistance to lamellar tearing
- Good internal soundness

The requirements for the characteristics of a HSLA steel depend on its application. This is certainly true for heavy sections, which are currently used for the following applications:
- Bearing piles in foundations
- Industrial equipments
- Buildings
- Nuclear power plants
- Offshore structures
- Arctic applications

The present paper covers steelmaking, thermomechanical rolling, properties and applications for the following 2 ARBED-HSLA steel grades:
- Fe E 460 Fritenar - presenting a minimum yield point of 460 MPa (67 ksi) and high toughness properties at -20°C (-4°F). This steel grade which is equivalent to ASTM A 572 Grade 65 is available in sections with thicknesses up to 60 mm (2,4 in.)

- ASTM A 572 Grade 50 Fritenar - developed especially for Jumbo sections to be used as tension members, combines a minimum yield point of 345 MPa (50 ksi) with good resistance to brittle fracture at a temperature < 0°C (+32°F). The heaviest section produced in grade Fritenar is the Jumbo beam WF 14"x16"x730 lbs with a flange thickness of 125 mm (4,9 in.).

2. FABRICATION ROUTE FOR SECTIONS - For the fabrication of structural steel sections, ARBED uses the following fabrication route:

Blast - furnace
↓
Oxygen steelmaking plant
↓
Ladle treatment
↓
Vacuum degassing
↓
Ingot casting
↓
Blooming mill
↓
Rolling mill
↓
Finishing + Inspection

At present a big part of world steel production is produced in continuous casting, because of its cost-effectiveness. This is certainly true for wire-rod and plates. For this reason ARBED uses this route for its whole wire production. Investigations carried out in order to study the possibility of producing also sections from continuously cast material came to the result that ARBED should maintain the ingot casting route for the following reasons:

- By remarkable progress made in its steelmaking and ingot casting technologies, an economic production of high quality sections, meeting the most severe customer requirements has been achieved.

Excellent user properties are obtained, mainly by a combination of high deformation ratios, typical for ingots, and application of advanced thermomechanical rolling techniques.

Moreover, ARBED sections produced by the ingot casting route show good internal soundness and high surface quality levels in accordance with the most stringent material specifications.

- By ingot casting it is possible to produce sections in a large range of geometrical dimensions, specially beams with depths up to 1100 mm (43"), flange thicknesses up to 125 mm (5") and flange widths up to 450 mm (17,7").

Thanks to the high deformation ratio, this high quality level is also obtained with extra-heavy sections.

- Finally ingot casting offers a high flexibility in producing special steel grades in small quantities with short delivery time.

3. STEELMAKING - In former times increased carbon content was the method to improve strength. This was easy and cheap, but it resulted in considerable deteriorations in toughness and weldability. Modern structural HSLA steels however are characterized by a low carbon content (< 0,20%), where the loss of strength due to the decreasing carbon content is balanced mainly by the use of microalloys and by thermomechanical rolling.

In addition to the lowering of carbon content, development of new metallurgical techniques was necessary to obtain an improvement of steel quality in respect to:

- Chemical composition: narrow range for the different elements
- Low oxygen and inclusion content
- Low sulphur content and shape control of the sulphides
- Low phosphorus content
- Low content of nitrogen and hydrogen
- Low content of tramp elements

4. ROLLING PROCESS - Since 1970, ARBED has continuously developed the thermomechanical rolling process for sections. The technology consists in applying well defined deformation ratios at precisely controlled temperatures during the different phases of the rolling process (fig. 1). During this treatment the flange-web intersection is selectively cooled (fig. 2) in order to decrease the temperature in the core areas and to equalize the temperature profile over the cross-section. The rolling is finished at a temperature just above the $Ar_3$ point (austenite → ferrite/pearlite), what is favourable for a fine-grained microstructure. The thermomechanical rolling process coupled with on-line selective cooling, named TM-SC-process, leads to improved and more homogeneous mechanical properties.

To be mentioned that the advantages of this thermomechanical rolling compared to normalizing are important. Thermomechanical rolling is more cost-effective and asks for a lower carbon equivalent for a given level of yield strength. A reduced carbon equivalent leads after welding to a lower underbead hardness and decreases the risk of cold cracking in the heat affected zone.

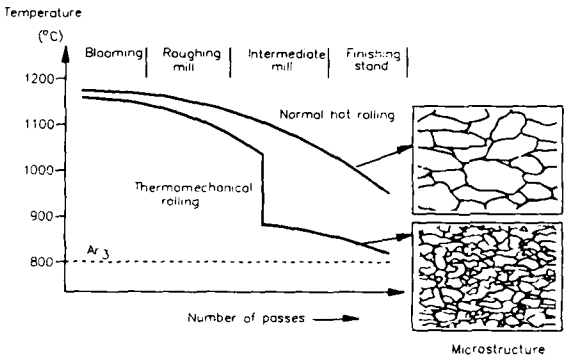


Fig. 1 - Comparison of thermomechanical and normal hot rolling (schematically)

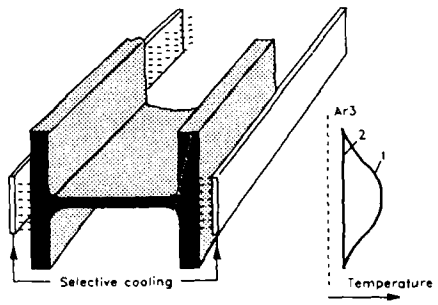


Temperature profile over flange width

1: Normal thermomechanical rolling

2: Thermomechanical rolling plus selective cooling

Fig. 2 - Principle of the selective cooling of beams during rolling

5. STEEL GRADE Fe E 460 - FRITENAR

5.1. Chemical composition - The chemical composition of grade Fe E 460-Fritenar is given in Table 1.

Table 1 - Chemical composition (ladle) of Fe E 460-Fritenar

| Elements | 1 | 1 | 1 |
|---|---|---|---|
| % C | < = 0,20 | < = 0,20 | < = 0,20 |
| % Si | 0,10-0,55 | 0,10-0,55 | 0,10-0,55 |
| % Mn | 1,10-1,70 | 1,10-1,70 | 1,10-1,70 |
| % P | < = 0,025 | < = 0,025 | < = 0,025 |
| % S | < = 0,020 | < = 0,020 | < = 0,020 |
| % Alsol | > = 0,020 | > = 0,020 | > = 0,020 |
| % N | < = 0,010 | < = 0,010 | < = 0,010 |
| % Nb | 0,02-0,06 | 0,02-0,06 | 0,02-0,06 |
| % V | - | 0,06-0,18 | 0,06-0,18 |
| % Ni | - | - | 0,20-0,70 |
| Material thickness | < = 10 mm (0,39 in.) | > 10 mm (0,34 in.) < = 20 mm (0,78 in.) | > 20 mm (0,78 in.) < = 60 mm (2,4 in.) |

The steel is Al-killed and micro-alloyed. The chemical composition is depending on the material thickness.

5.2. Tensile test - The tensile test properties of Fe E 460-Fritenar to be guaranteed in the flange (1/6 width) are prescribed in table 2.

The result of tests carried out on beams with material thicknesses from 10-60 mm (0,39 - 2,36 in.) is given in figure 3. It can be seen that the guaranteed values are largely obtained for all material thicknesses.

Table 2 - Tensile properties of Fe E 460-Fritenar

| Yield point MPa [ksi] | Tensile strength MPa [ksi] | Elongation (Lo = 5do) % |
|---|---|---|
| Material thickness in mm < 16 16<t<40 40<t≤60 | ≤ 60 | ≤ 60 |
| 460 min. [67] 450 min. [65] 440 min. [63] | 560 - 730 [81 - 106] | 17 min. |

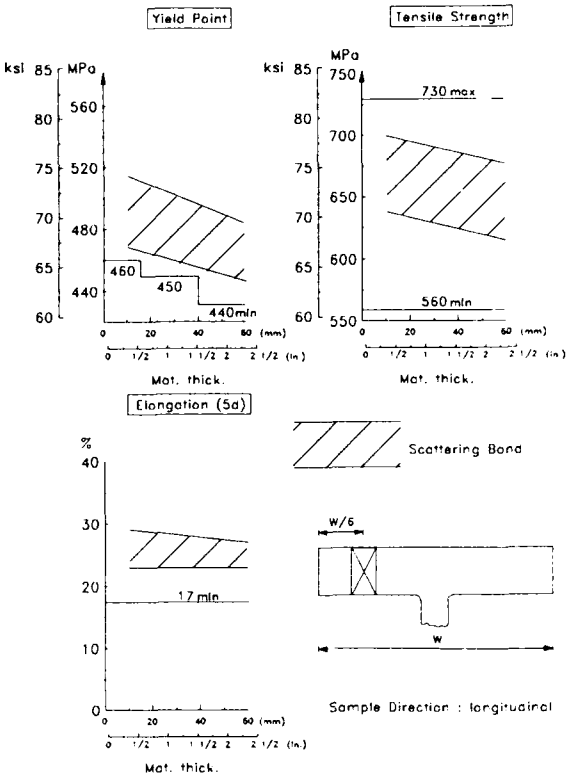


Fig. 3 - Result of tensile test on beams in grade Fe E 460-Fritenar

5.3. Notch-toughness properties - Notch toughness properties are characterized by Charpy V-notch impact test carried out on specimens taken in longitudinal direction. The impact values to be guaranteed for Fe E 460-Fritenar are indicated in table 3.

Figure 4 shows the test results obtained on an HE-beam with a flange thickness of 40 mm (1,57 in.) at the standard position (1/6 flange width) and at the intersection flange-web area. For both positions the impact values at -20°C (-4°F) are at a fairly high level, what is demonstrating the good resistance against brittle fracture of grade Fe E 460-Fritenar.

Table 3 - Charpy V-notch impact properties in longitudinal direction

| Absorbed Energy min. Joules [Ft. lbf] | | |
|---|---|---|
| -20°C [-4°F] | 0°C [+32°F] | +20°C [-68°F] |
| 40 [30] | 47 [35] | 55 [41] |

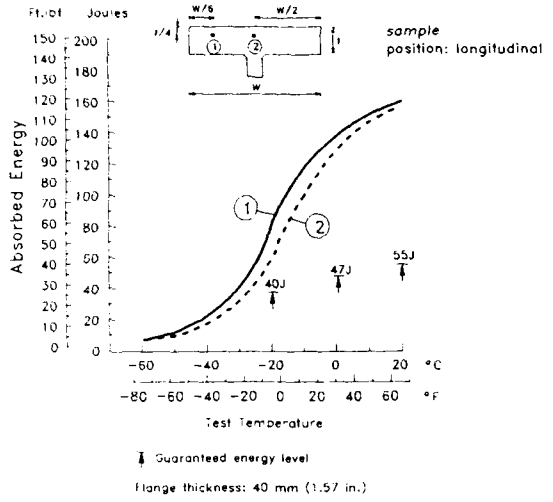


Fig. 4 - Charpy V-notch impact test on beams in grade Fe E 460-Fritenar

5.4. Weldability - Fe E 460-Fritenar can be welded with all manual and automatic welding processes like manual arc welding and submerged arc welding, provided that the general rules are respected.

The welding conditions depend on the welding process, the material thickness and the hydrogen content of the filler metal.

Welding trials carried out on different sections with heat-inputs situated between 18 and 25 kJ/cm (46-64 kJ/in) have shown that after welding, the ductility of the heat-affected zone remains at a high level. The test results are given in figure 5.

5.5. Stud welding - In the case of mixed (steel-concrete) constructions it may happen that studs have to be welded to a structural element by the drawn arc stud welding process.

Grade Fe E 460-Fritenar is suitable for such a welding process and an approval has been granted to ARBED by the "Schweisstechnische Lehr- und Versuchsanstalt Duisburg (F.R. of Germany)".

For the qualification test, studs of 13 mm (0,52 in.) and 22 mm (0,87 in.) have been welded to a 20,5 mm (0,81 in.) thick beam flange without preheating.

The results of the metallurgical examination, hardness test and shock bending test have been quite satisfactory and in accordance with the prescriptions of the german standard DIN 8563 Part 10.

5.6. Influence of stress-relieving - Stress-relieving at 580°C (1076°F) has been performed on material in the as-rolled condition and on butt-welded material.

For the as-rolled condition as well as for the welded condition (figure 6) there is no significant influence of stress-relieving on the yield strength, tensile-strength, elongation and the Charpy V-notch impact properties.

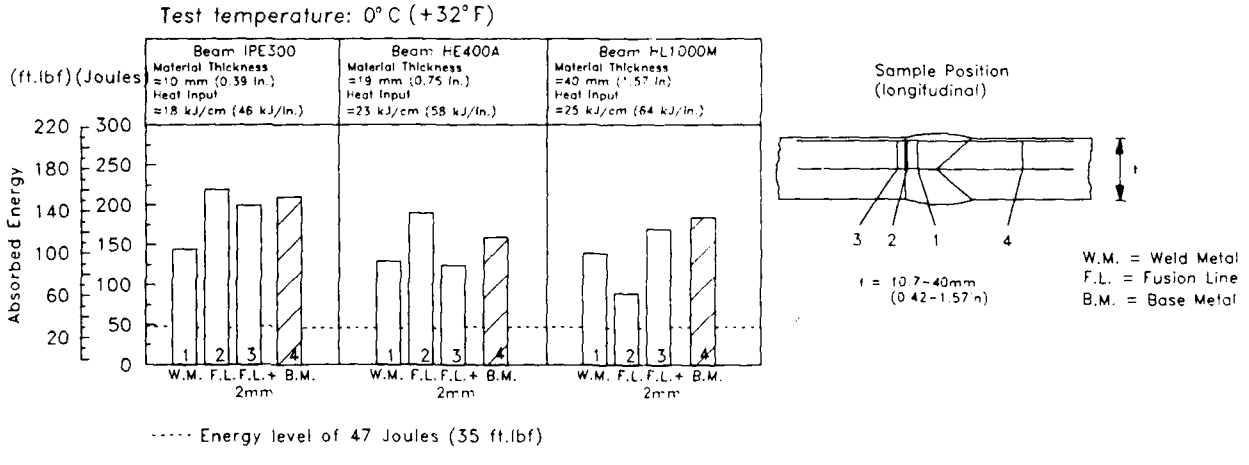


Fig. 5 - Charpy V-notch impact test on manual arc welded joints in Fe E 460-Fritenar

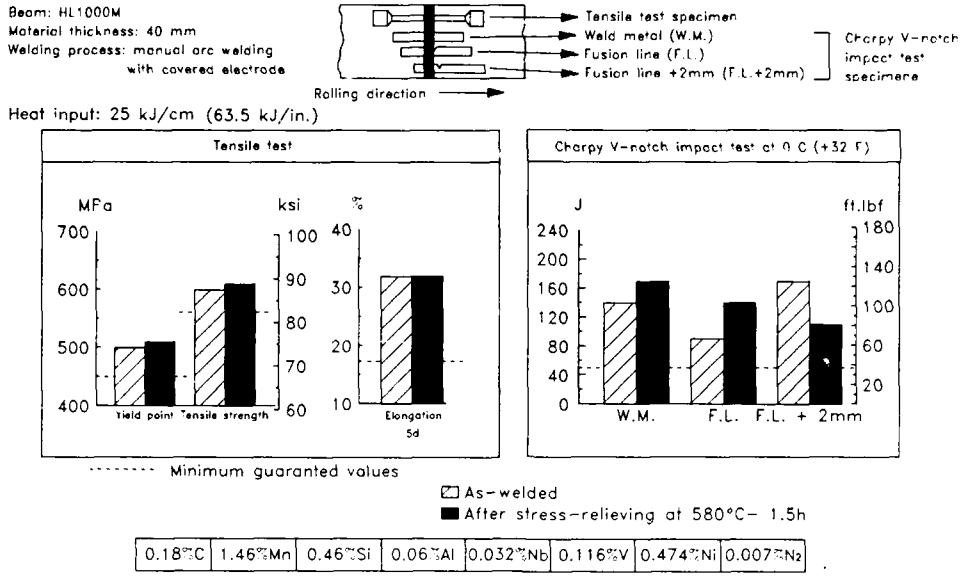


Fig. 6 - Influence of stress-relieving on the mechanical properties of welded joints in steel grade Fe E 460-Fritenar

5.7. Applications of Fe E 460-Fritenar in structural steelwork

5.7.1. General remark - Until now, the number of structures built with hot-rolled beams in high-strength steel Fe E 460 is rather limited. This is due to two major facts, namely:

- Most of the existing standards are limited to steel grades with yield strength less or equal 360 MPa.
- Engineers and steel constructors are very suspicious of new materials.

In future, these handicaps should be removed by introducing grade Fe E 460 in the most important national and international standards and by giving the customers arguments and data concerning the fabrication and the application of the new steel.

In order to succeed in this field and to create a scientific background, ARBED-Research is realizing a large research project with the aim to give the customer all the data he needs for using HSLA-steels.

5.7.2. Columns in Fe E 460-Fritenar - When using columns in steel grade Fe E 460, the average weight savings are about 22% as compared to grade Fe 510 (figure 7). In some cases, e.g. for certain buckling lengths or different steel shapes, the savings may be much more pronounced. At the same time, the total area of the column can be reduced by about 25% in average, increasing by this way the effective area of the building.

5.7.3. Beams in Fe E 460-Fritenar - Use of beams in Fe E 460 leads on the one side to weight savings of about 15% as compared to steel Fe 510 [Y.P. = 355 MPa (50 ksi)] when choosing the same beam depth, or on the other side to depth reduction of about 11%. Deflection problems can be solved by realizing composite beams, where the steel section is connected to a concrete slab by shear studs (figure 8). It should be noted, that stud welding can be performed by the usual way without preheating.

5.7.4. Frames in Fe E 460-Fritenar - In industrial frame buildings, weight savings reach 30% compared to grade Fe 360. In the past, ARBED realized several tests on frame-joints at the University of Karlsruhe (figure 9). In spite of the very high yield strength of 570 N/mm² obtained, the behaviour of the test specimen was astonishing, by reaching nearly the full plastic moment without local buckling. In fact, at the end of the tests, a plastic hinge could be visualized by special methods (figure 10).

5.7.5. Reference objects - Due to the reasons evoked above, the number of reference objects is rather limited. However some of them are worth mentionning:

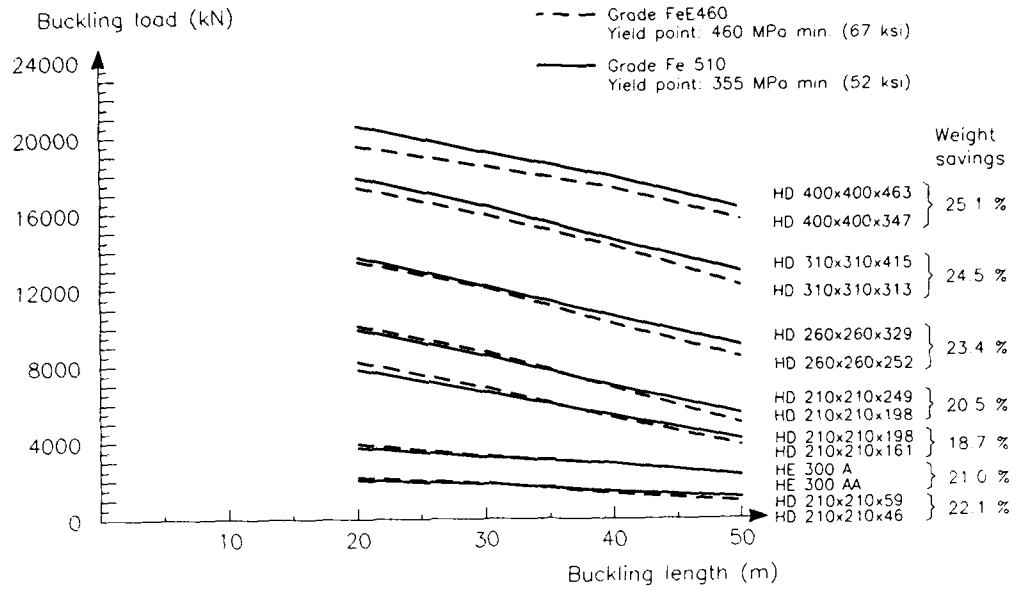


Fig. 7 - Comparison of the buckling load of columns in steel grades Fe 510 and Fe E 460

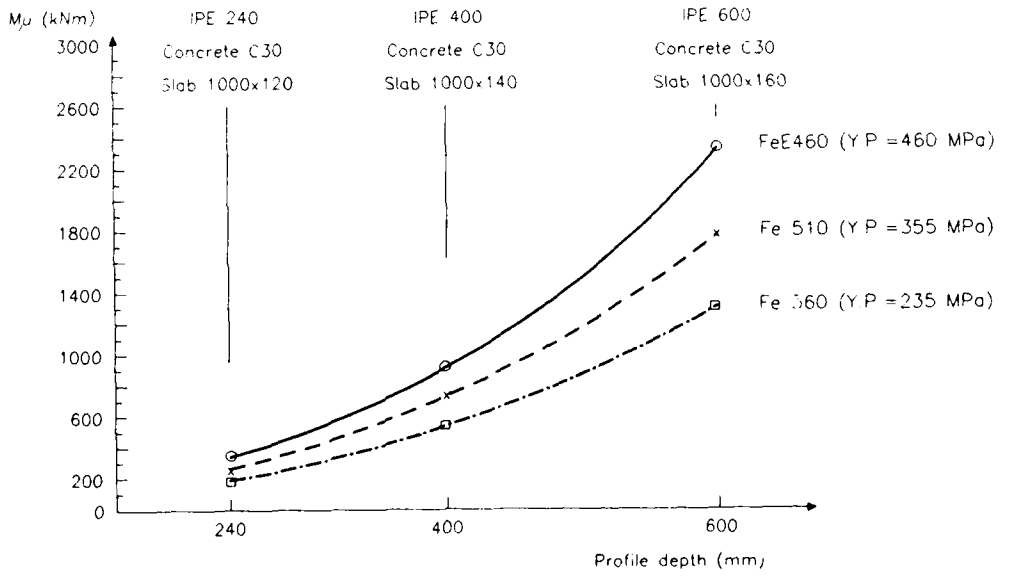


Fig. 8 - Ultimate bending moment of composite beams

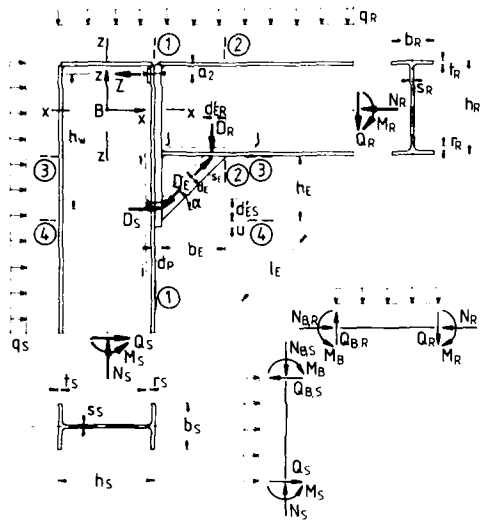

Fig. 9 - Calculation model for bolted joints

Fig. 10 - Test specimen in grade Fe E 460 after testing

A) Multi-storey building in Luxembourg - The public center for data processing in Luxembourg (figure 11), erected in 1987, is composed by a multi-storey steel frame. In order to have great facilities for later disposition, the column section should be reduced to a minimum. By using steel Fe E 460, the column area could be reduced by 40% compared to columns in steel Fe 510 (Y.P. = 355 MPa) At the same time, weight savings of about 30% could be realized. This two gains had of course a decisive influence on the economy of the object.

B) Multi-storey parkings in F.R. of Germany - In Germany, several objects were realized in Fe E 460. Beams with spans of 16 meters used in park-houses allowed the parking of two cars on each side with space for traffic inside (figure 12). Steel Fe E 460 was chosen for clearance problems and for money saving.

Nevertheless the slab was not connected to the HSLA-beams, deflection problems could be avoided by choosing IPEA-shapes, which present the best ratio inertia/weight.

This application was the first reference, where Fe E 460 elements became standardized structural elements.

Fig. 11 - Data Processing Center in Luxembourg

Fig. 12 - Park-house in Offenbach (F.R. of Germany)

C) Composite bridges for Turkey - As part of the construction of several bridges for a new line of the "Light Rapid Transport System" in Istanbul (figure 13), the requirements of the owner concerning clearance and span were leading to the application of tailor-made HL1000 beams with flange thicknesses of 55 mm in HSLA-steel according to ASTM 572 (Grade 65). The four main girders with a span of 34 meters support a concrete slab of 25 cm thickness.

The application of this steel grade in a railway-bridge proves also the good fatigue behaviour of HSLA-beams.

5.8. Synthesis - By progress in steelmaking and rolling techniques at ARBED, an economic production of sections presenting a combination of a high yield point (Re = 460 MPa) and high toughness at low temperature (-20°C) [-4°F] has become possible. The developed steel grade Fe E 460 is weldable with all usual welding processes. After welding, the toughness of the heat-affected zone remains at a sufficient high level. It should however be pointed out that during welding precautions are necessary in order to avoid cold cracking of the heat affected zone.

The material can be stress-relieved without altering significantly the mechanical properties.

Flame-cutting and machining can be performed without any major problems.

The development of a HSLA-steel like Fe E 460-Fritenar will help to improve the competitivity of structural steelwork. However the use of higher strength structural steels is in Europe at present limited by the fact that many standards and design rules for structural steelwork do not include those grades. This situation will certainly be improved by the introduction of Eurocode 3 for structural steelwork.

Fig. 13 - Light Rapid Transport System in Istanbul (Turkey)

## 6. DEVELOPEMENT OF HIGHLY WELDABLE JUMBO SHAPES FOR TENSION MEMBERS: STEEL ASTM A 572 GRADE 50-FRITENAR

6.1. Aim of the development - For many years Jumbo shapes have been used successfully as columns in high rise buildings where they had to support only axial compression loads, so that no special toughness requirements had to be specified.

However, when Jumbo sections were used as tension members in large trusses or bracings, cracking and even failures occured in groove-welded splices. An extensive study conducted at Lehigh University [4] lead to the conclusion that due to low toughness, mainly in the core area of Jumbo sections, bolted connections should be designed instead of welded joints when subjected to tension stresses.

In view of these results, ARBED started a research program to improve technological and mechanical properties of ASTM A 572 Grade 50 steel for Jumbo sections.

Based on ARBED's large experience as a supplier of high quality steel grades for offshore platforms in the North Sea, a special steel grade called ASTM A 572 Grade 50 Fritenar was developed for Jumbo shapes in tension applications. This steel combines standard properties of ASTM A 572 Grade 50 with improved toughness properties and high weldability.

6.2. Trials - Trials have been carried out on the 2 Jumbo beams indicated in table 4.

Table 4 - Test beams

| Beam type | ASTM A 6 Group | Material thickness | |
|---|---|---|---|
| | | Flange | Web |
| WF14"x16"x730 lbs | 5 | 125 mm (4,92 in.) | 78 mm (3,10 in.) |
| WF14"x16"x370 lbs | 4 | 68 mm (2,67 in.) | 42 mm (1,65 in.) |

For each beam 2 variants were tested:
Variant A: ASTM A 572 grade 50 - standard - quality (hot rolled)
Variant B: ASTM A 572 grade 50 - Fritenar (TM-SC-process)

Beams in ASTM A 572 grade 50 standard quality were hot rolled according to a normal rolling practice. Our new advanced thermomechanical rolling technique (TM-SC-process) has been used for the Fritenar quality with a modified chemical composition as indicated in table 5.

Table 5 - Chemical composition

| Variant | Grade 50 | % C | % Mn | % P | % S | % Si | % Al | % Nb | % V | % CE* |
|---|---|---|---|---|---|---|---|---|---|---|
| A | Standard | 0,201 | 1,24 | 0,030 | 0,014 | 0,23 | 0,011 | 0,033 | 0,064 | 0,42 |
| B | Fritenar | 0,146 | 1,41 | 0,023 | 0 010 | 0,29 | 0,032 | 0,037 | 0,086 | 0,40 |

* Carbon equivalent (IIW): $CE = C + \frac{Mn}{6} + \frac{Cr + Mo + V}{5} + \frac{Ni + Cu}{15}$

6.3. Results of the mechanical tests
6.3.1. Tensile properties - Tensile test specimens have been taken in the web in longitudinal direction in accordance with ASTM standard. The results are shown in table 6.

Table 6 - Tensile test results

| Beam type | Grade 50 | Yield point MPa (ksi) | Tensile strength MPa (ksi) | Elongation (Lo = 8") |
|---|---|---|---|---|
| W14"x16"x730 lbs | Standard | 402 (58,0) | 639 (91,3) | 21 |
| | Fritenar | 390 (56,5) | 520 (75,4) | 28 |
| W14"x16"x370 lbs | Standard | 419 (60,7) | 642 (93,0) | 20 |
| | Fritenar | 413 (59,8) | 541 (78,4) | 27 |
| ASTM A 572 grade 50 | | 345 (50) min. | 450 (65) min. | 18 min. |

All tested material is in compliance with the requirements for Grade 50 steel according to ASTM A 572. Fritenar steel has a considerably higher elongation.

6.3.2. Charpy V-notch impact properties - Toughness properties have been evaluated by Charpy V-notch impact tests in longitudinal direction, performed on samples taken from the flange. Figure 14 shows the sample locations and the test results.

For both test locations, Grade 50 Fritenar steel shows considerably improved toughness properties.

6.4. Full scale bend tests - The goal of the bend tests on full scale samples was to determine the loads which can be supported by Jumbo shapes in tension applications.

In these tests, performed at the University of Karlsruhe, a Jumbo shape in quality ASTM A 572 Grade 50 Fritenar with a groove-welded splice has been compared to 2 non welded reference shapes:
- 1 beam in ASTM A 572 Grade 50 - standard quality (variant A)
- 1 beam in ASTM A 572 Grade 50 - Fritenar (variant B)

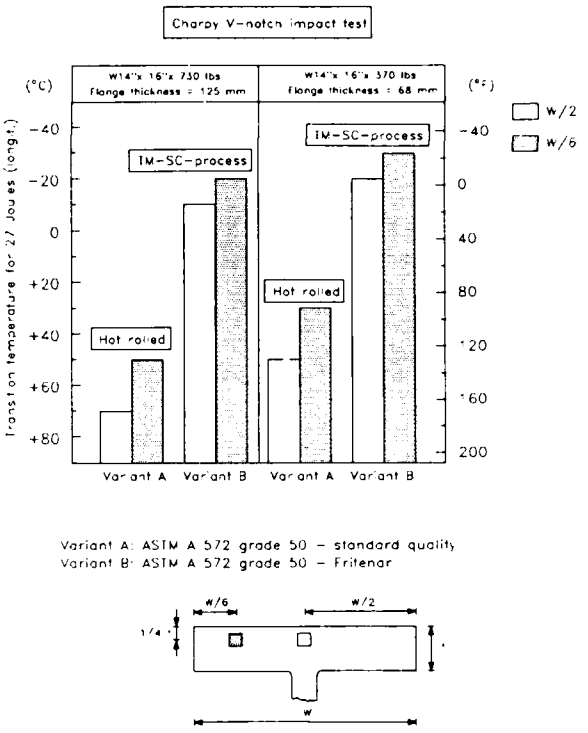


Fig. 14 - Influence of the TM-SC-process on the toughness of Jumbo beams in a steel grade with a yield point of 345 MPa min.

In figure 15, the test results are compared to theoretical values obtained on the basis of an ideal elasto-plastic design. It appears that experimental loads are considerably higher than the theoretical ones. For all 3 tests, the load corresponding to the beginning of plastification is clearly higher than the admissible load for design.

These tests show that groove-welded splices of Jumbo shapes in ASTM A 572 Grade 50 Fritenar meet all structural requirements and that they can be subjected to high tension stresses with large safety margins.

6.5. Synthesis - Based on the improved chemical composition and our new advanced thermomechanical rolling technology with selective cooling, Jumbo shapes have been developed, suitable for butt-welded connections in tension members.

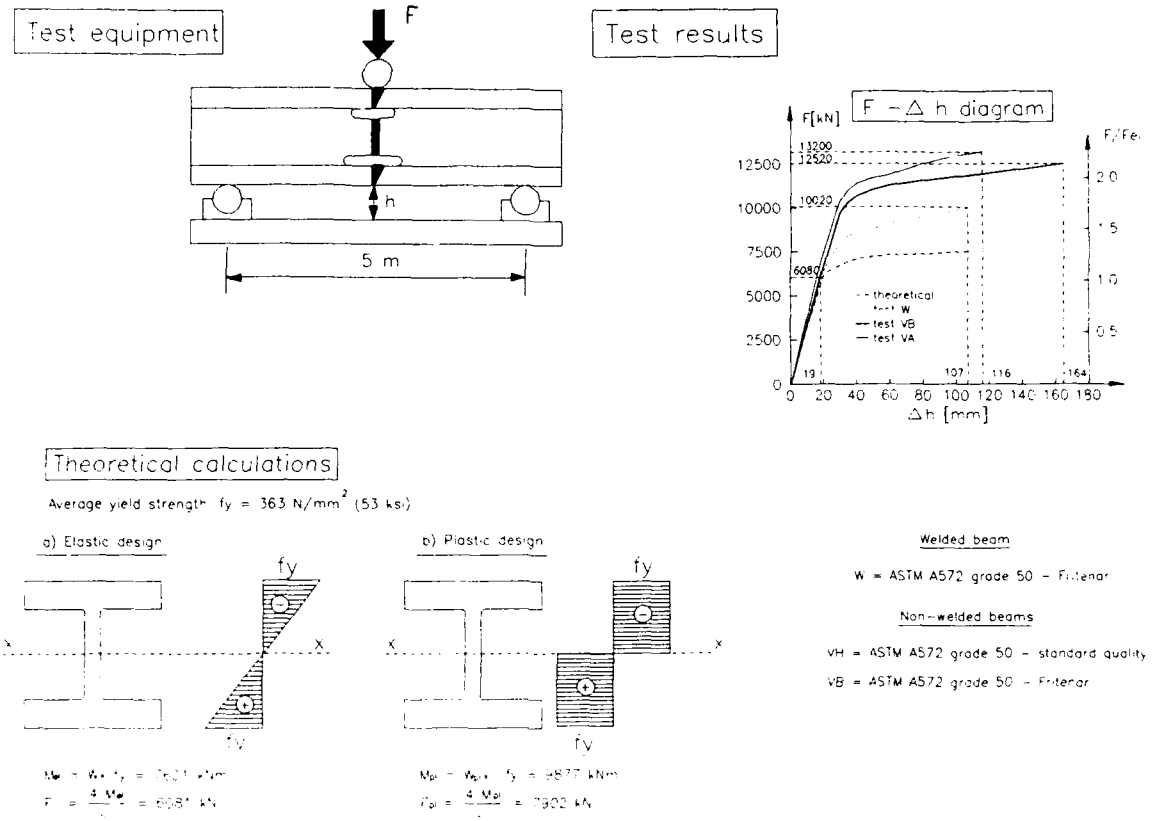


Fig. 15 - Bend test on reference and butt-welded Jumbo beams W14"x730

The new steel named ASTM A 572 Grade 50 Fritenar has the following properties:
- fine-grained microstructure over the entire cross-section
- improved notch toughness properties, particularly in the core area
- low carbon equivalent resulting in excellent weldability.

Large scale tests have shown that groove-welded splices of Jumbo shapes in ASTM A 572 Grade 50 Fritenar can be used as tension members.

This new product enables cost-effective design of steel structures and will contribute to improve their competitivity.

7. CONCLUSIONS - Technical progress in steelmaking and especially in thermomechanical rolling of sections has been important during the last decade. The developments resulted in an economic production of a new generation of HSLA structural sections combining properties formerly supposed to be contradictory:
- High yield strength
- Excellent weldability
- Good resistance to brittle fracture

For the users these developments have opened new possibilities in terms of weight savings and easier fabrication and by this way contributing to a considerable improvement of competitiveness of steel structures.

## REFERENCES

[1] Advanced Techniques for the Production of HSLA Steel Products.
J. de la Hamette, American Society for Metals 8520-017

[2] Thermomechanisches Walzen von schweren Trägerprofilen mit qualitativen Sonderansprüchen
J. de la Hamette, A. Zenner, Stahl und Eisen 104 (1984) Heft 23 S. 1225-1229

[3] Thermomechanische Behandlung von Profilen
J. de la Hamette, P. Belche, F. Becker, C. Panunzi, 16. Metalltagung in der DDR, Dresden, Mai 1987

[4] Experience with Use of Heavy W Shapes in Tension
J. Fisher and A. Pense, Lehigh University Bethlehem

# MICROALLOYED CARBON RAIL STEELS

**Harry Henderson Cornell**
Niobium Products Company Inc.
Pittsburgh, Pennsylvania, USA

## ABSTRACT

### MICROALLOYED CARBON RAIL STEELS

As rail trackage has decreased and car weights increased, the basic rail steel has been subject to conditions beyond its limits. This has lead to the development of methods of improving this eutectoid pearlitic steel to withstand present requirements. Heat treating. alloying and microalloying of basic steel has been investigated and the steels field tested over the last several decades. While each method has given major improvements, heat treating appears to be the most acceptable rail steel. However, recent work on head hardening of microalloyed (Nb), rail steel is an interesting possibility for future direction.

## INTRODUCTION

Since the first use of cast iron plate over wood runners around 1767, there has been a continuing search for improved rails. For the next 100 years the rails went throught minor change in composition but major change in design until a tee rail similar to that used today came into common use. It was in 1865 that the first bessemer steel rail was rolled in the United States. The next 100 years saw little change in design but a large change in cross-section as rails increased from 50 pounds per yard up to 155 pounds per yard. The increase in cross section was required to compensate for the increase in rail car capacity from less than 10 tons to 40-50 tons. In the last twenty years the load capacity has increased to the point where some rail cars exceed 100 tons. See Figure 1. (1,2)

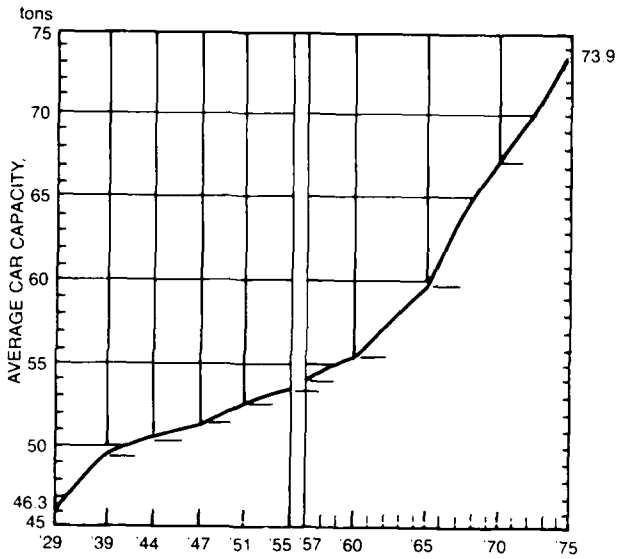

Figure 1 Increase in Freight Car Capacity from 1929 to 1975

This increase in load combined with higher speeds, longer trains, and reduced mainline trackage placed severe demands on the existing carbon rail steels. Since the turn of the century the standard rail steels had a composition of 0.69 to 0.82% carbon and 0.70 to 1.00% manganese with a fully pearlitic structure. See Table 1 (3,4). This as rolled steel has a fairly coarse pearlitic spacing, giving a yield strength of approximately 70ksi (482MPa), tensile strength of around 135Ksi (930MPa), and fracture toughness of about 36Ksi (248MPa). The steel had given good service, but modern conditions has resulted in accelerated wear, shelling, detail fracture, corrugations, and plastic deformation. Further increases in rail section size is not practical as the standard steel rails are now in service conditions where property limits are being exceeded.

TABLE 1 CHEMICAL REQUIREMENTS

| ELEMENT | COMPOSITION, % NOMINAL WEIGHT, LB/YD (KG/M) 60 to 80 (29.8 to 39.8), incl | 81 to 90 (40.3 to 44.7), incl | 91 to 120 (45.2 to 59.6), incl | 121 (60.1) and over |
|---|---|---|---|---|
| Carbon | 0.55-0.68 | 0.64-0.77 | 0.67-0.80 | 0.69-0.82 |
| Manganese | 0.60-0 90 | 0.60-0.90 | 0.70-1.00 | 0.70-1.00 |
| Phosphorus, max. | 0.04 | 0.04 | 0.40 | 0.40 |
| Sulfur, max. | 0.05 | 0.05 | 0.50 | 0.05 |
| Silicon | 0.10-0.25 | 0.10-0.25 | 0.10-0.25 | 0.10-0.25 |

High side rails on curves are deforming as a result of subsurface shear (shelling), while the heads of the low side rails are being crushed. Figure 2.

Lubrication can reduce wear to some extent, as can the modification of wheel and rail profiles. However, none of these changes can prevent failure due to the steel exceeding it property limits.

Increased material and maintenance cost as a result of accelerated replacement requirements (as often as six months on heavy haul ore trackage), required the development of premium quality steels with higher yields, higher fatigue strength, higher wear resistance, resistance to corrugations, good toughness, and good weldability. To this end the standard rail steel has been modified by quality refinement, alloy modification, microalloying, and combinations thereof.

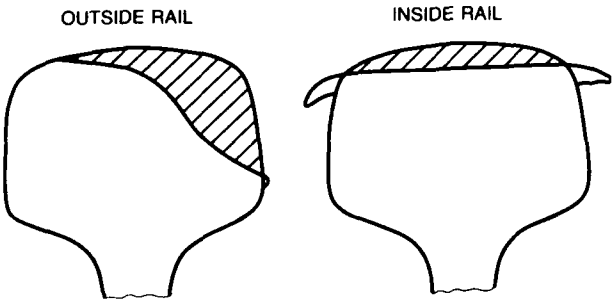


Figure 2. Difference in Wear of an Outside and Inside Rail

## QUALITY REFINEMENT

In non-lubricated rolling-sliding and sliding friction systems under large plastic deformation or on exceeding the deformation limits, cracks appear in the near surface region which can lead to very high wear rates. This type of cracking has been ascribed to non-metallic Mn-sul inclusions in some cases.

(5) In a number of reports from Russia, Zr and Ce additions increase resistance to development of fatigue cracks and increase toughness by 17% in through quenched rails by refinement of sulfides and globularization of the brittle fractured silicates; Si-Mn-Al additions instead of Si-Mn increased the degree of deoxidation, reduced the effects of stringer silicates and increased impact strength; Ti, nitrogen and rare earths additions changed the composition and shape of non-metallic inclusions, resulting in high strength and hardness, which gave wear resistance and contract fatigue strength rises of 150 - 200%.(6)

## HEAT TREATMENT

Although an improvement, clean steel practices can not raise the properties of carbon rail steel to an acceptable level for todays severe service. On the other hand, heat treatment of the standard carbon rail steel can give vastly improved properties. Austenising, quenching in air or oil, and tempering can improve both toughness and strength by decreasing the pearlite spacing and refinement of the prior austenitic grain size. As a result there can be up to a 50% improvement in yield (100/125Ksi-689/86 MPa), tensile strength (150/175Ksi-1033/1203 MPa), and hardness in the range of BHN 321/388. Thus wear life can be improved by a reported factor of three. Figure 3 and 4 are examples of the effect of pearlite spacing and prior austenitic grain size. (7,8).

Both fully heat treated rail and also rail head hardened by induction heating and air quenching, are used in many areas today.

Although heat treatment was a major step forward, there are limits to property improvements of the carbon steel. There are also the requirements of additional equipment and added operations. Thus as an alternative, modification of the steel composition to provide similar or improved properties as-rolled has been under taken by many companies and individuals.

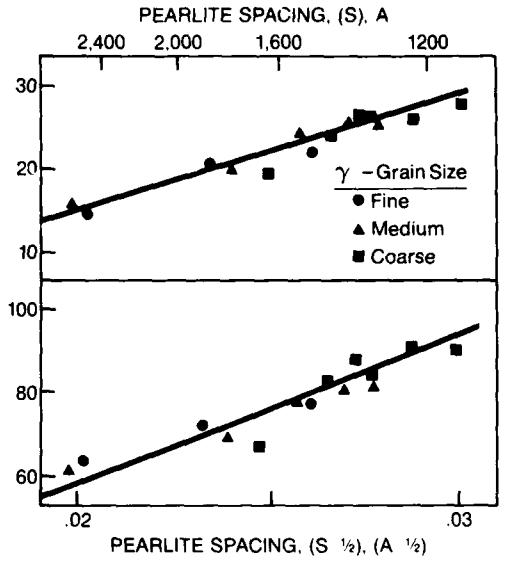


Figure 3

Yield Strength and Hardness
Vs Pearlite Spacing

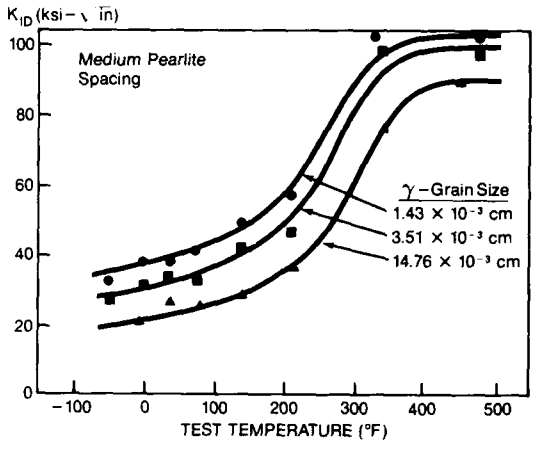


Figure 4

Dynamic Fracture Toughness as a Function
of Prior Austenitic Grain Size

## ALLOY MODIFICATION

The development of self hardening, highly wear-resistant rail steels with improved behavior in service through alloy additions to the standard carbon rail steel was started in the early sixties. (9)

The carbon level in the standard rail steel is based on the fact that the carbon controls the volume fraction of pearlite and is maximized at the eutectoid carbon content. Higher carbon contents would increase embrittlement. Lower carbons would increase ferrite with a decrease in strength and increased toughness. Lower carbon contents can be offset by additions of solid solution strengtheners. (10)

Manganese, by its effect on the eutectoid carbon, increases the volume fraction of pearlite, reduces austenitic grain size, and reduces the interlamellar spacing of the pearlite. It is also a ferritic solid solution strengthener. Manganese up to 1.35% can be tolerated in terms of toughness. Above 1.7% it can cause welding difficulties. (11)

Silicon improves the strength and wear resistance as it is also a ferrite solid solution strengthener. Up to 0.60% can be tolerated in terms of toughness. (12)

Chrome by lowering the transformation temperature for pearlite gives a refined pearlite structure and thus increases strength. Chrome precipitates help strengthen the ferrite laths. (13)

Molybdenum also lowers the transformation temperature and helps refine pearlite for higher strength. At higher levels (.30% 40%), the transformation temperature is lowered to a point where bainite is formed, resulting in lower strength and hardness. (14).

TABLE 2 - Ranges of chemical compositions of rail steels used in North America

| | Carbon | Manganese | Phosphorus | Sulfur | Silicon | Chromium |
|---|---|---|---|---|---|---|
| AREA Standard | 0.69/0.82 | 0.70/1.00 | >0.04 | >0.04 | 0.10 to 0.25 | *** |
| High Silicon | 0.69/0.82 | 0.70/1.00 | >0.04 | >0.04 | 0.50 to 1.00 | *** |
| Intermediate manganese | 0.65 | 1.37 | >0.04 | >0.04 | 0.10 to 0.25 | *** |
| Chromium | 0.72 | 0.78 | >0.04 | >0.04 | 0.25 | 1.31 |

Heat- treated rails are produce only from AREA Standard

TABLE 3 - Typical mechanical properties of rail steels used in North America at 21°C (75°F).

| | 0.2% Yield Strength | | Tensile Strength | | Elongation | Dynamic Fracture Toughness | |
|---|---|---|---|---|---|---|---|
| | ksi | MPa | ksi | MPa | % | $ksi\sqrt{in}$ | $MN \cdot m^{-3/2}$ |
| Standard | 69.9 | 481.9 | 135.9 | 937.0 | 9.5 | 26.0 | 28.6 |
| High Silicon | 70.8 | 488.2 | 137.0 | 944.6 | 10.3 | 19.0 | 20.9 |
| Intermediate Manganese | 76.2 | 525.5 | 133.4 | 920.1 | 13.5 | 27.0 | 29.7 |
| Chromium | 94.9 | 654.1 | 161.6 | 1114.0 | 9.2 | 19.0 | 20.9 |
| Heat-treated | 126.1 | 869.4 | 176.9 | 1219.7 | 9.5 | 34.0 | 37.4 |

Tables two and three show typical compositions and properties for some of the rail steels used in the seventies. Although the high silicon, intermediat manganese and chrome grades were superior to the as rolled carbon rail steel, they all proved inferior to the same steel when it was heat treated. An as-rolled steel equivalent to the heat treated steel was developed by reducing the chrome in the chrome steel and adding molybdenum. See Figure 5.

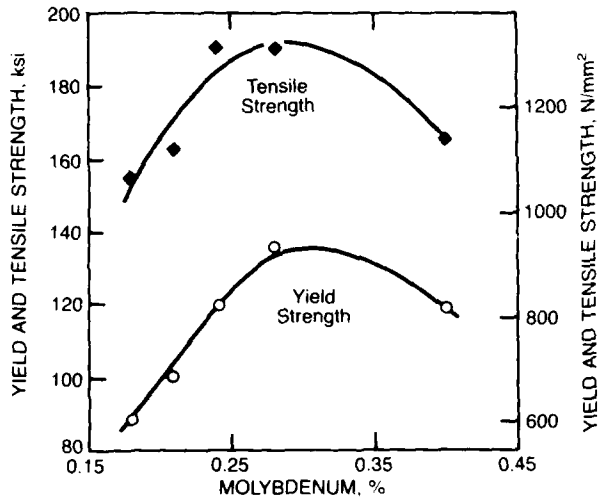


Figure 5. Influence of Molybdenum Content on Strength of Chromium-Molybdenum Rail Steels of Grain Size ASTM 10

One of the problems with alloy steels is the tendency for the elements to segregate during solidification. This has been reduced in part by steel producers continuous casting rail steels.

## MICROALLOYING

At the same time as the alloy rail steels were being developed, work was being done on the development of microalloyed rail steels.

Vanadium additions of from 0.01 to 0.30% have been made to standard carbon rail steel. As little as 0.03% reportly gives major improvements to wear resistance, strength and ductility, as pearlite spacing is refined and VC-V(CN) precipitates are dispersed through the ferrite laths. Vanadium produces an increase in yield strength of 15/22 Ksi (100/150MPa) with additions up to 0.15%, but higher additions are not beneficial. (15-18). On the other hand vanadium has been reported to raise the transformation temperature for pearlite, thus causing thicker pearlite lamellars, lowering impact strength and toughness. (19).

Chrome appears to offset the effect of vanadium on the transformation temperature and gives a lower temperature when in combination. Thus the pearlite thickness is finer than with vanadium alone and fatigue strengthens up to 65Ksi have been reported. Chrome levels of 0.4 - 1% and vanadium levels of 0.06 to 0.2% have been indicated. Service life of several times better than carbon rail steel has been shown for 1% Cr- 0.1% V steels. Good weldability and 2.5 life improvement has been reported for 1% Cr-0.15% V. Hardnesses up to BHN 400 were reported for.4%/6% Cr- 0.06/0.1% V with 115 Ksi (786 MPa) yield strength. (20-24)

In Europe a lower carbon (0.4%) rail steel with 0.4% Cr, 0.2% Ni, 0.17% V has been reported to give major service life improvements. The Ni is added to control hot shortness due to the copper. The Ni and Cu in combination gave a finer grain size and increased yield strength. As in the Cr-V steels, a 0.5% Cr addition intensified the V precipitates in the ferrite. This steel reportedly had good weldability. (25-26).

The microalloyed steel with the widest acceptance appears to be V-Cr-Mo rail steels, (0.07%V, 0.7%Cr, 0.2%Mo). These steels reportedly have yield strengths in the are of 121 Ksi (834 MPa), tensile strengths of 183 Ksi (1260 MPa), and hardnesses around BHN 376. See table 4. The chrome and manganese are kept low for better weldability. Also close

TABLE 4 - Comparison of Cr-Mo and Cr-Mo-V Steel Rails

| Steel | Composition, Wt. Percent | | | | | | 0.2% Yield Strength | | Ultimate Tensile Strength | | | | |
|---|---|---|---|---|---|---|---|---|---|---|---|---|---|
| | C | M | Si | Cr | Mo | V | MPa | (ksi) | Mpa | (ksi) | [1] | [2] | [3] |
| Cr-Mo | 0.75 | 0.81 | 0.26 | 0.69 | 0.18 | — | 785 | (114) | 1210 | (175) | 11 | 25 | 350 |
| Cr-Mo-V(I) | 0.66 | 0.90 | 0.23 | 1.02 | 0.06 | 0.09 | 675 | ( 98) | 1100 | (159) | 12 | 21 | 327 |
| Cr-Mo-V(II) | 0.78 | 0.85 | 0.39 | 0.75 | 0.20 | 0.07 | 835 | (121) | 1260 | (183) | 9 | 13 | 376 |

[1] Elongation,% [2] Reduction in Area,% [3] Head Hardness HB

control of the Mo-Cr-V content is needed to prevent bainite formation and thus decreased properties. (27).

Niobium additions of 0.01% to 0.1% have been made to carbon rail steels. As little as 0.028% Nb can give over a 25% increase in yield strength compared to carbon rail steel. A similar increase in hardness is reported (BHN 320). The niobium lowers the pearlite transformation temperature to produce finer pearlite lamellars and thus give higher strength. Niobium also lowers precipitates at high temperatures and acts to control prior austenitic grain size. This results in finer pearlite colony size and thus better toughness. Wear resistance compared to carbon steel is doubled with 0.028 Nb additions. Impact strength is greater or equal to steels of similar yield strengths and weldability is quite good. Reportedly service test gave equivalent life compared to heat treated rail. (28).

In comparative weld test a .006% Nb steel containing chrome exhibited less variation in the heat affected zone than Cr-V, carbon, and heat treated rail steels. See figures 6 & 7 and table 5. (29). Chrome in combination with niobium reportedly gives a steel with critical fracture stresses superior to heat treated rail steels. Pearlite lamellars are finer as is the pearlite spacing. This shows up in a 40% increase in yield strength over carbon rail steel, as shown in table. 6. (30-31).

Niobium-Molybdenum rail steels have not been fully investigated as early results produced a bainite structure at 0.25% Mo and 0.05% Nb, as a result of the pearlite transformation temperature being retarded. (32).

Vanadium additions to 0.5/0.1% Nb - 0.85/1.4%Cr Steel producted mixed results. Tensile strength was reduced with 0.1% V additions. However there was a 10Ksi (6$^{9}$ MPa) increase in yield strength, although no effect on ductility and toughness. A 0.2% V addition caused significant reductions in ductility and fracture toughness. (33).

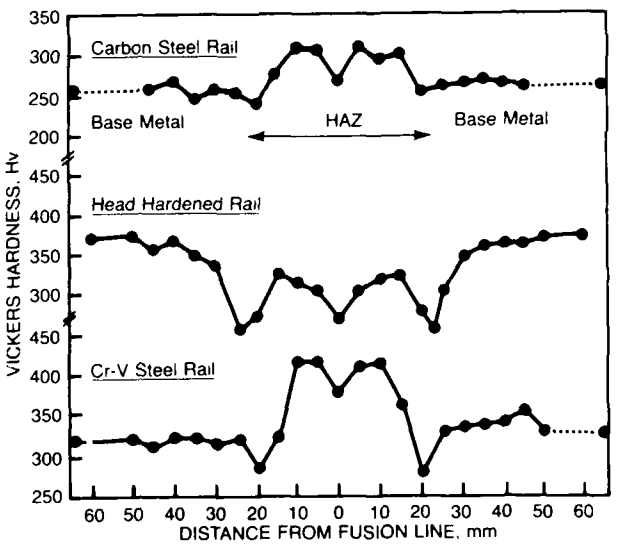


Figure 6. Hardness Distribution of Weld Joint Sections of Three Types of Rails

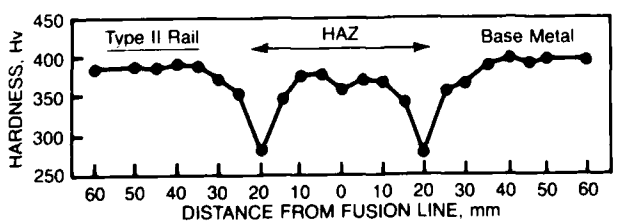


Figure 7. Hardness Distribution of Weld Joint of Type II Rail

TABLE 5 CHEMICAL COMPOSITIONS OF NEWLY DEVELOPED RAIL STEELS (%)

| | C | Si | Mn | Cr | Nb |
|---|---|---|---|---|---|
| Type I | 0.81 | 0.89 | 1.21 | — | 0.014 |
| Type II | 0.75 | 0.90 | 0.82 | 0.61 | 0.011 |

TABLE 6

| ELEMENT | CARBON STEEL | NIOBIAS 200 | SYDNEY STEEL |
|---|---|---|---|
| C | 0.74 | 0.78 | 0.70 |
| Mn | 0.80 | 1.33 | 1.10 |
| Si | 0.14 | 0.79 | 0.75 |
| Cr | - | - | 0.80 |
| Cb (Nb) | - | 0.028 | 0.06 |
| YS (MPa) | 510 | 645 | 705 |
| TS (MPa) | 920 | 1070 | 1040 |
| Elong (%) | 11 | 10 | 10 |
| Red of Area (%) | 18 | 15 | 16 |
| (HBN) | 267 | 320 | 340 |
| Yield\Tensile | 0.55 | 0.60 | 0.68 |

Columbium(Niobium) Rail Steel Comp (%) + Properties Ref. 30

Boron additions have also reportedly been made to microalloyed and alloyed rail steels. In Russia, boron-vanadium additions reportedly increased the hardness to BHN 450 and tensile strength to 235Ksi (1619MPa). (34). The English on the otherhand proposed a steel containing up to 3% Mn, 3% Mo and boron with optional additions of up to 6% Ni, Cr, Cu. These bainitic steels are reportedly tough and wear resistance. (35). Apparently no boron containing rail steels have been service tested.

## CONTROLLED ROLLING OF MICROALLOYED STEELS

Some of the more recent work on microalloyed rail steels has involved evaluation of the rolling temperature and more precisely the finishing temperature. High finishing temperatures promoted the retention of niobium in solution in the austenite and threfore increased the precipitation strengthening of the ferrite. (See figure 8). A low finishing temperature on the otherhand, enhances strain induced precipitation in the austenite with a resulting refinement of the pearlite colony size. (36).

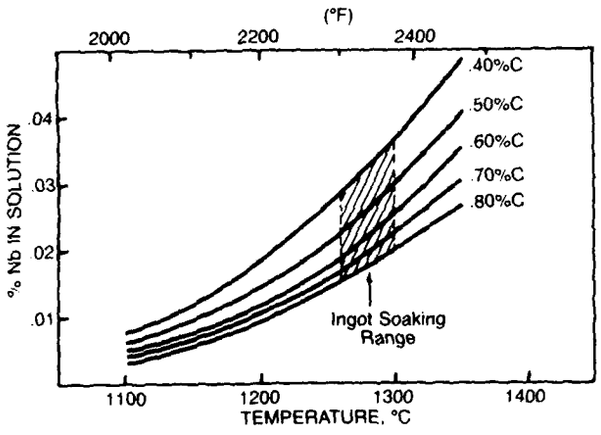


Figure 8. Nb(C,N) Solubility Curves in Austenite

With lower carbon and higher manganese the niobium in solution can be increased to give higher strength. Higher silicon contents can add to the strength and toughness, enhancing the effects of the low finishing temperatures. At the lower temperature the ductility is improved as a result of the elongated austenitic grains and the refinement of the pearlite cells. Reportedly, controlled rolled microalloyed steels can be superior to heat treated steels. (37-39).

## HEAD HARDENING OF MICROALLOYED (NB) RAIL STEELS

Head hardening is a method of obtaining high strengths by induction heating or flame heating of the rail head, followed by air quench and cooling by conduction into the lower portion of the rail. This method of hardening can produce a residual stress within the head and can be effective in preventing the generation and propogation of subsurface cracks.

Table 7 shows the composition of the steels head hardened (.005/.006% Cb), as well as the properties before and after head heardening. Head hardening in this work increased the yield strength by nearly 50% on the average. The tensile strength increased approximately 30%.

This steel is readily weldable and has a minimum of property variation within the heat affected zone. Service test indicated satisfactory results when last reported. (40-41).

TABLE 7 - Mechanical Properties of Newly Developed Steel Rails

| | C | Si | Mn | Cr | Nb |
|---|---|---|---|---|---|
| NSI | .76 | .84 | 1.24 | — | .006 |
| NSII | .76 | .82 | .82 | .49 | .005 |

| TYPE | YS | TS | ELONG | RED A |
|---|---|---|---|---|
| NSI | | | | |
| AS ROLLED | 608MPa | 1098MPa | 12% | 18% |
| HT | 873 | 1285 | 14 | 14 |
| NSII | | | | |
| AS ROLLED | 608 | 1127 | 14 | 19 |
| HT | 902 | 1324 | 19 | 50 |

## SUMMARY

While the first century of improvements in rail involved design of the rail cross section to meet demands of a growing transportation industry, the second century involved the introduction of the steel rail and its growth in cross section to meet increased weights and speeds of an industry that had spread throughout the world.

These first few decades of the third century of rail transportation has seen drastic reductions in rail line mileage, and increases in car weights and thus tonnage over the remaining trackage. This has brought about minor cross-section design changes but as previously mentioned, increasing the cross-section volume is impractical with the basic steel composition due to the steel being pushed beyond its limits of failure.

Improvements in the quality of steel can improve the resistance to shelling (subsurface shear), as can a fine grain structure. Also, it has been reported that a small amount of ferrite in a continuous network can work as a crack blunter. (42).

Heat treatment was a major improvement to rail steels, as was the modification of the composition, mainly through the addition of alloy and microalloying elements. Individually these changes in practice have resulted in major improvements in rail life by increasing the mechanical properties of the steels. Finer grain structures with finer interlamaller spacing such as show in Figure 9 have been achieved by lowering the pearlite transformation temperature. See Figure 10.

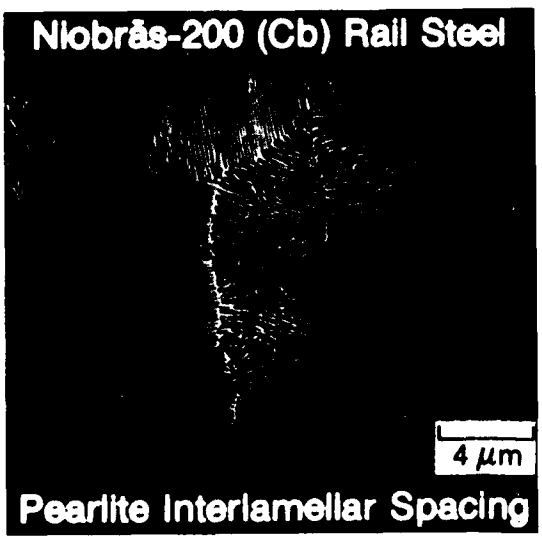


FIGURE 9

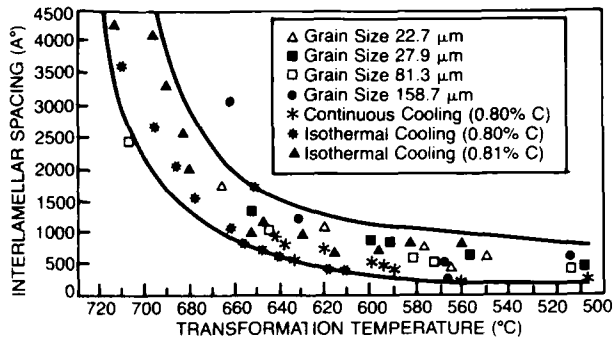


Figure 10. Transformation Temperature Effects on Interlamellar Spacing

While similar results could be achieved by controlled rolling, rail steel processing and rolling procedures make it impractical if not impossible.

Microalloying by itself does not appear to be the solution to rail steel requirements. It does provide major improvements in the presence of chrome as shown in Figure 11. However, some of the V steels reportedly require controlled cooling after heat treating to avoid martensite or bainite in the HAZ. Also, niobium solubility at the eutectoid carbon level is such as to be most beneficial as a precipitate in the ferrite lamellae. (43-44). With molybdenum, the microalloying elements must be maintained below a level that will produce unacceptable bainite or transition pearlite in the final microstructure.

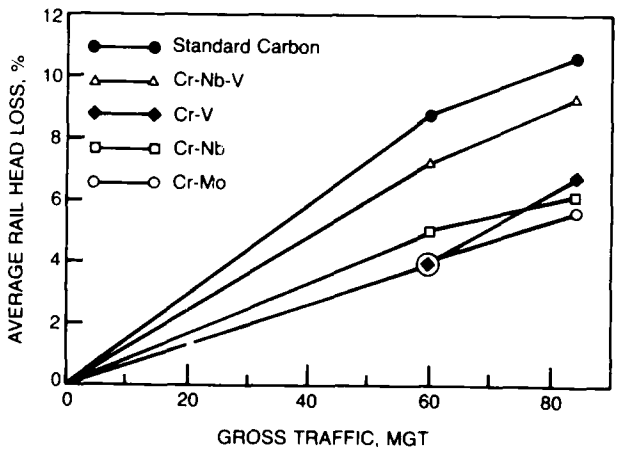


Figure 11. Wear Rates of Standard Carbon and Alloy Steel Rails on a Three-Degree (582 m Radius) Curve on the Mt. Newman Railway

## CONCLUSIONS

Reported research and field testing of niobium and vanadium microalloyed steels in the last few years is almost nil.

Chrome and molybdenym alloyed rail steels have some acceptance and have been in production.

The reduction in basic steel research and mill closings, including a number of rail mills, along with the downturn in the alloy industry, has resulted in the redirection of research and development into areas of more economic advantages.

Improved steel quality along with thermal treatment (full or head), appear to have taken the major share of the rail steel market to date.

From a development standpoint, the most interesting work in the last few years is a combination of microalloying and head hardening of a chrome rail steel, for maximum properties within the most severly stressed area of the rail. This steel has excellent potential for use on heavy haul trackage.

## REFERENCES


1. "Making and Shaping and Treating of Steel" United States Steel Corp., Pittsburgh, PA (1957) 7th Edition, 523-531.

2. G. G. Knupp, W. H. Chidley, J. L. Glove, H. H. Hartman, G. F. Morris, and C. W. Taylor, "A Review of the Manufacture, Processing and Use of Rail Steels in North America - A Report of AISI Technical Subcommittee on Rails and Accessories" ASTM Technical Publication No. 644, 1978, 7-20.

3. D. H. Stone and W. J. Harris Jr., "High Strength Steels for Rail Transportation", ASTM Technica Publications No. 644, 1978, 85-95.

4. Standard Specification for Carbon Steel Tee Rails ANSI/ASTM A1-76, 1978 Annual Book of ASTM Standards, Part 4, 1-6.

5. H. Krause and C. Schroelkamp, "Influence of Non-Metallic Inclusions on the Wear Behavior of Ferrous Materials in Nominally Dry Friction Systems", Wear 120 (3), 1987, 353-367.

6. V. I. Vorozhishchev, N. A. Fomin, M. S. Gordienki, "The Influence of Deoxidation and Modification on the Quality of Rail Steel", Stal' (1), 1987, 75-80.

7. Ibid, Ref. 3.

8. F. B. Fletcher, Y. E. Smith, V. A. Biss, "Fast-Welding Chromium-Molybdenum-Vanadium Extra-High Strength Rail Steels", Vanadium in Rail Steel Proceedings Conference, Chicago, ILL., Nov. 1979, )1980), 41-47.

9. H. Schmedders, "Use of Vanadium in High-Strength Rail Steels", Vanadium in Rail Steel Conference Proceedings, Chicago, ILL., Nov. 1979, (1980),

10. H. H. Cornell, "Improvement in Carbon Rail Steels by the Addition of Columbium (Niobium), Canadium Metallurgical Quarterly (22) (3), 347-351 (1983).

11. Ibid, Ref. 9.

12. T. Wada, K. Fukuda, "Effect of Rolling in Low Temperature Austenitic Region on Strength, Ductility and Toughness of Rail Steels", Journal Iron and Steel Institute of Japan (73), July 1987, 1162-1169.

13. Ibid, Ref. 8.

14. Y. E. Smith, F. B. Fletvher, "Alloy Steels for High Strength As-Rolled Rails, ASTM Technical Publication No. 644, 1978, 212-232.

15. V. D. Chervyakov, B. I. Tolychkanov, V. A. Palyanichka, A. V. Pan, G. S. Garheladze, "Melting Basic Oxygen Furnace Rail Steel From a Carbon Semi-Product With the Addition of Vanadium-Bearing Iron", Metallurgy, 1987 (2), 20-21.

16. M. Chen, J. Li, G. Chen, J. Ke, X. Wang, "The Effect of Residual Vanadium in Panzhihua Rail Steels", HSLA Steels Metallurgy and Applications, ASM International, 1986, 273-276.

17. G. K. Bouse, I. M. Bernstein, D. H. Stone, "Role of Alloying and Microstructure on the Strength and Toughness of Experimental Rail Steels", ASTM Technical Publication no. 644, 1978, 145-161.

18. D. E. Parsons, T. F. Malis, J. D. Boyd, "Microalloying and Precipitation in Cr-V Rail Steels", HSLA Steels and Technology and Applications, ASM International 1984, 1124-1135.

19. A. B. Dobuzhskaya, E. L. Kolosova, V. I. Syreishchikova, A. V. Velikanov, L. P. Shcherbakova, "Effect of Microalloying on the Impact Strength of Rail Steel", Fiz. Met. Metalloved, June 1985, 59, (6), 1228-1230.

20. A. M. Sage, W. Hodgson, D. H. Stone, "The Manufacture and Rail Trials With Chromium-Vanadium Steel for Heavy Duty Service", Vanadium in Rail Steels Proc. Conf, Chicago, IL, 1979, (1980) 12-22.

21. Ibid, Ref. 9.

22. "Chromium-Vanadium Rail Steels", Chromium Review, 1983 (1), 15.

23. A. W. Worth, "Special Rail Steels; The CN Experience", Railway Gaz. Int. Feb., 1985, 141, (2), 111-114.

24. J. Dilewwijns, L. Schetky, A. M. Sage, "Development of Low Carbon Vanadium-Copper-Chromium Rail Steel of Improved Weldability for Curves and Points in European Railways", Vanadium in Rail Steels Proc. Conf., Chicago, IL, Nov. 1979 (1080) 48-60.

25. Ibid, Ref. 24.

26. Ibid, Ref. 22.

27. Ibid, Ref. 8.

28. C. A. Nolasco, E. Q. Oliveira, G. Leonardos, J. P. Bordignon, "Niobium in Si-Mn Rail Steels", Niobium 81, (1984), 1041-1060.

29. D. Kageyama, K. Sugino, H. Masumoto, "Development of Alloying Elements for the Improvement of Rail Weldability, Trans of ISIJ (22) 5, (1982) 148-149.

30. Ibid, Ref. 10.

31. H. Kageyama, K. Sugino, H. Masumoto, C. Urashima, "Effect of Microstructure on the Basic Properties Requested for Rail Steels", Trans. of the ISIJ (22), 5, 1982, 147.

32. Ibid, Ref. 8.

33. D. E. Parsons, D. A. Munro, J. Ng-Yelim, "Vanadium/Nitrogen Modification of 1% Cr and Cr-Cb Rail Steels", Canadian Metallurgical Quarterly (22) (4), 1983, 475-483.

34. D. H. Stone, "Rail Practices in Russia; What US Group Found", Railway Track and Structures (72), 9, Sept. 1976, 20-22.

35. W. R. Callendar, K. J. Sawley, R. Brook, Europe Patent 0136004 July, 1984, 27.

36. J. G. Williams, I. D. Simpson, J. K. MacDonald, "Niobium in Rail Steels", Niobium 81, (1984) 1019-1039.

37. T. Wade, K. Fukuda, T. Kitada, "Effect of Controlled Rolling and Si, Nb additions on Ductility and Toughness of Eutectoid Steel", Trans. of the ISIJ (26), 1986, 109.

38. Ibid, Ref. 12.

39. I. Wade, K. Fukuda, T. Taira, "The Effect of Rolling Condition and Alloy Additions on Strength and Ductility of Eutectoid Steel", Trans. of the ISIJ (24), 1984, 277.

40. H. Kageyama, H. Masumoto, US Patent 4426236, May 12, 1978.

41. K. Sugino, H. Kageyama, H. Masumoto, "Development of Weldable High Strength Steel Rails", Second International Heavy Haul Rail Conf. Sept. 1982,

42. Ibid, Ref. 5.

43. H. D. Fricke, "Thermite Welding of Chromium-Vanadium Rail Steel", Vandium in Rail Steels Proc. Conf. Chicago, IL Nov. 1979, (1980) 63-69.

44. E. E. Laufer, D. M. Fegredo, "A Quantitative Electron Microscopic Examination of Nb and V (C,N) Precipitates in Eutectoid, Premium Rail Steels Transformed under Various Conditions", Canadian Metallurgical Quarterly (22) 2 (1983) 193-203.

# MICROALLOYED LOW CARBON Cb-B STEEL FOR HIGH STRENGTH BOLTS WITHOUT HEAT TREATMENT

**Gabor Jeszensky, Gilberto S. Gonzales, Sérvio R. M. Passos**
Siderúrgica N.S. Aparecida S.A.
Sorocaba, São Paulo, Brazil

**Rubens Cioto**
Matalac Indústria E Comércio S.A.
Sorocaba, São Paulo, Brazil

## INTRODUCTION

The high grade of process simplification inerent to the development of microalloyed steels for bolt making has been explored by many researches departaments in metalworking industries. The main task nowaday is to outline all factors concerned with cost reduction and quality reliability to be search from this technologycal innovation.

Bolts with high tensile strength that supersedes 800N/mm$^2$, as specified by ISO 898 and DIN 267 standards, can be produced by introducing of microalloyed steels. The microstructure of the wire rod in this material has a fundamental role in achieving the desired strength. Dual-phase bainitic structure is necessary to attend high strength levels. Low carbon microalloyed steel with boron and columbium is indicated for easier achieving these requirements.

In view of this subject, the Siderúrgica Nossa Senhora Aparecida, traditional special steelmaker in Brazil and Metalac, high technologycal Boltmanufacturer, are engaged together in the development of bolts class ISO 9.8, from a base composition of low carbon-manganese steel microalloyed with boron and columbium. The subject matter of this report is to stablish the main parameters related with microalloyed steel bolt manufacturing and to evaluate their mechanical properties, taking as reference the conventional quenched and tempered bolts.

MICROALLOYED STEELS FOR COLD HEADING BOLTS - The mechanical properties of microalloyed steels usually are developed by controlled cooling of the wire rod at the final stage of rolling. The cooling conditions are adjusted to promote very fine particle precipitation during the decomposition of austenite (1,2).

To select the steel composition it is worth note that for low carbon grades the columbium is more efficient than vanadium to increase yield strength (3).

Many published papers (1,2,4 to 7) shown that the austeno-martensite bainitic structure is more adequate to develope high tensile strengths by cold working. The additions of boron plus columbium changes the continuous cooling curve of the low carbon-manganese steels in away of that they retard the ferrite-perlite transformation, promoting better conditions to get bainitic structure by controlled cooling, as shown in figure 1.

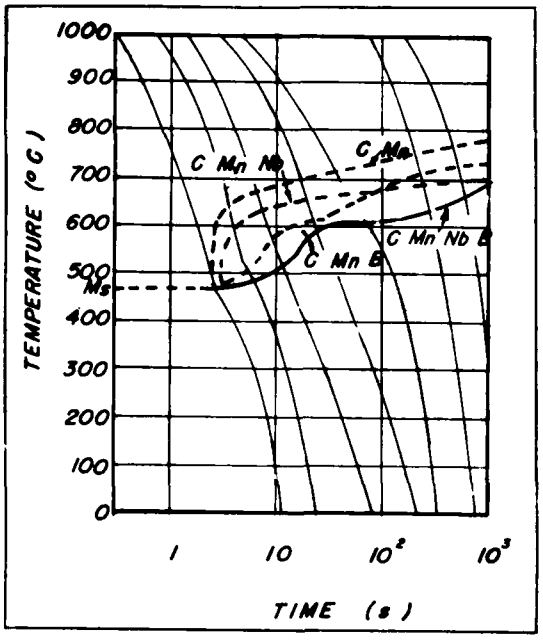


**Figure 1:** Continuous Cooling Transformation Diagram for Cb-B Microalloyed Steels after Ref. 1.

Usually, the desired microstructure is obtained directly from rolling, when controlled cooling is available at the finished rolling mill (1,4,6) Meanwhile, identical characteristics can be achieved by isotermal heat-treatment in continuous furnace.

Tensile Strengths of about 700-720N/$mm^2$ are required in wire rod to produce bolts with strength range from 900 to 1000 N/$mm^2$ by cold working without quenching and tempering final heat treatment (1,4, 6).

## EXPERIMENTAL PROCEDURES

PROCESS ROUTE FOR MANUFACTURING BOLTS CLASS ISO 9.8 FROM MICROALLOYED STEELS - The selected material (AP 15NB22) was a low carbon-manganese microalloyed steel with the following chemical composition:

| C | Mn | P | S | Cr |
|---|---|---|---|---|
| 0.19 | 1.62 | 0.019 | 0.017 | 0.10 |
| Al | Cb | B | $N_2$ | |
| 0.032 | 0.12 | 0.0012 | 0.0094 | |

The heat was melting in a eletric arc furnace of 25t, degassed in a VD system, and casting in ingots of 10t. The wire rod in roundness size of 1[illegible].49mm was produced from billets of 118mm square, in a looping mill with final speed of 5.8 m/s.

The wire rod was heat treated with isothermal cycle in a continuous furnace (austenitization temperature of 950°C followed by cooling in lead bath at 450°C).

The wire rod was drawing to size of Rd 10.9mm, coated with a zinc-phosphate layer of 9 up to 11g/$cm^2$. The bolts produced was the type DIN 912 with internal hexagonal cilindrical head ("Socket Head Cap Screws") using a progressive 4-stage cold heading machine, aiming tensile strength level from 900 up to 1000N/$mm^2$. Chemical oxidation was the final surface treatment. For comparison identical bolts of class ISO 10.9 were manufactured from quenched and tempered SAE 5135 steel at hardness level of 33 to 36 Rockwell C. In both cases the deformation process and the tools used were the same.

LABORACTORIES TESTING FOR EVALUATING THE WIRE ROD BEHAVIOR - First of all, the work-hardening curves was plotted to determine the workability of the material under progressive drawing reduction ratios.

In the same way, the Kf curve was plotted to know the material difficulty or ease in forming operations. This is required to manufacture a product from an unknow material. This can be compared with known materials using compressive

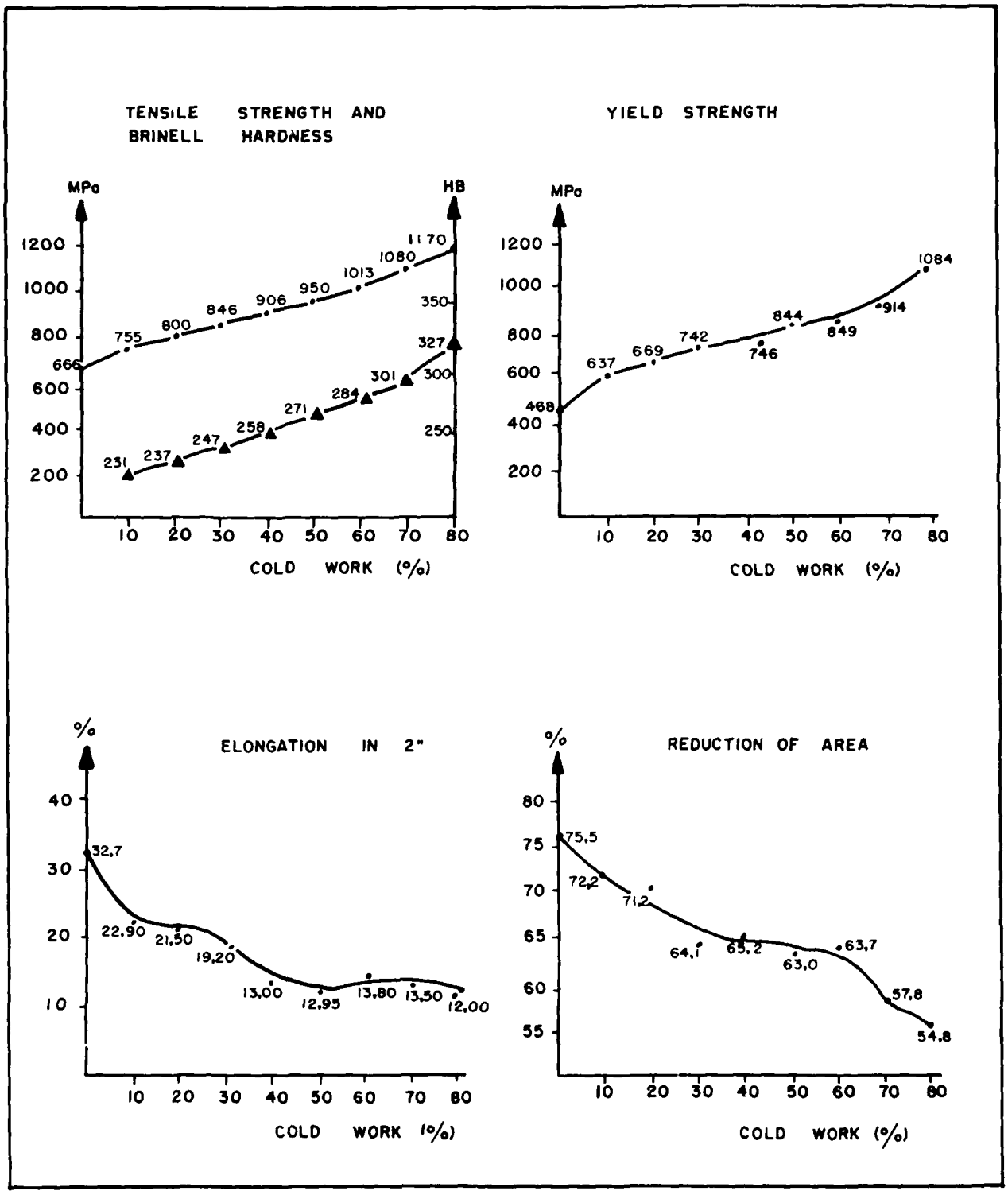


Figure 2: Work Hardening Curves by Wire Drawing for the AP 15NB22 Microalloyed Steel.

stress-strain curves and the manufacturing methods can be rank in the light of experience with known materials.

The microestructure was analysed by optical and scanning electron microscopy.

MECHANICAL TESTING FOR EVALUATING THE BOLTS PERFORMANCE

Tensile Tests - Tensile tests were carried out in the bolts in accordance with the norme ISO 898/I for measuring the tensile strength, yield stress, tensile strength under wedge, elongation, impact in the head. Brinell hardness was also measured.

Torque-Tension - Torque-tension relationships was plotted, using a 60KN maximum axial force machine and 200Nm maximum torque.

Fatique Tests - Fatique tests were performed in accordance with the norme ISO 3800/I aiming to plot wöhler curves. The applied stress function was the type tension-tension with median load of 23KN ($\sigma_m$ = 397N/mm$^2$), using five differents amplitudes, with a frequency of 100Hz. For each load it was used 5 specimens minimum.

## EXPERIMENTAL RESULTS AND DISCUSSION

WIRE ROD BEHAVIOR - The figure 2 shows the work hardening curves for the AP 15 NB22 steel. Tensile strength above than 900N/mm$^2$ are achieved with minimum reduction ratio of 40%. The material keeps high ductility even increasing the tensile strength at higher levels. This results agree with previous paper (1), using steel of similar composition. The wire rod has an austeno martensite bainitic structure as refered in the literature (Figure 3 and 4) (2).

The Kf curve of the wire rod is represented in figure 5. It is important

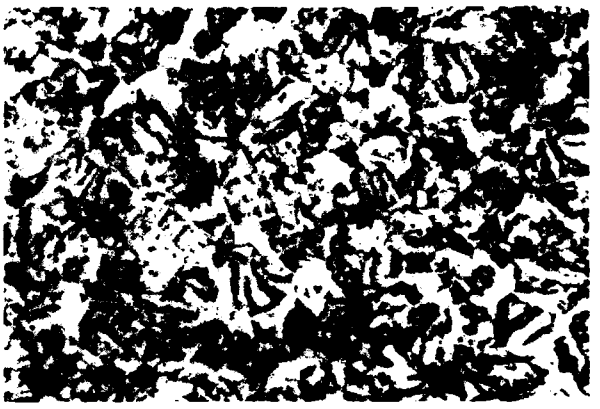

$HNO_3$ - 3% 1000 X

**Figure 3:** Optical Micrography Bainite Austeno-martensite in Wire Rod (Ø 13,49 mm = 17/32").

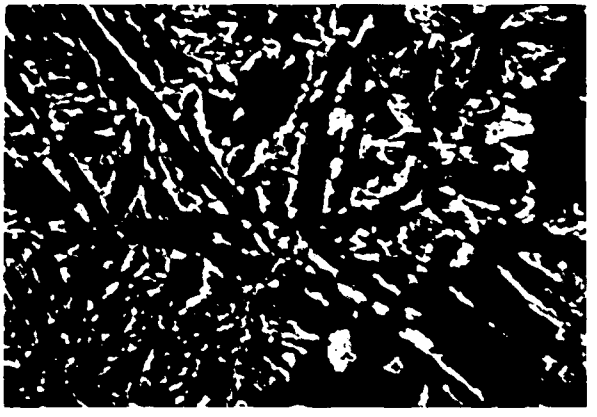

$HNO_3$ - 3% 1500 X

**Figure 4:** Scanning Micrography of Bainite Austeno-martensite in wire rod (Ø 13,49 mm = 17/32").

to consider that $Kf = a\varphi^n$ where $\varphi$ is the true strain;"a"is the stress strain for $\varphi = 1$; and n is the work hardening expoent. The work hardening expoent taken from this

curve is n = 0.135, then can be concluded that for the AP 15NB22 steel it is possible to achieve tensile strength levels higher than 900N/mm$^2$ from $\varphi$ higher than 0.83.

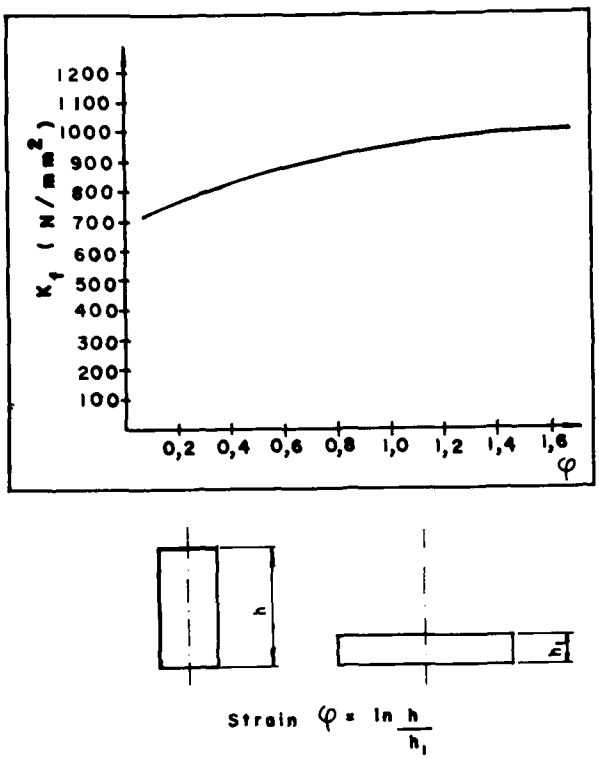


**Figure 5:** Microalloyed Steel AP 15NB22 - Characteristic Compression Test - Kf Curve.

BOLTS PERFORMANCE - The table 1 shows the results of tensile and hardness tests performed in accordance with the norme ISO I898/I and the figure 6 the macrograph aspect of the bolts. The figures 7 and 8 illustrate that the tensile strength and the tensile strength under wedge 6° have low scatter.

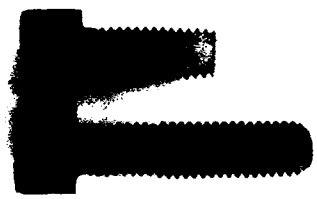

**Figure 6:** Macrograph Aspect of Bolts 9.8 AP 15NB22 Steel.

The data from table I point out that the microalloyed steel bolts attend the ISO standards class 9.8, as required for quenched and tempered steel bolts.

As shown in figure 9 the torque-tension relationships of microalloyed is at acceptable levels, although the mean and the scatter of torque coefficient are greater than usually found in quenched and tempered

**Table 1:** Mechanical Properties of Bolts as PER ISO 898/I.

| Mechanical Property | AP - 15NB22 | ISO class | | |
|---|---|---|---|---|
| | | 8.8 | 9.8 | 10.9 |
| Tensile Strenght $R_m$ ( N/mm$^2$ ) | 900 | 800 | 900 | 1040 |
| Brinell Hardness HB F = 30 D$^2$ | 255 . . . 285 | 219 . . . 285 | 242 . . . 319 | 295 . . . 363 |
| Stress at permanent set limit $R_p$ 0,2 ( N/mm$^2$ ) | 773 | 640 | 720 | 940 |
| Stress under proof load ( N/mm$^2$ ) | 650 | 580 | 650 | 830 |
| Head soudness | no fractured | no fracture | | |
| Nominal yeld stress / Nominal Tensile Strenght $\frac{R_p\,0,2}{R_m}$ | 0,86 | 0,80 | 0,80 | 0,90 |
| Elongation after fracture $A_5$ % min | 13,7 | 12 | 10 | 9 |

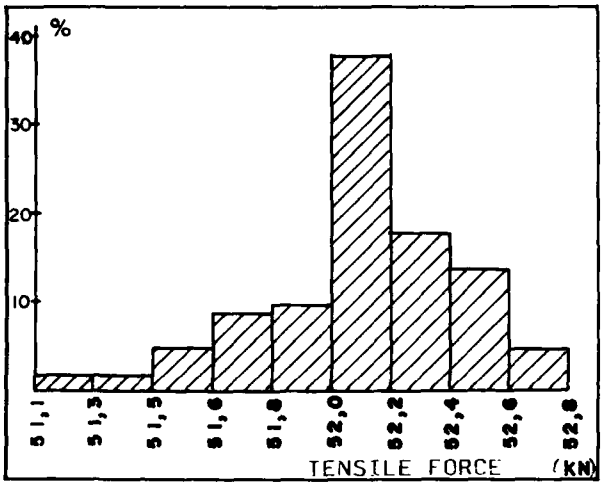


MEAN TENSILE FORCE (MTF): 52,2 KN
MTF + 3$\sigma$ = 53,1 KN
MTF - 3$\sigma$ = 51,2 KN

**Figure 7:** Distribution of Tensile Force for Bolts M10X1,5 - DIN 912 - AP 15NB22 Steel.

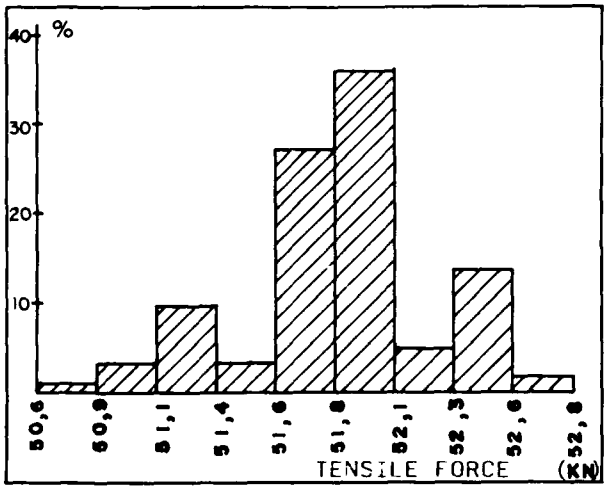


MEAN TENSILE FORCE (MTF): 51,9 KN
MTF + 3$\sigma$ = 53,0 KN
MTF - 3$\sigma$ = 50,7 KN

**Figure 8:** Distribution of Tensile Force Under Wedge 6°. for Bolts M10 X 1,5 - DIN 912 - AP 15NB22 Steel.

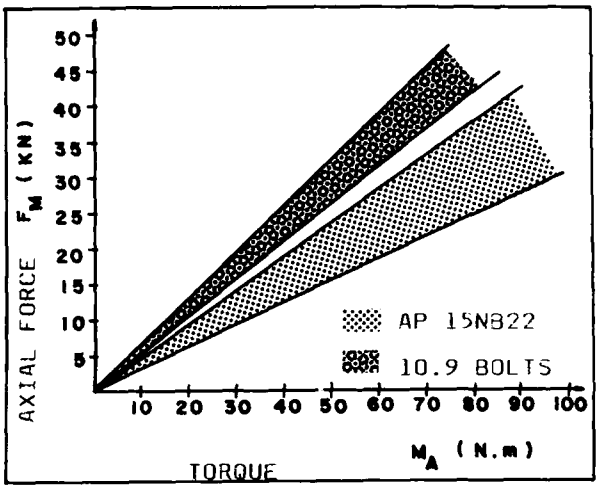


TEST CONDITIONS
BEARING SURFACE: HARDENED PLATE (40HRC)
FINISHED SURFACE: $R_z$ = 10um
FREQUENCY: 2 RPM

**Figure 9:** Torque Tension Relationship for Bolts M10X1.5 DIN 912 - Black Oxide Surface Treatment.

bolts. From this results can be concluded that in this case it is necessary higher momentum when tight system controlled by Torque is used. For modern tight system, controlled by angle, this aspect is not important.

The results of fatigue tests are illustrated in figure 10. The behavior of microalloyed bolts was better, even taking into account that the mean load (23 KN) used in both cases was more favorable for the 10.9 bolts that have higher yield point.

The curves show the endurance limite for microalloyed bolts achieve the amplitude of $\pm$ 84N/mm$^2$ for $10^7$ cycles while for the 10.9, in the same contition, achieve $\pm$ 52N/mm$^2$.

This conditions have been attributed to the effect of cold working that results in a residual compression stress in the root of the thread. The figure 11 shows the fiber texture that is preserved due

the absence of final heat treatment.

## CONCLUSIONS

The results of the performed tests show that it is possible to use microalloyed steels in the manufacturing of the socket head cap screws for the class ISO 9.8. Although the tools life was not evaluated it can be concluded by the work hardening curve that the behavior of this steel will be similar to the quenched and tempered bolts. Using the same argument, the production of bolts class ISO 10.9 will be possible, since the applied true strain achieve $\varphi = 1.3$.

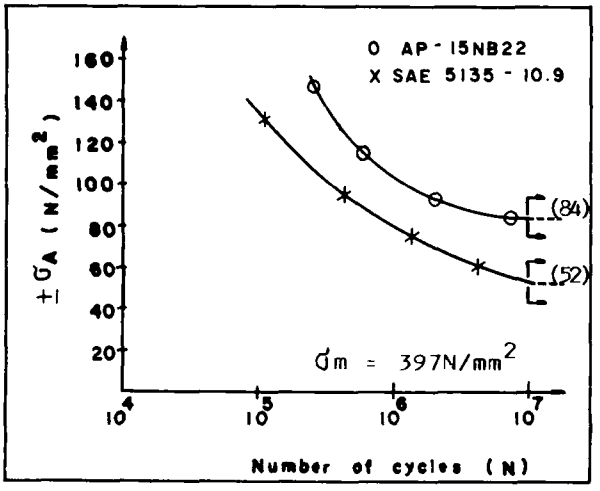


TEST CONDITIONS
TENSION-TENSION WITH LOAD $\sigma m \pm \sigma A$
LOAD FREQUENCY: 100Hz-HIDRAULIC MACHINE

**Figure 10:** Wöhler Diagram Relationship for Bolts M10x1.5 - DIN 912, Microalloyed AP 15NB22 Steel and 10.9 Quenched and Tempered.

**Figure 11:** Fiber Texture at the Root of the Thread in Bolts 9.8 - AP 15NB22 Steel.

## REFERENCES


1. Héritier B., Rofes-Vernis J, Wyckaert A. et Maitrepierre Ph, HSLA Steels Technology & Applications, Conference Proceedings, 3-6 October 1983, Philadelphia, Pensilvania, p. 981-989.
2. Backer L., Charlier P. et Hechelski R, Publication Métasafe: Les Aciers de Construction à Dispersoides, Juillet 1982.
3. Held J. F., Metal Progress, Dec. 1985, p. 17-23.
4. Héritier B, Rofes-Vernis J. et Maitrepierre Ph, Aciers Speciaux, 68, Nov. 1984, p. 5-10.
5. Serin B., Decalos Y, Maitrepierre Ph et Rofes-Vernis J, Mem. Scient. Revue de Metallurgie - Juin 1978, p.355-369.
6. Rofes -Vernis T., Heretier B., Maitre pierre Ph. Wychaërt A., Revue de Metallurgie, Nov. 1983, p. 879-885.
7. Rigant G., Tassis S., Wire Journal Internacional, v.18 (8), Aug. 1985, p. 34-42.

# DEVELOPMENT OF A MICROALLOYED JOINT BAR

**B. L. Bramfitt, S. S. Hansen**
Research Department
Bethlehem Steel Corporation
Bethlehem, Pennsylvania 18016 USA

**D. P. Wirick**
Steelton Plant
Bethlehem Steel Corporation
Steelton, Pennsylvania 17113 USA

**W. B. Collins**
Allegheny Rail Products Co.
Pittsburgh, Pennsylvania, USA

ABSTRACT

One of the important products supplied to the railways is a joint bar that is used to bolt the ends of two rails together. For over seven decades the American Railway Engineering Association (AREA) has specified a C-Mn steel (0.35 to 0.60% C and 1.20% Mn max.) that is rolled to section and then heat treated. The heat treatment, which consists of an austenitization and oil quench, is aimed at developing a ferrite/pearlite microstructure with a yield strength above 70 ksi, a tensile strength above 100 ksi, as well as adequate tensile and bend ductility. In order to provide a lower-cost product with mechanical properties at least equivalent to the current quenched product, we initiated work to develop an as-rolled microalloyed joint bar. A small laboratory program was conducted to develop the composition best suited to the thermomechanical treatment available on the 20" mill at the Steelton Plant. This study showed that a C-Mn-V-N grade could be hot-rolled to develop the desired mechanical properties. Subsequent mill trials demonstrated that similar results could be obtained consistently in the production environment. Testing of rail assemblies incorporating the new microalloyed joint bar is now in progress and, if successful, should provide more widespread application of this new technology.

JOINT BAR IS USED BY RAILWAYS to join the ends of two rails together (Figure 1), and provides both structural and electrical conductivity for the rail system. For over 75 years, either an as-rolled or oil-quenched C-Mn steel has been used for this application [1-3]. The current American Railway Engineering Association (AREA) specifications require a minimum carbon content of 0.45% for an as-rolled joint bar, and mandate a minimum tensile strength of 85 ksi and 15% total elongation for this product. For the oil-quenched joint bar the specification requires a carbon content between 0.35% and 0.60%, and a manganese content less than 1.20%. AREA specifications for the heat treated product require a 70 ksi minimum yield strength, a 100 ksi minimum tensile strength, a 12% minimum total elongation, a 25% minimum reduction in area and no cracking in a 90° minimum bend test (all tests are longitudinal). Today, the oil-quenched joint bar is more widely used by the railways because of its higher strength and better toughness than the as-rolled joint bar [4]. The typical composition of quenched joint bar is 0.45% C and 0.60% Mn, and the product is usually silicon-aluminum killed. With this composition, the microstructure after quenching in oil is fine pearlite with some proeutectoid ferrite at the prior austenite grain boundaries. The rails to which the joint bar is attached are fully pearlitic.

In an effort to reduce manufacturing, and hence final product cost, it was decided to evaluate the feasibility of producing an as-rolled joint bar with properties equivalent to the current quenched joint bar. Such processing would, of course, eliminate the heat treatment operation. In order to develop an optimum property combination, it was felt to be necessary to look beyond current AREA compositional specifications and evaluate the benefits of lower carbon and higher manganese levels on properties, particularly ductility and notch toughness. Although there are no AREA specifications for toughness, the railways are becoming more concerned about the toughness of both joint bar and rail in general. Two approaches were undertaken: (1) to develop an as-rolled joint bar within the compositional limits of the AREA specifications, and (2) to develop a lower carbon, higher manganese composition with improved properties. Microalloying is required in both approaches to compensate for the loss in strength in going from the as-quenched condition to an as-rolled condition and, in the latter case, going to a lower carbon content.

Because of the thermomechanical processing cycle for joint bar production on Steelton's 20" mill, where finishing temperatures are typically in excess of 1800°F, vanadium was the microalloying element of choice. In addition, nitrogen levels were increased to the range of 150-200 ppm to increase the intensity of precipitation hardening by the precipitation of vanadium carbonitride [5,6] during air cooling of the joint bar after hot rolling.

The alloy development program involved: (1) simulating production hot rolling in the laboratory, and (2) conducting a mill trial of the optimum alloy developed in the laboratory simulation. The details of the program are described below.

## EXPERIMENTAL PROCEDURE

LABORATORY SIMULATION - 500 lb air-induction melted ingots of three different microalloyed compositions were produced for the laboratory simulation. The C-Mn-V-N compositions are listed in Table I. The composition MA1 represents the same carbon level as the current joint bar but with higher manganese (0.15% above the maximum allowed by AREA). The vanadium and nitrogen levels were 0.11% and 0.019%, respectively. Composition MA2 represents a carbon level near the low end of the AREA specification limit and a manganese near the high end of the specification limit. The vanadium and nitrogen contents were 0.16% and 0.018%, respectively. Composition MA3 represents a lower carbon, higher manganese version with both elements outside the AREA specification. The vanadium and nitrogen contents of this steel were 0.17% and 0.016%, respectively. In all cases, the vanadium and nitrogen levels were adjusted to provide the degree of precipitation strengthening required to compensate for any loss in yield and tensile strength due to adjustments in carbon and manganese (and hence a reduced pearlite volume fraction). While the vanadium and nitrogen levels should ensure complete solubility of vanadium nitride above 1900°F, aluminum nitride solubility also had to be considered [7]. Evaluation of the rolling practices on Steelton's 20" mill showed that there was significant variation in bloom reheating temperature, with temperatures as low as 2150°F being possible. At 2150°F, AlN precipitates should only be completely soluble in steel MA3. In contrast, in both MA1 and MA2, some AlN should remain undissolved at 2150°F, leaving only about 0.012% and 0.017% N, respectively, available for subsequent precipitation as V(C,N). Of course, higher reheat temperatures will increase the amount of dissolved nitrogen in both steels MA1 and MA2.

The 500 lb ingots were initially hot-rolled to 4" thick plates. These plates were then reheated to 2150°F for 4 hours (to simulate lowest possible commercial reheating temperature) and hot-rolled in 5 passes to 1.38" thick plate. Finishing temperatures ranged from 1840 to 1875°F followed by air cooling. The soaking and finishing temperatures were typical of those used in production. The 5-pass rolling schedule simulated the production rolling of the head of the joint bar, which has an average final thickness of 1.38". The 5 passes represented reductions of 20, 25, 16, 22 and 16%, respectively.

PRODUCTION ROLLING - After the results of the laboratory rollings had been evaluated and discussed, a 10-ton electric arc furnace heat was produced with a C-Mn-V-N composition listed in Table II. This composition was designed for an optimum combination of strength, ductility and toughness, and while it is generally similar to the low-carbon, high-manganese steel evaluated in the laboratory (experimental composition MA3), the carbon, manganese and silicon levels of the 10-ton heat are somewhat higher than those of experimental composition MA3. In addition, the vanadium content of the 10-ton heat was lower than the laboratory heat MA3 (0.13% vs. 0.17%).

The 10-ton ingot was broken down on Steelton's 44" mill to produce eight rectangular blooms 10" x 7-3/4" in the cross-section. The blooms were then reheated (average temperature of 2375°F) and rolled into 90'-long joint bar sections on Steelton's 20" mill. The finishing temperature of the eight microalloyed joint bar sections ranged from 1885 to 1970°F. The eight microalloyed blooms were hot-rolled in a production run of current C-Mn joint bar, and no changes in hot rolling practices were mandated for the microalloyed grade. The as-rolled C-Mn joint bar was finished at 1870 to 1995°F. Samples of the microalloyed and C-Mn joint bars were taken at the hot saw and tested and the results compared with those of the C-Mn product after subsequent heat treatment.

PRODUCTION HEAT TREATMENT - The current oil-quenched C-Mn joint bar is produced by hot-rolling the composition (typical) listed in Table II on the Steelton 20" mill. The as-rolled sections are then cut into lengths of approximately 36" to 39", and subsequently placed into an austenitizing furnace for 4 hrs at 1800°F. Upon removal from the furnace, holes and/or slots may be punched into the joint bar, depending upon customer requirements; some customers cold-drill the joint bar. The hot bars are also slightly reshaped to correct for any distortion from the austenitizing cycle, and then are quenched into hot oil (100 to 160°F) to develop the required mechanical properties.

MECHANICAL PROPERTY MEASUREMENT -

Testing - Two standard 0.505" diameter tensile specimens, 12 full size Charpy V-notch bars, and a 1/2" square x 8" long bend test were machined from each laboratory plate, from the head of a microalloyed joint bar representing the middle portion of each bloom, from the head of as-rolled C-Mn joint bar prior to heat treatment and from the head of the same bars after heat treatment. All samples were taken longitudinally, and tests were run according to standard test procedures approved by the AREA.

Metallographic Analysis - Metallographic specimens were machined from the laboratory plates and from the head of both microalloyed and oil-quenched joint bars. Specimens were also taken from the as-rolled C-Mn joint bar prior to the heat treating operation. Microstructures were examined and the percent pearlite measured in all cases.

## RESULTS

LABORATORY SIMULATIONS - The mechanical properties of the three experimental as-rolled C-Mn-V-N compositions are listed in Table III compared to AREA specifications for this product. Full Charpy curves for these steels are shown in Figure 2. The two lower carbon versions (MA2 and MA3) met the AREA minimum specifications whereas the normal carbon (0.45%), higher manganese (1.35%) version failed to meet the minimum total elongation, reduction in area and bend test requirements. The ductility and notch toughness of the 0.25% carbon, 1.40% manganese (code MA3) steel far exceeded those of the higher carbon steels.

The microstructures of the experimental C-Mn-V-N steels are shown in Figure 3. The steels are all ferrite/pearlite aggregates with the ferrite volume fraction increasing with decreasing carbon content (e.g., there is 10% ferrite in MA1, 28% ferrite in MA2 and 52% ferrite in MA3). This increase in ferrite content is felt to be largely responsible for the increase in ductility with decreasing carbon level. To meet the 30 ksi spread between yield and tensile strength for this product, a microstructure with about 50% pearlite is necessary.

In view of the good combination of properties in composition MA3, a mill trial was conducted with a slightly modified composition (lower V, higher Mn). The results of the mill trial are discussed in the following section.

PRODUCTION ROLLING - The mechanical properties of the microalloyed joint bar processed in the mill trial are listed in Table IV, along with properties of the current joint bar, in both the as-rolled and oil-quenched conditions. Full Charpy curves for these three conditions are shown in Figure 4. As can be seen, the microalloyed joint bar had a somewhat better combination of properties than the oil-quenched joint bar. The tensile ductility (%TE and %RA) of the microalloyed joint bar was higher than the oil-quenched joint bar, even at a higher yield strength. Further adjustments in composition (e.g. lower V and N contents) would reduce the yield strength to a level similar to the oil-quenched product with some concomitant improvement in ductility. The notch toughness levels of the microalloyed and oil-quenched joint bar are comparable with indications of a higher shelf energy for the microalloyed joint bar.

Typical microstructures for the microalloyed and C-Mn (as-rolled and oil-quenched conditions) joint bars are shown in Figure 5. Again, in all cases the structures are mixtures of ferrite and pearlite. The microalloyed joint bar contains 43% ferrite, whereas the oil-quenched C-Mn joint bar contains 15% ferrite, and the as-rolled C-Mn joint bar 10% ferrite.

## DISCUSSION

The results of this limited investigation demonstrate that the current oil-quenched C-Mn joint bar can be replaced with a lower carbon, higher manganese, microalloyed joint bar with comparable strength and somewhat improved tensile ductility and notch toughness. While the oil-quenched joint bar derives its properties primarily from a high volume fraction of fine pearlite, the microalloyed joint bar has a more balanced ferrite/pearlite structure. Instead, V(C,N) precipitation is used to offset the loss in strength resulting from a reduced pearlite volume fraction. The substitution of precipitation strengthening for strengthening by pearlite is responsible for the improved ductility and toughness of the microalloyed joint bar.

The advantages of substituting a microalloyed joint bar for an oil-quenched joint bar are: (1) improved property consistency, (2) potentially lower production costs, and (3) improved ductility/toughness. The better consistency is derived from the inherent consistency of an as-rolled product vs. an austenitized and oil-quenched product. The composition of the microalloyed joint bar has been designed to be relatively insensitive to normal day to day variations in hot rolling practices. For example, in the present trial, although finishing temperatures for the eight bars varied by about 100°F, there was little change in the properties from bar to bar. With heat treatment, there are more processing variables to control, such as austenitization time and temperature, transfer time expended between the austenitization furnace and the quench and the oil temperature heat-up during an extended operation. Consequently, from a production viewpoint, the processing of a microalloyed joint, requiring only normal hot rolling, should provide an inherently more consistent product.

The lower production costs derive from the elimination of a labor-intensive heat treating operation. However, eliminating the heat treating operation also makes it impossible to hot-punch holes/slots in the joint bar. Instead, holes/slots will have to be milled or drilled. Currently most producers of finished joint bars have the capability of drilling holes or milling slots at their facilities and, in many cases, routinely drill/mill cold joint bar.

The improved ductility/toughness of the microalloyed joint bar may also be useful to the railways. Neither joint bar nor rail has current toughness specifications. However, the railways have expressed some concerns about toughness of trackwork and may eventually implement toughness requirements. With an as-rolled, microalloyed joint bar, conceivably the composition could be further modified to obtain additional improvements in tensile ductility and

notch toughness. On the other hand, the current oil-quenched joint bar needs the high volume fraction of pearlite to maintain the high strength levels required by AREA. However, the toughness of ferrite/pearlite steels is reduced as the volume fraction of pearlite increases [8]. This means that the current oil-quenched joint bar has little chance for an improved ductility/toughness combination, if present strength levels are to be maintained.

## SUMMARY

The current oil-quenched C-Mn joint bar can be replaced with an as-rolled microalloyed joint bar with an improved combination of properties. The microalloyed joint bar has the advantage of (1) improved property consistency, (2) lower production costs, and (3) improved tensile ductility and notch toughness. With the future trends to upgrade the properties and quality of trackwork economically, a microalloyed joint bar may eventually replace the current joint bar because of these advantages.

## ACKNOWLEDGMENTS

The authors wish to thank John Burkit for his intensive involvement in the laboratory simulation and mill trial. Thanks also go to Charles Wagner, James Petroff, and James Maglich for assisting with the mill trial.

## REFERENCES

(1) American Railway Engineering Association Bulletin, Vol. 16, 1915, p. 403.
(2) American Railway Engineering Association, "Specifications for High-Carbon-Steel Joint Bars," 1969.
(3) American Railway Engineering Association, "Specifications for Quenched Carbon-Steel Joint Bars," 1969.
(4) S. L. Hoyt, "Static Dynamic and Notch Toughness,", Trans. AIME, vol. 57, 1920, p. 480.
(5) P. S. Monckton, D. Whittaker and K. Sachs, Preprint from "Forging and Powder Metallurgy," International Congress on Metal Engineering, University of Aston, Birmingham, England (1981).
(6) M. Korchynsky, "Microalloyed High Carbon Wire Rod," 1986, Wire Association Meeting.
(7) K. J. Irvine, F. B. Pickering and T. Gladman, "Grain-Refined C-Mn Steels,", JISI, V, 1967, p. 161.
(8) F. B. Pickering, "The Optimization of Microstructures in Steel and Their Relationship to Mechanical Properties," in Hardenability Concepts with Application to Steel, D. V. Doane and J. S. Kirkaldy, editors, TMS-AIME, Warrendale, PA, 1978, p. 179.

Table I. Chemical Composition of Experimental Microalloyed Joint Bar

| Code | C | Mn | P | S | Si | V | Al | N | $N_{sol}$* |
|---|---|---|---|---|---|---|---|---|---|
| MA1 | 0.46 | 1.35 | 0.022 | 0.016 | 0.30 | 0.11 | 0.035 | 0.019 | 0.012 |
| MA2 | 0.38 | 1.18 | 0.010 | 0.008 | 0.25 | 0.16 | 0.017 | 0.018 | 0.017 |
| MA3 | 0.25 | 1.40 | 0.010 | 0.010 | 0.22 | 0.17 | 0.010 | 0.016 | 0.016 |

* Calculated amount of nitrogen in solution on reheating at 2150°F [7]

Table II. Chemical Composition of Production Joint Bar

| Code | C | Mn | P | S | Si | V | Al | N |
|---|---|---|---|---|---|---|---|---|
| Microalloyed | 0.27 | 1.65 | 0.021 | 0.020 | 0.32 | 0.13 | 0.022 | 0.017 |
| C-Mn | 0.50 | 0.92 | 0.023 | 0.014 | 0.23 | <0.003 | 0.018 | 0.009 |

Table III. Mechanical Properties of Experimental Microalloyed Joint Bar

| Code | Carbon, % | Yield Strength, ksi | Tensile Strength, ksi | Total Elongation % | Reduction in Area, % | 90° Bend Test | Charpy Energy @ RT ft-lb | 15 ft-lb Transition Temp., °F | Upper Shelf Energy ft-lb |
|---|---|---|---|---|---|---|---|---|---|
| MA1 | 0.46 | 90.7 | 135.8 | 11.8 | 23.7 | Failed | 8 | 175 | 35 |
| MA2 | 0.38 | 91.1 | 132.2 | 14.5 | 36.5 | Passed | 8 | 150 | 44 |
| MA3 | 0.25 | 87.1 | 118.5 | 18.3 | 45.9 | Passed | 24 | 25 | 73 |
| AREA Specification | | 70 min | 100 min | 12% min | 25% min | Pass | - | - | - |

Table IV. Mechanical Properties of Production Joint Bar

| Code | Condition | Yield Strength, ksi | Tensile Strength, ksi | Total Elongation % | Reduction in Area, % | 90° Bend Test | Charpy Energy @ RT ft-lb | 15 ft-lb Transition Temp., °F | Upper Shelf Energy ft-lb |
|---|---|---|---|---|---|---|---|---|---|
| Microalloyed | as-rolled | 91.1 | 124.3 | 20.6 | 55.1 | passed | 20 | 50 | 70 |
| C-Mn | oil-quenched | 86.1 | 128.5 | 19.4 | 48.4 | passed | 20 | 45 | 53 |
| C-Mn | as-rolled | 58.4 | 113.6 | 18.9 | 38.3 | Passed | 7 | 155 | 39 |

For the microalloyed joint bar, the data represents the average of 8 rolled sections, and for the C-Mn bar the average of 2 sections.

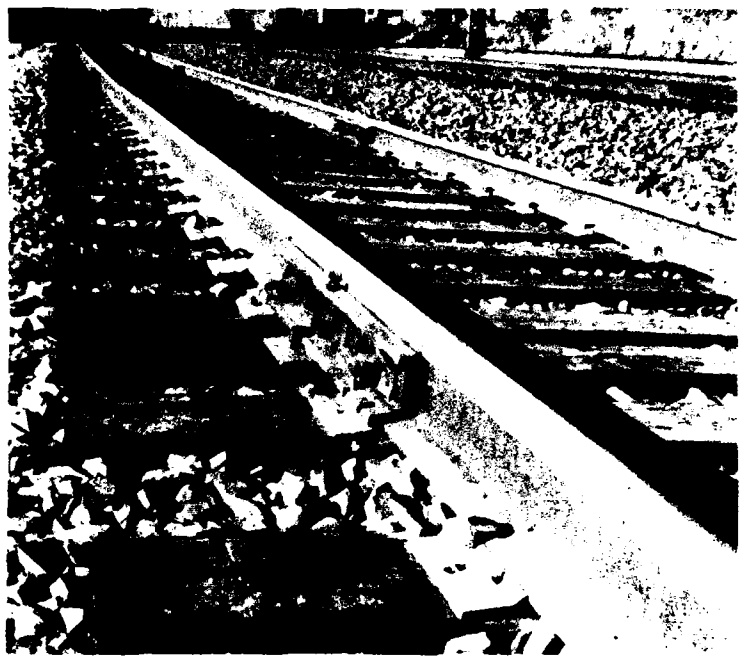

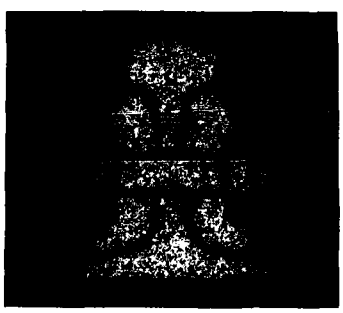

Figure 1.

Photo (above) shows placement of a joint bar on a railway track. Joint bar bolting arrangement is shown in cross-sectional view in diagram on the left.

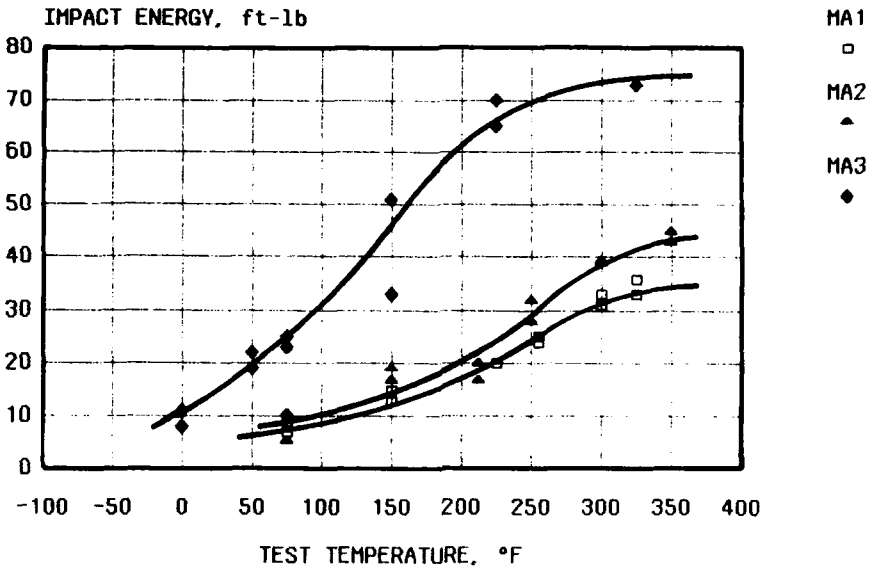


Figure 2. Charpy curves of experimental C-Mn-V-N alloys

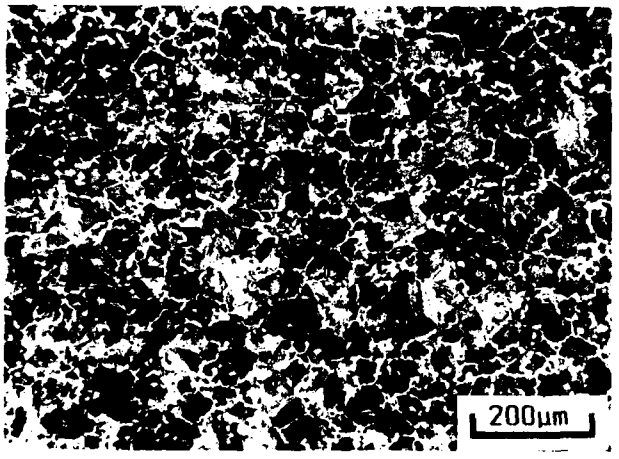


MA1

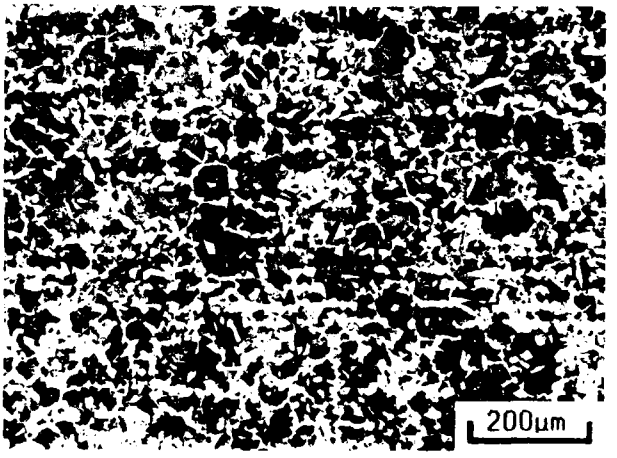


MA2

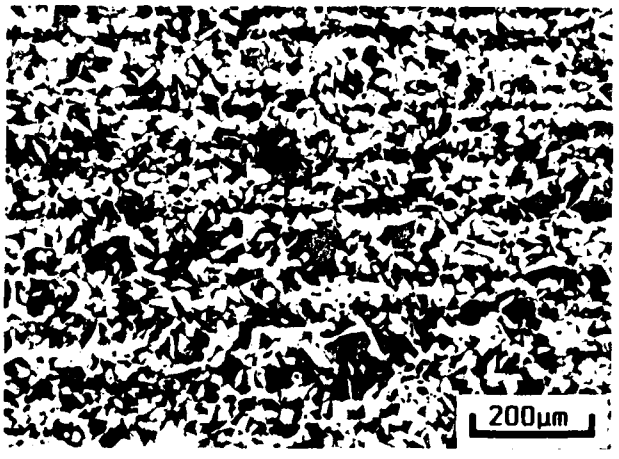


MA3

Figure 3. Microstructure of experimental C-Mn-V-N alloys. Picral etch.

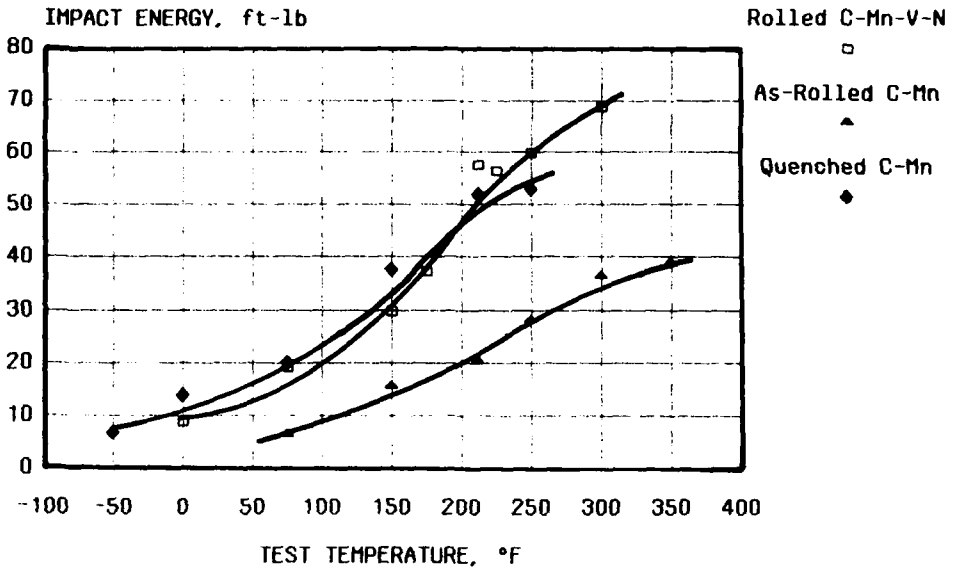


Figure 4. Charpy curves of production joint bar

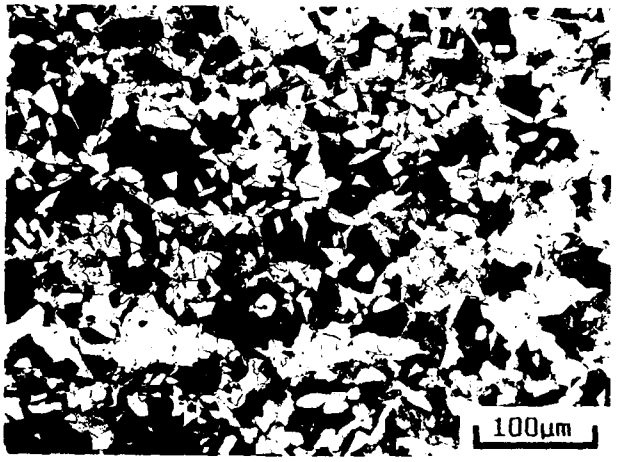


As-Rolled, C-Mn-V-N

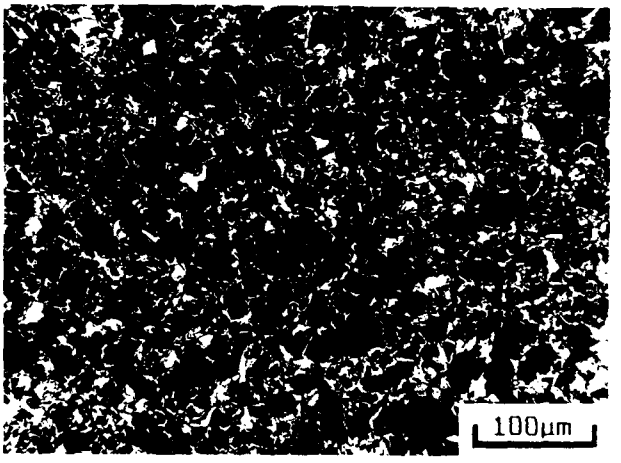


Quenched, C-Mn

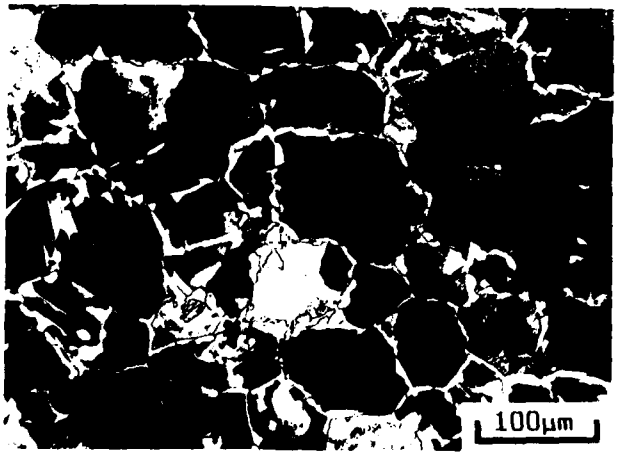


As-Rolled, C-Mn

Figure 5. Microstructure of production C-Mn-V-N and C-Mn joint bar. Picral etch.

# THE INFLUENCE OF VANADIUM AND COLUMBIUM ON THE INDUCTION HARDENABILITY OF STEEL

**Gregory A. Fett**
Dana Corporation
Ft. Wayne, Indiana, USA

**John F. Held**
LTV Steel Company
Massillon, Ohio, USA

ABSTRACT

Vanadium and columbium are commonly used in microalloyed steels to improve strength. These elements are also sometimes used as grain refiners in place of aluminum. This paper takes a look at the effect of these two elements on induction hardening. Several experimental heats were melted, rolled into bar, and induction hardened under constant parameters. The results indicate that both elements have a negative effect on induction hardenability, and that columbium has by far the greatest effect.

VANADIUM AND COLUMBIUM can be used in steels both as microalloying elements and as grain refiners. Vanadium is known to increase Jominy hardenability as can be seen by comparing 6100 series steels, containing vanadium, to 5100 series steels, without. However, the effect of these two elements on induction hardenability is relatively unknown. Compared to furnace hardening, the solution (austenitization) time for induction hardening is extremely short. The solution time for induction hardening is usually only a matter of seconds and in some cases may be only a fraction of a second. Since both vanadium and columbium readily combine with carbon, it was felt they may have a negative effect on induction hardening or induction hardenability.

To look at the effects of these elements, several laboratory heats were melted, hot rolled, machined, and induction hardened. The first series of heats is shown in figure 1. They are basically variants of SAE 1040, 1140, and 1137; some with vanadium, and some with columbium. These heats were rolled into 1.125" diameter bars and then turned down to a 1.000" diameter prior to induction hardening. Hardening was done on a ten kilocycle solid state induction unit with all conditions held constant except for the scan rate which was run at 30 sec./ft., 27 sec./ft., and 24 sec./ft. for each heat or group. The induction hardening results are shown in figure 2. The case depth on the diameter is measured in terms of effective case, which is depth below the surface to 40 RC; and total case, which is depth to 20 RC or the total visual heat affected zone if the core is 20 RC or harder. Looking at heats 167, 169 and 170 which all have the same chemistry except for vanadium and columbium, we can see that for constant induction hardening parameters .06 vanadium reduces the effective case depth by about 15 percent while .03 columbium reduces it by 35 percent.

Figure 3 shows the ideal diameter calculations for the heats based on the Grossman method. Manganese was adjusted in each case for sulphur. Since manganese combines with sulphur in a ratio of 1.7:1, 1.7 times the percent of sulphur was subtracted from the manganese and called the adjusted manganese. Also shown is the carbon content and the effective case for each heat at a scan rate of 30 sec./ft. Figure 4 shows a plot of the ideal diameter versus effective case depth. From this we can see that the heats with vanadium and columbium definitely have a lower case depth for the same ideal diameter, especially at deeper case depths. Of course, hardenability is also dependent on the carbon content, which is quite similar for many of these heats.

Figure 5 shows a second series of heats that were melted. All conditions were the same as the previous series except these heats were aluminum deoxidized, which is more typical of ingot cast fine grained practice, and there was an intermediate reheat during hot rolling. These heats are based on 1137 and 1141 with varying amounts of sulphur and vanadium. One heat also has .01 titanium and one has .11 aluminum. Again, figure 6 shows the adjusted manganese and ideal diameter, as well as the carbon content and other additions.

Figure 7 shows the ideal diameter versus effective case depth in graphical form. Unlike the previous series of heats, there does not appear to be a decrease in case depth or induction hardenability with vanadium. The heats with vanadium actually have better induction hardenability than those without. It appears .03-.04 aluminum counteracts the negative induction hardenability effect of vanadium. By increasing the aluminum beyond .03-.04 the induction hardenability increases further. For example, heat A401 with .11 aluminum had a deeper case depth for its ideal diameter than any other heat. However, the as rolled or air cooled hardness of this bar was also low compared to the other microalloyed bars. Too much aluminum may diminish the strengthening effect of the vanadium in the air cooled hot rolled condition.

From a more practical standpoint, three different trials of microalloyed steels were made into actual forgings and induction hardened. The component used was a front yoke shaft for a four wheel drive light truck which is shown in figure 8. Shown on the left of the figure is the forging which is normally made from SAE 1040 or 1137 steel and quench and tempered to 229-269 Brinell hardness. Essentially, the part is quench and tempered to strengthen the yoke ears. Next, the part is machined and the spline is rolled, which is shown in the center of figure 8. Finally the shaft portion, shown on the right of the figure, is induction hardened to provide the necessary torsional strength. It was hoped that by changing to a microalloyed steel, the part could be air cooled from the forging temperature to the desired hardness and the quench and the temper operation could be eliminated.

Three different grades of microalloyed steels were used for this forging. They are SAE 1141 with columbium, SAE 1541 with vanadium and SAE 1137 with vanadium. The compositions are shown in figure 9. All parts were forged between 2100-2350 F and still air cooled into the 229-269 BHN range, although the 1541 V was at the top end of the range or slightly over.

The 1141 Cb was induction hardened and tested first. With 1141 Cb the required case depth of .160" effective and .270" total was difficult to consistently obtain. Also, there was considerable variation in case depth from piece to piece. The outer case was martensite with ferrite and bainite at the grain boundaries rather than the normal all martensitic structure. This abnormal microstructure was something that had not shown up on the hot rolled bars before, probably because of the different thermal history. The grain size on the forgings was approximately ASTM #3 while that of the bars was approximately ASTM #8. Fully reversed torsional fatigue testing on these shafts gave results well below historic and the failure mode was intergranular. However, rehardening these shafts a second time brought the case depth and fatigue life into normal limits. Also, after rehardening the case was completely martensitic.

The 1137V shafts were forged and tested next. The 1137 V steel results were somewhat similar to the 1141 Cb except not to the same degree. The case depth did meet specification however, the case microstructure was still not completely martensitic. The fatigue life was within historic limits but at the low end.

The 1541 V results were considerably different. Case depths were more consistent. The case microstructures were fully martensitic, and the fatigue results were well within historic limits. Several differences exist between the 1541 V and the other two steels. First, the hardenability was higher. The ideal diameter of the 1541 V was 1.82" compared to 1.59" for the 1141 Cb and 1.37" for the 1137 V. Second, the 1541 V contained aluminum. And last, the 1541 V was not resulphurized.

As of this writing a fourth forging trial is underway with a grade of 1137 V with .087 aluminum. Like the previous steels, it did air cool into the 229-269 Brinell hardness range. In this forging, the aluminum did not appear to detract from the air cooled hardness. The yoke shafts have been machined and induction hardened. This time induction hardenability was greatly improved. The shafts were overcased when run on the same set up as the production parts. The power had to be reduced to bring the case depth back into range. However, when this was done the problem of ferrite and bainite at the prior austenite boundaries in the case showed up again (figure 10).

Several conclusions can be drawn from this data:

(1) Vanadium and columbium both reduce induction hardenability. However, columbium is much more potent in doing so. With a typical 1040 steel .06 vanadium reduces the hardenability about 15 percent while .03 columbium reduces it about 35 percent. The actual reduction on other steels will depend on the ideal diameter and the amount of vanadium or columbium.

(2) Aluminum in the amount of .03 or .04 percent appears to counteract the reduction in induction hardenability associated with vanadium. With this aluminum content this induction hardenability of steels containing vanadium is actually better than those with no vanadium. Further increases in aluminum can further improve the induction hardenability over normal steels. However, under specific rolling conditions or thermal histories high aluminum (.11) may reduce the strengthening effect of vanadium.

(3) With certain thermal histories such as in forging, vanadium or columbium steels can meet induction case depth and hardness specifications, but have inferior case microstructures. These microstructures may contain ferrite and bainite at the grain boundaries rather than all martensite. This has been shown to be detrimental to torsional fatigue life. It does appear the tendency to form these abnormal microstructures may be related to the ideal diameter and/or resulphurization.

| HEAT NO. | C | Mn | P | S | Si | Al | N | V | Cb | HB |
|---|---|---|---|---|---|---|---|---|---|---|
| A-160 | .38 | .84 | .015 | .023 | .23 | .002 | .008 | — | — | 187 |
| A-161 | .39 | .79 | .018 | .024 | .25 | .001 | .008 | — | — | 179 |
| A-162 | .43 | .77 | .018 | .024 | .25 | .001 | .008 | — | — | 192 |
| A-163 | .43 | .89 | .016 | .024 | .25 | .004 | .008 | — | — | 192 |
| A-164 | .35 | 1.47 | .016 | .10 | .28 | .002 | .009 | — | — | 197 |
| A-165 | .36 | 1.50 | .016 | .10 | .25 | .003 | .008 | .065 | — | 229 |
| A-166 | .39 | 1.48 | .015 | .10 | .25 | .004 | .008 | — | .031 | 217 |
| A-167 | .39 | .90 | .017 | .10 | .24 | .004 | .008 | — | — | 174 |
| A-168 | .38 | .90 | .014 | .10 | .25 | .003 | .009 | — | — | 167 |
| A-169 | .39 | .90 | .018 | .10 | .24 | .002 | .008 | .061 | — | 197 |
| A-170 | .40 | .91 | .018 | .10 | .25 | .004 | .009 | — | .031 | 192 |
| A-171 | .33 | .94 | .016 | .10 | .25 | .003 | .009 | .10 | — | 197 |
| A-172 | .38 | .78 | .017 | .071 | .23 | .004 | .009 | .090 | — | 201 |

FIG. 1 - Composition of Experimental Heats

| | SCAN RATE 30 SEC/FT | | SCAN RATE 27 SEC/FT | | SCAN RATE 24 SEC/FT | |
|---|---|---|---|---|---|---|
| HEAT NO | EFF/TOTAL | SURF/CORE | EFF/TOTAL | SURF/CORE | EFF/TOTAL | SURF/CORE |
| 160 | 204"/ 340" | 56 RC/22 RC | 163"/ 260" | 54 RC/22 RC | 131"/ 230" | 54 RC/12 RC |
| 161 | 184/ 310 | 54/25 | 163/ 270 | 54/20 | 133/ 220 | 54/8 |
| 162 | 205/ 310 | 56/26 | 183/ 290 | 56/24 | 147/ 220 | 55/10 |
| 163 | 231/ 360 | 56/27 | 200/ 300 | 56/24 | 158/ 230 | 56/9 |
| 164 | 273/THRU | 53/36 | 255/THRU | 53/32 | 206/ 330 | 53/13 |
| 165 | 247/THRU | 53/36 | 232/THRU | 53/34 | 197/ 340 | 53/19 |
| 166 | 235/THRU | 55/35 | 222/THRU | 55/34 | 192/ 380 | 55/19 |
| 167 | 192/ 310 | 54/24 | 166/ 290 | 55/18 | 147/ 220 | 54/6 |
| 168 | 165/ 300 | 54/22 | 152/ 260 | 54/18 | 134/ 220 | 53/6 |
| 169 | 167/ 280 | 54/23 | 139/ 280 | 54/21 | 126/ 250 | 54/12 |
| 170 | 126/ 240 | 54/24 | 105/ 240 | 54/23 | 108/ 210 | 54/11 |
| 171 | 147/ 300 | 52/23 | 112/ 260 | 51/19 | 111/ 210 | 51/9 |
| 172 | 154/ 300 | 54/24 | 138/ 260 | 54/22 | 115/ 200 | 54/12 |

FIG. 2 - Induction Case Depth and Hardness of Experimental Heats

| HEAT NO. | C | (1) ADJ MN | DI | (2) EFF CASE | ADDITIONS |
|---|---|---|---|---|---|
| A-160 | .38% | .80% | .82" | .204" | — |
| A-161 | .39 | .75 | .80 | .184 | — |
| A-162 | .43 | .73 | .83 | .205 | — |
| A-163 | .43 | .85 | .92 | .231 | — |
| A-164 | .35 | 1.30 | 1.21 | .273 | — |
| A-165 | .36 | 1.33 | 1.25 | .247 | V |
| A-166 | .39 | 1.31 | 1.27 | .235 | Cb |
| A-167 | .39 | .73 | .79 | .192 | — |
| A-168 | .38 | .73 | .78 | .165 | — |
| A-169 | .39 | .73 | .79 | .167 | V |
| A-170 | .40 | .74 | .81 | .126 | Cb |
| A-171 | .33 | .77 | .75 | .147 | V |
| A-172 | .38 | .66 | .72 | .154 | V |

(1) ADJ MN = MN-1.7(S)

(2) AT 30 SEC/FT SCAN RATE

FIG. 3 - Ideal Diameter of Experimental Heats

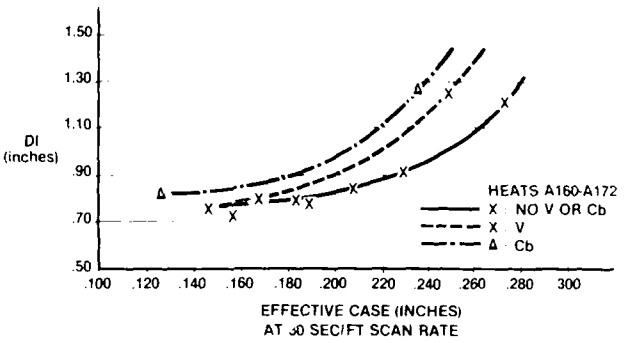


FIG. 4 - Effective Case Depth Versus Ideal Diameter for Experimental Heats

| HEAT NO. | C | Mn | P | S | Si | Al | N | V | Ti | HB |
|---|---|---|---|---|---|---|---|---|---|---|
| A-397 | .33 | 1.51 | .019 | .11 | .22 | .04 | .012 | .002 | — | 183 |
| A-398 | .34 | 1.47 | .019 | .11 | .23 | .04 | .012 | .080 | — | 187 |
| A-399 | .32 | 1.49 | .019 | .11 | .24 | .03 | .013 | .11 | — | 217 |
| A-400 | .33 | 1.48 | .020 | .11 | .23 | .03 | .012 | .082 | .012 | 201 |
| A-401 | .32 | 1.48 | .019 | .11 | .2[illegible] | .11 | .013 | .082 | — | 179 |
| A-402 | .35 | 1.34 | .019 | .028 | .20 | .03 | .012 | .074 | — | 201 |
| A-403 | .32 | 1.41 | .020 | .027 | .20 | .03 | .013 | .084 | — | 223 |
| A-404 | .37 | 1.50 | .020 | .11 | .25 | .03 | .013 | .041 | — | 217 |
| A-405 | .36 | 1.50 | .021 | .07 | .26 | .03 | .013 | .031 | — | 201 |
| A-406 | .38 | 1.62 | .020 | .11 | .26 | .03 | .013 | .11 | — | 235 |
| A-407 | .37 | 1.35 | .020 | .12 | .22 | .04 | .013 | .11 | — | 217 |
| A-408 | .37 | 1.42 | .019 | .11 | .22 | .03 | .012 | .11 | — | 223 |
| A-409 | .40 | 1.49 | .021 | .027 | .24 | .03 | .012 | .12 | — | 229 |
| A-410 | .39 | 1.35 | .020 | .027 | .22 | .03 | .012 | .041 | — | 217 |
| A-411 | .39 | 1.48 | .020 | .028 | .22 | .03 | .012 | .041 | — | 229 |

FIG. 5 - Composition of Experimental Heats

| HEAT NO. | C | (1) ADJ MN | DI | (2) EFF CASE | V | S |
|---|---|---|---|---|---|---|
| A-397 | .33% | 1.32 % | 1.16" | .210" | — | .11 |
| A-398 | .34 | 1.28 | 1.14 | .198 | .08 | .11 |
| A-399 | .32 | 1.30 | 1.13 | .200 | .11 | .11 |
| A-400 (3) | .33 | 1.29 | 1.14 | .204 | .08 | .11 |
| A-401 (4) | .32 | 1.29 | 1.12 | .255 | .08 | .11 |
| A-402 | .35 | 1.29 | 1.14 | .183 | .08 | .03 |
| A-403 | .32 | 1.36 | 1.17 | .183 | .08 | .03 |
| A-404 | .37 | 1.31 | 1.25 | .216 | .04 | .11 |
| A-405 | .36 | 1.38 | 1.31 | .360 | .04 | .07 |
| A-406 | .38 | 1.43 | 1.41 | .382 | .11 | .11 |
| A-407 | .37 | 1.16 | 1.15 | .198 | .11 | .11 |
| A-408 | .37 | 1.23 | 1.13 | .240 | .11 | .11 |
| A-409 | .40 | 1.44 | 1.43 | .380 | .11 | .03 |
| A-410 | .39 | 1.30 | 1.24 | .207 | .04 | .03 |
| A-411 | .39 | 1.43 | 1.40 | .300 | .04 | .03 |

(1) ADJ MN = MN-1.7(S)
(2) AT 30 SEC/FT SCAN RATE
(3) TITANIUM ADDED
(4) ALUMINUM ADDED

FIG. 6 - Ideal Diameter of Experimental Heats

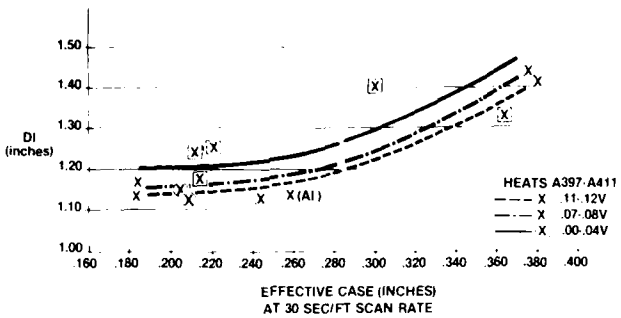


FIG. 7 - Effective Case Depth Versus Ideal Diameter for Experimental Heats

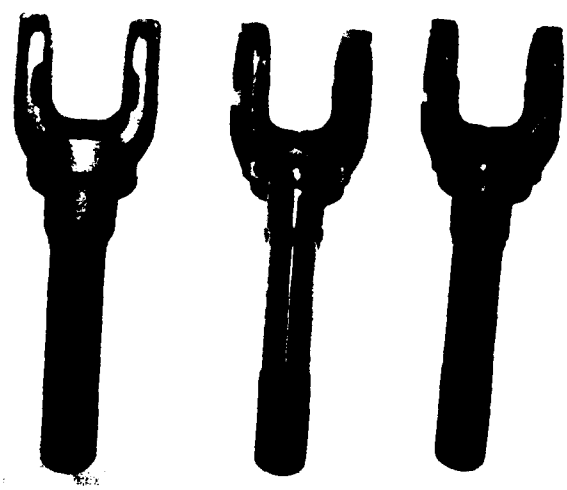

FIG. 8 - Front Yoke Shaft (Left to Right; Rough Forging, Machined Part, Induction Hardened Part)

| | 1141 Cb | 1541 V | 1137 V |
|---|---|---|---|
| C | .41 | .39 | .34 |
| Mn | 1.57 | 1.54 | 1.50 |
| P | .026 | .010 | .014 |
| S | .13 | .012 | .12 |
| Si | .22 | .21 | .19 |
| Ni | .02 | .04 | .03 |
| Cr | .07 | .08 | .07 |
| Mo | .008 | .008 | .013 |
| V | .00 | .09 | .08 |
| Cb | .05 | .00 | .00 |
| Cu | .017 | .022 | .018 |
| Al | .000 | .045 | .008 |
| DI | 1.59 | 1.82 | 1.37 |

FIG. 9 - Composition of Yoke Shaft Forgings

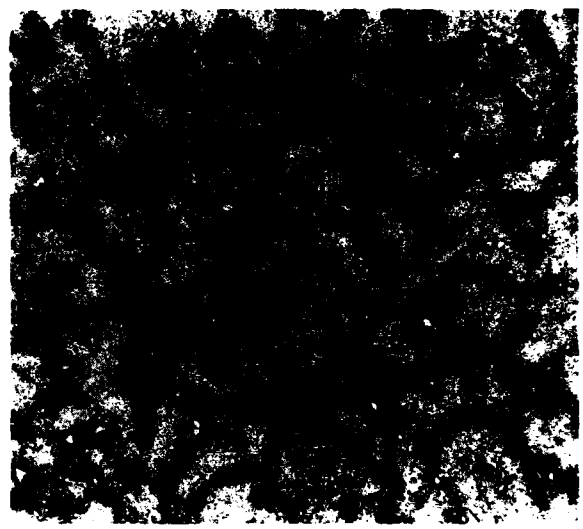

FIG. 10 - Induction Hardened Case Microstructure of 1137 V Yoke Shaft. Consists of Martensite with Ferrite and Bainite at the Prior Austenite Grain Boundaries (100X, Nital Etch)

# EFFECTS OF COMPOSITION AND HOT ROLLING CONDITIONS ON THE MECHANICAL PROPERTIES OF LOW CARBON BAINITIC STEELS

**O. Kwon, R. W. Chang**
Steel Products Department
Research Institute of Industrial Science and Technology
Pohang, Korea

**K. S. Ro, W. S. Lee**
Hot Rolling Department
Pohang Iron and Steel Company
Pohang, Korea

Abstract

The changes in microstructure and mechanical properties observed in low carbon bainitic steels were investigated under various alloying and hot rolling conditions. As carbon content was increased up to 0.05%, strength was increased but elongation and toughness were decreased. However, further increase in carbon content did not significantly affect the mechanical properties. The addition of 0.3% Mo resulted in a significantly increase in strength without deteriorating low temperature toughness. In contrast, the addition of 0.5% Cu had little influence on strength, but improved impact properties significantly. The combined addition of Mo with Cu or Ni resulted in an improvement in both strength and toughness. Little influence of reheating and finish rolling temperatures on strength was observed. But, toughness was slightly improved by decreasing the temperatures. A decrease in coiling temperature led to a little change in tensile strength. However, a significant improvement in low temperature toughness was observed as coiling temperature was lowered. The effect can be explained in terms of the microstructural refinement and the formation of ultra-fine polygonal ferrites.

Key Words; steels, microstructure, mechanical property, bainite, acicular ferrite, low carbon steel, hot coils, microalloying, hot rolling.

## 1. Introduction

Although the importance of bainitic steels with extra-low carbon had widely been recognized for the last 30 years, it was only recently that the steels found commercial applications. This was partly due to the difficulties in manufacturing steels of extra-low carbon content, i.e. 0.02%. However, the recent development in steel refining process using vacuum degassing with RH or RH-OB made it possible to manufacture steels with reduced carbon content commercially.

The advantage of the low carbon content was to improve low temperature toughness and weldability, resulting in the development of new grade high strength steels which can be used under severe environmental conditions. ULCB(Ultra-low carbon bainitic) steel of Nippon Steel corporation[1,2] and STAF steel of Nippon Kokan K.K.[3] are examples of the new steels. ULCB and STAF steels have found wide applications to oil industry for transporting oil and gas from arctic regions. These steels were alloyed with small amounts of Nb, Ti and B, and contained 1.0-2.0% Mn. Other alloying elements such as Mo, Ni, Cu and Cr were also added depending on the strength and toughness required.

However, most studies on low carbon bainitic steels have concentrated on heavy gage plates although the steels can be used as high strength strips with excellent toughness and weldability. The purpose of this

Table 1 Chemical composition of experimental steels.

(in weight %)

| Alloy | C | N | Si | Mn | Al | Nb | Ti | B | Mo | Ni | Cu |
|---|---|---|---|---|---|---|---|---|---|---|---|
| Alloy-A | 0.1 | 0.0014 | 0.22 | 1.41 | 0.0055 | 0.073 | 0.021 | 0.0008 | | | |
| Alloy-B | 0.05 | 0.0011 | 0.22 | 1.44 | 0.01 | 0.061 | 0.02 | 0.0006 | | | |
| Alloy-C | 0.018 | 0.0009 | 0.22 | 1.41 | 0.01 | 0.046 | 0.02 | 0.0009 | | | |
| Alloy-D | 0.0073 | 0.0014 | 0.22 | 1.44 | 0.0055 | 0.068 | 0.02 | 0.0007 | | | |
| Alloy-E | 0.019 | 0.0011 | 0.22 | 1.44 | 0.01 | 0.11 | 0.02 | 0.0009 | | | |
| Alloy-F | 0.022 | 0.0009 | 0.22 | 1.44 | 0.009 | 0.061 | 0.02 | 0.0011 | 0.34 | | |
| Alloy-G | 0.039 | 0.0023 | 0.15 | 1.47 | 0.024 | 0.066 | 0.024 | 0.0009 | | | 0.47 |
| Alloy-H | 0.035 | 0.0021 | 0.16 | 1.25 | 0.016 | 0.056 | 0.019 | 0.0009 | 0.28 | | 0.3 |
| Alloy-I | 0.023 | 0.0021 | 0.23 | 1.48 | 0.01 | 0.056 | 0.023 | 0.0006 | 0.32 | 0.34 | |

investigation was, by simulating the strip rolling process, to study the effects of alloy additions and processing parameters on the microstructure and mechanical properties of low carbon bainitic steels.

## 2. Experimental Procedures

The experimental steels were prepared by vacuum induction melting in 30Kg heats and casting in 110mm thick ingots. The chemical compositions of the steel are shown in Table 1. All steels were microalloyed with Ti, Nb and B. Varying amounts of C, Nb, Mo, Cu and Ni were added to study the effect of chemistry. Following casting, the ingots were forged to 50mm thick plates for hot rolling experiments. The plates were, then, hot rolled to 8mm thick sheets under various rolling conditions(see Fig.1). The reheating temperatures (RHT) employed were 1100 and 1250 °C, and the finish rolling temperatures (FT) were 750 and 820°C. To simulate coiling process, the hot rolled sheets were cooled to a desired coiling temperature(CT) of 500 or 600°C with a cooling rate of 15 °C/sec. and were isothermally treated at the temperature for one hour.

Mechanical properties were examined by tensile testing with subsize speimens(gage length = 25mm) and Charpy impact testing with 5mm thick sub-scale specimens. The microstructure was observed using both optical and transmission electron microscopes.

## 3. Results and Discussion

### 3.1 Effect of carbon content

Fig.2 shows the microstructures of low carbon bainite observed in transmission electron microscope. The microstructures are of typical low carbon bainite(Fig.2 a), which, according to Terazawa et.al.[3], consists of dislocation-loaded acicular ferrite and martensite island(M) formed along the grain boundary. The acicular ferrite was characterized by irregular, in some cases elongated, dislocation cells of about 0.5-1.0μm in size. Few dislocations existed inside the cells(Fig.2 b), but highly tangled dislocation networks existed along the cell boundaries(Fig.2 c).

The typical carbon content of ULCB steels ranged between 0.02 and 0.05%, much smaller than that of coventional ferrite-pearlite steels used for up to X-70 grade linepipes. The purpose of reducing carbon content was to improve weldability and low temperature toughness. In order to see the effect of carbon content, steels A, B, C and D were hot rolled under the identical condition and their mechanical properties were compared as shown in Fig.3. Tensile and yield strengths were increased and elongation was decreased steadily by increasing carbon content up to 0.05%. However, a further increase in carbon content did not exert appreciable effect on

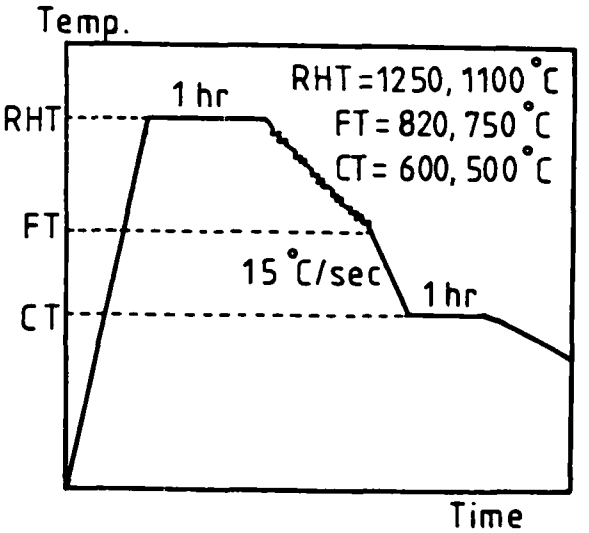


Fig.1 Schematic illustration of experimental hot rolling schedule.

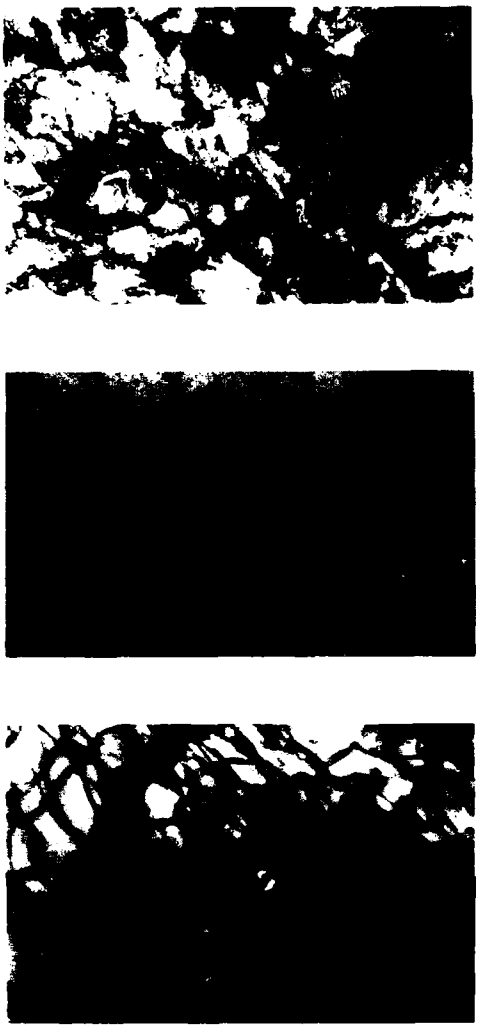

Fig.2 Transmission electron micro graphs of typical bainite structure at low(a) and high(b and c) magnifications.

both strength and elongation. It was also observed that impact properties were generally decreased by increasing carbon content although the change was relatively small in the carbon range of 0.02-0.05%. The present observation of carbon effect on mechanical properties appeared to be in agreement with the reported behavior in low carbon bainitic steel[1,4-7].

The effect of carbon content could be explained by observing the optical microstructures of four steels(A, B, C and D), which are shown in Fig.4. The results in Fig.4 indicated that the volume fraction of bainite was decreased as carbon content was increased more than 0.02%, resulting in the formation of polygonal ferrite at high carbon contents. Two opposing reactions took place when carbon content was increased; softening due to the reduction in the bainite volume fraction and strengthening due to the interstitial carbon. As a result, because of balancing between softening and hardening, little change in strength occurred when carbon content was increased higher than 0.05%. According to Tamehiro et.al.[6], the formation of ferrite was attributed to the loss of B by precipitating $Fe_{23}(CB)_6$ when excess carbon existed in the matrix.

### 3.2 Effect of alloy addition

The results of tensile and impact tests for steels with varying amounts of Nb, Mo, Cu and Ni are shown in Fig.5. The effect of increasing Nb content from 0.05 to 0.11% was a significant increase in strength without much loss in toughness. The addition of 0.3% Mo resulted in a

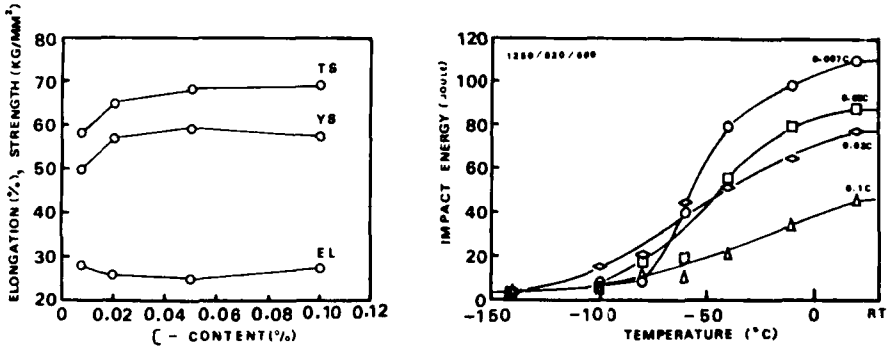


Fig.3 Effect of C-content on the mechanical properties of 1.5%Mn-0.05%Nb-0.02%Ti-0.001%B steel.

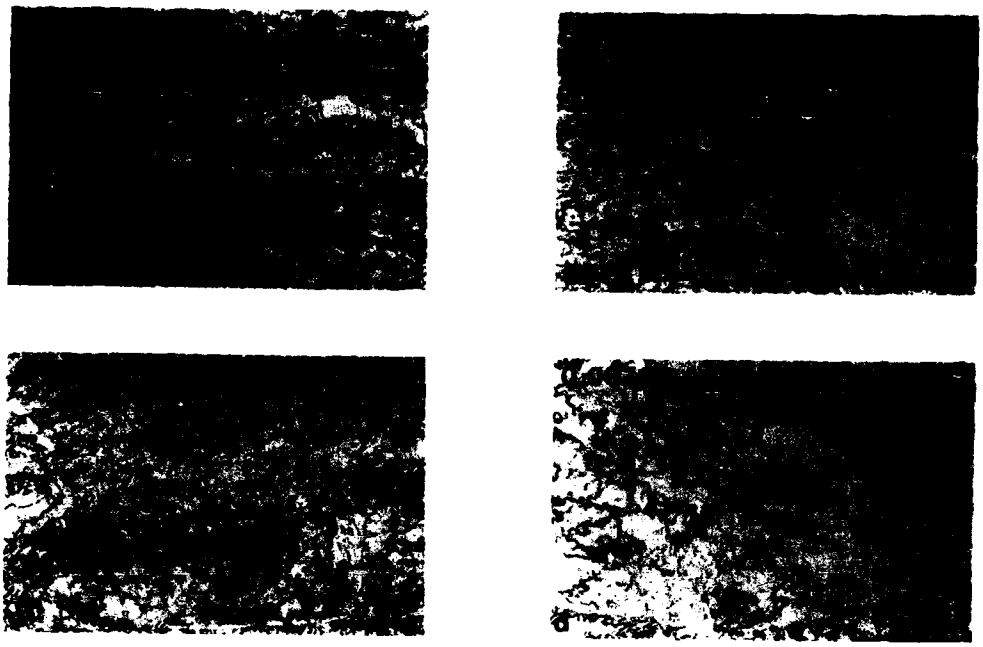

Fig.4 Optical micrographs showing the effect of carbon content.

significant increase in strength without impairing low temperature toughness. The addition of 0.5% Cu had little influence on strength, but improved low temperature toughness significantly. The combined addition of Cu or Ni with Mo(steels H or I, respectively) resulted in an improvement in both strength and toughness. Fig.6 shows the relationship between tensile strength and impact energy under various alloying conditions.

The typical content of Nb in high strength linepipe steels is 0.03-0.05%. Nb plays an important role in improving low temperature toughness by forming fine precipitates in austenite and, hence, retarding the progress of recrystallization. High Nb-content has been restricted because some Nb-precipitates remained undissolved in austenite after reheating. However, it would not be the case when C-content is extremely small, i.e. 0.02%.

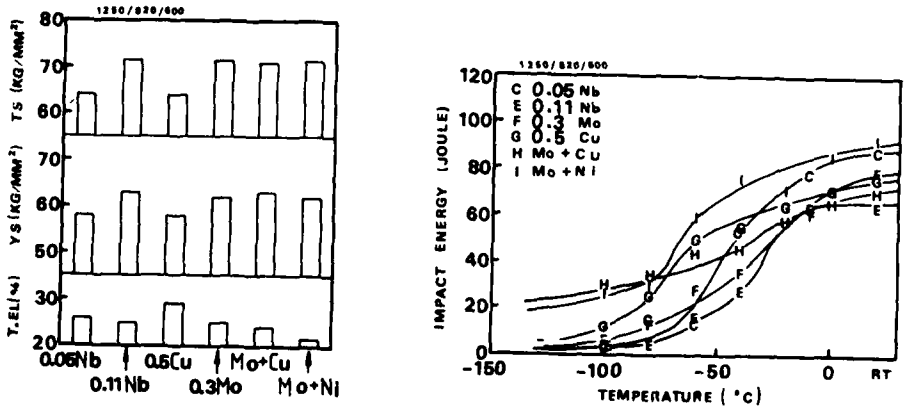


Fig.5 Effect of alloy additions on the mechanical properties of 0.02%C-1.5%Mn-0.05%Nb-0.02%Ti-0.001%B steel.

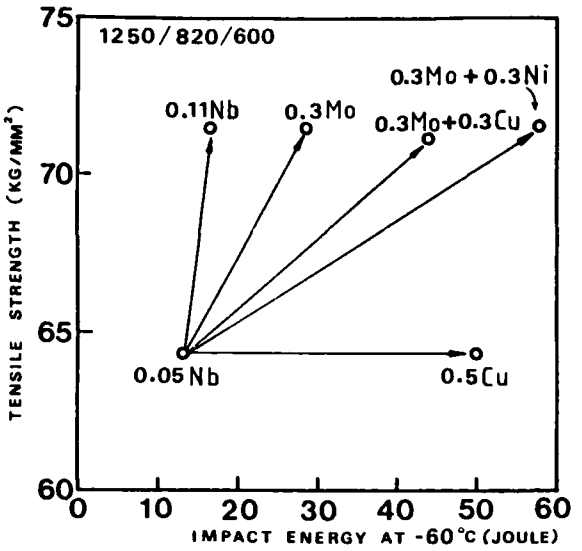


Fig.6 Relationship between tensile strength and Charpy impact energy under various alloying conditions.

Following the solubility relation of Irvine et.al.[8], the dissolution temperatures are 1339 and 1128 C for 0.11%Nb-0.005%N steels with 0.1 and 0.02% C, respectively. This indicates that all Nb-precipitates in the extra-low carbon steels will dissolve in austenite by heating at a temperature higher than 1128°C and the dissolved Nb can be fully utilized for improving the mechanical properties. The results in Fig.5. showed that increasing Nb-content from 0.05 to 0.11% was almost as effective as adding 0.3% Mo in strengthening. However, 0.11% Nb steel showed slightly inferior impact properties to 0.3% Mo steel.

Mo has been a popular alloying element used in low carbon bainitic steels[9-14]. In addition to the solution strengthening effect, Mo has been known to increase the period of incubation at the nose of the isothermal transformation diagram and to raise the temperature of the nose of the polygonal ferrite[10]. According to Bardgett and Reeve[9], strength of low carbon, boron containing steel was almost doubled by the addition of Mo up to 0.62%. In the present 0.3% Mo steel, both yield and tensile strengths were increased by 7 kg/mm² when compared with Mo-free steel without a loss in toughness. This indicates that, since the Mo-free steel satisfies the requirements of X-70 grade linepipes, the 0.3% Mo steel can be used as X-80 grade linepipes. It was also found that the low temperature impact properties of the Mo containing steel were improved significantly by adding Cu(steel H) and Ni(steel I). Therefore, these alloys are excellent candidate steels for X-80 grade linepipes of arctic service.

### 3.3 Effect of hot rolling condition

Fig.7 and Fig.8 show the effect of hot rolling variables on the mechanical properties of steels C and F, respectively. Eight different hot rolling conditions, which were the combinations of two RHT's(1250 and 1100 °C), two FT's(820 and 750°C) and two CT's(600 and 500°C), were employed to study the effect of processing variables. For impact properties, data obtained when RHT was 1250°C are shown in Fig.7 and Fig.8.

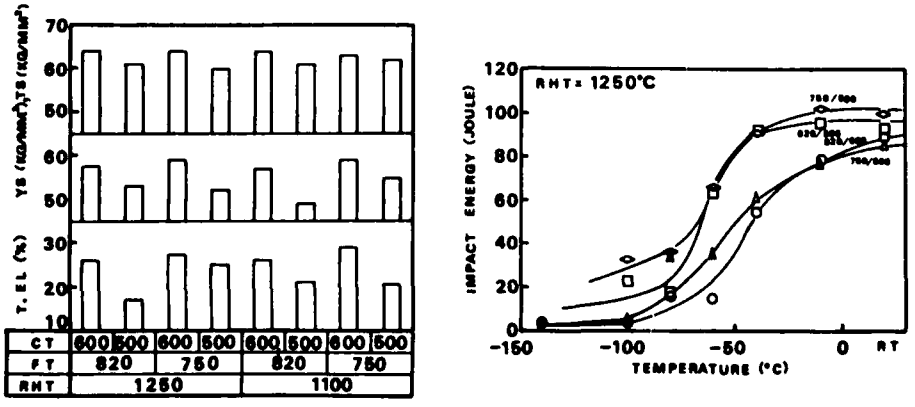


Fig.7 Effect of hot rolling conditions on the mechanical properties of steel C.

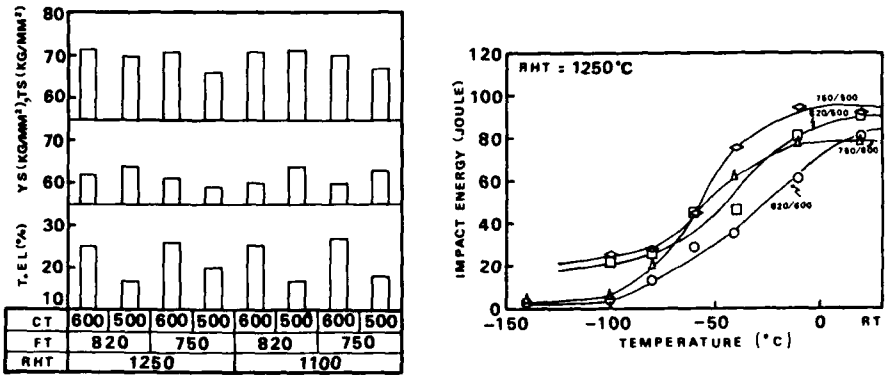


Fig.8 Effect of hot rolling conditions on the mechanical properties of steel F.

When RHT was lowered from 1250 to 1100 °C, strength did not seem to change significantly but toughness was slighly improved. This behavior appeared to be in agreement with the previous results of 0.02% C ULCB steels[1]. Two different structural changes could be cited when RHT was altered; austenite grain size and solute Nb in austenite. The slight improvement in toughness appeared to be attributed to the reduction in austenite grain size, and the change in strength was observed to be dependent on the amount of solute Nb. EDAX analysis of undissolved precipitates at two different RHT conditions showed that Nb was almost completely dissolved in the present steels. Therefore, little change in strength should be expected when RHT was altered. However, the data obtained in 0.046% C steel showed that strength abruptly decreased when RHT was lowered from 1200 to 1000 °C[6]. This follows from the fact that the amount of solute Nb rapidly decreased when the carbon content exceeded 0.04%.

The effect of FT on tensile and impact properties of C and F steels were similar to that of RHT; little change in tensile properties and slight improvement in impact properties when FT was changed from 820 to 750 °C. The difference in microstructures for two different FT conditions would be the effective retained strain energy in unrecrystallized austenite. Since the effective energy would be greater when FT was lower, the impact properties were expected to be improved. The previous investigations have already shown that increasing the total reduction below recrystallization temperature and, hence, increasing the effective energy exerted only slight effect on strength but improved low temperature toughness significantly[1,2,5,6,15,16].

The effect of CT on the mechanical properties was much greater than that of RHT or FT. CT did not have much effect on tensile strength, but had some influence on yield strength. In steel C, yield strength was slightly decreased when CT was changed from 600 to 500°C. This decrease was seen to be attributed to the disappearance of yield point elongation when CT was lowered. However, in steel F, a small increase in yield strength was observed when CT was decreased. Since both flow curves of steel F coiled at 600 and 500°C exhibited continuous yielding, the corresponding increase was thought to be due to the refinement of dislocation cell structure and the increase in dislocation density in low carbon bainite. An example is shown in Fig.9. The size of dislocation cell was smaller and the cell boundary was more diffuse when CT was 500 °C. Some dislocation-free polygonal ferrites with sharp grain boundaries were often observed. The size of ferrite grains, as shown in Fig.10, was 1-2 μm. The decrease in CT resulted in a sharp reduction in elongation, which may be attributed to higher dislocation density at 500°C. It was also observed that impact properties were significantly improved when CT was lowered from 600 to 500°C. Such an improvement has been explained in terms of fine grain size or bainite lath size[5,6,15,17]. But, Ohmori et.al.[18] argued that the size of the bunch of bainite laths which lay in almost same orientations, or the unit

crack path, was also important parameter determining low temperature toughness.

It has also been pointed out that the low temperature toughness of bainite steels was closely correlated with the facet size of cleavage fracture in the thickness direction [5,6]. The facet size has been known to be dependent on the prior austenite grain size and the effective retained strain after thermomechanical treatment. However, the present results of the CT effect on toughness suggested that the bainite lath size played a critical role in determining the impact properties. This follows from the fact that the main structural difference between steels treated at 500 and 600°C were the bainite lath size, not the prior austenite size or the effective strain energy. According to the recent report of Jizaimaru and Shirazawa[15], the toughness was almost independent of the bainite volume fraction. Instead, the toughness was a strong function of the presence of ultra fine polygonal ferrites of 1-2μm in size. The formation of ultra-fine ferrite was confirmed in the present study and has been shown in Fig.10.

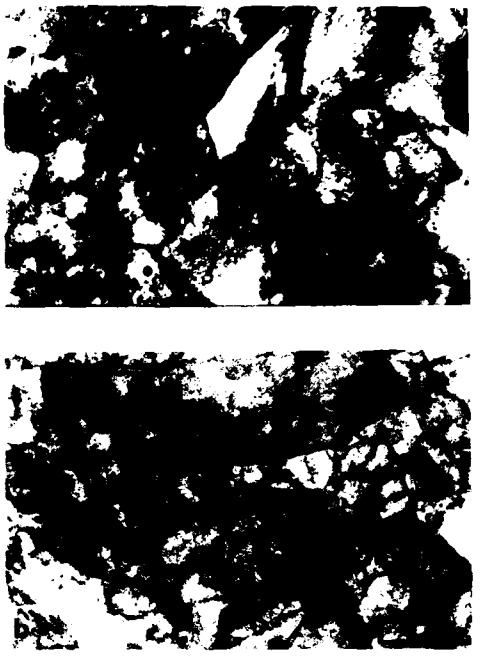

Fig.9 Typical dislocation cell structures of bainite observed in steels isothermally treated at (a) 600 and (b) 500°C.

Fig.10 Fine polygonal ferrites observed in the transmission electron microscope.

## 4.Conclusions

The effects of alloy additions and hot rolling variables on the mechanical properties of low carbon bainitic steels were studied in terms of structural changes occurring during processing. The following conclusions were obtained.

(1) The effect of carbon content up to 0.05% resulted in an increase in strength and a decrease in elongation and toughness. However, further increase in carbon content did not affect strength appreciably. This behavior resulted from the balancing effects of interstitial carbon and bainite volume fraction when the carbon content was varied.

(2) The addition of 0.3% Mo resulted in a significant increase in strength without deteriorating low temperature toughness. The addition of 0.5% Cu had little influence on strength, but improved impact properties significantly.

(3) The combined addition of Cu or Ni with Mo resulted in an improvement in both strength and toughness.

(4) When RHT and FT were lowered, tensile properties were not changed significantly but impact properties were slightly improved. The improvement in impact properties was attributed either to a reduction in austenite grain size or to an increase in retained strain energy in austenite.

(5) A decrease in CT led to a decrease in yield strength of Mo-free steel, but to a slight increase in yield strength of Mo-containing steel. In addition, the decrease in CT resulted in a sharp decrease in elongation and in a significant improvement in toughness. The latter effect can be explained in terms of the microstructural refinement.

## References


[1] H. Nakasugi, H. Matsuda and H. Tamehiro; "Alloys for the '80s", Climax Molybdenum Co, May, 1979, p213

[2] NKK Report, "Super Tough Acicular Ferrite Steel Line Pipe X-70", Sept., 1981

[3] T. Terazawa, H. Higashiyama and S. Sekino; "Toward Improved Ductility and Toughness", Kyoto, Japan, Oct. 1971, pp101-117

[4] T. Sawamura, T. Hashimoto Y. Komizo, Y. Yamaguchi and Y. Nakatsuka; Sumomoto Tech. Report, v37, 1984, pp57-70.

[5] M. Nikura, S. Yamamoto, C. Ouchi and I. Kozasu; Tetsu-to-Hagane, v70, 1984, pp1429-1436

[6] H. Tamehiro, M. Murata, R. Habu and M. Nagumo; Tetsu-to-Hagane, v72, 1986, pp466-473.

[7] H. Takechi, H, Matsuda, H. Tamehiro, M, Ohashi and H. Nagasugi; "Micon 82; Optimization of Processing, Properties and Service Performance through Microstructural Control", ASTM STP 792, 1982, pp149-171

[8] K.J. Irvine, F.B. Pickering and T. Gladman; JISI, v205, 1967, p161.

[9] W.E. Bandgett and L. Reeve; JISI, v63(1949), p277-294

[10] K.J. Irvine, F.B. Pickering, W.C. Hegelwood and M. Atkina; JISI, 1957, pp54-67

[11] K.J. Irvine and F.B. Pickering; JISI, Dec, 1957, pp292-309

[12] K.J. Irvine and F.B. Pickering; JISI, Feb.,1958, pp101-112

[13] A.J. McEvily, R.G. Davies, C.L. Magee and T.L. Johnston; "Transformation and Hardenability in Steels", Climax Molybdenum Co., Ann Arbor, Michigan, 1967, pp179-191

[14] A.J. McEvily and C.L. Magee; The Iron and Steel Institute Publication No.114, p147.

[15] J. Jizaimaru and H. Shirasawa; Tetsu-to-Hagane, v69, 1983, pp87-96

[16] K. Matsmoto, K. Akoa, T. Taira, M. Nikura and Y. Naganawa; Nippon Kokan Tech. Report No.46, 1986, pp35-43

[17] A.H. Cottrell; Trans. AIME, v212, 1958, p192.

[18] Y. Ohmori, H. Ohtani and T. Kunitake; Trans ISIJ, v12, 1972, p146.

# A SURVEY ON MICROSTRUCTURAL EVOLUTION OF TWO VANADIUM MICROALLOY STEELS IN THE THERMOMECHANICAL FORGING TREATMENT

**Carlos García, Manuel Carsí, Sebastián F. Medina, Miguel P. de Andrés**
Centro Nacional de Investigaciones Metalúrgicas
Madrid, España

ABSTRACT

Hot torsion testing is used to simulate the forging process of two vanadium microalloy steels, types 40MVS6 and 30MSiV62, having minimum strengths of the order of 900 and 800 MPa, respectively.

By establishing deformation parameters representative of the hot forging used for average automobile parts, the structural effects produced at different preheating and deformation temperatures are analyzed in order to attempt to obtain directly from the forging process an optimum final microstructure not requiring later heat treatment to attain the mechanical properties demanded in use.

---

THERE IS CURRENTLY A TENDENCY in the manufacturing of critical parts and components in the automobile industry to replace steel alloys for tempering, especially Cr and Cr-Mo steels, for C-Mn vanadium microalloy steels. This alternative is based on the lower manufacturing costs of these steels and on the possibility of their mechanical properties being obtained directly, via the shaping process itself. In this respect, this process should be analyzed as a real thermomechanical treatment in which application and definition of the corresponding controlled thermal and deformation cycles are capable of producing in the material thus shaped an optimum final structure permitting the expected mechanical characteristics to be obtained.

For several years microallyed steels have mainly been used in replacement for non-alloyed or low alloy, low resistance, thermally treated steels; however, the greatest potential for cost reduction occurs necessarily in using microalloyed steels instead of high resistance tempered alloy steels (1). This makes it possible to obtain similar levels of resistance without the presence of certain high cost alloy materials, such as chrome and molibdenum, and without the need for the steels to be subjected to post-forging heat treatments which, apart from increasing production costs may also give rise to serious dimensional problems in the product.

There are certain types of tests which make it possible to study thermomechanical forging processes in metallic materials - tension, compression and torsion - the last being the most widely used because of its specific characteristics, versatility and ease of execution. The hot torsion test allows any industrial forging process to be simulated at laboratory scale using samples of small dimensions.

The parameters that characterize any forging process are the degree of deformation and the temperature and rate at which these deformations are applied. The grounds for simulation of hot forging processes are based on the generalized concepts of stress ($\bar{\sigma}$) and deformation ($\bar{\varepsilon}$) derived from the principle of equivalence. According to this principle, if two metallic elements having identical chemical composition and initial structure are subjected over time to the same laws of generalized deformation and temperature, they will at any given moment be in one same state, regardless of the process giving rise to the deformation.

On the basis of these hot torsion tests, the present study has centred on consideration of the plastic behaviour of the two steels described above through the breaking point ductility curves. The industrial forging process has been simulated in two runs and applied to representative automobile parts (push rod, crankshaft, etc.), with reproduction of the values of deformation undergone during each forging stroke, the rate at which such deformations are applied and the parameters of the thermal cycles accompanying the shaping process - preheating and deformation temperatures, maintenance times between runs and cooling rate.

Maintaining the values of deformation ( $\bar{\varepsilon}$ ) and deformation rate ( $\dot{\bar{\varepsilon}}$ ) calculated in the industrial forging process for this type of parts, different torsion tests have been carried out varying the preheating and deformation temperatures, in order to analyze the influence of these thermal parameters on the final structure of both steels, the test samples being air cooled following application of the final deformation. The type of microstructure obtained and the shape, size and distribution of the phases and microconstituents present in this microstructure make it possible to estimate the degree of the different properties that can be achieved in these vanadium microalloy steels. Also, the results obtained from the study offer the possibility of gaining insight into the thermal cycles to be associated with the forging process in order to produce an adequate material structure under optimum operational conditions in the process itself.

## CHARACTERIZATION OF THE TESTED STEELS

Two Carbon Manganese Vanadium microalloyed steels hardened by air-induced precipitation were tested. Both of these steels are typified basically by standard 970/1983, and their chemical composition is shown in Table 1.

The test samples were obtained longitudinally from hot-rolled bars, this being the basis for the entire experimental study.

Both steels have very similar percentages of manganese and vanadium, and are distinguished fundamentally by their content in carbon, sulphur, nitrogen and silica; the two first of these elements are higher in 40MVS6 steel, while the content of nitrogen and silica is greater in the lower carbon content steel.

In order to favour the precipitation of vanadium nitrides in the 30MSiV62 steel, the nitrogen content of this steel was increased to the significantly high value of 164 ppm.

In spite of the fact that in the raw, hot transformation state these microalloyed steels show high tensile strengths (greater than 800 MPa for 30MSiV62 and than 900 in the case of 40MVS6 steel), when the shaping processes are performed using uncontrolled conventional techniques at equal values of resistance, the properties of ductility and toughness of the microalloyed steels are lower than those found in traditional alloyed steels subject to heat treatment tempering. Besides this, the elastic limit is also lower and the ferritic-perlitic structure, characteristic of microalloyed steels air cooled following hot shaping, shows a relationship between the elastic limit ($R_e$) and tensile strength ($R_m$) of $\frac{R_e}{R_m} = 0.65$,

while this ratio reaches a value of 0.90 in the case of tempered alloyed steels (2).

However, given the specific metallurgic characteristics of these vanadium microalloyed steels, which harden by precipitation during the cooldown that takes place after the hot transformations, study of the shaping processes on the basis of considering them as real thermomechanical treatments makes it possible to attain mechanical properties for these steels that are generally valid for numerous applications and perfectly comparable to those of tempered alloyed steels.

Table 1. Chemical Composition (% wt)

| | 40MVS6 | 30MSiV62 |
|---|---|---|
| C | 0.39 | 0.29 |
| Mn | 1.29 | 1.30 |
| Si | 0.22 | 0.43 |
| S | 0.073 | 0.026 |
| P | 0.014 | 0.019 |
| V | 0.10 | 0.11 |
| Al | 0.020 | 0.029 |
| $N_2$ | 70 ppm | 164 ppm |

## PLASTIC BEHAVIOUR. DUCTILITY

In order to acquire previous knowledge of the plastic behaviour of the two C-Mn-V steels under study, torsion tests were carried out at different temperatures, ranging from 900 ºC to 1,250 ºC, and applying deformations up to the breaking point at a constant rate of 2,000 rpm torsion, this being equivalent to a generalized deformation rate at the periphery of the sample equal to $\dot{\bar{\varepsilon}} = 7.25\ s^{-1}$, in accordance with the following expression:

$$\dot{\bar{\varepsilon}} = \frac{2\pi R}{\sqrt{3}\ L}\ \dot{N} \qquad (1)$$

where:

$\dot{N}$ - number of turns per second
R - radius of the sample (3 mm)
L - effective length of the sample (50 mm)

By expressing the values corresponding to the number of torsion turns withstood by the material prior to reaching the breaking point at each test temperature, it is possible to obtain the ductility curves shown in Figure 1. The diversity of metallurgical factors affecting the ductility of a metallic material - microstructural heterogeneity, residual elements, inclusions - demands that the information obtained from the curves showing ductility up to the breaking point be limited to suitable levels.

The expression linking the ductility of a material, represented by the value of deformation up to breaking point ($\bar{\varepsilon}_r$), with temperature approximates to a function of type (3):

$$\bar{\varepsilon}_r = A \exp - \frac{Q}{RT} \qquad (2)$$

where:

Q - activation constant
R - perfect gas constant
A - material-dependent constant

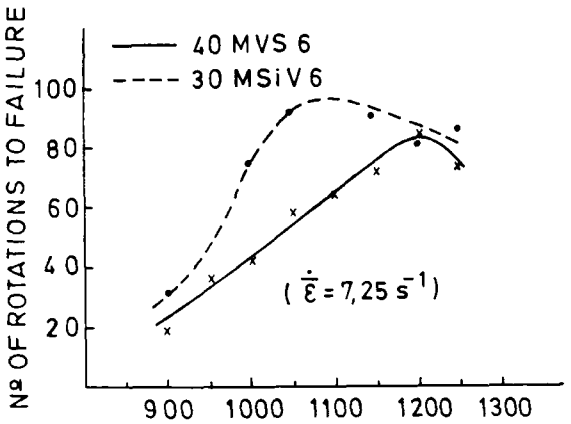

FIG.1_DUCTILITY CURVES

The increase in the deformation temperature gives rise to a progressive increase in ductility, this tendency being maintained in theory up to temperatures near to the melting point, where a sudden decrease is observed. However, the influence of the metallurgical factors mentioned above and the increase in temperature experienced in any deformation process favour the formation of cracks and defects and/or fusion of segregated microphases, this giving way to an appreciable reduction in the ductility of the material and breaking due to internal decohesion at temperatures quite a lot lower than the melting point.

However, in spite of these limitations, which are difficult to control experimentally, the ductility curves make it possible to determine the temperature zones in which the material shows maximum plastic flux and in which it is consequently more suitable for shaping.

According to the curves shown in Figure 1, the maximum ductility of the 40MVS6 steel occurs at a temperature of 1200 ºC, this being greater than the maximum point of ductility for the 30MSiV62 steel, which occurs at 1100 ºC. Although both steels show good plastic behaviour across a wide range of temperatures, the 30MSiV62 steel covers a greater range, which is also prolonged to lower temperatures.

If a torsion value of 40 turns is considered, this being equivalent to a generalized deformation of $\bar{\varepsilon} = 8.71$ (871%), which is much higher than the maximum accumulated deformations that would occur in any process of shaping ($\sim \Sigma \bar{\varepsilon} = 5$), this deformation could be achieved in the 30MSiV62 steel at an approximate temperature of 925 ºC, a lower temperature than that corresponding to the 40MVS6 steel, which is approximately 980 ºC. From the above it can be deduced that the high ductility zone of these steels extends from these temperatures to the maximum test temperature - 1,250 ºC - which it is not advisable to exceed in shaping processes.

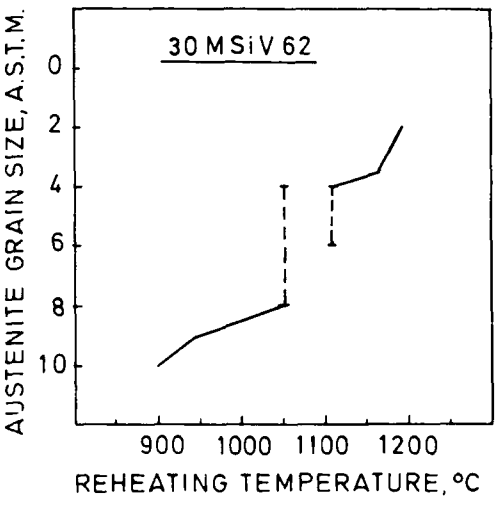


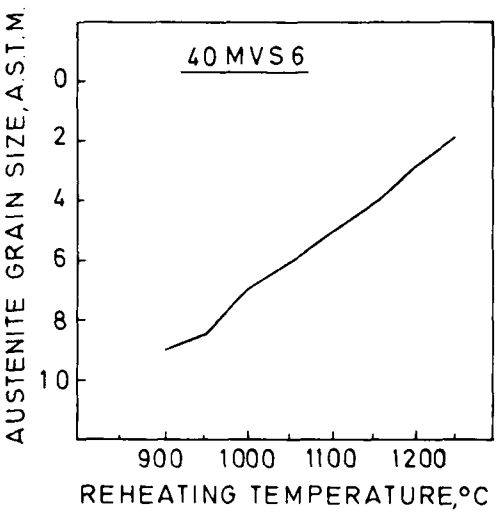

FIG.2_RELATIONSHIP BETWEEN AUSTENITE GRAIN SIZE UNDEFORMED AND REHEATING TEMPERATURE.

## SIZE OF THE INITIAL AUSTENITIC GRAIN

In order to know the size of the initial austenitic grain prior to deformation, small cylindrical samples were machined from both steels (Ø = 2 mm, L = 12mm) and subjected to heatup at a constant rate of 5ºC/s, followed by a period of temperature maintenance lasting 120 seconds and a cooldown at a rate of 200ºC/s.

Figure 2 shows the results of varying the size of the austenitic grain as a function of preheating temperature for the two steels tested.

From temperatures close to 1050 ºC up to temperatures above 1100 ºC the 30MSiV62 steel shows double austenitic grains. The grain growth curve corresponding to this steel, Figure 2, shows the maximum and minimum grain sizes observed over this range of temperatures. The maximum difference in the sizes of the austenitic grains present in the structure (max. 4 and min. 8 ASTM) is detected at a temperature of 1050 ºC; consequently, it can be deduced that this is the temperature at which the maximum growth of the austenitic grains commences in this steel.

The 40MVS6 steel, on the other hand, does not show double grains, and maintains a more uniform and regular growth in grain size with temperature.

Comparison of the grain growth curves for both steels makes it possible to detect the influence of nitrogen as the element responsible for formation of precipitates with the vanadium (VN), these having a high capacity for increase of the fineness of the austenitic grains, due to inhibition of their growth with temperature (4). In this respect, finer grain sizes are observed in the 30MSiV62 steel, with 164 ppm nitrogen, than in the 40MVS6 steel, up to the temperature of 1050 ºC at which formation of double grains commences.

## SIMULATION OF THE FORGING PROCESS

PREHEATING TEMPERATURES - Apart from several other considerations of an operational and structural nature, the preheating temperatures used in the microalloyed steel forging process should be adapted to the temperatures at which solubilization of the precipitates present in the material occurs. In the case of the C-Mn-V steels considered in this study, the precipitates that may be present are carbides of vanadium(VC), nitrates of vanadium (VN) and carbonitrates of vanadium V(C,N).

The effects of the slowing down of the recrystallization process, the inhibition of growth of austenitic grains, the increased fineness of ferritic grains and the hardening by precipitation produced by the action of these compounds, mainly VN and V(C,N) are well known (5). However, the beneficial effects of these precipitates, consisting of an increase in the mechanical characteristics, especially the elastic limit and impact resistance, would be enormously reduced if during the heatup prior to forging they were not put in solution in order to be able to precipitate later during the cooldown and act with maximum efficiency.

The solution temperatures of VC and VN as a function of the percent content in weight of these elements may be calculated respectively by the following equations:

$$\log (V)\,(C) = -\frac{9500}{T} + 6.72 \qquad (3)$$

and

$$\log (V)\,(N) = -\frac{8330}{T} + 3.46 \qquad (4)$$

where T represents the absolute temperature.

On the basis of these expressions o, and more easily via direct reading in Figure 3, it is possible to obtain the solid solution temperatures in the austenite of vanadium carburates and nitrates indicated in Table II.

TABLE II. VC and VN solution temperatures in the steels under study

| | 40MVS6 | 30MSiV62 |
|---|---|---|
| VC | 896 ºC | 883 ºC |
| VN | 986 ºC | 1070 ºC |

According to these data, the preheating temperatures normally applied in forging processes, located at around 1250 ºC, far exceed the VC and VN solution temperatures of these steels. However, as will be seen below, knowledge of these temperatures is also important in order to determine the temperatures at which the material should be deformed during the process.

DEFORMATION PARAMETERS - The basis used in order to establish the deformation parameters to be used in simulating the hot torsion tests was a two-run forging of an automobile pusl rod, in which the values of the deformations produced at each stroke and the average rate at which these deformations were applied were calculated by means of the following expressions (6):

$$\bar{\varepsilon} = \ln \frac{h_o}{h} \qquad (5)$$

$$\dot{\bar{\varepsilon}}_m = \frac{\Delta \varepsilon}{\Delta h}\, v_m \qquad (6)$$

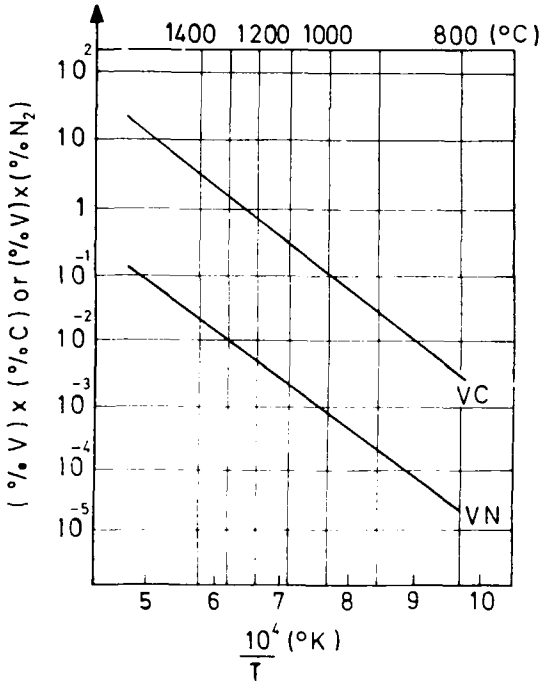


FIG.3. SOLUTION TEMPERATURES OF VC y VN

where

$h_o$ = initial height
$h$ = final height
$v_m$ = average speed of the hammer from commencement to termination of the deformation

On the basis of the above, and ignoring the small relative differences in the average generalized rates of deformation observed between the two runs, the deformation parameters shown in Table III were selected. Likewise, by applying the torsion equivalence equations given by the expression (1) (*), Table III includes the equivalent deformation parameters for the peripheral layer of the torsion sample used, expressed in terms of the number of turns (N) and the revolutions per minute ($\dot{N}$).

(*) From the expression (1) it is possible to arrive at the generalized torsion deformation equation: $\bar{\varepsilon} = \frac{2\pi R}{\sqrt{3}\, L} N$, where N is the number of turns and the remaining symbols have the same significance as in (1).

TABLE III. Deformation parameters used in simulation of the forging process

| | Forging | | Torsion | |
|---|---|---|---|---|
| | $\bar{\varepsilon}$ | $\dot{\bar{\varepsilon}}_m$ ($S^{-1}$) | N | $\dot{N}$ (rpm) |
| 1st run | 1.443 | 7.25 | 6.6 | 2000 |
| 2nd run | 0.779 | 7.25 | 3.6 | 2000 |

THERMAL PARAMETERS - In order to program simulation as faithfully as possible, the times and temperatures were directly measured during the development of the forging process in an industrial installation.

In this respect, different preheating temperatures were established, and the times between runs and temperatures of each batch were measured at the end of each deformation. The results are shown in Table IV.

TABLE IV. Thermal parameters directly measured during the forging process.

| Preheat Temp. Furn. (ºC) | 1st Run (ºC) | Time between runs | 2nd Run (ºC) | Cooling method |
|---|---|---|---|---|
| 1250 | 1180 | 3 | 1125 | air |
| 1200 | 1150 | 3 | 1102 | air |
| 1150 | 1120 | 3 | 1087 | air |
| 1100 | 1080 | 3 | 1050 | air |

All the parts were air cooled immediately after forging.

## EXPERIMENTAL RESULTS

Taking the real data arising from the industrial forging process described above as the basic model, a wide program of hot torsion tests was established, covering the entire practical range of preheating and deformation temperatures between 1250 ºC and 900 ºC.

In this way, and by exactly maintaining the same values of deformation (N) and deformation rate ($\dot{N}$) shown in Table III, torsion tests were performed on the basis of the thermal parameters shown in Table V, while maintaining the cooling law as close as possible to the industrial forging process under study.

STRUCTURAL ANALYSIS - Grooves of a depth of 0.3 mm were ground along the entire effective length of all the torsion samples tested for analysis of the corresponding final microstructures and determination of the grain sizes.

Table V indicates the grain sizes obtained in each of the samples tested. When precipitated ferrite exists at the old austenite grain boundaries, the austenitic size is given, and when the ferrite is present in the form of equiaxial grains, the ferritic grain size is given.

TABLE V. Thermal parameters used in simulating the described forging process by torsion

| Preheat. Furn. Temp. (ºC) | 1st Deform. (ºC) | 2nd Deform. (ºC) | Post-deform. Cooling | Final Grain Size (ASTM) (1) |
|---|---|---|---|---|
| | **40MVS6 STEEL** | | | |
| 1250 | 1225 | 1180 | air | 4/5 |
| | 1190 | 1130 | | 5 |
| | 1170 | 1120 | | 5/6 |
| | 1120 | 1075 | | 6 |
| | 1010 | 960 | | 7 |
| | 980 | 930 | | 8 |
| 1200 | 1180 | 1130 | air | 6/7 |
| | 1150 | 1110 | | 6/7 |
| | 1120 | 1080 | | 7 |
| | 1000 | 960 | | 7/8 |
| | 950 | 910 | | 8 |
| 1150 | 1130 | 1070 | air | 6/7 |
| | 1130 | 1055 | | 7 |
| | 1080 | 1010 | | 7/8 |
| 1100 | 1090 | 1050 | air | 7/8 |
| | 1090 | 1000 | | 7/8 |
| | **30MSiV62 STEEL** | | | |
| 1200 | 1175 | 1115 | air | 5/6 |
| | 1150 | 1055 | | 6 |
| | 1055 | 1010 | | (9/10) |
| | 1010 | 955 | | (9/10) |
| | 960 | 905 | | (10) |
| 1150 | 1110 | 1060 | air | 7 |
| | 1060 | 1005 | | (9/10) |
| | 1010 | 955 | | (9/10) |
| | 955 | 900 | | (10) |
| 1100 | 1085 | 1055 | air | (9/10) |
| | 1060 | 1000 | | (10) |
| 1050 | 1040 | 1005 | air | (10) |

(1) The numbers shown in brackets correspond to the values of ferritic grain sizes. The rest, not shown in brackets, correspond to the size of austenitic grains determined thanks to the presence of ferrite at the grain boundary.

Under all the test conditions encountered, the general microstructure of the 40MVS6 steel is made up of ferrite and perlite with a precipitation of proeutectoid ferrite at the old austenitic grain boundaries. In the case of the 30MSiV62 steel, the general microstructure is also ferritic-perlitic, although in this case there is a greater predisposition to the incipient formation of bainite, and ferrite is observed only at the grain boundaries in these samples whose last deformation terminated at higher temperatures, generally above 1050 ºC.

The deformation cycles applied under the different temperature conditions have given rise to totally recrystallized structures.

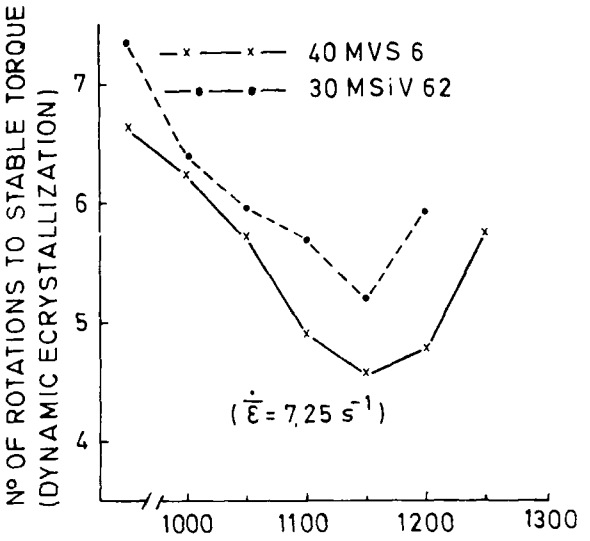


FIG.4_RELATIONSHIP BETWEEN FIRST DEFORMATION TEMPERATURE AND NUMBER OF ROTATIONS TO STABLE TORQUE (DYNAMIC RECRYSTALLIZATION)

Analysis of the recording curves for the different tests (torsion torque - number of turns) clearly shows that the extension of deformation in the first run ($\bar{\varepsilon}$ = 1.443 : N = 6.6 turns) is sufficient to produce total dynamic recrystallization in both steels when the temperature at which this deformation is accomplished is greater than 950 ºC. The graphs shown in Figure 4 represent the values of deformation necessary in order to reach the normal operational state (equilibrium between deformation hardening and recrystallization); the graphs also show that for temperatures exceeding 950 ºC the number of turns required in order to achieve recrystallization is fewer than that actually applied.

The second deformation, performed at a lower temperature and much lower intensity than the first ($\bar{\varepsilon}$ = 0.779 : N = 3.6 turns) is not capable of causing dynamic recrystallization in the structure; consequently, it can be deduced

that the recrystallization observed in the final microstructures has been fundamentally produced by static recrystallization during the cooldown following the second and last deformation. Only when the temperature of the second deformation is higher than 1070 ºC is it possible to detect signs of incipient dynamic recrystallization in both steels,, as a result of the deformation applied being slightly higher than that corresponding to maximum torque (deformation at maximum torque: $\bar{\varepsilon}$ max.).

These phenomena are shown in the recording curves included in Figures 5 and 6, which represent two extreme cases for the two steels: maximum and minimum temperature of the last deformation.

## CONCLUSIONS

The two vanadium microalloyed carbon-manganese steels considered in the present study are perfectly adequate for shaping by hot forging.

The wide temperature range over which these two steels show high values of ductility permit adaptation of the temperatures at which it is possible to apply the succesive deformations, in order to directly achieve from forging the final material structure best suited to the demands imposed by each application, without the need for costly subsequent thermal treatments.

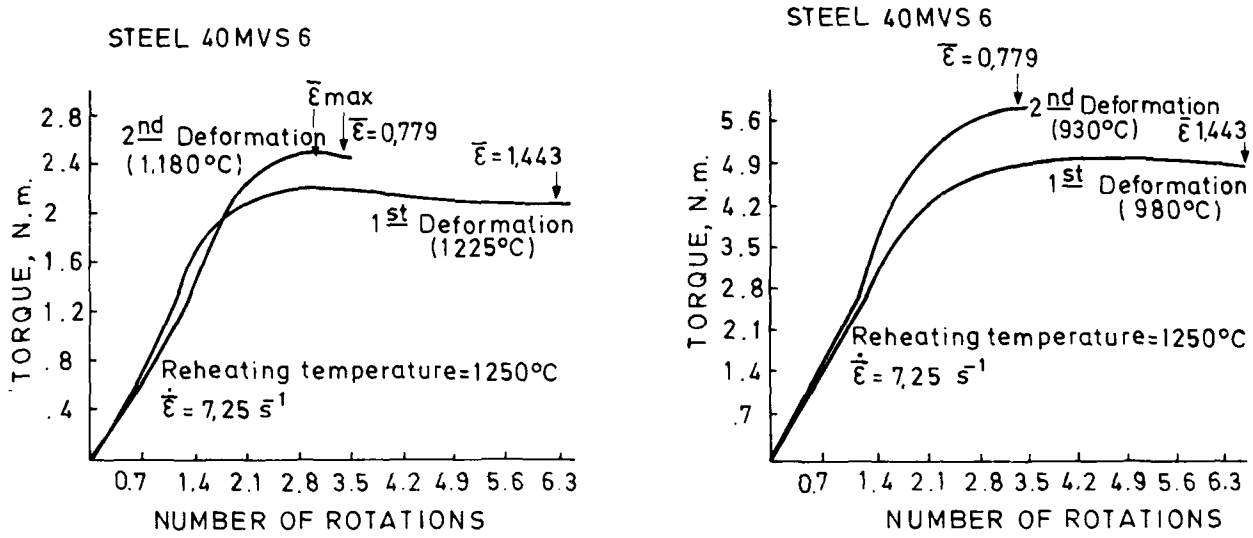


FIG.5_TORQUE-NUMBER OF ROTATIONS CURVES IN TWO EXTREME TEMPERATURES OF LAST DEFORMATION (STEEL 40MVS 6)

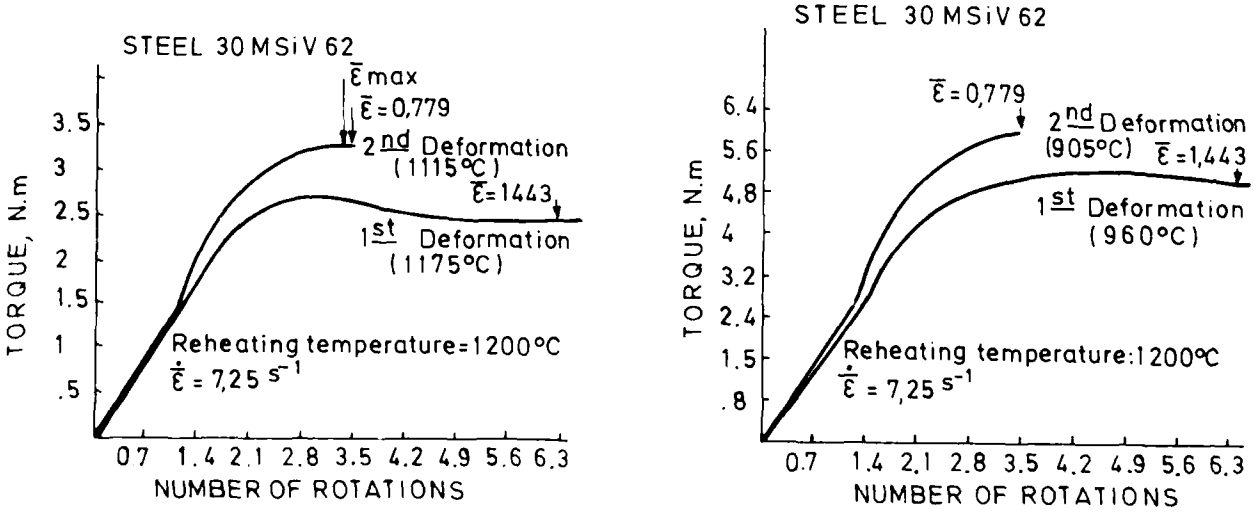


FIG 6_TORQUE-NUMBER OF ROTATIONS CURVES IN TWO EXTREME TEMPERATURES OF LAST DEFORMATION (STEEL 30 MSiV 62)

Centering simply on structural considerations, evaluation of the results presented in this study allows us to conclude that, in both steels, the optimum microstructure is obtained when final deformation is accomplished at low temperatures. Under these conditions, subsequent cooldowns by air are capable of generating fine grain ferritic-perlitic microstructures. In this respect, the higher level of nitrogen in the 30MSiV62 steel allows for the formation of greater quantities of precipitates which result in this steel attaining a considerably finer grain size than the 40MVS6 steel with identical temperature cycles associated with deformation.

Figure 7 shows the micrographs for both steels when subjected to an identical shaping process: Preheating temperature of 1200 ºC, initial deformation temperature ( $\bar{\varepsilon}$ = 1.443) at 1060 ºC, second deformation temperature of ($\bar{\varepsilon}$ = 0.779) at 1010 ºC, identical deformation rate in both cases at 7.25 $s^{-1}$ and air cooling under the same conditions.

In these micrographs the difference in grain size between the two steels can be appreciated: 7 ASTM for the 40MVS6 steel and 9/10 ASTM for 30MSiV62, as well as the precipitation of proeutectoid ferrite at the grain boundaries produced in the first of these steels. Although this type of microstructure can mean a reduction in the impact resistance of the material, the acceptable size of the grains achieved by cooling immediately after forging makes this steel a possible substitute for many thermally treated alloyed steels. This is undoubtedly the case for the 30MSiV62 steel which, with its ferritic-perlitic structure with grain sizes of 9 or 10 ASTM and a fine perlite, guarantees appropriate levels of strength, elastic limit and impact resistance for replacement of many alloyed steels in Q+T conditions, with important economical advantages.

The experimental results also show that the preheating temperature does not exercise an appreciable influence on the final grain size and microstructure, these depending exclusively on deformation temperatures when all other parameters are equal (magnitude of deformation in runs, deformation rate, time between runs and post-forging cooldown rates).

As a result of the above, apart from solubilization of the precipitates being assured in both steels from sufficiently low temperatures - ≃ 986 ºC for 40MVS6 and 1070 ºC for 30MSiV62 - the use of preheating temperatures lower than those usually utilized in forging will permit a series of important advantages to be achieved, quite apart from the clear energy saving implied. As regards the forging process itself, the possibility of reducing the preheating temperatures is a factor that impacts heavily on the prolongation of the service lifetime of the dies.

All the reasoning reflected above leads to the advisability of these steels being forged at the lowest temperatures possible. On the other hand, it would not appear to be advisable to reduce the preheating temperature below 1100 ºC, nor that the final deformation be accomplished below 1000 ºC. In both cases the action of the microalloying elements might be less effective and the operational difficulties encountered in the process would increase considerably.

On the basis of the above, it can be concluded that the optimum forging process for these microalloyed steels, considered as a real thermomechanical treatment, should be developed under the following conditions:

For 40MVS6 steel, which shows a maximum ductility temperature of 1200 ºC with high values as from 1,000 ºC, a regular austenitic grain growth rate, a precipitate solubilization temperature close to 1000 ºC and a minimum tem-

40 MVS 6 (x200)

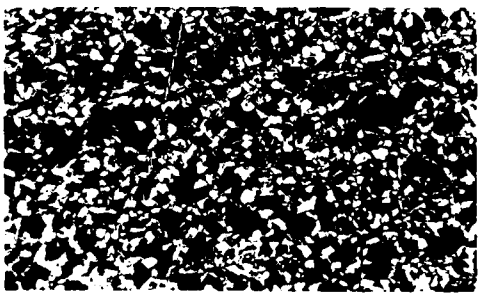

30MSiV 62 ( x 200)

FIG.7_ MICROSTRUCTURE OF BOTH STEELS TESTED IN THE SAME CONDITIONS

perature of $\simeq$ 1070 ºC for incipient dynamic recrystallization during the second deformation ($\bar{\varepsilon}$ = 0.779), the most adequate forging thermomechanical treatment for manufacturing of a piece of this steel, with the deformation parameters used in this study, might be developed under the following conditions: Preheating temperature = 1150 ºC; initial deformation temperature = $\sim$ 1120 ºC; temperature of the second and final deformation= 1090 ºC; and air cooling immediately following the final deformation, at a rate of between 50 and 250ºC/min. Under these conditions the final microstructure of the steel would be ferritic-perlitic, with a grain size of 6 or 7 ASTM, depending on the post-forging cooldown rate applied.

In the case of the 30MSiV62 steel, which has a maximum ductility temperature of 1100 ºC with high values being maintained as from 950 ºC, a fast grain growth rate above 1050 ºC, total precipitate solubilization at 1070 ºC and a minimum temperature of $\sim$ 1070 ºC for incipient dynamic recrystallization during the second deformation ($\bar{\varepsilon}$ = 0.779), the most adequate thermomechanical treatment in forging for production of a piece of this steel, with the deformation parameters established in this study, might be as follows: Preheating temperature = 1100 ºC; initial deformation temperature $\sim$ = 1080 ºC; temperature of the second and final deformation = 1050 ºC; and air cooling immediately following the final deformation at a rate of between 50 and 250ºC/min. Under these conditions, the 30MSiV62 steel would attain a very fine ferrite and perlite microstructure - 9/10 ASTM - of high characteristics.

Evidently, the decision to reduce the forging process temperatures of these steels requires adequate control of all the thermal and deformation parameters, and necessarily implies that the modification of certain operational and design aspects affected by this decision be suitably addressed.

## REFERENCES


(1) Ollilaimen, V., Hurmola, H. and Pontinen, H., J. Materials for Energy Systems. 5(4, 222-232 (1984).

(2) Bäcker, L. and Fombarlet, J., Aciers Speciaux, 72, 21-24 (1985).

(3) Urcola Galarza, J.J. and Fuentes Pérez, M., Rev. Metal, CENIM, 16(6), 337-342 (1980).

(4) Osuzu, H., Shiraga, T., Tsujimura, K., Shiroi, Y., Taniguchi, Y. and Kido, H., SAE Technical Paper Series, 860131, U.S.A. (1986).

(5) García, C., de Andrés, M.P., Medina, S.F. and Carsí, M., Jornadas Nacionales de Calidad Siderúrgica 85, UNISED (1985).

(6) STAHL-EISEN Prüfblätter (SEP) des Vereins Deutscher Eisenhüttenleute, Sep. 1123 (1986).

# DEVELOPMENT OF HIGH STRENGTH STEELS WITH LOW YIELD RATIO FOR LARGE SCALE STEEL STRUCTURES

**Nobuo Shikanai, Masayoshi Kurihara**
Steel Research Center
NKK Corporation
Kawasaki, Japan

**Hisatoshi Tagawa**
Research Administration Department
NKK Corporation
Kawasaki, Japan

**Shin Sakui, Itaru Watanabe**
Steel Research Center
NKK Corporation
Kawasaki, Japan

ABSTRACT

Uniform deformability of steel plates which relates to yield ratio is one of the important engineering properties for the safety of the large scale steel structures under severe loading conditions. In order to develop the heavy gauge 60 kgf/mm² class tensile strength steel plate with low yield ratio, the influences of heat treatment conditions and Thermo-Mechanical Control Process (TMCP) on yield and tensile strengthes and yield ratio were investigated. Test results of laboratory studies showed that both of high strength and low yield ratio can be achieved by quenching from appropriate dual-phase ($\alpha+\gamma$) temperature (Q') following after pre-treatment. On the basis of above studies, low YR 60 kgf/mm² class steel plate with 80 mm thickness was produced by QQ'T and TMCP-Q'T processes in a mill scale. The YR of mill trial steel plates was sufficiently low value below 80 %. In addition, fracture toughness and weldability were also sufficient as heavy gauge 60 kgf/mm² class steel plate.

YIELD RATIO OF STRUCTURAL STEEL PLATES is one of the important engineering properties[1] which controls uniform plastic deformability of steel structures under severe loading conditions (ex. seismic load). Lowering of yield ratio (YR: *yield strength/ultimate tensile strength*) is effective to improve the uniform deformability, however, YR of steels generally increases as tensile strength increases. The change of YR relates to microstructure. For example, the YR of tempered bainite and/or martensite steels is higher than that of ferrite-pearlite steels.

On the other hand, the high strength steel plates above 60 kgf/mm² class tensile strength produced by quenching and tempering (QT) process have many advantages of reducing component weight, saving welding cost and so on. It is expected that the development of high strength steel plate with low YR extends the application of high strength steel plate to larger scale steel structures which are required high resistance against catastrophic failure.

In the present paper, in order to develop the 60 kgf/mm² class tensile strength steel plates (tensile strength≥58 kgf/mm²) with low YR, influences of heat treatment and microstructures on YR were investigated. On the basis of these fundamental studies, 60 kgf/mm² class steel plates with low YR (plate thickness : 80mm) were manufactured in a mill scale, and mechanical properties of base matal and welded joints were examined in detail. Application of Thermo-Mechanical Control Process (TMCP) to manufacturing high strength steel plates with low YR was also investigated in this study.

## PRELIMINARY STUDIES ON LOW YR HIGH STRENGTH STEEL PLATE

Generally, YR of steel plate tends to decrease in the case of microstructure with high density of movable dislocations such as as-quenched bainite and martensite. Microstructure such as ferrite, which can easily initiate and multificate movable dislocations, also contributes to decrease YR. In such steels, *yield strength* (YS) can be decreased, because plastic deformation is induced by a little strain. On the other hand, metallurgical factors controlling tensile strength (TS) are different from those of YS. The TS of steels relates to solid-solution strengthening, volume fraction of the second phase, and work hardened ratio of matrix and second phase.

Since the controlling factors of TS are different from YS and YR, in order to produce the steel plates with high TS and low YR, it is

necessary to control YS and TS independently. From the considerations on dislocation behavior described above and from the studies[2) 4) 11)] carried out for the developement of 80 kgf/mm² class tensile strength steel plate with low YR, it is confirmed that control of the ferrite volume fraction and high strength second phase volume fraction is most effecient for lowering YR and obtaining high strength. The desirable mixed microstructures, which satisfy both of high strength and low YR, are bainitic microstructure containing ferrite. This mixed microstructure can be obtained by quenching from appropriate dual-phase ($\alpha+\gamma$ phases) temperature (Q' treatment).

Figure 1 shows the influence of Q' temperature on grain size and martensite volume fraction of the high strength steel plate[2)]. Ferrite grain size decreases as the Q' temperature increases. On the other hand, grain size of martensite and its volume fraction increase with an increase of Q' temperature. Therefore, in order to obtain the appropriate mixed microstructure, optimum Q' temperature should be determined by considering the change of dual-phase temperature range due to chemical composition.

In this study, rapid cooling treatment was performed as pre-treatment in order to refine the mixed microstructures uniformly. The rapid cooling treatment is effective to disperse refined carbides which can become austenite transformation sites during reheating at dual-phase region. In addition, the application of TMCP to pre-treatment was also investigated in a mill trial. One of the beneficial effects of TMCP is an increase of strength without contribution of additional alloying elements. It is expected that application of TMCP can also exert such profitable effect on the production of low YR high strength steel plates.

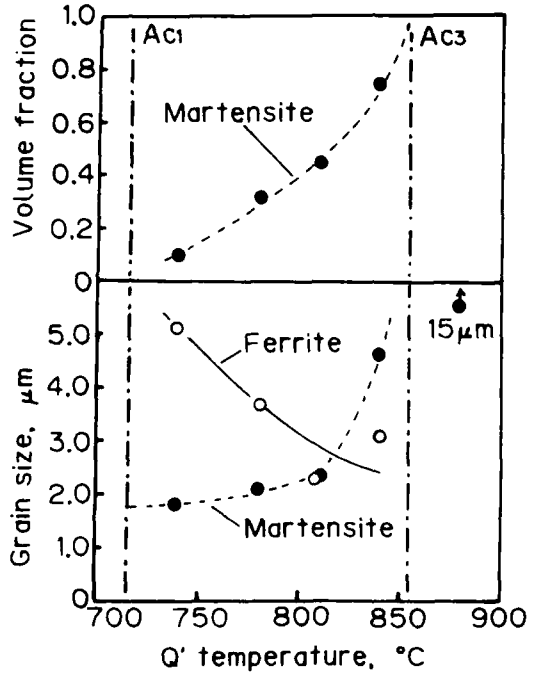


Fig. 1 Influence of Q' temperature on grain size and martensite volume fraction

## LABORATORY STUDIES

EXPERIMENTAL PROCEDURE - Table 1 shows the aimed mechanical properties of the 60 kgf/mm² class tensile strength steel plates with low YR. The plate thickness is determined as 80 mm by taking account of application to the large scale steel structures. The steel plates above 58 kgf/mm² tensile strength are included in the category of 60 kgf/mm² class steel plates as shown in Table 1, and YR is aimed to be below 85% in this study.

The steel plate prepared for the simulation of heat treatment is a 60 kgf/mm² class high strength low alloy steel plate with chemical composition shown in Table 2. The thickness was reduced from 90 mm to 80 mm by machining.

Table 1 Aimed properties of 60kgf/mm² class tensile strength steel plate

| YS kgf/mm² | TS kgf/mm² | YR % | $vE_0$ kgf·m | Thickness (mm) |
|---|---|---|---|---|
| > 44 | > 58 | < 85 | > 5.0 | 80 |

Table 2 Chemical composition of steel tested

wt%

| t mm | C | Si | Mn | P | S | Cu | Ni | Cr | Mo | V | Ceq |
|---|---|---|---|---|---|---|---|---|---|---|---|
| 90 | 0.13 | 0.25 | 1.48 | 0.012 | 0.002 | 0.18 | 0.19 | 0.08 | 0.17 | 0.04 | 0.45 |

NOTE : used for labo. simulation.

TEST RESULTS AND DISCUSSION - Fig. 2 shows the influence of Q' temperature on mechanical properties of the rapid-cooling-Q'T(QQ'T) processed steel plates. The YS, TS and YR slightly decrease at first and then increase with an increase of Q' temperature. With respect to toughness of Charpy-impact test, vTs (50%FATT) is sufficiently low (below -90 ℃) under Q' temperature from 740 to 810 ℃. The range of Q' temperature which satisfies the aimed mechanical properties (YS≦44 kgf/mm², TS>58 kgf/mm², YR≦85%) is wide enough to stably produce 60 kgf/mm² class steel plate with low YR. In addition to low YR, toughness is also improved through refinement of microstructures by Q' treatment.

Influence of Q' temperature on microstructures is shown in Fig. 3. The microstructure before Q' treatment is mainly bainite. The volume fraction of deeply etched microstructure tends to increase with an increase of Q' temperature. These microstructures are bainite or martensite which enriches alloying elements, and they were re-transformed from austenite which had transformed during reheating in dual-phase region. Fig. 4 shows the scanning electron micrographs (SEM) of the same heat-treated steel plates. Bainite and recrystallized ferrite with carbides can be observed in the Q' treated steels. The bainite with coarsened carbides is retained bainite which is tempered at dual-phase temperature.

The observations of microstructure indicate that the mixed microstructures obtained after Q' treatment are consisted of re-transformed bainite and/or martensite, bainite with coarsened carbides and recrystallized ferrite with carbides. It is confirmed that the Q' treatment is effective to obtain ferrite which can decrease YR.

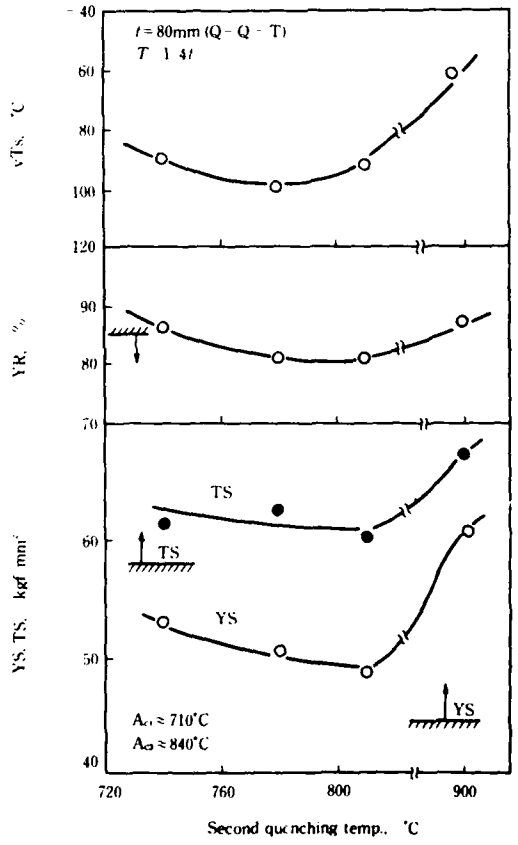


Fig. 2 Influence of Q' temperature on mechanical properties

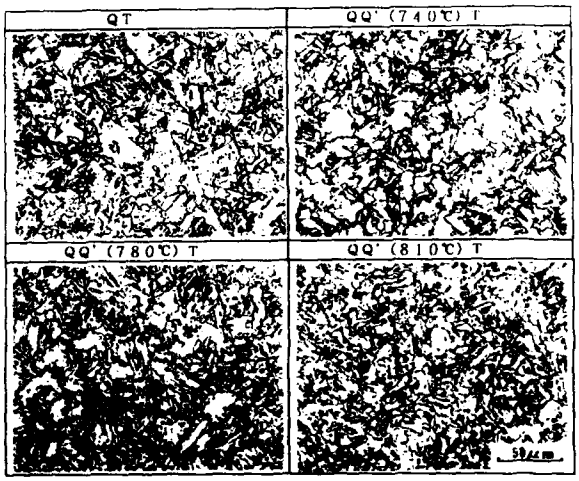


Fig. 3 Influence of Q' temperature on microstructure

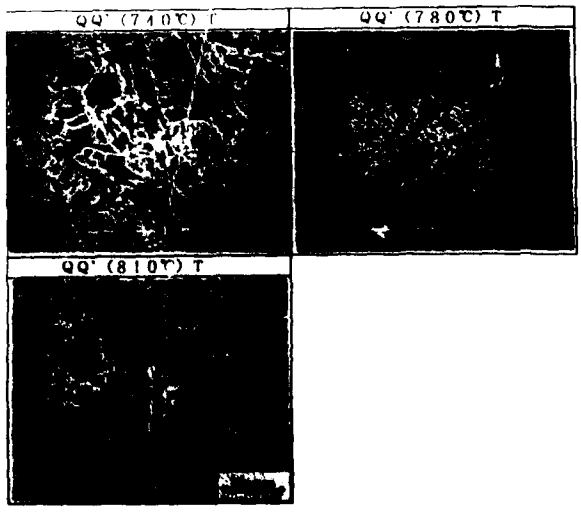


Fig. 4 Scanning electron micrographs (SEM) of the steel plates under various Q' conditions

## MILL TRIAL STEEL PLATES

MECHANICAL PROPERTIES OF BASE METAL - On the basis of laboratory studies described proceeding Chapter, mill trial was performed to manufacture 60 kgf/mm² class low YR steel plates. The chemical composition and manufacturing conditions of a mill trial steel plates with 80 mm thickness are shown in Table 3. Manufacturing processes employed were QQ'T and TMCP-Q'T processes. Conventional QT steel plate with 80 mm thickness was also produced by using the same heat for comparison.

Fig. 5 shows the microstructures of QQ'T, TMCP-Q'T and conventional QT steel plates. Bainite with re-transformed bainite and/or martensite and ferrite recrystallized by Q' treatment can be observed in microstructures of QQ'T and TMCP-Q'T steel plates. The grain size of TMCP-Q'T steel plate is slightly larger than that of QQ'T steel plate. Transmission electron micrographs of QQ'T steel plates are shown in Fig. 6. Ferrite with low dislocation density, and bainite with laths and carbides can be observed. It is confirmed that the bainitic microstructure with ferrite is also obtained in the mill trial steel plate produced by Q' treatment.

Figure 7 shows the results of tensile test and Charpy-impact test on QQ'T, TMCP-Q'T and conventional QT steel plates. The YS, TS and YR of QQ'T steel plate satisfy the aimed value listed in Table 1, and YR achieves below 80 %. In the case of conventional QT processed steel plate, their YS, TS and YR are higher than those of QQ'T and TMCP-Q'T ones. The strength of TMCP-Q'T steel plate is higher than that of QQ'T one, although the tempering temperature of TMCP-Q'T steel plate is higher than that of QQ'T one. This result indicates that an increase of strength caused by TMCP inherites even after Q' treatment.

The 50 % FATT of Charpy-impact test results of TMCP-Q'T steel plate is slightly higher than that of QQ'T one due to coarsening grain size as shown in Fig. 5. However, its 50 % FATT is low enough as heavy gauge 60 kgf/mm² class steel plate. It is possible to obtain finer grain size by control of TMCP conditions such as slab reheating temperature, finish-rolling temperature, water-cooling conditions and so on.

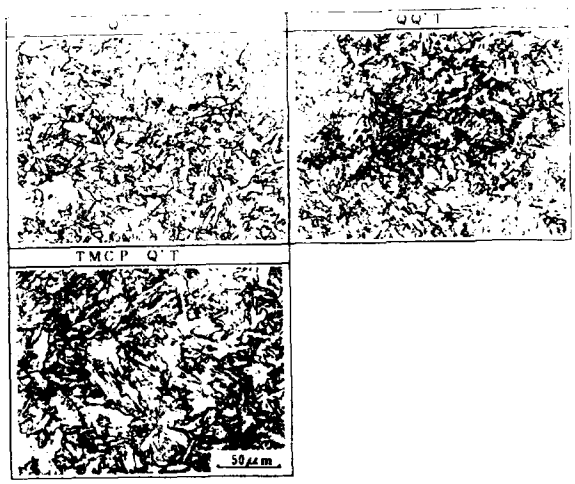


Fig. 5 Microstructures of QQ'T, TMCP-Q'T and conventional QT processed steel plates

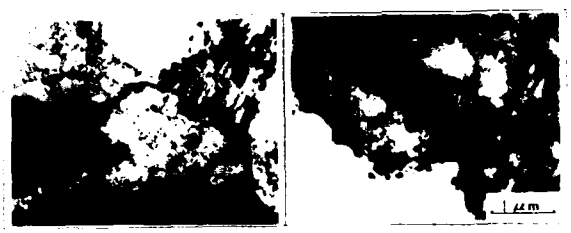


Fig. 6 Transmission electron micrographs of QQ'T processed steel plate

Table 3 Chemical composition and manufacturing conditions of mill trial steel plates

| | | | | | | | | wt% | | | |
|---|---|---|---|---|---|---|---|---|---|---|---|
| t mm | C | Si | Mn | P | S | Cu | Ni | Cr | Mo | V | Ceq |
| 80 | 0.13 | 0.25 | 1.44 | 0.012 | 0.002 | 0.21 | 0.20 | 0.08 | 0.17 | 0.04 | 0.45 |

Manufacturing conditions
tempering temp.: QQ'T ; 580℃, TMCP-Q'T ; 620℃, QT ; 600℃
Q' temp. : 780℃
TMCP condition : slab reheating temp. ; 1050℃
finish-rolling temp. ; 800℃
finish-cooling temp. ; <200℃

The examples of stress-strain curves of tested plates are shown in Fig. 8. The uniform elongation of QQ'T and TMCP-Q'T steel plates is improved up to 13~14 % in addition to low YR. On the other hand, the uniform elongation of conventional QT processed steel plate is about 9~10 %.

Figure 9 shows the tensile test results of small-size specimens sampled from seven locations in the thickness. The variation of YS, TS and YR of QQ'T and TMCP-Q'T steel plates in the thickness is much slighter compared with those of conventional QT one. Moreover, QQ'T and TMCP-Q'T steel plates achieves sufficiently low YR (YR<80%) at any location in the thickness. Despite heavy gauge steel plate, uniform mechanical properties of QQ'T steel plate are demonstrated by this mill trial.

Table 4 shows the results of drop weight test of QQ'T and TMCP-Q'T steel plates. Their NDT temperatures are -80 ℃ and -75 ℃ respectively. CTOD test results of QQ'T processed steel plate are shown in Fig. 10. It is shown that the CTOD value is larger than 0.6 mm even at -40℃.

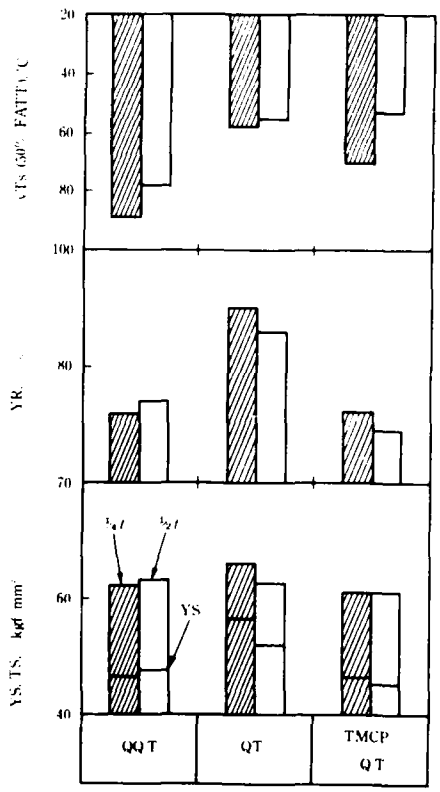


Fig. 7 Mechanical properties of QQ'T, TMCP-Q'T and conventional QT processed steel plates

As same as the tensile properties, sufficiently good properties as 60 kgf/mm² class steel plate with heavy gauge were obtained in both of drop weight test and CTOD test. The improvement of fracture toughness is attributed to refinement of microstructure and an increase of uniform elongation by Q' treatment. By this improvement of toughness, high strength steel plates with low YR can be applied not only to large scale steel-structures but also to other structures which are required high resistance against brittle fracture.

WELDABILITY OF QQ'T PROCESSED STEEL PLATES - Three types of welding and Tekken type Y-groove cracking test are performed for examination of the weldability of QQ'T steel plate.

Table 5 shows the welding conditions of Submerge Arc Welding (SAW) and $CO_2$-Gas Shielded Arc Welding ($CO_2$-GSAW). The heat input condition of SAW is 4.5 kJ/mm and that of $CO_2$-GSAW is 2.5 kJ/mm respectively. Table 6 shows the welding conditions of Electro Slag Welding (ESW) under high heat input at 133 kJ/mm. SAW and $CO_2$-GSAW are generally employed for construction of steel structures. ESW with high heat input is employed for construction of large scale steel structures using heavy gauge steel plates.

Table 7 shows the results of tensile test, Charpy-impact test and maximum hardness of SAW and $CO_2$-GSAW welded joints. Tensile strength and Charpy absorbed energy at 0 ℃ ($vE_0$) are high

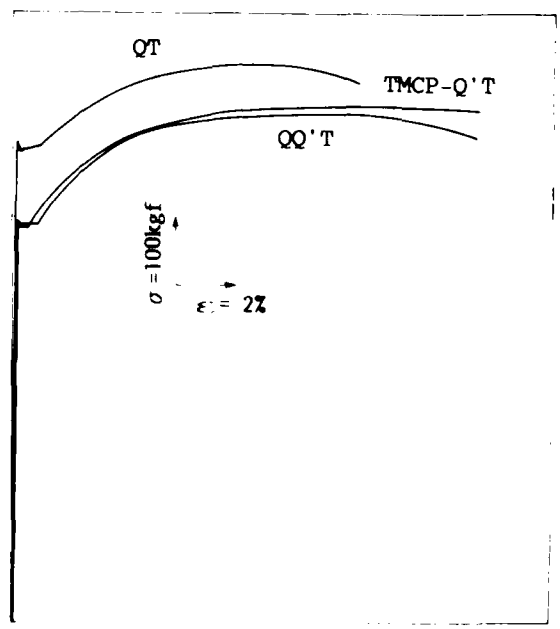


Fig. 8 Stress- strain curves of QQ'T, TMCP-Q'T and conventional QT processed steel plates (specimen : d=4mm)

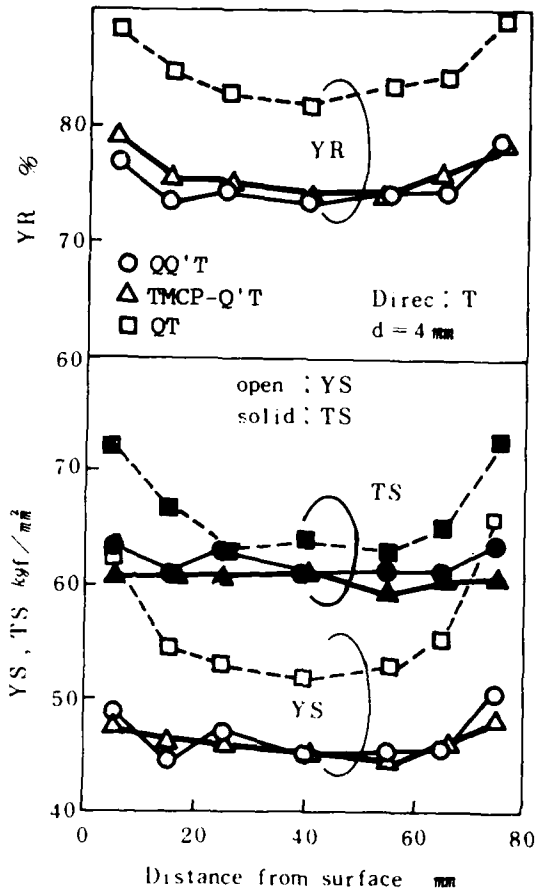


Fig. 9 Tensile properties of QQ'T, TMCP-Q'T and conventional QT processed steel plates

Table 4 Drop weight test results of QQ'T and TMCP-Q'T processed steel plates

| Process | Specimen | Direc. | Position | NDTT (℃) |
|---|---|---|---|---|
| QQ'T | P-1 | T | Surface | -80 |
| TMCP-Q'T | P-1 | T | Surface | -75 |

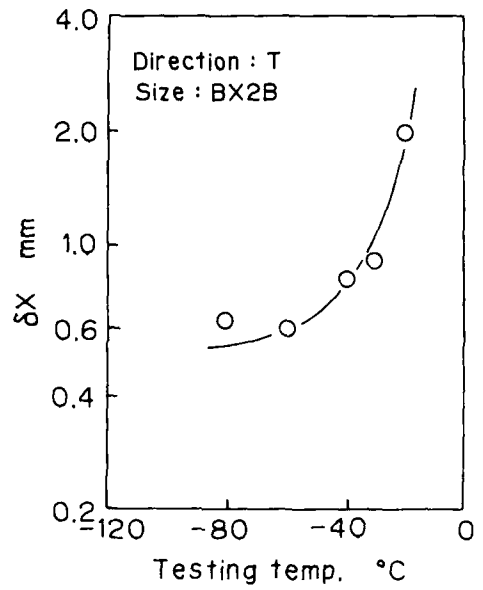


Fig. 10 CTOD test results of QQ'T processed steel plate

Table 5 Welding conditions of SAW and $CO_2$- GSAW

SAW

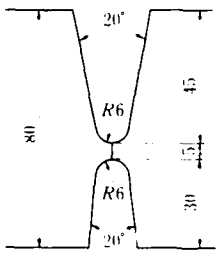


| | |
|---|---|
| Welding materials | US 49 (4.8ϕ) MF 38 |
| Preheat temp. | 150 °C |
| Interpass temp. | 150 ~ 200 °C |
| Arc voltage | 33 V |
| Welding current | 680 A |
| Speed | 300 mm min |
| Heat input | 4.5 kJ mm |
| B. side : 18 passes, 13 layers | |
| F. side : 16 passes, 10 layers | |

$CO_2$ GSAW

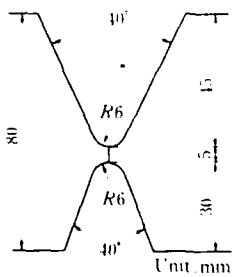


| | |
|---|---|
| Welding materials | MG 60 (1.2ϕ) 100 % $CO_2$ |
| Preheat temp. | 150°C |
| Interpass temp | 150 ~ 200 °C |
| Arc voltage | 37 V |
| Welding current | 310 A |
| Speed | 280 mm min |
| Heat input | 2.5 kJ mm |
| B. side : 21 passes, 9 layers | |
| F. side : 25 passes, 9 layers | |

enough and satisfy the aimed value. Maximum hardness of $CO_2$-GSAW joint is Hv 257.

Table 8 shows the mechanical properties of ESW welded joints. The tensile strengthes are above 60 kgf/mm² and toughnesses of Weld Metal(WM) and Heat Affected Zone(HAZ) satisfy the aimed value. The minimum hardness of ESW welded joint is Hv 171.

Tekken type Y-groove cracking test is also shown in Table 7. Pre-heating temperature for preventing from weld-cold cracking is sufficiently low temperature below 100 ℃.

Both of the mechanical properties of SAW, $CO_2$-GSAW and ESW, and results of Y-groove cracking test are sufficient as the heavy gauge 60 kgf/mm² class steel plate.

Table 6 Welding conditions of ESW with high heat input

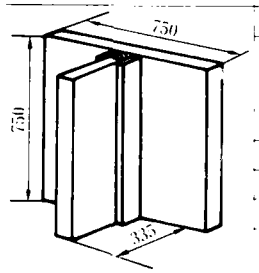


| | |
|---|---|
| Welding materials | US 49 (2.4ϕ) + MF 38 |
| Arc voltage* | 42 V |
| Welding current* | 450A |
| Speed | 17 mm/min |
| Heat input* | 133 kJ/mm |
| | *Two electrodes |

## CONCLUSION

The low YR steel plate with 60 kgf/mm² class tensile strength (TS>58 kgf/mm²) was developed on the basis of the investigations on the influences of heat treatment and TMCP conditions on YR. Test results obtained in this study are as follows.

(1) Ferrite which can easily initiate and multificate movable dislocations is effective to decrease YR. Both of low YR and high strength can be achieved by controlling bainitic microstructure with ferrite.

(2) The Q' heat treatment at appropriate dual-phase temperature makes it possible to obtain the desirable mixed microstructure. It was confirmed that low YR 60 kgf/mm² class steel plates can be produced by QQ'T and TMCP-Q'T processes.

(3) Despite heavy gauge steel plates (80 mm thickness), stably high strength and low YR of QQ'T and TMCP-Q'T steel plates are demonstrated by a mill trial.

(4) In addition, uniform elongation, Charpy-impact properties and fracture toughness are improved by Q' treatment through refinement of microstructure.

Table 7 Mechanical properties of welded joints (SAW and $CO_2$-GSAW) and Y-groove cracking test result

| Welding method | Heat input J/mm | Tensile test TS kgf/mm² | Frac. posi. | Charpy impact test Posi. | $vE_0$ kgf·m WM | FL | HAZ | Maximum hardness Hv(10) | Y-groove cracking test ℃ |
|---|---|---|---|---|---|---|---|---|---|
| SAW | 4.5 | 65.4 | WM | 1/4t | 10.7 | 12.1 | 28.8 | 251 | |
| | | 65.4 | WM | 1/2t | 10.1 | 11.4 | 32.2 | | 100 |
| $CO_2$-GSAW | 2.5 | 66.2 | BM | 1/4t | 13.7 | 18.8 | 33.5 | 257 | |
| | | 66.9 | WM | 1/2t | 10.0 | 32.7 | 36.4 | | |

Table 8 Mechanical properties of high heat input welded joints (ESW)

| Tensile test Posi. | TS kgf/mm² | Frac. posi. | Charpy impact test Posi. | $vE_0$ kgf·m | Minimum hardness Hv(10) |
|---|---|---|---|---|---|
| X | 64.6 | BM | ① | 8.6 | |
| | 64.6 | BM | ② | 15.9 | >171 |
| X | 61.8 | WM | ③ | 14.2 | |
| | 62.3 | WM | | | |

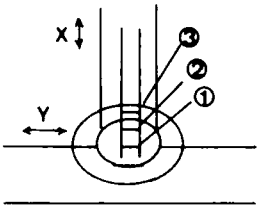

(5) Mechanical properties of welded joints of SAW, $CO_2$-GSAW, and ESW are sufficient as 60 kgf/mm² class tensile strength steel plates.

## REFERENCES


1) Sakuma,H et al. JISI, Vol.1, No.2, 351, (1988).
2) Kato,T. Seitetsu kenkyu. No.321, p.1-7(1986).
3) Tokuda,T. Kinzoku. No.12, p.2-7, (1986).
4) Sato,K et al. Quarterly J.JWS, Vol.3, No.2, p.153-159, (1986).
5) Tagawa,H et al. Quarterly J.JWS, Vol.3, No.2, p.160-167, (1986).
6) Sato,K et al. Quarterly J.JWS, Vol.4, No.1, p.170-175, (1987).
7) Tagawa,T et al. JISI, Vol.67, No.13, S1337, (1981).
8) Shikanai,N et al. JISI, Vol.73, No.4, S345, (1987).
9) Fukuda,Y. NIKKEI ARCHITECTURE. No.3/23, p.158-162, (1987).
10) Kokozo J. No.10, p.1, 28(1986)
11) Kagawa,H et al. JISI, Vol.1, No.2, 350, (1988).
12) Shikanai,N et al. JISI, Vol.73, No.13, S1312, (1987).

# COHERENT AND INCOHERENT PRECIPITATION FORMED DURING HOT PROCESSING AND PLATES AND STRIPS IN HSLA STEELS

**V. Leroy, J. C. Herman**
Centre de Recherches Metallurgiques, rue E. Solvay
11 B-4000 Liege, Belgium

It is now well accepted that grain refinement and precipitates size distribution play an important role in determining the mechanical properties of high strength microalloyed steels. As far as precipitation is concerned, the particle size distribution in the as-rolled condition is influenced by the thermo-mechanical parameters as well as steel composition (1 - 2 - 3 - 4).

After solid solution treatment during slab reheating, it is possible to form precipitates in the metallic matrix at each stage of the whole hot processing treatment; precipitates differ from one another in shape, size, distribution and interfacial energy according to the temperature at which they are formed (5).

In this problem, it is usual to make a distinction between :

- undissolved particles after reheating which contribute to prior austenite grain size control,
- the strain induced precipitation formed during hot deformation which controls to some extent the austenite recrystallisation process,
- the transformation induced precipitation which is formed at the $\gamma/\alpha$ transformation and appears random or aligned in the transformation interface
- the low temperature precipitation observed in the transformation products such as ferrite or acicular ferrite. This latest precipitation is formed at lower temperature during cooling, coiling or tempering.

It is generally accepted that strain or transformation induced precipitations formed at high temperature are incoherent with the metallic matrix and control the recrystallisation and grain growth of austenite or transformed ferrite. On the contrary, precipitates formed at lower temperature are coherent with the parent matrix and consequently such precipitation is particularly suited for improving tensile properties of the product in the as-rolled condition.

In addition, it may be assumed that the balance between incoherent and coherent fractions will be closely related to steel composition and processing parameters such as hot deformation temperature, cumulative strain and interpass time in the finishing mill, accelerated cooling on the run-out table and coiling temperature.

In a previous paper (6), we have shown how it is possible to quantify the influence of some processing parameters on the incoherent-coherent precipitation balance in the case of Ti bearing HSLA steels. This evaluation was mainly based on chemical analysis of selective electrolytic dissolved specimens previously deformed in a multi-pass hot compression testing equipment and quenched at different steps of the hot processing cycle.

This study has shown that finishing temperature near 950°C combined with large cumulative strain and longer interpass time increase the strain induced incoherent precipitation for Ti HSLA steels. Reducing the $\gamma/\alpha$ transformation temperature, for example by adjusting the steel composition, or increasing the cooling rate change part of the precipitation from incoherent to coherent type. In addition, it was shown that the hardening effect of the coherent Ti carbide precipitation is equal to 3000 MPa/%, what is rather in good agreement with theoretical evaluation.

The present study is mainly aimed to extend the work to the case of Nb microalloyed steels in view to quantify the kinetics of both incoherent and coherent precipitations. It is also intended to define the influence of some processing parameters as well as steel composition

## EXPERIMENTAL

The compositions of the steels used in this study are listed in table I. These materials were produced as vacuum induction melted laboratory ingots. After homogeneisation at 1200°C, the ingots were hot forged to plates 25 mm thick which were air cooled to room temperature.

Test specimens for hot deformation study were cylinders (20 mm in diameter, 20 mm in height) removed from the hot forged plates.

Simulation of the different thermomechanical process were carried out in compression on a TMT-S equipment (Thermo Mechanical Treatment-Simulator). This equipment based on a computer controlled MTS hydraulic machine performs multi-pass compression tests (strain rate $\dot{\varepsilon}$ = 30 $s^{-1}$ max, interpass time tip = 0.1 s min). The deformation law (strain rate versus strain) is adapted at each deformation step according to the simulated rolling schedule. Glass lubricant is applied to reduce friction and barrelling. A high speed manipulator is used for positioning test specimens equipped with thermocouple inserted in the mid-section. The transfer of specimens between the reheating furnace, the compression testing equipment, the cooling device (1 to 100°C/s) and the coiling furnace is made by means of the same manipulator. At any step of the thermomechanical cycle, the sample may be water quenched within 1 second for precipitation analysis. The amount of incoherent precipitates in test specimens is measured by selective electrolytic dissolution (15% KBr, 4% citric acid, pH = 2, - 0.150 V/SCE) of the metallic matrix, filtration on a millipore membrane with a rated pore size of 250 Å, alkaline fusion of filter residues and ICP analysis. For any quenched test specimen, the coherent fraction related to any microalloying element is assumed to be equal to the difference between the total soluble content as measured after reheating treatment and the measured incoherent fraction.

The precipitation hardening effect is deduced from hardness measurement made at the thermocouple location and expressed in terms of tensile strength after correction for grain size variation made by OTM 720.

## RESULTS AND DISCUSSION

KINETICS OF PRECIPITATION DURING HOT PROCESSING - After reheating at 1200°C, Nb steel 23 specimens were hot deformed with a constant deformation schedule (ε : 5 x 0.20 - $\dot{\varepsilon}$ = 2 $s^{-1}$ - tip = 2s). Figure 1 gives the evolution of incoherent precipitation as measured in test specimens quenched at different steps of the processing cycle. The deformation temperature was respectively 1075 and 950°C in these tests. For comparison purpose, the same figure gives the dependence of the incoherent Ti carbide fraction as measured in a previous work (6) for a Ti-steel (steel 12).

These results show that no precipitation is observed during cooling (1.5°C/s) from the reheating temperature to the start of hot deformation. As soon as deformation is applied, incoherent precipitation is detected which, for such reason, is called "strain induced precipitation". For both steels, it appears clearly that this strain induced precipitation increases by lowering the deformation temperature.

During cooling from finishing temperature to the $\gamma/\alpha$ transformation temperature the incoherent precipitation does not progress or just a few. Depending on deformation temperature (and other parameters to be precised later on), the kinetic of precipitation changes drastically within the transformation gap (750-700°C); the larger difference in terms of "transformation induced precipitation" is observed for Ti-steel. No more evolution is observed during additional cooling down to room temperature.

Table I - Chemical analysis of experimental steels $10^{-3}$%

| Index | Steel | C | Mn | Si | S | P | Al | $N_2$ | Nb | Ti |
|---|---|---|---|---|---|---|---|---|---|---|
| 23 | Ref Nb | 68 | 1090 | 195 | 6 | 4 | 40 | 2.9 | 45 | |
| 27 | Nb | 73 | 1015 | 150 | 1 | 4 | 40 | 0.1 | 43 | |
| 28 | Nb | 65 | 1055 | 190 | 1 | 5 | 40 | 1.7 | 44 | |
| 29 | Nb | 70 | 1070 | 95 | 1 | 4 | 38 | 4.8 | 52 | |
| 24 | Low Mn Nb | 68 | 320 | 187 | 5 | 4 | 40 | 4.4 | 43 | |
| 25 | Low C Nb | 38 | 1170 | 207 | 4 | 5 | 38 | 4.2 | 45 | |
| 26 | Low C Nb | 33 | 1010 | 170 | 1 | 4 | 34 | 0.1 | 49 | |
| 12 | Ref Ti | 79 | 1110 | 208 | 4 | 23 | 36 | 5.7 | 1 | 170 |
| 21 | Low Mn Ti | 69 | 290 | 195 | 5 | 4 | 47 | 4.2 | | 114 |
| 22 | Low C Ti | 41 | 1110 | 198 | 5 | 5 | 43 | 4.6 | | 115 |

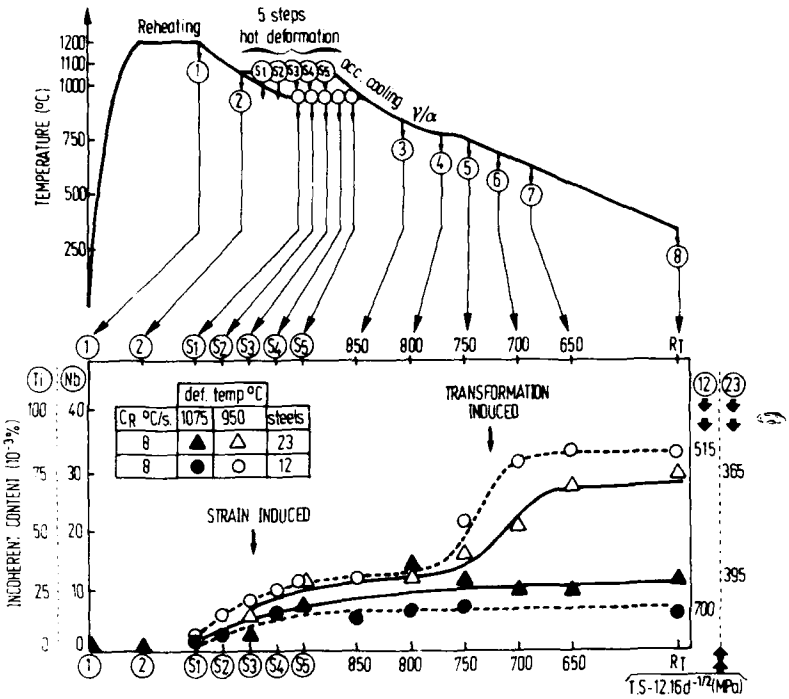


Fig. 1 - Kinetic of incoherent precipitation in Nb and Ti HSLA steels. Influence of deformation temperature.

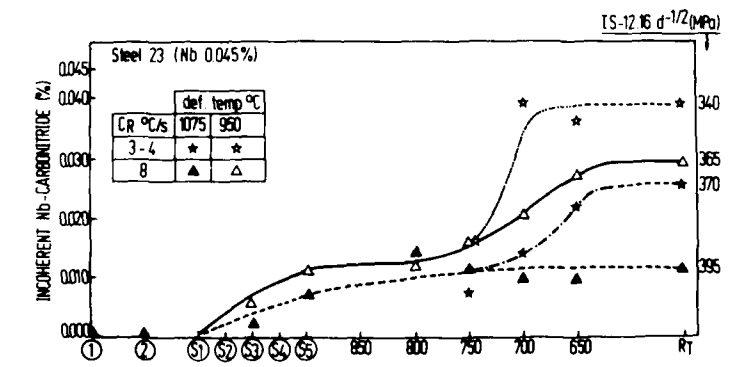


Fig. 2 - Kinetic of incoherent precipitation in Nb steel. Influence of cooling rate and deformation temperature.

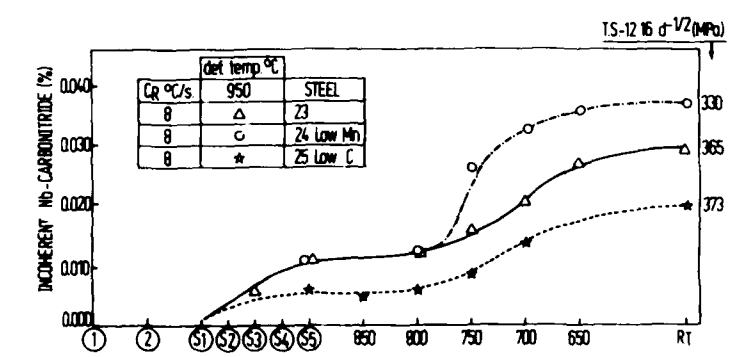


Fig. 3 - Kinetic of incoherent precipitation in Nb steels. Effect of steel composition (C, Mn).

At the same figure are reported the tensile strengths corrected for grain size ($TS - 12.16\ d^{-1/2}$) of the as-rolled products which appear to be inversely correlated to the incoherent precipitation fraction.

EFFECT OF COOLING RATE AND STEEL COMPOSITION - The same procedure was applied to Nb steel (23), low Mn-Nb steel (24) and low C-Nb steel (25) for which the total Nb content is approximately constant. Figure 2 gives for steel 23 the dependence of the incoherent carbo-nitride precipitation as measured for two different deformation temperatures and two different cooling rates.

The previous conclusion holds for all experimental conditions and it is observed in addition that an increase in cooling rate lowers the incoherent fraction measured on the end product.

As far as steel composition is concerned, it is clearly observed in figure 3 that lowering the manganese content (steel 24) results in an increase of the incoherent fraction due to the fact that the $\gamma/\alpha$ transformation temperature is higher for this steel.

It may be concluded that the effectiveness of the cooling treatment to promote coherent precipitation is increased when the $\gamma/\alpha$ transformation occurs at lower temperature what can also be related to the state of the strained austenite.

Comparing the reference Nb steel (23) to the low C-Nb steel (25), it is also evident that the amounts of strain induced precipitation as well as transformation induced precipitation are lower for the low C-Nb steel, owing to the limited niobium sursaturation in strained austenite and in ferrite.

In this respect, it is generally assumed that incoherent and coherent precipitation are carbo-nitride in the case of Nb HSLA steels. We have tried to check this assessment for strain induced precipitation by quenching test specimens with different Mn, C and N contents after a same reheating treatment (1200°C) and hot deformation process (950°C - $\varepsilon = 5 \times 0.20$ - $\dot{\varepsilon} = 2\ s^{-1}$ - tip = 2s).

Figure 4 gives the dependence of the strain induced precipitation as a function of the total nitrogen content for reference Nb steels, low Mn Nb steels and low C Nb steels. These results show clearly how nitrogen promotes the formation of the incoherent strain induced precipitation formed at rather high temperature; from such results, it can be also anticipated that nitrogen would lower the formation of coherent fraction responsible for steel hardening, as we discuss hereafter.

HARDENING DUE TO COHERENT PRECIPITATION - The amount of coherent precipitation in the end product is derived from the measurements of both the soluble content after

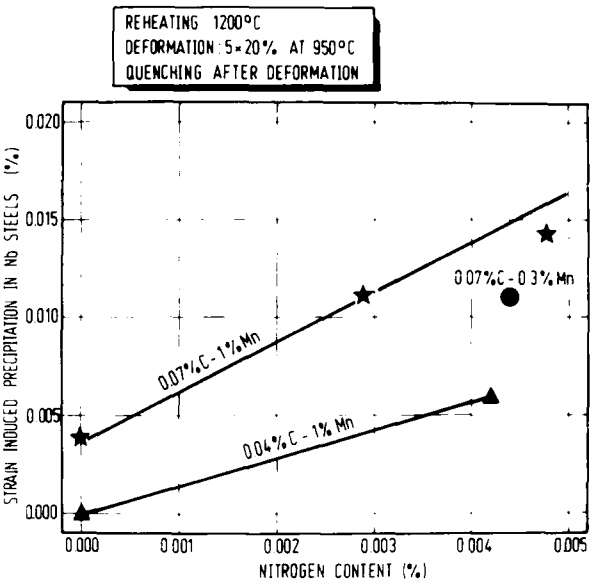


Fig. 4 - Effect of nitrogen and carbon contents on strain induced precipitation in Nb-steels.

reheating and the incoherent fraction in the as-rolled material. It is interesting to correlate this coherent fraction whith the precipitation hardening measured for the different test specimens processed in the present work.

Mixing all the results, taking into account the solid solution hardening due to actual Mn and Si contents as well as the phase hardening due to different perlite content (as measured by QTM 720), it is possible to deduce a mean precipitation hardening value equal to 2200 MPa/% for the coherent Nb carbo-nitride precipitation, as shown in figure 5.

It is interesting to observe that, in a previous work, the precipitation hardening coefficient of the coherent precipitation was measured equal to 3000 MPa/% for Ti-HSLA steels (6).

Such values are in good agreement with ASHBY-OROWAN theoretical assessments of maximum hardening effect due to optimized random distribution of particles 20-40 Å in diameter (7).

In conclusion, it appears that precipitation hardening is mainly improved by the increase of the coherent fraction which, in turn, is depending on deformation temperature, interpass-time during hot-rolling, cooling rate at the transformation temperature and chemical composition (C-N-Mn) of steels.

With respect to steel composition, the influence of carbon and manganese contents on mechanical properties in the as rolled condition, is well known; it is

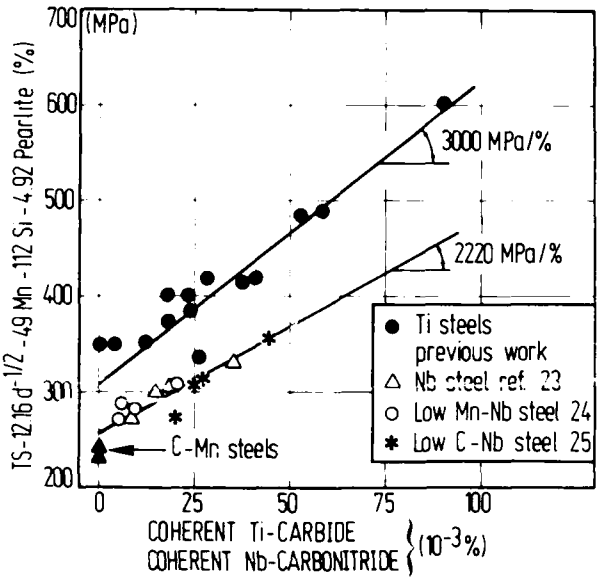


Fig. 5 - Hardening due to coherent precipitation in Nb and Ti HSLA steels.

perhaps more interesting to focus in some more details on the influence of nitrogen.

Figure 6 gives the tensile strength as a function of hot deformation temperature for several Nb steels with variable nitrogen content (reheating 1200°C - deformation schedule as above - cooling to room temperature). For both low and normal carbon contents, one observes that a reduced nitrogen content results in higher tensile strength for as-rolled steels. This effect is in qualitative agreement with the reduced formation of incoherent precipitation due to a lower nitrogen content (fig. 4). However the tensile strength increase is greater than it could be deduced by just transforming part of the incoherent fraction in a coherent precipitation taking into account a hardening coefficient equal to 2200 MPa/%. It probably means that the hardening coefficient of coherent precipitation could be greater for carbide than for carbo-nitride.

EFFECT OF ACCELERATED COOLING RATE - To investigate the possibilities of accelerated cooling on the run-out table of a hot strip mill, the preceding work has been extended to cooling rate ranging from 8 up to 80°C/s in the case of both Nb and Ti bearing steels.

The reheating temperature and hot deformation schedule were kept constant as in the here-above work, except for the deformation temperature equal to 900°C. The influence of cooling rate on the tensile strength is reported in figure 7 for all the steels.

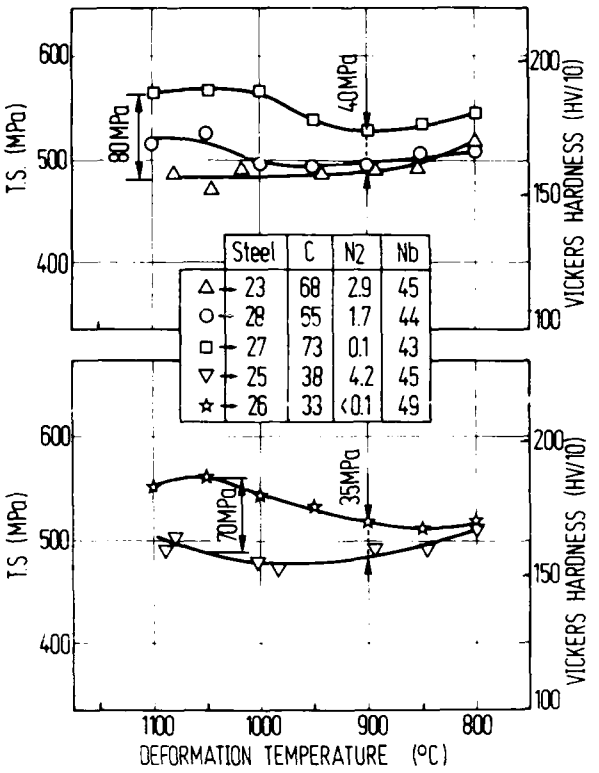


Fig. 6 - Effects of deformation temperature and nitrogen content on the resistance of Nb-steels. Reheating : 1200°C, deformation : 5 x 20%-tip : 2s, cooling rate : 3-4°C to room temperature.

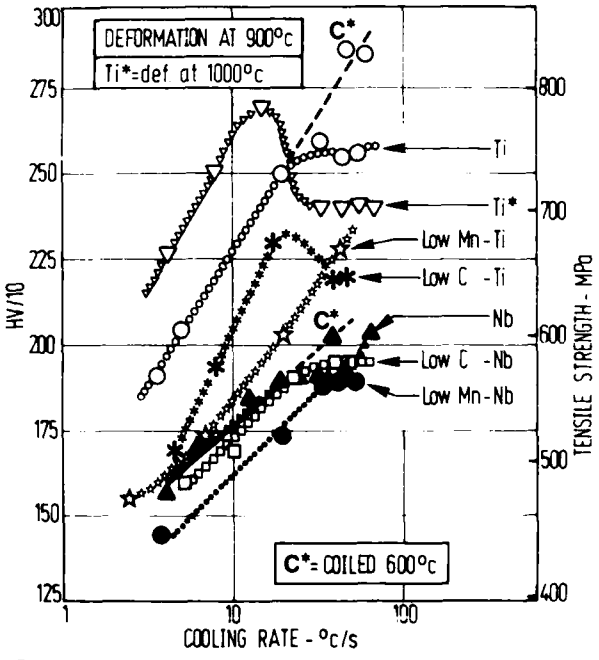


Fig. 7 - Effect of cooling rates on tensile strength of Nb and Ti HSLA steels cooled down to room temperature [except C* coiled at 600°C].

As expected, it appears that accclerated cooling increases the tensile strength as a consequence of a more extended coherent precipitation as well in Ti steels as in Nb HSLA steels. However experimental results show that for cooling rate in excess of 20°C/s, some distinction has to be made according to the manganese content of the steel.

For low Mn content, a continuous improvement of the tensile strength is observed for the whole range of cooling rates due to the precipitation change from incoherent to coherent (fig. 2) in a ferritic matrix.

On the contrary in a high Mn steel, as soon as the cooling rate reaches a value equal to 20°C/s, the tensile strength remains constant or even decreases for low C Ti steels cooled down to room temperature (fig. 7).

For such high Mn steel, it is quite evident that higher cooling rate causes acicular ferrite or bainite to replace progressively polygonal ferrite-perlite microstructure. This change in microstructure can certainly not justify the levelling or even the drop observed in the dependence of tensile strength on the cooling rate. For such reasons, we reach the conclusion that the strengthening due to bainite formation compete with an important loss in precipitation hardening. In fact, coherent precipitation is suppressed at cooling rates in excess of a critical value what, in turn, means that microalloying addition is retained in solid solution (4) for such bainitic microstructures.

As shown in figure 7, this reduction in precipitation hardening is more effective in Ti-bearing steels especially when deformation is performed at higher temperature (1000°C).

EFFECT OF COILING AFTER ACCELERATED COOLING - If part of alloying addition is retained in solid solution, it can be foreseen that a new hardening will be observed during subsequent tempering treatment such as self-tempering after interrupted cooling for plates or coiling for hot strips. This effect is shown in figure 7 for reference Nb and Ti steels after coiling at 600°C. The coiling treatment results in a tensile strength increase of 80 MPa for Ti steels hot deformed at 900°C and cooled to the coiling temperature at a rate of 60°C/s. This effect is not so important for Nb steel processed in the same condition as shown in the same figure.

In addition to that, it is also important to note that the effect of coiling is hardly depending on the coiling temperature. Coiling at high temperature after accelerated cooling will induce precipitation of alloying element as incoherent particles in the metallic matrix what in turns reduces the precipitation hardening : this new precipitation could be called "secondary incoherent precipitation".

Figure 8 gives the dependence of the incoherent Nb carbo-nitride content as measured for the reference Nb steel hot deformed at 900°C and cooled respectively down to room temperature or coiled at 650 or 680°C. This graph shows again how an increased cooling rate reduces the incoherent precipitation for test specimens cooled down to room temperature. Coiling at 650°C does not change the amount of incoherent precipitation. On the contrary, coiling at 680°C results in an increased amount of incoherent precipitation what is related to the formation of secondary incoherent precipitation during coiling at higher temperature.

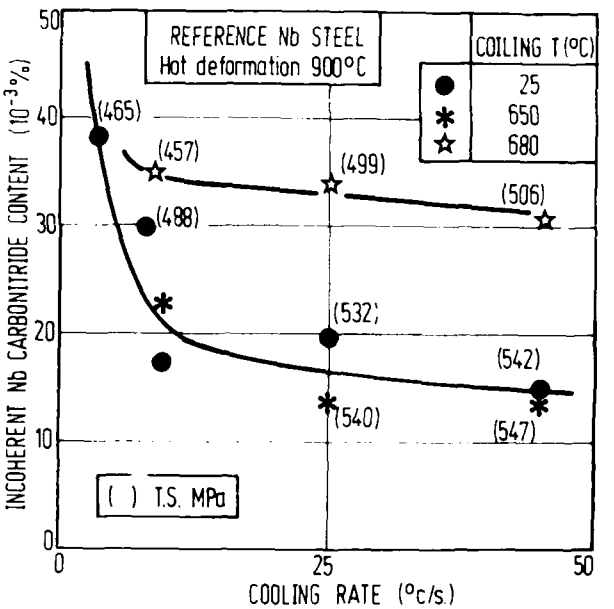


Fig. 8 - Influence of cooling rate and coiling temperature on incoherent precipitation for Nb steels deformed at 900°C.

Due to this additional precipitation, one observes that the tensile strength is lowered as shown by experimental results reported in the same figure. Based on a hardening coefficient equal to 2200MPa/% for coherent precipitation (fig. 5), it is interesting to note that the transformation of an amount equal to 20 $10^{-3}$% Nb carbonitride from the coherent to incoherent type must induce a drop of 40 MPa in tensile srength : this computed value is in good agreement with experimental data reported in the same figure.

## SUMMARY AND CONCLUSIONS

The present study was mainly aimed to determine the influence of processing parameters such as hot deformation temperature, cooling rate, coiling temperature and steel composition on the incoherent-coherent precipitation balance in HSLA steels.

The main conclusions may be summarized as follows :

1. Strain induced precipitation is clearly observed in Nb and Ti bearing steels, especially for deformation temperature around 950°C.
2. Transformation induced precipitation is formed during cooling to room temperature for cooling rates ranging between 4 and 10°C/s.
3. Strain and transformation induced precipitations are assumed to be incoherent with the parent metallic matrix.
4. Increasing the cooling rate results in a decrease of the transformation induced precipitation; in such conditions, coherent precipitation is now found in the saturated ferrite. For high cooling rate (20-80°C/s), as soon as acicular ferrite or bainitic structure are formed, there are some evidences that coherent precipitation does not appear anymore during cooling down to room temperature. It is assumed that the microalloying addition is retained in solid solution; this effect appears more clearly in Ti-bearing steel.
5. Coiling at low temperature (600°C) of accelerated cooled steels results in a very efficient hardening due to coherent precipitation; this effect is more limited in Nb steels as regards to Ti-steels. At higher coiling temperature (680°C), the hardening effect is lower due to the formation of a secondary incoherent precipitation.
6. In the experimented steels, the hardening coefficient of coherent precipitates is measured to be equal to 2200 or 3000 MPa/% respectively for Nb or Ti-bearing steels what seems to be in agreement with theoretical prediction for such precipitation.
7. As regards to steel composition, the Mn content plays a very important part owing its influence on the transformation temperature which in turns influences the amount of transformation induced precipitation. Experimental data show in addition that a low nitrogen content decreases the incoherent strain induced precipitation in Nb-bearing steels.

## ACKNOWLEDGEMENT

This research has been carried out with a financial support of IRSIA (the Belgian Institute for the Encouragement of Scientific Research in Industry and Agriculture) and under the sponsorship of ECSC (the European Coal and Steel Community).

## REFERENCES

1. Thermomechanical processing of microalloyed austenite, Proc. AIME Meeting, Pittsburgh 1981, Ed. A.J. DeArdo, G.A. Ratz, P.J. Wray.

2. DeArdo, A.J.; Gray, J.M. and Meyer, L., Niobium. Proceeding of the International symposium, Niobium Products Co Ltd, Pittsburgh 1981.

3. Lebon, A. et al, Metals Science, 9, 36 (1975).

4. Jonas, J.J. et al, Metals Science, 13, 238 (1979).

5. Burke, M.G.; Cuddy, L.J.; Piller; J. and Miller, M.K., Combined APFIM-TEM study of Nb(CN) precipitation in HSLA steels., ' terials Science and Technology, vol. 4, 113 (Feb. 1988).

6. J.C. Herman and V. Leroy, Incoherent and coherent precipitations induced by hot deformation and accelerated cooling in HSLA steels, Thermec 88, Tokyo, June 1988.

7. T. Gladman, D. Dulieu and I.D. Mc Ivor, Microalloying 75, M. Korschinsky et al, Ed. Union Carbide Corporation, New York, 1977.

# EFFECT OF NIOBIUM ON THE FORMATION OF M-A CONSTITUENT AND HAZ TOUGHNESS OF STEEL FOR OFFSHORE STRUCTURES

**Hiroaki Tsukamoto, Shigeru Endo, Masataka Suga**
Steel Research Center
NKK Corporation
Fukuyama, Japan

**Kazuaki Matsumoto**
Steel Research Center
NKK Corporation
Kawasaki, Japan

Abstract

The effect of Nb addition on the mechanical property in base metal and heat affected zone (HAZ) of steel plates for offshore structures manufactured with TMCP process was investigated. Nb deteriorates the HAZ toughness in as-welded condition through the formation of Martensite-Austenite (M-A) constituent. The toughness recovers with post weld heat treatment (PWHT). It is considered that the formation of M-A constituent with Nb addition is due to lowering of transformation temperature with the presence of solute Nb during welding. It is necessary to utilize Nb for the increase of strength and toughness in base metal, especially the strength after PWHT. Even small amount of Nb (ex. 0.01%) is effective for grain refinement and precipitation hardening. It is also effective to reduce Nb and carbon content (or carbon equivalent) for the prevention of the formation of M-A constituent. TS 500MPa grade (BS4360-50E Mod.) steel plate manufactured with TMCP process with the chemical composition of low C-Cu-Ni-low Nb(0.01%) has high strength and good toughness in base metal, and also good toughness in HAZ of submerged arc welding(SAW) with the heat input of 50kJ/cm.

AS ALREADY KNOWN[1] , Nb is effective for improving the strength and toughness of TMCP steel because Nb delays the recrystallization of deformed austenite grains and leads to grain refinement, and also has the precipitation hardening effect with carbide or carbo-nitride. So that, Nb is often used in linepipe steel, high strength steel plates for shipbuilding, steel plates for offshore structures with high strength and heavy gauge, and so on.

On the other hand, steel plates for structures in deep sea and cold water, such as in Arctic Ocean, require high toughness not only in base metal but also in heat affected zone (HAZ) of welded joint. The criterion of HAZ toughness, especially in crack tip opening displacement (CTOD) test, has become severe recently. For example, API RP 2Z[2] prescribes the CTOD test in HAZ in preproduction qualification weldability test, where the fatigue crack should be placed in coarse-grain HAZ material for at least 15% of specimen thickness. It is already known that the toughness in intercritically reheated coarse-grain HAZ deteriorates greatly owing to the Martensite-Austenite(M-A) constituent formed in coarse grains[3] . Therefore the effect of Nb on the formation of M-A constituent during welding and on the HAZ toughness in weldment was investigated.

## EXPERIMENTAL PROCEDURE

Firstly, the effect of Nb contant on the strength and toughness in base metal of TMCP steel was examined. The chemical composition of steel tested is shown in Table 1.
They were melted with 150kg vacuum remelting furnace in laboratory. Then they were reheated at 1000°C or 1100°C, and controlled rolled with the rolling mill in laboratory. 70% reduction below 820°C (1000°C soaking) or below 850°C (1100°C soaking) was done, and rolling was finished at 780°C with 25mm thickness. They were accelerated cooled just after rolling with the cooling equipment at the cooling rate of 4°C/sec. simulating the mid-thickness of 100mm thick plate. Then tensile and Charpy impact test was carried out.

Table 1 Chemical composition of TMCP steels manufactured in laboratory for the test of base metal wt.%

| C | Si | Mn | P | S | Cu | Ni | Nb | Ti | Sol Al | T N | $Ceq^{LR}$ |
|---|---|---|---|---|---|---|---|---|---|---|---|
| 007 | 030 | 149 | 0009 | 0001 | 020 | 041 | 0 | 0006 | 0027 | 00026 | 036 |
| ∫ | ∫ | ∫ | ∫ | ∫ | ∫ | ∫ | ∫ | ∫ | ∫ | ∫ | ∫ |
| 008 | 033 | 152 | 0012 | 0003 | 022 | 043 | 0033 | 0010 | 0034 | 00036 | 038 |

Secondly, the effect of chemical composition on the HAZ toughness was investigated. The chemical composition of steel tested is shown in Table 2. All of them are TS 500MPa grade steel plates manufactured with basic oxygen furnace(BOF) - continuous casting (CC) process. Steel A is a Nb free TMCP steel. Steel B and D are TMCP steels with small amount of Nb (approximately 0.01%). Steel D has extremely low carbon equivalent compared with other TMCP steels A and B. Steel C is a normalized one with 0.03%Nb. In order to investigate the effect of Nb on the HAZ toughness with large heat input, Charpy impact and CTOD test were carried out on the weldment with submerged arc welding (SAW) at 100kJ/cm heat input. The groove is a single bevel one as shown in Fig.1 and the sampling position of impact and CTOD test specimens is shown in Fig.2.

Thirdly, Charpy impact test was conducted on simulated HAZ with induction heating simulator. The thermal cycle is shown in Fig.3 which is based on the cooling curve measured during SAW with the heat input of 100kJ/cm as shown in Fig.4.

Furthermore, M-A constituent was observed by scanning electron microscope (SEM) after two-stage electrolytic etching [4] and the area fraction of M-A constituent was measured on several photographs.

Finally, typical TS 500 MPa grade TMCP steel plate with heavy thickness was welded with 50kJ/cm heat input of SAW and CTOD test in coarse-grain HAZ was carried out.

Table 2 Chemical composition of TS 500MPa grade heavy thick steel plates for the test of HAZ toughness wt.%

| Steel | C | Si | Mn | P | S | Cu | Ni | Ti | Nb | $Ceq^{LR}$ | Process |
|---|---|---|---|---|---|---|---|---|---|---|---|
| A | 007 | 030 | 150 | 0009 | 0001 | 019 | 036 | 0010 | — | 0356 | TMCP |
| B | 006 | 032 | 156 | 0008 | 0001 | 025 | 041 | 0007 | 0009 | 0364 | TMCP |
| C | 010 | 040 | 155 | 0003 | 0002 | 017 | 027 | — | 0027 | 0384 | Nor |
| D | 006 | 032 | 145 | 0007 | Tr | 026 | 036 | 0009 | 0007 | 0343 | TMCP |

$$CeqLR=C+Mn/6+(Cr+Mo+V)/5+(Cu+Ni)/15$$

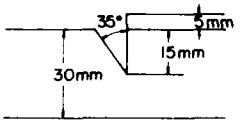


Fig.1 Groove configuration for SAW weldment

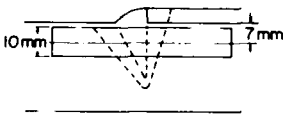


Fig.2 Sampling position of impact and CTOD test specimens

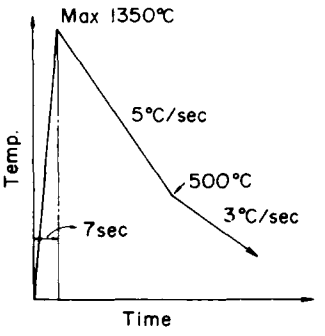


Fig.3 Thermal cycle for the simulation of SAW with the heat input of 100kJ/cm

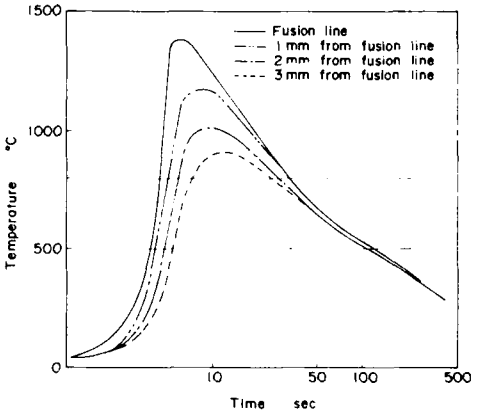


Fig.4 Thermal cycle during welding (SAW, 100kJ/cm)

## EFFECT OF NIOBIUM CONTENT ON THE MECHANICAL PROPERTY OF BASE METAL

Fig.5 shows the effect of Nb content and slab soaking temperature on the strength and toughness in base metal of 0.07/0.08%C-0.3%Si-1.5%Mn-0.2%Cu-0.4%Ni steel (Table 1) controlled rolled and accelerated cooled in laboratory. Both of strength and toughness increase with Nb addition, even with the content of 0.01%. Nb is especially effective to minimize the reduction of strength after PWHT. It is supposed to be due to precipitation hardening by Nb carbide. The strength and toughness level off with 0.01%Nb addition (1000°C soaking) or 0.02%Nb addition (1100°C soaking).

The microstructures with 1000°C soaking are shown in Fig.6. Microstructure of Nb free steel is composed of relatively coarse ferrite and pearlite. On the contrary, Nb added steel shows fine grains of ferritic and pearlitic structure, and small fraction of bainitic structure. The microstructure of 0.03% Nb steel is extremely fine.

The reduction of softening after PWHT with Nb addition is supposed to be owing to precipitation hardening which compensates the softening with the tempering effect of bainitic structure. The saturation of strength and toughness with 0.01% Nb addition (1000°C soaking) or 0.02% Nb addition (1100°C soaking) above mentioned can be explained with the solute Nb content during soaking before rolling which is calculated with the solubility product of Nb(CN) by Irvine.

$$\log[\%Nb][\%(C+12/14N)]=-6770/(T°C+273)+2.26 \quad ...(1)$$

That is, solute Nb content is estimated to be approximately 0.01% (at 1000°C) and 0.025% (at 1100°C).

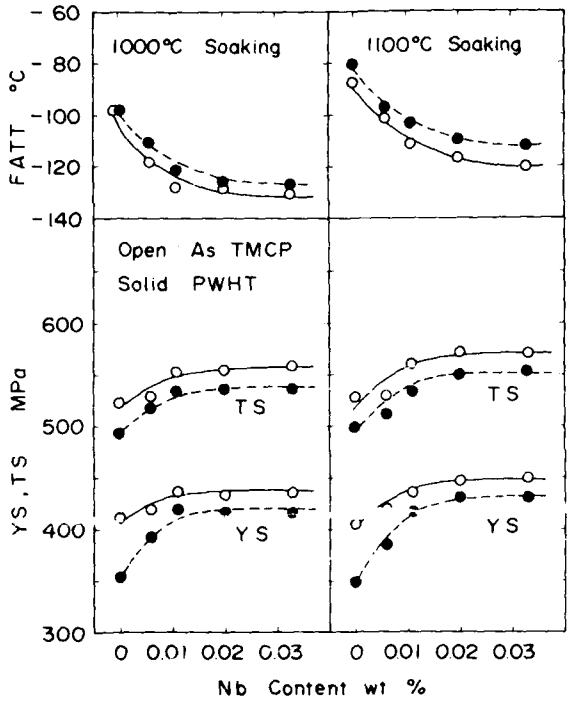


Fig.5 Effect of Nb content on the mechanical properties of base metal of TMCP steel plates (simulation of 100mm thickness)

The toughness with 1000°C soaking is better than 1100°C soaking due to grain refinement by unresolved precipitates which have pinning effect on austenite grain boundaries during slab soaking.

## MICROSTRUCTURE AND TOUGHNESS IN HAZ OF SAW WELDMENT

Microstructures in HAZ with SAW at the heat input of 100kJ/cm are shown in Fig.7. Microstructures on the fusion line of steel A (Nb free TMCP steel) and steel D (TMCP steel with 0.01% Nb and low carbon equivalent) are composed of upper bainite and ferrite on grain boundary. Those of steel B (TMCP steel with 0.01% Nb) and steel C (normalized steel with 0.03% Nb) are mainly upper bainite. Microstructures 3mm distant from fusion line of steel A, C and D are ferrite, pearlite and a small fraction of bainite. On the contrary, that of steel B is ferrite and bainite. Microstructures 5mm distant from fusion line are ferrite and pearite, which are almost the same as those of the base metal, but is supposed to have been reheated to $\alpha + \gamma$ region from the temperature measured during welding with the same welding condition.

FATT in Charpy impact test and CTOD value at -10°C in HAZ with SAW are shown in Fig.8 and Fig.9. The toughness on the fusion line of all the tested steels is the worst among all the test position. The toughness becomes better as the test position is apart from the fusion line.

Among the tested steels, normalized steel C with 0.03% Nb has the lowest toughness and TMCP steel D with 0.01% Nb and low carbon equivalent has the best toughness.

The relation between Nb content and the toughness on the fusion line is shown in Fig.10 and Fig.11. The increase of Nb addition enlarges the deterioration of HAZ toughness in as-welded condition. The toughness in Nb added steel recovers with PWHT. TMCP steel D containing 0.01% Nb and low carbon equivalent has relatively high toughness even on the fusion line in as-welded condition. There is no apparent correlation between Nb content and the toughness at the position 3mm and 5mm distant from the fusion line.

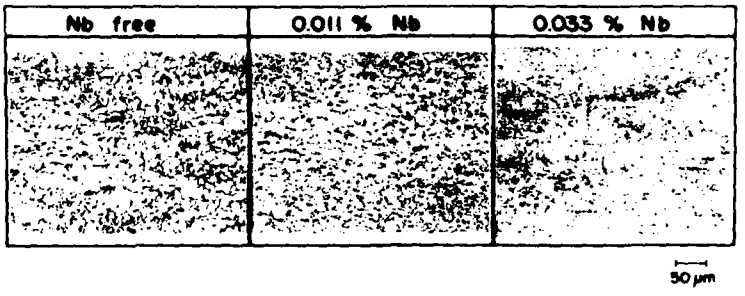


Fig.6 Effect of Nb content on the microstructure of TMCP steel (manufactured in laboratory, 1000°C soaking)

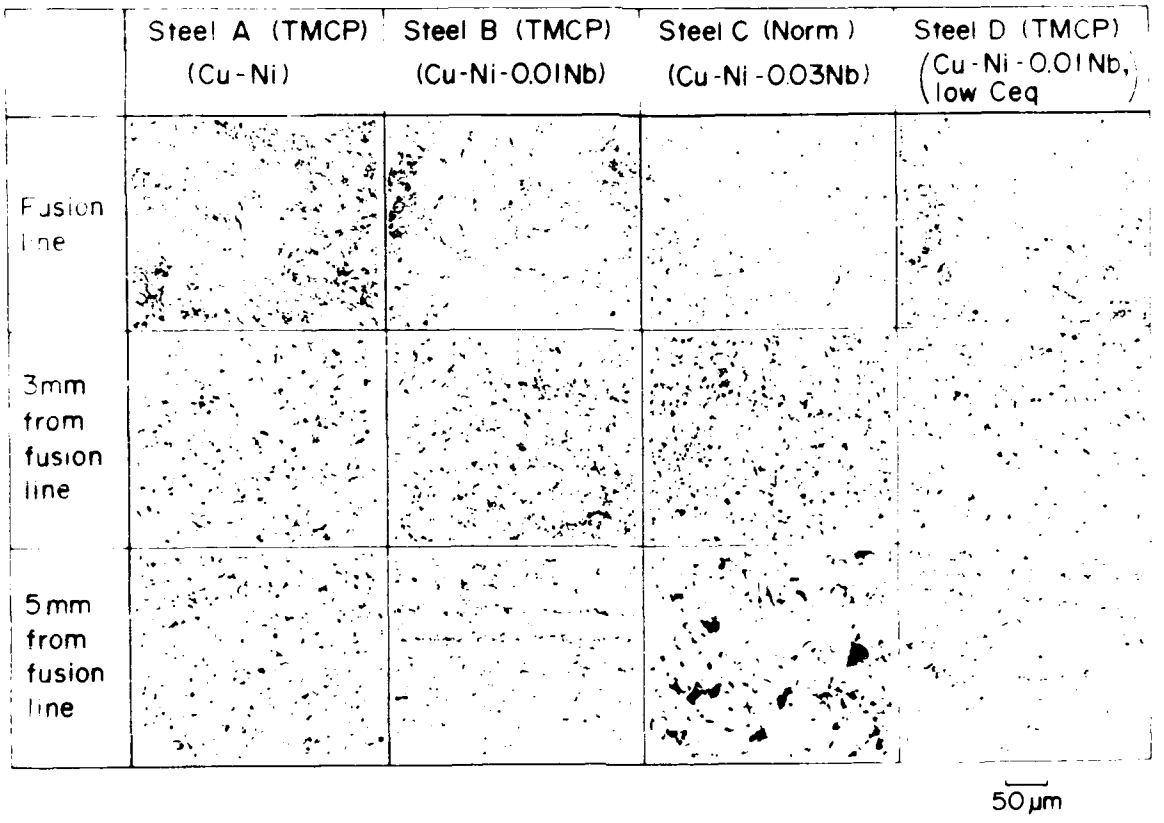


Fig.7 Microstructures in HAZ of SAW weldment (100kJ/cm)

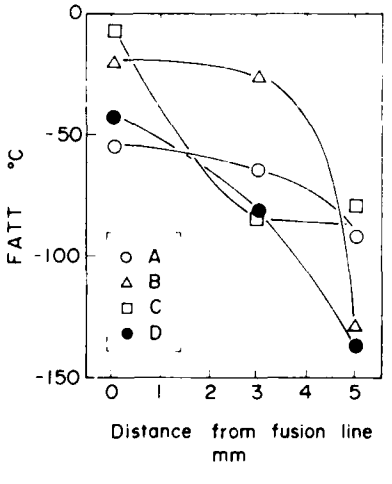


Fig.8 FATT in HAZ of SAW weldment (100kJ/cm, As welded)

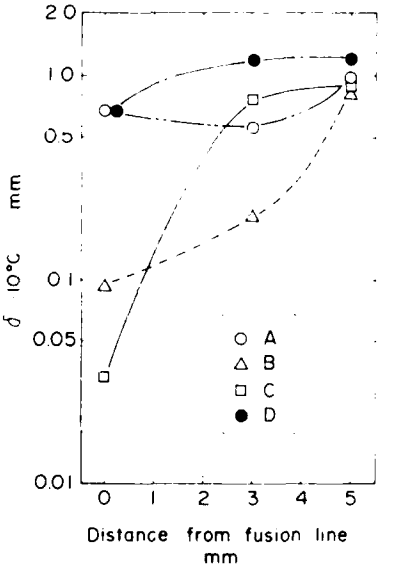


Fig.9 CTOD value in HAZ of SAW weldment (100kJ/cm, As welded)

## TOUGHNESS IN SIMULATED HAZ

Fig.12 shows the effect of peak temperature on the hardness and toughness of simulated HAZ. Peak temperature 1350, 900 and 800°C correspond to fusion line, 3mm and 5mm from the fusion line of SAW weldment respectively (Fig.4).

The toughness after 1350°C reheating is the worst and it becomes better as the peak temperature decreases. On the other hand, normalized steel C has the lowest toughness after 1350°C reheating. Those tendencies are the same as those in SAW weldment as above mentioned.

## M-A CONSTITUENT IN HAZ

Microstructures with SEM after two-stage electrolytic etching in SAW weldment are shown in Fig.13. White regions which are scarcely etched are supposed to be M-A constituent and deeply etched region is supposed to have contained cementite before etching [7]. Other regions are in ferrite grains.

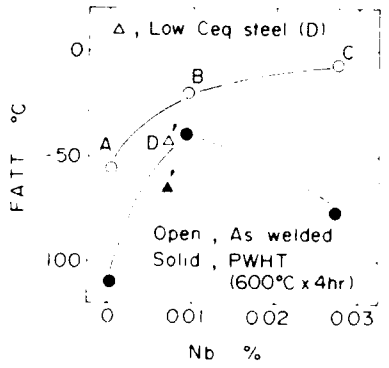


Fig.10 Relation between Nb content and the toughness on the fusion line of SAW (10kJ/cm, As welded and after PWHT)

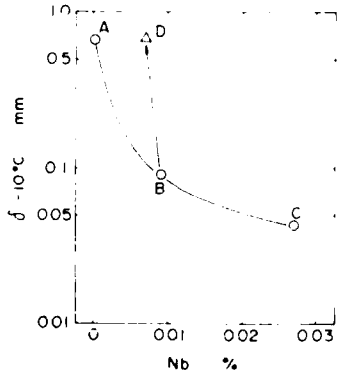


Fig.11 Relation between Nb content and the CTOD value on the fusion line of SAW (100kJ/cm, As welded)

The fusion line of steel B and C which have low toughness contain relatively high fraction of M-A constituent and steel A and D have only small fraction of M-A constituent. The area fraction of M-A constituent reduces as the position is apart from the fusion line. Although steel A,C and D contain little M-A constituent at the position 3mm distant from the fusion line, M-A constituent is still observed at the position 5mm distant from the fusion line of steel B.

Furthermore, the effect of the area fraction of M-A constituent which was measured on SEM photographs (Fig.13) on the HAZ toughness of SAW weldment is shown in Fig.14. There is the evident tendency that the toughness decreases as the area fraction of M-A constituent increases on the fusion line and also at 3mm distance from the fusion line. On the other hand, there is no correlation between M-A constituent and toughness at 5mm distance from fusion line where all the steels show relatively high toughness.

M-A constituent is supposed to be decomposed during PWHT because it is scarcely observed after PWHT.

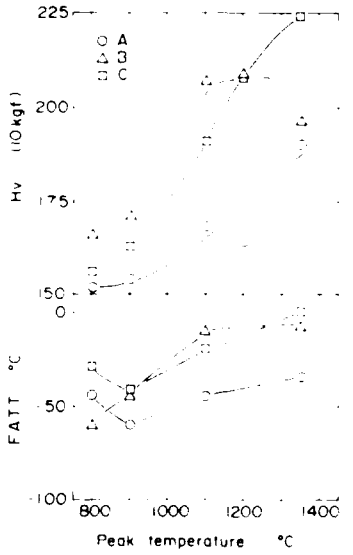


Fig.12 Effect of peak temperature on the hardness and toughness in simulated HAZ (simulation of 100kJ/cm, As welded)

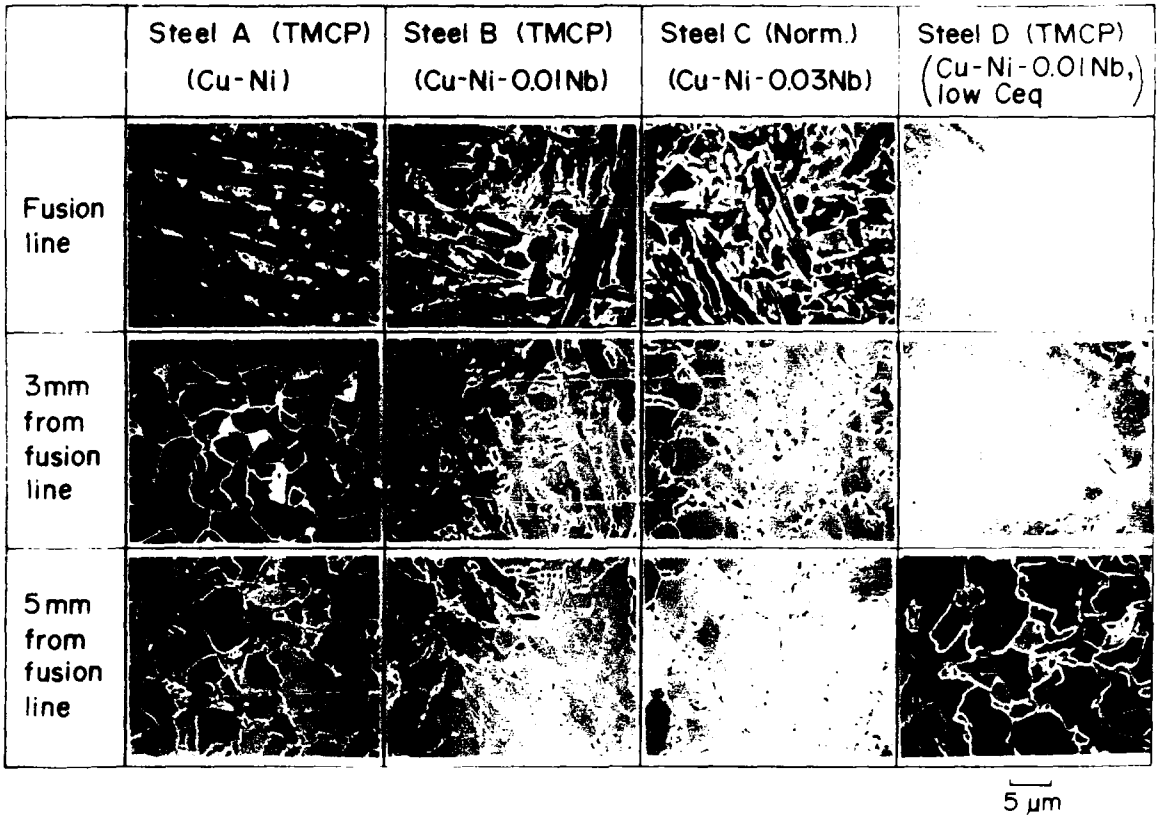


Fig.13 Microstructures in HAZ of SAW weldment with SEM with two-stage electrolytic etching (100kJ/cm, As welded)

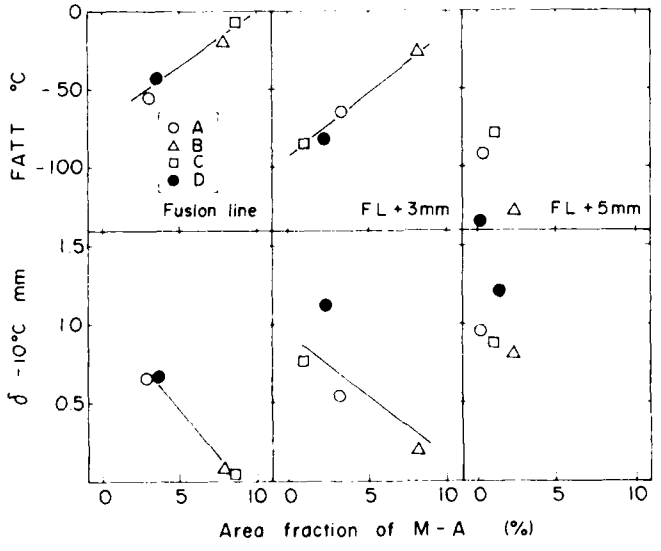


Fig.14 Effect of M-A constituent on the toughness in HAZ of SAW weldment (100kJ/cm, As welded)

## RESULT OF FULL THICKNESS CTOD TEST IN THE HAZ OF TMCP STEEL

As above mentioned, small amount of Nb (0.01%) in TS 500MPa grade TMCP steel is effective for the strength and toughness in base metal, and the deterioration of HAZ toughness is relatively little compared with further addition of Nb (0.03%). So, the HAZ toughness of heavy thick (100mm) TMCP steel plate with the composition of low C-Cu-Ni-0.01%Nb was tested. The chemical composition is shown in Table 3. They have high strength and good toughness as shown in Table 4. SAW was performed with the edge preparation of single bevel and the heat input of 50kJ/cm which is the typical condition of weldability test of steel plate for offshore structures. Then CTOD test in coarse-grain HAZ was carried out according to BS 5762 with Bx2B type specimen. Test result is shown in Table 5. Seven specimens among eight contain coarse-grains (larger than grain size No.7) and five specimens contain more than 15% region of coarse-grain HAZ. Low C-Cu-Ni-0.01%Nb steel has good weldability because all the CTOD values are high enough as shown in Table 5.

Table 3 Chemical composition of TS 500MPa grade heavy thick steel plate manufactured with TMCP process for the full thickness CTOD test in HAZ wt.%

| C | Si | Mn | P | S | Cu | Ni | Nb | Ti | Sol.Al | T.N |
|---|---|---|---|---|---|---|---|---|---|---|
| 0.08 | 0.15 | 1.55 | 0.004 | 0.001 | 0.25 | 0.44 | 0.010 | 0.009 | 0.040 | 0.0040 |

Table 4 Mechanical properties of TS 500MPa grade TMCP steel plate for the evaluation of CTOD value in HAZ

| Grade | Plate thick. mm | PWHT | YS MPa | TS MPa | El % | vE-80 J | vE-60 J | vE-40 J | FATT °C |
|---|---|---|---|---|---|---|---|---|---|
| BS 4360 -50E Mod | 100 | none | 445 | 524 | 37 | 312 | 342 | 382 | -90 |
| | | 600°C x 4hr | 426 | 509 | 38 | 315 | 335 | 380 | -81 |

Table 5 CTOD test results in coarse-grain HAZ of TS 500MPa grade TMCP steel plate

| PWHT | Test temp °C | Test No | Ratio of coarse-grain HAZ % (grain size No.≦7) | Critical CTOD value mm | Mode |
|---|---|---|---|---|---|
| none | -10 | 1 | 22 | >1.90 | No break |
| | | 2 | 1 | 0.82 | U |
| | | 3 | 9 | >1.91 | No break |
| | | 4 | 10 | 1.43 | U |
| | | 5 | 23 | >1.83 | No break |
| | | 6 | 47 | >1.89 | No break |
| | | 7 | 16 | 0.90 | U |
| | | 8 | 21 | 0.73 | U |

According to BS 5762
Test specimen - B x 2B

## DISCUSSION

EFFECT OF NIOBIUM ON M-A CONSTITUENT - In order to assertain the effect of Nb on M-A constituent, additional test was carried out. The relation between Nb content and area fraction of M-A constituent in simulated HAZ is shown in Fig.15. The area fraction of M-A constituent grows as Nb content increases in 1350°C reheated sample which simulates the fusion line of SAW weldment. However the area fraction of M-A constituent does not necessarily increases as Nb content increases in 900 ~ 1200°C reheated samples.

Then solute Nb content in simulated HAZ of steel B (TMCP steel containing 0.01% Nb) and steel C (normalized steel containing 0.03% Nb) was examined with electrolytically extracted residue. Although steel C contains higher solute Nb content after 1350°C reheating than steel B, it shows lower value after 900 ~ 1200°C reheating in spite of higher Nb addition as shown in Fig.16. Although measured values of solute Nb in both the steels are lower than the calculated one with eq.(1), measured value in steel C is extremely lower than the calculated one. It arises from that the equilibrium is not realized during welding. It also suggests that Nb carbide in normalized steel is large in size and thermaly stabilized compared with TMCP steel.

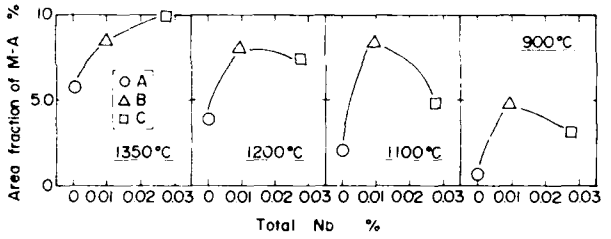


Fig.15 Effect of Total Nb content on the toughness in HAZ of SAW weldment (Simulation of 100kJ/cm, As welded)

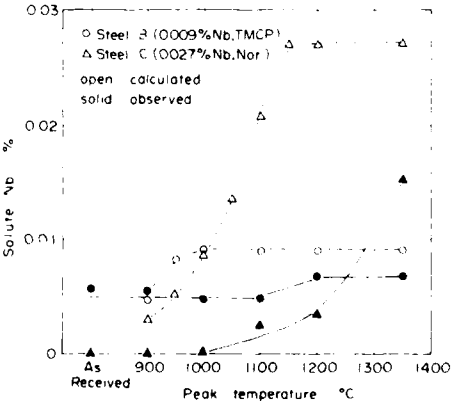


Fig.16 Relation between peak temperature and solute Nb content in simulated HAZ

Fig.17 shows the relation between solute Nb content and area fraction of M-A constituent in simulated HAZ, which shows the good correlation between those two factors among all the tested temperature region.

As above mentioned, the area fraction of M-A constituent increases as the solute Nb content increases after 900 ~1350°C reheating. In addition, solute Nb content is influenced not only with added Nb content and reheating temperature during welding, but also with manufacturing process of steel plates (i.e. TMCP or normalization).

MECHANISM OF THE FORMATION OF M-A CONSTITUENT WITH NIOBIUM ADDITION - One possible explanation for the formation of M-A constituent with Nb addition is the increase of hardenability. Fig.18 is the CCT diagram for welding in steel A and B. Although the critical cooling rate for ferrite formation is almost the same, steel B which contains 0.01% Nb and almost the same carbon equivalent as steel A shows lower transformation temperature than Nb free steel A. Fig.19 shows the effect of solute Nb content on the transformation starting temperature in simulated HAZ (peak temperature is 1350°C). The transformation starting temperature decreases linearly with the increase of solute Nb. Roughly speaking, hatched region in Fig.19 (500 ~ 600°C) is approximately the region where M-A constituent is formed [5) 6)].

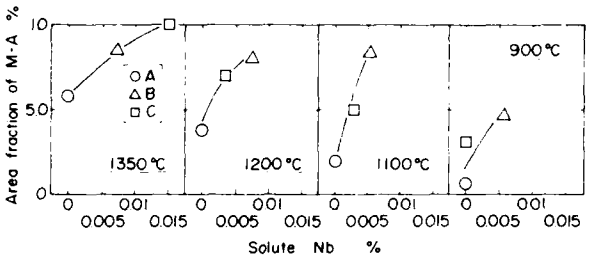


Fig.17 Effect of solute Nb content on the M-A constituent in simulated HAZ (simulation of 100kJ/cm)

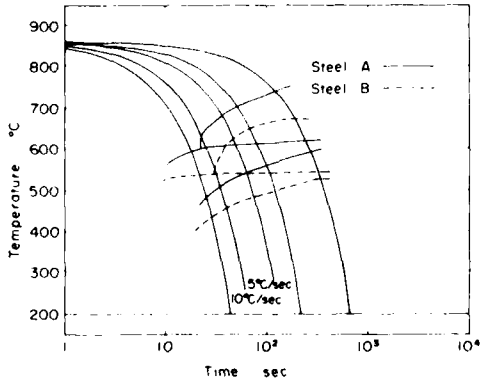


Fig.18 CCT diagram for welding (1350° reheated)

In order to ascertain the effect of transformation temperature on the formation of M-A constituent, thermal cycle for the isothermal transformation (shown in Fig.20) was conducted on 4 steels A,B,C and D using thermal induction simulator. Microstructures with optical microscope and SEM are shown in Fig. 21 and Fig. 22. All the tested steels are composed of upper bainitic structure, and all the steels including steel A (Nb free) contain great deal of M-A constituent. FATT in Charpy impact test after the thermal cycle above mentioned (isothermal transformation) is above -10°C and the deterioration of toughness is very large. Fig.23 shows the effect of transformation temperature and FATT in Charpy impact test in both the SAW weldment and simulated HAZ. The toughness is simply determined by transformation temperature irrespective of Nb content.

As above mentioned, addition of Nb decreases the transformation temperature during welding. It increases the area fraction of M-A constituent, and accordingly the toughness is deteriorated. So that the chemical composition should be carefully chosen in order not to decrease the transformation temperature, for example selecting the composition with low carbon equivalent and low Nb content.

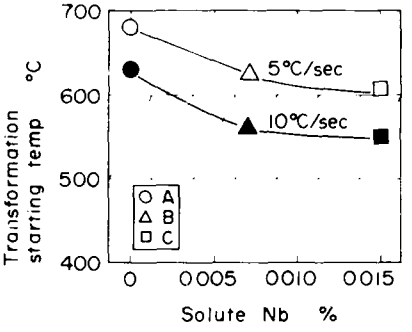


Fig.19 Effect of solute Nb content on the transformation starting temperature (1350°C reheated)

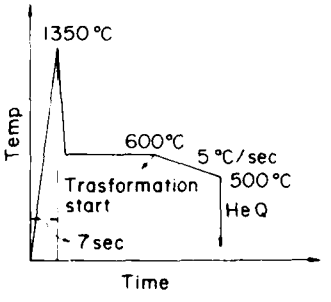


Fig.20 Thermal cycle for the isothermal transformtion with thermal induction simulator

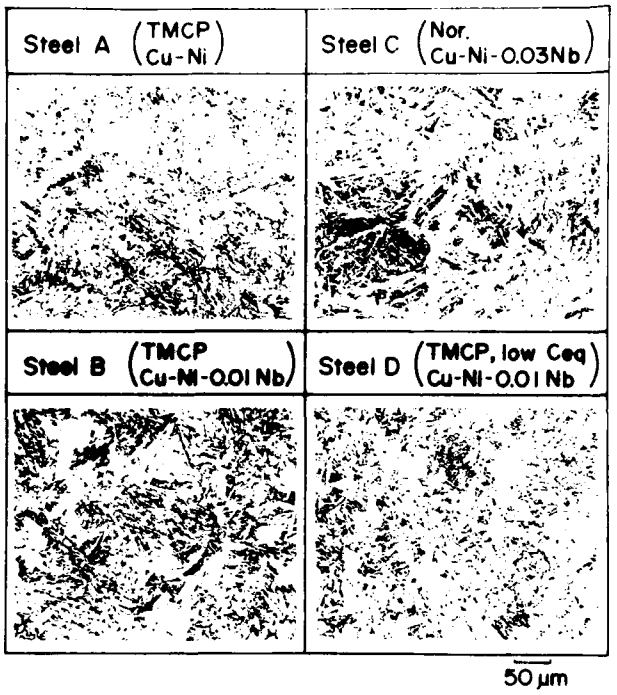


Fig.21 Microstructures with optical microscope after isothermal transformation as shown in Fig.20

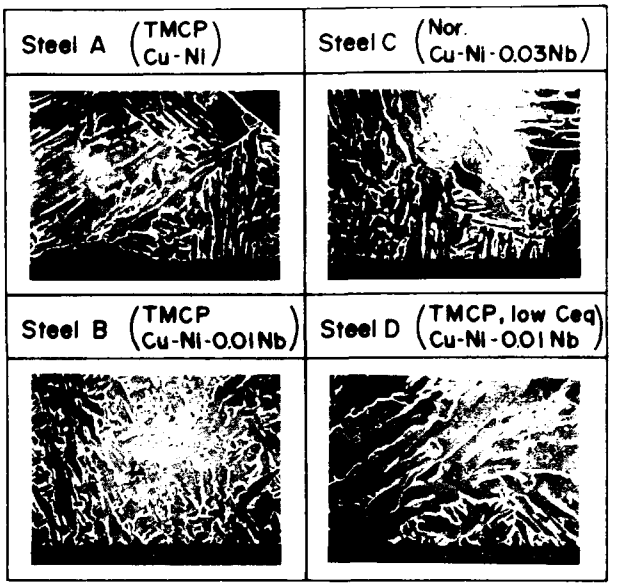


Fig.22 Microstructures with SEM after isothermal transformation as shown in Fig.20 (two-stage electrolytic etching)

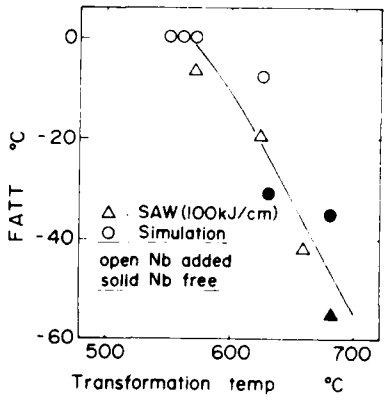


Fig.23 Effect of transformtion starting temperature on the HAZ toughness (SAW and simulation)

## CONCLUSION

1) Even the small amount of Nb (for example 0.01%) is effective for the increase of strength and toughness in base metal of TMCP steel, especially the strength after PWHT.
2) The toughness on the fusion line in as-welded condition is deteriorated with Nb addition. However it recovers with PWHT.
3) The toughness on the fusion line is mainly determined by the fraction of M-A constituent. It decomposes with PWHT.
4) The formation of M-A constituent with Nb addition is due to lowering of transformation temperature with the presence of solute Nb during welding. Even in the case of Nb free steel, when the transformation starts at low temperature (500 ~ 600°C) with isothermal heat treatment, M-A constituent is formed and the toughness is deteriorated.
5) The amount of solute Nb is affected not only by total Nb content but also by the manufacturing process.
6) It is necessary to utilize Nb for the increase of strength and toughness in the base metal of TMCP steel. It is also effective to reduce C and Nb content for the prevention of M-A constituent in HAZ in as-welded condition. TS 500MPa grade TMCP steel plate with the chemical composition of low C-Cu-Ni-low Nb (0.01%) has high strength and good toughness in base metal, and also high CTOD value in coarse-grain HAZ with SAW of 50kJ/cm heat input.

## REFERENCES


1) C. Ouchi, J. Tanaka, I. Kozasu and K. Tsukada, ASTM STP672, MiCon 78 (1978) p105
2) API RP 2Z "Recommended Practice for Preproduction Qualification for Steel Plates for Offshore Structures" (1987)
3) T. Haze and S. Aihara, IIW Document IX-1423-86
4) H. Ikawa, H. Oshige and T. Tanoue, J. Japan Welding Society, 49 (1980) 7, 467
5) J.W. Oblak and R.F. Heheman, Symposium "Transform and Hardenability in Steels", Mich (1967) 15
6) V. Biss and R.L. Cryderman, Met. Trans.2 (1971)2, 2267

# THE EFFECT OF SMALL AMOUNT OF NIOBIUM ON THE PROPERTIES OF STEEL C-Mn-Ti

**Wang Entao, Liu Rencai**
Institute of Iron & Steel Research
Anshan Iron & Steel Complex
Anshan, P.R.China

ABSTRACT

The effect of Nb-microalloying in the C-Mn-Ti HSLA steel has been studied after normalizing treatment. It was found that the ferrite grains were further refined, resulting in stabilizing the mechanical properties and improvement of impact toughness. In the meantime the coarsening temperature of austenite grains was raised and dynamic recrystallization in the steel was retarded.

## INTRODUCTION

The C-Mn-Ti HSLA steel has been produced for a number of years and found wide applications in the industries of automobiles, ship building and engineering machinery. It was found, however, that the properties of this steel were very sensitive to the variation of temperature and not very stable, bring difficulties in production, as well as their applications.

Several research works[1] have shown that addition of small amount of Nb has beneficial effect to the strength and toughness to the Ti-bearing HSLA steel. Experiments have been conducted by us in the addition of small amount of Nb to the Ti-bearing HSLA steel. The result indicated that the small amount of Nb improved the properties of Ti-bearing steel really, making them more stable. This addition of Nb has been used already in the production. The experiment work with regard to this subject will be described in this paper.

## EXPERIMENTAL MATERIALS

The experiment work consists of two parts. In the first part, the laboratory work, the steel studied was melted in the induction furnace of medium frequency, cast into ingots of 50 kg. The chemical compositions are given in Table 1. After reheated at 1200 ℃, the ingots were rolled into plates of 10 and 16 mm thick with finishing temperature of 1000 ℃. The plates were normalized at 950 ℃.

Table 1. Chemical compositions of experimental materials(Wt%)

| Steel | C | Si | Mn | S | P | Ti | Nb | Ne |
|---|---|---|---|---|---|---|---|---|
| A | 0.09 | 0.31 | 1.417 | 0.012 | 0.012 | 0.16 | | 0.007 |
| B | 0.09 | 0.33 | 1.42 | 0.020 | 0.014 | 0.16 | 0.02 | 0.006 |

In the second part of experiment work, the steel was made in the top blowing oxygen converter of 150 t in our steel-smelting shop, cast into ingots of 10.6 t, which were rolled into slabs of 120 mm thick and subsequently rolled, after reheated at 1300 °C, into plates of 10-16 mm thick. The final products were normalized at 950 °C also.

## EXPERIMENTAL RESULTS AND DISCUSSION

THE EFFECT OF SMALL AMOUNT OF Nb ON THE MICROSTRUCTURES - In the microstructures of the hot-rolled plates of both steels A and B, the ferrite grains were of irregular shapes and different sizes, with uniform distribution of pearlite colonies. The grain sizes of ferrite in steel A, ranging ASTM No. 7-8, were somewhat greater than those in steel B, being No. 8-9.

In the microstructures of the normalized specimens, the ferrite grains were of regular shapes with a few amount of pearlite, as shown in fig. 1. The grain sizes of ferrite in steel A, ranging ASTM No. 8-9, were still greater than those in steel B, being No. 10-11.

The observations under TEM indicated that there were dislocations of high density in the grains of the hot-rolled specimens of steel A, with the Ti(CN) particles of sizes about 5-20 nm distributed on the dislocation lines. Dislocations of lower density occurred in the grains of normalized specimens with Ti(CN) particles, which grew larger about 10-30 nm distributed uniformly within the grains. The

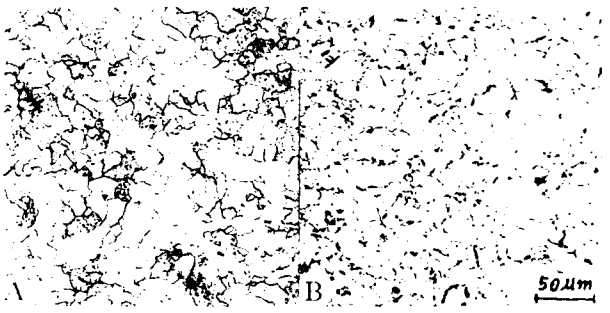


Fig. 1 - Microstructures of the normalized specimens of steels A and B.

dislocation density in the grains of the hot-rolled steel B was lower than that of steel A. Most of the second phase particles were of the complex ones (TiNb)(CN), while few of them of sizes 3-30 nm belonged to Ti(CN) and Nb(CN). Lower density of dislocations was in the grains of normalized specimens with second phase particles growing larger, being 8-30 nm.

MECHANICAL PROPERTIES - The mechanical properties of the hot-rolled and normalized specimens of steels A and B melted in laboratory are given in Table 2. From the data of this table, it can be seen that the strength of the hot-rolled steel A is somewhat higher than that of steel B, while the ductility of the former is lower than that of the latter. This fact means that the addition of small amount of Nb improved comparatively the combined properties of the hot-rolled steel. The data of the normalized specimens show that the addition of small amount of Nb does not in-

Table 2. The mechanical properties of test steels

| Steel | Condition | Thickness (mm) | $\sigma_s$ (N/mm²) | $\sigma_b$ (N/mm²) | $\delta_5$ (%) | $\psi$ (%) | $\alpha_{kv}$ J/cm² (-40°C) | grain size (ASTM No) |
|---|---|---|---|---|---|---|---|---|
| A | hot rolling | 10 | 670 | 815 | 20.5 | 49.5 | 2.5 | 8 |
| B | hot rolling | 10 | 565 | 715 | 21.5 | 62.5 | 5.0 | 9 |
| A | hot rolling | 16 | 590 | 720 | 20.5 | 60.5 | 2.5 | 7 |
| B | hot rolling | 16 | 550 | 710 | 21.5 | 64.5 | 4.0 | 8 |
| A | normalizing | 10 | 410 | 530 | 32.5 | 75.0 | 70.0 | 9 |
| B | normalizing | 10 | 395 | 530 | 33.0 | 75.0 | 85.0 | 11 |
| A | normalizing | 16 | 395 | 505 | 31.0 | 68.0 | 35.0 | 8 |
| B | normalizing | 16 | 410 | 505 | 31.0 | 71.0 | 45.0 | 10 |

Table 3. The chemical compositions and the variations in mechanical properties of the steels made in the steel smelting shop

| Steel | Chemical compositions (Wt%) | | | | | Variations in mechanical properties | | |
|---|---|---|---|---|---|---|---|---|
| | C | Mn | S | Ti | Nb | $\Delta\sigma_s$ (MPa) | $\Delta\sigma_b$ (MPa) | $a_{KV}$ J/cm² (-40°C) |
| Ti Steel | 0.07-0.14 | 0.8-1.6 | 0.010-0.030 | 0.08-0.20 | | 85 | 80 | 12-50 |
| Ti-Nb Steel | 0.07-0.14 | 0.8-1.6 | 0.010-0.030 | 0.08-0.20 | ≤0.04 | 55 | 50 | 42-109 |

crease the strength of the steel, but raises the toughness and lowers the ductile-brittle transition temperature. This is due to the effect of grain refinement caused by the small amount of Nb.

The amount of steel made in the steel plant reached 700 t already. The ranges of chemical compositions and the variations in the mechanical properties are shown in Table 3.

The addition of small amount of Nb reduced the variations of the mechanical properties of Ti-bearing steel, making them more stable. As will be discussed in the following, this was related to that during the normalizing treatment the complex (TiNb)(CN) particles were dissolved and coarsened not so easily and their sizes are kept more stabilized.

THE EFFECT OF THE DISSOLUTION AND COARSENING OF CARBONITRIDES ON THE GROWTH OF AUSTENITE GRAINS - The microalloying HSLA steels are characteristic essentially with their microstructures of fine grains, ensuring a good combination of strength and toughness. In order to obtain the microstructures of fine grains all stages and process variables during hot rolling should be controlled carefully after proper alloying design of the steel, such as the reheating of slabs, the rolling temperature, number of rolling passes, the amount of deformation of each pass and the finishing temperature. First of all it is of necessity to study under the laboratory conditions, the fundamental behavior of coarsening of austenite grains, which are associated with the influence rendered by the dissolution and coarsening property of the carbonitrides of Ti an Ti-Nb.

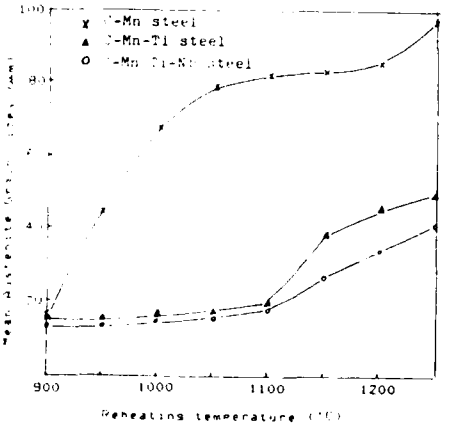


Fig. 2 - The relationship between the grain sizes of austenite and reheating temperatures.

The coarsening behavior of austenite grains of steels A and B appearing as abnormal grain growth was different from that of the C-Mn HSLA steel, which belonged to the normal grain growth. With increasing reheating temperature the grain growth of the austenite in steels A and B appeared discontinuous and there existed a coarsening temperature of grains, Tc. Below this temperature almost no grain growth of austenite was observed with increasing temperature. Even the soaking time reached 10 hrs, no distinct grain growth of austenite occurred. These appeared mixed grains consisting of different quantities of different sizes when the re-

Table 4. The coarsening temperature of the test steels

| Steel | Coarsening temperature | Temperature range of | Growing into coarse |
|---|---|---|---|
| A | of austenite grains(°C) | mixed grains(°C) | polygonal grains(°C) |
| A | 1100 | 1100-1200 | > 1200 |
| B | 1150 | 1150-1250 | > 1250 |

heating temperature (holding for 30 minutes) was within the range of 100 °C above Tc. At first, a part of austenite grains began to grow with the large grains extending to consume the small grains. It is worth noting that the coarsening temperature of austenite grains of steel B was higher than that of steel A by 50°C as shown in Table 4.

The mean sizes, interparticle spacings and volume fractions of the Ti- and Ti-Nb-

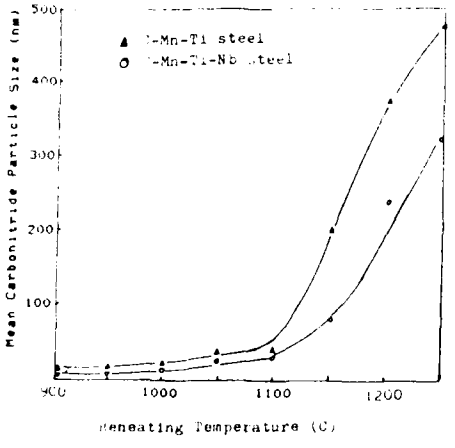


Fig. 3 - The relationship between the mean sizes of carbonitrides and the reheating temperatures.

carbonitrides in steels A and B at different reheating temperatures (holding for 30 minutes) have been determined by means of carbon replicas on electron microscope and quantitative metallography. The results of determination are shown in figures 3 and 4. It could be seen from the figures that the rates of

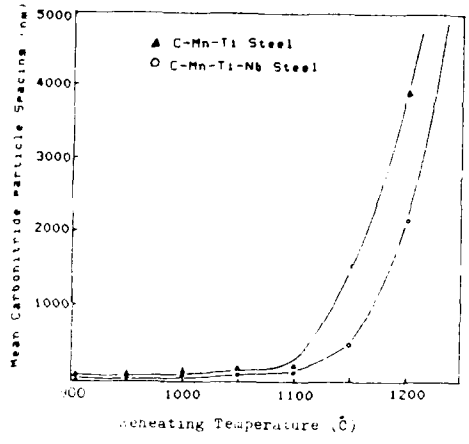


Fig. 4 - The relationship between the mean interparticle spacings and the reheating temperatures.

dissolving and coarsening of Ti- and Ti-Nb-carbonitrides at temperatures below 1100 °C for steel A and 1150 °C for steel B respec-

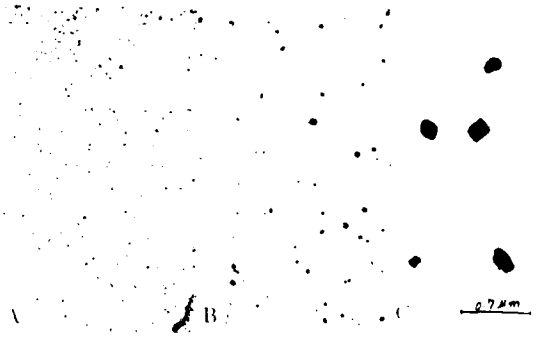


Fig. 5 - The distribution of Ti- and Ti-Nb-carbonitride particles of steel B at reheating temperatures 1000 °C (A), 1100 °C (B) and 1200 °C (C).

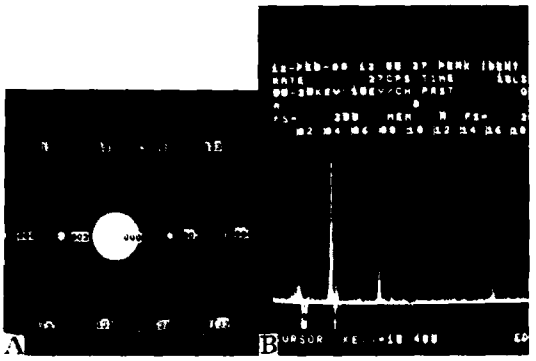

Fig. 6 - Identification of $(Ti,Nb)_4(CN)_3$ particles, (A) electron diffraction pattern, (B) energy dispersive spectrum.

tively was quite slow, while these rates became very rapid above these temperatures. The distributions of Ti- and Ti-Nb-carbonitrides of steel B at reheating temperatures 1000, 1100 and 1200 °C (holding for 30 minutes) are shown in fig. 5.

It should be pointed out that the onset temperature of rapid dissolving and coarsening of Ti- and Ti-Nb-carbonitrides of steel B has been raised, as compared with that of steel A, by 50 °C. The complex Ti-Nb carbonitrides of steel B have been identified as the ordered phase $(Ti,Nb)_4(CN)_3$ by means of electron diffraction and energy dispersive spectrum analysis.

According to the theory of the effect of second phase particles on the grain growth of austenite, the critical radius of the particle is given by

$$r_{crit} = \frac{6\bar{R}of}{\pi} \left( \frac{3}{2} - \frac{2}{Z} \right)^{-1}$$

For steel A at 1100 °C, $f_A$=0.16%, Z=3.0, and steel B at 1150 °C, $f_B$=0.17%, Z=3.0, the values of critical radii of the particles in steels A and B calculated from this expression were 30 and 40 nm, and those of the interparticle spacings are 600 and 700 nm respectively. These calculated values were almost coincident with the observed data obtained under TEM and by quantitative metallography.

The discontinuous behavior of the grain growth of austenite, which was different from that of C-Mn HSLA steel, of steels A and B in the reheating temperature range 900-1250 °C and the occurrence of a coarsening temperature can be attributed to the pinning of the austenite grain boundaries by the dispersive carbonitrides existed in the steel.[2-6]

In the case that the pinning force was less than the force of migration of grain boundary (activation energy, etc), the grains started to grow rapidly. Under constant value of volume fraction of the second phase particles, the pinning force, instead of depending on the critical radius of the particles, was actually controlled by the critical interparticle spacings and the density of the particles. The dense distribution of the second phase particles inhibited the migration of grain boundaries. Observations of steels A and B in the temperature range 100 °C above Tc under TEM indicated that not only the second phase particles were dissolved and coarsened rapidly, but their grain sizes and distribution became quite inhomogeneous. Thus it appeared that the particles were dense in some micro-regions, where the growth of austenite grains were impeded, and rare in other regions, where the austenite grains were able to grow, resulting in mixed grains. It was also observed that the second phase particles in steel B appeared denser and smaller than in steel A at the same reheating temperature (1100 °C). This might be attributed to the slow coarsening rate of the complex (Ti,Nb)(CN) particles of steel B, as compared with that rate of the Ti(CN) particles of steel A. That is the complex (Ti,Nb)(CN) particles were more stable than the Ti(CN) particles. This explains why the coarsening temperature Tc of austenite grain of steel B was higher than that of steel A by 50 °C.

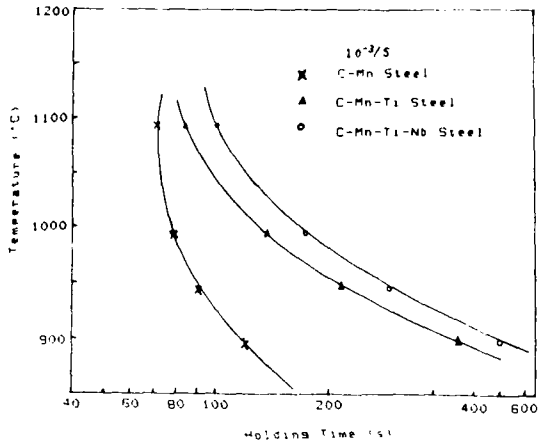


Fig. 7 - Dynamic RTT curves of C-Mn steel and steels A and B.

THE EFFECT OF Ti- AND Ti-Nb ON DYNAMIC RECRYSTALLIZATION - The experiments of dynamic recrystallization was conducted on the GLEEBLE-1500 testing machine. The specimens of $\phi 8 \times 12$ were heated to the austenite temperature 1250°C for 5 minutes, cooled to testing temperature within 35 s, kept isothermally for 30 s and subsequently compressed in the temperature range of 900-1100°C with the same strain rate $10^{-3}$/s and a total amount of reduction 60%. The flow curves $\sigma$-$\epsilon$ were recorded automatically. From the data obtained the dynamic RTT curves were plotted, as shown in fig. 6. It could be seen from the figure that the addition of Ti or Ti-Nb to the C-Mn steel resulted in retarding the dynamic recryctallization. It is worth noting that the addition of small amount of Nb somewhat retarded dynamic recrystallization so that the RTT curve moved towards the right side. In the low austenite temperature range, this retarding effect appeared more distinct. At present there is still dispute on the question whether the retarding effect on the recrystallization of austenite by Ti or Nb is due to the solute atoms or the precipitated particles. It is reported in literature that the PTT curve of Ti(CN),Nb(CN) has been determined.[7] We have observed the distributions of Ti(CN) and (Ti,Nb)(CN) particles resulting from strain-induced precipitation in the steels A and B, under TEM in detail. The observations indicated that it appeared a part of dispersed particles arisen from strain-induced precipitation in the temperature range of 900-1100°C, especially in that less than 1000°C. These precipitated particles has the influence of retarding the recovery and recrystallization in steels A and B. Therefore, the retardation of dynamic recrystallization in steels A and B arose primarily from the precipitation of Ti- or Ti-Nb particles, and the solute atoms had only secondary effect.

## CONCLUSIONS

(1) The addition of small amount of Nb to the C-Mn-Ti steels after normalizing treatment gave rise to the refinement of grains, stabilizing the mechanical properties and improvement of impact toughness at low temperatures.

(2) The rise of the coarsening temperature of austenite grains by 50°C in the C-Mn-Ti steel added with small amount of Nb can be attributed to the precipitation of complex (Ti,Nb)(CN) and the increase of the stability of carbonitride particles.

(3) The retardation of dynamic recrystallization in the C-Mn steel added with Ti or Ti-Nb, especially in the temperature range less than 1000°C, arose primarily from the strain-induced precipitation of Ti- or Ti-Nb-carbonitrides and the solute atoms had only secondary effect.

## REFERENCES

1. J. G. Williams, Conf. Proc. of Int. Conf. on "Technology and Applications of HSLA Steels", Philadelphia, 261-274 (1983).

2. C. S. Smith, Trans. AIME, 175, 15-51 (1948).
3. T. Gladman, Proc. Roy. Soc., 294A, 298-309 (1966).
4. T. Gladman and F. B. Pickering, JISI, 205, 653-664 (1967).
5. L. J. Cuddy and J. C. Raley, Met. Trans., 14A, 1983-1989 (1983).
6. J. Gladman and D. Dulieu, Metal Science, 8, 167-175 (1974).
7. M. G. Akben and J. J. Jonas, Conf. Proc. of Int. Con. on "Technology and Applications of HSLA Steels", PhiladelPhia, 149-161 (1983).

# DEVELOPMENT AND INVESTIGATION OF TITANIUM STEELS

**He Yongkang**
Department of Science and Technology
Anshan Iron and Steel Complex
Anshan, Liaoning, P.R.China

ABSTRACT

On the base of producing high-titanium steels (0.1%Ti), low-titanium and micro-titanium steels have also been developed by Anshan Iron and Steel Complex in recent years. Investigations have shown that even if the weight of ingot exceeds 10 tons, the size of TiN particles can still be controlled in the range of 10-50 nm. Thereafter, controlled cooling Ti-bearing reinforcing bars and steel strips produced by recrystallization controlled rolling process (RCR) were developed, and the combined adding of Nb-Ti was also investigated.

AS EARLY AS 1957, the first HSLA steel of our country—16Mn(ST52) was trial-produced by Anshan Iron and Steel Complex (AISC). In the sixties, micro-alloyed steels—niobium steel, vanadium steel and titanium steel were further developed. Thereafter in the eighties, the National Science and Technological Commission decided to reform AISC to a base of HSLA steels of our country, hence the production of HSLA steels of AISC increased rapidly (fig.1).

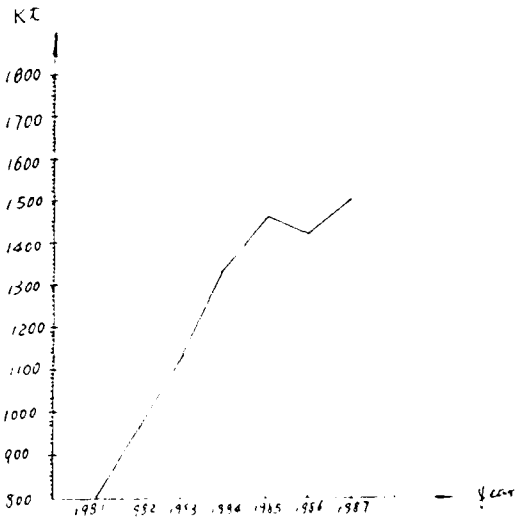


Fig. 1 - Annual output of HSLA steels

Vanadium steels: 14MnMoV steel for vessels and 15MnVN steel were developed in the sixties, and in recent years, vanadium steels have been well expanded. The largest bridge of our country—Changjiang Bridge across Jiujiang River is speeding up in the construction today and the main components are all made of 15MnVN provided by AISC.

Niobium steels: 18MnMoNb steel and 40MnMoNb steel were also developed in the sixties, but owing to ferroniobium is rather expensive in our country, the development of niobium steels are restricted. Since AISC cooperated with CBMM, niobium steels began to

develop rapidly, and the applying of niobium in high-carbon steels and low-carbon steels have all advanced significantly.

Titanium steels: AISC began to add micro-Ti (<0.03%) into 16Mn steel in the early of 1960 in order to promote grain-refinement and improve the properties of toughness and weldability, and the first microalloying steel of our country—15MnTi was successfully developed for the use in ship-building. Since 1973, a series of titanium steels represented by 10Ti, including 06Ti, 15Ti were developed to meet the demands of high-strength formable steels in automotive industry (fig.2), and a

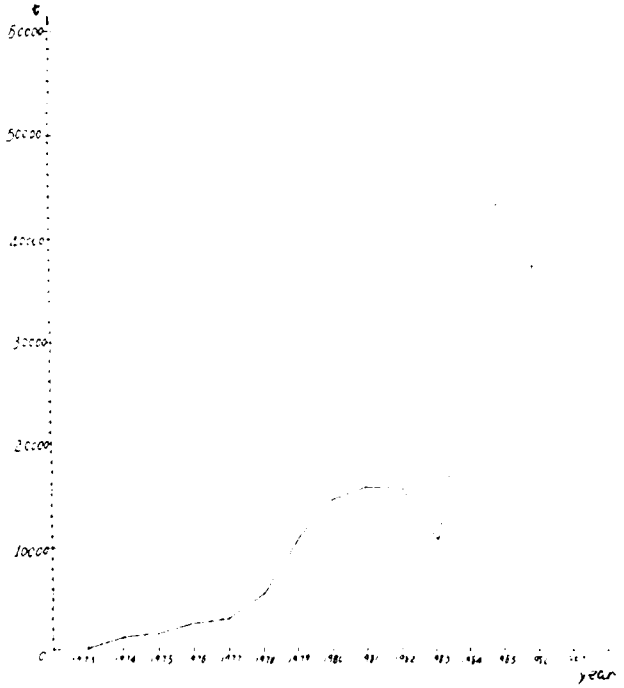

Fig. 2 - Annual output of low-carbon, low-manganese and titanium steels

series of Mn-Ti steels represented by 13MnTi, including 15MnTi for the use of mobiles and engineering machinery. All these steels achieved good results and millions of trucks manufactured of titanium steels are running throughout the country. The annual output of titanium steels of AISC was nearly 100 thousand tons last year (fig.3). However, owing to the fact that titanium steels (about 0.1% Ti) are easy to block up the sprue gate during pouring, and also due to the other problems such as titanium attenuation, low-titanium and micro-titanium steels and Ti-Nb steels were developed in recent years and all have advanced considerably.

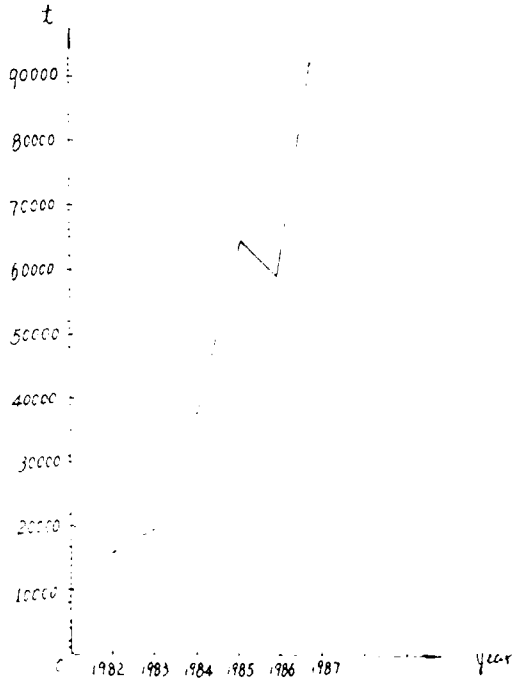


Fig. 3 - Curve of annual output of titanium steels

## Ti-BEARING REINFORCING BARS

The $TR_2$ Ti-bearing reinforcing bars are produced by the Temp-Core controlled cooling technique. The TiN particles sizes of 10-50 nm in $TR_2$ reinforcing bars can restrict the growth of austenite grains, retard the recrystallization and refine ferrite grains. In addition, the Ti(C,N) particles can strengthen the ferrite matrix. After Temp-Core processing, different micro-structures are formed across the section of $TR_2$ reinforcing bars, resulting in phase-transformation strengthening (fig.4).

According to formula IIW, the $C_{eq.}$ of $TR_2$ steel is 32.3, and that of 20MnSi steel, a traditional reinforcing bar steel used in China, is 44.3. This means that titanium will shift the nose cone of CCT to the shorter du-

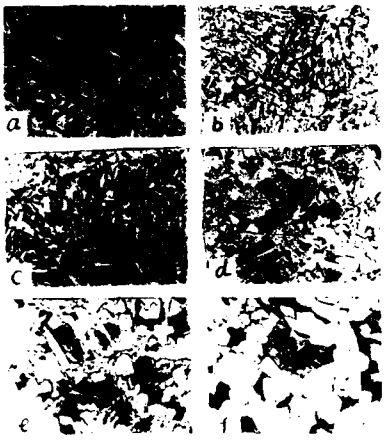


Fig. 4 - Different microstructures on the section of $TR_2$ reinforcing bars, 50×

ration time and hinder the formation of martensite, and resulting in the martensite of the outmost layer is less. This part will be squeezed to the convex positions of the weld during butt-welding and this will improve the weldability of reinforcing bars. Since aging of reinforcing bars is caused by nitrogen, therefore, adding element which bears strong combining capacity with nitrogen into reinforcing bars will decrease the sensivity to natural strain aging. The back-bending tests of $TR_2$ reinforcing bars after aging were all qualified, and the fatigue properties of $TR_2$ were better than that of 20MnSi steel, the $J^{-1}/\sigma b$ of low-cycle fatigue of the former is 0.52, while that of the latter is 0.45. The production cost of $TR_2$ reinforcing bars is lower than that of 20MnSi due to the save of Mn-Si alloys. Now $TR_2$ steel have been mass-produced and applied in many important engineerings.

## RECRYSTALLIZATION CONTROLLED ROLLING OF Mn-V-N-Ti STEEL

Strips of Mn-V-N-Ti steel containing 0.09%C have been produced in batches. Strips produced by RCR followed by controlled cooling (about 20 ℃/s) have better properties than that of the air-cooled strips, e.g., $D^{\alpha}$ reduced from 10 μm to 6.7-7.8 μm; $\sigma s$ increased by 98 MPa, and the banded structures have almost been eliminated (fig.5).

Fig. 5 - Microstructure of 09MnVTiN steel plates, 5 mm thick, (F+P), D=7.8 μm, 500×

Investigations indicated that there are four types of second-phase particles in the Mn-V-N-Ti steel:

a. Tiny TiN particles- of which the sizes can be controlled in the range of 10 to 50 μm (fig.6) even if the weight of ingots exceeds 10 tons. The temperature of austenite grain

30000×

Fig. 6 - Ti(C,N) particles

coarsening will be increased. The equi-axial ferrite grain sizes less than 10 μm can be obtained by controlled rolling even at finishing rolling temperature of about 930 ℃.

b. V(C,N) particles sizes of 7.5-25 nm- The strengthening effect on the ferrite matrix is mainly attributed to them.

c. Complex TiN phase- TiN particles with a black nuclei of $mCaO \cdot nAl_2O_3$ and an outer layer of MnS. This kind of complex inclusions which the bigger sizes are 3-10 μm, will be transformed to spindle-like shape after hot rolling, they are disadvantageous to both strength and toughness of the steel (fig.7).

Fig. 7 - Complex inclusions ($mCaO \cdot nAl_2O_3$+TiN+MnS) of TiN particles, 800×

By means of ladle refining treatment, e.g., injecting Ca-Si powder into the molten steel in the ladle, and form some low-melting point inclusions, which can be removed by injecting Ar into the ladle.

d. (V,Ti)N and (Ti,V)(C,N) particles sizes more than 50 nm. They consist of TiN nuclei grew according to epitaxial mechanism and VN+VC shells, which are formed during cooling of the ingots after casting. They will decrease the strengthening effect of ferrite.

The mechanical properties of continuous rolled Mn-V-N-Ti steel strips of 0.09%C are as follows:

| $\sigma_s$, MPa | $\sigma_b$, MPa | $a_k$(-40 ℃), J/cm$^2$ |
|---|---|---|
| 450 | 600 | 44 |

The strips are produced in batches and supplied to the automotive industry and engineering machinery.

## Mn-Ti-Nb PLATES

AISC has also investigated and developed the co-adding of niobium and titanium into the steels. Whether adding a slight amount of niobium into Mn-Ti steel, or adding a slight amount of titanium into Mn-Nb steel, products of good properties can all be obtained. Take 12Mn-Ti-Nb steel for example:

Chemical compositions

| C | Si | Mn | P | S | Ti | Nb |
|---|---|---|---|---|---|---|
| 0.13 | 0.48 | 1.52 | 0.016 | 0.005 | 0.15 | 0.024 |

Mechanical properties

| Plate-thick,mm | $\sigma_s$,MPa | $\sigma_b$,MPa | δ,% |
|---|---|---|---|
| 20 | 420 | 560 | 29 |

| $A_{kv}$, J | | $A_{ku}$, J | NDT |
|---|---|---|---|
| -20 ℃ | -40 ℃ | | |
| 129-137 | 78-94 | 90-110 | -65 ℃ |

It can be seen from the lists above that after adding niobium into Mn-Ti steel, we can acquire a fine-grain high-strength steel with comprehensive properties of good ductility, low transition temperature, good formability and good weldability. Considering from strict economic view point, the combined adding of Ti-Nb is desirable.

## THE ADVANTAGES OF MICRO-Ti STEELS

Micro-titanium was also added into carbon steel (boiler steel plate 20G), manganese steel (16Mn steel for vessels) and niobium steel. Investigations show that even in the case of large ingot mould-casting, there are still the following advantages:

1. Reducing free nitrogen, improving the aging property.

2. Reducing free nitrogen, increasing toughness.

3. Forming fine TiN particles, raising the temperature of grain coarsening of aus-

tenite (TGC).

4. Retarding austenite transformation, lowering the $\gamma \rightarrow \alpha$ transformation temperature, resulting in increasing the probability of ferrite nucleation and refining the ferrite grains.

5. Rolling deformation may induce the precipitation of Ti(C,N) and retard the recrystallization of austenite.

6. Precipitation of fine Ti(C,N) in ferrite may induce precipitation hardening and increase $\sigma_s$.

7. Improving the toughness of HAZ.

8. Increasing the strengthening effect of Nb in Nb-bearing steels and improving their ability to bear chilling and rapid heating. Combination of Ti and Nb microalloying may give better economic benefits.

The annual output of Ti-microalloyed steels in China have exceeded 300,000 tons in 1986.

## CONCLUSIONS

V-Ti steel, Nb-Ti steel and microalloyed steels containing small amount of titanium have developed extensively. We believe that this developement will be faster in the future as some new techniques, such as pretreatment of molten iron, top-bottom blowing converter, injecting metallurgy, continuous casting and controlled cooling, etc, are applied.

## ACKNOWLEDGEMENT

The author is grateful to Mr. Lin Zhihua, Mrs. Guo Jinru, Mr. Yan Jishi, Mr. Ji Yancheng and Mr. Hu Feibiao for their useful discussions.

# THE EFFECT OF COMBINED ADDITION OF NIOBIUM AND TITANIUM ON LOW CARBON-MANGANESE STEEL (FIRST REPORT)

**Yao Weixun, Xia Diepei, Ao Liege**
*Institute of Iron & Steel Research*
Anshan Iron and Steel Complex
Anshan, P.R.China

**Feng Zemin, Zhang Xiaogang***
*Department of Metallic Materials*
Northeast University of Technology
Shenyang, P.R.China

IT IS VERY IMPORTANT TO KNOW the behavior of grain coarsening and recrystallization of austenite under hot deformation in regulating a proper rolling schedule for microalloyed steels. A lot of research works about these topics have been carried out both in our country and abroad, and the effect of V, Ti and Nb elements on constraining the austenite grain growth and retarding recrystallization are affirmed unanimously. There are three opinions about the delay mechanism, i.e. (a) the solute drag effect; (b) the pinning effect of precipitates and (c) both (a) and (b) function at the same time. It becomes more complex as different microalloy elements are added simultaneously. This paper inquires into a low C-Mn steel with Nb and Ti added coalescently about the following aspects:

1. The tendency of austenite grain growth during reheating;

2. Effect on the precipitation kinetics of carbonitrides and on the recrystallization of austenite;

3. The mechanical properties attained under the present production condition in Anshan Iron and Steel Complex.

## MATERIALS AND PROCEDURES

MATERIALS - The chemical analysis of the steels studied in this work is given in table 1. Before rolling, the ingots were forged to 25 mm thick slabs, the slabs were homogenized at 1200°C and hot rolled in five passes to 7 mm thick plates with two different finishing temperatures which were 960-1000°C and 840-860 °C for steels 1 to 7 and steels 8 to 10 separately. For steels 8 to 10 only one finishing temperature ranges about 930-960 °C was adopted. After hot rolling, the plates were cooled to about 650 °C rapidly, and then held in a furnace of 600 °C for 0.5-1 hour and followed by furnace cooling to room temperature so as to simulate the coil cooling of steel strip after commercial rolling.

EXPERIMENTAL PROCEDURES - Tensile specimens of 5 mm dia. and Charpy V-notch impact specimens (1/2 size) were cut from the plate along transverse direction. Because the results of mechanical properties of steels 2 to 6 were not satisfied, so more detailed observations were merely dealt with samples 1 and 7, especially with samples 8 to 10.

The hot compression test were carried

*This paper is the master dissertation written by Zhang Xiaogang.

Table 1 . Chemical Composition of the Steels (Wt%)

| No | C | Mn | Si | P | S | Nb | Ti | Al | N | Method of Steelmaking |
|---|---|---|---|---|---|---|---|---|---|---|
| 1 | 0.16 | 1.20 | 0.39 | 0.011 | 0.006 | 0.027 | 0.029 | 0.39 | 0.002 | Vacuum Induction Furnace |
| 2 | 0.15 | 1.21 | 0.39 | 0.012 | 0.007 | 0.079 | 0.027 | 0.31 | " | " |
| 3 | 0.16 | 1.05 | 0.29 | 0.011 | 0.006 | 0.030 | 0.070 | 0.31 | " | " |
| 4 | 0.16 | 0.97 | 0.40 | 0.012 | 0.006 | 0.079 | 0.071 | 0.34 | " | " |
| 5 | 0.15 | 1.02 | 0.38 | 0.011 | 0.008 | 0.031 | 0.13 | 0.29 | " | " |
| 6 | 0.15 | 0.91 | 0.37 | 0.010 | 0.007 | 0.084 | 0.13 | 0.27 | " | " |
| 7 | 0.078 | 1.14 | 0.37 | 0.010 | 0.008 | 0.067 | 0.031 | 0.25 | " | " |
| 8 | 0.05 | 1.28 | 0.17 | 0.009 | 0.002 | 0.038 | 0.0275 | 0.013 | 0.088 | Induction Furnace |
| 9 | 0.055 | 1.28 | 0.18 | 0.016 | 0.016 | 0.94 | 0.027 | 0.014 | 0.083 | " |
| 10 | 0.068 | 1.09 | 0.12 | 0.009 | 0.030 | -- | 0.015 | 0.011 | 0.012 | " |
| 11 | 0.046 | 1.29 | 0.11 | 0.012 | 0.018 | -- | -- | 0.011 | | " |

out on Gleeble-1500 Tester, the sample size is $\phi$10X12 mm with $\phi$8x0.2 mm deep recesses on both ends. They are reheated at 1200 °C for 5 min and deformed at 925, 975 and 1025 °C with a series of strain rate from $10^{-4}$-$10^{-1}$/s, the strain is 40 %.

The microstructures of as rolled samples were observed with optical microscope and as-quenched deformation specimens, the austenite grain growth of steels 8 to 11 were observed under a HM-4 high temperature microscope between 900-1200 °C at intervals 50 °C and held 30 min at each temperature.

As the carbonitride particles which intensively affect the retardation of recrystallization and the growth of the austenite grains in microalloying steels are very fine, we adopt SPEED method to extract the precipitates smaller than 100 nm and examined under a H-700H electron microscope, with the aid of X-ray energy spectrometer and electron diffraction spots to analyse their structures and constituents. The morphology, distribution of the precipitated particles, the dislocations and substructures in steels were also observed with metal foils.

## RESULTS

MECHANICAL PROPER' Mechanical properties of the test st[illegible] showed table 2 with the exc[illegible] of steel 1 whose strength and toughness are slightly higher at lower FRT, the strengths of steel 2 to 6 are all higher at high FRT, but the toughness are quite lower. In spite of lower carbon content of steel 7, the strength is just the same as steels with higher carbon content and the toughness is good also. The steels 8 and 9 have better properties than steels 1 and 2 which possess much higher carbon contents and with approximately the same contents of other alloy elements. The steel 10 which contains Ti solely has the lowest strength.

As seen in table 2, despite of the condition of rolling and cooling, the steel that contains Ti only had very low strength, and the strengths increase significantly when combined aldition of Nb and Ti was used in the steels. The strength increases and toughness decreases with inereasing Nb, and the descending extend is greater at higher C level.

This investigation shows that it is possible for a low carbon (0.06%C) steel containing Nb and Ti to get the same strength

Table 2 . Mechanical Properties of Test Steels

| No | 0.2%Y.S. (MPa) | | T.S. (MPa) | | 0.2%Y.S./T.S. | | El. (%) | | R.A. (%) | | Impact Energy CVN(J) (½mm) | |
|---|---|---|---|---|---|---|---|---|---|---|---|---|
| | H | L | H | L | H | L | H | L | H | L | H | L |
| 1 | 462 | 486 | 615 | 627 | 0.74 | 0.78 | 27.5 | 26.3 | 71.0 | 72.8 | 51.5 | 60.0 |
| 2 | 566 | 514 | 699 | 649 | 0.81 | 0.79 | 22.3 | 26.3 | 67.0 | 69.5 | 33.5 | 46.0 |
| 3 | 607 | 546 | 742 | 684 | 0.82 | 0.80 | 20.0 | 25.0 | 68.0 | 68.0 | 19.0 | 34.0 |
| 4 | 589 | 477 | 726 | 637 | 0.80 | 0.75 | 21.7 | 25.3 | 67.3 | 70.5 | 22.5 | 55.0 |
| 5 | 665 | 558 | 783 | 681 | 0.85 | 0.82 | 22.3 | 24.3 | 66.5 | 70.5 | 21.5 | 39.0 |
| 6 | 656 | 552 | 777 | 662 | 0.85 | 0.83 | 19.0 | 26.0 | 66.0 | 69.5 | 16.0 | 45.5 |
| 7 | 591 | 558 | 684 | 676 | 0.86 | 0.83 | 21.7 | 23.3 | 72.5 | 70.5 | 60.5 | 54.0 |
| 8 | 470 | | 563 | | 0.83 | | 25.5 | | 72.0 | | 54.5 | |
| 9 | 553 | | 633 | | 0.87 | | 22.3 | | 72.8 | | 51.8 | |
| 10 | 320 | | 431 | | 0.74 | | 32.5 | | 77.0 | | 58.0 | |

H--- high FRT, L--- low FRT

as the steels with 0.16%C and much better toughness than those of high-C content steels, with conventional rolling and controlled cooling.

MICROSTRUCTURE - There are three kinds of microstructure in the steels after controlled rolling and cooling:

1) The microstructures in steels 1 to 6 are all ferrite and pearlite. The difference is that equiaxed polygonal ferrite grains from lower FRT, compared with that attaind at higher FRT are finer on the contrary. and there is a tendency for ferrite to become unequiaxed with less and disperse pearlite (fig.1).

2) In steel 7 with lower carbon content, the microstructure is consisted of fine acicular ferrite, which is quite different from steel 1 to 6. No matter what FRT is used, we can hardly see pearlite in it (fig.2a). However, at lower FRT, the acicular ferrite becomes a little coarser conversely.

3) The microstructures in steels 8 to 10 are composed of mixtures of unequiaxed and acicular ferrite (fig.2b). With decreasing of Nb and Ti contents and cooling rate, the grains become coarser. In addition, there are some cementite particles in these three steels, the amount of them are larger in steel 10 with higher carbon content (fig.3).

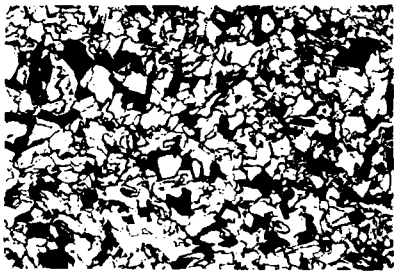

a. lower FRT 40 μm

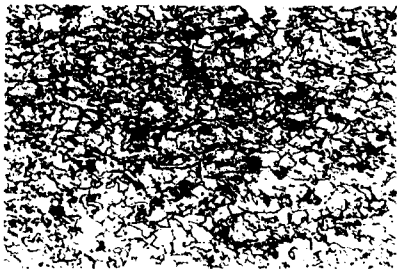

b. high FRT 40 μm

Fig. 1 - F+P in high carbon content steel

From the observation of thin foils for electron microscopy prepared along the rolling direction of the plates, it is found that most of the matrices of acicular and unequiaxed ferrite are composed of lath substructures with high dislocations. There

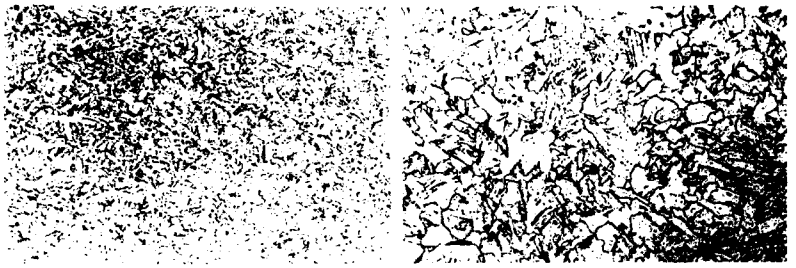

a. acicular F 40 μm b. unequiaxed F 20 μm

Fig. 2- Unequiaxed and acicular F

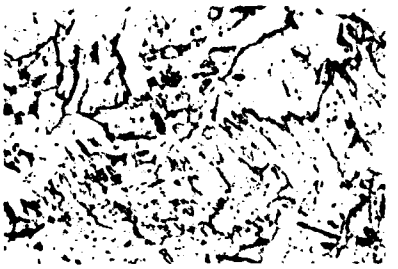

$F+Fe_3C$ 12 μm

Fig. 3 - Ferrite and Cementite Particles

are also some nearly equiaxed substructures in them (fig. 4). The dislocation density in cell-structures of two kinds of substructures are very similar, but with less dislocations in the center portion of the equiaxed substructures. It means that the crystal structure are relatively perfect in this region. There are some dislocations in the center area of the lath substructure, but the dislocation density is much smaller than that in the cell structure. The cell structure are net works composed of dislocation tangles as observed under higher magnifications (fig. 5). The dislocations are pinned by precipitates, and the higher the dislocation density is, the more the precipitates are. It is more evident in steel 9.

THE SIZE, DISTRIBUTION AND CHEMICAL ANALYSIS OF PRECIPITATES - Carbon extracted replicas for electronic microscopic examination of precipitates were prepared on metallographic specimens with SPEED method. Any precipitates are hardly seen in the hot compression specimens quenched from 1220°C.

With increasing Nb and Ti contents, the number of carbonitride become more and more in steels 8 to 10, which were controlled cooled after hot-rolling. The majority of the precipitates is fine in sizes of the order between 10-30 nm (see fig. 6a,b,c and table3). In the steel that contains 0.015%Ti only, not only the precipitates are less in quantity but also bigger in sizes. The precipitates in steels 8 and 9 are nearly the same in size, but the amount of particles in steel 9 was about three times of that in steel 8. A statistics on the size, distribution and mean spacing of precipitated particles is tabulated in table 3. It shows that most of the particles are smaller than 30 nm in diameter, the spacing between particles is smaller in steel 9 than in the other steels, and that of steel 10 is the biggest.

Chemistries of precipitates of different sizes in steel 8 and 9 were studied with the aid of EDAX, the results show that almost all particles whose sizes are between 50 and 150 nm contain both Nb and Ti simultaneously, and the amount of Ti reduces as the particle size decrease, but the Nb contents in particles nearly have no changes (fig. 7).

THE TENDENCY OF AUSTENITE GRAIN GROWTH IN THE STEELS - A high temperature microscope was used to observe the tendency of grain growth of austenite. The grain sizes of steels 8 to 11 during reheating were determined by linear intercept method and plotted versus temperature (fig. 8). The grain sizes of the common C-Mn steel and 0.015%Ti steel at 900°C are the same. The grain growth rate of steel 11 is about 3-6 μm/50°C between 900-1000°C and increases to 15-20 um/50°C above 1050°C. The grain sizes of the three kinds of steel with Nb or Ti additions almost have no change below 950°C, and grow up homogeneously and slowly till 1100°C. Even with steel 10, which

a. lath substructure 0.5μm b. equiaxed substructure

Fig. 4 - Two Kinds of Substructures

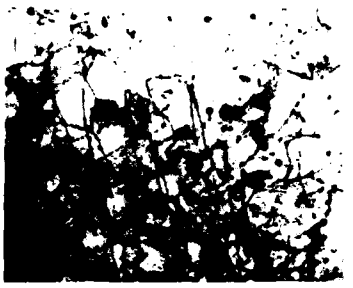

0.5 μm

Fig. 5 - Dislocation Networks

Table 3 . Precipitate Size,Distribution And Spacing

| No | size(nm) < 30 | 30-50 | 50-100 | 100-200 | average particle Spacing |
|---|---|---|---|---|---|
| 8 | 56.9 % | 29.4 % | 11.0 % | 2.8 % | 47 |
| 9 | 73.3 % | 19.2 % | 6.7 % | 0.9 % | 29 |
| 10 | 53.3 % | 31.1 % | 15.6 % | 0 | 280 |

a. 8# 0.5 μm b. 9# 0.5 μm c. 10# 0.5 μm

Fig. 6 - The Precipitates in Steels

contains small amount of Ti only, the grains also begin to coarsen obviously till 1150 °C. When the temperature raises to about 1100 °C, some abnormal grain growth appear in individual area in the steels, and is more evident in steel 10. The grains grow rapidly for all four kinds of steels between 1150-1200 °C, however, the rate of growth reduces along with increasing of Nb and Ti contents, and it becomes more obvious when Nb and Ti are added together, especially with the increasing Nb content.

INFORMATION OF DYNAMIC PRECIPITATION AND RECRYSTALLIZATION FROM THE TRUE STRAIN-STRESS CURVES

$\sigma$ -$\varepsilon$ Curves - The true stress and strain curves of steels 7,8,9 and 10 showed in fig. 9a were measured by hot compression tests on Gleeble-1500. Under the test condition adopted, the stresses in steel 1 and 7 increase continuously with ascending strains owing to the high contents of Al in them, this means that the resistances to deformation increase. The flow curves for other steels are typical of recrystallization. Figs.9b and 9c show the $\sigma$-$\varepsilon$ curves of steels obtained under the conditions of the same deformation temperature with different strain rate, and with the same strain rate at different deformation tempera-

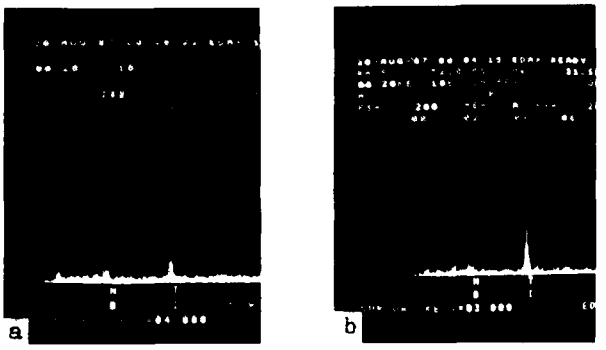


a. 50-80 nm precipitates b. 80-100 nm precipitates

Fig. 7 - The content of Nb and Ti in precipitates of different sizes

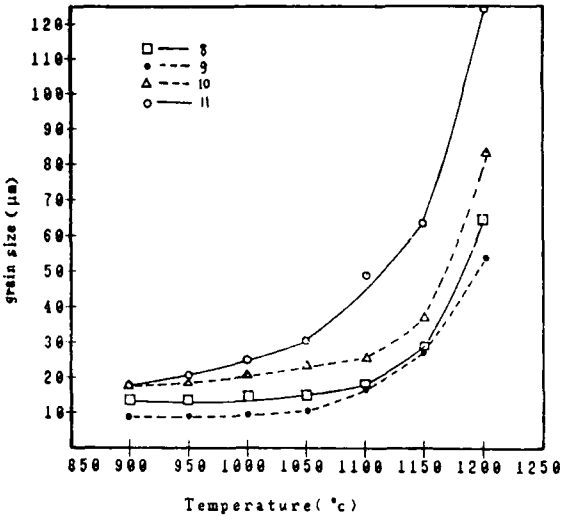


Fig. 8 - The relation between austenite grain size and temperature

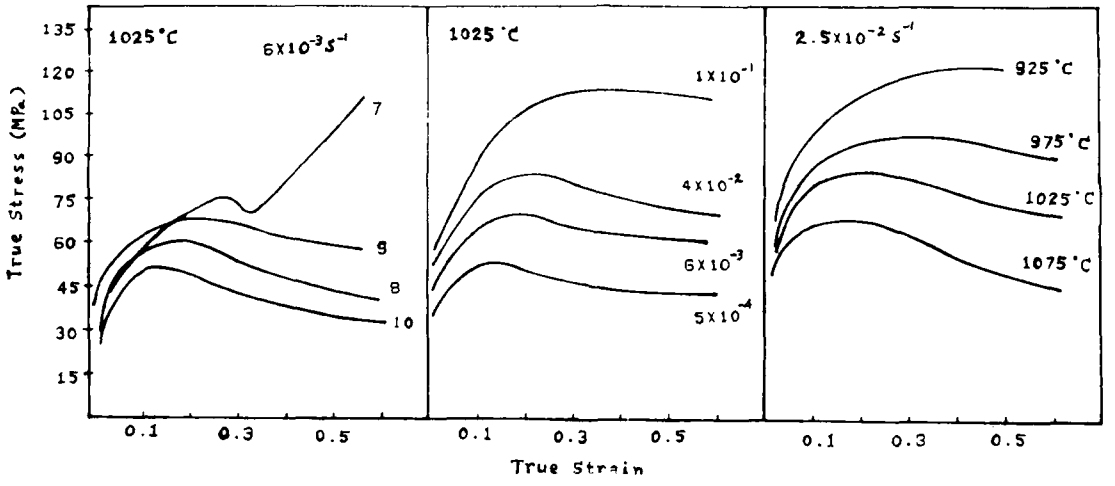


a. steels of different compositions b. same composition and temperature but different $\dot{\varepsilon}$ c. same $\dot{\varepsilon}$ and composition but different temperatures

Fig. 9 - True stress-strain curves

tures seperately. It can be seen that the peak stress is descending (ascending), and the peak shifts to the side of lower (higher) strain according to increasing (decreasing) deformation temperature. The process of high temperature deformation would not attain the dynamic recrystallization state and exhibits a typical characteristics of recovery when the temperature is below 925 °C or strain rate is higher than $10^{-1}/s$. It shows a similar behavior with the result of the earlier studies. On account of the $\varepsilon_p$ on the flow curves is approximately corresponding to the critical strain of dynamic recrystallization, the relation between $\varepsilon_p$ and $\dot{\varepsilon}$ may be used to study the effect of various chemical compositions and deformation conditions on dynamic recrystallization. Fig. 10 shows the $\varepsilon_p$-$\dot{\varepsilon}$ curves at 1025 °C of the conventional C-Mn steel and the steel which contains Nb and Ti. From the

curves we know that the steels microalloyed with Nb and Ti have higher peak strain than conventional C-Mn steel at any strain rate. This means the influence of Nb and Ti addition on retarding dynamic recrystallization. Fig. 10 also shows that in a certain range of strain rate an unusual peak appears on the $\varepsilon_p$-$\dot{\varepsilon}$ curves of Nb and Ti containing steel.

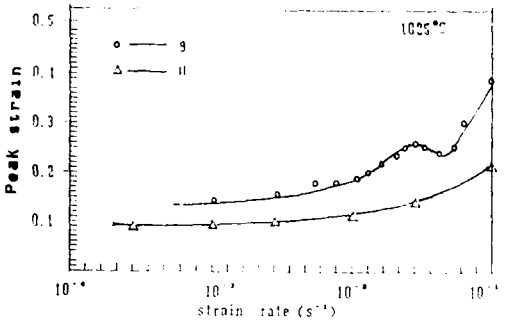


Fig. 10 - $\varepsilon_p$-$\dot{\varepsilon}$ curves in steel 9 and 10

RTT and PTT Curves - According to the influences of the same strain rate and different deformation-temperature on dynamic recrystallization of steels 8, 9 and 10, we obtained the curves of beginning of recrystallization, temperature and time (fig. 11). As in steel 10 with small amount of Ti, the peak strain is slightly higher than that of the conventional C-Mn steel, so the suppression effect on the recrystallization is not obvious. But combined addition of 0.03%Nb and 0.03%Ti to the steel exhibits an obvious retardation, although the effect on delaying recrystallization increase, the increasing degree become smaller along with continuously increasing Nb-content in steel.

Through calculation from the deformation parameters determined in steel 8, 9 and 10, the dynamic precipitation curves of carbonitrides are plotted in fig. 12. The fastest precipitation appears at 1090 ℃ in steel 10 which contains Ti only and the temperature range of precipitation is wide. The temperature of fastest precipitation reduced from 1090 °C to 1040 °C when Nb and Ti were added into the steel, the onset time of precipitation is shorter than the steel which contains Ti only, the temperature range of precipitation is smaller. The dynamic precipitation curves are quite the same for two kinds of steels containing Nb and Ti, when the amount of Nb increases from 0.038% to 0.094%, the curve moves towards the left direction.

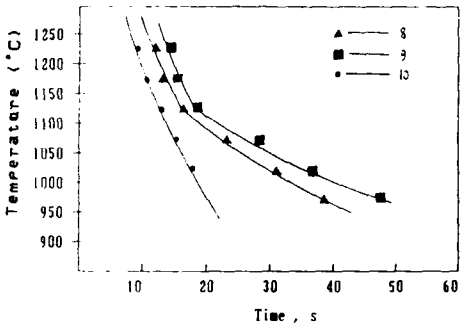


Fig. 11 - Affect of alloy element on recrystallization

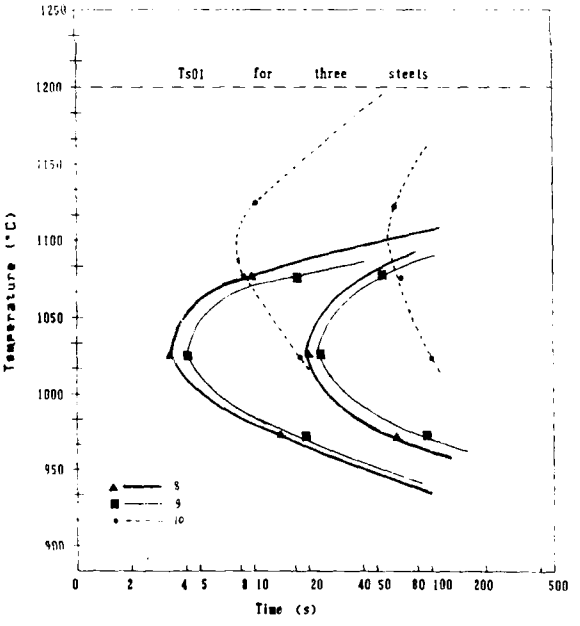


Fig. 12 - Dynamic precipitation curves

## DISCUSSION

### INFLUENCE OF ALLOY ELEMENTS AND ROLLING

SCHEDULES ON THE MICROSTRUCTURES AND PROPERTIES OF THE STEELS - A good combination of strength and toughness has been obtained for steels 7, 8 and 9 under conventional rolling followed by controlled cooling. The reasons are:

1) The austenite grain growth has been effectively controlled by Nb and Ti in the steels during the heating of the slabs (fig9). This effect results mainly from the hindrance to migration of grain boundaries exerted by finely dispersed particles of Nb, Ti carbonitrides. It has been shown by TEM observation that the amount of precipitated particles is propotional to the Nb and Ti contents in the steel. On that account, the degree of refinement of the austenite grains is correlated to the number, size and distribution of these particles. The grain sizes of steels containing Nb and Ti remain rather fine as they are heated up to 1100°C. A considerable carbonitride particles which contain predominately Nb begin to come into solid solution as the temperature is above 1100°C, this may be the reason why locally abnormal grain growth occurs at that time, while those Ti predominated whose solute temperature are higher may still act as obstacles to grain growth. The amount of precipitates in steel 10 is very small that they have minute ability to hinder the grains from coarsening. When the heating temperature is raised above 1200°C, the grain sizes of steels 8 and 9 with combined addition of Nb and Ti are approximate 60 and 50 $\mu$m respectively, that of the steel with Ti addition only is 82 $\mu$m, while the grains of the plain C-Mn steel grow up to about 130 $\mu$m. Consequently, the steels rolled from initial finer grains will have smaller grain sizes, and thus have greater strength.

2) The microstructures and CCT curves of the steels have been greatly changed. For a steel containing lower C, higher Mn and a certain amount of Nb, in adoption of controlled cooling soon after hot rolling, the transformation of austenite to polygonal ferrite and pearlite is hindered and the formation of an acicular ferrite structure may be promoted.[1][2] The latter is produced by a combined transformation mechanism of shear with diffusion, and has better strength and toughness than the F+P structure on account of the fact that there are higher dislocation density and finer cellular structure in its sub-structures. Smith et al has discovered that the steel has the best strength and toughness when it has a structure of fine acicular ferrite mixed with a smaller amount of polygonal ferrite.[3] The microstructures of steels 8 and 9 are essentially of this type. In view of the substructures of them observed by metal foils under TEM, there are a lot of high density dislocations and dislocation networks (fig. 4,5), which are quite different from those of polygonal ferrite.

3) When the steels are rapidly cooled from the finishing temperature to about 650°C, not only the coarsening of grains is highly hindered, but also the precipitation of Nb, Ti carbonitrides is restrained. In simulating the coiling of steel strip after commercial rolling, the water-cooled steel plates are held at 600°C and followed by furnace cooling, and the Nb, Ti carbonitrides may precipitate in this higher temperature region of $\alpha$-phase. According to K. Kunishige et al,[5] the fine particles precipitate in this temperature range will have a weak strengthening effect on the steel and no influence on the toughness. From the statistics of the amount, sizes and spacings of the precipitates observed by replica under TEM, the quantity of precipitates in steel 9 is the largest with the size the finest, so very good the strength and toughness are. The precipitates in steel 10 are very few and disperse sparsely, and hence the strength of it is rather low. These results are in coincidence with that of their investigation. Furthermore, the carbon in the

metastable structures formed in the steel during rapid cooling after hot rolling will precipitate as cementite and coalesce to spheric form, which will be additionally favourable for the toughness (table 3,figs.6, 2 and 3).

There are some differences between the basic chemical compositions of steels 1 to 7 and steels 8 to 10. This will unavoidably influence the microstructures and mechanical properties of the steels. In general, Mn lowers the $Ar_1$, $Ar_3$ points and the decomposition rate of austenite, and also has a promoting effect on precipitation hardening. The contents of carbon and microalloying elements must tally with the stoichiometric ratio of the precipitate. The largest number of particles could be obtained only when the heating temperature is well above the solubility curve of these precipitates. Under the condition of heating to 1200 ℃ in our experimental rolling, the Nb, Ti carbonitrides in steels 1 to 6 which have higher carbon contents could only dissolve partially, thus the number of carbonitride particles precipitated under cooling will reduce on the contrary, and hence the effect of precipitation hardening becomes weaker.

From the facts mentioned above we can realize why the steels 7 to 9 with much lower carbon contents than steels 1 to 6, but, have the same strength and better toughness. On account of low C and excessively high Al content, the acicular ferrite structure is very fine in steel 7, which exhibits an excellent toughness. As for steels 1 to 6, all of which contain very high Al, the common rule that the microstructures obtained at lower finishing temperatures are coarser than those rolled under higher temperatures may be attributed to the exceptional chemical compositions. This needs to study in detail further.

INFLUENCES OF COMBINDING ADDITION OF Nb AND Ti INTO STEEL ON THE PRECIPITATION KINETICS AND THE RECRYSTALLIZATION OF AUSTENITE — The free energy in the volume of a new phase is different from that in the matrix as the dynamic recrystallization occurs in a steel. Under a certain deformation condition, the amount of deformation energy in the microstructure is proportional to the area under the stress-strain curve. As can be seen from fig. 9a, that under the same $\varepsilon$, T and $\dot{\varepsilon}$, the areas beneath the curves are different depending on the variant alloying elements and the contents, i.e. much higher deformation energy is required for the occurrence of recrystallization in a steel containing more microalloying elements.

As Nb and Ti are added simultaneously into the steel, carbonitrides of nonstoichiometrical ratio are easily formed owing to the fact that Nb and Ti carbonitrides have the same crystalline lattice and can dissolve in each other. It can be seen from the dynamic precipitation curves that the precipitating temperature of carbonitrides in the steel only containing minute Ti is higher, and the curves for steels 8 and 9 have only one nose both, this means that the precipitation of Nb and Ti carbonitrides may all occur in this temperature range. It has been reported [6] that the activity of the carbonitrides in the steel will be lowered due to the interaction of Nb and Ti, and this causes their solubility to be increased, i.e. their stability in austenite may be relatively enhanced and the tendency of precipitation will be reduced, and the precipitation temperature is thus lowered. From our experimental result (fig. 13), we can see that the temperatures for fastest precipitation in steel with Nb and Ti are about 50 ℃ lower than that of the steel containing Ti only. This is in coincidence with these rules predicated by them.

On account of the higher precipitation temperature of Ti carbonitrides, it might be infered that the carbonitrides in which Ti predominates will precipitate firstly at higher temperature in the dynamic precipitation

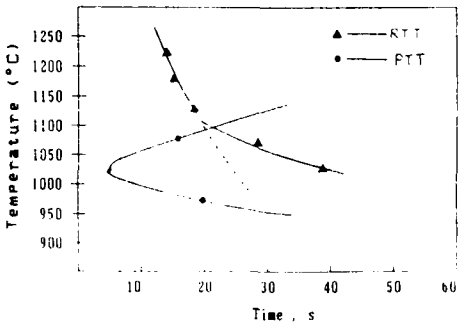


Fig. 13 - PTT and RTT curves in steel 9

curve during deformation, the sizes of them must be larger, while the carbonitrides containing Nb and Ti simultaneously as well as those in which Nb predominates will precipitate in order as the temperature decreases. The lower the precipitating temperature, the smaller the sizes of the particles will be. This deduction is semiquantitatively confirmed by analyzing Nb and Ti contents in the particles of different sizes ranging from 50 to 150 nm by EDAX accessory attached to TEM H-700H.

It is found from fig. 9, in which the PTT and RTT curves of steel 9 are superposedly plotted on the same graph, and as the initial dynamic recrystallization curve intersect with the initial PTT curve, the slope of the former varies greatly. This means that the delaying effect on the dynamic recrystallization is rather obvious owing to the occurence of dynamic precipitation of carbonitrides.

From observation under TEM of carbon extracted replica of the hot compression samples, which has been heated to 1220 °C and quenched after deformation with greater strain rate, no precipitated particles are discovered. It may be recognized that the carbonitrides are essentially dissolved at this temperature, and have not enough time to precipitate from the austenite under the high strain rate. In this case, the delaying effect on recrystallization dominantly results from solute hindrance of Nb and Ti elements owing to their greater size effects on the lattice deformation (right side of fig.10). For a certain range of strain rates, a peak appears on the $\varepsilon_p$-$\dot{\varepsilon}$ curve, this may be attributed to considerable precipitation of Nb, Ti carbonitrides, and results in intensification of delaying effect on recrystallization. On the left side of the $\varepsilon_p$-$\dot{\varepsilon}$ curve, deformation time is longer because the strain rate is small, so the firstly precipitated particles begin to coarsen, but they still have some effect on pinning the grain boundary and thus on delaying recrystallization. There are about half an amount of microalloying element remaining in the solid solution, it also contribute to the delaying of recrystallization.[7] Consequently, the retarding effect on dynamic recrystallization must be resulted from the combined contribution of solute hindrance and precipitated particles. At that time, both the larger sizes of particles and the diminution in solute atoms may combinedly weaken their impression on constraining recrystallization, hence the suppress effect exerted by microalloying elements on recrystallization at slower strain rate is smaller compared with that in other regions on the $\varepsilon_p$-$\dot{\varepsilon}$ curve.

## CONCLUSIONS

1. Addition of a minute amount of Nb or Ti to the low C-Mn steel will effectively suppress austenite grain growth during heating. This effect is more evident as they are added simultaneously.

2. The precipitation kinetics of Ti carbonitride changes and the temperature for dynamic precipitation decreases when Nb is added simultaneously. As the amount of Nb in steel increases, the time for the onset of carbonitride to precipitate is retarded. This is benificial for refining the precipitates and increasing precipitation in lower temperature region of austenite and also in higher temperature region of $\alpha$-phase.

3. The deformation energy required for recrystallization increases with increasing amount of Nb and Ti in steel, therefore the temperature for occurence of recrystallization is raised. The postponing effect on recrystallization before dynamic precipitation may be caused by solute hindrance of Nb and Ti atoms, while that after may result from combined effect of Ni, Ti carbonitrides and the elements remained in solid solution.

4. In this experiment, Nb, Ti carbonitrides may present as $(Nb_x, Ti_y)(C_m,N_n)$ in the form of continuous solid solution, in which the relative amount of each element at different temperature varies. The sizes of precipitating particles become larger and the contents of Ti increase also.

5. The preliminary result attained in our experiment is, a steel with compositions of C 0.05/0.09, Mn 1.0/1.3, Nb 0.03/0.05, Ti 0.01/0.03, $Al_{sol.}$ 0.02/0.3 may achieve a good combination of strength and toughness by conventional rolling followed by controlled cooling.

## REFERENCES


1. M.J. Crooks, J.M. Chilton, Metall. Trans. A. 15A, p.1137 (1984).
2. K. Amano, A. Kamada and N. Ohashi, Tetsu-to-Hagane, 65 A177 (1979).
3. Y.E. Smith, A.P. Coldren and R.L. Cryderman, in "Towards Improved Ductility and Toughness", p.119, Climax Molybdenum Company, Kyoto, Japan (1971).
4. N.J. Kim, J.Metals, 35, No.4, p.21 (1983).
5. K. Kunishige, T. Hashimoto and T. Yukitoshi, Tetsu-to-Hagane, 66, p.63 (1980).
6. M.G. Akben, I. Weiss and J.J. Jonas, Acta Metall, 29, p.111 (1981).
7. J.N. Cordea, Symposium on Low Alloy High Strength Steels, p.61, Metallurg. Companies, Nurnberg, BRD.

# AN INVESTIGATION OF LOW CARBON SILICON-NIOBIUM DUAL PHASE STEEL WIRES (SECOND REPORT)

**Yao Weixun, Zhang Li**
Institute of Iron & Steel Research
Anshan Iron & Steel Complex
Anshan, Liaoning, P.R.China

**Wang Quanshan, Sun Jianlun***
Department of Metallic Materials
Northeast University of Technology
Shenyang, Liaoning, P.R.China

ABSTRACT

A study has been made of the influence of different compositions, hot-rolling and heat-treatment processes on the micro-structures, mechanical properties and cold drawing properties of low carbon Si-Nb dual-phase steels containing 0.06-0.09%C, 1.5-1.9%Si and 0.03-0.05%Nb. The steel treated by firstly quenching from $\gamma$phase region and then heating to $\gamma+\alpha$ two-phase region and quenching again (hereinafter referred to as intermediate quenching) had better cold drawing ability than that treated by direct quenching from two phase region after hot rolling (hereinafter referred to as direct quenching), and no further heat treatment was needed when these steels were cold drawn into wires. A complete process of deformation and cracking to fracture was observed by in situ techniques under a HITACHI S-570 scanning electron microscope equipped with tensile accessories. It was found that dislocations piled up on the ferrite-martensite interfaces and ferrite grain boundaries, that led to the nucleation of cracks and finally to fracture.

DUAL PHASE STEELS have low yield strength, good ductility and high work hardening ability.[1-3] They can be easily formed and strenghtened in the meantime. The dual-phase steels extensively used in industry at present are those for stamping, while the studies on non-stamping ones are few. Professor G. Thomas has undergone many works in this respect. A "FERMAR" dual-phase steel has been developed for wires, chains, reinforced bars, etc., and a patent has been published.[4]

Since 1986 we have investigated into a low carbon Si-Nb steel. The objective of the present study is to investigate the structure-property relationships in the dual-phase steels produced by direct quenching and intermediate quenching, and discuss the feasibility of producing cold-drawing wires with these dual-phase steels.

## EXPERIMENTAL MATERIALS AND PROCEDURES

Chemical analysis of steels studied are listed in Table 1. Steel 22 was hot rolled to 90 mm square firstly, then homogenized at 1220°C and rolled to a wire-rod coil of 9 mm diameter by 7 passes on a commercial mill with finishing temperature about 1040°C. The whole coil was then transported to a water

* This paper is the master dissertation written by Sun Jianlun.

tank and quenched. The quenching temperatures of its outer and inner layers were not uniform and varied from 750 to 900 °C. The steels 4, 8 and 10 were hot rolled to 60 mm squares, and then forged to 40 mm squares. Forging cracks were found in the center portion of them because the deformation temperatures were too low. They were then reheated to 1220 °C and rolled to bars of 12 mm in diameter by 9 passes on a trial mill with finishing temperatures of 850 to 950 °C, and quenched immediately in water.

In the meanwhile, specimens were taken from each steel and heat treated in a laboratory furnace according to two systems (Fig. 1), namely, intermediate quenching and simulating direct quenching, so as to decide the appropriate quenching temperature that will be adopted in the $\gamma+\alpha$ region according to their mechanical properties obtained. Dynamic tensile specimens after heat treatment mentioned above were electrically polished and deep etched to reveal the microstructures and then stretched in a HITACHI S-570 scanning electromicroscope to observe the complete process of crack initiation and propagation to fracture in relation to the morphologies of microstructures.

The wire rods and bars treated by direct quenching and intermediate quenching were then cold drawn out into wires.

Mechanical properties and stress-strain curves were determined for all bars and wire rods thus prepared. For a part of them, the uniform elongation and work hardening index n was measured also.

The microstructures of specimens etched with 2% Nital or Lepera etchant[5] were observed with a Neophot-II optical microscope and a HITACHI-700H TEM. With the latter precipitates in steels extracted by carbon replica together with SPEED method were also examined.

## RESULTS AND DISCUSSIONS

MICROSTRUCTURE - The microstructures of steels heat treated by direct quenching and intermediate quenching are shown in Fig. 2. The microstructures of the former are consisted of fine equiaxed ferrite whose grain size number is about ASTM No. 10 to 11 and martensite islands which distribute along ferrite grain boundaries, and that of the latter are narrow fine lamellar martensite characterized by oriental distribution interspacing with ferrite. The formation of the lamellar martensite is related to the lamellar austenite which forms during heating a non-equilibrium structure in the two phase region, and is the result of heredity of microstructure.[6-7]

Table 1 - Chemical Analysis Of Tested Steels (wt %)

| No | C | Si | Mn | P | S | Nb |
|---|---|---|---|---|---|---|
| 22 | 0.12 | 0.99 | 0.33 | 0.016 | 0.02 | 0.041 |
| 4 | 0.08 | 1.35 | 0.34 | 0.009 | 0.014 | 0.033 |
| 8 | 0.06 | 2.0 | 0.42 | 0.01 | 0.01 | 0.045 |
| 10* | 0.05 | 2.08 | 0.23 | 0.006 | 0.016 | - |

*Refference steel

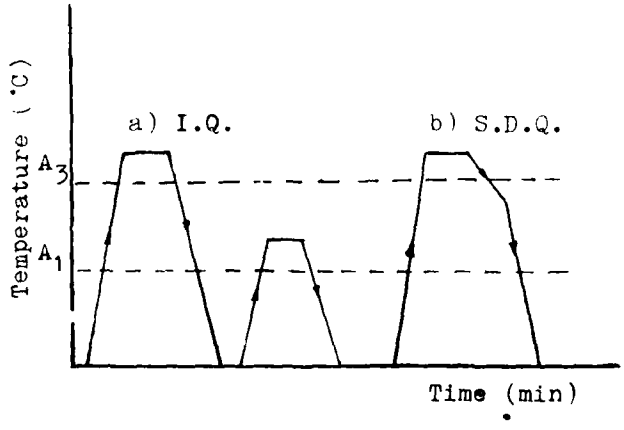


Fig. 1 - Schematic representation of dual-phase heat treatments
a. Intermediate quenching b. Simulating direct quenching

The details of island and lamellar mar-

tensite were observed under TEM. It is found that all the sub-structures of them have both twin and dislocation types, which are related to temperatures of quenching. It is composed mainly of dislocations when the quenching temperature is high. Along with the decrease of temperature, the carbon content of martensite increases, and so the substructure becomes predominately twins-dislocations as shown in Figs. 3 and 4.

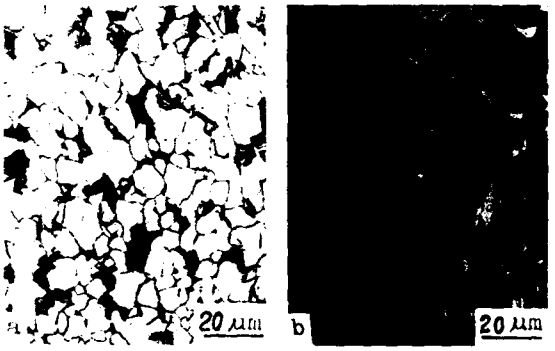


Fig. 2 - Optical micrographs of dual-phase steels
a. direct quenching, 2% Nital etch.
b. intermediate quenching, Lepera etch.

In the ferrite obtained by these two schemes of heat treatment, there are a lot of dislocations, cell substructures which are consisted of dislocation tangles, and some dispersed precipitates as shown in Fig. 5. These dislocations are essentially produced during the austenite/martensite deformation. The exsistence of dislocations and substructures enhances the strength of steels.

PROPERTIES - The stress-strain curves of all the tesile specimens heat treated by direct quenching and intermediate quenching are characterized by continuously yielding which is typical of dual-phase steel.

The relations between quenching temperatures and mechanical properties of niobium containing and reference steels heat treated by intermediate quenching are shown in Figure 6a. Generally, the strength increases and the ductility decreases as the quenching temperature is raised, but a good ductility still holds. The elongation is about 27% and the work hardening index is in the range of 0.18 to 0.20. In spite of the lower carbon content of steel 8 as compared with steel 4, its tensile strength is higher than that of the steel 4 and the yield strength and elongation of these two steels are approximately the same because of the higher silicon content of steel 8. Silicon is a strong solution hardening element and the presence of silicon in ferrite matrix can improve the ductility of steels. It has been reported that for a given strength level of dual-phase steels, a larger ductility may be attained in the steel with higher strength of ferrite.[8]

The contents of carbon and silicon in steel 8 and the reference steel are approximately the same, but the tensile strength and

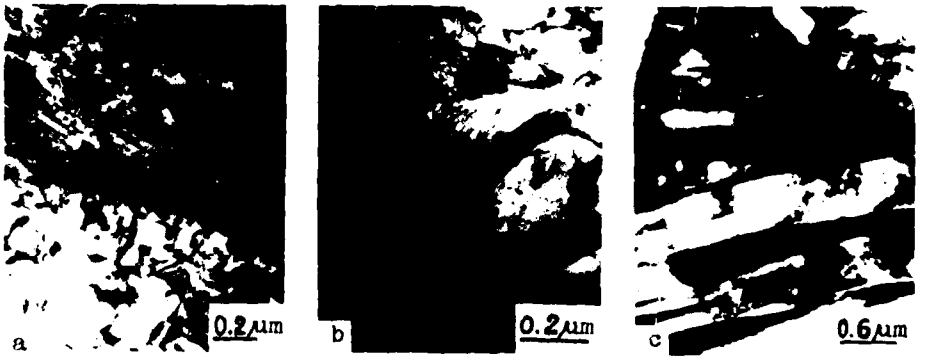


Fig. 3 - The martensite substructures of steels, intermediate quenching, TEM.
a. twin, quenched at 840 °C, b. twin+dislocation, quenched at 950 °C, c. dislocation, quenched at 950 °C,

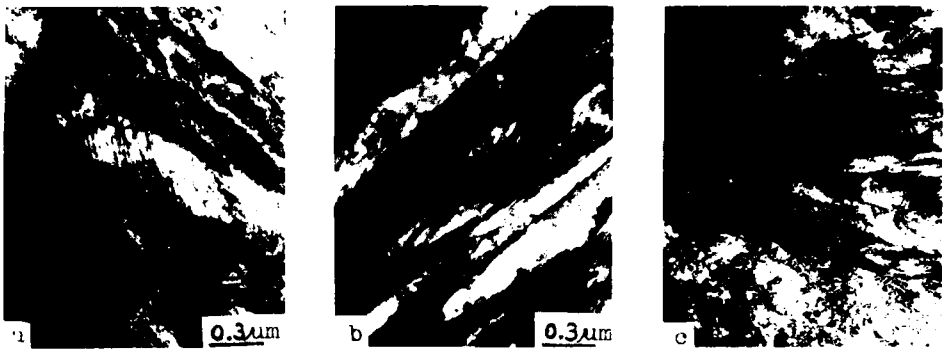


Fig. 4 - The martensite substructures of steels, direct quenching, TEM
a. twin. quenched at 850 ℃, b. twin+dislocation, quenched at 950 ℃, c. dislocation, quenched at 950 ℃,

elongation of niobium containg steel is obviously higher. This makes the ratio of yield strength to tensile strength decrease greatly and is beneficial for work hardening in cold drawing. In order to attain a better combination of strength and toughness, the quenching temperatures should be about at 900 to 950 ℃, as shown in Fig. 6a. A similar relationship also exists between the mechanical properties and quenching temperatures of steels treated by direct quenching as can be seen in Fig. 6b.

The influence of quenching temperature on the properties of dual-phase steels is achieved by virtue of the following aspects: the carbon content and the volume fraction of martensite thus obtained, the sub-structure of it, and the hardenability of austenite under this temperature. Evidently, it is an important factor which affects the strengthening of dual-phase steels.

DYNAMIC STRETCHING - Fig. 7a shows the microstructure of steels treated by simulating direct quenching before stretching (F+M island).

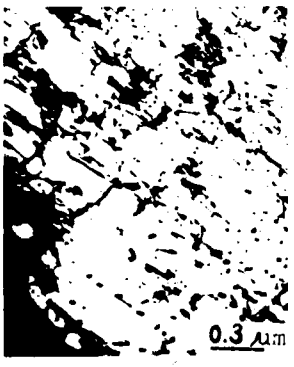


Fig. 5 - Dislocation substructures in ferrite.

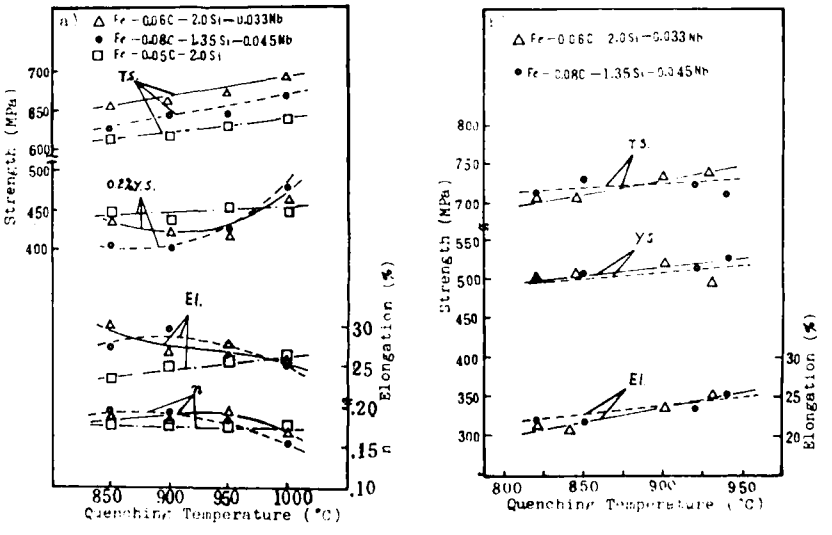


Fig. 6 - The relation between mechanical properties and quenching temperatures of dual-phase steels,
a. intermediate quenching b. direct quenching

There is a crack initiated on the ferrite side of a F/M interface and on the other side a crack is along the F-F boundary, as shown in Fig. 7b. These two cracks emerge just before necking of the specimen under stretching and the propagation of them under continuously increasing loading are shown in Fig. 7c. The F/M interface crack propagates by going round the M-island and entering the ferrite beside it. It seems that the martensite has an effect on hindering the crack propagation. However, the F/F boundary crack can not propagate further because the direction of propagation is almost parallel to the horizontal tensile axis and the M-island located in front of crack tip plays an important role in hindering the crack propagation. It shows that only the crack vertical to the tensile axis can propagate continuously.

No conspicuous deformation of M-islands could be discerned before necking, while the ferrite grains already deform greatly and the deformation is not uniform among various ferrite grains due to their different orientation. When the slip lines roughly parallel to the M-islands, the nearer to the M-island, the denser the distributions of slip lines are, and then they propagate by going round them. When slip lines intersect with the interfaces or ferrite grain boundaries, they pile up and converge to deformation bands as the deformation is increasing and microcracks initiate due to the intensification of strain concentration.

Araki et al[9] considered that the cracks had formed under a lower stress as the dual-phase steels were stretched, but the view of Shen Xianpu et al[10] was that all the cracks capable of propagating emerged only after

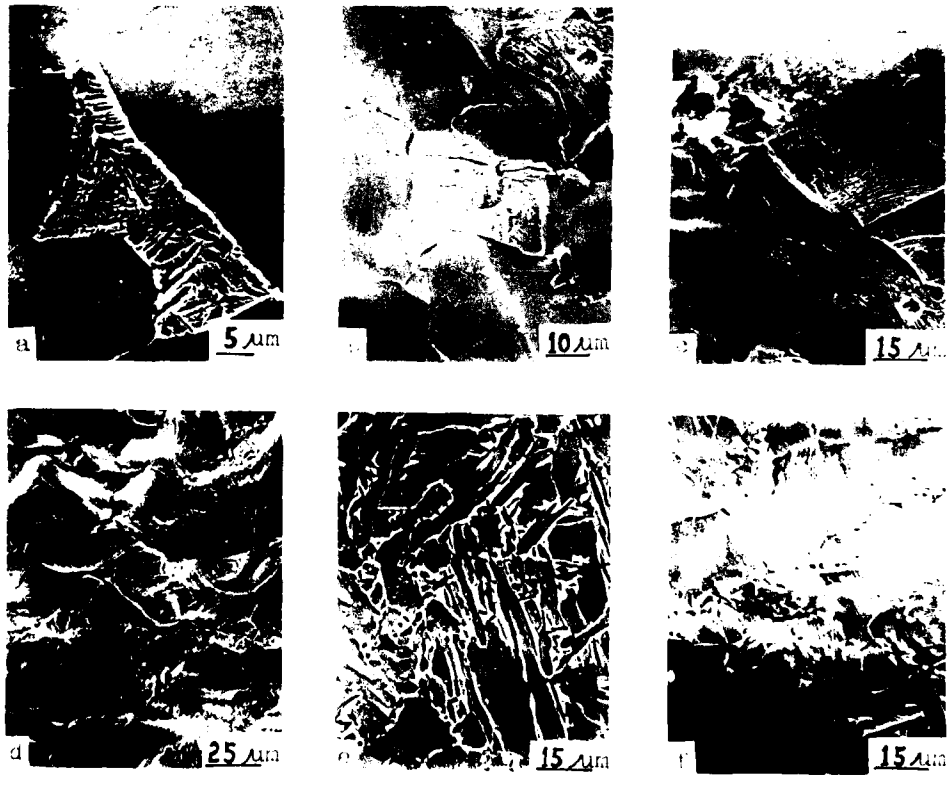


Fig. 7 - The initiation and propagation of cracks in dual-phase microstructures under SEM
a. direct quenching, microstructures before stretching b. direct quenching, F/M interface crack c. direct quenching, crack propagation d. direct quenching, the main crack before fracture e. intermediate quenching, microstructures before stretching f. intermediate quenching, microvoids.

necking. This work shows that cracks form essentially after necking, but also may emerge just before the necking will appear.

It is found that when the steel with F+M-island microstructures are stretched, the cracks will emerge mainly on the interfaces or boundaries, and also may be in ferrite grains and on the inclusions and so on. The microcracks originate just in the places where the slip lines are obstructed seriously. It shows that they form by the dislocation pile-up model. During the whole stretching process, the M-islands deform slightly and rotate as a whole under the shear stress towards the tensile axis. Generally, the main crack propagates on the ferrite side of the M-island by going round it, as shown in Fig. 7d. This may be the reason why dual-phase microstructures have good combination of strength and toughness.

Fig. 7e shows the microstructures after intermediate quenching before being stretched (F+lamellar-M). The microcracks do not appear until the later period after necking during stretching of this dual-phase steel. They form mainly at the F/M interfaces or on the inclusions and propagate in a manner of microvoid coalescing as shown in Fig. 7f. The amount of microcracks in this dual-phase steel is far less than that in the directly quenched steel, and the uniform and total elongations as well as necking of the latter are more greater than the former.

In the microstructures of steels by intermediate quenching, the interface between the two phases is coherent or a low angle boundary and crystallographic continuity of slip planes and directions may be maintained across the interfaces. But in the microstructures of steels treated by direct quenching, most of the F/M interfaces are high angle boundaries where voids are easily formed than in the former steels.[11] On the other hand, the lamellar martensite obtained by this way is finely dispersed and can be well deformed cooperately with the ferrite matrix.

PROPERTIES OF COLD DRAWING - Table 2 shows the final diameter, the total reduction of area and the ultimate strength of cold drawn wires. It can be seen that for a selected regime of heat treatment, steels of the same chemical analysis (8-1 and 8-2) quenched at higher temperatures have more better cold drawing capability than those quenched at lower temperatures, which is accordant with the result shown in Fig. 6b. When the quenching temperature is lower, the volume fraction of martensite is fewer and the carbon content in it is higher. Speich[12] had derived an empirical relation showing that the reduction of area is inversely propotional to the product of carbon content of the martensite and the square root of the volume fraction of it. The inferior cold drawing properties at lower quenching temperatures may be related to the transformation of martensite substructures from dislocation type to twin ones with increasing carbon content in them.

It can also be seen from Table 2 that steels treated by intermediate quenching have more better cold drawing properties and ultimate strengths than that by direct quenching. This verifies again that the microstructures of the former have better deformation ability as mentioned above.

The steel 10 treated by direct quenching or intermediate quenching fractured brittlely at 10.50 mm diameter just after they had been drawn two passes and exhibited crystalline fractures. The reason is that when this steel is heated and rolled at higher temperatures, the microstructures are very coarse due to the absence of niobium which can effectively prevent the deformed austenite grains from recrystallization and coarsening. The grain-size number of steel 10 treated in this way is about ASTM No. 5 to 6, but that of niobium

Table 2 - Cold Drawing Properties of Dual-Phase Steels

| No. | Heat Treatment | Quenching Temperature (°C) | Initial Diameter (mm) | Final Diameter (mm) | Total Reduction of Area (%) | Ultimate Strength (MPa) |
|---|---|---|---|---|---|---|
| 22 | D.Q. | 800 | 9.0 | 1.00 | 98.8 | 1669 |
| 8-1 | D.Q. | 840 | 12.0 | 3.00 | 93.8 | -- |
| 8-2 | D.Q. | 930 | 12.0 | 1.72 | 97.9 | 1688(φ2) |
| 4-1 | D.Q. | 920 | 12.0 | 2.20 | 96.6 | -- |
| 4-2 | I.Q. | 950 | 12.0 | 1.10 | 99.2 | 1790 |
| 10-1 | D.Q. | 860 | 12.0 | 10.50 | 12.5 | -- |
| 10-2 | I.Q. | 950 | 12.0 | 10.50 | 12.5 | -- |

D.Q. - Direct Quenching I.Q. - Intermediate Quenching

bearing steels is about ASTM No. 10 to 11.

It is found that there are some fine NbC or Nb(CN) particles whose sizes are about 10 to 50 nm, distribited mainly within the ferrite matrix and a minor of them scattered along the grain boundaries (Fig.8). The existance of precipitates enhances the strength of steels and make a good combination of strength and toughness because the amount of toughness decreased by precipitation hardening can be compensated by that increased in grain refinement. Therefore, it is beneficial to add some grain refinement elements in dual-phase steels.

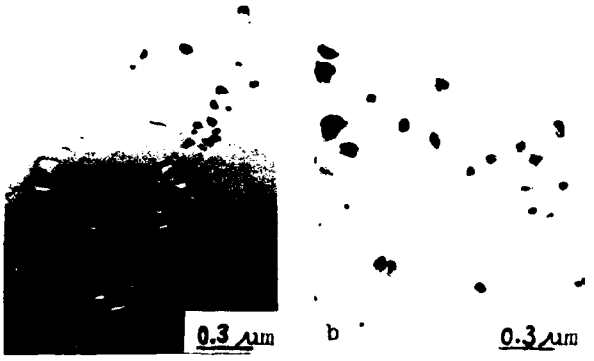


Fig. 8 - Distribution of precipitates in Nb-bearing dual-phase steels
a. at ferrite grain boundary,
b. within ferrite grains,

It can be seen from the changes of microstructures during cold drawing that with the increasing of the reduction of area the

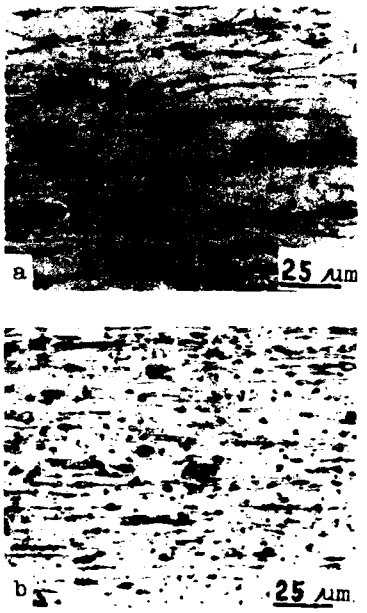


Fig. 9 - Deformation in steel 8-2 during cold drawing
a. φ6, b. φ2,

deformation of ferrite increases gradually and the larger martensite islands also deform and elongate along the drawing direction, but the smaller martensite islands deform only slightly and rotated towards the tensile axis. (*Fig.*9).

## CONCLUSIONS

An investigation has been made into the structure-property relations of dual-phase

steels containing 0.06-0.09%C, 1.5-1.9%Si and 0.03-0.05%Nb and wires drawn from them, the following conclusions may be drawn:

1. The direct quenching or intermediate quenching could be used to obtain ideal dual-phase structures in a wider range of quenching temperatures from 850 to 950 °C.

2. When these dual-phase steels are cold drawn into wires, no furthur heat treatment is needed. The steels treated by intermediate quenching have better col drawing capability than that produced by direct quenching.

3. When these dual-phase steels are stretched, the deformation undergoes mainly in the ferrite matrix, while the martensite rotates as a whole towards the tensile axis as the stress increases, but the deformation is less than that of ferrite. The pile-up of dislocations tends to fracture finally.

4. The cracks in steel by direct quenching initiate mainly at the F/M interfaces and propagate by going round the martensite islands, while in the steels of intermediate quenching the amount of cracks is less, and the fracture of them occurs only at the interfaces due to emerging and coalescing of microvoids.

5. The addition of niobium effectively refines the ferrite grains and is beneficial to cold drawing.

## ACKNOWLEDGMENTS

The authors are grateful to Mr. Cao Yinzhi for his critical review of this paper, Mr. Song Lan for hot rolling, Mr. Qi Baoxiang for cold drawing and to Mr. Xia Dianpei for TEM observations.

## REFERENCES

1. S. Hayami and T. Furukawa, Microalloying 75, Union Carbide Corp., New York, N.Y. 10017, 311 (1977).
2. J.Y. Koo and G. Thomas, Mater. Sci. Eng., 24, 187 (1976).
3. M.S. Rashid, SAE. Preprint 760206 (1976 Feb.).
4. G. Thomas, WO 84/02354.
5. F.S. Lepera, J. Met., 3, 38 (1980).
6. S. Kinoshita, ISIJ., 14, 411 (1974).
7. R. Homma, ISIJ., 14, 434 (1974).
8. R.G. Davies, Metall. Trans., 9A, 671 (1978).
9. K. Araki, Y. Takara and K. Nakaoka, Trans. ISIJ., 17, 710 (1977).
10. Shen Xianpu, Lei Tingquan and Liu Jianzhuang, Acta. Metallurgia, 21A, 228 (1985).
11. A. H. Nakagawa and G. Thomas, Metall. Trans., 16A, 831 (1985).
12. G.R. Speich and R.L. Miller, "Structure and Properties of Dual Phase Steels", p.145, R.A. Kot and J.W. Morris eds., TMS-AIME, Warrendale, PA (1979).

# DEVELOPMENT OF 100 kgf/mm² GRADE COLD-ROLLED SHEET STEEL CONTAINING RETAINED AUSTENITE WITH EXTRA-HIGH DUCTILITY

**I. Tsukatani, T. Kamei, T. Sakai, S. Hashimoto, K. Hosomi**
Iron & Steel Technology Center
Materials Research Laboratories
KOBE STEEL, LTD
Kobe, Japan

## ABSTRACT

A 100 kgf/mm² grade high strength sheet steel with a notably high product of tensile strength and elongation (TS x El = 2800) has been developed by introducing a large amount of retained austenite in 0.2%C -2.5%Si -1.5%Mn steel sheet by utilizing the heat cycle in a roll-quenching type continuous annealing line. This sheet steel shows not only good bendability and hole flangeability, but also excellent stretch formability when compared with conventional dual-phase sheet steels.

## INTRODUCTION

Various types of high strength sheet steels have been used as automotive materials for improving safety and for lowering fuel consumption by reducing vehicle weight. For example, 100 kgf/mm² grade cold-rolled dual-phase steels have been applied to door-guard-bars and bumpers.[1] Dual-phase steels have a number of unique properties, including the combination of high strength and easy formability.[2]

Recently, automobile industries have been trying to shorten the manufacturing process of those parts, which require steels with higher formability. In order to meet this requirement, multi-phase steels containing retained austenite are now being considered.[3]

The transformation of retained austenite during plastic straining and the resultant increase in work-hardening rate has been used to explain the higher ductility of metastable austenite stainless steels. Steels having transformation-induced plasticity (TRIP) due to retained austenite were found by Zackay.[4] Retained austenite was also found in dual-phase steels,[5] as first reported by Hayami et al.[2] It is well known that a significant amount of austenite is retained in steels containing about 2%Si when cooled to room temperature through the two-stage bainite transformation regime.[6] [7]

This cooling pattern is similar to the roll-quenching type continuous annealing process, which has become widely used in the production of sheet steels and includes two heat treatment stages: recrystallization annealing and overaging. Therefore, the process can be applied effectively to retain austenite.

It has been established that carbon is one of the most beneficial elements for retaining austenite. However, sheet steels with a high carbon content (over 0.2%) are disadvantageous in applications which require spot-welding. Therefore, it is necessary to establish an appropriate composition of sheet steel containing less than 0.2% carbon.

The present study has been undertaken to examine the mechanical properties of multi-phase sheets containing retained austenite produced on a roll-quenching type continuous annealing line (RQ-CAL), for the purpose of developing 100 kgf/mm² grade cold-rolled sheet steels with extra-high ductility.

## EXPERIMENTAL PROCEDURE

The chemical compositions of steels used in this experiment are shown in **Table 1**. A series of 0.2% carbon steels with silicon content of 1.5 ~ 2.5% and manganese content of 1.0 ~ 2.5% were hot-rolled to a thickness of 3.2 mm after being held at 1200 C for 1 hour. The hot-rolled sheets were

**Table 1** Chemical compositions of steels used (wt%)

| Steel | C | Si | Mn | P | S | Al | N |
|---|---|---|---|---|---|---|---|
| X1 | 0.40 | 0.97 | 1.51 | 0.008 | 0.007 | 0.043 | |
| X2 | 0.38 | 0.98 | 2.47 | 0.007 | 0.008 | 0.037 | |
| X3 | 0.21 | 1.01 | 1.52 | 0.007 | 0.0013 | 0.044 | 0.0039 |
| X4 | 0.20 | 1.70 | 1.49 | 0.005 | 0.0006 | 0.037 | 0.0008 |
| X5 | 0.21 | 2.51 | 1.51 | 0.005 | 0.0006 | 0.036 | 0.0009 |
| X6 | 0.21 | 0.99 | 1.96 | 0.004 | 0.0014 | 0.048 | 0.0035 |
| X7 | 0.20 | 1.67 | 1.98 | 0.004 | 0.0015 | 0.047 | 0.0035 |
| X8 | 0.20 | 2.00 | 1.99 | 0.014 | 0.0012 | 0.046 | 0.0008 |
| X9 | 0.21 | 2.44 | 1.90 | 0.003 | 0.0009 | 0.012 | 0.0014 |
| X10 | 0.17 | 1.34 | 1.86 | 0.017 | 0.0020 | 0.043 | 0.0035 |

reheated at 400, 440, 520, 600 and 680 C for 1 hour. After pickling, the hot-rolled sheets were cold-rolled to 0.85 mm thickness. The cold-rolled sheets were intercritically annealed at 770 ~ 860 C for 2 minutes, followed by cooling to 600 ~ 750 C ($T_1$) at rate of 6 to 12 C/s ($C_1$), quenched to 340 ~ 460 C, mainly 400 C ($T_2$) with a cooling rate of 100 C/s, and held at these temperatures for 3 minutes. This process simulates the thermal history of RQ-CAL.

The continuously annealed samples were tensile-tested without skin-pass rolling. Tensile specimens, 12.5 mm in width and 50 mm in gauge length (JIS No. 13B type) or 25 mm in width and 50 mm in gauge length (JIS No. 5 type), were prepared.

Microstructural examinations were made on a cross-section perpendicular to the rolling direction. The microstructure of each sample was examined by transmission and scanning electron microscopy. The volume fraction of martensite and bainite was determined by Quantimet image analysis.

Retained austenite measurements were made using an X-ray technique in the rolling plane of samples ground to half thickness, and were based on the integrated intensities of austenite 200 and 220 diffractions compared with that of ferrite 200 diffraction of Mo-K$\alpha$ radiation.

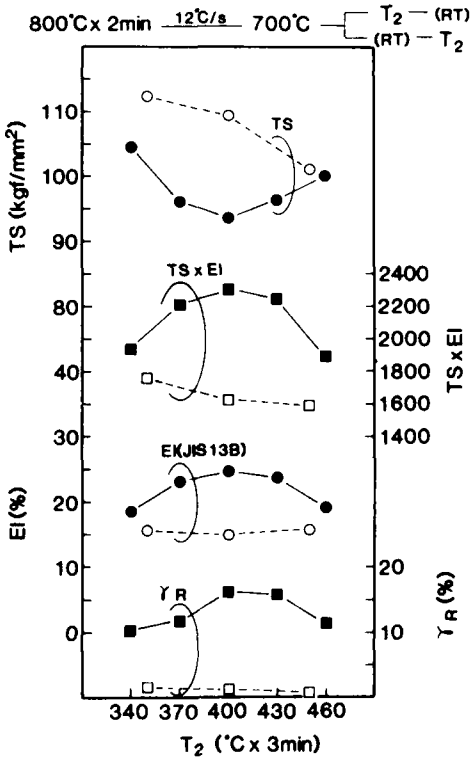


**Fig. 1** Effect of cooling pattern of continuous annealing on mechanical properties of steel X5 (Simulated coiling temp.: 680°C)
Solid marks: Roll-quenching type
Open marks: Water-quenching type

## RESULTS

**EFFECT OF COOLING PATTERN** For the purpose of clarifying the effect of cooling pattern after annealing, the mechanical properties of 0.2%C -2.5%Si -1.5%Mn steel sheets annealed with water-quenching to room temperature and then tempered at 350 ~ 450 C, and annealed with quenching interrupted at 340 ~ 460 C for 3 minutes were examined as shown in **Fig. 1.** An elevation in the tempering temperature decreases tensile strength in water-quenching type continuously annealed sheet. Total elongation remains a constant of about 15%. Consequently, a product of tensile strength and total elongation (TS x El) is about 1700. This may be due to the negligible amount of retained austenite in the water-quenching type continuonsly annealed sheet.

On the other hand, roll-quenching type continuously annealed sheet shows about 16% retained austenite and excellent tensile properties, i.e., tensile strength is about 94 kgf/mm$^2$, total elongation is 25% and the resultant TS x El is 2300 at an isothermal holding temperature of 400 C. The minimum tensile strength of the sheet is observed at an isothermal holding temperature of 400 C. The peak total elongation and peak TS x El are also observed at 400 C. The change in volume fraction of retained austenite shows the same tendency as that of total elongation.

**Photo 1** shows the change in microstructures as a function of isothermal holding temperature. The microconstituents of water-quenching type continuously annealed sheet are ferrite + martensite, though the photo is not illustrated.

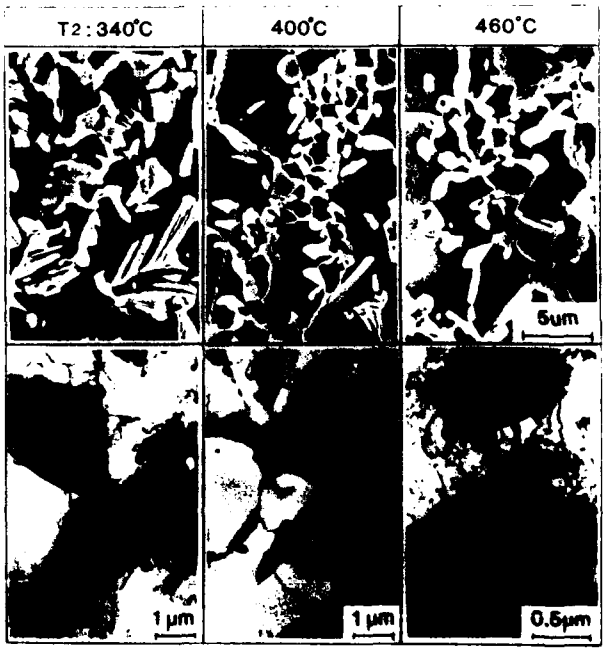


**Photo 1** Change in microstructure as a function of isothermal holding temperature of steel X5 after roll-quenching type continuous annealing at 800°C for 2 min with a first cooling rate of 12°C per second (Simulated coiling temp.: 680°C)

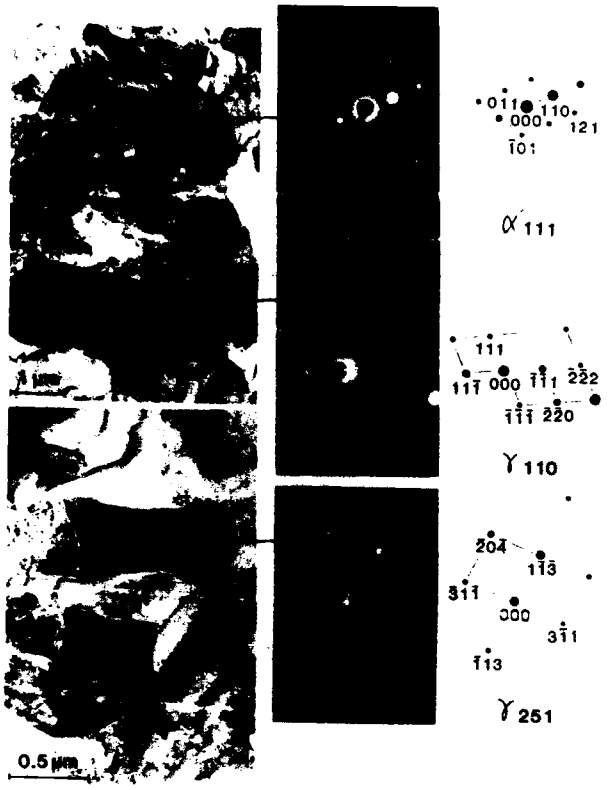


**Photo 2** Transmission electron micrograph of steel X5 after roll-quenching type continuous annealing

The microconstituent other than ferrite in roll-quenching type continuously annealed sheet is martensite with retained austenite of 10 ~ 16%. Retained austenite is observed not only as isolated particles within the ferrite grains, but also as aggregates with martensite, as shown in **Photo 2.** Some of the second phase looks like bainite under SEM observation. However, only bainitic ferrite is observed, and no "bainite" with carbide, under TEM examination.

As a result, an excellent combination of elongation and tensile strength is achieved in 0.2%C-2.5%Si-1.5%Mn steel by the roll-quenching type continuous annealing process.

**EFFECTS OF SILICON AND MANGANESE CONTENTS ON TENSILE PROPERTIES** The experiment has been undertaken to examine the effects of silicon and manganese contents on mechanical properties in 0.2% carbon steel, in order to achieve a good combination of strength and ductility by means of retained austenite without the use of expensive alloying elements in the roll-quenching type continuous annealing process. **Figure 2** shows the change in tensile properties and the volume fraction of retained austenite as a function of silicon content. The volume fraction of retained austenite increases as the silicon content increases in 1.5% manganese steel. The volume fraction of retained austenite in 2.0% manganese steel is almost independent of the silicon content, and is almost the same as that of 1.5% manganese steel having a silicon content of 1.7 to 2.5%. Each 1% addition of silicon increases tensile strength by 15 ~ 18 kgf/mm$^2$ in both 1.5% and 2.0% manganese steels. Total elongation remains almost constant for silicon contents of 1.0 to 1.7%. However, the increment in silicon from 1.7 to 2.5% deteriorates total elongation. TS x El in 1.5% manganese steel increases with the addition of silicon from 1.0% to 1.7% and remains constant for further increases of silicon. The optimum combination of tensile strength and ductility is obtained in steel having 1.5% manganese and 2.5% silicon.

The austenite fractions during intercritical annealing are different in steels used for examining the effect of silicon content due to the change in $Ac_1$ and $Ac_3$ temperatures, because all steels are annealed at 830 C for 2 minutes. However, it is confirmed that the addition of silicon also increases the volume fraction of retained austenite in sheets annealed at temperatures adjusted to obtain the same austenite fraction during intercritical holding.

**Figure 3** shows the relationship between volume fraction of retained austenite and TS x El. The increase in TS x El is closely related to the increase in volume fraction of retained austenite. The data are divided into three groups of relationship. It depends on manganese content of these steels. 1.5% manganese steel shows a TS x El of 1600, which is tensile strength of about 126 kgf/mm$^2$ and total elongation

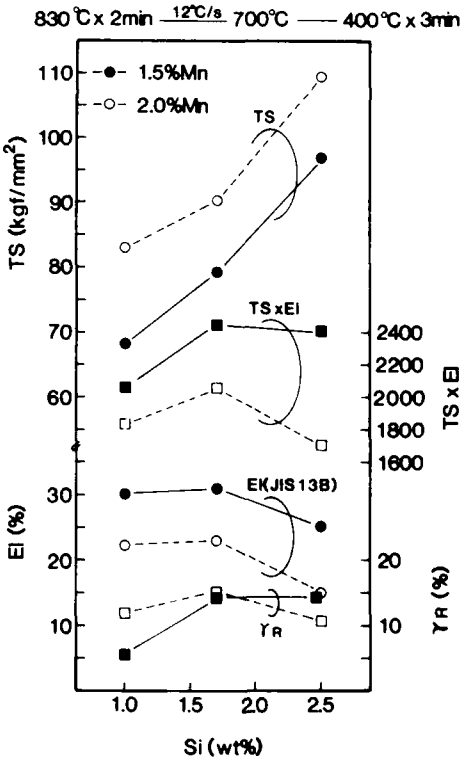


**Fig. 2** Effects of silicon and manganese contents on mechanical properties of sheets after roll-quenching type continuous annealing at 830 C for 2 min (Simulated coiling temp.: 680 C)

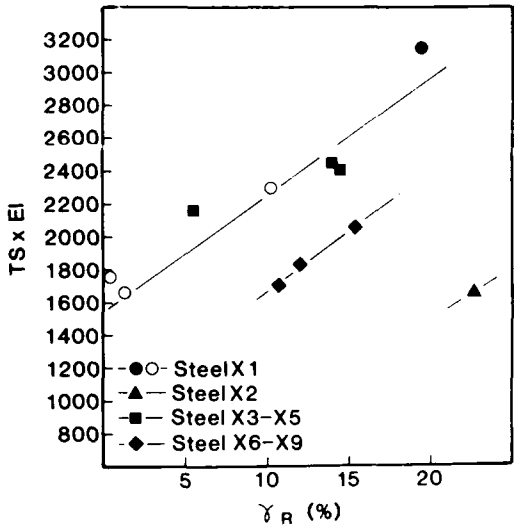


**Fig. 3** Relationship between volume fraction of retained austenite and product of tensile strength and elongation (by JIS 13B type tensile specimens)
Solid marks: Roll quenched
Open marks: Continuously cooled room temperature

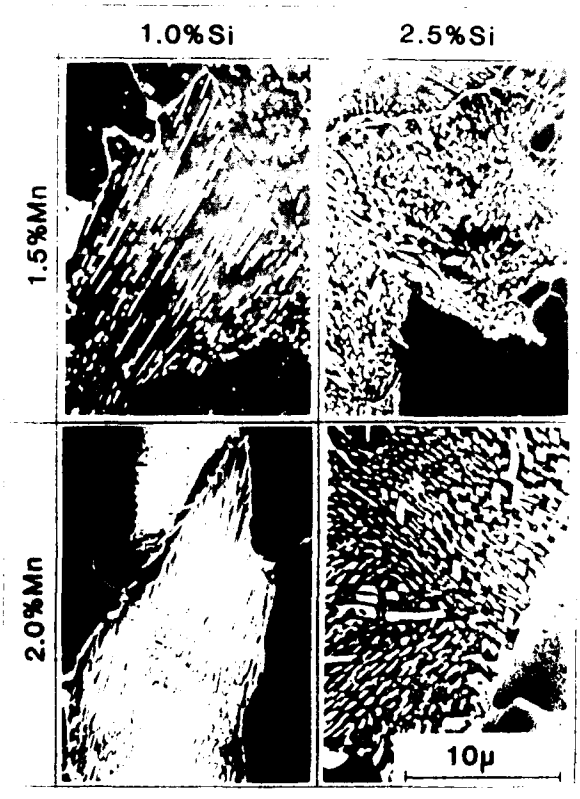


**Photo 3** Scanning electron micrographs of hot-rolled sheets coiled at 680 C

of about 12.5% in spite of as much as 23% retained austenite.

It is reasonable to assume that the change in ductility as a function of manganese contents has arisen from microstructural changes. The volume fraction of martensite increases as the manganese content increases. Therefore, the increase in volume fraction of martensite and consequential decrease in volume fraction of ferrite deteriorates TS x El in spite of a given volume fraction of retained austenite. It is expected that ferrite easily accepts the volume expansion of retained austenite which accompanies strain-induced transformation, leading to a better exhibition of TRIP.[3]

As the silicon content increases, the second phase becomes smaller in size with almost no change in the volume fraction of second phase though the volume fration of retained austenite increases slightly. Thus, the increase in tensile strength with silicon addition may be mostly attributed to solid solution hardening.

The change in microstructures of annealed sheets as functions of silicon and manganese contents may be due to that of hot-rolled sheets. **Photo 3** shows the change in microstructures of hot-rolled sheets as functions of silicon and manganese contents. The structure consists of ferrite + pearlite. As the manganese content increases, the volume fraction of pearlite increases and its lamella structure develops. On the contrary, as the silicon content increases, the size of pearlite decreases and the cementite in pearlite becomes globular.

**EFFETCS OF COILING TEMPERATURE AND *ANNEALING TEMPERATURE ON TENSILE PROPERTIES*** **Figure 4** shows the effects of simulated coiling temperature Tc and annealing temperature $T_1$ on the mechanical properties of steel X5 annealed by roll-quenching type continuous annealing. Elevating the simulated coiling temperature from 440 C to 680 C decreases tensile strength by 5 to 10 kgf mm$^{-2}$, increases total elongation by 3 to 7% and consequently increases TS x El. On the other hand, a low coiling temperature brings about an increase in tensile strength but a deterioration in TS x El. Therefore, a coiling temperature of about 520 C is suitable in terms of tensile strength and ductility.

**Photo 4** shows the change in scanning electron micrographs of hot-rolled sheets as a function of simulated coiling temperature. The lamella structure of pearlite develops in hot-rolled sheet with a lower simulated coiling temperature, whereas the cementite in pearlite becomes globular in hot-rolled sheet with a higher simulated coiling temperature. It is observed by metallographic examination that the nucleation of austenite in cold-rolled sheet with a lower simulated coiling temperature is more likely to occur at the pearlite particles during intercritical annealing, as shown in **Photo 4.** In cold-rolled sheet with a higher simulated coiling temperature, the transformation to austenite is initiated on the cementites distributed in rows. It is assumed that the difference of austenization results in changes of morphologies in martensite and retained austenite, though these differences become small by longer and higher annealing.

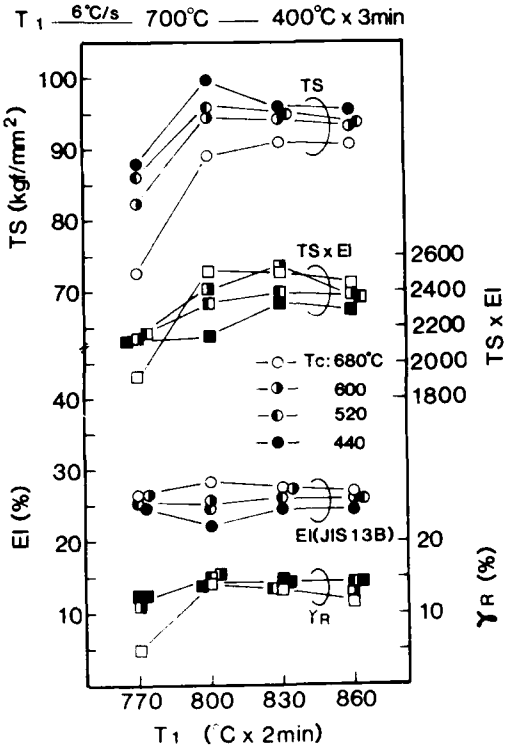


**Fig. 4** Effects of coiling ($T_c$) and annealing temperature ($T_2$) on mechanical properties of steel X5

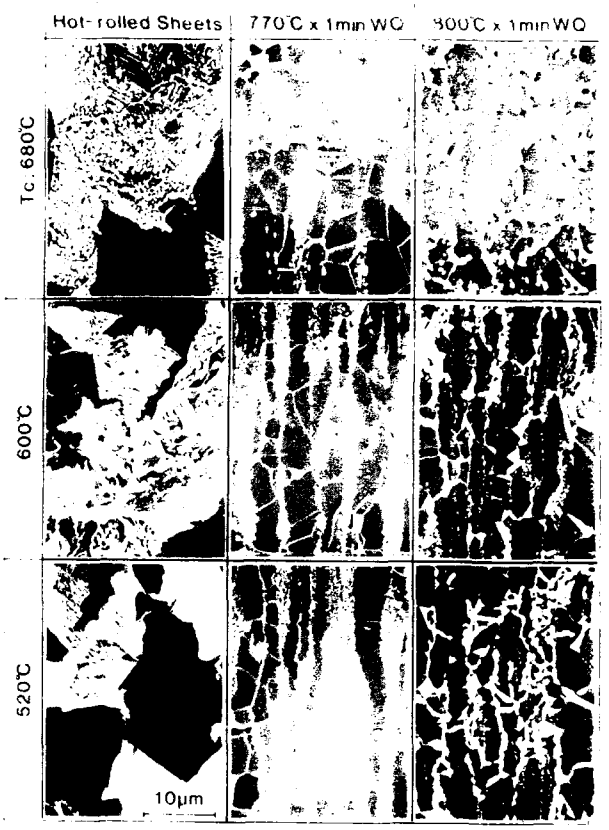


**Photo 4** Change in microstructures of steel X5 before and after anneal ing at 770 and 800 C for 1 min as a function of coiling temperature

Martensite increases slightly in volume fraction with a small change in retained austenite content as the coiling temperature decreases. Apparent differences of tensile strength and ductility due to change in the coiling temperature are believed to arise from the differences in martensite content and morphology, as well as the difference in retained austenite in stability against strain induced transformation.

A decrease in annealing temperature from 860 C to 800 C increases tensile strength and decreases total elongation, which are remarkable in sheets coiled at 440 C. A further decrease in annealing temperature rapidly decreases tensile strength and total elongation remains constant. The decrease in tensile strength at 770 C annealing may be due to incomplete austenization, as shown in **Photo 4.** The peak TS x El is obtained in sheets annealed at 800 C to 830 C. This peak is presumed to arise from the enrichment of austenite with carbon during intercritical annealing and from the stability of retained austenite.

**EFFETCS OF FIRST COOLING RATE AND QUENCHING TEMPERATURE ON TENSILE PROPERTIES** **Figure 5** shows the effects of the first cooling rate and quenching temperature $T_Q$ on the mechanical properties of steel X5 heated at 520 C for the simulated coiling treatment and annealed at 800 C for 2 min. In the case of a first cooling rate of 6 C per second, an excellent combination of 27% elongation (25 mm in width tensile specimen) and high strength of about 100 kgf mm² is achieved at a quenching temperature of 750 C. However, as the quenching temperature is lowered both tensile strength and total elongation deteriorate while yield strength increases.

**Photo 5** shows the change in transmission electron micrographs as a function of quenching temperature. The microstructures consist of ferrite with high density dislocation which may be bainitic ferrite, martensite and retained austenite. When the quenching temperature is lowered to 650 C, pearlite is observed though no change in the martensite distribution is observed. The introduction of pearlite deteriorates the strength and ductility. This results from the transformation from austenite to pearlite during the first cooling of 6 C per second.

On the other hand, in the case of a first cooling rate of 12 C per second, both tensile strength and total elongation remain at high levels in sheets annealed at temperature ranging from 750 to 650 C. Therefore, a high TS x El of 2900 is achieved even though the sheet is quenched at 650 C. A low quenching temperature is convenient for production on the actual process line.

As the simulated coiling temperature is lowered the quenching temperature at which high tensile strength and an excellent combination of strength and ductility are maintained decreases and tensile strength increases although total

elongation slightly decreases. Consequently, sheet heated at a simulated coiling temperature of 400 C and quenched from 600 C after cooling at a rate of 12 C per second shows a tensile strength of over 100 kgf/mm$^2$ and an excellent TS x El of 2700. Increasing the first cooling rate from 6 to 12 C per second results in the beneficial suppression of pearlite transformation without preventing the formation of polygonal ferrite during cooling.

**EFFECTS OF COILING TEMPERATURE AND QUENCHING TEMPERATURE ON HOLE EXPANDING LIMIT** It is thought that TRIP steel may not be suitable for commercial applications which demand stretch flangeability due to a lack of localized elongation, even though the steel shows high uniform elongation.[10] Thus, the following experiment was undertaken to improve the hole expanding limit as a characteristic parameter of stretch flangeability.

**Figure 6** shows the effects of the simulated coiling temperature and quenching temperature on the hole expanding limit of steel X5 annealed by roll-quenching type continuous annealing. An elevation in simulated coiling temperature brings about an increase in the hole expanding limit and lessens the effect of quenching temperature on the hole expanding limit. The hole expanding limits at simulated coiling temperatures of 400 to 520 C are low in value but are

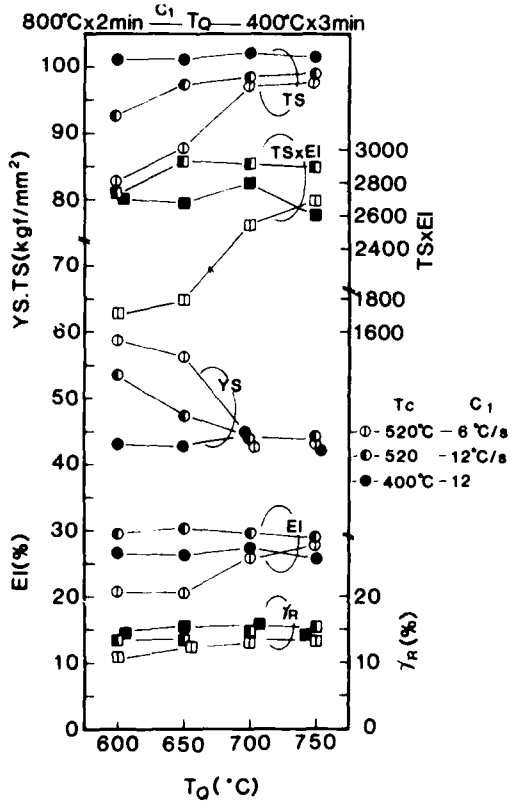


**Fig. 5** Effects of first cooling rate ($C_1$) and quenching temperature ($T_Q$) on mechanical properties of steel X5

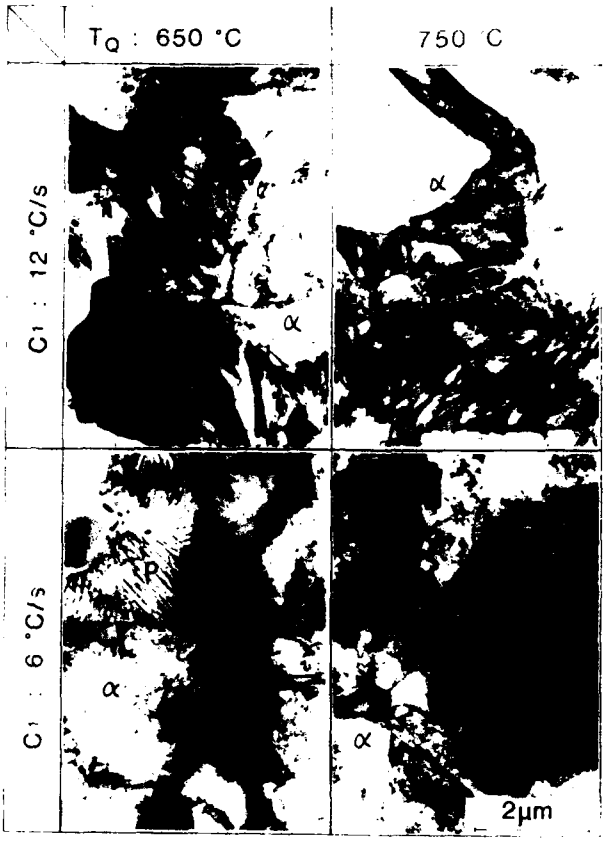


**Photo 5** Change in transmission electron micrographs as a function of quenching temperature of steel X5 after roll-quenching type continuous annealing at 800 C for 2 min with a first cooling rate of 6 C per second (Simulated coiling temp.: 520 C)

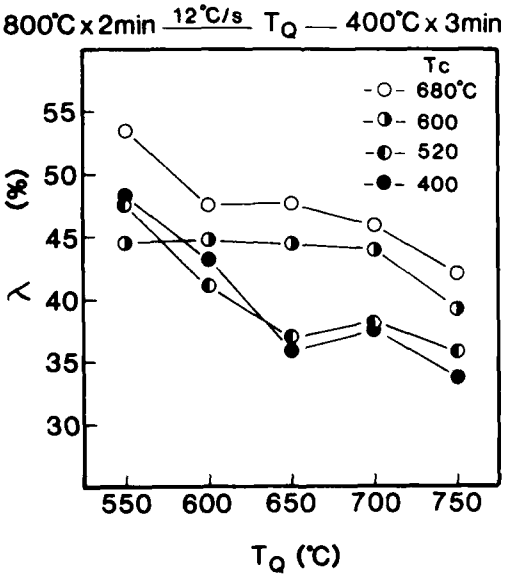


**Fig. 6** Effects of coiling temperature ($T_c$) and quenching temperature ($T_Q$) on hole expanding limit

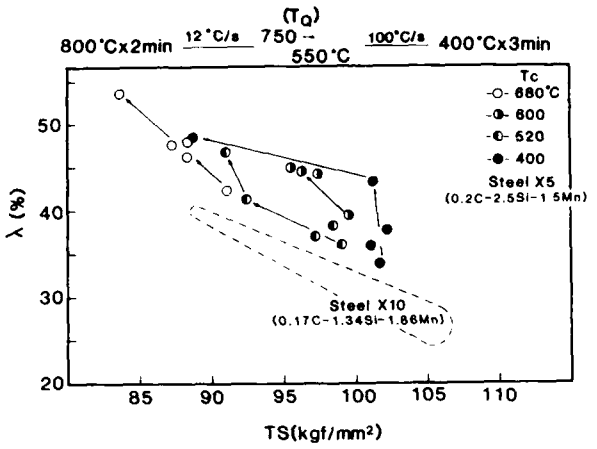


**Fig. 7** Relationship between hole expanding limit $\lambda$ and tensile strength

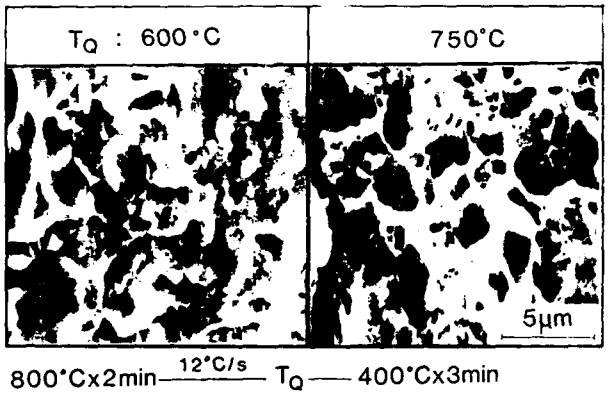


**Photo 6** Scanning electron micrographs of punched edge (Simulated coiling temp.: 400 C)

improved by decreasing the quenching temperature. The hole expanding limits are plotted against tensile strength in **Fig. 7**. At a simulated coiling temperature over 520 C, the hole expanding limit increases as tensile strength decreases. This relationship between the hole expanding limit and tensile strength is superior to that of conventional composition steel, steel X10, annealed by roll-quenching type continuous annealing. Furthermore, at a simulated coiling temperature of 400 C, a decrease in quenching temperature to 600 C improves the hole expanding limit at a given tensile strength. This may be due to the change in formation of the microcracks during punching caused by second phase, as shown in **Photo 6**, and the decrease in solute carbon content leading to beneficial suppression of the crack propagation in hole expansion.[11]

**PRESS FORMABILITY** As mentioned above a 100 kgf/mm$^2$ grade high strength steel with a notably high product of tensile strength and elongation has been developed by introducing a large amount of retained austenite in 0.2%C - 2.5%Si -1.5%Mn steel sheet by utilizing the heat cycle of RQ-CAL. An accumulation of press forming data is also required since practical applications usually involve various types of forming processes. The press formability of newly developed 100 kgf/mm$^2$ grade high strength sheet steel is evaluated by various press forming tests in the laboratory, and is compared with conventional 100 kgf mm$^2$ grade high strength cold-rolled dual-phase sheet steel produced by water-quenching type continuous annealing. This dual-phase sheet steel shows one of the best press formabilities of 100 kgf/mm$^2$ grade sheet steels put to practical use, such as in door-guard-bars and bumper reinforcement for automobile bodies.

Press formabilities investigated in this study were bendability, deep drawability, stretch formability, conical cup formability and hole flangeability. Tool dimensions, forming conditions and the experimental results of these press forming tests are summarized in **Table 2.** According to **Table 2.** it is apparent that the newly developed sheet steel having a superior combination of strength and ductility produced by roll-quenching type continuous annealing shows not only almost equal bendability and hole flangeability, but also excellent stretch formability compared with conventional dual-phase sheet steels. Therefore, the newly developed sheet steel is expected to be suitable for various applications requiring press forming.

## DISCUSSION

**EFFECT OF SILICON** Roll-quenching type continuously annealed sheets show extra-high ductility compared with sheets which are water-quenched to room temperature from intercritical annealing and then tempered at 350 ~ 450 C. Roll-quenching, followed by isothermal holding at 400 C for 3 minutes, is beneficially effective in introducing retained austenite. Silicon addition results in a significant increase in TS x El in roll-quenching type continously annealed sheets, indicating an improvement in ductility even though silicon increases the tensile strength by solid-solution hardening.

It has been reported that a significant amount of austenite is retained in sheets containing a middle to high carbon content by cooling to room temperature through the two-stage bainite transformation regime. However, there has been no investigation involving the 0.2% carbon steel used in this study, which is able to apply to spot welding.

Stabilization of the austenite at room temperature indicates that at some stage during the bainite reaction the austenite becomes enriched with respect to carbon. The isothermal transformation in the bainitic region does not always retain austenite. It depends on the presence of silicon. Silicon is known to inhibit cementite formation during the tempering reaction in steels.[12] This is generally explained by the relative insolubility of silicon in cementite requiring the diffusion controlled ejection of silicon at the transformation front which in turn results in a silicon concentration build-up during an early stage of growth. This locally increases the activity of carbon so that the carbon flux is reduced and further

development of the cementite embryos is inhibited[12].

Although details of bainite transformation in steels used in this study have not been clarified sufficiently, bainitic ferrite without carbide was observed. It is thought that this bainitic ferrite results in the inhibition of carbide precipitation due to silicon. The prevention of carbide formation correspondingly leads to a high concentration of carbon in austenite. The bainite transformation is a diffusionless transformation in which the growth of a sheaf occurs by the martensitic propagation of subunits, and the redistribution of carbon from these subunits to the residual austenite occurs after the actual transformation has taken place. Consequently, austenite is retained due to a lowered Ms point by the enrichment of carbon even after cooling to room temperature.

The retained austenite is observed not only as aggregate with martensite, but also as islands within ferrite grains. The former retained austenite can be explained by the above-mentioned hypothesis. However, the latter isolated retained-austenite particles may be caused by their small size since this inhibits their transformation to martensite, and may also be caused by the high carbon concentration of austenite, which even after sufficient intercritical annealing lowers the Ms point, since austenization is initiated on the carbides of pearlite.

**EFFECTS OF CONTINUOUS ANNEALING CONDITIONS** The peak volume fraction of retained austenite is obtained at an isothermal holding temperature (or austemper temperature) of 400 C in steel X5, as shown in **Fig. 1**. Shinoda et al[3] have examined the change in the volume fraction of retained austenite in a spring steel SUP 6 (0.6% C-1.7% Si-0.8% Mn) as a function of the isothermal holding temperature after an annealing at 850 C for 10 min. They have also showed the maximum content of retained austenite at 400 C, except in cases of extremely short or prolonged isothermal holding. According to Shinoda, the microconstituents are bainite + retained austenite + martensite at a lower isothermal holding temperature, and bainite + retained austenite at a higher temperature. And, the strength probably decreases as the isothemal holding temperature increases. However, it is important to note that the microconstituents are ferrite (including bainitic ferrite) + martensite + retained austenite, which are independent of the isothermal holding temperature within the present study, and the minimum tensile strength is obtained at an isothermal holding temperature of 400 C, as shown in **Fig. 1**. The transformation from austenite to bainitic ferrite contained no carbides due to the presence of silicon during the bainite reaction, which is assumed to be mostly promoted at a temperature just above the Ms point (380 C, calculated value). Consequently, the enrichment of carbon in austenite occurs and the peak volume fraction of retained austenite is thought to be obtained at 400 C. The elevation in isothermal holding temperature may decrease the carbon concentration in residual austenite, which is not enough to retain austenite at room temperature, caused by the retardation of bainitic ferrite transformation and the increase in the solute carbon content of ferrite. This residual austenite is thought to be transformed into twin-martensite during subsequent cooling and to bring about an increase in strength. On the other hand, if the isothermal holding temperature is lower then 400 C, it is reasonable to assume that lath-martensite is directly formed from austenite without the bainite reaction, and also brings about an increase in strength.

The low range of intercritical temperatures is applied

| Steel | Mechanical properties YS | TS | El (%) | Deep drawability | Stretch formability: flat punch | Stretch formability: Spherical punch | Conical cup formability (JIS17) | Hole flangeablity | Bendability |
|---|---|---|---|---|---|---|---|---|---|
| | | | |  | 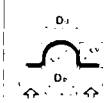 | | 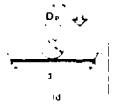 |  |  |
| | | | | $D_p$ : φ33mm, $D_d$ = 35mm, $r_p$ = 4mm<br>Blank size : φ66mm<br>B.H.F : 6.5ton | | | $D_p$ φ17.46mm<br>$d_2$ φ19.95mm<br>$r_p$ 1.2$D_p$<br>Blank size φ50mm<br>θ 60 | $D_p$ = φ33mm<br>$D_d$ = φ42mm<br>B.H.F = 6.5ton<br>θ 30 | t = 0.85mm<br>r = 0 ~ 4.4mm |
| | | | | Engelhardt method | | | | | |
| | | | | Limiting drawing ratio L.D.R | Maximum forming height $H_{max}$ (mm) | | Conical cup value $D_p$ (mm) | Hole expanding ratio | Minimum bending radius (mm) |
| X5 | 43.2 | 101.6 | 26.6 | 2.41<br>○ | 6.90<br>◎ | 11.7<br>◎ | 38.4<br>◎ | 43.3<br>◎ | 1.0<br>○ |
| X10 (Quenched) | 74.5 | 105.9 | 16.0 | 2.31<br>○ | 4.53<br>△ | 8.65<br>△ | Impossible to be formed<br>△ | 49.8<br>○ | 1.0<br>○ |

Excellent ←○←○←△ Poor

**Table 2** Tool dimensions, forming conditions and formabilities of steel sheets

for annealing in this experiment. When the annealing temperature is lower, slow dissolution of carbides becomes rate-controlling and it takes a long time to attain an equilibrium proportion of austenite. Undissolved carbides are found when the sheets are annealed at 770 C, just above the $Ac_1$ temperature, as shown in **Photo 4.** This implies an insufficient enrichment of austenite with carbon, and results in a small quantity and poor stability of retained austenite after the heat treatment that deteriorates both strength and elongation. On the contrary, excessive heating such as in the upper range of intercritical temperature and in the austenite single-phase range is thought to bring about a poor balance between strength and ductility. This is caused by the decrease in retained austenite content and the lowering of its stability due to an advance in the homogeneous distribution of carbon in austenite.

**RELATIONSHIP BETWEEN RETAINED AUSTENITE AND TRIP** The effects of retained austenite on ductility enhancement provement were discussed for dual-phase steels.[5),14)] However, the contributions of retained austenite have not been fully understood because it is doubtful that the relatively small amount of retained austenite and the completion of its transformation into martensite in the early stage of deformation could contribute to such improved ductility. In the present study, the contributions can be more clearly studied because of the large amount of austenite and the considerable increase in ductility.

**Figure 8** shows the change in the volume fraction of retained austenite and work-hardening rate as a function of tensile strain. Hot-rolled sheet of steel X5 was held at 400 C for 1 hour prior to cold-rolling. The simulated coiling temperature of steel X8 was 520 C. Both steels were heated at 800 C for 2 min, air-cooled at a rate of 12 C per second to 650 C, quenched at a rate of about 100 C per second to 400 C, held for 3 min and cooled to room temperature. The strength and ductility balance of steel X5 differed from that of steel X8, even though these steels provide the same volume fraction of retained austenite and almost the same tensile strength. The TS x El is 2681 for steel X5 and 2160 for steel X8. Steel X5 shows a large n-value even in a high strain of over 20%. The volume fraction of retained austenite decreases gradually with deformation from 14.6% before deformation to 2% after straining to uniform elongation. The decrease is caused by strain-induced transformation, and the accompanying large work-hardening results in improved elongation.

On the other hand, the decrease in the volume fraction of retained austenite of steel X8 is more rapid than that of steel X5, especially in the early stage of straining, and the rapid transformation from retained austenite to martensite probably deteriorates elongation. This difference may be attributed to the difference of retained austenite in the stability against strain-induced transformation as results of the different carbon content and second-phase distribution.

No apparent evidence with respect to the carbon content in austenite was detected by X-ray diffraction analysis, though it is expected that the carbon content in austenite of steel X5 is higher than that of steel X8 due to the different silicon and manganese contents. Accordingly, distribution of the martensite phases, as shown in **Photo 7,** must also influence the transformation behavior from retained austenite to martensite during tensile straining, and consequently influence ductility. Ferrite has a superior ductility because it is softer than martensite. Also, ferrite easily accepts the volume expansion of retained austenite which accompanies strain-induced transformation. Besides, the ferrite phase around isolated-retained austenite is presumed to relive external stress because the ferrite also accepts deformation. Therefore, strain-induced transformation occurs gradually, leading to a better exhibition of the TRIP effect. However, the presence of martensite is thought to diminish this effect. The retained austenite exists not only as aggregate with martensite, but also near martensite particles in addition to increasing martensite volume fraction in steel X8, in comparison with steel X5, as shown in **Photo 7.** Most of the

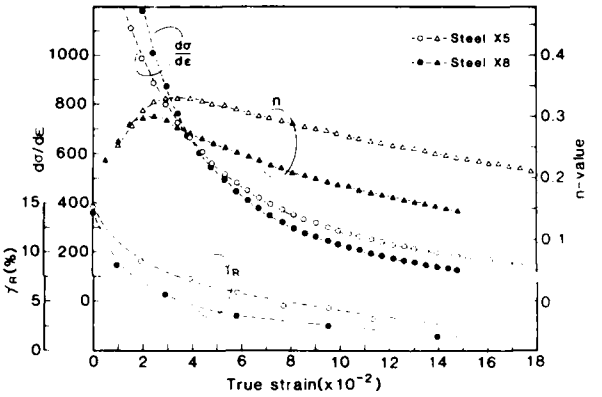


**Fig. 8** Changes in work-hardening rate and volume fraction of retained austenite as a function of tensile strain

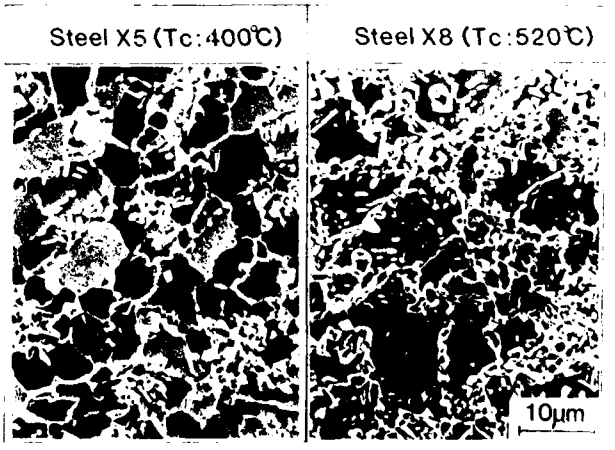


**Photo 7** Effects of silicon and manganese contents on microstructure of roll-quenching type continuously annealed sheets at 800 C for 2 min with a first coiling rate of 12 C per second

retained austenite in steel X8 may easily transform to martensite in the early stage of straining because the external stress directly propagates to retained austenite through the hard martensite phase. The presence of martensite is one of the reasons why strength-ductility balance is not good in spite of as much as 14% retained austenite before deformation.

## CONCLUSIONS

For the purpose of developing a 100 kgf/mm$^2$ grade high strength sheet steel with notably high elongation greater than 24% by utilizing transformation-induced plasticity of retained austenite, the effects of chemical compositions, hot-rolling conditions and continuous annealing conditions on the mechanical properties of 0.2% carbon steels were studied, and the key findings are:

1) Roll-quenching type continuously annealed sheets show extra-high ductility compared with sheets water-quenched to room temperature from the intercritical annealing temperature and then tempered at 350 ~ 450 C. Roll-quenching, followed by isothermal holding at 400 C for 3 minutes, is beneficially effective in introducing retained austenite. It is believed that the increment of elongation in sheets annealed by the RQ-CAL process results from the transformation of retained austenite during plastic straining and the resultant increase in work-hardening.
2) Silicon addition results in a significant increase in TS x El in roll-quenching type continuously annealed sheets, indicating an improvement in ductility even though silicon increases the tensile strength by solid-solution hardening. The effect of silicon may arise from the increase in appropriate stable retained austenite.

   On the other hand, it is observed that the addition of manganese deteriorates the total elongation though the amount of retained austenite remains unchanged. It is assumed that the effect of retained austenite on ductility is small, because the retained austenite transforms in the beginning of the straining process due to the presence of martensite.
3) As a result, a 100 kgf/mm$^2$ grade high strength sheet steel with a notably high product of tensile strength and elongation (TS x El = 2800) has been developed by introducing a large amount of retained austenite in 0.2%C-2.5%Si-1.5%Mn steel sheet by utilizing the heat cycle in an RQ-CAL process. This sheet steel shows not only equal bendability and hole flangeability, but also excellent stretch formability compared with conventional dual-phase sheet steels.

## REFERENCES


1) H. Shirasawa, Y. Tanaka, M. Miyahara and Y. Baba: Trans. ISIJ, 26(1986), p310
2) G.R. Seich: Fundamentals of Dual-Phase Steels, ed. by R.A. Kot and B.L.Bramfitt, AIME, Chicago, (1981). p3
3) O. Matsumura, Y. Sakuma and H. Takechi: Trans. ISIJ, 27 (1987), p570
4) V.F. Zackay, E.R.Parker, D.Fahr and R. Bush: Trans. Am. Soc. Mat., 60 (1967), p252
5) T. Furukawa, H. Morikawa, H. Takechi and K. Koyama: Structure and Properties of Dual-Phase Steels, ed. by R.A. Kot and J.W. Moris, AIME, New York, (1979), p281
6) S.J. Mates and R. F.Hehemann: Trans. Met. Soc. AIME, 221 (1961), 179.
7) R. Le Houilier, G. Begin and A. Dube: Metall. Trans., 2 (1971), 2645.
8) V.M. Pivovarov. I.A. Tananko and A.A. Levchenko: Phys. Met. Metallogr., 33 (1972), 116
9) H.K.D.H. Bhadeshia and D. V Edmonds: Metall. Trans. A, 10A (1979), 895.
10) J. Iwaya, Y. Tanaka, M. Miyahara, K. Korida: The Proceedings of 1988 IDDRG
11) M. Sudo, I. Tsukatani and Z. Shibata: Kobe Steel Enginieering Reports, Vol. 37, No. 2 (1987), p54
12) W.S. Owen: Trans. ASM. 1954, Vol. 46,p812
13) K. Shinoda and T. Yamada: Netsu shori (J. Jpn. Soc. Heat Treat.), 20(1980), 326.
14) A.R. Marder: Formable HSLA and Dual-Phase Steels, ed. by A.T. Davenport, AIME, Chicago, (1977), p89

# EFFECT OF COMPLEX PRECIPITATES ON MECHANICAL PROPERTIES IN Ti BEARING HSLA STEELS

**Shuji Okaguchi, Tamotsu Hashimoto, Hiroo Ohtani**
Technical Research Lab.
Sumitomo Metal Industries, Ltd.
Amagasaki, Japan

**Abstract**

The effects of Nb and V addition on mechanical properties and recrystallization behavior of austenite were investigated in Ti bearing steels, by comparing with the solubility and composition of precipitates. Addition of Nb decreases the tensile strength of Ti bearing steels reheated at a low temperature and increases the toughness of Ti bearing controlled rolled steels, whereas addition of V increases the tensile strength and scarcely increases the toughness. The addition of Nb is effective in increasing the solubility of precipitates in Ti bearing steels through the formation of complex precipitates, while the addition of V is little effective. It is concluded that the differences in the mechanical properties arise from the different solubility of the complex precipitates in Nb-Ti and V-Ti bearing steels.

## I. Introduction

In recent years Ti is more utilized in high strength low alloy (HSLA) steels to improve the mechanical properties of controlled rolled steels. Because microprecipitation of Ti carbonitrides brings about retardation of austenite recrystallization and precipitation strengthening of ferrite matrix. Addition of Ti increase both strength and toughness of low carbon steels.

Addition of Nb or V in Ti bearing steels can lead to formation of complex carbonitrides (which contains at least two metallic elements in precipitates), since the binary carbides and nitrides of these microalloying elements are mutually soluble because of their B1 type structure. Reports are available on the presence of complex precipitates in Nb-Ti[1,2] and V-Ti[1,3] steels. The formation of complex precipitates may change the stability of carbonitride precipitates, so that the addition of microalloys (Nb or Ti) is expected to influence the mechanical properties of Ti bearing steels. However, the characteristics of complex precipitates is not well understood and the effect of complex precipitates is not yet clear on mechanical properties of Ti bearing steels.

The main objective of the present work was to investigate the effect of Nb and V additions on the precipitation characteristics and recrystallization of austenite in Ti bearing steels in terms of microstructural and hot strength evaluation. And mechanical properties of Ti, Nb-Ti and V-Ti steels were examined considering the correlation among precipitation strengthening, recrystallization and complex precipitates with using thermodynamics model for complex precipitates.

## II. Experimental Procedures

(1) Materials

Three series of steels (Ti, V-Ti and Nb-Ti) with the chemical composition shown in Table 1 were melted as vacuum-induction melts and cast in 150 kg ingots with a base composition of 0.09wt%C-0.4wt%Si-1.6wt%Mn-0.03wt%Al-0.002wt%N. After soaking at 1250°C, the ingots were hot forged to 150 mm thick slabs.

Table 1. Chemical compositions of steels used (wt %)

| Steels | C | Si | Mn | Nb | V | Ti | N |
|---|---|---|---|---|---|---|---|
| Ti | 0.09 | 0.45 | 1.60 | | 0 | ~0.13 | 0.0024 |
| Nb-Ti | 0.09 | 0.44 | 1.57 | 0.027 | 0 | ~0.13 | 0.0023 |
| V-Ti | 0.09 | 0.43 | 1.56 | | 0.05 | 0.03~0.13 | 0.0022 |

(2) Precipitates in Ti bearing steels

After reheating to 1050~1250°C for 1h, the slabs were rolled to 80 mm, and cooled to 780°C for finishing rolling in a laboratory mill. The finish rolling reduced the plates from 80 to 20

mm, by finishing temperature at 700°C to be cooled in air. Some steels were solution treated besides controlled rolling. Test pieces machined from controlled rolled plates were reheated to 900~1250°C for 5h followed by water quenching.

Precipitates were extracted with carbon replicas from some specimens, for observation with TEM and quantitative microanalysis by STEM-EDX. Volume fraction of precipitates in solution treated specimens were extracted electrochemically for chemical analysis.

Tensile strength and Charpy 50% FATT were measured in the transverse direction of controlled rolled plates.

(3) Recrystallization of austenite

Static recovery and recrystallization kinetics after hot deformation of Ti-bearing steels were investigated by means of interrupted compression testing. By using the computerized hot deformation simulater equipped with induction heating system under a vacuum, the compression testing was performed.

From the true stress-strain curves, the percent softening taking place during the interval of the interrupted compression X was evaluated by following equation[4]:

$$X = \frac{\sigma_m - \sigma_{y_2}}{\sigma_m - \sigma_{y_1}} 100 \qquad (1)$$

where, $\sigma_{y_1}$, $\sigma_m$ : 0.2% offset yield stress and flow stress at a strain of 0.32 in the first compression

$\sigma_{y_2}$: 0.2% offset yield stress in the second compression

The cylindrical shape compression specimens with a diameter of 8 mm and height of 12 mm were machined from controlled rolled plates of the base (Si-Mn), 0.03wt%Nb, 0.07wt%Ti, 0.11wt%Ti and 0.03wt%Nb-0.05wt%Ti steels. After reheating at 1200 C for 5min., the specimens were kept at the deformation temperatures ranged from 850 to 1100°C for 1min., followed by the first compression with a strain of 0.32. The deformed specimens were kept isothermally in the various periods of time from 0.1 to 10000 s, and then the second compression was given in a strain of 0.32. The strain rate of first and second compression was 1 s.

## III. Results and Discussion

### III-1 Precipitates in Ti bearing steels

Figure 1 shows the distribution of precipitates in the three types of 0.13wt% Ti steels controlled rolled after reheating at 1150°C. The number of large precipitates (1000 A) is larger in Nb-Ti bearing steels than in Ti and V-Ti bearing steels. This difference in precipitates means that the addition of 0.03wt% Nb decreased the solubility of carbonitrides during reheating treatment, because large particles (>100 A), as shown Fig. 1, are usually formed in austenite at a high temperature. From Fig. 2, morphology of the precipitates in Ti bearing steels is classified into two types; spheroidal particles (a) and cuboidal particles (b). Cuboidal particles were mostly observed in the steels reheated at a above 1100°C, while spheroidal particles in those reheated at low temperatues. Both types produce identical electron diffraction patterns of the B1 type structure.

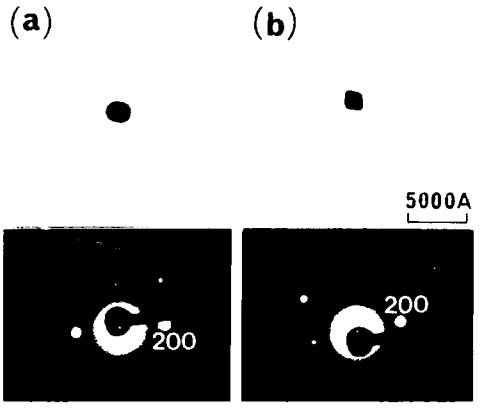


Fig. 2 Electron micrographs of extraction carbon replicas showing two types of precipitates particles ((a) spheroid, (b) cuboid) in 0.03wt%Nb-0.05wt%Ti reheated to 1100°C. Both have an identical diffraction patterns correponding to the B1 rock salt structure.

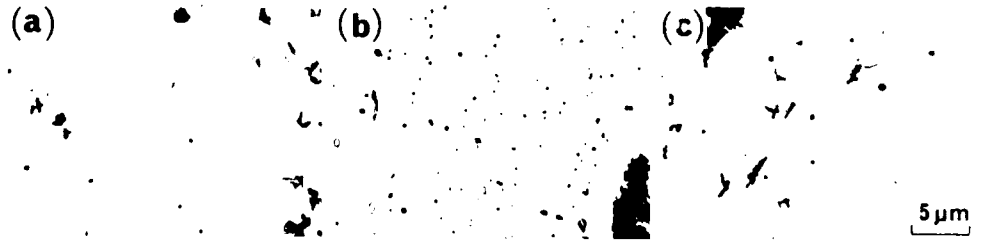


Fig. 1 Micrographs of extraction carbon replicas of: (a) 0.13wt%Ti, (b) 0.03wt%Nb-0.13wt%Ti and (c) 0.05wt%V-0.13wt%Ti bearing controlled rolled steels, reheated to 1150°C prior rolling.

Figure 3 shows the STEM-EDX analysis of Nb to Ti ratio in two types of particles for Nb-Ti bearing steels. Metallic elements were mutually soluble both cuboid and spheroid. The ratio of Nb/(Nb+Ti) in spheroid is relatively high and changes largely with Nb/Ti balance in steels and reheating temperature. On the other hand, Nb/(Nb+Ti) ratio in cuboid is fairly low and has little dependence on Nb/Ti balance and reheating temperature. Figure 4 shows the results of microanalysis of precipitates for V-Ti bearing steels reheating at 1050 and 1200 C. In contrast to the above, V/(V+Ti) ratio in both cuboid and spheroid in V-Ti bearing steels is extremely low and scarcely depends on V/Ti balance and reheating temperature. This suggests that Nb is significantly soluble in spheroid whereas V is only slightly soluble both in cuboids and spheroids.

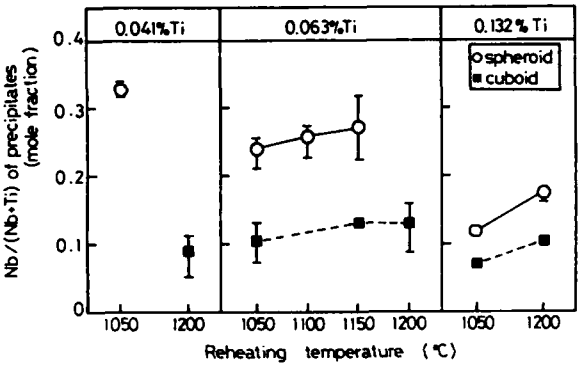


Fig. 3 contents of Nb in precipitate particles in 0.03wt%Nb-Ti bearing controlled rolled steels.

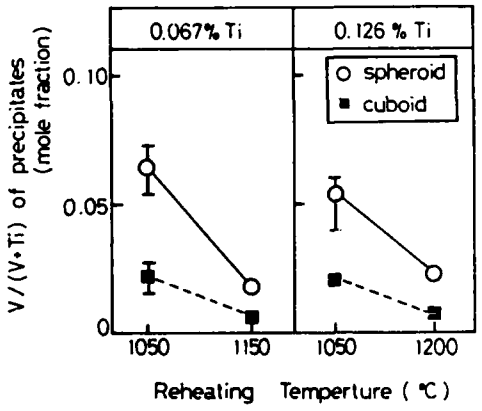


Fig. 4 Contents of V precipitate particle in 0.05wt%V-Ti bearing controlled rolled steels.

Figure 5 shows the amount of precipitates electro-chemically extracted from 0.05 and 0.13wt% Ti steels added 0.05wt% V and 0.03wt% Nb. The amount of precipitates decreases in all steels at higher temperatures: a significant increase by addition of 0.03wt% Nb both in 0.05wt% and 0.13wt% Ti steels below 1200 C. However, addition of 0.05% V makes a slight contribution. Above 1200°C, the amount of precipitates decreases to a level for all Ti bearing steels. The results of STEM-EDX microanalysis of precipitates show a considerable difference in solubility of complex precipitates between V and Nb. The V/(V+Ti) ratio of precipitates in V-Ti steels were extremely low while the Nb/(Nb+Ti) ratio of precipitates in Nb-Ti steels were relatively high.

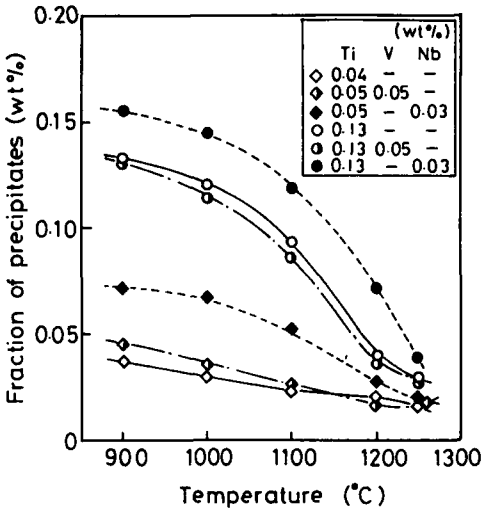


Fig. 5 Effect of 0.05wt%V and 0.03wt%Nb addition on the amount of precipitates in 0.05wt%Ti and 0.13wt%Ti bearing steels.

As described above, addition of Nb changed the precipitation characteristics in Ti bearing steels. Addition of 0.03wt% Nb increased the fraction of Ti carbonitrides and Nb were considerably soluble in the precipitates both in controlled rolled plates and solution treated specimens, while addition of 0.05wt% V were little effective in increasing the fraction of the precipitates and V were scarcely soluble in the precipitates.

These differences between Nb-Ti and V-Ti steels, can be related to the different solubility of carbonitride precipitates[5]. The 0.03wt% Nb addition in Ti bearing steels decreases the solubility of Ti carbonitrides in austenite corresponding to large solubility of Nb in the precipitates. Therefore, the amount of precipitates in Nb-Ti bearing steels will increase and consequently the amount of soluble elements in austenite matrix may be smaller in Nb-Ti bearing steels than Ti bearing steels. On the other hand, 0.05% V addition will have little influence on the solubility of precipitates since V is scarcely soluble in the precipitates.

The solubility of precipitates in austenite of Nb-Ti and V-Ti bearing steels can be estimated, by using an ideal solution model for quartenary precipitates. The model[5] assumed that precipitates was stoichiometric with Ti and

V or Nb on one sublattice, and C and N on the other, and that precipitation species had complete mutual solubility. The enthalpy of mixing and the charge configurational entropy of the matrix were neglected. The model can estimate the equilibrium chemical composition and fraction of precipitates at a given temperature.

Figure 6 compares the analyzed and calculated values of Nb, V and Ti in the precipitates of Nb-Ti and V-Ti bearing steels solution treated at a temperature between 900 and 1250°C. The chemical analysis of Nb, V and Ti agrees with the prediction based on the complex precipitates model. The model can predict both the low solubility of precipitates in Nb-Ti steels and the low V/(V+Ti) ratio of precipitates in V-Ti steels. And another calculation for the precipitate in controlled rolled steels, it is suggested that the cuboids and the spheroids may be the complex nitrides formed in the soaking (1250°C) before hot forging and the complex carbides formed in the soaking (1050~1150) before rolling.

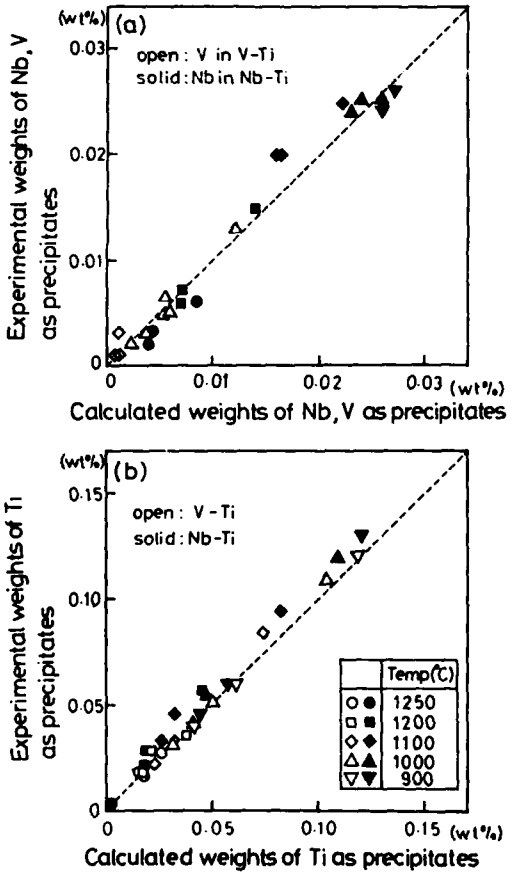


Fig. 6 (a) Nb, V as precipitates
(b) Ti as precipitates
Comparisons between the calculated and analyzed weights of microalloying elements as precipitates in V-Ti bearing (open mark) and Nb-Ti bearing steels (solid mark).

III-2 Recrystallization of Ti bearing steels

Softening kinetics after hot deformation of HSLA steels were investigated by means of the interrupted compression testing[4].

The dependence of the amount of softening taking place during the interval of unloading on the time of unloading is shown in Fig. 7 for the base (Si-Mn) and 0.11wt% Ti steels. Figure 7

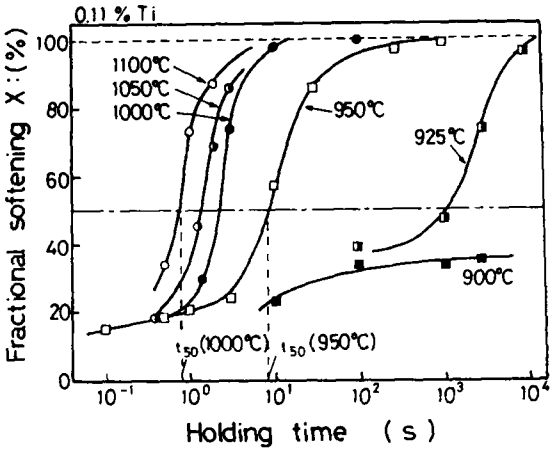


Fig. 7 Effect of holding time and temperature on isothermal softening after hot deformation of 0.11wt%Ti.

shows that retardation of softening due to static recovery and recrystallization in Ti bearing steels was small at temperature higher than 950°C, while retarding of softening became much more significant at the temperature lower than 950°C. It is infered that the marked retardation at the lower temperature is associated with TiC precipitation in austenite, while the weaker retardation at the higher temperature associated with solute drag effect of Ti. To compare retarding effects of microalloys, times for 50% softening ($t_{50}$) were estimated from softening curves and then used to produce Figs. 8.

The temperature dependence of $t_{50}$ are shown in Figs. 8 (a), (b) and (c) for the Ti, Nb and Nb-Ti bearing steels with comparing $t_{50}$ of the base steel (Si-Mn). In the case of Ti bearing steels, the slopes change corresoponded to temperatures of approximately 950°C (0.11wt% Ti) and 920°C (0.06wt% Ti). In the case of Nb steel, retardation of softening at high temperatures (>1050°C) is significant and the temperature of slope change (1030°C) is higher than the temperature of Ti bearing steels. This means that the dissolved Nb in austenite is more effective in retarding the austenite recrystallization than the dissolved Ti, and that the addition of Nb is more effective in raising the recrystallization stop temperature (corresponded to the temperature of slope change in Figs. 8[6]) than the addition of Ti. Addition of 0.03% Nb increased the temperature of slope change of Ti bearing steel (1040°C) and gave large retardation in high temperature.

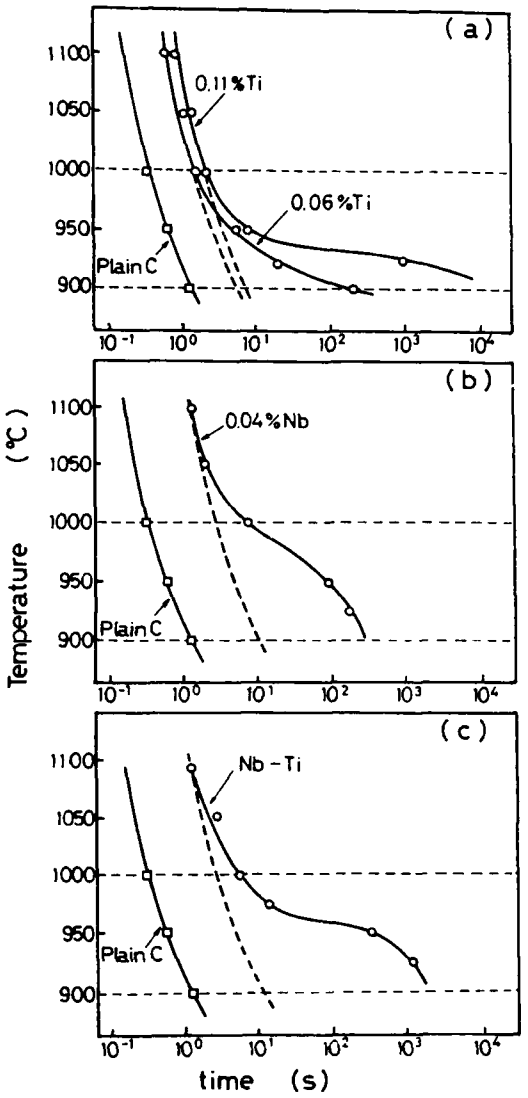


Fig. 8 Effect of temperature on 50% softening time ($t_{50}$) after hot deformation for (a) 0.06 and 0.11wt%Ti, (b) 0.04wt%Nb and 0.03wt%Nb-0.05wt%Ti steels, comparing $t_{50}$ for the base steel.

As mentioned above, the marked retardation of softening at lower temperature of microalloyed steels is associated with the formation of strain induced micro-precipitation, therefore the temperature of slope change depends on kinetics of the precipitation in austenite. The higher temperature of slope change in Nb bearing steels results from higher temperature precipitation of Nb (C, N), since Nb (C, N) is more stable than TiC in austenite[7]. For Nb-Ti steels, the addition of Nb increases the stability of Ti carbonitrides through the formation of Nb-Ti complex precipitates. Therefore, the temperature of slope change of Nb-Ti bearing steels is higher than the temperature of Ti or Nb steels.

III-3 Mechanical properties of Ti bearing steels

As discussed in III-1 and III-2, addition of Nb decreases the solubility of carbonitride precipitates and retards the softening due to static recovery and recrystallization after hot deformation of Ti bearing steels, while addition of V has little effect of changing the solubility of precipitates. In this part, we will show the effect of Nb and V on the mechanical properties of Ti bearing steels.

Figure 9 shows the variation of tensile strength with Ti content in the three types of steels reheated at a temperature between 1050°C and 1200°C. The tensile strength increases with increasing Ti content and reheating temperature. The results of steels reheated 1150 of above indicate an increase of tensile strength about 20kg/mm$^2$ by 0.1wt% Ti addition. This increment of strength due to Ti addition arised from the precipitation strengthening of Ti carbonitrides precipitated in ferrite matrix during cooling. Addition of 0.05wt% V always increases the strength of Ti bearing steels. However addition 0.03wt% Nb decreased the strength of Ti steels when the steels of higher Ti contents were reheated at a lower temperature (<1100°C). Since all steels are similar in the ferrite grain size and in the fraction and the lamella spacing of pearlite, the decrease in tensile strength of Nb-Ti steels may be due to poor precipitation

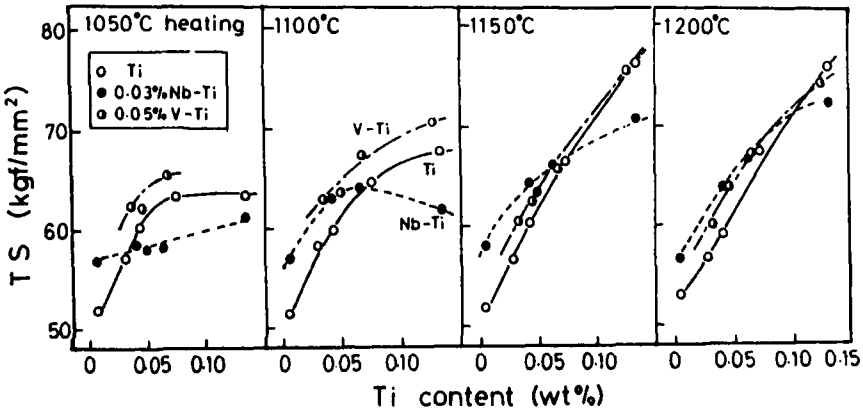


Fig. 9 The effect of Ti content on tensile strength of Ti, 0.03wt%Nb-Ti and 0.5wt%V-Ti bearing controlled rolled steels, for reheating temperatures between 1050 and 1200°C.

strengthening in ferrite matrix. The poor precipitation strengthening would result from decrease in amount of solute elements during reheating because of formation of complex precipitates. Therefore the tensile strength of Ti bearing steels can be predicted in terms of the solubility of complex precipitates; the relationship between the tensile strength and the calculated amount of elements soluble during the soakijng was summarized in Fig. 10. This shows that the tensile strength of all three Ti bearing steels can be predicted by the amount soluble elements calculated by the model. Thus, the

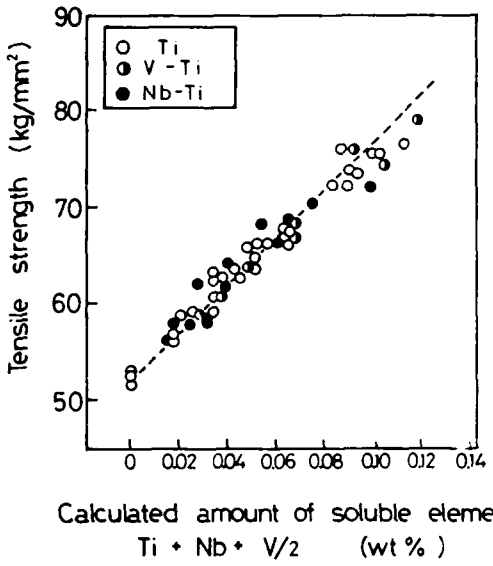


Fig. 10 A comparison between the tensile strength of Nb-Ti bearing controlled rolled steels and the calculated amount of microalloying elements in solution during reheating.

formation of complex precipitates should be taken into consideration in the design of chemical composition and reheating condition especially in the case of Nb-Ti bearing steels, since addition of Nb may decrease the solubility of carbonitrides in austenite during reheating.

Figure 11 shows the effect of total reduction below 950°C during controlled rolling reheated at 1200°C on Charpy 50% FATT of Ti, V-Ti and Nb-Ti bearing steels. For Ti bearing steel, smaller reduction than 67% was little effective in increasing the toughness of plates, and 75% reduction at least was necessary to give a good toughness to the steels. Such poor toughness of Ti bearing steels is thought to be associated with lower recrystallization stop temperature of the steels. Since the recrystallization stop temperature in Ti bearing steel is lower than the temperature in Nb bearing steel, the total reduction below 950°C in Ti bearing steels may be higher than the reduction in Nb bearing steels in order to make austenite grain pancaked. Addition of 0.02wt% Nb increased the toughness of Ti bearing steel with small reduc-

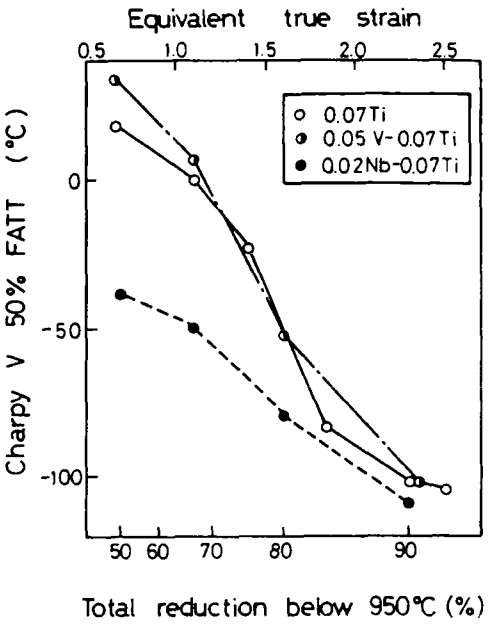


Fig. 11 Effect of total reduction below 950°C on Charpy 50% FATT of Ti, V-Ti and Nb-Ti bearing controlled rolled steels.

tion (<75%), while the addition of 0.05wt% V was little effective in improving the toughness. The addition of Nb in Ti bearing steels will increase the driving force of strain induced carbonitride precipitation since it makes the precipitates stable through the formation of the complex precipitates. Therefore, the addition of Nb raised the recrystallization stop temperature of Ti steels, so that it increased the toughness of the controlled rolled steels with small total reduction below 950°C. On the other hand, the addition of V was little effective in decreasing the solubility of the precipitates in Ti steels, so it is expected that V in Ti steels is little effective in raising the recrystallization stop temperature of the steels.

## IV. Conclusions

The changes in both mechanical properties and recrystallization of austenite with addition of Nb and V were investigated for Ti bearing steels, comparing the characteristics of precipitates in the steels.

1) Addition of 0.03wt% Nb decreased the tensile strength of Ti bearing controlled rolled steels if these steels were reheated to a low temperature (<1100°C) prior to rolling, while addition 0.05wt% V had no significant effect.
2) To obtain good toughness, higher total reduction below 950°C is necessary for Ti bearing steels than the reduction for Nb bearing steel, since the recrystallization stop temperature of Ti bearing steels is lower than the temperature of Nb bearing steels. However small amount of Nb addition

improved the toughness of Ti steels significantly, since the addition of Nb raised the recrystallization stop temperature of Ti steels.

3) The complex precipitates (which contain more than one metallic elements) was identified both in the V-Ti and Nb-Ti steels with electron diffraction and micro chemical analysis. However, there is a considerable difference in the solubility of elements in complex precipitates between these steels. The precipitates in Nb-Ti steels contain a significant amount of Nb (Nb/(Nb+Ti) = 0.1∿0.3 in atomic fraction), while V fraction in V-Ti steels was relative lower (V/(V+Ti) < 0.1). And the complex precipitates in Nb-Ti steels was stabler than in V-Ti steels.

4) The changes in both composition and amounts of complex precipitates can be predicted in these steels by an ideal solution model for quarternally precipitates. This model distinguishes the differences in formation of complex precipitates between Nb-Ti and V-Ti bearing steels. And the model is applicable to estimation of precipitation strengthening for the steels.

**References**


1) J. Strid and K.E. Eastering: Acta Met., 33 (1985), 2057
2) D.H. Houghton, G.C. Weatherly and J.P. Embury: Thermomechanical Processing of Microalloyed Austenite, ed. by A.J. DeArdo, G.A. Ratz and O.J. Wray, Met. Soc. AIME, New York, (1982), 267.
3) B. Loberg, A. Nordgren, J. Strid and K.E. Eastering: Met. Trans., 15A (1984), 33.
4) P.A.P. Djaic and J.J. Jonas: JISI, 210 (1972), 256.
5) S. Okaguchi and T. Hashimoto: Trans. ISIJ, 27 (1987), 467.
6) I. Weiss and J.J. Jonas: Met. Trans., 10A (1979), 831.
7) B. Aronsson: "Steel Strength Mechanism", Climax Molybdenum Company Symposium, p.77, Eilert Printing Co. Inc., Zurich, 1969.

# STRUCTURAL PREDICTION OF MECHANICAL PROPERTIES OF HSLA STEELS

**Ľudovít Parilák, Milan Šlesár, Blažej Štefan**
Slovenská Akadémia Vied Ústav Experimentálnej Metalurgie
Solovjevova, Czechoslovakia

OUR PHYSICO-METALLURGICAL approach was based on the logical relationships represented by the bonding triangle. Its vertices are: structure-properties-technology. The study of direct relationships between technology and properties gives no clue concerning the physical aspects of these relationships. In our opinion attention should be directed primarily to the technology-structure and structure-properties relations; the knowledge of these is indispensable for proposing structural and chemical conception of HSLA steels which would be able to describe the whole complex of required properties and to propose technological parameters for obtaining suitable structure.

The presented paper deals with the analysis of the structural basis of certain mechanical properties of HSLA steels, namely yield strength $R_e$, transition temperature and strain hardening exponent n. Attention was devoted chiefly to quantitative description of the influence of precipitation state on these properties taking into account the grain and subgrain sizes and manganese content, too. We will discuss some derived properties, such as tensile strength $R_m$ and actual fracture stress $R_{Fr}$. Statistical regression analyses are used together with physical principles in order to obtain simplified and practically usable relationships between structure and properties.

Decisive for obtaining of such relations is the knowledge and determination of the basic microstructure parameters. Because no unified approach to these questions exist yet, we shall briefly discuss some methodical aspects.

## CHARACTERISTICS OF STRUCTURAL PARAMETERS

HSLA steels exist in three basic modifications, namely:

a) polygonal, as a rule ferritic-pearlitic with reduced pearlite content, or ferritic;
b) non-polyhedral structures of the acicular pearlite, bainite, martensite or mixed type. This group comprises also quenched and tempered steels;
c) mixed structures of polygonal grains; e.g. dual phase steels.

Grain size - it is the basic structural parameter. In polygonal structures the determination of its quantity is usually a routine, especially when the structure is regular.

After controlled rolling, heterogenous grains in the cross-section tend to appear. In this case it is necessary to find a suitable value of representative grain size, especially in relation to sample size and its position in the volume of material. Another sources of grain size heterogeneity in HSLA steels are wrong parameters of controlled rolling and cooling, i.e. austenite recrystallization is not completed before finish rolling starts. Grain size heterogeneity could affect also the transition temperature. If average grain size is used only, it is necessary to consider another factors which could introduce imprecission. The microstructure is often morphologically anisotropic, the grains are nonequiaxed and banded pearlite is also frequent.

In nonpolygonal structures the determination of grain size is considerably more difficult, because both, original grains and block boundaries are high angle boundaries. In our opinion, grain size is best determined fractographically by evaluating the size of cleavage facets $d_F$ on brittle fractured surfaces at -196 °C, Fig. 1. The method is based on a promise that high angle boundaries control facets formation and their size. This

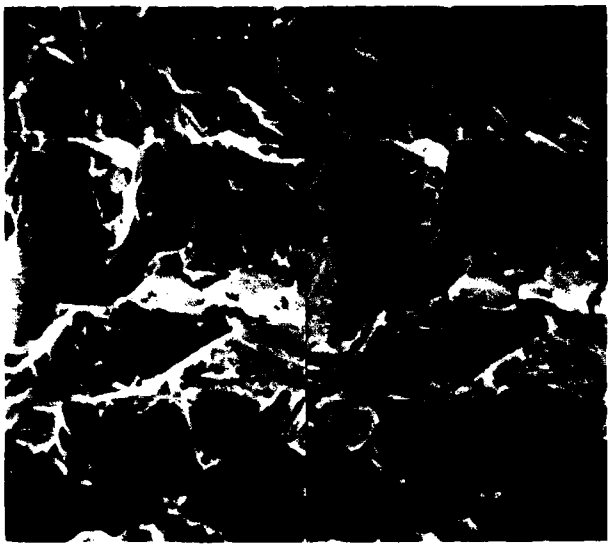

Fig.1 - Fractographic evaluation of mean cleavage facet size, $d_F$

hypothesis was verified on polygonal structures with various values of grain size, d. Obtained relation was linear, Fig. 2, :

$$d_F = 2.1 + 0.5\ d \qquad (1)$$

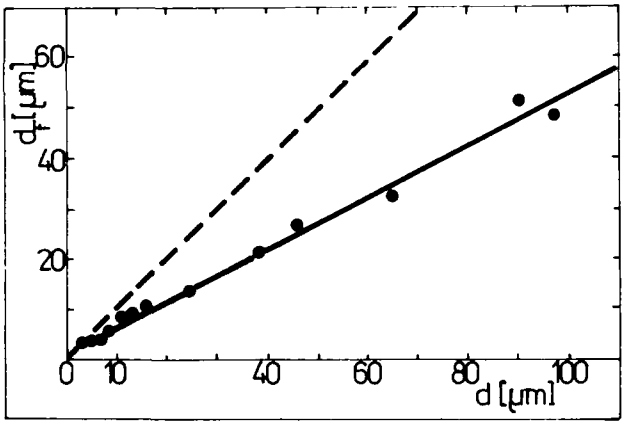


Fig. 2 - Relation between cleavage facet size $d_F$ and metallographic grain size d

One of the reasons for such a relationship is the dimensional factor. In case of coarse grains the fracture propagation is realized by bridging of cracks in neighbouring grains by cleavage - fragmentation occurs, Fig. 3b. In fine-grained structures the bridging in adjacent grains may be attained by plastic deformation - shearing, Fig. 3a. Quantitative fractographic analysis implies the detailed knowledge of fracture process micromechanisms and needs experience. Otherwise, there is the risk of errors caused by subjective factors. Our experiences show that the method is suitable for a wide scale of nonpolygonal and mixed microstructures.

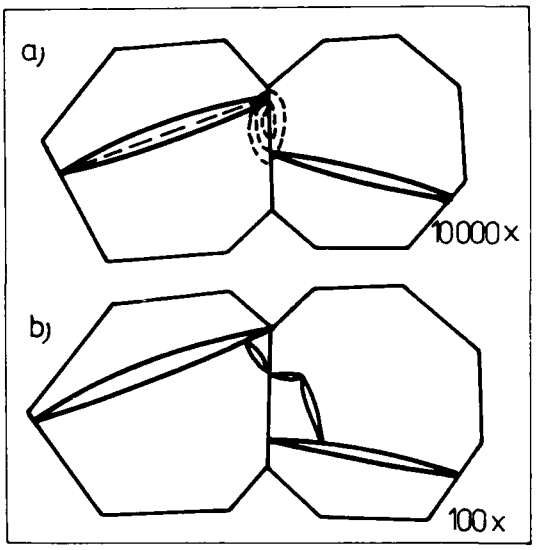


Fig.3 - a)Formation of a plastic step by bridge plastification in fine-grained material, b) Crack bridging by secondary cleavage cracks in coarse-grained material

Subgrain - Nonpolygonal structures are characterized by well developed subgrain structure. The individual subgrains are mostly laths, or discs (bainite, martensite), oval or irregular shaped (acicular ferrite, annealed structures). The views concerning measurements of the characteristic subgrain dimensions are different /1,2/. The evaluation of mean lath thickness $d_L$ on thin foils perpendicularly to the lath length we have found suitable for this purpose, Fig. 4. The effective mean lath size is larger than the mean thickness measured in this way; however, this disproportion can be adequately considered in regression constants for the strengthening calculations.

In mixed structures it is possible to determine microstructural parameters and the fraction of present phases using the well-known methods of statistical stereology.

Precipitation parameters - their measurement and definition presents certain problems. If we adopt Orowan's ideas of the interaction between dislocations and particles of secondary phases in the sliding plane, it is necessary to evaluate the mean planar interparticle distance $\lambda$ in the sliding plane. In our opinion, the most suitable method for measuring of these parameters is the determination of the number of precipitated particles in the unit area of the replica, N, and the mean size 2r of extracted particles. Then

$$\lambda = k \cdot N^{-1/2} \qquad (2)$$

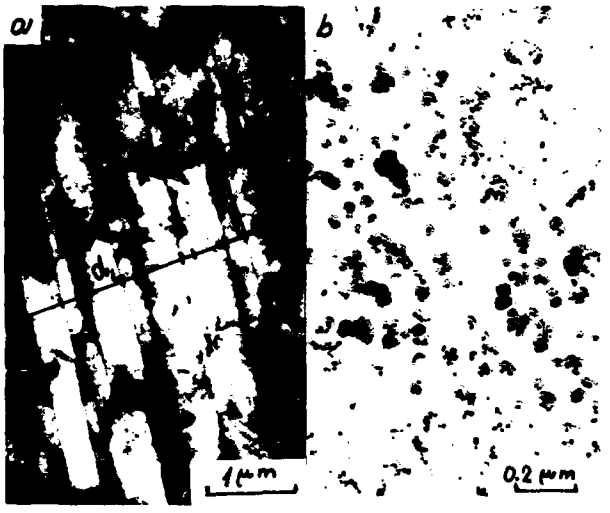


Fig. 4 - a)Lath size evaluation in the microstructure of upper bainite.

b) Homogeneous distribution of Ti/C,N/ particles in Ti-steel.

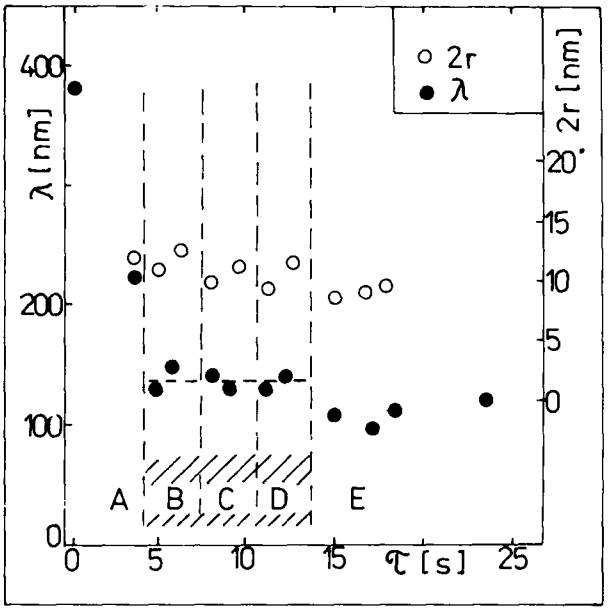


Fig. 5 -Influence of etching time on the measured size of Zr particles and on the mean interparticle distance

where the constant k depends in the type of particle ordering and its value is close to 1. Such a definition of mean interparticle distance is connected with certain stereological problems. However, the method does yield reproducible results, especially for uniformly distributed equiaxed carbidic and carbonitridic precipitates, Fig. 4b. Example on Fig. 5 documents the fact that the values of $\lambda$ are reproducible not only if the metallographic sample is etched correctly (region C) but even when the etching is slightly overdone (area D) or insufficient (area B). The value of the mean particle size 2r is less sensitive to the etching time. For nonequiaxed precipitates or clusters this procedure must be modified. The methods for determining $\lambda$ based on calculations using the volume fraction of the particles are, in our opinion, less exact.

## THE BASIC MODELS FOR HARDENING AND EMBRITTLEMENT

YIELD STRENGTH - In this field we start at well-known investigations of Gladman /3/, Pickering /4/, Prnka /5/ and others culminating in the middle of seventies.

The yield strength of alloys gains a value which depends on various contributions, among which we can count: $R_{PN}$- the contribution of the latice friction stress, $R_{IN}$ - the interstitial hardening from solute atoms, $R_D$ - dislocation hardening, $R_G$- contribution of the grain size and subgrain size $R_{SG}$,resp., $R_{PR}$ - pearlitic strengthening, $R_S$- substitutional hardening, $R_P$ - precipitation hardening. For their quantification the following equations are frequently used / 1 - 7/:

$$R_{IN} = k(\%C+N), \quad R_D = 2Gbq\varrho^{1/2},$$
$$R_G = k_y \cdot d^{-1/2}, \quad R_{PR} = k_{PR} \cdot X_{PR}, \qquad (3)$$
$$R_{SG} = k_{SG} \cdot d_L^{-1}, \quad R_S = \sum_{(i)} k_i \cdot x_i$$

$R_{PN}$ represents the temperature dependent component of yield strength, at 20 °C reaches a value of 40 MPa. In equations (3) %C+N corresponds with free carbon and nitrogen concentrations, $\varrho$ is the dislocation density, d and $d_{SG}$ are the grain and subgrain sizes, resp., $x_i$ is the concentration of i-th substitutionally dissolved element in the solid solution. The constants k, $k_y$, $k_{SG}$, $k_i$ express the intensity of influence the mentioned parameters on the individual strengthening contributions and they have a physical nature. However, their estimations are subjected to considerable scattering /8/ between following limits: $k_y$=13-24 Nmm$^{-3/2}$, $k_{SG}$=0.03-0.14 Nmm$^{-1}$, $k_{PR}$=2-3 MPa/%, $k_i$ for manganese $k_{Mn}$=33-100 MPa/%, for silicium $k_{Si}$=34-164 MPa/% This has an influence on accuracy and reliability of estimation of individual contributions.

Quantifying the $R_P$ contribution we encounter analytical relations based on the strict model approach of particle-dislocation interactions (Orowan, Orowan

-Ashby, Ansell-Lenel et al.) as well as with analyses of empirical nature (Edmons). The consequent model approach is subjected to inaccuracy in that it prefers one of the interaction mechanisms of particles with moving dislocations. However, it is evident that in a real material we have a statistically random type of interaction which is based on statistically random distribution of particles, their size, shape and properties. The empirical approach consider the precipitate-dislocation interaction in integral manner, but its quantification usually depends on the estimation of the other contributions to the yield strength. In most cases this relationship has no physical nature. In general, the precipitation hardening is the more intensive the more decreases the interparticle distance, increases the volume fraction of particles and the finer size of precipitated particles are present by the constant volume fraction of these. We recommend the use of the equation:

$$R_P = k_P^R \cdot f(PP) \qquad (4)$$

where f(PP) is a function dependent on precipitation parameters and $k_P^R$ expresses the intensity of precipitation strengthening; both quantities respect a statistically average state of precipitate-dislocation interaction. The function f(PP) should be analytically as simple as possible and must have a physical nature.

The dislocation hardening should be considered only for work hardened steels. After rolling or annealing the strengthening values calculated from dislocation density and from grain size are approximately equal as we have shown in /9/. That is why we hold both above mentioned strengthening contributions for interchangeable.

In our analyses we have accepted the principle of additivity of individual contributions to the yield strength in a form:

$$R_e = R_{PN}+R_{IN}+R_G+R_{SG}+R_S+R_{PR}+R_P \qquad (5)$$

From published dates and our own analyses follows that these contributions may be quantitatively divided according the character of their contribution to brittle fracture resistance. From this point of view the equation (5) may be written as:

$$R_e = R_G+(R_{SG}+k_{Mn}\cdot x_{Mn})+\Delta R \qquad (6)$$

Increasing the contribution of the grain size $R_G$, improves the transition temperature, too. Substitutional hardening of Mn and subgrain contribution have no significant influence on transit temperature and $\Delta R$ - the embrittling component, which comprises all contributions with an embrittling effect. In HSLA steels $\Delta R$ is predominantly influenced by precipitation strengthening.

TRANSITION TEMPERATURE - The basis for investigation of the relationship between the microstructure and the transition temperature is given by the original Petch's equation /9/, based on the equality of yield strength and fracture strength $R_{FR}$ at transition temperature $T_K$:

$$R_{FR} = R_{OFr} + k_f \cdot d^{-1/2} \qquad (7)$$

The microstructural parameters and the chemical composition have different intensity of influence on the friction stress value $R_{OFr}$, and in general influences each other. Therefore the expression of structural nature of transition temperature for HSLA steels is difficult. In /10/ we analysed this problem and proposed the following equation:

$$T_{35} = A-B.\ln d^{-1/2} + \sum_{(i)} r_i.f(y_i) =$$

$$A + \Delta T_G + \sum_I \Delta T_i \qquad (8)$$

where $A = B.\ln X$

$$X = K.(4G\gamma q/\kappa_y - k_f)^{-1}$$

The value of the constant A which represents the thershold value of brittleness must be determined experimentally because the value of q is unknown and the transition temperature is calculated at impact energy of 35 $J.cm^{-2}$ ($T_{35}$). The constant B reflects the temperature-dependent character of the yield strength. Constant $r_i$ represents the intensity of influence of i-th structural parameter $y_i$ on the transition temperature shift. In term $r_i.f(y_i) = \Delta T_i$ we consider the transition temperature shifts from: precipitates $\Delta T_P$, silicon $\Delta T_{Si}$, pearlite $\Delta T_{PR}$ and the intersticies $\Delta T_{IN}$. This contribution to the transition temperature shift may be expressed not only directly through structure parameters, but also indirectly through the corresponding hardening distributions, $R_i$, from precipitation, pearlite, silicon and interstices in form of $\Delta T_i = S_i.R_i$. It seems that the differences between the intensity of influence of the various hardening contributions $S_i$ on transition temperature are slight. In addition to it, in HSLA steels the influence of precipitation is dominant. This permits us to simplify the equation (8) for transition temperature into form:

$$T_{35} = A - B.\ln d^{-1/2} + C.\Delta R \qquad (9)$$

Together with (6), this equation is a starting point for further analysis.

## MATERIALS AND EXPERIMENTS

Our program included a relatively wide range of carbon micro-alloyed and low-alloyed steels manufactured in oxygen convertors and rolled on hot wide

strip rolling mills. The following steel types predominated:

a) Al-stabilized carbon steels with C content 0.06-0.18 % and 0.6-1.2 % Mn - designated as C-Mn steels;
b) Ti-microalloyed steels with 0.05-0.14 % Ti, 0.05-0.10 % C and about 0.6 % Mn - designed as Ti-steels;
c) Steels microalloyed with V up to 0.08 %, with Nb to 0.05 %, or with combination of these, in some cases with addition of Zr up to 0.06 %, with 0.09 to 0.13 % C and 1.0 - 1.5 % Mn - designed as V, Nb, V-Nb-Zr steels;
d) Low alloyed steels with about 0.3 % Mo, 0.09-0.13 % C and 1.5-2 % Mn, microalloyed with Nb, Ti, Zr individually, or in combination.

Steels were investigated after controlled rolling or thermal treatment. In addition to normalizing this comprises various types of annealing(from 700 to 1250 °C) with various cooling rates. The goal of this treatment was to form a wide spectrum of grain sizes and precipitation hardening. For the modelling of nonpolyhedral microstructures we used heating-up on 900 to 1250 °C, quenching using various brines and tempering up to 700 °C. This permitted us to obtain a wide variety of austenite grain sizes, blocks and subgrain sizes and values of precipitation hardening.

In all materials and microstructural states we determined the type of microstructure, the volume fractions of polygonal ferrite, acicular ferrite, upper and lower bainite or martensite. In all states the mean grain size was determined metallographically or (in nonpolyhedral structures) fractographically. Nonpolyhedral and mixed structures were defined by subgrain size determined on thin foils. In selected states the precipitation parameters $\lambda$ and 2r were measured on carbon extraction replicas, by statistical methods.

In static tensile test in addition to basic mechanical characteristics, the hardening exponent n and the constant k were determined, these follow from the equation:

$$R = k \cdot \varepsilon^{n} \qquad (10)$$

where R is the actual flow stress and the intensity of deformation. The actual fracture stress $R_{Fr}$ was also determined. The impact bending test was performed on samples with Charpy notch, at wide range of temperatures. Mechanical properties and notch toughness values were measured longitudinal to the rolling direction.

The following analyses include results from more than 250 microstructural states.

## ANALYSES

YIELD STRENGTH AND PRECIPITATION HARDENING - Fig. 6 Illustrates the dependence of yield strength for Ti-steels on the precipitation parameter $\lambda$. Material was heat treated in order to obtain two different grain sizes, 45.0 and 4.8 µm and different precipitation states. Even in such a simple experimental set can be seen a constant shift of yield strength for various values of $\lambda$ which can be an evidence for additivity of grain size and precipitation hardening contributions.

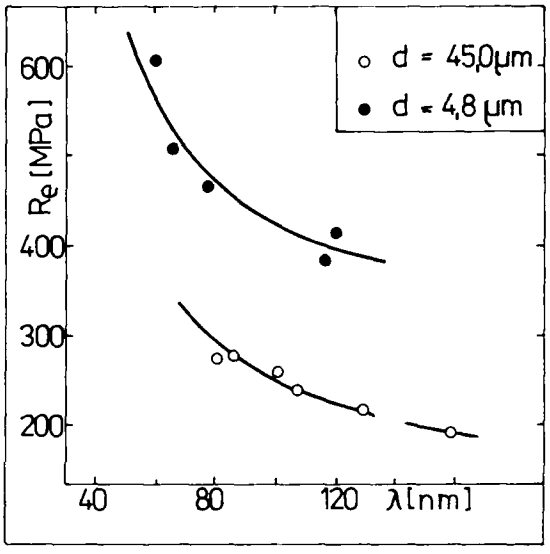


Fig. 6 - Influence of the precipitation parameter $\lambda$ on the $R_e$ values for different grain sizes, d

A set of 28 polygonal microstructural states of Ti-, Nb-V-, V-Nb-Zr- and Mn-Mo-Nb-steels, characterized by different grain sizes and different values of precipitation hardening, was obtained and used to determine the values of the mean interparticle distance $\lambda$ and mean particle diameter 2r. Using regression analyses and iteration methods, the following model for solution of yield strength was used:

$$R_e = R_{PN} + k_y d^{-1/2} + k_{Mn} \cdot x_{Mn} + 33.\%Si + 3.\%PR + k_{Pi} \cdot f_i(PP) \qquad (11)$$

that means, we look for optimal combinations of constants and an optimal function form for $f_i(PP)$. The following possibilities were considered in detail: $\lambda^{-1/2}$, $(\lambda - 2r)^{-1/2}$, $\lambda^{-1}$, $\ln \lambda$, $(\lambda - 2r)^{-1} \cdot \ln r$ and $\lambda^{-m}$ with an optimalization of exponent m. The best fit was obtained for $f_i(PP) = \lambda^{-2}$. Other functions either don't yield satisfactory correlation or necessitated replacing the Peierls-Nabarro stress ($R_{PN}$) by a negative threshold hardening

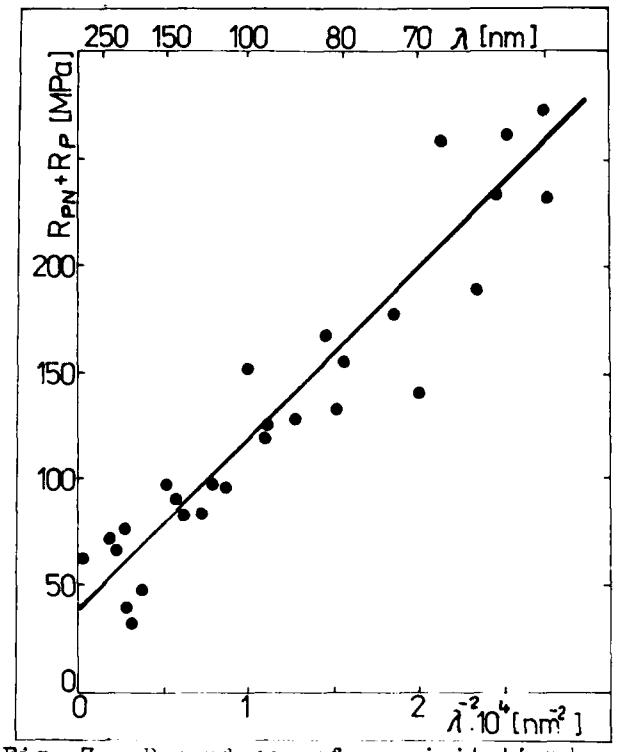


Fig. 7 - Dependence of precipitation hardening contribution on parameter $\lambda^{-2}$

value. The analysis yielded an optimum value for $k_y$ and $k_{Mn}$ of 15 Nmm$^{-3/2}$ and 50 MPa %, resp. Fig. 7 shows the optimized relation $R_P+R_{PN}$ vs. $\lambda^{-2}$. It can be seen that the correlation is very satisfactory and a realistic value of $R_{PN}$ = 38 MPa was reached. The constant $k_P$=76.8 .10$^{-8}$ N for $\lambda$ measured in /mm/.

The results show that the precipitation hardening is indirectly proportional to the slip surface dimension corresponding to one particle of precipitate.

TRANSITION TEMPERATURE AND PRECIPITATION STRENGTHENING - In a similar scheme as for yield strength analysis, Fig.8 shows the influence of precipitation on transition temperature for Ti-steel with two different grain sizes. Also in this case one can see that shifts influenced by grain size are equidistant; this supports the validity of the proposed model. Iterative methods were applied by the solution of equation:

$$T_{35} = A - B.\ln d^{-1/2} + 2.2.\%P_e + 8.3.\%Si + k_P^T.f_i(PP) \quad (12)$$

Here also the best suited function $f_i$(PP) was $\lambda^{-2}$. The optimum value for B is 110 °C which agrees with published results. The optimum value for A is 147 °C, $k_P$= 42.0.10$^{-8}$ N for d in /mm/.

Fig. 9 shows the dependence of precipitation embrittlement, i.e. the shift of transition temperature caused by precipitation, in dependence on $\lambda^{-2}$. The relatively good correlation indicates

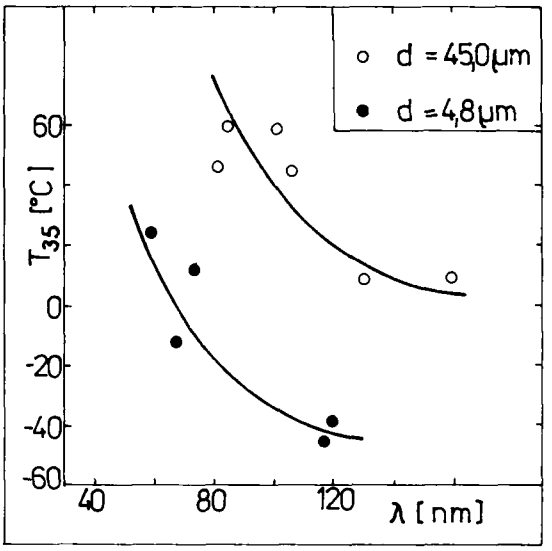


Fig.8 - Influence of precipitation parameter $\lambda$ on $T_{35}$ for two different values of grain size, d

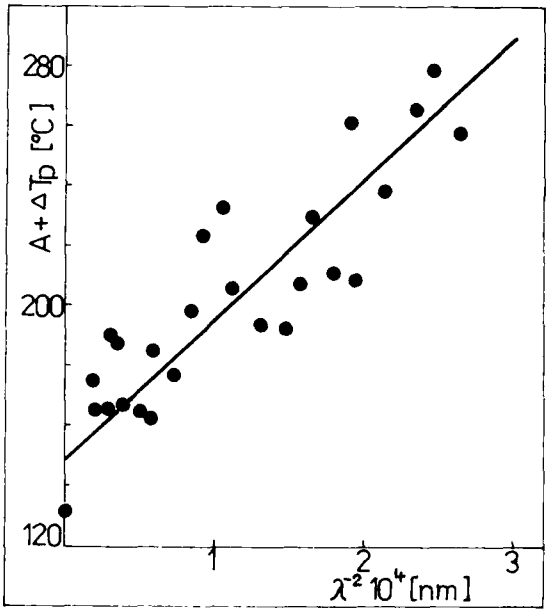


Fig. 9 - The dependence of precipitation embrittlement $\Delta T_p$ on $\lambda^{-2}$

that precipitation embrittlement is inversely proportional to the square of mean planar interparticle distance.

RELATIONS BETWEEN HARDENING AND EMBRITTLEMENT - At constant grain size the dependence of transition temperature vs. yield strength is approximately linear, Fig.10. The change of grain size has a strong influence on the position of curves without appreciable change of their slope. This is an indication of the va-

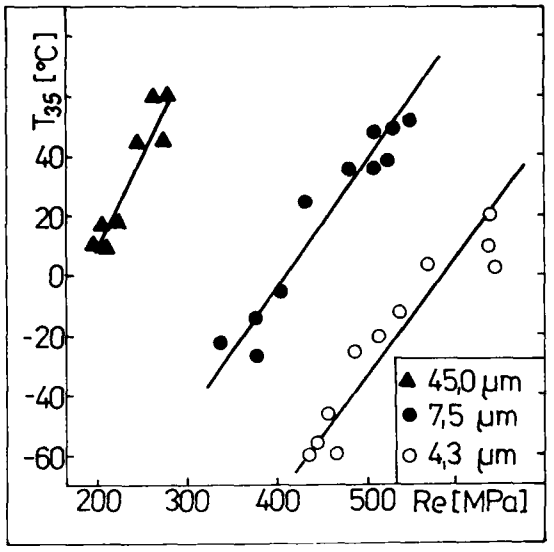


Fig.10 - Relations between $R_e$ and $T_{35}$ for three different values of grain size, d

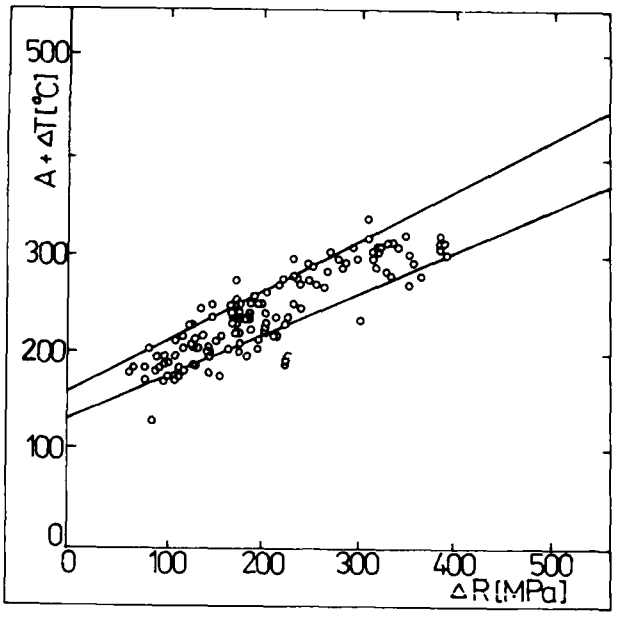


Fig.11 - The dependence of $T_{35}+B.\ln d^{-1/2}$ on ΔR for polygonal structures

lidity of model (9). The general solution was based on regression analyses supplemented by iterative methods. The goal was to test the validity of the model and to optimize the constants $k_y$, $k_{Mn}$, C, A. In the course of testing, various other alternatives beyond equations (6) and (9) were analyzed, such as including the embrittling effect of the subgrain and manganese, unification of the hardening effect of the grain and subgrain, etc. Various physical quantities were analyzed, such as $\gamma$, $k_f$ (8) and the relation $k_f = 1.92(G.\gamma)^{1/2}$, which agrees with /11,12/, derived. The results show that the models of (6) and (9) are well suited to the data. In polygonal structures it is possible to admit a slight direct positive effect of Mn on the transition temperature as proposed e.g. by Pickering /4/. The results, especially for polygonal microstructures, indicate that the interdependence between the embrittlement hardening ΔR and the corresponding embrittlement may be nonlinear with damping of embrittlement above the embrittlement hardening limit of 250-300 MPa. The improvement due to the introduction of nonlinear interdependence is relatively small. This will be the subject of further studies.

The character of our analyses is exemplyfied by Fig. 11 which shows the dependence between embrittlement hardening ($\Delta R = R_e - k_y.d^{-1/2} - k_{Mn}.\%Mn$) and the corresponding embrittlement ($A + \Delta T = T_{35} + B.\ln d^{-1/2}$). Fig.11 shows the results for polygonal structures with optimalized constants $k_y$=15 Nmm$^{-3/2}$, $k_{Mn}$ = 50 MPa/%, B = 110 °C. The regression equation is $\Delta T = 147 + 0.4.\Delta R$ with the correlation coeficient r = 0.884. This correlation seems to be low. However, if we consider that the accuracy of transition temperature determination is ±10 °C, the yield strength scattering is ± 4 %, the grain size measurement precision is ± 5 %, it is possible to surround the regression line by a natural scattering zone. After that only 4-6 % of results show a marked discrepancy.

Fig.12 shows the same dependence

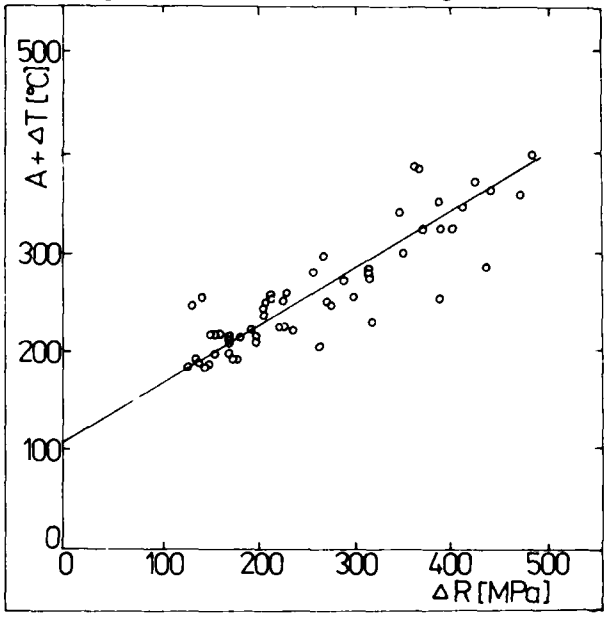


Fig.12 - The dependence of $T_{35}+B.\ln d^{-1/2}$ on ΔR for nonpolygonal structures

for nonpolygonal structures. In spite of fact that when comparing with the polygonal structures the microstructural parameters and ways of their evaluation (subgrain size is determined with the help of an electron microscope, the grain size is determined fractographically) are very different, we can see that the character of the interdependence does not change markedly. The position of the regression line is slightly different: $A+\Delta T = 108+0.566.\Delta R$ and the correlation coefficient is 0.871.

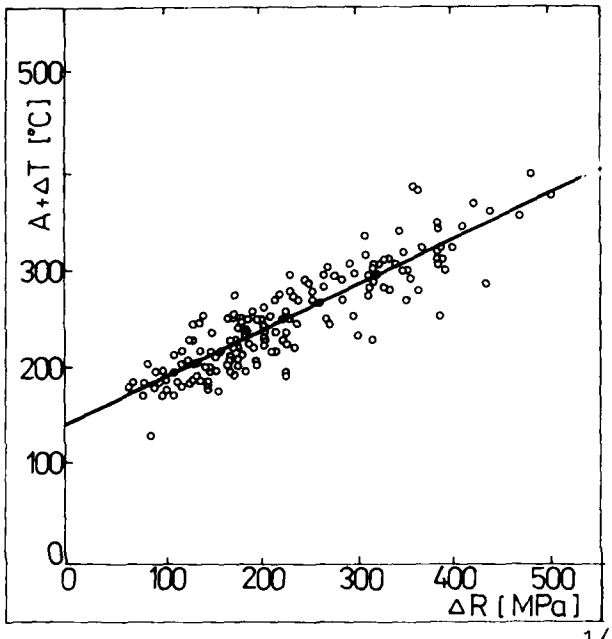


Fig. 13 - The dependence of $T_{35}+B.\ln d^{-1/2}$ on $\Delta R$ for polygonal and nonpolygonal structures

Fig.13 shows the unified set of results for polygonal and nonpolygonal structures. The regression equation is $A+\Delta T = 143+0.466.R$, the correlation coefficient is 0.870. The fall of correlation ciefficient is negligible. This leads us to accept a unified equation for all microstructural alternatives of HSLA steels, giving the relation between the yield strength, transition temperature and microstructural parameters in the form :

$$T_{35} - 0.47R_e = 143 - 23.\%Mn - 0.047\, d_L^{-1} - 7.05\,(d^{-1/2} + 15.6 \ln d^{-1/2}) \quad (13)$$

THE STRAIN HARDENING EXPONENT - The strain hardening exponent is habitually related to yield strength, when expressed parametrically by chemical composition or by grain size /4, 13-15/. In our analysis we shall start by investigating the influence of changes of precipitation parameters for three alternatives at the constant values of grain size. The values of n on Fig.14 are shown in dependence on the yield strength. We see that the curves are hyperbolical in character and are equidistantly shifted in relation to each other. This indicates that the influence of grain size is not marked and that precipitation plays a more significant role in the reduction of n with increasing of yield strength. This view is supported also by Fig.15 which

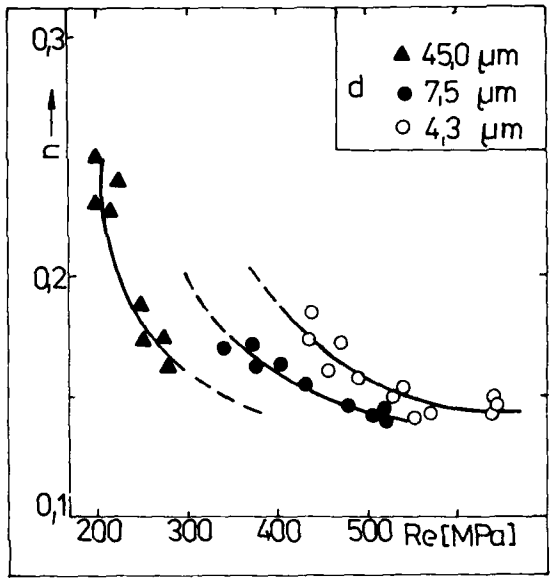


Fig.14 - Relation between $R_e$ and n for various values of d

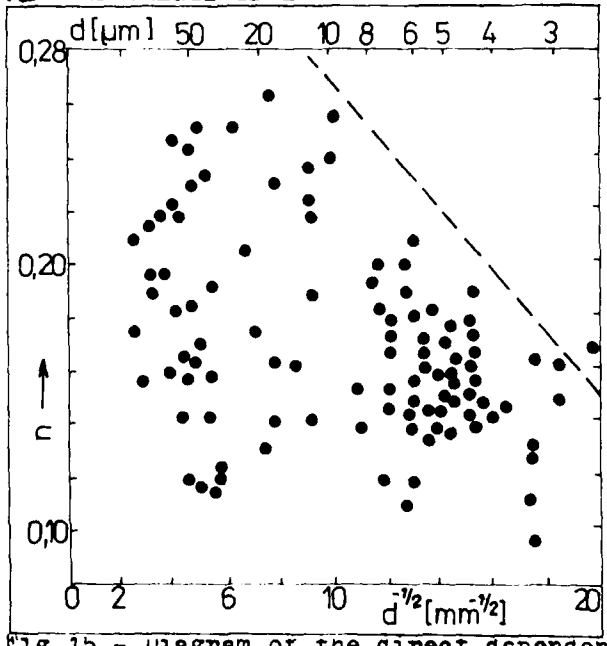


Fig.15 - Diagram of the direct dependence between n and d

shows the values of n in relation to grain size, for a representative measurement set . There is no observable dependence between these two quantities. The dashed line marks the region of fine grain sizes and higher values of n in which no measuring points are present. We admit the possibility that very fine grain may influence the formation of dislocation cells under strain and thus cause a decrease of the strain hardening exponent. The influence of precipitates is much more marked. Fig.16 shows values of n in relation to the precipitation parameter $\lambda^{-2}$. The validity of this dependence is supported by Figs. 17a,b,c which document the interaction between deformation dislocation substructure and precipitates. At low

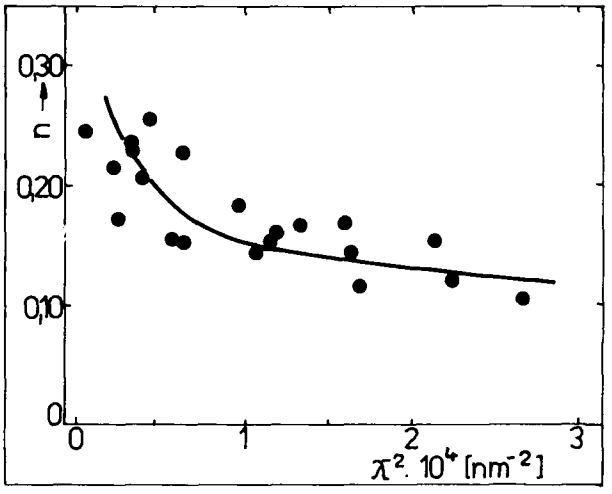


Fig.16 - Dependence of strain hardening exponent n on parameter $\lambda^{-2}$

precipitate density ( $\lambda$ = 212 nm) the formation of dislocation cells is independent of precipitates,Fig.17a. An intermediate density ( $\lambda$ = 103 nm) causes the formation of cells in the regions with sparse occurence of particles,in this case between the bands of interphase TiC precipitates, Fig.17b. A very high particle density ( $\lambda$ = 72 nm) has a homogenizing effect and retards cell formation, Fig. 17c.

In addition, regression analysis showed that pearlite in microstructure exerts a direct influence on the decrease of the exponent n. No influence of Mn was found. The measurement set is not sufficient with respect to Si content balance and therefore its influence could not be determined.

For polygonal microstructures the following equation was proposed for calculating of n :

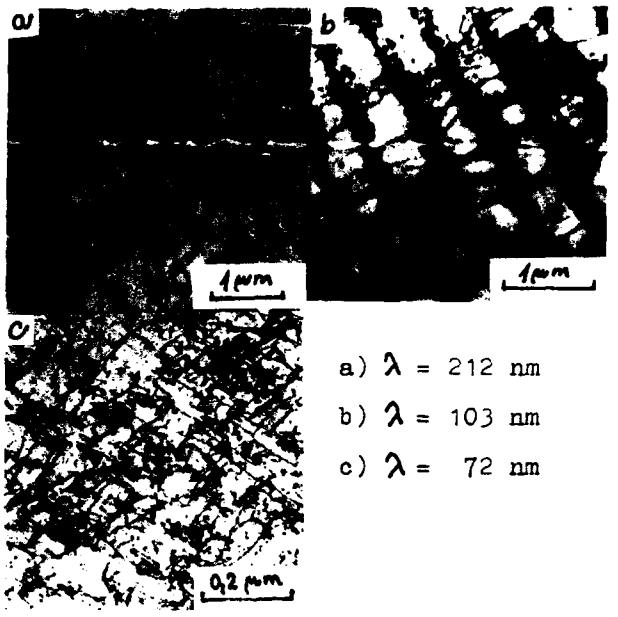


Fig.17 - Influence of precipitation state on the development of deformation dislocation substructure

$$n = \frac{a}{\Delta R} + b \qquad (13)$$

Fig.18 compares the measured values in relation to the regression hyperbola.The trend is clear, but the exactness of the relation is not yet completely satisfactory.

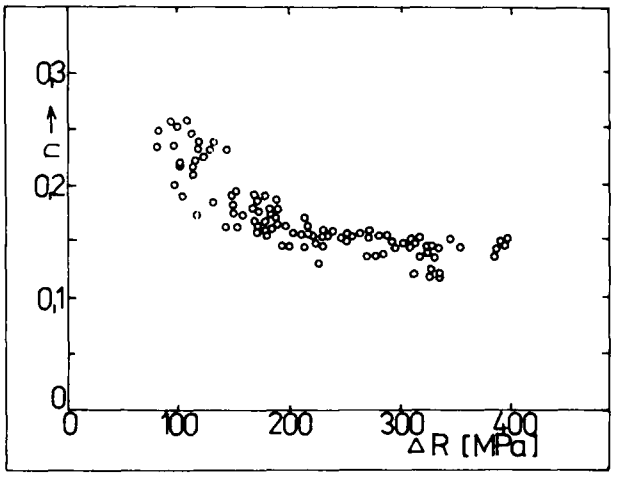


Fig.18 - The dependence of strain hardening exponent on the values of $\Delta R$

As for nonpolygonal structures, the influence of the subgrain size on the value of n is not marked, but there are many other influences of the microstructure, substructure and the solid solution composition which up to now have not been satisfactorily deciphered.

REDUCTION OF AREA - The reduction of area is influenced by those microstructural factors which during plastic deformation in the microvolumes serve as nuclei for defects formation. Therefore the influence of parameters such as grain and subgrain size and the solid solution characteristics are small. On the other hand, the influence of pearlite, inclusions and that of large carbides are significant. In /16/ we have proposed an anisotropic model for the mechanism of influence of rolled out inclusions on the ductile fracture mechanism. More recent statistical analyses /16/ have demonstrated the dependence of reduction of area on the planar fraction of nucleating particles of carbide and pearlite inclusions ($f_{Fr}$) on the fracture surface as follows:

$$Z = (1-1.2657.f_{Fr}^{1/3}).100\ \% \qquad (14)$$

The model is well suited for the determination of reduction of area in the transversal and normal direction to the sheet plane.

TENSILE STRENGTH AND FRACTURE STRESS - With respect to equation (10), the real stress $R_{m(r)}$ at tensile strength point is:

$$R_{m(r)} = k \cdot n^n \qquad (15)$$

If the steel has no marked yield strength and Lüder's strain, it is possible to express the constant k from yield strength and to calculate the tensile strength from $R_{P0.2}$ and n.

$$R_m = 1.002 \left(\frac{n}{0.0054}\right)^n \cdot R_{P0.2} \qquad 16)$$

In this case it is not necessary to look for a direct relationship between $R_m$ and microstructure; this should be expressed through the structural nature of $R_e$ and n.

The actual fracture stress at the static tensile test may be expressed using k, n and Z, as follows:

$$R_{Fr} = k\left(\ln \frac{100}{100-Z}\right)^n \Big/ (a-b.Z)(c+d.n) \qquad (17)$$

with regression constants a = 1.597, b = 0.013, c = 0.880, d = 1.460.

COMPLEX NOMOGRAM FOR RELATION BETWEEN MICROSTRUCTURAL PARAMETERS AND MECHANICAL PROPERTIES

The graphical processing of the above equations yields the nomogram shown in the Fig. 19. The nomogram is valid

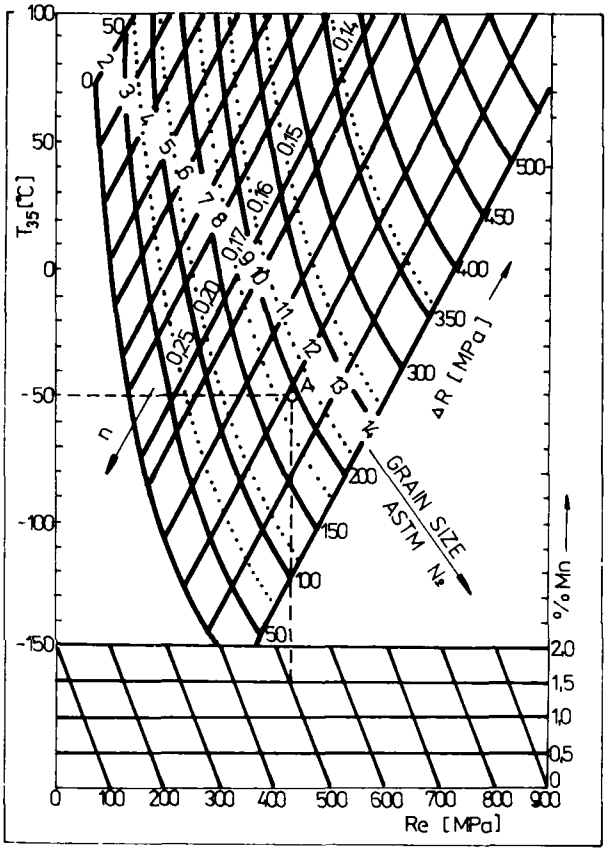


Fig. 19 - A complex nomogram for relations between yield strength and transition temperature

for polygonal microstructures. If it is used for nonpolygonal structures, then it is necessary to use instead of yield strength its corrected value, i.e. reduced by the contribution $R_{SG} = k_{SG}.d_L^{-1}$.

The nomogram permits using of any three parameters from the set ($R_e$, $T_{35}$, d, n, %Mn, $\Delta R$) to determine the remaining three. E.g. if the steel A has 1.5% Mn, $R_e$ = 500 MPa, the grain size according ASTM is 12, then the transition temperature will be -50 °C, $\Delta R$ = 200 MPa and the strain hardening exponent n = 0.165.

The nomogram permits an illustrative and fast orientation when predicting steel properties from its microstructure, designing the microstructure to ensure

the required property complex and helps in discovering the imperfections of the considered steel.

## CONCLUSION

A theoretical analysis of the problem led to the quantification of relationships between microstructural parameters, chemical composition and the yield strength, transition temperature and strain hardening exponent. Results were confirmed for a wide range of HSLA steels.

It was also possible to derive relationships expressing precipitation hardening and embrittlement.

Owing to the introduction of embrittlement hardening component it was possible to obtein usable relationships connecting HSLA steel structure and properties which were expressed nomographically.

## REFFERENCES


1. Rostoker, W. S., Dvorak, J. R., Interpretation of metallographic structures, Academia Press, London, 1965
2. Langford, G., Cohen, M., Trans. ASM, 62, 1969
3. Gladman, T. et al., Structure-property relationship in microalloyed steels, p. 25, Microalloying I, Washington, 1975
4. Pickering, F. B., High-strength,Low alloy steels-A decade of progress, p. 3, Microalloying I, Washington, 1975
5. Prnka, T., Hutnické aktuality, No. 4, 1976
6. Peierls, R., Proc. Roy. Soc., 52, 1940, p. 34
7. Ashby, M. F., The deformation of plastically non-homogenous alloys, p. 137, Strengthening methods in crystals, 1971
8. Parilák, Ľ., The precipation hardening and brittleness of HSLA steels, ÚEM SAV, Košice, 1982
9. Šlesár, M., Štefan, B., Parilák, Ľ., Structural parameters of ferrrite hardening and embrittlement, In: 5th Int. Symp. High purity materials in science and technology,III, Dresden, 1980, 261 - 282
10. Petch, N. J., Fracture I., Academia Press, New York-London, 1968, p.381
11. Stroh, A. N., Adv. Physics, 1957, No. 3, p. 418
12. Friedel, Z., Fizika metallov, Ed. Mir, 1972, p. 373
13. Keeler, S. P., Relationship between laboratory material characterization and press shop formability, p-21, Microalloying II, Washington, 1975
14. Takada, . et al., Trans. ISIJ, 20, 1980, No. 7, p. 280
15. Oberhauser, F. O. M. et al., Microalloying steels for light, cold formed sections, p. 16, Microalloying IV, Washington, 1975
16. Marek, P. et al., Ressearch project, ÚEM SAV, Košice, 1980

# OPTIMIZATION OF THE HOT ROLLING OF HIGH GRADE PIPELINE STEELS AT THE HOT STRIP MILL

**P. Choquet, H. Biausser**
IRSID
Saint-Germain-en-Laye, France

**S. Genet, J. J. Aernout**
SOLLAC
Dunkerque, France

**OPTIMIZATION OF THE HOT ROLLING OF HIGH GRADE PIPELINE STEELS AT THE HOT STRIP MILL**

P. CHOQUET*, S. GENET**
J.J. AERNOUT**, H. BIAUSSER*

* IRSID, Saint-Germain-en-Laye, France
** SOLLAC, Dunkerque, France

**ABSTRACT**

The aim of this work, which has been carried out by IRSID and SOLLAC Dunkirk, was to optimize the hot rolling of pipeline steels on the hot strip mill, in order to improve the toughness-strength compromise.

Hot torsion tests performed at IRSID enabled the effects of hot rolling parameters on the austenitic and ferritic microstructure of a C-Mn steel and a C-Mn-Nb steel to be quantified. One of the main results is that the ferritic grain size has been found to decrease with lower reheating temperature (through grain growth control) and with lower finishing temperature.

Rolling trials have been carried out on the pilot scale mill at IRSID and on the industrial scale SOLLAC Dunkirk hot strip mill. The main results of these investigations are :

- for both steels, a better strength and toughness compromise is obtained when lowering both reheating and finishing temperature,
- when rolling is finished in the $\gamma/\alpha$ range, mechanical properties of the C-Mn steel were further improved. As for the C-Mn-Nb steel, the toughness is improved if respective reductions in the austenitic and ferritic ranges are adequately balanced,
- for the C-Mn steel, a further improvement of mechanical properties is obtained when increasing the cooling rate and decreasing the coiling temperature.

These results permit the production of high toughness high grade hot rolled coils for pipes. An enlargement of the gauge capability has been possible at the SOLLAC Dunkirk hot strip mill for these products.

## 1. INTRODUCTION

As a consequence of the high hot strip mill productivity, which lowers costs, there is an increasing demand for high grade as rolled coils [1, 2]. However productivity requirements have greatly delayed the application to hot strip mill of controlled rolling techniques intensively developed in the seventies for plate mills. On the hot strip mill, high mechanical properties are often obtained by the use of alloying elements which combine precipitation, solid solution and structural hardening [2, 3, 4]. These elements allow relatively light rolling conditions [5, 6, 7] but have drawbacks: they are expensive and precipitation strengthening has a detrimental effect on toughness. Therefore the challenge is to obtain high grade coils with good toughness properties especially for thick gauge, at a competitive production cost. It is well known that the most effective way to improve both strengthening and toughness is the refinement of the ferritic grain size. This can be obtained by microalloying additions and/or modifications to the rolling process.

The objective of the present work, which has been carried out by IRSID and SOLLAC Dunkirk, was to optimize rolling conditions with a view to obtain a better strength and toughness compromise, through a balance between grain size and precipitation

hardening, within an acceptable range for technological facilities and mill capacity.

A C-Mn-Nb steel for X60 grade and a C-Mn steel for X42 grade were used, the compositions of which are given on Table I.

Steel C-Mn :

| C | Mn | Nb | Si | S | P | Al | $N_2$ |
|---|---|---|---|---|---|---|---|
| 149 | 1110 | | 281 | 5 | 13 | 47 | 6.3 |

Steel C-Mn-Nb :

| C | Mn | Nb | Si | S | P | Al | $N_2$ |
|---|---|---|---|---|---|---|---|
| 100 | 1250 | 27 | 200 | 1.5 | 24 | 30 | 10.6 |

Composition in $10^{-3}$ % weigth

TABLE I.

IRSID carried on the work by the means of hot torsion testing and rolling on a laboratory mill. Each aspect of the process has been separately studied by torsion testing, thereafter complete rolling schedules were performed on the experimental mill. An intensive use has been made of the structural model, recently developed at IRSID [8, 9], which proved to be effective for the prediction of the austenitic microstructure.

## 2. EXPERIMENTAL PROCEDURE

The hot torsion tests were performed on a fully computerized machine. Specimens were 6 mm dia. and 80 mm gauge length. The strain rate was 3.6 $s^{-1}$. Specimens are induction heated, cooled by argon or helium and can be quenched at any moment of the test.

The experimental mill is a three high mill with maximum speed 1 m/s. Minimum interpass time was 7 s. Products were 70 x 70 x 150 mm billets machined in 70 mm heavy plate and rolled to 12 mm final thickness. The temperature was controlled by a thermocouple embedded in a hole at the first pass. Cooling of the final product was obtained by pulsed air up to 10°C/s or water quenching for higher cooling rates. Coiling was simulated by 1 hour annealing, followed by slow cooling in vermiculite powder.

## 3. AUSTENITE AND FERRITE MICROSTRUCTURE

### 3.1. Reheating

The austenite grain size $d\gamma$ of torsion specimens has been observed after reheating whithin the 1080-1230°C range, simulated by a 20 mn isothermal holding at a choosen temperature $T\gamma$. Figures 1 and 2 show the evolution of $d\gamma$ (μm) with $T\gamma$ (°C), associated with the niobium carbonitride or aluminium nitride contents.

In both case (C-Mn-Nb and C-Mn steels) a low reheating temperature produces a fine austenitic grain size due to grain boundary pinning by nitride and carbonitride particles. At $T\gamma \simeq 1030$°C abnormal grain growth occurs because of unpinning, and the microstructure is heterogeneous. Above 1030°C normal grain growth takes place and because of the low temperature the grain size remains small until all of the particles are dissolved.

During the roughing stage, the austenitic structure is refined by recrystallization after each pass. Because of high temperature and large reductions, recrystallization is fast and grain growth occurs between passes. In the structural model developed in previous work at IRSID [8, 9], the grain growth is described by a logarithmic law : $d = dR\ (1 + \alpha \ln t/tR)$, where dR is the recrystallized grain size and tR the time for complete recrystallization. $\alpha$ is a parameter which depends on grain growth inhibitor factors such as niobium in solution or the presence of non dissolved particles.

The latter factor has been particularly studied in the present work and figure 3 shows the evolution of $\alpha$ with the reheating temperature.

From this data the following expressions for $\alpha$ could be derived :

C-Mn steel :

$$\alpha = 0.2\ (1 - f(AlN)) \qquad (1)$$

C-Mn-Nb steel :

$$\alpha = 0.1\ (1 - f(AlN))(1 - f(NbCN))^5 \qquad (2)$$

As shown in figure 3, the C-Mn-Nb steel exhibits a stronger control of grain and below 1080°C no grain growth occurs between passes.

Figure 4 shows the evolution of austenitic grain size in the whole roughing stage after reheating at 1230 an 1130°C. Lowering the reheating temperature produces a finer grain size at the entrance of the finishing stand due to finer recrystallized grain sizes after reductions at lower temperatures and slower grain growth between passes. The initial grain size has no effect on the final grain size as shown in figure 5 where grain sizes were computed and measured after the same roughing schedule from very different initial grain sizes.

Another way for refining austenitic microstructure is to increase the total reduction in the roughing stage, that is, decreasing the transfer bar thickness. Figure 6 shows the computed austenitic grain size at the entrance of stand F1 for C-Mn-Nb and C-Mn steels, according to bar thickness

steel C_Mn_Nb
$T_\gamma$ = 1230°C

| Pass n° | Δt (s) | H (mm) | ρ % | $\bar{\varepsilon}$ | $\dot{\bar{\varepsilon}}$ $s^{-1}$ | $X_R$(%) or $d_\gamma$ (μm) before pass — Rolling Temperature | | | | | |
|---|---|---|---|---|---|---|---|---|---|---|---|
| | | 36 | | | | 40 μm | 40 μm | 40 μm | 40 μm | 40 μm | 40 μm |
| 1 | | | 22 | 0,29 | 10 | 820 | 850 | 900 | 950 | 1000 | 1030 |
| | 3 | 28 | | | | 0 % | 0 % | 0 % | 8 % | 20 % | 45 % |
| 2 | | | 24 | 0,31 | 15 | 810 | 840 | 890 | 940 | 985 | 1035 |
| | 2,5 | 21,4 | | | | 0 % | 0 % | 0 % | 7 % | 20 % | 45 % |
| 3 | | | 21 | 0,27 | 20 | 800 | 830 | 880 | 925 | 970 | 1020 |
| | 2 | 17 | | | | 0 % | 0 % | 0 % | 0 % | 10 % | 30 % |
| 4 | | | 19 | 0,25 | 25 | 790 | 825 | 870 | 915 | 960 | 1005 |
| | 1,5 | 13,7 | | | | 0 % | 0 % | 0 % | 0 % | 7 % | 20 % |
| 5 | | | 12 | 0,15 | 30 | 780 | 820 | 860 | 905 | 950 | 990 |
| | | 12 | | | | | | | | | |
| | | | | | SCHEDULE N° | 1 | ② | 3 | 4 | ③ | 5 |

**TABLE II**

steel C_Mn
$T_\gamma$ = 1230°C

| Pass n° | Δt (s) | H (mm) | ρ % | $\bar{\varepsilon}$ | $\dot{\bar{\varepsilon}}$ $s^{-1}$ | $X_R$(%) or $d_\gamma$ (μm) before pass — Rolling Temperature | | | | | |
|---|---|---|---|---|---|---|---|---|---|---|---|
| | | 36 | | | | 60 μm | 60 μm | 60 μm | 60 μm | 60 μm | 60 μm |
| 1 | | | 22 | 0,29 | 10 | 820 | 850 | 900 | 950 | 1000 | 1030 |
| | 3 | 28 | | | | 0 % | 10 % | 40 % | 33 μm | 39 μm | 46 μm |
| 2 | | | 24 | 0,31 | 15 | 810 | 840 | 890 | 940 | 985 | 1035 |
| | 2,5 | 21,4 | | | | 0 % | 40 % | 80 % | 21 μm | 28 μm | 37 μm |
| 3 | | | 21 | 0,27 | 20 | 800 | 830 | 880 | 925 | 970 | 1020 |
| | 2 | 17 | | | | 0 % | 0 % | 40 % | 80 % | 23 μm | 31 μm |
| 4 | | | 19 | 0,25 | 25 | 790 | 825 | 870 | 915 | 960 | 1005 |
| | 1,5 | 13,7 | | | | 0 % | 0 % | 20 % | 60 % | 19 μm | 26 μm |
| 5 | | | 12 | 0,15 | 30 | 780 | 820 | 860 | 905 | 950 | 990 |
| | | 12 | | | | | | | | | |
| | | | | | SCHEDULE N° | 1 | ② | 3 | 4 | ③ | 6 |

**TABLE III**

and reheating temperature. As shown in this figure a finer grain size is obtained by decreasing the bar thickness with higher reduction in the roughing stage. This figure also shows that decreasing the reheating temperature has a more important effect on the austenitic grain size.

### 3.2. Finishing stage

In the finishing stage, the two steels have different behaviours : in the C-Mn-Nb steel, the austenite does not recrystallize between passes. However, in both cases structural evolution is strongly dependent on the rolling temperatures. Tables II and III show the computed recrystallized fraction XR or recrystallization grain size $d_\gamma$ at the entrance of each finishing stand, for the C-Mn-Nb and C-Mn steels respectively. With increasing temperature, recrystallization can occur for the C-Mn-Nb steel at the first stands of finishing stage. On the

contrary, with decreasing rolling temperature for the C-Mn steel, recrystallization may incomplete in the last stands or even supressed in the whole finishing stage if rolling temperatures are extremely low.

The figure 7 describes the complete microstructural evolution of both steels, between the stands, for schedules 2 and 5 of Tables II and III (finishing temperature equal respectively to 820 and 950°C). Figure 7 shows the evolution of the mean austenitic grain size $d\gamma$ and the residual strain $\bar{\varepsilon}^*$, which represents the mean amount of pancaking in the microstructure (for the computation of $d\bar{\gamma}$ and $\bar{\varepsilon}^*$ in a partially recrystallized structure, see ref. [8] and [9]. As can be seen, for both steels, when rolling temperatures are increased, the austenitic grain size is more refined by recrystallization, but pancaking decreases.

As the resulting ferritic grain size is dependant on both grain size and the amount of pancaking [9, 10] we performed complete simulations of rolling to investigate the influence of austenitic microstructure on the ferritic grain size.

### 3.3. Ferritic structure

Fine ferritic grain size results from the transformation of fine grained and strained austenite. Thereby the ferritic grain size is dependent on initial recrystallized grain size before straining, the temperature of rolling in the finishing stand and the total amount of straining.

As previously shown, a lowering of the reheating temperature and/or finishing temperature should produce a finer ferritic structure. This a confirmed by the results of figure 8 which gives the observed ferritic grain size of C-Mn-Nb and C-Mn steels according to reheating temperature produces a finer grain size, but this effect is relatively small for the C-Mn-Nb steel (figure 8). The effect of the finishing temperature is obviously stronger. It is important to note that at a finishing temperature of 780°C, both steels gave the same ferritic grains sizes. As can be seen in Table III for C-Mn steel finished at 780°C, recrystallization is suppressed over the whole of the finishing mill so this steel behaves like the C-Mn-Nb steel. This result is obvious from figure 9, where the observed ferritic grain size is plotted against the austenitic grain size calculated prior to the transformation. These results fit well the following relationship :

$$d\alpha = 0.58 \ln d\gamma - 2.12\bar{\varepsilon} + 0.00975\ FT - 3.33 \quad (3)$$

## 4. MECHANICAL PROPERTIES

### 4.1. Introduction

Complete rolling simulations have been performed on the experimental mill to investigate yield strength and toughness in the transverse direction. Processing parameters have been chosen as indicated below.

- Reheating temperature : $T\gamma$ 1080, 1130, 1180, 1230°C
- Total reduction in the finishing stage : $\rho F$ = 66 %, 75 %
- Finishing temperature : FT = 860, 820, 780, 760°C
- Cooling rate : CR = 1, 5, 10, 15, 20°C/s
- Cooling temperature : CT = 500, 550, 600, 650°C.

Thermal analysis of specimens after rolling were used to determine the austenite to ferrite transformation temperature $Ar_3^*$ which was found to be $Ar_3^*$ = 780°C for C-Mn-Nb steel, $Ar_3^*$ = 760°C for C-Mn steel. For C-Mn-Nb steel lamellar splitting occured in impact tests, whenever rolling was finished at low temperature. Therefore the 50% FATT could not be determined and toughness was assessed by the temperature for 28J/cm² impact energy : TK 28J.

### 4.2. Experimental results : C-Mn-Nb steel

Figure 10 shows the yield strength (YS) and toughness (TK28J) obtained after different reheating temperatures ($T\gamma$) and finishing temperatures (FT). The effect of finishing temperature and total reduction is more precisely shown by figure 11. Reduction of the reheating temperature results in lower yield strength but improved toughness. Lowering the finishing temperature to 820°C lead to higher yield strength and toughness. After finishing at 780°C however, toughness is strongly deteriorated but yield strength continues to increase.

Increasing the reduction in the finishing stage produces an improvement of toughness and only slightly affects the yield strength.

The effect of cooling rate after rolling has been investigated for $T\gamma$ = 1130°C ; $\rho F$ = 66 % ; FT = 820°C and CT = 600°C. The results are shown in figure 12. As can be seen, the yield strength and toughness are improved when the cooling rate varies from 1°C/s to 5°C/s, but no further improvement is obtained with higher cooling rates. The effect of coiling temperature between 500 and 650°C has been investigated and results are plotted in figure 13. No effect on the mechanical properties have been found when lowering the coiling temperature below

600°C. The yield strength is however deteriorated for CT = 650°C.

**4.3. Experimental results : C-Mn steel**

Similar trials have been performed with the C-Mn steel. Figure 14 shows the mechanical properties obtained after different reheating and finishing temperatures. The yield strength decreases with reheating temperature except at Tγ = 1080°C and FT = 780°C, where high yield strength is achieved. Lowering the reheating temperature resulted in improved toughness at FT = 780°C but had no effect on toughness at FT = 860°C.

When the finishing temperature is lowered down to 760°C, which is the transformation temperature, it is seen in figure 15 that both strength and toughness are further improved. Similar results are obtained with more severe cooling conditions either increasing the cooling rate up to 15°C/s or decreasing the coiling temperature down to 500°C.

**4.4. Discussion**

The results described above show clearly the competition between different strengthening effects.

The yield strength of C-Mn-Nb steel results from a combination of precipitation hardening and grain size effects. When the reheating temperature is lowered the amount of niobium which precipitates in the ferrite is reduced and the refinement of the ferritic grain size is not sufficient to compensate for the diminution of solid-solution strengthening. On the contrary, both effects produce an improvement of toughness. Improvement of both yield strength and toughness is achieved through grain refinement by lowering the finishing temperature. The transformation temperature $Ar_3^*$ is 780°C, therefore when rolling is finished at 780°C (measured at the center of the specimen) one can assume that deformation in the γ/α range is achieved through the thickness. Hence the impaired toughness and improvement of yield strength observed at FT = 780°C can be associated with rolling in the γ/α range. As can be seen in figure 11 when FT = 780°C, the toughness is improved by increasing the reduction in the finishing stage $\rho_F$. When FT = 760°C more reduction is achieved in the γ/α range and figure 11 shows that the yield strength is deteriorated.

These results confirm some of the conclusions of previous IRSID studies [11] :

- mechanical properties of steels rolled in the γ/α range are improved when strong reduction is achieved in the non recrystallized austenite,
- when reduction in the γ /α range exceeds a critical value, yield strength is decreased.

Mechanical properties of the C-Mn steel are mainly explained by the combined effects of ferritic grain size and solid solution strengthening due to soluble nitrogen. As shown in figure 2, the nitrogen content in solid solution is reduced by lowering the reheating temperature. A previous study carried on at IRSID [12], showed that the precipitation of AlN during coiling at temperatures under 650°C, is very slow. Therefore, in our rolling conditions, nitrogen should remain in solution from reheating to final cooling.

The ferritic grain size is refined by lowering finishing and reheating temperatures ; however that latter effect does not compensate the smaller solid solution hardening. Improved properties are also achieved through grain refinement when the cooling rate is increased from 10 to 15°C/s. The microstructure observed (figure 19) is fine equiaxed ferrite plus a small fraction of fine upper bainite. This is also observed (figure 16) at low coiling temperature (500°C) at which good properties are achieved.

In view of these results an experimental trial has been performed to obtain the best mechanical properties. The rolling parameters were :

Tγ = 1130°C
FT = 760°C
CR = 30°C/s
CT = 500°C.

The microstructure obtained is a mixture of fine ferrite and upper bainite. Resulting yield strength and temperature TK 50 % are :

YS = 460 N/mm² - TK 50% FATT = - 90°C

which constitutes, as seen in figure 16, the best strength-toughness compromise obtained for that steel.

| | C | Mn | Si | Nb | S | V |
|---|---|---|---|---|---|---|
| A | 95 | 1060 | 242 | 14 | 6 | - |
| B | 52 | 785 | 227 | 20 | 1 | - |
| C1 | 120 | 1370 | 335 | 40 | 5 | - |
| C2 | 120 | 1370 | 335 | 40 | 5 | - |
| D1 | 100 | 1400 | 250 | 35 | 7 | - |
| D2 | 100 | 1400 | 250 | 35 | 7 | - |
| CD | 132 | 1400 | 360 | 28 | 8 | - |
| E | 100 | 1400 | 320 | 50 | 2 | 78 |
| F | 79 | 1320 | 296 | 31 | 0.5 | - |
| G1 | 70 | 400 | - | 10 | - | - |
| G2 | 70 | 400 | - | 10 | - | - |
| H1 | 140 | 1200 | - | 10 | - | - |
| H2 | 140 | 1200 | - | 10 | - | - |

Composition in $10^{-3}$ % weight - TABLE IV (a)

| | ST | FT | CT | TH | YS | TK |
|---|---|---|---|---|---|---|
| A | 1200 | 880 | 620 | 10 | 400 | -20 |
| B | 1180 | 820 | 590 | 9,5 | 400 | -100 |
| C1 | 1160 | 840 | 660 | 10 | 430 | -90 |
| C2 | 1100 | 790 | 580 | 10 | 470 | -110 |
| D1 | 1230 | 860 | 610 | 8 | 490 | -45 |
| D2 | 1130 | 860 | 610 | 8 | 490 | -75 |
| CD | 1160 | 825 | 595 | 8 | 473 | -87 |
| E | 1160 | 820 | 610 | 10 | 530 | -85 |
| F | 1160 | 810 | 530 | 15 | 480 | -60 |
| G1 | - | 870 | 600 | 5 | 400 | -40 |
| G2 | - | 770 | 510/620 | 5 | 400 | -85 |
| H1 | - | 880 | 600 | 5 | 450 | -80 |
| H2 | - | 750 | 590/645 | 5 | 450 | -120 |

ST soaking temperature (°C)
FT finishing temperature (°C)
CT coiling temperature (°C)
TH coil thickness (mm)
YS yield strength ($N/mm^2$)
TK 50 % FATT (°C)

TABLE IV (b)

## 5. RESULTS ON THE SOLLAC DUNKIRK HOT STRIP MILL

Several trials have been performed on the industrial scale in order to confirm the major conclusions of the experimental study carried out at IRSID. The main results are summarized in table IV and figure 17, where the yield strength and the toughness (50 % FATT) have been plotted (each point represents the mean characteristics measured on several coils).

These results have to be described in terms of chemical composition (Nb content) rolling parameters and final thickness.

Steel A has a low niobium content ($14.10^{-3}$ %) and was rolled with high soaking and finishing temperature. As the final gauge is high (10 mm) the final microstructure is rather coarse and the properties are poor.

Steel B with the same final gauge, shows a considerably improved toughness compared to steel A. In this case the niobium content was greater and also the rolling conditions were more severe. Since the manganese and carbon content are lower the yield strength is the same as steel A.

With steel C, the influence of rolling and coiling temperature may be observed. Coils C1 were rolled and coiled at high temperature. Thanks to a higher niobium content the yield strength is higher than steel B (with the same gauge) but the toughness is lower. For coils C2 the finishing and coiling temperatures were lowered and this gives a drastic improvement of both strength and toughness.

The effect of reheating temperature has been investigated on steel D. Lowering the reheating temperature from 1230 to 1130°C improves the toughness without deteriorating the strength thank to a better control of the grain size.

Steel E is a niobium vanadium steel for X70 production. By means of low temperature rolling, good toughness is achieved with a very high strength.

Steel F was rolled to 15 mm final gauge; the mechanical properties are reasonably good for such a thickness on the hot strip mill.

With steels G and H the effect of very low temperature rolling - that is in the ferritic range - has been investigated. Because of the low final thickness (5 mm) a large amount of reduction was achieved in the austenitic range prior to deformation in the ferritic range. As a consequence, for both steels the toughness is drastically improved with no change in the yield strength. This confirms the results of the experimental works. Recrystallization of the ferrite may occur whenever too much reduction is performed in the ferrite and therefore the dislocation strengthening vanishes.

## 6. CONCLUSIONS

The present study clearly demonstrates the strong influence of processing parameters on microstructure and thus on mechanical properties of C-Mn and C-Mn-Nb steels rolled on the hot strip mill. Simulations by hot torsion tests and the use of a structural model help to explain the results observed. The main conclusions may be summarized as following :

C-Mn-Nb Steel

- an improved toughness is obtained by lowering the reheating temperature : therefore, to maintain a high yield strength, the finishing temperature should be reduced, but must be kept above the transformation temperature,
- when rolling is finished in the ferritic range, toughness is impaired, unless a higher reduction is achieved in the finishing stage,
- no significant influence of cooling rate from 5 to 20°C/s, nor of coiling temperature from 600 to 500°C were observed when finishing temperature is low (820°C).

C-Mn Steel

- toughness and yield strength are improved when both reheating temperature and finishing temperature are lowered,

- when rolling is finished in the ferritic range, both toughness and yield strength are still improved,

- both toughness and yield strength are further improved when the cooling rate is greater than 10°C/s and also when the coiling temperature is lowered to 500°C,

- excellent mechanical properties (YS = 460 N/mm² ; TK 50 % = - 90°C) are achieved with $T_\gamma$ = 1130°C ; FT = 760°C, CR = 30°C/s, CT = 500°C.

The results concerning the C-Mn-Nb steels have been confirmed by industrial trials. The attainment of attractive properties for thick gauge coils has been achieved through a close control of the temperature at each stage of the rolling process.

## LITTERATURE


[1] C. OUCHI and Al., Proc. of International Conference on Steel Rolling, TOKYO, Oct. 80.

[2] G. ARNCKON and Al., Proc. Steels for line pipe and pipeline fittings, London, 81.

[3] U. FELDMANN and Al., Proc. HSLA Steels, Philadelphia, 83.

[4] R. KASPAR and Al., Proc. Thermomechanical treatment of austenite, Pittsburgh 81.

[5] F. HEISTERKAMP and K. HULKA, Niobium technical report NbTR 04/83, Nov. 83.

[6] STUART and Al., ibid. [2]

[7] W. ROBERTS, ibid. [3]

[8] C. PERDRIX, ECSC Research 7210 EA/311

[9] P. CHOQUET, A. LE BON and C. PERDRIX, Proc. ICSMA 7, Montréal 1985.

[10] H. SEKINE, T. MARUYAMA, Seitetsu Kenkyü (1976), n° 289, p. 11920-11938

[11] T. JONCHERAY, ECSC Research 7210 MA/309

[12] J. GARCIA and A. LE BON, ECSC Research 7210 KD/310.



ACKNOWLEDGMENTS - The authors wish to express their gratitude to the European Communities (ECSC) for financial support of this work.


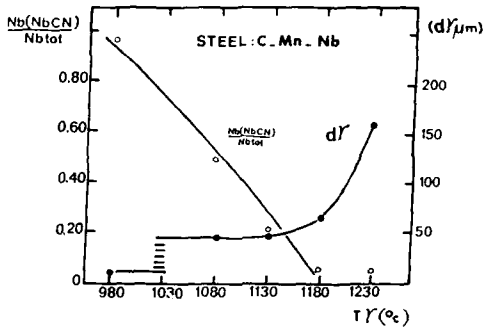


Fig. 1 - Austenitic grain size and dissolution of niobium after soaking.

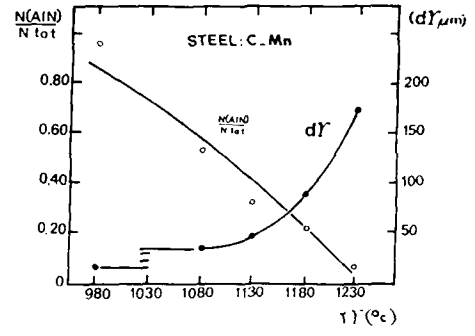


Fig. 2 - Austenitic grain size and dissolution of aluminium after soaking.

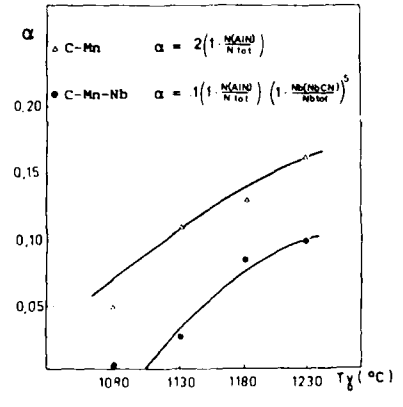


Fig. 3 - Grain growth parameter vs reheating temperature.

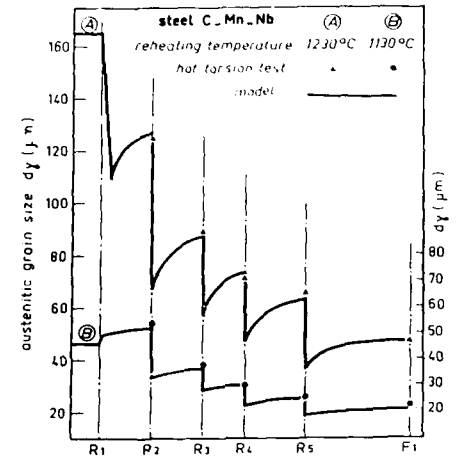


| H(mm) | 210 | 175 | 125 | 90 | 60 | 38 |
|---|---|---|---|---|---|---|
| ρ (%) | 17 | 23 | 28 | 33 | 37 | |
| T°C A | 1214 | 1205 | 1192 | 1178 | 1149 | 1076 |
| T°C B | 1117 | 1111 | 1102 | 1092 | 1070 | 1012 |
| t (s) | 22 | 22 | 20 | 28 | 48 | |

H sheet bar thickness ρ reduction T temperature
t time beetween passes

Fig. 4 Evolution of the grain size in the roughing mill.

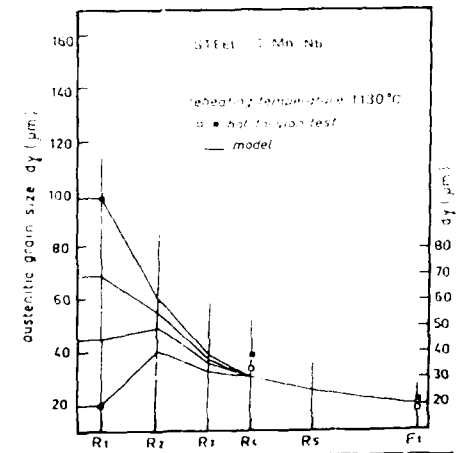


| H(mm) | 210 | 175 | 125 | 90 | 60 | 38 |
|---|---|---|---|---|---|---|
| ρ (%) | 17 | 23 | 28 | 33 | 37 | |
| T (°C) | 1117 | 1111 | 1102 | 1092 | 1070 | 1012 |
| t (s) | 22 | 22 | 20 | 28 | | |

H sheet bar thickness ρ reduction T temperature
t time beetween passes

Fig. 5 - Influence of the initial grain size.

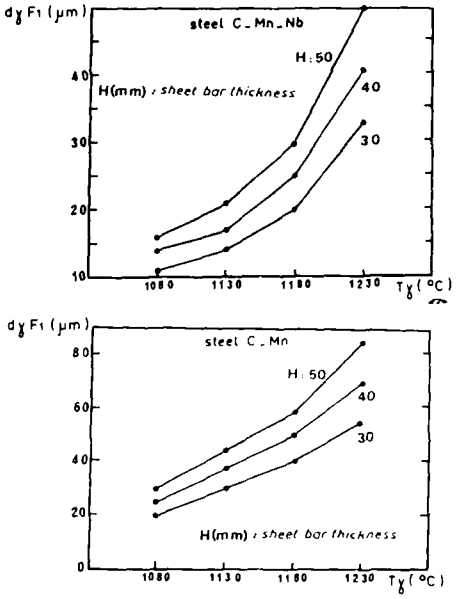


Fig. 6 - Calculated austenitic grain size of the bar.

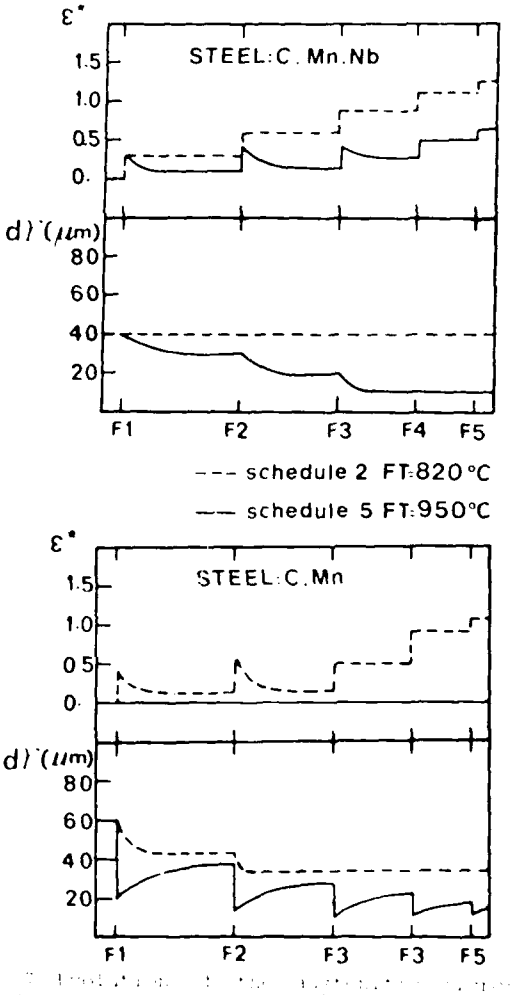


Fig. 7 [illegible]

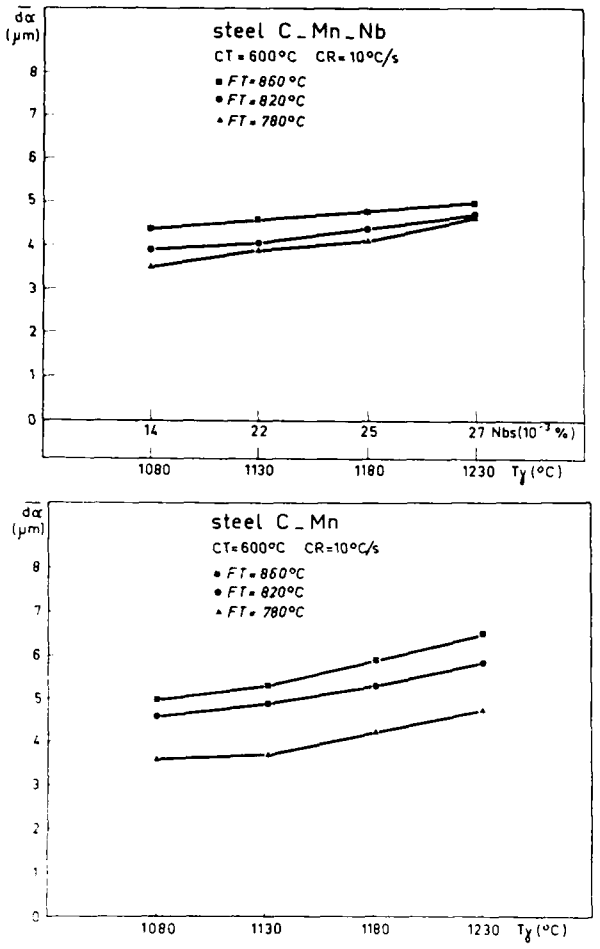


Fig.8 - Final ferritic grain size vs reheating temperature and finishing temperature.

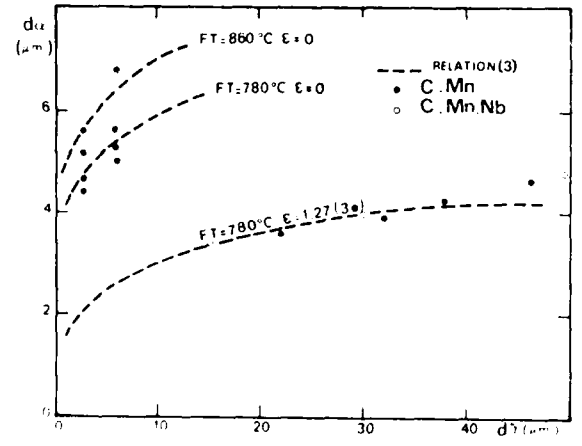


Fig. 9 - Ferritic grain size vs austenitic grain size and deformation temperature.

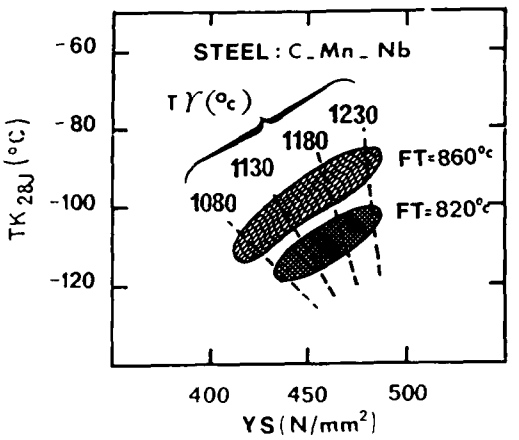


Fig. 10 - Mechanical properties of the C-Mn-Nb steel.

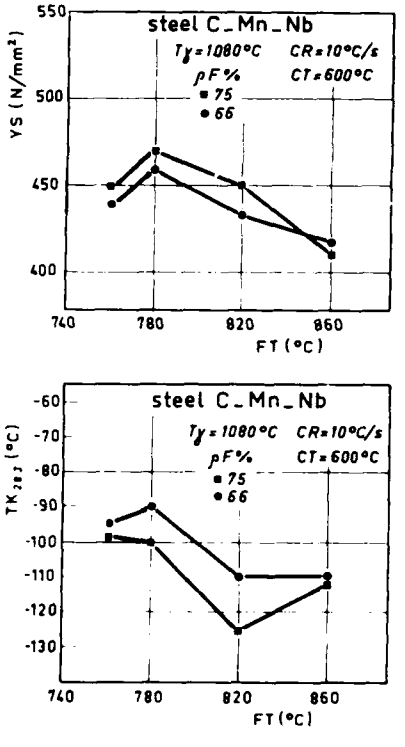


Fig. 11 - Effect of finishing temperature on the mechanical properties of the C-Mn-Nb steel.

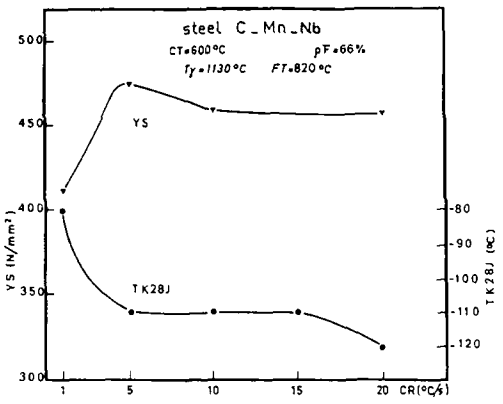


Fig.12 - Effect of cooling rate on the mechanical properties of the C-Mn-Nb steel.

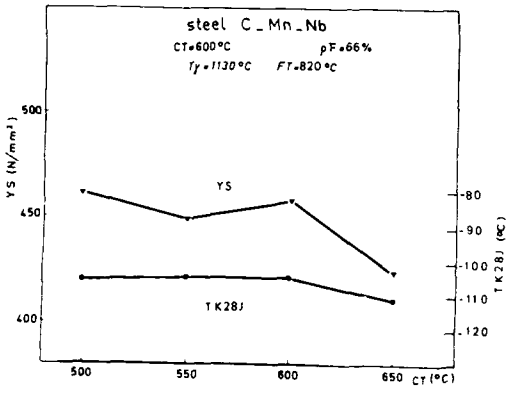


Fig. 13 - Effect of coiling temperature on the mechanical properties of the C-Mn-Nb steel.

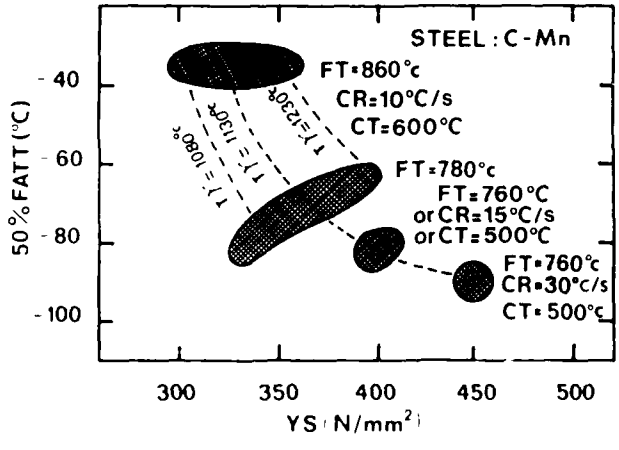


Fig. 14 - Mechanical properties of the C-Mn steel.

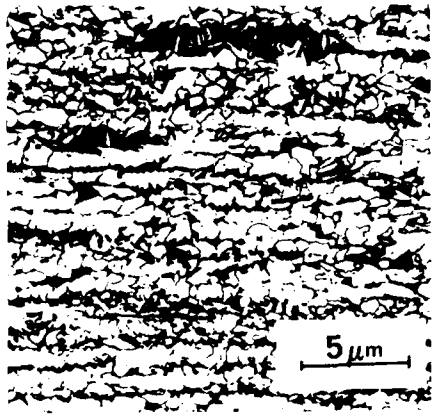


Fig. 15 - Microstructure of the C-Mn steel. after cooling rate - CR = 15°C/s.

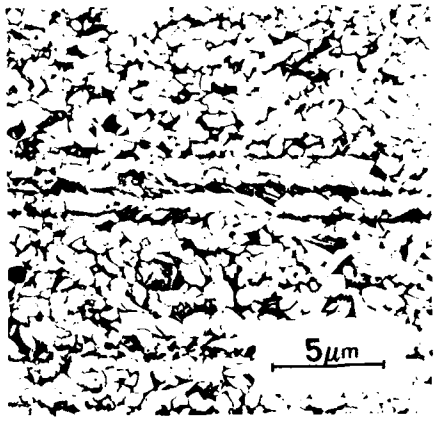


Fig. 16 - Microstructure of the C-Mn steel after coiling temperature - CT = 500°C.

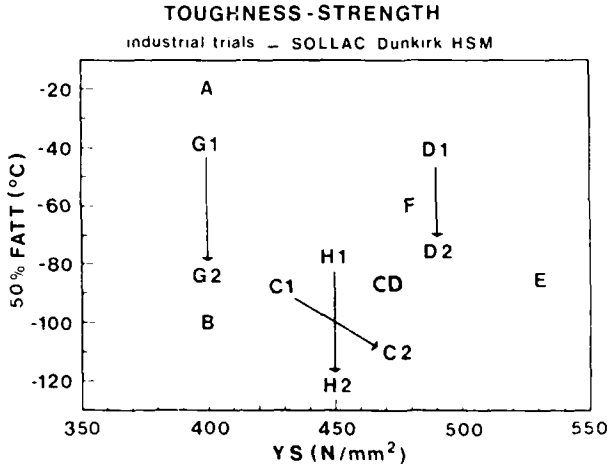


Fig. 17 - Mechanical properties of thick gauge high strength coils rolled at SOLLAC Dunkirk hot strip mill.

# THERMO-MECHANICALLY PROCESSED HIGH COPPER BEARING STEEL PLATES

**Takashi Abe, Masayoshi Kurihara, Hisatoshi Tagawa**
Steel Research Center
NKK Corporation
Kawasaki, Japan

Abstract

In order to develop YS460 grade steel plate for offshore structures, the effect of thermo-mechanical treatment on the mechanical properties of Cu bearing age hardenable steels was examined. Accelerated cooling and direct quenching after controlled rolling enhanced to produce the microstructure dominant of low carbon bainite which caused the improvement of strength and toughness. And addition of Cu over 1% was effective in both $\varepsilon$-Cu precipitation strengthening and microstructural control through its effects on hardenability. On the basis of studies on the combination of thermo-mechanical process and Cu addition over 1%, heavy gage steel plate contained 1% Cu has been developed with the process of accelerated cooling after controlled rolling. Despite high strength, this plate represents good toughness in HAZs of weldment and superior in weldability because of its lower carbon content ($C \leq 0.05\%$) and carbon equivalent ($Ceq^{IIW} \leq 0.40\%$).

FOR OFFSHORE STRUCTURES, increase in strength and thickness of steel plates, and improvement in toughness and weldability are required as operation environment becomes severer. And recently, steel plates with strength higher than YS460MPa are required. In order to improve the base metal properties and weldability of structural steel plates, TMCP(Thermo-Mechanical Control Process) technology has come to be used with a number of successful results[1)-5)]. However, to meet recent strict requirements on both strength and toughness, it is indispensable to introduce new technology in addition to TMCP.

It is known that addition of Cu about 1.0% to 1.2% in steels is effective in increase of strength by $\varepsilon$-Cu precipitation hardening. On the basis of this advantage, Cu age hardenable steels such as ASTM-A710 steel[6)] for hull structures and A710-modified steel[7)] for line pipe fittings have been developed. Because of lower carbon contents, these steels have excellent weldability in spite of their high strength, so that they are suitable for welded structures. Considering about application of high Cu steel as a structural steel plate in a wide range, application of the TMCP technology should be researched to exert a profitable effect on improvement of properties.

In the present paper, for the purpose of development of YS460MPa grade steels, firstly, mechanical properties of A710 and A710-modified steels were studied under conditions of controlled rolling, accelerated cooling and direct quenching after controlled rolling in comparison with the conventional heat treatments. Secondly, to make clear the effective factors in the improvement of the mechanical properties, the effects of chemical composition and conditions in rolling and cooling on the change of properties were examined in a laboratory. Finally, based on the results of these basic examination, a new kind of YS460MPa grade steel plate with a thickness of up to 75mm was successfully developed using the OLAC II (On-Line Accelerated Cooling II) plant. The properties of base metal and weldment of the developed steels are also introduced in this paper.

## LABORATORY STUDIES ON PROPERTIES OF TMCP Cu BEARING STEELS

EXPERIMENTAL PROCEDURE - Table 1 shows the chemical compositions of steels used in this study. Steel A is ASTM A710 steel which contains 1.2%Cu-0.7%Cr-0.2%Mo-0.03%Nb. Steel B, A710-modified steel, contains higher manganese in comparison with A710 steel to offset the elimination of Cr and Mo.

Table 1 Chemical composition, wt%

| Steel | C | Si | Mn | P | S | Cu | Ni | Cr | Mo | Nb | Ti | sol.Al | T.N |
|---|---|---|---|---|---|---|---|---|---|---|---|---|---|
| A | 0.03 | 0.27 | 0.41 | 0.004 | 0.001 | 0.17 | 0.84 | 0.65 | 0.18 | 0.031 | | 0.035 | 0.0043 |
| B | 0.06 | 0.30 | 1.40 | 0.016 | 0.003 | 1.16 | 0.70 | | | 0.029 | | 0.025 | 0.0042 |
| C | 0.046 | 0.28 | 1.02 | 0.006 | 0.004 | 1.01 | 0.55 | | | 0.010 | 0.010 | 0.025 | 0.0019 |
| D | 0.046 | 0.27 | 1.28 | 0.007 | 0.004 | 1.01 | 0.54 | | | 0.010 | 0.010 | 0.025 | 0.0020 |
| E | 0.048 | 0.27 | 1.52 | 0.006 | 0.004 | 1.00 | 0.54 | | | 0.010 | 0.010 | 0.025 | 0.0021 |

Steels C~E were used to confirm adequate composition for thermo-mechanically processed Cu bearing steels. The basic compositions of these steels were similar to that of steel B, however Nb content was reduced from 0.03 to 0.01%. The differences in properties according to plate thickness is adjusted by Mn content.

The conditions of multi-pass rolling with one pass reduction of 5~10% and heat treatments which involve aging are shown in Fig. 1. In the thermo-mechanical process, the finishing rolling temperature of controlled rolling was changed from 690 to 1000℃, which involved supercritical rolling ($\gamma$) and intercritical ($\gamma + \alpha$) rolling. After the rolling, various treatments such as air cooling (about: 0.8℃/s: CR), interruped accelerated cooling (10℃/s: AcC) and direct quenching (10~25℃/s: CR-DQ) were carried out. As the conventional heat treatments, quenching and normalizing were conducted after reheating to 900℃. Every plate was sbjected to aging treatment in the temperature range from 450 to 650℃. After aging, tensile properties, Charpy V-notch toughness and microstructure were examined. The longitudinal direction of every specimen was transverse to the rolling direction.

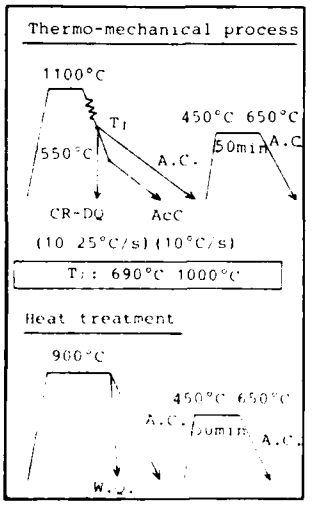


Fig. 1 Conditions of rolling, cooling and heat treatment in various process

EFFECT OF MANUFACTURINGE PROCESS ON THE PROPERTIES - To confirm the effect of thermo-mechanical process on the properties of Cu bearing steels, change in strength and toughness of variously processed A710 and A710-modified steels were examined. Figure 2 shows the aging response of variously processed A710 steel.

In this case, controlled rolling in the thermo-mechanical process was finished at 800℃ in austenite region. As shown in the figure, the maximum age hardening took place at a temperature around 500~550℃ with an increase of about 100-150MPa in TS regardless of the process. In the temperature range over 550℃, a decrease of strength caused by over-aging was observed. Concerning of the effects of processes, the TMCP type represented by half solid or solid mark has higher strength than the heat treatment type represented by open mark. To be specific, compared with normalized steel, the strength shows an increase of 50 to 100 MPa as a result of controlled rolling and 50 to 150MPa as a result of accelerated cooling. Comparison between quenched steel and CR-DQ steel shows that higher increase in strength by 30 to 70MPa is achieved as a result of DQ.

Toughness deteriorated as age-hardening increased and the lowest toughness was observed around 550℃. Over-aging was preferable for the improvement of toughness. Figure 3 shows an example of electron microscopic observation of fine $\varepsilon$-Cu precipitates as a result of aging. The age hardening described before is brought about by the precipitation hardening of this $\varepsilon$-Cu.

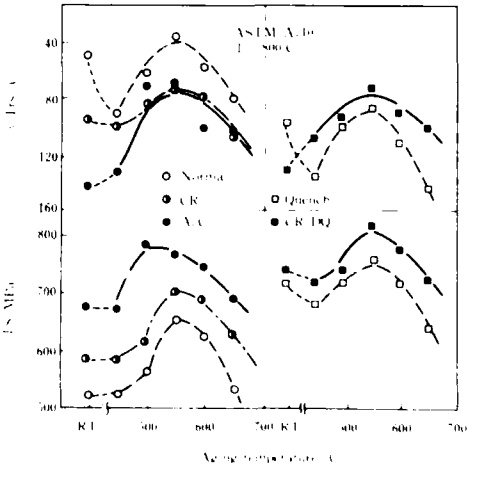

Fig. 2 Change in mechanical properties of variously processed A710 steel


Fig. 3 Observation of $\varepsilon$-Cu precipitates (Aging temperature: 600℃)

Figure 4 shows the relationship between tensile strength and Charpy transition temperature of variously processed A710 and A710-modified steels. The effect of thermo-mechanical process on the properties is obviously revealed in this figure. Compared with the conventional heat treatments, thermo-mechanical process brought about remarkable improvement in both strength and toughness. Especially, high strength and toughness such as tensile strength higher than 700MPa and vTrs lower than -80℃ were achieved by AcC or CR-DQ in both steels.

These changes in properties can be almost explained by the differences in microstructures shown in Fig. 5 Both normalized steel and CR steel show ferrite-pearlite microstructure, but the CR steel show finer ferrite grains. On the other hand, the steels processed under the condition where cooling is provided consist of mainly low-carbon bainitic structure containing some ferrite. Furthermore, this structure is characterized by extending in the rolling direction. The improvements in strength and toughness may be mainly attributed to this structural change. Cu brings about not only age precipitation hardening but also improvement in

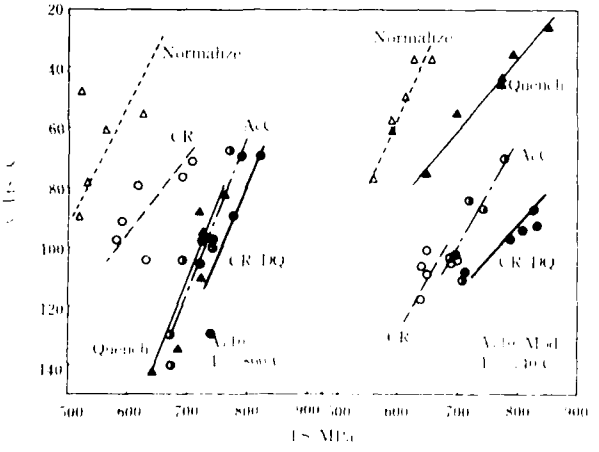


Fig. 4 Relationship between strength and toughness in variously processed A710 and A710-modified steels

hardenability and effectively works on transformation strengthening.

As a result, it was clarified that the combination of thermo-mechanical process and Cu addition over 1% was effective in improvement of the properties through the $\varepsilon$-Cu precipitaion strengthening and the microstructural improvement by grain refinement and formation of finer low carbon bainite.

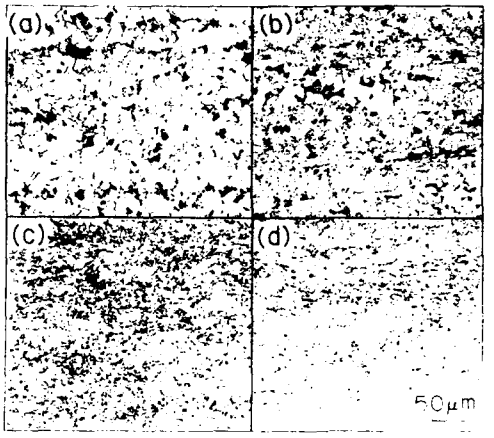


Fig. 5 Microstructure of variously processed A710 steel, (a) normalizing (b) controlled rolling (c) interrupted accelerated cooling (d) direct quenching after controlled rolling

EFFECT OF TMCP CONDITIONS AND COMPOSITION ON THE PROPERTIES - To clarify the effective factors for improvement of properties in thermo-mechanical process, the effect of rolling and cooling conditions on the properties was studied.

Figure 6 shows the change of properties of A710 steel with variation of finish-rolling temperature from 690 to 1000℃. The ferrite transformation temperature $Ar_3$ of A710 steel was around 780℃. Therefore, both supercritical and intercritical rolling were included in these conditions. In the supercritical rolling in which finish-rolling temperature was above $Ar_3$, little change of strength was observed with variation of finishing temperature. Nearly identical properties were obtained in a wide range of temperature except for 1000℃. Deterioration of toughness was observed in steel finish-rolled at 1000℃. Compared with the supercritical rolling, some decrease of strength was observed in the intercritical rolling finish-rolled below $Ar_3$.

The change of microstructure with variation of finish-rolling temperature is shown in Fig. 7. In the case of finish-rolling temperature at 1000℃, coarse grained upper bainite was observed, which caused deterioration of toughness. Under the conditions of finishi-rolling at 950 and 800℃ in supercritical

region, elongated and finer microstructures were obtained. Austenite grain refinement through hot working and deformation in unrecrystallization region which resulted in deformed microstructure were necessary to improve toughness.

On the other hand, in the intercritical rolling, the formation of coarse ferrite grain was observed. Although deformation was imposed to the transformed ferrite by the intercritical rolling, strength decreased as shown in Fig. 6. When accelerated cooling or direct quenching was applied, supercritical rolling was preferable because ferrite formation prior to the cooling

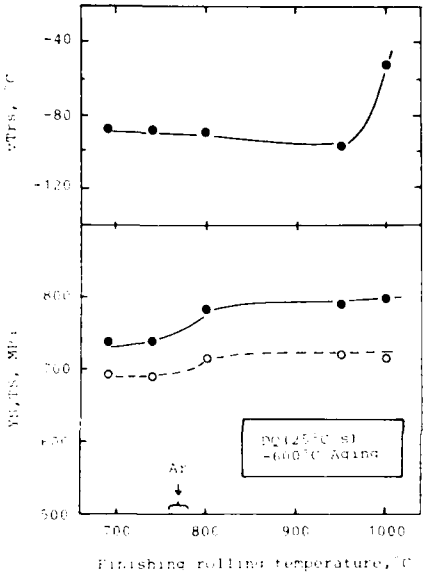


Fig. 6 Effect of finish-rolling temperature on mechanical properties in A710 steel

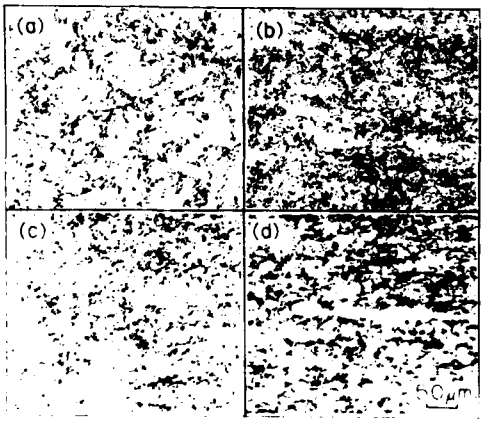


(a) 1000℃ (b) 950℃
(c) 800℃ (d) 740℃

Fig. 7 The change in microstructure of A710 steel with variation of finish-rolling temperature

resulted in deterioration of the mechanical properties. Producing bainite-dominant microstructure without coarse plolygonal ferrite by accelerated cooling is more effective for increase of strength than producing deformed ferrite by intercritical rolling.

The changes in property effected by changing the cooling rate in the accelerated cooling were examined using steels C to E and are shown in Fig. 8. The test was conducted under the conditons where finish rolling temperature was 810℃ and aging temperature 600℃. As to the cooling rate range, rather slow cooling rate of 4 to 10℃/s was applied, since the test was intended for thick plates. As shown in Fig. 8, strength and toughness improve with an increase in cooling rate. These effects are also obserbed in the slow cooling rate of about 4℃/s, and conspicuous was the effect of improvement in thoughness. CR steel almost satisfies the requirement of YS460MPa steel with regard to strength, but accelerated cooling is advantageous with regard to toughness.

Figure 9 shows the changes in microstructure resulting from accelerated cooling. Formation of polygonal ferrite with rather rough grains is observed in the steel on controlled rolling (CR steel), however, accelerated cooling suppresses polygonal ferrite formation with a resultant transformation of the structure into mainly consisting of low-carbon bainite with improved toughness.

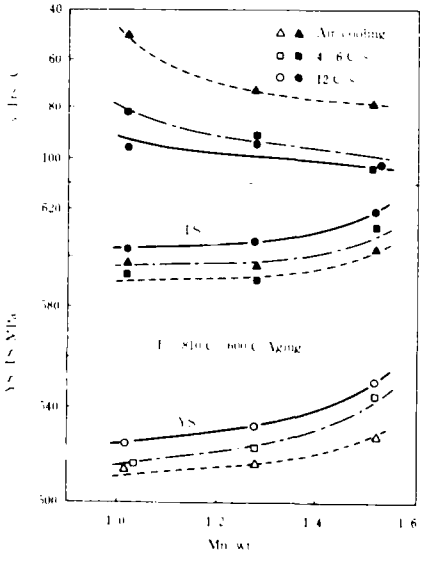


Fig. 8 Effect of cooling rate on mechanical properties

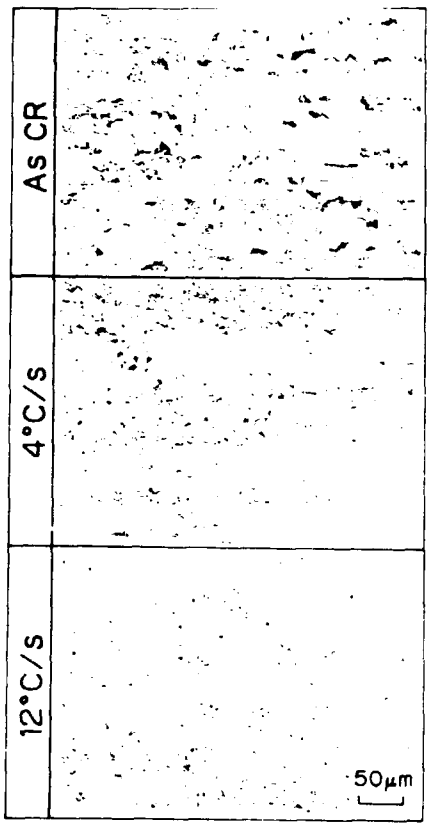


Fig. 9 Change in microstructure with variation of cooling rate (finishing rolling temp.: 810℃, 1.28%Mn)

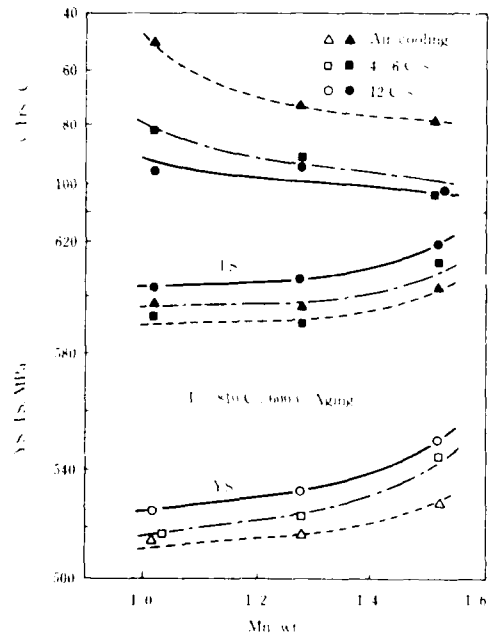


Fig. 10 Change in mechanical properties with variation of Mn content

Variation of properties with Mn content is shown in Fig. 10. As shown in the figure, it is possible to improve both strength and toughness by increasing Mn content. Although cooling rate for steel plate varies with plate thickness, the changes in property with the difference of cooling rate controllable through a adjustment of Mn content. It can be seen that about 1.0 to 1.3% of Mn needs to be added for plates of about 25 to 40mm thickness for which cooling rate of 10℃/s or higher may be applied and about 1.5% of Mn for thick plates (50 to 75mm) for which cooling rate of about 5℃/s is applied.

## PROPERTIES OF DEVELOPED STEELS

MANUFACTURING PROCESS - Based on the laboratory studies described in the preceding Chapter, mill trials were performed in order to develop YS460MPa grade steel plate. The aimed properties of trial plate are shown in Table 2. To manufacture the steel plates with thickness of 30mm and 75mm respectively, steels having the compositions shown in Table 3 were manufactured in a basic oxygen furnace. With the basic composition of 0.04%C-1.1%Cu-0.6%Ni-0.01%Nb-0.01%Ti, the 30mm thick steel had Mn content of 1.28% and the 75mm thick steel had that of 1.48%. Carbon equivalent in each steels was Ceq(IIW)$<$0.40 and Pcm=0.17% approx., which are relatively lower value despite that high strength steel is aimed at.

For these steels, the optimum condition of controlled rolling-direct quenching (CR-DQ) as described in the preceding Chapter was applied in the rolling mill. To get enough toughness of the base metal, the reheating temperature was kept as low as possible or in the range from 950 to 1000℃, so that even at such low temperature range, solute Nb can be maintained. The finish-rolling temperature was set in the range of austenitic single phase region with temperature higher than $Ar_3$ point.

Immediately after rolling, water cooling was conducted by OLAC II equipment. The cooling rate at that time was 28℃/s for the 30mm steel and 5℃/s for the 75mm steel, and the cooling stop temperature was lower than 200℃.

Table 2 Requirements for YS460MPa grade steel

| | | |
|---|---|---|
| Thickness, mm | | ~75 |
| Mechanical properties | YS, MPa | ≥460 |
| | TS, MPa | 570≤TS≤720 |
| | $vE_{-40}$, J | 40[Ave.] 27[min.] |
| | $vE_{-60}$, J | 34[Ave.] |
| Weldability | $\delta x_{10}$, mm | ≥0.20 |
| | preheating temp., ℃ | ≤25 |
| Chemical composition | | Pcm≤0.20 |

Table 3 Chemical composition (basic oxygen furnace), wt%

| Steel | C | Si | Mn | P | S | Cu | Ni | Nb | Ti | Sol. Al | T.N | C IIW eq | Pcm | Thick-ness |
|---|---|---|---|---|---|---|---|---|---|---|---|---|---|---|
| F | 0.036 | 0.25 | 1.28 | 0.007 | 0.004 | 1.09 | 0.57 | 0.012 | 0.011 | 0.030 | 0.0035 | 0.360 | 0.172 | 30 |
| G | 0.030 | 0.24 | 1.48 | 0.004 | 0.004 | 1.05 | 0.59 | 0.010 | 0.009 | 0.020 | 0.0024 | 0.386 | 0.174 | 75 |

BASE METAL PROPERTIES - The mechanical properties of the base metal after aging at temperature in the range from 550 to 650℃ are shown in Fig. 11, where the properties of the steel in the thickness direction classified by position (1/4t, 1/2t) are shown. First, a review of the properties of 30mm steel shows that strength of TS700MPa is obtained from aging at 550℃ and TS600MPa from 650℃.

In other words, varieties of strength levels in the range from 600 to 700MPa can be obtained by adjusting the aging temperatue. The yiled stress in this case is invariably higher than 550MPa. In the case the subject steel is YS460MPa, it is possible to get the required strength from the aging condition of 650℃. Examination of toughness (vTrs) shows the value of about -80℃ is obtained by aging at 550℃, and toughness improves with an increase in aging temperature. With the aging temperature of 650℃, the value of vTrs is about -120℃. The absolute values in all cases of conditions show excellent properties, which little vary with plate thickness positon.

On the other hand, the 75mm steel shows that the strength level is generally lower than the 30mm steel, because the cooling rate is reduced from 28℃/s to 5℃/s. However, its strength little varies with position in the thickness direction, and the required properties can be derived from the aging temperature in the range from 550 to 600℃. In this case, since the toughness (vTrs) of less than -80℃ is obtained at the center of plate thickness, the steel plate has sufficient Charpy impact toughness as the base metal property.

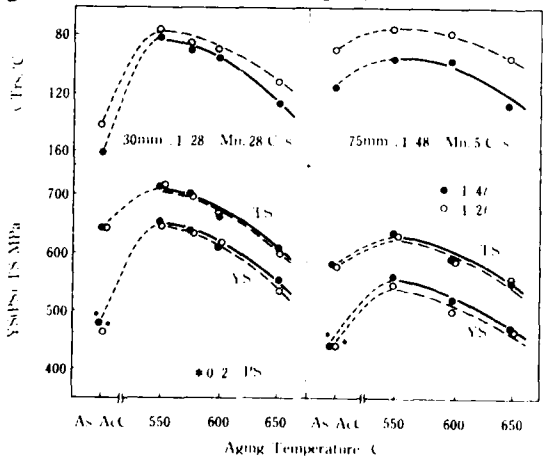


Fig. 11 Relationship between aging temperature and mechanical properties

To examine the toughness against brittle crack initiation, the base metal was also subjected to a CTOD test using a full-size (B×2B) test piece. Transition curves obtained from the test result are shown in Fig. 12. As is evident from the curves, both the 30mm steel and 75mm steel showed the critical CTOD value of larger than 1mm at -10℃. Even at a lower temperature, e.g. at -40℃, the value ($\delta$ x) was 0.4mm or more, showing excellent toughness against brittle crack initiation.

Results of NRL drop weight test are shown in Table 4. The tested material was a 30mm steel, and the test was conducted with one side of the plate reduced to a thickness of 25mm. As the direction of crack propagation, both the rolling direction (Direction L) and the direction perpendicular to the rolling direction (Direction T) were subjected to the test. The NDT temperature was -70 and -85℃ respectively. This level may be satisfactory as the steels with approximate strength of TS600MPa. This is the result of reflection of the controlled rolling effect and the microstructure improving effect achieved by application of accelerated cooling.

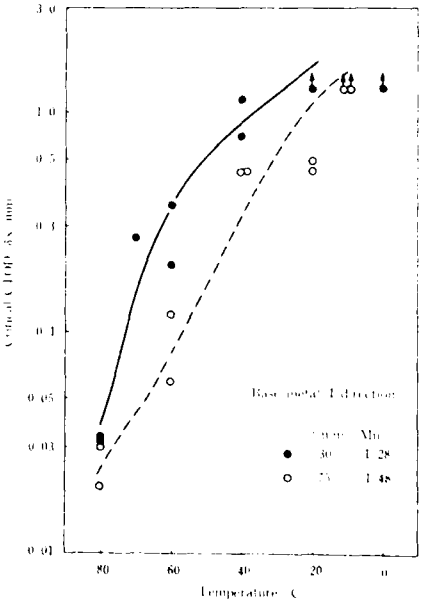


Fig. 12 CTOD test results of base metal

Table 4 Results of NRL drop weight test (30mm': 1.28%Mn)

| Direction | | -90°C | -85°C | -80°C | -70°C | -65°C | -60°C | NDTT, °C |
|---|---|---|---|---|---|---|---|---|
| 30 mm | L | | | ●● | ●● | ○○ | ○○ | -70 |
| | T | ●● | ●●○ | ○○ | | | | -85 |

WELDED JOINT PROPERTIES AND WELDABILITY - As the properties of welded joint, tensile strength, hardness distribution and the toughness (Charpy impact property, CTOD property) at each position of welded joint were measured. The welded joint was fabricated by the welding process, SAW with heat input of 45 to 50kJ/cm. Maximum hardness in weld heat-affected zone and Tekken Type Y-slit cracking test were also conducted to examin the weldability and low-temperature crack susceptibility.

The results of tensile tests conducted on the welded joint of the 30mm steel is shown in Table 5. It has sufficient welded joint strength, showing the tensile strength of about 610MPa. Also, since the ruptured position is located in the base metal, there occurs little softening in HAZ of welded joint. Figure 13 shows a hardness distribution at each position of welded joint. Due to the low-carbon composition, no detrimental hardening in the HAZ region was observed.

Table 5 Tensile test results of welded joint

| | TS, MPa | | Break point |
|---|---|---|---|
| As weld | 614.5 | 613.0 | Base metal |
| | 611.5 | | " |
| PWHT (600°C × 1 hr) | 603.7 | 606.8 | " |
| | 609.8 | | " |

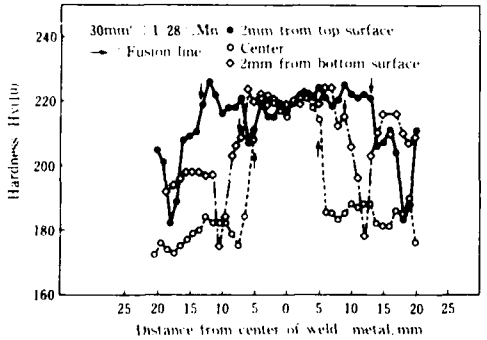


Fig. 13 Hardness distribution of weldment

The result of Charpy test conducted on welded joint is shown in Fig. 14 in terms of absorption evergy vE at -40°C. The test pieces were sampled from the position of 1/4t region of the final side. In the 30mm steel, in the region near the HAZ 1mm from the fusion line, a lower toughness value than those at other positions was observed. However, since absorption energy higher than 60J was obtained at even the lowest position, a satisfactry property is secured compared with the requirement in Table 2.

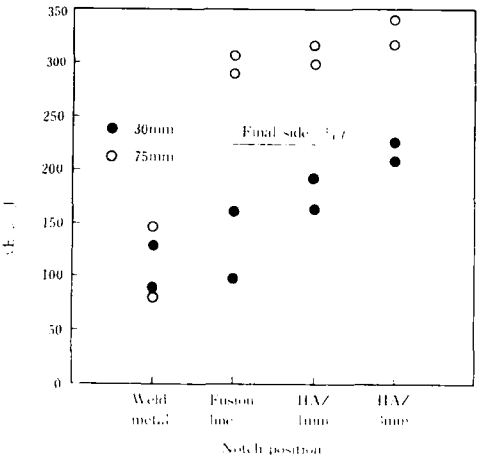


Fig. 14 Toughness of welded joint

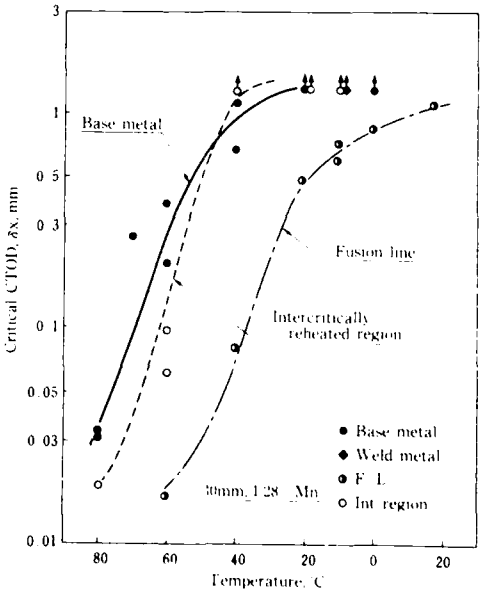


Fig. 15 CTOD test results of welded joint (30mm')

The results of CTOD tests conducted on welded joints are shown in Fig. 15 with respect to the 30mm. The test was conducted by introducing notches into the fusion line region and the HAZ boundary region corresponding to the intercritically reheatd region. As shown in Fig. 15, the test result for the HAZ boundary region shows the property almost equal to the base metal property provided as a reference in the figure, i.e. the test result shows a satisfactory value of $\delta x > 1.0$mm at -10℃. On the other hand, the transition curve for the fusion line region is located lower than that for base metal. However, it can be seen that the property is well exceeding the requirement even in the most brittle region, since the critical CTOD value at -10℃ is higher than 0.6mm. In the case of CTOD test results on welded joint of 75mm thickness plate, the fusion line region consisting of coarse grains also showed the lowest value, but a statisfactory property of $\delta x > 0.4$mm was obtained.

Maximum hardness test were conducted according to JIS-Z3101 (Testing Method of Maximum Hardness of in Weld Heat-affected Zone). NB2N was used as an electrode. The maximum hardness in that case showed Hv(10)=258. When the strength level of the base metal is taken into consideration, it may be a sufficiently low value.

To examine the low-temperature crack susceptibility as weldability, an oblique Y-slit cracking test was also conducted. The test reslts for the 30mm steel plate showed that no cracking occurred in the tested preheating temperature range from 75℃ down to 25℃. This results indicate the possibility of dispensation with preheating in the welding.

From the test result described above, it may be said that the developed steels have high toughness in HAZs including the CTOD property and excellent weldability where can be dispensed with preheating. This may be attributed to the low carbon composition in which carbon content is reduced as low as possible by effectively utilizing the age precipitaion of Cu.

## CONCLUSION

To develop YS460MPa grade steel plate for offshore structures, the effect of thermo-mechanical process on the mechanical properties of Cu bearing age-hardenable steels was exmained. After widely ranged research on the effect of its composition and processes on the properties, following results were obtained in this study.

(1) Application of accelerated cooling after contrleed rolling, and aging treatment to high Cu steel can achieve remarkable improvement of strength and toughness. Cu had effects on both age precipitaion hardening and microstructural improvement through controlled rolling and accelerated cooling.

(2) The basic composition of developed steels is 0.04%C-1.3/1.5%Mn-1.1%Cu-0.6%Ni-0.01%Nb-0.01%Ti system, and it is possible to obtained the required strength by appropriate aging treatment despite the low-carbon equvalent composition.

(3) Base metal toughness showed excellent values as a result of application of TMCP, i.e. Charpy $vTrs < -80$℃ was obtained even at the mid-thickness of plate, and the critical CTOD value showed $\delta x_{-10℃} > 1$mm.

(4) The properties of welded joint at the heat input of 5.0kJ/mm showed sufficient tensile strength and satisfactory values of $vE_{-40℃} > 60$J and $\delta x_{-10℃} > 0.4$mm even in the coarse grain region of HAZ.

(5) The result of low-temperature crack susceptibility test has proved that the developed steels can be dispensed with preheating.

## REFERENCES


1) Tsukada, K et al., Pro. 23rd Mech. Working & Steel Processing Conf., p.347 (1982).
2) Kozasu, I., Accelerated Cooling of Steel, TMS-AIME, p.15 (1985).
3) "Symposium of the Application of TMCP Steel to Welded Structures", Japan Society of Shipbuilding Engineering, (1983).
4) "Review on Properties of Thermo-mechanically Controlled Processed Steels", Iron and Steel Institute of Japan, (1986).
5) Harasawa, H et al., Int. Conf. on "Welding for Challenging Environments", Tront, Welding Institute of Canada, (1985).
6) Jesseman, R. J et al., HSLA Steels Technology and Applicaions, ASM, p.655-666 (1983).
7) Tsukada, K et al., Nippon Kokan Technical Report Overseas, No.32, p.1 (1981).

# PROPERTIES OF COLUMBIUM-MANGANESE HIGH STRENGTH STEELS WITH AN EXTRA-LOW CARBON

**Baltasar Hernández-Reyes, Cuauhtémoc Maldonado-Zepeda**
Instituto de Investigaciones Metalúrgicas Morelia
Michoacán. México

ABSTRACT

The principal objective of this research is to study two specific columbium-bearing steels with increasing manganese contents and to determine the effect of manganese using two types of cooling rates: air-cooling and water-quenching. Moreover, the influence of reheating temperature on the mechanical properties of these particular steels was analysed too. The studied steels have the following chemical composition Steels I(low-carbon): 0.12% C, 0.053% Cb, 0.23% Si, 1.10-4.71% Mn. Steels II (extra-low carbon): 0.037% C, 0.041% Cb, 0.15% Si, 0.96%-4.15% Mn. According to results Steels I show an increase in tensile properties when manganese addition is between 1.1% to 3% Mn but from 3% to 4.71% Mn, this element does not produce remarkable effect on the tensile properties of such steels. Microstructure of Steels I change with manganese content and cooling rate from ferrite-pearlite to bainite and martensite. Steels II show and increase of tensile properties as manganese content increases from 0.96% to 4.25% Mn. Microstructures change depending upon manganese content and the cooling rate, from polygonal ferrite to acicular ferrite and bainite.

## INTRODUCTION

STEELS WITH EXTRA-LOW CARBON contents have better toughness, weldability and formability than plain steels; there is a world tendency to decrease carbon content in order to improve all these properties. However, an extra-low carbon content produces a low-strength steel, unless it would be microalloyed with columbium, vanadium, titanium or alloyed with a large amount of elements such as manganese. These elements could strengthen steel by grain refining, precipitation hardening or by solid solution. Moreover, there are process techniques like controlled rolling or quenching and tempering which properly applied could be used in producing steels with improved properties. So that, for low-carbon contents, columbium microalloying, increasing manganese contents and cooling after rolling, may affect deeply the mechanical behaviour of steels. A properly combination of all these factors allow to obtain steels with a wide range of properties.

## METALLURGICAL FACTORS

EFFECT OF CARBON - Carbon is one of the most potent and cheapest strengthening elements. Carbon has a beneficial influence on yield and tensile strength but steels with high carbon amounts exhibit poor toughness and weldability. Compared to higher carbon steels, the lower carbon steels have a lower transition temperature and higher absorbed energy in an impact test for a given strength. Therefore, the carbon content should be kept low. Carbon is also the main contributing factor in all carbon-equivalent formulas. For alloy systems that produce acicular structures, carbon has a deleterious influence and must be further reduced to at least 0.10% maximum, and to 0.06% for the higher alloy systems. In small amounts, the principal role of carbon is to favor precipitation. Consequently, carbon could be specified between 0.01 and 0.02% required by columbium-carbide precipitation. Generally, any increase above this level is detrimental, but it is not practical to specify carbon contents lower than 0.06% for steelmaking. The decrease in toughness occurs because the high-carbon regions act as void-nucleation sites during impact loading[1]. Although higher carbon contents aid in depressing the ferrite-pearlite transformation and therefore contribute to the formation of acicular ferrite. The loss of toughness is easily compensated by increasing other alloy constituents having no effect on the loss of toughness. Grain refining and precipitation hardening have a helpful influence on the strength of steels; therefore, the levels of carbon and alloying elements can be decreased

in steels. Modern microalloyed steels use carbon contents lower than 0.10%.

EFFECT OF MANGANESE - This element is normally present in all commercial steels because it comes from used raw materials and is purposely added to combat the detrimental effect of sulfur and oxygen which are always present in steelmaking processes. Manganese is important in steelmaking because it deoxidizes the melt and facilitates the hot working of steel by reducing the susceptibility to hot shortness[2]. Manganese combines with sulfur to form manganese sulfide stringers, which improve the machinability of steels; otherwise, steels could not be hot worked because with no manganese in the melt, sulfur would react forming the sharply embrittling iron sulfide[3].

Manganese is a solid-solution strengthener and a good hardener that increases strength and does not impart brittleness to the steel. Thus this later retains its ductility. Also, manganese is a promoter of toughness. Most steels contain from 0.30 to 0.90% Mn. From 0.90 to 1.60% manganese is used to strengthen and harden steels while retaining their toughness. Manganese tends to form carbides but its tendency is weaker than in the case of elements such as chromium or titanium but stronger than iron. With low-carbon contents manganese dissolves itself in ferrite, strengthening it. Increasing manganese content decreases the carbon content of the eutectoid point and stabilizes austenite depressing the austenite-to-ferrite transformation temperature[3].

The lower the austenite-to-ferrite temperature the wider the potential temperature of controlled rolling. In mild steels in which the transformation temperature is higher than the recrystallization temperature of ferrite, normal controlled rolling often results in rolling after the austenite-to-ferrite transformation, which may produce coarse recrystallized ferrite grains[4]. The detrimental effect of carbon on ductility avoids its use for transformation-temperature control, as a result high manganese contents are desirable for controlled-rolled steels. Manganese delays the transformation temperature contributing to refine ferritic grain. Low-carbon and high-manganese steels tend to form acicular ferrite with high cooling rates[4].

If the temperature at which bainite starts to form could be depressed while maintaining a low-carbon weldable composition, steels of even higher strength could be developed forming fine-grained acicular ferrite. This temperature of transformation can be depressed by alloying elements such as manganese which is an attractive choice[5]. Too much manganese, however, would depress the transformation so much that bainite would be formed impairing yield strength and toughness. Manganese is usually limited to about 1.5 to 1.7%, but higher manganese can be tolerated by decreasing carbon content and cooling rate[5]. Manganese decreases the temperature at which martensite is formed during quenching; thus, it increases the likelihood of retained austenite in quenched steels.

Toughness could be improved by a reduction in carbon. However, low-carbon contents could cause the formation of embrittling-carbide filaments on the ferrite boundaries if they are accompanied by low manganese contents or slow-cooling rates from austenita. In order to avoid the growing of reducing-toughness elements, larger amounts of manganese or faster cooling rates must be used[6].

EFFECT OF COLUMBIUM - Columbium affects the three critical temperatures of austenite: the grain coarsening temperature, the recristallization temperature and the austenite-to-ferrite transformation temperature. An understanding of these factors allows the prediction of the response of austenite to thermomechanical processing[7].

When the reheating temperature of the ingot is kept below the grain coarsening temperature, the columbium carbonitride average size is very small and promotes grain refining of austenitic grain. The recrystallization temperature must be as high as possible to allow as much deformation as possible (the largest number of rolling passes) to occur below the recrystallization temperature; the induced precipitation of carbonitrides of columbium by strain prevents recrystallization of the heavily deformed austenitic grains during hot rolling[7]. Columbium is more efficient than titanium and vanadium to rise the recrystallization temperature; thus, columbium is generally used to increase the recrystallization temperature. Also, columbium strengthens steels by precipitation hardening. Although precipitation of columbium is important for proper conditioning of austenite during thermomechanical processing, enough columbium must be left in solution in the austenite to provide for precipitation hardening of ferrite. The amount of precipitates formed in the austenite should be the minimum required to produce this effect. The columbium contents must be enough so as it remains in solution to promote hardenability and hardening precipitation in steel thus helping grain refining[7].

## PROCESSING FACTORS

REHEATING TEMPERATURE - The ingot reheating temperature determine the initial austenitic grain size and the condition of microalloying elements. High reheating temperatures favor large starting austenitic grain sizes and dissolution of most microalloying elements. In general, high reheating temperatures are associated with higher strengths and poor resistance to brittle fracture. Low reheating temperatures produce the opposite results. Hence, thick sections should be rolled using lower reheating temperatures to produce optimum toughness. Thin strip, where high strength is an advantage, should be heated using higher reheating temperatures[7].

DIRECT QUENCHING - This process promotes important phase transformations of austenite,

leading to achieve structures such as acicular-ferrite, bainite or martensite, depending on the hardenability of steel and the cooling rate. Beneficial structures will be only obtained with a proper balance between hardenability which depends on chemical composition, and cooling rate which in turn depends on plate gage and the severity of the cooling medium.

## EXPERIMENTAL PROCEDURES

The produced steels have the following chemical composition: Steels I (low-carbon): 0.12%C, 0.053%Cb, 0.23%Si, 1.10-4.71%Mn. Steels II (extra-low carbon): 0.037%C, 0.041%Cb, 0.15% Si, 0.96-4.15%Mn. Both type of steels were molten in a 250-kg induction furnace. A scrap steel with 0.28% C was used, this scrap was decarburized adding oxygen to the bath. The melted steel was tapped at 1670°C and cast into 5-kg ingots, with the following dimensions: 37-mm thick, 50-mm wide and 250-mm high. Subsequently, the ingots were thermomechanically treated: each ingot was reheated at temperatures between 1050 and 1250°C and were rolled into plates in a 50-tons rolling mill, until getting a 57% reduction, using constant load and speed. The finish-rolling temperature was 850°C. After rolling the plates were air-cooled or water-quenched. Finally, specimens were taken from each plate for chemical and metallographic analyses, and also for mechanical testing. The temperature in the ingots during rolling was monitored with a thermocouple placed at the middle of the ingot thickness. Chemical compositions of studied laboratory steels are shown in Table I

Specimens were taken out from each ingot according to the ASTM A-370 specification Among the properties determined were: yield strength, tensile strength, elongation, Rockwell hardness and impact transition temperature which was determined for 20-Joules; all results are shown in Tables II and III.

## DISCUSSION OF EXPERIMENTAL RESULTS

COMBINED EFFECT OF MANGANESE AND QUENCHING - In general, increasing the manganese content improves strength but elongation decreases; the transition temperature increases with manganese content but this effect is related to the phase transformation induced by cooling.

In low-carbon steels I (Figure 1) for air-cooled steels, manganese produces an increase in yield strength of 147 MPa per 1% of manganese. In water-quenched steels, between 1.5% and 3% Mn, an increase of 372 MPa per 1% Mn is produced. Manganese contents from 3% to 4.71% does not increase the yield strength in water-quenched steels, because these steels reach a martensitic structure difficult to be hardened; thus, it is not very convenient to rise the manganese content above 3% in order to improve the yield strength. The elongation decreases as the manganese content becomes higher (Figure 2) in both; air-cooled and

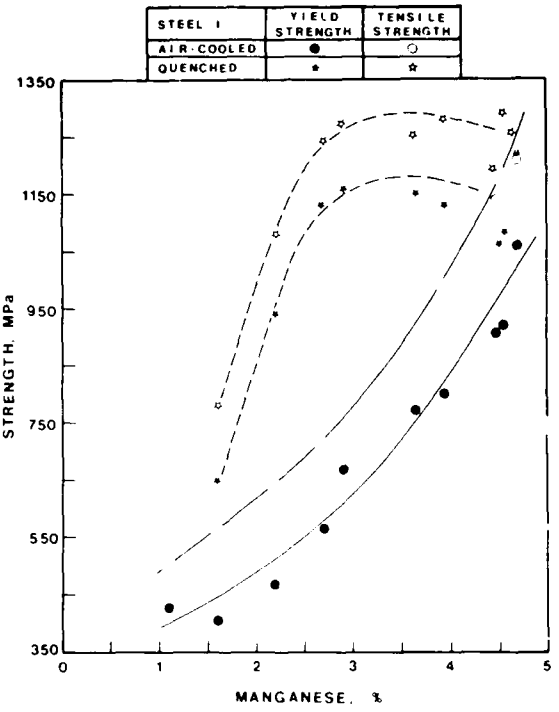


Figure 1. Influence of manganese on strength of low-carbon steels I. With 0.108% -0.132% C, 0.045% -0.066% Cb and manganese between 1.10% and 4.71% Mn

water-quenched steels The transition temperature of air-cooled steels depends upon the changes of microstructure (Figure 3). Initially, the matrix is ferrite-pearlite. As the manganese content increases, it appears acicular ferrite and bainite (Figure 4). Steels with a bainitic matrix have an increase in the transition temperature which decreases with the appearence of martensite. Water-quenched steels do not show a specific behaviour.

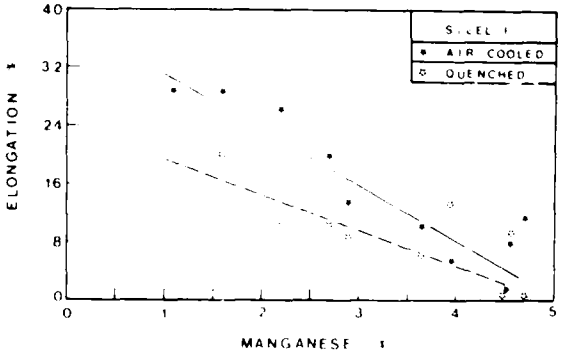


Figure 2 Influence of manganese on elongation of low-carbon steels I. With 0.11% -0.13% C, 0.045% -0.066% Cb and manganese between 1.10% and 4.71% Mn.

In extra-low carbon steels II, manganese increases the strength of air-cooled steels The

TABLE I. CHEMICAL COMPOSITION OF EXPERIMENTAL STEELS.

| STEEL | Carbon | Columbium | Manganese | Silicon | Aluminium | Phosphorus | Sulfur |
|---|---|---|---|---|---|---|---|
| I-A | 0.132 | 0.045 | 1.10 | 0.20 | 0.030 | 0.010 | 0.030 |
| I-B | 0.118 | 0.049 | 1.62 | 0.23 | 0.026 | 0.012 | 0.024 |
| I-C | 0.113 | 0.048 | 2.21 | 0.22 | 0.025 | 0.013 | 0.024 |
| I-D | 0.109 | 0.053 | 2.71 | 0.23 | 0.036 | 0.013 | 0.023 |
| I-E | 0.108 | 0.047 | 2.90 | 0.22 | 0.032 | 0.013 | 0.024 |
| I-F | 0.132 | 0.066 | 3.65 | 0.24 | 0.039 | 0.013 | 0.022 |
| I-G | 0.124 | 0.049 | 4.00 | 0.21 | 0.038 | 0.011 | 0.022 |
| I-H | 0.113 | 0.058 | 4.55 | 0.21 | 0.039 | 0.014 | 0.021 |
| I-1 | 0.129 | 0.058 | 4.52 | 0.21 | 0.039 | 0.014 | 0.020 |
| I-J | 0.122 | 0.060 | 4.71 | 0.20 | 0.039 | 0.014 | 0.015 |
| II-A | 0.037 | 0.037 | 0.96 | 0.15 | 0.014 | 0.011 | 0.026 |
| II-B | 0.038 | 0.038 | 1.55 | 0.14 | 0.021 | 0.010 | 0.024 |
| II-C | 0.038 | 0.042 | 2.27 | 0.15 | 0.023 | 0.011 | 0.022 |
| II-D | 0.038 | 0.043 | 2.81 | 0.15 | 0.023 | 0.011 | 0.022 |
| II-E | 0.035 | 0.053 | 3.40 | 0.15 | 0.029 | 0.012 | 0.021 |
| II-F | 0.037 | 0.061 | 3.89 | 0.16 | 0.034 | 0.012 | 0.020 |
| II-G | 0.034 | 0.058 | 4.15 | 0.17 | 0.028 | 0.013 | 0.018 |

TABLE II. MECHANICAL PROPERTIES OF LOW-CARBON STEELS I.

| STEEL | Reheating Temperature °C | Yield Strength MPa | Tensile Strength, MPa | Elongation % | Hardness | TT °C | Type of Cooling. |
|---|---|---|---|---|---|---|---|
| I-A1 | 1150 | 431 | 500 | 29 | 83HRB | -12 | A |
| I-A2 | 1250 | 451 | 510 | 32 | 81HRB | -25 | A |
| I-B1 | 1150 | 412 | 569 | 29 | 89HRB | -34 | A |
| I-B2 | 1150 | 657 | 784 | 20 | 26HRB | -25 | Q |
| I-B3 | 1250 | 431 | 578 | 30 | 88HRB | -34 | A |
| I-C1 | 1150 | 471 | 647 | 27 | 93HRB | -23 | A |
| I-C2 | 1150 | 941 | 1088 | 11 | 37HRC | -34 | Q |
| I-C3 | 1250 | 480 | 657 | 25 | 93HRB | -18 | A |
| I-D1 | 1150 | 578 | 716 | 20 | 20HRC | - 8 | A |
| I-D2 | 1150 | 1137 | 1245 | 11 | 41HRC | -24 | A |
| I-D3 | 1250 | 598 | 784 | 18 | 20HRC | - 8 | A |
| I-E1 | 1150 | 676 | 902 | 14 | 30HRC | 4 | A |
| I-E2 | 1150 | 1167 | 1274 | 9 | 40HRC | -59 | Q |
| I-E3 | 1250 | 578 | 784 | 11 | 38HRC | -- | A |
| I-F1 | 1150 | 774 | 951 | 11 | 30HRC | 11 | A |
| I-F2 | 1150 | 1157 | 1255 | 7 | 40HRC | -59 | Q |
| I-F3 | 1250 | 794 | 970 | 9 | 26HRC | -10 | A |
| I-G1 | 1150 | 804 | 990 | 6 | 35HRC | -25 | A |
| I-G2 | 1150 | 1137 | 1284 | 14 | 35HRC | 5 | Q |
| I-G3 | 1250 | 921 | 1067 | 9 | 42HRC | -- | A |
| I-H1 | 1150 | 921 | 1147 | 8 | 40HRC | -- | A |
| I-H2 | 1150 | 1088 | 1294 | 10 | 42HRC | -36 | Q |
| I-H3 | 1250 | 931 | 931 | 4 | 39HRC | -- | A |
| I-I1 | 1150 | 912 | 1186 | 2 | 40HRC | -- | A |
| I-I2 | 1150 | 1068 | 1068 | 1 | 42HRC | -- | Q |
| I-I3 | 1250 | 323 | 1039 | 1 | 39HRC | -- | A |
| I-J1 | 1150 | 1068 | 1216 | 12 | 40HRC | -- | A |
| I-J2 | 1150 | 1225 | 1225 | 1 | 43HRC | -- | Q |
| I-J3 | 1250 | 1157 | 1255 | 9 | 40HRC | -- | A |

A = Air - cooled steel. Q = Water - Quenched

TABLE III. MECHANICAL PROPERTIES OF EXTRA-LOW CARBON STEELS II.

| STEEL | Reheating Temperature °C | Yield Strength, MPa | Tensile Strength, MPa | Elongation % | Hardness | ITT °C | Type of Cooling |
|---|---|---|---|---|---|---|---|
| II-A1 | 1050 | 343 | 412 | 42 | 71HRB | -53 | A |
| II-A2 | 1050 | 421 | 510 | 28 | 89HRB | -76 | Q |
| II-A3 | 1100 | 363 | 431 | 39 | 73HRB | -53 | A |
| II-A4 | 1100 | 421 | 510 | 35 | 86HRB | -65 | Q |
| II-B1 | 1100 | 402 | 470 | 39 | 80HRB | -63 | A |
| II-B2 | 1100 | 451 | 588 | 28 | 90HRB | -77 | Q |
| II-B3 | 1175 | 402 | 490 | 35 | 80HRB | -53 | A |
| II-B4 | 1250 | 392 | 500 | 35 | 81HRB | -46 | A |
| II-C1 | 1100 | 421 | 559 | 27 | 88HRB | -17 | A |
| II-C2 | 1100 | 676 | 774 | 18 | 23HRB | -53 | Q |
| II-C3 | 1175 | 441 | 588 | 27 | 88HRB | -21 | A |
| II-C4 | 1250 | 441 | 559 | 25 | 86HRB | -- | A |
| II-D1 | 1100 | 500 | 657 | 26 | 93HRB | -28 | A |
| II-D2 | 1100 | 784 | 892 | 16 | 31HRC | -53 | Q |
| II-D3 | 1175 | 510 | 627 | 24 | 92HRB | - 8 | A |
| II-D4 | 1250 | 500 | 627 | 25 | 91HRB | - 4 | A |
| II-E1 | 1100 | 598 | 716 | 20 | 96HRB | -23 | A |
| II-E2 | 1100 | 892 | 980 | 14 | 36HRC | -30 | Q |
| II-E3 | 1175 | 578 | 706 | 23 | 97HRB | - 7 | A |
| II-E4 | 1175 | 882 | 990 | 14 | 32HRC | -42 | Q |
| II-E5 | 1250 | 588 | 725 | 18 | 96HRB | - 2 | A |
| II-F1 | 1100 | 637 | 765 | 18 | 21HRC | -20 | A |
| II-F2 | 1100 | 912 | 1000 | 10 | 33HRC | -12 | Q |
| II-F3 | 1175 | 618 | 765 | 17 | 21HRC | -13 | A |
| II-F4 | 1175 | 912 | 1010 | 11 | 34HRC | -- | Q |
| II-F5 | 1250 | 647 | 774 | 15 | 21HRC | -12 | A |
| II-G1 | 1100 | 706 | 843 | 12 | 25HRC | -- | A |
| II-G2 | 1100 | 961 | 1039 | 9 | 36HRC | 1 | Q |
| II-G3 | 1175 | 716 | 823 | 10 | 22HRC | -- | A |
| II-G4 | 1250 | 686 | 823 | 15 | 22HRC | 44 | A |

A = Air - cooled steel. Q = Water - quenched.

increase in yield strength is 108 MPa per 1% Mn; and the efficiency in water-quenched steels is 167 MPa per 1% Mn but elongation decreases (Figures 5-6). The transition temperature rises in both air-cooled, and water-quenched steels with the increase of manganese. Initially, steels have a ferritic structure (Figure 7) when the manganese content is low, but as manganese content increases structure becomes more acicular (Figure 8) being acicular ferrite with small amounts of manganese and bainitic when manganese content is increased or quenching is applied.

EFFECT OF QUENCHING - Quenching allows to get higher strength properties but it lowers ductility of steel. In general, water-quenched steels have lower transition temperature than air-cooled steels. Quenching involves faster cooling rates, which could promote finer and acicular structures. In steels II (Figure 7) the transition temperature of water-quenched steels is lower than air-cooled steels. In steel II, it is possible to reach transition temperatures as low as -77°C if quenching is applied, (Table III). The better transition temperature are obtained with manganese contents not higher than 2% in water-quenched steels.

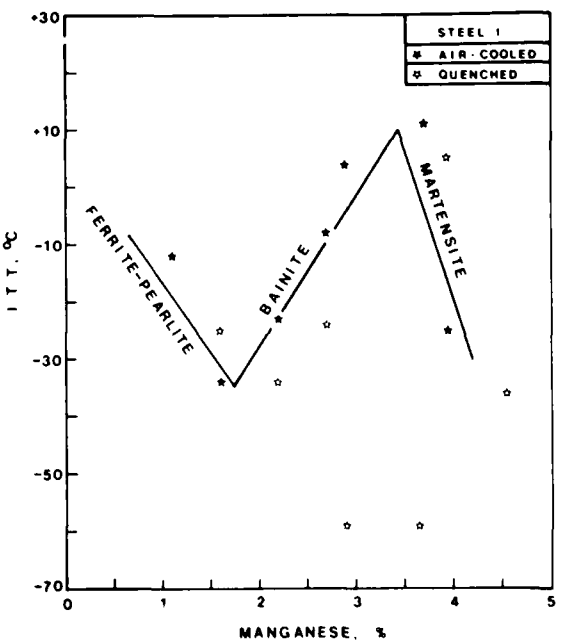


Figure 3. Influence of manganese on transition temperature of low-carbon steels I. With 0.11%-0.13% C, 0.045%-0.066% Cb and manganese between 1.10% and 4.71% Mn.

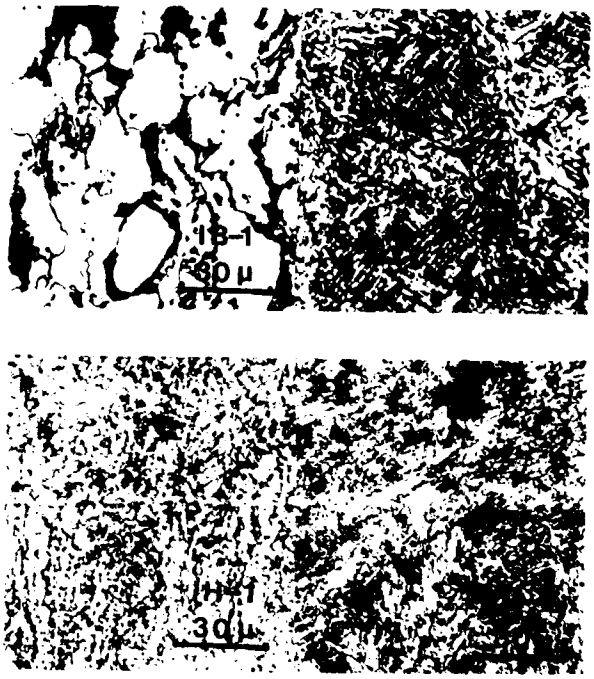


Figure 4. Microstructures of low-carbon steels I. I-B1 (air cooled with a ferrite-pearlite matrix) and I-B2 (quenched with a bainitic matrix) with 0.13% C, 0.049% Cb and 1.62% Mn. I-H1 (air-cooled with a bainitic matrix) and I-H2 (quenched with martensitic matrix) with 0.113% C, 0.058% Cb and 4.55% Mn.

EFFECT OF REHEATING TEMPERATURE - increasing the reheating temperature of the ingot, increases slightly the yield and tensile strength; although, the transition temperature decreases. Steels with the same composition, for instance, steel I-B1 with a reheating temperature of 1150°C, reaches a yield strength value of 412 MPa and I-B2, 431 MPa as shown in Table II; the transition temperature decreases showing small effect. Steels II have the same tendency. This effect is related to the more complete dissolution of carbonitrides at higher temperatures which enhances the hardening precipitation influence of columbium. In order to maintain lower transition temperatures where necessary, it is advisable to reheat the ingot at low temperatures.

## SUMMARY

1. Low-Carbon Steels I. Manganese contents in the range of 1.10 and 3% and for both, air-colled and water-quenched steels, increase yield and tensile strength and its influence on transition temperature depends on the phase transformation induced by quenching and the manganese level. For values of manganese between 3% and 4.71% in water-quenched steels manganese does not produce any increase in strength properties as its content is increased. On this range, martensitic

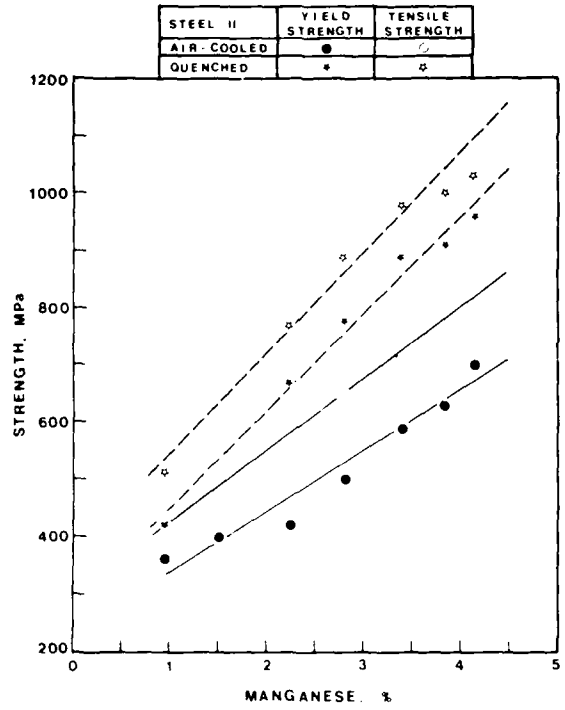


Figure 5 Influence of manganese on strength of extra-low carbon steels II. With 0.03%-0.05% C, 0.037-0.061 Cb and manganese between 0.96% and 4.15 Mn.

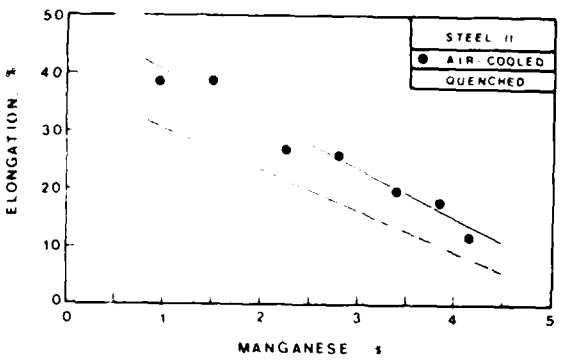


Figure 6. Influence of manganese on elongation of extra-low carbon steels II With 0.03%-0.04% C, 0.037-0.061% Cb and manganese between 0.96% and 4.15% Mn

structure are developed. For air-cooled steels, manganese increase the strength properties as its content is increased.

2. Extra-low carbon, Steels II. For manganese content between 0.96% and 4.15%, the yield and tensile strength increase as the manganese content is gradually rised. This tendency is observed in both, air-cooled and water-quenched steels. For low manganese contents a low transition temperature is reached, but increases with the manganese content; manganese and

quenching promote bainitic structures in steels as the manganese content increases from 0.96% to 4.25%.

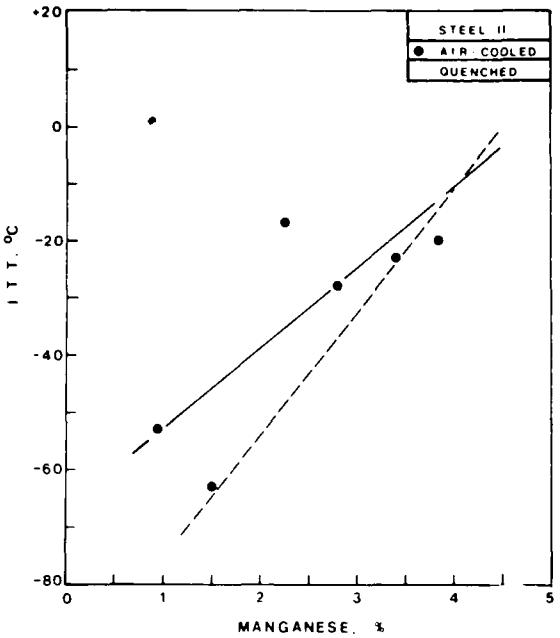


Figure 7 Influence on transition temperature of extra-low carbon steels II. With 0.03 -0.04 C, 0.037 -0.061 Cb and manganese between 0.96 and 4.15 Mn.

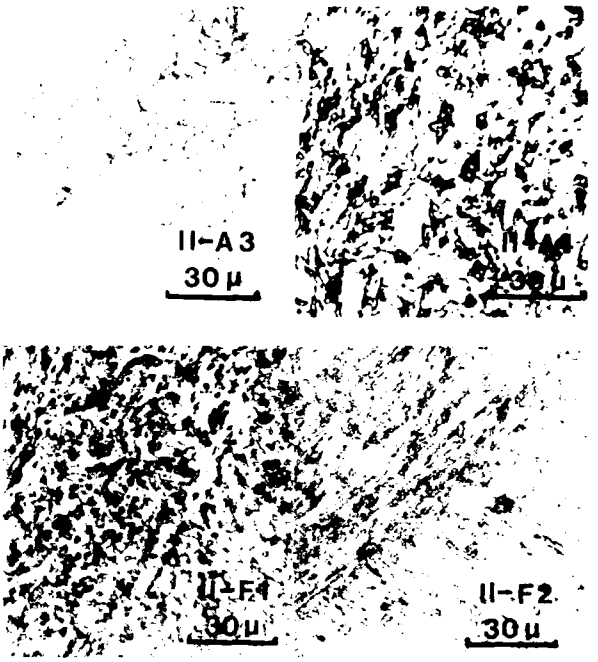


Figure 8. Microstructures of extra-low carbon steels II. II-A3 (air-cooled with polygonal ferritic matrix) and II-A4 (quenched with acicular-ferrite matrix) with 0.04 C, 0.037 Cb and 0.96 Mn. II-F1 (air-cooled with a ferrite-bainite matrix) and II-F2 (quenched with bainite matrix) with 0.037 C, 0.061 Cb and 3.89 Mn.


## ACKNOWLEDGMENTS

The authors wish to thank CONACYT (Consejo Nacional de Ciencia y Tecnología), SEP (Secretaría de Educación Pública), and UNIVERSIDAD MICHOACANA (MEXICO) for the financial support provided.


## REFERENCES


1. E.C. Hamre and A.M. Gilroy-Scott, "Acicular-Ferrite Steel for Large-Diameter Line Pipe" P. 375 in Microalloying '75 Proceedings, Union Carbide Corp., New York, New York. 1975.
2. Anthony T. Peters, "Ferrous Production Metallurgy", P. 78, Wiley-Interscience, U.S.A. 1982.
3. J.A. Barreiro, "Aceros Especiales", P. 61-89, Editorial Dossat, Madrid, España, 1982.
4. I. Kozasu, C. Ouchi, T. Sampel and T. Okita, "Hot Rolling as a High-Temperature Thermo-mechanical Process", P. 130, in Microalloying '75 Proceedings, Union Carbide Corp., New York, New York. 1975.
5. F.B. Pickering, "High-Strength, Low-Alloy Steels-A Decade of Progress", P. 20, in Microalloying '75 Proceedings, Union Carbide Corp., New York, New York. 1975.
6. Terry Gladman, "Structure-Property Relationships in High-Strength Microalloyed Steels", P. 42, in Microalloying '75 Proceedings, Union Carbide Corp., New York, New York. 1975.
7. A.J. DeArdo, "Thermomechanical Processing", P. 71-73, Advanced Materials & Progress, Vol. 133, Issue 1, January 1988.
8. T. Tanaka, N. Tabata and T. Hatomura, "Three Stages of the Controlled-Rolling Process", P. 110 in Microalloying '75 Proceedings, Union Carbide Corp., New York, New York. 1975.

# HIGH-STRENGTH TITANIUM-OXIDE BEARING LINE PIPE STEEL FOR LOW-TEMPERATURE SERVICE

**Kiyoshi Nishioka, Hiroshi Tamehiro**
Kimitsu R&D Laboratory
Nippon Steel Corporation
Kimitsu, Chiba, Japan

## ABSTRACT

A study was made on the improvement in toughness of high-strength, heavy-gauge line pipe steel for low-temperature service. It is difficult to obtain high-toughness in the weld heat-affected zone, particularly when strength is increased or large heat input welding is applied. Titanium-oxide steel has been developed for obtaining high HAZ toughness even for such cases, based on the finding that titanium-oxide particles, dispersed finely in the base material, can work as nuclei of fine acicular ferrite (intergranular ferrite plate), so that coarse grains near the fusion line of the HAZ can be effectively refined. In the present research, the effect of microalloying of Nb, Mo or B on the microstructure and toughness of the HAZ of titanium-oxide steel has been studied. It has been found that increasing alloying elements suppresses the growth of ferrite or ferrite sideplate from coarse $\gamma$ grain boundaries, increases area fraction of IFP, and as a result improves HAZ toughness. The line pipe steel manufactured based on the results of the present fundamental research has shown excellent toughness in the HAZ of large heat-input welding.

## INTRODUCTION

As offshore energy resources such as oil and natural gas are being exploited, the quality required for line pipe steel has become sophisticated. Since those energy resources are being extracted in deeper waters and colder districts, it is expected that higher strength line pipe of greater wall thickness with superior low-temperature toughness will be more and more required. As far as the base materials of line pipe are concerned, it is relatively easy to obtain the required strength and low-temperature toughness by applying the recently-developed thermomechanical process (accelerated cooling after controlled rolling)[1]. However, as for the weld of line pipe, particularly the heat-affected zone (HAZ), it is far from easy to attain the required level of low-temperature toughness. Metallurgical factors which govern the HAZ toughness include coarse grains near the fusion line (FL), hard phase (low-temperature transformation product, such as martensite-austenite constituent or high carbon martensite island, M*), intergranular embrittlement, hot strain embrittlement (HSE) and nonmetallic inclusios. Among these factors, the first two are particularly important. Many studies have been carried out on the refinement of HAZ microstructure. A typical example is the development of titanium-nitride (TiN) steel[2),3)]. TiN steel utilizes fine titanium-nitride particles dispersed in a steel for suppressing the coarsening of austenite ($\gamma$) grains in the HAZ, thereby enabling the HAZ microstructure to be refined. In the region reheated higher than 1400°C near the fusion line, however, TiN particles coarsen or dissolve and lose their effect, resulting in the formation of a local brittle zone (LBZ)[4)], which has been thought inevitable in any steel.

Titanium-oxide (TiO) steel is a newly-developed steel having excellent toughness in the entire HAZ. This new steel features fine HAZ microstructure made possible by dispersion of fine titanium-oxide particles, which are stable even at temperatures above 1400°C, and by formation of intragranular ferrite plate (IFP) nucleated from those particles. The technique of refining the microstructure by utilizing titanium-oxides as the nuclei of IFP has been established as a method of improving the toughness of weld metal[5)]. TiO steel is an innovative steel which applies this technique to the improvement in HAZ toughness by dispersing fine titanium-oxides in the steel making to continuous casting process. The present paper briefly introduces the toughness-improving mechanism of TiO steel, and then describes the effects of Nb, Mo and B on the properties of TiO steel. Also, the properties of Nb-microalloyed TiO steel (X80) are introduced together with the

examples of the practical application of TiO steel to heavy-gauge UOE pipe.

## TITANIUM-OXIDE (TiO) STEEL[6)-9)]

Since the HAZ is reheated to the high-temperature γ region during welding, γ grains coarsen markedly. Coarse γ grains tend to produce a coarse ferrite sideplate (FSP) and upper bainitic microstructure (Bu), causing the HAZ toughness to deteriorate significantly. Thus, in order to improve HAZ toughness, it is of prime importance to refine the HAZ microstructure. From the metallurgical viewpoint, there are two methods of refining the effective grain size of the HAZ microstructure. One is to prevent the coarsening of γ grains by fine precipitates. The other is to cause an intragranular transformation in coarse γ grains using fine precipitates as the nuclei, thereby making the ultimate microstructure fine. A typical example of practical application of the first method is TiN steel. As already mentioned, however, TiN steel cannot be a truly effective method of preventing the coarsening of γ grains near the fusion line, since TiN particles coarsen or dissolve in the HAZ reheated at high temperature above 1400°C. TiO steel is a new steel providing high HAZ toughness through the effect of both methods, particularly of the second one. TiO steel refines the microstructure transformed from coarse γ grains near FL by utilizing IFP nucleated radially from fine Ti-oxide particles dispersed in the steel, and at the same time, suppresses the coarsening of γ grains by the effect of fine TiN precipitates, as does TiN steel, at the temperature range below 1400°C. The concept of refining HAZ microstructure and basic characteristics of TiO steel are described below.

In order to utilize IFP in the HAZ, it is an essential prerequisite to disperse fine Ti-oxide particles in the steel so that IFP is nucleated from them. In the process of manufacturing TiO steel, it is therefore important to control the contents of Ti, N and O in proper balance and to minimize the Al content which impedes the formation of Ti-oxides (normally 30ppm or less). Figure 1 shows an example of IFP initiated from Ti-oxide particles in such low Al steel[8)]. This microstructure was obtained by quenching a specimen from 600°C during the cooling of a simulated HAZ test (peak temperature: 1400°C, cooling time from 800°C to 500°C: 192sec). The IFP nucleates and grows radially from the Ti-oxide particles dispersing inside a γ grain. The Ti-oxide was identified as $Ti_2O_3$ by electron diffraction. In most cases the Ti-oxide particles coexists with MnS, $Al_2O_3$ and (Mn, Si) O and are observed in the form of compound precipitates.

Figure 2 shows the effect of peak temperature on Charpy V-notch transition temperature (vTrs) of a simulated HAZ corresponding to large heat input welding[8)]. In the TiN steel, the vTrs remarkably rises as peak temperature rises because TiN begins to dissolve at a temperature higher than 1400°C. In contrast to this, the vTrs of the TiO steel changes little with peak temperature, indicating that the Ti-oxide is chemically stable even at a peak temperature of 1450°C and effectively serves as the nucleus of IFP.

Another feature of TiO steel is the formation of IFP over a wide range of cooling rates. For example, a study of the transformation characteristic of a TiO steel (0.08%C-1.6%Mn-0.013%Nb-0.014%Ti) showed that an IFP was formed over an extremely wide range of cooling rates, from 0.3°C sec to 50°C/sec[9)], suggesting wide applicability of TiO steel to various (from small to large) heat input welding.

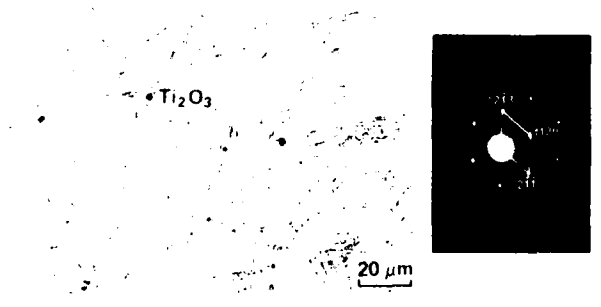


Fig. 1 IFP initiated from Ti-oxide particles in specimen quenched from 600°C during cooling of simulated thermal cycle test[8)]

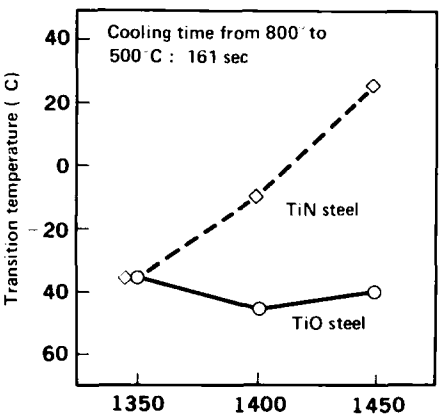


Chemical composition (wt%)

| Steel | C | Si | Mn | P | S | Al | Ti | N |
|---|---|---|---|---|---|---|---|---|
| TiO | 0.08 | 0.20 | 1.4 | 0.01 | 0.001 | 0.002 | 0.012 | 0.0020 |
| TiN | 0.08 | 0.20 | 1.4 | 0.01 | 0.001 | 0.020 | 0.018 | 0.0050 |

Fig. 2 Chang in Charpy-V notch transition temperature of simulated HAZ with peak temperature[8)]

## MICROALLOYING OF Nb, Mo AND B

### Experimental Procedure

The steels with various Nb, Mo and B contents shown in Table 1 were vacuum-melted in 300 kg heats and cast into 175mm thick ingots. All steels were TiO steel with low Al content. The ingots were controlled-rolled to 38mm thick plates after reheating at 1100°C for 1 hr, and accelerated cooled at a rate of 15°C/s to approximately 450°C and then air cooled. The rolling conditions were as follows: cumulative reduction below 900°C, 70%; finish rolling temperature, about 780°C. Plate tensile properties were examined by using full-thickness tensile specimens.

Each plate was welded by double submerged-arc welding method with a heat input of 115kJ/cm. The HAZ microstructures were examined using 3% nital etchant, and the formation of M* was examined using modified Lepera etchant[10]. Steels containing B were subjected to fission track etching (FTE) to reveal the distribution of B. HAZ toughness was evaluated by a 2mm V-notch Charpy test at different notch locations.

Table 1 Chemical compositions. (wt %)

| Steel | C | Si | Mn | P | S | Al | Ni | Mo | Nb | Ti | B | N |
|---|---|---|---|---|---|---|---|---|---|---|---|---|
| N1 | 0.055 | 0.08 | 1.55 | 0.003 | 0.002 | 0.002 | 0.35 | – | – | 0.014 | – | 0.0030 |
| N2 | 〃 | 〃 | 〃 | 〃 | 〃 | 〃 | 〃 | – | 0.010 | 〃 | – | 〃 |
| N3 | 〃 | 〃 | 〃 | 〃 | 〃 | 〃 | 〃 | – | 0.025 | 〃 | – | 〃 |
| N4 | 〃 | 〃 | 〃 | 〃 | 〃 | 〃 | 〃 | – | 0.038 | 〃 | – | 〃 |
| M1 | 〃 | 〃 | 〃 | 〃 | 〃 | 〃 | 〃 | – | 0.020 | 〃 | – | 〃 |
| M2 | 〃 | 〃 | 〃 | 〃 | 〃 | 〃 | 〃 | 0.07 | 〃 | 〃 | – | 〃 |
| M3 | 〃 | 〃 | 〃 | 〃 | 〃 | 〃 | 〃 | 0.15 | 〃 | 〃 | – | 〃 |
| M4 | 〃 | 〃 | 〃 | 〃 | 〃 | 〃 | 〃 | 0.23 | 〃 | 〃 | – | 〃 |
| B1 | 〃 | 〃 | 〃 | 〃 | 〃 | 〃 | 〃 | – | 〃 | 〃 | 0.0004 | 〃 |
| B2 | 〃 | 〃 | 〃 | 〃 | 〃 | 〃 | 〃 | – | 〃 | 〃 | 0.0009 | 〃 |
| B3 | 〃 | 〃 | 〃 | 〃 | 〃 | 〃 | 〃 | – | 〃 | 〃 | 0.0013 | 〃 |
| B4 | 〃 | 〃 | 〃 | 〃 | 〃 | 〃 | 〃 | – | 〃 | 〃 | 0.0017 | 〃 |

### Tensile Properties of Base Material

Figure 3 shows the effect of microalloying of Nb, Mo and B on the strength of base material. Typical microstrctures of base material are shown in Fig. 4. As the amount of Nb was increased, the tensile strength increased almost linearly, the increment being approximately 2kg/mm² per 0.01% Nb. As is evident from Fig. 4, with increasing Nb content, ferrite grains are markedly refined. The effects of Mo and B addition on the tensile strength of base material are also conspicuous. A marked increase in the strength was obtained with the formation of fine-grained bainitic ferrite (accicular ferrite).

From these results, it was found that the addition of Nb, Mo or B was very effective in improving the strength of TiO steel, as is the case with conventional steel.

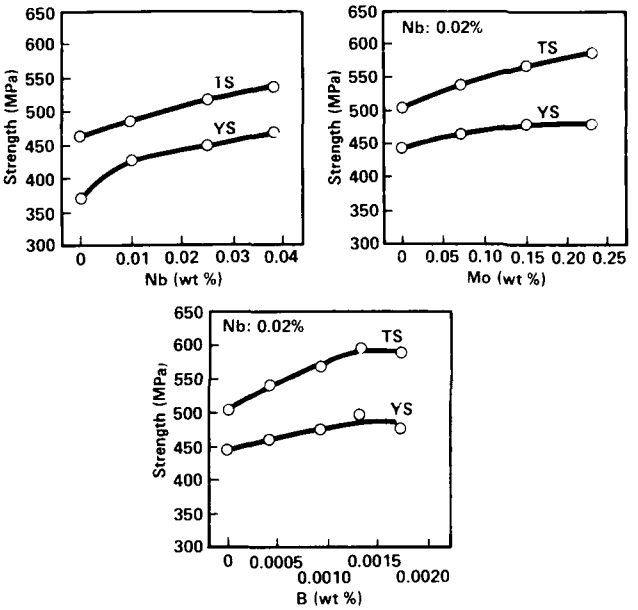


Fig. 3 Effect of microalloying of Nb, Mo and B on the strength of base material.

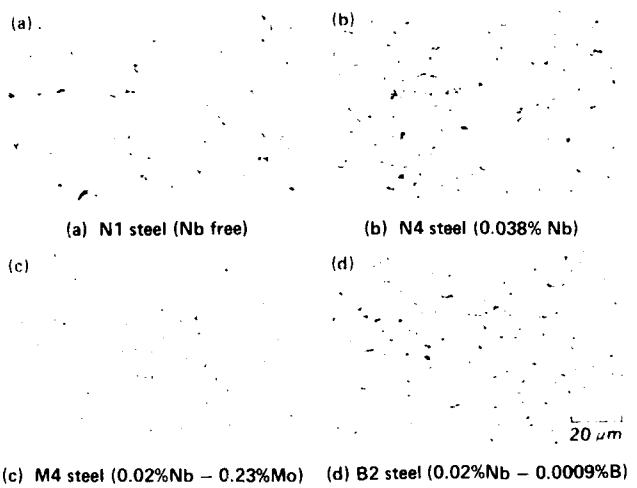


Fig. 4 Effect of microalloying of Nb, Mo and B on the microstructure of base material.

### HAZ Toughness and Microstructure

Figure 5 shows the effect of Nb content on HAZ toughness. The HAZ toughness shows a peak value at 0.010% Nb. It does not deteriorate even when the Nb content is increased to 0.038%. This is a unique characteristic of TiO steel considering that conventional steels having same chemistry show a tendency of deterioration in HAZ toughness when Nb content is increased. It has been known that the effect of Nb addition on HAZ toughness varies according to the C content and that, when the C content is approxiamately 0.06%, the HAZ toughness generally deteriorates with increasing Nb content[11,12]. This is considered due to the fact that the addition of Nb

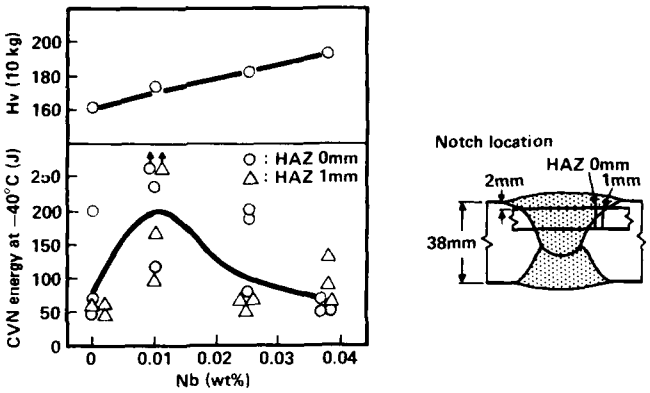


Fig. 5 Effect of Nb content on the hardness and toughness of the HAZ.

causes a marked growth of FSP, which is detrimental to toughness, while the formation of grain boundary allotriomorphs of ferrite ($F_A$) is suppressed by Nb addition. Yamamoto et al. studied the effect of a small amount of Nb addition (Nb≅0 to 0.01%) on TiO and TiN steels, each with 0.08%C-1.4%Mn as the base composition, using simulated HAZ test (cooling time from 800°C to 500°C, 161 sec)[8]. In the case of 0.01%Nb addition, TiN steel showed a toughness deterioration of about 40°C (vTrs), whereas TiO steel showed a slight improvement, rather than deterioration, in toughness. According toYamamoto, this is mainly due to the fact that the Nb addition causes a coarse-grained microstructure consisting of FPS to grow in TiN steel, whereas it promotes IFP formation in TiO steel. Figure 6 shows the effect of Nb content on HAZ microstructure. It can be seen that the improvement in toughness by the addition of 0.01%Nb is due to the suppression of coarse $F_A$ and FSP, resulting in increase in volume fraction of IFP (see Fig. 7). It should be noted that the IFP retains the major microstructure of the HAZ even when the Nb content is increased to approximately 0.04%. As a result, only a modest deterioration of HAZ toughness with increasing Nb content was observed despite the increase in HAZ hardness (see Fig. 5). Steel N4 with Nb content of 0.038% showed a HAZ toughness almost comparable to that of Nb-free steel N1.

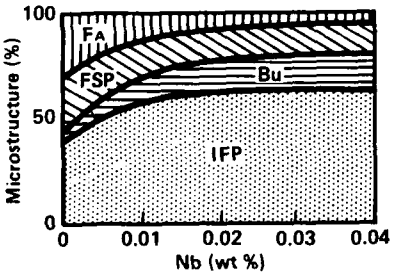


Fig. 6 Effect of Nb content on the microstructure (region within 150μm from FL) of the HAZ.

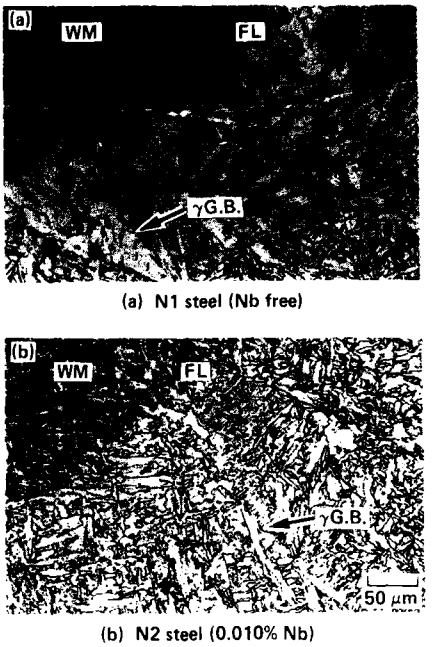


Fig. 7 Effect of Nb addition on the microstructure of the HAZ.

Figure 8 shows the effect of Mo content on the microstructure and toughness of the HAZ in 0.02% Nb steel. It can be seen that the HAZ toughness tends to improve as the Mo content is increased. As for the microstructure, the improvement in hardenability by Mo addition sufficiently suppresses coarse $F_A$ and FSP, and the marked formation of IFP is observed. The change in the HAZ microstructure corresponds to the change in the HAZ toughness. Figure 9 compares the HAZ microstructures of steels M1 and M4. Refinement of the IFP, as well as the suppression of coarse $F_A$ and FSP, can be observed. Thus, in addition to the increase in volume fraction of IFP, the refinement of IFP may partially contribute to improved HAZ toughness. As mentioned above, it was found that the addition of Mo was effective in improving the HAZ microstructure near the fusion line. However, excessive addition of Mo tends to increase the amount of M* in intercritically reheated coarse-grained HAZ. It is known that the presence of M* causes the HAZ toughness to deteriorate, since M* can originate brittle fracture[13]. In the present research, the amount of M* was observed to increase, in the above-mentioned region, with increasing Mo content. It should therefore be noted that there exists an appropriate Mo content corresponding to the required HAZ toughness level.

Figure 10 shows the effect of B content on the microstructure and toughness of the HAZ in 0.02% Nb steel. The HAZ toughness improves as B content is increased. However, after the HAZ toughness shows its peak value at 0.0009% B, it declines sharply with increasing B content. As for the microstructure, the addition of B noticeably suppresses coarse $F_A$

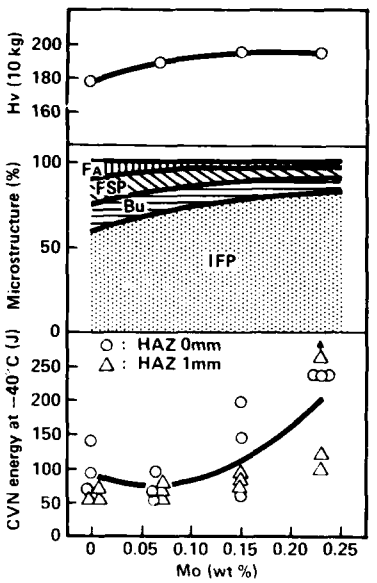


Fig. 8 Effect of Mo content on the hardness, microstructure (region within 150μm from FL) and toughness of the HAZ.

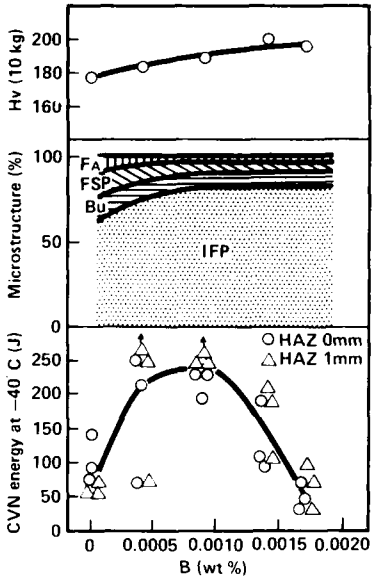


Fig. 10 Effect of B content on the hardness, microstructure (region within 150μm from FL) and toughness of the HAZ.


(a) M1 steel (0.02%Nb)

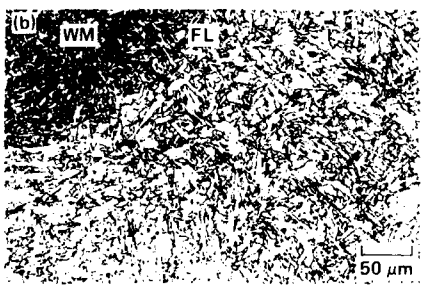


(b) M4 steel (0.02%Nb – 0.23%Mo)

Fig. 9 Effect of Mo addition on the microstructure of the HAZ.


(a) B1 steel (0.0004% B)

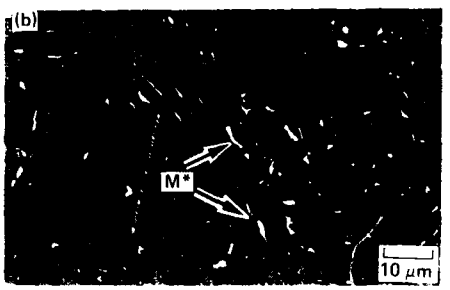


(b) B4 steel (0.0017% B)

Fig. 11 Effect of B content on the formation of M*.

and FSP and enhances the formation of IFP until B content reaches 0.0009%. This is considered due to the increased hardenability at γ grain boundary by B addition. The HAZ microstructure shows no marked change even when the B content is increased above 0.0009%, hence the deterioration of HAZ toughness above 0.0009% B cannot be explained by the change in HAZ microstructure. Possible causes of the toughness deterioration are the formation of M* and the coarse precipitates of B along the γ grain boundaries. The formation of M* in the HAZ near FL was examined by modified Lepera etching. The results in B1 and B4 steels are shown in Fig. 11. Steel B1 was almost free of M*, whereas steel B4 revelaed marked formation of M*. As already mentioned, a hard phase such as M* can initiate brittle cracking, hence the formation of M* can be considered a possible cause of the deterioration of HAZ toughness. As for the effect of B precipitates, it has been pointed out that the presence of coarse $Fe_{23}(CB)_6$ along γ grain boundaries can cause voids, which coalesce to initiate

brittle fracture, thereby deteriorating the HAZ toughness.[14] In the present research, steel B4 showed no intergranular fracture in a Charpy fracture surface. However, an FTE observation showed coarse precipitates of B in steel B4 (Fig. 12), suggesting that the precipitates of B may have some adverse effect on the HAZ toughness. Like Mo steels, B steels revealed the formation of M-A in the intercritically reheated coarse-grained HAZ when the B content was increased. This also suggests that excessive addition of B is undesirable. It should be noted that the optimum amount of B depends on the welding heat input, that is, the cooling rate after welding.

So far, the effects of Nb, Mo and B on HAZ toughness have been discussed. It was found that each of the elements was effective in improving the HAZ toughness by suppressing coarse $F_A$ and FSP through improvement in hardenability (suppression of $\gamma/\alpha$ transformation) and by increasing the volume fraction of IFP. The amount of addition of those elements is required to be optimized according to the required levels of strength and low-temperature toughness. It was confirmed that high-strength TiO line pipe having superior HAZ toughness can be manufactured by making the most effective use of those alloying elements.

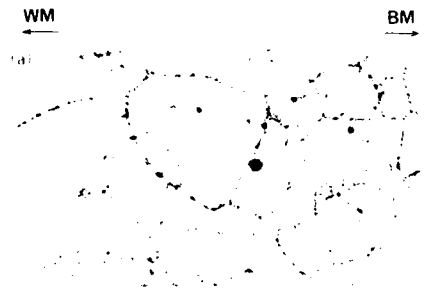


(a) B1 steel (0.0004% B)


(b) B4 steel (0.0017% B)

Fig. 12 Distribution of B in the HAZ near FL revealed by the FTE method.

## HIGH-STRENGTH (X80) TiO LINE PIPE STEEL

This section introduces the results of laboratory tests on Nb-microalloyed, high-strength (X80) line pipe steel. As described in the preceding section, the addition of Nb in TiO steel not only improves the strength of base material effectively, but also enhances the formation of IFP in the HAZ. Therefore, the deterioration of HAZ toughness due to increased strength is less conspicuous than in conventional Nb steels. Also, as can be seen in the case of Mo or B addition, TiO steel can produce sufficient amount of IFP even when its hardenability is relatively high. Shown below are properties of a high Mn-Nb X80 TiO line pipe steel, in comparison with those of TiN steel.

The chemical compositions of steels are shown in Table 2. While TiN steel contains the normal amount of Al, TiO steel has Al content reduced to such level as required to secure Ti-oxide particles as the nuclei for IFP formation. These two steels were vacuum-melted and controlled-rolled to 18 mm thick plates under the following thermo-mechanical processing conditions: reheating temperature 1150 C; cumulative reduction below 850 C about 78%; finish rolling temperature 730 C; cooling rate of accelerated cooling 30 C/sec; and stop temperature of accelerated cooling approximately 450 C. The mechanical properties of base materials are shown in Table 3. Both steels had fine ferrite-bainite microstructure and showed sufficient strength and toughness required for X80 steel. In order to study the HAZ toughness of each steel, the plates were welded by double submerged-arc welding method with a heat input of 38kJ/cm. The HAZ toughness is shown in Fig. 13. TiN steel showed low energy values at the notch locations of HAZ 1 and 2 mm, whereas TiO steel had high toughness at all notch locations. The HAZ microstructures

Table 2 Chemical compositions of TiO and TiN X80 line pipe steel.

| Steel | C | Si | Mn | P | S | Cu | Ni | Nb | Al | Ti | Ceq *) |
|---|---|---|---|---|---|---|---|---|---|---|---|
| TiO | 0.08 | 0.11 | 1.83 | 0.011 | 0.004 | 0.20 | 0.21 | 0.05 | 0.003 | 0.020 | 0.42 |
| TiN | 0.08 | 0.11 | 1.89 | 0.010 | 0.004 | 0.21 | 0.19 | 0.05 | 0.023 | 0.016 | 0.41 |

*) Ceq. = C + Mn/6 + (Ni + Cu)/15 + (Cr + Mo + V)/5

Table 3 Mechanical properties of TiO and TiN X80 steel plate.

| Steel | Thickness (mm) | Direction | Tensile properties | | | Charpy impact properties | | |
|---|---|---|---|---|---|---|---|---|
| | | | YS (MPa) | TS (MPa) | El (%) | Position | vE-40 (J) | vTrs (°C) |
| TiO | 18 | C | 620 | 698 | 36.3 | 1/2t | 19.8 | −110 |
| TiN | 18 | C | 606 | 694 | 36.0 | 1/2t | 18.4 | − 90 |

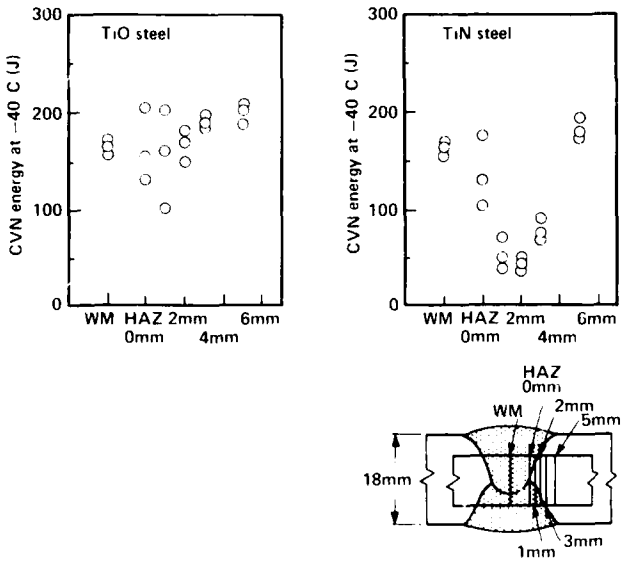


Fig. 13 Charpy V-notch impact energy at different notch locations of seam weld.

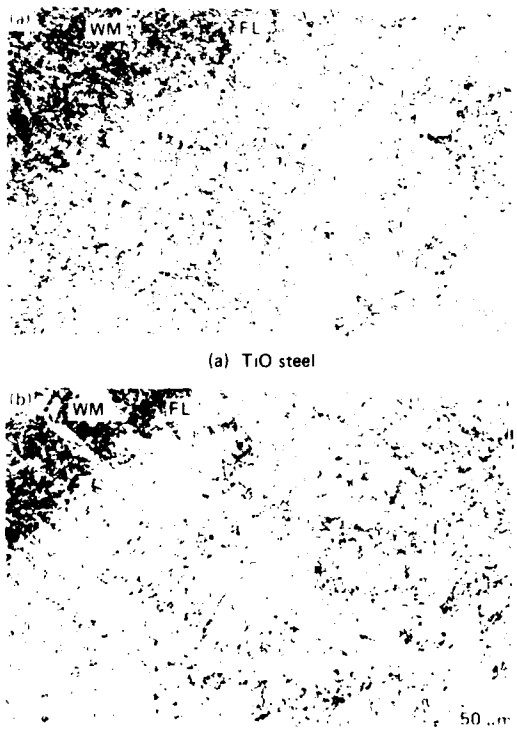


(a) TiO steel

(b) TiN steel

Fig. 14 Microstructures of the HAZ of X80 line pipe steel.

near FL are shown in Fig. 14. Despite the small heat input of 38kJ/cm, TiO steel showed the formation of IFP more markedly than TiN steel. From the above-mentioned results, it was found that even with high-strength line pipe, like X80, HAZ toughness can be improved by the formation of IFP, and that TiO steel can be a superior material for high-strength, high toughness line pipe.

## APPLICATION OF TiO STEEL TO ACTUAL PRODUCTION OF UOE PIPE

UOE pipes were manufactured commercially using the TiO steel, and their properties were examined. An outline of the manufacturing process of the steel plates for UOE pipe is shown in Fig. 15. In the refining process, special treatment was conducted to obtain Ti-oxide particles and ladle desulphurization and vacuum degassing were carried out in order to make the steel clean. In the plate rolling process, the steel was subjected to interrupted accelerated cooling after controlled rolling. The chemical composition of the steel is given in Table 4. To simultaneously form fine Ti-oxide and TiN particles, the Al content was reduced and an optimum Ti-O-N balance was ensured. Steels A and B are Nb-microalloyed and Nb, Mo microalloyed steels, respectively. Both steels have lower carbon equivalent (Ceq) and Pcm values than those of conventional steels and hence have good field weldability.

Table 5 shows typical examples of mechanical properties of base materials of UOE pipes with a size of 914mm (36 in.) OD x 38.1mm (1.5 in.) WT. Pipes A and B meet the strength

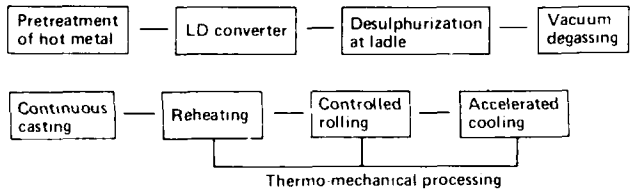


Fig. 15 Manufacturing process of plate.

Table 4 Chemical compositions of commercial steels (wt %).

| Steel | C | Si | Mn | P | S | Cu | Ni | Nb | Mo | Ti | Al | *1 Ceq | *2 Pcm |
|---|---|---|---|---|---|---|---|---|---|---|---|---|---|
| X52 (A) | 0.06 | 0.08 | 1.44 | 0.006 | 0.001 | | 0.36 | 0.012 | | 0.017 | 0.003 | 0.32 | 0.14 |
| X65 (B) | 0.05 | 0.07 | 1.49 | 0.008 | 0.004 | | 0.33 | 0.011 | 0.09 | 0.020 | 0.003 | 0.34 | 0.13 |

*1) Ceq = C + Mn/6+(Cr+Mo+V)/5+(Ni+Cu)/15(%)
*2) Pcm = C+Si/30+(Mn+Cu+Cr)/20+Ni/60+Mo/15+V/10+5B (%)

Table 5 Mechanical properties of base material of UOE pipe.

| Steel | Pipe size (mm) | Direction | Tensile properties*1 YS (MPa) | TS (MPa) | EL (%) | Charpy impact properties*2 vE-40 (J) | vTrs (°C) | BDWTT*3 85% shear FATT (°C) |
|---|---|---|---|---|---|---|---|---|
| X52 (A) | 914OD (36 in) x 38.1WT (1.5 in) | L | 448 | 520 | 64 | - | - | - |
| | | T | 443 | 527 | 62 | 442 | -80 | -50 |
| X65 (B) | 914OD (36 in) x 38.1WT (1.5 in) | L | 473 | 556 | 64 | - | - | - |
| | | T | 474 | 565 | 59 | 388 | -80 | -45 |

*1) Strap test of API rectangular specimen.
*2) Test position : 1/2 t.
*3) Reduced specimen (thickness = 19 mm).

specified for X52 and X65, respectively, and have only small anistropy. These steels are good in terms of Charpy impact energy and BDWTT properties and can withstand applications at −40°C. Figure 16 shows typical examples of Charpy V-notch impact energy at different notch locations of seam weld of both pipes. Seam welding was by double submerged-arc welding method. It can be seen that the Charpy impact energy is very high in all notch locations and that both pipes have superior HAZ toughness for low-temperature service. Nippon Steel manufactured 6000 tons of X52 conductor pipe used for offshore structure in the North Sea. As shown in Fig. 17, the energy in the HAZ of commercially manufactured conductor pipe is very high and more than double the specified value.

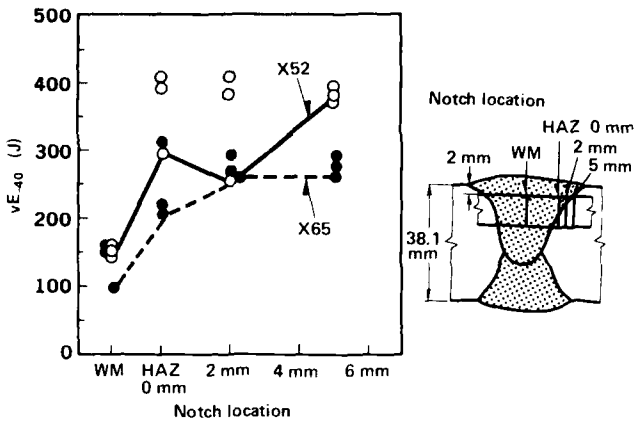


Fig. 16 Charpy V-notch impact energy at different notch locations of seam weld.

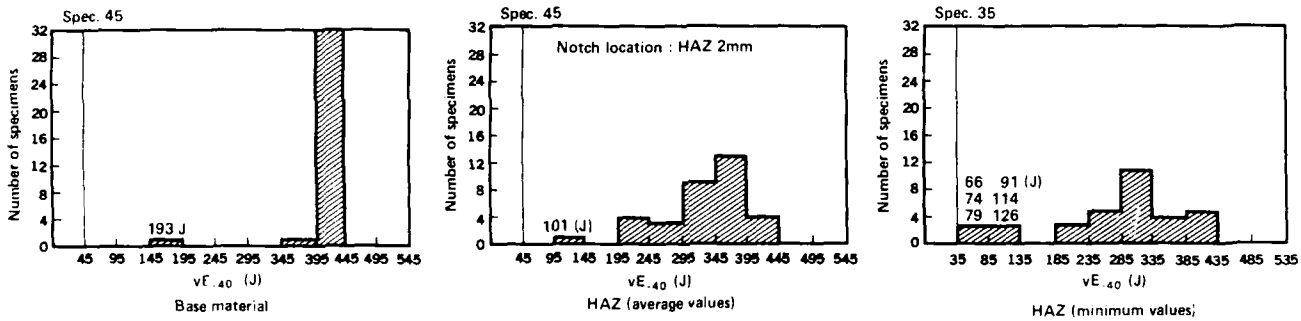


Fig. 17 Charpy V-notch impact energy of conductor pipes (X52).

## CONCLUSION

A study was made on the effects of Nb, Mo and B additions on the properties of TiO steel. The following conclusions were obtained.

1) The addition of Nb, Mo and B suppresses the formation of coarse grain boundary ferrite and ferrite sideplate in the HAZ near the fusion line and increases the volume fraction of IFP.

2) In conventional steel, the addition of Nb tends to cause the HAZ toughness to deteriorate. On the contrary, in TiO steel, the degree of HAZ deterioration is small due to the formation of IFP. From the viewpoint of HAZ toughness, the optimum amount of Nb is approximately 0.01%. It was also confirmed that good HAZ toughness could be obtained even with high Mn-Nb X80 steel.

3) It was found possible to manufacture high-strength steel having excellent HAZ toughness by the addition of Mo or B to Nb steel. The addition of Mo and B increases the volume fraction of IFP. However, the optimum amount of addition should be determined according to required levels of strength and toughness.

4) TiO steel applied to actual production showed excellent HAZ toughness and was supplied for conductor pipe in the North Sea.

## References


1) Accelerated Cooling of Steel edited by P.D. Southwick, AIME (1985)

2) S. Kanazawa, A. Nakajima, K. Okamoto and K. Kanaya: Tetsu-to-Hagané, *61*, 2589 (1975)

3) S. Matsuda and N. Okamura: Testu to-Hagané, *62*, 1209 (1987)

4) D.P. Fairchild: Local Brittle Zones in Structural Welds (1987)

5) N. Mori, H. Honma, S. Okita and M. Wakabayashi: Journal of Japan Welding Society, *50*, 174 (1981)

6) M. Imagunbai, R. Chijiiwa, N. Aikawa, M. Nagumo, H. Honma, S. Matsuda and H. Mimura: HSLA Steels edited by J.M. Gray et al., ASM & CSM, 557 (1985)

7) K. Yamamoto, T. Haze, T. Mukai, S. Matsuda and M. Imagunbai: Testu-to-Haganė, *72*, S626 (1986)
8) K. Yamamoto, R. Chijiiwa, T. Haze and H. Mimura: presented at "Symposium on Residual and Unspecified Elements in Steel", ASTM, Miami, Nov. (1987)
9) R. Chijiiwa, H. Tamehiro, M. Hirai, H. Matsuda and H. Mimura: presented at "OMAE' 88", Houston, Feb. (1988)
10) F.S. Lepera: Journal of Metals, March, 38 (1980)
11) T. Shioaku, M. Yamauchi, S. Takashima, H. Kaji and M. Kanou: Tetsu to-Haganė, *72*, S618 (1986)
12) S. Mukae, K. Nishio, M. Kato and H. Sakaguchi: The 104th Technical Commission on Welding Metallurgy, Japan Welding Society (1986)
13) T. Haze and S. Aihara: presented at "OMAE' 88", Houston, Feb. 1988
14) R. Habu: Dr. of Engng. Thesis, Tokyo University, Japan, April 1985)

# EFFECTS OF THERMOMECHANICAL PROCESSING ON MICROSTRUCTURE AND PROPERTIES OF ULTRA LOW CARBON BAINITIC STEELS

**L. E. Collins, J. D. Boyd, J. A. Jackman, L. Dignard-Bailey**
Metals Technology Laboratories
CANMET
Ottawa, Ontario, Canada

**M. R. Krishnadev, S. Dionne**
Department of Mining and Metallurgy
Lavel University
Quebec, P. Q., Canada

ABSTRACT

The role of impurity elements (O and S) and thermomechanical processing on the effectiveness of boron in suppressing ferrite formation in ultra low carbon bainitic (ULCB) steels has been investigated by means of laboratory rolling trials and dilatometer processing simulations. Secondary Ion Mass Spectroscopy (SIMS) and autoradiography were employed to examine boron distributions after various processing treatments. The addition of 20 ppm of B to a base alloy of composition 0.02 wt % C, 1.80 wt % Mn, and 0.05 wt % Nb suppressed transformation temperatures by 75 to 100°C; however, a fully bainitic microstructure was obtained only when the impurity content was low or when the steel was given a preliminary hot working treatment prior to final thermomechanical processing. It is suggested that the entrapment of boron at inclusions is a critical factor influencing the effectiveness of boron as a hardenability agent in these steels.

ULTRA LOW CARBON bainitic (ULCB) steels were developed in Japan in the early 1980's to meet the demand for high strength steels with good low temperature toughness and weldability for such applications as Arctic grade linepipe (1,2,3). In these steels, dislocation strengthening within the fine bainitic microstructure combines with Nb(C,N) precipitation strengthening to produce yield strengths in excess of 600 MPa. By employing carbon levels <0.03 wt %, formation of small islands of high carbon martensite is reduced, resulting in superior low temperature fracture toughness. Critical to the production of these steels is the addition of a small amount of boron, typically 10 to 20 ppm. During processing, the boron segregates to austenite grain boundaries where it inhibits ferrite nucleation, and thereby promotes formation of a fine baintic microstructure after controlled rolling and air cooling.

To effectively inhibit ferrite formation, boron must be retained in solid solution in the austenite. Boron has a strong affinity for nitrogen and, therefore, it is necessary to fix nitrogen to prevent the formation of BN. This is normally done by adding small amounts of titanium to form TiN precipitates which remove nitrogen from solid solution, and prevent austenite grain growth during controlled rolling. It is generally accepted that boron-containing steels should be clean i.e. contain minimal levels of S, O and other impurities, if the full effect of boron is to be achieved. However, the level of cleanliness has not been specified, nor are the mechanisms by which the impurities affect the behaviour of boron clearly understood.

In the present study, boron-containing steels were produced with both high (0.006 wt % S and 0.0085 wt % O) and low (0.004 wt % S and 0.0057 wt % O) levels of impurities by air and vacuum casting respectively. The microstructures of as-rolled plates were examined in detail and dilatometer studies were conducted to characterize the transformation behaviour of the steel. As well, the boron distributions resulting from various processing schedules were determined by Secondary Ion Mass Spectroscopy (SIMS) and autoradiography. The results are compared to those obtained for a steel of similar composition but containing no boron.

## EXPERIMENTAL

The alloys examined in this study had a base composition of 0.02 wt % C, 1.80 wt % Mn and 0.05 wt % Nb (Table 1). The boron-containing steels had an addition of 20 ppm B. The base alloy with no boron and two heats of the boron-containing steel were cast in air and a single heat of the boron-containing composition was cast in vacuum. All alloys were cast into 50 kg ingots with cross-section 125 mm x 150 mm. The ingots were controlled rolled to 12.7 mm thick plate according to the schedule in Table 2 and air cooled.

Table 1 - Steel compositions (wt%)

| Alloy | C | Mn | Nb | Si | S | Ti | Al | P | N | O | B | β |
|---|---|---|---|---|---|---|---|---|---|---|---|---|
| 1 (Air cast) | 0.020 | 1.65 | 0.045 | 0.31 | 0.006 | 0.020 | 0.025 | 0.005 | 0.0058 | 0.0050 | -- | -- |
| 2A (Air cast) | 0.019 | 1.85 | 0.040 | 0.41 | 0.0063 | 0.023 | 0.020 | 0.008 | 0.0032 | 0.0080 | 0.0016 | 0.0016 |
| 2B (Air cast) | 0.018 | 1.77 | 0.040 | 0.25 | 0.0060 | 0.020 | 0.020 | 0.006 | 0.0066 | 0.0085 | 0.0015 | 0.0010 |
| 2C (vacuum cast) | 0.021 | 1.83 | 0.057 | 0.32 | 0.0042 | 0.018 | 0.011 | 0.010 | 0.0062 | 0.0057 | 0.0019 | 0.0015 |

Effective boron = $\beta = [B - (N - 0.002 - Ti/5)]$

Dilatometer tests were carried out using an MMC deformation dilatometer. Specimens 8 mm long x 4 mm diam were machined from as-cast ingots and as-rolled plates. Specimens were austenitized in the dilatometer for 15 min at 1100°C, cooled to 825°C, deformed 50%, held 10 s and cooled according to a Newtonian cooling schedule such that the time between 800 and 500°C was 300 s (average cooling rate 1°C/s).

The microstructures of as-rolled plates and dilatometer specimens were examined after polishing and etching with a 2% nital solution. Inclusion counts were carried out on heats of the boron-containing steels in both the as-cast and controlled rolled conditions. A Cameca IMS-4F Secondary Ion Mass Spectrometer, operated in the direct-ion image mode with an $O_2^+$ beam, was used to examine boron distributions and identify inclusions. Boron distributions were also mapped by high resolution autoradiography carried out at the Research and Development Laboratories of Nippon Steel following standard techniques (4).

Table 2 - Rolling schedule

| Pass No. | Mill setting (cm) | Temperature (°C) |
|---|---|---|
| 1 | 11.57 | 1100 |
| 2 | 10.46 | 1060 |
| 3 | 9.45 | 1040 |
| 4 | 8.51 | 1020 |
| 5 | 7.65 | 1000 |
| 6 | 6.91 | 900 |
| 7 | 6.22 | 890 |
| 8 | 5.56 | 875 |
| 9 | 4.93 | 865 |
| 10 | 4.32 | 850 |
| 11 | 3.73 | 840 |
| 12 | 3.18 | 825 |
| 13 | 2.64 | 815 |
| 14 | 2.13 | 800 |
| 15 | 1.65 | 785 |
| 16 | 1.27 | 770 |

## RESULTS

ROLLING TRIALS - The microstructure of the as-rolled base alloy consisted of fine-grained polygonal ferrite and pearlite (Fig. 1a). In the air-cast boron alloy (2A), the boron failed to completely suppress ferrite formation. A banded microstructure was observed in which narrow bands, 20-40 μm in width, of fine polygonal ferrite lie parallel to the rolling plane interrupting the predominantly bainitic microstructure in the as-rolled condition (Fig. 1b). The boron distribution in this alloy, as revealed by SIMS and autoradiography, also showed evidence of banding with regions (up to 50 μm in width) in which little or no boron was detected (Fig. 1c). There was no clear evidence of boron segregation to austenite grain boundaries.

The microstructure of the as-rolled vacuum-cast material consisted almost entirely of bainite, although a few small regions of ferrite were evident (Fig 1d). The boron distribution of the vacuum-cast and rolled material appeared to be more homogeneous (Fig. 1e) than the air-cast material, but again there was little evidence of boron segregation to the grain boundaries.

Since S and O are present in the form of inclusions, analysis of inclusion contents was carried out on the as-cast and as-rolled boron steels (Table 3). It is seen that the volume

Table 3 - Inclusion content of steels

| Alloy | Condition | Oxides (vol %) | Sulphides (vol %) | Total inclusion content (vol %) |
|---|---|---|---|---|
| 2A | As-rolled | 0.038 | 0.085 | 0.123 |
| 2B | Air cast | 0.096 | 0.040 | 0.136 |
| 2B | Air cast + rolled | 0.071 | 0.073 | 0.144 |
| 2C | Vacuum cast | 0.051 | 0.027 | 0.078 |
| 2C | Vacuum cast + rolled | 0.031 | 0.044 | 0.075 |

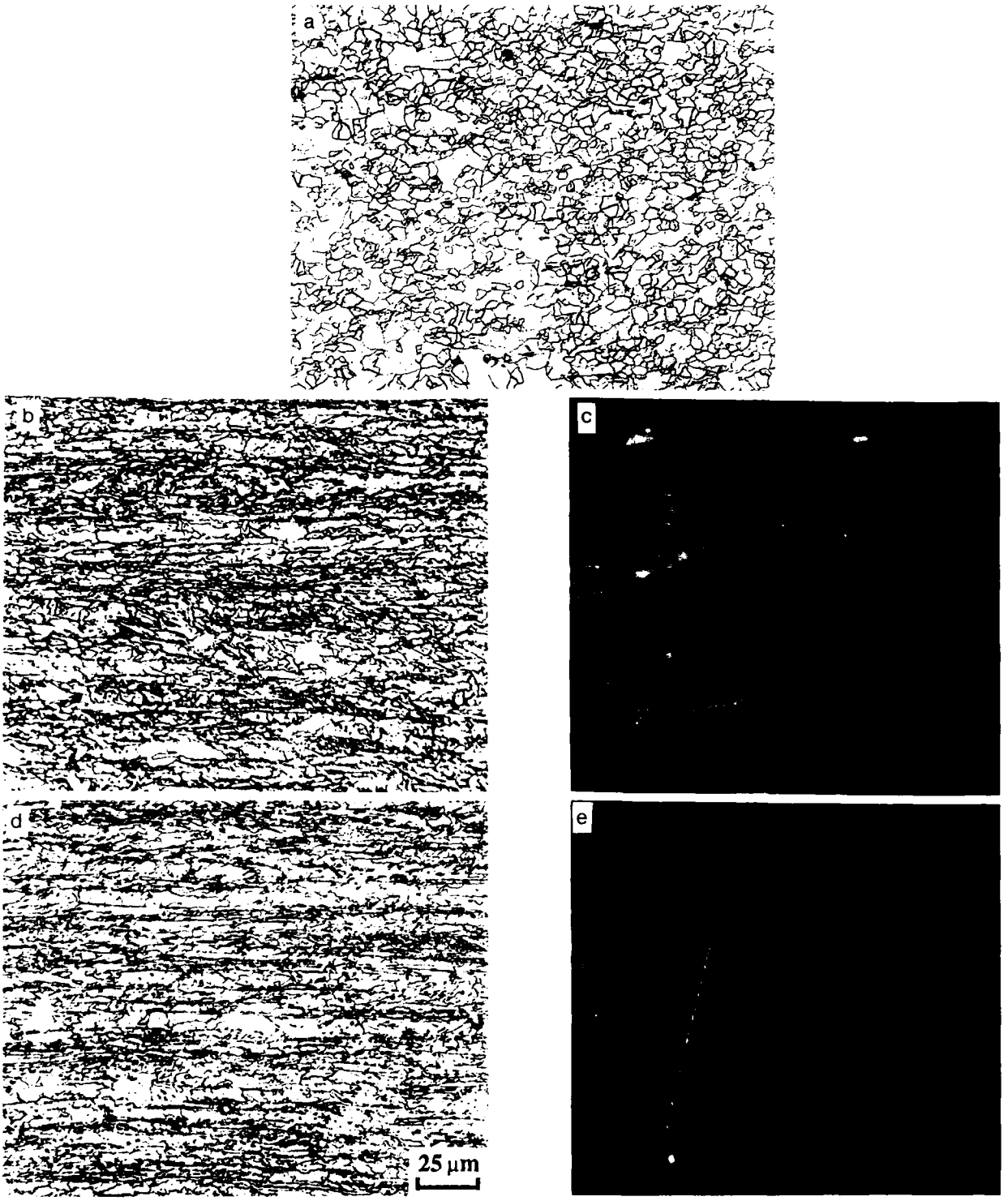


Fig. 1 - (a) Microstructure of base alloy 1 in the as-rolled condition.
(b) Microstructure of air-cast alloy 2A after controlled rolling.
(c) Boron distribution in air-cast alloy 2A after controlled rolling (SIMS).
(d) Microstructure of vacuum-cast alloy 2C after controlled rolling.
(e) Boron distribution in vacuum-cast alloy 2C after controlled rolling (SIMS).

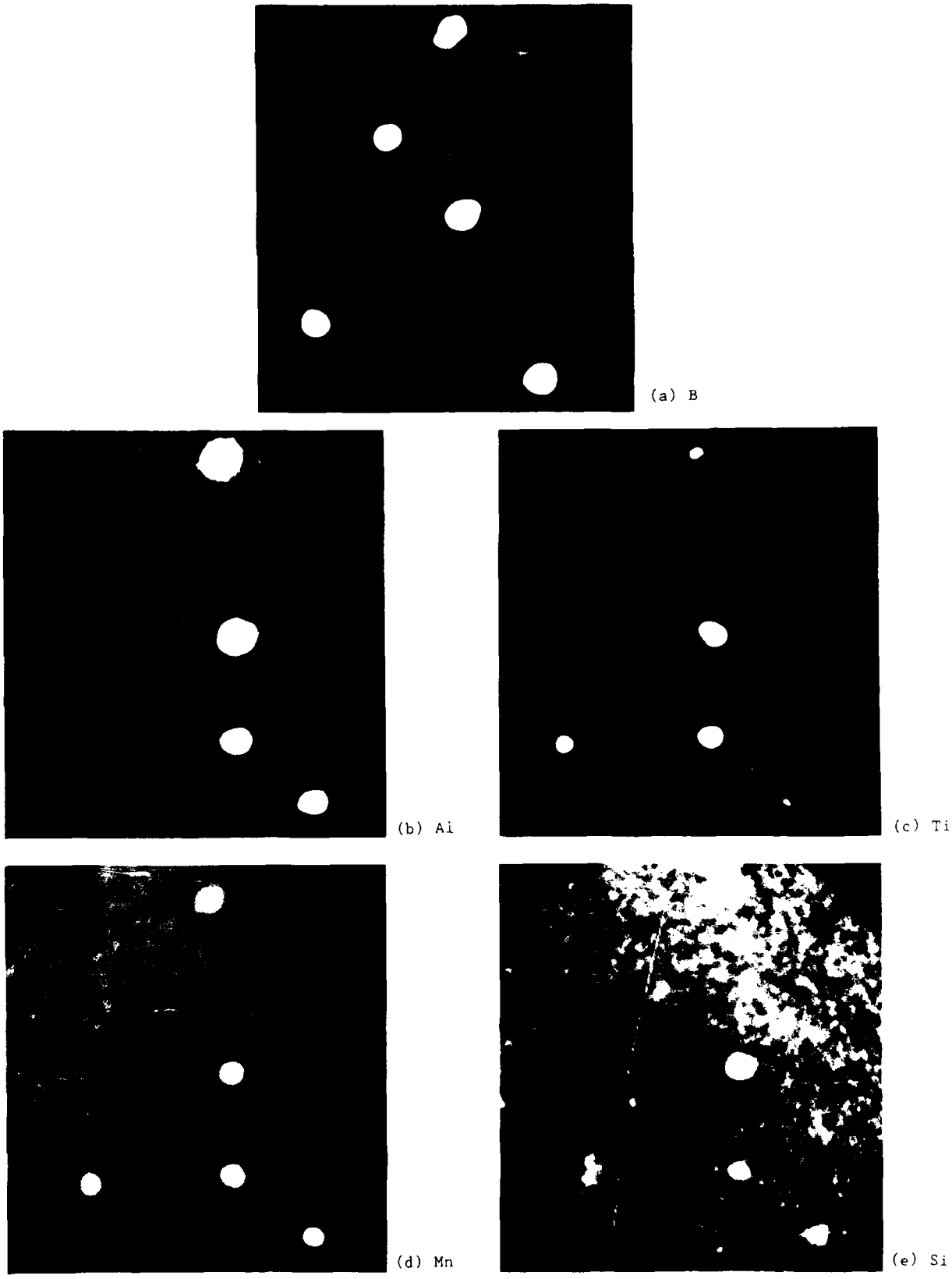


Fig. 2 - SIMS element distribution maps showing presence of boron in an inclusion array in the air-cast ingot 2B. (Field of view is 150 μm.)

(a) Mn

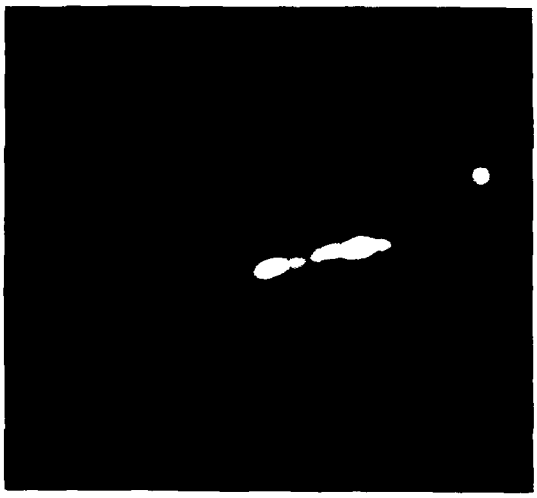

(b) Al

(c) Ti

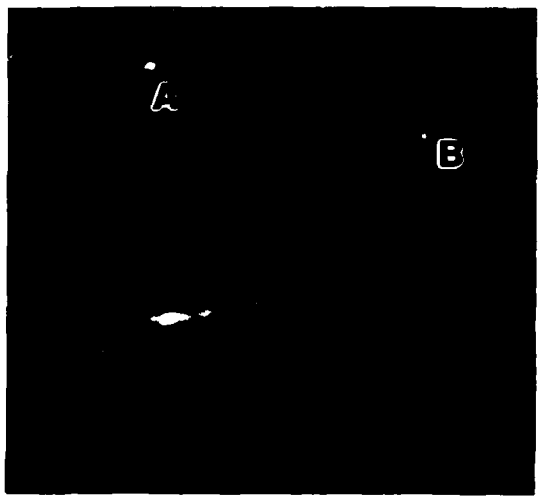


(d) B

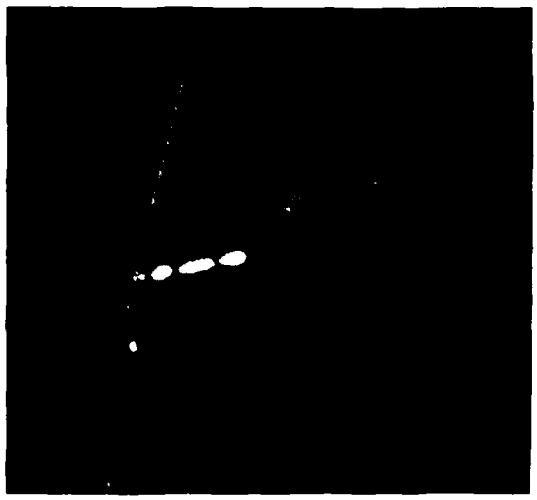

(e) Si

Fig. 3 - SIMS element distribution maps showing presence of boron at an elongated inclusion in the air-cast and as-rolled ingot 2A. (Field of view is 150 μm.)

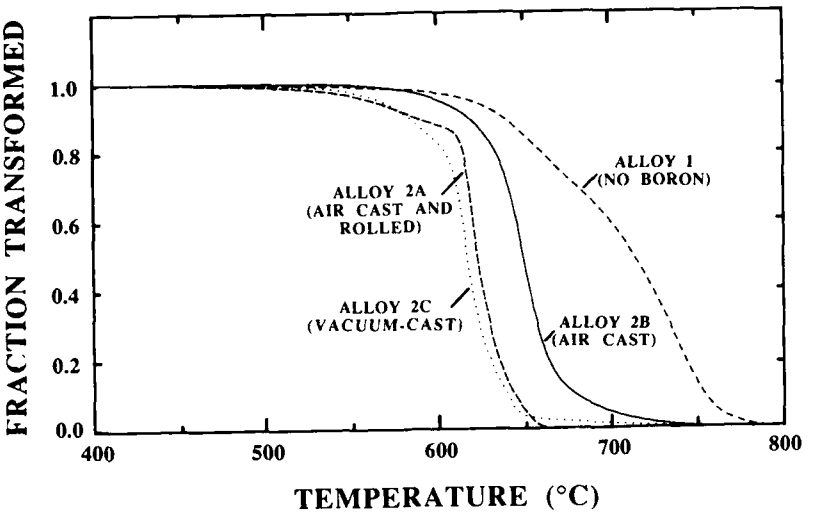


Fig. 4 - Plot of fraction transformed versus temperature for dilatometer specimens cooled at 1°C/s after deformation at 825°C. The starting condition of the material in each test is indicated.

fraction of inclusions in the air-cast material is approximately double that of the vacuum-cast material. It will be noted that the relative proportion of sulphides and oxides differs between the as-cast and as-rolled conditions for both air-cast and vacuum-cast materials. This is a consequence of the fact that samples used for analysis of the as-cast ingots were taken from near the ingot surface where the fraction of MnS is expected to be low, whereas the analysis of inclusion content was carried out on the full plate thickness in the as-rolled material and thus probably provides a more accurate measure of the true proportion of inclusions. Nonetheless, whether material in the as-cast or as-rolled condition is compared, the vacuum-cast material has a significantly lower volume fraction of inclusions than the air-cast alloy. There was no appreciable difference in the size of the inclusions between air-cast and vacuum-cast materials.

Samples from the air-cast ingot were examined by SIMS in an effort to determine if boron was associated with any particular inclusion type. Inclusion arrays were readily identified by SIMS as shown in Fig. 2. It was found that most inclusions contained Al, Ti, Si and Mn, although with SIMS analysis it was not possible to accurately identify the primary elements at any particular site. However, it was clear that boron was highly concentrated at inclusion sites in the as-cast material. In the as-rolled condition, some regions of high boron content appeared to correspond to inclusions (Fig. 3). As well, regions of high boron content were observed which did not appear to correspond to any type of Al, Mn or Si inclusion or to Ti precipitates (points A and B in Fig. 3d).

DILATOMETER SIMULATIONS - Plots of fraction transformed versus temperature for the dilatometer specimens, cooled at 1°C/s after deformation at 825°C are shown in Fig. 4. The addition of B to the base steel strongly suppresses ferrite formation and shifts the transformation downward by 75-100°C. Whereas a ferrite-pearlite microstructure was observed in the base alloy (Fig. 5a), the microstructures of the boron-containing specimens were primarily bainitic (Fig. 5b,c,e). Comparing the results for the boron-containing steels, some significant differences are observed depending upon the processing schedule. Transformation of specimens machined from the air-cast ingot proceeded at temperatures ~25°C higher than vacuum-cast samples; the beginning of transformation occured at 700°C for the air-cast and 675°C for the vacuum-cast material with the major portion of the transformation occuring between 675 and 650°C for the air-cast alloy and between 650 and 625 °C for the vacuum-cast material. This difference in the transformation temperatures is significant because the bainite-start temperature in this alloy is approximately 650°C. Consequently, a mixed ferrite-bainite microstructure was obtained from the air-cast specimens (Fig. 5c), whereas the microstructure of the vacuum-cast material was completely bainitic (Fig. 5b). In the air-cast condition, the boron distribution is inhomogeneous with only limited boron segregation to grain boundaries (Fig. 5d).

It is interesting that, in dilatometer tests on specimens taken from the air-cast and rolled plate, the transformation is shifted downward to a transformation temperature range similar to that of the vacuum-cast material, and a fully bainitic microstructure was obtained (Fig. 5e). Upon conclusion of the dilatometer test on air-cast and rolled material, boron clearly outlines most of the prior austenite grain boundaries (Fig. 5f). Evidence of boron segregation to grain boundaries has been observed in a wide range of dilatometer simulations when the starting material was in the air-cast and rolled condition (5). The results indicate a stronger effect of boron in suppressing ferrite formation in the vacuum-cast, and air-cast and

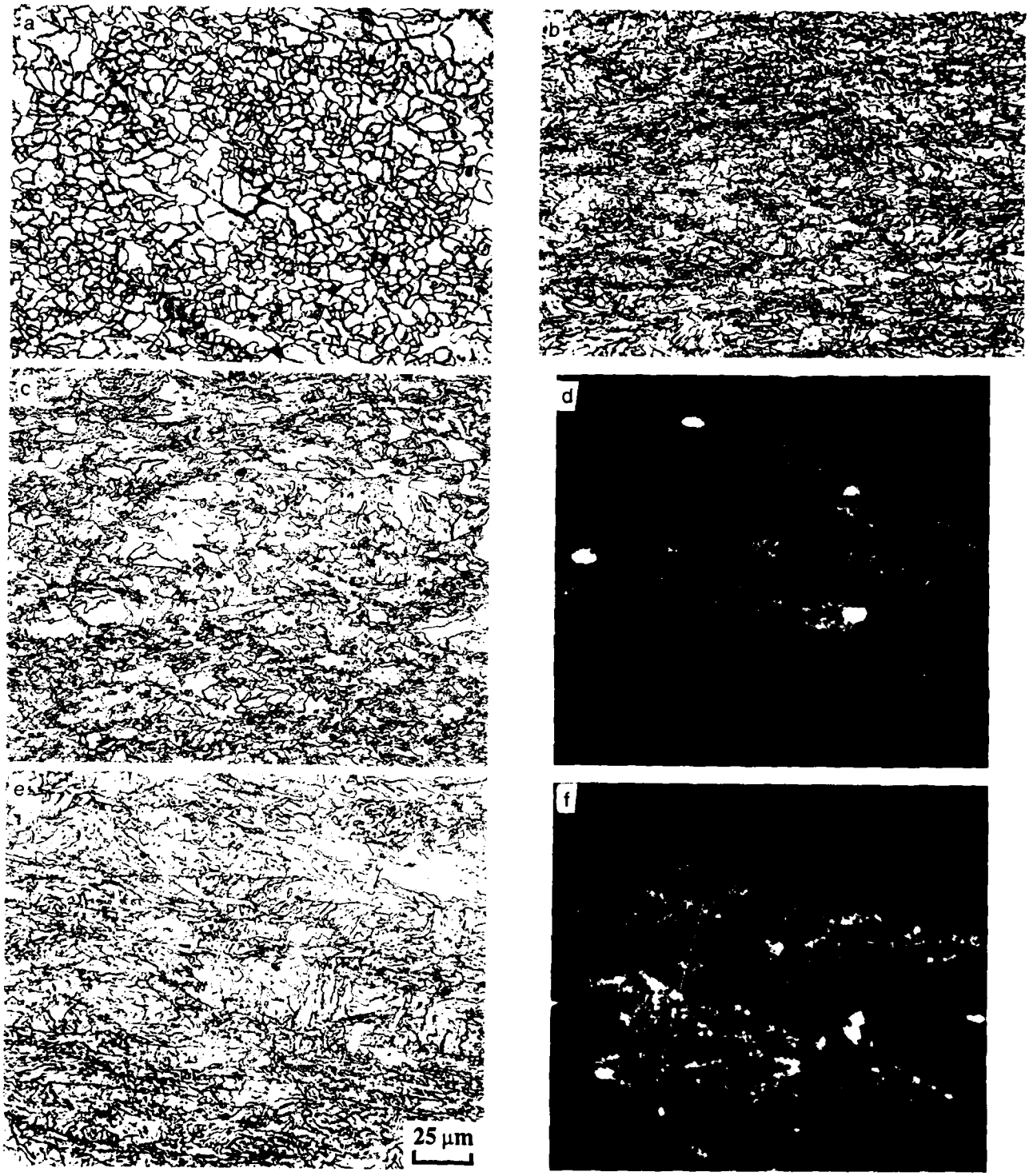


Fig. 5 - (a) Microstructure of alloy 1 after dilatometer simulation.
(b) Microstructure of vacuum-cast alloy 2C after dilatometer simulation.
(c) Microstructure of air-cast alloy 2A after dilatometer simulation.
(d) Boron distribution in material in (c). (SIMS - field of fiew is 150 µm.)
(e) Microstructure of alloy 2B after dilatometer simulation. Starting condition was as-rolled plate.
(f) Boron distribution in material in (e). (SIMS - field of view is 150µm.)

rolled materials, than in air-cast material tested without prior rolling.

The observation that transformation temperature shifted downward producing a fully bainitic microstructure when as-rolled, air-cast plate was tested in the dilatometer was surprising. A trial was conducted to ascertain whether a similar effect could be obtained by rolling. A piece of the as-rolled plate 2A was reheated at 1100°C for 20 min and then reduced in two passes of 25% each at 850 and 815°C prior to cooling at 1.2°C/s. The microstructure of the plate appeared to be 100% bainite (Fig. 6). Apparently, the boron hardenability effect in the air-cast material can be enhanced by a preliminary reheat and hot working treatment.

## DISCUSSION

The results of the present study indicate that the addition of 20 ppm of boron to a steel containing 0.006 wt % sulphur and 0.0085 wt % oxygen is only partially effective in suppressing ferrite formation. Although transformation temperatures are suppressed by 75-100°C compared with the alloy containing no boron, the transformation start temperature is still above the bainite-start temperature. When sulphur and oxygen contents are reduced to 0.004 wt % and 0.0057 wt % respectively, the transformation start temperature is reduced by another 25°C and a completely bainitic microstructure is obtained. It is also shown that similar transformation behaviour and microstructures can be obtained in air-cast steel containing high impurity contents if the cast steel is subjected to a double hot rolling process.

Although the precise mechanism is not fully understood, it is generally accepted that boron acts to suppress ferrite nucleation at austenite grain boundaries. Thus, if boron is to be fully effective, it must be distributed relatively uniformly to all austenite grain boundaries prior to the start of transformation. In the present study, the conditions which produce completely bainitic microstructures correlate with those which produce the most homogeneous boron distribution. Conversely, with an inhomogeneous boron distribution, such as in the as-rolled alloy 2A, the size and shape of the areas of ferrite in the final microstructure appear to coincide with the boron-free bands.

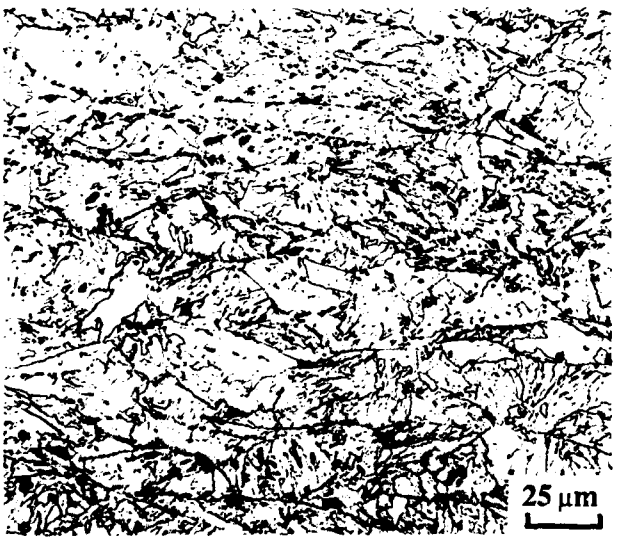


Fig. 6 - Microstructure of rerolled plated, austenitized 2 h at 1100°C, deformed 25% at 850 and 815°C, and cooled at 1.2°C/s.

The results of the present study indicate the importance of inclusion content and distribution in controlling the effectiveness of boron in suppressing ferrite formation. It is apparent from the SIMS analysis that boron migrates preferentially to inclusions during solidification and cooling of the ingot. Although the form the boron assumes at the inclusion has not been examined in this study, work has been reported (6) which demonstrates the precipitation of BN and $Fe_{23}(B,C)_6$ at MnS and $Al_2O_3$ inclusions. As well, it has been suggested that boron may exist in solution in stable oxide particles (7). Clearly, boron precipitation at inclusions reduces the amount of boron available for segregation to austenite grain boundaries. Consequently, the effectiveness of boron will depend upon its dissolution and homogenization in the austenite during austenitization and controlled rolling.

The homogenization of the boron distribution depends critically upon both the volume content and distribution of inclusions. By reducing the total number of inclusions, the number of preferred sites for boron precipitation during solidification and cooling is reduced and a greater quantity of boron will be left in solid solution or to precipitate at secondary sites such as grain boundaries, throughout the matrix. Thus reduced inclusion content results in a more uniform boron distribution in the as-cast material and facilitates the achievement of a homogeneous boron distribution during subsequent austenitization of the plate. The importance of inclusion content in determining the effectiveness of boron has previously been recognized and the hardenability of boron-containing steels has been correlated to such factors as sulfur content (6).

Even when the inclusion content of the boron-containing steel is relatively high, the use of a two stage processing schedule in which the steel is first heavily worked in the austenite region and cooled to room temperature prior to the final hot working treatment, can be used to improve the effectiveness of boron. Although there has been little discussion in the literature of the precise effects of deformation, hot-working is often performed as a preliminary step in many laboratory studies of boron-containing steels (see for example Ref. 8,9). Although results from the present study are ambiguous, a conjecture may be offered as to the effect of the preliminary hot working treatment on the effectiveness of boron. During the austenitizing treatments applied prior to rolling (2 h at 1100°C), any BN and $Fe_{23}(B,C)_6$ precipitates should dissolve. However, if the boron is in part dissolved in stable oxides or oxysulfides, it may not be fully dissolved into the steel matrix under these treatments. Indeed, in

(a) Air-cast ingot.

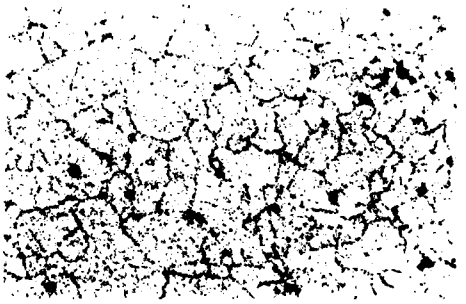

(b) Austenitized 2 h at 1100°C and quenched.

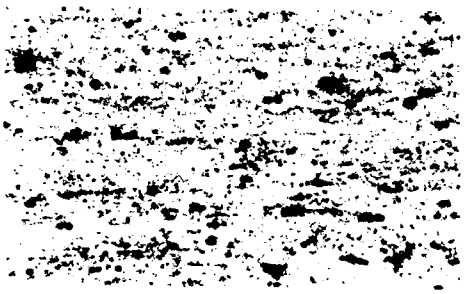

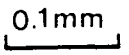


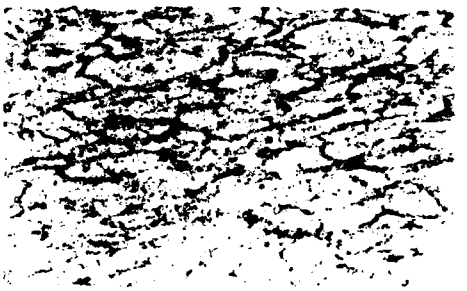

(c) As-rolled plate.

(d) Dilatometer specimen (starting condition - as-rolled plate).

Fig. 7 - Boron distribution in the as-cast material at different points in the processing schedule. (autoradiography)

studying BN precipitation in low carbon steels, Tanino et al. (7) observed a number of boron aggregates even after 1 h at 1250°C.

In the present study, large boron-rich precipitates are observed by autoradiography in the air-cast alloy (Fig. 7a) which would appear to correspond to the boron-containing inclusions observed by SIMS in the same material. After a 2 h austenitizing treatment at 1100°C followed by a water quench, the large boron-containing particles are still evident (Fig. 7b). (The obvious segregation of boron to austenite grain boundaries in this condition likely results from nonequilibrium segregation during quenching.) In the as-rolled plate, boron-containing particles are again present, although there is evidence that the particles have been broken into stringers of smaller particles during the large rolling reduction (Fig. 7c). When the as-rolled material is reaustenitized in the dilatometer, deformed and cooled to room temperature, no evidence of the coarse boron particles is found, and uniform segregation of boron to austenite grain boundaries is observed (Fig. 7d). It is suggested that boron exists in stable forms associated with inclusions, which are not readily dissolved under normal austenitizing conditions. Heavy deformation during rolling breaks down the coarse boron-containing particles and thereby facilitates the release of boron from these particles into the matrix during subsequent high temperature austenitizing treatments. The SIMS analysis of boron distribution in as-rolled plate has not yet provided conclusive evidence of the validity of this conjecture. Boron enrichment was observed at some, but not all inclusions in the air-cast and as-rolled plate (Fig. 3). Furthermore, it is not clear whether boron was retained at inclusions throughout austenitization and controlled rolling or whether it underwent dissolution and reprecipitation during thermomechanical processing.

If the full effectiveness of boron is to be achieved in ultra low carbon bainitic steels, efforts must be made to control inclusion distributions. Two strategies may be adopted. The first, and probably most practical approach, given the current industrial move toward production of clean steels, is to minimize the total inclusion content, thereby minimizing the number of sites at which boron will precipitate. The second approach is to ensure homogenization of boron by adoption of appropriate thermomechanical processing schedules. Although this approach has received little attention, the present study indicates the benefits of a preliminary hot-working treatment to improve the effectiveness of boron. As well, it is presumed that application of high temperature

austenitizing treatments would also assist to free boron from inclusions.

## CONCLUSIONS

The effects of inclusion content and thermomechanical treatment on the microstructure development of ULCB steels containing boron have been examined. The transformation temperature of vacuum-cast alloy (0.004 wt % S, 0.0057 wt % O) was approximately 25°C lower than that of a comparable air-cast alloy (0.006 wt % S, 0.0085 wt % O) resulting in a fully bainitic microstructure, whereas a mixed ferrite-bainite microstructure was obtained in air-cast material. The microstructure of the air-cast alloy was improved when as-rolled plate was reprocessed (reaustenitized, deformed and cooled). Such a treatment resulted in transformation behaviour similar to that of the vacuum-cast alloy.

Inclusions play a critical role in controlling the effectiveness of boron in these steels. By minimizing the total content of inclusions, at which boron preferentially precipitates, the boron available to segregate to austenite grain boundaries is maximized. Alternatively, the release of boron from relatively stable precipitates may be achieved by application of heavy deformation schedules which break up the inclusions into small particles from which boron is readily released during subsequent austenitizing treatments.

## ACKNOWLEDGEMENTS

The authors wish to thank Dr.M. Nagumo of Nippon Steel for his assistance in performing autoradiography. The assistance of Dr. M. Shehata and Mr. B. Casault in the characterization of inclusions and of Mr. B. Durocher in performing optical metallography is gratefully acknowledged.

## REFERENCES

1. Nakasugi, H., H. Matsuda and H. Tamehiro, "Alloys for the 80's", 213-224, Climax Molybdenum, Ann Arbour, Michigan (1980).
2. Taira, T., K. Matsumoto, Y. Kobayachi, K. Takestringe and I. Kozasu, "HSLA Steels-Technology and Applications", 723-731, ASM, Metals Park, Ohio, (1984).
3. Tamehiro, H., M. Murata and R. Habu, "HSLA Steels - Metallurgy and Applications", 325-333, ASM, Metals Park, Ohio, (1986).
4. He, X. L. and Y. Y. Chu, J. Phys. D: Appl. Phys., 16, 1145-1158, (1983).
5. Dionne, S., M. R. Krishnadev and L. E. Collins, to be published.
6. Saeki, M., F. Kurosawa and M. Matsuo, Trans. ISIJ 26, 1017-1035, (1986).
7. Tanino, M., S. Funaki, H. Komotsu and Y. Q. Zhang, Trans. ISIJ, 21, B-231, (1981).
8. Watanabe, S., H. Ohtani and T. Kunitake, Trans. ISIJ, 23, 122-128, (1983).
9. Yamanaka, K., and Y. Ohmoni, Trans. ISIJ, 17, 92-101, (1977).

# MEDIUM STRENGTH BAKE HARDENABLE STEELS FOR DRAWING

**João Francisco Batista Pereira, Haroldo Barcelos, Luiz Nelson Teixeira Klein**
Usiminas Steel Works
Ipatinga, MG, Brazil

Abstract

The effect of chemical composition (carbon, phosphorus, silicon and manganese) and coiling temperature on bake hardenability and drawability of laboratory produced aluminum killed steels have been studied. Based on these results a medium strength bake hardenable steel was produced on industrial scale using batch annealing process.
Results are presented on the performance of an automotive panel made from this new steel.

IN RECENT YEARS, increased emphasis has been given to the development of new steels for the automotive industry which have high strength and good ductility(1).

A successfull example of this effort are the so called bake hardenable steels, where the desired hardness is obtained by strain ageing during baking treatment in the painting line of automotive industry.

The efficiency of strain ageing, as hardening mechanism, is associated with the presence, in significant amounts, of interstitial elements in solid solution(2). This fact, in some way, has confined the production of bake hardenable steels to annealing process with high cooling rates(3,4).
Since batch annealing process has a low cooling rate, the steel composition(5), and coiling temperature(6) can strongly influence the total interstitial content of the steel at room temperature.

The laboratory experiments were performed to identify the main parameters that affect the production of bake hardenable steels by batch annealing process.

Based on these laboratory results an Al-killed bake hardenable industrial heat was produced. The laboratory bake hardenability parameters were compared with that of a finished panel produced in a automotive industry with the new product.

## MATERIALS AND EXPERIMENTAL METHODS

LABORATORY STUDIES - Eight 50 kg laboratory vacuum melted ingots were produced. The chemical compositions are shown in table I.

TABLE I - Chemical composition (wt %)

| SAMPLE No. | C | Mn | P | Si | Cr | $Al_{(s)}$ | $N_T$ | P + Si |
|---|---|---|---|---|---|---|---|---|
| 1 | 0.028 | 0.27 | 0.021 | 0.03 | 0.021 | 0.044 | 0.0024 | 0.051 |
| 2 | 0.019 | 0.18 | 0.097 | 0.06 | 0.019 | 0.042 | 0.0047 | 0.157 |
| 3 | 0.023 | 0.26 | 0.016 | 0.22 | 0.018 | 0.045 | 0.0038 | 0.236 |
| 4 | 0.026 | 0.18 | 0.079 | 0.29 | 0.014 | 0.067 | 0.0046 | 0.369 |
| 5 | 0.025 | 0.20 | 0.006 | 0.59 | 0.014 | 0.052 | 0.0063 | 0.596 |
| 6 | 0.030 | 0.21 | 0.059 | 0.52 | 0.018 | 0.039 | 0.0070 | 0.579 |
| 7 | 0.027 | 0.42 | 0.017 | 0.23 | 0.017 | 0.046 | 0.0046 | 0.247 |
| 8 | 0.050 | 0.25 | 0.020 | 0.22 | 0.018 | 0.051 | 0.0037 | 0.240 |

The composition (table I) was so chosen in such a way that the influence of carbon, manganese, silicon and phosphorus, on the mechanical properties could be studied.

Figure 1 shows schematically the route adopted to process ingots to cold rolled sheets.

The strain ageing sensitivity was evaluated according to figure 2. The load-extension curves were generated using tensile test pieces (ASTM-370) parallel to rolling direction. The test pieces were 6.0% tensile prestrained at a cross-head speed of 5mm/min and subsequently aged at 180°C for 20 minutes. The drawability was evaluated by using Lankford $\bar{R}$ value and strain hardening coefficient ($\bar{n}$).

INDUSTRIAL TRIALS - The chemical composition of experimental heat, based on pilot scale results, is shown in table II. The latter includes a D.D.Q. steel for comparison purposes.

The experimental heat was produced by the same process route adopted for D.D.Q. steel. Coiling temperature was fixed between 550 and 600°C, and subjected to a 1.0% skin pass. A 2.0% prestrain in tension was adopted instead of 6.0%

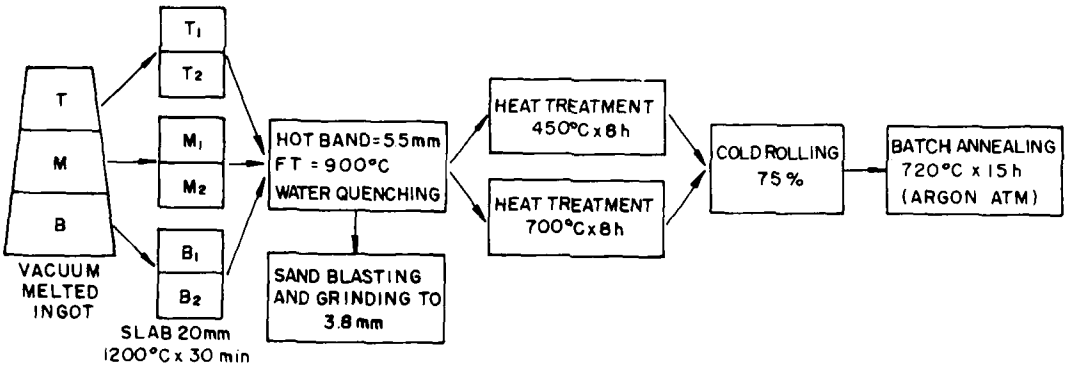


FIG.1 - Laboratory processing route

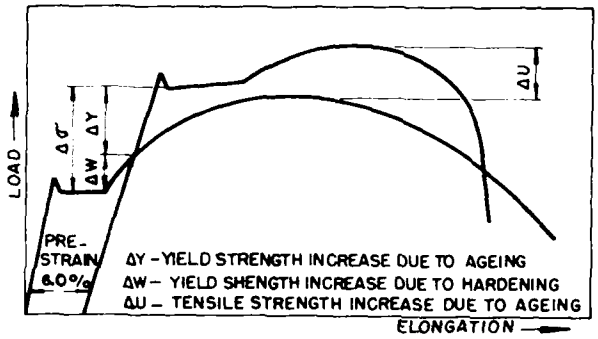


FIG.2 - Load-extension diagram

TABLE II - Chemical composition of industrial heat (wt %)

| ELEMENTS | C | Mn | S | Al(s) | N | O | P + Si |
|---|---|---|---|---|---|---|---|
| EXPERIMENTAL | 0.029 | 1.19 | 0.008 | 0.038 | .034 | 0.0054 | 0.11 |
| E.E.P. | 0.042 | 0.27 | 0.014 | 0.62 | 0.0054 | .027 | .34 |

used in laboratory samples, that weren't temper rolled. For better formability evaluation a forming limit diagram of new material was drawn(7).

Table III lists the tensile properties, drawability indices, bake hardenability parameters (2.0% prestrain plus 180 x 20 minutes) and results of metallographic examination of experimental and D.D.Q. steels.

PRODUCT PERFORMANCE - In laboratory studies the bake hardenability of materials is evaluated after a fixed prestrain followed by an ageing treatment of 180 C x 20 minutes. On an industrial painting line however, the pressed component is subjected to a sequence of heat treatments in the order listed in table IV.

TABLE IV - Thermal treatment at a continuous industrial painting line

| SCHEDULE NUMBER | DESCRIPTION | THERMAL TREATMENT |
|---|---|---|
| 1 | Pre-treatment - (De-greasing and Phosphatizing) | 180°C x 12 min |
| 2 | Electrophoretic painting | 185°C x 22 min |
| 3 | Primer coat | 160°C x 20 min |
| 4 | Protective coat | 185°C x 30 min |
| 5 | Finishing coat | 142°C x 20 min |

A laboratory simulation of these heat treatments resulted in the properties given in table V.

In order to estimate the strength changes due to strain ageing, under actual practical conditions, tests were carried out on a rear-quarter panel of a car. A gridded blank was formed in an automotive plant, under regular condition of panel production. This panel did not

TABLE III - Comparison of mechanical properties and territic grain size of experimental and D.D.Q steel

| STEEL | ORIGINAL MECHANICAL PROPERTIES (MPa) | | | BAKE HARDENABILITY 180°C x 20 min (MPa) | | | MECHANICAL PROPERTIES AFTER PRE-STRAIN AND BAKING (MPa) ** | | | DRAWABILITY | | | GRAIN SIZE |
|---|---|---|---|---|---|---|---|---|---|---|---|---|---|
| | Y.S. | T.S. | EL (%) * | ΔY | ΔW | Δσ | Y.E. | T.S. | EL. (%) * | $\bar{R}$ | $\bar{n}$ | ΔR | ASTM |
| EXPERIMENTAL | 238 | 374 | 39 | 41 | 44 | 85 | 322 | 383 | 36 | 1.80 | 0.20 | 0.25 | 9.0 |
| E.E.P. | 189 | 319 | 48 | 15 | 32 | 85 | 236 | 325 | 48 | 1.80 | 0.22 | 0.81 | 8.5 |

* Gage Length = 50 mm

** 2.0% pre-strain and 180°C x 20 minutes

TABLE V - Laboratory results simulation

| STAGES | Y.S. (MPa) | Y.S.A * (MPa) | EL(%) G.L.= 50 mm | T.S. (MPa) | ΔY (MPa) | Δσ (MPa) | ΔX (%) | CONDITION |
|---|---|---|---|---|---|---|---|---|
| 1 | 234 | 318 | 38 | 378 | 38 | 84 | 1.7 | 180°C x 12 min |
| 2 | 237 | 320 | 38 | 378 | 39 | 82 | 1.7 | 185°C x 22 min |
| 3 | 235 | 317 | 37 | 376 | 39 | 84 | 1.7 | 160°C x 22 min |
| 4 | 242 | 324 | 38 | 377 | 40 | 80 | 1.8 | 185°C x 7 min |
| 5 | 236 | 319 | 35 | 378 | 37 | 85 | 1.8 | 142°C x 27 min |

* Y.S.A. = Yield Strength after ageing
thickness = 0.8 mm

receive any surface coating, but was submitted to the same heat treatments of commercial panels. Figure 3 shows a sketch of the panel and the five positions from which tensile test pieces were extracted. These regions were selected because they had low deformation and they allowed flat tensile test pieces to be taken. The arrows (figure 3) indicate the major strain directions and the tensile test piece orientations.

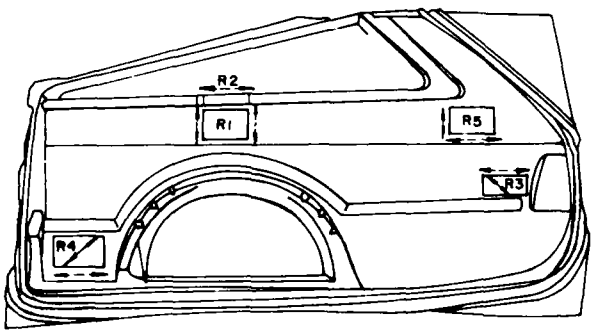


FIG.3 - Panel draw showing regions where test pieces were cut from

At least nine measurements were taken at each of the five locations and the mean equivalent strain values are given in table VI together with the tensile properties(23).

## RESULTS AND DISCUSSION

The effect of total phosphorus plus silicon content on the bake hardenability is shown in figure 4.

It is evident that for (P + Si) contents greater than 0.1%, it is possible to achieve ΔY and ΔU values higher than 30 MPa and 10 MPa respectively.

Grain boundary segregation in preference to carbon seems to be the reason why phosphorus increase bake hardenability(5). As for silicon it tends to form a barrier around the carbides and so retard its growth(5,8,9). The effect of carbon and manganese on the bake hardenability of samples heat treated to 450 C and 700°C for 8 hours is presented in figure 5. Data suggest that lower contents of carbon and manganese are beneficial to bake hardenability.

TABLE VI - Mechanical properties of panel after baking

| MATERIAL | REGION | PRESTRAIN (%) | (**) | Y.S. (MPa) | T.S. (MPa) | EL(%) G.L.= 50 mm | Δσ (MPa) | ΔU (MPa) |
|---|---|---|---|---|---|---|---|---|
| ORIGINAL | - | - | | 238 | 374 | 39 | - | - |
| PANEL(*) | 1 | 2.24 | | 323 | 387 | 37 | 85 | 13 |
| | 2 | 2.91 | | 337 | 393 | 38 | 99 | 19 |
| | 3 | 3.32 | | 364 | 395 | 36 | 126 | 21 |
| | 4 | 3.00 | | 372 | 397 | 35 | 134 | 23 |
| | 5 | 4.15 | | 368 | 398 | 34 | 120 | 24 |

* ASTM A-370 - sub-size
** Equivalent Strain

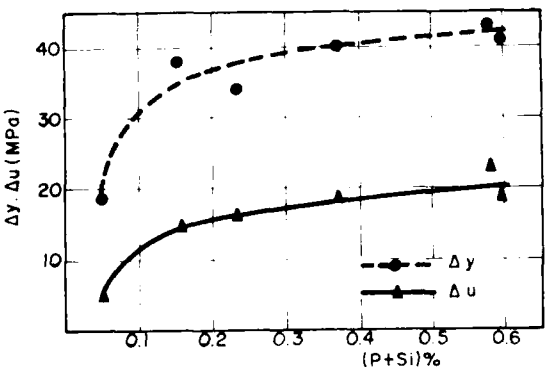


FIG.4 - Effect of (P + Si) Wt% on the bake hardenability samples heat treated 450 C x 8 hours

At room temperature, carbon in solid solution depends on the annealing temperature, amount of cementite and total carbon of steel(10, 11). If the total carbon is increased and annealing temperature is kept constant, the cementite acts as nuclei for carbon precipitation.

Manganese behaves as a cementite stabilizer and reduces the effect of carbon on age hardening sensitivity(5,8,11).

The influence of chemical composition on Lankford $\bar{R}$ value, for samples heat treated at 450°C and 700°C during 8 hours is shown in figure 6.

These data show that, at low carbon and manganese contents the steels exhibit better forming characteristics. This observation confirms the results of previous studies(12,14), where the deterioration of Lankford $\bar{R}$ value, due to the increased carbon and manganese contents, was associated with a decrease of

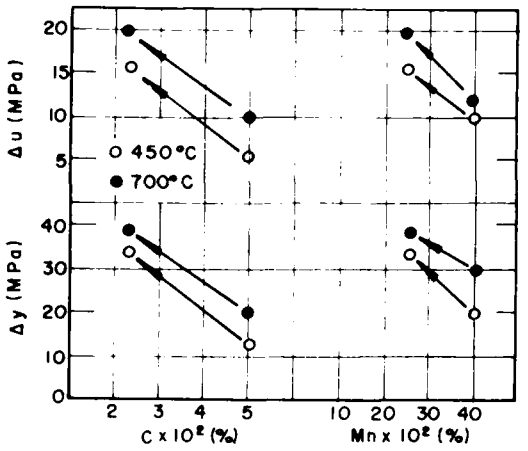


FIG.5 - Effect of carbon and manganese on the bake hardenability. Samples heat treated at (450°C and 700°C) x 8 h

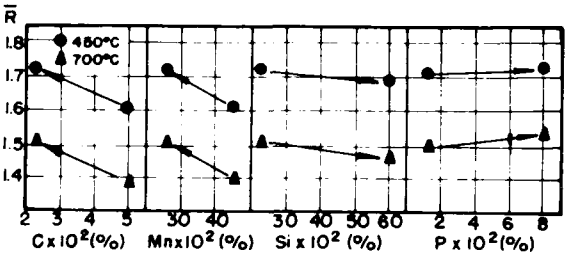


FIG.6 - Effect of chemical composition on $\bar{R}$ value, samples heat treated (450°C and 700°C) x 8 h

{111}<uvw> texture component and smaller recrystallized grains. The mechanism by which carbon and manganese affect texture is not completely clear yet. As for the influence of phosphorus, data published in the literature show that the drawability of the steel is superior to that of standard aluminum killed steels(15,16). However some authors have reported(17,18) contrary results. Present work has shown that the increase in Lankford value due to phosphorus is negligibly small. It appears that the role of phosphorus is to increase the mechanical strength of the steel without deteriorating its drawability. This behavior of phosphorus can be extended to silicon, in agreement with other papers(19).

Figure 5 showed an increase in bake hardenability when the coiling temperature increased from 450°C to 700°C. It seems that this behavior is related to cementite size, distribution and morphology, as observed in figure 7.

Considering sample 8 as a general case, cementite in material hot rolled and coiled at 450°C was found to be randomly distributed. The material coiled at 700°C showed coarse cementite with a tendency to concentrate preferentially along grain boundaries. After annealing the cementite characteristics kept a close relation with that observed in as hot rolled material.

The increase in mean free path of cementite in material coiled at 700°C, makes carbon atoms diffuse through larger distances to precipitate(6), favouring a large amount of this element in solid solution at room temperature.

Drawability is strongly decreased with increasing coiling temperature (figure 6). This observation agrees with the theory(20,21) that, if aluminum nitride precipitated during hot rolling for material processed by batch annealing it produces a texture unfavorable for drawing.

From the present study it was clear that the coiling temperature must be chosen as a compromise between bake hardenability and drawability.

From table III it follows that the new ma-

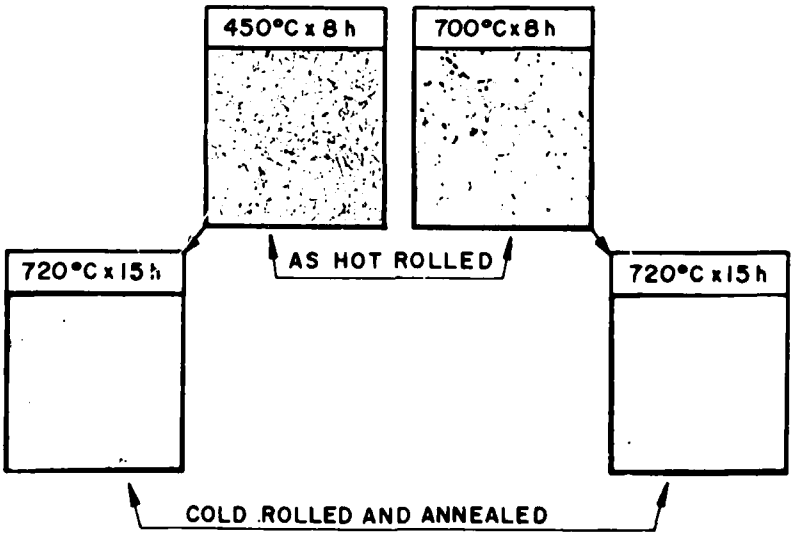


FIG.7 - Cementite morphology as a function of heat treatment Sample 8 - (Picral 4% - 200x)

terial gives a significant mechanical strength increase while mantaining the same formability capacity of D.D.Q. steel. An additional advantage was that the material gave an increase of about 40 MPa in $\Delta Y$, besides a lower planar anisotropy $\Delta \bar{R}$.

Figure 8 presents the F.L.D for both steels. As can be observed the curves are very similar, mainly in the drawing region. In the stretch region the difference can be attributed to coefficient n but both steels present excellent forming characteristics.

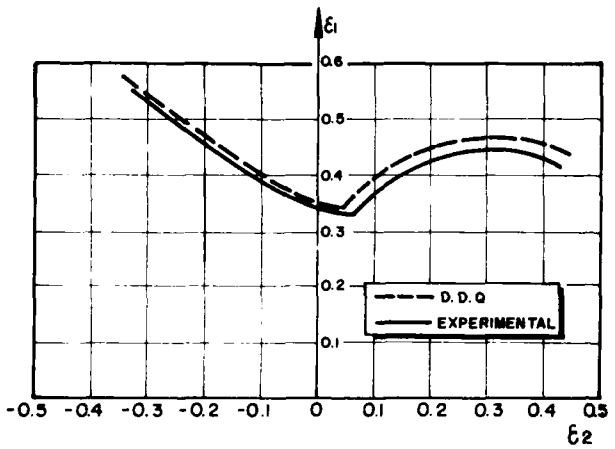


FIG.8-F.L.D for D.D.Q and experimental steels. thickness = 0.8 mm

The results of laboratory simulation of an industrial painting line (table V) show that after the first heat treatment no more changes in mechanical properties occur in material. Also the strength reaches its peak value in the initial treatment and no hardening of softening is observed in subsequent treatments. These results together with those of previous studies (22) lead to the conclusion that bake hardening can be simulated successfully by a single heat treatment of 180°C x 20 minutes in laboratory.

The test results of the industrial panel (table VI) show that the panel strength is appreciably improved by using experimental steel. It should be noted that the test pieces, for geometric reasons, were taken from flat regions of the panel which have suffered small deformations. Consequently the results given are considered as minimum values.

Table VI also shows, as general rule, that $\Delta\sigma$ increases with increasing strain. In effect it reflects the change of $\Delta W$ ($\Delta\sigma \simeq \Delta Y + \Delta W$) which is strongly strain dependent and $\Delta Y$ is practically constant(2). Neverthless an explanation was not found for $\Delta\sigma$ in regions 4 an 5. This discrepancy should be associated with factors such as different types and directions of strain path.

Another important aspect worth noting is that the gain in the strength of commercial panel at a equivalent strain of 2% was aproximately the same as that observed in the laboratory simulation test.

## CONCLUSIONS

The evaluation of the effect of chemical composition (carbon, manganese, silicon and phosphorus) and coiling temperature on the bake hardenability and drawability of aluminum killed steels gave the following conclusions:

- The bake hardenability is reasonably increased by lowering carbon and manganese contents and adding silicon and/or phosphorus, even for slow heating rates during annealing.
- The use of a steel with carbon content about 0.02% and manganese about 0.2% and silicon plus phosphorus in the range of 0.1 to 0.6% allows an increase of more than 30 MPa in yield strength and 10 MPa on tensile strength.
- The chemical composition studied produces a material with good drawing properties. Lowering carbon and manganese contents below the level of usual drawing quality steels improves Lankford $\bar{R}$ value. With the addition of silicon or phosphorus, $\bar{R}$ value is not apparently affected.
- The use of high coiling temperature increases the bake hardenability and decreases drawing characteristics ($\bar{R}$ value).
- It has been possible to produce on industrial scale a medium strength bake hardenable steel, with good drawing characteristics, using batch annealing process.
- Formed panels with small strains (2%) could achieve an increase in yield strength of 90 MPa after processing on the industrial line.
- The treatment of 180°C x 20 minutes adequately simulates an industrial painting line for this material, because no change in mechaical properties can be observed after this treatment.

## REFERENCES


1 - Takeshi, H. - Recent Developments in Production Technology of Automotive High Strength Steel Sheet, Nippon Steel Corporation - R&D Labs. II., Sagamihara City - Japan (1982)

2 - Baird, I.D. - Iron and Steel, 186, 326, 368, 400, 450, May to September, (1983)

3 - Wilson D.V. - Sheet Metal Industries, 61 (1) : 50-52, January, (1984)

4 - Irie, T., Satoh, S., Yasuda, A., Hashimoto, O. - Charles Hatchett Award Paper, (1984)

5 - Okamoto, A., Takahashi, M., Hino, T. - Transactions ISIJ, 24(11):17-23, (1984)

6 - Butler, J.F. - Transactions AIME, 224:89, (1962)

7 - Klein, L.N.T., Carvelin, F. - Metalurgia ABM 39(307):311-317, June, (1983)

8 - Leslie, W.C. - The Physical Metallurgy of Steels - Mc Graw-Hill Book Company, 79-80 (1981)

9 - Owen, W.S. - Transactions ASM, 46, p. 812 (1954)
10 - Takakai, T., Harada, S. - JIS, p. 191, (1968)
11 - Hanai, S., Takemoto, H., Tokinaga, Y., Misuyama, Y. - Transactions ISIJ ; 24 (1) : 17-23, (1984)
12 - Matsudo, K., Shimomura, T. - Transactions ISIJ, 10 : 448-58, (1970)
13 - Ichiyama, T., Yoshida, I., Ejima, M., Matsumura, O. - Transactions ISIJ, 15 : 69-78, (1975)
14 - Messien, P., Leval, T., Greday, T. - CRM, 39, June, (1974)
15 - Hu, H. - Texture of Crystalline Solids, 2 : 113-41, (1976)
16 - Hu, H. - Metallurgical Transactions, 8A : 1567-75, (1977)
17 - Matsudo, K., Shimomura, T., Osawa, K., Sakoh, M., Ono, S. - The Sixth International Conference on Texture of Materials : 759-68, Tokyo, (1981)
18 - Ono, S., Shimomura, T., Osawa, K., Matsudo, K. - Transactions ISIJ, 22(9) : 732-42, (1982)
19 - Hu, H. - Simposium Conformable HSLA and Dual Phase Steels : 109-25, (1977)
20 - Ichyama, T., Kovzumi, M., Ioshida, I., Watanabe, K. - Transactions ISIJ, 10 : 429-41, (1970)
21 - Parniere, P. - Mem. Scient. Revue de Metallurgie, 70(6) : 445-55, June,(1973)
22 - Pereira, J.F.B., Mirra, E.P.S. - II ETUAN, Rio de Janeiro, Brazil, May, (1987)
23 - Dieter, G.E. - Mechanical Metallurgy - McGraw-Hill Kogakosha, Ltd. II Ed. p. 80, (1976)